F 1103 04 64 R

ACADÉMIE DE LA RÉPUBLIQUE SOCIALISTE DE ROUMANIE

1986 FEB 1 1

REVUE ROUMAINE DE CHIMIE

MG

REFERALVA

TOME 31
Nº 1
Janvier 1986

Rev. Roumaine Chim.
RRCHAX, 31, *1*, p. 1–116 (1986), Bucarest
EDITURA ACADEMIEI REPUBLICII SOCIALISTE ROMÂNIA

ACADÉMIE DE LA RÉPUBLIQUE SOCIALISTE DE ROUMANIE

COMITÉ DE RÉDACTION

Rédacteur en chef:

I. G. MURGULESCU, membre de l'Académie de la République Socialiste de Roumanie

Rédacteurs en chef adjoints:

A. T. BALABAN et V. EM. SAHINI, membres correspondants de l'Académie de la République Socialiste de Roumanie

Collège de rédaction:

EM. BRATU, ELENA CEAUŞESCU, ECATERINA CIORĂNESCU-NENITZESCU, CR. SIMIONESCU, membres de l'Académie de la République Socialiste de Roumanie; S. SPACU, membre correspondant de l'Académie de la République Socialiste de Roumanie; M. BANCIU, M. D. GHEORGHIU, I. HAIDUC, D. I. MARCHIDAN, I. MOLDOVAN, G. NIAC et D. SĂNDULESCU

La Revue Roumaine de Chimie paraît 10 fois par an. Toute commande de l'étranger sera adressée à « ROMPRESFILATELIA » — sectorul Export-Import Presă, P.O. Box 12—201, télex 10376 prsfi r 78104, Calea Griviţei nr. 64—66, Bucureşti, Roumanie

Les manuscrits, les livres et les revue proposés en échange, ainsi que toute correspondance seront envoyés à la rédaction :

REVUE ROUMAINE DE CHIMIE

125, Calea Victoriei, 79717 Bucarest, Roumanie, téléphone 50 76 80

EDITURA ACADEMIEI REPUBLICII SOCIALISTE ROMÂNIA
125, Calea Victoriei, 79717 Bucarest, Roumanie, téléphone 50 78 60

REVUE ROUMAINE DE CHIMIE

Tome 31, N° 1 **Janvier, 1986**

S. STERNBERG, M. UNGUREANU and I. LINGVAY, Study of polarization of the semiconductor silicon electrodes in ammonium fluoride solutions 3 8

G. LÓPEZ CUETO and A. ALONSO MATEOS, Study on controlled-potential coulometric anodic oxidation of the binuclear Mn(III)-cyanide complex. III. Correction of positive and negative kinetic currents for its coulometric determination. Electrolytic formation of the binuclear cyanide complex of Mn(III) – Mn(IV). (in Spanish) 9 15

CLEOPATRA VASILIU OPREA and FELICIA WEINER, Modification of structure and properties of PVC-S by the processing on rollers in the presence of some new filling materials 17 23

GH. MANDRIC, GABRIELA NEAMŢU, SILVIA PECINCU and GETA RĂCARU, High temperature polymers. VI. Polybenzimidazole-amide-imides 25 30

CAMELIA BELDIE, NATALIA HURDUC, ANA ONU and IGNAT C. POINESCU, Thermal behavior of some styrene-methylmethacrylate copolymers 31 35

ALEXANDRU T. BALABAN, GEORGE MARTON and IOSIF SCHIKETANZ, Reaction of pyrylium salts with nucleophiles. XVIII. Synthesis of 4 (*p*-n-butoxyphenyl)-2,6-dimethylpyridine and of 2,6-dimethyl-4 (*p*-n-pentylphenyl)-pyridine 37 41

MIHAELA HILLEBRAND, MIRCEA IOVU, NADIA NICOLAU and ELENA VOLANSCHI, Spectral study of the anion-radicals provided by some nitro- and amino-ethers 43 49

C. I. CHIRIAC, A convenient method for the synthesis of 1,3,4-oxadiazoles from diaroylhydrazines under mild conditions using phosphorus trichloride-dimethylformamide adduct as reagent 51 55

NARENDRA NATH, R. C. DUBEY and U.S. MISRA, Kinetics of oxidation of digol by vanadium(V) in aqueous sulphuric and hydrochloric acid medium 57 62

R. P. VARMA and A. K. VIRMANI, Studies on physical properties of cadmium soaps. III. Dehydration and thermal decomposition studies of soaps by thermogravimetry 63 69

N. CALU, ELENA BĂLĂNESCU, I. BERDAN and I. SANDU, Complex compounds of Mn(III) and Mn(IV). II. The system Mn(III, IV) — 2-aminophenol-4-sulfone acid (in French) 71 78

Rev. Roumaine Chim. **31**, *1*, 1–116 (1986), Bucarest

FLORENŢA DOGAR, LUMINIŢA SILAGHI-DUMITRESCU, RODICA GRECU and IONEL HAIDUC, Amine adducts of nickel(II) diphenyldithiophosphinate with substituted ethylenediamines. 79 83

B. K. PURI, ATUL KUMAR and M. SATAKE, Spectrophotometric determination of cadmium and lead after adsorption of their n-butylxanthates onto microcrystalline naphthalene and replacement by copper 85 92

A. L. J. RAO and USHA GUPTA, Extraction spectrophotometric determination of nickel and palladium using cyclohexylthioglycolate (CyHTG) as a reagent 93 98

I. V. NICOLESCU, RODICA MĂNĂILĂ, M. A. CHAAR and G. FILOTI, Structure and properties of the $ZnO.nFe_2O_3$ catalysts system in the oxydehydrogenation reaction. I 99 104

E. CHIFU, I. ALBU, C. I. GHEORGHIU, EUGENIA GAVRILĂ, M. SĂLĂJAN and MARIA TOMOAIA-COTIŞEL, Marangoni flow — induced by temperature gradients — against gravity forces 105 112

BOOK REVIEWS 113 116

Revue Roumaine de Chimie, **31**, *1*, 3—8 (1986)

STUDY OF POLARIZATION OF THE SEMICONDUCTOR SILICON ELECTRODES IN AMMONIUM FLUORIDE SOLUTIONS

S. STERNBERG*, M. UNGUREANU* and I. LINGVAY**
* Department of Physical Chemistry and Electrochemical Technology,
Polytechnic Institute Bucharest, Calea Griviței 132
** Radio Parts and Semiconductors Factory, Bucharest, Romania

Received January 12, 1985

The present paper reports the study of the polarization behaviour in steady-state conditions of n- and p-type silicon semiconductor electrodes in ammonium fluoride. The influence of dopping and electrolyte concentration is also studied.

INTRODUCTION

The previous studies on the behaviour of the semiconductor silicon electrodes in aqueous sulphuric acid[12] and potassium hydroxide[3] solutions showed that at the anodic polarization small currents exist as the silicon surface is covered by an oxide layer. This layer is broken only at high polarizations. The present paper reports the behaviour of the semiconductor electrodes in aqueous ammonium fluoride solutions, which have an etching effect on the silicon dioxide.

EXPERIMENTAL PART

The potentiostatic determinations in steady-state conditions were performed by the usual technique using a Princeton Applied Research potentiostat 173-model. The working cell for the polarization of the n-type silicon electrodes was a classical one[2,4]. The working electrode was a disk of monocrystal silicon with a working surface of 1 cm^2, sealed in a Pyrom glass tube. The counter electrode was a bright platinum sheet, and the reference electrode was a saturated calomel electrode (SCE). The studies of polarization of the p-type semiconductor silicon electrodes were performed in an electrochemical cell with two compartments separated by means of a Vycor porous glass diaphragm. The n-type semiconductor electrodes were dopped with phosphorus from $POCl_3$ and the p-type semiconductor electrodes were dopped with boron, using the technique described in the previous papers.[3–5]

Prior to each experiment the surface renewal of the silicon disk was accomplished. The electrode was pretreated as follows: etched in a 1 : 1 mixture of HNO_3 (70%) and HF (50%), b) rinsed in distilled water for 3 or 4 times. Then the electrode was maintained for 15 minutes at a potential that assures the complete surface cleaning by an intense evolution of hydrogen. The electrode was polarized using potential steps of 50 mV.

Chemical reagents of p.a. grade quality were used. All experiments were carried out at constant temperature of 20°C, in dark.

RESULTS AND DISCUSSION

A. *n-Type electrodes*

Potentiostatic determinations on the behaviour of the n-type silicon electrodes with the resistivity of 0.01 Ω cm in 40 % aqueous NH_4F solutions were performed. The silicon electrode was polarized anodically in steps from −2V(SCE). At this potential an intense evolution of hydrogen occurs.

The polarization curve, shown in figure 1a, has the following characteristics :

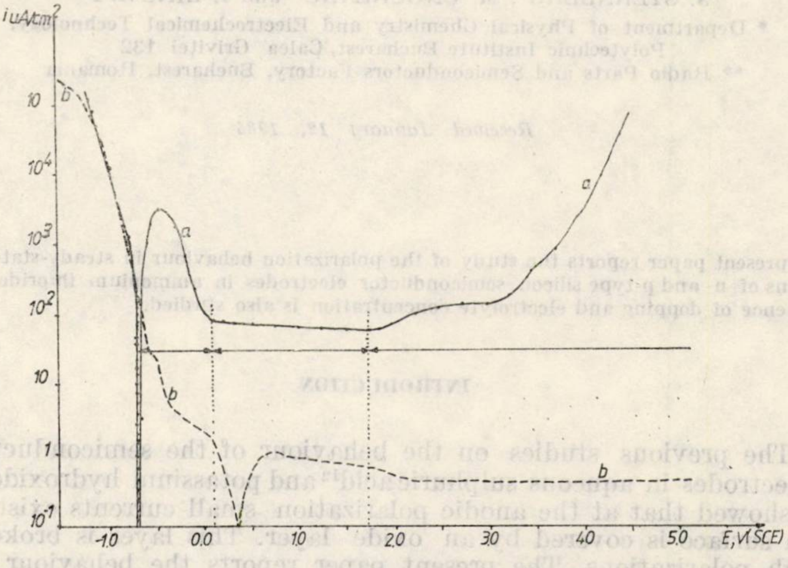

Fig. 1. — Polarization curves of the n-type 0.01 Ωcm silicon electrode in a) **40%** NH_4F and b) H_2SO_4 (d = 1.24 g/cm³) solutions.

a. The steady-state potential is $E_s = -0.85$ V(SCE) shifted with about 1 V more cathodically than the potential of the same electrode in sulphuric acid solutions [2,4] (see figure 1).

b. In the cathodic range, $\Delta E = E - E_s < 0$ (ΔE is the difference between the E potential imposed on the electrode and the E_s steady-state potential) the hydrogen discharge occurs with a Tafel slope of about 150 mV/decade.

c. In the anodic range, $\Delta E = E - E_s > 0$, the behaviour of the silicon electrode in NH_4F is very different from that in H_2SO_4, where the silicon is passivated and small passivation currents of about 1 μA/cm² are obtained ; the oxide layer is stable up to more than 5 V (SCE). The folllowing areas may be distinguished :

I (active) at $0 < \Delta E < 0.9$ V, with the maximum current of about 2600 μA/cm², corresponding to a $\Delta E = 0.4$V polarization ; II (passive) at $0.9 < \Delta E < 3.3$ V, with a constant passivation current of about 70μA/cm² (of about 70 times higher than the value of the passivation current in H_2SO_4 solutions) ; III (transpassive) within which the current increases again and the oxygen evolution occurs.

In more dilute 20 % NH_4F solutions the I (active) area appears within a smaller potential range with about 300 mV (see figure 2).

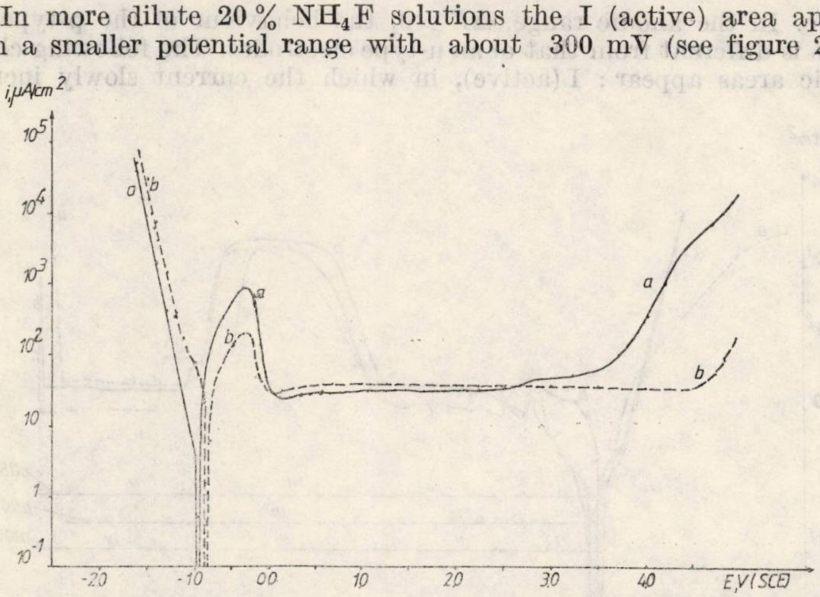

Fig. 2. — Polarization curves of the n-type 0.01 Ωcm silicon electrode in a) 40 % and b) 20 % NH_4F solutions.

The maximum value of the I(active) area current is smaller and the II (passive) area is more extended anodically up to 4.5 V(SCE). After that the current increases and oxygen evolution occurs (see figure 2). This behaviour could be explained in connection with the decrease of the etching effect of NH_4F simultaneously with the decrease of its concentration in electrolyte.

B. *p-Type electrodes*

Potentiostatic determinations were performed on the behaviour of the p-type silicon electrodes with resistivities of 0.01 ; 0.5 and 100 Ωcm respectively, in 40 % aqueous NH_4F solutions. Before each polarization the solution was deaerated by bubbling argon and the experiment was carried out in an inert atmosphere. After the previously described chemical treatment, p-type silcon electrodes were electrochemically cleaned by maintaining them at a potential of — 2 V(SCE), which assures an intense evolution of hydrogen. After that the electrodes were anodically polarized. The p 0.01 — type electrode was polarized at —3 V(SCE) in order to assure an intense evolution of hydrogen. After that the electrode was anodically polarized. The polarization curves are shown in figure 3 and have the following characteristics included in table 1.

a. The steady-state potential E_s has a value of about — 1 V (SCE), very different from that in $H_2SO_4^{2,4}$.

b. In the cathodic range, $\Delta E < 0$, the hydrogen ion discharge occurs, followed by the hydrogen evolution. In the case of small dopped 0.5 and 100 Ω cm electrodes, the Tafel slope is of about 160 mV/decade, and in the case of 0.01 Ωcm strongly dopped p-type electrode the hydrogen ion discharge is hindered (Tafel slope is of about 650 mV/decade).

c. In the anodic range, $\Delta E > 0$, the behaviour of the p-type electrodes is different from that of an n-type electrodes. The following characteristic areas appear : I (active), in which the current slowly increases and at polarization $\Delta E'$ a sudden increase of the current occurs up to values of about 60 $\mu A/cm^2$; II (passive) with small current of about 10 $\mu A/cm^2$; III (transpassive) with a high current of about 2000 $\mu A/cm^2$,

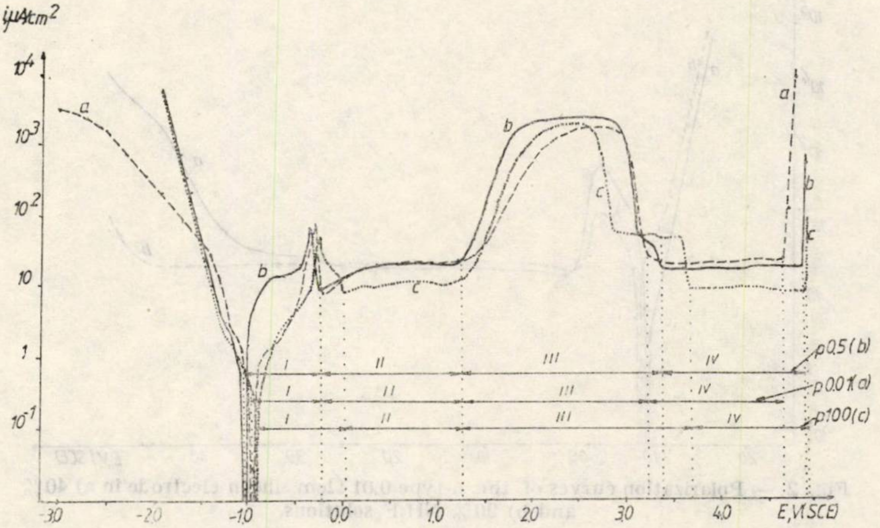

Fig. 3. — Polarization curves of the a) p-type 0.01 ; b) p-type 0.5 and c) p-type 100 Ωcm silicon electrode in 40 % NH_4F solutions.

Table 1

Experimental parameters	Silicon semiconductor resistivity (Ω cm)		
	p 0.01	p 0.5	p 100
1. Steady-state potential E_s(SCE), V	—0.950	—1.025	—0.875
2. Tafel slope, mV/decade	650	160	160
3. Potential range of the I (active) area, V	0—0.8	0—0.8	0—0.9
4. Maximum current potential of the I (active) area, $\Delta E'$, V	0.7	0.65	0.7
5. Potential range of the II (passive) area, V	0.8—2.2	0.8—2.3	0.9—2.2
6. Average current in the II (passive), area, $\mu A/cm^2$	27	12	11
7. Potential range of the III (transpassive) area, V	2.2—4.3	2.3—4.4	2.2—4.6
8. Maximum current in the III (transpassive) area, $\mu A/cm^2$ (after 3 minutes of polarization)	1800	2600	1800
9. Average current in the IV (passive) area, $\mu A/cm^2$	24	16	10

which remarkably increases in time. Figure 3 shows the current values after 3 minutes of polarization. This condition was imposed on all our experiments. IV (passive) with small current, which is broken at about $\Delta E'' = 6V$ polarization and the current suddenly increases. The examination of the electrodes after each polarization shows the appearance of pitting corrosion.

CONCLUSIONS

In ammonium fluoride solution the steady-state potential of silicon semiconductor electrodes is of about -1 V (SCE), a very different value from that in sulphuric acid solution. This fact could be explained not only by means of the pH difference of these aqueous solutions, but rather by means of the increase of the dissolution current of the silicon in NH_4F solution. This increase shifts the silicon corrosion potential towards more negative values.

In the cathodic range, in the case of the n-type electrodes as well as in the case of the p-type electrodes, the electrode reaction is the hydrogen ion discharge, followed by the hydrogen evolution. In the case of 0.01 strongly dopped p-type electrodes a hindering of the hydrogen ion discharge occurs. This could be explained by that the cathodic process occurs by means of conduction electrons which are, in this case, minority charge carriers. At the same 0.01 dopping no hindering effect exists at the n-type electrodes on the cathodic branch.

In the anodic range at small polarization a silicon oxidation process with the silicon dioxide formation occurs. The process could take place by means of two charge carriers; by holes (◦) or by electrons (e^-) following reaction (1):

$$Si + 2H_2O + m(\circ) = SiO_2 + 4H^+ + (4 - m)e^- \qquad (1)$$

where m, 4 and $(4 - m)$ are the number of holes, charges and electrons respectively involved in the process. If $m = 0$, the process takes place only by means of electrons and if $m = 4$, the process takes place only by holes.

In H_2SO_4 solutions the "active" area corresponding to this process is practically inexistent and the passivation occurs immediately, as a result of the formation of a SiO_2 adherent layer. This fact could explain the small anodic current. According to the data in literature,[6] the oxide layer formed in H_2SO_4 is stable up to about $+75$ V polarization. In NH_4F an etching effect exists, following reaction (2).

$$SiO_2 + 6F^- + 2H_2O \rightarrow SiF_6^{2-} + 4HO^- \qquad (2)$$

This effect allows the appearance of the I (active) area, which is absent in H_2SO_4. On the increasing branch of the active area, the SiO_2 layer formed by reaction (1) is dissoluted by reaction (2). At polarization $\Delta E'$, corresponding to the I (active) area maximum current the two phenomena have the same rate and at higher polarizations reaction (1) predominates. The electrode partially covers with an oxide layer, but the NH_4F etching effect leads within the II (passive) area to a current of about 50 times higher than in H_2SO_4. This range does not depend too much on the charge carriers nature (n or p). The electrode process could occur by a combined mechanism : electrons and holes.

At high polarizations there is a difference in the behavior of the n or p silicon semiconductor electrodes. In the case of n-type electrodes at polarization higher than 2.5 V, the current increases and the oxygen evolves. The appearance of the transpassive area of oxygen evolution could be explained by the etching effect of NH_4F, too, which decreases the length of the passive range in comparison with the behavior in H_2SO_4.

On p-type semiconductor electrodes a different behavior is obtained. In the 0—0.9 V potential range there is also a I (active) area followed by a II (passive) area, but at polarization ΔE of about 1.6 V a new III (transpassive) area begins, characterized by a high current which increases in time. This area corresponds to another mechanism of the silicon dissolution with a final soluble product (mechanism of anodic polishing)[1] :

$$\mathrm{Si} + 2\mathrm{F}^- + m(0) \rightarrow \mathrm{SiF}_2 + (2 - m)\mathrm{e}^- \qquad (3)$$

$$2\mathrm{SiF}_2 \rightarrow \mathrm{Si} + \mathrm{SiF}_4 \qquad (4)$$

$$\mathrm{SiF}_4 + 2\mathrm{F}^- \rightarrow \mathrm{SiF}_6^{2-} \qquad (5)$$

The silicon obtained through disproportion (see reaction 4) passivates and leads to the appearance of a IV new passive area :

$$\mathrm{Si} + 2\mathrm{H}_2\mathrm{O} \xrightarrow{\text{slowly}} \mathrm{SiO}_2 + 2\mathrm{H}_2 \qquad (6)$$

This new SiO_2 layer is suddenly broken at polarization $\Delta E''$ of about 5V, with oxygen evolution.

As a conclusion, ammonium fluoride is a moderate etching agent, in comparison with hydrofluoric acid, in which, accodring to the literature data,[7] no passive area, evidenced in this case, exists. Likewise, the appearance of the anodic polishing only on p-type silicon is an indication that reaction (3) takes place mainly by holes.

REFERENCES

[1] V. A. Myamlin and Yu. V. Pleskov, "Electrochemistry of semiconductors", Plenum Press, New York, 1967.

[2] S. Sternberg, V. Brânzoi, L. Apăteanu and M. Ungureanu, *Rev. de Metalurgie*, in press.

[3] I. Lingvay, Doctoral Thesis, Polytechnic Institute Bucharest, 1984.

[4] S. Sternberg, M. Ungureanu, V. Brânzoi and L. Apăteanu, *Rev. Roumaine Chim.*, in press.

[5] S. Sternberg, I. Lingvay and T. Vişan, *Rev. Roumaine Chim.*, **27**, 1085 (1982).

[6] S. O. Izidinov, T. I. Borisova and V. I. Veselovskii, *Zh. Fiz. Khim.*, **36**, 1246, (1962).

[7] E. A. Efimov and I. G. Erusalimchik, *Zh. Fiz. Khim.*, **35**, 384 (1961).

Revue Roumaine de Chimie, **31**, *1*, 9 — 15 (1986)

ESTUDIO CULOMBIMETRICO A POTENCIAL CONTROLADO DE LA OXIDACION ANODICA DEL COMPLEJO CIANURADO BINUCLEAR DE Mn(III).III*

CORRECCIÓN DE CORRIENTES CINÉTICAS POSITIVA Y NEGATIVA PARA SU DETERMINACIÓN CULOMBIMÉTRICA. OBTENCIÓN ELECTROLÍTICA DEL COMPLEJO CIANURADO BINUCLEAR DE Mn(III)—Mn(IV)

G. LÓPEZ CUETO y A. ALONSO MATEOS*

Departamento de Química Analítica, Facultad de Química, Universidad de Salamanca, España

Received January 29, 1982

Revised May, 19, 1985

Durante la oxidación culombimétrica del complejo cianurado binuclear de Mn(III) a + 0.20 voltios, se producen dos diferentes tipos de corrientes cinéticas : una de ellas positiva debida a una regeneración de la especie inicial y otra negativa debida a una reacción paralela de esta especie. La primera se corrige aplicando una modificación del tratamiento de Meites y Moros mientras que para la segunda, se propone un procedimiento de corrección. Se lleva a cabo la determinación de 5.6×10^{-5} equivalentes del complejo cianurado binuclear de Mn(III) con un error del orden de 0.2 a 0.4%. Se describe la preparación electrolítica del complejo cianurado binuclear de Mn(III)—Mn(IV) con un rendimiento superior al 99%.

During the controlled-potential (+0.20 volts vs S.C.E.) coulometric oxidation of the binuclear Mn(III)-cyanide complex in cyanide solution, two different kinetic currents appear : A positive kinetic current due to the regeneration of the initial species causing positive errors and a negative current due to a simultaneous reaction of the initial species causing negative errors. The total current is corrected according to a modification of the Meites and Moros procedure. There are no references relating a procedure to correct the total current when the negative kinetic current appears; in the present paper a correction procedure is proposed. The coulometric determination of 5.60×10^{-5} equivalents of the binuclear cyanide complex is carried out. For NaCN $\leqslant$ 2M the errors are lower than 0.5 per cent, being 1 or 2 per cent when the NaCN concentration of the temperature increase. The electrolytical preparation of the Mn(III)—Mn(IV) binuclear cyanide complex is realized at the optimal conditions : NaCN between 1.0 and 2.0 M, the ionic strength 5.0 and the temperature 10°C or minor. The efficiency is greater than 99 per cent.

---

* Part II, *Rev. Roumaine Chim.*, **31**, 237 (1986).

INTRODUCCION

El complejo Mn(III)—Mn(III) experimenta dos reacciones electroquímicas de oxidación, que conducen respectivamente a los complejos Mn(III)—Mn(IV) y Mn(IV)—Mn(IV), siendo 0.03 y 0.60 voltios (vs. S.C.E.) los correspondientes potenciales de semionda.[1] La determinación culombimétrica a potentical controlado del citado complejo cianurado de Mn(III) puede llevarse a cabo, por tanto, manteniendo el potencial anódico en cualquiera de las dos zonas de difusión, es decir, operando a + 0.20 o + 0.80 voltios, respectivamente.

Como se comprobó en trabajos anteriores, en ninguno de los dos casos tiene lugar la oxidación electrolítica con rendimiento en corriente y en producto del 100 %, debido a los efectos residuales o de fondo que simultaneamente se producen.

Durante la oxidación a +0.20 voltios tiene lugar una regeneración del complejo inicial Mn (III) — Mn(III), mediante reacción del Mn(III)—Mn(IV) con el CN^- del medio, regeneración que ocurre para concentraciones de CNNa 3M o superiores. Esta regeneración se traduce en una *corriente cinética*. Para CNNa $\leqslant$ 2M no tiene lugar apreciablemente la regeneración mencionada pero la especie inicial Mn(III)-Mn(III) experimenta una descomposición paralela hacia otra especie de Mn(III) pero mononuclear,[2] que disminuye el rendimiento en producto. Este efecto puede considerarse como una *corriente cinética negativa*.

Si la oxidación se lleva a cabo al potencial anódico de +0.80 voltios las corrientes de fondo son importantes en número y magnitud, efectivamente a dicho potencial el electrodo de platino experimenta una oxidación superficial que se traduce en la aparición de una corriente *faradaica exponencial*. Al mismo tiempo, el propio disolvente se oxida a este potenical, lo que produce una corriente faradaica continua. Finalmente, se observan dos diferentes *corrientes cinéticas* : las debidas a la regeneración de las especies Mn(III)—Mn(III) y Mn(III)—Mn(IV) siendo la segunda de ellas de mayor magnitud.

Aunque pueden proponerse correcciones para todos los tipos de corrientes de fondo, es evidente que la determinación culombimétrica del complejo Mn(III)—Mn(III) podrá llevarse a cabo con mas precisión al potencial anódico de +0.20 voltios, potencial en el que las corrientes de fondo no son importantes.

El objeto de este trabajo consiste en proponer procedimientos de corrección de la corriente consumida a lo largo de la oxidación electrolítica a +0.20 voltios para poder aplicar con exito la oxidación culombimétrica a la determinación del complejo cianurado Mn(III)—Mn(III).

Conocidos los procedimientos de corrección y las condiciones experimentales en que el rendimiento en producto es máximo, se ensaya la preparación electrolítica del complejo binuclear Mn(III)—Mn(IV).

PARTE EXPERIMENTAL

Los reactivos y aparatos así como los electrodos utilizados ya han sido descritos en la parte 1 de este serie de trabajos. Quizás conviene recordar que el complejo cianurado binuclear de Mn(III) ha sido preparado por el procedimiento descrito por Brauer.[3]

RESULTADOS Y DISCUSION

Durante la oxidación anódica del complejo binuclear Mn(III)—Mn(III) a +0.20 voltios pueden producirse dos diferentes corrientes de fondo:

— Corriente debida a la regeneración de la especie inicial Mn(III)—Mn(III), causante de errores por exceso (corriente cinética positiva). Este corriente aparece solo para $CN^- \geqslant 3M$.

— Corriente debida a la descomposición paralela de la especie inicial, causante de errores por defecto (corriente cinética negativa). Se observa solamente para $CN^- \leqslant 2M$.

Corriente cinética positiva

Las correcciones propuestas por Meites y Moros [4] para una corriente de este tipo se basan en la expresión:

$$Q_{\text{corr}} = \frac{Q^0_{\text{exp}}}{1 - \dfrac{aK}{(K+a)^2}} \tag{1}$$

donde: Q_{corr}, en la cantidad de corriente que realmente se invierte en la oxidación electrolítica; Q^0_{exp} es la cantidad de corriente obtenida por extrapolación de la curva Q frente a b, para tiempo cero; k, constante de proporcionalidad entre la intensidad de electrolisis y la concentración de reductor; a, constante de proporcionalidad entre la intensidad cinética, i_K y la concentración de oxidante.

Estas dos constantes a y k son proporcionales a k_1 y K por lo que igualemnte se cumple:

$$Q_{\text{corr}} = \frac{Q^0_{\text{exp}}}{1 - \dfrac{k_1 K}{(K + k_1)^2}} \tag{2}$$

Por otra parte, a partir de la ecuación que relaciona la concentración de Mn(III)—Mn(III) con el tiempo para $CN^- \geqslant 3M$:

$$[\text{Mn(III)}-\text{Mn(III)}] = [\text{Mn(III)}-\text{Mn(III)}]_0 \frac{1}{K + k_1} [k_1 + K.e^{-(K+k_1)t}] \tag{3}$$

para $t = \infty$ que es cuando se alcanza el estado estacionario y la concentración de [Mn(III)—Mn(III)] alcanza un valor constante, la ecuación (3) teniendo en cuenta la proporcionalidad entre concentraciones e intensidades de difusión, se llega a la expresión

$$k_1 = K \frac{i_k}{i_0 - i_k} \tag{4}$$

Sustituyendo esta expresión en (2) y simplificando, se obtiene:

$$Q_{\text{corr}} = \frac{Q^0_{\text{exp}}}{1 - \dfrac{i_k(i_0 - i_k)}{i_0^2}} \tag{5}$$

Mediante este expresión se puede [calcular Q_{corr} conociendo los valores inicial y final de la intensidad de corriente y Q^0_{exp} que se determina por extrapolación. Esta expresión es valida para disoluciones de CNNA 3 M o superior.

Corriente cinética negativa

Esta causa de error en las determinaciones culombimétricas a potencial controlado no figura entre las propuestas por Meites y Moros. En las condiciones citadas de $CN^- \leqslant 2M$ el complejo Mn(III)—Mn(III) evoluciona espontaneamente hacia otra forma compleja monómera de Mn(III) no oxidable Cuando se somete el complejo binuclear al potencial anódico de +0.20 voltios, la morfología de las curvas intensidad-tiempo es semejante a la que presentaría un proceso culombimétrico ideal. Asimismo,la representación de lg i frente al tiempo conduce a líneas rectas, pero de pendientes mayores que la teórica, por lo que el calculo de Q conduce a resultados por defecto.

La intensidad de la corriente en función del tiempo como ya fue deducida, viene dada por la ecuación

$$i = k_d[\mathrm{Mn(III)}-\mathrm{Mn(III)}]_0 \cdot e^{-(K+k_2)t} \qquad (6)$$

donde : k_2 es la constante de velocidad del proceso de evolución espontánea.

La integración de la ecuación (6) conduce a :

$$Q_{exp} = \frac{i_0}{K + k_2} \qquad (7)$$

y como

$$Q_{corr} = \frac{i_0}{K} \text{ y } K_{exp} = K + k_2$$

se obtiene finalmente :

$$Q_{exp} = Q_{corr} \frac{K_{exp} - k_2}{K_{exp}} \qquad (8)$$

Esta expresión permite el cálculo de Q_{corr} conociendo Q_{exp} y las constantes K_{exp} y k_2. El valor de K_{exp} se determina a partir de la pendiente de la recta obtenida al representar lg i frente al tiempo ($m = K_{exp}$ 0.434). Si no se conoce previamente el valor de k_2, su determinación experimental puede llevarse a cabo utilizando dos electrodos de platino de distinta superficie. Los correspondientes valores de K_{exp} para uno y otro electrodo estarán relacionados con K y k_2 mediante las expresiones :

$$K_{exp} = K + l_2 \qquad (9)$$
$$K'_{exp} = K' + k_2$$

Por otra parte, se cumplirá la proporcionalidad entre constantes de electrolisis, superficies e intensidades iniciales :

$$\frac{K}{K'} = \frac{S}{S'} = \frac{i_0}{i'_0} = \alpha \qquad (10)$$

A partir de las expresiones (9) y (10) se obtiene para k_2:

$$k_2 = \frac{K_{\text{exp}} - \alpha K'_{\text{exp}}}{1 - \alpha} \tag{11}$$

Resultados obtenidos

Para comprobar la validez de las ecuaciones (5) y (8) como métodos de corrección de corrientes de fondo catalíticas en determinaciones culombimétricas a potencial controlado se ha llevado a cabo la determinación de 5.6×10^{-2} miliequivalentes de manganeso en forma de complejo cianurado binuclear Mn(III)—Mn(III) en concentraciones de CNNa 1,2,3,4 y 5 M. Los resultados, que se muestran en las tablas 1,2,3, y 4 resultan ser plenamente satisfactorios, lo que indica que las expresiones propuestas son correctas.

Tabla 1

Determinación culombimétrica del complejo cianurado binuclear Mn(III)—Mn(III) para concentraciones de CNNa 2M.
f. iónica 5.0; $T < 25$°C
Mn(III)—(Mn(III) puesto: 5.6×10^{-5} equivalentes

CNNa M	$K_{\text{exp}} \cdot 10^3$ min^{-1}	$k_2 \cdot 10^3$ min^{-1}	Q_{exp} mFy·10^2	Mn(III)—Mn(III) eq·10^5	
				hallados	Error %
1.0	161	23	1.17	5.59	—0.2
2.0	150	13	1.10	5.62	+0.4

Tabla 2

Determinación culombimétrica del complejo cianurado binuclear de Mn(III)—Mn(III) para concentraciones de CNNa 2M.
CNNa 2.0 M; $T = 25$°C
Mn(III)—Mn(III) puesto: 5.60×10^{-5} equivalentes

f iónica	$k_{\text{exp}} \cdot 10^3$ min^{-1}	$k_2 \cdot 10^3$ min^{-1}	Q_{exp} mFy·10^2	Mn(III)—Mn(III) eq.10^5	
				hallados	Error %
1.0	391	236	2.22	5.59	—0.2
2.0	254	104	3.32	5.61	+0.2
3.0	219	71	3.81	5.64	+0.7
4.0	184	41	4.31	5.56	—0.7
5.0	161	23	4.78	5.59	—0.2

Tabla 3

Determinación culombimétrica del complejo cianurado binuclear
Mn(III)—Mn(III) para concentraciones de CNNa 2M.
CNNa 2.0M, fuerza iónica 5.0
Mn(III)—Mn(III) puesto : 5.60 × 10^{-5} equivalentes

T °C	$K_{exp}10^3$ min^{-1}	$k_2 . 10^3$ min^{-1}	Q_{exp} mFy.10^2	Mn(III)—Mn(III) e.10^2	
				hallados	Error, %
5	92	1	5.56	5.62	+0.4
15	115	4	5.44	5.66	+1.1
25	161	23	4.78	5.59	—0.2
30	196	39	4.46	5.58	—0.4
40	346	152	3.11	5.54	—1.1

Tabla 4

Determinación culombimétrica del complejo cianurado binuclear Mn(III)—
Mn(III) para concentraciones de CNNa 3 M
fuerza iónica 5.0 ; Tª = 25°C
Mn(III)—Mn(III) puesto : 5.60 × 10^{-5} equivalentes

CNNa M	i_0 mA	i_K mA	Q_{exp} mFy·10^2		Q_{exp} mFy.10^2	Mn(III)—Mn(III) eq.10^5	
			34 min	44 min		hallados	Er, %
3.0	12.4	0.2	5.69	5.81	5.42	5.53	—1.3
4.0	12.4	0.4	5.74	5.98	5.38	5.55	—0.9
5.0	12.4	0.6	5.87	6.24	5.29	5.47	—2.3

PREPARACION ELECTROLITICA DEL COMPLEJO CIANURADO BINUCLEAR Mn(III)—Mn(IV)

El procedimineto de preparación del complejo Mn(III)—Mn(IV) mediante oxidación electrolítica parece ser, en principio, el más adecuado presentando. por otra parte, la ventaja de no introducir sustancias extrañas en la disolución.

A partir de los estudios realizados acerca de la oxidación anódica del complejo Mn(III)—Mn(III) en disolución cianurada y de las variables que afectan al rendimiento en producto de dicha reacción electroquímica se deducen las condiciones experimentales más adecuadas para alcanzar el maximo rendimiento, condiciones que resultan ser las siguientes :

CNNa entre 1.0 y 2.0 M

Fuerza iónica elevada 5.0

Temperatura baja (10°C ó inferior)

Operando en las mencionadas condiciones y utilizando un electrodo de malla de platino de gran superficie sometido a un potencial de +0.20 voltios (vs. S.C.E.) se procedió a la oxidación anódica de cantidades crecientes del complejo Mn(III)—Mn(III). La electrolisis se considera completa cuando la intensidad alcanza un valor inferior a la milesima parte de la inicial. En las condiciones de trabajo el rendimiento en corriente es del 100 % por lo que el rendimiento en producto puede calcularse mediante el cociente entre la cantidad de corriente consumida (en milifaradays) y la cantidad de complejo puesta (en miliequivalentes). En las tablas 5 y 6 se muestran los resultados obtenidos para cantidades de complejo comprendidas entre 5×10^{-3} y 15×10^{-3} equivalentes y en disolución de CNNa 1.0 y 2.0 M. Como se aprecia, la oxidación puede considerarse practicamente cuantitativa.

Tabla 5

Preparación electrolítica del complejo cianurado binuclear Mn(III)—Mn(IV). Rendimientos obtenidos en CNNa 1.0 M, fuerza ionica 5.0 y $T = 5°C$

Mn(III)—Mn(III) eq.10^3	Q_{exp} mFy	R %
5.00	4.97	99.4
5.60	5.57	99.5
6.00	5.95	99.2
6.50	6.46	99.4
7.00	6.97	99.6
7.50	7.48	99.7
8.00	7.99	99.9
8.50	8.46	99.5
9.00	8.91	99.0
9.50	9.45	99.5
10.00	9.96	99.6
15.00	14.94	99.6

Tabla 6

Preparación electrolítical del complejo cianurado binuclear Mn(III)—Mn(IV). Rendimientos obtenidos en CNNa 2.0 M, fuerza ionica 5.0 y $T = 10°C$

Mn(III)—Mn(III) eq.10^3	Q_{exp} mFy	R %
5.00	4.98	99.6
5.60	5.58	99.6
6.00	5.96	99.3
6.50	6.48	99.7
7.00	6.95	99.3
7.50	7.48	99.7
8.00	8.00	100.0
8.50	8.46	99.5
9.00	8.95	99.4
9.50	9.46	99.6
10.00	14.97	99.8

BIBLIOGRAFIA

[1] G. Lopez Cueto y A. Alonso Mateos, *Anal. Lett.*, **28**, 106 (1974).
[2] G. Lopez Cueto, Tesis Doctoral. Salamanca 1972.
[3] G. Brauer, "Quimica Inorgánica Preparativa", Ed. Reverté, Barcelona 1958.
[4] L. Meites y S. A. Moros, *Analyt. Chem.*, **31**, 23 (1959).

Revue Roumaine de Chimie, 31, *1*, 17—23 (1986)

MODIFICATION OF STRUCTURE AND PROPERTIES OF PVC-S BY THE PROCESSING ON ROLLERS IN THE PRESENCE OF SOME NEW FILLING MATERIALS

CLEOPATRA VASILIU OPREA and FELICIA WEINER
Department of Organic and Macromolecular Chemistry
Polytechnic Institute of Jassy, 6600, Jassy, Romania

Received February 25, 1985

PVC-S processed on rollers (using as filling materials kaolin, volcanic tuff, mica, which were mechano-chemically grafted by vibratory milling with vinylic monomers (e.g. acrylonitrile, vinyl chloride, methyl methacrylate) is separated from the components by the dissolution in cyclohexanone and precipitation with methanol and physico-chemically analysed. The experimental results prove the base structure modification and explain the new properties of the prepared materials after roller mechanical processing.

INTRODUCTION

Our aim is to establish the structure of the PVC-S separated from the films resulted by the roller processing, using grafted polymers on the inorganic supports as filling materials which were mechano-chemically synthesized[1] and subsequently roller processed[2]; a series of the physico-chemical analyses were performed.

EXPERIMENTAL

1. Separation of PVC from the films obtained on rollers

The roller mixing of PVC-S in the presence of the filling materials, mechano-chemically synthesized by vibratory milling of volcanic tuff, mica, kaolin and vinylic monomers (acrylonitrile, vinyl chloride and methyl methacrylate) technology, methods and apparatus were previously presented.[2]

From the plates of PVC-S which were obtained on roller mixing in the presence of the inorganic supports, samples were removed, dissolved in cyclohexanone (5g in 300 mL of cyclohexanone) at 100°C, under stirring, for one hour. The obtained suspension was filtrated on a glass filter (G_4) in order to remove the other components, except polymer.

The filtrate was treated with methanol in order to precipitate the polymer. The obtained polymer was dried at constant weight.

2. Technique of Analyses Used to Characterize PVC-S Separated from Plates

In order to observe the changes which took place in the PVC-S structure after the mechanical processing on rollers in the presence of the mentioned filling materials, in the following analysis the physical methods were used : IR spectroscopy, photocolorimetric analysis, thermodifferential analysis, elemental analysis. The obtained data were plotted resulting in thermomechanical curves.

2.1. *IR-Spectroscopy*

The IR-Spectra were recorded on an IR Perkin Elmer apparatus, applying KBr pastil technique.

2.2. *Photocolorimetric Analysis*

The turbidimetric titration curves were obtained on the base of the experimental data recorded on a SPEKOL ZW, DDR apparatus.

2.3. *Thermodifferential Analysis*

The derivatograms were recorded on a Paulik-Erdely-Paulik apparatus, between 20—600°C, with a heating rate of 12°C/min and 50 sensitivity.

2.4. *Thermomechanical Curves*

The thermomechanical curves were performed on a Karghin balance, and the deformation variation vs. temperature was recorded at a constant load of 50 g.f.

2.5. *Elemental Analysis*

The determination of C, H and calcination residue contents was performed using a combustion oven. Nitrogen content was determined by Kjeldhal method, and chlorine content by Schöniger technique.

3. RESULTS AND DISCUSSION

3.1. Determination of C,H,N,Cl Contents

A sample from the following materials underwent a full elemental analysis :

a) PCV-S + PAN + volcanic tuff 10 p.g.

b) PVC-S + PVC + Kaolin 6 p.g.

c) PVC-S + PMeM + Kaolin 6 p.g.

The samples were previously purified by dissolutions in cyclohexanone and reprecipitatings with methanol.

The obtained results are given in Table 1.

Table 1

C, H, Cl, N content of polymer processed on rollers

Sample	C %	H %	N %	Cl%	Residue %
PAN grafted on volcanic tuff + PVC-S 10 p.g.	40.59	5.89	2.40	50.10	
PVC grafted on kaolin + PVC-S 6 p.g.	42.67	5.93	—	47.05	1.92
PMeM grafted on kaolin + PVC-S 6p.g.	43.33	3.05	—	43.44	—

Noteworthy are the experimental results obtained in the case when grafted PAN on the volcanic tuff is used as filling material, because from the elemental analysis results 2.40 % N which is only due to grafted PAN used in experiments.

Also, the decrease of Cl % from PVC-S after the processing of it with different filling materials shows the yielding of some materials with a new chemical structure.

3.2. Thermomechanical Curves

The improving of the features of PVC-S plates, rolled together with the filling materials obtained from the polymers grafted on the inorganic supports is a consequence of the increasing of the cohesion energy due to the intra- and intermolecular physical interactions.

The intensity of these interactions may be evaluated by plotting the thermomechanical curves (Figures 1—3).

Fig. 1 (curve 1) shows the thermomechanical curve of PVC-S + + PVC grafted on kaolin 3 p.g. The value of the glass temperature is 84.5°C.

In the case of the system PVC-S + PMeM grafted on kaolin 3 p.g. the glass temperature was 90°C (Fig. 3 Curve 1) and for the system PVC + + PAN grafted on kaolin 3 p.g. the glass temperature was smaller (about 80°C) (Fig. 2, curve 1).

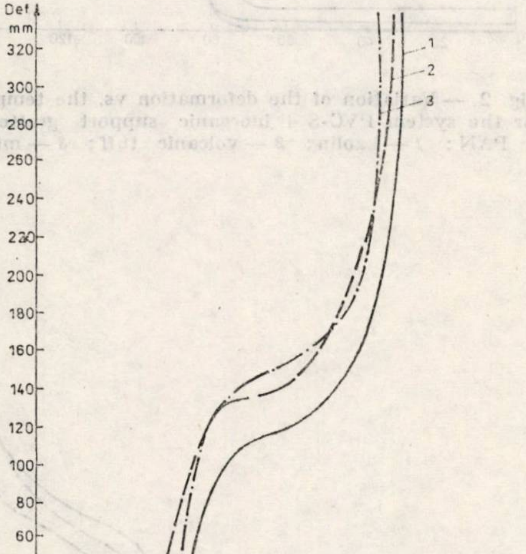

Fig. 1. — Variation of the deformation vs. the temperature for the system PVC—S + inorganic support grafted with PVC ; *1* — kaolin ; *2* — volcanic tuff ; *3* — mica.

These results are in good agreement with the physico-mechanical behavior of the systems. The last of them, which is characterized by the lowest glass temperature, represents an increased resistance at shock

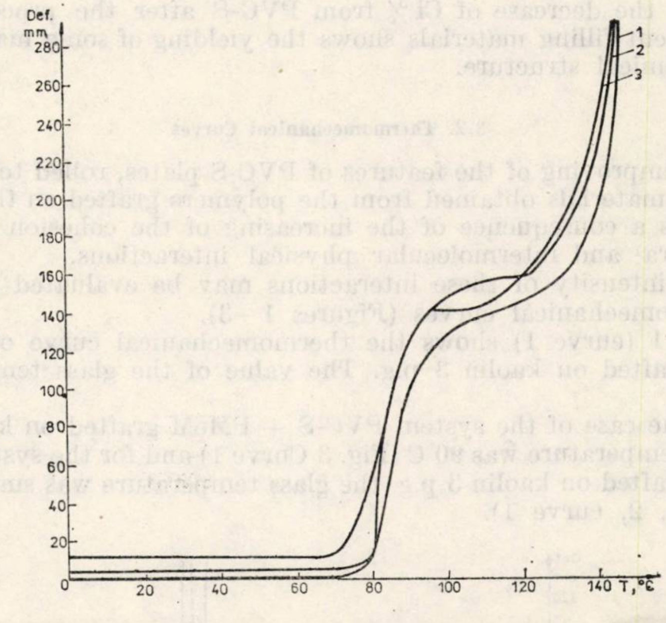

Fig. 2. — Variation of the deformation vs. the temperature for the system PVC-S + inorganic support grafted with PAN : *1* — kaolin ; *2* — volcanic tuff ; *3* — mica.

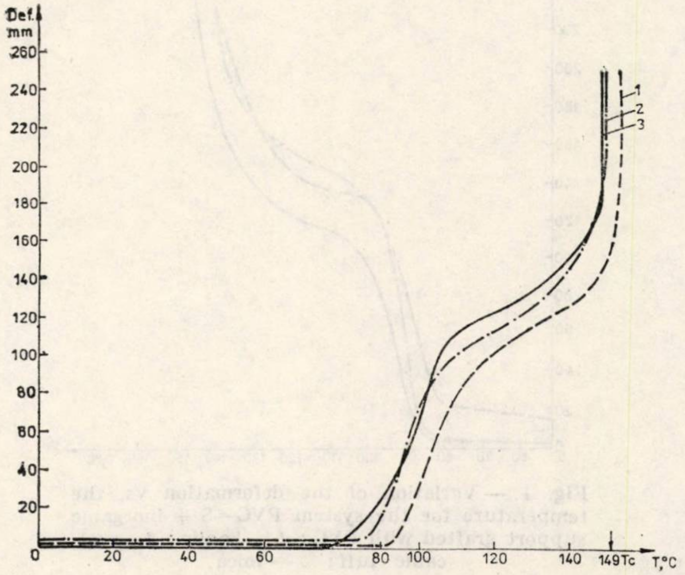

Fig. 3. — Variation of the deformation vs. the temperature for the system PVC-S + inorganic support grafted with PMeM : *1* — kaolin ; *2* — volcanic tuff ; *3* — mica.

by comparison with the standard polymer. This result might be explained by the increase of the flexibility of the macromolecules due to the annulment of the numerous intermolecular interactions produced by the presence of the grafted branches on the prepared polymer structure.

3.3. Thermostability

A feature quite important of PVC-S is its chemical stability, which was determined by DTA and GTA. The variations of losses in terms of the temperature were calculated from the recorded thermograms.

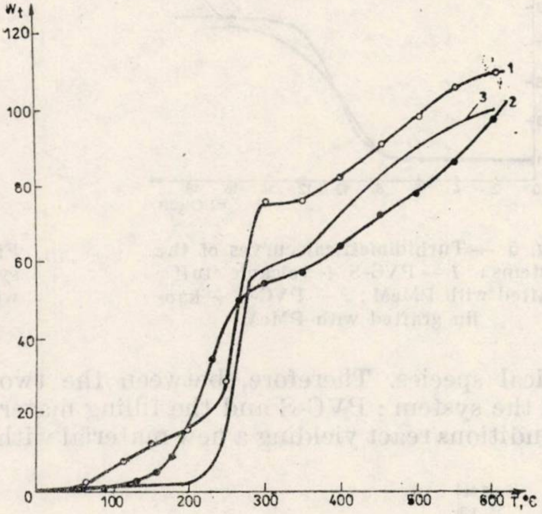

Fig. 4. — Variation of the losses vs. the temperature for the systems:
1 — PVC-S + kaolin grafted with PAN;
2 — PVC-S + kaolin grafted with PVC;
3 — PVC-S + kaolin grafted with PMeM.

From Fig. 4 curves 1—3, one can notice that the thermostability increases as follows:

$$\text{PVC-S} + \text{PMeM} + \text{kaolin} > \text{PVC-S} + \text{PAN} + \text{kaolin} > \text{PVC-S} + \text{PVC} + \text{kaolin}$$

So, at 300°C, the first system loses 66 %, while the second one loses 60 % and the third loses only 55 %. All materials are more thermostable than the PVC standard sample (which was not processed in the presence of the mentioned filling materials).

3.4. Turbidimetric Titration

The modified PVC-S plates by the introduction of some grafted polymers onto inorganic supports as filling materials, underwent a dissolution process in cyclohexanone and then reprecipitated polymer with methanol. As a result of the mechanical processing on the rollers in the presence of the used filling materials, it yielded PVC powder with modified structure.

From these PVC-powders, 0.5 % solutions in tetrahydrofuran were prepared and used for the turbidimetric titrations. The measured data were plotted. Methanol was used as nonsolvent and the measurements were performed at $\lambda = 700$ nm.

As results from the analyses performed, all turbidimetric titrations present only one slope (Fig. 5,6,7) that points out the presence of a chemical species. Therefore, between the two macromolecular components of the system : PVC-S and the filling materials which in the roller mixing conditions react yielding a new material with proper structure and features.

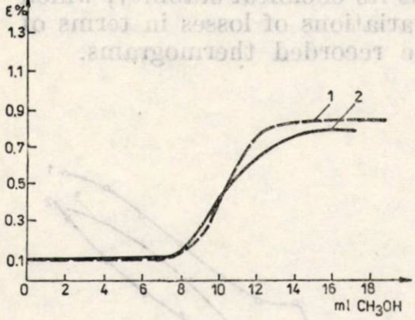

Fig. 5. — Turbidimetrical curves of the systems : *1* — PVC-S + volcanic tuff grafted with PMeM ; *2* — PVC-S + kaolin grafted with PMeM.

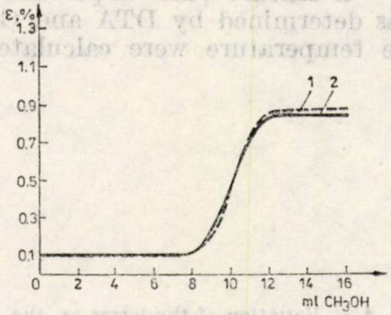

Fig. 6. — Turbidimetrical curves of the systems : *1* — PVC-S + kaolin grafted with PVC ; *2* — PVC-S + volcanic tuff grafted with PVC.

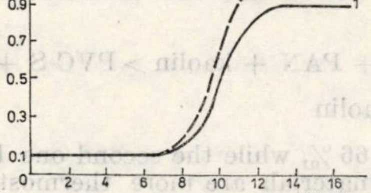

Fig. 7. — Turbidimetrical curves of the systems : *1* — PCV-S + kaolin grafted with PAN ; *2* — PVC-S + volcanic tuff grafted with PAN.

The elemental analysis and even IR spectroscopy data are in good agreement with this result.

3.5. IR-Spectroscopy

IR-spectra were performed using the polymer sample separated from the obtained products after the roller mixing with the filling materials (PAN grafted onto volcanic tuff, 10 p.g. ; PMeM grafted onto kaolin, 3 p.g. ; PVC grafted onto kaolin and PMeM grafted onto volcanic tuff, 6 p.g.)

From IR spectra one can notice the characteristic adsorption bands for ($C-Cl$ 360; $C-Cl$ 610; $C-Cl$ 640; $=CH_2-970$; $-C-C$ 1100; $\equiv C-H$ 1250 $-CH$ 1330 cm^{-1}). Besides these bands other ones can be noticed in the case of PMeM or PAN grafted onto kaolin. For instance: PMeM a band at 490 cm^{-1} assigned to the group $-C-CO-O$; at 1420 cm^{-1} due to $-O(CH_3)$ and at 1700 cm^{-1} thanks to the group $C = 0$. PAN it was noticed an adsorption at 3420 cm^{-1} band assigned to the nitril group.

These experimental results prove that during the roller mixing process of PVC-S together with the grafted polymer onto the inorganic supports, intensively chemical reactions take place and therefore the structure of the yielded polymer is quite modified, resulting materials with new physico-chemical and mechanical properties.

CONCLUSION

1. The use of the filling materials within the roller mixing process of PVC-S of the grafted polymers (PAN, PMeM, PVC) onto inorganic suppoprts (kaolin, volcanic tuff) allows to obtain rigid plates with modified physico-chemical properties.

2. The modification of the chemical structure of these polymers is in good agreement with the changing of the physico-mechanical properties. The modifications are based on the intensively developed interactions of physical nature as well as of some chemical reactions between the grafted products used as filling materials and polymer on the PVC-S basis.

REFERENCES

[1] Cl. Vasiliu Oprea and F. Weiner, J. Applied Polymer Sciences (in press).

[2] Cl. Vasiliu Oprea, M. Rusu, Gh. Adamescu and F. Weiner, Mehanika komp. mat. (in press)

Revue Roumaine de Chimie, **31**, *1*, 25—30 (1986)

HIGH TEMPERATURE POLYMERS. VI*

POLYBENZIMIDAZOLE-AMIDE-IMIDES

GH. MANDRIC, GABRIELA NEAMŢU, SILVIA PECINCU and GETA RĂCARU

Institute of Macromolecular Chemistry "P. Poni"
Aleea Gr. Ghica Vodă 41 A, Iaşi, Romania

Received December 3, 1984

The synthesis of a new series of ordered heterocyclic copolymers containing benzimidazole and imide rings with amide linkages in the macromolecular chain is described. The polybenzimidazole-amide-imides (PBI-A-I) obtained have a high thermal stability, up to 400°C, good solubility in aprotic dipolar solvents, high resistance to chemical reagents, high molecular weights ($\eta_{inh} = 0.28—1.93$) and these can be cast as transparent and elastic films with good mechanical and electrical properties.
The polymers were characterized by infrared spectroscopy, viscosity, elemental and thermogravimetric analysis.

INTRODUCTION

The synthesis of ordered copolymers is a route for obtaining polymers having a well-determined structure with superior flexibility, thoughness and high thermal stability.[1-8]

Previous papers in this series [9-12] have described the preparation and properties of some ordered copolymers containing benzimidazole or benzothiazole and imide rings and/or amide linkage in macromolecular chain.

In this paper we should like to report the preparation and the properties of a new ordered copolymer containing benzimidazole and imide rings with amide linkages in the macromolecular chain.

EXPERIMENTAL

Preparation of the Monomers

The synthesis of benzimidazoles containing diamines was carried out by reaction of an aromatic tetraamine with p- or m-aminobenzoic acid, using polyphosphoric acid (PPA) as solvent and condensing agent [13]:

---

* Part. V. ......

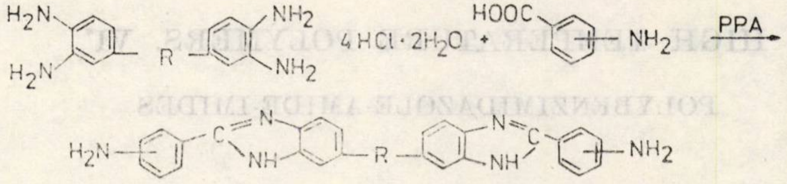

R = $-CH_2-$ (1)-para ; (2)-meta

R = — (3)-para

The benzimidazole-diamines were purified by methanol extraction, charcoal treatment and precipitation into water.

Elemental analysis of benzimidazole-diamines are summarized in table 1.

Table 1

Elemental analysis of benzimidazole-diamines

Compound	Condition	Formula	Melting point °C	Carbon, %		Hydrogen, %		Nitrogen, %	
				Calcd.	Found	Calcd.	Found	Calcd.	Found
(1)	Solvated				70.80		5.03		18.50
	Nonsolvated	$C_{27}H_{22}N_6$	321—323	75.33	75.21	5.15	5.07	19.52	19.43
(2)	Solvated				70.78		5.64		18.40
	Nonsolvated	$C_{27}H_{22}N_6$	204—208	75.33	74.90	5.15	5.23	19.52	19.28
(3)	Solvated				70.20		4.78		18.84
	Nonsolvated	$C_{26}H_{20}N_6$	320—322	74.99	74.78	4.80	4.96	20.19	19.64

The monomers containing imide rings were prepared by the reaction of dicarboxylic acids having imide units with thionyl chloride [13,14]:

$$HOOC-X-COOH + \xrightarrow[-SO_2,\,-HCl]{SOCl_2,\,reflux} ClOC-X-COCl$$

where X =

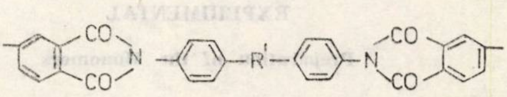

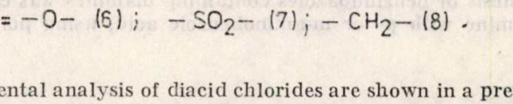

R' = —O— (6) ; $-SO_2-$ (7) ; $-CH_2-$ (8) .

Melting points and elemental analysis of diacid chlorides are shown in a previous paper.[12]

The dicarboxylic acids were obtained by condensation of trimellitic anhydride with m- and p-aminobenzoic acids[5,6] or aromatic diamines [7].

Preparation of the Polymers

The polymers were prepared by low temperature condensation of the benzimidazole rings containing diamines with diacid chlorides containing preformed imide units, as follows:

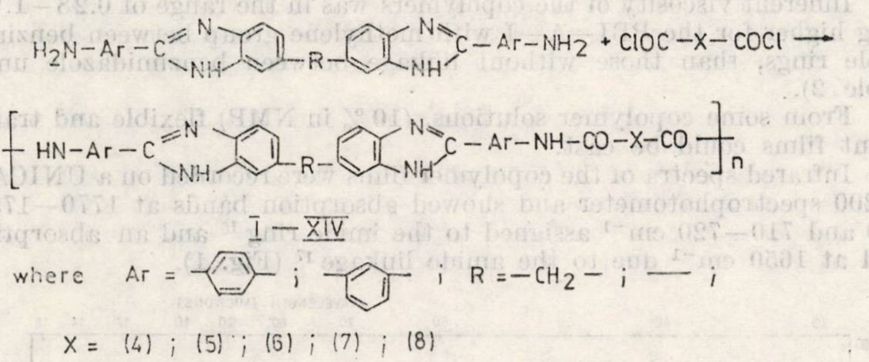

The polycondensation was carried out in solvents such as dimethylacetamide (DMAC) + + 5% LiCl or NMP, first at low temperature, then at room temperature, in inert atmosphere. In a typical polycondensation, a solution of 1.0750 g (0.0025 mole) diamine (1) in 22 ml DMAC + + 5% LiCl was cooled to —15°C and 1.4633 g (0.0025 mole) oxy-bis-N(4-phenylene)-4′(chloroformylphenyl)-phtalimide (6) finely powdered, were added all at once with stirring. The temperature of the solution was allowed to rise slowly to 25°C within 1 hour. Stirring was continued at room temperature for 1—2 hours. The resulting viscous polymer was neutralized with 0.38 g pyridine, diluted with one volume solvent and precipitated by pouring into acetone. Purification was made by washing with water and acetone. The polymer obtained was then dried at 150°C under reduced pressure.

Table 2 summarizes the principal characteristics of the copolymers:

Table 2

Characterization of the copolymers

Copolymer	Ar	R	X	η inh$^{1)}$ dl/g	ATG weight loss$^{2)}$, %		Nitrogen analysis, %	
					400°C	500°C	Calcd.	Found
I	p —C_6H_4—	—CH_2—	(4)	1.93	5	28	13.90	13.09
II	p —C_6H_4—	—CH_2—	(5)	1.85	6	34	13.90	12.98
III	p —C_6H_4—	—CH_2—	(6)	0.70	6	30	11.89	11.34
IV	p —C_6H_4—	—CH_2—	(7)	0.70	3	28	11.30	10.93
V	p —C_6H_4—	—CH_2—	(8)	1.10	4	26	11.92	11.78
VI	m—C_6H_4—	—CH_2—	(4)	0.94	3	37	13.90	13.41
VII	m—C_6H_4—	—CH_2—	(5)	1.15	3	24	13.90	12.93
VIII	m—C_6H_4—	—CH_2—	(6)	0.40	4	34	11.89	11.64
IX	m—C_6H_4—	—CH_2—	(7)	1.11	2	25	11.30	10.78
X	m—C_6H_4—	—CH_2—	(8)	1.60	2	21	11.92	11.79
XI	p —C_6H_4—	—	(5)	0.68	2	20	12.43	12.04
XII	p —C_6H_4—	—	(6)	0.70	2	23	10.73	10.44
XIII	p —C_6H_4—	—	(7)	0.28	4	17	10.20	9.88
XIV	p —C_6H_4—	—	(8)	0.40	0	9	10.76	10.70

1) Measured at a concentration of 0.5 g/100 mL N-Methylpyrrolidone (NMP) at 20°C.

2) Determined in air on "Paulik-Paulik Erderly Derivatograph" at a beating rate of 9°C/min.

RESULTS AND DISCUSSION

The copolymers obtained are yellow or cream coloured and have a linear structure being soluble in aprotic polar solvents.

Inherent viscosity of the copolymers was in the range of 0.28–1.93, being higher for the PBI–A–I with methylene group between benzimidazole rings, than those without linkage between benzimidazole units (Table 2).

From some copolymer solutions, (10 % in NMP) flexible and transparent films could be cast.

Infrared spectra of the copolymer films were recorded on a UNICAM SP-200 spectrophotometer and showed absorption bands at 1770–1780, 1710 and 710–720 cm^{-1} assigned to the imide ring [16] and an absorption band at 1650 cm^{-1} due to the amide linkage [17] (Fig. 1).

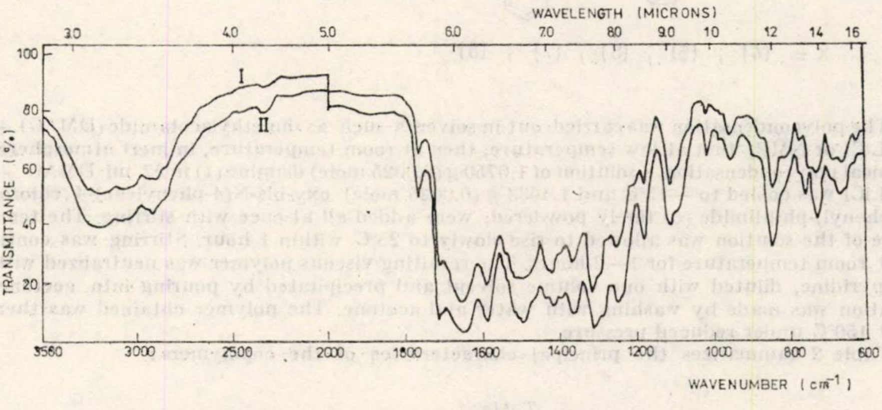

Fig. 1. — Infrared spectra of polybenzimidazole-amide-imides (I and II).

The copolymers obtained do not loose significantly up to 400°C and polybenzimidazole-amide-imides without linkage between benzimidazole rings (XI–XIV) have higher thermal stability than those with a methylene group between benzimidazole units (I–X) (Table 2).

Fig. 2 shows TGA of PBI–A–I (III) by comparing it with TGA of a polybenzimidazole-imide [10] (PBI-p) and an aromatic polyamide

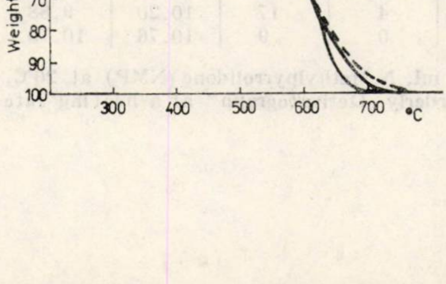

Fig. 2. — Thermogravimetric analysis: 1. polybenzimidazole-imide [10] (PBI-p); 2. polybenzimidazole-amide-imide (III); 3. aromatic polyamide [18] (P-M); (60 mg, heating rate: 9°C/min, in air).

(P—M)[18] (from 4,4′-diaminodiphenylmethane and tereftalic acid chloride).

By comparison with the other polymers, the following order of thermal stability was found : polybenzimidazole-imides[19] > polybenzimidazoles[19] > polybenzimidazole-amide-imides > polyimides.[20]

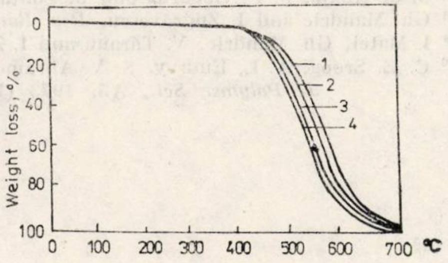

Fig. 3. Thermogravimetric analysis of PBI-A-I in comparison with other polymers : 1. polybenzimidazole- imide ; 2. — polybenzimidazole ; 3. — polybenzimidazole-amide-imide ; 4. — polyimide ; (50 mg. heating rate ; 9°C/min., in air).

Table 3 shows some electrical properties of polybenzimidazole-amide-imide III in comparison with polybenzothiazole-amide-imide[12] (7 f).

Table 3

Electrical properties of polybenzimidazole-amide-imide (III) and polybenzothiazole-amide-imide (7f) — films1)

Properties	Unit	III	7f
Dissipation factor			
0.3 kHz		2.1×10^{-2}	
1.0 kHz		1.2×10^{-2}	6.7×10^{-4}
10.0 kHz		1.5×10^{-2}	
Volume resistivity	ohm×cm	3.9×10^{16}	6.5×10^{15}
Dielectric strength	kv/mm	104	130

[2] All data were obtained on films of 30 μm.

REFERENCES

[1] F. Dobinson and J.Preston, *J. Polymer Sci.*, **A 1**, 2093 (1966).
[2] J. Preston, R. W. Smith and C. J. Stehman, *J. Polymer Sci.*, **C 19**, 7 (1967).
[3] J. Preston and R. W. Smith, *J. Polymer Sci.*, **B 4**, 1033 (1966).
[4] J. Preston and W. B. Black, *J. Polymer Sci.*, **B 3**, 845 (1965).
[5] J. Preston and W. B. Black, *J. Polymer Sci.*, **A-1, 5**, 2429 (1967).
[6] T. Kubota and R. Nakanishi, *J. Polymer Sci.*, **B, 2**, 665 (1964).
[7] P. M. Hergenrother, W. Wrasidlo and H. H. Levine, *J. Polymer Sci.*, **A, 3**, 1665 (1965).
[8] J. Preston, W. F. Dewinter and W. B. Black, *J. Polymer Sci.*, **A-1**, 7, 283 (1969).
[9] Gh. Mandric and I. Zugrăvescu, *Rev. Roumaine Chim.*, **16**, 1419 (1971).
[10] Gh. Mandric, A. I. Pavlov, V. V. Korshak and I. Zugrăvescu, *Rev. Roumaine Chim.*, **19**, 1783 (1974).
[11] V. V. Korshak, A. I. Pavlov, Gh. Mandric and I. Zugrăvescu, *Rev. Roumaine Chim.*, **22**, 1521 (1977).
[12] G. Neamțu, Gh. Mandric and I. Zugrăvescu, *Angew. Makromol. Chem.*, **103**, 29 (1982).

[13] Y. Iwakura, K. Uno, Y. Imai and M. Fukui, *Makromol. Chem.*, **22**, 41 (1964).
[14] M. Strul, G. Neamţu, E. Mănţăluţă and I. Zugrăvescu, *Rev. Roumaine Chim.*, **16**, 941 (1971).
[15] I. Zugrăvescu, M. Strul, E. Mănţăluţă and G. Neamţu, Rom., **56** 995 (1974); *Chem. Abstr.* **82**, 117430 q (1975).
[16] W. Wrasidlo and J. M. Angl, *J. Polymer Sci.*, **Part. A-1**, 321 (1969).
[17] J. de Abajo, J. P. Gobarda and J. Fontain, *Angew. Makromol. Chem.*, **71**, 143 (1978).
[18] Gh. Mandric and I. Zugrăvescu, *Rev. Roumaine Chim.*, **16**, 1419 (1971).
[19] I. Matei, Gh. Mandric, V. Tăranu and I. Zugrăvescu, *Rev. Roumaine Chim.*, **12**, 715 (1967).
[20] C. E. Sroog, A. L. Endrey, S. V. Abramo, C. E. Berr, W. M. Edwards and K. L. Olivier, *J. Polymer Sci.*, **A5**, 1973 (1965).

Revue Roumaine de Chimie, **31**, *1*, 31—35 (1986)

THERMAL BEHAVIOR OF SOME STYRENE-METHYLMETHACRYLATE COPOLYMERS

CAMELIA BELDIE, NATALIA HURDUC, ANA ONU and IGNAT C. POINESCU*

Polytechnic Institute "Gh. Asachi" of Jassy
Department of Physical Chemistry
*Institute of Macromolecular Chemistry
"P. Poni" Jassy, Romania

Received December 15, 1984

Two groups of styrene-methylmethacrylate copolymer samples keeping constant the monomer molar ratio and varying the percent of benzoyl peroxide (group A), or changing the monomer molar ratio while the quantity of initiator was kept constant (group B), were prepared.

The above samples were investigated using thermal analysis methods, (TG; DTG; DTA) in dynamic conditions of temperature.

Several conclusions were drawn on the experimental data referring to the thermal stability, copolymer structure and the activation energy of the thermal degradation process. It was also established the tight connection between the thermal stability and the copolymer structure.

On the basis of the performed researches, in practice, it is possible to predict the synthesis parameters in order to prepare copolymers with a higher (desired) thermal stability.

The thermal stability of copolymers as a function of its composition and structure has a large importance, both theoretical given by the relationships which are established between these magnitudes, and practical, according to the followed purpose, the choosing of the processing regime which has to be between the flow and decomposition temperatures and also to the establishing of the temperature range in which are used, in optimal conditions, the products obtained from different polymers and copolymers.[1]

There were several studies referring to the thermal behavior of some copolymers,[2] offering the possibility to obtain information concerning their structure, via the thermal methods.

This paper deals with the experimental results obtained during the thermal characterization in dynamical conditions of the temperature of some styrene-methylmethacrylate (S—MMA) copolymers, using the following methods : thermal gravimetry (TG), differential thermal gravimetry (DTG) and differential thermal analysis (DTA). This study allows to draw conclusions concerning the structure, the composition and the thermal stability of copolymers.

I. EXPERIMENTAL

1. Preparation of Copolymers

Styrene and methylmethacrylate (technical grade) were washed with a 5.0% NaOH aqueous solution and water to remove p-tertiary-butylcatechol used as polymerization inhibitor. The monomers were vacuum distilled before use. The suspension copolymerization technique[3] of the monomers was used. The bead-shape copolymers were performed in a glass suspension copolymerization apparatus, consisting of one liter, three, necked, round-bottomed vessel, fitted with a variable mechanical stirrer, a thermometer and a reflux condenser.

A solution of styrene and methylmethacrylate (1 : 1 ratio, w/w) and variable percents of benzyol peroxide was poured into the flask which contained an aqueous solution of ammonium salt of styrene-maleic anhydride copolymer (0.15% vs the volume of water) as dispersive agent and gelatine (0.07% vs the volume of water), as protective agent. The water organic phase ratio was 1 : 3 and the copolymerization process was carried out at 80°C for 12 hrs.

In this way, the copolymer samples from group A were obtained.

We also got copolymers with variable percents of styrene and methylmethacrylate using approximately 2.0% benzoyl peroxyde vs the quantity of monomers (group B).

The bead-shaped copolymers were washed with hot water and then dried at room temperature.

Copolymers samples were characterized from a chemical point of view and the numerical average molecular weights determined using a Knauer Electronic Membrane Osmometer, West Germany, and toluene as solvent at 37°C.

The measured data were listed in Table 1.

Table 1

Synthesis parameters and the $\overline{M}_n$ values of styrene methylmethacrilate copolymers

A					B				
Sample	Bz_2O_2	S (g)	MMA (g)	$\overline{M}_n$ ($g \cdot mol^{-1}$)	Sample	Bz_2O_2	S (g)	MMA (g)	$\overline{M}_n$ ($g \cdot mol^{-1}$)
1	0.2	52	50	110.450	6	2	100	—	26.400
2	0.5	52	50	78.900	7	2	80	20	31.300
3	1.0	52	50	69.300	9	2	40	60	44.300
4	2.0	52	50	55.400	10	2	20	80	69.200
5	5.0	52	50	20.900	11	2	—	100	99.300

2. Thermal characterization

The copolymer samples listed in Table 1 were analysed by DTG and DTA methods in dynamical conditions of temperature.

The apparatus allows simultaneous recording of the weight loss (TG), DTG, DTA and the increase of the temperature (T).

The weight of the searched samples ranged between about 80 to 90 mg, and the heating rate was of 10°C/min. α—Al_2O_3 (calcined at 1500°C) was used as a standard material. The sensibilities were: TG — 100 mg. DTG 1/30; DTA 1/20.

The working conditions were rigorously kept throughout the experiments, because the thermogram shapes may change function of the working parameters.

II. RESULTS AND DISCUSSION

The thermograms show the whole degradation of the analysed samples up to 700°C, with one prevailing stage.

The DTG of the copolymers from group A presented in Figure 1 are characterized by a peak (sample 1), two peaks (samples 2 and 3) and increasing asymmetry (samples 4 and 5).

More suggestive than the DTG curves are thoses corresponding to DTA analysis, presented in Fig. 2, which suggest a special behaviour for sample 1.

From Fig. 2 one can ascertain that the thermal degradation of sample 1 is accompanied by a strong exothermal effect, in comparison with the other samples at which the prevailing effect is endothermal.

The experimental results would suggest a modification of the copolymer structure depending on the initiator concentration.

Based both on the literature data, [2] and our measured experimental values, one might assert that the copolymers had different structures as for instance: a prevailing block structure (sample 1), a statistical structure (sample 2 and 3) and the appearance of a ordinate alternante structure (samples 4 and 5).

The kinetic parameters, estimated by the Freeman-Carroll method[3] presented in Table 2 supported strongly our assumption.

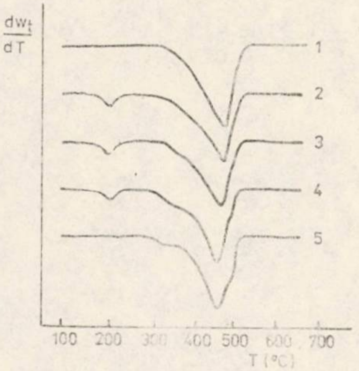

Fig. 1. — DTG curves for samples 1—5.

Although DTG curves show one degradation stage only, the calculations lead to two processes, a result which is in good agreement with the DTA data.

A carefull examination of the activation energy values of the degradation process suggests that sample 1 has the greatest thermostability, while samples 4 and 5, the smallest one.

Table 2

The kinetic characteristics of the copolymers listed in group A.

Sample	E_a (kJ·mol^{-1})	
	I	II
1	172	82
2	137	53
3	135	51
4	120	83
5	118	96

The decrease of the activation energy for the small degree of transformation (samples 4 and 5) suggests the prevailing depolymerization reaction, which is favoured by the presence of some ordinate (alternating) structures.

Taking into account the activation energy corresponding to the small degree of the transformation, in order to characterize thermostability, one could notice that it decreased simultaneously with the increase of the initiator concentration, and it might be explained by the appearance of some structural irregularity, resulted in the copolymerization reaction of the initiator with the monomers, as well as the appearance of the regular structures which favour the depolymerization process.

For the copolymers of group B, where the initiator concentration was kept constant and the ratio of the two monomers was varied, the DTG curves presented more obvious differences in comparison with group A of copolymers (Fig. 3).

These differences emerge from an approximate symmetrical curve recorded for sample 7 and then the asymmetry became visible at sample 4, it grew for the following copolymers, leading to an obvious separation in to two processes for sample 10.

Revue Roumaine de Chimie, **31**, *1*, 37—47 (1986)

REACTION OF PYRYLIUM SALTS WITH NUCLEOPHILES. XVIII[1]

SYNTHESIS OF 4 (*p*-n-BUTOXYPHENYL)-2,6-DIMETHYLPYRIDINE and of 2,6-DIMETHYL-4 (*p*-n-PENTYLPHENYL)-PYRIDINE

ALEXANDRU T. BALABAN, GEORGE MARTON and IOSIF SCHIKETANZ
Polytechnic Institute, Department of Organic Chemistry,
Splaiul Independenţei 313, 76206 Bucharest, Romania

Received April 2, 1985

By diacetylation of the corresponding p-substituted phenyl-dimethylcarbinols, *via* non-isolated pyrylium salts, the title pyridines were obtained. Their structure was confirmed by ^{1}H-NMR chemical shifts and by lanthanide induced shifts. Above room temperature, no mesophase was detected.

The literature of liquid crystals[2] indicates among the most useful nematic mesophases *p,p'*-disubstituted biphenyls **1** (AlkO = n-butoxy) and **2** (Alk = n-pentyl). Such materials exhibiting nematic liquid crystalline phases with $\varepsilon_{II} < \varepsilon_{\perp}$ at room temperature have been known since 1973, where the ε values refer to the anisotropy in the dielectric constant measured with the field parallel or orthogonal to the long axis of the molecule.

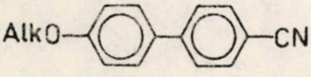

1

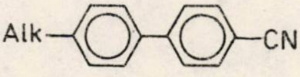

2

Taking into account the analogy between pyridines and benzenes substituted with electron-acceptor groups, we decided to investigate the related pyridines **3** and **4**, which might also lead to nematic mesophases. Such compounds have not yet been reported.

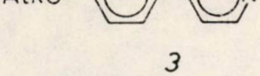

3

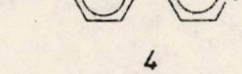

4

and the residue was poured into water. The organic layer was washed with aqueous sodium hydroxide, then with dilute sulphuric acid, dried over Na_2SO_4 and distilled at 160°/13 Torr; yield 81%.

p-n-Butoxyphenyl-dimethylcarbinol (**8**). The above bromoderivative was converted (0.1 mol) into the Grignard reagent in ethyl ether. Then 0.1 mol acetone was added, the mixture was refluxed for one hour, then decomposed and hydrolysed with saturated aqueous ammonium chloride. The crude carbinol was used directly after removing the solvent by distillation.

4-p-n-Butoxyphenyl-2,3,6-trimethylpyrylium perchlorate (**10**). Into a mixture of the above carbinol (0.1 mol) and 0.6 mol acetic anhydride, 70% perchloric acid (14.5 g, 0.1 mol) was added dropwise with caution under vigorous stirring without external cooling. The mixture became hot and dark brown, and was stirred for two hours. The product was not isolated.

4-(p-n-Butoxyphenyl)-2,3,6-trimethylpyridine (**11**). The above reaction mixture was poured with cooling into a large excess of aqueous ammonia. The resulting mixture was extracted three times with ethyl ether. The ethereal layer was treated with 20 ml 15% aqueous hydrochloric acid for extracting the pyridine. The aqueous acid layer was separated, extracted with ethyl ether, and made alkaline with aqueous sodium hydroxide, when the substituted pyridine was separated. It was extracted with ethyl ether, dried over sodium hydroxide, concentrated under reduced pressure and purified by chromatography on silica gel using chloroform as solvent. A liquid reddish product resulted which was characterized by its ¹H-NMR spectrum in $CDCl_3$. The coupling constant of the p-phenylene AA'BB' proton was 9 Hz.

p-Lauroyl-bromobenzene (**13**). To a solution of 95 g bromobenzene (0.61 mol) in 250 ml carbon disulphide was stirred with 54.4 g (0.41 mol) anhydrous aluminium chloride while adding dropwise 59.5 g (0.27 mol) lauroyl chloride. After one hour's refluxing, the solvent was distilled off and the residue was decomposed with ice and hydrochloric acid, to which benzene was added for extraction. After washing the organic layer with 10% sodium hydroxide and drying, the product was distilled under reduced pressure. Yield 69 g (59%), m.p. 34°, b.p. 178—182°/2 Torr.

p-Bromo-n-dodecylbenzene (**14**) was obtained by reducing 25 g (80 mmol) of the above product with 12 ml hydrazine hydrate and 8.4 g (150 mmol) KOH in 120 ml diethylene glycol. After dissolution of KOH at 100°, the temperature was raised to 180° and maintained for 3 hours. After cooling, the mixture was extracted with benzene, the organic layer was washed with water, dried and distilled under reduced pressure. Yield 12 g (58%) colourless liquid b.p. 120—125°/0.5 Torr.

p-n-Dodecylphenyl-dimethylcarbinol (**16**) was obtained by converting 1.3 g magnesium and 24 g (33 mmol) of the above product into the Grignard reagent in 25 ml anhydrous ethyl ether, and then by adding 2.5 g acetone (41 mmol). After decomposing with hydrochloric acid, the ethereal layer was washed with aqueous sodium hydrogen sulphite and the solvent was removed by gentle heating. The crude carbinol was used without further purification.

4-(p-n-Dodecylphenyl)-2,3,6-trimethylpyridine (**19**). The above carbinol was admixed with 36 g (0.35 mol) acetic anhydride and into the stirred mixture 70% perchloric acid (7.75 g, 54 mmol) was added dropwise with caution till the reaction started. The reaction mixture containing the pyrylium perchlorate **18** was introduced with cooling into an excess of aqueous ammonia. After one hour the solution was extracted with ethyl ether three times. The solution was shaken with 15% hydrochloric acid and the aqueous layer was separated and made alkaline with sodium hydroxide. The product was extracted with ethyl ether, the organic layer was separated, dried, concentrated and purified by TLC using chloroform as eluent. A liquid oily product was obtained. The ¹H-NMR spectrum (CCl_4) and the shifts induced by $Eu(fod)_3$ confirmed the structure of the product.

ACKNOWLEDGEMENT. Thanks are expressed to Dr. C. Draghici for the determination of NMR spectra

REFERENCES

1 Preceding part: E. Sliam and A. T. Balaban, *Rev. Roum. Chim.* 28, 707 (1983).
2 G. W. Gray, K. J. Harrison and J. A. Nash in "Liquid Crystals and Ordered Fluids" (eds. J. F. Johnson and R. S. Porter), Plenum Press, New York, vol. 2, 1974; G. W. Gray, "Molecular Structure and the Properties of Liquid Crystals", Aca-

off and the residue was poured into water. The organic layer was washed with aqueous sodium hydroxide, then with dilute sulphuric acid, dried over Na_2SO_4 and distilled at 150°/ /25 Torr; yield 61%.

p-(n-Butoxyphenyl)-dimethylcarbinol (**8**). The above bromoderivative was converted (0.1 mol) into the Grignard reagent in ethyl ether. Then 0.1 mol acetone was added, the mixture was refluexd for one hour, then cooled and hydrolyzed with saturated aqueous ammnoium chloride. The crude carbinol was used directly after removing the solvent by distillation.

4-(p-n-Butoxyphenyl)-2,6-dimethylpyrylium perchlorate (**10**). Into a mixture of the above carbinol (0.1 mol) and 0.6 mol acetic anhydride, 70%, perchloric acid (14.5 g,0.1 mol) was added dropwise with caution under vigorous stirring without external cooling. The mixture became hot and dark brown, and was stirred for two hours. The product was not isolated.

4-(p-n-Butoxyphenyl)-2,6-dimethylpyridine (**11**). The above reaction mixture was poured with cooling into a large excess of aqueous ammonia. The resulting mixture was extracted three times with ethyl ether. The ethereal layer was treated with 20 mL 15% aqueous hydrochloric acid for extracting the pyridine. The aqueous acid layer was separated, extracted with ethyl ether, and made alkaline with aqueous sodium hydroxide, when the substituted pyridine was separated. It was extracted with ethyl ether, dried over sodium hydroxide, concentrated under reduced pressure and purified by chromatography on silica gel using chloroform as solvent. A liquid reddish product resulted which was characterized by its ^1H-NMR spectrum in $CDCl_3$. The coupling constant of the *p*-phenylene AA′ BB′ proton was 9 Hz.

p-n-Pentanoyl-bromobenzene (**13**). A solution of 95 g bromobenzene (0.61 mol) in 250 mL carbon disulphide was stirred with 56.4 g (0.5 mol) anhydrous aluminium chloride while adding dropwise 56.5 g (0.47 mol) n-pentanoyl chloride. After one hour's refluxing, the solvent was distilled off and the residue was decomposed with ice and hydrochloric acid, to which benzene was added for extraction. After washing the organic layer with 10% sodium hydroxide and drying, the product was distilled under reduced pressure. Yield 67 g (59%), m.p. 34°, b.p. 118—119°/2 Torr.

p-Bromo-n-pentylbenzene (**14**) was obtained by reducing 22 g (90 mmol) of the above product with 12 mL hydrazine hydrate and 8.4 g (150 mmol) KOH in 120 mL diethyleneglycol. After dissolution of KOH at 100°, the temperature was raised to 180° and maintained for 3 hrs. After cooling, the mixture was extracted with benzene, the organic layer was washed with water, dried and distilled under reduced pressure. Yield 12 g (59%) colourless liquid b.p. 126—127°/25 Torr.

p-n-Pentylphenyl-dimethylcarbinol (**16**) was obtained by converting 1.3 g magnesium and 12 g (53 mmol) of the above product into the Grignard reagent in 25 mL anhydrous ethyl ether, and then by adding 2.3 g acetone (40 mmol). After decomposing with hydrochloric acid, the ethereal layer was washed with aqueous sodium hydrogen sulphite and the solvent was removed by gentle heating. The crude carbinol was used without further purification.

2,6-Dimethyl-4-(p-n-penthylphenyl)pyridine (**19**). The above carbinol was admixed with 33 g (0.33 mol) acetic anhydride, and into the stirred mixture 70% perchloric acid (7.75 g, 54 mmol) was added dropwise with caution till the reaction started. The reaction mixture containing the pyrylium perchlorate **18** was introduced with cooling into an excess of aqueous ammonia. After one hour the solution was extracted with ethyl ether three times. The solution was shaken with 15% hydrochloric acid and the aqueous layer was separated and made alkaline with sodium hydroxide. The product was extracted with ethyl ether, the organic layer was separated, dried, evaporated and purified by TLC using chloroform as eluent. A liquid oily product was obtained. The ^1H-NMR spectrum (CCl_4) and the shifts induced by $Eu(fod)_3$ confirmed the structure of the product.

ACKNOWLEDGEMENT. Thanks are expressded to Dr. C. Drăghici for the determination of NMR spectra.

REFERENCES

[1] Preceding part, E. Stepan and A. T. Balaban, *Rev. Roum. Chim.*, **28**, 707 (1983).

[2] G. W. Gray, K. J. Harrison and J. A. Nash in "Liquid Crystals and Ordered Fluids" (eds. J. F. Johnson and R. S. Porter), Plenum Press, New York, vol. 2, 1974; G. W. Gray, "Molecular Structure and the Properties of Liquid Crystals", Aca-

demic Press, New York, 1962; A. C. Griffin and J. F. Johnson (eds.), "Liquid Crystals and Ordered Fluids", Plenum Press, New York, 1984; H. Keller and R. Karz, "Handbook of Liquid Crystals", Verlag Chemie, Weinheim 1980.,

[3] A. T. Balaban, W. Schroth and G. W. Fischer *Adv. Heterocyclic Chem.*, **10**, 241 (1969).

[4] A. T. Balaban, A. Dinculescu, G. N. Dorofeenko, G. W. Fischer, A. V. Koblik, V. V. Mezheritskii and W. Schroth, "Pyrylium Salts", *Adv. Heterocyclic Chem.*, Suppl. Vol. 2, Academic Press, New York, 1982.

[5] A. T. Balaban, in "New Trends in Heterocyclic Chemistry", Studeis in Organic Chemistry, No. 3 (eds. R. B. Mitra et el.) Elsevier, Amsterdam, 1979, p. 79.

[6] A. T. Balaban and C. D. Nenitzescu, *Rev. Chim. Acad. R. P. Roumanie*, **6**, 269 (1961).

[7] A. T. Balaban and C. D. Nenitzescu, *Org. Synth.*, Coll. Vol. 5, 1106 (1973).

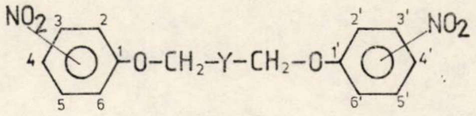

I – III

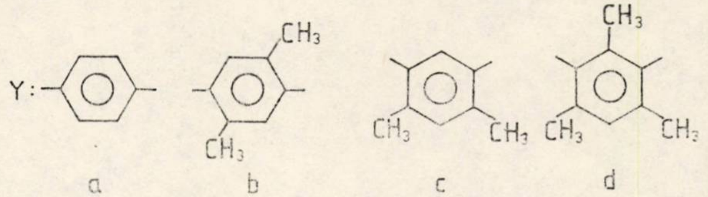

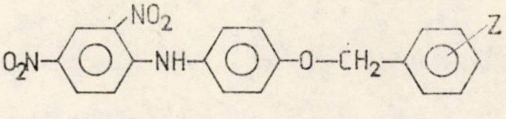

IV: $Z = H, Cl, CH_3$

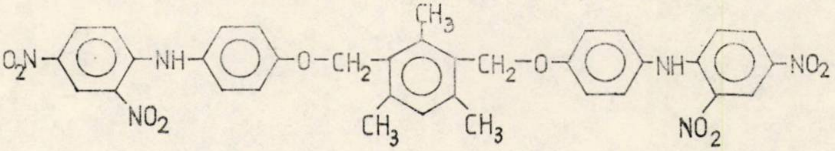

V

Class A : I : $2,2'—NO_2$; II : $3,3'—No_2$; III : $,44'—NO_2$
Class B : IV(e) : $Z=H$; (f) : $Z=4'—Cl$; (g) $Z=2'—CH_3$
(h) : $Z<3'—CH_3$; (i) : $Z=4'—CH_4$

EXPERIMENTAL PART

The anion-radicals were generated electrochemically, using an *in situ* technique for both optical and ESR measurements. The cells were equipped with platinum electrodes and a silver reference electrode[9]. Tetrabutylammonium perchlorate and dimethylsulfoxide were used, respectively, as supporting electrolyte and solvent.

The ESR spectra were registered at a JES-3B spectrometer and the electronic spectra at a SPECORD UV-VIS spectrophotometer.

The simulation of the ESR spectra and the spin density calculations were performed at the Calculus Center of the Polytechnic Institute of Bucharest.

RESULTS AND DISCUSSION

ESR spectra. From all the compounds belonging to class A, three different types of spectra were obtained, depending only on the position of the nitro group in the peripheric rings, and not on the Y bridge. The single effect of the Y moiety can be noted in the spectra of the anion-radicals (Ia) and (Id), characterised by a slightly different aspect.

In spite of the presence of two nitrosubstituted benzenic rings, the spectra presented in figures 1–4, reflect the typical triplet pattern of the mono-nitrosubstituted anion-radicals. The ESR spectra were rationalised in terms of the hyperfine splitting constants listed in Table 1.

The highest hfs. belongs in all cases to the nitro group nitrogen of one nitrosubstituted aromatic ring and no significant differences could be noted as a function of the position of the nitro group vs. the etheric bridge. The next hfs. were assigned in decreasing order to protons in *para*, *ortho* and *meta vs.* the nitro group.

As experimental data pointed out the spin localization on one benzenic ring, spin density calculations were performed considering only the nitrophenolic fragment of the molecule. The calculated splittings (Table 1) agree well with the experimental ones and were taken into account in the assignment given in Table 1, i.e. the assignment of the two nonequivalent *ortho* protons for II, etc.

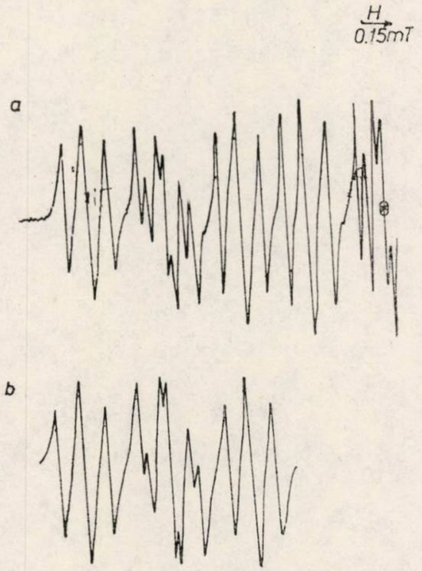

Fig. 1. — Lowest field half of the ESR spectrum of anion-radical Ia: (electrochemical reduction, DMSO) (a) experimental; (b) simulated: nitrogen line $M_N = -1$.

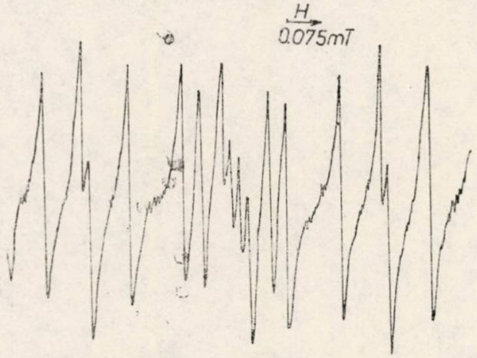

Fig. 2. — Central nitrogen line ($M_N = 0$) from the ESR spectrum of anion radical Id (electrochemical reduction, DMSO).

In the case of the anion-radicals IIIb, IIId, an extra splitting of 0.037 mT due to two equivalent protons was detected; this was obviously assigned to the pair of methylenic protons in the bridge (sites 7, 8). This is in agreement with the results of Maki and Geske,[11] who reported a splitting of 0.030 mT for the methyl protons in o-nitroanisole.

The literature data [5,6] referring to some symmetrically nitrosubstituted bridged systems (Y = CH_2, O, S) have stated that a single methylenic group, i.e. in *bis*(*p*-nitrophenyl)methane, can ensure the delocalization of the odd electron on the whole molecule; consequently, in this case the equivalence of the two nitrogen atoms, four *ortho* and respectively, *meta* protons was observed. The presence of the etheric and sulfide bridges determines either a spin localization on one aromatic moiety or a transfer between the two rings with a solvent dependent rate.

ESR behaviour of the anion-radicals provided by the 2,4-dinitroisopropylaniline have pointed out the further reduction of one nitro group, leading to a second radicalic species.[7] In view of its *g*-factor and the non-equivalence of the 3,5-proton splittings, this species was assigned to a nitroso anion radical. It was also stated that starting from dinitrotertiary amines both radicalic species (nitro and nitroso) were obtained, while starting from dinitro secondary amines only the nitroso anion radical was detected. We believe therefore that the ESR spectra registered in the present work starting from the compounds in class B belong, due to their experimental features and to the presence of the — NH — group rather to nitroso-type anion radicals than to nitro radicalic species. Therefore no MO calculations were performed on these compounds.

Table 2

Visible bands of the anion radicals

Anion radical	λ(mm)
I a	472 (electro, DMSO)
II b	432 ; 500 (electro, DMSO)
III b	435 (electro, DMSO)
V	435 (electro, DMSO) 426, 6 ; 500 (Na, DMF) 454 ; 500 (K, DMF)
2,4-dinitroisopropylaniline[7]	429 ;500 (electro, DMSO)

Electronic spectra. The anion radicals provided by compounds in class A are characterised by the appearance in the visible range of an appreciable absorption increasing during the electrolysis. The maxima of these new bands are listed in Table 2. After the interruption of the electro-

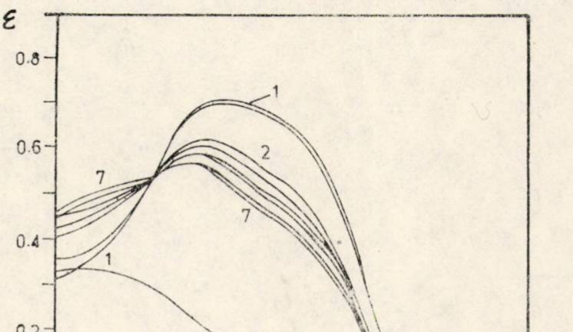

Fig. 5. — Visible spectra obtained at the decay of anion radical V, prepared by electrolytical reduction in DMSO : 1—7 — in time.

lysis the intensity of these bands decays and the initial neutral compounds were recovered, pointing out the reversible character of the reduction process.

In the case of anion radical V, the electrochemical reduction leads to two overlapped bands (Fig. 5). In order to see if these bands could be resolved, chemical reduction with alkali metals in dimethylformamide was also employed. Depending on the experimental conditions (reductive agent, time of reduction) the intensities of the two bands are different, indicating that they belong to two distinct species. The maxima of these bands obtained in various conditions are presented also in Table 2.

The optical spectra of anion-radical V are just like the ESR one, quite similar to those obtained in a previous work[7] starting from 2,4-dinitroisopropylaniline. We consider this fact is proving the same reaction sequence leading to the nitroso anion radical, as the ESR study has already outlined.

REFERENCES

[1] M. Hillebrand and M. Răileanu, *Rev. Roumaine Chim.*, **19**, 1227 (1974).

[2] A. Gioabă, V. E. Sahini and E. Volanschi, *J. Chem. Soc., Perkin Trans.*, **2**, 529, (1977).

[3] I. Baciu, M. Hillebrand, V. E. Sahini and E. Volanschi, *Rev. Roumaine Chim.*, **21**, 485 (1976).

[4] C. Cercasov, F. Cornea, M. Ciureanu, V. E. Sahini, M. Hillebrand and E. Volanschi, *Org. Magn. Reson.*, **20**, 217 (1980).

[5] H. M. McConnell, *J. Chem. Phys.*, **35**, 508 (1961).

[6] J. E. Harriman and A. H. Maki, *J. Chem. Phys.*, **39**, 778 (1963).

[7] M. Hillebrand, Em. Ionescu and E. Volanschi, to be published.

[8] M. Hillebrand, Em. Ionescu and E. Volanschi, submitted for publication to *Rev. Roumaine Chim.*

[9] I. B. Goldberg and A. J. Bard, *J. Phys. Chem.*, **75**, 3281 (1971).

[10] P. H. Rieger and G. K. Fraenkel, *J. Chem. Phys.*, **39**, 609 (1963).

[11] A. H. Maki and D. H. Geske, *J. Amer. Chem. Soc.*, **83**, 1852 (1961).

[12] I. Baciu, M. Hillebrand, O. Maior, V. E. Sahini and E. Volanschi, to be published.

[13] V. M. Kazakova and V. B. Piscov, *J. Strukt. Himii*, **14**, 734 (1973).

Revue Roumaine de Chimie, **31**, *1*, 51—55 (1986)

A CONVENIENT METHOD FOR THE SYNTHESIS OF 1,3,4-OXADIAZOLES FROM DIAROYLHYDRAZINES UNDER MILD CONDITIONS USING PHOSPHORUS TRICHLORIDE-DIMETHYLFORMAMIDE ADDUCT AS REAGENT

C. I. CHIRIAC
"P. Poni" Institute of Macromolecular Chemistry
Aleea Gr. Ghica-Vodă 41 A, Jassy, Romania

Received November 24, 1984

Various substituted 1,3,4-oxadiazoles are prepared in high yields by a cyclodehydration reaction of N,N′-diaroylhydrazines with the phosphorus trichloride-dimethylformamide adduct for 24 hours at room temperature or for 6 hours at 45—55°.

Since Stollé[1] first prepared 2,5-diphenyl-1,3,4-oxadiazoles from N, N′-dibenzoylhydrazine by dehydration at 250—300°, numerous dehydrating reagents have been used in an effort to decrease the hardness of the reaction conditions.

The dehydrating reagents which have been tested are: phosphorus oxychloride,[2–4] thionyl chloride,[5] ethyl ortoformate,[6] thionyl chloride in nitrobenzene,[7] aluminium chloride in nitrobenzene,[8] etc. From the various disadvantages associated with these reagents the following could be mentioned; the long reflux time, the high temperature of the low yields.

RESULTS AND DISCUSSION

A previous communication from this laboratory has shown[9] that the phenyldichlorophosphite-dimethilformamide adduct is a useful reagent for the dehydration of N,N′-diaroylhydrazine to the corresponding 1,3,4-oxadiazoles (on heating for four hours at 100—110°).

In this work we have found that the adduct between dimethylformamide (DMF) and phosphorus trichloride is a very suitable reagent for this reaction even at room temperature. Thus by stirring at room temperature for 24 hours one mole of N,N′-dibenzoylhydrazine with one mole of phosphorus trichloride in excess DMF, 2,5-diphenyl-1,3,4-oxadiazole resulted with yield 90 % (with smaller amount of phosphorus trichloride, the yield decreased). The same reaction performed at 100–110° for 2–3 hours gives a yield of 95–97 %. By heating at 100–110° for 2–3 hours 1 mole N,N'-dibenzoylhydrazine and 0.66 mole phosphorus trichloride in DMF, the yield was 92–96 % and decreased strongly when only 0.33 mole PCl_3 was used. Therefore, in PCl_3, only one chlorine atom reacts at room temperature, the second at 100–110° whereas the third is unreactive in these conditions, similar with other cases.[10]

For the structure of the adduct between one mole DMF and one mole phosphorus trichloride, Anderson and coworkers [10] proposed two uncertain structures : $(CH_3)_2N^+=CHP(O)Cl_2]\,Cl^-$ and $(CH_3)_2N^+=CCl]\,{}^-OPCl_2$. The first structure has pentavalent phosphorus, similar with the adduct between DMF and phosphorus oxychloride,[11] whereas the second structure has a C–Cl bond, similar with the adduct between DMF and $SOCl_2$.[12] Through the reaction between one mole N,N'-dibenzoylhydrazine and one mole $POCl_3$ in excess of DMF at room temperature (24 hours), 2,5-diphenyl-1,3,4-oxadiazole resulted with 13–15 % yield, whereas with one mole of $SOCl_2$ in the same conditions, the yield was only 14–18 %. Therefore, the adduct DMF–PCl_3 which gives a high yield in this reaction possesses another structure. We suppose that this adduct has the structure :

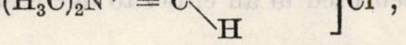

$$\left.(H_3C)_2N^+=C\begin{array}{l}\diagup O-PCl_2\\ \diagdown H\end{array}\right]Cl^-,$$

in which the phosphorus atom remains trivalent, being much more reactive than at valence five, similar with other cases.[9,11] We isolated this adduct as a very hygroscopic solid compound with m.p. 74–77°, by the reaction between DMF and PCl_3 in dry diethyl ether.

The IR spectrum of this adduct presents two bands at 1030 and 1110 cm^{-1}, which corresponds to the –P–O–C-group and a band at 1650 cm^{-1} for the $-C{=}N^+$ – group. This bands are present also in the spectrum of the adduct of DMF with $POCl_3$:

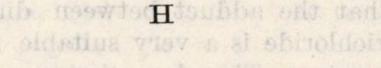

$$(H_3C)_2N^+=\underset{\displaystyle H}{\underset{|}{C}}-O-PCl_2]Cl^-$$ prepared by H. Bredereck.[11]

The structure of the above adduct will be extensively discussed in a separate communication.

In this cyclodehydration we used DMF in excess, because a small amount reacts with PCl_3 affording "in situ" the adduct and the remaining quantity serves as a solvent for the reaction products sparingly soluble. At the beginning, we used the adduct in pure state but in order to simplify the procedure, we worked with this reagent prepared "in situ".

We supposed, similar as in other cases,[9,13-15] that this reaction involves two transition states (II) and (III):

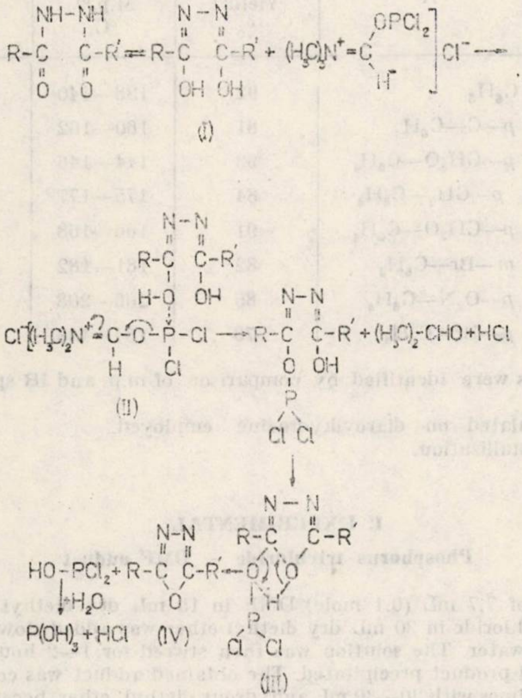

In a typical procedure 1 mole + 10 % excess PCl_3 was added slowly to dried DMF cooled to 0—5° (a small excess improves the yield). After one hour of stirring at room temperature, when the adduct DMF-PCl_3 resulted "in situ", one mole (I) was added and the obtained solution was stirred for 24 hours at room temperature or for 6 hours at 45—55° (these two procedures gave the same yield). The obtained product (IV) was precipitated with water and ice, when $HOPCl_2$ (by-product) was transformed in $P(OH)_3$. The yields obtained in this method ranged from 78 to 93 % (Table 1).

Using the adduct PCl_3—DMF, we obtained substituted 1,3,4-oxadiazoles by the cyclodehydration of the corresponding diaroylhydrazines under mild conditions with high yields even at room temperature.

Table 1

Substituted 1,3,4-oxadiazoles obtained from diaroylhydrazines using PCl_3-DMF adduct

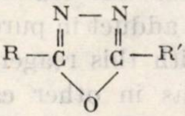

R	R′	Oxadiazoles[a]		
		Yield[b] %	M.p.[c] °C	Reported m.p. °C
C_6H_5	C_6H_5	92	138—140	139—140[1]
C_6H_5	p—C—C_6H_4	81	160—162	162[2]
C_6H_5	p—CH_3O—C_6H_4	93	144—146	145—146[2]
p—CH_3—C_6H_4	p—CH_3—C_6H_4	84	175—177	176[16]
p—CH_3O—C_6H_4	p—CH_3O—C_6H_4	91	166—168	166—167[16]
m—Br—C_6H_4	m—Br—C_6H_4	82	181—182	181—183[16]
C_6H_5	p—O_2N—C_6H_4	85	206—208	207—209[2]
C_6H_5	p—Br—C_6H_4	78	164—166	167[2]

a) The products were identified by comparison of m.p. and IR spectra with authentic samples.

b) Yields calculated on diaroylhydrazine employed.

c) After recrystallization.

I. EXPERIMENTAL

Phosphorus trichloride — DMF adduct

To a solution of 7.7 mL (0.1 mole) DMF in 15 mL dry diethyl ether, 8.58 mL (0.1 mole) phosphorus trichloride in 30 mL dry diethyl ether was added slowly under stirring and cooling with ice and water. The solution was then stirred for 1—2 hours at room temperature, when the desired product precipitated. The obtained adduct was collected by filtration, washed rapidly three times with 20—30 mL anhydrous diethyl ether, because it is hygroscopic. After drying for 3—4 hours under vacuum, 16.9 g (80.5%) adduct with m.p. 74—77° were obtained.

Anal. calculated for : $C_3H_7Cl_3PON$; C, 17.14 ; H, 3.33 ; N, 6.66 ; Cl, 50.71 ; P, 14.7%. Found : C, 16.21, H. 3.52 ; N, 6.28 ; Cl, 49.36 ; P, 14.10%.

2,5-Diphenyl-1,3,4-oxadiazole

To 10 ml dry DMF in a 50 mL three-necked flask, 1 mL (0.01 mole + 10% excess) of phosphorus trichloride was added slowly under stirring and cooling. After stirring for one hour at room temperature, 2.4 g. (0.01 mole) N,N′-dibenzoylhydrazine were added and then 5 ml DMF. This solution was stirred for 24 hours at room temperature or for 6 hours at 45—55°. At the end of the reaction, the obtained solution was poured into a large volume of water with ice (80—100 mL) under stirring, when the desired product precipitated. This mixture was treated with 10% NaOH solution till pH $<$ 9—10 and the product was collected by filtration, washed with 30—40 ml 7% HCl solution, three times, with 20—30 ml water and dried under vacuum at 100—120°, affording 2,5-diphenyl-1,3,4-oxadiazole (2.05 g) with m.p. 138—140° after recrystallisation from ethanol (mixed m.p. with pure product underpressed).

Anal. found: C, 75.11; H, 4.26; N, 12.39%. Calculated for $C_{14}H_{10}N_2O$; C, 75.60; H, 4.50; N, 12.60%.

Under similar conditions, the other oxadiazoles (presented in table 1) were prepared in high yields from the corresponding N,N'-diaroylhydrazines.

REFERENCES

[1] R. Stollé, *Ber. dtsch. chem. Ges.*, **32**, 797, (1897).

[2] A. P. Grekov and L. M. Kulakova, *Zhur. Obscei Khim.*, **29**, 3054 (1959); ***Chem. Abstr.*** **54,** 14108 (1960).

[3] R. S. Azen and A. P. Grekov, *Zhur. Obscei Khim.*, **29**, 1955 (1959); ***Chem. Abstr.***, **54, 9898** (1960).

[4] F. N. Hayes and B. S. Rogers, *J. Amer. Chem. Soc.*, **77**, 1850 (1955).

[5] Ciba Ltd. British patent 816, 750 (July 15, 1959); *Chem. Abstr.*, **54**, 3457 (1960).

[6] G. Ainsworth, U. S. Pat., 2, 733, 245; *Chem. Abstr.*, **50**, 12.115 (1956).

[7] N. S. Dokunikhin, *Zhur. priklad. Khim.*, **32**, 664 (1959).

[8] W. Müller, U. S. Pat., 2, 838, 520; *Chem. Abstr.* **52**, 17.290 (1958).

[9] C. I. Chiriac, *Rev. Roumaine Chim.*, **27**, 935 (1982).

[10] A. G. Anderson and D. Erickson, *Synthesis*, **1976**, 399.

[11] H. Bredereck, *Chem. Ber.*, **92**, 844 (1959).

[12] H. H. Bosshard and H. Zollinger, *Helv. Chim. Acta*, **42**, 1659 (1959).

[13] F. Gramer and M. Winter, *Chem. Ber.*, **94**, 990 (1961).

[14] H. M. Walborsky and G. E. Niznik, *J. Org. Chem.*, **37**, 187 (1972).

[15] E. A. Lawton and D. D. McRitchie, *J. Org. Chem.*, **24**, 26(1959).

[16] E. Baltazzi and A. Wysocki, *Chem. & Ind.* **26**, 1680 (1963).

Revue Roumaine de Chimie, 31, *1*, 57—62 (1986)

KINETICS OF OXIDATION OF DIGOL BY VANADIUM(V) IN AQUEOUS SULPHURIC AND HYDROCHLORIC ACID MEDIUM

NARENDRA NATH, R. C. DUBEY* and U.S. MISRA
Department of Chemistry, Shivapati Degree College,
Sohratgarh, Basti—272205, India

Received May 10, 1983
Revised July 1985

The kinetics of oxidation of digol by vanadium (V) in aqueous sulphuric and hydrochloric acid medium has been carried out. The order of reaction with respect to the oxidant and the substrate has been found to be unit within the range of their concentrations used. Hammett acidity function (—Ho) has been applied and a linear correlation between log *k* and —Ho has been obtained. The formation of an intermediate complex between vanadium (V) and substrate and the free radical formation during the course of reaction have also been indicated. The energy of activation and entropy of activation have been calculated. On the basis of experimental results a probable reaction mechanism has been proposed.

In the previous publication Nath and Dubey[1] carried out the kinetics of oxidation of substituted dihydric alcohols namely 2-methoxy ethanol, 2-ethoxyethanol and 2-butoxyethanol by vanadium(V) in aqueous acidic medium. They observed the reaction to be first order each with respect to the substrate and the oxidant. The reaction rate was found to be Hammett's acidity function ($-H_0$) dependent. On the basis of these results, the oxidation of these substituted dihydric alcohols was considered as proceeding through the formation of an intermediate complex between the substrate and vanadium(V) species in an equilibrium step followed by its rapid transformation to give the reaction product through a radical intermediate.

Vanadium(V) being one of the most versatile oxidizing agents, the interest arose of studying the kinetics of oxidation of different types of substituted dihydric alcohols namely diethyleneglycol (dihydroxydiethyl ether) commercially known as digol, methyl and ethyl digol and to see how its kinetics differs from the kinetics of simplest dihydric alcohol namely ethylene glycol reported earlier.[2]

The present communication deals with the kinetics of oxidation of digol ($CH_2OH.CH_2OCH_2CH_2OH$) by vanadium(V) in aqueous acid medium (in the presence of HCl and H_2SO_4) and to see in what way vanadium(V) oxidizes this substrate. Further work with respect to methyl digol and etyhl digol is in progress to establish the complete mechanism.

---

* Address for correspondence.

EXPERIMENTAL

All the chemicals used were of A.R. grade except digol (SD'S-Indian). The stock solution of ammonium-metavanadate was prepared by dissolving the sample in sulphuric and hydrochloric acid of known concentrations. Digol solution was prepared by weight. Mixed solution of ammonium metavanadate and sulphuric or hydrochloric acid of known strength and freshly prepared digol solution were taken in stoppered conical flasks and kept in an electrically operated thermostat maintained at the desired temperature with an accuracy of ±0.1°C. After allowing 30 min for the reactants to attain the temperature of the bath, requisite amount of digol was added to the mixed (vanadate-acid) solution. An aliquot (5 mL) was withdrawn immediately and quenched in a measured excess of ferrous ammonium sulphate solution. The unreacted solution was titrated against standard solution of cerric ammonium sulphate using N-phenylanthranilic acid as indicator.

RESULTS AND DISCUSSION

The reaction was carried under the condition $[S] \gg [\text{oxidant}]$. Pseudo first order rate constants did not vary much $(k_1 \times 10^3) = 1.12$ to $1.25\ \text{min}^{-1}$) at different initial vanadium(V) concentrations (0.02 to 0.10 M) indicating unit dependence on [V(V)]. The order in substrate was also one as revealed by negligible variation in the second order rate constant $\left(k_2 = \dfrac{k_1}{[S]}\right)$ at different initial [substrate] $(k_2 \times 10^3 = 1.70$ to $1.57)$ Litre $\text{mol}^{-1}\ \text{min}^{-1}$ at substrate concentration in the range of 0.6 to 2.2 M). The temperature dependence of the rate of the reaction has been studied at 30°, 35°, 40° and 45°C. The energy of activation (E_a) as calculated from the slope of the plot of log k_1 against $1/T$ is 68.9 kJ mol^{-1} and entropy of activation $\Delta S^{\neq}$ as -79.4 J $\text{degree}^{-1}\ \text{mol}^{-1}$.

Effect of Hydrogen Ion Concentration

The rate is not linear with respect to $[H^+]$. It has been observed that initially up to a certain $[H^+]$, both in HCl and H_2SO_4, there is very little change in reaction rate and after that the rate increases abruptly (Fig. 1). So under this condition where specific rates increase much faster than $[H^+]$ at high acid concentration, Hammett acidity function [3] has been applied. A linear correlation has been obtained between log k_1 and $-H_0$ (1 to 5 M sulphuric acid and 5 to 9.5 M hydrochloric acid; Fig. 2). The slope of the Hammett plot is 0.38 and 0.31 for sulphuric and hydrochloric acid respectively which is significantly less than the ideal slope of unity in such plots, but it is not uncommon in literature. [4,5] Probable reason for the deviation is that the reactant species for a rate study is occasionally very different from a typical Hammett indicator, whereas for establishment of H_0 scale itself the indicators were of fairly similar size and structure.[4,6] Further the reaction was studied with respect to Bunnett hypothesis.[7]

According to Bunnett, the plot of (log $k + H_0$) against log a_{H_2O} are generally linear and the slopes define a parameter ω. A ω value of -2.5 to 0 indicates non-participation of water molecules in the transition state, a value between $+1.2$ to 3.3 indicates that water acts as a nucleophile

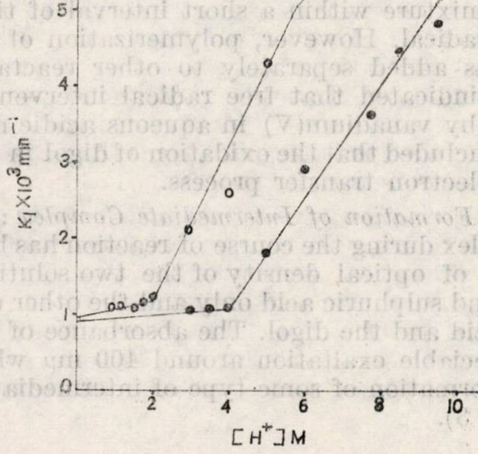

Fig. 1. — Plot of K_1 versus $[H^+]$
o H_2SO_4 ; ● HCl.

$[WH_4VO_3] = 0.04$ M; [DIGOL] =
= 1.0M; $T = 35$°C.

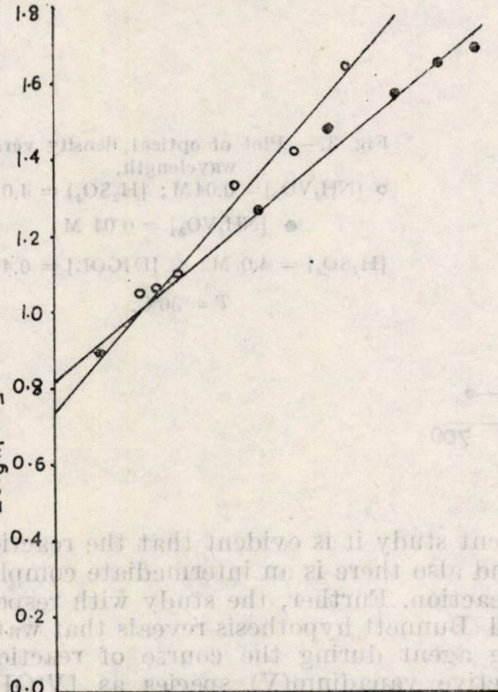

Fig. 2. — Plot of log K_1 ; versus
$[-H_0]$
o H_2SO_4 ; ● HCL
$[NH_4VO_3] = 0.04$M ;
[DIGOL] = 1.0M ; $T = 35$°C.

and a value greater than 3.3 indicates that water acts as a proton abstracting agent. The value of ω in the present study has been found to be 9.2 (in aqueous sulphuric acid) and 14.5 (in aqueous hydrochloric acid).

Presence of free radical. Polymerization tests were carried out with pure acrylonitrile to detect the presence of free radical during the course of reaction. The induced polymerization of acrylonitrile added to the reaction mixture within a short interval of time indicated the formation of free radical. However, polymerization of monomer did not occur when it was added separately to other reactants of the oxidation reaction. This indicated that free radical intervenes in the oxidation reaction of digol by vanadium(V) in aqueous acidic medium. In other words, it may be concluded that the oxidation of digol in aqueous acidic medium involves one electron transfer process.

Formation of Intermediate Complex : The formation of intermediate complex during the course of reaction has been established by the measurement of optical density of the two solutions — one containing vanadium (V) and sulphuric acid only and the other containing vanadium(V) sulphuric acid and the digol. The absorbance of the reaction mixture showed an appreciable exaltation around 400 mμ which gives positive evidence for the formation of some type of intermediate during the course of reaction (Fig. 3).

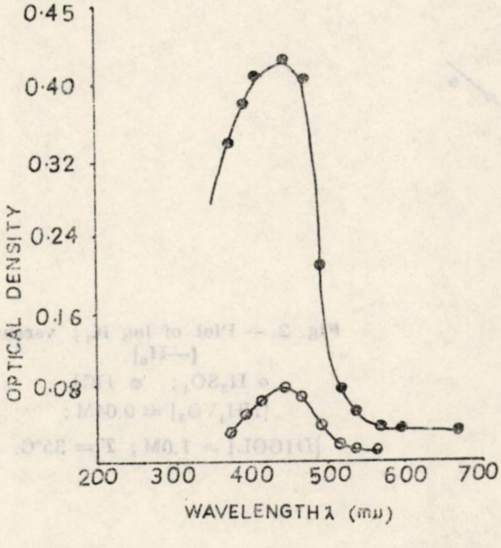

Fig. 3. — Plot of optical density versus wavelength.
○ $[NH_4VO_3] = 0.04$ M ; $[H_2SO_4] = 4.0$ M
● $[NH_4VO_3] = 0.04$ M ;
$[H_2SO_4] = 4.0$ M ; [DIGOL] = 0.4 M
$T = 30$°C.

Mechanism : From the present study it is evident that the reaction involves free radical formation and also there is an intermediate complex formation during the course of reaction. Further, the study with respect to Hammett acidity function and Bunnett hypothesis reveals that water would act as proton abstracting agent during the course of reaction. Further, the participation of active vanadium(V) species as $[V(OH)_3 HSO_4]^+$ in the presence of aqueous sulphuric acid has been well established by previous workers. Taking these evidences into consideration the following probable mechanism is being proposed for the oxidation of digol by vanadium(V) in aqueous sulphuric acid medium :

$$VO_2^+ + H_2O + H^+ \underset{}{\overset{K_1}{\rightleftharpoons}} [V(OH)_3]^{+2} \tag{1}$$

$$[V(OH)_3]^{+2} + [HSO_4]^- \overset{K_2}{\rightleftharpoons} [V(OH)_3 . HSO_4]^+ \tag{2}$$

$$[V(OH_3) . HSO_4]^+ + \text{Digol} \overset{K_3}{\rightleftharpoons} [VO_2 . \text{Digol} . H_2SO_4]^+ + H_2O \tag{3}$$

Intermediate complex

$$\text{Intermediate complex} \xrightarrow[\text{slov}]{k} \text{Radical intermediate} + V(V) + H^+ \tag{4}$$

$$\text{Radical Intermediate} + V(V) + H_2O \xrightarrow{\text{fast}} \text{Product} + V(IV) + H^+ \tag{5}$$

Based on steps (1—5) :

$$\text{Rate} = k[\text{Intermediate complex}]$$

$$= k\,K_1K_2K_3[VO_2]^+\,[H^+][HSO_4]\,^-[H_2O][\text{Digol}]$$

$$= kK_1'K_2K_3[VO_2]^+[H_2SO_4][\text{Digol}]\,;\ \text{where } K_1' = K_1[H_2O] \tag{6}$$

Replacing $[VO_2]^+$ by $[V(V)]_T$ equation 6 becomes :

$$\frac{-\,d[V(V)]}{dt} = \frac{kK_1'K_2K_3[H_2 . SO_4][\text{Digol}][V(V)]_T}{1 + K_1'[H^+] + K_1'K_2[H_2SO_4] + K_1'K_2K_3[H_2SO_4][\text{Digol}]} \tag{7}$$

assuming K_1' to be negligibly small :

$$-\frac{d[V(V)]}{dt} = \frac{k\,K_1'K_2K_3[H_2SO_4][\text{Digol}][V(V)]_T}{1 + K_1'K_2K_3[H_2SO_4](1 + K_3[\text{Digol}])} \tag{8}$$

assuming the inequality $1 \gg K_3$ [Digol], under the present experimental conditions the rate law 8 reduces to

$$\frac{-\,d[V(V)]}{dt} = \frac{k\,K_1'K_2K_3[H_2SO_4][\text{Digol}][V(V)]_T}{1 + K_1'K_2[H_2SO_4]} \tag{9}$$

Equation 9 substantiates a first order kinetics with respect to vanadium(V) and digol. A plot of $\frac{1}{k_{\text{obs}}}$ and $\frac{1}{[H_2SO_4]}$ should be linear. This has been experimentally verified which supports the above postulated mechanism (Fig. 4).

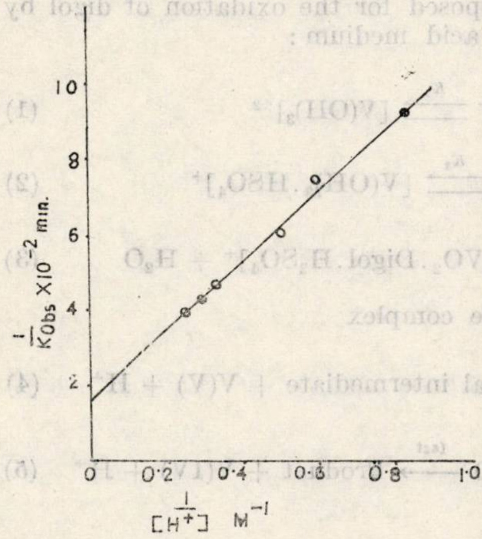

Fig. 4. — Plot of $\frac{1}{[H^+]}$ versus $\frac{1}{k_{Obs}}$

$[\mathrm{DIGOL}] = 1.0$ M

$[NH_4VO_3] = 0.04$ M ; $T = 35°C$

REFERENCES

[1] N. Nath and R. C. Dubey, (a) *Colloid Polym. Sci.*, **258**, 944 (1980); (b) *Indian J. Chem.* **21A**, 244 (1982).

[2] J. S. Littler, A. I. Mellet and W. A. Waters, *J. Chem. Soc.*, **1960**, 2761.

[3] L. P. Hammett, "Physical Organic Chemistry", Mc-Graw Hill, New York, 1970, Chapter IX.

[4] R. N. Mehrotra, *J. Chem. Soc.*, **1963**, 1564.

[5] G. C. Pillai, J. Rajaram and J. C. Kuriacose, *Indian J. Chem.*, **15A**, 680 (1977).

[6] L. P. Hammett and A. J. Dyrup, *J. Am. Chem. Soc.*, **54**, 2721 (1932).

[7] J. F. Bunnett, *J. Am. Chem. Soc.*, **83**, 4956 (1961).

Revue Roumaine de Chimie, **31** *1*, 63—69 (1986)

STUDIES ON PHYSICAL PROPERTIES OF CADMIUM SOAPS. III*

DEHYDRATION AND THERMAL DECOMPOSITION STUDIES OF SOAPS BY THERMOGRAVIMETRY

R. P. VARMA and A. K. VIRMANI **
Department of Chemistry, D. A. V. College, Muzaffarnagar-251001, India

Received October 1, 1984

Dehydration and thermal decomposition of cadmium valerate and caproate have been studied by T.G. Soaps are found to lose their weights (7%) below 180°C due to loss of crystallization water. Above 180°C, these soaps undergo rapid change and finally yield CdO as residue. The activation energy, ΔE, order of reaction, n frequency factor, Z, entropy, ΔS and free energy, ΔG have been calculated for both dehydration and decomposition processes and a probable mechanism has been proposed.

INTRODUCTION

Thermal decomposition of soaps has been widely studied by T.G. data in recent years. [1-6] In our previous paper,[7] we have reported the IR of cadmium valerate and caproate. When these soaps are recrystallized in water, the spectra show a peak between 3590 and 3650 cm^{-1} indicating crystallization water, which gets full support from the chemical analysis of samples. In view of the above fact, it was considered of interest to study their thermal stability. Therefore, in the present paper, dehydration and thermal decomposition of these soaps have been studied in order to explore the mechanism of dehydration and decomposition and to evaluate the various kinetic parameters by T.G. data.

EXPERIMENTAL

Materials

The chemicals were purified and the soaps prepared by the method described earlier.[7,8] These sopas were recrystallized from water and then dried in vacuum.

---

* Part II, *Polish Journal of Chemistry*, **55**, 1617 (1981).

** Present address: Department of Chemistry, S.D. College, Muzaffarnagar-251001, India

Apparatus and Procedure

Thermograms were obtained by Derivatograph, MOM Budapest (Hungary), model No. OD-103. The samples were well powdered before the start of each run and heated in air at the heating rate of 10°C min^{-1}.

RESULTS AND DISCUSSION

Dehydration and thermal decomposition of cadmium soaps viz. valerate and caproate have been studied. It is observed from thermograms (Fig. 1). that both these soaps show an appreciable loss (Approx. 7 %) from 80 to 180°C due to crystallization water in these soaps. The presence of crystallization water in soaps has been confirmed by chemical and IR analysis. On further heating these soaps decompose slowly up to 320°C and then rapidly up to 410°C and finally become almost constant at about 520°C. The plots of weight per cent of soap residue vs. temperature (Fig. 1) indicate that these soaps lose the weight in three steps. Thus from the loss in weight in different steps, the dehydration and decomposition of cadmium soaps can be written as follows :

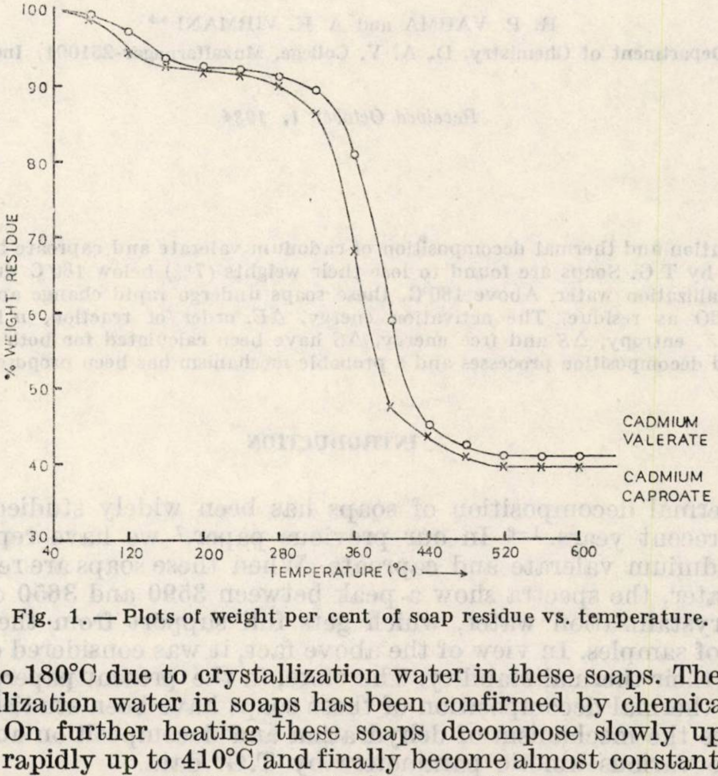

Fig. 1. — Plots of weight per cent of soap residue vs. temperature.

$$(RCOO)_2Cd.H_2O \longrightarrow (RCOO)_2Cd + H_2O$$

(where $R = C_4H_9$ and C_5H_{11})

$$(RCOO)_2Cd \longrightarrow \underset{\text{ketone}}{RCOR} + CdCO_3$$

$$CdCO_3 \longrightarrow CdO + CO_2$$

EXPERIMENTAL PART

The diphenyldithiophosphinic acid was obtained [10] by the reaction of benzene and phosphorus pentasulfide in the presence of anhydrous $AlCl_3$. Nickel(II) diphenyldithiophosphinate was prepared according to the literature.[11]

The amine adducts of $Ni(S_2PPh_2)_2$ were synthesized by mixing the required amounts of the reagents (the amine and nickel(II) diphenyldithiophosphinate) in an appropriate solvent (acetone). Some physical properties and analytical data are shown in Table 1.

Table 1

Physical properties and elemental analysis of the synthesized compounds

Compound	Colour	M.p. (°)	%C found / calcd.	%H found / calcd.	%N found / calcd.
$Ni(S_2PPh_2)_2.EDA$	green	244	49.98 50.59	4.42 4.54	4.38 4.54
$Ni(S_2PPh_2)_2.EDA$	blue	(190—220) 242—244	49.20 49.65	5.22 5.32	8.32 8.27
$Ni(S_2PPh_2)_2.3EDA$	pink	260	50.17 48.87	6.25 5.97	11.52 11.40
$Ni(S_2PPh_2)_2.DMEDA$	green	214	50.17 52.11	5.10 4.97	4.28 4.34
$Ni(S_2PPh_2)_2.2DMEDA$	blue	(200) 212—214	52.37 52.40	5.85 6.00	7.52 7.64
$2Ni(S_2PPh_2)_2.TMEDA$*	brick-red	230	52.35 52.70	3.28 3.41	2.19 2.27

The values in parentheses represent the colour-change temperature from blue to green.
*) Also: Ni found 9.12%, calcd. 9.55%; P found 10.36%, calcd. 10.08%

Infrared sepctra were recorded as KBr pellets in the range 4000—400 cm^{-1} on a UR 10 Carl Zeiss Jena spectrophotometer. Electronic spectra were recorded as MgO pellets using a VSU-2G Carl Zeiss Jena spectrophitometer,

RESULTS AND DISCUSSION

In order to establish the coordination behavior of diphenyldithiophosphinic ligand, IR and electronic spectra of the synthesized compounds were recorded.

The infrared spectra of the dithiophosphinic derivatives exhibit two characteristic bands in the range 680—480 cm^{-1}, due to the stretchings of the PS_2 group. The position of these bands differs with the coordination pattern of the dithio group. In the spectra of iso- and anisobidentate dithio-ligands, the two bands are assigned to $\nu_{sym\ PS_2}$ and $\nu_{antisym\ PS_2}$ while for monodentate PS_2 group they are assigned to ν_{P-S} and $\nu_{P=S}$. It was shown earlier that even if the phosphorus-sulphur stretchings are coupled with the phosphorus-carbon frequencies[12,13] in the same class of compounds, the difference between the two phosphorus-sulphur

Revue Roumaine de Chimie, **31**, *1*, 79—83 (1986)

AMINE ADDUCTS OF NICKEL(II) DIPHENYLDITHIOPHOSPHINATE WITH SUBSTITUTED ETHYLENEDIAMINES

FLORENȚA DOGAR[a], LUMINIȚA SILAGHI-DUMITRESCU[a],
RODICA GRECU[a] and IONEL HAIDUC[b]*
[a]Institute of Chemistry Cluj-Napoca
[b]Babeș-Bolyai University,
R—3400 Cluj-Napoca, Romania

Received March 26, 1985

Adducts of the type $Ni(S_2PPh_2)_2.nL$, where $Ph = C_6H_5$, and $n = 1,2,3$, L = ethylenediamine (EDA); $n = 1,2$, L = N,N′-dimethyl-ethylenediamine (DMEDA) and $n = 1$, L = N,N,N′, N′—tetramethylethylenediamine (TMEDA) were synthesized and investigated by their infrared and electronic spectra. Bidentate diphenyldithiophosphinato groups were found in 1Ni : 1L adducts, monodentate in 1Ni : 2L adducts and ionic in 1Ni : 3L adducts, in accordance with the relative position of phosphorus-sulphur stretchings in the IR spectra and crystal field parameters (10 Dq, B′ and β) in the electronic spectra. A pentacoordinate dimeric structure was proposed for $2Ni(S_2PPh_2)_2$ TMEDA.

INTRODUCTION

The phosphorodithioic anions (dithiophosphates, dithiophosphonates, dithiophosphinates) were found to be very good ligands towards transition and nontransition metals.[1,2]

Particularly, nickel(II) dithioderivatives were intensively investigated due to their adduct forming properties. Nickel(II)-bis(diphenyldithiophosphinate) readily forms adducts with primary and secondary amines.[3,4] There are X-ray diffraction studies on HS_2PPh_2 [5], $Ni(S_2PPh_2)_2$ [6] and the pyridine (Py) adduct [7] $Ni(S_2PPh_2)_2.2Py$.

In this paper we report the synthesis and spectral properties of some amine adducts of $Ni(S_2PPh_2)_2$ with ethylenediamine, N,N′-dimethylethylenediamine and N,N,N′,N′-tetramethylethylenediamine.

These diamines were used as ligands in some nickel(II) dithiophosphate adducts, whose structures were determined by X-ray diffraction and demonstrated the bidentate character of both dithiophosphate and diamine ligands.[8,9]

---

* **Address all correspondence to this author.**

la valeur $D_q = 1{,}219{,}5$ cm^{-1}, on obtient $\beta_{35} = 0{,}62$. Cette dernière valeur signifie que la liaison métal-ligand du complexe Mn(IV).2L présente un caractère covalent assez élevé.

4. CONCLUSIONS

Dans la réaction entre l'ion $[Mn(H_2P_2O_7)_3]^{3-}$ et l'acide 2-aminophénol-4-sulfonique se forme, par suite d'un processus de dismutation du Mn(III), les complexes Mn(IV).L et Mn(IV).2L.

La constante globale de formation est $\beta_2 = 1{,}202.10^4$ l^2.mole^{-2}.

Les paramètres cinétiques de formation du complexe Mn(IV).2L sont : $k = 1{,}805.10^{-1}$ l.mole^{-1} et $E_a = 56{,}062$ kJ/mole.

L'interprétation des spectres champ cristallin du complexe à nombre maximum de coordinance a permis le calcul du paramètre de scission, $D_q = 1219{,}5$ cm^{-1}, et celui néphélauxétique dont la valeur $\beta_{35} = 0{,}63$ indique un caractère covalent assez élevé de la liaison métal-ligand du complexe Mn(IV).2L.

BIBLIOGRAPHIE

[1] T. U. Mikhailova, K. V. Astachov et N. M. Zhirnova, *Zhur. fiz. Khim.*, **45**, 2345 (1971).
[2] N. Calu, A. Popa-Rang et M. Calenciuc, *Rev. Roumaine Chim.*, **19**, 12, 1889 (1974).
[3] P. Job, *Ann. Chim.*, **9**, 10, 113 (1928).
[4] J. Joe et A. Jones, *Ind. Eng. Chem. Analyt. Ed.*, **16**, 11 (1944).
[5] J. Bjerrum, *Kgl. Danske Videnskab. Selskab. mat. phys. medd.*, **21**, 4, 1944); **22**, 18 (1946).
[6] S. Fronaeus, *Acta. Chem. Scand.*, **5**, 139 (1951).
[7] S. Edmonds et N. Birnbaum, *J. Amer. Chem. Soc.*, **63**, 1471 (1941).
[8] A. B. P. Lever, "Inorganic Electronic Spectroscopy", Elsevier Amsterdam, 1968, p. 216, 392.

Tableau 3

Les bandes d'absorption ν_i de type champ cristallin du complexe Mn(IV).2L

ν_i / Caractéristiques spectrales	ν_1	ν_2	ν_3	Bande à transfert de charge
$\lambda_{max.}$ (cm^{-1} ; nm.)	12.195 820	18.181 550	22.624 442	25.316 395
$\varepsilon_{mex.}$ (l·mole^{-1}·cm^{-1})	30	165	220	4290

Tableau 4

Les caractéristiques de la bande ν_1, de type champ cristallin, de l'ion complexe $[Mn(H_2P_2O_7)_3]^{3-}$

ν_1	$\lambda_{max.}$ (cm^{-1} ; nm)	$\varepsilon_{max.}$ l·mole^{-1}·cm^{-1}
	19.380 ; 516	264

Les valeurs un peu plus élevées des coefficients molaires d'absorption des bandes champ cristallin sont dues à l'état élevé d'oxydation du générateur de complexe.

Les bandes champ cristallin des complexes Mn(IV).2L sont interprétées en s'appuyant sur le diagramme à niveaux énergétiques propre au cas $d^3(O_h)$ (fig. 8).

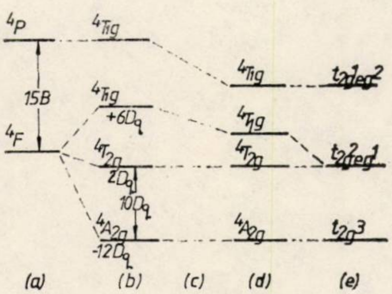

Fig. 8. — Diagramme de corélation pour un ion d^3 ($S = 3/2$; $M_S = 3/2$) dans un champ octaédrique : a. Termes spectroscopiques de l'ion libre, sphérique, perturbé ; b. Termes dans le champ, faible, octaédrique ; c. Configurations électroniques dans le champ octaédrique fort (en negligeant les intéractions électroniques) ; d. Termes dans le champ octaédrique fort, en tenant compte des intéractions électroniques ; e. Zone de champ intermédiare.

Le paramètre néphélauxétique β_{35} pour le complexe Mn(IV).2L a été calculé par une méthode graphique, [8] à la base des représentations :

$$\nu_m/\nu_n = f(D_q/B) \tag{6}$$

$$\nu_3/\nu_n = f(E\nu_3/B) \tag{7}$$

où : $m = 2$ et 3 ; $n = 1$ et 2 ; E_{ν_3} = énergie de la transition qui correspond à la bande avec $\lambda_{max.} = 22.624$ cm^{-1} ; B = paramètre Racah. Avec

Les valeurs ainsi obtenues sont portées dans le tableau 2.

Tableau 2

Données concernant la détermination de la constante de vitesse de la réaction de formation du complexe Mn(IV).2L

No	Température °C	tgα	k (l·mole^{-1}·s^{-1})
1	16	$tg\alpha_1 = 3,57.10^{-4}$	$1,371.10^{-1}$
2	20	$tg\alpha_2 = 4,70.10^{-4}$	$1,805.10^{-1}$
3	26	$tg\alpha_3 = 8.37.10^{-4}$	$3.215.10^{-1}$

L'énergie d'activation correspondante a été déterminée à partir de la pente de la droite obtenue en représentant graphiquement la fonction $\lg k = f(1/T)$ (fig. 7). La valeur obtenue est $E_a = 56,062$ kJ/mole.

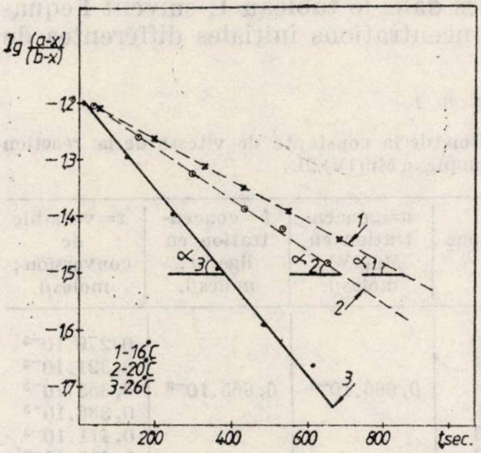

Fig. 6. — Représentation graphique de $\lg(a-x)/(b-x)$ en fonction de temps, dans le cas de la formation du complexe Mn(IV).2L.

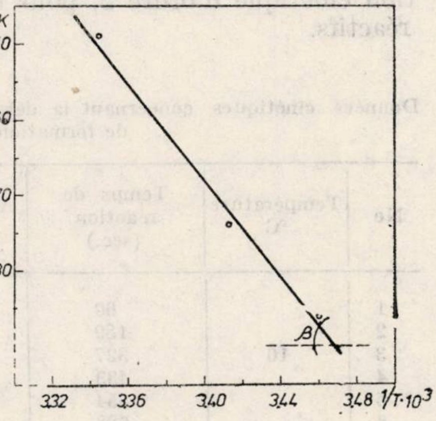

Fig. 7. — Représentation graphique de la fonction $\lg k = f(1/T)$.

3.6. Spectres champ cristallin du complexe Mn(IV). 2L

Bien que la microsymétrie réelle du complexe Mn(IV).2L soit inférieure à celle de type O_h, pratiquement, son spectre champ cristallin peut être interprété sur la base d'un diagramme de termes propres à la symétrie O_h. Ainsi, on admet que dans la symétrie plus basse, la scission des niveaux énergétiques est beaucoup plus faible et, par conséquent, elle n'apparaît plus dans le spectre.

Dans les tableaux 3 et 4 on présente les caractéristiques des bandes d'absorption, de type champ cristallin, du complexe Mn(IV). 2L ainsi que celles de l'ion $[Mn(H_2P_2O_7)_3]^{3-}$, à partir duquel on a préparé le complexe du Mn(IV).

3.5. Cinétique globale de la réaction de formation du complexe Mn(IV). 2L

Les données cinétiques concernant le processus de formation du complexe Mn(IV).2L ont été obtenues par une méthode spectrophotométrique, en se basant sur la bande d'absorption avec $\lambda_{\text{max.}} = 395$ nm (fig. 1).

Ainsi, au cours de la réaction de formation du complexe, on a déterminé la variable de conversion, x, selon les relations :

$$C_i = A_i/\varepsilon.d \quad \text{et} \quad x = C_i/\nu \tag{4}$$

où : $C_i =$ concentration transformée à l'instant «i» de la réaction ;
$A_i =$ absorbance de la prise d'essai, à $\lambda_{\text{max.}} = 395$ nm, à l'instant «i» de la réaction ;
$\varepsilon = 4{,}29.10^{-3}$ l.mole^{-1}, coefficient molaire d'absorption ;
$d = 0{,}5$ cm, épaisseur de la couche absorbante ;
$\nu = 1$, coefficient stoechiométrique du complexe, selon l'équation (1).

Les données obtenues, présentées dans le tableau 1, suivent l'équation cinétique d'ordre 2, pour des concentrations initiales différentes de réactifs.

Tableau 1

Données cinétiques concernant la détermination de la constante de vitesse de la réaction de formation du complexe Mn(IV).2L

No	Température °C	Temps de réaction (sec.)	Absorbance A	a=concentration en Mn(IV) ; moles/l.	b=concentration en ligand ; moles/l.	x=variable de conversion ; moles/l.
1	16	60	0,600	$0{,}666.10^{-3}$	$6{,}665.10^{-3}$	$0{,}279.10^{-3}$
2		189	0,689			$0{,}321.10^{-3}$
3		327	0,759			$0{,}353.10^{-3}$
4		433	0,829			$0{,}386.10^{-3}$
5		554	0,883			$0{,}411.10^{-3}$
6		688	0,942			$0{,}439.10^{-3}$
1	20	39	0,573	$0{,}666.10^{-3}$	$6{,}665.10^{-3}$	$0{,}267.10^{-3}$
2		162	0,697			$0{,}324.10^{-3}$
3		293	0,797			$0{,}371.10^{-3}$
4		420	0,872			$0{,}406.10^{-3}$
5		546	0,933			$0{,}434.10^{-3}$
6		663	1,008			$0{,}469.10^{-3}$
1	26	20	0,580	$0{,}666.10^{-3}$	$6.665.10^{-3}$	$0{,}270.10^{-3}$
2		125	0,740			$0{,}344.10^{-3}$
3		244	0,898			$0{,}418.10^{-3}$
4		359	1,007			$0{,}469.10^{-3}$
5		483	1,092			$0{,}509.10^{-3}$
6		603	1,152			$0{,}537.10^{-3}$

A la représentation graphique de $\lg(a - x)/(b - x)$ en fonction du temps, à des températures différentes, on obtient des droites (fig. 6), dont les pentes (tgα) permettent de calculer la constante de vitesse suivant l'expression :

$$k = \text{tg}\alpha/0{,}434(\text{a}-\text{b}) \tag{5}$$

A partir de la courbe d'étalonnage, on a établi des séries de solutions correspondantes (caractérisées par la même valeur de ε) avec lesquelles on a calculé le nombre moyen de ligands, $\bar{n}$, et la concentration du ligand à l'équilibre, $[L_{\acute{e}q.}]$. A l'aide de ces paramètres, en représentant graphiquement la fonction $\bar{n} = f(pL_{\acute{e}q.})$ (3) on obtient la courbe de formation (fig. 5).

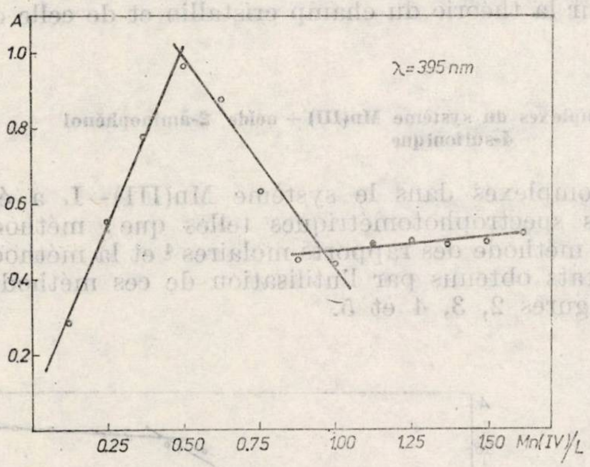

Fig. 4. — Données concernant la composition des complexes du système Mn(III)—L, obtenues par la méthode des rapports molaires (titrage indirect); $A = f[\mathrm{Mn(IV)/L}]$; concentration de L : $2{,}5 \cdot 10^{-3}$ moles/l; cuve : 0,2 cm; temps de réaction : 80′.

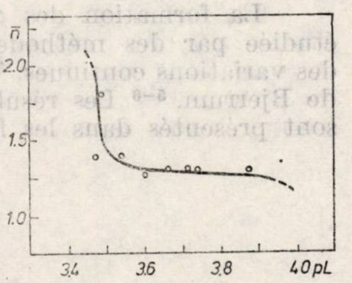

Fig. 5. — Courbe de formation $\bar{n} = f(pL_{\acute{e}q.})$ pour certains complexes du système Mn(IV)—L.

Les résultats obtenus par l'application de la méthode de Bjerrum montre que dans le système Mn(III)—acide 2-aminophénol 4-sulfonique. se forment successivement les complexes : Mn(IV). L et Mn(IV).2L

3.3. Séparation et identification du complexe Mn(IV). 2L par chromatographie sur papier

Les composés, résultés à la suite de la dismutation de Mn(III) de l'ion complexe $[\mathrm{Mn(H_2P_2O_7)_3}]^{3-}$ en présence du ligand L, ont été séparés et identifiés par chromatographie sur papier.

Ainsi, sur le chromatogramme le Mn(IV) apparaît comme une tache jaune-orange avec $R_f = 0{,}53$. Le cation $\mathrm{Mn^{2+}}$, incolore, est mis en évidence par oxydation (avec $\mathrm{H_2O_2}$, en milieu alcalin) à l'état de $\mathrm{MnO_2}$, dont la présence sur le chromatogramme est indiquée par une tache brune de $R_f = 0{,}83$. L'ion complexe $[\mathrm{Mn(H_2P_2O_7)_3}]^{3-}$ apparaît comme une tache rose de $R_f = 0{,}81$.

3.4. Stabilité du complexe Mn(IV). 2L

La constante de formation globale, β_2, du complexe à nombre maximum de coordinance, Mn(IV). 2L, obtenu en grande excès de ligand, a été déterminée par la méthode de Edmonds-Birnbaum.[7] La valeur obtenue est $\beta_2 = 1{,}202.10^4\ \mathrm{l^2.mole^{-2}}$.

La cinétique globale du processus de formation des complexes du Mn(IV) a été établie à partir des données spectrophotométriques.

Les spectres d'absorption électronique de ces complexes ont été interprétés en se basant sur la théorie du champ cristallin et de celle du champ des ligands.

3.2. Composition des complexes du système Mn(III) — acide 2-aminophénol 4-sulfonique

La formation des complexes dans le système Mn(III)—L a été étudiée par des méthodes spectrophotométriques telles que : méthode des variations continues, [3] méthode des rapports molaires [4] et la méthode de Bjerrum. [5-6] Les résultats obtenus par l'utilisation de ces méthodes sont présentés dans les figures 2, 3, 4 et 5.

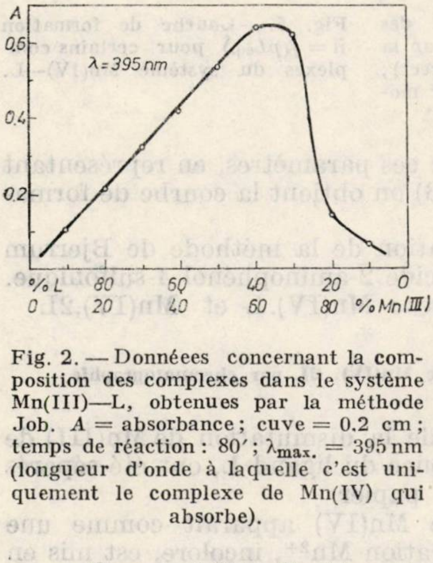

Fig. 2. — Donnéees concernant la composition des complexes dans le système Mn(III)—L, obtenues par la méthode Job. A = absorbance ; cuve = 0.2 cm ; temps de réaction : 80′ ; $\lambda_{\text{max.}} = 395$ nm (longueur d'onde à laquelle c'est uniquement le complexe de Mn(IV) qui absorbe).

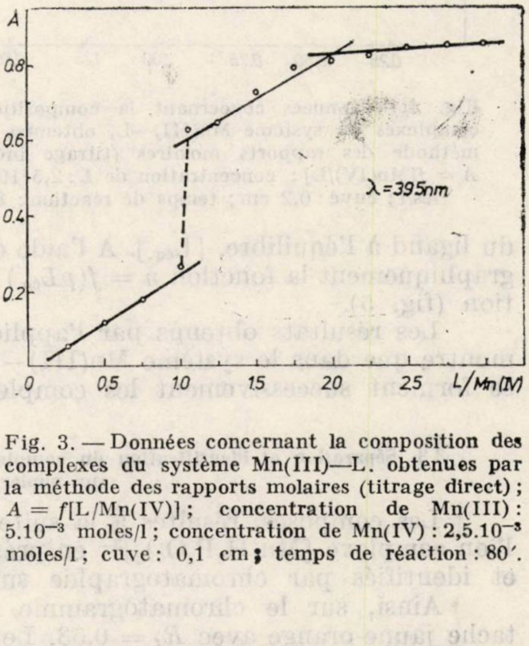

Fig. 3. — Données concernant la composition des complexes du système Mn(III)—L. obtenues par la méthode des rapports molaires (titrage direct) ; $A = f[\mathrm{L}/\mathrm{Mn(IV)}]$; concentration de Mn(III) : 5.10^{-3} moles/l ; concentration de Mn(IV) : $2{,}5.10^{-3}$ moles/l ; cuve : 0,1 cm ; temps de réaction : 80′.

Quant à l'application de la méthode de Bjerrum, on a utilisé la variante dite « de la courbe d'étalonnage ». Cette variante repose sur la représentation graphique de la fonction :

$$\varepsilon = f(C_{\mathrm{L}}) \tag{2}$$

où : ε = coefficient molaire d'absorption pour $\lambda_{\text{max.}} = 395$ nm ;
C_{L} = concentration du ligand.

Pour deux séries de solutions, les concentrations du métal ont été : $C'_{\mathrm{M}} = 1{,}666.10^{-3}$moles/l et $C''_{\mathrm{M}} = 2{,}5.10^{-3}$ moles/l.

2. PARTIE EXPÉRIMENTALE

Le Mn(III) a été utilisé sous forme d'ion complexe $[Mn(H_2P_2O_7)_3]^{3-}$, stable en solution aqueuse, préparé en chauffant le mélange Mn_2O_3—$K_2H_2P_2O_7$—H_2SO_4 en solution aqueuse, à pH = 2,5. [2]

La concentration initiale du complexe formé a été d'environ 2.10^{-2} moles/l, à partir de laquelle on a préparé, par dilution, des solutions étendues de concentrations comprises entre 1.10^{-3} moles/l et 5.10^{-3}moles/l.

L'acide 2-aminophénol-4-sulfonique (L) a été utilisé sous forme de solution aqueuse, de concentration variable : $2{,}5 \cdot 10^{-3}$— $6{,}66 \cdot 10^{-4}$ moles/l.

Les déterminations spectrophotométriques ont été effectuées à l'aide d'un spectrophotomètre de type Spekord —V-VIS, Carl Zeiss, Jena.

Les séparations chromatographiques ont été faites par la variante ascendante, en utilisant du papier Whatman-1.

3. RÉSULTATS ET DISCUSSIONS

3.1. Réaction de l'ion complexe $[Mn(H_2P_2O_7)_3]^{3-}$ avec l'acide 2-aminophénol-4-sulfonique

En solution aqueuse, à des pH allant de 2 à 4, l'ion complexe $[Mn(H_2P_2O_7)_3]^{3-}$ réagit avec l'acide 2-aminophénol 4-sulfonique, en donnant, finalement, par dismutation, le complexe du Mn(IV) selon le processus :

$$2\,Mn(III) + 2\,L \rightleftharpoons Mn(IV).2L + Mn^{2+}. \tag{1}$$

Les essais de laboratoire montrent que l'ion Mn^{2+} ne forme pas des complexes avec le ligand L.

L'évolution, dans le temps, du système Mn(III) – L a été suivie au moyen de ses spectres d'absorption, dans le domaine visible, présentés dans la figure 1.

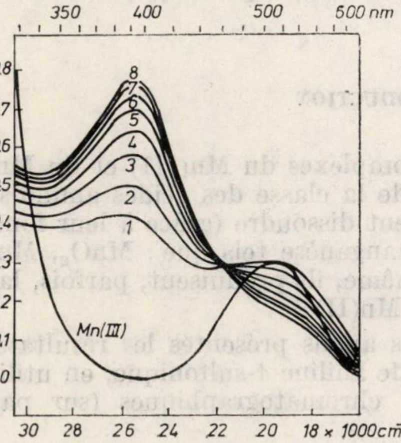

Fig. 1. — Spectres d'absorption, enregistrés dans le temps sur le système 1 Mn(III) : 1 L ; concentration de Mn(III) : $2{,}5 \cdot 10^{-3}$ moles/l ; concentration de Mn(IV) (après la dismutation) : $1{,}25 \cdot 10^{-3}$ moles/l ; cuve : 0,5 cm ; $t_1 = 1'30''$; $t_2 = 3'5''$; $t_3 = 5'2''$; $t_4 = 7'5''$; $t_5 = 9'39''$; $t_6 = 12'33''$; $t_7 = 15'59''$; $t_8 = 22'5''$.

Le point isobestique obtenu sur le graphe de la figure 1 signifie le processus décrit par l'équation (1).

Les complexes du Mn(IV) ont été séparés et identifiés par chromatographie sur papier.

Revue Roumaine de Chimie, 31, *1*, 71—78 (1986)

COMBINAISONS COMPLEXES DU Mn(III) ET DU Mn(IV). II*

LE SYSTÈME Mn(III, IV)—ACIDE 2-AMINOPHÉNOL-4-SULFONIQUE

N. CALU, ELENA BĂLĂNESCU, I. BERDAN et I. SANDU
Institut Polytechnique « Gh. Asachi », Iaşi
71, Splai Bahlui, Roumanie

Reçu le 22 juin 1983

The paper reports on the spectrophotometric and chromatographic study of the Mn(III, IV) — 2-aminophenol-4-sulfonic acid(L) system. The interaction between Mn(IV) ions and ligand (L) gives two complex compounds namely Mn(IV).L and Mn(IV).2L. The crystal-field spectra of the Mn(IV).2L is characterized by splitting parameter $D_q = 1219.5$ cm^{-1} and nephelauxetic parameter $\beta_{35} = 0.63$.

On a étudié, par spectrophotométrie et chromatographie sur papier, les complexes formés en solution aqueuse, de types : Mn(IV). L et Mn(IV). 2L, où L est l'acide 2-aminophénol 4-sulfonique. Les complexes ont été obtenus par la dismutation du Mn(III) de l'ion $[Mn(H_2P_2O_7)_3]^{3-}$, en présence du ligand L. Le complexe Mn(IV).2L se forme selon une réaction du second ordre, avec la constante de vitesse $k = 1,806 \cdot 10^{-1}$ l.mol.$^{-1}$ (à 20°C) et l'énergie d'activation $E_a = 56,062$ kJ/mole. La constante globale de formation du complexe est $\beta_2 = 1,202.10^4 1^2$. mole^{-2} et son spectre champ cristallin este caractérisé par le paramètre de scission $D_q = 1219,5$ cm^{-1} et le paramètre néphélauxétique $\beta_{35} = 0.63$.

1. INTRODUCTION

Nos recherches concernent les complexes du Mn(III) et du Mn(IV) avec les ligands, à fonctions mixtes, de la classe des acides amino-sulfoniques aromatiques. Ces ligands peuvent dissoudre (grâce à leur fonction acide, $-SO_3H$) certains oxydes du manganèse tels que : MnO_2, Mn_2O_3 ; avec la formation de complexes. De même, ils produisent, parfois, la dismutation du Mn(III) en Mn(IV) et Mn(II).[1]

Dans un travail antérieur [2] nous avons présentés les résultats obtenus sur le système Mn(III, IV)—acide aniline-4-sulfonique, en utilisant des méthodes spectrophotométriques, chromatographiques (sur papier) et polarographiques.

Dans cette Note on présente les données obtenues sur le système Mn(III, IV) — acide 2-aminophénol-4-sulfonique.

---

* Part I. Rev. Roum. Chim., *19*, 1889 (1974)

It is noted that entropy change ΔS is negative, so the values of free energy obtained are positive.

According to the mechanistic treatment, the mode of decomposition of cadmium soaps follows the Mampel[15] equation i.e. $-\ln(1-\alpha)$ for $g(\alpha)$. This shows that decomposition occurs by a random nucleation process.

ACKNOWLEDGEMENT. The authors thank Prof. K. N. Mehrotra for his valuable criticism and to the College authorities for providing laboratory facilities. Financial assistance to one of the authors (A.K.V.) from U.G.C., New Delhi is gratefully acknowledged.

REFERENCES

[1] K. N. Mehrotra and R. Kachhwaha, *Bull. Inst. Politeh Iasi*, Sect. 2, **24** 45 (1978) (Eng.).
[2] R. P. Varma and S. Shukla, *Tenside Detergents*, **20**, 192 (1983).
[3] R. P. Varma and I. Singh, *Transition Met. Chem.*, **5**, 39 (1980).
[4] A. Rasheed and R. A. Bhobe, *J. Indian Chem. Soc.*, **LIII**, 442 (1976).
[5] R. P. Varma and H. K. Bhargava, *Revue Roumaine de Chimie.*, **24,** 537 (1979).
[6] K. N. Mehrotra, V. P. Mehta and T. N. Nagar, *J. Naturforsch. Teit. D.*, **28**, 254 (1973).
[7] R. P. Varma and A. K. Virmani, *Revue Roumaine de Chimie*, **27**, 1109 (1982).
[8] R. P. Varma and A. K. Virmani, *Polish Journal of Chemistry*, **55**, 1617 (1981).
[9] R. P. Varma and P. K. Jain, *Transition Met. Chem.*, **7**, 129 (1982).
[10] V. Satava and J. Sestak, *Anal. Chem.*, **54**, 154 (1973).
[11] J. R. MacCallum and J. Tanner, *Eur. Polym. J.*, **6**, 1033 (1970).
[12] A. W. Coats and J. P. Redfern, *Nature*, **201**, 68 (1964).
[13] H. H. Horowitz and G. Metzger, *Anal. Chem.*, **35**, 1464 (1963).
[14] S. Glasstone, K. J. Laidler and H. Eyring, "The Theory of Rate Process". McGraw Hill Book Co. p. 184 (1941).
[15] K. L. Mampel, *Z. Phys. Chem.*, **A. 187,** 235 (1940).

The overall order of reaction is determined by Horowitz-Metzger equation[13] :

$$\ln \ln(1 - \alpha)^{-1} = \frac{E}{RTs^2} \cdot \Phi \qquad \text{(v)}$$

where Ts is the temperature at the point of inflexion in T.G. curve and Φ is equal to $(T - Ts)$. The plots of $\ln \ln(1 - \alpha)^{-1}$ vs. Φ give an intersection of two straight lines for decomposition of cadmium soaps and a straight line for dehydration of these soaps, as observed earlier.

The activation energies, E, for loss of water of crystallization (Table 1) and for the decomposition of cadmium soaps (Table 2) obtained by Horowitz-Metzger equation are comparable with previous equations.

The values of E for the loss of crystallization water of cadmium valerate are slightly higher than cadmium caproate. When the values of E of decomposition of soaps are compared, it is found that the values of valerate are higher than caproate in the first step, but these are almost constant in the second step.

The kinetic parameters i.e. freyuency factor, Z, entropy of activation, ΔS and free energy, ΔG for dehydration and decomposition of cadmium soaps have been calculated from Mac-Galum Tanner, Eyring[14] and Gibbs equation (Tables 3, 4). The values of frequency factor, Z, for cadmium caproate are higher than valerate in the first step of decomposition. For loss of crystallization water at 393K and decomposition of soaps in the second step, these values for valerate are higher than caproate.

Table 3

Values of frequency factor, $Z(\mathrm{S}^{-1})$, entropies ΔS $(\mathrm{JK}^{-1}\ \mathrm{mol}^{-1})$ and free energies, ΔG $(\mathrm{kJ\ mol}^{-1})$ for crystallization water of cadmium soaps (at temperature 393 K)

Parameter	Valerate	Caproate
$Z(\mathrm{S}^{-1})$	2.232×10^6	2.142×10^2
$-\Delta S(\mathrm{JK}^{-1}\ \mathrm{mol}^{-1})$	0.1256	0.1451
$\Delta G(\mathrm{kJ\ mol}^{-1})$	114.003	110.094

Table 4

Values of frequency factor, $Z(S^{-1})$, entropies, $\Delta S(\mathrm{JK}^{-1}\ \mathrm{mol}^{-1})$ and free energies, ΔG $(\mathrm{kJ\ mol}^{-1})$ for cadmium soaps

Parameter	Valerate		Caproate	
	Step I 653 K	Step II 733 K	Step I 653 K	Step II 733 K
$Z(S^{-1})$	6.992×10^6	2.865	8.321×10^6	1.046
$\Delta S(\mathrm{JK}^{-1}\mathrm{mol}^{-1})$	0.1204	0.2436	0.1189	0.2520
ΔG $(\mathrm{kJ\ mol}^{-1})$	195.291	214.826	191.033	214.620

Table 2

Activation energies, E (kJ mol^{-1}) obtained from different equations for cadmium soaps.

Equation	Valerate		Caproate	
	Step I	Step II	Step I	Step II
Mechanistic				
$-\ln(1-\alpha)$	124.45	44.61	121.19	38.29
$[-\ln(1-\alpha)]^{1/2}$	63.75	19.14	60.61	19.14
$[-\ln(1-\alpha)]^{1/3}$	44.61	12.77	38.29	12.77
Mac-Callum Tanner				
$-\ln(1-\alpha)$	116.67	36.26	113.39	29.90
$[-\ln(1-\alpha)]^{1/2}$	55.54	10.62	52.38	10.62
$[-\ln(1-\alpha)]^{1/3}$	36.26	4.20	29.90	4.20
Coats and Redfern				
$n = 1$	114.87	35.09	113.28	28.71
Horowitz and Meztger	124.13	34.48	117.82	29 45

where Φ is the heating rate. The slopes of the plots of log $g(\alpha)$ vs. $1/T$ are equated to $(0.449 + 0.217\ E) \times 10^3$ to yield the value of E. These values for loss of crystallization water and for decomposition of soaps are tabulated in Tables 1 and 2, respectively. It is found that energy of activation, E, for loss of water of crystallization and for decomposition of soaps is lower than the values obtained from mechanistic models.

The activation energy has also been determined by Coats-Redfern equation [12] :

$$\log\left[\frac{1-(1-\alpha)^{1-n}}{(1-n)\ T^2}\right] = \log\frac{ZR}{\Phi E}\left[1-\frac{2RT}{E}\right] - \frac{E}{2.303\ RT} \qquad \text{(iii)}$$

where n is the order of reaction. This equation may be derived for $n = 1$ in the following form :

$$\log\left[\frac{-\ln(1-\alpha)}{T^2}\right] = \log\frac{ZR}{\Phi E}\left[1-\frac{2RT}{E}\right] - \frac{E}{2.303RT} \qquad \text{(iv)}$$

This equation has been applied by simple graphical technique. Since there is a theoretical justification for $n = 0, \frac{1}{2}, \frac{2}{3}$ and 1 in solid state kinetics, it is possible to substitute $0, \frac{1}{2}, \frac{2}{3}$ and 1 values in equation (iii) to obtain the plots. The plots of different orders represent an intersection of two straight lines for decomposition of cadmium soaps, whereas it is almost linear for loss of crystallization water. However, the plots for $n = 0$ are non-linear.

It is observed that the values of activation energy for $n = 1$ (Tables 1 and 2) correspond with the values obtained for the model : $-\ln(1-\alpha)$ from Mac-Callum Tanner equation for both the decomposition steps and for crystallization water.

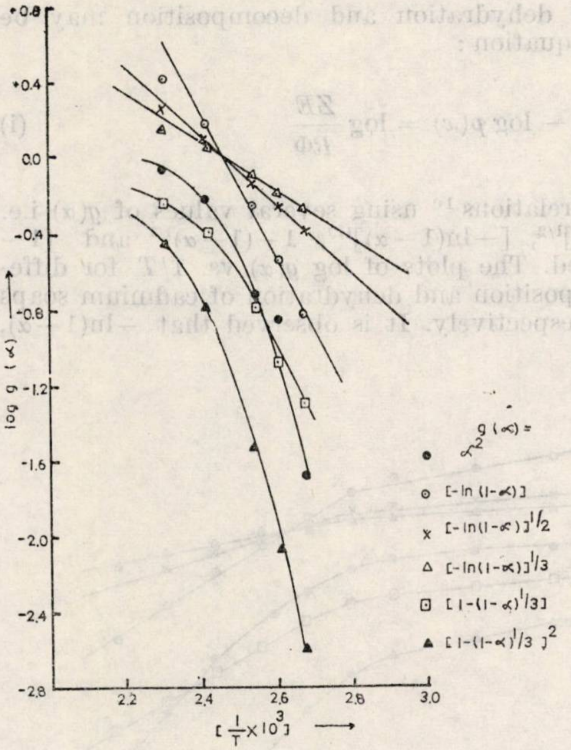

Fig. 3. — Plots of log $g(\alpha)$ vs. $1/T$ for dehydration of cadmium valerate.

Table 1

Activation energies, E (kJ mol^{-1}) obtained from different equations for crystallization water of cadmium soaps

Equation	Valerate	Caproate
Mechanistic		
$-\ln(1-\alpha)$	72.75	61.26
$[-\ln(1-\alpha)]^{1/2}$	34.46	42.12
$[-\ln(1-\alpha)]^{1/3}$	22.97	19.14
Mac-Callum Tanner		
$-\ln(1-\alpha)$	64.61	53.04
$[-\ln(1-\alpha)]^{1/2}$	26.04	33.76
$[-\ln(1-\alpha)]^{1/3}$	14.48	10.62
Coats and Redfern		
$n = 1$	64.13	53.60
Horowitz and Metzger	64.82	53.04

Max-Callum Tanner[11] equation was used to calculate the value of activation of energy E as :

$$\log g(\alpha) = \log \frac{ZE}{\Phi R} - 0.48E^{0.44} - \left(\frac{0.449 + 0.217E}{T}\right) \times 10^3 \qquad \text{(ii)}$$

The kinetic process of dehydration and decomposition may be described by the following[9] equation :

$$\log g(\alpha) - \log p(x) = \log \frac{ZE}{R\Phi} \tag{i}$$

Different mechanistic model relations[10] using several values of $g(\alpha)$ i.e. α^2, $-\ln(1-\alpha)$, $[-\ln(1-\alpha)]^{1/2}$, $[-\ln(1-\alpha)]^{1/3}$, $1-(1-\alpha)^{1/3}$ and $[1-(1-\alpha)^{1/3}]^2$ have been plotted. The plots of $\log g(\alpha)$ vs. $1/T$ for different possible modes of decomposition and dehydration of cadmium soaps are shown in Figs. 2 and 3, respectively. It is observed that $-\ln(1-\alpha)$, $[-\ln(1-\alpha)]^{1/2}$ and $[-\ln(1-\alpha)]^{1/3}$ models show an intersection of two straight lines for these cadmium soaps at a point and almost straight lines for loss of crystallization water for cadmium valerate and caproate. The activation energies for dehydration (Table 1) and decomposition (Table 2) of cadmium soaps have been calculated. Since more than one linear plot are obtained for different values of $g(\alpha)$, the probable operating mechanism has been proposed by comparing the value of E (Table 1, 2) for such plots with those obtainable from other equations.

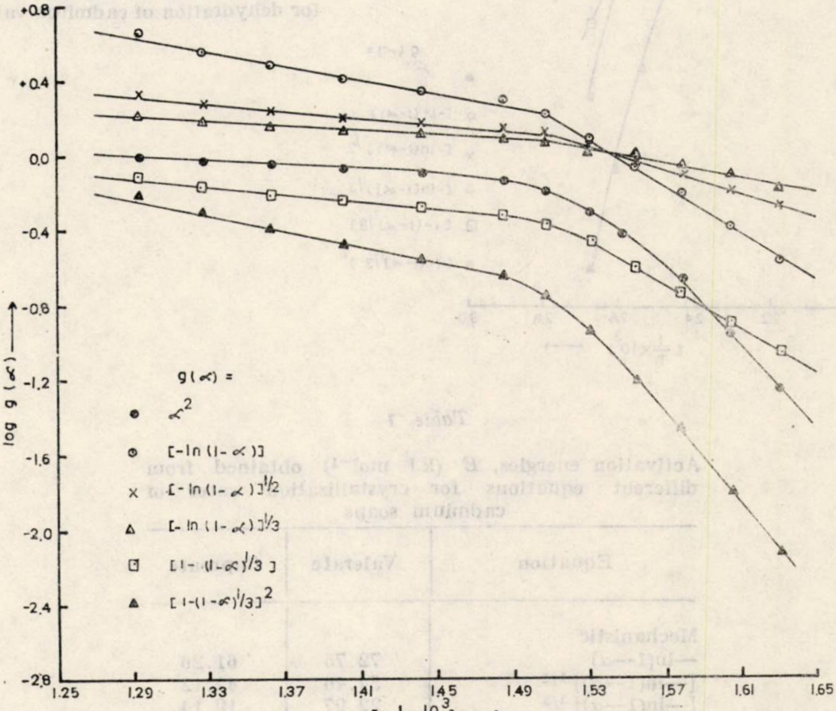

Fig. 2. — Plots of $\log g(\alpha)$ vs. $1/T$ for thermal decomposition of cadmium caproate.

bands can be correlated with the coordination mode of the ligands. So, $\Delta\nu_{PS} = \nu_{\text{antisym PS}} - \nu_{\text{sym PS}}$ (or $\Delta\nu_{PS} = \nu_{PS} - \nu_{PS}$) differences of $45-75$ cm^{-1}, $80-90$ cm^{-1} and larger than 95 cm^{-1} are found in the infrared spectra of the compounds containing isobidentate, anisobidentate and monodentate dithiophosphinic ligands, respectively.[14]

Table 2

Infrared bands assigned to stretching vibrations of PS_2 and NH_2 groups (cm^{-1})

Compound	ν_1^*	ν_2^*	$\Delta\nu_{PS}$	ν_{sNH_2}	ν_{asNH_2}	Ref.
HS_2PPh_2	530s	650vs	120	—	—	15
$Na^+(S_2PPh_2)^-$	565s	648s	83	—	—	15
$Ni(S_2PPh_2)_2$	574s	622s	48	—	—	16
$Ni(S_2PPh_2)_2$.EDA	573vs	645s	72	3230m	3295ms	
$Ni(S_2PPh_2)_2$.2EDA	560vs	643s	90	3113m	3253ms	
$Ni(S_2PPh_2)_2$.3EDA	572vs	743vs	71	3139m 3118m 3210m	3290ms 3260s 3270s	
$Ni(S_2PPh_2)_2$. DMEDA	572s	645vs	73	3148m		
$Ni(S_2PPh_2)_2$.2DMEDA	557vs	643vs	96	3178m 3208m		
$2Ni(S_2PPh_2)_2$.TMEDA	572vs	650vs	78	—	—	

*) ν_1, $\nu_2 = \nu_{P-S}$ and $\nu_{P=S}$ for monodentate, respectively ν_{symPS_2} and $\nu_{\text{antisymPS}_2}$ for bidentate coordination of diphenyldithiophosphinic group.

m = medium, s = strong, vs = very strong, ms = medium-strong

Taking into account the above considerations, as well as the comparison between the infrared spectra of the amine adducts, diphenyldithiophosphinic acid[15] its sodium salt[15] and nickel(II) bis(diphenyldithiophosphniate)[16] (see Table 2), we can assume an isobidentate coordination of the dithiophosphinic ligand in the compounds $Ni(S_2PPh_2)_2$. EDA, $Ni(S_2PPh_2)_2$.DMEDA, $2Ni(S_2PPh_2)$. TMEDA and monodentate in the compounds $Ni(S_2PPh_2)_2$.2EDA and $Ni(S_2PPh_2)_2$.2DMEDA. Although the $\Delta\nu_{PS}$ is 71 cm^{-1} in the spectrum of $Ni(S_2PPh_2)_2$.3EDA, the presence of ionic rather than bidentate diphenyldithiophosphinic groups is supported by the electronic spectra (see below).

The N—H stretching frequencies ($3300-3100$ cm^{-1}) are shifted towards lower values compared with the free (uncoordinated) amines spectra (Table 2) in accordance with the coordination of all nitrogen atoms to the metal.

The electronic spectra of amine adducts are significantly different from that of nickel(II) diphenyldithiophosphinate. The last one exhibits a typical D_{4h} square planar electronic spectrum,[17] while the spectra of the adducts can be correlated with an octahderal environment of the nickel.

The colour of the synthesized compounds is that usual for sixcoordinate Ni(II) derivatives, depending on the chromophore: green — NiS_4N_2, blue — NiS_2N_4, pink — NiN_6.[3,4,18,19] The same chromophores were found in our compounds. It is worth noticing that the compounds with two molecules of amine, blue coloured, are changing their colour to green when heated. The changing of the colour can be due to the formation of two different compounds :

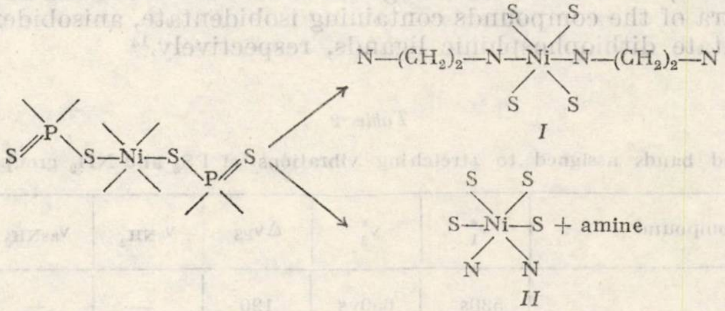

The melting point of the green product being the same with that of the directly synthesized green compound, we can assume that the structure II is the right one.

The assignment of the transition bands is presented in Table 3, together with the crystal field parameters calculated by a graphic method.[18] The values are close to those reported for other amine adducts of nickel(II) diphenyldithiophosphinate.[3,4,19] The value of the 10 Dq increases as follows :

$$NiS_4N_2 < NiS_2N_4 < NiN_6$$

in accordance with the values of the nephelauxetic parameter.

The electronic spectrum of the $Ni(S_2PPh_2)_2.3EDA$ is quite similar to the spectra of the compounds containing the $[Ni(EDA)_3]^{2+}$ cation [20]; hence anionic dithiophosphinate groups are supposed to be present.

Table 3

Eletcronic spectra and crystal field parameters

Compound	ν_1 (cm^{-1})	ν_2 (cm^{-1})	ν_3 (cm^{-1})	10 Dq (cm^{-1})	B'	β
$Ni(S_2PPh_2)_2.EDA$	—	14450	22400	9470	557	0.52
$Ni(S_2PPh_2)_2.2EDA$	10400	16100	25900	10360	740	0.70
$Ni(S_2PPh_2)_2.3EDA$	11800	17400	—	11660	865	0.82
$Ni(S_2PPh_2)_2.DMEDA$	—	15000	24800	9240	660	0.62
$Ni(S_2PPh_2)_2.2DMEDA$	10300	15700	24500	10780	770	0.72

$\nu_1 : {}^3T_{2g}(F) \leftarrow {}^3A_{2g}(F)$; $\nu_2 : {}^3T_{1g}(F) \leftarrow {}^3A_{2g}(F)$; $\nu_3 : {}^3T_{1g}(P) \leftarrow {}^3A_{2g}(F)$

The value of Racah paarmeter B : 1060 cm^{-1}

For $[Ni(EDA)_3]^{2+}$: 10 Dq = 11500, $B' = 855$ and $\beta = 0.81$ (ref. 20).

The bands for square planar (D_{4h}) $Ni(S_2PPh_2)_2$ (assigned according to ref. 21) are[17] :

ν_1 : 13900 ; $({}^1A_{2g} \rightarrow {}^1A_{1g})$

ν_2 : 18300 ; $({}^1B_{1g} \rightarrow {}^1A_{1g})$

The values of the electronic transitions in the spectrum of $2Ni(S_2PPh_2)_2.TMEDA$ (14800 and 23800 cm^{-1}) support a pentacoordinate environment around the nickel atom,[4] possibly in a dimeric structure (due to the steric hinderance). The proposed structure for this compound is :

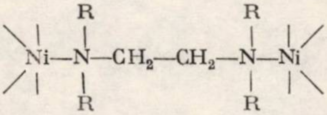

It should be noticed that the colour of $2Ni(S_2PPh_2)_2$.TMEDA is brick-red (as with other five coordinate Ni(II) dithio-complexes [22]) while the other dithiophosphinato complexes reported in this work are green or blue, typical of six-coordinate Ni(II) dithiophosphate adducts.[3,4,8,9]

REFERENCES

[1] I. Haiduc, *Revs. Inorg. Chem.*, **3**, 353 (1982).
[2] R. Wasson, G. W. Woltermann and H. J. Stoklosa, *Fortschr. Chem. Forsch.*, **35**, 65 (1973).
[3] A. Sgamellotti, C. Furlani and F. Magrini, *J. Inorg. Nucl. Chem.*, **30**, 2655 (1968).
[4] J. R. Angus, G. M. Woltermann and J. R. Wasson, *J. Inorg. Nucl. Chem.*, **33**, 3967 (1971)
[5] B. Krebs and G. Henkel, *Z. anorg. Chem.*, **475**, 143 (1981).
[6] P. Porta, A. Sgamellotti and N. Vinciguerra, *Inorg. Chem.*, **7**, 2625 (1968).
[7] P. Porta, A. Sgamellotti and N. Vinciguerra, *Inorg. Chem.*, **10**, 545 (1971).
[8] D. B. Sowerby and I. Haiduc, *Inorg. Chim. Acta*, **17**, L15 (1976).
[9] D. B. Sowerby and I. Haiduc, *Inorg. Nucl. Chem. Letters*, **12**, 791 (1976).
[10] W. A. Higgins, P. W. Vogel and W. G. Craig, *J. Am. Chem. Soc.*, **77**, 1864 (1955).
[11] W. Kuchen, J. Metten and A. Judat, *Chem. Ber.*, **97**, 2306 (1964).
[12] I. Silaghi-Dumitrescu and I. Haiduc, *Rev. Roumaine Chim.*, **25**, 815 (1980).
[13] I. Silaghi-Dumitrescu and I. Haiduc, *Rev. Roumaine Chim.*, **25**, 823 (1980).
[14] I. Haiduc, I. Silaghi-Dumitrescu, R. Grecu, R. Constantinescu and L. Silaghi-Dumitrescu, *J. Mol. Structure*, **114**, 467 (1984).
[15] A. Müller, V. Krishna Rao and G. Klinksiek, *Chem. Ber.*, **104**, 1982 (1971).
[16] R. N. Mukherjee, V. V. Krishna Rao and J. Gupta, *Indian J. Chem.*, **4**, 209 (1966).
[17] A. G. Tomlison and C. Furlani, *Inorg. Chim. Acta*, **3**, 487 (1969).
[18] A.B.P. Lever, *J. Chem. Educ.*, **45**, 711 (1968).
[19] R. N. Mukherjee, M. S. Venkateshan and M. D. Zingde, *J. Inorg. Nucl. Chem.*, **36**, 1043 (1974).
[20] A. B. P. Lever, "Inorganic Electronic Spectra" Elsevier Publ. Comp., Amsterdam, New-York, 1968.
[21] G. Maki, *J. Chem. Phys.*, **28**, 651 (1958).
[22] P. S. Shetty, R. E. Ballard and Q. Fernando, *Chem. Commun.*, **1969**, 717.

Revue Roumaine de Chimie, 31, *1*, 85—92 (1986)

SPECTROPHOTOMETRIC DETERMINATION OF CADMIUM AND LEAD AFTER ADSORPTION OF THEIR n-BUTYLXANTHATES ONTO MICROCRYSTALLINE NAPHTHALENE AND REPLACEMENT BY COPPER

B. K. PURI, ATUL KUMAR and M. SATAKE*
Department of Chemistry, Indian Institute of Technology, Hauz Khas,
New Delhi—110016
*** Faculty of Engineering, Fukui University, Fukui 910, Japan**

Received March 13, 1984

Cadmium and lead form water insolubile complexes with potassium n-butylxanthate which are quantitatively adsorbed onto microcrystalline naphthalene in the pH ranges Cd : 2.6—9.7 and Pb : 4.8—10.4 respectively. The solid naphthalene containing the colourless metal complex is dissolved in chloroform and then replaced by copper to develop a yellow colour in the chloroform layer. The absorbance in each case is measured at 423 nm against the reagent blank. Beer's law is obeyed over the concentration ranges Cd : 2.0—115.0 μg and Pb : 3.0—200.0 μg per 10 mL of the final chloroform solution. The molar absorptivities and sensitivities in terms of Sandell's, definition are calculated to be Cd : 8.206×10^3 l mol^{-1} cm^{-1}, 0.013 μg/cm^2 and Pb : 8.170×10^3 l mol^{-1} cm^{-1}, 0.025μg/cm^2. Aliquots containing 40 μg of cadmium and 52 μg of lead give mean absorbance of 0.292 and 0.205 with standard deviations 0.0028 and 0.0018 and relative standard deviations 0.95% and 0.87% respectively. The interference of various ions have been studied and the conditions are being developed for the determination of these metals in various synthetic mixtures and also in certain reference materials.

Xanthates have been widely used as reagents in the extraction of a number of metal ions.[1-3] We have already developed a new method of extraction, i.e. "Solid-liquid separation after liquid-metal ions".[4-6] Although there are many advantages of this method over the usual liquid-liquid extraction [7] but it cannot be applied for the extraction of thermally unstable complex e.g. xanthates in the present case. Recently, we found that most of the metal chelates in aqueous solution can be easily adsorbed onto microcrystalline naphthalene.[8-9] This method is more convenient (since it is carried out at room temperature) more rapid (no need of heating naphthalene), economical (only 0.4 g of naphthalene is required) more sensitive and can be applied to many types of the complexes. So far, this technique has been applied only to those metal ions which form coloured complexes but no attempt has been made in the absorption of colourless metal complexes. Therefore, in the present communication conditions have been developed for the adsorption of cadmium and lead n-butyl xanthates onto microcrystalline naphthalene and subsequently determined spectrophotometrically after dissolution of the solid naphthalene containing the metal complex in chloroform and replacing by copper to develop a yellow colour. The interference of various ions has been studied and the method has been applied to the determination of these metals in certain standard reference materials.

EXPERIMENTAL

Reagents and Chemicals : Solutions of cadmium nitrate, lead nitrate and copper nitrate were prepared in double distilled water from their analytical grade samples and standardized by known methods.[10] Potassium n-butylxanthate (PBX) was prepared and purified according to the method given in the literature[11] and its 0.2% solution was prepared in distilled water. Naphthalene, chloroform and acetone were of analytical grade sample and tested spectrophotometrically before use. Solutions of alkali metal salts (1%) and various metal salts (0.1%) were used to study the interference of anions and cations respectively. Ammonium acetate/acetic acid buffer (0.2 M) and dilute solutions of perchloric acid and ammonia were used for pH adjustment.

Equipment : An Elico pH meter, SP-500/700 Spectrophotometers and a Pye Unicam Atomic Absorption Spectrophotometer (A.A.S.) were used.

General Procedure. To aliquots of the metal ion solutions taken in stoppered Erlenmeyer flask separately were added 2.0 mL of PBX to each and adjusted the pH (Fig. 1) by adding 2.0 ml of the acetate buffer in case of cadmium and perchloric acid-ammonia for lead. These solutions were shaken thoroughly and allowed to stand for 5—10 min. Then to each 2.0 mL of a 20% solution of naphthalene in acetone was added in a fast stream and the solutions were shaken vigorously for 1—2 min. The solid mass formed was filtered off on a Whatman No. 1042 filter paper, washed 2—3 times with distilled water, drained dry, dissolved in chloroform and made up to the volume in a 10 mL standard flask. This 10 mL solution was transfered to a separatory funnel and 10 mL of 10^{-3}M copper nitrate solution was added to it in order to develop a yellow colour in chloroform layer. These solutions were shaken vigorously for about 5 min and then the chloroform layer was poured onto anhydrous sodium sulphate (2 g) taken in a beaker in order to remove the last traces of water. A portion of this solution was taken in a 1-cm cell and the absorbance was measured at 423 nm against the reagent blank.

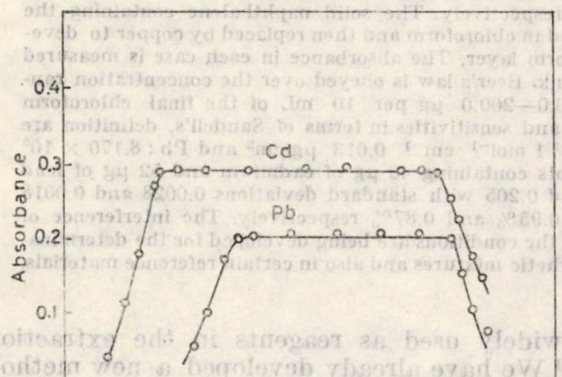

Fig. 1. — Effect of pH : Cd = = 40.0 μg, Pb = 52.0 μg, Reagent = = 2.0 mL (0.2%), digestion time = = 10 min, naphthalene = 2.0 mL (20%), Copper nitrate used for replacement = 10 mL of 10^{-3}M, wavelength = 423 nm and reference = reagent blank.

RESULTS AND DISCUSSION

Preliminary observations have revealed neither the reagent nor the metal ion is adsorbed onto naphthalene when taken individually. It has already been reported that copper is quantitatively extracted into molten naphthalene or adsorbed onto microcrystalline in the pH range of 1.5—5.5, $\varepsilon = 8.260 \times 10^3 \, \mathrm{l \, mol^{-1} \, cm^{-1}}$ and has an absorption maximum of 420—425 nm.[12] The stability constant of copper n-butylxanthate is much higher than these n-butyl xanthates,[13-14] naturally these metals will be quantitatively replaced by copper from the chloroform into aqueous phase according to the equation :

$$MR_{2(or)} + Cu^{2+}_{(aq)} \rightleftharpoons CuR_{2(or)} + M^{2+}_{(aq)}$$

where M is Cd or Pb. Preliminary observations have revealed, though stoechiometric amount of copper can be used for the quantitative replacement of these metals but for safe side 10 mL of 10^{-3}M copper nitrate has been added in each case.

REACTION CONDITIONS

Cadmium and lead complexes are quantitatively formed in the pH ranges of 2.6—9.7 and 4.8—10.4 respectively (Fig. 1). The spectra measured for reaction at various pH values show that only one type of complex is formed.

It was found that for 40 μg of cadmium and 52 μg of lead a minimum of 0.7 mL of reagent was necessary for complete reaction. A minimum standing time of 5 min for digestion of the complex is recommended. The adsorption is very rapid, being practically complete in less than 10 sec, and a standing time of 1—2 min gives an ample safety margin. A minimum of 0.7 mL of 20 % naphthalene solution in acetone is required for complete adsorption. Therefore, 2.0 ml is recommended in all cases.

Since only a small amount of the organic phase (0.4 g) is required, the volume of the aqueous phase is important. The absorbance is maximum and constant if the aqueous phase volume is less than 75 mL for cadmium and 50 mL for lead and is best kept to 30—35 mL.

Under these conditions, 0.5—5.0 mL of the acetate buffer has no effect in case of cadmium while the pH was only adjusted with perchloric acid and ammonia solution in case of lead.

The absorbance of the copper n-butyl xanthate complex(after replacement of Cd or Pb) in naphthalene chloroform was constant for more than 20 h.

Under the optimum conditions described above calibration curves were constructed at 423 nm in each case. Beer's law holds in the concentration ranges Cd : 2.0—115.0 μg and Pb : 3.0—200.0 μg per 10 ml of the final chloroform solutions. The molar absorptivities in terms of Sandell's definition are calculated to be Cd : $8.206 \times 10^3 \mathrm{L \, mol^{-1} \, cm^{-1}}$, 0.013 μg/cm² and Pb : $8.170 \times 10^4 \, \mathrm{l \, mol^{-1} \, cm^{-1}}$, 0.025 μg/cm². Aliquots containing 40 μg of cadmium and 52 μg of lead gave mean absorbances 0.292 and 0.205 with standard deviations 0.0028 and 0.0018 and relative standard deviations 0.95 % and 0.87 respectively. The percentage of absorption was established in each case by back extracting the metal from chloroform layer before replacing by copper with 20 ml of 2 M HNO_3

Table 1

Effect of diverse anions on the determination of cadmium and lead.
Cadmium : 40.0 μg, Lead : 52.0 μg, Reagent : 2.0 mL of 0.2% solution in each case,
λ max : 423 nm

Alkali salt added	Anion added (mg)	Absorbance 423 nm		Remarks
		Cadmium	Lead	
	—	0.292	0.205	—
Sodium fluoride	100	0.290	0.205	
	75	0.292	0.205	—
Sodium chloride	100	0.293	0.195	Interfered only in case of lead
	25	0.291	0.202	Relatively low amount could be tolerated
Potasium bromide	100	0.292	0.190	,,
	20	0.293	0.202	
Potasium iodide	100	0.292	0.188	,,
	15	0.293	0.201	
Sodium acetate	100	0.292	0.196	,,
	25	0.292	0.203	
Sodium oxalate	100	0.280	0.195	Interfered in both cases
	20	0.290	0.201	Relatively low amount could be tolerated
Sodium citrate	100	0.285	0.196	,,
	20	0.291	0.203	
Potassium sodium tartrate	100	0.286	0.195	,,
	25	0.291	0.201	,,
Sodium ortho-phosphate	100	0.288	0.197	,,
	20	0.291	0.203	
Sodium thiosulphate	100	0.292	0.200	—
	50	0.292	0.205	
Sodium carbonate	100	0.243	0.204	—
	75	0.292	0.204	
Sodium azide	100	0.290	0.203	—
	50	0.292	0.205	
Potassium thio-cyanate	100	0.291	0.203	—
	75	0.293	0.205	
Potassium nitrate	100	0.292	0.205	—
	75	0.292	0.206	
Sodium sulfate	100	0.293	0.178	Interfered only in case of lead
	10	0.293	0.202	Relatively low amount could be tolerated
Disodium EDTA	100	0.024	0.020	Interfered in both cases
	5	0.065	0.075	,,

Table 2

Effect of diverse cations on the determination of cadmium and lead

Metal salt	Metal ion added (μg)	Absorbance at 423 nm		Remarks
		Cadmium	Lead	
	—	0.292	0.205	—
Ammonium meta-vandate	500	0.294	0.203	—
	250	0.294	0.204	
Chromium(III) nitrate	500	0.293	0.204	—
	200	0.293	0.205	
Manganese(III) acetate	500	0.293	0.203	—
	250	0.293	0.203	
Iron(III) chloride	500	0.320 0.295*	0.240 0.208*	Interfered in both. *After masking with 5 ml of 5% hydroxylaminehydrochloride solution
	100	0.298 0.292*	0.210 0.206	
Cobalt(II) nitrate	500	0.360	0.245 0.210*	Interfered in both. Relatively low amount could be tolerated, Can be masked in case of lead with 5 ml of 5% sodium cyanide solution
	100	0.298	0.210 0.204*	
Nickel(II) nitrate	500	0.310	0.210	Interfered in case of cadmium
	250	0.296	0.206	Relatively low amount could be tolerated
Mercury(II) chloride	500	0.288	0.200	—
	250	0.291	0.202	
Copper(II) nitrate	500	0.300	0.210	—
	250	0.294	0.207	
Zinc nitrate	500	0.300	0.208	
	250	0.293	0.206	
Cadmium nitrate	500	—	0.280 0.207*	Interfered. *After masking with 5 ml of NaCN solution
	250		0.235 0.205*	
Lead(II) nitrate	500	0.300	—	
	250	0.295	—	
Aluminium nitrate	500	0.294	0.206	—
	200	0.293	0.204	
Bismuth nitrate	500	0.300	0.210	—
	250	0.295	0.206	
Ammonium molybdate	500	0.290	0.202	—
	200	0.292	0.204	
Platinum(IV) chloride	500	0.292	0.200	—
	250	0.292	0.204	
Sodium tungstate	500	0.290	0.202	—
	250	0.291	0.204	
Thorium(IV) nitrate	500	0.292	0.203	—
	250	0.292	0.205	
Beryllium(II) nitrate	500	0.294	0.205	
	250	0.293	0.205	
Uranyl acetate	500	0.292	0.205	
	250	0.292	0.204	

Table 3

Determination of cadmium and lead in standard reference materials

Metal to be determined	Name of the sample	Certified (%) Composition	Metal taken (μg)	Metal found by AAS(μg)	Metal found by present method (μg)	Average (μg)	Error (%)
Cadmium	N.B.S., SRM 94C Zn-alloy	Cd : 0.003, Pb : 0.006 Sn : 0.006, Ni : 0.006 Mn : 0.14, Fe* : 0.018 Mg : 0.042, Cu : 0.01 Al : 0.407	21.0	21.15	21.30 21.15 21.25 21.10 21.20	21.2	0.95
Cadmium	,,	,,	63.0	63.4	63.65 63.70 63.90 63.70 63.60	63.7	1.1
Lead	,,	,,	30.0	30.20	30.20 30.30 30.20 30.40 30.10	30.26	0.86
Lead			45.6	45.40	45.40 45.70 45.50 45.30 45.40	45.46	1.02
Cadmium	N.B.S., SRM 629 Zn-base die-casting alloy E	Cd : 0.0155 Pb : 0.0155 Cu : 1.50, Al : 5.15 Mg : 0.094, Fe : 0.017* Sn : 0.012, Cr : 0.0008 Mn : 0.0017, Ni : 0.0075 Si : 0.078	31.0	31.15	31.40 31.00 31.20 31.40 31.60	31.32	1.03
Cadmium	,,	,,	46.50	46.95	46.70 47.00 47.40 47.20 46.70	47.00	1.07
Lead	,,	,,	37.2	37.45	37.60 37.50 37.80 37.40 37.60	57.58	1.01
Lead	,,	,,	62.0	62.6	62.45 62.80 62.60 62.70 62.50	62.61	0.98

* Fe(III) was masked with 5 ml of 5% hydroxylamine hydrochloride solution.

and determining the metal by atomic absorption spectrophotometry. It was found to be Cd : 99.2 % and Pb : 98.70 % respectively.

Effect of diverse ions : Effect of diverse anions in the determination of these metals has been studied by preparing synthetic solutions containing 40 μg of cadmium or 52 μg of lead taken individually and varying amount of anions. The tolerance limit for the anions is given in (Table 1). Only EDTA interfered seriously probably due to the larger stability constants of these metal EDTA complexes than their xanthates.[15] Among the cations studied (Table 2) Fe(III) and Co(II) interfered in both the cases. Although a relatively low amount of these ions could be tolerated in both cases but Fe(III) was masked by reducing Fe(III) to Fe(II) with 5 ml of 5 % hydroxylamine solution.[15] Co(II) was also masked in case of lead with the addition of 5 ml of 5 % sodium cyanide solution. Ni(II) only interfered in case of cadmium but its relatively low amounts could be tolerated. In case of lead only Cd(II) interfered but it was safely masked with 5 mL of 5 % sodium cyanide solution. Thus the methods are fairly selective and were applied to the determination of these metals in standard reference materials.

Determination of cadmium and lead in some standard reference materials : The proposed method is tested in the determination of these metals in standardised reference materials (Table 3). The analytical procedures are as follow : 1–2 g sample of the alloy was taken in a 250 ml beaker and added to it 50–60 mL of HCl (1+1) and 5–10 mL of concentrated HNO_3. This was heated on a hot plate for about 30 min, the mixture dissolved completely. After cooling, the volume of the sample was made 100 mL exact in a standard flask. An aliquot of this sample solution was taken and analysed according to the general procedure. The results are given in Table 3.

CONCLUSION

This study revealed that these metal complexes are easily adsorbed onto microcrystalline naphthalene and can be successfully applied in analytical determination. The sensitivity can be further increased by separating the metal from a larger volume of the aqueous phase (50–70 mL) by adsorption over 0.4 g of naphthalene. This small amount of naphthalene containing the metal complex can be dissolved in 1–2 mL of the organic phase and whole of it can be taken for the analysis.

The method will be especially useful for those metal complexes which have low solubility in the organic solvents.

REFERENCES

[1] E. M. Donaldson, *Talanta*, **23**, 417 (1976).

[2] E. M. Donaldson and E. Mark, *Talanta*, **29**, 663 (1982).

[3] A. L. J. Rao and S. Singh, *J. Indian Chem. Soc.*, **51**, 503, (1974).

[4] M. Gautam, R. K. Bansal and B. K. Puri, *Bull. Chem. Soc. Japan*, **54**, 3178 (1981).

[5] M. Gautam and B. K. Puri, *Mikrochim. Acta (Wein)* **1**, 515 (1979).

[6] A. Kumar, C. L. Sethi, M. Satake and B. K. Puri, *Japan Analyst*, **32**, E 67(1983).

[7] B. K. Puri and M. Gautam, *Talanta*, **25**, 484 (1978).

[8] B. K. Puri, C. L. Sethi and A. Kumar, *Mikrochim. Acta, (Wein)* **2**, 361 (1983).

[9] M. Satake, B. K. Puri, J. C. Yuh and L. F. Chang, *Mem. Fac. Engg. Fukui Univ*, **30**, 69 (1982).

[10] Vogel A. I., "A Text book of Quantitative Inorganic Analysis" 3rd Ed., Longmans London, 1966.

[11] S. R. Rao "Xanthates and Related Compounds", Marcel Dekker Inc., New York, 1971.

[12] B. K. Puri, A. Kumar, A. L. J. Rao and M. Satake, *Croatica. Chem. Acta* (In press).

[13] Z. A. Shaka and E. E. Kriss, *Roboty Khim. Rastvorov. Kompleks, Soedinenii*, Ákad-Nauk. Ukr. SSR, **135** (1959), *Chem. Abstr.*, **54**, 16249h (1960).

[14] R. J. Magee, *Rev. Anal. Chem.*, **1**, 335 (1978).

[15] D. D. Perrin, "Masking and Demasking of Chemical Reaction", Willey-Interscience, New York, 1970.

Revue Roumaine de Chimie, **31**, *1*, 93—98 1986)

EXTRACTION SPECTROPHOTOMETRIC DETERMINATION OF NICKEL AND PALLADIUM USING CYCLOHEXYLTHIOGLYCOLATE (CyHTG) AS A REAGENT

A.L.J. RAO and USHA GUPTA
Department of Chemistry, Punjabi University,
Patiala—147002, India

Received October 1, 1984

Conditions have been developed for the spectrophotometric determination of nickel and palladium after extraction of their cyclohexylthioglycolate (CyHTG) complexes with chloroform. Nickel and palladium reacts with CyHTG to form coloured water insoluble complexes which are quantitatively extracted into chloroform in pH ranges of Ni : 7.5—9.0 and Pd : 4.0—9.0. The complexes were extracted into chloroform and trace amounts of these metals are determined spectrophotometrically by measuring the absorbances : Ni at 410 nm and Pd at 385 nm respectively. Beer's law holds in the concentration ranges of 5.9—70.8 μg for nickel and 2.12—37.1 μg for palladium in 10 mL of the final solution. The molar absorptivities and Sandell's sensitivities were calculated to be 4.44×10^3 L mol^{-1} cm^{-1} and 0.013 μg/cm^2 (410 nm) for nickel and 1.67×10^4 L. mol^{-1} cm^{-1} and 0.0064 μg/cm^2 (385 nm) for palladium respectively. Aliquots containing 47.2 μg of nickel and 31.8 μg of palladium gave mean absorbances of 0.355 and 0.500 with standard deviations of 0.0066 and 0.008 and relative standard deviations 1.86% and 1.6% respectively. Interferences of various ions were studied.

Nickel and palladium react with a large number of organic reagents. For example, nickel form complexes with acetothioacetanilide,[1] 2-nitroso-1-naphathol-4-sulphonic acid,[2] dimethylglyoxime,[3] 1-phenyl-3-thiobenzoylthiocarbamide,[4] ethylthioxanthate,[5] chlorethylthioglycolate.[6] Palladium is complexed with 2-mercaptobenzothiazole.[7] 2,3-quinoxaline-d-dithiol,[8] bismuthol,[7] mercaptoacetoacetanilide,[9] ethyltrithicarbonate,[10] and dibenzylidene-thiocarbohydrazide.[11] In the present communicat-ion a simple, rapid and more sensitive spectrophotometric method has been developed for the determination of nickel and palladium using CyHTG as the complexing agent.

EXPERIMENTAL

Apparatus. All absorbance measurements were made with SP-20 spectronic spectrophotometer. The measurements of pH were carried out with a digital pH meter.

Reagents. Standard solutions of nickel chloride and palladium chloride were prepared in distilled water and standardized.[12] Cyclohexylthioglycolate was synthesized by the method given by Gambarov for the preparation of esters of thioglycolic acid.[13] CyHTG has a density of 0.9448 and refractive index ($n=1.4825$) at room temperature. Results of elemental analysis were in good agreement with the theoretical ones.

A 0.1% solution of CyHTG was made in distilled alcohol.

0.2 M ammonium acetate — 0.2 M ammonia solutions were made for pH 8 — 11 and 0.2M ammonium acetate + 0.2 M acetic acid solutions were used for pH 3—6.

Alkali salts and metal salt solutions were prepared to study interferences.

General procedure

An aliquot of metal ions containing 5.9—70.8 µg Ni. 2.12—37.1 µg Pd was taken in a beaker individually. 1 mL of CyHTG (0.1%) solution was added and pH was adjusted (8.0 for Ni and 4.0 for Pd). 2 mL of corresponding buffer solution was added. Then appropriate amount of molar potassium nitrate was added to these solutions to give 0.1 M concentration of the electrolyte in 10 mL of the final solution. The solution was transferred into separatory funnel and 10 mL of chloroform was added. The solution was shaken vigorously for 2 minutes and allowed to stand for 5 min, then the chloroform layer poured over anhydrous sodium sulphate (2g) in order to remove the last traces of water. The absorbance was measured at 410 nm (for Ni) and 385 nm (for Pd).

RESULTS AND DISCUSSION

Absorption spectra

The spectra of cyclohexylthioglycolate, nickel and palladiumhexylthioglycolates were recorded against ethanolic alcohol and the reagent blank respectively (Fig. 1). It was found that complexes of nickel and palladium absorbed at 410 nm and 385 nm respectively. The reagent absorbed negligibly in this wavelength region.

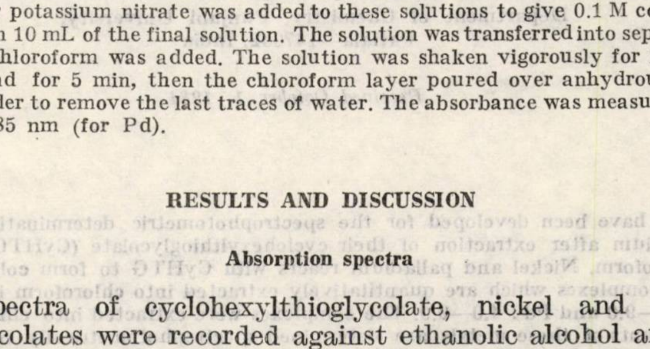

Fig. 1. — Absorption spectra of reagent (CyHTG) against ethanolic alcohol, and cyclohexyltbioglycolates of nickel and palladium in chloroform solution againts reagent blank: Ni: 47.2 µg; Pd: 31.8 µg; CyHTG (0.1%): 1.0 mL; pH Ni: 8.0; Pd: 4.0; Potassium nitrate: 0.1M

Effect of pH

The effect of pH on the absorbance of these metal complexes was studied over a wide range of pH (Fig. 2). The nature of the spectral curves remained the same in all the cases (for both metals) indicating the formation of one complex under these conditions. Optimum pH range for Ni is (7.5—9.0) and for Pd it 4.0—9.0 respectively.

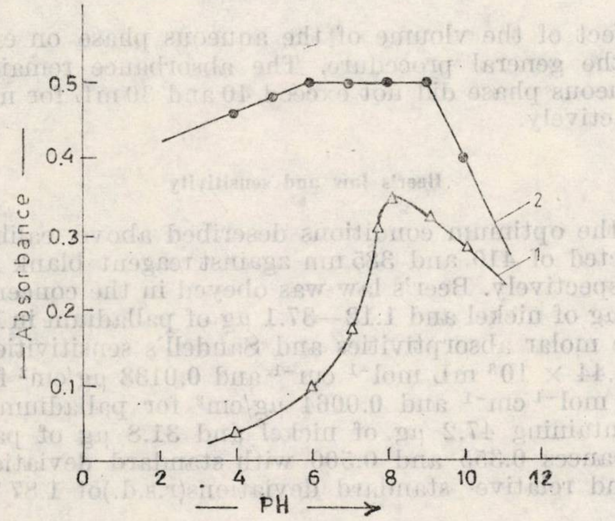

Fig. 2. — Effect of pH on absorbance: Ni : 47.2 μg; Pd : 31.8 μg; CyHTG (0.1 %) : 1.0 mL ; (1) Ni; (2) Pd.

Effect of reagent concentration

Keeping other conditions constant extractions were carried out by varying the reagent concentration (0.1 % CyHTG). It was found that absorbance was constant for 0.6—2.0 mL of reagent for nickel and 0.4—1.6 mL of reagent for palladium. In all the experiments, 1 mL of 0.1 % CyHTG was used.

Effect of shaking time

The effect of shaking time on extraction of these complexes was studied by applying the general procedure. The absorbance remained constant for shaking from 1—10 min. in both cases. Hence 2 min. of shaking time was chosen for further work.

Effect of electrolytes

The effect of various electrolytes such as sodium acetate, sodium chloride and potassium nitrate (0.01—1.0 M) was studied on the extraction of the complexes. It was found that the absorbance was almost constant when the strength of the electrolyte was in the range of 0.05—0.4 M indicating the salting out effect. Extraction was incomplete below and above this range of the electrolyte. So in all the cases the overall concentration of the electrolyte (KNO_3) was kept at 0.1M.

Effect of volume of aqueous phase

The effect of the vloume of the aqueous phase on extraction was studied by the general procedure. The absorbance remained constant when the aqueous phase did not exceed 40 and 30 mL for nickel and palladium respectively.

Beer's law and sensitivity

Under the optimum conditions described above, calibration curves were constructed of 410 and 385 nm against reagent blank for nickel and palladium respectively. Beer's law was obeyed in the concentration range of 5.9—70.8 μg of nickel and 1.12—37.1 μg of palladium in 10 mL of final solution. The molar absorptivities and Sandell's sensitivities were calculated to be 4.44×10^3 mL mol^{-1} cm^{-1} and 0.0133 μg/cm^2 for nickel and 1.67×10^4 l mol^{-1} cm^{-1} and 0.0064 μg/cm^2 for palladium respectively. Solutions containing 47.2 μg of nickel and 31.8 μg of palladium gave mean absorbances 0.355 and 0.500 with standard deviations of 0.0066 and 0.008 and relative standard deviations(r.s.d.)of 1.87 % and 1.6 % respectively.

Composition of the complex

The composition of nickel and palladium-cyclohexylthioglycolates was established by the Job's method of continuous variation and by the Mole Ratio method. A sharp peak at 0.33 mole fraction in Job's curve and a break at 1 : 2 metal ligand ratio in the plot confirmed the formation of $M(CyHTG)_2$ complex (both in case of nickel and palladium).

Effect of diverse ions

The effect of various salts on the extraction of these metals was studied. The following species gave no interference with the determination even at 50 mg amount level; potassium bromide, potassium iodide, sodium acetate, potassium chloride, sodium phosphate, sodium citrate, and sodium oxalate for nickel, and lower amounts (25 mg) of these anions for palladium. EDTA interfered in case of nickel whereas its lower amount (0.2——0.5 mg) was tolerable in case of palladium. But thiosulfate (500 μg) interfered in case of palladium, but was tolerable (50 mg) in case of nickel. Among the cations examined Co(II), Fe(II) and Pd(II) interfered in the determination of Ni(II). Interference due to Fe(II) was eliminated with the addition of 2 mL of 5 % NaF. Interference due to palladium was removed by pre-extraction of pH 4.0, but Co(II) interfered seriously in the determination of Ni. In the case of palladium, interference due to Fe was eliminated as above. Co(II) and Ni(II) were extractable at higher pH and thus did not interfere.

Determination of nickel and palladium in some alloys

The alloy sample (0.1 g) was taken in a beaker to which were added 15–20 mL of concentrated hydrochloric acid along with a few mL of concentrated nitric acid. It was heated on a hot plate till the mixture dissolved completely and the solution was reduced to about 5 mL. This solution was cooled, 15 mL of hydrochloric acid being added to it. This solution was diluted with distilled water, filtered and the final volume was made 500 mL exact in a standard flask. An aliquot cotaining appropriate amount of nickel was taken and followed the general procedure. The results of this determination are given in Table 1.

Table 1
Determination of nickel and palladium in some alloys

Metal to be determiied	Name of the alloy	Certified % composition	Amount of metal taken (μg)	Amount of metal found (μg)	Average (μg)	% Error
Ni	Monel-400	Ni : 63.0, C : 0.15 S : 0.0023, Mn : 0.01 Si : 0.50, Fe : 2.5 Cu : 31.0	63.0	62.50 63.50 63.50 63.00 64.00	63.30	0.48
Ni	Palau	Ni : 60.0, Pt : 20.0 V : 9.5, Pd : 10.5	54.0	54.50 54.50 55.00 54.00 54.50	54.50	0.93
Pd	Palau	,,	9.45	9.0 9.45 10.0 9.80 9.65	9.58	1.38

Simultaneous determination of nickel and palladium

An aliquot containing 54.0 μg of nickel and 9.45 μg of palladium was taken in a beaker. 1 mL of (0.1 %) CyHTG solution was added and pH was adjusted to 4.0 and then 2.0 mL of buffer solution (0.2 M ammonium acetate + 0.2 M acetic acid) was added. To it 1 mL of M KNO_3 was added. Total aqueous volume was made to 10 mL. The yellow complex of palladium was extracted with 10 ml of chloroform after shaking for 2 min. and allowing to stand for 5 min. The absorbance was measured at 385 nm and referred to the calibration curve constructed under similar conditions. Now, 5 ml of the aqueous phase were taken to which 1 mL of CyHTG (0.1 %) was added and pH adjusted to 8.0 with 2.0 mL of buffer. The total volume was made to 10 mL and the nickel complex was extracted with chloroform. The absorbance was measured at 410 nm and referred to the calibration curve prepared under similar conditions. Thus nickel and palladium were determined in the presence of each other.

Sincere thanks of the authors are due to CSIR for the award of SRF to one of us (UG). The help of Prof. N. K. Ralhan during the synthesis of the reagent is also acknowledged.

REFERENCES

[1] K. D. Dutta and J. Das, *J. Ind. Chem. Soc.*, **52**, 1026 (1975).

[2] S. Motomizh and K. Toei, *Anal. Chem. Acta.*, **97**, 335 (1978).

[3] F. D. Snell and C. T. Snell, "Colorimetric methods of analysis", D. van Nostrand, London, Vol. II (1949).

[4] S.Q.R. Ilyas and A. P. Joshi, *J. Ind. Chim. Soc.*, **58**, 360 (1981).

[5] P. K. Paria, S. Dutta and S. K. Majumdar, *J. Ind. Chem. Soc.*, **56**, 314 (1979).

[6] D. G. Gambarov, A. M. Ayubova and S. R. Azimova, *Azerb. Khim. Zh.*, **2**, 122 (1981).

[7] S. I. Ginzburg; N. A. Ezerskaya, I. V. Prokofeva, N. V. Fedorenko, V. I.Shlenskaya and N. K. Belskii, "The Analytical Chemistry of Platinum Metals", ed. by P. Schelnitz, Willey, New York (1975).

[8] H. S. Gowda and B. Keshawan, *J. Ind. Chem. Soc.*, **53**, 688 (1976).

[9] K. D. Arabinda and Jyotirmov Das. *Ind. J. Chem.*, **22**, 93 (1983).

[10] A. L. J. Rao and Chander Shekhar, *Ind. J. Chem.*, **16**, 463, (1978).

[11] J. Pramanik and H. R. Das. *J. Ind. Chem. Soc.*, **59**, 397 (1982).

[12] A. I. Vogel, ,,A. Textbook of Quantitative Inorganic Analysis".

[13] D. G. Gambarov, K. Z. Guseinov, and R. Fatizade. *Organic Reagentry Anal. Khim.* (Tezisy. Dokl. Vses. Konf. 4th) 1976, **1**, 111. (*C.A.* **87**, 193132x)

Revue Roumaine de Chimie, **31**, *1*, 99–104 (1986)

STRUCTURE AND PROPERTIES OF THE ZnO.nFe$_2$O$_3$ CATALYSTS SYSTEM IN THE OXYDEHYDROGENATION REACTION (I)

I. V. NICOLESCU*, RODICA MĂNĂILĂ**, M. A. CHAAR* and G. FILOTI**
* Polytechnical Institute, Dept. of Chemical Technology, Bucharest
** Institute of Physics and Technology of Materials, Bucharest, Romania

Received August 27, 1984

The crystalline structure and magnetic interactions in the ZnO.nFe$_2$O$_3$ system were investigated by X-ray diffraction and Mossbauer spectrometry. The stoichiometry of the ferritic phase as well as the Fe valence are reported for the fresh, reduced and tested states of the catalysts used in the *n*-butene oxydehydrogenation to butadiene.

1. INTRODUCTION

The search for new ferritic catalysts, with a high efficiency in the butene oxydehydrogenation to butadiene processes, has led to complex oxidic systems.

This type of catalysts usually show several crystalline phases in their fresh (oxidized) state. In the investigated ZnO.nFe$_2$O$_3$ system ($1 \leqslant n \leqslant 7$), the atomic ratio Fe/Zn is mostly greater than 2 (Fe excess over the ferrite stoichiometry). As a consequence, the spinelic Zn ferrite phase is accompanied by an amount of free $\alpha - Fe_2O_3$, with the equilibrium rhombohedral structure.

This system was chosen in view of its good catalytic properties in the above-mentioned reaction and taking also into account the possibility of obtaining ferritic lattices with a high concentration of structural defects.

The samples were submitted to a complex structural investigation by X-ray diffraction and Mossbauer spectrometry.

2. RESULTS AND DISCUSSION

2.1. Fresh (oxidized) samples

The samples comprised two crystalline phases: ZnFe$_2$O$_4$ and free $\alpha - Fe_2O_3$.

2.1.1. *X-ray diffraction results.* Fig. 1 displays the variation with *n* of the amounts of ZnFe$_2$O$_4$ and free $\alpha - Fe_2O_3$, as represented by the integrated intensities I_Z (diffraction line (220) of $ZnFe_2O_4$) and I_α (line (104) of $\alpha-Fe_2O_3$). For $n = 1$ (no Fe excess), a small amount of non-reacted $\alpha-Fe_2O_3$ is noticeable, as well as occasional traces of ZnO. This shows that the synthesis of $ZnFe_2O_4$ at 900 °C proceeds rather slowly.

---

* Present address: Faculty of Chemical and Petroleum Engineering, Al-Baath University, Homs, Syria.

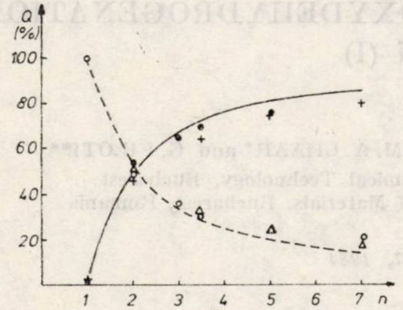

Fig. 1. — Fraction Q of the total Fe amount in α—Fe_2O_3 (● : M, + : XRD(I_α)) and in $ZnFe_2O_4$ (○ : M, Δ : XRD(I_Z)) *vs.* compositional parameter n. M : Mössbauer spectrometry, XRD : X-ray diffraction. —, ... : data calculated from the composition. The XRD data were calibrated to the M values at $n = 7$ (I_α) and $n = 1$ (I_Z).

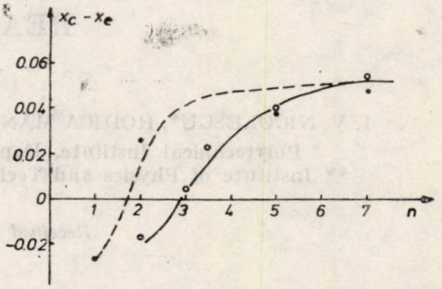

Fig. 2. — Excess Fe_2O_3 in the $ZnFe_2O_4$ lattice (molar concentration), ● : XRD, ○ : M.

The XRD data are in general agreement with the Mossbauer-derived concentrations of the phases, both showing a deficit of $\alpha-Fe_2O_3$ for $n > 3$. This fact suggests the presence of a Fe excess in the ferrite lattice.

The integrated intensities ratio I_α/I_Z (which is also free of absorption corrections) gives further information about the stoichiometry of the ferrite phase:

$$\frac{I}{I_Z} = 1.955 \frac{A_\alpha x_e}{A_Z(1 - x_e)} \tag{1}$$

Here A are the molar weights of the two phases, x_e is the molar free $\alpha-Fe_2O_3$ concentration and 1.955 is the intensity ratio I_α/I_Z in the case of equal weight concentrations.[1] The difference between the x_e value inferred from eq. 1 and $x_c = (n - 1)/n$, evaluated from the global composition, is shown on Fig. 2 and in table 1.

It must be stressed that for n close to 1 (stoichiometric ferrite with $x_c = 0$), the non-reacted amount of $\alpha - Fe_2O_3$ gives rise to the negative $(x_c—x_e)$ values. For $n>2$, fig. 2 indicates the presence of less free $\alpha - Fe_2O_3$ in comparison with the calculated value, *i.e.* of a Fe excess in the $ZnFe_2O_4$ lattice, which increases with n. This is to be understood as a Fe_2O_3 dissolution in the spinelic lattice, which must give rise to cation vacancies, by a charge compensation effect. For the Fe-rich compositions ($n > 5$), the non-stoichiometry levels off.

The phase diagram of the $ZnO—Fe_3O_4—Fe_2O_3$ system [2] supports our explanation by suggesting a narrow zone of spinelic solid solution on the axis $ZnFe_2O_4—Fe_2O_3$. The present results establish the outer limit of this zone at a molar Fe_2O_3 excess of about 5 %, which corresponds to the composition $0.45ZnO.0.55Fe_2O_3$. All the compositions with $n > 2—3$

Table 1

Lattice constants of the cubic spinelic phases (experimental a(Å) and calculated a_c(Å) for a solid solution), haematite excess in Zn ferrite (molar fractions), average crystallite dimension D(Å) of the spinelic phases.

n	Lattice constant a(Å)			a_c(Å)	$\varepsilon < x_c - x_e$	D(Å)
	Oxidized	Reduced	Tested			
1	$8.445 \pm 1 \cdot 10^{-3}$	8.446	8.443	8.446	$-0.025 \pm 5 \cdot 10^{-3}$	210
2	8.447	8.446[1]	8.410	8.427	0.026	200
3	8.446		8.396	8.419		230
3.5	8.445	8.446 + 8.403[2]	8.403	8.417	0.059	200
5	8.447		8.402	8.412	0.037	230
7	8.442	8.399[3]	8.431[2]	8.408	0.048	220

[1] Small amounts of magnetite also present

[2] Zn ferrite + magnetite

[3] Small amounts of Zn ferrite also present

[4] Zn-doped magnetite.

will therefore consist of a mixture between this defective Zn ferrite and free $\alpha-Fe_2O_3$.

The Fe excess accommodated by the Zn ferrite lattice would cause a decrease of the lattice constant of $2 \cdot 10^{-3}$ Å only (as estimated after [2]) which is the accuracy limit of the measurements reported here.

The average crystallite size of $ZnFe_2O_4$, as determined from the integral widths of the (220)line, lies in the range 200–250 Å (Table 1) without any systematic dependence on the sample composition.

2.1.2. *Mössbauer spectrometry results.* The Mössbauer spectra display at room temperature two components : a quadrupolar doublet, characteristic for the Zn ferrite and a sextet, assigned to $\alpha-Fe_2O_3$.

Fig. 1 shows the concentrations of the two phases, measured by the area ratio of the components, in comparison with those calculated from the initial composition.

The ratio between the areas of the two components gives the stoichiometry deviations in the Zn ferrite (Fig. 2). It can be noticed that for $n < 3$ there is a non-reacted $\alpha-Fe_2O_3$ excess, while for $n > 3$ a Fe excess is dissolved in the spinelic lattice of $ZnFe_2O_4$, in good agreement with the diffraction data.

These phenomena can be also related to the width of the absorption line of the Zn ferrite, which decreases with increasing n (Fig. 3), suggesting an increasing degree of perfection. The region around $n = 3$ (the border between Fe deficit and Fe excess in $ZnFe_2O_4$), corresponds to a lower degree of structural ordering.

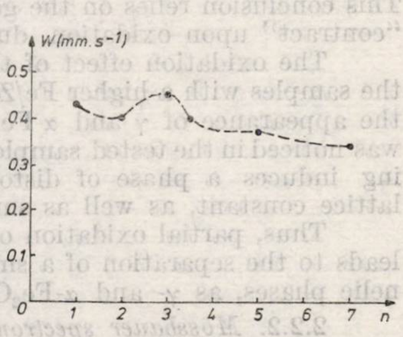

Fig. 3. — Width W of the Mössbauer absorption line corresponding to the Zn ferrite *vs.* compositional parameter n.

2.1.3. *Comparison of the results.* The results obtained by both X-ray diffraction and Mössbauer spectrometry point to the presence of a two-phase system. The Zn ferrite is formed incompletely below $n = 2-3$.

Above this value, the ferrite accommodates a slight Fe excess, as required by the equilibrium phase diagram.

In $ZnFe_2O_4$ the Fe ions occupy the octahedral sites and are in the 3^+ valence state, as inferred from the values of the quadrupole splitting and of the isomer shift. Cation distribution determinations, performed by X-ray diffraction on the basis of the intensity ratios (111)/(400) and (220)/ /(400) for the samples with $n = 2$,3.5 and 5 support the normal character of the $ZnFe_2O_4$, the Zn ions occupying the tetrahedral sites.

2.2. Reduced and tested samples

The reduced as well as the tested samples contain usually spinelic phases only ($ZnFe_2O_4$ and Fe_3O_4), present as distinct compounds or forming solid sloutions. Occasional traces of γ- and α-Fe_2O_3 in the tested samples can be accounted for by partial oxidation processes, as will be mentioned below.

2.2.1. *X-ray diffraction results.* Reduction in butenes at 500°C gives rise to Fe^{2+} ions, thereby transforming the free haematite of the oxidized sample into magnetite with a cubic spinelic structure, coexisting with the Zn ferrite phase.

The reduction process does not affect noticeably the Zn ferrite, as can be seen from the insignificant lattice constant variations between the oxidized and the reduced samples (Table 1). Also, the testing of the sample with $n = 1$ in the oxydehydrogenation reaction of n-butenes does not bring about significant changes in the $ZnFe_2O_4$ phase.

On the contrary, the reduced samples with $n = 2$;3;3.5 and 5 tend to develop after testing a spinelic solid solution $ZnFe_2O_4$—Fe_3O_4. The highly disordered state of this phase can be due partly to local compositional inhomogeneities. This phase is partially oxidized, as can be seen from its decreased lattice constant, in comparison with the value calculated after Végard's law (Table 1) for a $ZnFe_2O_4$—Fe_3O_4 solid solution. This conclusion relies on the general behaviour of spinelic lattices, which "contract" upon oxidation, due to the appearance of cation vacancies.

The oxidation effect of the reaction process is particularly clear in the samples with a higher Fe/Zn ratio. For $n = 3$, the testing brings about the appearance of γ and α-Fe_2O_3 in small amounts, while γ-Fe_2O_3 only was noticed in the tested samples with $n = 3.5$ and 5. For $n = 7$, the testing induces a phase of distorted Fe-deficient magnetite, with a large lattice constant, as well as small amounts of haematite.

Thus, partial oxidation of the catalytic material during the testing leads to the separation of a small amount of iron from the catalytic spinelic phases, as γ- and α-Fe_2O_3.

2.2.2. *Mössbauer spectrometry data.* In all of the reduced samples $ZnFe_2O_4$ was identified as a separate phase. The compositions containing α-Fe_2O_3 in the fresh state showed after reduction amounts of magnetite, as well as $ZnFe_2I_4$.

The tested sample with $n = 1$ contains $ZnFe_2O_4$ only, but for $n =$ $= 2$,3.5 and 7, the testing leads to the formation of a distorted magnetite phase, in various oxidation states up to γ- and α-Fe_2O_3. In the sample with $n = 7$, γ-Fe_2O_3 is clearly noticeable.

The lattice distortion (Fig. 4a) increases when the sample changes from the oxidized (fresh) state to the reduced and tested one. At the same time, the Zn ferrite concentration decreases during the same succession of catalytic phases (Fig. 4b), pointing to a partial dissolution of $ZnFe_2O_4$ in Fe_3O_4 at the granular interfaces.

Fig. 4-a. — The distortion of the ferrite lattice, as reflected by the Mossbauer line width W in different catalytic states; b. — The Zn ferrite concentration Z in different catalytic states (oxidized 0, reduced R, tested T for the samples with $n = 2$ and 7.

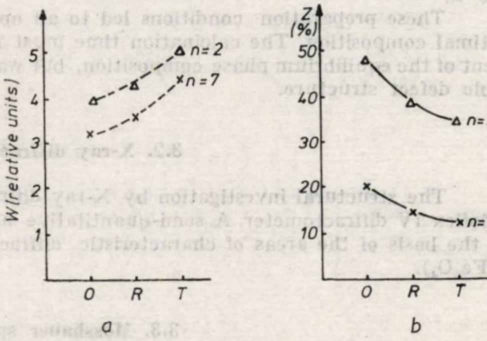

2.2.3. *Catalytic activity*. Fig. 5 displays the dependence of the catalytic activity, in the *n*-butene oxidohydrogenation to butadiene, on sample composition, showing a broad maximum at $n = 2-3{,}5$[5]. A comparison with Fig. 2 and 3 strongly suggests that a high activity is related to a quasi-stoichiometric, non-equilibrium Zn ferrite, which is fromed in the compositional range $n = 2-3{,}5$ with a high degree of structural disorder. In the reduced and tested states, this ferrite retains a higher disorder than for higher Fe content (compare $n = 2$ and 7 in Fig. 4a, b).

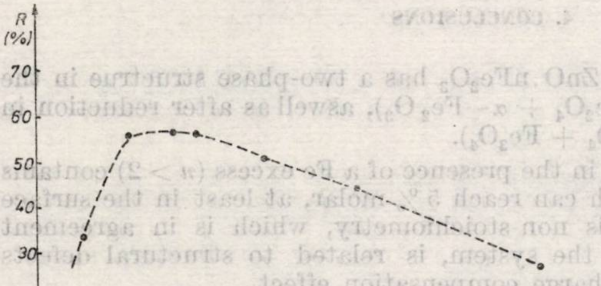

Fig. 5. — Catalytic yield of the $ZnO.nFe_2O_3$ samples in the n-butene oxydehydrogenation to butadiene.

The catalytic activity of the Fe-rich compositions ($n > 3.5$) could also be diminished by the tendency towards a partial oxidation in the reaction. This oxidation would decrease the concentration of anion vacancies, which are generally held responsible for the fixation of the reagent molecules on the surface of the catalyst.

3. EXPERIMENTAL

3.1. Preparation

The samples in the $ZnO \cdot nFe_2O_3$ system (with $n = 1,2,3,3.5$ and 7) were prepared starting from Zn nitrate and α—Fe_2O_3 (haematite). They were calcined for 90 minutes at 900 °C.

These preparation conditions led to an optimal catalytic activity for a sample of optimal composition. The calcination time must not correspond necessarily to the establishment of the equilibrium phase composition, but was proved experimentally to ensure a favourable defect structure.

3.2. X-ray diffraction (XRD)

The structural investigation by X-ray diffraction was performed with a Siemens Kristalloflex IV diffractometer. A semi-quantitative analysis of the phase composition was made on the basis of the areas of characteristic diffraction lines ((104) for α-Fe_2O_3 and (220) for $ZnFe_2O_4$).

3.3. Mössbauer spectrometry

The Mössbauer spectra were recorded with a laboratory-built spectrometer.[3] The data were computer-processed by a specially adapted program.[4] The isomeric shift was determined by comparison with a ^{57}Co source (activity $\simeq$ 20 mCi), in a Cu matrix. The Mössbauer absorbants had a thickness corresponding to $\simeq 25$ mg/cm^2.

4. CONCLUSIONS

The catalytic system $ZnO \,.\, nFe_2O_3$ has a two-phase structrue in the fresh (oxidized) state ($ZnFe_2O_4 + \alpha{-}Fe_2O_3$), aswell as after reduction in butenes at 500 °C ($ZnFe_2O_4 + Fe_3O_4$).

The Zn ferrite formed in the presence of a Fe excess ($n > 2$) contains a lattice Fe_2O_3 excess which can reach 5 % molar, at least in the surface layer of the particles. This non-stoichiometry, which is in agreement with the phase diagram of the system, is related to structural defects (cationic vacancies) by a charge compensation effect.

During the testing in the butene oxydehydrogenation to butadiene reaction a catalytic phase is formed, consisting of a distorted magnetite, which partially dissolves the Zn as a solid solution. Thus, the formation of the catalytically active phase, characterized by a high concentration of structural defects, takes place during the first stages of the reaction only.

REFERENCES

Powder Diffraction File Search Manual, Alphabetical Listing (inorganic), p. 657, Joint Committee on Powder Diffraction Standards, 1973, Swarthmore (USA).

[2] S. Kaida, T. Suzuki, T. Yamazaki, and Y. Mita, *J. Phys. C, Solid state Phys.*, **8**, 617 (1975).

[3] R. Ruscu, *Rev. Roumaine Phys.*, **14**, 1171 (1969).

[4] G. Filoti, Ph. D. Thesis, Bucharest (1971).

[5] M. A. Chaar, Ph. D. Thesis, Bucharest 1979).

Revue Roumaine de Chimie, 31, *1*, 105–112 (1986)

MARANGONI FLOW – INDUCED BY TEMPERATURE GRADIENTS – AGAINST GRAVITY FORCES

E. CHIFU*,[1] I. ALBU*, C. I. GHEORGHIU**, EUGENIA GAVRILĂ*,
M. SĂLĂJAN* and MARIA TOMOAIA-COTIŞEL*
* University of Cluj-Napoca
** Polytechnic Institute of Cluj-Napoca, Romania

Received November 24, 1984

In the present work a comparison is made between the authors' experimental and numerically calculated data obtained in studying the Marangoni-type flow induced by temperature gradients, in competition with the gravity flow, for a thin liquid pellicle of trinagular section found on an inclined plane.
The equation with partial derivatives, appearing in the proposed theoretical model, is integrated by the method of the finite element in the simplex form. The order of magnitude of the calculated rates of flow for the two types of flow through the thin liquid pellicle is close to the one experimentally determined.

INTRODUCTION

In previous papers the Marangoni flow caused by interfacial tension gradients induced by surfactants [1,2] has been studied. In the present work the flow induced by temperature gradients is investigated when competing with the flow due to gravity forces. This latter arises because the examined liquid pellicle is placed on an inclined solid plane.

THEORY

It is supposed that the fluid (liquid) moving inside the pellicle is viscous and incompressible and the flow is stationary and laminar.

In these conditions the equation of motion is the Navier-Stokes equation :

$$\mu \Delta \vec{v} - \operatorname{grad} p + \rho \vec{F} = 0 \qquad (1)$$

where μ is the viscosity of the fluid inside the pellicle, ρ the density, $\vec{v}(v_x, v_y, v_z)$ is the velocity, p the pressure, and $\vec{F}(F_x, F_y, F_z)$ the external force vector.

---

[1] To whom correspondence should be sent : Department of Physical Chemistry, str. Arany, J. No. 11, 3400 Cluj-Napoca, Romania

According to the model sketched in Fig. 1, S denotes the solid/ /liquid interface (the walls of the canal), L the liquid/gas interface and $\vec{n}$ the vector (oriented to the outside) normal to L.

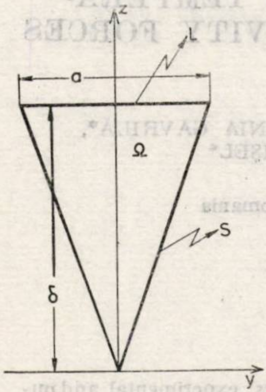

Fig. 1. — The transverse section of the liquid pellicle considered in the numerical calculations.

Taking into account the hydrodynamic and the geometric symmery of the problem (the movement occurs only along the Ox ayxis), we have :

$$v_y = v_z = 0 \tag{2}$$

From relationships (2) and the continuity equation for an incompressible fluid it results :

$$v_x = v_x(y,\ z) \tag{3}$$

Also supposing that p is constant, Eq. (1) becomes :

$$-\mu\left(\frac{\partial^2 v_x}{\partial y^2} + \frac{\partial^2 v_x}{\partial z^2}\right) = \rho F_x \tag{4}$$

Because the fluid is assumed viscous, it adheres to the surface of the canal walls, therefore :

$$v_x = 0 \text{ on } S.$$

In order to find the boundary condition on L we write the equation of motion [3] for the liquid/gas interface. It is :

$$\Gamma\frac{\mathrm{d}\vec{w}}{\mathrm{d}t} = \Gamma\vec{g} + \vec{T}_l - \vec{T}_g + \operatorname{grad}\sigma + (\varepsilon + k)\Delta\vec{w} \tag{5}$$

where $\vec{w} = (\vec{v})_{z=\delta}$. The magnitudes in Eq. (5) have the following meanings :

Γ — the surface density of the liquid/gas interface ($\Gamma \cong 10^{-7}\mathrm{g\ cm^{-2}}$)
ε — the shear surface viscosity
k — the dilational surface viscosity

$\vec{T}_l$ and $\vec{T}_g$ — represent the tractions exerted by the two phases contacting the interface, in our case the inner liquid on one side ($\vec{T}_l$), and the gas on the other ($\vec{T}_g$).

For $\vec{T}_l$ we have, in addition

$$\vec{T}_l = -\mu\left(\frac{\partial v}{\partial z}\right)_{z=\delta} \tag{6}$$

By considering, in Eq. (5), only the effect of the surface tension gradient and the interaction between the liquid inside the pellicle and the interface, the boundary condition on L will be written as:

$$\frac{\partial v_x}{\partial n} = \frac{1}{\mu}\frac{\partial \sigma}{\partial x} \tag{7}$$

As mentioned in the experimental part, the surface tension gradient is induced by a temperature difference $(T_0 - T_1)$. Mathematically this dependence is expressed by

$$\sigma(x) = \sigma(T(x)). \tag{8}$$

Like this, the boundary condition on L becomes:

$$\frac{\partial v_x}{\partial n} = \frac{1}{\mu}\frac{\mathrm{d}\sigma}{\mathrm{d}T}\frac{\mathrm{d}T}{\mathrm{d}x}$$

or, assuming the constancy of the temperature gradient created between the two reservoirs, I and II – see Fig. 2., we shall have, finally:

$$\frac{\partial v_x}{\partial n} = -\frac{1}{\mu}\frac{\mathrm{d}\sigma}{\mathrm{d}T}\frac{(T_0 - T_1)}{H} \tag{9}$$

where H represents the length of the pellicle.

Then the following problem is to be numerically solved:

$$-\mu\left(\frac{\partial^2 v_x}{\partial y^2} + \frac{\partial^2 v_x}{\partial z^2}\right) = \rho F_x \text{ in } \Omega$$

$$v_x = 0 \text{ on } S \tag{10}$$

$$\frac{\partial v_x}{\partial n} = -\frac{1}{\mu}\frac{\mathrm{d}\sigma}{\mathrm{d}T}\frac{(T_0 - T_1)}{H} \text{ on } L$$

where

$$F_x = g\frac{h}{H} = g \sin\alpha \tag{11}$$

h stands for the level difference between the reservoirs and α is the angle between the inclined plane and the horizontal.

The method used to solve this problem is that of the finite element, in the "simplex" form, and the effective algorithm utilized in the calculus has been described in our previous work.[2]

The surface tension gradient being induced by a temperature difference, in a rigorous approach of the phenomenon also the equation of the energy should have been taken into consideration. But, in a first approximation, and having in mind that the thermal processes inside the pellicle are unimportant, we — likewise other authors[4] — have not taken the energy equation into account. Therefore the temperature is present only in the expression of the surface tension — relationship (8).

EXPERIMENTAL

The interfacial mobility of thin liquid layers situated on an inclined solid plane and acted by temperature gradients has been determined by means of a method presented in a previous work[1] and fit for creating the temperature difference $(T_0 - T_1)$.

The reservoir I — Fig. 2. — is thermostated at temperature T_1, and the reservoir II is maintained at a lower temperature T_0. Corresponding to these temperatures, the surface tension of the liquid in reservoir I is σ_1 and that of the liquid in reservoir II σ_0. The two liquid surfaces are connected by an open surface canal along which a temperature gradient arises and simultaneously induces a surface tension gradient.

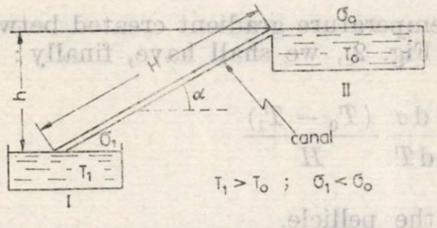

Fig. 2. — The schematic plotting of the experimental device.

Table 1

The dimensions of the thin liquid pellicles

Canal	$\delta \times 10^2$, cm	$a \times 10^2$, cm
A	2.99	4.19
B	2.39	4.19
C	2.69	4.49

The transverse section of the canal is an isosceles triangle the sides of which are slightly curved. In the calculus the transverse section of the pellicle is assumed to be properly triangular. The sizes of the pellicle for the different canals used in the work are listed in Table 1.

Marangoni (Q_-) and gravity (Q_+) rates of flow have been measured. We mention that these rates of flow do not result from pure effects but are reciprocally influenced.

The experiments have been run at three values of the temperature gradient, corresponding to $(T_1 - T_0)$: 20°, 30°, and 50°C, with three canals (see Table 1); and at various level differences h between the reservoirs. Making use of the variable hydrostatic level difference h is the same as if a variable gravity field is realized, since like this the product gh can be modulated (see Eq. 11). Practically, the range of the desired level differences was obtained by modifying the length of the pellicle (H) and keeping constant the inclination of the canal $(\alpha = 20° — Fig. 2.)$. The temperature T_0 was always 20°C. In these conditions the influence of the two parameters : the temperature difference and the hydrostatic level difference on the rates of flow could be studied.

The liquid used in this investigation was water. The values of the surface tension differences $(\sigma_0 - \sigma_1)$ (determined by the method of the maximum pressure in the gas bubble), corresponding to the temperature differences $(T_0 - T_1)$, are given in Table 2.

In order to visualize the movement and to determine the rates of flow, 0.02% aqueous methylene blue was used. The surface tension temperature coefficient of this solution is

$$(\mathrm{d}\sigma/\mathrm{d}T)_{\mathrm{m.b.sol}} = -0.176\ \mathrm{mN/m\ K}$$

i.e. close to that of water $(\mathrm{d}\sigma/\mathrm{d}T)_{H_2O} = -0.155$ mN/m K. This similarity of the coefficients $\mathrm{d}\sigma/\mathrm{d}T$ allowed us to consider that the presence of methylene blue did not disturb the studied phenomenon.

The rates of flow Q_- and Q_+ have been determined as described in the previous work,[1] by making use of the relationship :

$$Q_- = \frac{V_0}{t}\,\frac{c_0}{c_1}\left(1 - \frac{c_0}{c_1}\right)^{-1}\ \mathrm{cm^3 s^{-1}} \qquad (12)$$

c_1 and c_0 represent the concentrations in reservoir I and II, respectively. They were measured by the spectrophotometric method, at the wavelength $\lambda = 665$ nm, with a Spekol ZV apparatus. V_0 is the volume of water in reservoir II, thermostated at 20°C, t is the duration of the flow and it was determined by timing, from the moment the two reservoirs were linked by the canal.

The rate of flow Q_+ from reservoir II to reservoir I has been measured likewise but, in this case, V_0 represents the volume of water in reservoir I, thermostated at 40°, 50° or 70° in dependence of the desired temperature difference, experimentally established and c_1, c_0 represent the concentrations in reservoir II and I, respectively.

Table 2

The temperature differences $(T_0 - T_1)$ and the corresponding surface tension differences $(\sigma_0 - \sigma_1)$

$(T_0 - T_1)$, °C	$(\sigma_0 - \sigma_1)$, mN/m
—20	3.52
—30	5.29
—50	8.82

RESULTS AND DISCUSSION

The experimental values of the rates of flow Q_+ and Q_-, determined in the described conditions, are listed in Tables 3a, 4a, and 5a.

The theoretical values of the rates of flow, obtained by the numerical integration of (10), are also listed in Tables 3b, 4b, 5b, for the same conditions as in the experiment.

Unlike the case when the flow through canals is influenced by surface tension gradients caused by surfactants, the present case, in which these gradients are induced by temperature differences, creates the problem of evaluating the density and the viscosity. It arises as a consequence of the temperature profile existing along the canal.

Table 3

The dependence : a) $Q_{exp} = f(h)$ and b) $Q_{calc} = f(h)$ for the canal C, $(T_0 - T_1) = -30$°C, $(\sigma_0 - \sigma_1) = 5.29$ mN/m.

a)				b)		
h, cm	$Q_{-exp} \times 10^4$, $\mathrm{cm^3 s^{-1}}$	h, cm	$Q_{+exp} \times 10^4$, $\mathrm{cm^3 s^{-1}}$	h, cm	$Q_{-calc} \times 10^4$, $\mathrm{cm^3 s^{-1}}$	$Q_{+calc} \times 10^4$, $\mathrm{cm^3 s^{-1}}$
0.60	4.15	0·68	0·50	0.2	19.94	0.082
0.66	3.08	0.81	1·60	0.4	4.23	1.17
0.74	1.69	0.92	1.95	0.6	0.77	2.91
0.76	1.68	1.24	3.03	0.8	0.102	4.56
1.00	0.38	1.53	2.95	1.0	0.022	5.70
1.02	0.70	1.60	2.35	1.2	0.006	6.35
1.13	0.67	1.75	2.75	1.4	0.002	6.72
1.14	0.65	2.01	2.54	1.6	0.001	6.92
1.20	0.85	—	—	1.8	0.0004	7.01
				2.0	0.00	7.03

Table 4

The dependence: a) $Q_{\text{exp}} = f(h)$ and b) $Q_{\text{calc}} = f(h)$ for the canal C, $(T_0 - T_1) = -50°\text{C}$, $(\sigma_0 - \sigma_1) = 8.82 \text{mN/m}$.

a)				b)		
h, cm	$Q_{-\text{exp}} \times 10^4$, cm^3s^{-1}	h, cm	$Q_{+\text{exp}} \times 10^4$, cm^3s^{-1}	h, cm	$Q_{-\text{calc}} \times 10^4$, cm^3s^{-1}	$Q_{+\text{calc}} \times 10^4$, cm^3s^{-1}
0.52	7.16	0.74	1.49	0.2	58.93	0.0033
0.60	4.43	0.78	1.89	0.4	18.65	0.254
0.69	4.88	0.80	2.27	0.6	7.07	1.05
1.07	0.89	0.98	1.71	0.8	2.65	2.17
1.10	0.84	1.12	2.42	1.0	0.88	3.29
1.18	1.47	1.28	2.14	1.2	0.22	4.28
1.20	1.13	1.47	2.26	1.4	0.076	5.10
1.28	1.60	1.66	2.55	1.6	0.030	5.63
1.34	0.40	1.85	2.47	1.8	0.013	5.95
1.46	0.17	2.01	1.99	2.0	0.006	6.12

Table 5

The dependence: a) $Q_{\text{exp}} = f(h)$ and b) $Q_{\text{calc}} = f(h)$ for canal A, $(T_0 - T_1) = -50°\text{C}$, $(\sigma_0 - \sigma_1) = 8.82 \text{mN/m}$

a)				b)		
h, cm	$Q_{-\text{exp}} \times 10^4$, cm^3s^{-1}	h, cm	$Q_{+\text{exp}} \times 10^4$, cm^3s^{-1}	h, cm	$Q_{-\text{calc}} \times 10^4$, cm^3s^{-1}	$Q_{+\text{calc}} \times 10^4$, cm^3s^{-1}
0.63	5.74	0.67	0.48	0.2	61.60	0.02
0.65	3.89	0.77	1.09	0.4	18.90	0.53
0.68	5.78	0.78	1.07	0.6	6.80	1.69
0.77	3.11	0.83	1.25	0.8	2.82	3.08
0.83	4.44	1.10	2.48	1.0	0.61	4.42
0.91	2.75	1.61	3.28	1.2	0.16	5.56
1.09	1.34	1.93	2.32	1.4	0.04	6.42
1.12	2.36	2.24	2.58	1.6	0.02	6.94
1.38	0.71	2.32	2.66	1.8	0.009	7.24
1.52	0.17	2.42	3.53	2.0	0.004	7.40

Taking into account that the densities of the liquids in reservoirs I and II found at temperatures T_1 and T_0 respectively, are relatively close, we considered it reasonable to use an average density in the calculus. In what the viscosity is concerned, its variation with the temperature being rather significant ($\mu_{20} = 1.005$ cP; $\mu_{70} = 0.4061$ cP), a linear variation of this magnitude with the level difference h has been used, as a first approximation:

$$\mu = \frac{\mu_1 - \mu_0}{h_{\text{total}}} h + \mu_0 \tag{13}$$

where $h_{\text{total}} = 3$ cm and μ_0 and μ_1 stand for the viscosities of the liquids in reservoir II, respectively I.

It can be seen that the level difference h does influence the values of the rates of flow, Q_+ and Q_- experimentally determined or calculated in the predicted sense.

The values of the rates of flow obtained with the three canals are close to one another, probably due to the similar dimensions of the pellicles (see Tables 4 and 5). This agreement reflects the reproducibility of the phenomenon.

It is to be noticed that, in accordance with the theory of the process, the coexistence of the two types of flow is experimentally ascertained in a given domain of the level difference h (see Tables 3–5 and Fig. 3). Outside this domain, at smaller values of h, it is the Marangoni flow which predominates and determines the rate of flow Q_-. In this situation practically the whole liquid from the pellicle is dragged upward the canal; while at greater level differences h the flow due to gravity forces is preponderent, with the corresponding rate of flow, Q_+.

The influence of the interfacial tension gradient, induced by the temperature difference $(T_0 - T_1)$ between the reservoirs, is illustrated in Tables 3 and 4 for a given canal.

As was to be expected, the increase of the temperature gradient significantly influences the ascending (Marangoni) rate of flow Q_- and has a smaller effect on the descending (gravity) rate of flow Q_+ (see Tables 3b and 4b).

The experimental data for the rates of flow generally agree with the calculated ones from the qualitative point of view. We specifiy that the experimentally determined rates of flow represent values averaged along the entire canal and over all the time interval in which the flow was watched, while the calculated rates of flow represent instantaneous values taken only for the terminal part of the canal. In these conditions we are not able to do a better correlation between the two groups of data.

Taking into consideration that the theoretical rates of flow refer to the upper terminal section of the canal, an additional calculation has been done for these rates in the case of canal B at three gradients, by assigning, this time, unique values for the viscosities. For the calculation of the ascending rate of flow it seemed plausible to adopt the viscosity of the warmer liquid μ_1, and for that of the descending rate of flow the viscosity of the colder liquid μ_0. The results obtained for a given temperature difference are represented, together with the experimental ones, in Fig. 3. It can be seen that the experimental rates of flow are closer to the values calculated in this way, what does not alter the conclusions above.

An interesting feature is revealed by the numerical calculation: the movement of the liquid/gas interface produced by the surface tension gradient arises in the close vicinity of the solid wall (S) — Fig. 4. This behavior can be explained by the fact that the thickness of the pellicle is smaller close to the wall, and therefore the drag effect produced thereon by the interface is important.

By examining again the data here presented, it can be concluded that the theoretical model proposed, — even simplified by considering

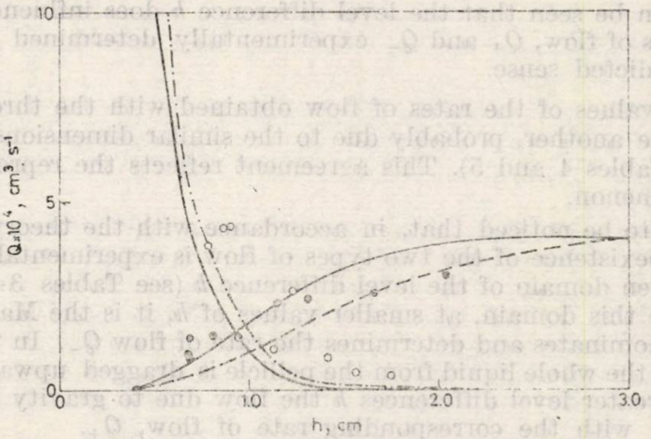

Fig. 3. — The dependence $Q = f(h)$ for the canal B. $(T_0 - T_1) = -50°C$, $(\sigma_0 - \sigma_1) = 8.82$ mN/m : —— $Q_{-calc} = f(h)$, $Q_{+calc} = f(h)$ assuming the linear variation of the viscosity, according to Eq. (13) ; —·—· $Q_{-calc} = f(h)$ supposing that $\mu = \mu_1$; – – – $Q_{+calc} = f(h)$ supposing that $\mu = \mu_0$; ○ experimental values of $Q_- = f(h)$; ● experimental values of $Q_+ = f(h)$.

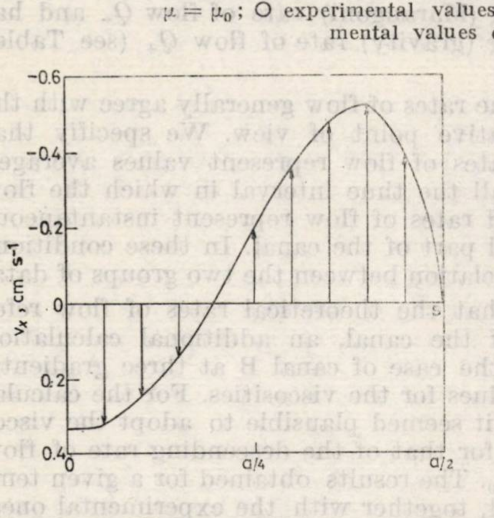

Fig. 4. — The velocity profile on the liquid/gas interface for the thin pellicle of triangular section (canal B, $(T_0 - T_1) = -20°C$, $(\sigma_0 - \sigma_1) = 3.52$ mN/m, $h = 0.6$ cm, $\mu = 0.00656$ P, $z = \delta = 0.0239$ cm, $a = 0{,}0419$ cm)

the thermal effect only upon the liquid/gas interface, by approximating the liquid viscosity, and by making use of simplex finite elements — satisfactorily describes the studied phenomenon.

REFERENCES

[1] E. Chifu, I. Albu, *Studia Univ. Babeş-Bolyai, Chem.*, **13** (1), 99 (1968).

[2] E. Chifu, C. Gheorghiu, I. Stan, *Rev. Roumaine Chim.*, **29**, 31 (1984).

[3] L. E. Scriven, *Chem. Engl. Sci.*, **12**, 98 (1960).

[4] V. G. Levich, "Physicochemical Hydrodynamics", Prentice-Hall, New York., 1962, p. 384–390.

Revue Roumaine de Chimie, **31**, *1*, 113—116 (1986)

COMPTES RENDUS

K. YOSHIHARA, H. KUDO and T. SEKINE, "*Periodic Table with Nuclides and References Data*", Springer-Verlag, Berlin, 1985, 451 pages, hard-cover, DM 198

The book of the three Japanese authors provides an up-to-date information on nuclides and radiochemistry, in more detail than may do any chart of nuclides.

Most pages of the book are devoted to extended tables; however, the corresponding captions, introductory text and literature references provide sufficient background data for enabling any reader to make good use of the book. The 53 tables and 47 figures of the book are grouped in eight chapters: I, Periodic table with nuclides; II, Nuclear properties, disintegration and standards; III, Nuclear reactions; IV, Interaction of radiation with matter and its detection; V, Radioactive nuclides in chemistry and related fields; VI, Nuclear fusion in science and technology; VII, Radioactive nuclides in life-science; VIII, Environmental radioactivity and radiation safety.

The first two chapters constitute more than half of the book. Chapter I contains Fig. I.1 (13 pages) which lists separately the periods of Mendeleev's system indicating under each element its isotopes with their characteristic data and with the β-stability line. One may note in passing that the authors do not mention that both the A—B designations of subgroups in the periodic table, and the names of elements with $Z > 101$, are at present highly controversial. The subsequent Table 1.2 (86 pages) presents stability of isobaric nuclides (mass excesses and binding energies) in the ascending order of mass number values. Both Fig. I.1 and table 1.2 are easy to use and indicate by boldface characters or by a black dot, respectively, the stable nuclides.

Chapter II presents in Table II.1 (20 pages) nuclear properties (isotopic mass, spin and parity, magnetic dipole moment and electric quadrupole moment) for all radioactive and stable nuclides. Table II.2 (120 pages) lists the energies and intensities of gamma-rays emitted by radionuclides. Other figures and tables of chapter II indicate characteristics and standards for other particles emitted by radionuclides.

Chapter III includes data on cross sections for nuclear reactions such as radioactivation, production of radioisotopes, neutron fission of heavy nuclides.

Chapter IV has tables for range and stopping power of various media for different nuclear radiations, as well as data on efficiency of various detectors such as NaI (T1) or Ge(Li).

Chapter V contains tables which are useful for radionuclides as tracers in chemistry, for isotope dilution analysis, for radioactivation analysis, for hot atom chemistry, for Mössbauer spectroscopy and for pertubed angular correlation (PAC).

A brief chapter VI is devoted to nuclear fusion, including data for hydrogen isotopes. A quite interesting chapter VII presents in tabellar form applications of radionuclides in life science; tables VII.1 and VII.2 present medium-and short-lived nuclides and corresponding labelled compounds for radiopharmaceutical use, together with the dose administered to various organs. There are some omissions in table VII.1b, namely ^{85}Sr, ^{87}Sr, ^{117}In and ^{197}Hg. Chapter VIII has up-to-date information on maximum permissible dose, internal exposure, etc.

The appendix contains tables with fundamental constants (both in SI and CGS systems), energy conversion factors, statistical and numerical functions.

The book is reproduced directly from the typewritten manuscript so that it is practically error-free; the reviewer has spotted, however, on p. 386 the word bladder misspelt as blasser, and a missing slash on p. 385 in mrad/μCi; in the subsequent table instead of radiation dose (in mrad/μCi administered) the same information is indicated as: dose (rad/mCi) administered.

The book is very useful to have at hand in all radiochemical/radioisotope/labelled compounds/radiopharmaceutical laboratories. It is also of assistance for teaching purposes and for users in various branches benefiting from employing radioisotopes.

A. T. Balaban

J. R. THURNLUND and P. E. JOHNSON (eds.), *"Stable Isotopes in Nutrition"* ACS Symposium Series No. 258, Amer. Chem. Soc., Washington, DC, 1984, hard cover, 230 pages, \$ 47.95 (overseas)

Three incentives exist for the growing interest in biomedical applications of stable isotopes : (i) they do not expose the human body to radioactivity, yet (ii) newer instrumentation allows their detection in amounts not very much higher than for their radionuclidic isotopes, allowing in addition their precise localization in the. molecule; (iii) some of the most interesting elements have not suitable radioisotopes of convenient half-life, such as nitrogen or oxygen.

The fourteen chapters contributed by the symposium participants in 1983 analyze various aspects of the use of stable isotopes for studying human feeding. Technically centered problems are discussed by L. J. Moore (Thermal and Resonance Ionization Mass Spectrometry), J. R. Turnlund (Trace Element Utilization in Humans Studied with Enriched Stable Isotopes and Thermal Ionization Mass Spectrometry), and L. May (Mössbauer Spectroscopy). Other contributions are centered on a certain element : A.L. Yergey et al. (calcium metabolism) ; C. M. Weaver (trace elements such as zinc, iron and selenium *via* hydroponic intrinsic labeling of edible plants) ; R. Schwartz (magnesium) ; C. Veillon (selenium, measured by GC/MS) ; N. S. Shaw et al. (iron absorption in young women estimated by MS of a volatile iron chelate) ; D. B. Christie et al. (trace metals analyzed by MS at the sub-ppb range *via* chelates) ; P. E. Johnson (iron, zinc, and copper). The final four chapters are devoted to ^{13}C analysis in connection with the human diet. Taking advantage that maize starch has a different C_{13}/C_{12} ratoi than wheat or potato starch (the former is a "C_4 plant" producing glucose photosynthetically *via* a C_4 intermediate, whereas the latter are "C_3 plants" whose glucose is formed *via* a C_3 intermediate)*, T. W. Boutton, P. D. Klein et al. found by MS analysis of prehistoric bone collagen that maize culture in Missouri and Arkansas started later than it had been believed, namely around 1000 AD, but then it spread rapidly so that 35—72% of human diet from 1000 to 1600 AD consisted of maize. H W. Krueger, and C. H. Sullivan studied carbon isotope fractionation between diet and bone. Using the $\delta^{13}C$ value relative to the international PBD limestone standard (a $CaCO_3$ marine shell that is rich in ^{13}C, whose $\delta^{13}C$ is $0^0/_{00}$.) defined as

$$\delta^{13}C = \left[\frac{(C^{13}/^{12}C)_{\text{sample}}}{(^{13}C/^{12}C)_{\text{PDB}}} - 1 \right] \times 1000$$

one obtains for C_3 plants $\delta^{13}C \cong -26.5^0/_{00}$ and for C_4 plants $\delta^{13}C \cong -11.5^0/_{00}$. The collagen in the corresponding diets has less negative values by $+5^0/_{00}$ in both cases, which are easily detectable by a triple-collecting mass spectrometer (overall precision is better than $\pm$ $\pm 0.2^0/_{00}$). Eight possible diets were modelled : C_3 plants ; C_3 plants + C_3 meat ; C_4 plants ; C_4 plants + C_4 meat ; mixed, mainly maize ; marine food ; C_3 plants + C_4 meat ; etc. Analysis of both collagen and hydroxyapatite carbon isotopic ratios gives considerable information on the total diet. J. R. Brainard, J. Y. Hutson, P. E. London and N. A. Matwiyoff used a ^{13}C-enriched substrate, 3-^{13}C-L-alanine, for in vivo studies by ^{13}C-NMR in perfused hamster liver for metabolic profiling of gluconeogenesis and of glucogen formation. It is expected that similarly to the present diagnosing of physiological and biochemical disorders by means of non-invasive ^{31}P-NMR in humans, in the near future ^{13}C-methodology will be amenable to a similar performance. R. P. Wolfe, M. H. Wolfe and G. Shulman report a study of glucose metabolism in humans using MS analysis by primed constant infusion with U-^{13}C-glucose ; hypo/hyper-thyroid volunteers give distinct patterns from normal volunteers indicating significant reduction of cycling in hypothyroid patients.

The volume is excellently produced by direct reproduction of authors' manuscripts ; the literature is up-to-date. It has an index of contributing authors and a subject index. The book is essential for food scientists, nutritionists, chemists, and isotope chemists interested in biological applications.

Alexandru T. Balaban

---

* The C_3 (Calvin-Benson) photosynthetic pathway fixes CO_2 to C_3 phosphoglycerate *via* catalysis by ribulose biphosphate carboxylase which discriminates strongly against $^{13}CO_2$. By contrast, the C_4 (Hatch-Slack) pathway fixes CO_2 into the C_4 malic or aspartic acids *via.* catalysis by phosphoenolpyruvate carboxylase which is less discriminatory against $^{13}CO_2$.

K. L. MITTAL (ed.), "Polyimides: Synthesis, Characterization, and Applications", Plenum Publishing Corporation, New York, 1984, 1182 pages, 155 dollars.

This two-volume set represents the first comprehensive monograph in the field, providing a wealth of material on different aspects of current research and development in polyimides. It contains the proceedings of the First Technical Conference on Polyimides: Synthesis, Characterization and Applications held under the auspices of the Mid — Hudson Section of the Society of Plastics Engineers at Ellenville, New York, November 10—12, 1982.

During the last two decades, there has been a growing interest in the use of polyimides for a variety of applications in widely different technologies. The applications of polyimides range from aerospace to microelectronics and medicine and this is due to their outstanding properties (high temperature stability, electrical insulation, flexibility at low temperature, chemical resistance, etc.) and due to the advantageous method of synthesizing them in two steps. Polyimides are used as organic insulators, as adhesives, as coatings, in composities, etc. and this is why they have been given a special attention.

In this book one hundred and sixty-four scientists and technologists hailing from academic, government and industrial laboratories present interdisciplinary papers on the state of knowledge of each topic under consideration through combination of overviews and original unpublished research. Volume 1 focuses on synthesis, properties and characterization of a variety of polyimides; metal-containing polyimides; cure kinetics of polyimides; structure — — property relationship; polyimide adhestion. Volume 2 covers the mechanical properties of polyimides both in bulk state and in thin film form, microelectronic applications, photosensitive polyimides. polyimides as adhesives, aerospace applications, polyimides blends, electrophoretic deposition of polyimides and electrochemical and medical applications. Each volume has a subject index for easy reference to this important class of materials.

As an important source of up-to-date information on the subject. "Polyimides: Synthesis, Characterization and Applications" will meet the requirements of the scientists and technologists who work particularly in this field, as well as of those who are generally concerned with heterocyclic thermostable polymers. The book denotes a high level editorial effort and all the contributions are of high standard. The diagrams and formulas are presented clearly. The printing is excellent.

Maria Brumă

V. BALEK and J. TÖLGYESSY, *"Emanation Thermal Analysis and Other Radiometric Emanation Methods"*, Akadémiai Kiadó, Budapest, 1984, 304 p.

The book authored by Dr. V. Balek and Professor J. Tölgyessy is actually an exhaustive work dedicated to the emanation thermal analysis (ETA) and to other related methods, which enriched in the past two decades the family of thermoanalytical methods.

This method is based on inert gas release from solids and has undergone in recent years a particular development in theory, instrumentation and applications. The development of emanation thermal analysis was determined by the requirements of more sensitive experimental techniques in the investigation of solid state processes together with modern nuclear instrumentation. On the other hand, the increasing interest in the radiometric methods is due to their high versality and sensitivity in comparison with other chemical or physical methods.

The material is divided into 8 chapters. The first of them is an introductory chapter, which gives definition, terminology and historical development of the method.

The second chapter deals with the techniques used for the labelling of solids by inert gases with special emphasis on techniques introducing the inert gas (without parent nuclid) and of the parent nuclid of inert gas.

Chapters 3 and 4 are devoted to the theories of inert gas release from solids in case of introducing inert gas or its parent into the solid. Chapter 5 treats the measurement of inert gases, presenting in detail the schemes of some instruments permitting the simultaneous measurements using the following thermoanalytical methods: ETA—DTA, ETA—DTA-dilatometry, ETA-DTA-EGA and ETA-DTA-TG/DTG.

The last three chapters are devoted to the most common applications of radiometric methods in analytical chemistry (determination of natural radioelements, analysis of non radioactive gases, with special emphasis on determination of air and water pollutants, analysis of solution) and various branches of technology: characterization of material properties, non-stoichiometry, solid state reactions, the study of physical changes in multi-phase systems, determination of the rate constant of corrosion, testing of building materials.

The radiometric emanation method becomes an important tool in basic research as well as in the solution of practical problems of chemical technology, metallurgy, production of plastics, pharmaceuticals, in nuclear science and technology, in environmental research; therefore, the book is useful and interesting for various researchers working in different fields.

The book contains 196 figures drawn with care and the quality of printing is excellent.

Marius Andruh

NOTE POUR LES AUTEURS

La Reuve Roumaine de Chimie publie des articles en anglais, français, russe, allemand ou espagnol. Les auteurs sont priés d'envoyer des articles et des comptes rendus inédits.

Les manuscrits seront dactylographiés à double interligne. La bibliographie, les tableaux et la légende des figures seront placés après le texte.

Si l'article fait partie d'une série numérotée, la partie précédente sera donnée comme première référence.

Chaque article sera précédé d'un résumé comprenant quinze lignes au maximum.

Les références bibliographiques dans le texte seront faites par des exposants sans parenthèses et paraîtront à la fin de l'ouvrage.

Les publications périodiques mentionnées dans la bibliographie seront présentées suivant les prescriptions internationales : le nom de l'auteur précédé de l'initiale du prénom, le titre du périodique abrégé conformément à « Chemical Abstracts » et souligné par une ligne, le numéro du tome indiqué par des chiffres arabes et souligné par deux lignes, suivi de la première page de l'article : à la fin, l'année de la parution sera placée entre parenthèses. Le numéro de la revue ne sera pas indiqué si les pages du volume sont numérotées consécutivement.

Les textes des livres ou traités inclueront : le nom des auteurs, l'initiale du prénom, le titre du livre entre guillemets et sans être souligné, le numéro du tome précédé par l'abréviation « vol. » (ou « Bd. »), le numéro de l'édition, les éditions (the publisher), la localité de la parution du livre, l'année de la parution et la page de la référence précédée(s) par l'abréviation « p. » (ou S. »).

Les brevets seront indiqués comme suit : l'auteur ou la firme, le pays et le numéro du brevet, la date et la revue *(Chem. Abstr.)*. Par ex. : M. Jones (to Union Carbide Co), Brit. Pat 601 238, 2 Sept. 1959 ; cf. *Chem. Abstr.*, 54, 12808 (1960).

Si la référence n'a pas été lue en original, on indiquera aussi la revue de référence consultée.

Les diagrammes seront tracés à l'encre de Chine sur papier calque. Les tableaux et les figures (en nombre strictement nécessaire) ainsi que les courbes dans les figures seront numérotés par des chiffres arabes. Leur explication sera donnée dans la légende des figures. Prière de ne pas inscrire les mêmes données dans les tableaux et les figures. Chaque tableau aura un titre. On indiquera dans le texte la place approximative des tableaux et des figures. Les formules chimiques seront incluses dans le texte ; en outre, elles seront transcrites sur papier calque, à l'encre de Chine.

Les auteurs sont priés d'indiquer les caractères italiques (en soulignant les lettres au crayon), ainsi que tout autre caractère spécial : les préfixes *ortho*, *meta*, *para*, *cis*, *trans*, etc. seront soulignés pour indiquer leurs caractères italiques et ne seront jamais écrits avec des majuscules.

Aucune correction à la main ne sera admise sur le manuscrit. Les corrections seront tapées à la machine. Les lettres grecques ou d'autres symboles spéciaux seront insérés à la main à l'encre clairement.

Le manuscrit sera signé par l'auteur.

Le titre-courant aura 50 lettres au maximum.

L'entière responsabilité du contenu des articles appartient aux auteurs.

Sur demande ou peut obtenir une note plus complète.

PRINTED IN ROMANIA

TRAVAUX PARUS AUX ÉDITIONS DE L'ACADÉMIE DE LA RÉPUBLIQUE SOCIALISTE DE ROUMANIE

V. DRĂGUȚAN A. T. BALABAN M. DIMONIE, **Olefin methathesis and ring-opening polymerization of cyclo-olefins** coédition avec John Wiley and Sons, 1985, 544 p.

GH. MARCU, **Chimia compuşilor coordinativi**, 1984, 415 p.

E. CORDOŞ, C. MANOLIU, **Spectrometria de absorbție și fluorescență atomică**, 1984, 178 p.

C. BODEA editeur, **Tratat de biochimie vegetală**, p. I, vol. 5, 1984, 438 p.

ELENA CEAUŞESCU, **Cercetări în chimia şi tehnologia polimerilor**, 1983, 519, p.

N. ASANDEI, A. GRIGORIU, **Chimia şi structura fibrelor**, 1983, 39 p.

N. IONESCU, M. CĂLDĂRARU, **Oxidarea catalitică a olefinelor inferioare**, 1983.

C. CAŞCAVAL, **Studiul polimerilor prin piroliză și cromatografie de gaze**, 1983, 220 p.

C. I. SIMIONESCU, F. DANEŞ, **Originea vieții**, 1983, 110 p.

C. BODEA (editeur), **Tratat de biochimie vegetală**, p. II, vol. IV, 1982, p. 408.

I. G. MURGULESCU, RODICA VÎLCU, **Introducere în chimia fizică Vol. III. Termodinamica chimică**, 1982, 624 p.

I. G. MURGULESCU, J. PĂUN. **Introducere în chimia fizică. Vol. I.3.Nucleul atomic, reacții nucleare, particule elementare**, 1982, 606 p.

ELENA JERCAN, **Analiza cromatografică**, 1982, 286 p.

ELENA CEAUŞESCU, **Noi cercetări în domeniul compuşilor macromoleculari**, 1981, 536 p.

I. G. MURGULESCU, TATIANA ONCESCU, E. SEGAL, **Introducere în chimia fizică, Vol. II. 2. Cinematică chimică și cataliză**, 1981, 1024 p.

LYDIA-MARIA VAICUM, **Epurarea apelor uzate cu nămol activ. Bazele biochimice**, 1981, 218 p.

I. GĂLĂȚEANU, **Procese şi metode radiochimice în energetica nucleară**, 1981, 234 p.

O. IORDACHE, **Procese polistocastice aplicate la fenomenele de transfer**, 1981, 186 p.

CR. SIMIONESCU, VALERIA GORDUZA, **Polimeri biocompatibili şi biologic activi**, 1980, 479 p.

ELENA CEAUŞESCU, **Polimerizarea stereospecifică a izoprenului**, 1979, 307 p.

CONST. GH. MACAROVICI, **Analiza chimică cantitativă anorganică**, 1979, 457 p.

M. FLORESCU, **Metode ştiinţifice în dezvoltarea industriei chimice moderne**, 1979, 256 p.

A. T. BALABAN, I. GĂLĂȚEANU, G. GEORGESCU, LIGIA SIMIONESCU **Compuşi marcați și radiofarmaceutici cu aplicații în medicina nucleară**, 1979, 495 p.

I. G. MURGULESCU, E. SEGAL, **Introducere în chimia fizică. Vol. II. I. Teoria molecular-cinetică a materiei**, 1979, 1036 p.

S. STERNBERG, FL. DANEŞ, **Termodinamica chimică aplicată**, 1978, 400 p.

I. G. MURGULESCU, V. EM. SAHINI, **Introducere în chimia fizică. Vol. I.2. Structura şi proprietățile moleculare**, 1978, 604 p.

I. ZUGRĂVESCU, MAGDA PETROVANU, **N-ylid chemistry**, coédition avec McGraw-Hill International Book Company, U.S.A., 1977, 396 p.

I. G. MURGULESCU, **Introducere în chimia fizică. Vol. I.1. Atomi, molecule, legătură chimică**, 1976, 560 p.

ELENA CEAUŞESCU, **Research work on synthesis and characterization of macromolecular compounds. Contributions**, 1974, 251 p.

CR. SIMIONESCU, VIORICA RUSAN, V. POPA, **Chimia algelor marine**, 1974, 212 p., 1 pl.

ISSN 0035 – 4090

I. P. INFORMAȚIA c. 1607

43426

1986 ILB 2

LEI 40

$ 80 (pour un abonnement annuel)

F 1103

66

ACADÉMIE DE LA RÉPUBLIQUE SOCIALISTE DE ROUMANIE

04

REVUE ROUMAINE DE CHIMIE

REFERALVA

R 1986 APR 7

MG

TOME 31

N° 2

Février 1986

Rev. Roumaine Chim.

RRCHAX, 31, 2, p. 117–258 (1986), Bucarest

EDITURA ACADEMIEI REPUBLICII SOCIALISTE ROMÂNIA

ACADÉMIE DE LA RÉPUBLIQUE SOCIALISTE DE ROUMANIE

COMITÉ DE RÉDACTION

Rédacteur en chef:

I. G. MURGULESCU, membre de l'Académie de la République Socialiste de Roumanie

Rédacteurs en chef adjoints:

A. T. BALABAN et V. EM. SAHINI, membres correspondants de l'Académie de la République Socialiste de Roumanie

Collège de rédaction:

EM. BRATU, ELENA CEAUȘESCU, ECATERINA CIORĂNESCU-NENITZESCU, CR. SIMIONESCU, membres de l'Académie de la République Socialiste de Roumanie, P. SPACU, membre correspondant de l'Académie de la République Socialiste de Roumanie; M. BANCIU, M. D. GHEORGHIU, I. HAIDUC, D. I. MARCHIDAN, I. MOLDOVAN, G. NIAC et D. SĂNDULESCU

La Revue Roumaine de Chimie paraît 10 fois par an. Toute commande de l'étranger sera adressée à ROMPRESFILATELIA — sectorul Export-Import Presă, P.O. Box 12—201, télex 10376 prsfi r, Bucharest, Calea Griviței nr. 64—66, Roumanie.

Les manuscrits, les livres et les revues proposés en échange, ainsi que toute correspondance seront envoyés à la rédaction.

REVUE ROUMAINE DE CHIMIE

125, Calea Victoriei, 79717 Bucarest, Roumanie, téléphone 50 76 80

EDITURA ACADEMIEI REPUBLICII SOCIALISTE ROMÂNIA
125, Calea Victoriei, 79717 Bucarest, Roumanie, téléphone 50 76 80

REVUE ROUMAINE DE CHIMIE

Tome 31, N° 2 **Février 1986**

FLORIN BADEA, ALEXANDRU T. BALABAN, ADRIAN DIMITRIU, FLORIN IORDACHE, AURELIA MEGHEA and LUCIAN STOENESCU, Carbanions and free radicals derived from 1,2-diphenylpyrazolidine-3,5-diones. II[1]. Trapping of the free radicals derived from diethyl fluoro-malonate, n-butyl-, and phenyl-malonate . . . . 119 – 130

ROBERT SCHWARTZ and ANIKÓ JUHÁSZ, The synthesis of some 3-oxo-4-ene-B-nor-derivatives. Oppenauer oxidation of 3β-hydroxy-5-ene-B-nor-steroids with Al_2O_3 . . . . 131 – 136

MARIUS H. TERDIC, Disubstituted phenothiazones. IV. Chloro-4-nitro- and -7-nitro-3H-phenothiazin-3-ones . . . . 137 – 141

A. XICLUNA and J. E. ROBERT, ^{1}H-NMR Spectral study of ethyl 3,5-diphenyl-3,5-dihydrothiophene-2-carboxylate (in French) . . . . 143 – 147

HOCINE KADI and D. P. LAZĂR, Identification of aromatic hydrocarbons in petroleum fractions. IV. IR Spectral analysis (in French). . . . . 149 – 157

C. I. CHIRIAC, Phosphorous acid – iodine as reagent for the synthesis of 1,3,4-oxadiazoles from diacylhydrazines . . . . 159 – 162

MARIA BRUMĂ, GHEORGHE DUMITRESCU and ELENA DUMITRESCU, Modified copolymers with radioprotective action . . . . 163 – 168

RADU VLĂDEA, Catalytic influences in electrooxidation of olefins in non-aqueous solutions. IV. Reaction mechanism for olefin oxidation in methanol. . . 169 – 174

DAN CARTIANU, Dissipative structures in reaction-diffusion systems as synchronization phenomena. . . . . 175 – 197

RODICA VĂŢULESCU, T. BUDIU, GH. MARCU and IRINA PAL, Heteropolytungstates with Ti(IV) and Ni(II). VI. The behaviour of the Ni(II)-undecatungstotitanate(IV) and Ni(II)- pentatungstotitanate(IV) anions towards cationites, in acidic and neutral media . . . . 199 – 207

RODICA VĂŢULESCU, T. BUDIU, GH. MARCU and IRINA PAL, Heteropolytungstates with Ti(IV) and Ni(II). VII. The stability of Ni(II)-undecatungstotitanate(IV) and Ni(II)-pentatungstotitanate(IV) anions in aqueous solution . . . . 209 – 216

NICOLAE CALU, ION SANDU and IOAN BERDAN, Preparation and characterization of active forms of manganese dioxide for dry galvanic elements and systems (in French) . . . . 217 – 226

Revue Roumaine Chim. 31, 2, 117–258 (1986), Bucares

GH. MARCU, A. HANTZ, MAGDA SOMAY, CS. VÁRHELYI and F. TOLEA, Study on some cobalt(III) dioximine chelate adducts with tertiary phosphines . . . . 227 – 235

G. LÓPEZ CUETO and A. ALONSO MATEOS, Coulometric study at controlled potential of the anodic oxidation of the binuclear cyanide complex of Mn(III). Part II. Oxidation at + 0.80 volts vs. SCE ; Faraday currents, kinetic currents (in Spanish) . . . . 237 – 253

BOOK REVIEWS . . . . 255 – 257

Revue Roumaine de Chimie, **31**, 2, 119—130 (1986)

CARBANIONS AND FREE RADICALS DERIVED FROM 1,2-DIPHENYLPYRAZOLIDINE-3,5-DIONES. II[1]

TRAPPING OF THE FREE RADICALS DERIVED FROM DIETHYL FLUORO-MALONATE, n-BUTYL-, and PHENYL-MALONATE

FLORIN BADEA, ALEXANDRU T. BALABAN, ADRIAN DIMITRIU,
FLORIN IORDACHE, AURELIA MEGHEA and LUCIAN STOENESCU

Polytechnic Institute, Department of Organic Chemistry, Splaiul Independenţei 313, 76206
Bucharest, Romania

Received August 2, 1985

Diethyl fluoro-, n-butyl-, and phenyl-malonate were converted into nitroxides either by oxidation to the corresponding free radicals and spin-trapping with a nitrosoarene (nitrosobenzene or 3,5-di-t-butylnitrosobenzene), or by condensation of the malonate with the nitroso compound, followed by oxidation of the resulted hydroxylamine. The ESR spectra of the free radicals were recorded and the characteristic coupling constants (a_F, a_N and a_H) were measured. Diethyl phenylmalonate was condensed with hydrazobenzene to 1,2,4-triphenylpyrazolidine-3,5-dione. In conditions in which the n-butyl analog (phenylbutazone) was readily converted to a nitroxide,[1] 1,2,4-triphenylpyrazolidine-3,5-dione forms no radical detectable by ESR spetrometry. It is considered that the present results provide a new experimental proof for the steric repulsion in spin-trapping reactions of crowded free radicals with nitroso compounds. The reactivity of diethyl fluoromalonate is discussed.

1. INTRODUCTION

In the previous paper in this series[1] we have generated the nitroxide, radicals **4** in two ways. In route (i), the carbanion **2** derived from phenylbutazone **1** was either condensed with nitrosobenzene (**a**, Ar = =Ph) or with 3,5-di-*t*-butylnitrosobenzene (**b**, Ar= t-$Bu_2C_6H_3$) and the resulted hydroxylamines were oxidized to **4**. Both radicals **4a** and **4b** were thus identified by their ESR spectra :

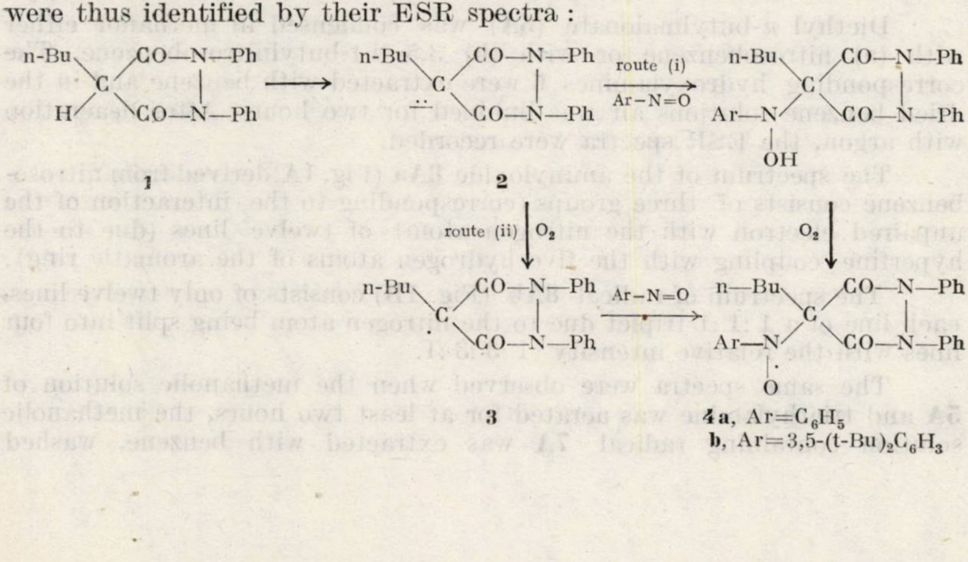

3 **4a**, Ar=C_6H_5
b, Ar=3,5-(t-Bu)$_2$$C_6H_3$

In route (ii), the carbanion **2** was oxidized to radical **3**, which was spin-trapped with the same nitroso compounds. Only radical **4a** was observed in this way by the ESR technique. We considered that the unreactivity of radical **3** must be due to the steric repulsion between the remote t-butyl groups from the nitrosoarene and the n-butyl group of radical **3**; the latter group is constrained by the bulky phenyl substituents of the pyrazolidinedione ring in a conformation which is unfavourable to the approach of the nitroso derivative to the radical centre.

In order to find other support to our interpretation, in this work we have tried to obtain new nitroxide radicals from precursors of the pyrazolidinedione ring, *i.e.* from malonic esters **5**:

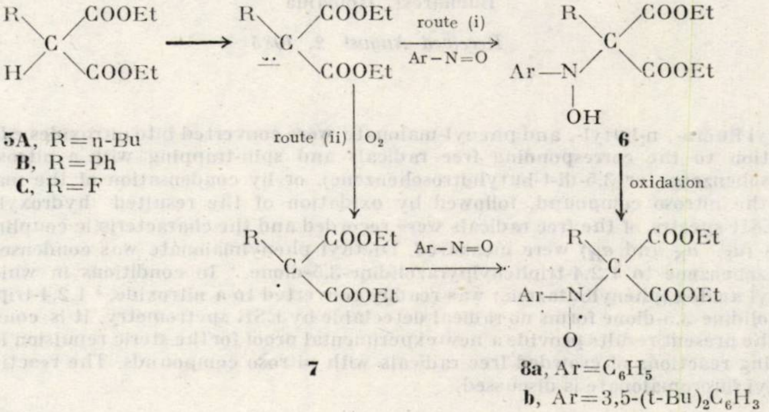

5A, R=n-Bu
B, R=Ph
C, R=F

6

7

8a, Ar=C_6H_5
b, Ar=3,5-$(t\text{-}Bu)_2C_6H_3$

Radicals **8** were generated by the two pathways, developed by us earlier.[1]

2. RESULTS

Diethyl *n*-butylmalonate (**5A**) was condensed in methanol either with (**a**) nitrosobenzene or with (**b**) 3,5-di-t-butylnitrosobenzene. The corresponding hydroxylamines **6** were extracted with benzene and in the dried benzene solutions air was bubbled for two hours. After deaeration with argon, the ESR spectra were recorded.

The spectrum of the aminyloxide **8Aa** (Fig. 1A)derived from nitrosobenzene consists of three groups (corresponding to the interaction of the unpaired electron with the nitrogen atom) of twelve lines (due to the hyperfine coupling with the five hydrogen atoms of the aromatic ring).

The spectrum of radical **8Ab** (Fig. 1B) consists of only twelve lines, each line of a 1 :1 :1 triplet due to the nitrogen atom being split into four lines with the relative intensity 1 :3 :3 :1.

The same spectra were observed when the methanolic solution of **5A** and triethylamine was aerated for at least two hours, the methanolic solution containing radical **7A** was extracted with benzene, washed with dilute acid to remove Et_3N, dried over $CaCl_2$ and finally radical **7A** was trapped either with nitrosobenzene or with di-t-butylnitrosobenzene. The characteristic coupling constants are given in table 1. Thus,

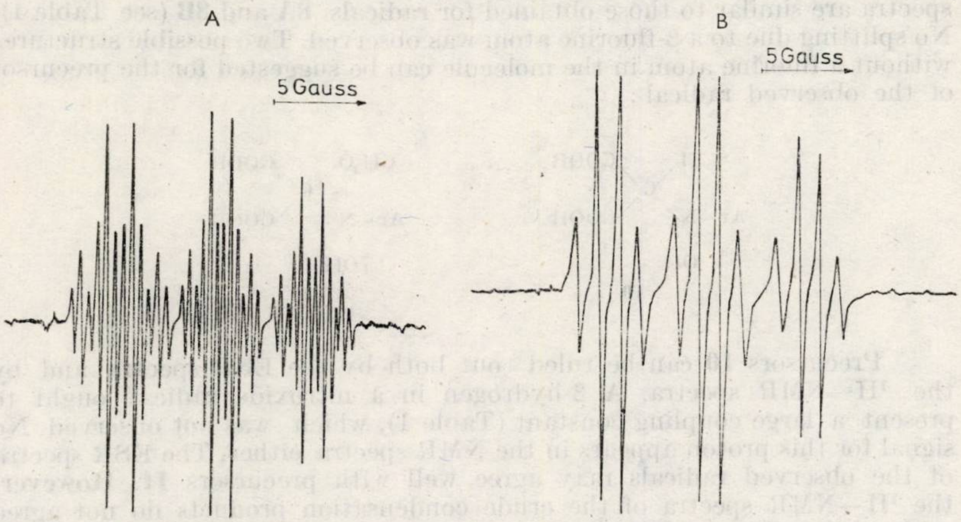

Fig. 1.A. — First derivative ESR spectra of the free radical **8Aa** formed from **7A** and nitrosobenzene;
B. — ESR spectrum of the free radical **8Ab** formed from **7A** and 3,5-di-*t*-butylnitrosobenzene.

n-butylmalonic ester **5A** behaves differently from phenylbutazone **1**, yielding in route (ii) the expected aminyloxides with both nitrosocompounds. Diethyl phenylmalonate (**5B**) manifests the same behaviour as diethyl n-butylmalonate **5A**. Radicals **8Ba** and **8Bb** were obtained readily in both routes; the coupling constants of these radicals are given in table 1. The ester was also condensed with hydrazobenzene to the pyrazolidinedione **9**:

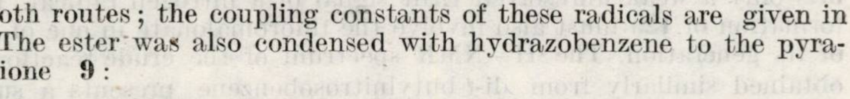

$$C_6H_5(H)C(COOEt)_2 + \begin{matrix}HN{-}Ph\\HN{-}Ph\end{matrix} \xrightarrow{-2\,EtOH} C_6H_5(H)C\begin{matrix}CO{-}N{-}Ph\\ |\\ CO{-}N{-}Ph\end{matrix}$$

In contrast with ester **5B** and phenylbutazone **1**, no nitroxide radical was detected when starting from 1,2,4-triphenylpyrazolidine-3,5-dione **9**.

Diethyl fluoromalonate **5C** was also used in this work in order to observe the fluorine coupling constant a_F due to the β-fluorine atom from the aminyloxides **8C**:

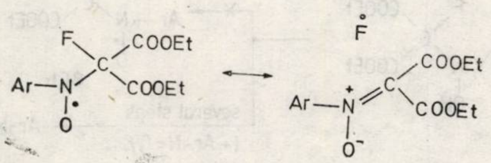

8c

By condensing the fluoromalonate with nitrosoarene in methanol in the presence of triethylamine, after oxidation of the resulted product, a nitrogen radical was identified by ESR spectrometry. The recorded spectra are similar to those obtained for radicals **8A** and **8B** (see Table 1). No splitting due to a β-fluorine atom was observed. Two possible structures without a fluorine atom in the molecule can be suggested for the precursor of the observed radical :

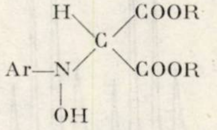

10

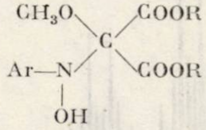

11

Precursors **10** can be ruled out both by the ESR spectra and by the ^{1}H—NMR spectra. A β-hydrogen in a nitroxide radical ought to present a large coupling constant (Table 1), which was not observed. No signal for this proton appears in the NMR spectra either. The ESR spectra of the observed radicals may agree well with precursors **11**. However, the ^{1}H—NMR spectra of the crude condensation products do not agree with the methoxy derivatives **11**. More precisely, the compound with Ar = Ph presents two triplets at δ 1.10 ppm and 1.35 ppm, respectively (6H), two ill-resolved quadruplets centered at δ 4.18 ppm (4 H) and a multiplet centered at δ 7.46 ppm (5H).

If the condensation of diethyl fluoromalonate is performed in benzene, in the presence of triethylamine, diphenylaminyloxide (**12a**) was identified by ESR spectrometry. Control experiments have shown that nitrosobenzene refluxed in benzene in the condensation conditions exhibits only a weak unresolved ESR signal of a nitrogen radical. Thus, the formation of **12a** must also involve the fluoromalonate in one of the steps of its generation. The ^{1}H—NMR spectrum of the crude reaction product obtained similarly from di-*t*-butylnitrosobenzene presents a superposed singlet (18H) and triplet (6H) at δ1.40 ppm, a quadruplet (4H) at δ4.3 ppm and two peaks in the aromatic region (2H at 7.30 ppm and 1H at 7.80 ppm). Another signal (δ 8.05 ppm, 1H) can be assigned to the hydroxylaminic proton. It seemed thus that the hydroxylamine **6Cb** was obtained but in the oxidation conditions used by us for the generation of the other mentioned radicals it does not form the expected radical **8Cb** :

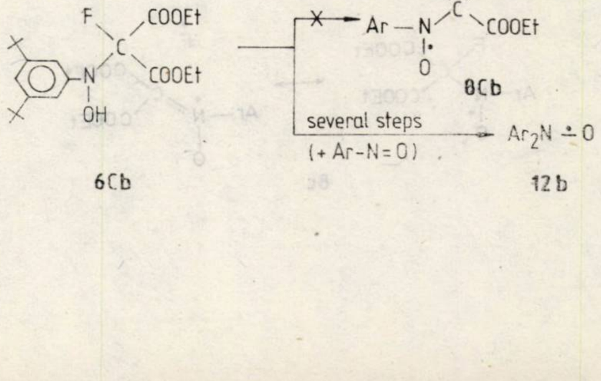

Radical **8Cb** has been observed, however, (Fig. 2) if a benzene solution of diethyl fluoromalonate and 3,5-di-t-butylnitrosobenzene was treated with lead tetracetate and the ESR spectrum was immediately recorded. The coupling constants of nitrogen (a_N) and of hydrogen (a_H) have comparable values with the values of the other known aminyloxides (Table 1), but the fluorine atom has a surprisingly large value ($a_F = 30.02$ Gauss). All nitroxide radicals obtained by us are fairly stable and can be detected even after 2–3 days.

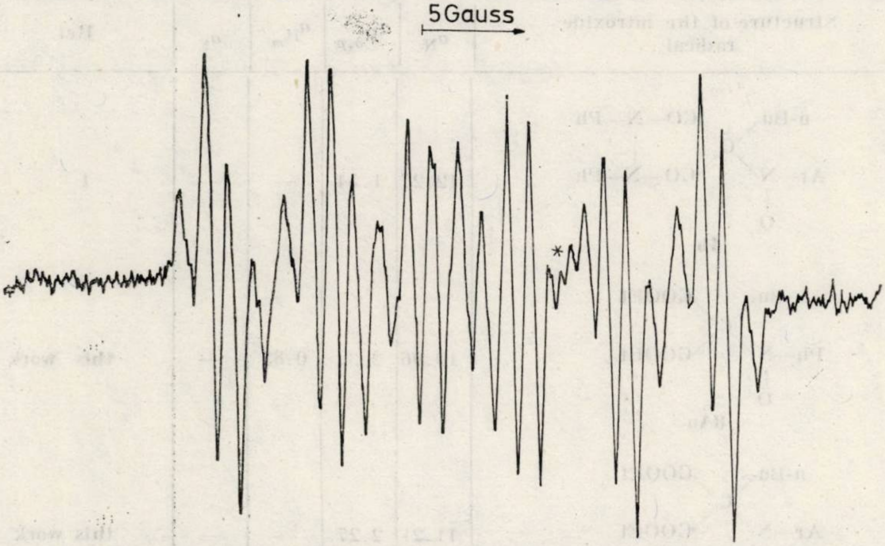

Fig. 2. — First derivative ESR spectrum of the free radical **8Cb**, resulted from the lead tetracetate oxidation of diethyl fluoromalonate in the presence of 3,5-di-*t*-butyl-nitroso-benzene. The asterisk indicates impurity peaks.

DISCUSSIONS

1. *The two routes in generation aminyloxides from malonic esters.* In this and the previous paper [1] we have generated nitroxide radicals in two ways.

In route (i) we prepared a hydroxylamine by condensation of the corresponding malonic acid derivative with a nitrosoarene, followed by oxidation to the stable aminyloxide. In route (ii), the carbanion resulted by treating the malonic ester with triethylamine, usually in methanolic solution, was aerated for at least two hours, extracted with benzene, then to the benzene solution a drop of the nitrosoarene solution was added, and the ESR spectrum was recorded immediately. The identity between the ESR spectra observed in both procedures implies the easy oxidation of the carbanions to the corresponding free radicals. In order to be able to use the experimental difference between these procedures as an argument for the following discussions, a few other comments are

Table 1

Hyperfine coupling constants (hfc's) of some nitroxide radicals (in Gauss; 10 G = 1 mT)

Structure of the nitroxide radical	a_N	$a_{H_{o,p}}$	a_{H_m}	a_F	Ref.
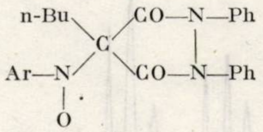 **4b**	12.27	1.54	—	—	1
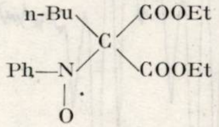 **8Aa**	10.96	2.32	0.83	—	this work
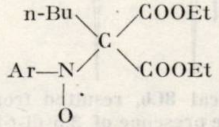 **8Ab**	11.21	2.27	—	—	this work
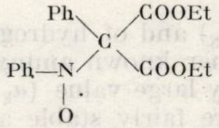 **8Ba**	11.01	2.46	0.87	—	this work
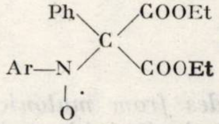 **8Bb**	11.20	2.44	—	—	this work
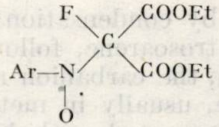 **8Cb**	10.11	2.28	—	30.02	this work
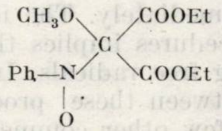 (?) **8Da**	10.42	2.42	0.35	—	this work

Table 1 (continued)

Structure of the nitroxide radical	a_N	$a_{H_{o,p}}$	a_{H_m}	a_F	Ref.
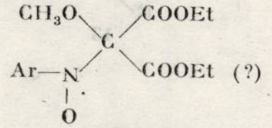 (?) **8Db**	10.70	2.41	—	—	this work
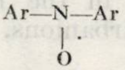 $Ar—\overset{\textstyle\cdot}{N}(O)—Ar$ **12b**	9.74	1.83	—	—	4
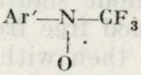 $Ar'—N(O^{\cdot})—CF_3$ **16**	9.44	—	0.70	9.44	5
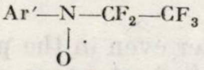 $Ar'—N(O^{\cdot})—CF_2—CF_3$ **17**	9.63	—	0.69	27.02	5
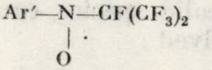 $Ar'—N(O^{\cdot})—CF(CF_3)_2$ **18**	9.73			48.4	5
a 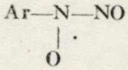 $Ar—N(O^{\cdot})—NO$ **19**	10.2	3.75	—	—	6
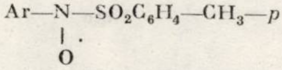 $Ar—N(O^{\cdot})—SO_2C_6H_4—CH_3—p$ **20**	11.7	1.71	—	—	6
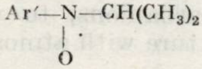 $Ar'—N(O^{\cdot})—CH(CH_3)_2$	13.07	—	0.76	22.11*	4

$Ar = 3.5—(t\text{-}Bu)_2C_6H_3$; $Ar' = 2.4.6—(t\text{-}Bu)_3C_6H_2$.

Hfc for β-fluorine

*Hfc for β-hydrogen

necessary. Thus, in using a nitroso compound as a spin trap[2] (route ii), the formation of an aminyloxide does not definitely allow the conclusion that an intermediate radical was actually trapped (reaction (1)). A carbanionic species may also react with the nitrosoarene to yield an anion **14**, which is then rapidly oxidized[3] to the nitroxide **13** (reaction (2)):

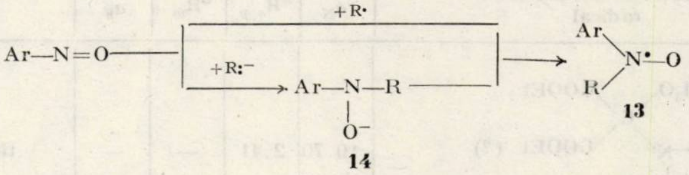

(1)

(2)

However, we consider that in route (ii) applied by us for the generation of radicals **4** and **8**, the reactive species involved in the reaction are radicals **3** and **7**, rather than the corresponding carbanions, on the basis of the following arguments:

The most convincing argument in our opinion is the procedure itself. Indeed, after prolonged aeration of the methanolic solution and extraction with benzene, the benzene extract was washed free from any base present in solution with dilute hydrochloric acid, then with water, with calcium chloride solution and finally dried over calcium chloride. No carbanion could be present in the mixture before adding the nitroso compound.

Secondly, the condensation of the malonic ester even in the presence of triethylamine with the nitrosoarene is not an instantaneous process; it requires several hours for completion.

However, in our procedure (ii) other radicalic species cannot be ruled out. Reactions (3) and (4) may also be involved:

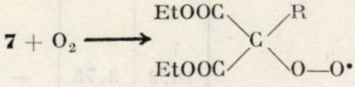

15

(3)

$$\mathbf{15} + \mathbf{5} \longrightarrow (EtOOC)_2CR{-}OOH + \mathbf{7} \qquad (4)$$

etc.

Anyway, our results indicate the easy oxidation of the carbanions derived from malonic esters to the corresponding radicals. Thus, it is not superfluous, even in working with stable carbanions, to exclude carefully the intimate contact of the reaction mixture with atmospheric oxygen.

2. *The ESR spectra of the observed aminyloxides* **8**. The interpretation of ESR spectra is straightforward: the spectrum of radical **8Aa** consists of a 1:1:1 triplet of phenyl proton multiplets (12 lines forming a 1:3:3:1 quartet of 1:2:1 triplets). In this decreasing order of magnitude the hyperfine coupling constants are ascribed to the nitrogen atom, the three *o*-, *p*-protons, and the two *m*-protons (Table 1). The spectrum of radical **8Ab** consists of a 1:1:1 triplet of 1:3:3:1 quartets; the splittings are assigned to the nitrogen atom and to the three *o*-, *p*- protons, respectively (Table 1).

The ESR spectrum of radical **8Cb** (Fig. 2) is much more extended than the preceding spectra and has four marginal 1 :3 :3 :1 quadruplets and an overlapping central region. It can be easily seen that this spectrum is a 1 :1 doublet of 1 :1 :1 triplets of 1 :3 :3 :1 quadruplets. The large splitting due to ^{19}F (1 :1 doublet) can be measured from the centre of the second quadruplet to the centre of the last but one multiplet. The triplet splitting is a_N and the quadruplet splitting is the *o*-, *p*-hydrogen splitting.

3. *Remote steric effects in spin-trapping reactions.* The rigidity of the 1,2- diphenylpyrazolidine-3,5-dione ring and the bulkiness of the phenyl substituents were considered by us[1] as responsible for the lack of reactivity of radical **3** towards 3,5-di-t-butyl-nitrosobenzene. The 1,2-diphenyl groups constrain the butyl substituent to point in a direction which may interfere with the t-butyl groups from the nitroso compound. If this interpretation is correct, it follows that in the less rigid radical **7A** derived from n-butylmalonic ester, the access of the nitroso reagent to the radicalic centre will be facilitated so that both nitrosobenzene and 3,5-di-t-butylnitrosobenzene may yield a nitroxide radical. This was actually observed.

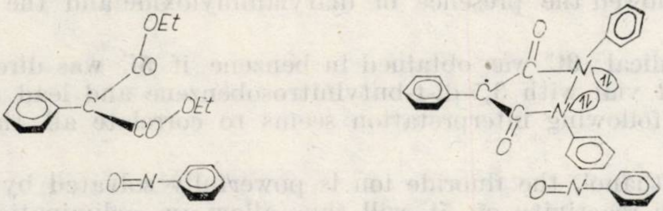

Fig. 3. — Model of the attack by the nitroso compound on the free radical **7B** and on the free radical derived from 1,2,4-tri-phenylpyrazolidine-3,5-dione.

Diethyl phenylmalonate **5B** and the corresponding pyrazolidinedione **9** deserve a special discussion. The radical **7B** derived from phenylmalonate is easily trapped by both nitrosoarenes. Conversely, both the carbanion and the radical generated from **9** do not react even with nitrosobenzene. A possible interpretation is shown in Fig. 3. In order to avoid the bulky phenyl group, the nitroso compound attacks the radicalic centre in **7B** from the esteric part of the molecule. In the pyrazolidinedione system neither direction of attack is favourable. The present results confirm the previous assumed steric effects in spin-trapping reactions.

4. *The reactivity of the fluoromalonate ester.* Our efforts to generate the aminyloxide **8C** can be summarized as follows : a) In methanol, **5C** with nitroso compound and in the presence of triethylamine yields a product which according to its ^1H-NMR spectrum has two ethyl groups and an aryl group, but not a β-fluorine or a β-hydrogen (according to the ESR spectrum of the oxidation product). However, the oxidation product exhibits an ESR spectrum which agrees well with a methoxy radical

8D, even if the structure of its precursor (**11**) was not confirmed by NMR.

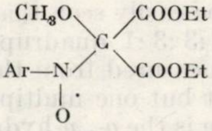

8D

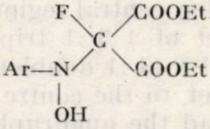

22

b) The condensation of **5C** with the nitroso compound in benzene and in the presence of triethylamine yields a product which according to its NMR spectrum may correspond to the hydroxylamine **22**. However, after bubbling air in the benzene solution of **22**, the recorded ESR spectrum showed the presence of diarylaminyloxide and the absence of radical **8C**.

c) Radical **8C** was obtained in benzene if **5C** was directly mixed in the ESR vial with 3,5-di-t-butylnitrosobenzene and lead tetracetate.

The following interpretation seems to correlate all the observed results :

In methanol, the fluoride ion is powerfully solvated by the protic solvent. The reactivity of **5C** will thus allow an α-elimination to yield carbene **23**. A rapid insertion reaction will lead to the methoxy ester **5D** :

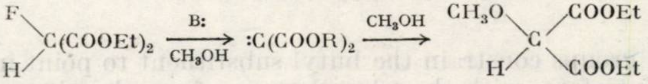

5C **23** **5D**

Ester **5D** will behave similarly with the other esters **5A**–**C** and will lead to radical **8D**. However, in the experiments in which the isolation of the intermediate hydroxylamine was tried, the intermediate carbene **23** was trapped by the nitrosobenzene, forming a nitrone **24**. It is well known that nitrones may be obtained from nitroso compounds with precursors of carbenes :[7]

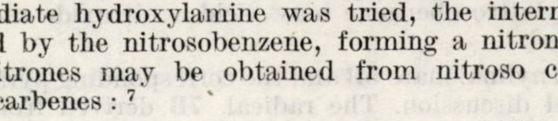

23 **24**

The ^1H–NMR spectrum of the condensation product agrees well with the structure of nitrone **24**.

In benzene, an aprotic solvent, fluorine would have no tendency to ionize. Hydroxylamine **22** can be thus isolated, as shown by its ^1H–NMR spectrum. However, if **22** is further aerated, due to the presence of triethylamine and to a lower reactivity of the compound, an elimination reaction takes place leading to the same nitrone **24** :

$$\mathbf{22a} \xrightarrow[-Et_3NH^+F^-]{+Et_3N} \mathbf{24a} \longrightarrow \cdot O{-}N{=}C((COOEt)_2 + C_6H_5\cdot$$

$$C_6H_5\cdot + C_6H_5{-}N{=}O \longrightarrow \underset{\mathbf{12a}}{(C_6H_5)_2N{\dot{-}}O}$$

The nitrone **24** may be responsible for the generation of diphenylaminyloxide **12a**. Actually, the ESR spectrum in which **12a** was detected shows the presence of another nitrogen radical.

EXPERIMENTAL

Diethyl phenylmalonate was prepared by the known procedure[8] from ethyl phenyl acetate and diethyl oxalate. *Diethyl n-butylmalonate* was obtained by alkylation of diethyl malonate with n-butylbromide. *Diethyl fluoromalonate* was from Riedel-De Haën. All products were gas-chromatographically pure.

Condensation of diethyl phenylmalonate with hydrazobenzene. The method of Ruhkopf[9] was applied in the synthesis of pyrazolidinedione **9**. The crude condensation product was recrystallized from ethanol, mp. 137°, in perfect agreement with literature.[10].

Preparation of radicals **8** *by route* (*i*). The procedure described previously[1] was applied, with the difference that no attempt was made in order to isolate the intermediate hydroxylamine. The benzene solution containing **6** was vigorously shaken with air and the ESR spectra were recorded (Fig. 1). The calculated coupling constants of the observed radicals are given in table 1.

Trapping of radicals **7A—7B** *with nitrosoarenes* by route (ii). Diethyl malonate **5A** or **5B** (0.01 mol) was dissolved in 20 mL methanol and 1 mL (0.01 mol) triethylamine was added. Air was bubbled in to the methanolic solution for 3 hours. The yellowish solution was then diluted with benzene, was washed with water (2 × 25 mL), then the solution was washed with dilute hydrochloric acid (2 × 10 mL) and with 10 % calcium chloride solution and finally it was dried over $CaCl_2$. The benzene solution was concentrated to about 10 mL *in vacuo*, a drop of a benzene solution of the nitrosoarene was added and, after deaeration with argon, the ESR spectra were immediately recorded. The same spectra as those obtained in route (i) were observed.

Condensation of diethyl fluoromalonate with nitrosoarenes in methanol. Diethyl fluoromalonate (0.1 mL, about 1 mmol) treated either with nitrosobenzene or with 3,5-di-t-butylnitrosobenzene,[11] according to the procedure described for route (i), yields ESR spectra corresponding to radicals **8Da** and **8Db**, respectively (Table 1). In a preparative run, with about 0.5 ml fluoromalonate, the residue obtained after removing *in vacuo* the solvent gave a ^1H—NMR spectrum which may be attributed to nitrone **24** (see text).

Condensation of diethyl fluoromalonate with nitrosoarenes in benzene. Diethyl fluoromalonate (0.25 mL, about 2 mmol) was dissolved in 20 mL benzene containing 0.4 g (2 mmol) 3,5-di-t-butylnitrosobenzene and 0.2 mL triethylamine. The solution was refluxed for 1.5 hours, then it was washed with water, dried over $CaCl_2$, and benzene was removed *in vacuo*. The ^1H—NMR spectrum of the residue corresponds to the hydroxylamine **6C** (a superposed singlet and triplet at δ 1.40 ppm, 18H; a quadruplet (4H) at $\delta = 4.3$ ppm, 2H at $\delta = 7.30$ ppm, 1H at $\delta = 7.80$ ppm and 1H at $\delta = 8.05$ ppm). The solid residue was dissolved in dry benzene, air was bubbled for two hours and the ESR spectrum was recorded. The spectrum reveals the presence of two nitrogen radicals, one of them being a 1 :1 :1 triplet and the other having the characteristics of diarylaminyloxide **12b** (Table 1).

Preparation of radical **8Cb**. In an ESR vial, 0.3 mL benzene was mixed with one crystal of 3,5-di-t-butylnitrosobenzene and 0.05 mL diethyl fluoromalonate. After homogenization of the solution, 2—3 crystals of lead tetracetate were added and the ESR spectrum was recorded.

The ESR determination of the radicals. The spectra were recorded on a Romanian-made ART-5 spectrometer, in the X-band frequency (9060 MHz), using peroxylamine disulphonate as internal standard ($a_N = 13$ Gauss; $g = 2.0055$).

ACKNOWLEDGEMENTS. The authors are indebted to Dr. F. Chiraleu for recording the ^1H—NMR spectra and to Dr. M. T. Căproiu for a kind supply of 3,5-di-t-butylnitrosobenzene. A generous gift of diethyl fluoromalonate from Riedel-De Haën is gratefully acknowledged.

REFERENCES

[1] F. Badea, F. Iordache, A. Meghea, A. T. Balaban, R. Marinescu and A. M. Ghivirigă, *Rev. Roumaine Chim.*, **30**, 189 (1985).

[2] E. G. Janzen, *Acc. Chem.Res.*, **4**, 31 (1971).

[3] A. R. Forrester and S. P. Hepburn, *J. Chem.Soc.*, (C) *1971*, 701 ; H. G. Aurich and W. Weiss,, *Topics Current Chem.*, **59**, 65 (1975).

[4] Th. A. J. W. Wajer, A. Mackor, Th. J de Boer and J.D.W. van Voorst, *Tetrahedron*, **23**, 4021 (1967).

[5] Sh. Terabe and R. Konaka, *Bull. Chem.Soc.Japan*, **46**, 825 (1973).

[6] M. T. Căproiu, Ph. D. Thesis, Bucharest, 1984 ; M. T. Căproiu, N. Negoiță and A. T. Balaban, *Tetrahedron Lett.*, **1977**, 1825.

[7] F. Sachs and H. Barschall, *Ber. dtsch. chem. Ges.*, **35**, 1238 (1902) ; A. Kaufmann and L. G. Valette, *ibid.*, **45**, 1793 (1912) ; F. Barrow and F. J. Thorneycroft, *J. Chem. Soc.*, **1934**, 722 ; T. D. Perrine and L. S. Sargent, *J. Org. Chem.*, **14**, 583 (1949).

[8] P.A. Levene and G. M. Mayer, Org. Synth., Coll. Vol. **2**, 288 (1943).

[9] H. Ruhkopf, *Ber. dtsch. chem. Ges.*, **73**, 820 (1940).

[10] R. Takaganaki and K. Fujii, Japan Pat. 3226 (1955) ; cf. *Chem. Abstr.*, **51**, 16561 (1957).

[11] H. G. Aurich, *Chem.Ber.*, **101**, 1761 (1968).

Revue Roumaine de Chimie, **31**, *2*, 131—136 (1986)

THE SYNTHESIS OF SOME 3-OXO-4-ENE-B-NOR-DERIVATIVES. OPPENAUER OXIDATION OF 3β-HYDROXY-5-ENE-B-NOR-STEROIDS WITH Al_2O_3

ROBERT SCHWARTZ and ANIKÓ JUHÁSZ
Chemical and Pharmaceutics Research Institute
Str. Fabricii Nr. 126, 3400 Cluj-Napoca, Romania

Received March 8, 1985

The synthesis of some 3-oxo-4-ene-B-nor-derivatives starting from the corresponding 3β-hydroxy-5-ene-B-nor-derivatives is presented. The oxidation was attempted with aluminium oxide as oxidizing agent. The reaction conditions and some factors influencing the reaction time and hence the reaction rate are discussed.

INTRODUCTION

A modified Oppenauer oxidation of some 3β-hydroxy-5-ene steroids using aluminium oxide (II—III activity on the Brockmann scale) as oxidizing agent was studied in a previous paper. [1] The promising results prompted us to try also the synthesis of 3-oxo-4-ene-B-nor-derivatives using this oxidant (Al_2O_3). The literature data [2–14] indicate the synthesis of 3-oxo-4-ene-B-nor-derivatives starting from 3β-hydroxy-5-ene-B-nor-derivatives using the classic Oppenauer oxidation, that is with an aluminium alkoxide (isopropoxide or t-butoxide) which is soluble in the reaction medium.

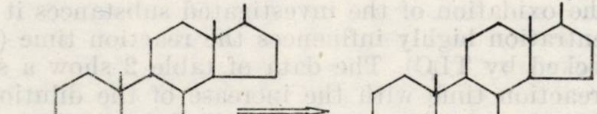

RESULTS AND DISCUSSION

The main problem was the choice of the most adequate working conditions, that is: the best solvent, the Al_2O_3/steroid ratio and the hydride-acceptor.

The tentative experiences demonstrated that one of o-, m- or-p-xylene was the adequate solvent as the oxidation process takes place easier at the boiling temperature of these solvents (at the boiling temperature of benzene or toluene the course of the oxidation was very slow).

The experiences made in order to establish the Al_2O_3/steroid ratio indicated a decrease of the reaction time with the increase of the quantity of aluminium oxide (Table 1). On the basis of these experiences we chose a 2 :1 proportion. This ratio permitted the use of a relatively reduced quantity of Al_2O_3, the decrease of the reaction time to a satisfactory value and the complete transformation of the starting material.

Table 1

The influence of the Al_2O_3/steroid ratio on the reaction time

No	3β-Hydroxy-B-nor-5-cholestene g	Al_2O_3 g	Acetone mL	o-Xylene mL	Reaction time min.
1	1.0	1.0	1.0	100.0	960
2	1.0	2.0	2.0	100.0	150
3	1.0	3.0	2.0	100.0	60
4	1.0	3.0	3.0	100.0	35
5	1.0	4.0	4.0	100.0	35

The initial experiences were accomplished according to the literature data [1–16] using cyclohexanone as hydride-acceptor. Acetone was also used for this purpose. The redox potential of acetone proved to be suited for this oxidation and it had also the advantage to permit an easier working-up of the reaction mixture. The oxidation with acetone failed in the case of 17ß-benzoyloxy-B-nor-5-androstene-3ß-ol and of the lactone of 3-(3ß, 17ß-dihydroxy-B-nor-5-androstene-17α-yl) propanoic acid. The complete oxidation of these derivatives was feasible only with cyclohexanone.

During the oxidation of the investigated substances it was observed that the concentration highly influences the reaction time (the oxidation course was checked by TLC). The data of table 2 show a significant decrease of the reaction time with the increase of the dilution till a given value, after this the reaction time remained approximately the same. At a very large dilution an increase of the reaction time was observed.

The oxidation of 3ß-hydroxy-B-nor-5-cholestene and of 3ß-hydroxy--B-nor-5-androstene-17-one was also attempted without a hydride-acceptor. The steroid and Al_2O_3 were refluxed under stirring and the water trapped in the active centers of Al_2O_3 was azeotropically distilled off. In both cases the "oxidation" or more exactly the action of Al_2O_3 was pointed on chromatographic plates (TLC). The starting material dissapeared completely and the reaction products could be visualised. In the case of 3ß-hydroxy-B-nor-5-cholestene the separation (by crystallization from methanol) and the identification of B-nor-3,5-cholestadiene, m.p. : $[\alpha]_D^{20}$ 72–74°C, −112° (c = 1, $CHCl_3$) (literature [17,18] : m. p. : 73–74 resp. 76°C, $[\alpha]_D^{20}$: −116 ± 1°, c = 1,14, $CHCl_3$) as main reaction product

Table 2

The influence of the concentration on the reaction time

No.	3 β-Hydroxy--B-nor-5--cholestene g	Al_2O_3 g	Acetone mL	o-Xylene mL	Conc. % (w/v)	Reaction time min.
1	1.0	2.0	2.0	20.0	5.00	600
2	1.0	2.0	2.0	25.0	4.00	240
3	1.0	2.0	2.0	33.0	3.00	120
4	1.0	2.0	2.0	50.0	2.00	120
5	1.0	2.0	2.0	65.0	1.56	120
6	1.0	2.0	2.0	100.0	1.00	120
7	1.0	2.0	2.0	100.0[a]	1.00	600
8	1.0	2.0	2.0	125.0	0,80	60
9	1.0	2.0	2.0	150.0	0.66	60
10	1.0	2.0	2.0	200.0	0.50	60
11	1.0	2.0	2.0	250.0	0.40	60
12	1.0	2.0	2.0	256.0	0.39	[b]
13	1.0	2.0	2.0	263.0	0.38	[b]
14	1.0	2.0	2.0	280.0	0.35	[b]
15	1.0	2 0	2.0	350.0	0.28	[c]
16	1.0	2.0	2.0	1000.0	0.10	[c]

[a] toluene; [b] the oxidation was stopped at a conversion of 80—90%, the complete transformation being not feasible; [c] the oxidation was not possible.

was feasible. The separation and identification of the other products was not possible.

In the case of 3β-hydroxy-B-nor-5-androstene-17-one the separation and the identification of the reaction products failed. However a substance having the same Rf value as the 3,17-dione obtained through an oxidation with a hydride-acceptor was visualised from the reaction mixture. These observations confirm the necessity of the presence of a ketone as hydride-acceptor.

In order to make a preliminary study regarding the effect of the Al_2O_3 activity on the oxidation course, experiences with Al_2O_3 having I and II—III activities were accomplished. A few drops of water were also added to the reaction mixture with or without the azeotropic distillation of the water during the oxidation. The obtained results suggest that if the elimination of the water during the reaction is achieved the initial water content of Al_2O_3 is not important. The experiences accomplished without removing the water (using only refluxing without a water-separator) failed.

CONCLUSIONS

The observations that the oxidation of steroids can be achieved only if the water attached to the Al_2O_3 surface is removed and that the incomplete poisoning of Al_2O_3 with pyridine exaggerately lengthens the reaction time suggest that the active centres with acidic character (Brönsted or Lewis) on the aluminium oxide surface play an important part in the oxidation. The imperative necessity of a ketone as hydride-acceptor

Table 3

Some of the prepared 3-oxo-4-ene-B-nor-derivatives

No	Starting material	Reaction product	Analytical data	Yield in pure subst. %
1	2	3	4	5
1	3 β-Hydroxy-B-nor-5-cholestene	B-nor-4-Cholestene-3-one	m.p.: 68—70°C $[\alpha]_D^{20}$: —1.5° E_1^1: 500 $\lambda_{max.}$: 243 nm	66—70
2	B-nor-Diosgenin	B-nor-4-Diosgenin-3-one	m.p.: 178—181 °C $[\alpha]_D^{20}$: —108.4°* E_1^1: 388 $\lambda_{max.}$: 240 nm	73—75
3	3 β-Hydroxy-B-nor-5-pregnene-20-one	B-nor-Progesterone	m.p.: 145—147 °C $[\alpha]_D^{20}$: + 68.6° E_1^1: 474 $\lambda_{max.}$: 242 nm	54—60
4	3 β-Hydroxy-B-nor-5-androstene-17-one	B-nor-4-Endrostene-3,17-dione	m.p.: 142—143°C $[\alpha]_D^{20}$: + 63° E_1^1: 549 $\lambda_{max.}$: 240 nm	65—70
5	3 β,17β-Dihydroxy-B-nor-5-androstene-			
6	17 α-Methyl-3β, 17β-dihydroxy-B-nor-5-androstene	17α-Methyl-B-nor-testosterone	m.p.: 151—154°C $[\alpha]_D^{20}$: — 32.8° E_1^1: 498 $\lambda_{max.}$: 240 nm	60—65
7	17 α-Ethyl-3β, 17β-dihydroxy-B-nor-5-androstene	17 α-Ethyl-B-nor-testosterone	m.p.: 126—127°C $[\alpha]_D^{20}$: — 37.6° E_1^1: 467 $\lambda_{max.}$: 240 nm	60—65
8	17 α-Ethynyl-3β, 17 β-dihydroxy-B-nor-5-andros tene	17α-Ethynyl-B-nor-testosterone	m.p.: 244—247°C $[\alpha]_D^{20}$: — 54. 2° E_1^1: 512 $\lambda_{max.}$: 240 nm	60—65
9	17 α-Allyl-3-β,17 β-dihydroxy-B-nor-5-androstene	17α-Allyl-B-nor-testosterone	m.p.: 147—148°C $[\alpha]_D^{20}$: — 18.5° E_1^1: 436 $\lambda_{max.}$: 242 nm	65—70
10	3 β-hydroxy-17β-benzoyloxy-B-nor-5-androstene	B-nor-Testosterone-17β-benzoate	m.p.: 214—216°C $[\alpha]_D^{20}$: + 45.6° E_1^1: 680 $\lambda_{max.}$: 243 nm	63—66

The specific optical rotations are for chloroform solutions, c = 1
*c = 4

Table 3 (cont inued)

1	2	3	4	5
11	3-(3β,17 β-Dihydroxy-B-nor-5-androstene-17α-yl) propanoic acid lactone	3-(3-oxo-17β-hydroxy-B-nor-4-androstene-17α-yl) propanoic acid lactone	m.p. : 156—158°C $[\alpha]_D^{20}$: — 30.3° E_1^1 : 407 $\lambda_{max.}$: 240 nm	70—75
12	2β-hydroxy-B-nor-5-androstene-17-ketal	B-nor-4-Androstene-3,17-dione-17-ketal	m.p. : 122—124°C $[\alpha]_D^{20}$: —29.5° E_1^1 : 380 $\lambda_{max.}$: 243 nm	74—77

confirms the Oppenauer character of this oxidation, i.e. the probability that an intermediary six-membered cyclic complex could be formed.

Table 3 presents some of the synthesized 3-oxo-4-ene-B-nor-derivatives (17α-allyl-B-nor-testosterone and the lactone of 3-(3-oxo-B-nor-4-androstene-17β-ol-17α-yl) propanoic acid are not described in the literature). The obtained yields are comparable with those presented in the literature.

EXPERIMENTAL

Melting points are uncorrected. The ^{1}H—NMR and ^{13}C—NMR spectra were recorded with a Varian XL 100 spectrophotometer. The substances were dissolved in $CDCl_3$ and as internal reference standard TMS was used. The UV spectra (in ethanol) were recorded with a Specord UV VIS C. Zeiss Jena spectrophotometer. The completion of the reaction and the purity of the prepared compounds were checked by TLC.

To a stirred solution of 1 part (g) of 3β-hydroxy-5-ene-B-nor-derivative in 100 parts (mL) of xylene 2 parts (g) of Al_2O_3 (II — III activity) and 2 parts (mL of acetone are added. The reaction mixture was refluxed and the water was eliminated (distilled off azeotropically). The end of the oxidation was controlled by TLC. After cooling the aluminium oxide was filtered off. The filtrate was concentrated on the water-bath in vacuo. The crude product was crystallized from the adequate solvent.

Example 1

1 g (0.003 mol) of) of 3β -hydroxy-B-nor-5-pregnene-20-one were dissolved in 100 mL of p-xylene. To the obtained solution 2 g (0.020 mol) of aluminium oxide and 2 mL (0.026 mol) of acetone were added. The mixture was refluxed 2 hours with the simultaneous elimination of the water. After cooling, the Al_2O_3 was filtered off and the filtrate was concentrated. The crude product (a pale-yellow oil) was crystallized from ligroine and purified from methanol yielding 0.7 g of B-nor-progesterone, ^{1}H—NMR δ, ppm, $cDCl_3$, TMS :5.78 m C(4)H, 0.69 s C(18) H_3, 1.08 s C(19)H_3, 2.13 s C(21)H_3 ^{13}C—NMR δ, ppm, $CDCl_3$, TMS : 35 · 31 C_1, 33 · 55 C_2, 199 · 05 C_3, 122 · 59 C_4, 178.14 C_5, 34.34 C_6, 38.17 C_8,58.09 C_9, 48.85 C_{10}, 20.77 C_{11}, 38.52 C_{12}, 45.55 C_{13}, 56.03 C_{14}, 24.64 C_{15}, 23.20 C_{16}, 62.90 C_{17}, 13.79 C_{18}, 17.41 C_{19}, 209.06 C_{20}, 31.46 C_{21}.

Example 2

To a stirred solution of 2 g (0.006 mol) of 17 α-ethynyl-B-nor-5-androstene-3β, 17 β-diol in 200 mL of p-xylene 4 g (0.040 mol) of aluminium oxide (II—III activity) and 4 mL (0.050 mol) of acetone were added. The mixture was refluxed 2.5 hours with elimination of the water. The crude product was crystallized from acetone to yield 1.25 g 17 α-ethynyl-B-nor-testosterone, ^{1}H—NMR δ, ppm, $CDCl_3$TMS : 5 .72mC(4)H, 0.90 sC(18)H_3, 1.08 s C(19) H_3, 2.53 s≡C(21)H ; δ, ppm, $CDCl_3$, TMS ; ^{13}C—NMR, δ, ppm, $CDCl_3$TMS : 35.36 C_1, 34.30 C_2, 199.79 C_3, 122.85 C_4, 178.77 C_5, 39.19 C_6, 38.97 C_8, 58.02 C_9, 43.87 C_{10}, 20.48 C_{11}, 32.65 C_{12}, 48.61 C_{13}, 50.22 C_{14}, 23.47 C_{15}, 33.64 C_{16}, 79.42 C_{17}, 13.07 C_{18}. 17.46 C_{19}, 87.66 C_{20}, 74.16 C_{21}.

REFERENCES

[1] A. Bodor, R. Schwartz and D. Breazu ; *Revista de Chimie*, **27** (11), 929(1976).

[2] J. Joska, J. Fajkos and F. Sorm ; *Chem. and Ind.*, 1665 (1958).

[3] J. Joska, J. Fajkos and F. Sorm ; *Coll.Czech. Chem. Comm.*, **25**, 1086 (1960).

[4] J. Joska, A, A. Ahrem, J. Fajkos and F. Sorm ; *Coll.Czech.Chem., Comm.*, **26**, 2050 (1961).

[5] J. F. Kerwin ; U.S. Pat. 3072681/1963 ; *C.A.*, **59**, 1723 (1963).

[6] J. Joska, J. Fajkos and F. Sorm ; *Coll. Czech. Chem. Comm.*, **31**(1), 298 (1966).

[7] K. G. Holden and J. F. Kerwin ; Belg. Pat. 665.116/1965 ; *C.A.*, **65**, 7739(1966).

[8] J. F. Kerwin ; U.S. Pat.3334140/1967 ; *C.A.*, **67**, 100332m (1967).

[9] K. G. Holden ; U.S.Pat. 3300489/1967 ; *C.A.*, **66**, 115887z (1967).

[10] K. G. Holden and J. F. Kerwin ; U. S. Pat. 3375280/1968 ; *C. A.*, **69**, 7763 on (1968).

[11] V. Sanda, J. Fajkos and F. Sorm ; *Coll. Czech. Chem. Comm.*, **35**, 3445 (1970).

[12] J. Joska, J. Fajkos and F. Sorm ; *Coll. Czech. Chem. Comm.*, **38** (7), 2121 (1973).

[13] V. Sanda, J. Fajkos and F. Sorm ; *Coll. Czech. Chem. Comm.*, **39** (5), 1377 (1974).

[14] J. Joska and J. Fajkos ; *Coll. Czech. Chem. Comm.*, **42**, 1045 (1977).

[15] K. R. Bharucha ; *Experimentia*, **14**, 5 (1958).

[16] F. Hodoşan, N. Şerban, A. Balogh and I. Jude ; R.S.R. Pat. 57740/1974 ; *C. A.*, **84**, 165117, (1976).

[17] J. Joska and J. Fajkos ; *Coll. Czech. Chem. Comm.*, **32** (11), 3941 (1967).

[18] F. Sorm ; *Coll. Czech. Chem. Comm.*, **12**, 436 (1947).

Revue Roumaine de Chimie, **31**, *2*, 137—141 (1986)

DISUBSTITUTED PHENOTHIAZONES. IV[1]

CHLORO-4-NITRO- AND -7-NITRO-3H-PHENOTHIAZIN-3-ONES

MARIUS H. TERDIC
Institute of Chemistry, str. Fintinele 30,
3400 — Cluj-Napoca, Romania

Received March 4, 1985

The preparation of four isomeric chloro-4-nitro-3H-phenothiazin-3-ones by direct nitration of the corresponding chloro-derivatives was described. The 7-nitro- and 2-chloro-7-nitro-3H-phenothiazin-3-ones were also synthetized by oxidation of the corresponding nitro-phenothiazines (Table 1). The IR and UV/Vis spectra present clear differences between 4-nitro- and 7-nitro-3H-phenothiazin-3-ones.

In recent works [2,3] the preparation of some monochloro-3H-phenothiazin-3-ones (chloro-phenothiazones) was described. It was pointed out that these substances may serve as starting compounds for other reactions such as the selective halogenation in the position 4. Carrying on these investigations we subjected the compounds to the selective nitration which also took place in position 4. This reaction, known from our previous works[4,5] was now applied with some modifications.

Thus, chloro-phenothiazones **1a — d** by treating with nitric acid at room temperature were transformed into chloro-4-nitrophenothiazones **2a — d**.

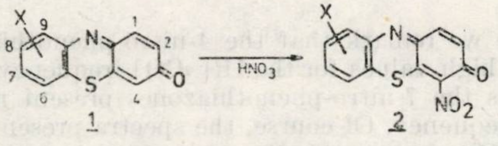

a · X = 1-Cl
b · X = 6-Cl
c · X = 8-Cl
d · X = 9-Cl

We obtained in this way four new isomers with good yields (see Table 1). These isomers are important for the phenothiazone chemistry because they have completed the chloro-4-nitro-phenothiazone series. The colour of the substances **2a — d** in methanol or acetone solution is orange.

By direct nitration it was not possible to introduce the NO_2-group in other positions of the phenothiazone ring. In order to obtain phenothiazones carring the nitro-group in the position 7 we have operated inversely: first it was prepared the 3-nitro-phenothiazines **3a** — **b** which were then oxidized in the usual way with potassium dichromate in glacial acetic acid in order to obtain the corresponding 7-nitro-phenothiazones **4a** — **b**. (The positions 3 and 7 in the phenothiazine are equivalent).

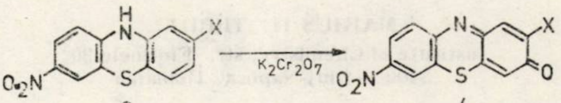

3   4

a . X = H
b . X = Cl

The compounds **4a** — **b** are the first representatives of a new series of phenothiazone-derivatives carring the nitro-group in the position 7. The methanol or acetone solutions of the compounds **4a** — **b** are red-coloured. Table 1 presents the yield, melting points, analyses and the IR[νCO] values of the synthetized compounds.

Table 1

Chloro-nitro-phenothiazones obtained by nitration and oxidation

Substituted phenothiazone (substituent)		Yield %	m.p. °C	Nitrogen %		IR[ν CO] cm^{-1}
				calc.	found	
1-Chloro-4-nitro-	(**2a**)	41	255—9	9.57	10.02	1654
6-Chloro-4-nitro-	(**2b**)	63	264—8	9.57	9.40	1651
8-Chloro-4-nitro-	(**2c**)	65	240—1	9.57	9.89	1655
9-Chloro-4-nitro-	(**2d**)	61	263—5	9.57	10.84	1656
7-Nitro-	(**4a**)	19	221—3	10.85	10.72	1631
2-Chloro-7-nitro-	(**4b**)	30	263—5	9.57	9.40	1619

In this table we remark that the 4-nitro-phenothiazone derivatives present unusually high values for the IR[νCO] frequency, between 1651—1656 cm^{-1} whereas the 7-nitro-phenothiazones present normal values for the IR carbonyl frequency. Of course, the spectra present also the characteristic bands of NO_2-group at 1560—1500 cm^{-1} but the examination of these bands does not show differences between 4-nitro- and 7-nitro-phenothiazones.

3-Nitro-phenothiazine (**3a**) was prepared according to Daneke and Wanzlick[6] but the reaction product contained considerable amounts of iron hydroxide, so that the chromatographic purification was necessary (see the experimental part).

The UV/Vis spectra were recorded in methanol solution. Beside the compounds whose preparation is described in this work, the spectra of phenothiazone, 4-nitro-, 2-chloro- and 7-chloro-4-nitrophenothiazones known from our previous works[4,5] were also recorded; their spectra in methanol have not been published yet. In Fig. 1 the spectra of phenothiazone, 4-nitro- and 7-nitro-phenothiazone are compared.

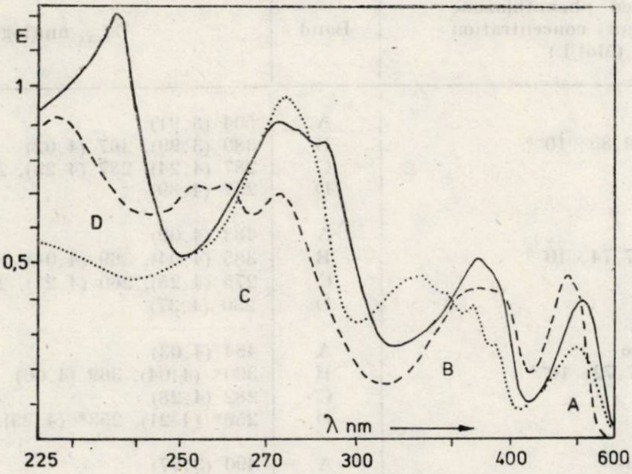

Fig. 1. — UV/Vis spectra of phenothiazone(———), 4-nitro- (— — —) and 7-nitro-phenothiazone (. . . . . . .).

All compounds present four bands noted A,B,C and D. The nitro-group from the position 4 produces a strong hipsochromic effect (upon the band A), therefore these substances are orange. If the nitro-group is substituted in position 7 the hypsochromic effect is very weak, therefore the substances belonging to this series give red coloured solutions. In Table 2 the UV/Vis spectra of all known chloro-nitro-phenothiazones are presented.

The A band is in all cases an isolated band situated at the longest wavelength, in visible region. Chloro-4-nitro-phenothiazones have this band at 485 ± 9 nm. An interesting observation is that the A band of all compounds of this series presents a weak shoulder on the longer wavelength side which was not observed with any other compound. This detail together with the orange colour of the methanolic solution permit the reliable identification of the nitro-group in the position 4.

In Table 2 we observe further that 2-chloro-7-nitro-phenothiazone has the A band at 510 nm, presenting hence a bathochromic effect toward the unsubstituted phenothiazone. However this effect is due to the chlorine atom located in position 2 and not to the NO_2-group substituted in the position 7.

The bands B and C are complex being constituted from several bands (or shoulders), whereas the D-band is with some exceptions, an isolated, very flat band. These bands were not studied because we have not observed relations to the structure.

Summarizing, we conclude that the position of the νIR[νCO] band and the position and shape of the A band of the UV/Vis spectra permit a clear differentiation of the location of the nitro-group in the position 4 or 7 of the phenothiazone ring.

Table 2

UV/Vis Spectra of some chloro-nitro-phenothiazones in methanol

Substituted phenothiazone (substituent) concentration (Mol/L)	Band	λ_{max} nm(logε)
none 9.85×10^{-5}	A	504 (3.91)
	B	380 (3.99), 367 (4.02)
	C	287 (4.24), 287 (4.25), 272 (4.26)
	D	237 (4.39)
4- Nitro- 7.74×10^{-5}	A	483 (4.09)
	B	385 (4.04), 369 (4.04)
	C	275 (4.25), 260 (4.27), 254 (4.27)
	D	230 (4.37)
1-Chloro-4-nitro- 7.72×10^{-5}	A	494 (4.03)
	B	390* (4.04), 369 (4.06)
	C	282 (4.28)
	D	259* (4.21), 253* (4. 23), 232 (4.35)
2-Chloro-4-nitro- 7.79×10^{-5}	A	490 (3.97)
	B	403 (4.01)
	C	280 (4.20), 265 (4.12), 257 (4.14)
	D	233 (4.32)
6-Chloro-4-nitro- 7.79×10^{-5}	A	476 (4.00)
	B	395 (4.04)
	C	277 (4.73), 262 (4.20), 255 (4.22)
	D	208 (4.20)
7-Chloro-4-nitro- 7.38×10^{-5}	A	476 (4.08)
	B	393 (3.99)
	C	267 (4.34), 260 (4.33)
	D	230 (4.39), 211 (4.23)
8-Chloro-4-nitro- 7.17×10^{-5}	A	490 (4.05)
	B	363 (4.10)
	C	276 (4.29), 264 (4.30), 256 (4.29)
	D	235 (4.33), 207 (4.25)
9-Chloro-4-nitro 6.83×10^{-5}	A	482 (4.00)
	B	410 (4.08), 360 (3.94)
	C	279 (4.25), 266 (4.20), 258 (4.20)
	D	235 (4.36)
7-Nitro- 7.67×10^{-5}	A	501 (3.83)
	B	385 (3.85), 367 (4.00), 345 (4.04) 331 (4.08), 322* (4.06)
	C	277 (4.40)
	D	225 (1.16)
2-Chloro-7-nitro $7.38=10^{-5}$	A	510 (3.84)
	B	390 (4.09), 376 (4.16), 358 (4.09) 337 (4.11)
	C	278 (4.46)
	D	230 (4.25)

* Shoulder

EXPERIMENTAL

Melting points are corected. The IR spectra were recorded with a Carl Zeiss Jena UR-10 spectrophotometer ; the substances were prepared as KBr pellets. The UV/Vis spectra were recorded with a Beckman DK–2A spectrophotometer ; the substances were dissolved in methanol.

Starting compounds

1-Chloro- (**Ia**)[2], *6-chloro-* (**1b**)[3], *8-chloro-* (**1c**)[2] and *9-chloro-phenothiazone* (**1d**)[3] were obtained following our previously published methods.

3-Nitro-phenothiazine (**3a**) (improved method). The mixture of 2 g (10 m Mol) phenothiazine, 2 g (20 mMol) potassium acetate and 200 mL methanol was heated in a large baker at 60°C then it was allowed to cool. A solution of 5 g (72 mMol) sodium nitrite in 10 mL water was added and under stirring 3.5 g (31 mMol) anhydrous iron chloride dissolved in 50 mL methanol were then added dropwise during 30 minutes. The reaction mixture was allowed to stay at room temperature over night. The next day the mixture was poured into water and the precipitate filtered off, washed with water and dried. The product was boiled with 400 mL toluene, cooled and filtered. On the filter paper remains the iron hydroxide which was insoluble in toluene. The filtrate was then distilled to a volume of about 200 mL, cooled and chromatographed on 1 kg aluminium oxide (activity III). On the column a wide orange zone of **3a** is formed. 3-Nitro-phenothiazine (**3a**) was obtained as brown-black agglomerated prisms with m.p. 198–199°C (decomp., lit.[6] m. p. 212°C). Yield 0.765 g or 31.2%.

2-Chloro-7-nitro-phenothiazine (**3b**)[7] was prepared according to the method described in the literature.

Nitration of chloro-phenothiazones

General method. 0.3 g (1.2 mMol) Chloro-pheothiazone **1a** – **d** was introduced under stirring in 50 mL nitric acid (d = 1.40) during 10 minutes. After 1 hour the reaction mixture was poured onto ice and water, the brick coloured precipitate filtered off, washed with water and dried on filter paper in air. The substance was dissolved in 60–70 mL toluene and chromatographed on 250 g silicagel (deactivated with 13% water). The Al_2O_3 column descomposed the reaction product. After concentration of the toluene solution to a small volume the chloro-4-nitro-phenothiazones **2a** – **d** were obtained as brick crystalls. The results of our experiments are presented in Table 1.

Oxidation of 3-nitro-phenothiazines

General method. 0.5 g (2 mMol) *3-Nitro-phenothiazine* **3a** – **b**, 0.6 g (2 mMol) potassium dichromate and 25 mL glacial acetic acid were boiled for 5 minutes. The red solution was poured into water, extracted with toluene and the solution was worked-up as usual and chromatographed on 250 g Al_2O_3 (deactivated with 6% water). After concentration of the toluene solution to a small volume the 7-nitro-phenothiazones **4a** – **b** crystallized as glossy leaflets. The results of our experiments are presented in Table 1 .

ACKNOWLEDGEMENTS. The author is indebted to Mrs. Ileana Roşu and Maria Duma for the microanalytical determinations, and to Mr. Rodica Grecu and Magdalena Schoplocher for recording the IR and UV/Vis spectra.

REFERENCES

[1] Part III. M. H. Terdic and V. A. Smarandache, *Rev. Roum. Chim.*, **30**, 135 (1985).
[2] M. H. Terdic and C. Bodea, *Rev. Roum. Chim.*, **13**, 833 (1968).
[3] M. H. Terdic, *Rev. Roum. Chim.*, **29**, 489 (1984).
[4] C. Bodea, M.H. Terdic and E. Broser, *Liebigs Ann. Chem.*, **740**, 122 (1968).
[5] E. Broser and C. Bodea, *Rev. Roum. Chim.*, **17**, 1747 (1972).
[6] J. Danecke and H. W. Wanzlick, *Liebigs Ann. Chem.*, **740**, 52 (1970)
[7] Gh. Rusu, patent, *Rom.* 64116, *Chem. Abstr.* **92**, 94414(1980)

Revue Roumaine de Chimie, **31**, 2, 143–147 (1986)

ÉTUDE ^{1}H-RMN DU DIPHENYL-3,5 DIHYDRO-2,5 THIOPHÈNE CARBOXYLATE-2 D'ÉTHYLE

A. XICLUNA et J. E. ROBERT

Laboratoire de Chimie Pharmaceutique, U.E.R. des Sciences Médicales et
Pharmaceutiques, Place Saint Jacques, 25030 BESANÇON Cédex, France

Reçu le 14 janvier, 1985

The dehydration of ethyl 3,5-diphenyl 3-hydroxy tetrahydrothiophene 2-carboxylate gives a corresponding Δ_3-dihydrothiophene which is in agreement with ^{1}H–NMR data. The determination of relative signs of J couplings was realised by double resonance. The absolute J couplings signs were determined by comparison of 2,5-dihydrothiophene, 2,5-dihydrofuranne and 2-5-dihydropyrrole compounds

La condensation entre le thioglycolate d'éthyle **1** et la benzylidène acétophénone **2** et certains de ses dérivés de substitution conduit, selon les conditions opératoires, à des composés de type **3** qui résultent d'une addition de Michael[1,2] ou à des dérivés tétrahydrothiophéniques de type **4** dont certains ont été décrits par Tilak et coll. [3,4]. Le rôle de la pipéridine est prépondérant pour le passage de **3** à **4**[1].

La présence d'un hydroxy en **4** permet une déshydratation qui, a priori, peut conduire à deux dihydrothiophènes isomères **5** et **6**.

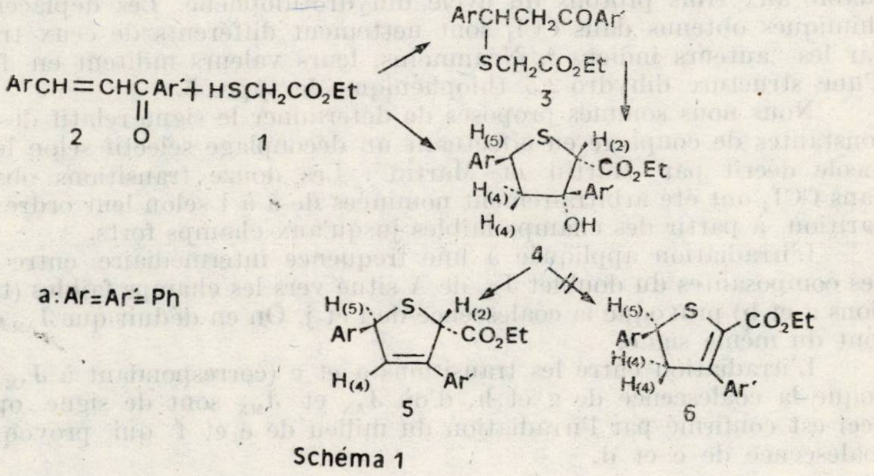

Schéma 1

Tilak, et coll. ont traité **4a** par l'acide polyphosphorique et ont attribué la structure **5** au composé qu'ils ont obtenu à l'appui des déplacements chimiques des trois protons du cycle thiophène partiellement réduit, sans utiliser les valeurs des constantes de couplage [4].

Il nous a paru intéressant de reprendre l'étude NMR protonique (PMR) du produit de déshydratation du diphényl-3,5 hydroxy-3 tétrahydrothiophène carboxylate-2 d'éthyle **4a** dont la stéréochimie est connue [5,6] et que nous avons représentée sur le schéma 1.

RÉSULTATS

Nous avons réalisé l'enregistrement du composé de déshydratation de **4a**, obtenu selon le procédé décrit par Tilak, et coll.[4], dans six solvants de polarité différente (cf. tableau 1).

Tableau 1

Déplacements chimiques (δ ppm) et constantes de couplage (J Hz) en valeur absolue des trois protons dihydrothiophéniques

Solvants	δ_A	δ_M	δ_X	J_{AX}	J_{AM}	J_{MX}
CCl_4	6,23	5,53	5,07	1,16	2,20	4,50
CCl_4*	6,85	6,15	5,75	—	—	—
C_6D_6	6,02	5,56	5,28	1,16	2,16	4,33
$CDCL_3$	6,36	5,66	5,26	1,12	2,25	4,50
CD_3COCD_3	6,48	5,68	5,40	1,25	2,50	4,75
CD_3OD	6,43	5,66	5,36	1,25	2,25	4,66
DMSO d_6	6,57	5,68	5,50	1,08	2,25	4,66

* Valeurs données par TILAK et coll. [4]

On observe dans tous les cas l'existence d'un système AMX attribuable aux trois protons du cycle dihydrothiophène. Les déplacements chimiques obtenus dans CCl_4 sont nettement différents de ceux trouvés par les auteurs indiens [4]. Néanmoins, leurs valeurs militent en faveur d'une structure dihydro-2,5 thiophénique de type **5**.

Nous nous sommes proposés de déterminer le signe relatif des trois constantes de couplage en effectuant un découplage sélectif selon le protocole décrit par Martin et Martin [7]. Les douze transitions observés dans CCI_4 ont été arbitrairement nommées de a à l selon leur ordre d'apparition à partir des champs faibles jusqu'aux champs forts.

L'irradiation appliquée à une fréquence intermédiaire entre celles des composantes du doublet J_{AX} de A situé vers les champs faibles (transitions a et b) provoque la coalescence de i et j. On en déduit que J_{AM} et J_{MX} sont du même signe.

L'irradiation entre les transitions a et c (correspondant à J_{AM}) provoque la coalescence de g et h, d'où J_{AX} et J_{MX} sont de signe opposé. Ceci est confirmé par l'irradiation du milieu de e et f qui provoque la coalescence de c et d.

Enfin, l'irradiation au milieu de e et g (correspondant à J_{MX}) provoque la coalescence de j et 1. On en déduit que J_{AX} et J_{AM} sont de signe opposé.

En conséquence on peut proposer deux hypothèses : soit $J_{AX}=1{,}16$, $J_{AM}=-2{,}20$, $J_{MX}=-4{,}50$, soit $J_{AX}=-1{,}16$, $J_{AM}=2{,}20$, $J_{MX}=4{,}50$Hz. Les états de spins associés à chaque transition, déduites de ces différentes irradiations sont consignés dans le tableau 2.

Tableau 2

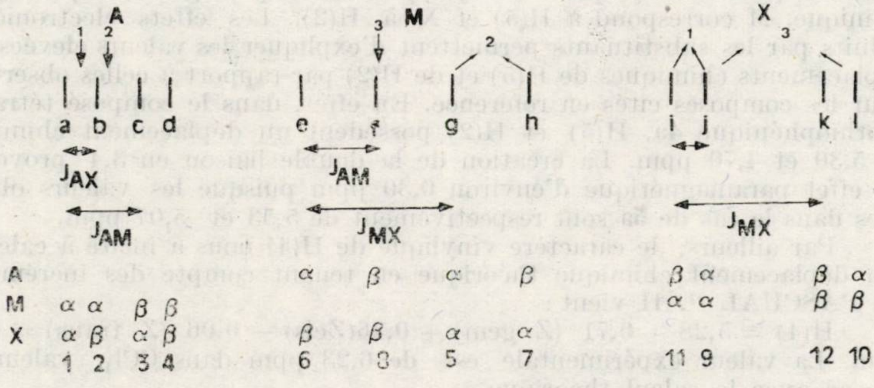

Tableau 3

Déplacements chimiques (ppm) et constantes de couplage (Hz) de protons en 2,4 et 5 de dihydro-2,5 thiophènes, de dihydro-2,5 furannes et de dihydro-2,5 pyrroles

COMPOSÉS	δH_2	δH_4	δH_5	$J_{H_2H_4}$	$J_{H_4H_5}$	$J_{H_2H_5}$	Ref
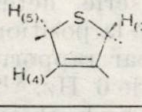	3,66	5,79	3,66	−2,25	2,52	3,24	8
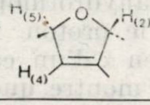	4,51	5,85	4,51	−2,51	1,63	4,59	8
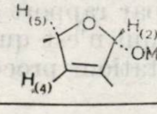	5,78	5,99	5,78	−1,20	1,20	4,00	9
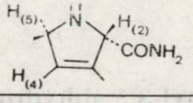	4,55	5,86	3,79	−2,54	1,99	5,81	10
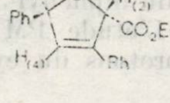	5,75 5,07	6,86 6,23	6,15 5,53	 −1,16	 2,20	 4,50	4

Afin d'attribuer sans ambiguité les déplacements chimiques et les constantes de couplage avec leur signe absolu nous avons confronté nos résultats avec ceux décrits dans la littérature dans le cas de dihydro-2,5 thiophènes[8], de dihydro-2,5 furannes[8,9] et de dihydro-2,5 pyrroles[10] (cf. tableau 3).

DISCUSSION

D'après les données du tableau 3, on peut conclure que A correspond au proton vinylique H(4) qui possède le plus grand déplacement chimique. M correspond à H(5) et X à H(2). Les effets électroniques induits par les substituants permettent d'expliquer les valeurs élevées des déplacements chimiques de H(5) et de H(2) par rapport à celles observées pour les composés cités en référence. En effet, dans le composé tétrahydrothiophénique **4a**, H(5) et H(2) possèdent un déplacement chimique de 5,30 et 4,70 ppm. La création de la double liaison en 3,4 provoque un effet paramagnétique d'environ 0,30 ppm puisque les valeurs observées dans le cas de **5a** sont respectivement de 5,53 et 5,07 ppm.

Par ailleurs, le caractère vinylique de H(4) nous a incité à calculer son déplacement chimique théorique en tenant compte des incréments de PASCUAL[11]. Il vient :

H(4) = 5,28 + 0,71 (Z gem) + 0,36(Zcis) — 0,06 (Z trans) = 6,29 ppm. La valeur expérimentale est de 6,23 ppm dans CCl_4, valeur en accord avec le calcul théorique.

Les valeurs des constantes de couplage sont également en accord avec une structure dihydro-2,5 thiophénique de type **5**. En effet, $J_{H(2)H(5)}$ correspond à un couplage allylique normalement faible et négatif[12]. La valeur de $J_{H(4)H(5)}$, voisine de 2 Hz, correspond à un angle dièdre d'environ 60° si l'on tient compte des relations de Karplus. Cet angle est celui que font ces deux protons étant donné la planéité du cycle dihydrothiophénique[8]. La valeur apparemment élevée de $J_{H(2)H(5)}$ est également conforme à un couplage à longue distance ^4J en série hétérocyclique pentaatomique (cf. tableau 3). De plus, elle confirme la position trans de ces deux protons. Si ces derniers étaient en cis l'un par rapport à l'autre on serait en droit d'observer une valeur de ^4J voisine de 6 Hz.[8,10]

Sur le plan chimique, la déshydratation du tétrahydrothiophène met en jeu l'hydroxyle en 3 et le proton H(4) et non le proton H(2) qui, a priori, paraît être le plus mobile des deux car situé en α d'un carbéthoxy et d'un atome de soufre. La conformation de **4a**[5,6] montre que l'un des hydrogène en 4 occupe une position trans diaxiale par rapport à l'hydroxyle en 3, conformation que ne présente pas H(2) qui n'est que pseudoaxiale. On peut donc en conclure que la déshydratation procède d'une réaction de trans élimination.

CONCLUSION

Cette étude confirme l'obtention du diphényl-3,5 dihydro-2,5 thiophène carboxylate-2 d'éthyle par déshydratation du diphényl-3,5 hydroxy-3 tétrahydrothiophène carboxylate-2-d'éthyle. L'étude PMR permet l'attribution non ambiguë des signaux des trois protons du cycle dihydrothiophénique. Les valeurs observées sont en parfait accord avec celles décrites à propos d'hétérocycles isostères présentant la même insaturation en 3,4.

PARTIE EXPÉRIMENTALE

Les spectres ^1H-RMN ont été effectués sur un appareil Perkin. Elmer R 24 A muni d'un accessoire de double résonance. Les échantillons ont été dissous dans les solvants à raison de 5%. Les déplacements chimiques sont exprimés en ppm par rapport au TMS utilisé comme étalon interne.

Diphényl-3,5 hydroxy-3 tétrahydrothiophène carboxylate-2 d'éthyle **4a** Préparé selon[1] à partir d'un mélange équimoléculaire de thioglycolate d'éthyle **1** de benzylidèneacétophénone **2** et de pipéridine.

Diphényl-3,5 dihydro-2,5 thiophène carboxylate-2 d éthyle **5a** Préparé selon[4].

BIBLIOGRAPHIE

[1] A. Xicluna, C. Guinchard, J. F. Robert et J. J. Panouse, *C. R. Acad. Sci. Ser. C*, **280**, 287 (1975).

[2] A. Xicluna, J. F. Robert et J. J. Panouse. Comm. XVIèmes Rencontres Internationales de Chimie Thérapeutique, Marseille, 9—11 juillet 1980.

[3] B. D. Tilak, H. S. Desai et S. S. Gupte, *Tetrahedron Letters*, 1609 (1964).

[4] B. D. Tilak et S. S. Gupte, *Indian J. Chem.*, **7**, 9 (1969).

[5] A. Xicluna, Thèse de Doctorat ès Sciences Pharmaceutiques, Besançon, Mars 1981.

[6] A. Xicluna, J. F. Robert, J. J. Panouse, M. Baud, L. Pizalla et H. Bodot, à paraître. A. Xicluna, B. Baud, R. Bazin, J. F. Robert, L. Pizalla, J. C. Cardot, J. J Panouse et H. Bodot, Comm. XVIèmes Rencontres Internationales de Chimie. Thérapeutique, Marseille, 9—11 juillet 1980.

[7] M. L. Martin et G.J. Martin, Manuel de Résonance Magnétique Nucléaire (édité par Azoulay) p. 128 Paris (1971).

[8] R. Lozac'H et B. Braillon, *J. Magn. Résonance*, **12** (3) 244 (1973).

[9] C. Barbier, D. Gagnaire et P. Vottero, *Bull. Soc. Chim.*, 2230 (1968).

[10] T. J. Batterham, NMR Spectra of Simple Heterocycles, Wiley-Interscience Publ., and Sons (edited by E. C. Taylor and A. Weissenber), New York (1973) p. 160.

[11] C. Pascual, J. Meier et W. Simson, *Helv. Chim. Acta*, **49**, 164 (1966).

[12] A. Gaudemer, Determination of Configurations by Spectrometric Methods, Georg Thieme Publ. (edited by H. B. Kagan) Stuttgart 1977, p. 47.

Revue Roumaine de Chimie, **31**, 2, 149–157 (1986)

IDENTIFICATION D'HYDROCARBURES AROMATIQUES DE QUELQUES FRACTIONS PÉTROLIÈRES. IV$^{1-3}$

ANALYSE SPECTRALE IR

HOCINE KADI et D.P. LAZĂR

Département de Génie chimique, Ecole Polytechnique, Université d'Alger, Algérie

Département de Chimie physique, Faculté de technologie chimique, Splai Bahlui 71, 6600 Jassy, Romania

Reçu le 3 septembre, 1984

The IR spectral analysis of the 23 oil fractions obtained after the TBP (True Boiling Point) distillation has been intended to strengthen the previous quantitative results provided by the methods previously reported, i.e. HPLC^{1,2} and n.d.PA^3. With that purpose in view and moreover supposing that each oil fraction represents itself a complex mixture of alkanes, cycloalkanes and aromatics, it became possibile to use IR analysis technique to confirm the qualitative composition in most of the 23 fractions. Using qualitative procedures which are specific for the empiric IR, analysis, it was possible to formulate a quantitative appreciation of each oil fraction under the form of percentage composition in alkanes ($\% C_P$), in cycloalkanes ($\% C_N$) and respectively in aromatics ($\% C_A$).

L'analyse spectrale IR de 23 fractions, obtenues par distillation VPE a pour but la confirmation générale des résultats fournis par les méthodes décrites antérieurement, HPLC^{1,2} et n.d.PA^3 (n = indice de réfraction, n_{20}^{D}, d = densité relative, d_4^{20}, PA = « point d'aniline »).

Dans ce sens, on a considéré que chaque fraction pétrolière est un mélange complexe d'hydrocarbures aliphatiques, naphténiques et aromatiques et que chaque classe d'hydrocarbures présente, dans le spectre IR, des bandes d'absorbtion spécifiques. En utilisant les procédés spécifiques de calcul quantitatif de l'analyse spectrale IR empirique, il est possible d'apprécier quantitativement chaque fraction pétrolière, sous la forme de la composition, en pourcentage, des hydrocarbures aliphatiques ($\% C_P$), naphténiques ($\% C_N$) et aromatiques ($\% C_A$).

1. PRÉSENTATION DE LA MÉTHODE

Dans les notes antérieures, on a montré que toutes les 23 fractions seconddmaires obtenues par distillation VPE de la fraction primaire entre 90°C et 209°C possèdent des pourcentages élevés en hydrocarbures paraffiniques, moyens en hydrocarbures naphténiques et assez bas en hydrocarbures aromatiques.

L'analyse spectrale IR, appliquée à toutes les fractions, a pour but de confirmer, globalement, la composition générale établie par les méthodes HPLC et n.d.Pa. L'application des procédés de calcul de l'analyse spectrale empirique se base sur l'établissement des positions des bandes d'absorbtion (ou groupes de bandes) dans le spectre IR et des valeurs des intensités relatives des pics de ces bandes, attribuées aux différents types de vibrations des liaisons C—H, C—C ou C=C, dans les molécules des hydrocarbures présents dans chaque fraction (voir Tableaux 1 et 2, colonne 5, classé par groupes des bandes).

Autrement dit, la méthode d'analyse spectrale IR a été utilisée pour la confirmation des valeurs (% C_P, % C_N) et % C_A, raportées antérieurement[1-3], en utilisant le procédé de l'identification qualitative et d'approximation quantitative indiqué dans la littérature[4,5].

L'analyse spectrale IR a été appliquée à toutes les fractions tant à l'état dilué, ainsi qu'à l'état non-dilué.

2. MÉTHODE DE TRAVAIL

Les spectres IR de ces 23 fractions diluées et non diluées, ont été analysés à l'aide d'un spectromètre PERKIN ELMER 283, en utilisant des cellules avec fenêtres de NaCl d'une épaisseur de 0,027 mm.

Pour les fractions non diluées, l'atténuation de l'amplification du signal a été de 1/10. La dilution des fractions est faite avec du CCl_4 (Uvasol) à un rapport fraction/solvant = 1/3 ; pour l'enregistrement des spectres on a utilisé une amplification nominale 1/1.

3. DISCUSSION DES RÉSULTATS EXPÉRIMENTAUX

Les spectres IR des fractions non diluées présentent, en général, un aspect commun, suivant le tableau 1 :

a) groupe de bandes à forte intensité, situé dans le domaine de fréquence 3100—2840 cm^{-1};

b) groupe de bandes à moyenne intensité, situé dans le domaine de vibrations 1609—1340 cm^{-1};

c) bandes isolées, faibles, situées, pour la majorité des fractions, entre 1090 et 980 cm^{-1};

d) groupe de bandes spécifiques au benzène et de ses homologues, situé, suivant les fractions, entre 830 et 685 cm^{-1}.

L'attribution de ces bandes d'absorbtion par types de liaisons chimiques et par types de vibrations, pour un nombre de cinq fractions sélectionnées (4, 11, 14, 16 et 21), est présentée dans le tableau 1.

Les spectres des fractions diluées présentent aussi un aspect général commun, avec un nombre plus réduit de bandes d'absorbtion de faible intensités, groupées de la même manière (voir Tableau 2) :

a) groupe de bandes à forte intensité, situé dans le domaine 2925—2985 cm^{-1};

b) groupe de bandes à moyenne intensité, situé dans le domaine 1375—1460 cm^{-1};

c) groupe de bandes spécifiques au benzène et à ses homologues, situé dans la zone spectrale 700—835 cm^{-1}.

L'attribution empirique des pics des bandes d'absorbtion des deux séries de spectre est présenté dans les tableaux 1 et 2, colonne 5.

Les pics des bandes à forte intensité (3020 — 2840 cm^{-1}) sont attribués spécialement aux vibrations longitudinale des liaisons C—H (ν_{CH}), symétriques et antisymétriques, dans les molécules des hydrocarbures paraffiniques et naphténiques.

Les pics de la zone médiane des spectres (1606 — 1445 cm^{-1}) sont attribués aux vibrations longitudinales des liaisons C = C ($\nu_{C=C}$) des hydrocarbures naphténiques et aromatiques et ceux de la zone spectrale spécifique (1470—1340 cm^{-1}) sont attribués aux vibrations de déformation (δ) des liaisons C—H des hydrocarbures paraffiniques.

Les pics isolés du domaine 1090—980 cm^{-1} sont attribués aux vibrations des noyaux aromatiques avec 1, 2 ou 3 atomes de H substitués.

Enfin, les pics de la zone spectrale 830—685 cm^{-1} sont spécifiques pour les vibrations de déformation en dehors du plan (γ) dans les noyaux aromatiques mono-, di- ou tri-substitués.

4. CALCUL DE VALEURS (% C_P + % C_N) ET % C_A

4.1. Si on prend en considération seulement les pics les plus elevés de chaque bande d'absorbtion, alors pour les valeurs (% C_P, % C_N) et respectivement % C_A, on trouve des valeurs assez différentes par rapport aux calculs de la méthode n.d.PA. Par contre, si on tient compte de tous les pics (d'intensités différentes) de chaque bande d'absorbtion, on obtient des résultats satisfaisants, concordant avec ceux obtenus par la méthode n.d.PA.

Par la suite, nous présentons un exemple de calcul à l'aide des données spectrales obtenues pour la fraction 4, non diluée et diluée.

On utilise les notations suivantes :

x = pourcentage d'atomes de carbon des hydrocarbures aromatiques de la prise d'essai (fraction 4);

y = pourcentage d'atomes de carbon des paraffines et des naphtènes de la prise d'essai.

Donc,

1. A partir du spectre IR de la fraction 4 non diluée, on obtient

$\sum_{i=1}^{23} h_{i,P.N}$ = la somme des hauteurs des pics de la bande d'absorbtion intense, attribuée aux vibrations longitudinales (ν_{CH}) des liaisons C—H paraffiniques et naptheniques;

$h^{d}_{i,P.N}$ = hauteur des pics de la bande d'absorbtion d'intensité moyenne, attribuée aux vibrations de déformation (δ_{CH}) des liaisons C—H des hydrocarbures paraffiniques et napthéniques;

$\sum_{i=1}^{23} h_{i,A}$ = somme des hauteurs des pics de la bande d'absorbtion de faible intensité, attribuée aux vibrations de deformation (γ_{CH}) des noyaux aromatiques avec de différents degrés de substitution.

Tableau 1

Données spectrales IR et attribution empirique par classes d'hydrocarbures pour certaines fractions non diluées (4, 11, 14, 16 et 21)

Fréquence (cm^{-1})	Intensité 1)	Fractions secondaires	Groupe 2) polyatomique	Type de 3) vibration	Attribution empirique	Observations
1	2	3	4	5	6	7
			A. Groupe des bandes à fortes intensités			
3100 – 3020	t.i	4, 14, 16	$>C-H$	ν_{CH}	aromatiques	benzène substitué ; bandes multiples
3015	t.i	4, 11, 14, 16, 21	a) $C=C$	$\nu_{C=C}$	alkènes cycliques	cyclohexane
			b) $C-H$	ν_{CH}	noyaux aromatiques	vibration de valence
2962	i	4, 11, 14, 16, 21	$-CH_3$	ν_{CH_3as}	paraffines et cycloparaffines	vibration de valence antisymétriques
2925	i	4, 11, 14, 16, 21	$>CH_2$	ν_{CH_2as}	paraffines et cycloparaffines	vibration de valence antisymétrique
2890	f	4, 11, 14, 21	$>-CH$	ν_{CH}	paraffines	vibration de valence
2872	m	4, 11, 14, 21	$-CH_3$	ν_{CH_3s}	paraffines	vibration de valence
2840	f	11, 16	—	—	non attribué	—
			B. Groupe des bandes avec une intensité moyenne			
1606 – 1609	m – f	11, 14, 16, 21	$>C=C<$	$\nu_{C=C}$	benzène monosubstitué et ortho-disubstitué	
1588 – 1575	i – m	11, 14, 16, 21	$>C=C<$	$\nu_{C=C}$	idem	
1500 – 1490	i	11, 14, 16, 21	$>C=C<$	$\nu_{C=C}$	idem	

~1470	i	4, 11, 14, 16, 21	a) $>CH_2$	δ_{CH_2}	paraffines	vibration de cisaillement
			b) $>CH_2$	δ_{CH_2}	cycloparaffines	idem
			c) $-CH_3$	δ_{CH_3as}	paraffines	attribution non certaine
1380	m	4, 11, 14, 16, 21	$-CH_3$	δ_{CH_3s}	paraffines	vibration de déformation dans le plan
1340	f	4, 11, 14, 16, 21	$-\!\!>CH$	δ_{CH}	idem	
			C. Bandes isolées			
1090 – 980	f	4, 11, 14, 16, 21	a) noyaux aromatiques	—	benzène substitué	vibration du noyaux benzéniques
			b) idem	δ_{CH}	idem	bandes multiples ; superposition avec les vibrations de noyaux benzéniques
			c) $>CH_2$	γ_{CH_2} (wagging)	cycloparaffines	
			D. Groupe des bandes spécifiques du benzène substitué			
830 – 800	m	11, 14, 16, 21	$>CH$	γ_{CH}	benzène nono-substitué ;	entre 1260 – 680 cm^{-1} peuvent aussi exister des vibrations des noyaux aromatiques.
805 – 770	m	16				
770 – 725	m	11, 14, 16, 21				
760 – 730	m	14, 16			benzène orthodisubstitué ; benzène 1,2,3 et 1,3,5 trisubstitué	
720 – 685	m					
710 – 685	m					

Légende : 1) Symboles pour l'appréciation qualitative de l'intensité des bandes I.R. :t.i. = très intense ; i = intense ; m = moyenne ; f = faible

2) a), b), c) = variantes d'attributions

3) ν_s ; ν_{as} = vibrations de valence (d'allongement) symétriques, respectivement asymétriques,

δ; γ = vibration de déformation dans le plan, respectivement en dehors du plan.

4) Observations : sur les spectrogrammes IR on n'a pas observé les harmoniques des vibrations du domaine 685 – 830 cm^{-1} (donc dans la région 1660 – 2 000 cm^{-1}) ; de plus, les vibrations antisymétriques γ_{CH} ne sont pas mises en évidence

Tableau 2

Données spectrales IR et attribution empirique par classes d'hydrocarbures pour certaines fractions diluées (4, 11, 14, 16 et 21)

Fréquence (cm^{-1})	Intensité 1)	Fractions secondaires	Groupe 2) polyatomique	Type de 3) vibration	Attribution empirique	Observations
1	2	3	4	5	6	7
A. Groupe des bandes à fortes intensités						
2985	i	4, 11, 14, 16, 21	$>CH$	ν_{CH}	non attribué	(noyaux aromatiques ?)
2962	i	4, 11, 14, 16, 21	$-CH_3$	ν_{CH_3as}	paraffines et cycloparaffines	
2925	i	4, 11, 14, 16, 21	$>CH_2$	ν_{CH_2as}	idem	
B. Groupe des bandes avec une intensité moyenne						
1460	m	4, 11, 14, 16, 21	a) $>CH_2$	δ_{CH_2}	cycloparaffines	(cyclohexane ?)
			b) $-CH_3$	δ_{CH_3as}	paraffines	
1380—1375	m	4, 11, 14, 16, 21	$-CH_3$	δ_{CH_3s}	idem	doublet
C. Bandes isolées — n'apparaissent pas						
D. Groupe des bandes spécifiques du benzène substitué						
835—700	f	4, 11, 14, 16	$>CH$	γ_{CH}	benzène substitué	1—2 bandes

Légende : voir Tableau 1

2. Du spectre IR de la fraction 4 diluée on obtient :

$$\sum_{i=1}^{23} h'_{i,P.N}, \quad h'^{d}_{i,P.N} \quad \text{et} \quad \sum_{i=1}^{23} h'_{i,A}.$$

Des mesures quantitatives effectuées sur spectrogramme on obtient les valeurs suivantes :
$\sum_{i=1}^{23} h'_{i,P.N}$, $h'_{i,P.N}$, $h_{i,P.N}$ et $h'^{d}_{i,P.N}$, à partir desquelles on calcule la valeur $\sum_{i=1}^{23} h_{i,P.N}$ correspondant aux hauteurs des pics paraffiniques et naphténiques de la prise d'essai 4 non diluée (qui apparait tronqué sur le spectrogramme).

En supposant que l'hauteur des pics, qui varie en fonction de la concentration des atomes de carbon (%C) suit une même loi, on peut écrire que :

$$\sum_{i=1}^{23} h_{i,P.N} = \frac{h^{d}_{i,P.N}}{h'^{d}_{i,P.N}} \sum_{i=1}^{23} h_{i,P,N} \qquad (1)$$

et, conformément aux notations convenues, $x = \sum_{i=1}^{23} h_{i,A}$, et $y = \sum_{i=1}^{23} h_{i,P.N}$.

Pour le cas particulier de la fraction 4, oú i = 4, les mesures effectuées sur le spectrogramme donnent :

$\sum_{i=4} h'_{4,P.N} = 49{,}00$ cm ; $h^{d}_{4,P.N} = 11{,}00$ cm ; $h'^{d}_{4,P.N} = 4{,}90$ cm et $\sum_{i=4} h_{4,A} = 14{,}70$ cm.

En tenant compte du fait que le spectre IR de la fraction 4, non diluée, a été enregistré avec un attenuation du signal égal à 1/10, on écrit : $\sum_{i=4} h_{4,P.N} = \frac{110}{49} \cdot 490 = 1100$ cm.

Puisque x = 147 cm et y = 1100 cm, il résulte que :

$$\frac{x}{y} = \frac{147}{1100}.$$

Mais, d'autre part, x + y = 100, alors que :

$$x = 88{,}21\ (\%\,C_P + \%\,C_N) \text{ et } y = 11{,}79\ \%\,C_A.$$

4.2. Appréciation des résultats obtenus en utilisant la spectroscopie d'absorbtion IR par rapport à ceux obtenus par méthode n.d.PA. Considérons, de nouveau, la fraction 4 comme référence.

Les méthodes n.d.PA et IR donnent les pourcentages suivants pour les valeurs $\% C_A$:

. méthode n.d.PA. . . . . 11,40 $\% \ C_A$

. méthode IR . . . . . . 11,79 $\% \ C_A$

d'où, l'erreur relative, sera :

$$\varepsilon_R = \frac{\% C_{A,n.d.PA} - \% C_{A,IR}}{\% C_{A,n.d.PA}} \cdot 100 \qquad (2)$$

par conséquent, pour la fraction 4, la relations (2) indique :

$$\varepsilon_R = \frac{11,40 - 11,79}{11,40} \cdot 100 = -3.42 \ \%.$$

À la suite du calcul de l'appréciation—en utilisant la relation (2)—on a établi que pour toutes les fractions 1—23, la méthode spectrale IR présente uu erreur relative moyene de 5%, par rapport à la méthode n.d.PA, considérée exacte et précise.

Pour certaines fractions (2, 3, 6, 7 et 22) les erreurs individuelles sont, en quelque sorte, plus grandes (voir Tableau 3).

Tableau 3

Valeurs, en $\% C_A$ fournies par la méthode n.d.PA et respectivement IR

Fraction	$\% C_{A,n.d.PA}$	$\% C_{A,IR}$	$\varepsilon_R = \frac{\% C_{A,n.d.PA} - \% C_{A,IR}}{\% C_{A,n.d.PA}} \cdot 100$
1	9,50	9,97	−4,95
2	6,50	6,89	−6,00
3	11,90	12,63	−6,13
4	11,40	11,79	−3,42
5	9,90	10,49	−5,96
6	14,60	15,49	−6,10
7	16,20	17,18	−6,05
8	10,20	10,80	−5,88
9	13,70	14,47	−5,62
10	16,60	17,40	−4,82
11	17,60	18,44	−4,77
12	17,20	18,14	−5,47
13	17,60	17,08	+2,95
14	17,40	17,92	−2,99
15	16,50	17,28	−4,73
16	16,90	16,26	+3,79
17	16,30	16,94	−3,93
18	16,10	15,35	+4,66
19	16,40	15,51	+5,43
20	16,30	15,47	+5,09
21	16,40	15,50	+5,49
22	17,00	15,98	+5,98
23	17,50	16,64	+4,91
			$\bar{\varepsilon}_R = 5,00 \%$

CONCLUSIONS

1°. Les trois méthodes d'analyse — HPLC, n.d.PA et IR — présentées antérieurement[1-3], permettent de formuler quelques indications globales sur la composition, en pourcentage, par les classes des hydrocarbures, de chaque fraction séparée, ainsi que celle de la fraction primaire initiale, distillée entre 90°—209°C.

2°. La méthode HPLC nous a permis de conaître le nombre d'hydrocarbures aromatiques se trouvant dans chaque fraction 1—23.

3°. La méthode n.d.PA a permis le calcul du pourcentage en atomes de carbon aliphatiques + naphténiques et aromatiques.

4°. L'analyse spectrale IR a confirmé les conclusions formulées par deux premières méthodes.

BIBLIOGRAPHIE

[1] H. Kadi et D. P. Lazăr, Rev. Roumaine Chim., **29**, 497 (1984)
[2] H. Kadi et D. P. Lazăr, Rev. Roumaine Chim., **30**, 80 (1985)
[3] H. Kadi et D. P. Lazăr, Rev. Roumaine Chim., **30**, 365 (1985)
[4] Collectif, «Organicum. Chimie organică practică», Editura Ştiinţifică şi Enciclopedică, Bucureşti, 1982, p. 112—118 (traduit de l'allemand)
[5] A. T. Balaban, M. Banciu et I. Pogany, «Aplicaţii ale metodelor fizice în chimia organică», Editura ştiinţifică şi enciclopedică, Bucureşti, 1983, p. 13—37.
[6] I. Pogany et M. Banciu, «Metode fizice în chimia organică», Editura ştiinţifică, Bucureşti, 1972, p. 109—114.

Revue Roumaine de Chimie, **31**, 2, 159–162 (1986)

PHOSPHOROUS ACID–IODINE AS REAGENT FOR THE SYNTHESIS OF 1,3,4-OXADIAZOLES FROM DIACYLHYDRAZINES

C. I. CHIRIAC
"P. Poni" Institute of Macromolecular Chemistry,
Aleea Ghica-Vodă 41 A Jassy, Romania

Received February 25, 1985

A series of substituted 1,3,4-oxadiazoles are prepared by a cyclodehydration reaction of N, N′-diacylhydrazines with a reagent formed from phosphorous acid and iodine in dimethylformamide (at reflux for 6—7 hours).

For the preparation of substituted 1,3,4-oxadiazoles from N, N′-diacylhydrazines, a series of dehydration reagents were used, such as: thionyl chloride,[1] ethyl ortoformate,[2] phosphorus oxychloride,[3] aluminium chloride,[4] etc.

RESULTS AND DISCUSSION

Previous communication from this laboratory has shown that the adduct phenyldichlorophosphite — dimethylformamide is a useful reagent for the dehydration of N,N′-diaroylhydrazines to the corresponding 1,3,4-oxadiazoles.[5] On the other hand, in a recent paper, we have found that the reagent formed from phosphorous acid and iodine in pyridine is useful for the synthesis of amides.[6]

In this work we have found that this reagent in dimethylformamide (DMF) as solvent is also suitable for the cyclodehydration of the diacylhydrazines to oxadiazoles. Thus by stirring at reflux for 6–7 hours, one mole + 15% excess phosphorous acid, one mole iodine and one mole dibenzoylhydrazine in DMF, 2,5-diphenyl-1,3,4-oxadiazole resulted with 68% yield (at lower temperature, the yield decreased).

In the reaction of $P(OH)_3$ with I_2, iodophosphoric acid resulted "in situ",[6,7] which acts as reagent having reactive P–I bond. We used DMF in this cyclodehydration, because it is a very good solvent for the reaction products.

We supposed, similar as in other cases,[5,8] that this reaction involves the following mechanisms :

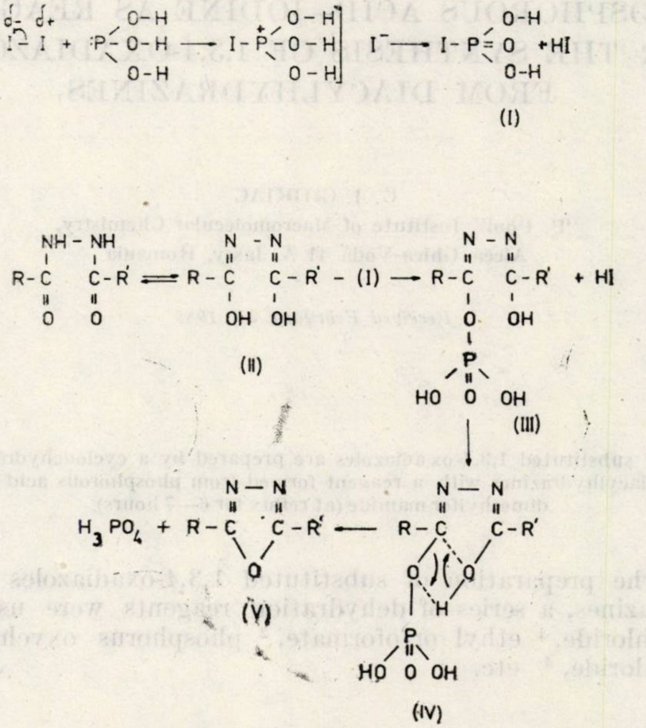

The formation of the iodophosphoric acid involves an electrophylic attack of iodine atom at the phosphor atom of phosphorous acid. The "in situ" formed iodophosphoric acid (I) reacts with the tautomeric form of the diacylhydrazine (II) affording reactive intermediate (III) which, by a transition state (IV) gives the corresponding oxadiazole (V) and phosphore acid as by-product.

In a typical procedure to a solution of one mole + 15% excess $P(OH)_3$ in DMF, under stirring, one mole of iodine was added. At the beginning, the obtained solution has a black-violet colour owing to iodine. Then the reaction becomes exothermic and the colour of the solution changes to light yellow. This is an indication that iodine has reacted with $P(OH)_3$, affording "in situ" the reagent (I) in DMF solution. Over this solution, one mole of diacylhydrazine (II) was added and the obtained mixture was refluxed and the final product (V) was separated by precipitation. The oxadiazoles (V) obtained by this method are presented in table 1.

The yields obtained using this method ranged from 66 to 78%.

In conclusion, we have found a new method for the synthesis of 1,3,4-oxadiazoles by the cyclodehydration of the corresponding diacylhydrazines with the reagent formed from $P(OH)_3$ and iodine in DMF solution at reflux.

Table 1

Substituted 1,3,4-oxadiazoles obtained from diacylhydrazines using $P(OH)_3$-I_2as cyclodehydrating reagent.

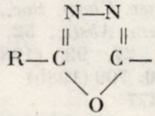

R	R′	Oxadiazoles[a]		
		yield[b] %	M,p.[c] °C	Reported m.p.[d] °C
C_6H_5	C_6H_5	78	138—140	139—140[9]
C_6H_5	p-CH_3O—C_6H_4	75	145—147	145—146[10]
p-CH_3—C_6H_4	p-CH_3—C_6H_4	67	174—176	176[11]
C_6H_5—CH_2	C_6H_5—CH_2	76	97—99	98— 99[d]
p-CH_3O—C_6H_4	p-CH_3O—C_6H_4	73	165—166	166—167[11]
C_6H_5	p-O_2N—C_6H_4	66	205—207	207—209[10]
C_6H_5	p-Cl—C_6H_4	68	161—163	162[10]
C_6H_5	p-Br—C_6H_4	70	165—167	167[10]

[a] The products were identified by comparison of m.p. and IR spectra with authentic samples.

[b] Yield calculated on diacylhydrazine employed.

[c] After recrystallization.

[d] From *Beilstein Handbuch der Organischen Chemie*, **27**, 595.

EXPERIMENTAL

2,5 Diphenyl-1,3,4-oxadiazole

To a solution of 1 g (0.01 mole + 15% excess) $P(OH)_3$ in 10 mL dry DMF, 2.52 g (0.01 mole) I_2 was added under stirring. After 10—20 minutes, the reaction becomes exothermic and the colour of the solution changes from black-violet to light yellow. The obtained solution which contains iodophosphoric acid resulted "in situ" was stirred for 20—30 minutes at room temperature. Over this solution, 2.4 g (0.01 mole) N,N′-dibenzylhydrazine were added and then 2 mL dry DMF in order to dissolve the hydrazide remained on the neck of the flask. The solution was stirred at reflux for 6—7 hours. At the end of reaction, the obtained solution was poured into 70—80 mL of water with ice under stirring, when the desired product precipitated. This mixture was treated with 10% NaOH solution till pH = 9 — 10 and the product was collected by filtration, washed with 30—40 mL 7% HCl solution, three times with 20—30 mL water and dried under vacuum at 100—120°. 2,5 Diphenyl-1,3,4-oxadiazole (1.73 g) was obtained with 78% yield (calculated on dibenzoylhydrazine employed). The melting point was 138—140° after recrystallization from ethanol (mixed m.p. with a pure sample obtained by a classical method underpressed).

Anal. Found : C, 75.43 : H, 4.31 ; N, 12.25%. Calculated for $C_{14}H_{10}N_2O$; C, 75.60 ; H, 4.50 ; N, 12.25%.

Under similar conditions, the other oxadiazoles presented in table 1, were prepared from the corresponding N, N′-diacylhydrazines.

REFERENCES

[1] N. S. Dokunikhin, *Zhur. prikland. Khim.*, **32**, 664 (1959).
[2] G. Ainsworth, U. S. Pat., 2, 733, 245 ; *Chem. Abstr.*, **50**, 12. 115 (1956).
[3] F. N. Hayes and B. S. Rogers, *J. Amer. Chem. Soc.*, **77**, 1850 (1955).
[4] W. Müeller, U. S. Pat. 2,838, 520 ; *Chem. Abstr.*, **52**, 17.290 (1958)
[5] C. I. Chiriac, *Rev. Roumaine Chim.*, **27**, 935 (1982).
[6] C. I. Chiriac, *Rev. Roumaine Chim.*, **30**, 799 (1985)
[7] A. J. Kirby, *Chem. & Ind.* **1963**, 1877
[8] F. Cramer and M. Winter, *Chem.Ber.*, **94**, 990 (1961).
[9] R. Stollé, *Ber. dtsch. chem. Ges.*, **32**, 797 (1897).
[10] A. P. Grekov and L. M. Kulakova, *Zhur. Obscei Khim.*, **29**, 3054 1959) ; *Chem. Abstr.*, **54**, 13. 108 (1960).
[11] E. Baltazzi and A. Wysocki, *Chem. & Ind.*, **26**, 1680 (1963).

Revue Roumaine de Chimie, **31**, 2, 163–168 (1986)

MODIFIED COPOLYMERS WITH RADIOPROTECTIVE ACTION

MARIA BRUMĂ, GHEORGHE DUMITRESCU and ELENA DUMITRESCU
Institute of Macromolecular Chemistry "Petru Poni",
Aleea Gr. Ghica-Vodă 41 A, Iaşi, Romania

Received March 8, 1985

The synthesis of new chemical radioprotectors with improved effectiveness and long term protective action is described. The reaction of micromolecular radioprotective compounds containing free amino groups with N-vinylpyrrolidone—maleic anhydride copolymer was used. The modified copolymers thus obtained have been tested for their ability to protect against ionizing radiations.

The irradiation of the human body with ionizing radiations produces a series of structural and functional modifications, the more complex the more developed the treated subject on biological scale is. Therefore appears the necessity to elaborate protective methods and means against noxious effects induced by ionizing radiations. Among these an important place is occupied by chemical protection utilizing radioprotective compounds. [1] On the basis of the results obtained so far in the literature it can be considered that the most efficient radioprotectors are thiolic compounds. Among these the most interesting are β-mercaptoethyl amine, β,β′-diaminodiethyl sulphide and certain substituted derivatives.[2]

The present paper describes the synthesis of new chemical radioprotectors with improved effectiveness whose radioprotective action should last for a long time. For this purpose we studied the reaction of micromolecular radioprotective compounds containing free amino groups with N-vinylpyrrolidone – maleic anhydride copolymer, taking into account the radioprotective effect of N-vinylpyrrolidone itself.[3] The modified copolymers thus obtained are soluble in dimethylsulfoxide and can be used as a solution in this solvent, being known the radioprotective properties of dimethylsulfoxide, as well. [4]

RESULTS AND DISCUSSION

N-vinylpyrrolidone – maleic anhydride copolymer (NVP–AM) has been synthesized by copolymerization of the two monomers taken into equimolecular quantities. [5] The mechanism of this copolymerization consists of the formation of a donor-acceptor complex which acts as a new monomer:

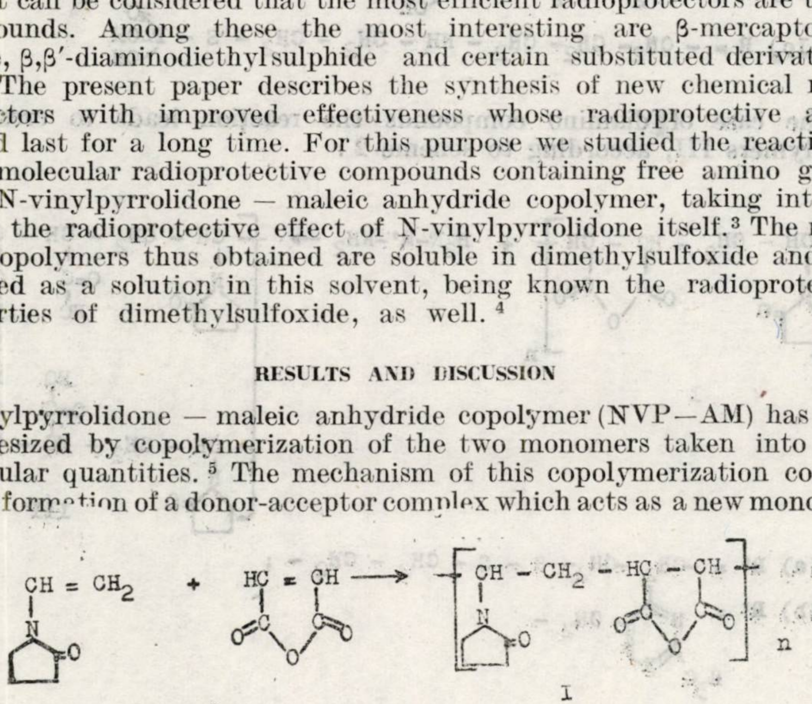

I

Regardless of the composition of the initial mixture the copolymerization leads to the formation of a copolymer with constant composition 1 :1, in which the units of the two monomers alternate in a very rigorous way.

As the macromolecular chain of N-vinylpyrrolidone — maleic anhydride copolymer contains anhydride groups, we have selected for the reaction those micromolecular radioprotective compounds which contained amino groups capable to give polymer — analogous reactions with anhydride groups. These compounds are : β-mercaptoethyl amine, 2-methyl-4-amino-5-aminomethyl-pyrimidine, β,β′-diaminodiethyl sulphide, β-aminoethyl-thiophosphoric acid and γ-aminopropyl-β-aminoethyl thiophosphoric acid. On the action of amino groups in these compounds, the anhydride groups of copolymer I open and lead to polyamidic acids II and III. In the case of monoamino compounds the reaction takes place according to scheme 1 :

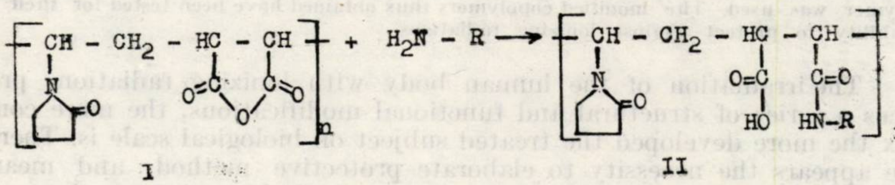
I

II

IIa) R = $-CH_2-CH_2-SH$;

IIb)
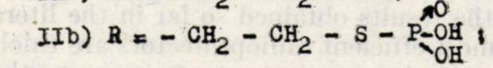
$R = -CH_2-CH_2-S-P(=O)(OH)OH$;

IIc)
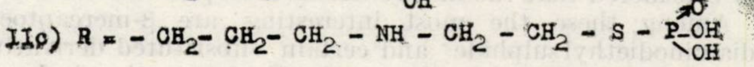
$R = -CH_2-CH_2-CH_2-NH-CH_2-CH_2-S-P(=O)(OH)OH$

In the case of diamino compounds the reaction leads to crosslinked copolymers III, according to scheme 2 :

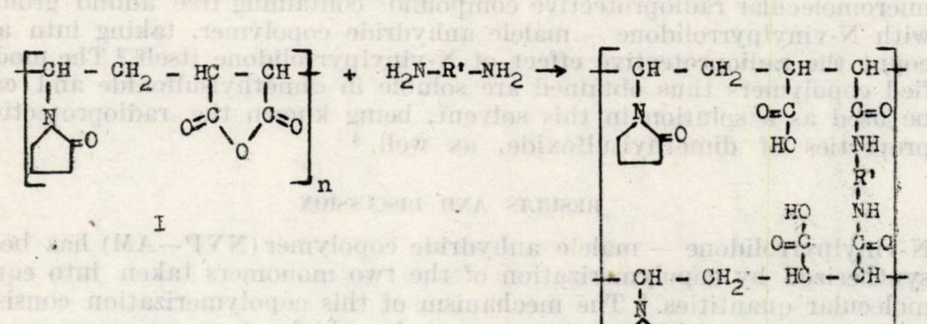
I

III

IIIa) R' = $-CH_2-CH_2-S-S-CH_2-CH_2-$;

IIIb)
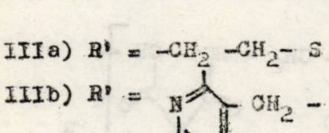

Table 1

Preparation of modified copolymers

Modified copolymer	Copolymer NVP-AM		Amino compound			N-methyl-pyrrolidone mL	Temp. °C.	Triethyl-amine		Solvent for separation	Yield %
	g.	mol.		g.	mol.			g.	mol.		
IIa	20,9	0.1	β-mercaptoethyl amine	7.7	0.1	150	40	—	—	Acetone	93
IIb	20.9	0.05	β-aminoethyl thiophosphoric acid chlorhydrate	19.35	0.1	180	40	10.1	0.1	Ethylic ether	90
IIc	10.45	0.1	γ-aminopropyl-β-aminoethyl thiophosphoric acid chlorhydrate	12.50	0.05	100	45	5.05	0.05	Ethylic ether	87
IIIa	41.8	0.2	β, β′-diaminodiethylsulphide chlorhydrate	22.50	0.1	320	50	20.2	0.2	Ethylic ether	89
IIIb	20.9	0.1	2-methyl-4-amino-5-aminomethyl pyrimidine chlorhydrate	10.55	0.05	225	50	10.1	0.1	Acetone	90

These reactions have been carried out in dipolar aprotic solvents such as N-methylpyrrolidone or dimethylformamide at 40–50°. The molar ratio between the quantities of copolymer I and amino compound is 1 :1 in the case of modified copolymers II, and 2 :1 în the case of modified copolymers III. When amino compounds were used as chlorhydrates, it was necessary to add triethylamine to the reaction mixture and eliberate the free amino base. In table 1 the preparation of modified copolymers is shown.

The final products are soluble in dipolar aprotic solvents and can be isolated from solution by precipitation with acetone or ether.

The structure of modified copolymers II and III was confirmed by elemental analyses, infrared spectra and imidization reactions. By heating in N-methylpyrrolidone under reflux they gave rise to the compounds II′ and III′ which showed characteristic absorption bands for imide cycle .[6] These latter compounds can only appear as a result of cyclodehydration of compounds II, respectively III, as shown in scheme 3 :

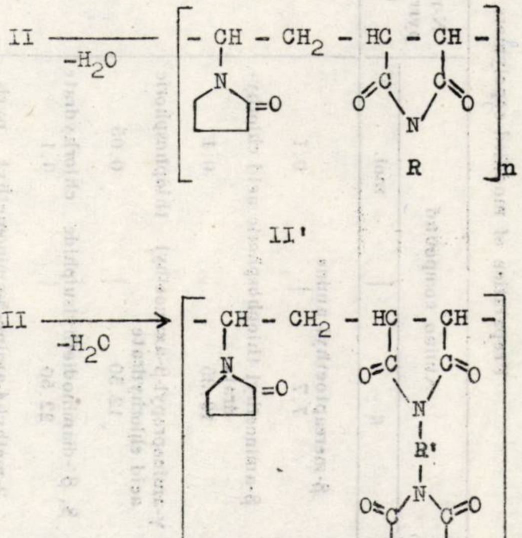

II'

III'

The modified copolymers II and III are white powders soluble in dipolar aprotic solvents such as : N-methylpyrrolidone, dimethylformamide, dimethylsulfoxide. They do not melt under 300°. Their infrared spectra show characteristic absorption bands for carboxylic OH at 3060 cm^{-1} and amidic NH at 3340 cm^{-1}. IR spectrum of the product IIa shows a weak absorption band[7] – characteristic for C–S bond at 700 cm^{-1} and another weak band characteristic for S–H bond at 2560 cm^{-1}. The product IIIb shows characteristic absorption bands[8] for pyrimidine cycle at 850 cm^{-1} and 1020 cm^{-1}.

All the modified copolymers synthesized in this paper have been tested for their ability to protect against ionizing radiations.[9] The following studies have been carried out: modification of cellular ultrastructure, modification of radioinduced genetic processes and survival of irradiated animals.

The study of the influence of gamma radiations on cellular ultrastructure of bacteria which have been irradiated in the presence of our compounds showed an attenuation of the destructive effect of radiations on cellular organites, also a decreased percentage of cells having severe ultrastructural alterations compared to the experiments which have been carried out in the absence of these chemical products.

The study of lethal effect induced by radiations at bacteria and yeast treated with our modified copolymers showed a decrease of induced lethality compared to untreated samples, the radioprotective effect being more pronounced at high doses of irradiation.

The survival test of irradiated rats in the presence of these polymers gave a survival of ten times higher than in the case of irradiated but untreated animals.

All these experiments showed that modified copolymers synthesized in this paper possess radioprotective action by attenuation of the noxious effect induced by radiations, decrease of induced lethality, increase of viability of irradiated organisms and increase of the percentage of survival. Copolymers modified with β-mercaptoethyl amine and 2-methyl-4-amino-5-aminomethyl pyrimidine showed remarkable and long-term radioprotective properties. The mechanism of radioprotective effect of these modified copolymers can be explained by delayed hydrolysis to micromolecules with protective groups and by the special properties resulting from the macromolecular structure which contains in the main chain N-vinylpyrrolidone units. The use of these polymers as a solution in dimethylsulfoxide leads to the intensification of radioprotective effect.

EXPERIMENTAL

Preparation of N-vinylpyrrolidone — maleic anhydride copolymer. In a three-necked flask equipped with mechanical stirrer, reflux condenser and N_2-inlet and outlet, were placed 19.6 g (0.2 mol) maleic anhydride and 110 mL dioxane dried and distilled over sodium wire. To the stirred solution 22.2 g (0.2 mol) N-vinylpyrolidone and 0.4 g azoisobutyronitrile were added. The reaction mixture was heated under stirring on a water bath for 7 h at 70—80°. The resulted copolymer was filtered off, washed with dioxane and ethylic ether. Elemental analysis ($C_{10}H_{11}NO_4$) : C% calcd : 57.41, found 57.09 : H% calcd : 5.21, found 5.04 ; N% calcd : 6.70, found 6.57.

Preparation of modified copolymers.

Table 1 shows the preparation of modified copolymers. The following example illustrates the general procedure : In a reaction flask fitted with stirrer, reflux condenser and N_2-atmosphere, 20.9 g (0.1 mol) vinypyrrolidone — maleic anhydride copolymer and 150 mL N-methylpyrrolidone dried and distilled over phosphorus pentoxide were introduced. The mixture was stirred until complete dissolution. Then 7.7 g (0.1 mol) β-mercaptoethyl amine were added and stirring was continued for 2 h at 40—45°. The viscous yellow solution was precipitated by pouring into acetone. The white product was filtered, washed with acetone and dried under vacuum at 60°.

Elemental analysis $C_{12}H_{18}N_2SO_4$) : C % calcd. 50.35, found 50.45 ; H % calcd. 6.30, found 6.75 ; N % calcd. 9.80, found 8.97 ; S % calcd. 11.25, found 10.95. IR spectrum shows characteristic absorption bands for carboxylic OH at 3060 cm $^{-1}$ and amidic NH at 3340 cm $^{-1}$.

The modified copolymers IIb and IIc have been prepared in a similar way using 1 mol of N vinylpyrrolidone — maleic anhydride copolymer to 1 mol of amino compound.

The modified copolymes IIIa and IIIb have been prepared using 2 mol copolymer to 1 mol of diamino compound.

Testing of radioprotective action. Radioprotective properties have been tested in the Institute of Biological Sciences — Bucharest. An irradiation source Co^{60} has been used. The experiments have been carried out on three groups of organisms : microorganisms (*Corynebacterium melasecola, Brevibacterium lactofermentum* and *Saccharomices cerevisiae*), plants (*Allium cepa*) and animals (*Mesocricetus auratus*). Radioprotective effect was evidenced in two ways : by comparing the percetange of mutalions induced by radiations in the presence of our modified copolymers and in the absence of them ; by comparing the radioprotective effect of our polymers with the effect of classic radioprotectors as cysteamine and cystamine.

CONCLUSIONS

By the research done in this paper the range of radioprotective compounds has been extended with a series of modified copolymers which have been synthesized by the reaction of micromolecular radioprotective amino compounds with N-vinylpyrrolidone-maleic anhydride copolymer. The final products are soluble in dimethylsulfoxide and can be used as a solution in this solvent which leads to the intensification of the radioprotective effect. Biological experiments carried out with these compounds showed remarkable, long-term radioprotective properties.

REFERENCES

[1] N. N. Suvorov and V. S. Shashkov, "Himiya i farmakologiya sredstv profilaktiki radiatzionnih porazheniy", Atomizdat, Moskow, 1975, p. 7.

[2] A. S. Mozzhuhin and F. Yu. Rachinskiy, "Himicheskaya profilaktika radiatzionnyh porazheniy", Atomizdat, Moskow, 1979, p. 78.

[3]. I. M. Parkhomenko, *Radiobiologiya*, **3**, 467 (1963).

[4] D. Martin, "Dimethylsulfoxide", Akademie — Verlag, Berlin, 1971, p. 445.

[5] A. F. Nikolaev, V. N. Bondarenko and N. K. Sakalova, *Vysokomol. Soedineniya*, Ser. B, **15**, 737 (1973).

[6] C. E. Sroog, *J. Polymer Sci., Macromol. Reviews*, **11**, 161 (1976).

[7] L. J. Bellamy, "*The Infrared Spectra in Organic Sulfur Compounds*" Pergamon Press., London, 1961, p. 47.

[8] A. R. Katritzky, "Physical Methods in Heterocyclic Chemistry", Vol. 2, Academic Press, New York, 1963, p. 292.

[9] G. Dumitrescu, *Doctoral Thesis*, Polytechnic Institute of Iaşi, Romania, 1979, p. 124.

Revue Roumaine de Chimie, **31**, *2*, **169—174 (1986)**

CATALYTIC INFLUENCES IN ELECTROOXIDATION OF OLEFINS IN NON-AQUEOUS SOLUTIONS. IV*

REACTION MECHANISM FOR OLEFIN OXIDATION IN METHANOL

RADU VLĂDEA
"Traian Vuia" Polytechnic Institute Timişoara Blvd. 30 Decembrie
No. 2 Timişoara, Romania

Received October 13, 1982
Revised February 15, 1985

The products compositions of the preparative anodic oxidations of diisobutylene and styrene as well as structural and kinetic data were used as arguments for a unitary oxidation mechanism of olefins in methanol.

Mechanistic studies, though not directly related to synthetic work, often provide valuable information regarding the paths of electrochemical oxidation processes; the synthetic organic chemist can then control his reaction conditions to achieve the desired effect or product.

All authors agree so for olefins may react either by a direct or an indirect oxidation mechanism.

Since the influence of anion nature on the yield of methoxylated products was observed, the following mechanism was assumed [1]

$$X^- \longrightarrow X^\bullet + e \tag{1}$$

$$RH + X^\bullet \longrightarrow R^\bullet + HX \tag{2}$$

$$CH_3OH \longrightarrow CH_3O^\bullet + H^+ + e^- \tag{3}$$

$$R^\bullet + CH_3O^\bullet \longrightarrow ROCH_3 \tag{4}$$

where X^- is the supporting electrolyte anion. The influence of the anion nature on the olefin oxidation process has been also demonstrated by several other groups [2-4] but it is rather difficult to assume more than a replacement electrosorption on the electrode surface since, on the one hand anions like F^-, ClO_4^- are very stable, and on the other hand the process is independent of the presence of inhibitors, e.g. oxygen [4,5].

Another indirect mechanism has been suggested for some alcoxylation reactions. [6,7] An interesting mechanism was assumed in the case of ester α-methoxylations using sodium methoxide in methanol [2]:

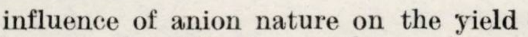

$$RO{-}\underset{|}{\overset{|}{C}}H + MeO^- \longrightarrow RO{-}\underset{|}{\overset{|}{C}}{-}OMe + 2e + H^+ \tag{5}$$

---

* Part III in. Rev. Roumaine Chim., **30**, **249** (**1985**)

An indirect mechanism which assumes an intermediate methoxy radical has been suggested for tetraline α-methoxylation (in methanol and NaCN) since the tetraline half-wave potential is ca. 1.9 V vs. SCE whilst the reaction takes place at $+0.5$ V.[3]

The second mechanistic pathway assumes a direct oxidation of the organic substrate when a radical-cation is formed in the first step. The next steps involve either an electron transfer following a proton elimination or a proton elimination followed by a reaction with a nucleophile :

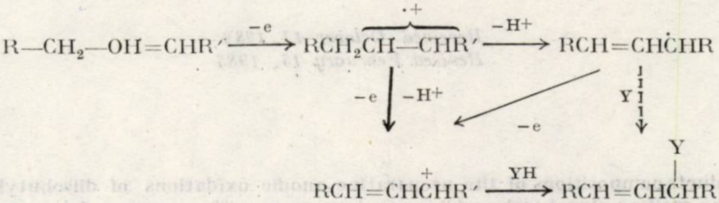

(6)

Shono and Ikeda [8] have demonstrated this mechanism for the olefin oxidation in very stable solvents (CH_3CN, CH_3COOH) but, at the same time, have recognized that the olefin methoxylation may have a different mechanism.

It is the aim of this paper to suggest another mechanism supported by kinetic and structural data.

The first step is the electrochemical oxidation of methanol to the radical-cation **1** :

$$CH_3—O—H \xrightarrow{-e} CH_3—\overset{\cdot+}{O}—H \qquad (7)$$

1

In the absence of a nucleophile the course of the reaction could explain the formaldehyde generation :

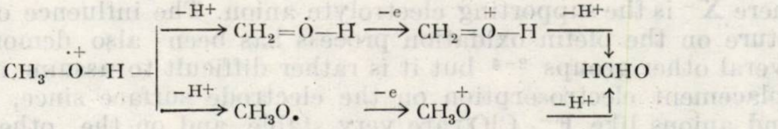

(8)

The presence of CH_2O as a side product was also mentioned by other authors.[5,9]

The methanol oxidation follows an electrochemical-chemical-electrochemical-chemical (ECEC) pathway, frequently met in organic electrochemistry.

The presence of an olefin in the close proximity of the electrode surface drastically alters the course of the reaction. An olefin, e.g. DIB will react with the radical cation **1** or perhaps, with a methoxy radical in one of the following pathways :

a)

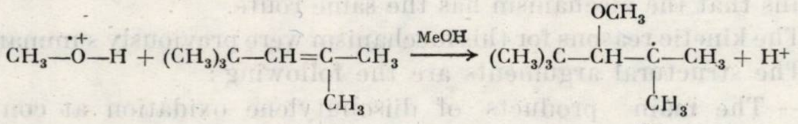

$$CH_3-\overset{+}{O}-H + (CH_3)_3C-CH=\underset{\displaystyle CH_3}{C}-CH_3 \xrightarrow{MeOH} (CH_3)_3C-CH-\underset{\displaystyle CH_3}{\overset{\displaystyle OCH_3}{C}}-CH_3 + H^+ \qquad (9)$$

2

b)

$$CH_3-\overset{+}{O}-H \longrightarrow CH_3O^{\bullet} + H^+$$

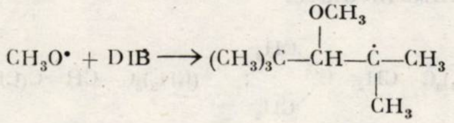

$$CH_3O^{\bullet} + DIB \longrightarrow (CH_3)_3C-\overset{\displaystyle OCH_3}{CH}-\underset{\displaystyle CH_3}{\dot{C}}-CH_3 \qquad (10)$$

3

c)

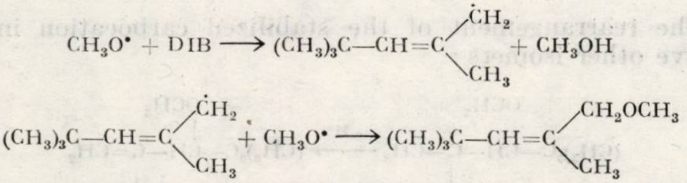

$$CH_3O^{\bullet} + DIB \longrightarrow (CH_3)_3C-CH=C\begin{matrix}\dot{C}H_2\\ CH_3\end{matrix} + CH_3OH \qquad (11)$$

$$(CH_3)_3C-CH=C\begin{matrix}\dot{C}H_2\\ CH_3\end{matrix} + CH_3O^{\bullet} \longrightarrow (CH_3)_3C-CH=C\begin{matrix}CH_2OCH_3\\ CH_3\end{matrix}$$

Kinetic reasons, especially the independence of the half-wave potentials of the olefin nature, have supported the consideration of route a) as rather unlikely. The route c) is probable but it assumes a radicalic reaction in solution where it should be hindered by oxygen presence; working under dry nitrogen atmosphere did not change the results obtained under normal conditions in the presence of air .[4,10]

The best convergence of kinetic and structural data should be obtained with the route b). Radical **3** is quickly oxidized [8] giving a stabilized carbocation **4**

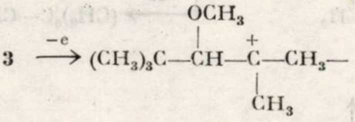

$$3 \xrightarrow{-e} (CH_3)_3C-\overset{\displaystyle OCH_3}{CH}-\underset{\displaystyle CH_3}{\overset{+}{C}}-CH_3- \qquad (12)$$

4

The rearrangements of this carbocation could account for the isomers of 142 molecular weight.[11]

It means that the anodic oxidation of DIB in methanol is of ECEC type.

The first intermediate in the case of styrene is radical **5**

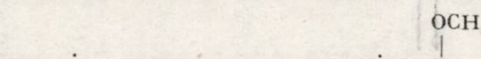

$$CH_3-\dot{O} + C_6H_5CH=CH_2 \longrightarrow C_6H_5\dot{C}H-\overset{\displaystyle OCH_3}{CH_2} \qquad (13)$$

5

when a simultaneous proton exclusion is supposed.

Radical **5** is oxidized giving a very stable carbocation :

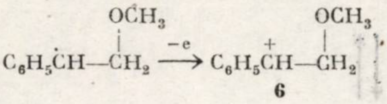

$$C_6H_5\dot{C}H-\overset{\displaystyle OCH_3}{CH_2} \xrightarrow{-e} C_6H_5\overset{+}{C}H-\overset{\displaystyle OCH_3}{CH_2} \qquad (14)$$

6

Carbocation **6** could account for the main identified products.[11] It means that the mechanism has the same route.

The kinetic reasons for this mechanism were previously summarized.[12] The structural arguments are the following:

— The main products of diisobutylene oxidation at controlled potential electrolysis were irrespective of the initial mixture composition of DIB (mixtures of **7** and **8**), indicating that they derive from a common stabilized radical intermediate.

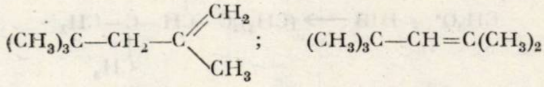

7 **8**

— The rearrangement of the stabilized carbocation intermediate **4** could give other isomers:

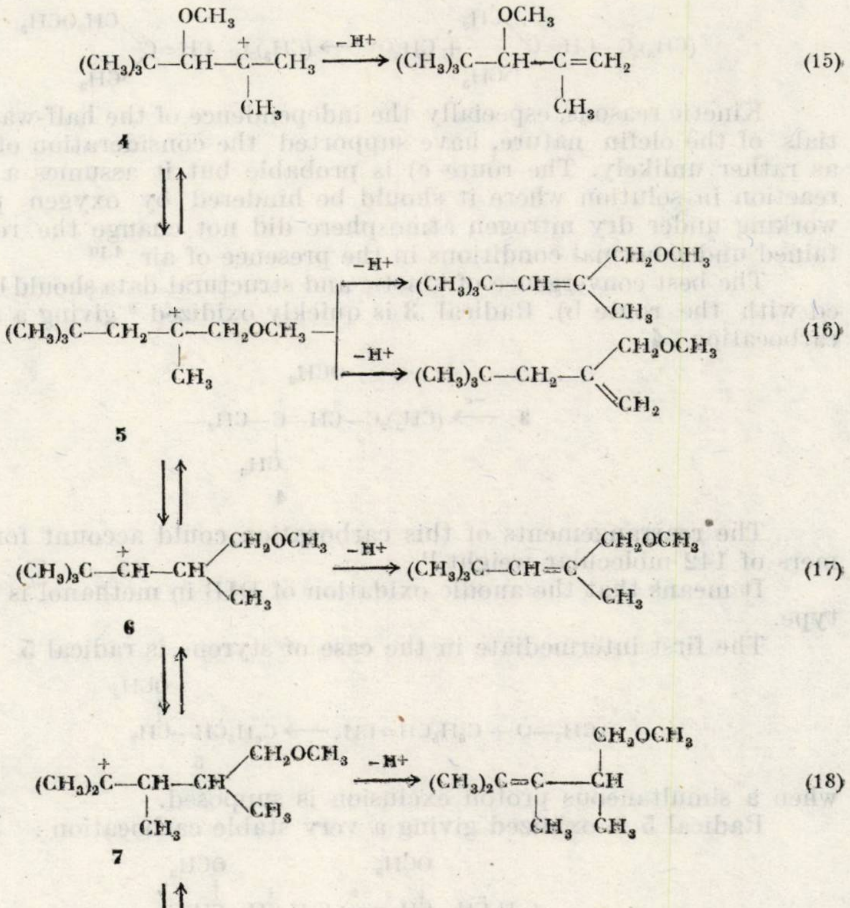

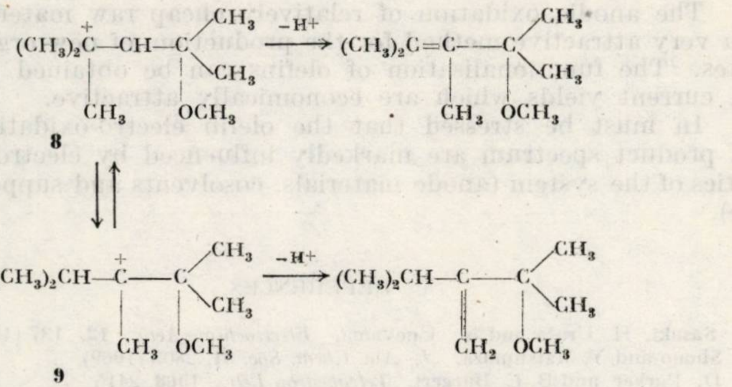

(19)

(20)

The other components could be likely explained.

The styrene oxidation on carbon electrode has given some different products [4,11] in comparison with the results of Wendt.[10]

The presence of a carbocation intermediate can afford all previously identified products.[11]

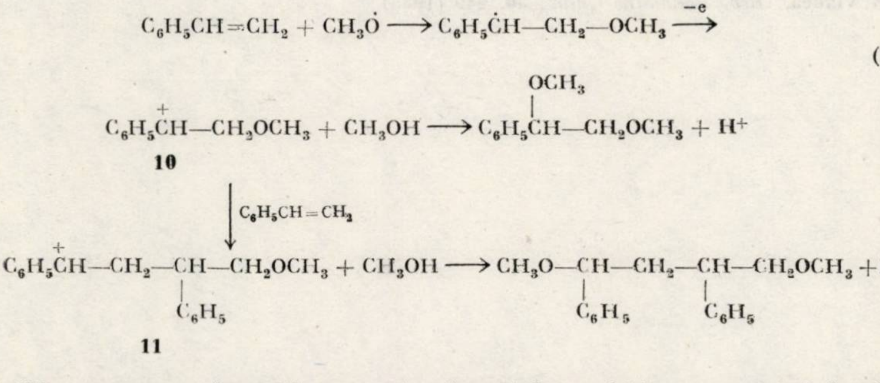

$$C_6H_5CH{=}CH_2 + CH_3\dot{O} \longrightarrow C_6H_5\dot{C}H{-}CH_2{-}OCH_3 \xrightarrow{-e}$$

$$C_6H_5\overset{+}{C}H{-}CH_2OCH_3 + CH_3OH \longrightarrow C_6H_5\overset{\overset{OCH_3}{|}}{C}H{-}CH_2OCH_3 + H^+ \qquad (21)$$

10

$$\Big\downarrow C_6H_5CH{=}CH_2$$

$$C_6H_5\overset{+}{C}H{-}CH_2{-}\underset{\underset{C_6H_5}{|}}{CH}{-}CH_2OCH_3 + CH_3OH \longrightarrow CH_3O{-}\underset{\underset{C_6H_5}{|}}{CH}{-}CH_2{-}\underset{\underset{C_6H_5}{|}}{CH}{-}CH_2OCH_3 + H^+$$

11

The presence of small amounts of acetals could be accounted for by a radicalic mechanism. The methoxy radical $CH_3O^{\bullet}$ may react with 1,2-dimethoxy-etylbenzene giving an ether-acetal:

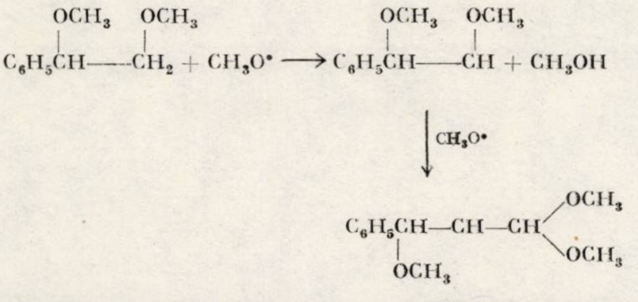

(22)

This mechanism provides a good correlation between the products spectrum and the kinetic and structural data.

The anodic oxidation of relatively cheap raw materials seems to be a very attractive method for the production of new organic intermediates. The functionalisation of olefins can be obtained with material and current yields which are economically attractive.

In must be stressed that the olefin electro-oxidation selectivity and product spectrum are markedly influenced by electrocatalytic properties of the system (anode materials, cosolvents and supporting electrolyte).

REFERENCES

[1] K. Sasaki, H. Urata and K. Uneyama, *Electrochim. Acta,* **12**, 137 (1967).

[2] T. Shono and Y. Matsumura, *J. Am. Chem. Soc.* **91**, 2803 (1969).

[3] V. D. Parker and B. E. Burgert, *Tetrahedron Lett.*, **1968**, 2415.

[4] Gh. Facsko and R. Vlădea, Conf. Rep. Ch. Fiz., București, 1976.

[5] M. Katz, Oe. Saygin and H. Wendt, *Electrochem. Acta,* **19**, 193 (1974).

[6] S. D. Ross, M. Finkelstein and R. C. Peterson, *J. Am. Chem. Soc.*, **88**, 4657 (1967).

[7] E. J. Rudd, M. Finkelstein and S. D. Ross, *J. Org. Chem.*, **37**, 1763 (1972).

[8] T. Shono and A. Ikeda, *J. Amer. Chem. Soc.*, **94**, 7892 (1972).

[9] M. Katz, P. Riemenschneider and H. Wendt, *Electrochim. Acta,* **17**, 1595 (1972).

[10] V. Plzak, H. Schneider and H. Wendt, *Ber. Bunsenges. physik. Chem.*, **78**, 1373 (1974).

[11] R. Vlădea and P. Kerek, *Rev. Roumaine Chim.*, **30**, 157 (1985).

[12] R. Vlădea, *Rev. Roumaine Chim.*, **30**, 249 (1985).

Revue Roumaine de Chimie, **31**, 2, 175—197 (1986)

DISSIPATIVE STRUCTURES IN REACTION-DIFFUSION SYSTEMS AS SYNCHRONIZATION PHENOMENA

DAN CARTIANU

ICECHIM — Centre of Physical Chemistry,
Splaiul Independenței 202, Bucharest, Romania

Received November 10, 1984

Two kinds of dissipative structures, phase waves and trigger waves in the Belousov-Zhabotinskii reaction-diffusion system have been described as phase and frequency synchronization phenomena of adjacent oscillatory domains of the reagent. An equation has been derived for the time evolution of the phase difference between two adjacent reaction cells, coupled by diffusion, in which two concentrations of intermediates oscillate. The phase distribution function for ensembles of coupled oscillators is determined in the harmonic approximation. Its evolution is established. The time evolution of the synchronized and unsynchronized ensembles of oscillators is also determined. Trigger waves are considered as originating from the break up of the gradient of frequency into several plateaux of synchrony, within which all oscillators are entrained by the fastest one. In the harmonic approximation an equation is derived for the phase shift of the local oscillators with respect to the frequency-synchronized state.

INTRODUCTION

In the present paper I will demonstrate that the concept of synchronization explains several forms of self-organization of matter.

Two kinds of dynamic dissipative structures, phase waves and trigger waves are described in this paper as arising in systems consisting of many oscillatory compartments coupled with each other by diffusion. For systems of several such oscillators two forms of coupling, parallel coupling and series coupling, are considered. The latter form of coupling arises in a finite-difference approximation of the reaction-diffusion equations in distributed chemical systems. $^{1-4}$

An equation is derived for the time evolution of the phase shift between two oscillatory two-variable reaction systems coupled by diffusion, thus permitting an understanding of the phenomenon of phase waves.

On the basis of the equation derived for two coupled oscillators, the phase synchronization of ensembles of chemical reaction oscillators coupled by diffusion is studied, in the case of harmonic oscillations.

The distribution of phases is calculated in terms of a function, given by a differential equation which is exactly solvable for the case of a uniform initial distribution of phases, but which has a Dirac-function peak at the origin of the coordinate space. corresponding to a pacemaker of the trigger waves which synchronizes the adjacent reagent volumes.

The frequency synchronization condition is established for a system of parallel-coupled Van der Pol oscillators in the harmonic approximation.

A frequency drift with respect to the synchronized state was found. The assumed Lorentzian distribution of frequencies exhibits a frequency-synchronized Dirac function component and a nonsynchronized background. These formulas form the basis of the understanding of phase and trigger waves as phase and frequency synchronization phenomena.

2. THE INTERPRETATION OF DISSIPATIVE STRUCTURES IN THE BELOUSOV-ZHABOTINSKII REAGENT AS SYNCHRONIZATION PHENOMENA

The discovery of dynamic patterns in the BZ reaction : the metal ion catalyzed oxidation and bromination of certain organic compounds by bromate ions, has triggered a significant new research direction for finding stable wave-like solutions of reaction-diffusion equations.

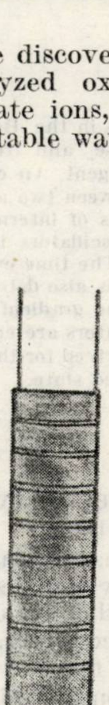

Fig. 1. — Phase waves in the Belousov-Zhabotinskii reagent.

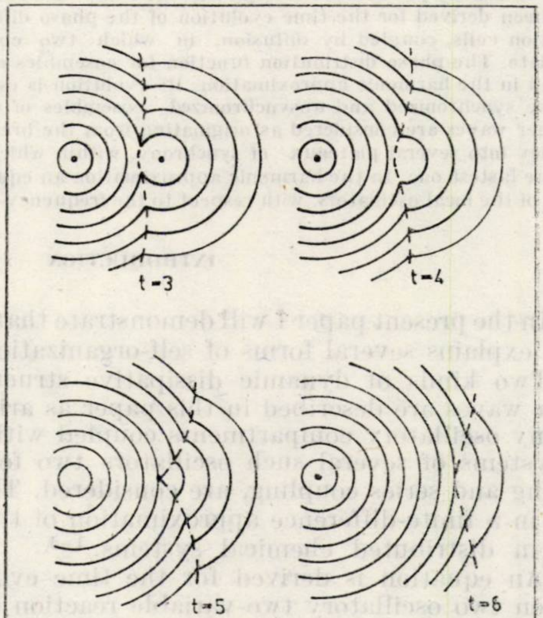

Fig. 2. — Propagation of trigger waves at time intervals of one minute. The target patterns propagate starting from the region with greatest frequency. They entrain the lower frequency patterns.

The phenomena observed in the unstirred BZ reagent are of two kinds. Kinematic waves ^{5} appear only in the oscillatory reagent and propagate independently of diffusion along a phase gradient which develops in an unstirred medium of large extent. Such waves are independent of diffusion since they are not stopped by obstacles. Trigger waves [6] propagate by means of the interaction of chemical reaction and diffusion of intermediate species in oscillatory reagents as well as in quiescent but excitable reagents.

If the phase of the oscillation with period T of an oscillatory reagent in a tall cylinder varies linearly over the length of the cylinder, the waves' velocity is inversely proportional to the phase gradient :

$$\varphi(z, t) = \varphi_0(z) + 2\pi t/T \tag{2.1}$$

The wave velocity

$$v = \left.\frac{\mathrm{d}z}{\mathrm{d}t}\right|_{\varphi=\mathrm{const}} = \frac{\partial\varphi/\partial t}{\partial\varphi_0/\partial z} = -\frac{2\pi}{T}\cdot\frac{1}{\partial\varphi_0/\partial z} \tag{2.2}$$

is equal to the reciprocal of the phase gradient. The range of possible phase wave velocities in a particular reagent is very large. If $\partial\varphi_0/\partial z < 0$, then $v > 0$ and the oxidation bands move upward.

Kinematic waves which are packed ever closer together as phase gradients steepen and velocities decrease in time, are observed in BZ reagents with frequency gradients. In tall cylinder it is possible to create frequency gradients by applying a temperature gradient.

The phase

$$\varphi(z, t) = \varphi_0(z) + \Psi(z, t) \tag{2.3}$$

where $\varphi_0(z)$ is the initial phase distribution and $\Psi(z, t)$ satisfies :

$$\Psi(z, 0) = 0, \quad \Psi(z, t + T(z)) = \Psi(z, t) + 2\pi \tag{2.4}$$

where $T(z)$ is the local autonomous period. Suppose $\varphi_0(z) = 0$. Define $t_k(z)$ by

$$\varphi(z, t_k(z)) = 2\pi k, \quad 0 < z < 1, \tag{2.5}$$

i.e. $t_k(z)$ is the time at which the k-th wave front reaches position z. Calling the initial synchronous oscillations the $k = 0$ wave, we have :

$$t_k(z) = kT(z) \tag{2.6}$$

and the velocity of the k-th wave is :

$$\mathrm{v}_k = \left.\frac{\mathrm{d}z}{\mathrm{d}t}\right|_{\varphi=2\pi k} = \left(\frac{\mathrm{d}t_k(z)}{\mathrm{d}z}\right)^{-1} = \frac{1}{kT'(z)} \tag{2.7}$$

If $T(z)$ is monotone increasing, $T' > 0$ and the k-th blue oxidation zone enters at $z = 0$, $t = kT(0)$, propagates up the tube at $1/k$ times the velocity of the first wave, and leaves at $z = 1$, $t = kT(1)$. Since the velocity decreases as k increases, the waves are packed ever closer together in the vicinity of $z = 0$.

The waves which depend on the interaction of reaction and diffusion or trigger waves are of two kinds : target patterns and scroll waves. Target patterns are axisymmetric periodic travelling waves which appear around a heterogeneous nucleus, the pacemaker of the pattern. Frequency and wavelength may vary from pattern to pattern. The patterns of greater frequency propagate through the ones with lower frequency, i.e. synchronize the oscillation at their own frequency. Scroll waves [7] are observed in carefully filtered reagents under proper initial conditions and are of several kinds : symmetric spirals, elongated spirals, elongated rings, scroll rings. They can arise in excitable reagents from target patterns by tilting the recipient containing the reagent, due also to the refractary state which follows upon an excited state.

In a thin layer (2 mm) of reagent which is not oscillatory, due to the inhibitory role of the oxygen in the air, the distinctive feature of excitability can be analyzed : in response to finite disturbances of the concentrations the system makes a large loop in the space on the intermediate substances, i.e. the perturbations are greatly amplified. The system is refractary just behind the propagating colored excitation wave. This refractariness explains the mutual destruction of trigger waves upon collision. The mechanistic details of the BZ system and the waveforms for target patterns, spiral waves, etc. for the Oregonator model [1] for the three intermediates concentrations are described in [8].

Mathematically it is not necessary that the target patterns be produced by pacemakers, as [9] one can construct axisymmetric periodic travelling waves for a simplified so called $\lambda - \omega$ model of the reaction term, which are completely regular at the origin.

Trigger waves travel at a unique velocity defined by the reaction and diffusion properties of the system. They propagate through the diffusion of the autocatalytically produced species ($HBrO_2$) in the region with high Br^- ion concentration. If k is the rate constant of the autocatalytic step, the velocity

$$v = \sqrt{kD} = \sqrt{k_0 D_0} \exp\left(-\frac{E_k + E_D}{2k_B T}\right), \tag{2.8}$$ [10]

k_B being Boltzmann's constant and T the absolute temperature.

The core of the spiral wave which originates not necessarily from heterogeneous pacemakers shows complicated, even chaotic time evolution.

In an oscillatory reagent trigger wave velocity may be variable as a result of spatial gradients in bromide ion concentration residual from an initially present phase gradient. If a phase wave is moving more slowly than a trigger wave would move under the same conditions, the phase wave will initiate this trigger wave. Trigger waves do not require an oscillatory medium. In the case of a nonoscillatory BZ reagent with a stable but excitable kinetic steady state, the initial pulse of a trigger wave occurs at a pacemaker center probably as the result of heterogeneous catalysis at a gas bubble, a particle, or scratch in the recipient, the reagent being very sensitive to perturbations.

A well stirred BZ reagent will oscillate synchronously throughout its volume. In the unstirred reagent there is no requirement for all parts of the reagent to oscillate synchronously. This fact is the basis of the appearance of phase waves, waves of oxidation. There is a maximum velocity at which a phase wave can travel.

In an oscillatory BZ reagent, phase waves and trigger waves coexist. One expects the minimum phase wave velocity in a particular BZ reagent to be that of a trigger wave propagation under the same conditions with an initial phase wave. By a similar mechanism a pacemaker may initiate a single trigger wave in a synchronously but slowly oscillatory reagent. Passage of this initial trigger wave will generate a phase gradient, and it will be followed by phase waves travelling at the velocity of the initial trigger waves, but appearing at the frequency of temporal oscillation in the medium. The first wave may not be identical with a trigger wave propagating in a nonoscillatory medium. Furthermore while the following waves will have all the properties of a phase wave they will be travelling slowly enough to be influenced by diffusion.

By numerically integrating the partial differential equations of the three-variable kinetic model called Oregonator [1], with diffusion terms for each intermediates' concentrations, in [11] travelling wave solutions are found which are identifiable as either phase waves or trigger waves mainly on the basis of whether their mechanism of propagation is critically dependent on diffusion. In [12] it is shown that all phase waves of sufficiently slow velocity (steep phase gradient) initiate trigger waves which travel at a velocity mainly characteristic of the particular BZ reagent. For phase gradients $|\nabla \varphi| = 0.1$ s/mm, a phase wave appears with a velocity of 600 mm/min. For $|\nabla \varphi| \sim 1$ s/mm the effects of diffusion become apparent and at $|\nabla \varphi| > 10$ s/mm they become dominant. For $|\nabla \varphi| = 25$ s/mm the expected phase wave velocity is 2.4 mm/min. The calculated wave velocity increases rapidly from the expected phase wave velocity of 2.4 mm/min to about 50 mm/min. The increase in propagation velocity is accompanied by a large increase in pulse width. This means that a faster, diffusion-dependent wave is initiated by a slower phase wave. The trigger wave velocity is not constant but is affected by spatial changes in bromide ion concentration residual from the phase gradient that initial phase wave was propagating along.

A common feature of the dissipative structures described above is the initial synchronization of the phases. The spontaneous phase synchronization of the oscillations occurring in various volume elements of the system is characteristic of the phase waves. A characteristic of trigger waves is that the gradient of frequency breaks up into several plateaux of synchrony within which all oscillators are entrained by the fastest one. This produces a gradient of phase parallelling the gradient of frequency. The wave propagating down this gradient has the velocity of a phase wave, but unlike it its passage is blocked by any transverse obstacle which breaks the synchronizing interactions i.e. the coupling by diffusion

3. PHASE SHIFT EVOLUTION EQUATION FOR TWO OSCILLATORY TWO-VARIABLE REACTION SYSTEMS COUPLED BY DIFFUSION

I will derive now an equation for the phase shift evolution.

A Brusselator-type model [1] with only two variables can be written as :

$$\begin{aligned} \dot{x}_1 &= f(x_1, y_1) + \lambda[k(x_2 - x_1) + \delta f_1(x_1, y_1)] \\ \dot{y}_1 &= g(x_1, y_1) + \lambda[k(y_2 - y_1) + \delta g_1(x_1, y_1)] \\ \dot{x}_2 &= f(x_2, y_2) + \lambda k(x_1 - x_2) \\ \dot{y}_2 &= g(x_2, y_2) + \lambda k(y_1 - y_2) \end{aligned} \tag{3.1}$$

where $0 < \lambda \ll 1$, and $k = D_1 = D_2$ and $\delta \neq 0$ distinguishes the case when two different oscillations are coupled, $\lambda = 0$ corresponds to the case of uncoupled oscillations, λ being a small parameter of the order of magnitude of the diffusion coefficients. Equal diffusion coefficients are assumed, just as in the criterion for phase synchronization derived in [1].

The assumption is made that the uncoupled systems have a stable T-periodic limit cycle :

$$x_1 = X(t + \Psi_i), \quad y_i = Y(t + \Psi_i), \quad i = 1, 2 \tag{3.2}$$

The $O(\lambda)$ diffusion terms in (3.1) determine on the orbit $(x_i(t), y_i(t))$ displacements of order $O(\lambda)$ from the trajectory of the limit cycle (3.2). By a change of variable $(x, y) \rightarrow (M, \theta)$ defined by :

$$x = X(\theta) + \lambda M Y'(\theta), \quad y = Y(\theta) - \lambda M X'(\theta) \tag{3.3}$$

where θ parametrizes the limit cycle and λM measures orthogonal displacements from the limit cycle of the uncoupled systems, (3.1) becomes :

$$\begin{aligned} \dot{M}_1 &= R(\theta_1)M_1 + kU(\theta_1, \theta_2) + \delta S(\theta_1) + \lambda N_1(\mathbf{M}, \boldsymbol{\theta}) + O(\lambda^2) \\ \dot{\theta}_1 &= 1 + \lambda[\Lambda(\theta_1)M_1 + \delta\Lambda_1(\theta_1) + kr(\theta_1) + kV(\theta_1, \theta_2)] + O(\lambda^2) \\ M_2 &= R(\theta_2)M_2 + kU(\theta_2, \theta_1) + \lambda N_2(\mathbf{M}, \boldsymbol{\theta}) + O(\lambda^2) \\ \dot{\theta}_2 &= 1 + \lambda[\Lambda(\theta_2)M_2 + kr(\theta_2) + kV(\theta_1, \theta_2)] + O(\lambda^2) \end{aligned} \tag{3.4}$$

where : $U(\theta_1, \theta_2) = [X(\theta_2)Y'(\theta_1) - Y(\theta_2)X'(\theta_1)]/R_1^2(\theta_1)$

$$V(\theta_1, \theta_2) = [X(\theta_2)X'(\theta_1) + Y(\theta_2)Y'(\theta_1)]/R_1^2(\theta_1).$$

$$R_1^2(\theta) = X'^2(\theta) + Y'^2(\theta).$$

The form of the other functions of (3.4) does not appear in the derivation. They are all T-periodic in θ_1 and θ_2.

For a uniform solution, equal in the two identical reaction cells :

$$\dot{M}_1 = R(\theta_1)M_1 + O(\lambda), \quad \frac{\mathrm{d}\theta_1}{\mathrm{d}t} = 1 + O(\lambda) \tag{3.5}$$

hence :

$$\frac{\mathrm{d}M_1}{\mathrm{d}t} = R(t)M_1 + O(\lambda) \tag{3.6}$$

for time intervals with length $O(1)$. Integration of this equation gives :

$$\frac{M_1(t+T)}{M(t)} = (1 + O(\lambda)) \exp\left(\int_0^T R(\zeta)\,\mathrm{d}\zeta\right) \tag{3.7}$$

because by the periodicity of R, $\int_t^{t+T} R(\zeta)\,\mathrm{d}\zeta = \int_0^T R(\zeta)\mathrm{d}\zeta$. In (M_1, θ_1) coordinates the limit cycle is given by $M_1 = 0$, $\theta_1 = t + \Psi_1$. Stability of the limit cycle means that $M_1(t) \to 0$, as $t \to \infty$. This implies

$$\int_0^T R(\zeta)\mathrm{d}\zeta < 0 \tag{3.8}$$

To leading order in λ, the asymptotic expression of the solution of (3.4) has the form :

$$M^i \sim M_i^0 + \lambda M_i^1, \quad \theta_i = \theta_i^0 + \lambda\theta_i^1 \tag{3.9}$$

We obtain the following hierarchy of equations to order $O(1)$:

$$\frac{\partial M_1^0}{\partial t} - R(\theta_1^0) = kU(\theta_1^0, \theta_2^0) + \lambda S(\theta_1^0)$$

$$\frac{\partial \theta_1^0}{\partial t} = 1 \tag{3.10}$$

$$\frac{\partial M_2^0}{\partial t} - R(\theta_2^0)M_2^0 = kU(\theta_2^0, \theta_1^0)$$

$$\frac{\partial \theta_2^0}{\partial t} = 1$$

and to order $O(\lambda)$, introducing the slow variable $\tau = \lambda t$:

$$\frac{\partial M_1^1}{\partial t} - R(\theta_1^0)M_1^1 = \left[R'(\theta_1^0)M_1^0 + k\frac{\partial U}{\partial \theta_1}(\theta_1^0, \theta_2^0) + \lambda S'(\theta_1^0)\right]\theta_1^1 +$$

$$+ k\frac{\partial U}{\partial \theta_2}(\theta_1^0, \theta_2^0)\theta_2^1 + N_1(\mathbf{M}^0, \boldsymbol{\theta}^0) - \frac{\partial M_1^0}{\partial \tau}$$

$$\frac{\partial \theta_1^1}{\partial t} = \Lambda(\theta_1^0)M_1^0 + \lambda\Lambda_1(\theta_1^0) + kr(\theta_1^0) + kV(\theta_1^0, \theta_2^0) - \frac{\partial \theta_1^0}{\partial \tau} \tag{3.11}$$

$$\frac{\partial M_2^1}{\partial t} - R(\theta_2^0)M_2^1 = \left[R'(\theta_2^0)M_2^0 + k\frac{\partial U}{\partial \theta_1}(\theta_2^0, \theta_1^0)\right]\theta_2^1 + k\frac{\partial U}{\partial \theta_2}(\theta_2^0, \theta_1^0)\theta_1^1 +$$

$$+ N_2(\mathbf{M}^0, \boldsymbol{\theta}^0) - \frac{\partial M_2^0}{\partial \tau}$$

$$\frac{\partial \theta_2^1}{\partial t} = \Lambda(\theta_2^0)M_2^0 + kV(\theta_2^0, \theta_1^0) + kr(\theta_2^0) - \frac{\partial \theta_2^0}{\partial \tau}.$$

From the order $O(1)$ equations we deduce:

$$\theta_i^0 = t + \Psi_i(\tau),\ i = 1, 2 \tag{3.12}$$

Introducing these values into the other $O(1)$ equations (3.10), the following equations will result:

$$\frac{\partial M_1^0}{\partial t} - R(t + \Psi_1)M_1^0 = kU(t + \Psi_1, t + \Psi_2) + \lambda S(t + \Psi_1) \tag{3.13}$$

$$\frac{\partial M_2^0}{\partial t} - R(t + \Psi_2)M_2^0 = kU(t + \Psi_2, t + \Psi_1)$$

The homogenous solution: $\exp\left(\int^{\zeta} R(\zeta)\mathrm{d}\zeta\right)$ is decaying due to the stability condition (3.8) of the limit cycle. The equations (3.13) with periodic coefficients and nonhomogenous terms:

$$\frac{\mathrm{d}x}{\mathrm{d}\zeta} - R(\zeta)x = S(\zeta) \tag{3.14}$$

$$\frac{\mathrm{d}y}{\mathrm{d}\zeta} - R(\zeta)y = U(\zeta, \zeta - \Psi)$$

where $\Psi = \Psi_2 - \Psi_1$, have thus unique T-periodic solutions :

$$x = \rho(\zeta), \quad y = \rho(\zeta, \Psi), \tag{3.15}$$

The general solutions of (3.13) become :

$$\begin{aligned} M_1^0 &= k\rho(t + \Psi_1, \Psi) + \lambda\rho(t + \Psi_1) + h_1(\tau)\exp\left(v(t + \Psi_1)\right) \\ M_2^0 &= k\rho(t + \Psi_2, -\Psi) + h_2(\tau)\exp\left(v(t + \Psi_2)\right) \end{aligned} \tag{3.16}$$

Introducing (3.16) into the order $O(\lambda)$ equations (3.11) the following equations will result :

$$\begin{aligned} \frac{\partial\theta_1^1}{\partial t} &= [k\rho(t + \Psi_1, \Psi) + \lambda\rho(t + \Psi_1)]\Lambda(t + \Psi_1) + \lambda\Lambda_1(t + \Psi_1) + kr(t + \Psi_1) + \\ &\quad + kV(t + \Psi_1, t + \Psi_2) - \frac{d\Psi_1}{d\tau} + h_1(\tau)\Lambda(t + \Psi_1)\exp(v(t + \Psi_1)) \\ \frac{\partial\theta_2^1}{\partial t} &= k\rho(t + \Psi_2, -\Psi)\Lambda(t + \Psi_2) + kV(t + \Psi_2, t + \Psi_1) - \frac{d\Psi_2}{d\tau} + \\ &\quad + h_2(\tau)\Lambda(t + \Psi_2)\exp(v(t + \Psi_2)) \end{aligned} \tag{3.17}$$

By writing a T-periodic function $f(t)$ as $\mu + \omega(t)$, where $\mu = \dfrac{1}{T}\displaystyle\int_0^T f(\zeta)\,d\zeta$ and $\omega(t)$ is T-periodic with zero mean, the equations (3.17) become :

$$\begin{aligned} \frac{\partial\theta_1^1}{\partial t} &= \mu_1(\Psi) + \omega_1(t, \tau) \\ \frac{\partial\theta_2^1}{\partial t} &= \mu_2(\Psi) + \omega_2(t, \tau) \end{aligned} \tag{3.18}$$

where

$$\begin{aligned} \mu_1 &= kH(\Psi) + \lambda\beta - d\Psi_1/d\tau \\ \mu_2 &= kH(-\Psi) - d\Psi_2/d\tau \end{aligned} \tag{3.19}$$

with

$$\beta = \frac{1}{T}\int_0^T [\rho(\zeta)\Lambda(\zeta) + \Lambda_1(\zeta)]\,d\zeta$$

$$H(\Psi) = \frac{1}{T}\int_0^T [\rho(\zeta, \Psi)\Lambda(\zeta) + V(\zeta, \zeta + \Psi) + r(\zeta)]\,d\zeta \tag{3.20}$$

The solutions of equations (3.18) are :

$$\theta_1^1 = \mu_1(\Psi)t + W_1(t, \tau)$$

$$\theta_2^1 = \mu_2(\Psi)t + W_2(t, \tau) \tag{3.21}$$

where W_1 and W_2 are bounded.

Introducing this into the order $O(\lambda)$ equations (3.11) one obtains :

$$\frac{\partial M_2^1}{\partial t} - R(t + \Psi_2)M_2^1 = [S_1(t, \tau)\mu_1 + S_2(t, \tau)\mu_2]t + B(t, \tau) \tag{3.22}$$

where :

$$S_1 = k\frac{\partial U}{\partial \theta_2}(t + \Psi_1,\ t + \Psi_2)$$

$$S_2 = k\frac{\partial U}{\partial \theta_1}(t + \Psi_2,\ t + \Psi_1) + k\rho(t + \Psi_2,\ -\Psi)R'(t + \Psi_2)$$

The quantity M_2^1 must be bounded for all t, so that :

$$S_1(t, \tau)\,\mu_1 + S_2(t, \tau)\mu_2 = 0 \tag{3.23}$$

S_1 and S_2 being different T-periodic functions. One concludes that $\mu_1 = \mu_2 = 0$, i.e.

$$\frac{\mathrm{d}\Psi_1}{\mathrm{d}\tau} = kH(\Psi) + \lambda\beta$$

$$\frac{\mathrm{d}\Psi_2}{\mathrm{d}\tau} = kH(-\Psi), \tag{3.24}$$

where $\Psi = \Psi_2 - \Psi_1$, and :

$$\frac{\mathrm{d}\Psi}{\mathrm{d}\tau} = kP(\Psi) + \lambda\beta \tag{3.25}$$

where $P(\Psi) = H(-\Psi) - H(\Psi)$.

A similar formula was mentioned in [13]. We see that $H(\Psi)$ is T-periodic, hence also $P(\Psi)$ is T-periodic. The equality $P(\Psi = 0) = 0$ also holds. The derivative of H is :

$$H'(0) = \frac{1}{T}\int_0^T \left[\frac{\partial \rho}{\partial \Psi}(\zeta, 0)\Lambda(\zeta) + \frac{\partial V}{\partial \theta_2}(\zeta,\ \zeta)\right]\mathrm{d}\zeta \tag{3.26}$$

$\rho(\zeta, \Psi)$ is defined in (3.15) by the T-periodic solution of (3.14). Differentiating (3.14) with respect to Ψ, at $\Psi = 0$, one obtains :

$$\frac{\partial}{\partial \zeta}\left(\frac{\partial \rho}{\partial \Psi}(\zeta, 0)\right) - R(\zeta)\,\frac{\partial \rho}{\partial \Psi}(\zeta, 0) = \frac{\partial U}{\partial \theta_2}(\zeta_1, \zeta) \tag{3.27}$$

From the definition of U in (3.4) one deduces $\frac{\partial U}{\partial \theta_2}(\zeta, \zeta) = 0$. The only periodic solution of (3.27) is $\frac{\partial \rho_1}{\partial \Psi_1}(\zeta, 0) = 0$. From the definition of V in (3.4) the relation $\frac{\partial V}{\partial \theta_2}(\zeta, \zeta) = 1$ results. Introducing these values in (3.26) one obtains:

$$H'(0) = \frac{1}{T}\int_0^T [0 \cdot \Lambda(\zeta) + 1]\mathrm{d}\zeta = 1 \tag{3.28}$$

Hence $P'(0) = -2$, another general property of the equation for the phase shift.

The solution is nearly constant at values $\Psi = \Psi_m - nT$, n integer, where Ψ_m is the phase difference for which $P(\Psi_m)$ is minium.

The frequency of oscillations in x_2 is:

$$\omega = \frac{\mathrm{d}}{\mathrm{d}t}(t + \Psi_2) = 1 + \lambda k H(-\Psi) \tag{3.29}$$

4. PHASE SYNCHRONIZATION OF CHEMICAL REACTION OSCILLATORS COUPLED BY DIFFUSION. THE HARMONIC APPROXIMATION

I have analyzed the dissipative structures in distributed systems, dynamic patterns as chemical waves, in terms of local oscillatory or excitable, diffusion-coupled devices.

Different types of coupling can be assumed: coupling in parallel, in which the evolution equations for each of the N local concentration variables W_n are added an interaction term defined by

$$I_n(\{W_k\}) = \frac{1}{N}\sum_{k=1}^{N}(W_k - W_n) \tag{4.1}$$

in which the coupling is realized e.g. via a common medium or by the communicating vessels principle; coupling in series for which:

$$I_n(\{W_k\}) = W_{n+1} + W_{n-1} - 2W_n \tag{4.2}$$

in which the coupling is on a line, with simple, difference, nearest-neighbor interactions. Coupling can happen also on a circle as in the experiment reported in [14]. One can imagine also for a compartmented system with periodic boundary conditions coupling on a circle and for the two-dimensional array of coupled cells with periodic boundary conditions coupling on a torus. If one interprets the series coupling formula (4.2) as a finite difference approximation for each coordinate axis of a partition in cells of linear dimension d, the interaction term :

$$\frac{D(W_{n+1} + W_{n-1} - 2W_n)}{2d^2} \tag{4.3}$$

for the line of cells on each coordinate axis is the finite-difference form of the mass balance equation [1], with coupling term

$$D(W_2 - W_1). \tag{4.4}$$

I have thus demonstrated also the correctness of the form assumed in (3.1) for the coupling through diffusion of two reaction cells with a plane separation surface.

A mode analysis [15] of the system consisting of a large number of mutually coupled Van der Pol oscillators coupled on a circle and described by an equation with series coupling of the type :

$$\ddot{x}_n - \varepsilon(1 - x_n^2)\dot{x}_n + (1 + \alpha)x_n - \alpha x_{n-1} - \alpha x_{n+1} = 0 \tag{4.5}$$

is done by diagonalizing the coupling matrix of the unperturbed equations ($\varepsilon = 0$) and using the averaging method [1,3], for the diagonalized normal modes of the complete nonlinear equation. The averaging method assumes quasiharmonic oscillators (ε small). For larger ε the oscillations are relaxation oscillations, however, one does not expect the synchronization phenomenon to depend strongly on the detailed form of the limit cycles.

Entrainment phenomena in the chain of several Van der Pol oscillators with $x - \dot{x}$ series coupling, represented by the equations :

$$\ddot{x}_n + \lambda_n \dot{x}_{n+1} + \lambda_{n-1}\dot{x}_{n-1} - c_n(1 - x_n^2)(\dot{x} + \lambda_n x_{n+1} + \lambda_{n-1}x_{n-1}) + \omega_n^2 x_n = 0 \tag{4.6}$$

have been analyzed by the averaging method in [16] assuming also entrained quasiharmonic oscillations.

The Van der Pol equations considered as a model for a two-variable oscillator in the variables x and $y = \dot{x}$, are just like the oscillations in chemical reaction systems, relaxation oscillations, but behave harmonically for small ε.

The two-variable equations for each oscillator i of the ensemble with parallel coupling are written thus :

$$\dot{x}_i = f(x_i, y_i) + \frac{\lambda}{N}\sum_l K(\mathbf{d}_{il})x_l \tag{4.7}$$

$$\dot{y}_i = g(x_i, y_i) + \frac{\lambda}{N}\sum_l K(\mathbf{d}_{il})y_l$$

where $0 < \lambda \ll 1$, and $\mathbf{d}_{il}$ is the spatial displacement between the i-th and the l-the oscillators. N is the total number of oscillators.

The solutions in the two time scales expansion method of chapter 2 are :

$$x_i = X(t + \Psi_i(\tau)), \quad y_i = Y(t + \Psi_i(\tau)), \quad \tau = \lambda t \tag{4.8}$$

where $x_i = X(t + \Psi), y_i = Y(t + \Psi)$ is the limit cycle solution of the uncoupled systems :

$$\frac{d\Psi_i}{d\tau} = \frac{1}{N}\sum_l K(\mathbf{d}_{il})H(\Psi_l - \Psi_i) \tag{4.9}$$

H has the property $H'(0) = 1$.

I will derive an equation for the distribution of phases. Assuming that the points $(\mathbf{q}_i, \Psi_i(\tau)) = X_i$ are distributed according to a density $n(X, \tau)$, a discrete sum $\frac{1}{N}\sum_l F(x_l)$ has an expected value $\int F(x)n(x)dx$, in the limit $N \to \infty$.

The evolution of the phase is given by :

$$\frac{d\Psi}{d\tau} = \int K(\mathbf{q}' - \mathbf{q})H(\varphi - \Psi)n(\varphi, \mathbf{q}', \tau)d\varphi d\mathbf{q}' \tag{4.10}$$

For a given spatial position $\mathbf{q}$, the right hand side can be considered as the velocity of a flow in the space of the phases Ψ. The equation of continuity which expresses the conservation of oscillators is :

$$\frac{\partial n}{\partial \tau} + \frac{\partial}{\partial \Psi}(nE) = 0 \tag{4.11}$$

can be written in characteristic form :

$$\frac{dn}{d\tau} = -n\frac{\partial E}{\partial \Psi}, \tag{4.12}$$

along the characteristics :

$$\frac{d\Psi}{d\tau} = E \tag{4.13}$$

In the harmonic case, assuming :

$$x = \cos(t + \Psi), \; y = \sin(t + \Psi), \tag{4.14}$$

the function $H(\theta)$ satisfying $H'(0) = 1$, is in this case : $H(\theta) = \sin\theta$. The function $E(\Psi, \mathbf{q}, \tau)$ in (4.13) is given then by :

$$E(\Psi, \mathbf{q}, \tau) = \alpha(\mathbf{q}, \tau)\cos\Psi + \beta(\mathbf{q}, \tau)\sin\Psi \tag{4.15}$$

where $\alpha(\mathbf{q}, \tau) = \int\int_{-\pi}^{\pi} K(\mathbf{q}' - \mathbf{q})\sin\zeta \, n(\zeta, \mathbf{q}', \tau) \, d\zeta d\mathbf{q}'$

$$\beta(\mathbf{q}, \tau) = -\int\int_{-\pi}^{\pi} K(\mathbf{q}' - \mathbf{q})\cos\zeta \, n(\zeta, \mathbf{q}', \tau) \, d\zeta d\mathbf{q}'$$

The equation for the characteristics is :

$$\frac{d\Psi}{d\tau} = \alpha(\mathbf{q}, \tau)\cos\Psi + \beta(\mathbf{q}, \tau)\sin\Psi \tag{4.16}$$

If one seeks solutions $n(\Psi, \mathbf{q}, \tau)$ that are even in Ψ, then $\alpha(\mathbf{q}, \tau) = 0$ and the equation (4.16) becomes

$$\frac{d\Psi}{d\tau} = \beta(\mathbf{q}, \tau)\sin\Psi \tag{4.17}$$

By integrating this equation the following relation results :

$$\operatorname{tg}\frac{\Psi}{2} = \exp(B(\mathbf{q}, \tau))\operatorname{tg}\frac{\Psi_0}{2} \tag{4.18}$$

where

$$\Psi_0 = \Psi(\tau = 0) \text{ and } B(\mathbf{q}, \tau) = \int_0^{\tau} \beta(\mathbf{q}, u)du \tag{4.19}$$

If the function $B(\mathbf{q},\tau) \to -\infty$ as $\tau \to \infty$, then the characteristics defined by equation (4.17) converge to $\Psi = 0$ as $\tau \to \infty$ if $-\pi < \Psi(0) < \pi$. This corresponds to the phase synchronization of the oscillators to the value $\Psi = 0$. If $B(\mathbf{q}, \tau) \to \infty$ as $\tau \to \infty$, then the phases of the oscillators synchronize to $\Psi = -\pi$ or $\Psi = \pi$, which corresponds to the same point on the limit cycle.

The phases in the interval $d\Psi_0$ around Ψ_0 are transformed via characteristics to the interval $d\Psi$ around Ψ in time τ, hence the density at $(\Psi, \mathbf{q}, \tau)$ is related to the initial value $(\Psi_0, \mathbf{q}, 0)$ through :

$$n(\Psi, \mathbf{q}, \tau)d\Psi = n_0(\Psi_0, \mathbf{q}, 0)d\Psi_0 \tag{4.20}$$

By using the expression (4.18) of the characteristics, the density becomes :

$$n(\Psi, \mathbf{q}, \tau) = \nu(\Psi, \mathbf{q}, B(\mathbf{q}, \tau)) \tag{4.21}$$

where :

$$\nu(\Psi, \mathbf{q}, \tau) = \frac{n_0(2\operatorname{arc\,tg}(e^{-B}\operatorname{tg}(\Psi/2)), \mathbf{q})}{\cosh B + \sinh B \cos\Psi} \tag{4.22}$$

From the definition of β in (4.15), and noticing that by (4.19): : $\beta = \partial B / \partial \tau$ using (4 21) the following equation for B with initial condition $B(q, 0) = 0$ results :

$$\frac{\partial B}{\partial \tau} = -\int \int_{-\pi}^{\pi} K(\mathbf{q}' - \mathbf{q}) \cos \zeta \cdot \nu(\zeta, \mathbf{q}', B(\mathbf{q}', \tau)) \mathrm{d}\zeta \, \mathrm{d}\mathbf{q}'. \tag{4.23}$$

When a fraction of the oscillators are phase-synchronized and the other have a random distribution of phases, the initial distribution is :

$$n_0(\Psi, \mathbf{q}) = \frac{p(\mathbf{q})}{2\pi} + u(\mathbf{q}) \, \delta(\Psi) \tag{4.24}$$

The first term represents the random part and the second Dirac-function term the synchronized part. By using the identity [17] (if $a > b$) :

$$\int \frac{\mathrm{d}x}{a + b \cos x} = \frac{2}{\sqrt{a^2 - b^2}} \operatorname{arc\,tg} \left(\sqrt{\frac{a - b}{a + b}} \operatorname{tg} \frac{x}{2} \right) + C \tag{4.25}$$

the equation for B becomes :

$$\frac{\partial B}{\partial \tau} = \int K(\mathbf{q}' - \mathbf{q}) (p(\mathbf{q}') \tanh \frac{B}{2} - u(\mathbf{q}')) \mathrm{d}\mathbf{q}' \tag{4.26}$$

When the coupling between any two oscillators is independent of the positions, $K(\mathbf{q}' - \mathbf{q}) = 1$ for all $\mathbf{q}'$ and $\mathbf{q}$. Assuming $p \gg u$, the random component is initially dominant. Equation (4.26) becomes :

$$\frac{\mathrm{d}B}{\mathrm{d}\tau} = \tanh \frac{B}{2} - uV \tag{4.27}$$

with initial condition $B(0) = 0$, where V is the volume of the system.

If there is a completely random initial distribution of phases ($u = 0$), then the solution of (4.27) is $B = 0$. The characteristics given by (4.18) are straight lines and the initial random distribution persists for every t.

The coupling terms in (4.7) are :

$$\begin{aligned} \lambda \sum_l K(\mathbf{d}_{il}) x_l(t) &\sim \lambda \sum_l \cos(t + \Psi_l) \\ \lambda \sum_l K(\mathbf{d}_{il}) y_l(t) &\sim \lambda \sum_l \sin(t + \Psi_l) \end{aligned} \tag{4.28}$$

If the phases Ψ_l vary randomly over $(-\pi, \pi)$, then these coupling terms are nearly zero. This steady state solution with random phases is unstable. If $0 < u \ll 1$, then $|B(\tau)|$ grows until its evolution is determined by equation (4.27) without the uV term. The solution with $B \to -\infty$ has $B \to -\tau + \text{const}$, as $\tau \to \infty$. By introducing this into the equation for the characteristics (4.18), as $\tau \to \infty$, all characteristics converge to $\Psi = 0$. The system evolves towards a state in which all oscillators are synchronized.

If the oscillations are coupled by diffusion, $K(\mathbf{d}) = \nabla^2 \delta(\mathbf{d})$ which is equivalent to the series coupling for a line of oscillators, the evolution equations are written replacing the interaction terms in (4.7) by averages of $x(\mathbf{q}, t)$ over the distribution $K(\mathbf{q}' - \mathbf{q})$:

$$\frac{\partial x}{\partial t} = f(x, y) + \lambda \nabla^2 x \tag{4.29}$$

$$\frac{\partial y}{\partial t} = g(x, y) + \lambda \nabla^2 y$$

If initially the phases are distributed uniformly in $[-\pi, \pi)]$ except for those oscillators in an infinitesimal neighborhood of spatial position $q = 0$ which have $\Psi = 0$ for all slow times $\tau > 0$, then :

$$n(\Psi, \mathbf{q}, \tau) \to \delta(\Psi) \tag{4.30}$$

as $\mathbf{q} \to 0$ for fixed $\tau > 0$, and $n(\Psi, \mathbf{q}, 0) = n_0(\Psi, \mathbf{q}) = 1/2\,\pi$ for $\mathbf{q} \neq 0$. The oscillators at $\mathbf{q} = 0$ are the pacemakers that produce synchronization in the rest of the medium. Comparing with the initial condition (4.24) the parameters in the initial distribution are : $p(\mathbf{q}) = 1$, $u(\mathbf{q}) = 0$, for $\mathbf{q} \neq 0$.

The equation for $B(\mathbf{q}, \tau)$ related to the equations (4.29) is :

$$\frac{\partial B}{\partial \tau} = \nabla^2 \left(\tanh \frac{B}{2} \right) \tag{4.31}$$

The initial condition is $B(\mathbf{q}, 0) = 0$ for $\mathbf{q} \neq 0$, At $\mathbf{q} = 0$, we utilize the fact that the distribution of phases becomes sharply peaked around $\Psi = 0$ as $B \to -\infty$. Since $n(\Psi, \mathbf{q}, \tau) = \delta(\Psi)$ as $\mathbf{q} \to 0$, we require $B(\mathbf{q}, \tau) \to -\infty$ as $\mathbf{q} \to 0$ for fixed $\tau > 0$. This is the condition for B at $\mathbf{q} = 0$.

Utilizing the variable $U = \tanh(B/2)$ we obtain from (4.31) :

$$\frac{\partial U}{\partial \tau} = \frac{1}{2} (1 - U^2) \nabla^2 U, \tau > 0 \tag{4.32}$$

with initial conditions : $U(\mathbf{q}, 0) = 0$, $U(0, \tau) = -1$ for $\tau > 0$. In the one-dimensional case : for oscillators coupled in a line, the solution $U = X(s)$, $s = |\mathbf{q}|/\sqrt{\tau}$ satisfies the equations :

$$X'' = \frac{s}{1 - X^2} X' \tag{4.33}$$

on $0 \leqslant x < \infty$, with $X(0) = -1$, $\lim_{s \to \infty} X(s) = 0$. It follows that :

$$B(\mathbf{q}, \tau) = \frac{1}{2} \ln \frac{1 + X(|\mathbf{q}|/\sqrt{\tau})}{1 - X(|\mathbf{q}|/\sqrt{\tau})} \tag{4.34}$$

As $\tau \to \infty$ with $\mathbf{q}$ fixed, $X(|\mathbf{q}|/\sqrt{\tau}) \to -1$ and $B \to -\infty$. Hence the characteristics (Ψ, τ) converge to $\Psi = 0$. The rate of synchronization determined by the position $\mathbf{q}$ of the oscillator in the line, decreases as $|\mathbf{q}| \to \infty$.

5. FREQUENCY SYNCHRONIZATION OF ENSEMBLES OF COUPLED OSCILLATORS. THE HARMONIC APPROXIMATION

As I have previously mentioned, a system of coupled Van der Pol oscillators can be regarded as a model of distributed dissipative oscillatory chemical reaction-diffusion systems. [18]

The coupled Van der Pol oscillators are assumed to be of the form :

$$\frac{\mathrm{d}^2 X_n}{\mathrm{d}t^2} + \omega_n^2 X_n - 2\varepsilon(1 - 4X_n^2)\frac{\mathrm{d}X_n}{\mathrm{d}t} = 2\varepsilon\lambda I_n(\{X_k, \dot{X}_k\}) \tag{5.1}$$

Then $\varepsilon \ll 1$, in the quasiharmonic approximation, by means of the transformation :

$$W_n \exp(\mathrm{i}\omega t) = \sqrt{2}\,((\dot{X}_n/\mathrm{i}\omega) + \mathrm{i}X_n),\ \omega_n = \omega + \varepsilon\Delta_n,\ \tau = \varepsilon t, \tag{5.2}$$

the equation (5.1) becomes, denoting by

$$P_n(W_n) = W_n(1 - |W_n|)^2 \tag{5.3}$$

$$\frac{\mathrm{d}W_n}{\mathrm{d}\tau} = \mathrm{i}\Delta_n W_n + P_n(W_n) + \lambda I_n(W_1 W_2, \ldots, W_n) \tag{5.4}$$

This is a rotational wave approximation ($\varepsilon \ll 1$) as one sees from the structure of the right hand side of this equations.

When the distribution function of the frequencies $n(\omega) = \delta(\omega - \omega_0)$ the exact synchronized solution is :

$$W_n = \exp(\mathrm{i}\omega_0 + \mathrm{i}\varphi_0) \tag{5.5}$$

in which the mean frequency is

$$\omega_0 = \int_{-\infty}^{\infty} \omega\, n(\omega)\mathrm{d}\omega \tag{5.6}$$

In polar coordinates defined by :

$$W_n = \rho_n \exp(\mathrm{i}\varphi_n), \tag{5.7}$$

equation (5.4) becomes :

$$\frac{\mathrm{d}\rho_n}{\mathrm{d}t} = P_n(\rho_n) + \lambda\rho_n \operatorname{Re}(I_n(\{W_k\})/W_n) \tag{5.8}$$

$$\frac{\mathrm{d}\varphi_n}{\mathrm{d}t} = \omega_n + \lambda \operatorname{Im}(I_n(\{W_n\})/W_n) \tag{5.8}$$

One notices that $P_n(1) = 0$.

In the neighborhood of the synchronized solution, $(\exp(\mathrm{i}\varphi_n) \simeq 1 - \mathrm{i}\varphi_n)$ this is approximated quasiharmonically in the form :

$$\rho_n = 1$$

$$\frac{\mathrm{d}\varphi_n}{\mathrm{d}t} = \omega_n + \lambda \operatorname{Im}(\mathrm{e}^{-\mathrm{i}\varphi_n} I_n(\{\mathrm{e}^{\mathrm{i}\varphi_k}\})) \tag{5.9}$$

If the frequency distribution $n(\omega)$ is sharply peaked at the mean frequency

$$\omega_0 = \frac{1}{N}\sum_{k=1}^{N}\omega_k \tag{5.10}$$

the equation (5.9) can be written for parallel coupling of the form (4.1) :

$$\frac{\mathrm{d}\Psi_n}{\mathrm{d}t} = \Delta_n + \lambda\sum_{m=0}^{N} A_{nm}\Psi_m + O(\{\Psi_l\Psi_k\}) \tag{5.11}$$

where $\Psi_n = \varphi_n - \omega_0 t - \varphi_0$, cf. equation (2.1), $\Delta_n = \omega_n - \omega_0$, $(n = 1 \ldots \ldots, N)$ and $A_{nm} = \operatorname{Re}(\partial I_n(\{W_k\})/\partial W_m)$. This$_m$ form is valid for parallel coupling since $\sum_{k=1}^{N} I_k = 0$ and hence $\sum_{m=1}^{N} A_{nm} = 0$. If the exact synchronized solution is stable then the eigenvalues of the matrix A_{nm} are non-positive. The steady solution Ψ_n, denoted Ψ_n^s determines then uniquely the synchronized state. Approximating $\rho_k = 1$, $\Psi_k = \Psi_k^s$, except for Ψ_n, in the coupling term, the system of equations results :

$$\frac{\mathrm{d}\rho_n}{\mathrm{d}t} = P_n(\rho_n) + \lambda\rho_n \operatorname{Re}((\mathrm{e}^{-\mathrm{i}\Psi_n}\tilde{I}_n(\{\mathrm{e}^{\mathrm{i}\Psi_k^0}\})) \tag{5.12}$$

$$\frac{\mathrm{d}\Psi_n}{\mathrm{d}t} = \Delta_n + \lambda \operatorname{Im}(\mathrm{e}^{-\mathrm{i}\Psi_n}\tilde{I}_n(\{\mathrm{e}^{\mathrm{i}\Psi_k^s}\}))$$

which is simply written if

$$\tilde{I}_n(\{e^{i\Psi_k^s}\})) = |\tilde{I}_n|e^{i\varphi_n^0} \tag{5.13}$$

On this system of equations the self-synchronization of the ensemble of coupled oscillators can be analyzed in terms of an externally stimulated system with a stimulus of frequency ω_0, equal to the syncronized frequency.

The frequency-synchronized state of the entrained modes, defining entrainment by :

$$|\Delta_n| < \lambda|\tilde{I}_n| \tag{5.14}$$

is given by :

$$d\rho_n/dt = d\Psi_n/dt = 0 \tag{5.15}$$

In the case of parallel coupling (4.1) the asymptotic solution $\Psi_k^s = \Psi_k(t\rightarrow\infty)$ of equation (5.11) is given by $(-\Delta_k/\lambda + \overline{\Psi}_0)$, $\overline{\Psi}_0$ constant. One notices that in the limit of the continuous spectrum ($N \rightarrow \infty$ one can use the average of this solution over the Lorentzian distribution

$$n(\Delta) = \frac{\gamma}{\pi}\frac{1}{\Delta^2 + \gamma^2} \tag{5.16}$$

The average of $\exp(i\Psi_k^s(\Delta))$ is :

$$\int_{-\infty}^{\infty} n(\Delta)\exp(i\Psi_k^s(\Delta))d\Delta = s^{-\gamma/\lambda} \tag{5.17}$$

Denoting $\Delta_0 = \lambda e^{-\gamma/\lambda}$ one notices that $\Delta_0 = \lambda|\tilde{I}_n|$.

The equation for the phase shift Ψ_n of local oscillators with respect to the synchronized phase is :

$$\frac{d\Psi_n}{dt} = \Delta_n + \Delta_0\sin(\varphi_n^0 - \Psi_n) \tag{5.18}$$

Therefore in the frequency-synchronized state defined by $d\varphi_n/dt = \omega_0$, or by (5.15) : $d\Psi_n/dt = 0$. The phase of the modes evolves according to :

$$\varphi_n = \omega_0 t + \arcsin\frac{\Delta_n}{\Delta_0} + \overline{\Psi}_0 \tag{5.19}$$

where $\overline{\Psi}_0$ is a constant phase. The relation $P_n(\rho_n) = \rho_n(1 - \rho_n^2)$ implies

$$\rho_n = \sqrt{1 + \lambda|\tilde{I}_n|\cos(\Psi_n - \varphi_n^0)} \tag{5.20}$$

The number of entrained modes, with $|\Delta_k| \leqslant \lambda\,|\tilde{I}_n|$, is given by the order parameter σ : (θ being here Heaviside's step function).

$$\sigma = \frac{1}{N}\sum_{n=1}^{N} \theta(\lambda\,|\tilde{I}_n| - |\Delta_n|) = \int_{-\infty}^{\infty} n(\Delta)\,\theta(\mathrm{e}^{-\gamma/\lambda} - \Delta)\mathrm{d}\Delta \qquad (5.21)$$

For the Lorentzian distribution (6.16) the order parameter σ is :

$$\sigma = \frac{2}{\pi}\operatorname{arc\,tg}\left(\frac{\lambda}{\gamma}\mathrm{e}^{-\gamma/\lambda}\right) \qquad (5.22)$$

By using the integral formula (4.25), and solving the equation (5.18) for phases Ψ_n which are not synchronized to the frequency ω_0, for which

$$|\Delta_n| > |\Delta_0| = \lambda|\tilde{I}_n| \qquad (5.23)$$

one obtains :

$$\frac{2}{\sqrt{\Delta_n^2 - \Delta_0^2}}\operatorname{arc\,tg}\frac{\Delta_n \operatorname{tg}(\Psi - \varphi_n^0) + \Delta_0}{\sqrt{\Delta_n^2 - \Delta_0^2}} = t - t_0, \qquad (5.24)$$

where t_0 is the initial time, or :

$$\Psi_n = \varphi_n - \omega_0 t = -2\operatorname{arc\,tg}\left(\frac{\Delta_0}{\Delta_n} + \frac{\sqrt{\Delta_n^2 - \Delta_0^2}}{\Delta_n}\operatorname{tg}\frac{\sqrt{\Delta_n^2 - \Delta_0^2}}{2}(t - t_0)\right), \qquad (5.25)$$

This shows that the phase φ_n of the n-th mode which is not synchronized to the frequency ω_0 drifts with an effective frequency :

$$\omega_n = \frac{\sqrt{\Delta_n^2 - \Delta_0^2}}{2} \qquad (5.26)$$

The effective frequency distribution $n_1(\omega)$ is obtained by subtracting the fraction of entrained modes :

[illegible]$(\omega) = \sigma\delta(\omega - \omega_0) + n_1(\omega - \omega_0) \qquad (5.27)$

and is :

$$n_1(\Delta) = \frac{\gamma}{\pi}\,\frac{|\Delta|}{(\gamma^2 + \Delta^2 + \Delta_0^2)\sqrt{\Delta^2 + \Delta_0^2}} \qquad (5.28)$$

The formulas derived above show that in the harmonic approximation, a system of interacting Van de Pol oscillators has a frequency-synchronized state. The number of entrained modes grows with the strength of the interaction λ. There are in addition nonsynchronized modes whose frequency distribution is determined in the limit of a continuous distribution of oscillators, which can model a spatially distributed oscillatory chemical system.

6. DISCUSSION AND OUTLOOK

In this paper a new point of view is promoted for the study of dissipative structures. The phase waves and trigger waves in the Belousov-Zhabotinskii reaction-diffusion system are regarded as phase synchronization viz. frequency synchronization phenomena of adjacent oscillatory domains of the reagent. This synchronization states have been described mathematically in [1–3].

The explanation of dissipative structures proposed here does not asume any extrinsic mechanism as origin of spatial differentiation as e.g. the influence of gravity and of sedimentation processes. In [19] the influence of gravity and centrifugal force together with surface tension of the free surface have been described, and experiments in imponderability have been proposed which should demonstrate that the dissipative structures occur independently of these external gradients.

The general problem of stability of compartmented system has been analyzed in[20] where the stability of many oscillatory systems coupled in different ways with each other is determined by the Liapunov second method.

In the present paper I described phase waves by deriving an equation for the time evolution of the phase difference between two adjacent reaction cells coupled by diffusion in which two intermediates concentrations oscillate. For several oscillatory reaction systems coupled with each other by diffusion, an equation was derived for the distribution function of the total phase of the coupled system which in the case of harmonic oscillators can be solved exactly. The phase distribution function consists initially of a sum of a random distribution and of a Dirac-shaped synchronized part. Its time evolution can be thus determined permitting the description of phase-synchronized states. The criterion for phase synchronization of two coupled systems derived in [1]: the equality of the diffusion coefficient D of the two systems, has been assumed to be fulfilled in the above derivations.

In [21] an equation for the phase gradient has been derived which can be regarded as the continuous variant of the analysis given here.

A contribution to the experimental description of phase waves in distributed chemical systems has been given in[22] and for trigger waves in [23].

I consider trigger waves as originating from the break up of the gradient of frequency into several plateaux of synchrony within which all oscillators are entrained by the fastest one as has been demonstrated in[1]. Target patterns are explained in the present paper through the derivation in the same harmonic approximation of an equation for the phase shift of the local oscillators with respect to the synchronized phase. Parallel coupling of the local oscillators is assumed, each oscillator being coupled by diffusion with every other, as for the case of phase waves. By solving this equation a phase drift is determined for the synchronized harmonic modes of the initial nonlinear system. By assuming a Lorentzian distribution for the frequencies of the harmonic modes, and computing the number of entrained modes an effective frequency distribution of the nonsynchronized modes is also determined.

In [24] and [25] the problem of the center of the trigger waves is analyzed and how its dynamics couples with the outer plane-wave-like nature of these phenomena such as spiral or circular waves. The various phenomena found in nonlinear oscillations can be ecountered : periodic and aperiodic centers, multiple centers compatible with a given outer frequency and centers which oscillate at the outer plane wave frequency or at a fraction of the outer plane wave frequency i.e. subharmonic resonance.

Some applications of the trigger wave dissipative structures are proposed in [26] if a reagent of reduced sensitivity could be realized such that only trigger waves initiated at will, at certain electrodes, appear. The application put forward in [26] might include smoothing the interval between repetitive pulses, designing a circuit with discontinuous advance of the time at which a chemical signal in transit will be received. Time scales in this chemical system are however of the order of one minute so that these useful applications can be accomplished more effectively with conventional electronic circuits. The phenomenon is however useful as a model of biochemical communication.

The synchronization phenomenon is mentioned in the context of autowave processes in distributed chemical systems, also in [27] but without any detailed mathematical description.

The problem of coupling excitable, nonoscillatory devices has been discussed in [28]. The oscillatory devices are excitable in the acceptance that certain parameter thresholds exist above which a large loop in the configuration space is being described.

It has been shown in [29] that two adjacent cells, neither of which alone is oscillatory may excite each other so that a chemical pulse echoes back and forth between the two compartments. In the BZ reagent one observes such echo waves at the center of the above described spiral wave[30]. This is a mechanism which explains the formation of trigger waves in excitable but nonoscillatory BZ reagents.

The interested reader may find related material in [31-33].

A confirmation of the equation derived in this paper is that it coincides with the equation studied and solved iteratively in [34] with a view to the description of the synchronization or phase-lock looping of electrical circuits.

REFERENCES

[1] D. Cartianu, *Rev. Roum. Phys.*, **30**, 327 (1985).
[2] D. Cartianu, *Rev. Chim.*, **30**, 126 (1985).
[3] D. Cartianu, *Stud. Cerc. fiz.*, **36**, 762 (1984).
[4] D. Cartianu, *Stud. Cerc. Fiz.*, **35**, 360 (1983).
[5] H. G. Busse, *J. Phys. Chem.*, **73**, 750 (1969).
[6] A. N. Zaikin and A. M. Zhabotinskii, *Nature*, **225**, 535 (1970).
[7] A. T. Winfree, "The Geometry of Biological Time", Springer, Berlin, 1980.
[8] J. J. Tyson, "The Belousov-Zhabotinskii Reaction", Springer, Berlin, 1976.

[9] J. Greenberg, *SIAM J. Appl. Math.*, **34**, 391 (1978).

[10] K. W. Pehl., L. Kuhnert and H. Linde, *Nature*, **282**, 198 (1979).

[11] R. J. Field and R. M. Noyes, *J. Chem.Phys.*, **60**, 1877 (1975).

[12] E. J. Reusser and R. J. Field, *J. Amer. Chem. Soc.*, **101**, 1063 (1979).

[13] D. S. Cohen and J. C. Neu, in "Bifurcation Theory and Applications in Scientific Disciplines", eds., O. Gurel and O. E. Roessler, Ann. New York Acad. Sci., **316**, 332 (1979).

[14] P. Raschman, M. Kubicek and M. Marek, in "New Approaches to Nonlinear Problems in Dynamics", ed., P. J. Holmes, SIAM, Philadelphia, 1980.

[15] T. Endo and S. More, *IEEE Trans. Circ. Syst.*, CAS — **25**, 7 (1978).

[16] D. A. Linkens, *IEEE Trans. Circ. Syst.*, CAS — **21**, 294 (1974).

[17] M. I. Rîjik and S. I. Gradstein, "Tabele de integrale, sume, serii şi produse", Ed. Tehnică, Bucureşti, 1955.

[18] Y. Kuramoto, in "Mathematical Problems in Theoretical Physics", ed., H. Araki, *Lecture Notes in Physics, Vol.* **39**, Springer, Berlin, 1975.

[19] M. H. Kaufmann, G. Nicolis and A. Nazarea, *Z. Flugwiss. Weltraumforsch.*, **2**, 379 (1978).

[20] G. S. Ladde, *Math. Biosci.*, **29**, 309 (1976) ; **30**, 1(1976).

[21] P. Ortoleva, *J. Chem. Phys.*, **64**, 1395 (1976).

[22] M. L. Smoes, *J. Chem. Phys.*, **71**, 4669 (1979).

[23] A. T. Winfree, in *Lecture Notes in Biomath., Vol.* **2**, ed. P. van den Driessche. Springer, Berlin, 1974.

[24] P. Ortoleva, *J. Chem. Phys.*, **69**, 300 (1978).

[25] S. Bose, S. Bose and P. Ortoleva, *J. Chem. Phys.*, **72**, 4258 (1980).

[26]. K. Showalter, R. M. Noyes and H. Turner, *J. Amer. Chem. Soc.*, **101**, 7463 (1979).

[27] V. Vasiliev, Iu. M. Romanovskii and S. Iahno, *Uspehl Fiziceskih Nauk*, **128**, 625 (1979).

[28] G. Bard Ermentrout and J. Rinzel, *J. Math. Biol.*, **11**, 269 (1981).

[29] G. P. Ivaniţkii, V. I. Krinskii and E. E. Selkov, "Matematiceskaia biofizika kletki", Nauka, Moscow, 1978.

[30] J. J. Tyson, *Ann. New York Acad. Sci.*, **316**, 279(1979).

[31] D. Cartianu, *Stud. Cerc. Fiz.*, **29**, 735 (1977).

[32] D. Cartianu, *Rev. Chim.*, **29**, 1158 (1978).

[33] D. Cartianu, *Rev. Roum. Phys.*, **23**, 393 (1978).

[34] R. Donocik, "Theory of Phase-Controlled Oscillations", Academia, Praha, 1969.

Revue Roumaine de Chimie, **31**, *2*, 199—207 (1986)

HETEROPOLYTUNGSTATES WITH Ti(IV) AND Ni(II). VI[1]

THE BEHAVIOUR OF THE Ni(II)-UNDECATUNGSTOTITANATE(IV) AND Ni(II)-PENTATUNGSTOTITANATE(IV) ANIONS TOWARDS CATIONITES, IN ACIDIC AND NEUTRAL MEDIA

RODICA VĂŢULESCU, T. BUDIU, GH. MARCU and IRINA PAL
Institute of Chemistry, 30, Fintinele Street,
3400 Cluj-Napoca, Romania

Received March 3, 1985

The behaviour of the potassium and ammonium salts of the anion $[H_2ONiTiW_{11}O_{39}]^{6-}$ (I) and of the sodium salt of the anion $[H_2ONiTiW_5O_{20}]^{4-}$ (II) towards the Amberlite IR—120 and Zerolite 225, in the K^+, NH_4^+ and H^+-form and respectively Na^+ and H^+ has been studied by means of analytical methods and UV spectrophotometry. The results obtained demonstrated that the two heteroatoms (titanium and nickel) are an integral part of the heteropolytungstic anion, but they are not structurally equivalent.

1. INTRODUCTION

The heteropolycompounds of the series 1 :1 :11, of general formula $[H_hM^{m+}O_6X^{x+}O_4W_{11}O_{30}]^{(14-m-x-h)-}$, possess two heteroatoms in the anion; one tetrahedrally coordinated, occupying a central position and a second one, octahedrally coordinated, occupying a peripheral position by replacing a tungsten atom.[2]

When the "outer" heteroatom is a divalent metal ion, the structural nonequivalence of the two heteroatoms is reflected by a different behaviour towards the H^+ ions, in solution. Thus, some authors[3–6] report that, in the case of the compounds of the series 1 :1 : 11 with a divalent "outer" heteroatom M, the ion M^{2+} is totally removed from the heteropolytungstic anion, when treated with a H^+-form ion-exchanger, as well as when attacked by strong acids. Consequently, it is impossible to obtain the corresponding free acid, even in solution; in each case, an acid of the series 1 : 12[3–7] is obtained.

2. EXPERIMENTAL

In the ion exchange experiments, two strongly acidic cationites were used, namely, Amberlite IR—120 and Zerolite 225 (sulphonated polystyrene resins). Both resins were used in the H^+-form, as well as in the K^+ and NH_4^+ form for the anion $[H_2ONiTiW_{11}O_{39}]^{6-}$, and in the Na^+ form for the anion $[H_2ONiTiW_5O_{20}]^{4-}$

The resins of 0.1—0.2 mm granulations were prepared by means of the usual operations of swelling in water for 24 hours, followed by washing with 4N HCl and then with water, up to neutral reaction of the effluent. Thus the resins in the H^+-form were obtained.

Solutions of approximately 2N NaOH, KOH and respectively NH_4OH were used for their transformation into the Na^+, K^+ and NH_4^+ forms. These solutions were kept in contact with a H^+-form resin for three hours, and then washed with distilled water until the pH of the effluent was the same as the pH of the distilled water.

2.1. The ion exchange on Amberlite IR—120 and Zerolite 225, in the K^+, NH_4^+ and Na^+ forms

For this series of experiments, volumes of 25 mL solution were measured: $K_8[H_2ONiTiW_{11}O_{39}]$ with $T_W = 0.005307$, $(NH_4)_6[H_2ONiTiW_{11}O_{39}]$ with $T_W = 0.005129$ and $Na_4[H_2ONiTiW_5O_{20}]$ with $T_W = 0.009187$; these were stirred for 60 minutes with 6 g of Amberlite IR—120 in the K^+ and NH_4^+ form, and respectively Na^+ form, and similarly, with 6 g of Zerolite 225 in the K^+, NH_4^+ and Na^+ forms.

The solutions of the complex salts subjected to ion exchange experiments were quantitatively analysed for the components (titanium, nickel, tungsten), before and after the exchange.

Tungsten was gravimetrically determined by precipitation with HCl and cinchonine and calcination to WO_3, according to the method described by Kolthoff and Sandell.[8]

Nickel was determined complexometrically in the presence of murexide, according to the method described by Liteanu.[9]

Titanium was determined photocolorimetrically with H_2O_2 and H_2SO_4, according to the method given by Sandell.[10]

2.2. The ion exchange on Amberlite IR—120 and Zerolite 225 in the H^+-form

In another series of experiments, volumes of 25 mL solution of $K_8[H_2ONiTiW_{11}O_{39}]$ with $T_W = 0.005307$, $(NH_4)_6[H_2ONiTiW_{11}O_{39}]$ with $T_W = 0.005129$ and respectively $Na_4[H_2ONiTiW_5O_{20}]$ with $T_W = 0.009187$ were stirred with 6 g resin Amberlite IR—120 and Zerolite 225 in the H^+-form.

The experiments were conducted as a function of the contact time the resin — solution of complex (the exchange developed in a beaker under continuous stirring). From time to time (15 to 60 minutes) the resin was filtered and the elements (Ti, Ni and W) were analysed in the effluent, according to the methods mentioned above.

The modifications taking place with the anions I and II as a result of the exchange, on contact with a cationite in the H^+-form, were also examined spectrophotometrically. The UV absorption spectra of the solutions subjected to exchange were recorded before and after the exchange, and then they were compared with the spectra of other known compounds.

The recording of the spectra was carried out on an automatic UV-VIS Specord Spectrophotometer. At the same time, the heteropolyacids obtained as a result of the exchange were isolated and separated as guanidinium salts. The precipitation was carried out with an excess of a 40% solution of guanidinium hydrochloride, followed by multiple washing with warm water. The products obtained were quantitatively analysed for the components, according to the methods previously quoted (the guanidinium cation was determined by means of C and N microanalysis).

3. RESULTS AND DISCUSSIONS

3.1. The ionic exchange on Amberlite IR—120 and Zerolite 225 in the Na^+, K^+ and NH_4^+ forms

As a result of the exchange of the K^+ and NH_4^+ salts of the anion I and respectively of the Na^+ salt of the anion II on the mentioned cationites, the effluents resulted preserved their yellow-greenish colour and the pH they exhibited before the exchange, namely: pH=5.5 for the solutions of the potassium and ammonium salts of the anion $[H_2ONiTiW_{11}O_{39}]^{6-}$ and pH=7.2 for the solution of the complex $Na_4[H_2ONiTiW_5O_{20}]$.

The chemical analyses carried out on the solutions of the salts of the two anions, before and after the exchange, demonstrated that after the exchange the stoichiometric ratio Ti : Ni : W remained unchanged, namely, 1 :1 :11 in the case of the anion I and respectively 1 :1 :5 for the anion II.

In table 1 are given the analytical data obtained as a result of the ion exchange of the complex salts mentioned, with the cationite Amberlite IR−120 in the Na^+, K^+ and NH_4^+ forms (Table 1). Actually, the same results were obtained as in the case of Zerolite 225 resin in the Na^+, K^+ and NH_4^+ forms.

Table 1

The results of the ion exchange experiments in solution of $K_6[H_2ONiTiW_{11}O_{39}]$, $(NH_4)_6[H_2ONiTiW_{11}O_{39}]$ and $Na_4[H_2ONiTiW_5O_{20}]$ on Amberlite IR—120 in the K^+, NH_4^+, and Na^+ form, respectively

Compound		$K^+[H_2ONiTiW_{11}O_{39}]^{6-}$	NH_4^+	$Na_4[H_2ONiTiW_5O_{20}]$
Before the exchange	Ti g/mL Ni g/mL W g/mL	0.0001245 0.0001495 0.005307	0.0001188 0.0001496 0.005129	0.0004646 0.0005752 0.009187
After the exchange	Ti g/mL Ni g/mL W g/mL	0.0001203 0.0001489 0.005131	0.0001167 0.0001464 0.005021	0.0004412 0.0005472 0.008668
Experimental stoichiometric ratio Ti :Ni :W before the exchange		1 :0.98 :11.15	1 :1.03 :11.25	1 :1.021 :5.1
Experimental stoichiometric ratio Ti :Ni :W after the exchange		1 :1.01 :11.12	1 :1.023 :11.23	1 :1.012 :5.12

This first series of ion exchange experiments demonstrate that the transition metals titanium and nickel are an integral part of the complex anion I and II respectively and they do not actually participate in the ion exchange in neutral medium. The exchange takes place in the external coordination sphere without determining any modification in the inner heteropolyanion framework.

The paper electrophoresis of the solutions containing the anions I and II, carried out in a buffered solution having pH = 5.02 and pH = = 7.24 respectively, led us to the same conclusion.

3.2. The ion exchange on Amberlite IR−120 and Zerolite 225 in the H^+-form

The effluents obtained after the complete exchange as a result of the second series of exchange experiments are colourless, having a pH = 2 in the case of the solution obtained from the anion $[H_2ONiTiW_{11}O_{39}]^{6-}$

and the pH = 2.5 for the anion $[H_2ONiTiW_5O_{20}]^{4-}$. The experiment was as a function of the contact time : resin-complex solution.

The chemical analyses of the elements in the effluent were compared with those of the solutions before the exchange. The analytical results are given in table 2.

3.2.1. The anion $[H_2ONiTiW_{11}O_{39}]^{6-}$. From the data given in table 2 it is obvious, that in the case of the heteropolyanion I contacted with any of the two resins in the H^+-form, there is no evidence for the presence of the Ni ion in the effluent, as a result of the complete exchange. The Ni ion was completely retained on the resin, but Ti and W were found every time in a 1 :12 stoichiometric ratio. The behaviour of the heteropolyanion $[H_2ONiTiW_{11}O_{39}]^{6-}$ is analogous in the presence of the resins Amberlite IR—120 in the H^+-form and Zerolite 225 in the H^+-form. The only difference between them concerns the rate of exchange, namely, the cationite Amberlite IR—120 in the H^+-form retains completely the Ni ions more rapidly (30 minutes) than the cationite Zerolite 225 in the H^+-form (60 minutes).

In the effluent only the elements Ti and W in 1 :12 ratio were identified, and the newly formed acid was isolated as guanidinium salt. The attempt to isolate it as alkali metal salts failed. Otherwise, it was noticed that the 12-tungstotitanic acid, formed as a result of the exchange, is stable in solution only for a limited period of time ($\simeq$ 2 hours); this is the reason why its isolation and the recording of the UV absorption spectra were performed immediately after the exchange (30 minutes in the case of the resin Amberlite IR—120 in the H^+-form).

The analysis of the guanidinium salt of the 12-tungstotitanic acid indicates no evidence for Ni (negative reaction with dimethylglyoxime) and shows that the Ti and W elements are in a 1 :12 stoichiometric ratio (Table 3). This fact denotes that the Ni ions were retained by the ion exchange resin in the H^+-form, simultaneously with the transformation of the anion I into 12-tungstotitanate(IV) anion.

From the data given in table 3 the following experimental stoichiometric ratio is deduced for the guanidinium compound : 1Ti :12W :4C :12N or 4G :1Ti :12W. (G = guanidinium). Thus, the isolation of the compound $G_4[TiW_{12}O_{40}]$ leads to the conclusion that, at least in solution, a 12-tungstotitanic acid can be obtained on a H^+-cationite by ion exchange, but this acid is only little stable. The basicity found was 4, in accordance with the formulation of the acids of the heteropolytungstic class 1 :12.

The UV absorption spectrum of the acid $H_4[TiW_{12}O_{40}]$ in the effluent was recorded after the total exchange, and compared with the spectrum of the 12-tungstosilicic acid and with that of the anion I before the exchange (Fig. 1).

As it can be seen from figure 1, the spectrum of $H_4[TiW_{12}O_{40}]$ has the same shape as the spectrum of $H_4[SiW_{12}O_{40}]$ and presents an absorption maximum at 37400 cm^{-1}. (The absorption maximum characteristic for the heteropolytungstates of the 1 :12 series is estimated at approximately 37800 cm^{-1}. [11,12])

Table 2

The results of the ion exchange experiments in solution of the potassium and [ammonium salt of the anion I ($[H_2ONiTiW_{11}O_{39}]^{6-}$) and of the sodium salt of the anion II($[H_2ONiTiW_5O_{20}]^{4-}$) on Amberlite IR—120 and Zerolite 225 in the H^+-form

Resin		Amberlite IR—120, H^+-form			Zerolite 225, H^+-form		
Compound		Anion I		Anion II	Anion I		Anion II
		K^+ salt	NH_4^+ salt	Na^+ salt	K^+ salt	NH_4^+ salt	Na^+ salt
Before the exchange	Ti	0.0001245	0.0001188	0.0004646	0.0001245	0.0001188	0.0004646
	Ni	0.0001495	0.0001496	0.0005752	0.0001495	0.0001496	0.0005752
	W	0.005307	0.005129	0.009187	0.005307	0.005129	0.009187
Ratio Ti:Ni:W		1 :0.98 : 11.15	1 :1.03 :11.25	1 :1.021 :5.1	1 :0.98 :11.15	1 :1.03 :11.25	1 :1.021 :5.1
Exchange 5 minutes	Ti	0.0001182	0.0001108	0.000403	0.0001121	0.000109	0.000372
	Ni	0.00007222	0.00006104	0.0002958	0.00008928	0.00008218	0.0003322
	W	0.005127	0.004848	0.008348	0.004862	0.004736	0.007490
Ratio Ti:Ni:W		1 :0.5 :11.34	1 :0.45 :11.40	1 :0.6 :5.40	1 :0.65 :11.30	1 :0.62 :11.35	1 :0.73 :5.25
Exchange 30 minutes	Ti	0.0001114	0.000104	0.000368	0.000116	0.000112	0.000421
	Ni	—	—	0.0001127	0.00002817	0.00003017	0.000196
	W	0.005096	0.004815	0.007962	0.005163	0.005007	0.009071
Ratio Ti:NiW		1Ti :11.95W	1Ti :12.07W	1 :0.25 :5.64	1 :0.2 :11.60	1 :0.22 :11.65	1 :0.38 :5.62
Exchange 60 minutes	Ti			0.0000369	0.000112	0.000108	0.000385
	Ni			—	—	—	slight traces
	W			0.0008563	0.005157	0.004975	0.008797
Ratio Ti: W				1Ti :6.05W	1Ti :12.04W	1Ti :12.03W	1Ti :5.96W

Table 3

The results of the chemical analysis of the guanidinium salts of the 12-tungstotitanate(IV) and 6-tungstotitanate(IV) anions

Compound	W%		Ti%		C%		N%		Experimental stoichiometric ratio
	calc.	found	calc.	found	calc.	found	calc.	found	
$G_4^*[TiW_{12}O_{40}]$	70.39	70.72	1.52	1.53	1.53	1.56	5.36	5.45	1Ti :12.04W :4.07C :12.18N or 4G :1Ti :12.04W
$G_2^*[TiW_6O_{24}H_6]$	66.41	66.72	2.88	2.85	1.44	1.50	5.06	5.15	1Ti :6.09W :2.06C :6.07N or 2G :1Ti :6.09W

$G^* = [CN_3H_6]^+$ (guanidinium cation)

The spectrum of the anion I before the exchange (Fig. 1, curve 3) is different from that of the acid obtained as a result of the exchange (curve 2). The anion I absorbs at $\simeq 38500$ cm^{-1}, that is its absorption maximum is shifted with about 1100 cm^{-1} towards lower wavelengths as compared with the absorption maximum of the acid $H_4[TiW_{12}O_{40}]$ obtained after the exchange. This behaviour is also mentioned in the literature in general for the compounds of the series 1 : 1 : 11 as compared with the compounds of the series 1 : 12.[6]

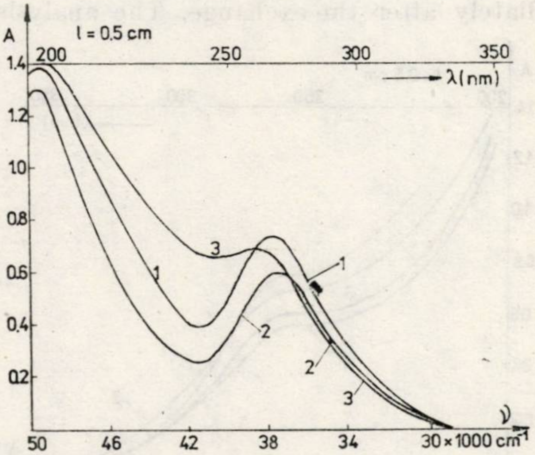

Fig. 1. — The UV absorption spectra recorded in solution for the complexes : *1* — $H_4[SiW_{12}O_{40}]$ $C = 4 \cdot 10^{-4} M_W$; *2* — $H_4[TiW_{12}O_{40}]$ $C = 3.4 \cdot 10^{-4}$ M_W, obtained as a result of the exchange on the H^+-form cationite ; *3* — $(NH_4)_6[H_2ONiTiW_{11}O_{39}]$ $C = 3.6 \cdot 10^{-4} M_W$, before the exchange.

From the data presented it can be concluded that the behaviour of the anion $[H_2ONiTiW_{11}O_{39}]^{6-}$ in the presence of ion exchangers, is analogous to the behaviour of other representatives of the series 1 :1 :11.[3-6]

These studies and the octahedral coordination of nickel (established with the help of the visible absorption spectra)[13] suggest that titanium is the central tetrahedrally coordinated heteroatom, and the nickel occupies, at random, the place of a tungsten atom in the heteropolyanion (modified Keggin structure [14]).

On acidic attack (by means of the cationic resin in the H^+-form) the nickel ion is expelled from the anion and retained by the resin. It is replaced by a tungsten atom and a heteropolyacid of the 1 :12 series is obtained.

3.2.2. The anion $[H_2ONiTiW_5O_{20}]^{4-}$. The behaviour of the anion $[H_2ONiTiW_5O_{20}]^{4-}$ on ion exchangers in the H^+-form (Amberlite IR—120 and Zerolite 225) is similar to that of the anion I, in the sense that the nickel ions are totally retained following the exchange.

The chemical analyses (Table 2) indicate that the exchange is not complete after 15 and 30 minutes respectively, but there was no evidence of the nickel ions after 60 minutes in the effluent, the nickel ions being completely retained on the H^+-form cationite. Titanium and tungsten were detected in 1 :6 stoichiometric ratio, which means that nickel is more weakly bonded in the heteropolytungstic structure of the anion II as compared with titanium. It follows that the two heteroatoms occupy nonequivalent positions within the anion and it is not possible to obtain, even in solution, the acid corresponding to the anion $[H_2ONiTiW_5O_{20}]^{4-}$.

Following the complete exchange on the H^+-form cationite, attempts were made to isolate, in solid state, the compound from the effluent formed as a result of the exchange.

The guanidinium compound was isolated by precipitation, immediately after the exchange. The analysis of the guanidinium compound (Table 3) shows that titanium and tungsten are in a 1 : 6 stoichiometric ratio and the guanidinium ion is in a 2 : 1 ratio towards titanium. Admitting that a single heteropolyacid is formed as a result of the exchange, this corresponds to the basicity 2.

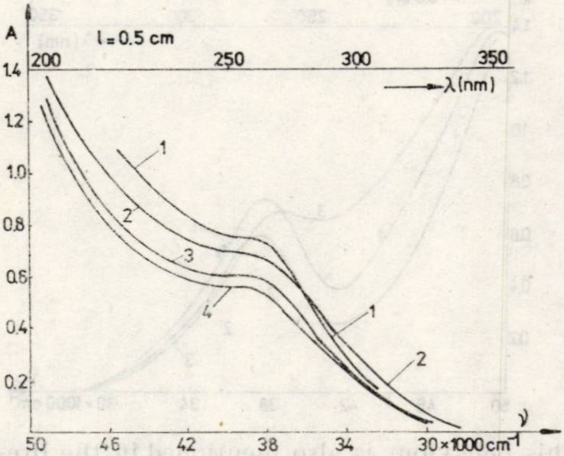

Fig. 2. — The UV absorption spectra recorded in solution for the compounds : *1* — The compound $SeMo_6$[16] ; 2 — The hypothetical acid TiW_6 $C = 6.6 \cdot 10^{-4} M_W$, obtained as a result of the exchange on the H^+-form cationite ; *3* — The compound TiW_6 $C = 5 \cdot 10^{-4} M_W$, obtained at pH = 6 ; *4* — The compound TiW_6 obtained in the same way as 3- and acidified at pH = 2.5 ($C = 5 \cdot 10^{-4} M_W$)

According to Baker[15] and to the data mentioned above, the acid containing titanium and tungsten in ratio of 1 :6, formed as a result of the exchange on the cationite in the H^+-form, can be tentatively formulated as $H_2[TiW_6O_{24}H_6]$.

The presence in solution of a little stable heteropolyanion of 1 : 6 ratio, as a result of the exchange, was demonstrated by means of the UV absorption spectra, and is presented in figure 2, curve 2. This spectrum was compared with the spectrum of a heteropolymolybdate, containing selenium and molybdenum in 1 :6 ratio[16] (curve 1) ; it can be seen that the two spectra are similar. There is no literature reference concerning the 6-tungstotitanate system. Therefore, for comparison purposes, a compound was prepared in solution at pH = 6 by adding the elements in stoichiometric ratio of 1 :6.

The UV absorption spectrum of the compound of ratio 1Ti : 6W of pH = 6 (curve 3) was recorded, as well as the spectrum of this compound acidified at pH = 2.5 (curve *4*) in order to have conditions similar to those obtained in exchange experiments with anion II on the H^+-form cationite. In both cases, spectra of similar shape as the previous ones were obtained, suggesting that the solution obtained as a result of the exchange on the H^+-form cationite contains the same condensed anion as the solution obtained by direct synthesis between the Ti ions and tungstate, in a stoichiometric ratio of 1 :6.

From the results obtained one may conclude that within the anion II the titanium and nickel heteroatoms are not structurally equivalent; nickel is more weakly bonded and is expelled from the polyanion under acidic attack. As a result of the exchange, a little stable 6-tungstotitanic acid is formed in solution, which proves that titanium is the central heteroatom.

In both heteropolytungstates (I and II) investigated, nickel is octahedrally coordinated,[13] and is the "outer" heteroatom in both anions.

REFERENCES

[1] R. Vățulescu, T. Budiu, Gh. Marcu and I. Pal, part V, Rev. Roumaine Chim., **30**, 639 (1985).

[2] L. C. W. Baker, V. Simmons-Baker, K. Eriks, M. T. Pope, M. Shibata, O. W. Rollins, J. H. Fang and L. L. Koh, *J. Amer. Chem. Soc.*, **88**, 2329 (1966).

[3] T. J. R. Weakley and S. A. Malik, *J. Inorg. Nuclear Chem.*, **29**, 2935 (1967).

[4] S. A. Malik and T. J. R. Weakley, *J. Chem. Soc*, *A*, **9**, 2647 (1968).

[5] C. M. Tourné, *Compt.rend.*, **266**, 702 (1968).

[6] C. M. Tourné, G. F. Tourné, S. A. Malik and T. J. R. Weakley, *J. Inorg. Nuclear Chem.*, **32**, 3875 (1970).

[7] M. Pușcașiu, *Dokl. Akad. Nauk. S.S.S.R.*, **182**, 634 (1968).

[8] I. M. Kolthoff and E. B. Sandell, "Textbook of Quantitative Inorganic Analysis", Macmillan Company, New York, 1949, p. 728.

[9] C. Liteanu, "Chimie Analitică Cantitativă", Ed. Tehnică, Bucharest, second edition, 1959, p. 539.

[10] E. B. Sandell, "Colorimetric Determination of Traces of Metals", Interscience Publishers Inc., New York, third edition, 1959, p. 870.

[11] D. H. Brown, *Spectrochim. Acta*, **19**, 1683 (1963).

[12] G. M. Varga Jr., E. Papaconstantinou and M. T. Pope, *Inorg. Chem.*, **9**, 662 (1970).

[13] R. Vățulescu, T. Budiu, Gh. Marcu and I. Pal, part III, *Rev. Roumaine Chim.*, **30**, 823 (1985).

[14] L. C. W. Baker, J. S. Figgis, *J. Amer. Chem. Soc.*, **92**, 3794 (1970).

[15] L. C. W. Baker, "Advances in the Chemistry of the Coordination Compounds" (Proceedings 6th. I.C.C.C. Detroit, Michigan), edited by S. Kirschner, Macmillan Comp. New York, 1961, p. 604–612.

[16] P. Souchay, M. Cadiot and C. Volfovsky, *Compt. rend.*, **269**, 826 (1969).

Revue Roumaine de Chimie, **31**, *2*, 209—216 (1986)

HETEROPOLYTUNGSTATES WITH Ti(IV) AND Ni(II) .VII[1]

THE STABILITY OF Ni(II)-UNDECATUNGSTOTITANATE(IV) AND Ni(II)-PENTATUNGSTOTITANATE(IV) ANIONS IN AQUEOUS SOLUTION

RODICA VĂȚULESCU, T. BUDIU, GH. MARCU and IRINA PAL
Institute of Chemistry, 30 Fintinele Street, 3400 Cluj-Napoca, Romania

Received March 3, 1985

The behaviour of heteropolyanions $[H_2ONiTiW_{11}O_{39}]^{6-}$(I) and $[H_2ONiTiW_5O_{20}]^{4-}$(II) towards H^+ and OH^- ions has been investigated in aqueous solution at room temperature, by means of UV spectrophotometry.

1. INTRODUCTION

It is well known that the heteropolyanions are formed by reactions of condensation between the oxyanions of certain heavy metals (Mo, W, V) in the presence of a "heteroatom", at particular pH values of the solution.[2] At the same time, their stability in solution depends mainly on the pH. By the variation of this parameter important transformations of the framework of the respective heteropolyanions take place, leading to a higher condensation degree or, on the contrary to the degradation to representatives of the series with lower condensation degree. This behaviour is a function of the nature of the heteropolyanion and of the direction of the pH variation. [3,4]

On treating with a strong acid the heteropolytungstates of the series 1 :1 :11 (of general formula $[H_hM^{m+}O_6X^{x+}O_4W_{11}O_{30}]^{(14-h-m-x)-}$), containing an "outer" heteroatom M = divalent metal ion,[1,5–8] it is not possible to obtain the corresponding heteropolyacids, but they are rapidly converted into compounds of the series 12. The stability of the heteropolytungstates in acid medium depends to a greater extent on the nature of M and to a lesser extent on the nature of the central heteroatom. [7] These heteropolyanions are gradually degraded by alkaline hydroxides, to simple tungstates ; sometimes the degradation may proceed stepwise.

2. EXPERIMENTAL

The behaviour of the heteropolyanions $[H_2ONiTiW_1\,O_{39}]^{6-}$(I) and $[H_2ONiTiW_5O_{20}]^{4-}$(II) towards acids and bases has been investigated by means of UV absorption spectra.

The UV absorption spectra were recorded on a UV—VIS Specord automatic spectrophotometer.

We used solutions of anions I and II of 10^{-2}M concentration ($C_I = 6.6 \cdot 10^{-2}M_W$ and $C_{II} = 6\cdot2 \cdot 10^{-2}M_W$, respectively), to which various amounts of HCl ($T_{HCl} = 4.4 \cdot 10^{-3}$) or NaOH ($T_{NaOH} = 1.2 \cdot 10^{-2}$) were added, allowing for the stoichiometry of their degradation reactions in acid or alkaline medium (according to equations 1,2 and 3,4, respectively).

Upon acid degradation of anions I and II, we recorded the UV absorption spectra after a reaction time of one hour. As it was observed when salts of anions I and II were treated with strongly acid cation exchangers in the H+-form,[1] a reaction time longer than 1.5—2 hours leads to the decomposition of the new heteropolytungstic species formed.

In order to investigate the degradation in acid medium, we added to the solutions various amounts of hydrochloric acid, as follows:

— in amounts smaller than required by the stoichiometry of reactions 1 and 2;

— in stoichiometric amounts;

— in amounts larger than the stoichiometry of the degradation reactions of anions I and II.

The degradation in alkaline medium was investigated by the same procedure as in the case of the degradation in acid medium; the amounts of sodium hydroxide which are to be added were calculated allowing for the reactions of complete degradation 3 and 4. Since the alkaline degradation occurs slower, in this case an investigation as a function of the reaction time is carried out.

The UV absorption spectra were recorded from time to time, during a period of 10—97 days for anion I, and 10—60 days for anion II. The samples were diluted to concentrations in the range of $10^{-4}M_W$, approximately 30 minutes before recording the UV spectra, both in the case of the acid and in the alkaline degradation.

The pH measurements on the systems under study were performed with a pH-meter of type LPU—01, one hour after hydrochloric acid or sodium hydroxide was added. The pH-values are given in table 1 for anion I and in table 2 for anion II.

Table 1

pH-Values of the systems $[H_2ONiTiW_{11}O_{39}]^{6-}$/acid(base), after a reaction time of one hour

No.	Molar ratio complex anion : $H^+(OH^-)$	pH, after one hour	Obs.
1	$12[H_2ONiTiW_{11}O_{39}]^{6-} : 10\ H^+$	4.50	
2	$12[H_2ONiTiW_{11}O_{39}]^{6-} : 24\ H$	3.80	
3	$12[H_2ONiTiW_{11}O_{39}]^{6-} : 56\ H^+$	2.50	3 = stoichiometric system
4	$12[H_2ONiTiW_{11}O_{39}]^{6-} : 75\ H^+$	1.80	
5	$12[H_2ONiTiW_{11}O_{39}]^{6-} ; 100\ H^+$	1.20	
6	$[H_2ONiTiW_{11}O_{39}]^{6-} : 5\ OH^-$	6.60	
7	$[H_2ONiTiW_{11}O_{39}]^{6-} : 10\ OH^-$	7.20	8 = stoichiometric system
8	$[H_2ONiTiW_{11}O_{39}]^{6-} : 16\ OH^-$	8.35	
9	$[H_2ONiTiW_{11}O_{39}]^{6-} : 20\ OH^-$	9.30	
10	$[H_2ONiTiW_{11}O_{39}]^{6-} : 25\ OH^-$	10.50	

Table 2

pH-Values of the systems $[H_2ONiTiW_5O_{20}]^{4-}$/acid (base), after a reaction time of one hour

No.	Molar ratio complex anion : $H^+(OH^-)$	pH, after one hour	Obs.
1	$6[H_2ONiTiW_5O_{20}]^{4-} : 12\ H^+$	5.50	
2	$6[H_2ONiTiW_5O_{20}]^{4-} : 20\ H^+$	4.40	
3	$6[H_2ONiTiW_5O_{20}]^{4-} : 30\ H^+$	3.20	3 = stoichiometric system
4	$6[H_2ONiTiW_5O_{20}]^{4-} : 40\ H^+$	2.60	
5	$6[H_2ONiTiW_5O_{20}]^{4-} : 50\ H^+$	1.70	
6	$[H_2ONiTiW_5O_{20}]^{4-} : 2\ OH^-$	7.80	
7	$[H_2ONiTiW_5O_{20}]^{4-} : 4\ OH^-$	8.00	
8	$[H_2ONiTiW_5O_{20}]^{4-} : 6\ OH^-$	8.40	8 = stoichiometric system
9	$[H_2ONiTiW_5O_{20}]^{4-} : 8\ OH^-$	9.00	
10	$[H_2ONiTiW_5O_{20}]^{4-} : 10\ OH^-$	9.50	

3. RESULTS AND DISCUSSIONS

The literature data[5-8] as well as our results concerning the behaviour of the anions $[H_2ONiTiW_{11}O_{39}]^{6-}$ and $[H_2ONiTiW_5O_{20}]^{4-}$ towards ion exchangers in the H^+-form, [1] allow us to consider that upon acid attack of anions I and II, the following degradation reactions take place :

$$12[H_2ONiTiW_{11}O_{39}]^{6-} + 56H^+ \longrightarrow 12Ni^{2+} + Ti^{4+} + 11[TiW_{12}O_{40}]^{4-} + 40H_2O$$

or (1)

$$[H_2ONiTiW_{11}O_{39}]^{6-} + 4.66H^+ \longrightarrow Ni^{2+}1/12Ti^{4+} + 11/12[TiW_{12}O_{40}]^{4-} + 3.33\,H_2O$$

$$6[H_2ONiTiW_5O_{20}]^{4-} + 30H^+ \longrightarrow 6Ni^{2+} + Ti^{4+} + 5[TiW_6O_{24}H_6]^{2-} + 6H_2O$$

or (2)

$$[H_2ONiTiW_5O_{20}]^{4-} + 5H^+ \longrightarrow Ni^{2+} + 1/6Ti^{4+}5/6[TiW_6O_{24}H_6]^{2-} + H_2O$$

It should be mentioned that we assigned to the anion obtained from the acid degradation of anion II, the formula $[TiW_6O_{24}H_6]^{2-}$, according to Baker[9] and to the results of our investigations concerning the behaviour of anion II on ion exchangers in the H^+-form. [1] It was thus found that the basicity of hexatungstotitanate (IV) ion is two.

We took into consideration the following equations of the complete decomposition reactions of anions I and II on alkaline degradation, under the action of OH^- ions, at room temperature :

$$[H_2ONiTiW_{11}O_{39}]^{6-} + 16OH^- \longrightarrow Ni(OH)_2 + Ti(OH)_4 + 11\,WO_4^{2-} + 6\,H_2O \qquad (3)$$

$$[H_2ONiTiW_5O_{20}]^{4-} + 6OH^- \longrightarrow Ni(OH)_2 + Ti(OH)_4 + 5WO_4^{2-} + H_2O \qquad (4)$$

We recorded the UV absorption spectra of anion $[H_2ONiTiW_{11}O_{39}]^{6-}$ (I), when subjected to acid degradation. The absorption curves obtained for the systems corresponding to the ratios anion I : H^+ given under positions 2, 3 and 4 in table 1, are to be seen in figure 1.

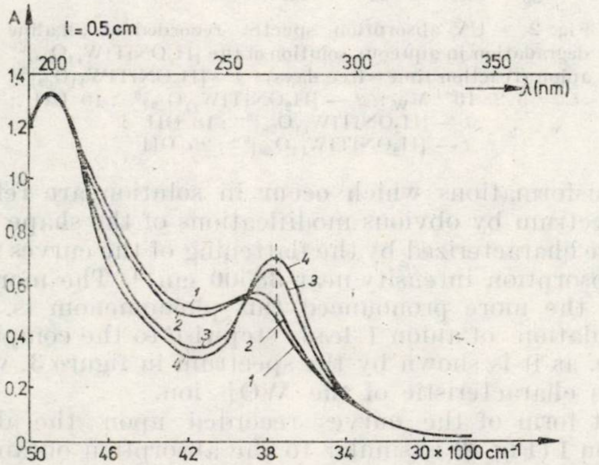

Fig. 1. — The UV absorption spectra recorded in aqueous solution of the $[H_2ONiTiW_{11}O_{39}]^{6-}$ anion subjected to the acid degradation (reaction time = one hour) :
1 — $[H_2ONiTiW_{11}O_{39}]^{6-}$ $C = 3.3 \cdot 10^{-4} M_W$;
2 — $[H_2ONiTiW_{11}O_{39}]^{6-}$: $2H^+$;
3 — $[H_2ONiTiW_{11}O_{39}]^{6-}$: 4.66 H^+ ;
4 — $[H_2ONiTiW_{11}O_{39}]^{6-}$:6.25 H^+.

It is to be noted that the degradation leads to the formation of the heteropolyanion $[TiW_{12}O_{40}]^{4-}$, which was identified by means of the absorption maximum characteristic of the acids of the series 1 :12 (curves 3 and 4). At the same time the absorption maximum is shifted towards lower frequencies (from 38500 cm^{-1} to 37400 cm^{-1}). A similar behaviour was observed for anion I when treated with an ion exchanger in the H^+-form.[1]

The UV absorption spectra recorded in the degradation process of anion I in alkaline medium are shown in figure 2. (The spectra of the systems 7, 8 and 10 in table 1 are represented in Fig. 2.)

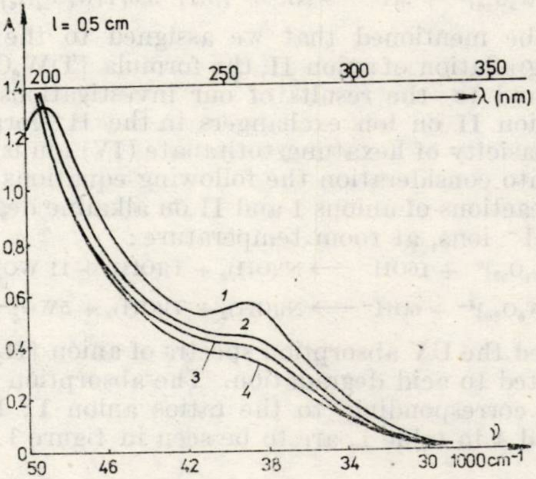

Fig. 2. — UV absorption spectra recorded on alkaline degradation in aqueous solution of the $[H_2ONiTiW_{11}O_{39}]^{6-}$ anion (reaction time=five days) : *1*—$[H_2ONiTiW_{11}O_{39}]^{6-}$ $C = 3.3 \cdot 10^{-4}\ M_W$; *2* — $[H_2ONiTiW_{11}O_{39}]^{6-}$: 10 OH^-; *3* — $[H_2ONiTiW_{11}O_{39}]^{6-}$: 16 OH^-: *4* — $[H_2ONiTiW_{11}O_{39}]^{6-}$: 25 OH^-.

The transformations which occur in solution are reflected in the absorption spectrum by obvious modifications of the shape of the curves. The spectra are characterized by the flattening of the curves and the lowering of the absorption intensity near 38500 cm^{-1}. The more alkaline the solutions are, the more pronounced this phenomenom is. In time, the alkaline degradation of anion I leads stepwise to the complete formation of a tungstate, as it is shown by the spectrum in figure 3, which exhibits the absorption characteristic of the WO_4^{2-} ion.

The flat form of the curves recorded upon the alkaline degradation of anion I (Fig. 2) is similar to the absorption obtained for anion II $([H_2ONiTiW_5O_{20})]^{4-})$.[10]

Indeed, taking into consideration the molar ratio $[H_2ONiTiW_{11}O_{39}]^{6-}$: 10 OH^-(pH = 7.2) we may assume that the degradation of anion I to WO_4^{2-} proceeds stepwise, whereas the anion $[H_2ONiTiW_5O_{20}]^{4-}$ constitutes a stable intermediate of this degradation reaction.

The equation of the reaction is as follows:

$$[H_2ONiTiW_{11}O_{39}]^{6-} + 10\,OH^- \longrightarrow [H_2ONiTiW_5O_{20}]^{4-} + 6WO_4^{2-} + 5\,H_2O \qquad (5)$$

As it was pointed out in the case of the formation of the $[H_2ONiTiW_5O_{20}]^{4-}$ anion as a function of pH,[11] this is actually formed in a relatively narrow pH-range. Under the conditions described by us[12] it can be obtained and isolated in the form of salts, at pH = 7.2−7.5.

A behaviour similar to that of anion I when subjected to alkaline attack (which means a stepwise degradation resulting in a heteropolyanion with lower condensation degree) was reported in literature for other heteropolycompounds of the series 1 : 1 : 11[7] and 1 :11.[13]

Thus, Tourné[7] has shown that with heteropolycompounds of the 1 :1 :11 series, when the "outer" heteroatom M is a divalent metal ion, essential modifications are to be seen in the spectrum at pH = 7−7.5, without formation of metal hydroxides. These modifications are reproducible both in the spectra and in the crystalline products obtained. This behaviour is accounted for by the alkaline degradation which, in the case of the compounds discussed, occurs stepwise, the heteropolytungstic framework being partly preserved.

The existence of the anion $[H_2ONiTiW_5O_{20}]^{4-}$ (II) confirms the above mentioned statements, since it was identified as an intermediate in the partial alkaline degradation of anion $[H_2ONiTiW_{11}O_{39}]^{6-}$ (I), on the basis of the characteristic absorption in the UV spectrum, near 38000 cm^{-1} ;[10] anion II was prepared and isolated by us under the form of salts, as a stable, unitary compound.[11,12]

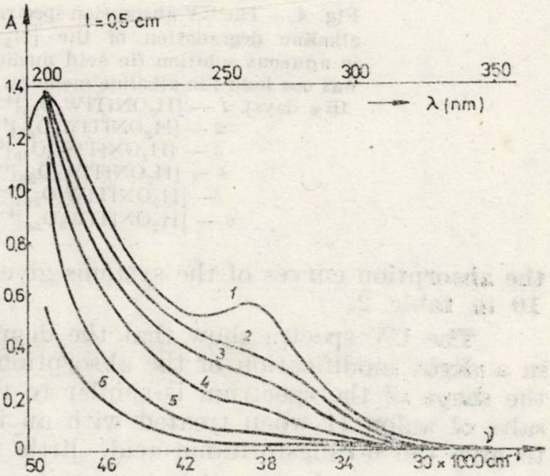

Fig. 3. — The UV absorption spectra recorded at the alkaline degradation in time, in aqueous solution of the $[H_2ONiTiW_{11}O_{39}]^{6-}$ anion, at room temperature: *1*—$[H_2ONiTiW_{11}O_{39}]^{6-}$ $C = 3.3 \cdot 10^{-4}\,M_W$; *2* — $[H_2ONiTiW_{11}O_{39}]^{6-}$: 16 OH^-, after 10 days; *3* — $[H_2ONiTiW_{11}O_{39}]^{6-}$:16 OH^-, after 30 days; *4*—$[H_2ONiTiW_{11}O_{39}]^{6-}$: 16 OH^-, after 60 days; *5* — $[H_2ONiTiW_{11}O_{39}]^{6-}$: 16 OH^-, after 97 days; *6* — Na_2WO_4 $C = 3.8 \cdot 10^{-4} M_W$.

In view of the fact that the alkaline degradation of the heteropolyanions is slow, we recorded the UV absorption spectra of aqueous solutions of the stoichiometric system $[H_2ONiTiW_{11}O_{39}]^{6-}$:16OH^- after 10, 30, 60 and 97 days, at room temperature (Fig. 3).

On examining the spectra in figure 3 we observed that the flat shape of the curves becomes more pronounced on ageing of the solutions.

It results that, in the case of the system with stoichiometric ratio OH^- : anion I, a long period of time is necessary at room temperature, for the complete decomposition of anion I in alkaline medium. The time of decomposition may be reduced by using an excess of hydroxide and by heating.

Similarly, the behaviour of anion $[H_2ONiTiW_5O_{20}]^{4-}$(II) towards H^+ and OH^- ions at room temperature was investigated.

The UV absorption spectra recorded on the acid and alkaline degradation of anion II are presented in figure 4. We selected for representation the absorption curves of the systems given under positions 1, 3, 7, 8 and 10 in table 2.

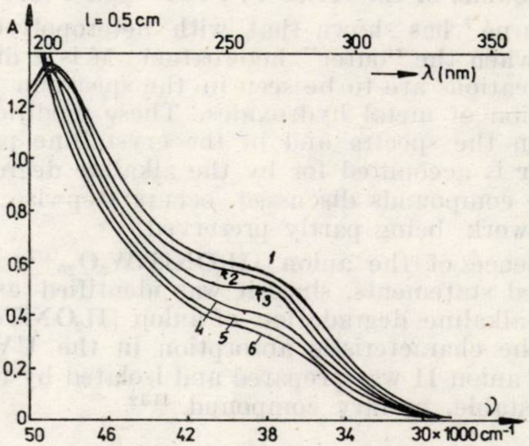

Fig. 4.— The UV absorption spectra recorded on acid and alkaline degradation of the $[H_2ONiTiW_5O_{20}]^{4-}$ anion in aqueous solution (in acid medium, the reaction time was one hour ; in alkaline medium, the reaction time was five days). *1* — $[H_2ONiTiW_5O_{20}]^{4-}$ $C = 3.1 \cdot 10^{-4} M_W$;
2 — $[H_2ONiTiW_5O_{20}]^{4-}$: $2H^+$;
3 — $[H_2ONiTiW_5O_{20}]^{4-}$: $5H^+$;
4 — $[H_2ONiTiW_5O_{20}]^{4-}$: $4OH^-$;
5—$[H_2ONiTiW_5O_{20}]^{4-}$: $6OH^-$;
6 — $[H_2ONiTiW_5O_{20}]^{4-}$: $10\,OH^-$.

The UV spectra show that the degradation in acid medium results in a slight modification of the absorption curve (curve 3). In this case, the shape of the spectrum is similar to that obtained with solutions of salts of anion II when treated with an ion exchanger in the H^+ -form[1] to give the 6-tungstotitanic acid, little stable.

On ion exchange with a strongly acid cation exchanger, we observed that the Ni^{2+} ion was expelled from the complex anion and no acid of the 2 :5 series corresponding to anion II could be obtained.

The curves 4,5, and 6 in figure 4 present the transformations occurring in the spectrum when the $[H_2ONiTiW_5O_{20}]^{4-}$ anion undergoes alkaline degradation. In this case too, a modification of the shape of the absorption curves is observed, namely a flattening accompanied by the lowering of the absorption, as the alkalinity of the solution is increased.

In order to follow in time the process of alkaline degradation of anion II, we recorded the UV absorption spectra (Figure 5). It may be seen that the flat form of the curves becomes more pronounced on ageing of the solutions and finally an absorption characteristic of the WO_4^{2-} ion is obtained.

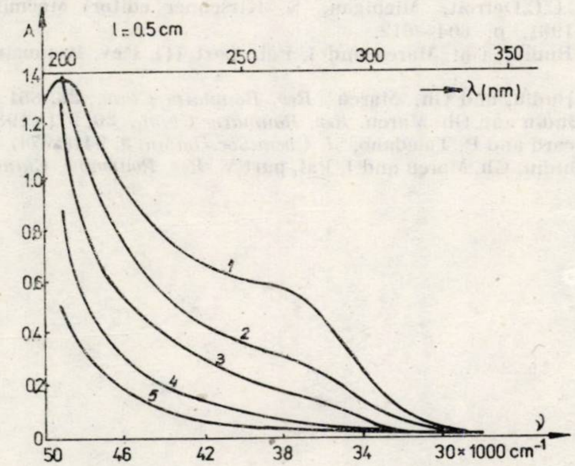

Fig. 5. — The UV absorption spectra recorded on alkaline degradation of the $[H_2ONiTiW_5O_{20}]^{4-}$ anion in time, in aqueous solution: *1* — $[H_2ONiTiW_5O_{20}]^{4-}$ $C = 3.1 \cdot 10^{-4} M_W$; *2* — $[H_2ONiTiW_5O_{20}]^{4-} : 6\,OH^-$, after 10 days; *3* — $[H_2ONiTiW_5O_{20}]^{4-} : 6\,OH^-$, after 30 days; *4* — $[H_2ONiTiW_5O_{20}]^{4-} : 6\,OH^-$, after 60 days; *5* — Na_2WO_4 $C = 3.8 \cdot 10^{-4} M_W$.

We concluded that the pH limits of stability can be estimated in the range of 3.5—7 for anion I and 6.5—8 for anion II.

As a result of the present study and of the investigations on the behaviour of anions I and II towards ion exchangers in the H^+ -form, we established that it is not possible to obtain the acids corresponding to anions I and II in solution.

Although anion II was detected to be an intermediate in the partial degradation of anion I, the former is a well defined heteropolytungstic species, since both the stability range and formation range have limits which allow it to be obtained. The salts of anion II could be isolated in crystalline state and every study we have carried out [1, 10, 11, 14] confirm the existence of the $[H_2ONiTiW_5O_{20}]^{4-}$ anion, affording evidence that it is a unitary product belonging to the 2:5 heteropolytungstic series.

REFERENCES

[1] R. Vățulescu, T. Budiu, Gh. Marcu and I. Pal, part VI, *Rev. Roum. Chim.*, **31**, 199 (1986).

[2] F. G. R. Gimblett, "Inorganic Polymer Chemistry", Butterworth Scientific Publications, London, 1963, p. 199—206.

[3] R. Ripan, A. Duca, R. Palade, D. Stănescu and A. Mager, *Bull. Soc. Chim. France*, **1958**, 1514.
[4] R. Ripan, A. Duca and D. Stănescu, *Bull.Soc.Chim. France*, **1959**, 1984.
[5] T. J. R. Weakley and S. A. Malik, *J. Inorg. Nuclear Chem.*, **29**, 2935 (1967).
[6] C. M. Tourné, *Compt. rend.*, **266**, 702 (1968).
[7] C. M. Tourné and G. F. Tourné, *Bull. Soc.Chim.France*, **4**, 1124 (1969).
[8] C. M. Tourné, G. F. Tourné, S. A. Malik and T. J. R. Weakley, *J. Inorg. Nuclear Chem.*, **32**, 3875 (1970).
[9] L. C. W. Baker, "Advances in the Chemistry of the Coordination Compounds" (Proceedings 6th I.C.C.C.Detroit, Michigan, S. Kirschner editor) Macmillan Comp., New York, 1961, p. 604–612.
[10] R. Văţulescu, T. Budiu, Gh. Marcu and I. Pal, part III, Rev. Roumaine. Chim., **30**, 823 (1985).
[11] R. Văţulescu, T. Budiu, and Gh. Marcu, *Rev. Roumaine Chim.*, **26**, 851 (1981).
[12] R. Văţulescu, T. Budiu and Gh. Marcu, *Rev. Roumaine Chim.*, **26**, 971 (1981).
[13] J. Fischer, L. Ricard and P. Toledano, *J. Chem.Soc.Dalton*, **9**, 941(1974).
[14] R. Văţulescu, T. Budiu, Gh. Marcu and I. Pal, part V. *Rev. Roumaine Chim.*, **30**, 639, (1985).

Revue Roumaine de Chimie, **31**, *2*, 217—226 (1986)

PRÉPARATION ET CARACTÉRISATION DE QUELQUES FORMES ACTIVES DE DIOXYDE DE MANGANÈSE POUR LES ÉLÉMENTS ET PILES GALVANIQUES SÈCHES

NICOLAE CALU, ION SANDU et IOAN BERDAN
Faculté de Technologie Chimique
Institut Polytechnique « Gh. Asachi », Iassy
Chaire de Chimie et Technologie anorganique,
Splai Bahlui 71, 6600 — Iassy — 10

Reçu le 13 mai, 1985

Dans ce travail on présente certains aspects concernant les processus de synthèse et d'activation du dioxyde de manganèse utilisé dans la structure des systèmes électrochimiques et électroniques. Ainsi, on insiste sur deux produits actifs obtenus par des méthodes différentes : l'un des produits obtenu par activation des minerais riches en MnO_2 par fusion alcaline ($NaOH + Na_2CO_3$), suivie de la décomposition du manganite de natrium formé par de l'acide sulfurique ; l'autre — obtenu par le changement de l'état d'oxydation du manganèse de $+IV$ à $+II$ et $+VI$ dont l'interaction conduit à MnO_2 actif de forme : $MnO_2 \cdot MnO(OH)_r \cdot n\,H_2O$. Les nouveaux produits actifs, de type γ-MnO_2, impurifiés avec les formes δ — et α-MnO_2, sont caractérisés par des méthodes chimiques, physiques et électrochimiques. En raison de leur activité électrochimique élevée, ces produits peuvent être utilisés comme masses électrochimiques actives pour les éléments et piles galvaniques sèches.

Aspects of synthesis and activation of the manganese dioxide used in the structure of electrochemical and electronic systems are presented.
Two active products obtained by different methods are described : one is obtained by activating MnO_2 rich ores by alkaline fusion ($NaOH + Na_2CO_3$), followed by the decomposition of natrium manganite formed by sulphuric acid ; the other is got by changing the oxidation state of manganese from $+IV$ to $+II$ and $+VI$, whose interaction leads to an active MnO_2 of a $MnO_2 . MnO(OH)_r \cdot nH_2O$ form. The new active products of a γ-MnO_2 type, impurified with δ- and α-MnO_2 are characterized by chemical, physical and electrochemical methods.
Due to their high electrochemical activity, these products may be used as active electrochemical masses for dry galvanic elements and piles.

1. INTRODUCTION

Dans la fabrication du mélange cathodique à base d'oxydes supérieurs de manganèse, l'industrie des éléments et piles sèches utilise, tant pour les systèmes salins que pour ceux alcalins, du MnO_2 artificiel obtenu par procédés électrochimiques (DME) ou chimiques (DMC), comme tel ou mélangé avec du MnO_2 naturel (DMN) à forte activité [1].

Les propriétés et le comportement particulier des oxydes supérieurs de manganèse dans de différents systèmes chimiques ou électrochimiques sont influencées par une série de facteurs tels que : la composition chimique, la structure cristalline, les défauts de structure, la surface active et la morphologie des particules, le contenu en groupement — OH de surface et d'intérieur, la présence des impurités etc. [2-5]. Ces facteurs influent l'activité chimique et électrochimique, la conductivité électrique, la capacité d'absorption, d'adsorption et d'échange ionique, la porosité et le pH des échantillons de MnO_2.

La corrélation entre les propriétés physico-chimiques et l'activité électrochimique, respectivement celle entre le mode de préparation et le comportement cathodiques de MnO_2, est encore compliquée par le fait que tous les types de MnO_2 (DME, DMC et DMN) représentent des systèmes rédox monophasiques, sumatifs de deux ou plusieurs modifications cristallines. Ces systèmes présentent un large domaine de composition et de distributions statistique des phases dans la solution solide qui dépend du mode de préparation (nature et concentration des réactifs, température, pH etc.) ainsi que du traitement chimique, thermique et mécanique, appliqués ultérieurement.

Toutes les formes actives obtenues par voie chimique ont une structure zéolitique désordonnée qui présente trois types d'activité : de surface, intercristalline et de «retassure» intercristalline. Ces trois types d'activité confèrent aux produits actifs des propriétés intéressantes tant du point de vue rédox que du celui acido-basique.

En dépit des nombreuses études, on ne connaît pas une rélation quantitative entre la composition et les propriétés physico-chimiques des solutions solides contenant MnO_2 et leur activité électrochimique. Même pour une seule variété allotropique, cette relation n'est pas rigoureuse. En revanche, on sait que parmi toutes les modifications connues, la forme γ-MnO_2, obtenue par oxydation anodique ou chimique de l'ion Mn^{2+}, en milieu acide, à 70 — 90°C, est la plus active. Souvent, les échantillons contenant la même forme de γ-MnO_2 présentent un comportement physico-chimique et électrochimique différent dû à l'impurification avec d'autres modifications actives qui peuvent affecter même le modèle Debye — Scherrer de diffractions des rayons X.

Les procédés d'obtention du dioxyde de manganèse actif, élaborés dans le cadre de nos recherches se classifient ainsi :

1. Procédés chimiques qui partent des sels du manganèse et impliquent les processus suivants :

a. Oxydation des ions Mn^{2+} ;

b. Réduction des ions MnO_4^- et MnO_4^{2-} ;

c. Traitement thermique de certains sels de l'ion Mn^{2+}.

2. Procédés d'activation du dioxyde de manganèse des minerais par voie chimique ou physico-chimique, avec ou sans modification de l'état d'oxydation du Mn(IV).

Les procédés chimiques d'obtention du dioxyde de manganèse actif présentent une série d'avantages par rapport à ceux électrochimiques, tant sous l'aspect de la qualité que par l'aspect du coût du produit actif.

D'autre part, nos recherches ont eu comme but la caractérisation détaillée des différentes modifications cristallines (tout en tenant compte de leur degré d'impurification) des produits DMC préparés par voie chimique. Ainsi, l'étude apporte des données concernant la composition chimique (pureté, contenu en : Mn-total, Mn(IV), Mn(III), Mn(II), autre cations, eau etc.), les caractéristiques microstructurales (variété cristalline, système cristallin, surface active, distribution des groupements —OH et des cations Mn(IV), Mn(III), H(I) etc.) et le comportement cathodique de deux produits de MnO_2 actif obtenus par un procédé chimique de type 2, appliqué aux minerais à faible activité.

Les produits actifs de MnO_2 représentent des solutions solides de deux ou plusieurs modifications allotropiques avec des répartitions statistiques et compositions chimiques nonstöechiométriques qui englobent de l'eau de constitution et du manganèse sous différents états d'oxydation. Leur formule brute, suggérée par Brenet et colab. [11] est de type $MnO_{x-y}(OH)_{2y} \cdot n\, H_2O$, dans laquelle, pour la variété γ-MnO_2 (pur), « y » doit prendre la valeur $y = 2 - x$ correspondant à la formule : $(MnO_2)_{2y-3}$ $(MnOOH)_{4-2y}$. $z\, H_2O$ avec $y \in [1{,}5 - 2]$. L'activité électrochimique de ces produits étant assez élevée, ceux-ci peuvent être utilisés comme masses électrochimiques actives pour les piles galvaniques sèches.

2. PARTIE EXPÉRIMENTALE

Afin d'améliorer les qualités des oxydes de manganèse à faible activité, nous avons élaboré, en partant des minerais indigènes, deux procédés d'obtention du MnO_2 à forte activité, tout en suivant la diminution de leur contenu en oxydes de fer et dioxyde de silicium.

2.1. Préparation des produits actifs

Dans ce qui suit, on présente la préparation de deux produits :

2.1.1. *Préparation du produit I* [12]. Une certaine quantité de minerais de manganèse, préalablement homogéneisée, est dispersée dans une solution de H_2SO_4 10—20% suivie de l'addition, sous agitation continue, d'un mélange Na_2MnO_4 — $NaMnO_4$, à 90°C, durant 6 heures Après la concentration de la solution, le produit est filtré, lavé à l'eau jusqu'à $pH = 5$ Ensuite le produit séché, est traité par fusion alcaline avec du mélange NaOH 45% — Na_2CO_4 35%, 450 °C pour 1 heure. Le Na_2MnO_3 formé est repris à l'état divisé avec une solution de H_2SO_4 10—15%. La température est maintenue constante, $t = 15$ °C et le $pH < 3$. La suspension obtenue est filtrée, lavée et séchée à l'air, à température ordinaire.

2.1.2. *Préparation du produit II* [13]. Le procédé de préparation du produit II, appliqué aux minerais de MnO_2 à faible activité, se base sur une série de processus physico-chimiques qui consiste dans un traitement parallèle de l'essai partagé en deux fractions. Une fraction est traitée, à l'état fondu, par le mélange NaOH—$KClO_3$, lorsqu'on obtient du Na_2MnO_4. L'autre fraction, chauffée préalablement à 700 °C — pour réaliser la réduction du Mn(IV) à Mn(III) — est traitée par de l'acide chlorhidrique conc. Dans ces condi^{3}ions, il en résulte du $MnCl_2$. Dans une deuxième étape, le Na_2MnO_4, sous forme d'une solution alcaline, est ajouté, graduellement, sous agitation, à la solution de $MnCl_2$, à $pH \simeq 1$. Durant la réaction, le pH de la solution est maintenu à une valeur constante, $pH \simeq 3{,}5$; l'ajustement du pH se réalise par addition de l'acide nitrique. A la suite de la réaction entre les ions MnO_4^{2-} et Mn^{2+} se forme, avec un rendement satisfaisant, du MnO_2 de haute pureté et forte activité.

Les produits sont d'abord lavés à l'eau distillée jusqu'à l'absence des ions provenant des réactifs, puis séchés en étuve, pendant 2—4 heures à 60 °C. Après séchage, les épreuves sont homogénéisées et passées par un set complet de tamis vibratoires. La fraction qui reste sur le tamis de 0,0042 (Standard 1077/1976) est conservée dans une fiole de pesage hermétiquement fermée, dans un dessicateur à $CaCl_2$sic.

2.2. Analyse chimique

Les produits synthétisés contiennent, en dehors des oxydes de manganèse en différents états d'oxydation, une quantité variable d'eau de constitution et d'humidité. Le contenu en oxydes de manganèse exprimé en pourcentages de Mn(IV), Mn(III) et Mn(II), a été déterminé par les méthodes : complexonométrique, Volhard et rédox [14,15].

Pour déterminer le contenu en H(I), correspondant aux groupements acides de l'unité $Mn (\geqslant IV)—0]^{-}H^{+}$, on a utilisé une méthode acido-basique qui repose sur la variation du pH des solution de LiOH, NaOH ou KOH de concentration différentes à la suite de l'addition d'une certaine quantité de MnO_2 actif.

L'activité chimique du produit à été déterminée d'après le STAS 1314/19—1975, qui utilise la méthode de Drotschmann [16], corrélée avec la composition gravimétrique du produit.

2.3. Analyse thermogravimétrique

L'analyse thermique en régime statique, isotherme, à été effectuée à l'aide d'un four qui a permis l'investigation du comportement thermique du produit dans un domaine de température situé entre 60°C et 1000°C. Les déterminations ont été faites sur des essais en contact avec l'air atmosphérique.

L'analyse thermogravimétrique non-isotherme à été réalisée en utilisant un dérivatographe MOM — Budapest, type Paulik-Erdey, en étudiant tant des échantillons de MnO_2 fraîchement préparés, que des essais conservés pour un certain temps, à des vitesses différentes de chauffage.

2.4. Spectroscopie des rayons X.

Les spectres de difraction des rayons X ont été obtenus à l'aide d'un appareil de type TUR—M 62, en utilisant la radiation $Fe_{k\alpha}$ avec $\lambda = 1{,}937$ Å et le filtre à manganèse. Les conditions opératoires ont été établis comme suit : potentiel d'excitation 30—45 KV, intensité du courant de 8—10 mA, vitesse du goniomètre : $1/2$ grad $\cdot$ min^{-1}, la vitesse du déplacement du papier 600 mm/h. La comparaison des paramètres θ_{hkl} et d_{hkl} observés et des intensités des lignes de diffraction avec les données présentées dans le catalogue «Powder Diffraction File-Search Manual Inorganic Compounds», ICPDS, USA—1973 et les fiches ASTM, a permis l'identification des espèces cristallines existantes dans les produits actifs. L'établissement du système de cristallisation a été fait par indexation des lignes de diffraction à base de comparaison des valeurs d_{hkl} observées avec celles calculées. L'application de la méthode des plus petits carrés a été réalisée en utilisant un programme FORTRAN IV adéquat, pour chacun des systèmes cristallins, qui a permis l'évaluation des valeurs a_0, b_0, c_0.

2.5. Densité des produits

La densité á été déterminée à l'aide d'un picnomètre de 25 ml, par déplacement du toluène dont la densité, à 26°C, est 0,8601 $g \cdot cm^{-3}$. La pesée des essais a été réalisée à 26—27°C.

2.6. Activité électrochimique

L'activité électrochimique à été déterminée à l'aide d'un dispositif à base de cellule polyfonctionnelle connectée dans un circuit électrique adéquat. La méthode repose sur la mesure de la tension de décharge d'une pastille contenant 0,2 g mélange cathodique (0,16 g MnO_2 et 0,4 g masses graphitiques colloïdales) par rapport à une anode de zinc de suface active constante, sous un courant de décharge constant de 0,1 $A \cdot g^{-1}$ MnO_2.

3. RÉSULTATS ET DISCUSSIONS

Les résultats de l'analyse chimique concernant les pourcentages de Mn(IV), Mn(III), Mn(II), H(I), H_2O et autre cations sont présentés dans la tableau 1.

A partir des données expérimentales, on a evalué «x» de MnO_x. Les valeurs trouvées correspondent aux formules approximatives : $MnO_{1,815} \cdot 0{,}42H_2O$ (produit I) et $MnO_{1,898} \cdot 0{,}51\ H_2O$ (produit II) ou encore : $9MnO_2 \cdot 2mnO\ (OH) \cdot 3H_2O$ et respectivement $11\ MnO_2 \cdot 2MnO(OH)4{,}5H_2O$.

Les déterminations pH-métriques effectuées dans le système hétérogène : solution aqueuse de NaOH — MnO_2 solide, concernant le contenu en groupement acides, présentées dans la fig. 1, indiquent l'apparition d'un saut de pH pour le rapport : 0,9 — 1,0 HO^-/1 Mn (IV). Les protons mis en évidence sont attribués aux groupements acides $Mn(\geqslant IV)-O]^-H^+$ de surface.

Tableau 1

Données expérimentales concernant la composition des produits I et II (en %)

Constituants (%)	I	II
Mn(IV)	41,54	48,34
Mn(III)	9,18	8,64
Mn(II)	1,13	0,85
H(I)	0,37	0,34
Na(I)	2,06	2,23
SiO_2	12,93	—
H_2O de constit.	5,23	7,67
O_2, calculé par différence	27,56	31,93

Les nouveaux produits actifs (I et II) présentent une activité chimique assez élevée : 110—115 ml N_2 (I) et 122—135 ml N_2 (II) qui se conserve dans le temps.

L'activité chimique dépend de la structure des produits et du contenu en eau et H(I). C'est la raison pour laquelle nous avons suivi la variation de l'activité remanente en fonction de la perte spécifique avec la température ; fig. 2. Dans ce but, les produits ont été chauffés, à des températures différentes, pendant 2 heures, jusqu'à pond constant. En déterminant l'activité remanente et la perte spécifique ΔG_{sp}, on constate qu'à 110°C les produits perdent cca 8 % de l'activité. Cette perte est

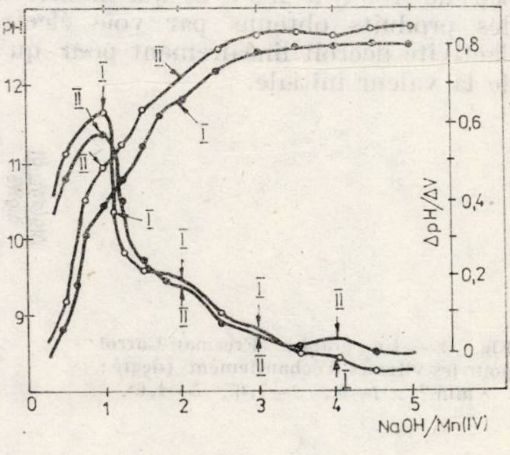

Fig. 1. — Représentation graphique de la fonction pH = f (c_{NaOH}) pour le système $NaOH_{aq}$ — MnO_2 actif, solide; temps de réaction : 144 h.

corrélée avec l'élimination de l'eau hydroscopique qui influe négativement sur l'activité des produits[7].

Entre 100°C et 200°C, les produits perdent 30 % de l'activité ; dans ce domaine c'est l'eau physique et une partie de celle de constitution qui s'élimine. Ensuite, l'activité rémanente et la perte spécifique varient peu de 180°C à 290°C ce qui montre une stabilité plus grande que celle des produits obtenus par voie électrochimique.. Au-dessus de 300°C, l'activité décroît linéairement pour qu'à 400°C la diminution soit 80 % de la valeur initiale.

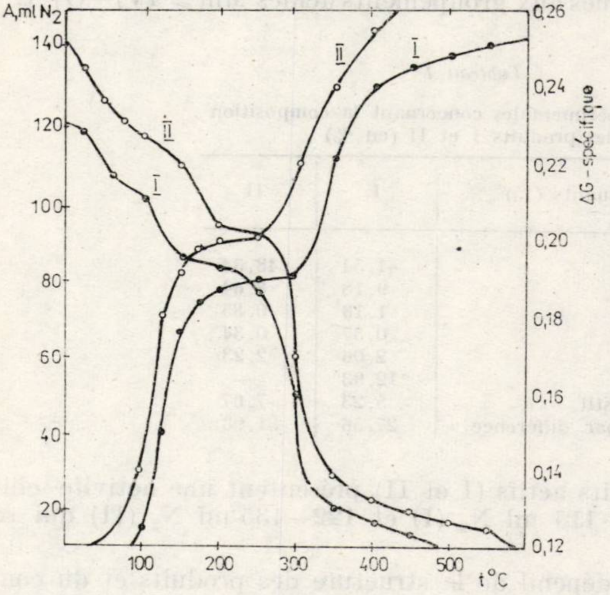

Fig. 2. — Données expérimentales concernant la perte spécifique et l'activité remanente déterminées par échauffement en régime statique.

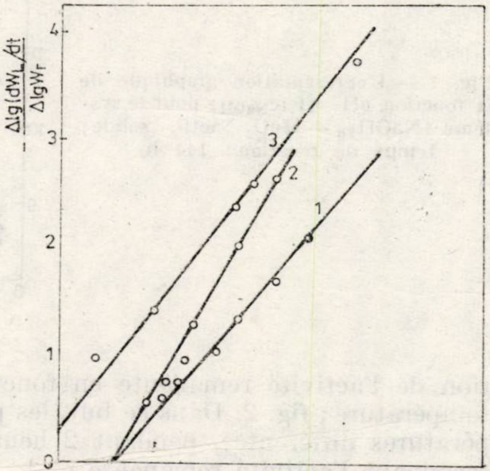

Fig. 3. — Le graphe Freeman-Carrol pour les vitesses d'échauffement (degré · · min^{-1}) : *1*—9°, *2*—7,6°, *3*—4,6°.

L'étude dérivatographique des produits actifs, en régime dynamique, fig. 3 et 4, et tableau 2, nous à permis de tirer les conclusions suivantes.

— Dans le domaine 30°C — 90°C, le processus exothermique avec le maximum à 48°C, pour I, et 40°C, pour II, correspond à l'oxydation partielle du Mn(III) à Mn(IV).

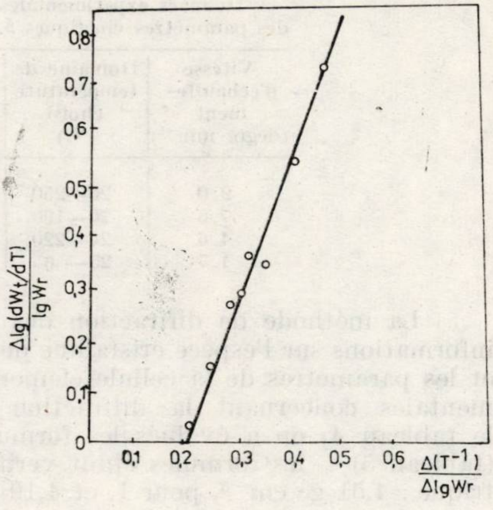

Fig. 4. — Le graphe Freeman-Carrol pour la vitesse d'échauffement de 1,7 degré · $\cdot$ min^{-1}.

— Entre 90°C et 180°C, le processus faiblement endothermique, avec le minimum à 165°C, pour I, et 150°C, pour II, correspond à la perte de l'eau d'humidité et à une partie de l'eau de constitution.

Tableau 2

Données expérimentales concernant la perte en poids des produits actifs, à chaud, en régime dynamique nonisotherme

Produit	Composition			Perte en poids jusqu'à 250°C (%)	Perte en poids lors de la transf. Mn(IV) → Mn(III)		
	MnO_2 (%)	Mn_2O_3 (%)	H_2O (%)		calc. (%)	exp. (%)	dif. (%)
I	65,70	12,46	5,23	4,75	6,04	7,04	1,00
II	75,46	12,41	7,67	6,00	7,03	7,80	0,77

— Entre 180°C et 320°C, le processus exothermique avec le maximum à 270°C, pour I, et 260°C, pour II, est dû à la diffusion de l'oxygène de la surface et à l'oxydation lente du Mn (III) à Mn (IV).

— Enfin, dans le domaine 320°C — 600°C, le processus endothermique continu, avec le minimum à 520°C, pour I, et 510°C, pour II, correspond à la reduction thermique du MnO_2 à Mn_2O_3.

L'influence de la vitesse d'échauffement sur les paramètres cinétiques « n » et « E » a été suivie en enregistrant des dérivatogrammes à des différentes vitesses d'échauffement ; tableau 3. Les valeurs des paramètres cinétiques calculés pour les quatre vitesses, indiquent le fait que la perte de l'eau a lieu en régime « cinético-diffusional ».

Tableau 3

Données expérimentales concernant le calcul des paramètres cinétiques à 4 vitesses d'échauffement

Vitesse d'échauffement (degré · min^{-1})	Domaine de température choisi (°C)	E_a ($kcal \cdot mol^{-1}$)	n
9,0	20—250	9,30	0,61
7,6	20—190	13,54	0,86
4,6	24—220	10,08	0,26
1,7	25— 65	12,97	0,53

La méthode de diffraction des rayons X a permis d'obtenir des informations sur l'espèce cristalline de base, son système de cristallisation et les paramètres de la cellule élémentaire. A partir des données expérimentales concernant la diffraction des rayons X, présentées dans le tableau 4, on a évalués les formules empiriques des produits actifs (tableau 5) — les formules étant verifiées à l'aide de la densité picnométrique : 4,51 g · cm^{-3}, pour I, et 4,19 g · cm^{-3}, pour II.

Tableau 4

Modèle de diffraction des rayons X sur des essais en poudre de γ-MnO_2

Produit I						Produit II					
$d_{obs.}$ (Å)	I/I_0	Système orthorhombique pour γ-MnO_2		Système tetragonal pour α-MnO_2		$d_{obs.}$ (Å)	I/I_0	Système orthorhombique pour γ-MnO_2		Système hexagonal pour δ-MnO_2	
		$d_{cal.}$	hkl	$d_{cal.}$	hkl			$d_{cal.}$	hkl	$d_{cal.}$	hkl
4,862	tb	4,848	020	4,867	200	3,993	th, l	3,998	110	3,994	101
3,971	th	3,998	110	—	—	3,276	tb	3,258	120	—	—
3,165	tb	3,173	120	3,154	310	3,093	tb	—	—	3,092	201
3,090	b	—	—	3,065	320	2,580	b	2,578	130	2,593	211
2,581	b	2,598	130	2,576	111	2,541	tb	2,541	021	2,434	301
2,434	b	2,434	021	2,418	201	2,312	b	2,324	111	—	—
2,130	h	2,132	121	2,124	301	2,135	h	2,141	121	2,129	221
1,627	h	1,627	221	1,623	600	1,640	h	1,637	221	1,650	222
1,426	tb	1,428	231	1,424	601	1,428	tb	1,428	231	—	—

t — très, *b* — basse, *h* — haute, *l* — large.

En connaissant les paramètres de la cellule élémentaire on a calculé ensuite le volume de la cellule.

L'analyse de diffraction des rayons X a permis de constater que les deux produits présentent, en dehors des lignes caractéristiques au système orthorombique, et d'autres lignes propres au système tétragonal (pour I) et hexagonal (pour II). Ceci montre que les deux produits sont impurifiés avec des modifications α- et, respectivement, δ-MnO_2.

L'activité électrochimique des produits est de 66 minutes (I) et respectivement 70 minutes (II) — temps nécessaire pour atteindre $U =$ $= 0,9$ V — des valeurs approximativement égales à celles de meilleur produit obtenu par voie chimique.

Tableau 5

Les formules empiriques et quelques paramètres structurals des produits actifs I et II

Produit	Fomule empirique évaluée à partir de :		Paramètres de la cellule (en Å)				Densité		
							évaluée par picnomètre ($g \cdot cm^{-3}$)	calculée * par le :	
	l'analyse chimique	la diffraction des rayons X	a_0 (Å)	b_0 (Å)	c_0 (Å)	$V_{cell.}$ ($Å^3$)		trou anionique	trou cationique
I	$Mn_{3,3}O_{6,0} \cdot H_2O$	$Mn_{3,3}O_{6,5}0,7H_2O$	4,397	9,577	2,761	116,273	4,51	4,45	4,53
II	$Mn_{3,5}O_{6,7} \cdot 1,4HO$	$Mn_{3,5}O_{7,0}0,8H_2O$	4,449	9,629	2,877	123,245	4,19	4,15	4,20

* — Dans le système hexagonal.

4. CONCLUSIONS

Les nouveaux produits obtenu par deux procédés chimiques différents qui se basent sur des processus rédox associés aux processus acido-basiques, présentent une activité chimique et électrochimique élevé. La composition des produits, déterminée par méthodes physico-chimiques, met en évidence la structure complexe et permet d'établir certaines corrélations avec leur comportement dans différents systèmes chimiques et électrochimiques.

Les résultats de l'étude conduisent à la conclusion que les produits actifs sont de type γ-MnO_2, impurifiés avec les formes α-et δ-MnO_2.

BIBLIOGRAPHIE

[1] A. Kozawa et R. J. Brodd , « Manganese Dioxide Symposium », vol. I, I. C. Samples Office, Union Carbide Corp., Cleveland. Ohio, 1975, p. 12, 47, 111, 306, 328 et 470.

[2] T. Takahashi et A. Kozawa, « Electrochemistry of Manganese Dioxide and Manganese Dioxide in Japan », Vol. I et II, Union Carbide Corporation, Cleveland, Ohio, 1973, p. 7, 115, 131, 219 (vol I) et 189 (vol II).

[3] A. Kozawa, « Batteries », Vol. I, « Manganese Dioxide », Éditeur K. V. Kordesch, Marcel Dekker, Inc., New York, 1974, p. 310 et 385.

[4] A. Kozawa, « 11 th International Power Sources Symposium », **30**, 1978, p. 67.

[5] N. Calu, P. Onu, I. Sandu, D. Gânju et I. Berdan, Symposium « Zeoliţii în tehnologia modernă » Institut Polytechnique Gh. Asachi, Iassy, 1983, p. 202.

[6] N. Calu, S. Bălănescu et I. Sandu, Symposium « Contribuţii ştiinţifice în chimie", Université « Babeş-Bolyai » de Cluj-Napoca, p. 12.

[7] I. Sandu, Thèse de doctorat, Institut Polytechnique Gh. Asachi, Iassy, 1984, p. 55.

[8] T. Takahashi et A. Kozawa, »Applications of Solid Electrolytes », Jet Press, Cleveland Ohio, 1980, p. 23.

[9] G. V. Vinal, « Primary Batteries », John Wiley, New York, 1950, p. 58.

[10] W. W. Nye, S. B. Levin, N. H. Kedesy, *Proc. Annual Power Sources Conf.*, **13**, 125 (1969).

[11] J. Brenet, P. C. Picquet et J. Y. Welsh, « Progress in Batteries & Solar Cells », Vol. I, J. E. C. Press, New York, 1978, p. 119.

[12] N. Calu et collab., Brevet R.S.R., nr. 75.270/1981.

[13] E. Bălănescu, Thèse de Doctorat, Institutu Polytechnique Gh. Assachi, Iassy, 1982,

[14] C. Liteanu et E. Hopîrtean, « Chimie analitică cantitativă », ed.a VI-a, Editura didactică şi pedagogică, Bucureşti, 1972, p. 358, 586, 592.

[15] A. I. Vogel, « Quantitative Inorganic Chemical Analysis », Longmans Green, London, 1961, p. 297.

[16] C. Drotschmann, *Batterien*, **20**, (2), 887, (1966) ; ibid, **18** (6), 651, (1964) ; ibid., **19** (1), 768, (1966) ; ibid, **18** (12), 721, (1965) et dans « Modern Primary Batteries », Vol. III, Trocken Batterien, Leipzig, 1957, p. 133.

Revue Roumaine de Chimie, **31**, *2*, 227–235 (1986)

STUDY ON SOME COBALT(III) DIOXIMINE CHELATE ADDUCTS WITH TERTIARY PHOSPHINES

GH. MARCU*, A. HANTZ**, MAGDA SOMAY*, CS. VÁRHELYI*
and F. TOLEA*
* Faculty of Chemical Technology, "Babeş-Bolyai" University, Cluj-Napoca, Romania
** Chemical Institute, Cluj-Napoca, Romania

Received January 12, 1985

A number of 27 new binary complex salts oi type: $[Co(DH)_2(phosphine)_2]X$ and 8 nonelectrolytes of type: $[Co(DH)_2$ (phosphine)X](DH_2= dimethylglyoxine, phosphine: Et_2PhP, Et_2(p-tol)P, Bu_2PhP and Ph_2EtP) were obtained and characterized by IR and UV spectra. The thermal decomposition of some derivatives of these types was followed by means of derivatographic measurements.

INTRODUCTION

The coordination chemistry of mixed phosphine complexes of cobalt has been expanded considerably, especially in the last 2–3 decades[1,2]. A great number of complexes of type $[CoX_2(R_3P)_2]$ (R_3P = tertiary phosphine[3,4], carbonyl-complexes: $[CoX_2(CO)(R_3P)_2]$[5,6], $[Co(CO)_3(R_3P)]^-$, nitrosyl-derivatives: $[Co(CO)_2(NO)(R_3P)]$[7,8] were obtained and characterized. Bidentate chelating agents, e.g. $R_2P(CH_2)_n PR_2$, $Ph_2P(CH_2)_nPPh_2$ (n = 2, 3, 4) were also used for the synthesis of cobalt chelates. [9,10].

Mixed polydentate phosphine-amine ligands (L″), e.g. $N(CH_2-CH_2-PPh_2)_3$,[11] $N(CH_2-CH_2-PPh_2)_2(CH_2-CH_2-OCH_3)$[12] were also used for preparative purposes, e.g. for the preparation of $CoLX_2^+$ type chelates (X = Cl, Br). [13,14]

Tertiary phosphines exhibit weaker basical properties than the analogous amines, nevertheless their nucleophilic properties are more significant than those of the amines.

These compounds form various aquo-, halogeno- and pseudohalogeno-complexes of Co(III) and Cr(III) by reacting with $[Co(NH_3)_5(H_2O)]^{3+}$, $[Co(en)_2Cl_2]^+$, $[Co(ec)(H_2O_2)]^+$ (ec.H_2 = ethylenediimino-bis-acetylacetone),[15] $[Cr(NCS)_6]^{3-}$.[16]

The first phosphino-complexes in the class of cobalt(III)-dioximino-chelates, $[Co(DH)_2(R_3P)(MeOH)]^+$ have been described by Trogler and Marzilli.[27] Some derivatives of this type were studied by means of ^{31}P NMR, ESCA and x-ray measurements.

The reduction of Co(III) phosphine-complexes with $NaBH_4$ leads to the formation of Co(I) derivatives.[18]

RESULTS AND DISCUSSION

We have observed that the oxidation of cobalt (II) salts in the presence of aliphatic or alycyclic α-dioximes and tertiary alkylarylphosphines, e.g. diethylphenylphosphine (Et_2PhP), dietyl-p-tolylphosphine (Et_2(p-tol)P), diphenylethylphosphine (Ph_2EtP) and dibutylphenylphosphine (Bu_2PhP) leads to the formation of $[Co(Diox.H)_2(phosphine)_2]^+$ type complexes following the equation :

$$2\ Co^{2+} + 4\ Diox.\ H_2 + 4\ phosphine + 1/2\ O_2 =$$
$$2[Co(Diox.H)_2(phosphine)_2]^+ + H_2O + 2\ H^+$$

The composition of the chelate cations with dimethylglyoxime as chelating agent, was proved by a series of double decomposition reactions with mineral- and organic aromatic acids or their sodium salts and with various complex acids of Co(III), Cr(III) and Pt(IV).

Some new complex salts of the above mentioned type were characterized in Tables 1—4.

The salts of the platinum (IV) acids: $H_2[PtCl_6]$, $H_2[PtBr_6]$, $H_2[Pt(SCN)_6]$ and $H_2[Pt(SeCN)_6]$ are slightly soluble in water. The derivatives of the Reinecke-salt ($K[Cr(NCS)_4(NH_3)_2]$) and analogous compounds (amine. H $[Cr(NCS)_4(amine)_2]$) : $[Co(DH)_2\ (phosphine)_2]\ [Cr(NCS)_4(NH_3)_2]$, etc. are insoluble in aqueous media and soluble in acetone and dimethylformamide.

Table 1

New complex salts of the $[Co(DH)_2(diethylphenylphosphine)_2]$ X type

Formula	Yield (%)	Appearance	Analysis	Calcd.	Found
A. Br. 2 H_2O	60	orange needles	Co	7.98	7.66
			H_2O	4.88	4.70
A. I	75	rhombohedral orange plates	Co	7.87	8.03
			I	16.95	16.70
A. NO_3	75	rhombohedral orange plates	Co	8.62	8.84
			N	10.24	10.00
A. ClO_4	80	yellow irregular crystalline aggregates	Co	8.17	8.46
A. picrate	95	limone yellow sparkling thin plates	Co	6.94	7.12
			N	11.53	11.30
A. $[Co(NH_3)_2(NO_2)_4]$	90	rhombohedral orange prisms	Co	13.11	13.21
			C	37.43	37.48
			H	5.68	5.79
A. $[Co(DH)_2(NCS)_2]$	75	sparkling brown prisms	Co	11.47	11.52
			C	44.44	44.18
A. $[Co(DH)_2(NO_2)_2]$	65	short orange prisms	Co	11.75	11.70
			C	43.11	43.70
			H	5.83	6.30

A = $[Co(DH)_2(Et_2PhP)_2]^+$

Table 2

New complex salts of the $[Co(DH)_2(\text{diethyl-p-tolylphosphine})_2]$ X type

Formula	Yield (%)	Appearance	Analysis		
				Calcd.	Found
B. Br. 2 H_2O	55	rhombohedral orange plates	Co H_2O	7.70 4.70	7.65 4.55
B.I.	75	sparkling yellow-brown plates	Co I	7.59 16.34	7.95 16.25
B. NO_3	60	sparkling rhombohedral orange plates	Co N	8.28 9.84	7.92 9.77
B. ClO_4	75	yellow-brown short irregular prisms	Co	7.87	7.97
B. picrate	90	limone yellow irregular crystals	Co C H	6.72 49.26 5.74	6.43 48.83 5.86
B. $[Co(NH_3)_2(NO_2)_4]$	80	sparkling yellow-brown plates	Co	12.73	12.88
B.$[Co(DH)_2(NO_2)_2]$	85	orange prisms	Co C H	11.43 44.26 6.06	11.41 44.68 6.08
B. $[Co(DH)_2(NCS)_2]$	60	sparkling brown plates	Co C H	11.18 45.54 5.92	11.30 45.55 5.85

$B = [Co(DH)_2(Et_2((p\text{-}tol)P)_2]^+$; $DH = C_4H_7N_2O_2$

Table 3

New complex salts of the $[Co(DH)_2(\text{dibutylphenylphosphine})_2]$ X type

Formula	Yield (%)	Appearance	Analysis		
				Calcd.	Found
C. ClO_4	85	yellow-brown short prisms	Co	7.07	7.01
C. Picrate	90	limone yellow prisms	Co N	6.12 11.56	5.95 11.40
C. $[Co(NH_3)_2(NO_2)_4]$	80	irregular dark yellow crystals (from acetone, needles)	Co N C	11.68 13.87 42.77	11.98 14.18 43.40
C. $[Co(DH)_2(NCS)_2]$	75	brown prisms (from acetone, needles)	Co S	10.35 5.63	10.44 5.90
C. $[Co(DH)_2I(N_3)]$	50	sparkling brown needles	Co N	9.89 12.92	10.18 13.10

$C = [Co(DH)_2(Bu_2PhP)_2]^+$

The same oxidation reaction in the presence of triarylphosphines leads to the formation of aquo-phosphino-complexes, e.g. $[Co(DH)_2(H_2O)(Ph_3P)]^+$.

Table 4

New complex salts of the $[Co(DH)_2(diphenylethylphosphine)_2]X$ type

Formula	Yield (%)	Appearance	Analysis		
				Calcd.	Found
$D.ClO_4$	75	green-yellow plates	Co C H	7.25 52.92 5.42	7.45 52.97 5.40
D. picrate	90	orange prisms	Co N	6.24 10.37	6.52 10.45
$D.\ [Co(NH_3)_2(NO_2)_4]$	85	short orange prisms	Co C H	11.85 43.47 5.06	11.88 43.55 5.05
$D.\ [Co(DH)_2(NCS)_2]$	60	sparkling brown long plates	Co C H	10.50 49.20 5.20	10.60 49.16 5.02
$D.\ [Co(DH)_2I(N_3)]$	60	aggregates from brown fine prisms	Co C H	10.02 43.95 4.97	9.91 44.42 4.52
$D.\ [Co(DH)_2(N_3)_2]$	55	aggregates from irregular brown cryst.	Co N	10.80 15.43	10.60 15.24

$D = [Co(DH)_2(Ph_2EtP)_2]^+$

The alkylarylphosphines participate in various substitution reactions with Co(III)-dioximine chelates :

$$[Co(Diox.H)_2X_2]^- + \text{phosphine} = [Co(Diox.H)_2X(\text{phosphine})] + X^-$$

Generally a single X-ligand is exchanged by phosphine molecules. The presence of ammonium acetate at 60—80° favours the formation of the corresponding nonelectrolytes.

The electrical conductivity measurements show the obtained binary salts : $[Co(DH)_2(\text{phosphine})_2]X$ to have a molar conductivity of 90—110 $ohm^{-1}\ cm^2$ and the nonelectrolytes values of 3—10 $ohm^{-1}\ cm^2$ at a dilution of $V = 1\ 000$ L/mole.

The new nonelectrolytes were characterized in Table 5.

Infrared spectra. In the IR spectra of the phosphino-complexes obtained the characteristic ν_{O-H} and $\delta_{O-H..O}$ frequencies of the inner O—H. . O hydrogen bridges appear 2350 cm^{-1} (m) and 1700—1750 cm^{-1} (w), as in the case of the analogous amine derivatives ($[Co(DH)_2(amine)_2]X$ and $[Co(DH)_2(amine)X]$) indicating an analogous trans geometric structure. [19] The characteristic vibration frequencies of the coordinated, deprotonated dimethylglyoxime appear at the following wavenumbers : $\nu_{C=N}$: 1560 — 1570 cm^{-1} (v.s.) ; ν_{N-O} : 1240 cm^{-1} (v.s.) and 1090—1100 cm^{-1} (v.s.) (strong covalent Co—N bondings).

The $\nu_{C=N}$ stretching vibrations of the coordinated NCS group at 2080—2090 cm^{-1} (v.s.) and the ν_{C-S} vibrations at 780 — 800 cm^{-1} (m) show the formation of cobalt-isothiocyanate bond : Co—NCS.[20] The characteristic phosphine vibrations (ν_{P-C}, ν_{C-H}, δ_{CH_2}) are not influenced by coordination effect.

The *thermal decomposition* of three $[Co(DH)_2(phosphine)_2]X$ type complexes has been studied by means of derivatography. The compounds studied contain crystallization water. Both TG and DTA curve have a similar shape for all the three complexes studied. The first decomposition stage, up to 80–90°, corresponds to the loss of 2 water molecules. This process is marked by a well defined endothermal peak on the DTA curves (Figs 1–3).

Table 5

New nonelectrolytes of the $[CO(DH)_2(phosphine)\ X]$ type

Formula	Yield (%)	Appearance	Analysis		
				Calcd.	Found
$[Co(DH)_2Cl(Et_2PhP)]$	80	yellow-brown irregular prisms	Co N	12.01 11.40	12.00 11.25
$[Co(DH)_2Cl(Et_2)p\text{-}tol)P)]$	80	light brown sparkling prisms	Co N	11.68 11.10	11.90 11.03
$[Co(DH)_2Br(Et_2PhP)]$	85	gold-brown irregular plates	Co Br	11.00 14.93	11.21 14.77
$[Co(DH)_2Br(Et_2(p\text{-}tol)P]$	88	sparkling brown irregular plates	Co Br	10.73 14.50	10.90 14.70
$[Co(DH)_2I(Et_2PhP)]$	90	brown prisms	Co I	10.12 21.80	9.90 22.16
$[Co(DH)_2I(Et_2(p\text{-}tol)P)]$	90	sparkling dark brown irregular prisms	Co I	9.88 21.28	9.44 20.98
$[Co(DH)_2(NCS)\ (Et_2PhP)]$	80	dark brown rhomb. prisms .	Co S	11.48 6.24	11:51 6.35
$[Co(DH)_2(NCS)\ (Et_2(p\text{-}tol)P)]$	85	short, brown irregular prisms	Co S	11.17 6.07	11.36 6.26

Et_2PhP = diethylphenylphosphine

$Et_2(p\text{-}tol)P$ = diethyl-p-tolyl-phosphine

The eliberation of the phosphine ligands are endothermal processes marked by two endothermal peaks on the DTA curves at 220° and 280–300°, respectively. The Br^- and I^- anions present a little influence on this decomposition stage. The corresponding perchlorates and nitrates decompose suddenly, in any cases with explosion, without formation of any stoichiometric or non-stoichiometric (intermediate products. At higher temperatures, in air atmosphere the oxidation of the ligands takes place (strong exothermal peaks at 450, 500°C on the DTA curves). The formation of the stoichiometric intermediates : $[Co(DH)_2X\ (phosphine)]$, $[Co(DH)_2X(phosphine)_{0.5}]$ and the pentacoordinated $[Co(DH)_2X]$[21,22] cannot be observed on the thermograms.

The *electronic spectra* of the phosphine complexes studied exhibit 4–5 bands. Their wavelengths are given in Table 6.

The A and B bands appear as very weak crystal field (CF) transition bands. Their position depends on the nature of the acidic ligand X in the inner coordination sphere.

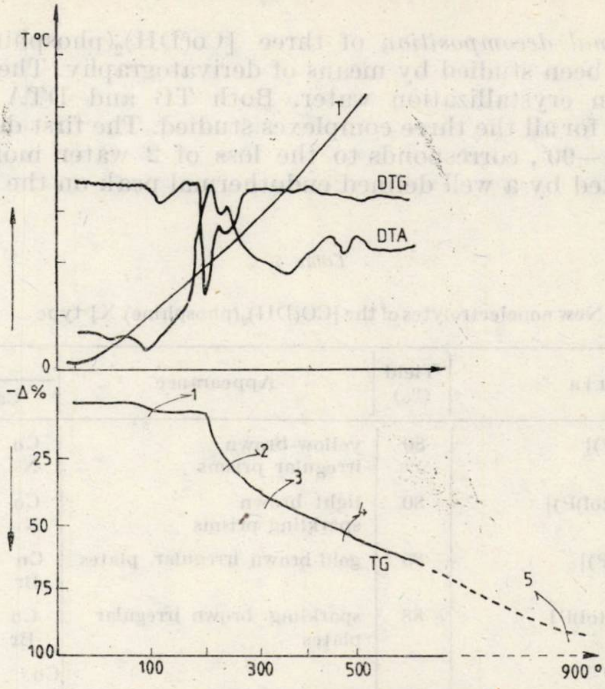

Fig. 1. — Derivatogram of $[Co(DH)_2(Et_2Ph.P)_2]Br.\ 2\ H_2O$

1 — calcd. mass of $[Co(DH)_2(Et_2Ph \cdot P)_2]$ Br
2 — calcd. mass of $[Co(DH)_2(Et_2Ph \cdot P)Br]$
3 — calcd. mass of $[Co(DH)_2(Et_2PhP)_{0.5} \cdot Br]$
4 — calcd. mass of $[Co(DH)_2Br]$
5 — calcd. mass of $1/3\ Co_3O_4$

Table 6

Electronic spectral data of the $[Co(DH)_2$ (phosphine) A*]-complexes

Phosphine	A*	A	B	C	D	E
Et_2PhP	Cl	18.5i	22.1i	31.0	40.3	—
	Br	16.2i	22.2i	31.6	39.9	46i
		18.0i	22.3	31.2	40.0	
	I	16.2i	24.6	30.9	40.1	46i
	NCS	18.1	22i	30.3	40.2	—
	NO_2	22.2	22.2	32.2	40.4	45i
	Et_2PhP	—	—	30.3	40.4	45i
$Et_2(p\text{-}tol)P$	I	16i	24i	30.2	40.1	46i
	Br	16i	21.8	31.6	40.0	45.8i
	$Et_2(p\text{-}tol)P$	—	—	29.6	41.0	45
Ph_3P	Br	18i	21i	28.3	40.1	44.5
Bu_2PhP	Bu_2PhP	—	—	29.9	40.3	45.8
Bu_3P	I	17i	22.7	31.3	40.3	
	NCS	18.4	22.5i	31.8	39.7	45.5i

i = inflexion point

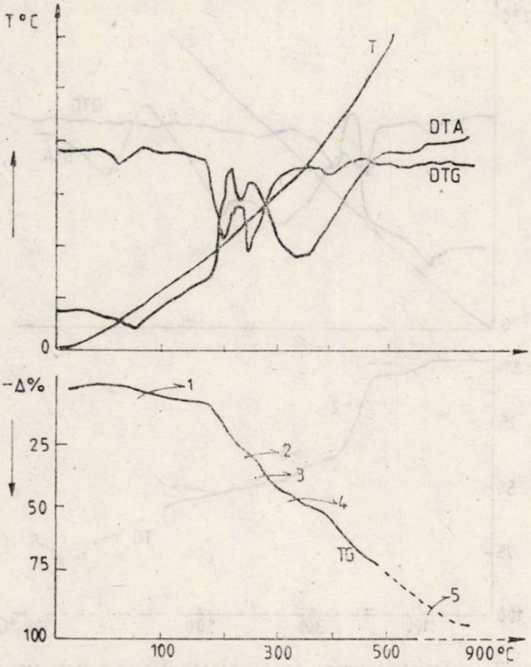

Fig. 2. — Derivatogram of $[Co(DH)_2(Et_2Ph.P)_2]\ I.2\ H_2O$

1 — calcd. mass of $[Co(DH)_2(Et_2Ph.P)_2]I$
2 — calcd. mass of $[Co(DH)_2(Et_2Ph.P)I]$
3 — calcd. mass of $[Co(DH)_2(Et_2Ph.P)_{0.5}.I]$
4 — calcd. mass of $[Co(DH)_2I]$
5 — calcd. mass of $1/3\ Co_3O_4$

The lowest $\tilde{\nu}$ values were observed in the case of the iodine nonelectrolytes. The A and B bands are completely absent in the case of the $[Co(DH)_2(phosphine)_2]X$ binary complex salts. An analogous phenomenon can also be observed for the corresponding diamine-complex bases: $[Co(DH)_2(amine)_2]^+$ and $[Co(ec)(amine)_2]^+$ (ecH_2 = ethylenediimino-bis-acetylacetone).

The C band at 28—32 kK can be considered as a Co^{3+} to ligand charge transfer band.

In the case of the $[Co(DH)_2X(amine)]$ and $[Co(DH)_2(amine)_2]^+$ type derivatives this band appears at higher wavenumber values: 33—— 34.5 kK.[23] The data given in Table 6 suggest that the position of C band depends on the number of aromatic rings linked to the P atoms. ($[Co(DH)_2X(R_3P)]$: 31.6, $[Co(DH)_2\ X(R_2ArP)]$: 31.1, $[Co(DH)_2\ (R_2ArP)_2)^+$: 29.9, $[Co(DH)_2X(Ar_3P)]$: 28.3 ; R = alkyl, Ar = aryl). The wave number of band C decreases with an increasing number of arylic substituents in the phosphine ligand.

This seems to be in agreement with the above hypothesis, that the C band is due to a Co^{3+} to ligand charge transfer transition, since the increase of the number of arylic substituents might lower the energy of the first empty ligand orbital.

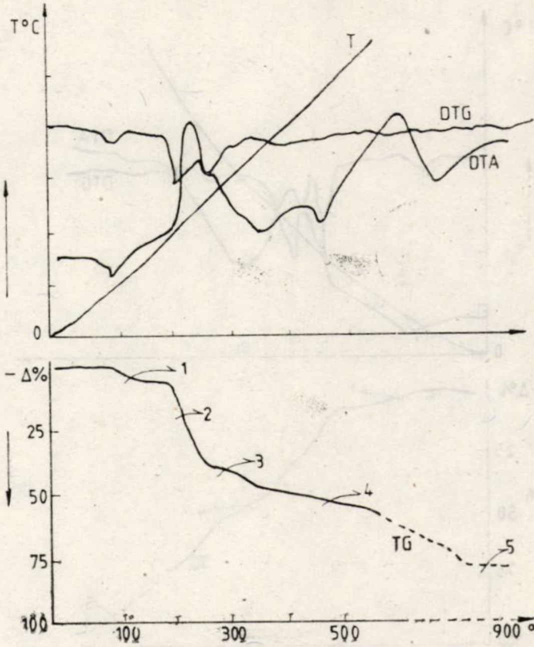

Fig. 3. — Derivatogram of $[Co(DH)_2(Et_2(p\text{-}tol)P)_2]Br.2\,H_2O$
1 — calcd. mass of $[Co(DH)_2(Et_2(p\text{-}tol)P)_2)]Br$
2 — calcd. mass of $[Co(DH)_2(Et_2(p\text{-}tol)P)Br]$
3 — calcd. mass of $[Co(DH)_2(Et_2(p\text{-}tol)P)_{0.5}\ Br]$
4 — calcd. mass of $[Co(DH)_2Br]$
5 — calcd. mass of 1/3 Co_3O_4
(T = temperature, TG, DTA, DTG (thermogravimetrical-, differential thermal — and differential thermogravimetrical curves),

The D band at 39.7—40.4 kK appears invariable in the spectra of all phosphine-complexes studied and is due probably to the presence of the Co $(DH)_2$ planar group, in agreement with the observation of Ablov and Filippov[24] in the case of the analogous amine derivatives.

The D and E bands might be ligand or charge transfer transition bands and their position does not differ very much for different types of Co- bis- dimethylglyoximine complexes.

EXPERIMENTAL

$[Co(DH)_2(phosphine)_2]$acetate solutions. 0.1 mol cobalt (II) acetate in 250 mL water were treated with a mixture of 0.2 mol dimethylglyoxime and 0.25 mole phosphine in 500 mL dil. methanol (1 : 1). The mixture was oxidized by air bubbling during 6—8 hours, filtered off, and the brown solutions used for double decomposition reactions.

$[Co(DH)_2(phosphine)_2]X$. 10 mmoles of $[Co(DH)_2\ (phosphine)_2]$—acetate in 50 mL solution were treated with an excess of 2—10 % KBr, KI, $NaClO_4$, picric acid, $NH_4[Co(NH_3)_2\ (NO_2)_4]$, $H[Co(DH)_2X_2]$ ($X = Cl$, Br, I, NCS, NO_2, N_3), in water and in dilute methanol (1 :3), respectively. The crystalline products obtained were filtered after 14—30 min. standing, washed with ice cooled water and dried in air.

[Co(DH)$_2$X(phosphine)] nonelectrolytes. 10 mmoles of H[Co(DH)$_2$X$_2$] monobasic complex acids or their sodium salts (X = Cl, Br, I, NCS, NO$_2$) were dissolved in 100 mL dilute methanol (1 :1) and after adding of 3—4 g ammonium acetate were treated with 10—12 mmol phosphine in 25—30 mL methanol. The mixture was evaporated down to a volume of 30—50 mL on a water bath. The crystalline products formed were filtered off, washed with dilute methanol and dried in air.

The *derivatograms* were recorded with a Derivatograph MOM (Hungary). Sample weight: 100 mg, heating rate: 10°/min.

The *electronic spectra* were recorded in methanol by means of a Specord recording spectrophotometer. Concentration : 2×10^{-3} mole/L (visible region) and 2×10^{-5} mole/L (UV region).

REFERENCES

[1] C. Booth, "Complexes of the transition metals with phosphines, arsines and stibines", in "Advances in Inorganic Chemistry and Radiochemistry", vol. 6, Academic Press, New-York, 1964, p. 10.

[2] C. A. Mc. Auliffe and W. Lewason, "Phosphine, arsine and stibine complexes of the transition elements", Elsevier, 1979, p. 2.

[3] J. Chatt and B. L. Shaw, *J. Chem. Soc.*, **1961**, 285.

[4] K. A. Jensen, *Z. anorg. Chem.*, **229**, 225, 282 (1932).

[5] W. Hieber and J. Sedlmeier, *Chem.Ber.*, **87**, 789 (1954).

[6] W. Hieber, and K. Heinicke, *Z. Naturforsch.*, **16 b**, 553 (1961).

[7] L. Malatesta and A. Araneo, *J. Chem. Soc.*, **1957**, 3803.

[8] A. Sacco and B. Freni, *J. Inorg. nuclear Chem.*, **8**, 566 (1958).

[9] J. Bosnich, W. G. Jackson and S.T.D. Lo, *Inorg.Chem.*, **13**, 2598 (1974).

[10] J. Bosnich, W. G. Jackson and W. J. Mc Lauren, *Inorg. Chem.*, **13**, 1133 (1974).

[11] G. R. Dobson, R. C. Taylor and T. D. Wals, *JCS. Chem. Commun.*, **1966**, 281.

[12] N. E. Takach, E. M. Holt, N. W. Alcoock, R. A. Henry and J. H. Nelson, *J.Amer.Chem. Soc.*, **102**, 2968 (1980).

[13] J. A. Kargol, R. W. Crecely, J. L. Burmeister, P. J. Toscano and L. G. Marzilli, *Inorg. Chim.Acta.*, **40**, 79 (1982).

[14] R. C. Stewart and L. G. Marzilli, *J.Amer.Chem.Soc.*, **100**, 817 (1978).

[15] G. Marcu, Cs. Várhelyi, M. Abdel Salam El Absy and A. Hantz, Academia RSR, Memoriile Secțiilor Științ. Ser. IV., Tom. IV. (2). 43 (1981).

[16] I. Gănescu, Cs. Varhelyi, A. Hantz and I. Papa, *Z. anorg. Chem.*, 1984 in press.

[17] W. C. Trogler and L. G. Marzilli, *Inorg. Chem.*, **14**, 2942 (1975).

[18] L. Sacconi, C. A. Ghilardi, C. Mealli and F. Zambini, *Inorg. Chem.*, **14**, 1380 (1975).

[19] R. Blinc and D. Hadzi, *J.Chem.Soc.*, **1958**, 4536.

[20] M. Chamberlain and J. C. Bailar, *J.Amer.Chem.Soc.*, **81**, 6412 (1959).

[21] J. Zsakó, J. Horák and Cs. Várhelyi, *J. Thermal Anal.*, **20**, 435 (1981).

[22] J. Zsakó, J. Horák and Cs. Várhelyi, *Monatsh.*, **112**, 945 (1981).

[23] J. Zsakó, J. Sata and Cs. Várhelyi, *Rev. Roumaine Chim.*, **18**, 1759 (1973).

[24] A. V. Ablov and M. P. Filippov, *Zhur. neorg. Khim.*, **3**, 1565 (1958) ; **4**, 2204, 2213 (1959).

Revue Roumaine de Chimie, **31**, *2*, 237–253 (1986)

ESTUDIO CULOMBIMETRICO A POTENCIAL CONTROLADO DE LA OXIDACION ANODICA DEL COMPLEJO CIANURADO BINUCLEAR DE Mn(III). II*

OXIDACION A +0.80 VOLTIOS (vs. S.C.E.): CORRIENTES FARADAICAS, CORRIENTES CINETICAS

G. LÓPEZ CUETO y A. ALONSO MATEOS*
Departamento de Química Analítica, Facultad de Química,
Universidad de Salamanca, España

Received January 29, 1982
Revised December 18, 1985

Se realiza un estudio sobre la oxidación electrolítica a potencial controlado de +0.80 voltios (vs. S.E.C.) del complejo cianurado binuclear de Mn(III) en medio cianurado. A este potencial de trabajo se producen corrientes faradaicas. Se observa la aparicíon de una corriente cinética. Se propone el siguente mecanismo: Durante la oxidación anódica tiene lugar la formación de los complejos cianurados binucleares de Mn(III)—Mn(IV) y Mn(IV) — Mn(IV). Ambos complejos reaccionan químicamente con el CN^- regenerando las especies inciales y al mismo tiempo reaccionan entre si pues son incompatibles. Se calculan las ecuaciones que relacionan la intensidad de corriente con el tiempo asi como los valores de la constante de velocidad de la reacción interferente.

A study has been made of the electrolytical oxidation of the Mn(III) brown binuclear cyanide complex in cyanide solution to constant-potential of +0.80 volts (vs. S.C.E.). Faradaic currents due to electrode and dissolvent oxidation are measured. A kinetic current is observed. From the experimental results a mechanism is proposed: The electrolytical oxidation guides to the formation of a Mn (III) — Mn(IV) and Mn(IV — Mn(IV) binuclear complexes which react with the cyanide of the solution regenerating the initial complexes. On the other hand binuclear complexes between reacts. The equation which relates the current with the time and the rate constant of the interferent reaction has been calculated.

INTRODUCCION

El complejo cianurado de Mn (III) obtenido según Brauer,[1] presenta en solución cianurada y en electrodo de platino dos ondas anódicas reversibles a 0.03 y 0.60 voltios respectivemente. En un trabajo ya comunicado [2] se expusieron los resultados obtenidos de un estudio voltamétrico sobre la naturaleza de los procesos anódicos: La primera onda anódica corresponde a la oxidación de un complejo binuclear Mn(III) —Mn(III) hasta otro también binuclear Mn(III)—Mn(IV), esta especie en la segunda reacción se oxida hasta Mn(IV)—Mn(IV). Las propriedades diamagnéticas del complejo de partida confirman su estructura binuclear.

---

* Part I: *Revue Roumaine de Chimie*, 000—000, *1985*

A la vista de los resultados anteriormente mencionados, pareció interesante realizar un estudio culombimétrico de la oxidación electrolítica del complejo cianurado binuclear de Mn(III) manteniendo el potencial constante precisamente a valores comprendidos en la zona de diffusión de las dos ondas anódicas ya mencionadas. En un primer trabajo se expusieron los resultados obtenidos durante la oxidación a + 0.20 voltios (vs. S.C.E.), se muestran a continuación los resultados obtenidos durante la oxidación a + 0.80 voltios.

La finalidad del presente estudio culombimétrico, es por tanto, comprobar la naturaleza de los productos de la oxidación electrolítica, así como la extensión de la misma. Es decir, determinar su estequiometría y grado de cuantitatividad, características representadas por los rendimientos en corriente y producto.

PARTE EXPERIMENTAL

Los reactivos, apparatos y electrodos así como el procedimiento utilizado para el pretratamiento del electrodo son los mismos que los descritos en la Parte 1.

EVALUACION DE LAS CORRIENTES FARADAICAS

La zona de difusión de la primera onda anódica está comprendida en el margen de potenciales de + 0.10 a + 0.40 voltios (vs. E.C.S.) aparoximadamente, siendo de +0.70 a + 0.90 voltios los límites de la zona de difusión corespondiente a la segunda onda. Las curvas intensidad-potencial obtenidas en ausencia de cualquier otra especie electrolizable (fuera del propio electrolito soporte) registradas para CNNa desde 1M hasta 5M, muestran que al aumentar la concentración de cianuro las corrientes de fondo se producen a potenciales menos positivos, lo cual es debido sin duda a la variación del potencial de oxidación del sistema O_2/OH^- con el pH.

En la oxidación culombimétrica a los potenciales de la zona de difusión de la segunda onda anódica si se precisan correccione, pues las corrientes faradaicas de fondo son importantes en magnitud. Estas corrientes faradaicas pueden atribuirse, por una parte a la oxidación superficial del electrodo de platino, [3] proceso que daría lugar a una intensidad decreciente de forma exponencial, y por otra a la oxidación de los iones OH del disolvente, lo que se manifestaria en una intensidad de corriente constante.

Para determinar la magnitud de las corrientes faradaicas del fondo al potencial de trabajo correspondientes a la zona de difusión de la segunda onda anódica —potencial que se ha establecido en + 0.80 voltios— se han registrado las curvas intensidad-tiempo para diferentes condiciones. Las curvas experimentales presentan una disminución inicial de la intensidad hasta que ésta alcanza un valor constante distinto de cero. En la figura 1 se ha representado esquemáticamente la forma de estas curves :

la intensidad decreciente corresponde a una *corriente faradaica exponenal** debida a la oxidación de la superficie del electrodo de platino, la intensidad constante final representa una *corriente faradaica continua* debida a la electrolisis del disolvente.

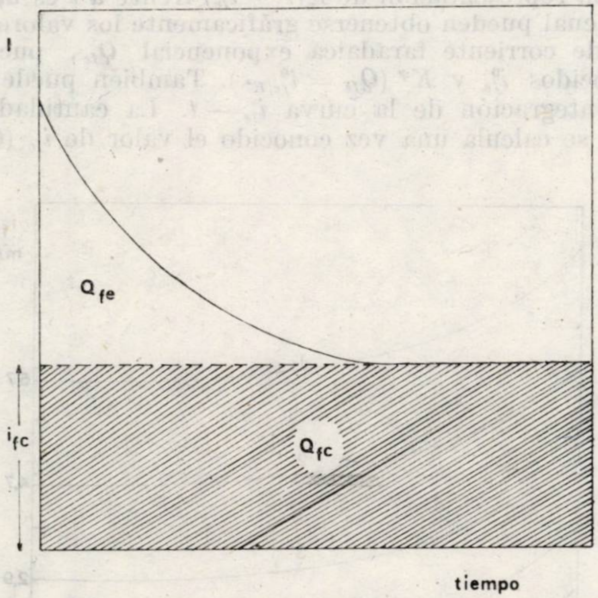

Fig. 1. — Curva intensidad-tiempo en presencia de una corriente faradaica continua.

La intensidad de la corriente faradaica exponencial vendrá dada en todo momento por la diferencia entre la intensidad total y la intensidad de la corriente faradaica continua :

$$i_{fe} = i - i_{fc} \tag{1}$$

port otra parte y seqún la ecuación de Lingane :

$$i_{fe} = i_{fe} \cdot e^{-K^*t} \tag{2}$$

donde K^* tiene un sentido físico diferente al de la constante K de la ecuación de Lingane. Teniendo en cuenta (2), la expresión (1) se transforma en :

$$i - i_{fc} = i^0_{fe} \cdot e^{-K^*t} \tag{3}$$

---

* En la terminología de Meites y Moros[4] esta corriente se denomina *corriente faradaica de impurezas* („faradaic impurity current"). En el presente trabajo se ha considerado mas adecuado el termino *corriente faradaica exponencial* y se representarán por i_{fe} y Q_{fe} la la intensidad y la cantidad de corriente correspondientes, con esta denominación se hace alusión al tipo de función a que se ajusta la intensidad de dicha corriente y por otra parte el término mas general, pues incluye las corrientes faradaicas debidas a la electrolisis superficial del electrodo, lo cual no debe en rigor ser calificado de impureza.

o bien tomando logaritmos se llega a la ecuación:

$$\lg (i - i_{fc}) = \lg i_{fe} - 0.434\, K^{*t} \tag{4}$$

según la cual la representación de $\lg(i - i_{fc})$ frente a t es una línea recta a partir de la cual pueden obtenerse gráficamente los valores de i^0_{fe} y K^*. La cantidad de corriente faradaica exponencial $Q_{fe'}$, puede calcularse una vez conocidos i^0_{fe} y K^* ($Q_{fe} = i^0_{fe/K^*}$). También puede determinarse Q_{fe} mediante integración de la curva $i_{fe} - t$. La cantidad de corriente continua, $Q_{fc'}$, se calcula una vez conocido el valor de $i_{fc'}$ ($Q_{fc} = i_{fc} \cdot t$).

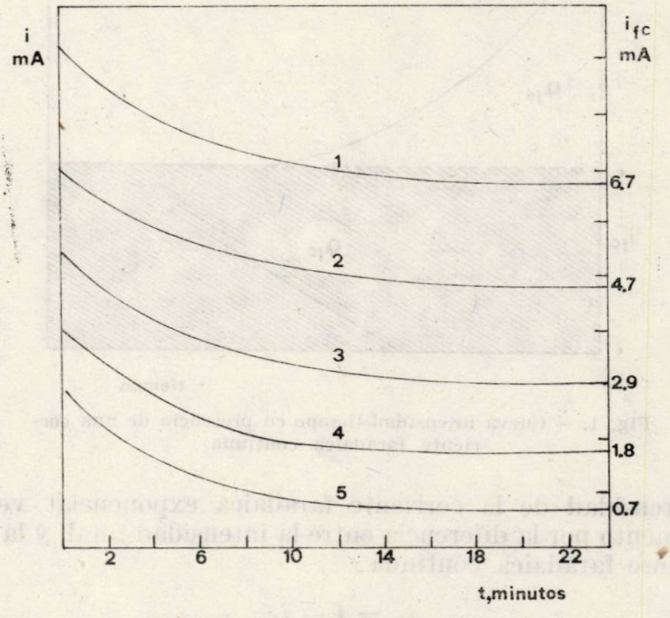

Fig. 2. Curvas intensidad-tiempo de la disolución fondo. Influencia de la concentración de CNNa: 1. CNNa 50 M; 2. CNNA 4.0 M; 3. CNNA 3.0 M; 4. CNNA 2.0 M; 5. CNNAa 1.0 M.

En la figura 2 se muestran las curvas intensidad-tiempo obtenidas para diferentes concentraciones de *cianuro sódico*, manteniendo constantes la fuerza iónica y la temperatura. El incremento de la intensidad final, $i_{fc'}$ al aumentar la concentración de cianuro se debe a la disminución del potencial de oxidación del disolvente al aumentar el pH. Representando los valores de lg $(i - i_{fc})$ frente al tiempo se obtienen siempre líneas rectas (Figura 3). En la Tabla 1 se muestran los valores de Q_{fe} calculados a partir de dichas rectas y por medio de integración, pudiendose advertir la constancia de Q_{fe} en todas las experiencias realizadas.

Al aumentar la *fuerza iónica* se observa una disminución de $i_{fc'}$ debida a la modificación que experimenta el coeficiente de difusión a fuerza iónica elevada. La representación de los valores de lf $(i - i_{fc})$

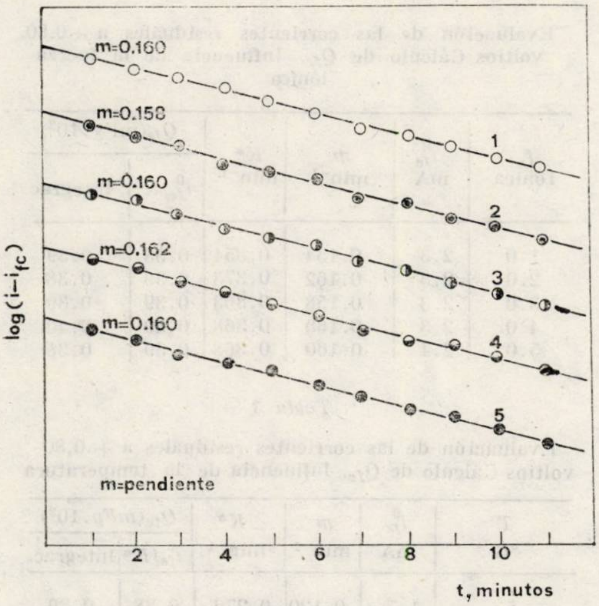

Fig. 3. — Curvas $\lg(i - i_{fc})$ frente al tiempo de la disolución fondo. Influencia de la concentración de CNNa : 1. CNNa 5.0 M ; 2. CNNa 4.0 M ; 3. CNNa 3.0 M ; 4. CNNa 2.0 M ; 5. CNNa 1.0 M.

Tabla 1

Evaluación de las corrientes residuales a + 0.80 voltios Cálculo de Q_{fe}. Influencia de la concentración de CNNa

CNNa M	i^0_{fe} mA	m min^{-1}	K^* min^{-1}	$Q_{fe}(mF \cdot 10^2)$ i^0_{fe}/K^*	Integrac.
1.0	2.4	0.160	0.368	0.39	0.38
2.0	2.3	0.158	0.363	0.39	0.40
3.0	2.3	0.160	0.368	0.39	0.39
4.0	2.3	0.162	0.373	0.39	0.39
5.0	2.3	0.160	0.368	0.39	0.39

frente al tiempo conduce en todos los casos a lineas reactas y el valor de Q_{fe} calculado por los procedimientos antes mencionados se mantiene sensiblemente constante (Tabla 2).

Un aumento de la *temperatura* se traduce también en un aumento de la intensidad final i_{fc}. Los valores de Q_{fe} calculados a partir de las rectas lg $(i - i_{fc})$ frente al tiempo, resultan ser practicamente iguales (Tabla 3).

Tabla 2

Evaluación de las corrientes residuales a +0.80 voltios Cálculo de Q_{fe}. Influencia de la fuerza iónica

f. iónica	i^0_{fe} mA	m min^{-1}	K^* min^{-1}	Q_{fe}(mFy.10^2)	
				i^0_{fe}/K^*	Integrac.
1.0	2.3	0.154	0.354	0.38	0.39
2.0	2.3	0.162	0.373	0.39	0.38
3.0	2.3	0.158	0.363	0.39	0.39
4.0	2.3	0.160	0.368	0.39	0.40
5.0	2.4	0.160	0.368	0.39	0.38

Tabla 3

Evaluación de las corrientes residuales a + 0,80 voltios Cálculo de Q_{fe}. Influencia de la temperatura

T °C	i^0_{fe} mA	m min^{-1}	K^* min^{-1}	Q_{fe}(mFy.10^2)	
				i^0_{fe}/K^*	Integrac.
5	1.7	0.120	0.276	0.38	0.39
15	2.1	0.140	0.322	0.40	0.37
25	2.4	0.160	0.368	0.39	0.39
30	2.6	0.180	0.414	0.39	0.38
40	3.1	0.220	0.506	0.38	0.40

EVOLUCION DE LAS CURVAS INTENSIDAD-POTENCIAL DURANTE LA OXIDACION A + 0.80 VOLTIOS

Fijando el potencial de trabajo en + 0.80 voltios (vs. E.C.S.) se llevó a cabo la oxidación electrolítica de una disolución reciente de $Mn(CN)_6^{3-}$ 1.12×10^{-3}M en CNNa 2.0 M y fuerza iónica 5.0 manteniendo la temperatura en 25°C y registrando las curvas intensidad-potencial en diferentes momentos de la oxidación.Como puede apreciarse en la Figura 4 la intensidad de difusión de la primera onda anódica disminuye progresivamente, al mismo tiempo que aparece una onda catódica de intensidad de difusión creciente. Por su parte la sequnda onda anódica no modifica aparentemente su altura aunque la electrolisis se mantenga durante tiempo prolongado.

Este hecho resulta sorprendente, ya que por el circuito pasa en todo momento intensidad de corriente de magnitude apreciable, corriente que, cuando la primera onda anódica ha desaparecido por completo, se invierte necesariamente en el proceso :

$$Mn(III)-Mn(IV) - 1e^- \rightarrow Mn(IV)-Mn(IV)$$

A la vista de este resultado, parece que el complejo Mn(IV)—Mn(IV) formado como producto de la reacción electroquímica es sumamente inestable y reacciona rápidamente con el cianuro, regenerando el Mn (III)—Mn(IV).

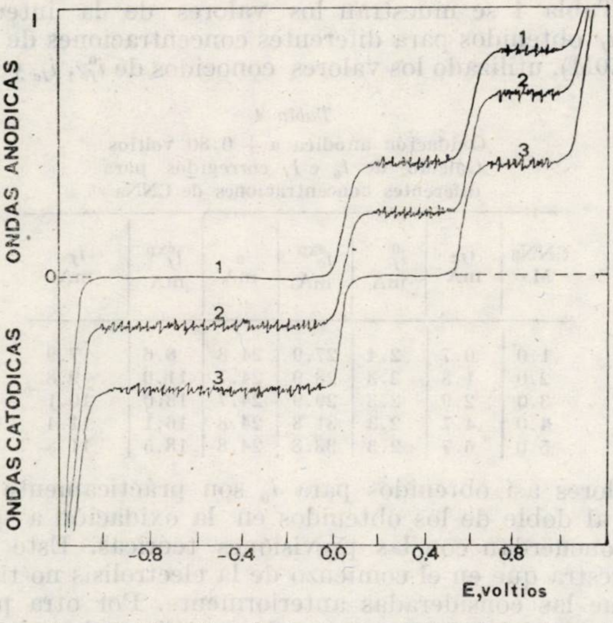

Fig. 4. — Modificación de las curvas intensidad-potencial durante la oxidación eectrolítica a ± 0.80 volts : 1. Antes de la oxidación ; 2. Durante a oxidación ; 3. Al final de la oxidación.

CURVAS INTENSIDAD-TIEMPO DURANTE LA ELECTROLISIS

Las curvas intensidad-tiempo durante la electrolisis a + 0.80 voltios se registraron todas en las mismas condiciones experimentales, CNNa 1.0M, fuerza iónica 5.0 y temperatura de 25°C, exceptuando naturalmente la variable en estudio.

Durante la oxidación a + 0.80 voltios deberá tenerse en cuenta la existencia de corrientes de fondo, debidas por una parte a la oxidación superficial del electrodo (corriente faradaica exponencial, i_{fe}) por otra parte a la oxidación del OH^- (corriente faradaica continua, i_{fc}). Por otro lado, la corriente cinética i_K debida a la regeneración del Mn(III)—Mn(III) mediante reducción del Mn(III)—Mn(IV) con el cianuro, alcanza también valores apreciables para $CN^- \geqslant 3M$. Los valores de $i_{fe'}$ i_{fc} y i_K son conocidos para las distintas condiciones experimentales, los dos primeros a partir de las curvas intensidad-tiempo del electrolito fondo y i_K a partir de las curvas intensidad-tiempo en la oxidación a + 0.20 voltios. Conocidos estos valores, se podrán efectuar las correcciones oportunas en los valores experimentales i_0^{exp}, i_f^{exp} (corriente inicial y final experimental) para conocer los valores de i_0 e i_f que pertenecen realmente a la oxidación electrolítica de la especie $Mn(CN)_6^{3-}$:

$$i_0 = i_0^{\text{exp}} - i_{fc} - i_{fe}^0 \tag{5}$$

$$i_f = i_f^{\text{exp}} - i_{fe} - i_K \tag{6}$$

En la Tabla 4 se muestran los valores de la intensidad inicial, $i_{0'}$ y la final $i_{f'}$ obtenidos para diferentes concentraciones de CNNa (desde 1.0M hasta 5.0M), utilizado los valores conocidos de $i^0_{fe'}$, i_{fc} y i_K.

Tabla 4

Oxidación anódica a + 0.80 voltios
Cálculo de I_0 e I_f corregidos para diferentes concentraciones de CNNa

CNNa M	i_{fc} mA	i^0_{fe} mA	i_0^{exp} mA	i_0 mA	i_f^{exp} mA	i_f mA
1.0	0.7	2.4	27.9	24.8	8.6	7.9
2.0	1.8	2.3	28.9	24.7	11.6	9.8
3.0	2.9	2.3	29.9	24.7	13.0	10.1
4.0	4.7	2.3	31.8	24.8	16.1	11.4
5.0	6.7	2.3	33.8	24.8	18.5	11.8

Los valores así obtenidos para i_0 son prácticamente constantes y equivalentes al doble de los obtenidos en la oxidación a + 0.20 voltios, por lo que concuerdan con las previsiónes teóricas. Este hecho experimental demuestra que en el comienzo de la electrolisis no tiene lugar mas reacciones que las consideradas anteriormente. Por otra parte, el valor obtenido de i_f distinto de cero pone de manifiesto la existencia de una nueva corriente cinética además de la anteriormente considerada. Parece evidente que esta nueva corriente cinética se debe a la reducción del Mn(IV)—Mn(IV) con el cianuro. La intensidad de difusión correspondiente a la onda anódica de 0.60 voltios, lo que justifica que esta no modifique prácticamente su altura a lo largo de la electrolisis.

Al representar lg $(i - i_{fc})$ frente al tiempo (Figura 5) no se obtienen líneas rectas mas que al principio del proceso, debido a la presencia de corrientes cinéticas. Midiendo la pendente en el origen (m) se pueden hallar los valores de K_{exp} $(n = 0.434\ K_{\text{exp}})$. En la Tabla 5, se muestran los valores de K_{exp} obtenidos en la oxidación a + 0.80 voltios, pudiéndose comprobar que siempre son superiores a los obtenidos en la oxidación a + 0.20 voltios, diferenciándose precisamente en el valor de K^*, constante física correspondiente a la oxidación de la superficie del electrodo, proceso que, como es sabido, da lugar a una corriente faradaica exponencial.

Los resultados obtenidos al estudiar las otras variables, fuerza iónica, temperatura, son concordantes con los obtenidos y expuestos anteriormente por lo que no se indican los valores va que no aportan nueva información.

RENDIMIENTO EN CORRIENTE Y PRODUCTO

Cuando el complejo cianurado de Mn(III) en estudio, se oxida a un potencial anódico de + 0.80 voltios, pueden tener lugar succesivamente, las siquientes reacciones electroquímicas :

$$\text{Mn(III)}-\text{Mn(III)}-\text{le}^{-}\rightarrow \text{Mn(III)}-\text{Mn(IV)}$$

$$\text{y Mn(III)}-\text{Nn(IV)}-\text{le}^{-}\rightarrow \text{Mn(IV)}-\text{Mn(IV)}$$

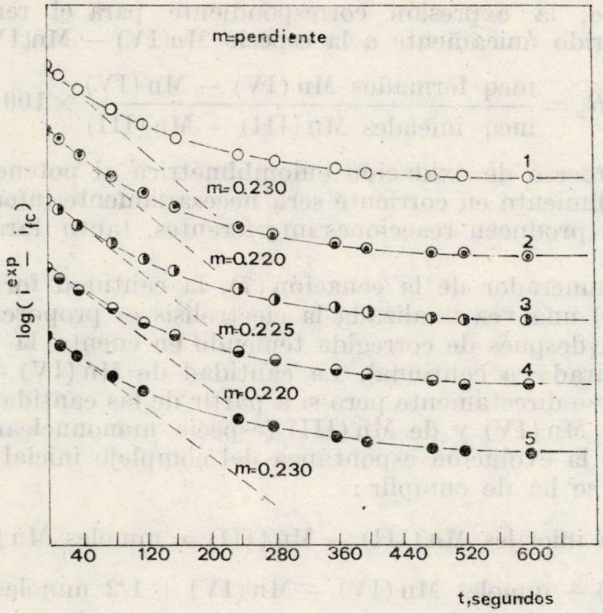

Fig. 5. — Curvas Intensidad-tiempo durante la oxidación electolítica a + 0.80 volts del complejo cianurado binuclear Mn(III)—Mn(III). Influencia de la concentración de CNNa: 1. CNNa 5.0 M; 2. CNNa 4.0 M; 3. CNNa 3.0 M; 4. CNNa 2.0 M; 5. CNNa 1.0 M.

Tabla 5

Oxidación anódica a + 0.80 voltios
Influencia de la concentración de CNNa. Valores de K_{exp}

CNNa M	m min^{-1}	$K_{\text{exp}}^{0.80}$ min^{-1}	$K_{\text{exp}}^{0.80} - K_{\text{exp}}^{0.20}$ min^{-1}	K^* min^{-1}
1.0	0.230	0.529	0.368	0.368
2.0	0.220	0.506	0.356	0.363
3.0	0.225	0.517	0.379	0.368
4.0	0.220	0.506	0.368	0.373
5.0	0.230	0.506	0.391	0.368

La segunda de las reacciones solamente se produce cuando el Mn(III)—Mn(III) inicial ha sido oxidado por completo a la forma intermedia Mn(III)—Mn(IV).

El rendimiento en corriente, en tanto por ciento, vendrá dado por la expresión:

$$R_C = \\ = \frac{\text{meq formados Mn(III)}-\text{Mn(IV)} + \text{meq formados Mn(IV)}-\text{Mn(IV)}}{\text{mF de corriente consumidos}} \times 100 \qquad (7)$$

por otra parte, la expresión correspondiente para el rendimiento en producto, referido únicamente a la especie Mn(IV) — Mn(IV), será:

$$R_p = \frac{\text{meq formados Mn (IV)} - \text{Mn (IV)}}{\text{meq iniciales Mn (III)} - \text{Mn (III)}} \times 100 \qquad (8)$$

En el proceso de oxidación culombimétrica al potencial de +0.80 voltios el rendimiento en corriente será necesariamente inferior al 100 %, puesto que se producen reacciones interferentes, tanto faradaicas como cinéticas.

En el numerador de la ecuación (7), la cantidad formada de Mn (III)—Mn (IV) una vez finalizada la electrolisis es proporcional a la intensidad final (después de corregida teniendo en cuenta la intensidad de la corriente faradaica continua). La cantidad de Mn (IV) — Mn (IV) no puede calcularse directamente pero si a partir de las cantidades formadas de Mn (III) — Mn (IV) y de Mn (III) (especie mononuclear no oxidable procedente de la evolución espontánea del complejo inicial). Al final de la electrolisis se ha de cumplir:

$$\begin{aligned} &\text{mmoles iniciales Mn (III)} - \text{Mn (III)} = \text{mmoles Mn (III)} - \\ &- \text{Mn (IV)} + \text{mmoles Mn (IV)} - \text{Mn (IV)} + 1/2 \text{ mmoles Mn (III)} \qquad (9) \end{aligned}$$

La especie Mn (III) es producto de una sola reacción química, por lo que la cantidad formada podría calcularse conociendo la cinética de la reacción:

$$\frac{d\,\text{Mn(III)}}{dt} = -2\,\frac{d\,\text{Mn(III)} - \text{Mn(III)}}{dt} = 2\,k_2\,[\text{Mn (III)} - \text{Mn(III)}] \qquad (10)$$

Esta reacción no puede integrarse, pues se desconoce la expresión que indica la dependencia de [Mn (III) — Mn (III)] con respecto al tiempo. Por tanto, la cantidad formada de Mn (IV) — Mn (IV) sólo podrá calcularse, según la ecuación (9), en condiciones en que la descomposición paralela del Mn (III) — Mn (III) pueda despreciarse. En estas condiciones ($[\text{Cn}^-] \geqslant 3\text{M}$), la ecuación (9) queda simplificada:

$$\begin{aligned} &\text{mmoles Mn (IV)} - \text{Mn (IV)} = \text{mmoles iniciales Mn (III)} - \text{Mn (III)} - \\ &\qquad - \text{mmoles Mn (III)} - \text{Mn (IV)} \qquad (11) \end{aligned}$$

Teniendo en cuenta el número de electrones invertidos en cada reacción:

$$\text{meq Mn (IV)} - \text{Mn (IV)} = 2 \times \text{mmoles Mn (IV)} - \text{Mn (IV)}$$

$$\text{meq Mn (III)} - \text{Mn (IV)} = \text{mmoles Mn (III)} - \text{Mn (IV)}$$

$$\text{meq Mn (III)} - \text{Mn (III)} = 2 \times \text{mmoles Mn (III)} - \text{Mn (III)}$$

la ecuación (11) se transforma en:

$$\begin{aligned} &\text{meq Mn (IV)} - \text{Mn (IV)} = \text{meq iniciales Mn (III)} - \text{Mn (III)} \\ &\qquad - 2 \times \text{meq Mn (III)} - \text{Mn (IV)} \qquad (12) \end{aligned}$$

El numerador de la expressión (7) tomará la forma :

$$\text{meq formados Mn (III)} - \text{Mn (IV)} + \text{meq formados Mn (IV)} - \text{Mn(IV)} =$$

$$\text{meq iniciales Mn (III)} - \text{Mn (III)} - \text{meq formados Mn (III)} - \text{Mn(IV)} \tag{13}$$

o bien en función de las intensidades de difusión :

$$\text{meq formados Mn (III)} - \text{Mn (IV)} - \text{meq formados Mn (IV)} - \text{Mn(IV)} =$$

$$\text{meq iniciales Mn (III)} - \text{Mn (III)}\ 1 - \frac{i_f}{i_0} =$$

$$\text{meq iniciales Mn (III)} - \text{Mn (III)}\ \frac{i - i_f}{i_0} \tag{14}$$

De donde el rendimiento en corriente según la ecuación (7) vendrá dado por :

$$R_C = \frac{\text{meq iniciales Mn (III)} - \text{Mn (III)}}{Q_{\text{exp}}} \left(\frac{i_0 - i_f}{i_0} \right) \times 100 \tag{15}$$

La ecuación anterior solamente es válida para concentraciones de cianuro elevadas (⩾ 3M), condiciones en las que puede despreciarse la cantidad de Mn (III) – Mn (III) que evoluciona paralelamente hacia la formación del complejo mononuclear no oxidable.

Sustituyendo en (8) el numerador por la expresión (12) se obiene :

$$\frac{\text{meq iniciales Mn(III)} - \text{Mn(III)} - 2 \times \text{meq formados Mn(III)} - \text{Mn(IV)}}{\text{meq iniciales Mn (III)} - \text{Mn (III)}} \times 100 \tag{16}$$

expresión que se transforma, en función de las intensidades de difusión en :

$$R_p = \frac{i_0 - 2\, i_f}{i_0} \times 100 \tag{17}$$

Esta ecuación permite el cálculo del rendimiento en producto para concentraciones elevadas de cianuro, basándose en la medida de las intensidades inicial y final.

Utilizando las ecuaciones (15) y (17) se han calculado los rendimientos en corriente y producto para disoluciones de cianuro 3.0, 4.0 y 5.0 M. Como puede comprobarse en la Tabla 6 los resultados son muy bajos e inferiores a los obtenidos en la oxidación a + 0.20 voltios, debido a la inestabilidad del complejo Mn (IV) – Mn (IV) en disolución cianurada.

Tabla 6

Oxidación anódica a +0.80 voltios. Rendimiento en corriente y producto. Influencia de la concentración de CNNa

CNNa M	Mn(III)−Mn(III) meq.10^2	Q_{exp} mFy.10^2	$\frac{i_0-i_f}{i_0}$	Rendimientos %	
				R_c	R_p
3.0	11.2	8.3	0.59	79.6	18.2
4.0	11.2	9.4	0.54	64.3	8.1
5.0	11.2	10.6	0.52	57.3	4.9

MECANISMOS

Durante la oxidación anódica del complejo cianurado binuclear de manganeso (III) al potencial de +0.80 voltios tienen lugar las dos reacciones siguientes:

$$\mathrm{Mn\,(III) - Mn\,(III)} - 1e^- \xrightarrow{K} \mathrm{(Mn\,(III) - Mn\,(IV)} \qquad (18)$$

$$\mathrm{Mn\,(III) - Mn\,(IV)} - 1e^- \xrightarrow{K} \mathrm{Mn\,(IV) - Mn\,(IV)} \qquad (19)$$

La velocidad de la primera está controlada por la difusión de la especie Mn (III) — Mn (III) hacia el electrodo, y la de la segunda por la difusión de las especies Mn (III) — Mn (III) y Mn (III) — Mn (IV), puesto que en este caso el complejo que reacciona en el electrodo, el Mn (III) — Mn (IV), proviene, por una parte, de la primera de las reacciones electroquímicas y, por otra, de la difusión de dicha especie. En consecuencia, la velocidad de cada una de estas reacciones electroquímicas, controladas por difusión, será:

$$v_{e1} = K\,[\mathrm{Mn\,(III) - Mn\,(III)}] \qquad (20)$$

$$v_{e2} = [\mathrm{Mn\,(III) - Mn\,(III)}] + K\,[\mathrm{Mn\,(III) - Mn\,(IV)}] \qquad (21)$$

Además de las dos reacciones electroquímicas mencionadas pueden producirse las siguientes reacciones químicas:

$$2\,\mathrm{Mn\,(III) - Mn\,(IV)} + \mathrm{Cn^-} + 2\mathrm{OH^-} \xrightarrow{k_1}$$

$$2\,\mathrm{Mn\,(III) - Mn\,(III)} + \mathrm{CNO^-} + \mathrm{H_2O} \qquad (22)$$

$$2\,\mathrm{Mn\,(IV) - Mn\,(IV)} + \mathrm{CN^-} + 2\mathrm{OH^-} \xrightarrow{k_2}$$

$$2\,\mathrm{Mn\,(III) - Mn\,(IV)} + \mathrm{CNO^-} + \mathrm{H_2O} \qquad (23)$$

Cuyas velocidades vendrán dadas, respectivamente, por las expresiones:

$$v_1 = k_1[\mathrm{Mn\,(III) - Mn\,(IV)}] \qquad (24)$$

$$v_3 = k_3[\mathrm{Mn\,(IV) - Mn\,(IV)}] \qquad (25)$$

Por otra parte, el producto de la segunda de las reacciones, electroquímicas, el complejo Mn (IV) – Mn (IV), será inestable en presencia de Mn (III) – Mn (III):

$$\mathrm{Mn\,(IV) - Mn\,(IV) + Mn\,(III) - Mn\,(III)} \xrightarrow{\text{rápida}} \mathrm{2Mn\,(III) - Mn\,(IV)} \qquad (26)$$

Esta reacción es rápida, por lo que su velocidad, $v_{4'}$ estará controlada por la velocidad de formación de la especie Mn (IV) – Mn (IV) (cuando esta especie no tenga existencia en disolución, es decir para $t < \tau$).

Por tanto:

$$v_4 = v_{e2} = K\,[\mathrm{Mn\,(III) - Mn\,(III)}] + K\,[\mathrm{Mn\,(III) - Mn\,(IV)}] \qquad (27)$$

o bien por la velocidad de formación de Mn (III) – Mn (III), para $t > \tau$:

$$v_4 = v_1 = k_1\,[\mathrm{Mn\,(III) - Mn\,(IV)}] \qquad (28)$$

Finalmente es preciso contar con la descomposición que el complejo binuclear experimenta paralelamente:

$$\mathrm{Mn\,(III) - Mn\,(III)} \xrightarrow{k_2} \mathrm{2Mn\,(III)} \qquad (29)$$

Reacción cuya velocidad viene dada por:

$$v_2 = k_2\,[\mathrm{Mn\,(III) - Mn\,(III)}] \qquad (30)$$

Las diferentes reacciones consideradas se pueden resumir en el siguiente esquema:

$$\begin{tikzcd}
\mathrm{Mn\,(III) - Mn\,(III)} \arrow[r, "k_2"] \arrow[d, shift right, "K"'] & \mathrm{Mn\,(III)} \\
\mathrm{Mn\,(III) - Mn\,(IV)} \arrow[u, shift right, "k_2"'] \arrow[d, shift right, "K"'] & \mathrm{Mn(III) - Mn\,(III)} \arrow[ul] \\
\mathrm{Mn\,(IV) - Mn\,(IV)} \arrow[u, shift right, "k_3"'] \arrow[ur, dash] &
\end{tikzcd}$$

La intensidad de la corriente será en todo momento proporcional a la suma de las velocidades de las dos reacciones electroquímicas, y se cumplirá:

$$i = 2k_d[\mathrm{Mn\,(III) - Mn\,(III)}] + k_d\,[\mathrm{Mn\,(III) - Mn\,(IV)}] \qquad (31)$$

Siendo k_d la constante de proporcionalidad entre concentración e intensidad de difusión, constante, que según ya se ha dicho tiene practicamente el mismo valor para las dos ondas anódicas en estudio.

Si se representa por τ el tiempo necesario para que la concentración de Mn (III) – Mn (III) se haga cero, la expresión anterior adoptará la forma simplificada para $t > \tau$:

$$i = k_d[\mathrm{Mn\,(III) - Mn\,(IV)}] \qquad (32)$$

a) Intensidad para $t \leqslant \tau$

Para deducir la ecuación que representa la intensidad en función del tiempo es preciso hallar la dependencia de [Mn (III) – Mn (III] y [Mn (III) – Mn (IV)] frente al tiempo. Según las ecuaciones (20), (24), (27) y (29), la variación de la concentración de la especie inicial Mn (III) – Mn (III) con respecto al tiempo será:

$$-\frac{\mathrm{d\,Mn\,(III) - Mn\,(III)}}{\mathrm{d}t} = K[\mathrm{Mn(III) - Mn(III)}] - k[\mathrm{Mn(III) - Mn(III)}] +$$

$$+ K[\mathrm{Mn(III) - Mn(III)}] + K[\mathrm{Mn(III) - Mn(IV)}] + k_2[\mathrm{Mn(III) - Mn(III)}] \qquad (33)$$

Para integrar esta ecuación se necesita expresar Mn (III) – Mn (IV) en función de Mn (III) – Mn (III). En todo momento se ha de cumplir:

$$[\mathrm{Mn\,(III) - Mn\,(IV)}] = [\mathrm{Mn\,(III) - Mn\,(III)}]_0 - \mathrm{Mn\,(III) - Mn\,(III)}] -$$

$$- [\mathrm{Mn\,(IV) - Mn\,(IV)}] - 1/2\,[\mathrm{Mn\,(III)}] - 1/2\,[\mathrm{Mn\,(III)}] \qquad (34)$$

donde $[\mathrm{Mn\,(III) - Mn\,(III)}]_0$ es la comcemtración inicial antes de la electrolisis.

Para $t \leqslant \tau$, $[\mathrm{Mn\,(IV) - Mn\,(IV)}] = 0$ y para concentraciones de cianuro $\geqslant$ 3M, $[\mathrm{Mn\,(III)}] = 0$, por lo que la ecuación (34) se transforma en:

$$\mathrm{Mn\,(III) - Mn\,(IV)} = [\mathrm{Mn\,(III) - Mn\,(III)}]_0 - [\mathrm{Mn\,(III)\;Mn\,(III)}] \qquad (35)$$

Sustituyendo en (33) y teniendo en cuenta que para $[\mathrm{CN}^-] \geqslant 3\mathrm{M}$, $K \geqslant\geqslant k_2$, después de simplificar:

$$-\frac{\mathrm{d\,Mn\,(III) - Mn\,(III)}}{\mathrm{d}t} = (K + k_1)\,[\mathrm{Mn\,(III) - [Mn\,(III)]} + [(K - k_1)$$

$$[\mathrm{Mn\,(III) - Mn\,(III)}]_0 \qquad (36)$$

Integrando esta ecuación diferencial y sustituyendo en (35) resulta:

$$[\mathrm{Mn\,(III) - Mn\,(IV)}] = [\mathrm{Mn\,(III) - Mn\,(III)}_0\,\frac{2K}{K + K_1}\,[K \cdot \mathrm{e}^{-(K+k_1)t}] \qquad (37)$$

Sustituyendo los valores obtenidos para [Mn (III) – Mn (III)] por integración de (36) y [Mn (III) – mn (IV)] en (31):

$$i = k_a[\mathrm{Mn\,(III) - Mn\,(III)}]_0\,\frac{2}{K + k_1}\,[\mathrm{K}\mathrm{e}^{-(K+k_1)t} + k_1] \qquad (38)$$

Esta ecuación representa la dependencia de la intensidad con el tiempo en el intervalo $t \leqslant \tau$ y para concentraciones de cianuro $\geqslant 3.0$ M.

b) Intensidad para $t \geqslant \tau$

La intensidad de la corriente para $t \geqslant \tau$ se deducirá a partir de la ecuación (32). Para ello se expresa la variación de la concentración de la especie Mn (III) – Mn (IV) en función del tiempo. Según las ecuaciones (21), (24), (25) y (28), la variación de la concetración de la especie antes mencionada con respecto al tiempo será :

$$-\frac{\mathrm{d\,Mn(III) - Mn(IV)}}{\mathrm{d}t} = K[\mathrm{Mn(III) - Mn(IV)}] + k_1[\mathrm{Mn(III)} -$$

$$- \mathrm{Mn(IV)}] - k_3[\mathrm{Mn(IV) - Mn(IV)}] - 2[k_1\mathrm{Mn(III) - Mn(IV)}] \quad (39)$$

A partir de la ecuación (34) y teniendo en cuenta que para $t \geqslant \tau$, $[\mathrm{Mn(III) - Mn(III)}] = 0$ y para $[\mathrm{CN}] \geqslant 3.0\mathrm{M}$, $[\mathrm{Mn\,(III)}] = 0$; se transforma en :

$$[\mathrm{Mn(IV) - Mn(IV)}] = [\mathrm{Mn(III) - Mn(III)}] - [\mathrm{Mn(III) - Mn(IV)}] \quad (40)$$

Llevando esta expresión a la ecuación (39) y teniendo en cuenta las simplificaciones :

$$-\frac{\mathrm{d\,Mn(III) - Mn(IV)}}{\mathrm{d}t} = (K - k_1 + k_3)[\mathrm{Mn(III) - Mn(IV)}]$$

$$- k_3[\mathrm{Mn(III) - Mn(II)}]_0 \quad (41)$$

Integrando esta ecuación y llevando su resultado a (32) :

$$i = k_a[\mathrm{Mn(III) - Mn(III)}]_0 \cdot$$

$$\cdot \frac{1}{K - k_1 + k_3}\left[k_3 + (K - k_1)\left(\frac{2K}{K - k_1}\right)\frac{K - k_1 + k_3}{K + k_1} \cdot \mathrm{e}^{-(K - k_1 + k_3)t}\right] \quad (42)$$

Ecuación que representa la dependencia de la intensidad frente al tiempo en el intervalo $t \geqslant \tau$ y para $\mathrm{CN}^- \geqslant 3\mathrm{M}$.

Comprobación

La validez de las ecuaciones (38) y (42), que representan la intensidad de la corriente frente al tiempo para $t \leqslant \tau$ y $t \geqslant \tau$ en disolución de CNNa 3, 4 y 5 M se ha comprobado obteniendo a partir de ellas los valores de i a diferentes tiempos y comparándolos con los experimentales. La concordancia es satisfactoria como puede comprobarse en la Figura 6.

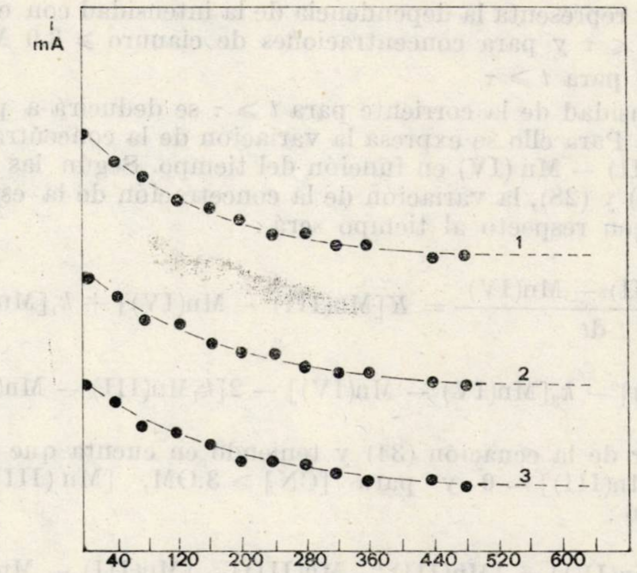

Fig. 6. — Valores de *i* experimentales y calculados para distintas concentraciones de CNNa : 1. CNNa 5.0 M ; 2. CNNa 4.0 M ; 3. CNNa 3.0 M ; — Valores experimentales ; ● Valores calculados.

CALCULO DE LAS CONSTANTES DE LAS REACCIONES INTERFERENTES

Durante la oxidación anódica del complejo binuclear Mn(III) — Mn(III) al potencial de + 0.80 voltios tiene lugar una nueva reacción además de las anteriormente mencionadas : la reducción del complejo Mn(IV) — Mn(IV) con el CN^-, representada por la ecuación (23) y cuya velocidad viene dada por la expresión (25). La constante de velocidad de dicha reacción puede calcularse a partir de la ecuación (41) integrada. Para $t = \infty$ se alcanza una situación de regimen estacionario en la que la concentración de Mn(III) — Mn(IV) alcanza un valor constante :

$$[\mathrm{Mn(III)} - \mathrm{Mn(IV)}] = [\mathrm{Mn(III)} - \mathrm{Mn(III)}\,\frac{k_3}{K - k_1 + k_3} \qquad (43)$$

Teniendo en cuenta la proporcionalidad entre concentraciones e intensidades, representada por la expresiones (31) y (32), se obtiene :

$$k_3 = (K - k_1)\frac{2i_k}{i_0 - 2\,i_k} \qquad (44)$$

Ecuación en la que i_0 e i_k son los valores inicial y final de la intensidad de difusión medida a +0.80 voltios (después de corregidos de las corrientes faradaicas). Los valores así calculados para k_3 para concentraciones de cianuro $\geqslant$ 3M, se muestran en la tabla 7.

Tabla 7

Oxidación anódica a + 0.80 voltios
Cálculo de la constante k_3 para diferentes concentraciones de CNNa

CNNA M	$K.10^3$ min^{-1}	$k_3.10^3$ min^{-1}	$(K-k_3).10^3$ min^{-1}	i_0 mA	$2i_f$ mA	k_3 min^{-1}
3.0	138	2.3	135.7	24.7	20.2	0.6
4.0	138	4.6	133.4	24.8	22.8	1.6
5.0	138	7.0	131.0	24.8	23.6	2.8

BIBLIOGRAFIA

[1] G. Brauer, „Química Inorgánica Preparativa", Ed. Reverté, Barcelona, 1958.
[2] G. Lopez Cueto y A. Alonso Mateos, *Anal.Lett.*, **11**, 43 (1978).
[3] F. C. Anson y J. J. Lingane, *J. Amer. Chem. Soc.*, **79**, 4901 (1957).
[4] L. Meites y S. A. Moros, *Analyt. Chem.*, **31**, 23 (1959).

Revue Roumaine de Chimie, **31**, *2*, 255–257 (1986)

COMPTES RENDUS

M. B. HOCKING, "Modern Chemical Technology and Emission Control", Springer, Berlin 1984; 460 pp., 152 figures, hard cover (cloth-bound), 98 DM

Chemical industry is considered to be one of the main sources of environmental pollution, yet the present book shows that this need not be so, and presents means to curb noxious emissions due to chemical processes.

The first chapter presents an overview on technical aspects of the chemical industry. The USA investment (in thousands of US dollars, TD) in chemical plant per employee is 30 TD per worker whereas the average for all manufacturing is at 14 TD per worker, because of the higher degree of automation in chemical plants. Inter-country comparisons indicate in the USA the value added per employee 59 TD in 1978, in West Germany and Netherlands 44—46 TD, in Sweden, Belgium and Canada 36—39 TD, in France 32 TD, in Italy and UK 20 TD and in Spain 17.8 TD. At the interface between chemistry and chemical engineering, one has to select batch processes for Third World nations due to relative costs of capital versus labor, while developed countries opt for high degree of automation and continuous processes despite the higher capital costs.

The second and third chapters review the air/water quality and emission control, respectively. The author's 8 years of experience in industry followed by 12 years in teaching is reflected in the clear, systematic and comprehensive exposition of the main aspects involved. Controversial issues are not hidden under the carpet but presented with an extensive bibliography.

The following 13 chapters discuss the main chemical or petrochemical processes and their gaseous, liquid and solid wastes: sodium and potassium salts; calcium and sodium hydroxide and carbonate; salt electrolysis; sulfur and sulfuric acid; phosphorus and phosphoric acid; ammonia, nitric acid and their derivatives; aluminium; ore enrichment and copper smelting; iron and steel; pulp and paper; fermentations; petroleum production and transport; petroleum refining.

Each chapter ends with a section entitled "Relevant Bibliography" which presenst about a dozen general book titles, followed by the references cited in the text with an average of about 100 references per chapter, although two chapters have 32–38 references (for the production of calcium and sodium bases, and for iron/steel) and the 2nd and 3rd chapters, have 286 and 306 references, respectively.

A table of conversion formulae and a subject index conclude the book.

The book is richly illustrated by schemes and photographs. Much tabullar material accompanies the text. Although cement manufacture and radioactive wastes are not treated in the book, the rich perspective provided by the author for all other main branches of the chemical industry makes this excellent book a valuable and essential tool for obtaining a better and safer environment.

Alexandru T. Balaban

I. HARGITTAI, "The Structure of Volatile Sulphur Compounds", Akadémiai Kiadó, Budapest, 1985 and D. Reidel Publ. Comp., Dordrecht, 316 pp., cloth-bound

The revised English edition of the Hungarian version which appeared in 1981 as vol. 50 in the series "A kémia újabb eredményei (Recent Results in Chemistry)" presents a thorough compilation of molecular structures for sulphur compounds. Data were obtained by two main methods: electron diffraction and microwave spectroscopy; many of the electron diffraction data are due to the authour, either with his research associates in Budapest, or in collaboration with foreign scientists from 12 countries.

The sulphur compounds which were selected for discussion were limited to those which are *volatile* in order to restrict the number of atoms in the molecules on one hand, and to provide structural data determined solely by intramolecular forces (free of packing forces). However, occasionally crystal data are also provided for comparison, although such data are not exhaustive. On the other hand, the umbrella of volatile compounds includes even inorganic sulphates (such as Cs_2SO_4) which have been studied by high-temperature electron diffraction.

The five chapters of the book discuss molecules with (i) one-coordinated sulphur, (ii) two-coordinated sulphur, (iii) three-coordinated sulphur, (iv) four-coordinated sulphur, (v) five- and six-coordinated sulphur. In all but the first chapter, sulphur is the central atom.

The geometries exhibited by the molecules are explained by the Valence Shell Electron Pair Repulsion (VSEPR) model of Gillespie and by considering also the non-bonded interactions leading to the "1,3-radii" postulated by Bartell and later by Glidewell. Even when apparently the VSEPR model fails to account for some experimental data, such as the angles in Hal_2SO_2 (96–100° for Hal-S-Hal, 108° for $Hal-S=O$, and 123–124° for $O=S=O$), in the series X_2S, X_2, SO and X_2SO_2 (where X is Me_2N, Me, Cl, F) or in the series MX_4 (where M is $C \rightarrow N \rightarrow O$, or $Si \rightarrow P \rightarrow S$, and X is H, F, Cl), or finally for equatorial bond angles in SF_4, $(F_3C)_2SF_2$ and $H_2C=SF_4$, careful consideration of non-bonded interactions and of the space requirements of the shared or non-shared electron pairs does accomodate all known data.

Theoretical calculations, including *ab-initio* ones when the molecules are small enough. are frequently mentioned.

Several interesting aspects deserve to be highlighted : structural variations in the RSR' series include the tilt and the hindered rotation of CH_3-S groups ; the two stable isomeric S_2F_2 molecules (the 1,2-difluorodisulphane has a lower energy than 1,1-difluorodisulphide with one S(II) and one S(IV) atom) have no analogues with other ligands than F ; compounds with a triple bond at S(IV) are the thiazyl chloride and fluoroide $N \equiv S-Hal$, while the structures $Hal-N=S$ are still unknown ; the structure of F_3NS is neither $FS-NF_2$, nor $FN=SF_2$ but $F_3S \equiv N$ with S(VI). Actually the book makes no comments on the oxidation state of sulphur atoms but considers only the coordination number.

The systematic treatment of a vast number or references reflects the author's involvement in the field for more than 15 years. The book is well illustrated with clear structure diagrams, numerous tables, and many radial distributions enabling chemists to see how the experimental information is translated into structural information. The author mentions in footnotes several cases when he corected misprints or inversions in figure captions encountered in the literature. When (as in microwave spectroscopy with too few isotopic species for multiatomic molecules) insufficient data are available, the data are presented critically, emphasizing the uncertainties which persist. In several instances, the author indicates which molecules should be (re)investigated.

An interesting section concerns empirical correlations of geometrical (bond distances, bond angles) and vibrational parameters (ν_{as}, ν_s, δ) for $S=O$ bonds in sulphones and related molecules. By means of such correlations an error was spotted in the reported (1967) $S=O$ bond length and $O=S=O$ bond angle in $ClSO_2CCl_3$; reinvestigation in 1978 by the author with his coworkers fully confirmed the correctness of the correlation.

The literature coverage is up to 1980 with a few post-1980 references of the author. An author and a formula index facilitate access to sections of the book. The excellent printing, easy reading, and especially the fact that chemical structures obey simple rules, make this book of high interest for organic, inorganic, physical and theoretical chemists who are interested in structural and stereochemical problems.

Alexandru T. Balaban

Dahlem Workshop Reports
Life Sciences Research Report
Editor : Bernhard,S.
Vol. 31
"Microbial Adhesion and Aggregation". Editor : Marshall, K. C. Report of the Dahlem Workshop on Microbial Adhesion and Aggregation.
Berlin, 1984, January 15–20.
Rapporteurs : Breznak, J. A. ; Calleja, G. B. ; McFeters, G.A. ; Rutter, P. R.
Springer Verlag, Berlin, Heidelberg, New York, Tokio, 1984, 424 pages.

The Stifterverband für die Deutsche Wissenschaft (The Donors Association for the Promotion of Sciences and Humanities) in cooperation with the Deutsche Forschungsgemeinschaft (German Science Foundation) founded the Dahlem Konferenzen in 1974. The task of Dahlem Konferenzen is to promote international, interdisciplinary exchange of scientific information and ideas to stimulate international cooperation in research and to develop and test new models conducive to more effective communication between scientists.

Dahlem Konferenzen organizes four workshops per year. The main work of the Dahlem Workshop is done in four interdisciplinary discussion groups. During the workshop the members of the four groups prepare reports reflecting their discussions and providing suggestions for future research needs.

The results of the workshops are published in two series :
(1). Life Sciences Research Reporst and (2) Physical, Chemical and Earth Sciences Research Reports

Adhesion and/or aggregation of microorganisms are involved in certain diseases of humans and animals, in industrial processes, in fouling of man-made surfaces, in syntrophic and other community interactions between microorganisms, and so on.

The goal of this workshop was to explore the mechanisms and consequences of microbial adhesion and aggregation with the participation of microbial physiologists, ecologists and geneticists, industrial microbiologists, physical and polymer chemists and bioengineers, in an attempt to develop new approaches and concepts as a result of the interdisciplinary discussions.

The workshop was planned to consider following major aspects :

a) the mechanisms whereby microorganism adhere to surfaces,

b) the development of biofilms and the consequences of such films formation.

c) the process and consequences of microbial aggregation

One of the ultimate aims in studying these aspects is to evolve the means for manipulating adhesion and aggregation of microorganisms to our own advantage. This may be to control the fouling of ship hulls or heat exchanger surfaces, to control periodontal disease, to control cholera and other intestinal diseases, to enhance aggregation in activated sludge processes, to enhance biofilm development in fixed film fermenters, etc.

Each aspect was considered by a group consisting of representatives of different disciplines who attempted to evolve new concepts based on the context of its discussions, followed by reports detailing the main object, exposed by world known specialists.

The first aspect "Mechanisms of Adhesion" includes the following items : Physicochemical interactions of the substratum, Microorganisms and the Fluid Phase, Stereo biochemistry and Function of Polymers, Adhesion to Inanimate Surfaces, Adhesion to Animal Surfaces, Bacterial Adhesion to Plant Root Surfaces, Genetic control of Bacterial Adhesion.

The second aspect "Biofilm Development and its Consequences" is particularized by the following reports : Surface Colonization Parameters from Cell Density and Distribution, Biofilm Development : A process Analysis, Chemical Characterization of Films, Effects of Network Structure on the Phase Transition of Acrylamide Sodium Acrylate Copolymer Gels, Colonization by Higher organisms.

The aspect "Activity on Surfaces" comprises : Comparative Physiology of Attached and Free living Bacteria, Activities of Microorganisms Attached to Living Surfaces, Utilization of Substrates and Transformation of Solid Substrata, Attachment of Bacteria : Advantage or Disadvantage for Survival in the Aquatic Environment.

In the last considered aspect "Aggregation" the subjects Physiology of Cell Aggregation : Flocculation by Sacharomyces Cerevisiae As a Model System ; Aggregation, Choesion, Adhesion, Phagocytosis and Morphogenesis in Dictyostelium — Mechanisms and Implications ; Consequence of Aggregation ; Microcolony Fromation and Consortia, are included.

Each subject is clear and concise and, where needed, accompanied by graphs, tables and expressive iconography.

Taking into account the novelty of this field and its interdisciplinary feature, a Glossary was included.

By comparison with other Symposia and a number of books that have been devoted to the subject of adhesion and aggregation in recent years, the Dahlem Konferenzen had to create its own concept known as Dahlem Workshop Model. This Model provides the framework for the utmost possible interdisciplinary communication and cooperation between scientists in a given time period.

The extensive bibliography adds to the usefulness of the book to all interested in the particular areas under discussion.

Radu Ghiocel

Dahlem Konferenzen organizes four workshops per year. The main work of the Dahlem Workshop is done in four interdisciplinary discussion groups. During the workshop the members of the four groups prepare reports reflecting their discussions and providing suggestions for future research needs.

The results of the workshops are published in two series (1) Life Sciences Research Reports and (2) Physical, Chemical and Earth Sciences Research Reports.

Adhesion and/or aggregation of microorganisms are involved in certain diseases of humans and animals, in industrial processes, in fouling of man-made surfaces, in syntrophic and other community interactions between microorganisms, and so on.

The goal of this workshop was to explore the mechanisms and consequences of microbial adhesion and aggregation with the participation of microbial physiologists, ecologists and geneticists, industrial microbiologists, physical and polymer chemists and bioengineers, in an attempt to develop new approaches and concepts as a result of the interdisciplinary discussions.

The workshop was planned to consider following major aspects:

a) the mechanisms whereby microorganism adhere to surfaces,

b) the development of biofilms and the consequences of such films formation,

c) the process and consequences of microbial aggregation.

One of the ultimate aims in studying these aspects is to evolve the means for manipulating adhesion and aggregation of microorganisms to our own advantage. This may be to control the fouling of ship hulls or heat exchanger surfaces, to control periodontal disease, to control cholera and other intestinal diseases, to enhance aggregation in activated sludge processes, to enhance biofilm development in fixed film fermenters, etc.

Each aspect was considered by a group consisting of representatives of different disciplines who attempted to evolve new concepts based on the content of its discussions, followed by reports delivered by [illegible], exposed by world known specialists.

The first aspect "Mechanisms of Adhesion" includes the following items: Physicochemical Interactions of the Substratum, Microorganisms and the Liquid Phase, Stereo Biochemistry and Functions of Polymers, Adhesion to Inanimate Surfaces, Adhesion to Animal Surfaces, Bacterial Adhesion to Plant Host Surfaces, Genetic control of Bacterial Adhesion.

The second aspect "Biofilm Development and its Consequences" is particularized in following reports: Surface Colonization, Parameters from Cell Density and Distribution, Biofilm Development: A process Analysis, Chemical Characterization of Films, Effects of Kinetic Structure on the Phase Transition of [illegible], Sessile Versus Planktonic Cells, Colonization by Higher organisms.

The aspect "Activity at Surfaces" groups Compartive Physiology of Attached and Free-living Bacteria, Activities of Microorganisms Attached to Living Surfaces, Utilization of Substrates and Transformation of Solid Substrata, Attachment of Bacteria: Advantage or Disadvantage for Survival in the Aquatic Environment.

In the last considered aspect "Aggregation" the stages Physiology of Cell Aggregation, Flocculation by Colloidal [illegible] the Yeast System, Aggregation Processes, Adhesion, Linkage and Arrangements in [illegible], Mechanisms for Modification, Consequences of Aggregation, Microcolony Formation and [illegible] are included.

Each subject is clear and concise and, where needed, accompanied by graphs, tables and expressive iconography.

Taking into account the novelty of this field and its interdisciplinary feature, a Glossary was included.

By comparison with other symposia and a number of books that have been devoted to the subject of adhesion and aggregation in recent years, the Dahlem Konferenzen had to create its own concept known as Dahlem Workshop Model. This Model provides the framework for the utmost possible interdisciplinary communication and cooperation between scientists in a given time period.

The extensive bibliography adds to the usefulness of the book to all interested in the particular areas under discussion.

Rodica [illegible]

NOTE POUR LES AUTEURS

La Revue Roumaine de Chimie publie des articles en anglais, français, russe, allemand ou espagnol. Les auteurs sont priés d'envoyer des articles et des comptes rendus inédits.

Les manuscrits seront dactylographiés à double interligne. La bibliographie, les tableaux et la légende des figures seront placés après le texte.

Si l'article fait partie d'une série numérotée, la partie précédente sera donnée comme première référence.

Chaque articlé sera précéde d'un résumé comprenant quinze lignes au maximum.

Les références bibliographiques dans le texte seront faites par des exposants sans parenthèses et paraîtront à la fin de l'ouvrage.

Les publications périodiques mentionnées dans la bibliographie seront présentées suivant les prescriptions internationales : le nom de l'auteur précédé de l'initiale du prénom, le titre du périodique abrégé conformément à « Chemical Abstracts » et souligné par une ligne, le numéro du tome indiqué par des chiffres arabes et souligné par deux lignes, suivi de la première page de l'article ; à la fin, l'année de la parution sera placée entre parenthèses. Le numéro de la revue ne sera pas indiqué si les pages du volume sont numérotées consécutivement.

Les textes des livres ou traités inclueront : le nom des auteurs, l'initiale du prénom, le titre du livre entre guillemets et sans être souligné, le numéro du tome précédé par l'abréviation « vol. » (ou « Bd »), le numéro de l'édition, les éditions (the publisher), la localité de la parution du livre, l'année de la parution et la page de la référence précédée(s) par l'abreviation « p » (ou « S. »).

Les brevets seront indiqué comme suit : l'auteur ou la firme, le pays et le numéro du brevet, la date et la revue (*Chem. Abstr.*) Par. ex : M. Jones (to Union Carbide Co,) Brit. Pat. 601 238, 2 Sept. 1959 ; cf. *Chem. Abstr.*, *54*, 12808 (1960).

Si la référence n'a pas été lue en original, on indiquera aussi la revue de référence consultée.

Les diagrammes seront tracés à l'encre de Chine sur papier calque. Les tableaux et les figures (en nombre strictement nécessaire) ainsi que les courbes dans les figures seront numérotés par des chiffres arabes. Leur explication sera donnée dans la légende des figures. Prière de ne pas inscrire les mêmes données dans les tableaux et les figures. Chaque tableau aura un titre. On indiquera dans le texte la place approximative des tableaux et des figures. Les formules chimiques seront incluses dans le texte ; en outre, elles seront transcrites sur papier calque, à l'encre de Chine.

Les auteurs sont priés d'indiquer les caractères italiques (en soulignant les lettres au crayon), ainsi que tout autre caractère spécial ; les préfixes *ortho*, *meta*, *para*, *cis*, *trans*, etc. seront soulignés pour indiquer leurs caractères italiques et ne seront jamais écrits avec des majuscules.

Aucune correction à la main ne sera admise sur le manuscrit. Les corrections seront tapées à la machine. Les lettres grecques ou d'autres symboles spéciaux seront insérés à la main à l'encre clairement.

Le manuscrit sera signé par l'auteur.

Le titre-courant aura 50 lettres au maximum.

L'entière responsabilité du contenu des articles appartient aux auteurs.

Sur demande on peut obtenir une note plus complète.

PRINTED IN ROMANIA

TRAVAUX PARUS AUX ÉDITIONS DE L'ACADÉMIE DE LA RÉPUBLIQUE SOCIALISTE DE ROUMANIE

1986 APR 2 4

V. DRĂGUŢAN, A. T. BALABAN, M. DIMONIE, **Olefin Metathesis and Ring-Opening Polymerization of Cyclo-olefins**, coédition avec John Wiley and Sons, 1985, 544 p.
C. LITEANU, I. RÎCA, **Optimizarea proceselor analitice**, 1985, 360 p.
N. PERESCU, **Chimia extracţiei cu solvenţi şi aplicaţii**, 1985, 212 p.
V. E. SAHINI, M. HILLEBRAND, **Chimie cuantică în exemple şi aplicaţii**, 1985, 378 p.
GH. MARCU, **Chimia compuşilor coordinativi**, 1984, 415 p.
E. CORDOŞ, C. MANOLIU, **Spectrometria de absorbţie şi fluorescenţă atomică**, 1984, 178 p.
C. BODEA, **Tratat de biochimie vegetală**, p.II, vol. 5. 1984, 438 p.
ELENA CEAUŞESCU, **Cercetări în chimia şi tehnologia polimerilor**, 1983, 519 p.
N. ASANDEI, A. GRIGORIU, **Chimia şi structura fibrelor**, 1983, 395 p.
N. IONESCU, M. CĂLDĂRARU, **Oxidarea catalitică a olefinelor inferioare**, 1983, 178 p.
C. CAŞCAVAL, **Studiul polimerilor prin piroliză şi cromatografie de gaze**, 1983, 220 p.
C. I. SIMIONESCU, F. DANEŞ. **Originea vieţii**, 1983, 110 p.
C. BODEA (sous la direction). **Tratat de biochimie vegetală**, 2^{e} partie, t. IV. 1982, 408 p.
I. G. MURGULESCU, RODICA VÎLCU, **Introducere la chimia fizică. Vol. III. Termodinamica chimică**, 1982, 624 p.
I. G. MURGULESCU, J. PĂUN, **Introducere în chimia fizică. Vol. I.3. Nucleul atomic, reacţii nucleare, particule elementare**, 1982, 606 p.
ELENA CEAUŞESCU, **Noi cercetări în domeniul compuşilor macromoleculari**, 1981, 536 p.
I. G. MURGULESCU, TATIANA ONCESCU, E. SEGAL, **Introducere în chimia fizică. Vol. II. 2, Cinematică chimică şi cataliză**, 1981, 1024 p.
LYDIA-MARIA VAICUM, **Epurarea apelor uzate cu nămol activ. Bazele biochimice**, 1981, 218 p.
I. GĂLĂŢEANU, **Procese şi metode radiochimice în energetica nucleară**, 1981, 234 p.
O. IORDACHE, **Procese polistocastice aplicate în fenomenele de transfer**, 1981, 186 p.
CR. SIMIONESCU, VALERIA GORDUZA, **Polimeri biocompatibili şi biologic activi**, 1980, 479 p.
ELENA CEAUŞESCU, **Polimerizarea stereospecifică a izoprenului**, 1979, 307 p.
C. GH. MACAROVICI, **Analiza chimică cantitativă anorganică**, 1979, 457 p.
M. FLORESCU, **Metode ştiinţifice în dezvoltarea industriei chimice moderne**, 1979, 256 p.
A. T. BALABAN, I. GĂLĂŢEANU, G. GEORGESCU, LIGIA SIMIONESCU, **Compuşi marcaţi şi radiofarmaceutici cu aplicaţii în medicina nucleară** 1979, 495 p.
I. G. MURGULESCU, E SEGAL., **Introducere în chimia fizică. Vol. II. 1. Teoria molecular-cinetică a materiei**, 1979, 1036 p.
S. STERNBERG, FL. DANEŞ, **Termodinamica chimică aplicată**, 1978, 400 p.
I. G. MURGULESCU, V. EM. SAHINI, **Introducere în chimia fizică, Vol. I. 2. Structura şi proprietăţile moleculelor**, 1978, 604 p.
I. ZUGRĂVESCU, MAGDA PETROVANU, **N-ylid chemistry**, coédition avec McGraw Hill International Book Company. U.S.A., 1977, 396 p.
I. G. MURGULESCU, **Introducere în chimia fizică. Vol. I, 1. Atomi, legătură chimică**, 1976, 560 p.
ELENA CEAUŞESCU, **Research work on synthesis and characterization of macromolecular compounds. Contributions**, 1974, 251 p.
CR. SIMIONESCU, VIORICA RUSAN, V. POPA, **Chimia algelor marine** 1974, 212 p. 1 pl.

ISSN 0035—3930

c. 1660—I. P. INFORMAŢIA

43426

Lei 40

$ 80 (pour un abonnement annuel)

F 1103

ACADÉMIE DE LA RÉPUBLIQUE SOCIALISTE DE ROUMANIE

REVUE ROUMAINE DE CHIMIE

REFERÁLVA

R 1986 APR 7

M5

TOME 31

N° 3

Mars 1986

Rev. Roumaine Chim.

RRCHAX, 31 *3*, p. 259–362 (1986), Bucarest

EDITURA ACADEMIEI REPUBLICII SOCIALISTE ROMÂNIA

ACADÉMIE DE LA RÉPUBLIQUE SOCIALISTE DE ROUMANIE

COMITÉ DE RÉDACTION

Rédacteur en chef :

I. G. MURGULESCU, membre de l'Académie de la République Sodialiste de Roumanie

Rédacteurs en chef adjoints :

A. T. BALABAN et V. EM. SAHINI, membres correspondants de l'Académie de la République Socialiste de Roumanie

Collège de rédaction:

EM. BRATU, ELENA CEAUŞESCU, ECATERINA CIORĂNESCU-NENITZESCU, CR. SIMIONESCU, membres de l'Académie de la République Socialiste de Roumanie; P. SPACU, membre correspondant de l'Académie de la République Socialiste de Roumanie; M. BANCIU, M. D. GHEORGHIU, I. HAIDUC, D. I. MARCHIDAN, I. MOLDOVAN, G. NIAC et D. SĂNDULESCU

La Revue Roumanie de Chimie parait 10 fois par an. Toute commande de l'étranger sera adressée à ROMPRESFILATELIA – sectorul Export-Import, Presă, P. O. Box 12–201, télex 10376 prsfir 78104 Bucarest, Calea Griviţei nr. 64–66, Roumanie.

Les manuscrits, les livres et les revues proposés en échange, ainsi que toute correspondance seront envoyés à la rédaction.

REVUE ROUMAINE DE CHIMIE

125, Calea Victoriei, 79717 Bucarest, Roumanie, téléphone 50 76 80

EDITURA ACADEMIEI REPUBLICII SOCIALISTE ROMÂNIA
125, Calea Victoriei 79717 Bucarest, Roumanie, téléphone 50 76 80

REVUE ROUMAINE DE CHIMIE

Tome 31, N° 3 **Mars 1986**

F. IORDACHE, F. CHIRALEU, LIGIA STĂNESCU, F. BADEA and MARGARETA AVRAM, Bicyclo[2.2.2]octane derivatives. III. Stereoisomeric 2,3,5,6,-tetracarbomethoxy-bicyclo[2.2.2]octanes 261–267

MIHAELA ȘTEFAN and CĂLIN STOICESCU, Kinetics of the methoxylation of *o*-chloronitrobenzene 269–272

HANS-HORST GLATT, MAMADOU FOULA BARRY, CAROL CSUNDERLIK, RADU BACALOGLU, MIRCEA BOTOACĂ, SIMONA SAVU-BOTOACĂ and DIANA FECHETE, Imines of aminoazoles II. Synthesis and characterization of some imines of 2-amino-benzothiazoles benzoxazole thiazole and 3-amino-1,2,4-triazole (in German) 273–282

RADU BACALOGLU, HANS-HORST GLATT, MAMADOU FOULA BARRY and CAROL CSUNDERLIK, Imines of aminoazoles III. Basicity constants of heterocyclic imines in the series of benzylidene-amino-benzothiazoles, -benzoxazole, benzimidazoles, -thiazole and -triazole (in German). . 283–289

CS. VÁRHELYI, I. GĂNESCU, A. HANTZ and I. PAPA, A new Reinecke salt analogues with dibutylphenylphosphine and diphenylethylphosphine (in German) 291–296

R. AGARWAL and P. BAHADUR, Study of α-diazoketones from nicotinyl and furoyl chlorides and higher diazoalkanes 297–303

H. K. SHARMA, A. K. YADAV and S. P. S. JADON, Characterization of the complexes of Ti(III) and Zr(IV) with tetrathiazyl hydrofluoride by UV, EPR and XRD spectra 305–308

ADRIAN O. FULEA, Concerning "The relation between moments of inertia, steric crowding and librational motion in molecules. Effects on NMR spectra" 309–322

MARCOS CAROLI REZENDE and LILIAM INÊS DAL SASSO, Polarity of salt solutions : a general empirical equation 323–326

I. M. SIDAHMED, H. SADEK and S. M. SALEM, Types of solvent interactions in water-glycerol mixtures 327–334

LUMINIȚA SILAGHI-DUMITRESCU, LUIS ALBERTO AVILA-DIAZ and IONEL HAIDUC, Dimethyl- and diphenyldithioarsinates of some main group metals 335–340

Rev. Roumaine Chim. 31, *3*, 259–362(1986), Bucarest

LUMINIŢA PATRON, ADRIANA CONŢESCU, GH. ROLEA and CONSTANŢA GHEORGHIU, Preparation and properties of a novel Pd(II)–Sn(II) complex 341–344

RODICA VĂŢULESCU, T. BUDIU, GH. MARCU and GH. MORARU, Heteropolytungstates with Ti(IV) and Ni(II). VIII. Crystal data for the potassium and ammonium salts of the Ni(II)- undecatungstotitanate(IV) anion 345–351

N. LEÓN, J. L. BURGUERA, M. BURGUERA and O. M. ALARCÓN, Determination of cobalt and manganese in blood serum by flow injection analysis and atomic absorption spectroscopy 353–360

COMPTES RENDUS 361–362

Revue Roumaine de Chimie, **31**, *3*, 261–267(1986)

BICYCLO[2.2.2]OCTANE DERIVATIVES. III.[1]

STEREOISOMERIC 2,3,5,6-TETRACARBOMETHOXY-BICYCLO-[2.2.2]OCTANES

F. IORDACHE[a], F. CHIRALEU[b], LIGIA STĂNESCU[b], F. BADEA[a] an
MARGARETA AVRAM[a] *

[a]Laboratory of Organic Chemistry, Polytechnic Institute-T.C.H, 77208 Bucharest,
Splaiul Independenţei 313, Romania
[b]Centre of Organic Chemistry, Splaiul Independenţei 202 B, 76300 Bucharest, Romania

Received September 12, 1984

The base-catalysed isomerization of *all-exo*-ester **1** and of stereoisomeric esters **2**, **3** and **4**, to an equilibrium mixture of **1**, **2**, **3**, and **4**, is described. The structure of these esters is established by means of ^{1}H-NMR spectroscopy. A mechanism for the isomerization of these esters is proposed.

INTRODUCTION

There are several possible stereoisomeric 2,3,5,6-tetracarbo-methoxybicyclo [2.2.2] octanes (**1 ÷ 7**); four of these formulas (**1**,**4**,**6** and **7**) have a plane of symmetry and lead to achiral structures, while the remaining three (**2**,**3** and **5**) are chiral, leading to a total of ten stereoisomers.

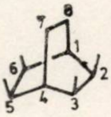

1

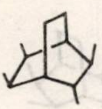

2

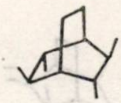

3

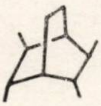

4

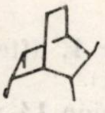

5

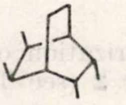

6

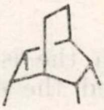

7

Only the achiral isomer **1** is described in the literature; it was obtained by Diels and Alder,[2] by hydrogenation of *all-exo*-2,3,5,6-tetracarbomethoxy-bicyclo [2.2.2]oct-2-ene (*all-exo*, **11**). Alkene **11** was prepared[2] through a diene reaction between dihydrophthalic anhydride (**8**) and maleic anhydride (**9**), followed by the esterification with methanol of the resulting dianhydride **10**.

---

* Deceased 28 October, 1983

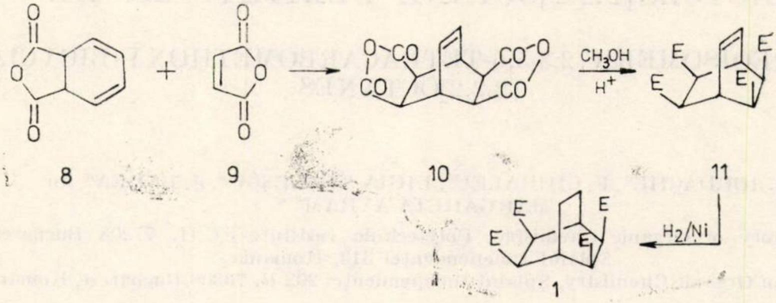

8 9 10 11 1

In the present paper we report the preparation of stereoisomeric (±) 2,5,6-*exo*-3-*endo* (**2**), (±) 3,6-*exo*-2,5-*endo* (*all-trans*) (**3**) and of the achiral 2,6-*exo*-3,5-*endo* (**4**) derivatives.

RESULTS

On treatment at various reaction times and temperatures with sodium methoxide in methanol, the *all-exo* ester **1** is readily isomerized. The reaction mixture was analysed gas-chromatographically and the resulting compounds **2**,**3** and **4** were isolated through preparative gas-chromatography.

Assuming that the formation of esters **3** and **4** from the *all-exo* ester **1** is not a primary process (which would involve the formation of improbable dianions of type **12** or **13**) but a stepwise one, the reaction time was shortened in order to evidence possible intermediates.

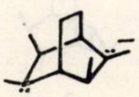
12

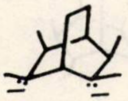
13

As expected in the isomerization of ester **1**, after 20 minutes we detected and isolated the ester **2** (see Table 1).

Ester **2** is formed from **1** *via* the carbanion **14** resulted from the attack of the base on any of the four equivalent hydrogens.

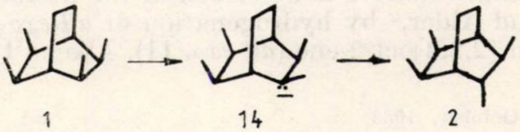
1 14 2

Table 1

Isomerization of ester **1** (at 20°)

Time min.	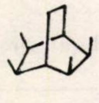 1	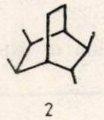 2	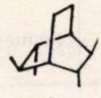 3	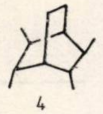 4
5	30%	70%	—	—
10	19.8%	80.2%	—	—
15	15.3%	84.7%		
20	12.86%	87.42%	—	—
30	18%	82%	—	—

In ester **2**, the hydrogen atoms are no longer sterically equivalent. We may assume that the base prefers to attack H-6 rather than H-5, which is hindered by the neighbouring *endo*-carbomethoxy group from the position 3.

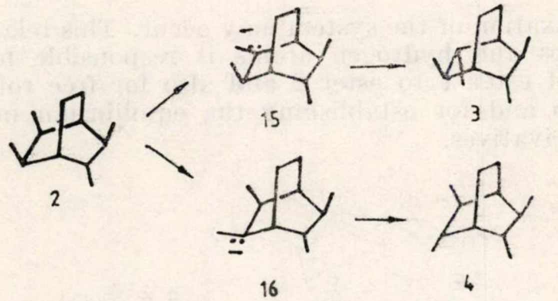

From this reason the isomer **3** was expected to be formed preferentially in addition to a minor proportion of isomer **4**. The isomerization of ester **1** was compared with the isomerization of the unsaturated ester **11**[1] (see Table 2).

Data in the Table 2 indicate a rapid decrease of the *all-exo* isomer **11**, accompanied by the formation of *exo-endo* isomer **17**; when the latter reaches high concentration, the *all-trans* isomer **18** appears as the major compound, together with minor amounts of **19**.

On the contrary, data in Table 1 indicate a slower decrease of *all-exo* isomer **1**, accompanied by the formation of the *exo-endo* isomer **2**.

Simultaneously after 20 minutes reaction time, isomer **2** reverts to **1**. This fact indicates a possible free rotation of carbomethoxy groups explaining the isomerization of ester **1**.

Comparatively with isomerization of esters **11**, where a stereochemically rigidity of the system is determined by through-space interaction of the double bond with carbomethoxy groups,[3] in the saturated ester **1** a sterical relaxation of the system may occur. This relaxation of carbomethoxy groups and hydrogen atoms is responsible for the delay of isomerization of ester **1** to ester **2** and also for free rotation of carbomethoxy group and for establishing the equilibrium mixture between **1**,**2**,**3** and **4** derivatives.

Table 2

Isomerization of ester **11** (at 20°)

Time min.	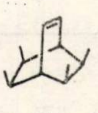 11	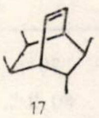 17	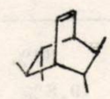 18	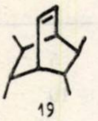 19
1.5	76.76%	23.24%	—	—
1.9	66.13%	33.87%	—	—
3	57.33%	42.27%	0.4%	—
4.8	19.1%	76.70%	4.2%	
7.8	5.2%	86.75%	7.3%	.0.75%
12	3.47%	83.69%	9.57%	0.27%

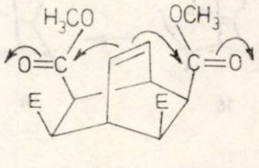

E = COOCH$_3$

Thus, the isomerization of ester **1** carried out at 25°, for 100 hours, led to an equilibrium mixture of 60 % **3**, 36.8 % **4**, 2.1 % **2** and only 1.1 % **1**.

The isomerization of ester **3** carried out for 5.5 hours at 55° led to an equilibrium mixture of 67.8 % **3**, 28.2 % **4**, 3.2 % **2** and only 0.8 % **1**.

The isomerization of ester **4** carried out for 9 hours at 55° led to an equilibrium mixture of 68.6 % **3**, 27.8 % **4**, 2.5 % **2** and only 1.1 % **1**.

DISCUSSION

On the basis of the above experimental facts we proposed the following mechanism. In the presence of sodium methoxide in methanol, ester **1** is isomerized to ester **2**, which is the intermediate of the transformation of esters **1,3** and **4** in the equilibrium mixture.

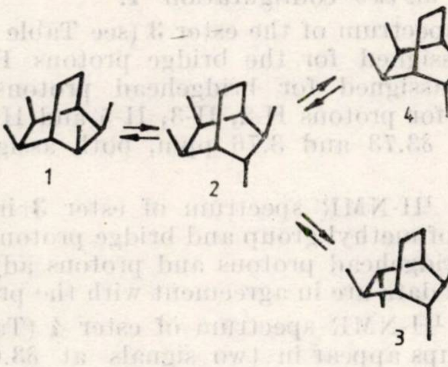

Configuration of esters 1, 2, 3 and 4

In order to establish the configuration of these compounds we used ^{1}H-NMR data, mainly the chemical shifts (Table 3) of protons.

Table 3

Chemical shifts of the esters 1—4 ($CDCl_3$, ppm)

Structure of ester	Position of protons			
	—$COOCH_3$	2.3.5.6.	1.4	7.8
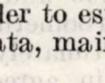 1	3.67	2.90	2.54	1.67
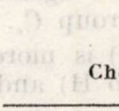 2	3.74(2) 3.68(1) 3.65(1)	3.16 2.88 3.10	2.55	1.30 2.10
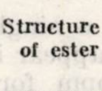 3	3.76 3.73	3.11	2.60	1.53
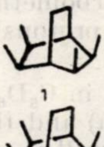 4	3.73 3.63	3.25 3.08	2.78 2.60	1.20 1.80

In the ^{1}H-NMR spectrum of ester **1** (see Table 3) the protons H-2, H-3, H-5 and H-6 appear as a singlet at $\delta = 2.90$ ppm. The signals of bridge protons H-7 (two H) and H-8 (two H) appear as singlet at $\delta = 1.67$ ppm, the bridgehead protons H-1 and H-4 signal appear at $\delta = 2.54$

ppm and the carbomethoxy signals appear as a singlet at $\delta = 3.67$ ppm. In this case, the equivalence of the protons adjacent to the carbomethoxy groups support the *all-exo* configuration **1**.

The ^{1}H-NMR spectrum of the ester **3** (see Table 3) presents signals at: δ1.53 ppm, assigned for the bridge protons H-7 (2H) and H-8 (2H), δ2.60 ppm, assigned for bridgehead protons H-1 and H-4, δ3.13 ppm, assigned for protons H-2, H-3, H-5 and H-6 adjacent to carbomethoxy groups, δ3.73 and 3.76 ppm, both assigned to the methyl groups of esters.

Recording the ^{1}H-NMR spectrum of ester **3** in C_6D_6 we noticed the high-field shifts of methyl group and bridge protons together with the low-field shifts of bridgehead protons and protons adjacent to carbomethoxy groups. These data are in agreement with the proposed structure **3**.

Analysing the ^{1}H-NMR spectrum of ester **4** (Table 3) we noticed that the methyl groups appear in two signals at δ3.63 and 3.73 ppm.

The chemical shifts of the bridge proton H-7 (two H) and H-8 (two H) are noticed between δ1.20 and 1.80 ppm. The bridgehead protons are not equivalent and appear in ^{1}H-NMR spectrum at δ2.60 and 2.78 ppm. The chemical shifts of the protons adjacent to carbomethoxy groups are noticed between δ3.08 and 3.25 ppm, but unfortunately cannot be resolved. The above values of chemical shifts are in agreement with the structure **4**, proposed, which possesses a point group C_s.

The ^{1}H-NMR spectrum of ester **2** (see Table 3) is more complex, containing nine signals. The bridge protons H-7 (two H) and H-8 (two H) afford a signal between δ1.30 and 2.10 ppm.

The bridgehead protons H-1 and H-4 appear as a singlet at δ2.55 ppm. The protons adjacent to carbomethoxy groups appear in three signals: δ3.16 ppm for H-5 and H-6 protons, δ3.10 ppm for H-2 (*endo* position) and δ2.88 ppm for H-3 (*exo* position). The carbomethoxy groups appear also in three distinct signals: δ3.74 ppm (6 protons) δ3.68 ppm (3 protons) and δ3.65 ppm (3 protons).

Recording the ^{1}H-NMR spectrum of the ester **2** in C_6D_6 we noticed the shielding of methyl groups and H-2 (*endo* position) and the deshielding of H-3 (*exo* position), of the bridgehead protons as well as of the bridge protons.

EXPERIMENTAL

Gas-chromatographic analyses were carried out on a Carlo-Erba model D gas-cromatograph. The columns contain 3% neopenthylglycol succinate on sylanized chromosorb W (60—80 mesh) $l = 2$ m; $\emptyset = 2$ mm; the column temperature was 220°C; vaporizer temperature was 290°C; hydrogen as carrier gas with a rate-flow of 32.2 mL/min.

Isolation of the esters **2**, **3** and **4**, through preparative gas-chromatography, was carried out on a Carlo-Erba model G.V.

The ^{1}H-NMP spectra were recorded on a VARIAN A-60A spectrometer, using TMS as an internal standard.

Isomerization of esters **1**, **2**, **3** *and* **4**. General procedure. A 0.36 N solution of sodium methoxide in methanol (50 mL) was treated with 10 g (3 mmoles) of ester **1** (**2**, **3**, or **4**) and the mixture was stirred at constant temperature. The reaction was stopped by bubbling gaseous anhydrous hydrochloric acid. The solution was then evaporated *in vacuo* and the residue was extracted with dichloromethane. The solid sodium chloride was filtered off and the solvent was evaporated, yielding 0.90—0.95 g (90—95%) crude product, which are analysed by gas-chromatography. The results were presented in Table 1.

The new esters **2, 3** and **4** were separated by preparative gas-chromatography and their m.p. and elemental analyses are presented in Table 4.

Table 4

Mycroanalyses of ester **2, 3, 4**

Ester	m.p.	calculated	found
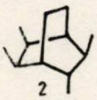 2	65°	C 56.13% H 6.48%	C 56.07% H 6.64%
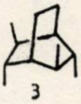 3	132°	C 56.13% H 6.48%	C 56.19% H 6.58%
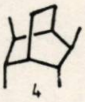 4	165°	C 56.13% H 6.48%	C 56.20% H 6.52%

ACKNOWLEDGEMENT. We express our thanks to Miss. E. Şliam for performing the elemental analyses.

REFERENCES

[1] Part. II, F. Iordache, F. Chiraleu and M. Avram, *Rev. Roumaine Chim.*, **20**, 233 (1975).
[2] O. Diels and K. Alder, *Liebigs Ann. Chem.*, **490**, 257 (1931).
[3] F. Iordache, P. Filip and T. Constantinescu, *Rev. Chim. Bucharest*, **29**, 1154 (1978).

Revue Roumaine de Chimie, 31, 3, 269–272(1986)

KINETICS OF THE METHOXYLATION OF *o*-CHLORONITROBENZENE

MIHAELA ŞTEFAN and CĂLIN STOICESCU
Chemical and Pharmaceutical Research Institute, 112, Sos. Vitan, Bucharest, Romania

Received March 30, 1985

The kinetics of the methoxylation of *o*-chloronitrobenzene in a methanol—dimethylsulphoxide solution in the presence of sodium hydroxide was studied within the temperature range from 60 to 80°C. The rate constant was correlated with the dielectric constant of the solvent mixture in order to explain the accelerating effect of dimethylsulphoxide.

The nucleophilic substitution of the aromatic halogen atoms with amino- or alkoxy-groups is more easily performed in such compounds where the halogen atom is activated by the presence of electron-attracting substituents placed in appropriate positions. Hence, the method is a synthetic tool for the preparation of certain aromatic compounds.

The alkoxylation of nitro- or polynitrohalobenzenes is a method applied with good results for the synthesis of nitro- or polynitroalkoxybenzenes. Both preparative and kinetic studies of these reactions have been performed. The methoxylation of *o*- and *p*-chloronitrobenzenes is highly interesting for the preparation of the corresponding *o*- and *p*-nitroanisoles, which may be further converted by reduction into *o*- and *p*-anisidines which are versatile intermediates for the dye and drug industries.

The methoxylation of *o*-chloronitrobenzene is usually carried out with methanolic solutions of alkaline methoxide[1] sor hydroxides.[2] In order to avoid secondary reactions, especially to prevent the reduction of the nitro group in basic conditions, the methoxylation was run in the presence of various metal oxides (MnO_2, PbO_2, Cu_2O).[3]

Kinetic studies of chloronitrobenzene methoxylation with methanolic solutions of sodium methoxide account for a second-order reaction in agreement with the generally accepted S_NAr reaction mechanism involving the activating effect of the nitro group on the halogen atom reactivity.[4,5] However, the accelerating effect of polar aprotic solvents on S_NAr reactions is well-known. Among such solvents, dimethylsulphoxide (DMSO) shows a remarkable effect; the rate of the aminolysis reactions of the aromatic halides is increased about 10^3 times in the presence of DMSO.[6]

In this paper we have studied the kinetics of *o*-chloronitrobenzene methoxylation with natrium hydroxide in methanol—dimethylsulphoxide solution, which is the industrial process for *o*-nitroanisole preparation.

The product formed in the reaction of halonitrobenzenes with alcoholic solutions of alkaline hydroxides is the corresponding ether, according to the equilibrium[7]:

$$HO^- + ROH \rightleftarrows RO^- + H_2O$$

In the reaction run in methanol, nitroanisole is the unique product, as the nitrophenol formation is negligible. However, in higher alcohols, phenol formation and nitro group reduction are competitive with the alkoxylation. The presence of DMSO in the reaction mixture shifts the equilibrium towards the alkoxy ion owing to the strong association between DMSO and water molecules.

RESULTS AND DISCUSSION

The methoxylation reaction of *o*-chloronitrobenzene (*o*-CNB) with NaOH in methanol — DMSO solution was studied within the temperature range of 60—80°C, at reagent concentrations of about 0.1 molar. From the logarithmic plots of the reaction rate *vs.* the reagent concentration, the corresponding reaction orders with respect to *o*-chloronitrobenzene and NaOH, respectively, have been determined, confirming the second-order kinetic equation characteristic for S_NAr reactions. The dependence of the reaction rate on the reagent concentrations is shown in Table 1. From these data, the rate constant $k = 5.4 \times 10^{-4} L.M^{-1} \cdot s^{-1}$ was calculated.

Table 1

The dependence of the reaction rate on the reagent concentration

$v \cdot 10^6$	[*o*-CNB]	[NaOH]
11.1	0.1	0.2
8.88	0.1	0.16
6.93	0.1	0.125
5.55	0.1	0.1
8.67	0.125	0.125
4.97	0.07	0.125

$t = 70°C$, DMSO : MeOH = 1 : 1(v/v)

Table 2

The dependence of the reaction constant on the temperature

$k \times 10^4$, $L.M^{-1} \cdot s^{-1}$	*T, K*
2.02	333
5.4	343
10.0	353

[*o*-CNB] = 0.1 M,
[NaOH] = 0.125 M
DMSO : MeOH = 1 : 1(v/v)

The dependence of the rate constant on the temperature is shown in Table 2. From the slope of the plot log *k* *vs.* $1/T$ the activation energy, $E_a = 18.97$ kcal/mole, was calculated. The pre-exponential factor, log $PZ = 7.4$, was determined. The activation energies reported in the literature for the methoxylation of *o*-chloronitrobenzene with MeONa/MeOH are 23.5[4] and 26.0[5] kcal/mole. The activation parameters calculated from the plot of log k/T *vs.* $1/T$ are: $\Delta H^{\neq} = 18.29$ kcal/mole and $\Delta S^{\neq} = -20.63$ e.u., respectively.

Further we have checked the influence of DMSO concentration on the rate constant. The results are listed in Table 3. The rate constant increases proportionally to the DMSO concentration. The rate constant of the reaction in pure methyl alcohol at 70°C, k_{MeOH} 1.35×10^{-5} $\mathrm{L.M^{-1} \cdot s^{-1}}$ was calculated by extrapolation. The calculated value is of the same order as those reported by other authors for the methoxylation of *o*-chloronitro-benzene with MeONa/MeOH (2.12×10^{-5} $\mathrm{L.M^{-1} \cdot s^{-1}}$[4] and 1.92×10^{-5} $\mathrm{L.M^{-1} \cdot s^{-1}}$[5]). The rate constant in pure DMSO, k_{DMSO} 0.37 $\mathrm{L.M^{-1} \cdot s^{-1}}$, of about 2.7×10^4 times higher than the value determined for the reaction in pure methanol, was similarly calculated. The accelerating effect of the reaction rate produced by DMSO is remarkable. It was not possible to perform the kinetic measurements at a molar concentration of 83 % DMSO (MeOH : DMSO 10 : 90 v/v) since the reaction was too fast. In order to explain the acceleration effect exerted by DMSO, we have tried to correlate the rate constant with the dielectric constant of the solvent mixture. The result is presented in Table 3. We observe a good linear dependence of the rate constant logarithm on the dielectric constant of the solvent mixture.

Table 3

The dependence of the rate constant on the dielectric constant of the solvent mixture

$k \times 10^4$, $\mathrm{L.M^{-1} \cdot s^{-1}}$	DMSO : MeOH (molar ratio)	ε
0.25	0.06	33.3
1.04	0.24	35.0
5.55	0.56	37.1
48.23	1.32	39.6

$t = 70$°C, [*o*-CNB] = 0.1 M, [NaOH] = 0.125 M

According to the generally accepted S_NAr mechanism shown in the following equation :

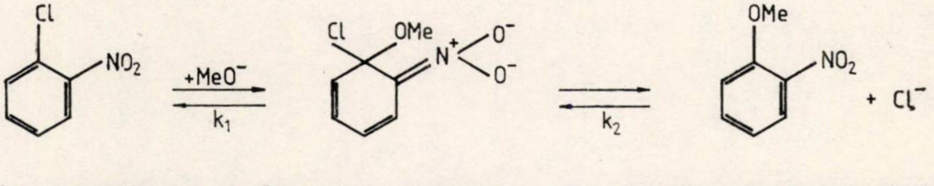

the dependence of the rate constant on the dielectric constant of the solvent mixture is determined by an electrostatic interaction between the solvent and the addition intermediate which is thus stabilized. Therefore, the slow addition step is markedly accelerated. This stabilization of the reaction intermediate through interaction with the solvent also accounts for the decrease of the activation energy of the reaction in the given solvent mixture.

EXPERIMENTAL

Apparatus and method. The kinetic measurements have been performed in an ultrathermostat at temperatures of 60, 70 and 80°C. The substitution reaction was followed by the potentiometric determination of the chloride ion with a 0.01 N $AgNO_3$ solution using the calomel electrode as reference electrode and the Ag^+-selective electrode (ORION) as indicator. The potentiometric titration was performed with an automatic titration device including a titrator TTT2, an autobiurette ABU12 and a recorder SBR20 (Radiometer, Copenhagen).

Reagents. Methanol and dimethylsulphoxide used as solvents were of analytical grade. *o*-Chloronitrobenzene and sodium hydroxide were min. 99% purity.

The concentration range of the reagents used in the kinetic determinations were : $0.66 \times \times 10^{-1}$—$1.25 \times 10^{-1}$M/L *o*-chloronitrobenzene and 1×10^{-1}—2×10^{-1}M/L NaOH, respectively.

REFERENCES

[1] S. G. Riklis, *Zhur. obshchei Khim.*, **17**, 1511 (1947).

[2] O. Manabe and H. Hiyama, *J. Chem. Soc. Japan*, **55**, 366 (1952) ; **56**, 203 (1953).

[3] B. B. Dey, T. R. Govindachari and H. V. Udupa, *J. Sci. Ind. Res., India*, **4**, 369 (1945) ; **5**, 258 (1946).

[4] J. Miller, *J. Chem. Soc.*, **1952**, 3550.

[5] T. O. Bamkele, J. Hirst and E. J. Udoessien, *J. Chem. Soc. Perkin Trans. II*, **1973**, 110.

[6] H. Suhr, *Chem. Ber.*, **97**, 3277 (1964).

[7] J. F. Bunnett and R. E. Zahler, *Chem. Rev.*, **49**, 273 (1951).

Revue Roumaine de Chimie, 31, 3, 273—282 (1986)

IMINE DER AMINOAZOLE II.[1]

SYNTHESE UND CHARAKTERISIERUNG EINIGER IMINE DES 2-AMINO-THIAZOLS, -BENZOTHIAZOLS, -BENZOXAZOLS UND DES 3-AMINO-1,2,4-TRIAZOLS

HANS-HORST GLATT, MAMADOU FOULA BARRY, CAROL CSUNDERLIK, RADU BACALOGLU, MIRCEA BOTOACĂ, SIMONA SAVU-BOTOACĂ und DIANA FECHETE
Technische Hochschule "Traian Vuia" Timişoara, Laboratorium für Organische Chemie,
str. Bocşa 6, 1900 Timişoara, SR Rumänien

Eingegangen am 25. März, 1985

Es wird die Synthese von 16 Iminen aus der Reihe der Benzyliden-2-aminobenzothiazole, des -benzoxazols, -thiazols und -triazols anhand der Reaktion der heterocyclischen Amine mit den entsprechenden substituierten Benzaldehyden beschrieben. Die dargestellten Verbindungen, unter denen sich auch 12 in der Literatur nicht beschriebene befinden, wurden durch Schmelzpunkt, Elementaranalyse, Infrarot-, Ultraviolett- und ^{1}H-NMR-Spektroskopie charakterisiert. Es wird dabei bewiesen, dass die Moleküle in allen untersuchten Fällen eine ebene Konfiguration und eine erweiterte Konjugierung aufweisen.

Sixten benzylidene 2-amino-benzothiazoles, -benzoxazoles, -thiazoles and -triazoles have been obtained from the corresponding heterocyclic amines and benzaldehydes. The products, of which twelve are new, were characterized by their melting point, elemental analysis, IR-, UV- and ^{1} H-NMR-spectra. It has been proved, that all compounds have a planar configuration and an extended conjugation.

EINLEITUNG

Heterocyclische Imine aus der Reihe der Benzyliden-2-aminobenzothiazole, des -thiazols, -des Benzoxazols und des -triazols sind nur selten in der Literatur beschrieben worden. So zum Beispiel wurden die Synthesen einiger Imine des 2-Aminothiazols, des 2-Aminobenzothiazols und des 5-Chlor-2-aminobenzoxazols[2,3] untersucht, ohne auf spektroskopische Eigenheiten einzugehen. In der vorangehenden Arbeit dieser Reihe[1] wurde eine systematische Untersuchung der Synthesen und der spektroskopischen Eigenschaften der 5(6)-substituierten Benzyliden-2-aminobenzimidazole vorgenommen. Vorliegende Arbeit befasst sich mit der Synthese und Charakterisierung von Iminen der 2-Aminobenzothiazole, -thiazols, -benzoxazols und des 3-Amino-1,2,4-triazols.

ERGEBNISSE

Die Imine aus der Reihe der Benzyliden-2-aminobenzothiazole, des -thiazols, des -benzoxazols und des -triazols wurden anhand folgender

Reaktion dargestellt :

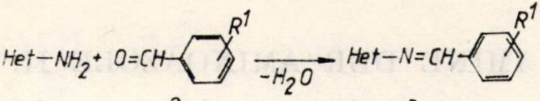

1 2 3

Het :

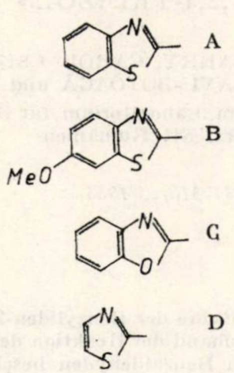

R¹	
4—NMe₂	a
4—OMe	b
4—Cl	c
2—NO₂	d
3—NO₂	e
4—NO₂	f
2.4 di—NO₂	g
2—OH	h

Das aus den heterocyclischen Amin **1** und dem Benzaldehyd **2** gebildete äquimolare Gemisch wurde in Toluen, Dioxan oder Pyridin gelöst und in der Abwesenheit oder im Beisein katalytischer Mengen von *p*-Toluensulphonsäure unter Rückfluss gekocht. Von den 16 dargestellten Verbindungen sind 12 (3Ba, 3Bb, 3Bc, 3Bd, 3Be, 3Bg, 3Ca, 3Ea, 3Eb, 3Ec, 3Ef, 3Eh) in der Literatur nicht angegeben. So wie im Falle der heterocyclischen Imine der Benzimidazolreihe, [1] sind auch im Falle der Imine der Benzyliden-2-aminobenzothiazole die IR-Spektren wegen der grossen Bandenanzahl des Benzothiazol systems, des Benzenkerns, sowie der Substituenten äusserst komplex. Überaus bandenreich ist der 1400—1610 cm^{-1}-Bereich, im dem nebst den Skelettbanden des Benzensystems[4] und des Benzothiazolsystems[5] auch die der C=N—Valenzschwingung zuzuschreibenden Banden auftreten.

In diesem Bereich erscheinen so wie es aus den in Tab. 1. enthaltenen Daten hervorgeht. 4 bis 6 Banden mittlerer oder sogar hoher Intensität, deren genaue Zuordnung durch die Methode der empirischen IR-Spektroskopie unsicher ist.

Die dem Benzothiazolsystem entsprechenden Banden sind jedoch relativ leicht erkennbar. Es erscheinen so drei mittelstarke Absorptionen in den 1555—1565—(1570[5]), 1525—1550—(1530[5]) und 1420—1460 —(1435[5])—cm^{-1} Bereichen, die den Skelettschwingungen des Benzothiazolsystems entsprechen. Die starke Bande von 1050—1060 cm^{-1} enspricht

Tabelle 1

Charakteristische Banden aus den IR-Spektren der Imine der Benzyliden-aminobenzothiazole, des — benzoxazols, des-thiazols und des — 1,2,4-triazols

Verbindung	ν_{NH}	1580—1610[a]	1500—1570	1400—1480	1050	700—800
3Aa	—	1607	1527	1467,1427	1060	700
3Ba	—	1583	1525	1453,1431	1052	702
3Bb	—	1588	1553,1502	1456,1420	1047	687
3Bc	—	1611	1551,1498	1453,1429	1056	711
3Bd	—	1600	1553	1467,1429	1051	703
3Be	—	1600	1569,1551	1456,1429	1053	711
3Bf	—	1611,1593	1540	1447,1427	1051	703
3Bg	—	1593	1567	1448,1427	1051	698
3Bh	—	1613,1591	1553	1451,1429	1059	727
3Ca	—	1603,1592	1559,1513	1443,1427	1059,1056	737
3Da	—	1609,1583	1525	1430	1056	773
3Ea	3100	1603,1583	1524	1440,1408	1056	811
3Eb	3126	1580	1510	1437,1411	1080	816
3Ec	3129	1577		1467,1420	1080,1000	796
3Ef	3138	1602,1581		1450,1430	1000	857,769
3Eh	3108	1611	1569	1468,1425	1027	821,754

a) erscheinen zusammen mit der C=N—Valenzschwingung

der Deformationsschwingung in der Ebene (1070[5]) und die schwache Bande von 690—710 cm^{-1} ist der Deformationsschwingung der CH-Gruppen des Benzothiazolsystems ausserhalb der Ebene (708[5]) zuzuschreiben.

Die IR-Spektren der Benzyliden-3-amino-1,2,4-triazole weisen im 3100—3140 cm^{-1} Bereich eine breite, mittelstarke Bande auf, die der Valenzschwingung der heterocyclischen NH-Gruppe zuzuschreiben ist. Im 1570—1615 cm^{-1} Bereich erscheinen die Benzenskelettbanden sowie mit ihnen überlargert die Valenzschwingungsbande der Imin-C=N— Gruppe (1590—1620[4,6]).

Nebst den oben angegebenen Banden erscheinen in den IR-Spektren der untersuchten Verbindungen auch die den funktionellen Gruppen entsprechenden Banden.

In den UV-Spektren der untersuchten heterocyclischen Imine, erscheint, so wie es aus Tab. 2. ersichtlich ist, ein Absorptions maximum im 370—410 nm Bereich mit molaren Extinktionskoeffizienten von 13000—45000 1/Mol cm. Die Absorptionsmaxima der Imine sind im Vergleich mit jenen der heterocyclischen Amine und bzw. der entsprechend substituierten Benzaldehyde bedeutend bathochrom verschoben. Dies legt den Schluss nahe, dass so wie es auch für andere Benzylidenimine gezeigt wurde, [1,7,8] diese Moleküle eine ebene Konfiguration haben und eine erweiterte Konjugation aufweisen. Je bedeutender der elektronenspendende Charakter des Substituenten am Benzenkern ist, um so bathochromer ist die Verschiebung des Absorptionsmaximus (Verbindungen 3Ba — 3Bc, Tab. 2.). Dies beweist eindeutig, dass der Benzenkern im Vergleich mit dem heterocyclischen System die Rolle des Elektronenspenders spielt. Diese Rolle kann mit Hilfe folgender Grenzstrukturen

Tabelle 2

UV-Spektren der heterocyclischen Imine

Verbindung	$\lambda^{a}_{\mathrm{Max}}$ (nm)	$\lambda^{b}_{\mathrm{Max}}$ (nm)	$\lambda^{c}_{\mathrm{Max}}$ (nm)	$\lambda^{d}_{\mathrm{Max}}$ (nm)	$\varepsilon^{a}_{\mathrm{Max}}\,10^{-4}$ (1/Mol·cm)	f
3Aa	404	480	293 261 222	340 242	4.099	1.145
3Ba	409	481	267 226	340 242	4.083	0.803
3Bb	373	373	267 226	273	2.436	0.683
3Bc	376	376	267 226	254	1.911	0.541
3Bd	390	390	367 226	252	1.208	0.424
3Be	380	380	267 226	233	1.685	0.474
3Bf	402	402	267 226	265	1.718	0.446
3Bg	423	423	267 226	328	1.284	0.411
3Bh	384	384	267 226	328 259	2.008	0.549
3Ca	405	469	280 240	340 242	4.465	0.820
3Da	391	470	256	340 242	3.372	0.722
3Ea	371	435	208	340 242	3.271	—
3Eb	319		208	273	1.714	—
3Ef	316		208	265	2.073	—
3Eh	389		208	328 259	1.833 1.487	—
3Fa[e]	392	454	258 232	340 242	4.316	0.835

[a] in dioxanischer Lösung

[b] in 0.4 Mol/1 CF_3COOH in Dioxan

[c] Absorptionsmaxima des entsprechenden Amino-Heterocyclus

[d] Absorptionsmaxima des entsprechenden Benzaldehyds

[e] *p*-Dimethylaminobenzyliden-2-aminobenzimidazol[1]

veranschaulicht werden:

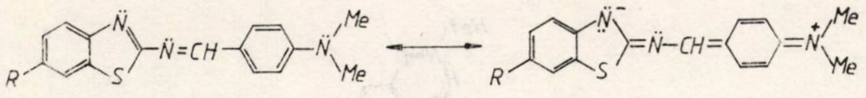

Die Imine mit Nitrogruppen am Benzenkern (z.B. 3Bd, 3Be, 3Bf, 3Bg) zeigen jedoch eine wichtigere bathochrome Verschiebung als das Chlor-Derivat (3Bc). Die lässt erkennen, dass der Benzenkern in diesen Fällen im Vergleich zum Benzothiazolkern elektronenanziehend wird:

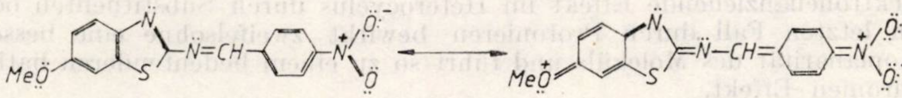

Durch Protonieren der Verbindungen 3Aa, 3Ba, 3Ca, 3Da und 3Ea tritt eine bedeutende bathochrome Verschiebung des Absorptionsmaximums auf, das die Rolle des heterocyclischen Systems als Elektronenanzieher im Vergleich zum Benzenkern bestättigt. Durch Protonieren des Heterocyclus am endocyclischer Stickstoffatom wird natürlich sein elektronenanziehender Charakter ausgeprägter:

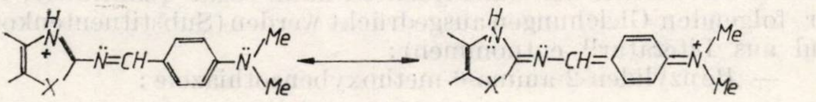

Vergleicht man die Absorptionsmaxima der vom *p*-Dimethylamino benzaldehyd herrührenden Imine (3Aa, 3Ba, 3Ca, 3Da, 3Ea und 3Fa) lässt sich leicht feststellen, dass die Maxima der Benzazole bathochromer liegen als jene der einfachen Azole. Der Benzenkern bewirkt zweifelsohne eine erhöhte Konjugation im Benzazolsystem. Das Benzoxazol- und Benzothiazolderivat weisen fast gleiche bathochrome Verschiebungen auf, die jedoch bedeutender sind als die im Falle des Benzimidazolsystems was im Einklang mit dem elektronenanziehenden Effekt des Heterocyclus im System ist. Der Thiazolring scheint einen bedeutenderen elektronenanziehenden Charakter zu haben als das Triazolsystem.

Ebefalls aus Tab. 2. ist ersichtlich, dass die Stärke des harmonischen Oszillators, f, mit dem zunehmenden elektronenanziehenden Charakter der Substituenten am Benzenkern fällt. Dies kann als neuer Beweis der erweiterten Konjugierung dieser Imine ausgelegt werden. Solche elektronenanziehende Substituenten vermindern in bedeutendem Masse die Konjugierung.

Bemerkenswert ist die besonders hohe bathochrome Verschiebung der Absorptionsmaxima der Verbindungen mit *ortho*-ständiger Hydroxylgruppe im Benzenkern (3Bh, 3Eh), obzwar dieser Substituent keinen starken elektronenanziehenden Effekt aufweisen kann. Dieser bathochrome Effekt lässt sich nur anhand einer intramolekularen Assozierung erklären, die die Planarität des Systems vorantreibt und den elektronenaziehenden Charakter des Imin-Stickstoffatoms vergrössert:

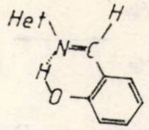

Dies legt den Schluss nahe, dass obzwar das System erweiterte Konjugierung aufweist, und so in grossen Zügen koplanar ist, kann diese Koplanarität doch noch durch Assozierung verbessert werden.

Der zunehmende elektronenstossende Effekt im Benzenkern und elektronenanziehende Effekt im Heterocyclus durch Substituenten oder im letzten Fall durch Protonieren bewirkt zweifelsohne eine bessere Koplanarität des Moleküls und führt so zu einem bedeutenderen bathochromen Effekt.

Die ^{1}H-NMR-Spektren der Verbindungen beweisen die ihnen zugeschriebenen Strukturen (Tabelle 3).

So erscheint das stark entschirmte Signal des Aldiminprotons im Falle der vom 2-Aminobenzothiazol abstammenden Imine im δ 8,9–9,6 ppm Bereich als Singulett. Der zunehmende elektronenanziehende Charakter der Substituenten am Benzenkern der Imine führt erwartungsgemäss zu einer bedeutenden Tieffeldverschiebung des Signals (3Ba, 3Bc). Dieser Effekt der Substituenten kann sogar quantitativ, mit Hilfe der folgenden Gleichungen ausgedrückt werden (Substituentenkonstanten sind aus Literatur[11] entnommen):

— Benzyliden-2-amino-6-methoxybenzothiazole:

$$\delta_{\mathrm{CH}} = 0{,}22\sigma_{\mathrm{R}}1 + 8{,}97 \quad (r = 0{,}98)$$

— Benzyliden-3-amino-1,2,4-triazole:

$$\delta_{\mathrm{CH}} = 0{,}20\sigma_{\mathrm{R}}1 + 9{,}14 \quad (r = 0{,}98)$$

Aus diesen Beziehungen folgt, dass der Anstieg dieser Korrelierungen praktisch für beide Verbindungsklassen der selbe ist, und gleich mit jenem der 5(6)-substituierten Benzyliden-2-aminobenzimidazolen (0,22[1]).

Im Prinzip ist die chemische Verschiebung des Protons der Imingruppe auch ein Mass des elektronenanziehenden Effektes des heterocyclischen Systems. Dieses Proton befindet sich wegen der *trans*-Konfiguration des Iminmoleküls in der Nähe des Heteroatoms und wird zweifelsohne von dessen Anisotropiekegel beeinflusst. Aus dem Vergleich der chemischen Verschiebung des Iminprotons folgt, dass die Benzazolderivate eine grössere Verschiebung aufweisen als die einfachen Azole (3Aa, 3Ca, 3Fa im Vergleich zu 3Da und 3Ea). Das Benzothiazol scheint elektronenanziehender zu wirken als das Benzimidazol (3Ba und 3Fa) während das Benzoxazol weniger elektronenanziehend wirkt. Im letzteren Fall kann jedoch ein Anisotropieeffekt nicht ausgeschlossen werden. Das Triazolsystem scheint wiederum elektronenanziehender zu sein als das Thiazol (3Ea und 3Da).

Die Signale der Protonen der aromatischen Systeme ergeben komplexe Multiplette mit erwarteten chemischen Verschiebungen. So erschei-

Tabelle 3

^{1}H-NMR-Spektren der heterocyclischen Imine

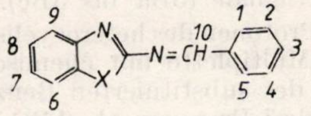

Verbindung^a	chemische Verschiebung δ (ppm)									
	1	2	3	4	5	6	7	8	9	10
3Aa	7.61	6.71	3.15 NMe_2	6.71	7.61	ABCD :	7.00	—	7.83	9.59
3Ba	7.86	6.80	3.15 NMe_2	6.80	7.86	7.40	3.75 OMe	7.05	7.68	8.79
3Bb	7.93	7.03	3.16 OMe	7.03	7.93	7.48	3.83 OMe	7.03	7.70	8.83
3Bc	7.93	7.35	Cl	7.35	7.93	7.35	3.75 OMe	7.00	7.68	8.98
3Bd	NO_2	8.13	7.55	7.63	7.98	7.50	3.78 OMe	7.03	7.73	9.30
3Be	8.73	NO_2	7.51	8.33	7.79	7.28	3.78 OMe	7.08	7.71	9.15
3Bh	11.46 OH	7.00	7.42	7.00	7.77	7.37	3.78 OMe	7.45	7.75	9.27
3Ca	7.83	6.80	3.06 NMe_2	6.80	7.83	ABCD :	7.00	—	7.93	9.08
3Fa^b	7.80	6.76	3.00	6.76	7.80	ABCD :	7.08	—	7.39	9.16

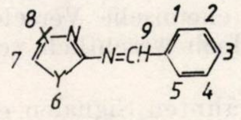

	1	2	3	4	5	6	7	8	9
3Da	7.73	6.71	2.96 NMe_2	6.71	7.44	S	7.37	7.55 CH	8.74
3Ea	7.74	6.73	2.96 NMe_2	6.73	7.74	13.7 NH	8.02	N	8.95
3Eb	7.92	7.06	3.81 OMe	7.06	7.92	8.00 NH	8.20	N	9.11
3Ec	8.00	7.60	Cl	7.60	8.00	10.0 NH	8.25	N	9.20
3Ef	8.12	8.32	NO_2	8.32	8.12	14.3 NH	8.36	N	9.27
3Eh	12.80 OH	6.94	7.40	6.89	7.71	12.8 NH	8.44	N	9.35

a) die Verbindungen 3Bf und 3Bg sind unlőslich ; Lősungsmittel : DMSO-d_6 ; Standard HMDS (Hexamethyldisiloxan)

b) *p*-Dimethylaminobenzyliden-2-aminobenzimidazol (siehe L.c. 1.).

nen die vier aromatischen Protonen des 1,4-disubstituierten Benzenkerns als AB-Multiplett mit chemischen Verschiebungen von 7,6-7,9 und bzw. 6,7 – 7,4 ppm. Elektronenanziehende Substituenten bewirken ein Tieffeldverschiebung dieser Signale (3Ba bis 3Bc).

Die aromatischen Protonen des heterocyclischen Systems erscheinen ebenfalls als komplexe Multiplette mit chemischen Verschiebungen von 6,9 – 7,8 ppm. Im Falle des substituierten Benzothiazolsystems (3Ba bis 3Bh) erscheinen dessen drei Protonen als ABC-Multiplett bei 7,68 – 7,75, 7,28 – 7,50 und 7,0 – 7,1 ppm. Die Lage dieser Signale wird von den elektronischen Effekten der Substituenten am Benzenkern nur in unbedeutendem Masse beeinflusst. Im Falle der Imine 3Aa und 3Ca erscheinen die aromatischen Protonen als ABCD-Multiplett im 7,00 – 7,93 ppm Bereich.

Im Falle der Imine der Triazolreihe erscheint auch das Signal des aromatischen Protons des Heterocyclus bei chemischen Verschiebungen von 8,00 – 8,50 ppm. Bemerkenswert ist dass dieses Signal von elektronenanziehenden Substituenten am Benzensystem tieffeldverschoben und bzw. von elektronenabstossenden hochfeldverschoben wird. Folgende Gleichung widergibt quantitativ diese Einflüsse :

$$\delta_{\mathrm{CH}} = 0{,}20\sigma_{\mathrm{R}}\,1 + 8{,}21 \quad (r = 0{,}98)$$

Diese Gleichung ähnelt der für den Fall des Aldiminprotons gefundenen Gleichung, was darauf hinweist, dass die Elektroneneffekte der Substituenten am aromatischen Kern in gleicher Weise den zwei Protonen übertragen werden. Mesomere Effekte können jedoch zum heterocyclischen System nur in ebenen Molekülen übetragen werden.

Die NH-Gruppe des Triazolsystems lässt sich in den ^{1}H-NMR-Spektren ebenfalls lokalisieren (chemische Verschiebung σ, 8 – 14 ppm), die Lage ihres Signals wird jedoch wesentlich von der Temperatur und der Konzentration beeinflusst.

Nebst den bisher erwähnten Signalen erscheinen in den ^{1}H-NMR-Spektren der Imine auch die den Substituenten entsprechenden Signale. So erscheint die Dimethylaminogruppe als sechs-Protonen-Singulett bei 3 – 3,15 ppm. Die Methoxygruppe des Benzothiazolsystems weist eine chemische Verschiebung von 3,78 – 3,90 ppm auf. Die Lage dieses Signals wird von elektronenspendenden Substituenten im Benzenkern tieffeldverschoben.

BESCHREIBUNG DER VERSUCHE

Die IR-Spektren der KBr-Presslinge wurden mit einem IR 75 SPECORD (Carl Zeiss Jena) aufgenommen. Die UV-Spektren wurden mit einem CARY 17 (Varian) aufgezeichnet. Die ^{1}H-NMR-Untersuchungen fanden mit einem TESLA BS 487 C (80 MHz) statt. Die Proben wurden in Dimethylsulfoxyd (DMSO-d_6) gelöst. Als Standard wurde Hexamethylendisiloxan (HMDS) benützt. Die Multiplette der aromatischen Protonen wurden als Systeme erster Ordnung angenommen und so konnten annähernde Werte der chemischen Verschiebungen und der Kopplungskonstanten bestimmt werden. Die Elementaranalysen wurden mit einem Elemental Analyser Modell 240 B (Perkin Elmer) ausgeführt.

Darstellung von Benzyliden-aminobenzothiazolen, -benzoxazolen, -thiazolen (allgemeine Vorschrift).

Man löst 9 mMol des heterocyclischen Amins **1** und 9 mMol Benzaldehyd **2** in 50 mL Toluol, versetzt mit 0,004 mMol *p*-Toluensulphonsäure und kocht 2—9 Std am Wasserabscheider unter Rückfluss. Dannach wird das Reaktionsgemisch auf etwa die Hälfte des Ausgangsvolumens eingeengt. Während des Erkaltens fällt das Produkt aus. Es wird abgesogen, mit etwas P. Ae gewaschen und umkristallisiert. Die Ausbeute beträgt 60—98%. Weiteres Imin kann aus der Mutterlauge durch Fällen mit P.Ae gewonnen werden. Folgende Verbindungen wurden nach dieser Vorschrift erhalten:

p-Dimethylaminobenzyliden-2-aminobenzothiazol 3Aa, aus 1A und 2a, Rückfluss 6 Std, Ausbeute 91,2%; goldgelbe Prismen, Schmp (Toluol) 284,5—7° (184—6[2]); $C_{16}H_{18}N_3S$ (M=281,38) ber. %C 68,30, %H 5,37, %N 14,93; gef. %C 68,33, %H 5,33, %N 14,81.

p-Dimethylaminobenzyliden-2-amino-6-methoxybenzothiazol 3Ba. aus **1B** und 2a, Rückfluss 9 Std ohne Katalysator Ausbeute 8,9%; Rückfluss 5 Std ohne Entfernen des Reaktionswassers 70,6%; Rückfluss 5 Std am Wasserabscheider 82,2%; goldgelbe Nadeln, Schmp (Äthanol) 196,5—197,5°; $C_{17}H_{17}N_3OS$ (M=311,41); ber. %C 65,57, %H 5,50, %N 13.49; gef. %C 64,47, %H 5,34, %N 13,68.

p-Methoxybenzyliden-2-amino-6-methoxybenzothiazol 3Bb, aus 1B und 2b, Rückfluss, 8 Std, Ausbeute 52,6%, gelbe Nadeln, Schmp 145,5—6,5°; $C_{16}H_{14}N_2O_2S$ (M=298,37); ber. %C 64,41, %H 4,73, %N 9,39; gef. %C 63,59, %H, 4,71, %N 9,30.

p-Chlorbenzyliden-2-amino-6-methoxybenzothiazol 3Bc, aus 1B und 2c, 7,5 Std Rückfluss, 91%-ige Ausbeute; gelbe Kristalle, Schmp (Toluol) 145—6°; $C_{15}H_{11}ClN_2OS$ (M=302,79); ber. %C 59,50, %H 3,66, %N 9,25; gef. %C 59,40, %H 3,56, %N 9,21.

o-Nitrobenzyliden-2-amino-6-methoxybenzothiazol 3Bd, aus 1B und 2d, 4,5 Std Rückfluss, 91%-ige Ausbeute; rote Nadeln, Schmp (Toluol) 178—181°; $C_{15}H_{11}N_3O_3S$ (M=313,34); ber. %C 57,50, %H 3,54, %N 13,41; gef. %C 57,30, %H 3,52, %N 13,55.

m-Nitrobenzyliden-2-amino-6-methoxybenzothiazol 3Be, aus 1B und 2e 7 Std Rückfluss, 87,5-%ige Ausbeute; goldgelbe Kristalle, Schmp (Toluol) 197—9°; $C_{15}H_{11}N_3O_3S$ (M=313,34); ber. %C 57,50, %H 3,54, %N 13,41; gef. %C 57,14, %H 3,42, %N 13,49.

p-Nitrobenzyliden-2-amino-6-methoxybenzothiazol 3Bf, aus 1B und 2f, 0,5 Std Rückfluss, Ausbeute 80%; gelbe Stäbchen, Schmp (Toluol) 250—2° (253—5[3]); $C_{15}H_{11}N_3O_3S$ (*M*=313,34); ber. %C 57,50, %H 3,54, %N 13,41; gef. %C 56,81, %H 3,56, %N 13,62.

o, p-Dinitrobenzyliden-2-amino-6-methoxybenzothiazol 3Bg, aus 1B und 2 g; 2,5 Std Rückfluss, Ausbeute 88%; rote Nadeln, Schmp (Toluol) 190—2°.

o-Hydroxybenzyliden-2-amino-6-methoxybenzothiazol 3Bh, aus 1B und 2h, Rückfluss in Äthanol, ohne Katalysator 7 Std Ausbeute 14,6%; 2 Std mit Katalysator, Ausbeute 77,3%; 8 Std in Benzol, Ausbeute 60,4%; gelbe Nadeln, Schmp (Äthanol) 148,5—149° (147—9[3]).

p-Dimethylaminobenzyliden-2-aminobenzoxazol 3Ca, aus 1C und 2a, Rückfluss in *o*-Xylol 8 Std, Ausbeute 50,2% (ohne Katalysator) goldgelbe Plättchen, Schmp (*o*-Xylol) 221—3°; $C_{16}H_{15}N_3O$ (M=265,32); ber. %C 72,43, %H 5,70, %N 15,84; gef. %C 72,40, %H 5,54, %N 16,40.

p-Dimethylaminobenzyliden-2-aminothiazol 3Da, aus 1D und 2a, Rückfluss in Toluol-Dioxan (1 : 1) 3,5 Std, 3 Extraktionen mit n-Hexan; goldgelbe Kristalle, Schmp (Hexan) 118—9° (118—9[2])

Darstellung der Benzyliden-3-amino-1,2,4-triazole (allgemeine Vorschrift)

Man löst 12 mMol 3-Amino-1,2,4-triazol, 12 mMol des entsprechenden Benzaldehyds in 50 ml Pyridin und kocht unter Rückfluss 6—10 Std. Das Reaktionsgemisch wird auf cca 1/4 des Anfangsvolumens eingeengt. Beim Erkalten fällt das Produkt meist rein aus. Die Ausbeute beträgt 74—95%. Folgende Verbindungen wurden auf dieser Weise hergestellt:

p-Dimethylaminobenzyliden-3-amino-1,2,4-triazol 3Ea aus 1E und 2a, 10 Std, 74,3% %-ige Ausbeute, grünliche Kristalle, Schmp 234—5°; $C_{11}H_{13}N_5$ (M=215,26); ber. %C 61,38, %H 6,09, %N 34,53; gef. %C 61,34, %H 6,18, %N 32,10.

p-Methoxybenzyliden-3-amino-1,2,4-triazol 3Eb, aus 1E und 2b, 6 Std, 79,5%-ige Ausbeute, gelbliche Kristalle, Schmp 201—3°; $C_{10}H_{10}N_4O$ (M=202,22); ber. %C 59,40, %H 4,98, %N 27,71; gef. %C 59,96, %H 5,26, %N 28,21.

p-Chlorbenzyliden-3-amino-1,2,4-triazol 3Ec, aus 1E und 2c, 6 Std, 80,9 %-ige Ausbeute, Schmp 188—90°.

p-Nitrobenzyliden-3-amino-1,2,4-triazol 3Ef, aus 1E und 2f, 6 Std, 74,3 %-ige Ausbeute; gelbliche Nadeln, Schmp 240—2°; $C_9H_7N_5O_2$ (M=217,19); ber. %C 49,77, %H 3,25, %N 32,25; gef. %C 50,18, %H 3,43, %n 32,47.

o-Hydroxybenzyliden-3-amino-1,2,4-triazol, 3Eh, aus 1E und 2h, 8 Std, 96,1 %-ige Ausbeute, gelbliche Nadeln, Schmp 135—7°; $C_9H_8N_4O$ (M=188,19); ber. %C 57,44, %H 4,29, %N 29,77; gef. %C 57,59, %H 4,71, %N 28,57.

LITERATURÜBERSICHT

[1] Erste Mitteilung dieser Reihe: H. H. Glatt, M. F. Barry, C. Csunderlik, R. Bacaloglu, M. Medeleanu und M. Lantos, *Rev. Roum. Chim.*, **30**, 125 (1985).

[2] J. Bödeker und K. Courault, *J. prakt. Chem.*, **322** (2), 336 (1980).

[3] H. O. Hankovsky und K. Hideg, *Acta chim. Acad. Sci. Hung.*, **53** (4), 405 (1967).

[4] K. Nakanishi und P. H. Solomon, *Infrared Absorption Spectroscopy* Holden-Day, San Francisco 1977, S. 19.

[5] A. R. Katritzky, *Physical Methods in Heterocyclic Chemistry*, Academic Press, London, 1963.

[6] A. T. Balaban, M. Banciu und I. Pogany, *Aplicații ale metodelor fizice în chimia organică*, Ed. Științifică și Enciclopedică, București 1983, S. 44.

[7] R. Gawinecki und F. Muzalewski, *Polish J. Chem.*, **54**, 1177 (1980).

[8] F. Muzalewski und R. Gawinecki, *Polish J. Chem.*, **55**, 565 (1981).

Revue Roumaine de Chimie, 31, 3, 283—289 (1986)

IMINE DER AMINOAZOLE III[1].

BASIZITÄTSKONSTANTEN HETEROCYCLISCHER IMINE AUS DER REIHE DER BENZYLIDEN-AMINO-BENZOTHIAZOLE, DES -BENZOXAZOLS, DER -BENZIMIDAZOLE, DES -THIAZOLS UND DES -TRIAZOLS

RADU BACALOGLU, HANS-HORST GLATT, MAMADOU FOULA BARRY
und CAROL CSUNDERLIK
Technische Hochschule "Traian Vuia" Timişoara, Laboratorium für organische Chemie,
str. Bocşa 6, 1900 Timişoara, SR Rumänien

Eingegangen am 25. März, 1985

pK_a-Werte von 19 heterocyclischen Iminen aus der Reihe der Benzyliden-amino-benzothiazole, des -benzoxazols, der -benzimidazole, des -thiazols und des -triazols wurden bestimmt und der Einfluss der Substituenten am Benzylidenrest sowie jener des Heterocyclus und seiner Substituenten auf diese Werte untersucht.

The basicity constants for 19 heterocyclic imines from the benzylidene aminobenzothiazole, benzoxazole, benzimidazole, thiazole and triazole series were determined. The electronic influence of the benzylidene substitutens and of the substituted heterocycles was established.

In vorangehenden Arbeiten dieser Reihe[1,2] wurden die Synthesen und die spektroskopischen Eigenschaften von heterocyclischen Iminen der Benzyliden-2-aminobenzimidazole, des -benzoxazols, der -benzothiazole, des -thiazols und -3-amino-1,2,4-triazols untersucht. Da wir am Studium der sauren Hydrolyse dieser Imine interessiert waren, haben wir vorerst ihre Basizitätskonstanten bestimmt, um sie dann mit Geschwindigkeitskonstanten zu korrelieren.

ERGEBNISSE UND DISKUSSION

Zur Bestimmung der Basizitätskonstanten der heterocyclischen Imine wurde die Indikatoren-Methode [3,4] herangezogen. Als Indikatoren wurden Krysoidin ($pK_a = 5.30^5$) sowie 4-Dimethylaminoazobenzen ($pK_a = 3{,}17^5$) verwendet. Für diese Indikatoren wurde die Aciditätsfunktion *H* bestimmt, wobei die Konzentration des freien und des protonierten Indikators in dioxanischer Lösung im Beisein von Trifluoressigsäure UV-spektroskopisch gemessen wurde (siehe Versuchsteil). Anhand dieser Aciditätsfunktionen und anhand der ebenfalls UV-spektroskopisch bestimmten Konzentrationen der freien und protonierten Imine in dioxanischer Lösung im Beisein von verschiedenen Mengen von Trifluoressigsäure wurden die Besizitätskonstanten der heterocyclischen Imine berechnet. Diese Konstanten sind in Tabelle 1 zusammengefasst.

Tabelle 1

pK_a — Werte der heterocyclischen Imine

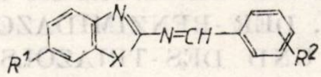

X	R_1	R_2	pK_a	$\pm\sigma$	n^a	Indikator^b
NH	H	*p*-NMe_2	6,64	—	1	K
NH	H	*p*-Cl	5,82	—	1	K
NH	H	*m*-NO_2	5,43	0.20	5	K
NH	H	*p*-NO_2	5.39	—	1	K
NH	Me	*p*-NMe_2	6,67	—	1	K
NH	Cl	*p*-NMe_2	6,21	0.03	4	K
NH	NO_2	*p*-NMe_2	6.11	0.16	4	K
S	H	*p*-NMe_2	3.94	0.04	3	D
S	MeO	*p*-NMe_2	3.99	0.09	4	D
S	MeO	*p*-OMe	3.54	0.03	3	D
S	MeO	*p*-Cl	3.26	0.22	3	D
S	MeO	*o*-NO_2	2.46	0.30	3	D
S	MeO	*m*-NO_2	2.47	0.30	4	D
S	MeO	*p*-NO^{+2}	2.97	0.04	3	D
S	MeO	*o,p*-diNO_2	1.85	0.09	2	D
S	MeO	*o*-OH	0.93	—	1	D
O	H	*p*-NMe_2	3.42	0.03	3	D

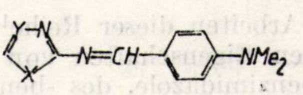

X	**Y**	**pK_a**	**$\pm\sigma$**	**n^a**	**Indikator^b**
S	CH	4.22	0.13	4	D
NH	N	5.42	0.07	6	K

a Anzahl der Messungen;
b K-Krysoidin; D-Dimethylaminoazobenzol.

Die pK_a-Werte dieser Imine sind von der Art der Substituenten am Benzylidenkern sowie am Heterocyclus bedingt. Folgende Hammett Gleichungen wurden für die Verbindungen aus Tab. 1 erhalten:

— am Benzylidenkern substituierte Benzimidazolimine:
$pK_a = -0{,}78\ \sigma_{R_2} + 5{,}99\ (r = 0{,}999)\ (R_1 = H;\ X = NH)$
— am Benzimidazolkern substituierte Benzimidazolimine:
$pK_a = -0{,}71\ \sigma_{R_2} + 6{,}57\ (r = 0{,}967)\ (R_2 = p\text{-}NMe_2;\ X{=}NH)$

— am Benzylidenkern substituierte Benzothiazolimine:
$pK_a = -0{,}79\ \sigma_{R_2} + 3{,}34\ (r = 0{,}935)\ (R_1 = OMe;\ X{=}S)$

Eine besondere Lage in der Reihe der Basizitäten weist das 2-Hydroxybenzyliden-2-amino-6-methoxybenzothiazol ($pK_a{=}0{,}93$) auf. Die bedeutend niedrigera Basizität dieser Verbindung kann nur anhand einer intramolekularen Assoziation der phenolischen HO-Gruppe mit der Imin C=N-Gruppe verstanden werden. Eine solche Assoziation verringert beträchtlich den elektronenspendenden Effekt der exocyclischen Aminogruppe

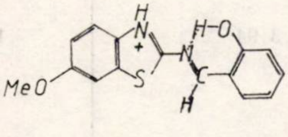

Vergleicht man die Basizitäten der *p*-dimethylaminobenzylidenaminoheterocyclischen Imine mit der des Benzylidenanilins (Tab. 2) folgt dass, obzwar der Heterocyclus einen offensichtlich bedeutenderen elektronenanziehenden Effekt aufweist als der Benzolkern. die Basizität des Benzylidenanilins um fast 2—3 Ordnungsgrössen kleiner ist. Dies kann nur dann verstanden werden. wenn man annimmt. dass die Protonierung der heterocyclischen Benzyliden-amine am heterocyclischen N-Atom und nicht am Imin-N-Atom stattfindet.

Diese Annahme wird vom ^{1}H-NMR-spektroskopischen Vergleich des protonierten *p*-Methoxybenzyliden-2-aminobenzimidazols mit jenem des 2-Aminobenzimidazols untermauert (Tab. 3.).

Durch Protonieren des heterocyclischen Imins verschieben sich die den Benzolkern-Protonen (A. B. C) entsprechenden Signale nur unwesentlich tieffelds (0.05—0.07 ppm), während sich das Signal des Aldiminprotons (D) um 0.13 ppm nach höheren Feldern verschiebt. Eine Protonierung an diesem N-Atom hätte zweifelsohne eine sehr wichtige Tieffeldverschiebung des entsprechenden Signals verursacht. Das Signal des Protons des Imidazolsystems (E) wird jedoch um 3,9 ppm tieffelds verschoben. Diese Verschiebung ist mit jener des Imidazolprotons aus 2-Aminobenzimidazol, einer Verbindung die sich bekanntlich[7] am endocyclisch ständigen N-Atom protoniert, vergleichbar.

Die Basizität der heterocyclischen Imine liegt in allen studierten Fällen höher als die der entsprechenden Azole (Tab. 2). Dies ist verständlich, wenn man den elektronenspendenden Charakter der Benzylidenaminogruppe in Betracht zieht. Dieser Effekt wurde von uns auch anhand der UV- und ^{1}H-NMR Spektren[1,2] bewiesen.

Die Basizität der heterocyclischen Imine ist jedoch im allgemeinen kleiner als jene der entsprechenden 2-Aminoazole (Tab. 2.), was auf den bedeutenderen elektronenspendenden Effekt der Aminogruppe im Vergleich mit der Benzylidenaminogruppe hinweist.

Eine besondere Stellung nimmt das *p*-Dimethylaminobenzyliden-3-amino-1,2,4-triazol ein, das basischer als das 3-Amino-1,2,4-triazol ist.

Tabelle 2

pK_a-Werte einiger Azole, Aminoazole und der entsprechenden p-Dimethylaminobenzyliden-aminoazole

Verbindung	pK_a-Werte $R=N=CH-C_6H_4-NMe_2(p)$	$R=H^a$	$R=NH_2^a$
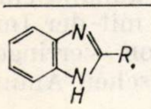	6.65	5.53	7.51
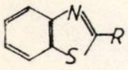	3.94	1.20	4.48
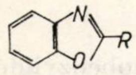	3.42	−0.50	3.70
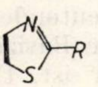	4.22	2.53	5.36
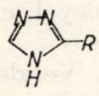	5.43	2.27	4.04
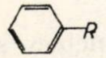	2.27^b	—	4.60

a pK_a-Werte sind aus l.c. 5 entnommen
b $R = -N=CH-C_6H_6$ aus l.c. 6

Tabelle 3

^1H-NMR Spektren von freien und protonierten Benzimid-azolen

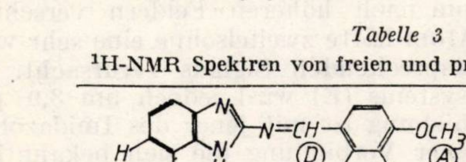

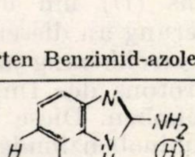

Protonentyp	δ(ppm) frei$^{a)}$	δ(ppm) protoniert$^{b)}$	δ(ppm) frei$^{a)}$	δ(ppm) protoniert$^{b)}$
A	3.80	3.85	—	—
B	7.05	7.12	—	—
C	7.95	8.01	—	—
D	9.30	9.17	—	—
E	7.00	10.88	8.13	10.58
F	7.08	7.42	6.84	7.16
G	7.44	7.65	7.07	7.32
H	—	—	6.15	8.47

a in DMSO-d_6 bei 30°C; Standard Hexamethyldisiloxan
b Verhältnis DMSO-d_6 : CF_3COOH = 1 : 1 (Vol : Vol)

Vergleicht man die Basizitätskonstanten der heterocyclischen Imine untereinander (Tab. 1.) so ergibt sich folgende Reihung:

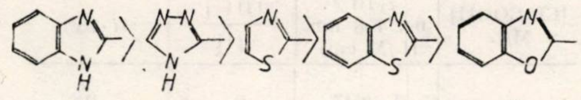

I II III IV V

In der Reihe der Benzazole ist die Verminderung der Basizität mit dem Anstieg der Elektronegativität des zweiten Heteroatoms (I, IV, V) klar verständlich. Die Einführung eines weiteren Heteroatoms führt anhand dessen Elektronegativität zum Absinken der Basizität (I, II). Durch Kondensierung eines Benzolkerns an den Heterocyclus steigt die Konjugierung des Systems, und so fällt dessen Basizität.

Beschreibung der Versuche

Messgeräte

Die UV-spektroskopischen Untersuchungen wurden mit einem CARY 17 (Varian) ausgeführt. Die ^{1}H-NMR-Spektren der DMSO-d_6 Lősungen (im Beisein oder in der Abwesenheit des CF_3COOH) wurden mit einem TESLA BS 487 C (80 MHz) aufgezeichnet. Als Standard wurde HMDS (Hexamethylendisiloxan) verwendet.

Bestimmung der Aciditätsfunktion H der Indikatoren

Die UV-Spektren der Indikatorlösungen (Krysoidin, *p*-Dimethylaminoazobenzol) in Dioxan ($[I]_T = 10^{-5}$M/L) im Beisein verschiedener Mengen von wasserfreier Trifluoressigsäure ($[CF_3COOH] = 0 - 23$ M/L) bei 25° wurden aufgezeichnet. Aus diesen wurden die Extinktionskoeffizienten in der Abwesenheit und im Beisein variabler Mengen von CF_3COOH bestimmt und anhand Gleichung (1) wurde das Konzentrationsverhältnis $[IH^+]/[I]$ berechnet.

$$\frac{[IH^+]}{[I]} = \frac{\varepsilon_I - \varepsilon_T}{\varepsilon_T - \varepsilon_{IH^+}} \qquad (1)$$

wobei $[I]$ und $[IH^+]$ Konzentration des freien und des protonierten Indikators sind.

$\varepsilon_I \cdot \varepsilon_{IH}{}^+$ und ε_T-Extinktionskoeffizienten des Indikators in der Abwesenheit, im Beisein eines grossen Überschusses, sowie in der Gegenwart verschiedener CF_3COOH – Konzentrationen sind.

Gleichung (2) ermöglicht nun anhand dieses Verhältnisses sowie der Basizitätskonstante des Indikators (K_{IH^+}) den *H*-Wert bei einer gewissen CF_3COOH-Konzentration zu berechnen.

$$H = K_{IH^+} \cdot \frac{[IH^+]}{[I]} \qquad (2)$$

Sowie es aus dem in Tab. 4. angegebenen Rechenbeispiel hervorgeht hängt *H* von der CF_3COOH-Konzentration ab. Fur Krysoidin ist diese Abhängigkeit von der Form :

$$H = 1{,}733 \cdot 10^{-5}\ [CF_3COOH] + 6.20 \cdot 10^{-7}\ (r = 0{,}996) \qquad (3)$$

Für den Fall des *p*-Dimethylaminoazobenzol wurde folgende Aciditätsfunktion erhalten :

$$H = 4{,}0813 \cdot 10^{-4}\ [CF_3COOH]^2 - 2{,}54 \cdot 10^{-6}\ (r = 0{,}997) \qquad (4)$$

Tabelle 4

Bestimmung der Aciditätsfunktion *H* für Krysoidin bei 25°C.

$[CF_3COOH]$ M/L	$\varepsilon_T 10^{-3}$ bei 458 nm (L/M cm)	$\frac{[IH^+]}{[I]}$	$H \cdot 10^6$
—	1.9643	0	0
0.0670	3.1299	0.432	2.164
0.1333	3.4629	0.633	3.173
0.1990	3.7555	0.863	4.327
0.2640	4.0290	1.146	5.745
0.5799	4.4935	1.892	9.484
1.1683	5.0918	4.236	21.231
2.1973	5.8301	—	—

Bestimmung der Basizitätskonstanten der heterocyclischen Imine

Unsere Vorversuche hatten gezeigt, dass die heterocyclischen Imine ohne Ausnahme beim Hinzufühgen von CF_3COOH zu ihrer dioxanischen Lösungen schnell eine Hydrolysereaktion erleiden. Aus diesem Grund wurden die molaren Extinktionskoeffizienten bei konstanten dem Absorptionsmaximum der der nichtprotonierten Imine entsprechenden Wellenlänge durch Extrapolieren zum Zeitpunkt Null, dem Moment der Einfuhrung der Trifluoressigsäure in die dioxanische Iminlüsung, bestimmt. Das Konzentrationsverhältnis [B]/[BH⁺] wurde aus der Gleichung (5) berechnet :

$$\frac{[B]}{[BH^+]} = \frac{\varepsilon_T - \varepsilon_{BH^+}}{\varepsilon_B - \varepsilon_T} \tag{5}$$

wobei [B], [BH⁺]die Konzentrationen des nichtprotonierten und bzw. des protonierten Imins und

ε_B, ε_{BH^+} ε_T die molaren Extinktionskoeffizienten des Imins in der Abwesenheit, in der Anwesenheit eines bedeutenden Überschusses und bzw. bei verschiedenen Konzentrationen der Trifluoressigsäure sind. Die Basizitätskonstanten wurden dann nach Gleichung (6) berechnet wobei die für einen der Indikatoren bestimmten *H*-Werte verwendet wurden.

$$K_{BH^+} = H \cdot \frac{[B]}{[BH^+]} \tag{6}$$

Ein Rechenbeispiel ist in Tab. 5. zusammengefasst. Die mittleren pK_a-Werte verschiedener Imine sind aus Tab. 1. ersichtlich.

Tabelle 5

Rechenbeispiel des mittleren pK_a-Wertes des *p*-Dimethylaminobenzyliden-3-amino-1.2.4-triazols

$[CF_3COOH]$ M/L	$\varepsilon_T 10^{-4}$ L/M cm	$\frac{[B]}{[BH^+]}$	$pK_a^{a)}$	$pK_{amed.} \pm \sigma$
0	3.2194	—	—	5.42±0.07
0.0440	2.8780	6.590	5.30	
0.0877	2.3332	1.924	5.53	
0.1312	2.2890	1.785	5.39	
0.1743	2.0779	1.270	5.42	
0.2598	1.8104	0.839	5.42	
0.4275	1.4942	0.502	5.43	
2.1375	0.6282	—	—	

a) Indikator : Krysoidin; Temperatur : 25° C.

LITERATURÜBERSICHT

[1] II-te Mitt. : H. H. Glatt, M. F. Barry, C. Csunderlik, R. Bacaloglu, M. Botoacă, S. Savu-Botoacă und D. Fechete. *Rev. Roum. Chim.*, **1985, 31**, 273 (1986).

[2] H. H. Glatt, M. F. Barry, C. Csunderlik, R. Bacaloglu, M. Medeleanu und M. Lantos, *Rev. Roum. Chim.*, **30**, 125 (1985).

[3] F. Badea, "Mecanisme de reacţie în chimia organică", Edit. Ştiinţifică Bucureşti 1973, S. 82.

[4] L. P. Hammett, ,,Physical Organic Chemistry. Reaction Rates, Equilibria and Mechanisms", 2-nd Ed., Mc Graw-Hill, New York 1970, S. 266.

[5] D. D. Perrin, ,,Dissociation Constants of Organic Bases in aqueous Solution". Butterworth, London 1965.

[6] I. R. Bellobono und G. Favini, *Tetrahedron*, **25**, 57 (1969).

[7] H. Lettau, ,,Chemie der Heterocyclen", Vlg. Grundstoffindustrie Leipzig 1980, S. 215.

Revue Roumaine de Chimie, **31**, *3*, 291–296 (1986)

NEUE REINECKESALZÄHNLICHE VERBINDUNGEN MIT DIBUTYL-PHENYLPHOSPHIN und DIPHENYLETHYLPHOSPHIN

CS. VÁRHELYI*, I. GĂNESCU**, A. HANTZ* und I. PAPA**

* Fakultät der Chemischen Technologie, "Babeş-Bolyai Universität", 3400 — Cluj-Napoca, Str. Arany János 11, Rumänien

** Chemische Fakultät der Universität, 1100 — Craiova, Str. Al. Ioan Cuza 13, Rumänien

Eingegangen am 17. XI. 1984

Es wurden neue Substitutionsreaktionen des $K_3[Cr(NCS)_6]$ mit einigen tertiären gemischten Phosphinen (Dibutyl-phenylphosphin und Diphenylethylphosphin) in n-Butanol durchgeführt. Die Herstellung von 24 Salzen mit den Chlorhydraten einiger organischen N-Basen, Metallen und mit Metall(III)-amin-Komplexen bestätigt die Zusammensetzung der neuen Komplexanionen : $[Cr(NCS)_4(\text{Dibutylphenylphosphin})_2]^-$ und $[Cr(NCS)_4(\text{Diphenylethylphosphin})_2]^-$. Zur Klärung einiger Strukturfragen es wurden UV und IR spektrophotometrische Untersuchungen durchgeführt.

New substitution reactions of $K_3[Cr(NCS)_6]$ with mixed tertiary phosphines in n-butanol were carried out. The formulas of the new anions : $[Cr(NCS)_4\ (\text{dibuthylphenylphosphine})_2]^-$ and $[Cr(NCS)_4\ (\text{diphenylethylphosphine})_2]^-$ were established by preparation of 24 new derivatives with the hydrochlorides of some organic N-bases, metals, and metal (III)-ammines. Electronic and IR spectral data are communicated.

EINLEITUNG

Als basische Substanzen bilden die tertiären Phosphine Phosphoniumsalze mit verschiedenen Komplexsäuren, wie z.B. $H_2PtCl_6]$, $H_2[PtBr_6]$, $H_2[Pt(SCN)_6]$, $H[Co(DH)_2(NCS)_2]$, $H_3[Cr(NCS)_6]$, usw.

Reineckate vom (Phosphin) $H[Cr(NCS)_4(NH_3)_2]$ Typ wurden aus Phosphomiumchloride oder — Bromide durch doppelten Umsetzungsreaktionen mit $K[Cr(NCS)_4(NH_3)_2]$ erhalten[1–3].

Issleib und Mitarbeiter[4,5] haben beobachtet dass die sekundären und tertiären aliphatischen Phosphinen mit $K_3[Cr(NCS)_6]$ in siedendem Isopropanol, unter teilweiser Substitution der Thiocyanato-liganden, unter Bildung von reineckesalzanalogen Phosphinkomplexen reagieren. Einige Derivate vom Typ : $K[Cr(NCS)_4(L)_2]$ $(L = (C_2H_5)_2PH$, $(C_2H_5)_3P$, $(C_4H_9)_3P$, $(C_5H_{11})_3P$, $HP(C_6H_{11})_2$ wurden wegen Luftempfindlichkeit der Phosphine in Stickstoffatmosphäre präpariert.

Diese Substitutionsreaktion mit Phosphinoxyden in Isopropanol erzielt Nichtelektrolyte mit der Zusammensetzung : $[Cr(NCS)_3(L)_3]$ $(L = (C_2H_5)_3P{=}O$, $(C_4H_9)_3P{=}O$, $(C_6H_{11})_3P{=}0$[4,5]

In einer Reihe von früheren Arbeiten [6,7] haber wir über die Bildung von Reineckesalzanaloga mit verschiedenen organischen primären und tertiären Aminen und $K_3[Cr(NCS)_6]$ im Schmelzzustand berichtet. Es wurden binäre Komplexsalze des Typs $M[Cr(NCS)_4(Am)_2]$ (Am = Alkylaniline, Alkoxy-aniline, hetero-cyclische N-Base, wie z.B. Pyridin, β- und γ-Picolin, 2,2,-Dipyridyl, 1,10-Phenanthrolin), Benzylamin, usw.) isoliert und charakterisiert.

In Fortsetzung dieser Arbeit haben wir die Wechselwirkung von $K_3[Cr(NCS)_6]$ mit gemischten Alkyl-aryl-phosphinen in verschiedenen Alkoholen, als Lösungsmitteln, untersucht.

Wir haben beobachtet, dass die obenerwähnte Substitutionsreaktion in Methanol und Ethanol wegen komplizierten Solvolysen nicht durchgeführt werden kann.

Es ist bemerkenswert, dass die nukleophilen Eigenschaften der aliphatischen Alkohole gegen Cr(III) in der folgenden Reihe abnimmt.

$$CH_3OH < C_2H_5OH < C_3H_7OH < C_4H_9OH < C_5H_{11}OH$$

Die Alkyl-aryl-phosphine, wie das Dibuthylphenyl-phosphin und das Diphenylethyl-phosphin bilden leicht Reineckesalz-ähnliche Verbindungen nach der Gleichung:

$$K_3[Cr(NCS)_6] + 2\,\text{Phosphin} = K[Cr(NCS)_4(\text{Phosphin})_2] + 2\,KCNS$$

Die verdünnte Lösung der gebildeten Komplexe in einer Mischung von n-Buthanol – Methanol (1 : 5) gibt eine Reihe von Fällungsreaktionen mit Übergangsmetallionen wie Cu(I), Ag(I), Tl(I), Pd(II), Au(I), mit anderen Schwermetallionen (Hg(II), Pb(II), Bi(III)), mit den Chlorhydraten einiger heterocyclischen N-Basen, und insbesonders mit Metal(III)-aminen von verschiedenen Typs (Hexammine, Monoacidopentamine und Diacido-tetramine).

Die erhaltenen neuen Substanzen sind in den Tabellen 1 und 2 charakterisiert.

Diese Komplexsalze sind unlöslich im Wasser, in verdünntem Methanol und Ethanol, lösen sich aber leicht in einigen organischen polaren Lösungsmitteln, wie Aceton, Methyl-ethylketon, Acetonitril, Dimethylformamid und Dimethylsulfoxid.

Die thermische Stabilität der obenerwähnten Komplexsalze ist von der Natur des äusseren Kations und von der Zusammensetung des Komplexanions beeinflusst. Diese Reineckesalzanaloga zersetzen sich beim Erhitzen über 180–240° ohne einem wohlbestimmten Schmelzpunkt, unter freiwerden von Phosphin, HCNS, HCN, CO, CO_2 in nichtstöchiometrischen Verhältnissen.

Der Rückstand bei 650–700° ist eine stöchiometrische Menge von Cr_2O_3, Cr_2O_3+M, bzw. $Cr_2O_3+M_2O$ in Funktion der Natur des Kations.

Die derivatographischen Messungen zeigen, dass die Dezaminierung der $\text{Amin}.H[Cr(NCS)_4(\text{Phosphin})_2]$-Salze ein endothermer Prozess ist. Die Zersetzung des $[Cr(NCS)_4(\text{Phosphin})_2]^-$ Anions geht über 2–3 exothermen oxidativen Processen hervor (300–500°).

Tabelle 1

Neue Komplexsalze des Typs $M[Cr(NCS)_4(Bu_2Ph \cdot P)_2]$

Nr.	Formel	Ausb. %	Charakteristik	Analyse		
					Ber.	Gef.
1	Ag.A	92	Rotviolette mikrokrist. Masse	Ag Cr S	12,93 6,24 15,37	12,72 6,09 15,11
2	Tl.A	91	Rotviolette kurze Prismen	Tl Cr S	21,94 5,60 13,78	21.58 5,51 13,68
3	$Hg.A_2$	94	Gelbbraune unregelmässige Platten	Hg Cr S	12,13 6,29 15,50	12,00 6,20 15,22
4	$Bi.A_3$	88	Braune unregelmässige, kleine Krist.	Bi+3Cr S	15,27 16,09	15,18 15,96
5	Pyridin.HA	79	Rotviolette mikrokrist. Masse	Cr S	6,46 15,90	6,38 15,71
6	γ-Picolin.HA	81	Rotviolette kleine unregelmäss. Prismen	Cr S	6,37 15,63	6,28 15,44
7	sym.-Collidin. HA	77	Rotviolette, dünne Platten	Cr S	6,20 15,28	6,09 15,11
8	o-Phenanthrolin. HA	84	Rotviolette mikrokrist. Masse	Cr S	5,75 14,15	5,66 14,00
9	o-Oxy-Chinolein. HA	91	Gelbbraune grosse Tafeln	Cr S	6,00 14,73	5,88 14,54
10	Cinchonin. HA	92	Rotviolette, dünne Platten	Cr S	5,11 12,57	5,00 12,31
11	$[Co(DH)_2(NH_3)_2]$.A	89	Rotbraune quadratische Prismen	Co+Cr S	10,56 12,21	10,43 12,05
12	$[Co(DH)_2$(p-Toluidin$)_2]$A	87	Braune mikrokrist. Masse	Co+Cr S	9,03 10,43	8,91 10,18
13	$[Co(DH)_2$(m-Amino-Phenol$)_2]$.A	81	Rotbraune quadratische Platten	Co+Cr S	9,01 10,41	8,86 10,22
14	$[Co(DH)_2$(m-Xylidin $)_2]$.A	80	Rotbraune quadratische Platten	Co+Cr S	8,82 10,19	8,71 10,06
15	$[Co(DH)_2$(Thiouree$)_2]$.A	82	Braune mikrokrist. Masse	Co+Cr	9,59	9,43

„A": $[Cr(NCS)_4(Bu)_2PhP)_2]$; $(Bu)_2PhP$ = Dibuthylphenyl-Phosphin DH = Dimethylglyoximrest ($C_4H_7N_2O_2$)

Tabelle 2

Neue Komplexsalze des Typs $M[Cr(NCS)_4(Et(Ph)_2P)_2]$

Nr.	Formel	Ausb. (%)	Charakteristik	Analyse		
					Ber.	Gef.
1	Ag.B	93	Rotviolette mikrokrist. Masse	Ag	13,13	13,05
				Cr	6,33	6,22
				S	15,61	15,44
2	Tl.B	90	Rotviolette, dünne Platten	Tl	22,26	22,18
				Cr	5,67	5,60
				S	13,96	13,81
3	$Hg.B_2$	90	Rotbraune mikrokrist. Masse	Hg	12,29	12,20
				Cr	6,39	6,26
				S	15,74	15,66
4	Pyridin.HB	78	Rotviolette unregelmässige Prismen	Cr	6,55	6,50
				S	16,15	16,02
5	γ-Picolin.HB	80	Rotviolette, dünne Platten	Cr	6,44	6,33
				S	15,81	15,70
6	sym.-Collidin.HB	79	Rotviolette Nadeln	Cr	6,30	6,23
				S	15,53	15,38
7	o-Oxy-Chinolein.HB	92	Gelbbraune dünne Platten	Cr	6,06	6,00
				S	14,95	14,81
8	$[Co(DH)_2(NH_3)_2].B$	90	Rotbraune Nadeln	Co+Cr	10,68	10,57
				S	12,40	12,20
9	$[Co(DH)_2(p\text{-}Toluidin)_2].B$	88	Rotbraune Sternen	Co+Cr	9,11	9,03
				S	10,52	10,26

$B = [Cr(NCS)_4(Et(Ph)_2P)_2]$: $Et(Ph)_2P$ = Diphenylethyl-phosphin

Die Ultrarotspektren der neuen Reineckesalzanaloga wurden in KBr-Presslingen mit einem UR-20 Spektrophotometer (VEB) Carl Zeiss Jena) aufgenommen.

In den Ultrarotspektren wurden die Schwingungsfrequenzen der NCS-gruppe verfolgt.

Von Chamberlain und Bailar[8] sowie von Fujita und Mitarb. [9] wurde festgestellt, dass die $^{\nu}C{=}N$ — Valenzschwingungsfrequenzen der NCS-Gruppe bei den Isothiocyanato-Komplexen des Kobalts um 2110—2140 cm^{-I}, und die entsprechenden $^{\nu}C-S$ — Valenzschwingungsfrequenzen bei 760—810 cm^{-I} auftreten.
Diese Frequenzen erscheinen bei $[Cr(NH_3)_5(NCS)]Cl_2$,

$[Cr(en)_2(NCS)_2]Cl$ bei 2060—2080 cm^{-I}, bzw. bei 730—760 cm^{-I}.

Diese Verschiebung nach niederen Werten bezeichnet die Steigerung des kovalenten Charakters der M-NCS Bindung von Co(III) nach Cr(III).

Im Fall der untersuchten $Ag[Cr(NCS)_4$(Dibuthylphenyl-phosphin)$_2]$ und phosphin $H[Cr(NCS)_4$(Diphenylethyl-phosphin)$_2]$ erscheinen die $^{\nu}C{=}N$—Valenzschwingungsfrequenzen um 2085—2095, bzw. um 2090 cm^{-1} und die $^{\nu}C-S$—Frequenzen bei 755 und 730 cm^{-I}, bzw. 760 und 730 cm^{-I}.

Diese Erscheinung bestätigt, dass im Gegensatz zu den Thiocyanato-Komplexen des Quecksilbers, Platins und Palladiums mit M-SCN – Bindungen, die Chrom-Thiocyanat-Bindung in den Reineckesalz-analoga über das Stickstoffatom erfolgt. (Isothiocyanato-komplexe).

In den Elektronenspektren der $Py.H[Cr(NCS)_4(Bu_2Ph.P)_2]$ und $Py.H[Cr(NCS)_4(EtPh_2P)_2]$ erscheinen 4 Absorptionsbanden, wie im Falle der Reineckesalzanaloga mit N-Basen:

Bu_2PhP – Derivat : 18,000, 25,200, 30,500 und 41,600 cm^{-1}

$EtPh_2P$ – Derivat : 17,700, 25,200, 30,400 und 41,500 cm^{-1} (siehe Abb. 1.)

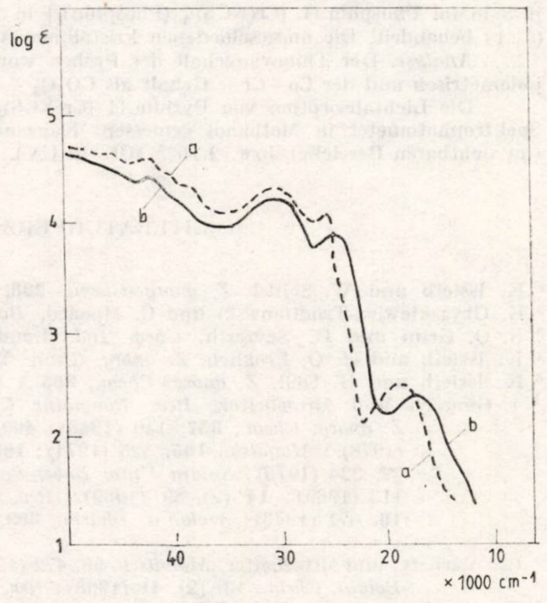

Abb. 1 – Elektronenspektrum von : a. $Py.H[Cr(NCS)_4(Ph_2EtP)_2]$ b. $Py.H[Cr(NCS)_4(Bu_2PhP)_2]$ (in Methanol)

Die Banden im sichtbaren Bereiche entsprechen zu Krystallfeldübergänge (d–d Übergänge) und die letzten zwei Bänden können zu Ladungsüberführung (CT-Übergänge) zugeschrieben werden. Ihre Position ändert sich in gleicher Weise wie im Falle anderer reineckesalzähnlichen Verbindungen. Die neutralen Ligandmoleküle (L in den $[Cr(NCS)_4L_2]^-$-Komplexen) üben einen Einfluss auf die Lage der Kristallfeldbanden (z.B. im Falle : L = m-Toluidin : 17,500, 25,300, L = p-Toluidin : 17,650, 24,800, Pyridin : 17,050, 25,150).

EXPERIMENTELLER TEIL

Phosphin . $H[Cr(NCS)_4 (Phosphin)_2]$ – Lösungen

In einem verschliessbaren Erlenmeyerkolben werden 0,1 Mol entwässertes $K_3[Cr(NCS)_6]$ (54 g) und 0,3 Mol Dibutyl-phenylphosphin (53 g), bzw. Diphenyl-ethyl-phosphin (66 g) in 300 ml n Buthanol innig vermischt und etwa 5–6 Stunden auf dem Wasserbade unter mehrmaligen Umschütteln erhitzt, wodurch die anfangs blauviolette Farbe der Masse in eine dunkelrote übergeht. Nach Abkühlen wird in Methanol auf 1,5 Liter Volumen verdünnt und das rotviolette (Phosphin. H)$_3$ [Cr(NCS)$_6$] Nebenprodukt abfiltriert. Die rotviolette Lösung des Phosphin. H [Cr(NCS)$_4$(Phosphin)$_2$] wird für doppelte Umsetzungsreaktionen verwendet.

Amin.H[Cr(NCS)$_4$(Phosphin)$_2$]. Je 20 mMol des betr. Amins werden mit 10 mL konz. Salzsäure behandelt und das Chlorhydrat in 80—100 ml Wasser gelöst. Die Lösung wird mit 10 mMol Reineckesalzanalog in 50—60 mL Methanol-Buthanol Mischung (5 : 1) behandelt. Nach 10—15 Minuten werden die ausgeschiedenen Kristalle abgesaugt, mit verd. Methanol (1 : 3) gewaschen und dann bei Raumtemperatur an der Luft getrocknet.

Derivate der [Cr(NCS)$_4$ Phosphin)$_2$]$^-$ mit Metallen und Metall (III)-aminen

Je 15—25 mMol MNO$_3$, bzw. je 10 mMol Kobalt(III) — und Chrom(III) — aminsalze von verschiedenem Typ in 100 mL Wasser, oder in verdünntem Methanol (1 : 2) werden mit je 5 mMol Phosphin.H [Cr(NCS)$_4$ (Phosphin)$_2$] in 30—35 mL Methanol-Buthanol-Mischung (5 : 1) behandelt. Die ausgeschiedenen kristallinen Massen werden, wie oben verarbeitet.

Analyse. Der Thiocyangehalt der Proben wurde gravimetrisch als BaSO$_4$, das Chrom jodometrisch und der Co+Cr— Gehalt als CO$_3$O$_4$ + Cr$_2$O$_3$ bestimmt.

Die Lichtabsorption von Pyridin.H [Cr(NCS)$_4$(Phosphin)$_2$] wurde mit einem Specord-Spektrophotometer in Methanol gemessen. Konzentration der Probelösungen : 2.10^{-3} M/L (im sichtbaren Bereiche), bzw. 2.10^{-5} M/L (in UV).

LITERATURVERZEICHNIS

[1] K. Issleib und W. Seidel, *Z. anorg. Chem.*, **288**, 201 (1956).

[2] E. Gryszkiewicz-Trodimowski und C. Monard, *Bull. soc. chim.* (France), **1961**, 2408.

[3] S. O. Grim und D. Seyferth, *Chem. Ind.* (London), **1959**, 849.

[4] K. Issleib und H. O. Fröhlich, *Z. anorg. Chem.*, **298**, 84 (1959).

[5] K. Issleib und G. Döll, *Z. anorg. Chem.*, **305** ,1 (1960).

[6] I. Gănescu und Mitarbeiter, *Rev. Roumaine Chim.*, **12**, 395 (1967) ; **13**, 321 (1968) ; *Z. anorg. Chem.*, **357**, 140 (1968) ; **409**, 121 (1974) ; **423**, 259 (1976) ; **439**, 282 (1978). ; *Monatsh.*, **105**, 525 (1974) ; **106**, 1071 (1975) ; *J. Inorg. Nuclear Chem.*, **37**, 324 (1975) ; *Studia Univ. Babeş-Bolyai, Chem.*, **12**, (1), 103 (1967), **14**, (1), 113 (1969) ; **14** (2), 89 (1969) ; *Rev. Chim. Minérale* (Paris), **6**, 765 (1969), **10**, 671 (1973) ; *Archiv d. Pharm.*, **309**, 887 (1976).

[7] Cs. Várhelyi und Mitarbeiter, *Monatsch.* **98**, 472 (1967), **100**, 106 (1969) ; *Studia Univ. Babeş-Bolyai, Chem.*, **13**, (2), 41 (1968) ; *Rev. Roumaine Chim.*, 16, 695 (1971).

[8] M. Chamberlain und J. C. Bailar, *E. Amer. Chem. Soc.*, **81**, 6412 (1959).

[9] Y. Fujita, K. Nakamoto und M. Kobayashi, *J. Amer. Chem. Soc.*, **78**, 3295 (1956).

Revue Roumaine de Chimie, **31**, *3*, 297—303 (1986)

STUDY OF α-DIAZOKETONES FROM NICOTINYL AND FUROYL CHLORIDES AND HIGHER DIAZOALKANES

R. AGARWAL* and P. BAHADUR
Department of Chemistry, South Gujarat University, Surat — 395 000, India

Received September 23, 1983
Revised September 20, 1985

α-Diazoketones have been synthesized from nicotinyl and furoyl chlorides by the action of higher diazoalkanes and characterized by the action of various reagents on them.

INTRODUCTION

Adopting the method of Arndt and Eister, [1] α-diazoketones have been synthesized, starting from nicotinyl chloride hydrochloride and furoyl chloride and diazoethane, diazopropane and diazobutane in dry ether at 0°C, thus affording ω-diazo-ω-alkyl-β-acetyl pyridine (I) and ω-diazo-ω-alkyl-α-acetyl-furane (II) as thin mobile yellow liquids. Purification even by vacuum distillation was not feasible due to their decomposition.

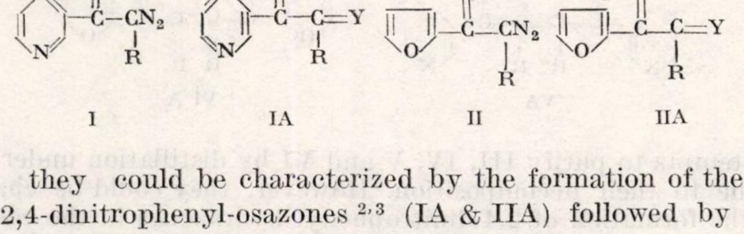

I IA II IIA

However, they could be characterized by the formation of the corresponding 2,4-dinitrophenyl-osazones [2,3] (IA & IIA) followed by element analysis and infrared studies in them (IA & IIA).[4–6]

---

* Correspondence address — R. Agarwal, Chemist, Oil & Natural Gas Commission, Chemistry Section, Sabarmati Ahmedabad-380 005 Gujarat (India).

All the diazoketones with dry hydrogen chloride[7,8] afforded the corresponding chloroketones (III, IV : X = Cl ; R = $-CH_3$, $-C_2H_5$, n$-C_3H_7$)

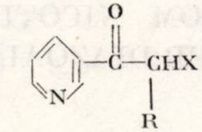
III

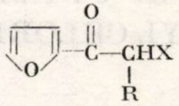
IV

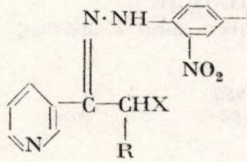
III A

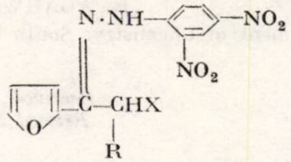
IV A

and similarly on warming in molten phenol[7,8] and benzoic acid[7,8] the corresponding phenoxy (III, IV ; X = $-OC_6H_5$, R = $-CH_3$, $-C_2H_5$, n$-C_3H_7$) and benzoyloxy (III, IV ; X = $-OCOC_6H_5$, R = $-CH_3$, $-C_2H_5$, n $-$ C_3H_7) derivatives as liquids.

On heating the diazoketones in dioxan in the presence of copper powder,[7,8] after loss of nitrogen, the resulting radicals dimerised to V and VI, (R = $-CH_3$, $-C_2H_5$, n$-C_3H_7$), also as liquids.

where Yis =

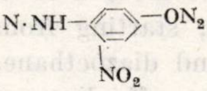

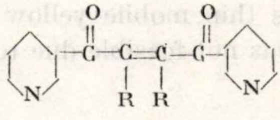
V

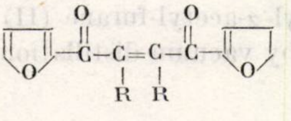
VI

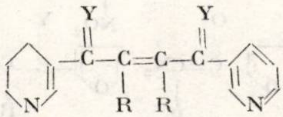
VA

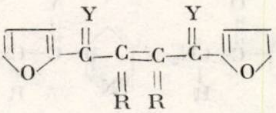
VI A

Attempts to purify III, IV, V and VI by distillation under vacuum failed due to their decomposition. However, they could be characterized by the formation of 2,4-dinitrophenyl hydrazones in the case of III, IV as IIIA and IVA (X = Cl, $-OC_6H_5$, $-OCOC_6H_5$; R = $-CH_3$, $-C_2H_5$, n$-C_3H_7$) and di-2,4 dinitrophenyl-hydrazones in the case of V, VI as VA and VIA (R = $-CH_3$, $-C_2H_5$, n$-C_3H_7$), followed by element analysis and infra-red studies in IIIA, IVA, VA and VIA as given in the experimental part.

EXPERIMENTAL

ω-Diazo-ω-alkyl-β-acetyl-pyridine I ($R= -CH_3$, C_2H_5, $n-C_3H_7$) : An alcoholic solution of nicotinyl chloride — hydrochloride, m.p.156°, (4.42 g, .025 mole ; 4.42 g, .025 mol ; 3.56 g, 020 mol respectively) was added gradually to an ethereal solution of preestimated diazoethane (4.2 g, .074 mol), diazopropane (5.25 g, .075 mol) and diazobutane (5.04 g, .06 mol) at 0°, under dry conditions.

On keeping overnight and removal of the solvent the diazoketones I (3.2 g, 80 % ; 3.65 g, 85 % ; 3.14 g, 85 % respectively) were obtained as yellow mobile liquids. Purification even under vacuum was not possible, due to their decomposition.

ω-Diazo-ω-alkyl-α-acetyl-furane II ($R= -CH_3$, $-C_2H_5$, $n-C_3H_7$) : The ethereal solution of furoyl chloride, b.p. 173°, (5.22 g, .044 mol ; 4.56 g, .038 mol ; 3.91 g, .033 mol respectively) was added gradually to an ethereal solution of pre-estimated diazo-ethane (4.48 g, .088 mol), diazopropane (4.9 g, .076 mol) and diazobutane (5.04 g, .066 mols) at 0° under dry conditions.

On keeping overnight and removal of the solvent the diazoketones II (5.94 g, 90 % ; 4.56 g, 74 % ; 4.75 g, 82 % respectively) were obtained as yellow mobile liquids. Purification even under vacuum was not possible, due to their decomposition.

ω-Chloro-ω-alkyl-β-acetyl-pyridine III ($X=C1$; $R= -CH_3$, $n-C_3H_7$) *and ω-chloro-ω--alkyl-α-acetyl-furane IV* ($X=C1$; $R=CH_3$, C_2H_5, n-C_3H_7) : Dry hydrogen chloride gas was passed into the solution of diazoketones I and II (1 g each) in glacial acetic acid for half an hour. On keeping overnight and working out, afforded III (0.746 g, 71 % ; 0.70 g, 67 %) and IV (0.812 g, 77 % ; 0.77 g, 74 % ; 0.69 g, 67 %) as yellow liquids.

ω-Phenoxy-ω-alkyl-β-acetyl-pyridine III ($X= -OC_6H_5$; $R= -CH_3$) *and ω-phenoxy-ω-alkyl-α-acetyl-furane IV* ($X=OC_6H_5$; $R= -CH_3$, $-C_2H_5$) : On warming the diazoketones I and II (1 g each) with molten phenol (1 g), eliminated nitrogen, after washing with 1 % NaOH afforded III (0.868 g, 62 %) and IV (0.986 g, 76 % ; 0.91 g, 65 %) as yellow liquids.

ω-Benzoyloxy-ω-alkyl-β-acetyl-pyridine III($X= -OCOC_6H_5$; $R=CH_3$, $n-C_3H_7$) and ω-benzoylexy-ω-alkyl-α-acetyl-furane IV ($X=OCOC_6H_5$; $R = -CH_3$, $-C_2H_5$) : The diazoketones I and II (1 g each) when heated with molten benzoic acid (1 g), eliminated nitrogen ; after washing with 5 % sodium carbonate solution afforded III (1.16 g, 74 % ; 0.98 g, 65 %) and IV(1.26 g, 78 % ; 0.96 g, 62 %) as yellow liquids.

1,2-Dialkyl-1,2-β-β′-dinicotinyl-ethene V ($R= -CH_3$, n-C_3H_7) *and 1,2-dialkyl-1,2-α-α′-difuroyl-ethene VI* ($R= -CH_3$, $-C_2H_5$) : When the diazoketones I and II (0.8 g each) were refluxed for three hours in dioxan in the presence of pinch of copper powder, eliminated nitrogen and the resulting radicals dimerised to V (0.62 %g, 76 % ; 0.572 g, 69 %) and VI (0.60 g, 74 % ; 0.51 g, 62 %) as red liquids.

I and II with aq-alcoholic-sulphuric acid solution of 2,4-dinitrophenyl hydrazine afforded the Osazones as I A & II A, III and IV afforded hydrazones as III A & IV A and V and VI di-2,4-dinitrophenyl hydrazones as V A & VI A, followed by their element analysis and infra-red spectra, as described in table 1. The infra-red spectra were recorded on Perkin Elmer 157 model.

INFERENCE

The above series of experiments concludes that heterocyclic ring also undergoes in reaction to give α-diazoketones.

ACKNOWLEDGEMENT. The authors are thankful to the Vice-Chancellor, South Gujarat University, Surat, for providing necessary facilities to carry out the above work.

Table 1

Compound	2,4-DNP derivatives, m.p.	Molecular formula of derivative	Element				Analysis				I.R. frequencies—cm^{-1} in 2,4 DNP derivative
			Calculated				Experimental				
			C%	H%	N%	Cl %	C%	H%	N%	Cl %	
I,R= $-CH_3$	320°C	$C_{20}H_{15}O_8N_9$	47.15	2.95	24.75	—	47.51	3.24	24.58	—	1620(C=N), 1418(C=CH_3), 1330(C—NO_2).
I,R= $-C_2H_5$	262°C	$C_{21}H_{17}O_8N_9$	48.10	3.25	24.09	—	47.68	2.91	23.68	—	1620(C=N), 1342(C—NO_2), 748 (ethyl group.)
I,R= $-n-C_3H_7$	224°C	$C_{22}H_{19}O_9N_9$	49.16	3.54	23.44	—	49.98	3.84	22.98	—	1620(C=N), 1340(C—NO_2), 747(n-propyl group)
II,R=$.CH_3$	172°C	$C_{19}H_{14}O_9N_8$	45.78	2.81	22.48	—	46.29	3.08	22.88	—	1610(C=N), 1380(C—CH_3), 1325(C—NO_2).
II,R= $-C_2H_5$	C	$C_{20}H_{16}O_9N_8$	47.78	3.12	21.87	—	46.97	3.32	21.51	—	1618(C=N), 1327(C—NO_2), 750(ethyl group)
II,R=$n-C_3H_7$	209°C	$C_{21}H_{18}O_9N_8$	47.87	3.42	21.29	—	47.66	3.28	20.91	—	1612(C=N) 1340(C—NO_2), 735(n-propyl group)
III,X=Cl R=CH_3	248°	$C_{14}H_{12}O_4N_5Cl$	48.07	3.43	20.28	10.13	47.88	3.08	21.12	10.73	1620(C=N), 1632(C—CH_3), 1340(C—NO_2). 680(C—Cl).
III,X=Cl R=$n-C_3H_7$	256°	$C_{16}H_{16}O_4N_5Cl$	50.86	4.24	18.54	9.40	50.44	4.48	18.48	9.11	1620(C=N), 1340(C—NO_2), 680(C—Cl), 754(n-propyl group).

IV,X=Cl R=$-CH_3$	72°	$C_{13}H_{11}O_5N_4Cl$	46.08	3.24	16.69	14.88	46.99	3.46	16.81	14.24	1620 (C=N) 1380 ($C-CH_3$), 1340 ($C-NO_2$), 690 (C−Cl).
IV,X=Cl R=C_2H_5	176°	$C_{14}H_{13}O_5N_4Cl$	47.69	3.68	15.88	14.05	47.43	3.41	15.63	14.60	1620 (C=N), 1340 ($C-NO_2$), 690 (C−Cl) 737 (ethyl group)
IV,X=Cl R=n−C_3H_7	98°	$C_{15}H_{15}O_5N_4Cl$	49.11	4.09	15.27	13.32	49.36	4.16	15.53	13.61	1620 (C=N), 1338 ($C-NO_2$), 687 (C−Cl), 730 (n-propyl group).
III,X=$-OC_6H_5$ R=$-CH_3$	226°C	$C_{20}H_{17}O_5N_5$	58.97	4.18	17.20	—	58.67	4.29	17.68	—	1618 (C=N), 1428 ($C-CH_3$) 1065 (OC_6H_5), 1340 ($C-HO_2$)
IV,X=$-OC_5H_5$ R=$-CH_3$	221°	$C_{19}H_{16}O_6N_4$	57.57	4.06	14.14	—	57.87	4.26	14.56	—	1605 (C=N) 1380 (C−CH3), 1070 ($-OC_6H_5$) 1325 ($C-HO_2$)
IV,X=OC_6H_5 R=$-C_2H_5$	136-8°	$C_{20}H_{18}O_6N_4$	58.53	4.39	13.65	—	58.79	4.52	13.43	—	1620 (C=N), 1082 ($-OC_5H_5$) 1340 ($C-NO_2$) 780 (ethyl group)
III,X=$OCOC_5H_5$ R=CH_3	199°	$C_{21}H_{17}O_6N_5$	58.06	3.69	16.13	—	58.48	3.80	16.40	—	1615 (C=N), 1421 ($C-CH_3$), 1338 ($C-NO_2$), 1218 ($-OCOC_6H_5$)
III,X=$OCOC_6H_5$ R=n−C_3H_7	226°	$C_{23}H_{21}O_6N_5$	59.61	4.54	15.12	—	59.87	4.43	14.96	—	1617 (C=N), 1330 ($C-NO_2$), 1240 ($-OCOC_5H_5$) 760 (n-propyl group)
IV,X=OCO_6H_5 R=$-CH_3$	182°	$C_{20}H_{16}O_7N_4$	56.60	3.77	13.20	—	56.36	3.98	13.43	—	1620 (C=N) 1735 ($-OCOC_5H_5$) 1338 ($C-NO_2$)

Table 1 (continued)

Compound	2,4-DNP derivatives, m.p.	Molecular formula of derivative	Element Analyses Calculated				Experimental				I.R, frequencies Cm^{-1} in 2,4 DNP derivative
			C%	H%	N%	C1%	C%	H%	N%	C1%	
IV, X= — $-OCOC_6H_5$ R= $-C_2H_5$	136°	$C_{21}H_{18}O_7N_4$	57.53	4.11	12.77	—	57.21	3.93	12.62	—	1617 (C=N), 1720 ($-OCOC_6H_5$) 1338 ($C-NO_2$)
V, R= $-CH_3$	232°	$C_{28}H_{22}O_8N_{10}$	53.67	3.40	21.67	—	53.48	3.17	21.44	—	1620 (C=N) 1430 ($C-CH_3$) 1340 ($C-NO_2$) 1670 (C=C)
V, R= n $-C_3H_7$	240°	$C_{32}H_{30}O_8N_{10}$	56.45	4.39	20.52	—	56.83	4.16	20.36	—	1618 (C=N), 1338 ($C-NO_2$), 1660 (C=C), 745 (n-propyl group)
VI, R= $-CH_3$	191-2°	$C_{26}H_{20}O_{11}N_8$	51.65	3.31	18.54	—	51.44	3.67	18.20	—	1610 (C=N), 1380 ($C-CH_3$), 1325 ($C-NO_2$), 1670 (C=C)
VI, R= C_2H_5	162°	$C_{28}H_{24}O_{10}N_8$	53.16	3.79	17.72	—	53.36	3.62	18.08	—	1610 (C=N), 1330 ($C-NO_2$), 748 (ethyl group) 1670 (C=C).

REFERENCES

[1] Arndt. Eistert and Partale, *Ber.*, **60**, 1364 (1927).
[2] Satish Kumar and S. M. Gupta, *E. Indian Chem. Soc.*, **43**, 2, 95 (1966).
[3] L. Canorica, *Gazz. Chim. Ital.*, **80**, 412 (1950).
[4] L. J. Ballamy, "Introduction to infra-red spectra of complex molecules "Methuna & Co. London, 1968.
[5] Norman B. Colthup, H. Daly Lowrence, E. Wiberley, Stephen, "Introduction to infra-red and Raman spectroscopy", Academic Press, New York and London, 1964.
[6] John R. Dyer, "Application of absorption spectroscopy of organic compcunds", Prentice Hall of India Ltd., New Delhi, 1978).
[7] L. Wolff, *Ana,* **394**, 23 (1912).
[8] K. C. Mathur, Ph. D. Thesis, Agra University, Agra, India, 1977.

Revue Roumaine de Chimie, **31**, *3*, 305—308 (1986)

CHARACTERIZATION OF THE COMPLEXES OF Ti(III) AND Zr(IV) WITH TETRATHIAZYL HYDROFLUORIDE BY UV, EPR AND XRD SPECTRA

H. K. SHARMA, A. K. YADAV and S. P. S. JADON*
Department of Chemistry, S. V. College, Aligarh-202001, India

Received September 3, 1984

Tetrathiazyl hydrofluoride (TTAHF) was prepared, studied and used as ligand (L) to prepare its complexes with Ti(III) and Zr(IV) compounds. The complexes were studied with the help of electronic, EPR and X-ray diffraction spectra. "TTAHF" is found to be semiconductor and paramagnetism with σ band. The complexes show spin allowed Laporte forbidden transitions with charge transfer environment, diamagnetic and semiconductive nature. The $L.Ti_2(SO_4)_3$ has face-centered cubic (fcc) (hexagonal) structure, while the complex $L.ZrOCl_2$, with permitive lattice (triclinic) structure is a polymeric complex.

Halogen derivatives of S_4N_4 have been reported[1-7] and their complexes with metal compounds have been prepared [8]. However an adduct (S_4N_4 with H_2F_2) which is denominated as tetrathiazyl hydrofluoride [9] (TTAHF), was neither prepared, nor used as ligand to prepare its complexes with metal compounds. In the present communication the complexes of "TTAHF" with Ti(III) and Zr(IV) compounds are investigated, and their UV, EPR and XRD spectra are reported.

EXPERIMENTAL

Doubly distilled, free from water, AnalaR grade chemicals were used for all preparations, S_4N_4 was prepared as described[10] and its adduct, TTAHF was prepared by passing dry hydrogen fluoride gas into benzene solution of S_4N_4 at 290 K with constant mechanical stirring for about 4—5 hrs till a reddish yellow precipitate was obtained. The reddish yellow mass was separated by filtration and washed with benzene, followed by ether and dried in dry air.

Alcoholic solutions of $Ti_2(SO_4)_3$ and $ZrOCl_2$ were mixed separately with alcoholic solution of "TTAHF" and refluxed for about 24 hrs. Different coloured products were found; they were filtered and successively washed with alcohol and ether. The complexes formed were dried in vacuo.

TTAHF and its complexes with $Ti_2(SO_4)_3$ and $ZrOCl_2$ were qualitatively and quantitatively analysed by well known methods.[11] Electronic (reflectance) and EPR spectra were recorded on VSU-22 UV spectrophotometer and X—E—4 band spectrometer respectively at room temperature. XRD spectra of the complexes were carried out on XDR-6 model G.M. 11 diffractometer by using CuK_α ($\lambda = 1 \cdot 5418A$) as source of radiations.

---

* For correspondence, 3/206, Shyam Nagar, Aligarh (U.P.) 202001.

RESULTS

The factors, oscillator strength (f), Racah parameter (B) and ratio, ν_2/ν_1, calculated from the electronic spectra of the complexes and 'TTAHF' are given in Table 1.

EPR spectrum of 'TTAHF' has a single peak with $g = 1{\cdot}994$, $\mu_{eff} = 1{\cdot}73$ BM, $X_A = 1{\cdot}232 \times 10^{-3}$ and $A = 40$G, while the EPR spectra of the complexes do not show any signal.

From the X–RD powder diffraction spectra of the complexes, the Miller indices, *hkl*, I/I_0 and d(Å) are calculated (Tables 2 and 3).

Table 1

Electronic spectra of complexes of 'TTAHF' with $Ti_2(SO_4)_3$ and $ZrOCl_2$

Complexes	Assignments (cm^{-1})	Transitions	'f'	D_q (cm^{-1})	B (cm^{-1}	ΔE (e.v.	ν_2/ν_1
$L.Ti_2(SO_4)_3$	30303(v_1) 32553(v_2)	$^2E_g(D) \rightarrow {}^2T_{2g}(D)$ c.T.	2.32×10^{-5}	1225.0	2450	1.52	1.07
$[L.ZrOCl_2]_{1,98}$	27777(v_1) 38461($v)_2$	$^3T_{1g}(F) \rightarrow {}^3T_{2g}(F)$ C.T.	2.16×10^{-4}	1068.4	1335.5	1.32	1.38

Abbreviation : $L = S_4N_4H_2F_2$

Table 2

X-ray powder diffraction data of $L.Ti_2(SO_4)_3$ complex

2 O	Sin O	*hkl*	d(Å)	I/I_0
23.2	0.2011	111	3.8306	5.80
26.6	0.2300	200	3.3482	4.34
38.3	0.3280	220	2.3480	100.00
44.5	0.3787	311	2.0342	95.60
48.0	0.4067	222	1.8937	2.90
55.9	0.4687	400	1.6434	1.45

Table 3

X-ray powder diffraction data of $[L.ZrOCl_2]_{1.98}$, polymeric complex

2 O	Sin O	*hkl*	d(Å)	I/I_0
13.2	0.1149	100	6.7015	42.86
18.8	0.1633	110	4.7160	14.29
23.3	0.2019	111	3.8144	28.57
26.2	0.2266	200	3.3984	57.14
30.0	0.2588	210	2.9760	21.42
33.0	0.3146	211	2.7120	100.00
37.8	0.3239	220	2.3779	28.57
40.8	0.3485	221	2.2097	14.29
42.9	0.3657	310	2.1063	28.57
45.3	0.3851	311	2.0001	21.42
46.4	0.3939	222	1.9552	28.57
48.1	0.4075	320	1.8900	35.71
50.7	0.4282	321	1.7958	21.42
54.7	0.4594	400	1.6765	35.71
57.5	0.4810	410	1.6014	35.71
59.3	0.4947	411	1.5570	14.29

DISCUSSION

From the quantitative estimation, molecular weights determination and I.R. spectral studies,[12] the molecular formulae of TTAHF and its complexes with $Ti_2(SO_4)_3$ and $ZrOCl_2$ are expressed as $S_4N_4H_2F_2$, $[S_4N_4H_2F_2 \cdot \cdot Ti_2(SO_4)_3]$ and $[S_4N_4H_2F_2,\ ZrOCl_2]_{1 \cdot 98}$.

Electronic Spectra

Electronic spectrum of $S_4N_4H_2F_2$ (TTAHF) possesses the peaks according to 3·26 and 3·64 e.v., indicating the absence of ionisation environment and formation of σ bond in it. The oscillator strength ($f = 4 \cdot 34 - 5 \cdot 06 \times 10^{-5}$) suggests the spin allowed Loparate forbidden transition in it. The value of band gap energy ($\Delta E = 0 \cdot 38$ e.v.) testifies its semiconductivity.

UV spectrum of complex $L.Ti_2(SO_4)_3$ has two peaks corresponding to 30303 (ν_1) and 42553 (ν_2) cm^{-1}, out of which the former vibration is due to the ${}^2E_g\,(D) \leftarrow {}^2T_{2g}\,(D)$ transition of Ti atom while the latter frequency suggests the charge transfer due to coordination of ligand to Ti atom in the complex. The occurrence of charge transfer is also inferred by ratio $\nu_2/\nu_1 = 1 \cdot 07$ which lies in the range of $1 \sim 2$. The electronic spectrum of the complex, $L.ZrOCl_2$, is somewhat similar to spectrum of $L.Ti_2(SO_4)_3$, showing only two peaks at 27777 and 38461 cm^{-1}. Out of these absorptions, the band at 38461 cm^{-1} is due to a charge transfer which is also confirmed by the ratio $\nu_2/\nu_1 = 1 \cdot 38$ $(1 \sim 2)$.

Theoretically zirconium must have three (d — d) transitions ${}^3T_{1g}(f) \rightarrow {}^3A_{2g}(F)$; ${}^3T_{1g}(F) \rightarrow {}^3T_{2g}(F)$ and ${}^3T_{1g}(F) \rightarrow {}^3T_{2g}(F)$. But ony the middle transition ${}^3T_{1g}(F) \rightarrow {}^3T_{2g}(F)$ (at 27777 cm^{-1}) appears at a slightly higher frequency while the other two transitions have disappeared inferring polymerization in the complex.

The values of oscillator strength, f, for both complexes are found of the order of 10^{-5} to 10^{-4}, showing the presence of spin allowed Laporte forbidden transitions in them. The band gap energy, (ΔE) calculated (Table 1) for the complexes, explains that both complexes appear to be semiconductor.

EPR Spectra

EPR spectra of the ,,TTAHF'' suggest that it is paramagnetic in character with an unpaired electron, which may cause the hydrogen bonding in it.

No signals are found for the complexes, indicating that both complexes are diamagnetic and formed due to spin orbital coupling between metal and ligand. But the blurring in EPR spectrum of the complex, $L.ZrOCl_2$ suggests its polymeric form.

X-ray Powder Diffraction Pattern of the Complexes

The X-ray powder diffraction spectra of the complexes were obtained over the 2θ range 6° to 60°. Miller indices, I/I_0 and d(Å) values were determined and compared to the values calculated for S_4N_4.[13] The decrease in the intensities of the (111) and (100) to other peaks leads to suppose the less crystallization of the complexes. The *hkl* found for L.$Ti_2(SO_4)_3$ correspond to the hexagonal (fcc) structure of each unit cell with semiconductivity along the (111) direction. The complex L.$ZrOCl_2$, for which *hkl* are according to triclinic structure in permitive lattice, is a polymeric complex showing the semiconductivity to (100) direction.

ACKNOWLEDGEMENT. Authors are thankful to CSIR (India) for its financial support to KHS.

REFERENCES

[1] G. Wolmershaeuser, G. B. Street. and R. D. Smith, *Inorganic Chem.*, **18**, 383 (1979).

[2] L. Zborilova and P. Gebauer, *Z. Anorg. All. gem. Chem.*, **448**, 5, (1979).

[3] A. J. Banister, J. A. Durrant et al., *J. Chem. Soc. Dalton Trans.*, **10**, 928, (1976).

[4] R. D. Harcourt, *J. Inorg. Nucl. Chem.*, **39**, 237 (1977).

[5] L. Zborilova and P. Gebauer, *Z. Chem.*, **19**, 32 (1979).

[6] Y. Monteil, H. Vincent and M. P. Berthet, *Ann. Chem.* (Paris), **5**, 431, (1980): *Synth. Inorg. Met. Org. Chem.*, **10**, 99 (1980).

[7] H. W. Roesky, O. Glemser et al., *Chem. Ber.*, **101**, 1215 (1968).

[8] R. C. Paul, R. P. Sharma, R. D. Verma and J. K. Puri, *Indian J. of Chemistry* (Sec. A), **18**, 516 (1979).

[9] S. P. S. Jadon and H. K. Sharma, *Proc. Indian Chem. Soc.*, **20**, 10 (1983).

[11] M. Goehring, *Chem. Ber.*, **80**, 110 (1947).

[10] A Text Book of Quantitative Inorganic Analysis, ELBS Publication (1968).

[12] S. P. S. Jadon and H. K. Sharma, Rev. Roumaine Chimie (Communicated).

[13] Shuichi Hamada, A. Takanashi and T. Shirai, *Bull. Chem. Soc. Japan*, **44**, 1433 (1971).

Revue Roumaine de Chimie, **31**, *3*, 309—322 (1986)

CONCERNING "THE RELATION BETWEEN MOMENTS OF INERTIA, STERIC CROWDING AND LIBRATIONAL MOTION IN MOLECULES. EFFECTS ON NMR SPECTRA"[1]

ADRIAN O. FULEA

Department of Physical Chemistry and Electrochemical
Technology, Polytechnic Institute of Bucharest, Bd. Republicii 13
Bucharest, Romania

Received October 6, 1982
Revised May 15, 1985

An analysis of the main factor in which originates the major contribution to the magnitude of the chemical shift difference of the diastereotopic *ortho* protons in *para* substituted N-thiobenzoylmorpholines indicates the existence of three different diastereomers. For *meta* substituted analogous, the NMR spectra and molecular models indicate six different diastereomers. It is presented an elaboration of the explanation of the coalescence of the geminal anisochronous protons by librational motion, but it is withdrawn the interpretation[1] which proposed line broadening by librational motion.

INTRODUCTION

In a series of papers we have introduced the theory of the effects of the librational motion in NMR spectra,[1–4] starting from an earlier note of Kurland and Wise,[5] which demonstrated that the librational motion can substantially change the chemical shifts in some systems. Our interpretations of some of the spectral features, on the basis of which we proposed our theory, were proved to be erroneous by Fraser and Taymaz,[6] Berg[7] and Jennings and Randall.[8]

In the present paper we are reinterpreting some other spectra[1] in the light of Berg criticisms[7]; our reinterpretation led us to interesting conclusions in regard to the stereochemistry of these compounds. Further to our paper[1] a more specifical and documented presentation of our theory of the coalescence of geminal chemical shift nonequivalent protons by librational motion was thought to be indicated, because this phenomenon is not yet accepted as valid in the literature.[8]

In this paper we will discuss the NMR data* for the following compounds :

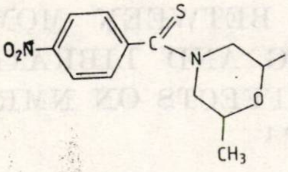

1(cis)

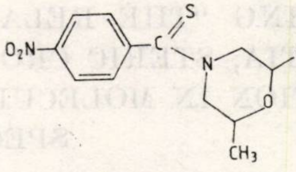

2(trans)

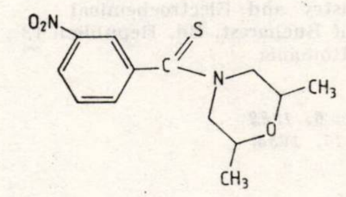

3(cis)

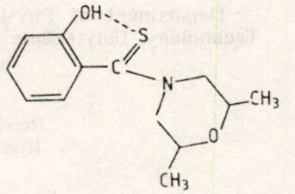

4(cis)

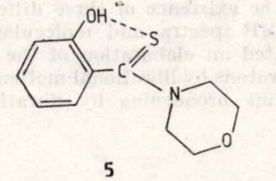

5

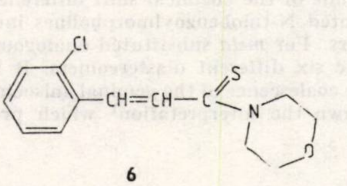

6

The abbreviations and notations throughout the paper are : a = axial, e = equatorial ; *syn* and *anti* denote the position in regard to the sulphur.

CONFORMERS OF THE *CIS* ISOMER OF 2,6-DIMETHYL-4-(4′-NITROTHIOBENZOYL) MORPHOLINE, 1

To begin with we have to withdraw our claiming that for the *trans* isomer of 2,6-dimethyl-4-(4′-nitrothiobenzoyl) morpholine, **2,** the barrier E_{steric} [2] cannot in principle be determined[9] ; although the two *ortho* protons exchange places during the rapid ring inversion, they remain still diastereotopic on NMR time scale. Therefore Berg[7] was correct claiming that E_{steric} [2] was seen frozen for this compound in ^{13}C NMR spectra contrary to our assertion.[9]

What we think that still needs explanation is the chemical shift difference for the two *ortho* phenyl protons, after the freezing of the rotation around aryl-C(S) bond, E_{steric}, for **1**. As Lyle and Pridgen underlined, the diastereotopic relationship of two hydrogens is a necessary but not a sufficient requirement for them to have ^1H NMR signals showing different chemical shifts.[10] The part of **1**, which renders diastereotopic on NMR time scale the *ortho* phenyl protons, is far apart by them and contains only groups with a very small anisotropy. Thus we think that the magnetic influence on the *ortho* protons from this part cannot explain their difference of chemical shift of around 25 cps at 300 MHz*. We are proposing a conformer populations effect to explain it.

---

* The spectra published in the present work were published by us previously [1,4] and we republished them here at the request of the Editor.

According to Fig. 1, the compound **1** can exist either in two conformers A and C, or in three conformers A, B, C. We cannot predict only form Dreiding models if the B conformer exists because the conformation B might involve a rather large steric interaction between the *anti ortho* phenyl hydrogen and both *anti* NCH_2 hydrogens.

Because of the small overlapping between the Van der Waals radii of the *anti ortho* proton and the *anti* axial NCH proton, the process $B \rightleftarrows C$ should be rapid on NMR time scale at all the temperatures which can be reached in NMR experiments.

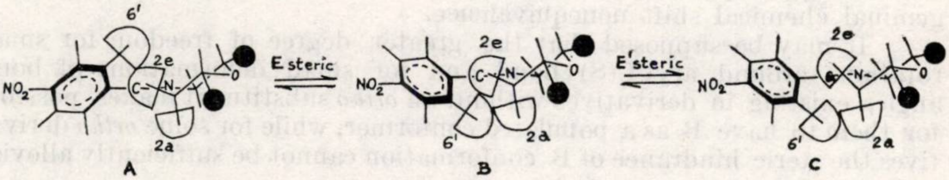

Fig. 1. — The conformers of *cis* isomer of 2,6-dimethyl-4-(4'-nitrothyobenzoyl) morpholine, **1**.

We are presuming that the two *ortho* phenyl hydrogens have quite close values of chemical shift in the A, B and C conformers, which is reasonable; their chemical shifts are therefore determined by the position *syn* or *anti* to the sulphur; in this approximation we can write:

a) in the case that two conformers A and C exist:

$$\Delta \nu_{ortho} = (p_C - p_A)(\nu_{syn} - \nu_{anti}) \tag{1}$$

b) in the case of the existence of B, A and C conformers:

$$\Delta \nu_{ortho} = (p_B + p_C - p_A)(\nu_{syn} - \nu_{anti}) \tag{2}$$

The phenyl moiety is titled by more than 45° in regard to the CSN plane, and $(\nu_{syn} - \nu_{anti})$ should have a rather small value, so we believe that the real case is described by equation (2), rather than by equation (1), i.e. all three conformations depicted in Fig. 1 exist as equilibrium conformations.

Another support for our proposal of a conformer populations effect causing $\Delta\nu_{ortho} \neq 0$ is the finding that, in ^1H NMR spectra, for the *trans* isomer of 2,6—dimethyl-4-(3'-nitrothiobenzoyl)morpholine, $\Delta \nu_{ortho} = 0$, after the barrier E_{steric} was frozen, at 220 MHz[2,7] for **1**. For **2** the type of conformer equilibrium $A \rightleftarrows B$ is rapid through ring inversion* so, at NMR time scale, a molecule will exist in all three types of conformers, A, B and C and an *ortho* phenyl proton will be found in both positions *syn* and *anti* to the sulphur atom**, in this way remaining only the difference in the magnetic influence from the part $CH(CH_3)OCH(CH_3)$ for the two *ortho* protons, but this influence is so small if any, that cannot be sensed by ^1H NMR spectroscopy even at 220MHz resolution and Berg had to rely on ^{13}C NMR in order to determine the barrier E_{steric} for **2**.[6]

---

* The experimentally observed $\Delta\nu_{ortho}$ for the *cis* isomer of 2,6-dimethyl-4-(3'-nitrothiobenzoyl)morpholine and 4-methyl-1-(3'-nitrothiobenzoyl) piperidine respectively, practically the same, 26 cps[1] shows indeed that it is not the magnetic influence of $CH(CH_3)$ $OCH(CH_3)$ or $CH_2CH(CH_2)CH_2$ which is responsible for the $\Delta\nu_{ortho} \neq 0$.

The present discussion of the conformer populations effect as the main factor which contributes to the magnitude of $\Delta\nu_{ortho}$ in ^1H NMR spectra is resembling the problem of the origin of the geminal chemical shift nonequivalence of *syn* NCH_2 diastereotopic protons in *ortho* (thio)benzamides.[11a], [11b]. The similarity of the two problems was observed previously by Fraser and Taymaz[6], but unfortunately they failed to see all the aspects of the problems.***

The fact that, for the geminal *syn* NCH_2 protons in *ortho* thiobenzoylmorpholines and -piperidines, $\Delta\nu^{syn} \neq 0$ was found[11a] even when only two different conformers were detected experimentally[14] is explained by the fact that $\nu^{syn}_a - \nu^{syn}_c$ is very large, so the conformer population difference $|(p_C - p_A)|$ can be small and still the NCH_2 protons exhibit a geminal chemical shift nonequivalence.

It may be supposed that the greater degree of freedom for small rotations around aryl-C(S) bond and for small deformations of bond angles existing in derivatives without an *ortho* substituent makes possible for them to have B as a populated conformer, while for some *ortho* derivatives the steric hindrance of B conformation cannot be sufficiently alleviaed in order to have B as a populated equilibrium conformation, because of the constrain imposed by the *ortho* substituent.

---

* For **1** this $A \leftrightarrows B$ equilibrium, although rapid from the kinetic point of view, is restricted in the thermodynamic sense.

** The $E\pi$ barrier is overpassed rapidly on NMR time scale for both **1** and **2**.

*** Recently some inconsistent proposals were also advanced by Cercasov, Ciureanu et al.[12] in regard to the 1-(4′-nitrothiobenzoyl)homopiperidine. These authors found experimentally that "the signals of the *syn* and *anti* "NCH_2" protons have different patterns; the former is a triplet, whereas the latter is a broad singlet".

The authors state that "it is difficult to assess whether this difference is due to the existence of two rotameric conformations with unequal populations, or to intrinsic molecular asymmetry". Firstly the spectrum does not support a geminal chemical shift nonequivalence of any of the two NCH_2, groups the broadening of the *anti* NCH_2 protons being due to a so-called virtual coupling with the C_5 protons. Such a phenomenon was found already by us for the *syn* NCH_2 protons in thiobenzoylpiperidines. [13] Probably there are three conformers, analogues to the conformers A, B and C described here for **1**. Because the barrier E_π is overpassed rapidly on NMR time scale the geminal NCH_2 protons are rendred enantiotopic, so no phenomenon of geminal chemical shift nonequivalence could be suspected as being involved and, to our best knowledge, only for this phenomenon is possible such a statement as the authors propsed.[12] By the same token the intrinsic asymmetry is il on NMR time scale. It should be noted that, to our knowledge, no geminal chemical shift nonequivalence of NCH_2 geminal protons was found to date for any *para* substituted (thio)benzamide. In relation to our above remark we have to correct also an errer appearing in our paper[1]. Thus, based on Fig.4,[1] the NCH_2 geminal protons, in 4-(4′-nitrothiobenzoyl) morpholine should remain diastereotopic on the NMR time scale whereas the rotation $E\pi$ (ΔE^{1}_{conj}) is rapid. The same might therefore be expected by one, for 1-(4-nitrothiobenzoyl) homopiperidine by analogy. However, Fig. 4[1] is erroneous. The real conformational process through the rotation $E\pi$i s $A \rightleftharpoons B'$ for both 4-(4′-nitrothiobenzoil)morpholine and 2,6-dimethyl 4-(4′-nitrothiobenzoyl)morpholine, as can be easy seen looking on the models. For the former compound Fig. 4[1] indicates erroneously the process $A \overset{E\pi}{\rightleftharpoons} A'$.

The force which sets in the Van der Waals contacts between the *ortho* phenyl proton and the *anti* NCH_2 proton(s) in A, B and C conformers of **1** is due to the existing conjugation between the π electrons of the phenyl and thioamide moieties. We are making this point because of a somewhat different opinion expressed by Berg and Sandström,[15] which were asserting that the above conformers are existing only in the case of *ortho* OH...S hydrogen bonded systems. Fraser and Taymaz[6] were also claiming that there is no conjugation in our class of compounds.[2] Such a conjugation does exist even in N,N-dimethyl-2-methoxythiobenzamide and N,N-dimethyl-2,4-dimethoxythiobenzamide, as shown by the results obtained by Berg, which found the barrier to rotation around C—N bond smaller in the latter compound than in the former;[16] this requires in turn the existence of the conjugation between phenyl and thioamide even in *ortho* methoxythiobenzamides; in our compounds this conjugation should be stronger.

In the NMR spectra of **1** will be seen only one signal for each proton, because this signal accounts for the proton in A+B+C conformers, E_π being overpassed rapidly on NMR time scale[7] and $B \rightleftarrows C$ is rapid too*.

CONFORMERS OF THE *CIS* ISOMER OF 2,6-DIMETHYL-4-(3′-NITROTHIOBENZOYL) MORPHOLINE, 3

The spectra from Fig. 2 were interpreted by us previously as showing the freezing of the rotation around aryl—C(S) bond, E_π,[1] from Fig. 3. In the light of Berg's criticism[7] of one of our earlier papers[2] we are reinterpreting

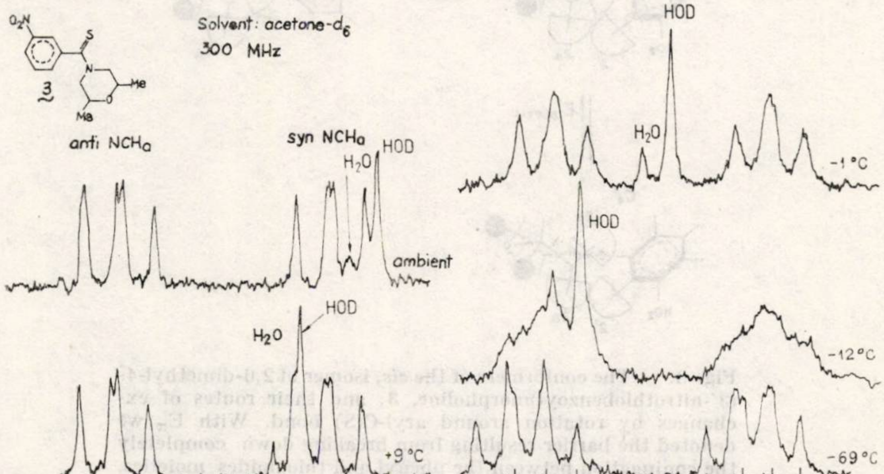

Fig. 2. — 300 MHz ^1H NMR spectra of *cis* isomer of 2,6-dimethyl-4-(3′-nitrothiobenzoyl) morpholine, **3**.

---

* We asserted previously erroneously that only one signal was seen in the spectrum for each proton, because the A and B conformers were equienergetic and very much alike.[1] Although A, B and C conformers could have very close energies, they are diastereomers and, in general, they may have different energies.

these spectral features as indicating the freezing of E_{steric}. Thus one of the two overlapping triplets of each NCH_a proton of the *cis* isomer of 2,6-dimethyl-4-(3′-nitrothiobenzoyl)morpholine, **3**, in the spectrum at −69°C, is due to $A_1 + B_1 + C_1$ conformers, whereas the other one is

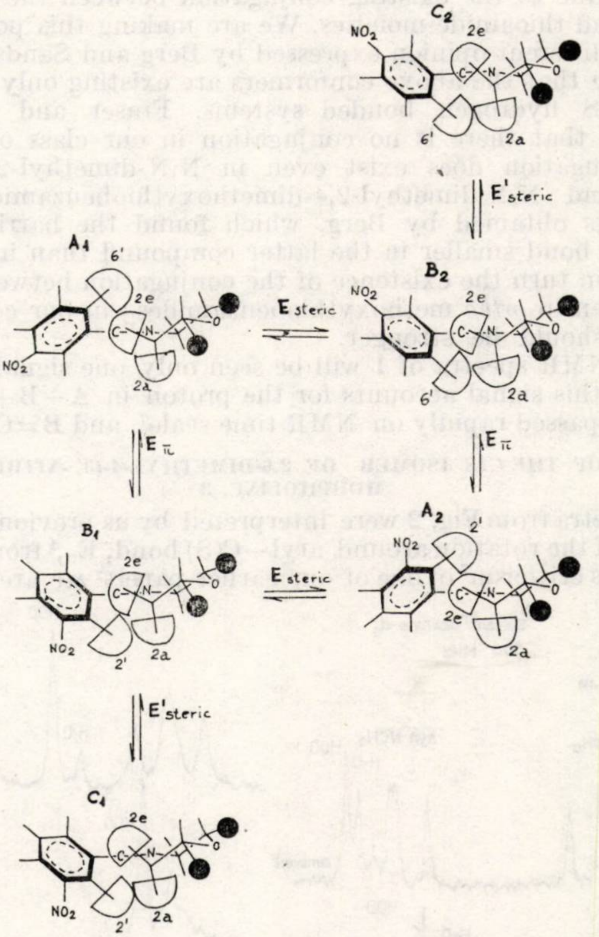
C2
NO2
2e
6'
2a
E'steric
A1
6'
2e
NO2
2A
E steric
B2
NO2
2e
6'
2a
Eπ
Eπ
A2
NO2
2
B1
2e
NO2
2'
2a
E steric
2e
2a
E'steric
C1
2e
NO2
2'
2a

Fig. 3. — The conformers of the *cis*, isomer of 2,6-dimethyl-4-(3′-nitrothiobenzoyl)morpholine, **3**, and their routes of exchanges by rotation around aryl-C(S) bond. With E_π we denoted the barrier resulting from breaking down completely the conjugation between the phenyl and thioamides moieties, whereas E_{steric} is the barrier resulting from overlapping of the Van der Waals radius of the *ortho* phenyl proton with the *anti* equatorial NCH proton radius.

corresponding to $A_2 + B_2 + C_2$. Each of the six conformers A_1, A_2, B_1, B_2, C_1, C_2, from Fig. 3, has an enantiomer : A_1', A_2', B_1', B_2', C_1', C_2', but this is irrelevant for our NMR spectra, because they were obtained using an achiral solvent. The type of conformers denoted with 1 and 2, in Fig. 3, should have close energies, having very similar structures and the spectrum at −69°C, from Fig. 2, seems to indicate very close energies indeed.

THE COALESCENCE OF THE GHEMINAL CHEMICAL SHIFT NONEQUIVALENT PROTONS DUE TO LIBRATION MOTION

In Fig. 4 the *syn* NCH_e proton of the *cis* isomer of 2,6-dimethyl-4-(2′-hydroxythiobenzoyl)morpholine, **4**, has two signals corresponding to the two conformers A and C from Fig. 5, whereas the *syn* NCH_a proton of the same compound has the same chemical shift in both conformers, as Fig. 6 shows. The conformer populations p_A and p_C seem equal from the intensity of the two signals of the *syn* NCH_e proton. For **4** the ring inversion is restricted from the thermodynamic point of view,[7] but for 4-(2′-hydroxythiobenzoyl)morpholine, **5**, the ring inversion is

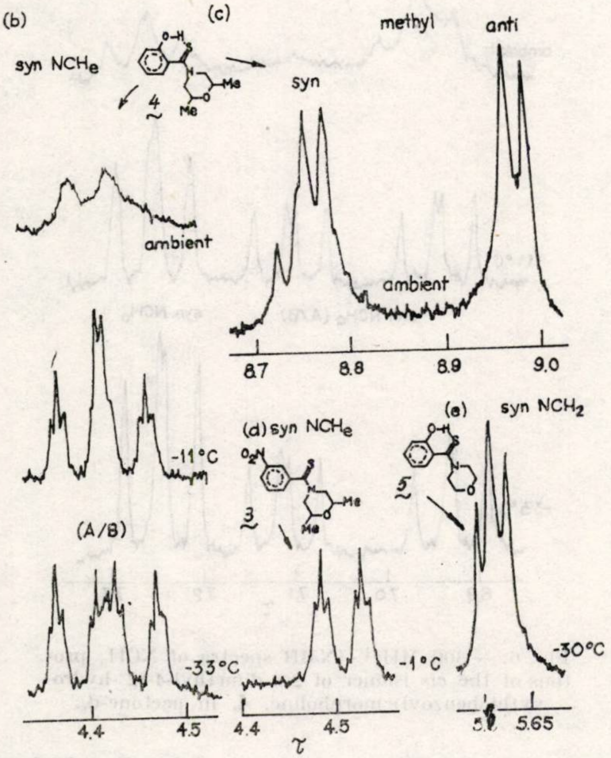

Fig. 4 — Selected 300 MHz ^1H NMR spectral features of the *cis* isomers of 2,6-dimethyl-(2′-hydroxythiobenzoyl) morpholine, **4,** 2,6-dimethyl-(3′-nitrothiobenzoyl)morpholine, **3**, and of 4-(2′-hydroxythiobenzoyl)morpholine, **5**, in acetone-d_6. Other explanations are given in the figure. Compare the signal of *syn* NCH_e proton in **3** and **4**.

rapid at all the temperatures searched, A′ and C conformers interchanging by ring inversion, as shown in Fig. 7. Because the conformer populations p_A and p_C should be the same in **4** and **5** it would be expected

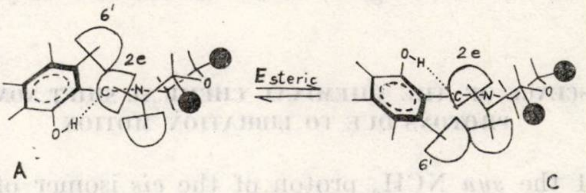

Fig. 5. — The conformers A and C of the *cis* isomer of 2,6-dimethyl-4-(2′-hydroxythiobenzoyl)morpholine, **4**, and their interchange route by rotation around aryl-C(S) bond.

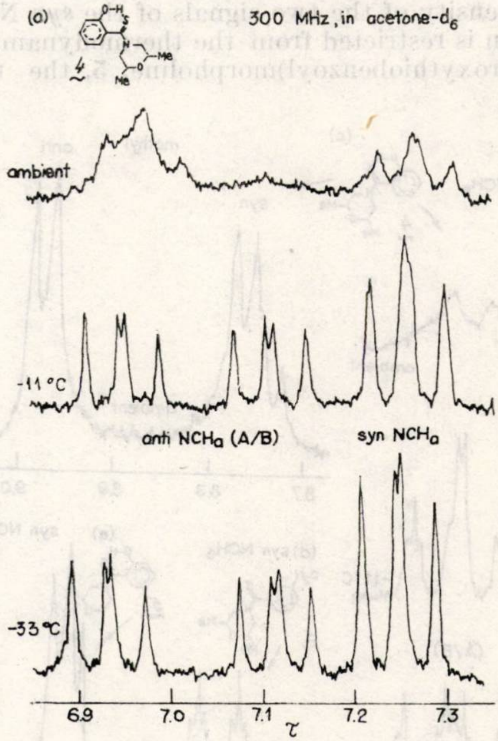

Fig. 6. — 300 MHz¹ HNMR spectra of NCH_a protons of the *cis* isomer of 2,6-dimethyl-4-(2′-hydroxythiobenzoyl) morpholine, **4**, in acetone-d_6.

that the *syn* NCH_2 protons of **5**, in acetone — d_6 be chemical shift nonequivalent : $\Delta\nu_{12}^{syn} = \frac{1}{2}\left|\nu_{A,e}^{syn} - \nu_{C,e}^{syn}\right|$; this is not the case, the *syn* NCH_2 protons of **5** being chemical shift equivalent at 300 MHz resolution. Even if there is a small difference in the populations p_A and p_C, which cannot be sensed from the intensity of NMR signals, affecting the value of $\Delta \nu_{12}^{syn}$ of *syn* NCH_2 protons of **5**, it is hard to believe that the interplay between the populations of the conformers p_A and p_C and the chemical shifts $\nu_{A,e}^{syn}$, $\nu_{C,e}^{syn}$, $\nu_{A,a}^{syn}$ and $\nu_{C,a}^{syn}$ can cause, at different temperatures, $\Delta \nu_{12}^{syn} = 0$, for **5**, in acetone-$d_6$, at 300 MHz.

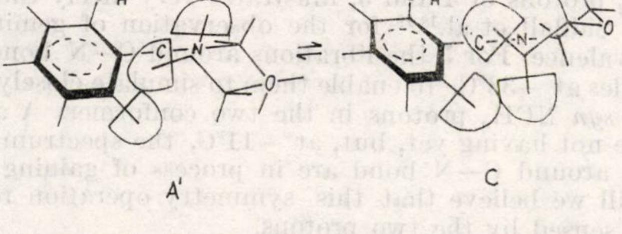

Fig. 7. — The interchange of A′ and C conformers of 4-(2′-hydroxythiobenzoyl) morpholine, **5**, through ring inversion ; A′ is the enantiomer of the A conformer.

Jennings et al, suggested that the perturbation introduced by the methyl groups in **4**, might not be neglected, when comparing the data of **4** and **5**, for *syn* NHC_2 group.[17] Even supposing a perturbation of the chemical shifts of NCH_2 protons, we still cannot explain by such an effect the chemical shift equivalence of *syn* NCH_2 protons of **5**. Thus for both A and C conformers, there is the same spatial relationship between the NCH_e hydrogen atom and the CH_3 groups in **4** and therefore the methyls will have the same magnetic influence on the chemical shifts of NCH_e proton in A and C conformers ; by this token $(\nu_{A,e}^{syn} - \nu_{C,e}^{syn})$ should be the same in **4** and **5**.

The results from Fig. 4 for *syn* NCH_2 protons of **4** and **5** could be explained, in our view, only as an effect of the librational motion on NMR spectra, as we already proposed.[1] Such an effect was discovered by Kurland and Wise,[8] the changing of the chemical shift, because of the librational motion, taking place while the NMR lines remain sharp. The experimental finding that $|\nu_{A,e}^{syn} - \nu_{C,e}^{syn}| \simeq 20$ cps at 300 MHz, at −33°C, for **4**, whereas $\nu_{A,e}^{syn} = \nu_{C,e}^{syn}$ for **5**, is thus explained by us by the decreasing of the amplitude of libration around C−N bond, after introducing the two methyl groups, while comparing **4** with **5**.

The spectrum of **4** at −11°C, where the separation between the signals of the *syn* NCH_e proton in the two conformers A and C decreased, as compared to that at −33°C, in Fig. 4, could lend support to our interpretation, proving that, even for **4**, the process of equalizing $\nu_{A,e}^{syn}$ and $\nu_{C,e}^{syn}$ is taking place, of course, at a higher temperature. If we are correct in regard to this interpretation, it could be expected that, at temperatures lower than −33°C, the *syn* NCH_2 protons of **5** exhibit geminal chemical shift nonenquivalence in acetone -d_6, at 300 MHz, even if p_A and p_C are equal.

Therefore we are still claiming that, for such systems, the librational motion can, in principle, coalesce geminal anisochronous protons, contrary to the statement of Jennings et al[8] *.

We would like to point out that this phenomenon, observed for the *syn* NCH_2 protons of **4** and **5**, illustrates very nicely the condition 3 envisaged by Siddall et al.[18,19] for the observation of geminal chemical shift nonequivalence. For **5** the librations around C—N bond are having large amplitudes at −33°C, to enable them to simulate closely a symmetry operation for *syn* NCH_e protons in the two conformers A and C, while for **4** they are not having yet, but, at −11°C, the spectrum shows that the librations around C—N bond are in process of gaining such amplitudes too. Still we believe that this symmetry operation refers to the *magnetic field* sensed by the two protons.

The comparison of the spectra of *syn* NCH_e proton at −33°C and −11°C respectively is also relevant in regard to the relation between the condition 2 and condition 3, stated by Siddall et al.[18,19] for geminal chemical shift nonequivalence. At a smaller gradient field, say 100 MHz resolution, the librations around C—N bond would simulate a symmetry operation (more precisely a symmetry plane) at an even lower temperature. On the other hand a smaller field gradient should exist for the *anti* NCH_a protons in the two conformers, for which almost no detectable change in the chemical shifts is observed between −33°C and −11°C, in the spectra from Fig. 6.

This different behaviour of the *syn* NCH_e proton signals as compared to that of the *anti* NCH_a proton signals, in regard to the same molecular motion, the libration around C—N bond, indicates that the field gradient which causes the difference in the chemical shifts of the *syn* NCH_e signals in the two conformers is due to the CSN group, while the separation between the *anti* NCH proton signals is due to the anisotropy of the phenyl ring, a fact which we already pointed out based on other considerations.[11a] The thioamide group is very anisotropic and close to the *syn* NCH_2 group, but the difference in the deshielding cone of the CSN group of the two equatorial positions is very small. In fact, if an intramolecular hydrogen bond OH. . .S had not existed in **4** and **5**, this difference would have been nil, the CSN plane being a symmetry plane for the two equatorial positions; the hydrogen bond, having different strengths in the conformers A and C,[14] pulls the sulphur atom a little from the conjugation with nitrogen, this being somehow more accentuated in one of the conformers probably in C, although the nitrogen remains still planar in both A and C.

There is a very small decrease in the chemical shift difference of the *anti* NCH_a proton signals going from − 33°C to −11°C in Fig. 6, but here the librational motion is still far from simulating a symmetry operation; although the phenyl ring is having a smaller anisotropy than CSN group, the two axial positions are quite different in regard to the phenyl ring.

---

* We agree with these authors that our explanation based on such a phenomenon for the case discussed by us previously[4] was wrong and that their explanation[8] is the one valid.

The finding that the intensities of the two signals of *syn* NCH_e proton in **4** are equal at −33°C and at −11°C is a valuable NMR indication that, for **4**, in acetone-d_6, there are indeed only two populated equilibrium conformations—this in connection with the possibility of existing three conformers for **1** discussed above.

If three populated conformers A, B, C had existed for **4** in acetone-d_6, with $A \rightleftarrows B$ slow and $B \rightleftarrows C$ rapid on NMR time scale, through rotation around aryl-C(S) bond, for the B+C corresponding signal should have been expected in general a greater intensity and furthermore the intensities might have been functions of the temperature.*

Our assertion that **5**, in acetone-d_6, should exhibit (a small) geminal chemical shift nonequivalence, if we could perform measurements at sufficiently low temperatures, at 300 MHz resolution, could raise another interesting question in regard to the origin of the geminal chemical shift nonequivalence** of *syn* NCH_2 diastereotopic protons in *ortho* (thio) benzamides. We have pointed out[11a,11b] that the published NMR studies support the assertion that the conformer populations factor is the origin of the geminal chemical shift nonequivalence of *syn* NCH_2 diastereotopic protons in *ortho* (thio)benzamides, in agreement with some earlier claimings.[22]

Here may be still a case where only the experimental difficulties, such as low temperature measurements, coupled perhaps with a still insuficient resolution power of the instrument, seem to prevent detecting a small $\Delta\nu_{12}^{syn}$, when $p_A = p_C$. The origin of geminal chemical shift nonequivalence in this case would not be the conformer populations factor, but the magnetic asymmetry in the field of the highly anisotropic CSN group, sensed by the *syn* NCH_2 protons while being in the equatorial position in the two different conformers A and C.

We conclude this point stressing the importance of knowing the conformers in which the molecule exists, in discussing both the chirality on NMR time scale and the origin of the geminal chemical shift nonequivalence; without such knowledge we may fail to draw the right conclusions.

Our claiming that NMR bands can be broadened by librational motion was based in part[1] on spectra subjected to artefacts and we have to withdraw these proposals.

---

* We should observe that the above NMR finding for **4** in acetone-d_6 does not preclude that conformation B to exist in a well potential energy, but this minimum would be much higher than the minima A and C. Up to −11°C the population of B could be thus sufficiently low as not to be sensed by NMR spectra.

** We use the term "origin of the geminal chemical shift nonequivalence" in the sense which is prevalently accepted in the literature, i.e. the most important factor in determining the magnitude of the chemical shift between the geminal methylene protons, in what originates the major contribution to $(\nu_1 - \nu_2)$.[20] Jennings, Berg et al.[17,21] understood on the other hand by the origin(s) of the geminal chemical shift nonequivalence the conformational motion which, by becoming rapid, renders the geminal NCH_2 protons enantiotopic. The ambiguity still existing in the literature for this terminology and which was unfortunately overlooked both by Jennings at al.[17,21] and by us[11a,11b] is in fact partially responsible for the criticism[17] and its reiteration[21] of the conclusion of our preliminary communication,[11a] whereas the NMR results of Berg, Jennings et al. obtained for N,N-di(isobutyl)-o-hydroxythiobenzamide[21] lend further support to our conclusion.[11a]

Thus the spectrum from Fig. 6 at ambient temperature does not show the broadening due to librational motion of *anti* NCH_a proton signals* in one conformer, as we submitted,[1] but the already rapid passage $A \overset{E_{steric}}{\rightleftarrows} C$, admitting also that this spectrum was recorded at a smaller amplitude or, more probably, at a lower concentration of the probe than the other two spectra from Fig. 6, at −11°C and −33°C. There is also a problem with the chemical shift of the *anti* NCH_a proton signals* which seems to suffer a downfield shift from −11°C to the ambient temperature, although no change is observed between −33°C and −11°C.

We have claimed the possibility of the broadening of the bands by ibr ational motion, in molecules with no severe steric crowding, based on the selective sharpening observed in Fig. 8**. Our explanation is wrong, being in disagreement with the very short relaxation time of the torsional vibrations[23] while the spectra themselves were in fact not showing a real phenomenon, but probably artefacts in obtaining them, because of instrumental problems with positioning the irradiation frequency to simultaneously decouple both *syn* and *anti* signals*** if we also admit a decrease with the temperature increase in the difference of the chemical shifts of C_3 and C_5 proton signals.

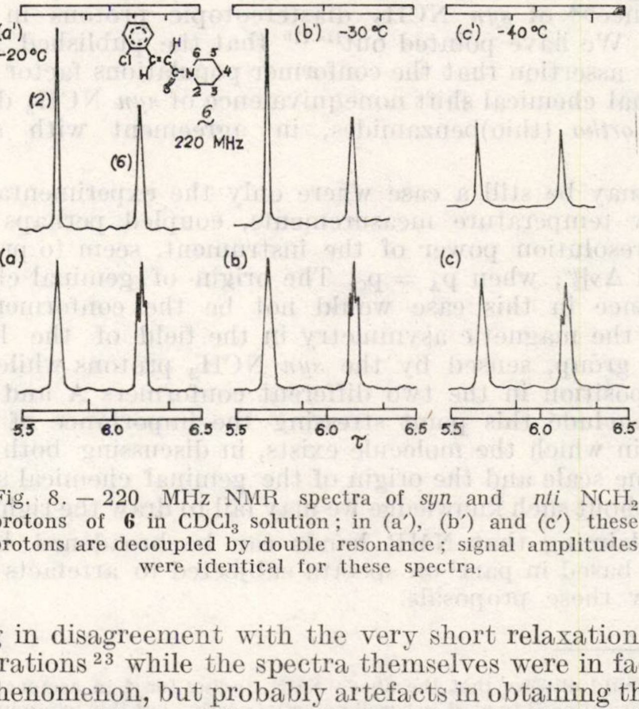

Fig. 8. — 220 MHz NMR spectra of *syn* and *nti* NCH_2 protons of **6** in $CDCl_3$ solution ; in (a′), (b′) and (c′) these protons are decoupled by double resonance ; signal amplitudes were identical for these spectra.

---

* We attributed the two downfield signals in Fig. 6, to the *anti* NCH_a proton, mainly because it is for the *anti* position more probable the splitting of the signal for the A and C conformers, than for *syn* NCH_a proton, the former being much closer to the phenyl ring ; we anticipated this possibility for the *anti* NCH_a proton previously.[11a]

** These spectra were published previously by us.[4]

*** The author is owing this explanation to Dr. W.B. Jennings.

In order to rationalize the experimental data from,[3] discussed also in[1] (p. 1286) we think that further NMR studies, especially of 1-(2′-hydroxythiobenzoyl)-3,4,5-$d_6$piperidine, should be done. All we can say now is that $\Delta(\tau_a^{syn} - \tau_e^{syn})$ of around 1.6 ppm,[1] in the temperature interval (−60°C, 0°C), from our interpretation of the coalescing of *syn* NCH_2 protons[1] seems unrealistically high. On the other hand, if we are presuming that the observed coalescence of the *syn* NCH_2 protons of 1-(2′-hydroxythiobenzoyl) piperidine in $CDCl_3$ was taking place because of variation of the populations of two conformers, we get an estimated $\Delta S_0 \sim$ 3 e.u. This figure may be also unrealistically high.[24] In the light of a suggestion of Berg el al.[21] that two conformational processes with different $\Delta H_0 : \Delta S_0$ ratios may be an alternative explanation for a single conformational process which would give an unrealistically high ΔS_0 between two conformers, we might suspect that, in the case of 1-(2′-hydroxythiobenzoyl)piperidine in $CDCl_3$, all three conformations A, B, C are in fact populated conformers in the range of temperature (−60°C, 0°C). The two conformational processes, rapid on NMR time scale would be then : $A \rightleftarrows B$ by ring inversion and $B \rightleftarrows C$ by small rotations around Ph-C(S). If this is true, it may lend further support to our supposition from the beginning of this paper of the existence of three populated conformers for thiobenzoylmorpholines and -piperidines without an *ortho* substituent.

It may be that, besides of the variation with the temperature of populations of the conformers, the variation of the chemical shifts of axial and equatorial hydrogens plays a role too.

ACKNOWLEDGEMENTS: We are acknowledging helpful communications with Dr. U. Berg (University of Lund) and Dr. W.B. Jennings (University of Birmingham) in regard to some matters contained in this paper.

Note added in proof: Fortunately, we have recently come across the general principle of symmetry in Physics[25] formulated by Pierre Curie (1893—1895). We hawe thus found that some of our ideas, contained in the present paper, are in fact backed also by this principle if applied in the area of NMR spectroscopy. A full paper dealing specifically with the geminal chemical shift nonequivalence in the light of Curie's principle is forthcoming shortly. Some of the ideas emerging also from an our recent paper[26] are in fact an illustration of the general principle of symmetry in the vibrational spectroscopy; one knowing Curie's principle and our paper[26] might have envisaged very well that the principle of Pierre Curie would have proved estremly helpful in improving our present understanding of the vibrational spectroscopy of polymers. We plan to discuss this topic too in the future.

REFERENCES

[1] A. O. Fulea, *Rev. Roum. Chim.*, **24**, 1265 (1979).
[2] A. O. Fulea and P. J. Krueger, *Can. J. Chem.*, **53**, 3315 (1975).
[3] A. O. Fulea and P. J. Krueger, *Spectroscopy Lett.*, **8**, 375 (1975).
[4] A. O. Fulea and P. J. Krueger, *Chem. Phys. Lett.*, **35**, 480 (1975).
[5] P. J. Kurland and W. B. Wise, *J. Am. Chem. Soc.*, **86**, 1877 (1964).
[6] R. R. Fraser and K. Taymaz, *Tetrahedron Lett.*, 4573 (1976).
[7] U. Berg, *Can. J. Chem.*, **55**, 2297 (1977).
[8] W. B. Jennings and D. Randall, *Chem. Phys. Lett.*, **55**, 479 (1978).

[9] A. O. Fulea, *Rev. Roum. Chim.*, **24**, 1439 (1979).

[10] R. E. Lyle and L. N. Pridgen, *J. Org. Chem.*, **38**, 1618 (1973).

[11a] A. O. Fulea and P. J. Krueger, *Tetrahedron Lett.*, 3135 (1975).

[11b] A. O. Fulea, *Rev. Roum. Chim.*, **24**, 1107 (1979).

[12] C. Cercasov, F. Cornea, M. Ciureanu, M. Hillebrand, V. E. Sahini and E. Volanschi, *Rev. Roum. Chim.*, **29**, 25 (1984).

[13] P. J. Krueger, A. O. Fulea, C. Fulea and F. Cornea, *Spectroscopy Lett.*, **8**, 141 (1975).

[14] A. O. Fulea and P. J. Krueger, *Can. J. Chem.*, **55**, 227 (1977).

[15] U. Berg and J. Sandström, *Tetrahedron Lett.*, 3197 (1976).

[16] U. Berg, *Acta Chim. Scand.*, B**30**, 695 (1976).

[17] W. B. Jennings and M. S. Tolley, *Tetrahedron Lett.*, 695 (1976).

[18] T. H. Siddall, III, *J. Phys. Chem.*, **70**, 2249 (1966).

[19] T. H. Siddall and W. E. Stewart, Progr. NMR Spectroscopy, **5**, 3 (1969).

[20] G. M. Whitesides, J. J. Grocki, D. Holtz, H. Steinberg, and J. D. Roberts, *J. Am. Chem Soc.*, **87**, 1058 (1965).

[21] U. Berg, J. Sandström, W. B. Jennings and D. Randall, *J. Chem. Soc. Perkin II*, 949 (1980).

[22] G. R. Bedford, G. Greatbanks and D. B. Rogers, *Chem. Comm.*, 330 (1966).

[23] A. B. Callear and J. D. Lambert in "Comprehensive Chemical Kinetics", Ed. C.H. Bamford and C. F. Tipper, Elsevier, Amsterdam, 1969, p. 215.

[24] C. Piccini-Leopardi, O. Fabre, D. Zimmermann J. Reisse, F. Cornea and C. Fulea, *Can. J. Chem.*, **55**, 2649 (1977) and the references cited therein.

[25] I.I. Sirotin and M.P. Shaskolskaia, "Fizica cristalelor", Editura Ştiinţifică şi Enciclopedică, Bucharest, 1981, p.209.

[26] A.O. Fulea, *Rev. Roum. Chim.*, **30**, 357 (1985) ; compare for example eq. (3) with the eqs. (6) and (8) in our paper.

Revue Roumaine de Chimie, **31**, *3*, 323–326 (1986)

POLARITY OF SALT SOLUTIONS: A GENERAL EMPIRICAL EQUATION

MARCOS CAROLI REZENDE and LILIAM INÊS DAL SASSO
Departamento de Química, Universidade Federal de S. Catarina, Florianópolis 88000, SC, Brasil

Received March 23, 1985

Variations of the polarity of a solvent by the addition of an electrolte are readily predicted by means of a general empirical expression which relates they polarity of the medium to the molar concentration of added salt.

The addition of an electrolyte to a solvent is generally assumed to change the polarity of the medium. Variations of the rates of many reactions by the addition of a salt to the medium are frequently rationalized as arising from these polarity changes. As far as we are aware, little systematic work has been done with the object of testing this assumption or quantifying these polarity changes for various salts.

We have reported that the rates of many reactions in solution, which vary with the addition of a particular salt, follow a general empirical expression which correlates the rate constant with the molar concentration of the added salt.[1] This empirical equation was derived with the assumption that the added electrolyte affects the reaction rates by changing the polarity of the medium. We now provide evidence which substantiates this hypothesis, and show that a similar equation, relating the polarity of the medium to the molar concentration of added salt, holds for a variety of solvents and electrolytes.

The present treatment stems from Langhals original proposal[2] of a general empirical expression to describe the polarity of a binary liquid mixture as a function of the molar concentration of the more polar component. By applying the proposed equation to electrolyte solutions and treating the added salt as the more polar "co-solvent", equation (1) can be written, which relates the polarity value $E_T(1)$ of a given salt solution to the molar concentration of added electrolyte.

$$E_T(1) = E_T^0(1) + A \cdot \ln(c/c^* + 1) \qquad (1)$$

$E_T^0(1)$ is the polarity value of the pure solvent, A and c^* are adjustable parameters. In principle, any polarity scale can be used in equation (1).[2] Though largely superseded by the $E_T(30)$ scale,[3] the $E_T(1)$ scale[4] was chosen by us because of the easy availability of the N-(4-hydroxyphenyl)-2,4,6-triphenylpyridinium betaine used as reference.[4]

The constant A in equation (1) measures the susceptibility of a certain milieu to polarity changes by the addition of a particular salt. For dilute electrolyte solutions, the polarity is linearly dependent on the concentration of salt, but as more salt is added, the polarity may eventually become a function of the logarithm of the electrolyte concentration. The constant c^* is a threshold concentration value which separates these two regions. In most cases this transition lies within the investigated range of salt concentrations. This can be readily seen by applying limit conditions to equation (1). When $c^* \gg c$, equation (2) is a good approximation to (1)[1,2]

$$E_T(1) = E_T^0(1) + \mathrm{A.c/c^*} \tag{2}$$

Examples of such behaviour, with large values of c^*, are given in table 1, entries (g) and (l). A second approximation to (1) results when $c^* \ll c$.

$$E_T(1) = E_T^0(1) + A \cdot \ln\ c/c^* \tag{3}$$

We have not observed this behaviour with the range of salts and solvents investigated, but there is no reason why it should not occur.

Sixteen examples of successful application of equation (1) to experimental data are given in the Table. Figure 1 illustrates graphically with a particular example the good linearity obtained in all cases, when $E_T^0(1)-E_T^0(1)$ values are plotted against $\ln(c/c^* + 1)$.

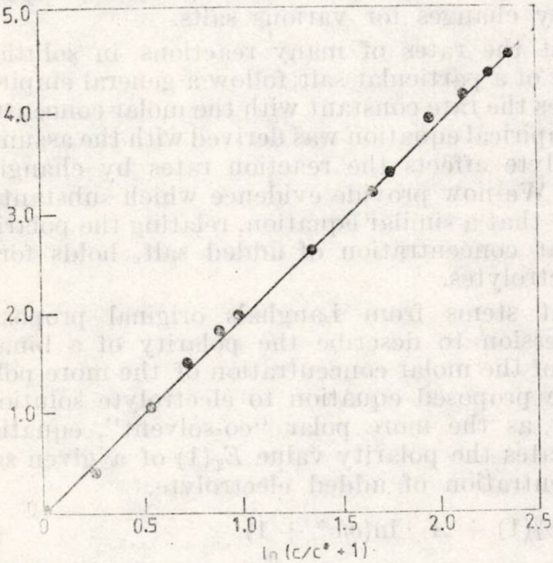

Fig. 1. — Variation of the polarity with the addition of a salt. Sodium iodide solutions in ethanol at 25°C (see Table 1, entry (a)).

The majority of examples presented involve organic solutions of electrolytes. Aqueous solutions of inorganic salts had always the same $E_T(1)$ value of pure water. This does not mean that the addition of water does not change the polarity of the medium. The constancy of $E_T(1)$ values of aqueous salt solutions, irrespective of the nature of the amount of added electrolyte, probably stems from limitations of the polarity scale employed. In fact, a plot of $E_T(1)$ values against the corresponding dielectric constants, for various solvents (graph not shown) yields a curve which rises steeply for apolar solvents, reaching a plateau in the more polar region. Variations of the dielectric constant of aqueous solutions should not be detected by the $E_T(1)$ scale, unless they corresponded to a decrease in the polarity of the medium. This is the case of aqueous solutions of benzyltrialkylammonium chlorides (entries (e), (f) and (g) in Table 1) which are remarkable in that they are less polar than the pure solvent. The $E_T(1)$ value of a 2.5 M aqueous solution of benzyltributylammonium chloride is 59.3, close to the value of 59.2 observed for n-butanol. This observation is to be compared to Kosower's report[5] of an increase in the polarity of the medium when tetrabutylammonium salts are added to non-aqueous solvents which include acetonitrile, 1,2-dimethoxyethane, acetone, chloroform and dichloromethane, all of them less polar than either water or ethanol. Our results complement Kosower's observations and show that tetraalkylammonium salts in solution may be treated as organic "co-solvents" of intermediate polarity, in contrast to the much more polar inorganic salts.

Table 1

Application of equation (1) to various electrolyte solutions

Solvent	Salt (Concentration range, M)	c^*,M	A	Number of points (Correlation coefficient
(a) EtOH	NaI(0–2.1)	0.25	2.28	13(0.9981)
(b) MeOH	NaI(0–2.1)	0.17	0.17	12(0.9928)
(c) i-PrOH : H_2O(9 : 1)	NaI(0–2.0)	0.05	1.56	13(0.9994)
(d) $(CH_3)_2CO$: H_2O(9 : 1)	LiI(0–2.0)	0.07	1.71	14(0.9966)
(e) H_2O	BTA[a](0–2.5)	1.95	−11.96	11(0.9991)
(f) H_2O	TEBA[b](0–1.6)	0.30	−1.22	11(0.9927)
(g) EtOH : H_2O(1 : 1)	BTA[a](0–1.9)	1500	−3150	12(0.9970)
(h) $(CH_3)_2CO$: H_2O(4 : 1)	NaBr(0–1.8)	0.28	0.36	16(0.9966)
(i) $(CH_3)_2CO$: H_2O(3 : 2)	NaBr(0–2.0)	0.80	1.54	17(0.9842)
(j) DMSO : H_2O(4 : 1)	NaBr(0–2.0)	2.15	2.77	13(0.9957)
(k) $(CH_3)_2CO$: H_2O(4 : 1)	NaI(0–2.5)	1.15	2.97	19(0.9959)
(l) DMSO : H_2O(4 : 1)	NaI(0–2.2)	2.55	431.40	15(0.9987)
(m) DMF : H_2O(4 : 1)	NaI(0–2.0)	1.57	6.12	12(0.9990)
(n) DMF : H_2O(4 : 1)	KI(0–1.2)	4.65	16.18	9(0.9971)
(o) DMF : H_2O(4 : 1)	NaBr(0–2.0)	1.15	2.71	14(0.9977)
(p) DMF : H_2O(4 : 1)	$NaNO_3$(0–2.0)	0.26	1.42	20(0.9952)

[a] — Benzyltributylammonium chloride
[b] — Benzyltriethylammonium chloride

We suggest that equation (1) will be very useful in all those cases where the presence of an electrolyte affects the polarity and the rates of chemical processes in solution. By relating these polarity changes to the amount of added salt, this relationship provides a general, unifying framework for quantifying hypotheses and observations which have rested so far on purely qualitative grounds.

ACKNOWLEDGEMENT: We are indebted to the Conselho Nacional de Desenvolvimento Científico e Tecnológico — CNPq for financial support.

EXPERIMENTAL

All salts and solvents employed were analytically pure. Solvents were distilled before use. Aqueous solutions were made up with deionized, CO_2-free water. The *N*-(4-hydroxyphenyl)-2,4,6-triphenylpyridinium perchlorate was prepared by a reported procedure. [4]

The spectroscopic measurements were carried out on a Shimadzu ultraviolet spectrophotometer equipped with a thermostated (25.0±0.1°C) water-jacketed cell compartment.

All salt solutions contained, besides the added electrolyte, a constant concentration of sodium hydroxide (2×10^{-2} M). Measurements were made on samples prepared by adding 10μL of a 5×10^{-2} M methanolic solution of the *N*-(4-hydroxyphenyl)-2,4,6-triphenylpyridinium perchlorate to 3 mL of the basic salt solutions. The $E_T(l)$ values were calculated[4] from the maxima of such samples, recorded in the range of 410—550 nm.

REFERENCES

[1] M. C. Rezende, D. Zanette and C. Zucco, *Tet. Letters*, **25**, 3423, (1984); M. C. Rezende, D. Zanette and C. Zucco, *Tetrahedron* **41**, 87 (1985).

[2] H. Langhals, *Angew. Chem. Int. Ed. Engl.*, **21**, 724 (1982).

[3] H. Langhals, *Chem. Ber.*, **114**, 2907 (1981).

[4] K. Dimroth, C. Reichardt, T. Siepmann and F. Bohlmann, *Justus Liebigs Ann. Chem.*, **661**, 1 (1963).

[5] E. M. Kosower and M. Mohammad, *J. Phys. Chem.*, **74**, 1153, (1970).

Revue Roumaine de Chimie, **31**, *3*, 327—334 (1986)

TYPES OF SOLVENT INTERACTIONS IN WATER-GLYCEROL MIXTURES

I. M. SIDAHMED, H. SADEK and S. M. SALEM

Department of Chemistry, Faculty of Science, Alexandria University, Alexandria, Egypt

Received March 8, 1985

The thermodynamic ionization constant of *p*-nitroanilinium ion, pK_{BH^+}, was determined in aqueous glycerol. The changes in pK_{BH^+} were found to be negligibly small as the dielectric medium was changed. This observation has been used to show the types of interaction between the solvent and the different species in the initial and the activated states for the acid hydrolysis of formamide in the same solvent mixtures. A specific interaction has been postulated in the initial state which is stable and unaffected by the solvent composition while the change in rate is due to the direct electrostatic interaction between the solvent and the activated complex.

INTRODUCTION

The acid ionization constant of *p*-nitroanilinium ion:

$$O_2N-C_6H_4NH_3^+ \rightleftharpoons O_2N-C_6H_4-NH_2 + H^+ \qquad (1)$$

is given by the relation,

$$pK_{BH^+} = -\log\frac{a_{H^+}a_B}{a_{BH^+}} = -\log\frac{C_{H^+}C_B}{C_{BH^+}} - \log\frac{f_{H^+}f_B}{f_{BH^+}} \qquad (2)$$

where a_{BH^+}, a_B and a_{BH^+} are the activities of the proton, the unprotonated base and the protonated base respectively.

All measurements for the ionization constant of *p*-nitroanilinium ion, particularly in water-alcohol mixtures, [1] showed that the proton availability is affected to a great extent by changing the medium composition. Such a considerable change in the proton availability cannot be concluded from the nearly constant values of $pK_{BH}{}^+$, measured in water-glycerol mixtures; this indicates that the species is not affected by changing the medium composition.

However, rate measurements for example in the acid hydrolysis of formamide [2] in the latter solvent mixtures, showed considerable variations when glycerol was added to water. These observations have drawn the attention to investigate the interaction of the solvent mixtures with the ground and the activated states.

The rate of the reaction is not only affected by the non-specific solvation caused by the electrostatic and dispersion forces in which the solvent can be regarded as an isotropic continuum, but also by the specific solvation caused by hydrogen bonding and electron pair donor (EPD)-electron pair acceptor (EPA), complexation. From the solvation type point of view, the reaction kinetics for any particular reaction in a given solvent should change according to the predominating type of solvation for the reaction.

The electrostatic and non-electrostatic solvation types concerning the initial and the activated states in water-glycerol mixtures, will be discussed in the light of medium effects on the ionization of *p*-nitroanilinium ion and the rate of acid hydrolysis of formamide.

EXPERIMENTAL

Materials

p-Nitroaniline of "B.D.H." grade was crystallized twice from ethyl alcohol.

Glycerol of pure "Merck" grade was purified[2] by distillation under reduced pressure (3–4 mm Hg, at 175°C).

Constant boiling hydrochloric acid was prepared from Carlo Erba concentrated acid [3].

Spectrophotometric measurements

A Carl-Zeiss spectrophotometer (model PMQ II) was used for the optical density measurements which were carried out at 25°C$\pm$0.05, in a 1 cm cell using distilled water or the mixed solvent as a blank. The solutions always have an absorption maximum at 380 nm, at which the optical densities were compared.

The indicator ratio I, was calculated from the relation,

$$I = \frac{C_{BH^+}}{C_B} = \frac{D_1 - D}{D - D_2}$$

where D, D_1 and D_2 are the optical densities of the solutions of the partially protonated base, the basic form of the indicator molecules and that of the completely acidic form respectively. It should be pointed out that D_2 in water is actually zero while in the mixed solvent it was found to be so small that it can be neglected.

RESULTS AND DISCUSSION

To avoid the complexity arising from the change in the activity coefficient term with the solvent composition, Paul's procedure [4] has been applied by using equation (2) in the form :

$$\mathrm{pK}_{BH^+} = \lim_{C_{H^+} \to 0} \left[\log\left(\frac{C_{BH^+}}{C_B}\right) - \log C_{H^+} \right] \qquad (3)$$

The expression in brackets on the RHS of equation (3) varies linearly with the concentration of the acid as shown in Fig. 1 ; the intercept at $C_{H^+} = 0$ denotes pK_{BH^+} .

The thermodynamic ionization constant previously determined by this method [5] has been found to be consistent with that obtained by other methods.

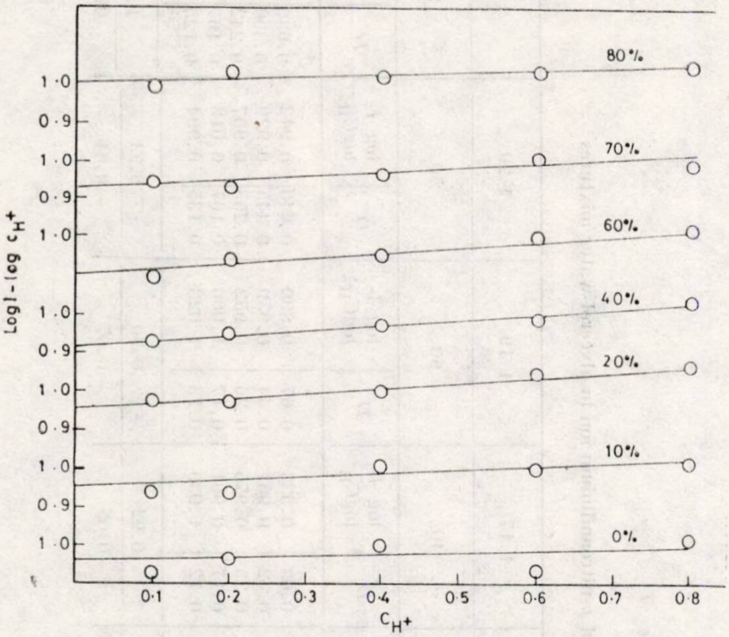

Fig. 1. — Determination of $p^{K}_{BH^+}$ for *p*-nitroanilinium ion in glycerol-water mixtures by Paul's method.

The data compiled in Table 1, show that there is a very small change in $pK_{BH}{}^+$, since it has steadily changed from 0.97 in water to 0.90 in 60wt% glycerol then increased steadily till it reached the value 1.00 at 80 wt.%.

The data, in terms of medium effect, have been compared with other solvent systems [1,6] as shown in Fig. 2. It can be readily seen that large variations with the dielectric constant occur with most of the solvent mixtures, which decrease to a great extent in ethylene glycol and glycerol. Higher Δ pK values measure the departure of the system from the basic nature of water as reference. Therefore, the small differences observed in water-glycerol mixtures indicate a basic reaction of the solvent system close to that of water.

Generally, variations of pK_{BH^+} with solvent composition have been ascribed to the breakdown of water structure as the alcohol content is increased, [7] the relative basicities of alcohol and water molecules in a particular solvent mixture [5] and the existence of different forms of solvated protons [8], for example $(H_2O)_4H^+$ and $ROH(H_2O)_3H^+$. Mixed hydration and solvation have been recently reported in water-ethylene carbonate mixtures. [9]

However, the acidic nature of glycerol [10] (in the sense that it accepts electrons from neighbouring water molecules) requires the proposal of a chemical interaction between the proton and water molecules forming

Table 1

Determination of the dissociation constant of *p*-nitroanilinium ion in glycerol-water mixtures

D_1	1.05		1.12		1.15		1.17		1.19		1.20		1.25	
Wt% solvent	0		10		20		40		60		70		80	
C_{H^+} M/L	*D*	log *I*- log G_{H^+}	*D*	log *I*- logC_{H^+}	*D*	log *I*- logC_{H^+}	*D*	log *I*- logC_{H^+}	*D*	log I- logC_{H+}	*D*	log *I*- logC_{H^+}	*D*	log *I*- logC_{H^+}
0.1	0.57	0.925	0.60	0.9379	0.59	0.977	0.63	0.933	0.67	0.890	0.640	0.942	0.630	0.993
0.2	0.37	0.963	0.41	0.9375	0.40	0.972	0.42	0.951	0.44	0.939	0.445	0.929	0.396	1.033
0.4	0.21	1.000	0.22	1.0097	0.23	1.000	0.25	0.975	0.26	0.952	0.255	0.967	0.242	1.018
0.6	0.17	0.936	0.16	1.0000	0.15	1.049	0.17	0.991	0.17	1.000	0.167	0.013	0.167	1.034
0.8	0.11	1.029	0.12	1.0178	0.11	1.073	0.12	1.039	0.13	1.023	0.135	0.994	0.125	1.051
pK_{BH^+}	0.97		0.95		0.96		0.92		0.90		0.93		1.00	
ΔpK	0		−0.02		−0.01		−0.05		−0.07		−0.04		0.03	

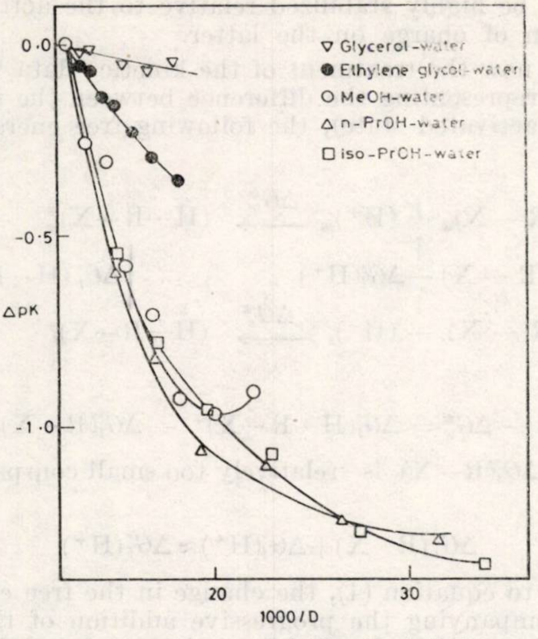

Fig. 2. — Change of ΔpK with 1/D in different aqueous-organic solvents.

solvation sheats in such a manner which makes the proton unaffected with the bulk electrostatic forces in which the solvent can be regarded as an isotropic continuum. By another treatment, Wells[11] has reached the same conclusion concerning the solvation of the proton in the same solvent mixtures.

The problem of making quantitative allowances for solvent induced changes in the rate constant of a reaction, is reduced to the calculation of the difference between the partial free energies of solvation of the activated complex and the initial reactants.[12] According to the results of these calculations one can predict the influence of the different solvents on reaction rate, say of the type:

$$R - \overset{\frown}{X} + \bar{Y} \rightarrow R - Y + \bar{X}$$

For reactions which are being carried out in acidic solutions, there may be in addition a preliminary step which represents the initial state:

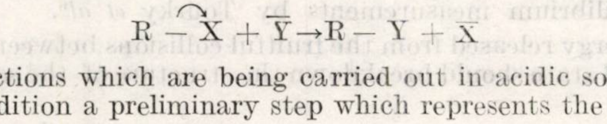

$$\underset{\displaystyle O}{\underset{\|}{R - C}} - X + H^{+} \rightarrow [\underset{\displaystyle {}^{+}OH}{\underset{\|}{R - C}} - X \leftrightarrow R - \underset{\displaystyle OH}{\underset{|}{\overset{+}{C}}} - X]$$

followed by the formation of the activated complex, *via* other intermediate steps, giving the products which represent the final state.

If the same reaction is carried out in aqueous mixed solvents, the rate will be diminished by increasing the polarity of the solvent, since the initial state will be highly stabilized relative to the activated state due to the dispersion of charge on the latter.

Considering now the treatment of the kinetic data which is usually based on terms representing the difference between the initial state and the final state (activated state), the following free energy cycle can be considered :

$$\begin{tikzcd}
(\mathrm{R}-\mathrm{X})_w + (\mathrm{H}^+)_w \arrow[r, "\Delta G^*_w"] & (\mathrm{H}\text{---}\mathrm{R}\text{---}\mathrm{X})^+_w \arrow[d, "\Delta G^\circ_t(\mathrm{H}\text{---}\mathrm{R}\text{---}\mathrm{X})^+"] \\
(\mathrm{R}-\mathrm{X})_s + (\mathrm{H}^+)_s \arrow[u, "-\Delta G^\circ_t(\mathrm{R}-\mathrm{X})-\Delta G^\circ_t(\mathrm{H}^+)"] \arrow[r, "\Delta G^*_s"] & (\mathrm{H}\text{---}\mathrm{R}\text{---}\mathrm{X})^+_s
\end{tikzcd}$$

from which,

$$\Delta\Delta G^* = \Delta G^*_s - \Delta G^*_w = \Delta G^\circ_t(\mathrm{H}\text{---}\mathrm{R}\text{---}\mathrm{X})^+ - \Delta G^\circ_t(\mathrm{R}-\mathrm{X}) - \Delta G^\circ_t(\mathrm{H}^+) \quad (4)$$

Assuming $\Delta G^\circ_t(\mathrm{R}-\mathrm{X})$ is relatively too small compared to $\Delta G^\circ_t(\mathrm{H}^+)$, therefore,

$$\Delta G^\circ_t(\mathrm{R}-\mathrm{X}) + \Delta G^\circ_t(\mathrm{H}^+) \approx \Delta G^\circ_t(\mathrm{H}^+)$$

According to equation (4), the change in the free energy of activation $\Delta\Delta G^*$, accompanying the progressive addition of the organic component, should be entirely due to the variation of $\Delta G^\circ_t(\mathrm{H}\text{---}\mathrm{R}\text{---}\mathrm{X})^+$ with the solvent composition as compared to the accompanying variations in $\Delta G^\circ_t(\mathrm{H}^+)$.

To test the validity of these assumptions, plots of $\Delta\Delta G^*$ against 1/D for the acid hydrolysis of formamide in aqueous-, glycerol,[2] glycol,[13] methanol,[13] *n*-propanol,[14] isopropanol[14] and *t*-butanol[14] were compared. Straight lines were obtained only for the reaction in aqueous-glycol and -glycerol while other solvent mixtures showed deviations from linearity as shown in Fig. 3. The linear relations in the case of glycerol and glycol indicate that the contribution of the electrostatic interaction between the solvent and the activated complex is a predominating factor affecting the magnitude of $\Delta\Delta G^*$.

The linearity observed in aqueous glycol is in agreement with the results of $\Delta G^\circ_t(H^+)$ in the latter solvent obtained by Wells[15] and proton transfer equilibrium measurements by Tourky *et al*[6].

The energy released from the fruitful collisions between the reactants in the ground state should breakdown the structure of the solvation sheats

Table

Velocity constants (in litre-mole^{-1} hr^{-1})

wt.% / Cosolvent	0.00	8.03	9.80	10.74	16.35	19.18	21.38	33.74	36.84	41.75
Glycerol[(a)]	0.5107	—	0.5370	—	—	0.5599	—	—	0.6060	—
Ethylene glycol[(b)]	0.5107	—	—	0.5667	—	—	0.5932	—	—	0.6500
Methanol[(b)]	0.5107	0.7184	—	—	0.8113	—	—	0.9594	—	—

around the proton; glycerol molecules enhance the free water molecules to reach a position of minimum potential energy by hydrogen bonding, forming the continuum dielectric. Such arrangement limited the dual

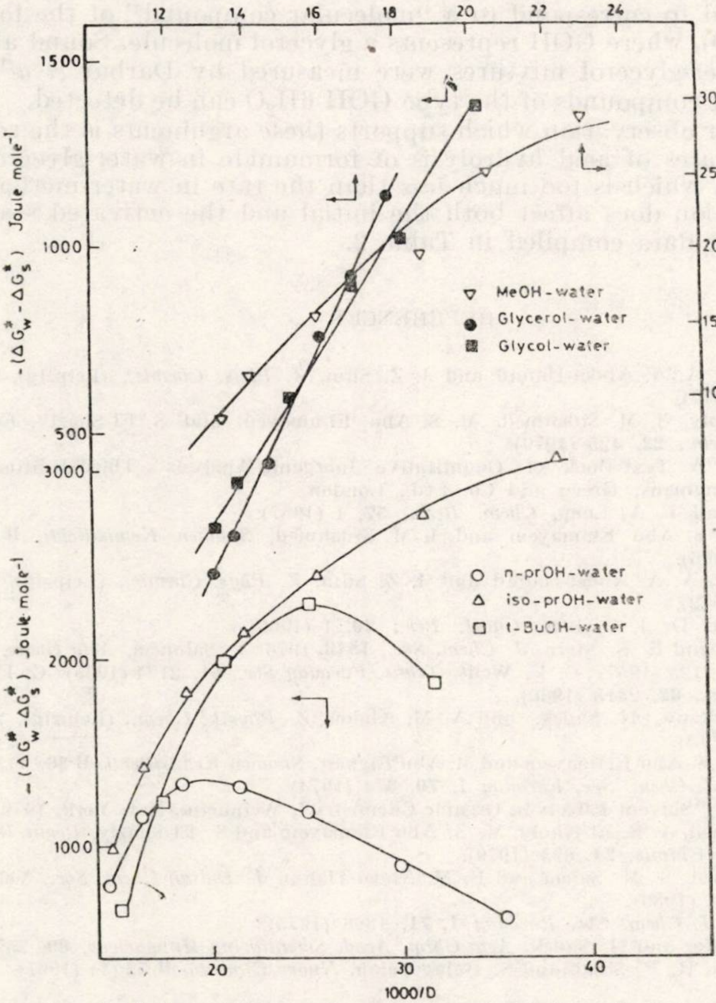

Fig. 3. — Variation of the free energy of transfer of the activated complex with 1/D.

2

in water + cosolvents, at 25°C

52.54	53.32	60.84	61.19	62.95	68.83	70.68	74.12	80.27
—	0.6958	0.7404	—	—	0.8100	—	—	—
—	—	—	0.7324	—	—	0.7729	—	0.8944
1.1204	—	—	—	1.4129	—	—	1.6396	—

nature of water, since it can act as EPD as well as EPA, and this prevents any specific interaction which may occur between the solvent molecules andt he activated state. This view is in agreement with viscosity and density measurements.[16] The maximum contraction at ($X_1 = 0.25$) may be considered to correspond to a "molecular compound" of the formula (GOH, $3H_2O$), where GOH represents a glycerol molecule. Sound absorptions in water-glycerol mixtures were measured by Darbar *et al*[17] who deduced that compounds of the type GOH $6H_2O$ can be detected.

Another observation which supports these arguments is the relative increase of rates of acid hydrolysis of formamide in water-glycerol and water-glycol, which is too much less than the rate in water-methanol in which solvation does affect both the initial and the activated states as shown in the data compiled in Table 2.

REFERENCES

[1] A. R. Tourky, A. A. Abdel-Hamid and I. Z. Slim, *Z. Phys. Chemie.*, (Leipzig), **250**, 49 (1972).

[2] E. A. El-Kholy, I. M. Sidahmed, M. S. Abu El-amayem and S. El-Shazly, *Egypt. J. Chem.*, **22**, 425 (1979).

[3] A. I. Vogel, "A Text-Book of Quantitative Inorganic Analysis", Third Edition, 1961, Longmans, Green and Co. Ltd., London.

[4] M. A. Paul and F. A. Long, *Chem. Revs.*, **57**, 1 (1957).

[5] H. Sadek, M. S. Abu Elamayem and I. M. Sidahmed, *Suomen Kemistilehti*, **B 39**, 225 (1966).

[6] A. R. Tourky, A. A. Abdel-Hamid and I. Z. Slim, *Z. Phys. Chemie.*, (Leipzig), **250**, 61 (1972).

[7] F. Franks and D. J. G. Ives, *Quart. Rev.*, **20**, 1 (1966).

[8] E. A. Braude and E. S. Stern, *J. Chem. Soc.*, **1948**, 1976 ; P. Salomaa, *Acta Chem. Scand.*, **11**, 125 (1957) ; C. F. Wells, *Trans. Faraday Soc.*, **61**, 2194 (1965) : C. F. Wells, *ibid.*, **62**, 2815 (1966).

[9] A. A. El-Harakany, H. Sadek, and A. M. Abdou, *Z. Physik. Chem.*, (Leipzig), **264**, 785 (1983).

[10] H. Sadek, M. S. Abu Elamayem and M. Abu Elgheit, *Suomen Kemistilehti*, **B 36**, 115 (1963).

[11] C. F. Wells, *J. Chem. Soc. Faraday I*, **70**, 674 (1974).

[12] C. Reichardt, "Solvent Effects in Organic Chemistry", Weinheim, New York, 1979.

[13] I. M. Sidahmed, A. E. El-Kholy, M. S. Abu Elamayem and S. El-Shazly, *Revue Roumaine de Chimie*, **24**, 695 (1979).

[14] I. M. Sidahmed, S. M. Salem and F. M. Abdel Halim, *J. Indian Chem. Soc.*, Vol. *LVII*, 624 (1980).

[15] C. F. Wells, *J. Chem. Soc. Faraday I*, **71**, 1868 (1975).

[16] Amina M. Hafez and H. Sadek, *Acta Chim. Acad. Scientiarum Hungaricae*, **89**, 257 (1976).

[17] G. S. Darbari, R. P. Singh and S. Rajagopalan, *Nuovo Cimento*, **B 52** (1) (1961).

Revue Roumaine de Chimie, **31**, 3, 335—340 (1986)

DIMETHYL- AND DIPHENYLDITHIOARSINATES OF SOME MAIN GROUP METALS

LUMINIŢA SILAGHI-DUMITRESCU[a], LUIS ALBERTO AVILA-DIAZ[b]* and IONEL HAIDUC[b] **

[a] Institute of Chemistry, Cluj-Napoca
[b] Chemistry Department, Cluj-Napoca University, R-3400 Cluj-Napoca, Romania

Received March 26, 1985

Metallic dimethyl- and diphenyldithioarsinates of the type $M(S_2AsR_2)_n$, where n = the valence of the metal, M = Sn(IV), Pb(II), As(III), Sb(III), Bi(III) and R = CH_3, C_6H_5, were synthesised and characterised by their IR and ^{1}H-NMR spectra. According to spectral data anisobidentate dithioarsinic groups are present in the Group V metal derivatives and isobidentate ligands in the lead compounds. Both mono- and isobidentate R_2AsS_2 units were found in $Sn[S_2As(C_6H_5)_2]_4$.

INTRODUCTION

Dithioarsinic anions, $R_2AsS_2^-$, were found to be very good chelating reagents towards transition metals. [1-10] We were interested in the coordination ability of these anions in relation to less known and investigated main group element derivatives. In this respect some organometallic dimethyl- and diphenyldithioarsinates were reported so far, [11-14] as well as tin(IV)[11] and lead(II)[6] dimethyldithioarsinates. Anisobidentate, monodentate and triconnective bridging ligands were proved to be present in organometallic dithioarsinates. [11-15]

In this paper we report the synthesis and spectral behavior of some other main group metal dimethyl- and diphenyldithioarsinates, namely: $Sn[S_2As(C_6H_5)_2]_4$; $Pb[S_2As(C_6H_5)_2]_2$; $As(S_2AsR_2)_3$; $Sb(S_2AsR_2)_3$; $Bi(S_2AsR_2)_3$

RESULTS AND DISCUSSION

The main group metal dimethyl- and diphenyldithioarsinates were synthesised by mixing the sodium salt of the dithioarsinic acid with an appropriate salt of the metal, in a solvent or in a mixture of solvents (see Experimental Part). The antimony and bismuth derivatives were also obtained starting from the metal powders, sodium dithioarsinates and nitric acid in an organic solvent.

---

* Present address: Instituto di Metallurgica, Caracas, Venezuela
** Address all correspondence to this author.

The infrared spectra, recorded for all synthesised compounds in the 4000—400 cm^{-1} range, exhibit characteristic bands between 700—400 cm^{-1} for dimethyldithioarsinates and 1 450—400 cm^{-1} for diphenyldithioarsinates.

The most important frequencies for establishing the coordination behavior of the dithioarsinic ligands are the As—S stretchings. As shown earlier [16] these frequencies are due to group type vibrations, uncoupled with As—C modes. Taking into account these results and comparing the spectra of the title compounds with those of the starting materials and other dithioarsinates we selected the bands presented in Table 1.

Table 1

Spectral data: As—S stretchings (IR spectra) and chemical shifts (^{1}H-NMR spectra) of the title compounds

Compound	$\overset{1}{\nu}_{AsS}$ (cm^{-1})	$\overset{2}{\nu}_{AsS}$ (cm^{-1})	δ (ppm)
$Pb(S_2AsMe_2)_2$	428 m	465 ms 475 sh	2.05 s
$As(S_2AsMe_2)_3$	405 ms 420 sh	475 ms 454 sh	2.05 s
$Sb(S_2AsMe_2)_3$	405 w 449 m	460 m 470 ms	2.05 s
$Bi(S_2AsMe_2)_3$	410 vw 427 m	452 m 465 ms	2.05 s
$Sn(S_2AsPh_2)_4$	416w 438 m	465 m 490 ms	7.15—7.90 m
$Pb(S_2AsPh_2)_2$	438 m	470 ms 480 sh	7.10—7.89 m
$As(S_2AsPh_2)_3$	428 m 435sh	485ms 465 sh	7.15—7.95 m
$Sb(S_2AsPh_2)_3$	415w 450m	465 ms 480 m	7.15—7.96 m
$Bi(S_2AsPh_2)_3$	420vw 435m	465 ms 480 sh	7.15—7.94 m

vw = very weak, w = weak, m = medium, ms = medium-strong, sh = shoulder, s = singlet, m = multiplet

It is obvious that the metal atom has a quite important influence upon the spectral feature while the R group does not affect the coordination behavior of the dithio group. Although the number of the bands assigned to the arsenic-sulfur stretchings is the same in the spectra of our compounds, the relative position and, consequently, the coordination of the R_2AsS_2 units, are different.

The four bands in the IR spectra of $Sn(S_2AsPh_2)_4$ (where $Ph = C_6H_5$) grouped in two pairs, are characteristic for monodentate (416 cm^{-1}, ν_{As-S} and 490 cm^{-1}, $\nu_{As=S}$) and isobidentate ligands (438 cm^{-1}, ν_{symAs2} and

465 cm^{-1}, $\nu_{\text{antisym AsS}_2}$). The structure is similar to that of $Sn(S_2AsMe_2)_4$[11] (where Me=CH_3) and $Sn(S_2CNEt_2)_4$ (where Et = C_2H_5)[17]. Monodentate diphenyldithioarsinic groups, with the same position of the arsenic-sulfur stretchings were found earlier in organo-silicon, and organogermanium dithioarsinates,[14] while isobidentate ligands are present in transition metal dithioarsinates.[1–4]

The spectra of the lead compounds exhibit two bands, one wearing a shoulder. Isobidentate dithio groups are consistent with the position of the As—S stretchings. Monomeric or polymeric structures cannot be proved at this stage, because of the low solubility of the compounds, which does not permit molecular weight determination. There are examples for both structures in the dithiophosphoric class of compounds: the polymer[18] $\{Pb[S_2P(O-iC_3H_7)_2]_2\}_n$ and the monomer[19] $Pb[S_2P(OC_2H_5)_2]_2$.

The chemistry of heavy Group V elements in the low oxidation state (As(III), Sb(III), Bi(III)) is a good field to check the activity or inactivity of the lone pair (unshared electron pair). Both VSEPR theory[20] of "hard" and ,,soft" acids and bases (HSAB) concept[21] are explaining the behavior of the lone pair in a certain configuration. "Soft" ligands (as the dithio-ligands) generaly lead to a stereochemicaly inactive (inert) lone pair in AB_6E systems.[21] The dithioarsinic ligands, containing sulfur as donor atom, can be considered "soft" ligands (sulfur atom has available orbitals into which the lone pair may be partially delocalized, decreasing lone pair — bonded pair repulsion). On the other hand, the possibility to form small rings (chelates) activates the lone pair (makes it stereochemically active). The competition of these two effects is "influenced" by the metal, different structures being found for the same group metals with the same ligands. Small sized atoms, with low acceptor power facilitate higher lone pair—bonded pair repulsion, the geometry of the molecule being somehow unusual (as for example arsenic (III) N,N′-diethyldithiocarbamate[22] and arsenic (III) xanthate[23] — have distorted trigonal antiprism geometry, the lone pair presumably occupying the triangular face formed by the less tightly bonded sulfur).

With this in mind we tried to deduce the structure of the Group V metal dithioarsinates from their spectral behavior. The general features of the infrared spectra in the As—S stretchings region are similar for all discussed compounds (Table 1). Four bands were found in this region, suggesting at least two different As—S bonds.

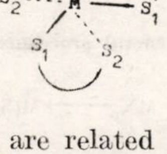

The three As—S_1 bonds are related to "normal" covalent M—S_1 bonds. M—S_2 interactions are not as strong as a covalent bond, therefore, As—S_2 keeps certain double character. The π electrons are, however, less localised than in monodentate dithio-groups: the $\nu_{As=S}$ is shifted to lower energies in the spectra of Group V element dithioarsinates.

Two of the four bands assigned to arsenic-sulfur stretchings have high intensity, the other being shoulders or bands of medium intensity (Table 1). The larger the differences between the two main bands, the weaker the $M-S_2$ interactions are. In the arsenic(III) dithioarsinates the $M-S_2$ interactions are the weakest, while in the bismuth(III) dithioarsinates the coordination of the ligand is almost isobidentate, in accordance with increasing metallic character of the Group V elements.

The infrared spectra of the antimony(III) dithioarsinates show similarities with the dithiophosphinic derivative, $Sb[S_2P(C_6H_5)_2]_3$, whose structure was determined by X-ray diffraction.[24] The geometry of the latest is pentagonal bipyramidal, with the seventh coordinative position occupied by the lone pair of antimony. Taking into account the similarity of the infrared spectra, we tentatively suggest that antimony(III) dithioarsinates have also a pentagonal bipyramidal geometry.

Based on the above theoretical and experimental (spectral) considerations, we may conclude that the activity of the lone pair is decreasing from As(III) derivatives to Bi(III) derivatives, the geometries probably passing from a trigonal antiprism (distorted, of course), through a pentagonal bipyramid to a distorted octahedron.

EXPERIMENTAL PART

The reagents used were of analytical grade purity. Dithioarsinic sodium salts were synthesised using literature data.[1,3]

Infrared spectra were recorded on a SPECORD IR 75, C. Zeiss Jena DDR, spectrophotometer, within the range 4000–400 cm^{-1}, in KBr pellets. ^{1}H-NMR spectra were recorded on a TESLA 487 instrument in $CDCl_3$ or CCl_4 using HMDSO as internal standard. Carbon and hydrogen microanalyses were performed on a Perkin-Elmer 240 B microanalyser.

The synthesis of metal dimethyl- and diphenyldithioarsinates

The title compounds were synthesised in two general ways:

a) the reaction of sodium dimethyl- and diphenyldithioarsinate with a metal salt (used to obtain all dithioarsinates reported here) and

b) the reaction of the metallic powders of antimony and bismuth with the sodium dithioarsinates in the presence of the nitric acid. General procedures for the two methods are presented bellow.

General procedure (a)

$$n\ NaS_2AsR_2 + MX_n \longrightarrow M(S_2AsR_2)_n + n\ NaX$$

A stoichiometric amount of the sodium dimethyldithioarsinate or sodium diphenyldithioarsinate, in ethanol or CCl_4, was mixed under stirring with the required amount of $SnCl_4$, $Pb(OCOCH_3)_2$, $AsCl_3$, $SbCl_3$ or $Bi(NO_3)_3 \cdot 6H_2O$ (in ethanol). 0.3 mL HNO_3 2N were added to the reaction mixture containing Sb(III), Pb(II) and Bi(III). No heating is recommended. Microcrystalline precipitates are formed shortly (10–30′) in all cases.

Several extractions with CCl_4 were needed in order to obtain pure compounds from the reaction mixtures. The yields and physical properties of the synthesised compounds are shown in Table 2.

Table 2

Properties and elemental analysis of metallic dithioarsinates

Compound	Net formula	g NaS_2AsR_2/ mL solvent	g MX_n/ ml solvent	Yield	M.p (°)	Elemental analysis (%)found/calcd.		
						C	H	As
$As(S_2AsMe_2)_3$	$C_6H_{18}As_4S_6$	0.18/5 mL benzene	0.64/15 mL ethanol	32	(226– 234)	12.01 12.37	3.42 3.09	51.16 51.55
$Sb(S_2AsMe_2)_3$	$C_6H_{18}As_3S_6Sb$	0.45/10 mL ethanol	1.35/20 mL ethanol	27 (48)	228	11.14 11.45	2.57 2.86	35.38 35.78
$Bi(S_2AsMe_2)_3$	$C_6H_{18}As_3S_6Bi$	0.74/15 mL ethanol	1.35/20 mL ethanol	43 (58)	127	9.53 9.98	2.27 2.51	31.16 31.42
$Sn(S_2AsPh_2)_4$	$C_{48}H_{40}As_4S_8Sn$	0.26/15 mL benzene	1.34/20 mL acetone	70	108	43.96 44.31	3.38 3.09	22.84 23.24
$Pb(S_2AsPh_2)_2$	$C_{24}H_{20}As_2S_4Pb$	0.59/25 mL ethanol	1.26/20 mL CCl_4	43	(157)	36.02 36.31	2.75 2.52	18.36 18.91
$As(S_2AsPh_2)_3$	$C_{36}H_{30}As_4S_6$	0.18/5 mL benzene	0.96/20 mL acetone	38	(185– 197)	44.92 45.37	3.58 3.14	31.02 31.44
$Sb(S_2AsPh_2)_3$	$C_{36}H_{30}As_3S_6Sb$	0.23/10 mL benzene	0.96/20 mL CCl_4	37 (35)	217	42.72 43.17	2.61 3.00	22.07 22.48
$Bi(S_2AsPh_2)_3$	$C_{36}H_{30}As_3S_6Bi$	0.37/10 mL ethanol	0.96/20 mL CCl_4	40 (52)	143	39.52 39.82	2.49 2.76	20.26 20.74

General procedure (b)

$$M + 3\ NaS_2AsR_2 \xrightarrow{HNO_3} M(S_2AsR_2)_3 + 3NaNO_3$$

A suspension of sodium dimethyldithioarsinate or sodium diphenyldithioarsinate in CCl_4 was mixed with 1 g of Sb or Bi metal powders in the presence of 1 mL HNO_3, 2N, under energic stirring. After one hour the solution is separated from the unreacted metal powder and concentrated. Yellow solids are obtained with the same physical properties as in previous methods (data collected in Table 2). The yields and the purity of the compounds are higher than in method (a).

REFERENCES

[1] M. Forster, H. Hertel and W. Kuchen, *Angew. Chem. Int. Ed. Engl.*, **9**, 811 (1970).

[2] A. T. Casey, N. S. Ham, D. J. Mackey and R. L. Martin, *Austral. J. Chem.*, **23**, 1117, (1970).

[3] A. Mueller and P. Werle, *Chem. Ber.*, **104**, 3872 (1971).

[4] A. T. Casey, D. J. Mackey and R. L. Martin, *Austral. J. Chem.*, **24**, 1587 (1971).

[5] W. Kuchen, M. Forster and H. Hertel, *Chem. Ber.*, **105**, 3310 (1972).

[6] A. Mueller, P. Werle, P. Cristophliemk and I. Tossidis, *Chem. Ber.*, **106**, 3601 (1973).

[7] Z. R. Baratova, P. M. Solozhenkin and E. V. Semenov, *Dokl. Akad. Nauk SSSR, Fiz.–Khim.*, **236**, 1137 (1977).

[8] E. Lindner and H. M. Ebinger, *J. Organometal. Chem.*, **66**, 103 (1974).

[9] B. J. McCormick, J. L. Featherstone, H. L. Stocklosa and J. R. Wasson, *Inorg. Chem.*, **12**, 692 (1973).

[10] Z. R. Baratova, E. V. Semenov, P. M. Solozhenkin and B. S. Prahbanda, *Inorg. Chem.*, **21**, 57 (1982).

[11] I. Haiduc and L. Silaghi-Dumitrescu, *J. Organometal. Chem.*, **225**, 225 (1982).

[12] L. Silaghi-Dumitrescu and I. Haiduc, *J. Organometal. Chem.*, **252**, 295 (1983).

[13] L. Silaghi-Dumitrescu and I. Haiduc, *J. Organometal. Chem.*, **259**, 65 (1983).

[14] L. Silaghi-Dumitrescu, I. Haiduc and J. Weiss, *E. Organometal. Chem.*, **263**, 159 (1984).

[15] C. Silvestru, L. Silaghi-Dumitrescu, I. Haiduc, M. J. Begley, D. B. Sowerby, *J. Chem., Soc., Dalton Trans.*, in press.

[16] I. Silaghi-Dumitrescu, L. Silaghi-Dumitrescu and I. Haiduc, *Rev. Roumaine Chim.*, **27**, 911 (1982).

[17] C. S. Harreld and E. O. Schlemper, *Acta Cryst.*, **B27**, 1964 (1964).

[18] S. L. Lawton and G. T. Kokotailo, *Inorg. Chem.*, **11**, 363 (1972).

[19] T. Ito, *Acta Cryst.*, **B28**, 1034 (1972).

[20] R. J. Gillespie, *J. Chem. Educ.*, **47**, 18 (1970).

[21] J. K. Wynne, *J. Chem. Educ.*, **50**, 330 (1973).

[22] M. Colapietro, A. Domenicano, L. Scaramuzza and A. Vaciago, *Chem. Commun.*, **1968**, 302.

[23] G. Carrai and G. Gottardi, *Z. Kristallogr.*, **113**, 373 (1960).

[24] M. J. Begley, D. B. Sowerby and I. Haiduc, *J. Chem. Soc., Chem. Commun.*, **1980**, 64.

Revue Roumaine de Chimie, **31**, *3*, 341—344 (1986)

PREPARATION AND PROPERTIES OF A NOVEL Pd(II)— Sn(II) COMPLEX

LUMINIȚA PATRON*, ADRIANA CONȚESCU*, GH. ROLEA** and CONSTANȚA GHEORGHIU+

* Center of Physical Chemistry, Bucharest, Romania
** ICECHIM, Bucharest, Romania

Received March 30, 1985

The synthesis of complex compounds with mixed ligands of the system $PdCl_2 - SnCl_2 - (C_4H_9)_4N$ was studied. Elemental chemical analysis, electronic and IR spectra, determinations of molecular electric conductivity and magnetic susceptibility are in agreement with the following formula : $[(C_4H_9)_4N]_2[Pd(SnCl_3)_2I_2]$.

The complex compounds with Sn—M and Ge—M bonds, where M is a platinum group metal exhibit catalytic activity in hydrogenation and isomerization of hydrocarbons, acids and polyunsaturated esters ; they have focused an increasing attention lately.[1,2]

In order to elucidate the catalytic activity of complex compounds with $SnCl_3^-$ ligand, studies have been conducted on the chemistry of these combinations. Therefore complex compounds of the elements in the 2nd and 3rd transition series, especially those with d^6 and d^8 electron configurations, were obtained. [3-9]

The platinum metals form in solution as well as in solid state, coordination compounds with the $SnCl_3^-$ ligand. [10,11]
The existence of some complex combinations of Pd(I), of $[Pd(C_3H_5)P(C_6H_5)_3)(SnCl_3)]$[12] or $[Pd(SnCl_3)_2Cl]_2^{4-}$[13] type is mentioned in the literature. While the structure of the first kind of complex compounds was established by X-ray difraction, the second kind is only partially characterized, its structural formula being assigned by analogy with Rh(I) compound, $[RhCl(SnCl_3)_2]_2^{4-}$.

A few such compounds are known for Pd(II). These complex compounds containing Pd(II) — MCl_3 bond are characterized by the general formula $[PdL_2(MX_3)_2]$, where $L=PPh_3$; $AsPh_3$; $M^{II} = Sn$, Ge ; $X^- = Cl$, Br.[14] All attempts of isolating the anion complex : $[Pd(SnCl_3)_nCl_{4-n}]^{2-}$ with quaternary ammonium salts have failed. [13]

We studied the separation of complex compounds with mixed ligands of the system :

$$PdCl_2 - SnCl_2 - [(C_4H_9)_4N]I$$

+ Deceased March 27, 1983

The study of the solution equilibria of Pd(II) halogenated complexes supports the hypothesis that Pd(II) ion is a type "b" acceptor for which the affinity for halogen coordination increases in the sequence $Cl^- < Br^- < I^-$[15] The preference of Pd(II) ion to coordinate I^- determines the use of tetrabutylammonium iodide. The crystalline, dark-violet compound, $[(C_4H_9)_4N]_2\ [Pd(SnCl_3)_2I_2]$ is obtained. It decomposes at 50–60°.

The determination of molecular electric conductivity in acetone solutions confirmed the nature of the compound. The value obtained 178.5 $\Omega^{-1}cm^2mol^{-1}$ is in the range 170–200$\Omega^{-1}cm^2mol^{-1}$, that corresponds to a 2 :1 electrolyte.[16]

Further information was obtained from infrared spectra. The complex compounds containing $SnCl_3^-$ group as ligand exhibit two bands characteristic of σ-coordinated $SnCl_3^-$ group, in the infrared region (300–350 cm^{-1}).[14] The far infrared spectrum recorded for the combination $[(C_4H_9)_4N]_2[Pd(SnCl_3)_2I_2]$ exhibits two bands at 320 cm^{-1} and 340 cm^{-1} assigned to ν_{sym} and ν_{asym} of $SnCl_3^-$ σ – coordinated group (Fig. 1). The vibration frequencies characteristic of Pd–$SnCl_3$ and Pd–I bonds lie in the 190–220 cm^{-1} range which were outside the range of our apparatus.

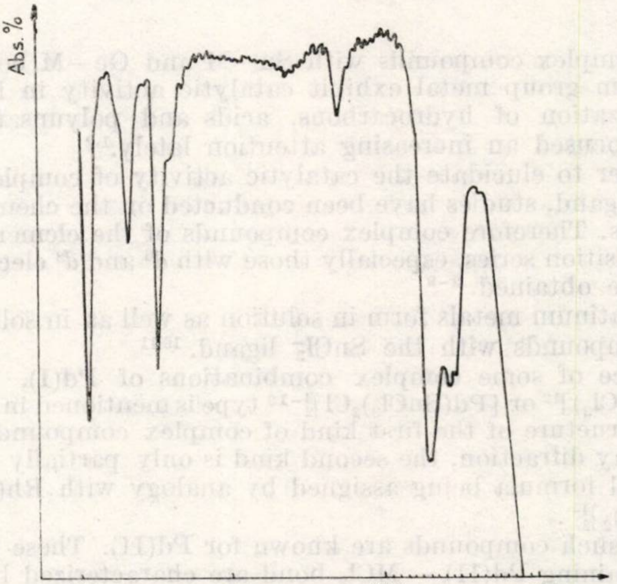

Fig. 1. – IR spectra of $[(C_4H_9)_4N]_2[Pd\ (SnCl_3)_2I_2]$.

The UV–VIS spectra recorded for the compound prepared both in absorption and reflection, confirm the square-planar configuration of Pd(II) (d^8) ion. Table 1 lists the main bands from 13,000–40,000 cm^{-1} range and the corresponding assignments. The assignment of bands in the spectra was made by comparison with the data reported for $[PdI_4]^{2-}$

Table 1

Reflectance spectra and spectra in solution of $[(C_4H_9)_4N]_2[Pd(SnCl_3)_2I_2]$

$[(C_4H_9)_4N]_2[Pd(SnCl_3)_2I_2]$			$[PdI_4]^{2-}$ Acetone sol. 18	$[PdBr_4]^{2-}$ Refl. 20	Assign. 18 .20
Reflectance cm^{-1}	Acetone sol. cm^{-1}	Chloroform sol. cm^{-1}			
15400			16000	16000	$^1A_{1g} \rightarrow {}^1E_g$ $d_{xy} \rightarrow d_{x^2-y^2}$
18500	18500	19100	18500	20000	$^1A_{1g} \rightarrow {}^1E_g$ $d_{xy}d_{yz} \rightarrow d_{x^2-y^2}$
26000	22900		22300	26000	$^1A_{1g} \rightarrow {}^1B_{1g}$ $d_{z^2} \rightarrow d_{x^2-y^2}$
	30400	29200	29400	30400*	$^1A_{1g} \rightarrow E_u$ $Cl_p \rightarrow d_{x^2-y^2}$
	38000 37700	38500 36900		36500^a	$^1A_{1g} \rightarrow E_u$ $Cl_p \rightarrow d_{x^2-y^2}$

^{a}Spectra in aqueous solution with Br^- excess.

and $[PdBr_4]^{2-}$.[17-19] The bands observed for acetone and chloroform solutions, in the 30,000—38,000 cm^{-1} range were assigned to ligand→metal charge transfer transitions; this agrees with Gray and Balhausen's data.[19]

The diamagnetism recorded for this combination is in agreement with the square-planar structure.

EXPERIMENTAL

Preparation of the complexes

The compound $[(C_4H_9)_4N]_2$ $[Pd(SnCl_3)_2I_2]$ is obtained from methanol-HCl 10 M (5 : 1) solution which contains Pd(II) and Sn(II) at a 1 : 5 ratio, on addition of methanol solution of tetrabutylammonium iodide (10%) at pH = 1—2.

Found : Sn % :18.36 ; Cl % : 16.60 ; I % : 20.00 ; C % : 30.00 ; N % : 2.20 ; H % : 5.56. $[(C_4H_9)_4N]_2$ $[Pd(SnCl_3)_2I_2]$ requires : Sn % : 18.39 ; Cl % : 16.46 ; I % : 19.62 ; C % : 29.67 ; N % : 2.16 ; H % : 5.56.

Physical measurements

Electronic spectra were recorded on VSU-1 Zeiss Jena spectrophotometer within a 260—1100 nm range. IR spectra were recorded on a UR-10 Zeiss-Jena spectrophotometer. Magnetic susceptibilities of solid samples were measured by the Faraday method using Mohr salt as standard. Molecular electrical conductivities were determined in acetone at 25° by means of an OK-102/1 radelkis conductometer with a 0.1 μS — 0.25 S measuring range.

REFERENCES

[1] R. D. Cramer, *J. Amer. Chem. Soc.*, **85**, 1691 (1963).
[2] J. C. Bayllar, jr., *J. Amer. Chem. Soc.*, **89**, 1592 (1967).
[3] R. D. Cramer and R. V. Lindsey, *J. Amer. Chem. Soc.*, **87**, 658 (1965).
[4] J. F. Young, *J. Chem. Soc.* (*A*), **1964**, 5179.

[5] R. V. Lindsey and R. Parshall, *J. Amer. Chem. Soc.*, **86**, 5367 (1964).
[6] J. Chatt, *J. Chem. Soc.*, **1962**, 5075.
[7] J. Davies, *J. Amer. Chem. Soc.*, **85**, 1692 (1963).
[8] G. Wilkinson, *J. Inorg. Nucl. Chem.*, **28**, 2708 (1968).
[9] R. C. Tayllor and J. F. Young, *Inorg. Chem.*, **6**, 20 (1966).
[10] J. S. Young and G. Wilkinson, *J. Chem. Soc.*, **1964**, 5176.
[11] J. S. Young and G. Wilkinson, *J. Chem. Soc.*, **1964**, 992.
[12] R. Mason and O. P. Whimp, *J. Chem. Soc.*, **1969**, 2709.
[13] M. A. Kattak and R. J. Magu, *J. Chem. Soc., Chem. Commun.*, **1965**, 400.
[14] B. Crociani, F. Boschi and M. Nicollini, *Inorg. Chim. Acta.*, **4**, 577 (1970).
[15] D. J. Phillys and S. Tyree, *J. Amer. Chem. Soc.*, **83**, 1806 (1961).
[16] F.R. Hartley, "The chemistry of platinum and palladium", Appl. Sci. Publ. LTD, London, 1973, p. 238.
[17] P. Day, A. F. Orchard, A. J. Thomson and R. J. P. Williams, *J. Chem. Phys.*, **42**, 1973 (1965).
[18] P. Day, M. J. Smith and R. J. P. Willliams, *J. Chem. Soc (A)*, **1968**, 668.
[19] H. B. Gray, C. J. Balhausen, *J. Amer. Chem. Soc.*, **85**, 260 (1963).

Revue Roumaine de Chimie, **31**, *3*, 345—351 (1986)

HETEROPOLYTUNGSTATES WITH Ti(IV) AND Ni(II). VIII[1]

CRYSTAL DATA FOR THE POTASSIUM AND AMMONIUM SALTS OF THE Ni(II)-UNDECATUNGSTOTITANATE(IV) ANION

RODICA VĂȚULESCU, T. BUDIU, GH. MARCU and GH. MORARU
Institute of Chemistry, 30 Fîntînele Street, 3400 Cluj-Napoca, Romania

Received February 14, 1985

The results of the X-ray powder diffraction analysis and of the picnometer density determinations of $K_6[H_2ONiTiW_{11}O_{39}] \cdot 13H_2O$ (I_K) and $(NH_4)_6[H_2ONiTiW_{11}O_{39}] \cdot 11.5H_2O$ (I_{NH_4}) are reported. Both salts crystallize in the face centered cubic system, with the possible space groups: Fm3m, $F\overline{42}m$, F432 or F23; the lattice constant is a = 12.3364 Å and respectively a = 21.9218Å and the number of molecules per unit cell, Z = 8.

1. INTRODUCTION

In early papers of Baker and co-workers [2] concerning the heteropolytungstic series 1 : 1 : 11, a primitive cubic crystalline structure was assigned to the first representatives of this series, which they formulated as dodecatungstates. Subsequently, the same authors [3] reported that the actual symmetry of these heteropolytungstates was face centered cubic and they assigned them a modified Keggin-type structure. (The face centering of the unit cell is explained by the fact that two adjacent Keggin units differ in orientation with a 90° rotation; this arrangement is similar to the NaCl structure, the Na^+ and Cl^- ions being replaced by Keggin-type units).

By obtaining and characterizing new heteropolyanions of the type 1 : 1 : 11, isomorphous with those described by Baker and co-workers,[2,3] subsequent studies [4–8] confirmed and completed their assertions.

2. EXPERIMENTAL

The X-ray powder diffraction spectra were recorded at room temperature on a 1050 PW Philips X-ray spectrometer, using a Cu anode tube and a Ni β filter. The diffraction diagrams were recorded on paper in the usual manner, with a scanning rate of 1° 2θ/min and a rotation speed of the sample of 60 rot/min. The intensity was measured by means of a proportional detector with Xe, coupled with a pulse height analyser.

The picnometer density determinations were carried out in acetone as picnometric liguid, at 20°C, with an accuracy of ± 0.05 g/cm³.

RESULTS AND DISCUSSIONS

The X-ray diffraction diagrams for the potassium and ammonium salt of the $[H_2ONiTiW_{11}O_{39}]^{6-}$ anion were recorded in the coordinates: Bragg angle θ (in fact 2θ value) as a function of the intensity of the diffraction lines. The relative intensities of the diffraction lines and the interplanar spacings d were calculated by means of Bragg's relation:

$$\lambda = 2d \sin\theta \tag{1}$$

The data obtained are given in table 1.

Table 1

The interplanar spacings and the relative intensities of the diffraction lines for the potassium (I_K) and ammonium (I_{NH_4}) salts of the anion $[H_2ONiTiW_{11}O_{39}]^{6-}$

I_K				I_{NH_4}			
d(Å)	$I_r = \frac{I}{I_{max.}}$	d(Å)	I_r	d(Å)	I_r	d(Å)	I_r
12.2581	5	2.3861	2	12.5530	4	3.0374	12
10.6524	100	2.3284	3	10.9149	100	2.9284	4
7.5185	16	2.2740	4	7.7410	28	2.8553	3
5.3276	12	2.2364	22	6.5889	3	2.7403	31
4.7702	60	2.1780	2	6.3481	2	2.6590	46
4.3527	7	2.1333	2	5.4644	23	2.5829	4
3.7701	14	2.0924	3	5.0240	5	2.5298	2
3.5532	25	1.9890	5	4.9009	70	2.4515	4
3.2152	60			4.4665	50	2.3926	5
3.08102	79			4.2158	3	2.3378	7
2.9592	11			3.8783	19	2.2381	2
2.6671	28			3.6553	19	2.2033	5
2.5886	35			3.4653	3	2.1503	5
2.5140	3			3.1662	61		

The diffraction diagrams were indexed by means of the analytical indexing method.[9,10] As a first step, the correspondence with the cubic symmetry system was verified; in this aim, the proportionality of the values $1/d^2$ with the sequence of values of the whole numbers N, which can be taken by the sum of Miller's indices ($h^2 + k^2 + l^2 = N$), was checked for every reflection apart, according to the relation:

$$\frac{1}{d^2} = \frac{1}{a^2}(h^2 + k^2 + l^2) = \frac{N}{a^2} \tag{2}$$

where: d = the interplanar spacing;
h, k, l = Miller's indices;
a = the lattice constant.

The first 22 reflections were taken into consideration for indexing the X-ray diagram of compound I_K and the first 27 reflections for compound I_{NH_4}. The crystal structural data obtained for the compounds $K_6[H_2ONiTiW_{11}O_{39}]\cdot 13H_2O$ and $(NH_4)_6[H_2ONiTiW_{11}O_{39}]\cdot 11.5H_2O$ are given in tables 2 and 3 respectively.

Table 2

The experimental crystal data obtained for $K_6\ [H_2ONiTiW_{11}O_{39}] \cdot 13H_2O$, compared with the calculated values

h	k	l	$N_{exp.}$	N	$1/d^2_{exp.}$	$1/d^2_{calc.}$	$a_{exp.}$ (Å)
1,	1,	1	3.03	3	0.006655	0.006589	21.3376
2,	0,	0	4.01	4	0.008810	0.008786	21.3345
2,	2,	0	8.05	8	0.017690	0.017570	21.3321
4,	0,	0	16.04	16	0.035231	0.035144	21.3373
4,	2,	0	20.0	20	0.043950	0.043930	21.3321
4.	2,	2	24.03	24	0.052781	0.052716	21.3372
4,	4,	0	32.03	32	0.070353	0.070288	21.3371
6, 0, 0	4,	4, 2	36.06	36	0.079205	0.079074	21.3371
6,	2,	2	44.04	44	0.096735	0.096646	21.3369
4,	4,	4	47.96	48	0.105344	0.105432	21.3370
6,	4,	0	51.99	52	0.114200	0.114218	21.3366
8,	0,	0	64.0	64	0.140576	0.140576	21.3370
8, 2, 0	6,	4, 4	67.94	68	0.149230	0.149362	21.3370
8, 2, 2	6,	6, 0	72.03	72	0.158214	0.158148	21.3370
8.	4,	0	79.96	80	0.175632	0.175720	21.3370
8,	4,	2	83.97	84	0.184440	0.184506	21.3357
6,	6,	4	88.04	88	0.193383	0.193292	21.3368
9,	3,	1	91.02	91	0.199925	0.199881	21.3370
8,	4,	4	95.97	96	0.210798	0.210864	21.3370
10, 0, 0	8,	6, 0	100.03	100	0.219715	0.219650	21.3370
10, 2. 0	8,	6, 2	103.98	104	0.228392	0.228436	21.3370
9,	5,	3	115.07	115	0.252751	0.252597	21.3370

Table 3

The experimental crystal data obtained for $(NH_4)_6\ [H_2ONiTiW_{11}O_{39}]\ 11.5H_2O$ compared with the calculated values

h	k	l	$N_{exp.}$	N	$1/d^2_{exp.}$	$1/d^2_{calc.}$	$a_{exp.}$ (Å)
1,	1,	1,	3.05	3	0.006346	0.006242	21.9229
2,	0,	0	4.03	4	0.008394	0.008323	21.9112
2,	2,	0	8.02	8	0.016688	0.016646	21.9222
3,	1,	1	11.07	11	0.023034	0.022888	21.9224
2,	2,	2	11.93	12	0.024815	0.024969	21.9261
4,	0,	0	16.09	16	0.033490	0.033292	21.9189
3,	3,	1	19.04	19	0.039618	0.039535	21.9223
4,	2,	0	20.01	20	0.041634	0.041616	21.9229
4,	2,	2	24.09	24	0.050126	0.049939	21.9223
5, 1, 1	3,	3, 3	27.04	27	0.056264	0.056181	21.9223
4,	4,	0	31.95	32	0.066483	0.066585	21.9219
6, 0, 0	4,	4, 2	35.97	36	0.074845	0.074908	21.9224
6,	2,	0	40.02	40	0.083273	0.083232	21.9223
4,	4,	4	47.94	48	0.099755	0.099878	21.9220
6,	4,	0	52.09	52	0.108392	0.108201	21.9219
6,	4,	2	56.04	56	0.116614	0.116524	21.9216
7, 3, 1	5,	5, 3	58.95	59	0.122657	0.122767	21.9227
8,	0,	0	64.0	64	0.133172	0.133172	21.9221
8, 2, 0	6,	4, 4	67.97	68	0.141432	0.141494	21.9222
8, 2, 2	6,	6, 0	72.03	72	0.149891	0.149817	21.9214
7, 5, 1	5,	5, 5	75.09	75	0.156247	0.156060	21.9222
8,	4,	0	79.96	80	0.166380	0.166464	21.9222
8, 8	4,	2	83.95	84	0.174692	0.174787	21.9216
6,	6,	4	87.93	88	0.182964	0.183110	21 9222
8,	4,	4	95.94	96	0.199632	0.199756	21.9222
9, 3. 3	7, 7, 1	7, 5, 5	98 99	99	0.205978	0 205999	21.9222
10, 2, 0	8	6 2	103 94	104	0.216278	0.216403	21.9222

The concordance of the experimental and calculated values $1/d^2$ verifies the indexing corectness and the fact that the samples examined contain a single phase, a unitary compound.[9]

The values obtained for the sum of the squares of Miller's indices (N) for the compounds I_K and I_{NH_4} are rangedwithin the series of N values characteristic for the structure of the face centered cube. This fact enables us to attribute a crystalline structure of face centered cube to the potassium and ammonium salts of the anion $[H_2ONiTiW_{11}O_{39}]^{6-}$.

From the experimental values $1/d^2$ and N we calculated the lattice constant a according to the relation (2). From the mean of all the values a (tables 2 and 3) the value $\bar{a} = 21.3364$ Å for the compound $K_6[H_2ONiTiW_{11}O_{39}]\cdot 13H_2O$ and the value $\bar{a} = 21.9218$ Å for the salt $(NH_4)_6[H_2ONiTiW_{11}O_{39}]\cdot 11.5H_2O$ were obtained; both these compounds are isomorphous with other heteropolytungstates with 2 metal central ions, [3-8,11] having the same face centered cubic structure and similar structural parameters.

The parameter Z (the number of complex molecules in the unit cell) as well as the molecular weights of the compounds I_K and I_{NH_4} were calculated, on the basis of the experimental values obtained for the densities and of the following roentgenographic relation:

$$M = \frac{a^3 \cdot \rho \cdot N_A}{Z} \tag{3}$$

where: a = the lattice constant;
ρ = the density;
N_A = Avogadro's number;
M = the molecular weight.

The values of the densities experimentally obtained as well as the values of the parameter Z and of the molecular weights are presented in table 4.

Table 4

The values of the lattice constant a, of the density ρ, of the parameter Z and of the molecular weight M obtained for $K_6[H_2ONiTiW_{11}O_{39}]\cdot 13H_2O$ and $(NH_4)_6[H_2ONiTiW_{11}O_{39}]\cdot 11.5H_2O$

Compound	a(Å)	exp. (g/cm³)	$M_{exp.}$	$M_{theor.}$	Z
$K_6[H_2ONiTiW_{11}O_{39}]\cdot 13H_2O$	21.3364	4.4	3217.46	3239.77	$7.945 \simeq 8$
$(NH_4)_6[H_2ONiTiW_{11}O_{39}]\cdot 11.5H_2O$	21.9218	3.9	3093.07	3085.97	$8.01 \simeq 8$

Since the X-ray powder diffraction method has serious limitations when applied to determining the space groups of a crystal structure unambiguously, we only may indicate as possible space groups for the face centered cubic system the following: Fm3m, $F\bar{4}2m$, F432 or F23. Each of these requires 8 complex molecules, with the characteristic four threefold axes of symmetry of a Keggin-type anion, in its crystallographic unit cell.

Our experimental values 7.94 and 8.01 of the parameter Z obtained for potassium — respectively ammonium nickel (II)—undecatungstotitanate (IV) are thus in good agreement.

The molecular weights determined on the basis of the roentgenographic data are in agreement with the theoretical values calculated from the formulae assigned as a result of the chemical analysis. The error was $-$ 0.6 % for the potassium salt and +0.3 % for the ammonium salt of anion $[H_2ONiTiW_{11}O_{39}]^{6-}$ thus confirming the formulation of both complexes.

As a result of the roentgenographic analysis and according to the data obtained in solution concerning the nickel coordination[12] and the coordinative nonequivalence of the titanium and nickel heteroatoms,[1,13] it may be assumed that the heteropolytungstic anion $[H_2ONiTiW_{11}O_{39}]^{6-}$ has a modified Keggin-type structure, of general formula :

$$[H_hM^{m+}O_6X^{x+}O_4W_{11}O_{30}]^{(14-m-x-h)-}$$ [3]

or

$$[Y^{y-}M^{m+}O_5X^{x+}O_4W_{11}O_{30}]^{(12-m-x+y)-}$$ [14]

Allowing for the above mentioned assumption concerning the ,,molecular" structure of the $[H_2ONiTiW_{11}O_{39}]^{6-}$ anion, the tetrahedrally coordinated titanium atom is likely to be the central heteroatom, according to a classical Keggin structure. In every complex anion, the nickel atom, which is hexacoordinated,[12] is likely to occupy randomly one of the 12 positions of the ligand tungsten atoms of a conventional Keggin structure. The other 11 positions will be occupied by 11 tungsten atoms, like in the usual Keggin structure.

In accordance with other researchers[3, 11, 14] we consider that the constitutional water molecule is most probably placed at nickel, the "outer" heteroatom ocupying the 6-th coordinative site (that one orientated towards the exterior).

In our previous notes,[1, 12, 13, 15, 16] we reported on the anion $[H_2ONiTiW_{11}O_{39}]^{6-}$, as well as on the preparation and study of another heteropolytungstic anion, $[H_2ONiTiW_5O_{20}]^{4-}$, belonging to the series 1 : 1 : 5.

The studies concerning the structure of the compounds of the series 2 : 5 were carried out by Strandberg[17] and Fischer and co-workers[18] on molybdenum representatives with two identical heteroatoms. In both cases, the above mentioned authors formulate the complex anion $[P_2Mo_5O_{23}]^{5-}$ as a ring of five distortioned MoO_6 octahedra out of which four have common edges. The ring is closed at the fifth MoO_6 octahedron by sharing a corner. The phosphorus atoms, both tetrahedrally coordinated by oxygen atoms, are placed on both sides of the cavity surrounded by the five molybdenum octahedra, since the cavity formed in the inside structure is smaller than necessary for a tetrahedral coordination. Thus, such a structure supposes two structurally equivalent heteroatoms, with an identical or very similar chemical behaviour.

The structure shortly described above, may also be compared to the structure of 6 molybdenum or 6 tungsten rings, taking into consideration that the interatomic Mo—Mo distances are very close to those which are to be found in the compound $(NH_4)_6[TeMo_6O_{24}]\cdot 7H_2O$,[19] which is known to have the structural model proposed by Anderson.[20]

Taking into consideration the structural model described for the anion $[P_2Mo_5O_{23}]^{6-}$,[17,18] as well as the studies on the behaviour or the anion $[H_2ONiTiW_5O_{20}]^{4-}$[1, 12, 13, 15, 16] in solution, we consider that we cannot assign to the latter the same structural model as to the anion $[P_2Mo_5O_{23}]^{6-}$, for the following reasons:

— in the structural model described for the anion $[P_2Mo_5O_{23}]^{6-}$ both heteroatoms are tetrahedrally coordinated, while in the case of the anion $[H_2ONiTiW_5O_{20}]^{4-}$, nickel is proved to be octahedrally coordinated.[12]

— the two phosphorus atoms in the pentamolybdodiphosphate anion are structurally equivalent and are expected to have an identical behaviour from the chemical point of view; but the two heteroatoms (titanium and nickel) in the Ni(II)-pentatungstotitanate (IV) anion exhibit a different behaviour, namely titanium is more strongly bonded in the structure as compared with nickel. The nickel ion is expelled from the complex anion on acid degradation[1] or when it is treated with ion exchangers in the H^+ form;[13] in each case a heteropolyacid with titanium and tungsten of ratio 1 : 6 is obtained. Therein it follows that the two heteroatoms are not identical from the structural point of view.

Having in view the similar behaviour in solution of the anion $[H_2ONiTiW_{11}O_{39}]^{6-}$, derived from a lacunar structure and of the anion $[H_2ONiTiW_5O_{20}]^{4-}$, as well as the fact that on alkaline degradation the anion Ni(II)-pentatungstotitanate(IV) was observed to be an intermediate stage of the alkaline degradation of the former, we may suppose that the structure of the anion $[H_2ONiTiW_5O_{20}]^{4-}$ is of lacunar type. Michelon and Hervé,[21] stated the same concerning the anion $[Sb_2W_5O_{20}]^{4-}$, without further relations with regard to the structure of this anion.

Taking into consideration the data reported above, as well as the possible parallelism between the structure of P_2Mo_5 and the Anderson-type XMO_6 structures,[17] we propose for the anion $[H_2ONiTiW_5O_{20}]^{4-}$ a new possible structural model, namely, a lacunar structure derived from the Anderson classical model of the heteropolycompounds of ratio 1 : 6. This would mean that the nickel ion, octahedrally coordinated, occupies randomly the place of a tungsten atom in the ring of $6WO_6$ octahedra of the Anderson model. According to the Anderson model, titanium is supposed to be octahedrally coordinated. In various chemical combinations as well as in heteropolycompounds, titanium may also be octahedrally coordinated,[4,5,8,22,23] but in the case of the heteropolytungstates we dealt with, we have not established the type of the titanium coordination.

Further studies are to elucidate some of the problems not yet solved concerning these new compounds.

REFERENCES

[1] R. Vățulescu, T. Budiu, Gh. Marcu and I. Pal, note VII, *Rev. Roumaine Chim.*, **31**, 209 (1986).

[2] L. C. W. Baker and T. P. Mc Cutcheon, *J. Am. Chem. Soc.*, **78**, 4503 (1956).

[3] L. C. W. Baker, V. Simmons-Baker, K. Eriks, M. T. Pope, M. Shibata, O. W. Rollins, J. H. Fang and L. L. Koh, *J. Am. Chem. Soc.*, **88**, 2329 (1966).

[4] R. Ripan and M. Pușcașiu, *Z. Anorg. Allg. Chem.*, **358**, 82 (1968).

[5] T. J. R. Weakley and S. A. Malik, *J. Inorg. Nuclear Chem.*, **29**, 2935 (1967).

[6] C. M. Tourne, G. F. Tourne, S. A. Malik and T. J. R. Weakley, *J. Inorg. Nuclear Chem* **32**, 3875 (1970).

[7] O. W. Rollins and Ch. R. Skolds, *J. Inorg. Nuclear Chem.*, **42**, 371 (1980).

[8] O. W. Rollins, *J. Inorg. Nuclear Chem.*, **42**, 1368 (1980).

[9] R. W. M. D'Eye and E. Wait, "X-Ray Powder Photography in Inorganic Chemistry", Butterworth Scientific Publications, London, 1960, p. 80, 117, 183.

[10] L. V. Azaroff and M. J. Buerger, "The Powder Method in X-Ray Crystallography", Mc. Graw Hill Book Company, Inc., New York, Toronto, London, 1958, p. 79.

[11] T. J. R. Weakley, *J. Chem. Soc. Dalton Trans.*, **3**, 341 (1973).

[12] R. Vățulescu, T. Budiu, Gh. Marcu and I. Pal, note III, *Rev. Roumaine Chim.*, **30**, 823 (1986).

[13] R. Vățulescu, T. Budiu, Gh. Marcu and I. Pal, note VI, *Rev. Roumaine Chim.*, **31**, 199 (1986).

[14] L. C. W. Baker and J. S. Figgis, *J. Am. Chem. Soc.*, **92**, 3794 (1970).

[15] R. Vățulescu, T. Budiu and Gh. Marcu, *Rev. Roumaine Chim.*, **26**, 851 (1981).

[16] R. Vățulescu, T. Budiu and Gh. Marcu, *Rev. Roumaine Chim.*, **26**, 971 (1981).

[17] R. Strandberg, *Acta Chem. Scand.*, **27**, 1004 (1973).

[18] J. Fischer, L. Ricard and P. Toledano, *J. Chem. Soc. Dalton*, **9**, 941 (1974).

[19] H. Evans, *J. Am. Chem. Soc.*, **70**, 1291 (1948).

[20] J. S. Anderson, *Nature*, **140**, 850 (1937).

[21] M. Michelon and G. Hervé, *Compt. rend.*, **274**, 209 (1972).

[22] C. M. Tourne, *Compt. rend.*, **266**, 702 (1968).

[23] F. A. Cotton and G. Wilkinson, "Advances Inorganic Chemistry", New York, London, Sydney Interscience Publishers, (a Division of John Wiley and Sons), second ed., 1966, p. 799.

Revue Roumaine de Chimie, **31**, *3*, 353—360 (1986)

DETERMINATION OF COBALT AND MANGANESE IN BLOOD SERUM BY FLOW INJECTION ANALYSIS AND ATOMIC ABSORPTION SPECTROSCOPY

N. LEÓN, J. L. BURGUERA, M. BURGUERA and O. M. ALARCÓN*
Departamento de Química, Facultad de Ciencias, Universidad de Los Andes, Apartado 542, Mérida, Venezuela
*Departamento de Bioquímica, Facultad de Medicina, Universidad de Los Andes, Mérida, Venezuela

Received February 25, 1985

The determination of serum cobalt and manganese has been shown to be feasible by the use of flow injection analysis combined with atomic absorption spectrophotometry. The sample is injected into a continuously aspirated analytical stream which is fed into the nebulizer of an atomic absorption spectrometer. Matrix problems are overcome by preparing the standard solutions in 20% (V/V) glycerol containing physiological amounts of albumin, sodium, phosphate, chloride and sulphate. A sample throughput of ca. 120 measurements per hour is possible. The coefficients of variation for within-batch and between-batch are ca. 3.5 and 2.9% for cobalt, and ca. 3.2 and 3.4% for manganese, respectively, in serum samples ($n=12$). The proposed method takes less time to perform and was found to give similar precise results in comparison with a conventional method based on standard addition. However, the flow injection method uses microsamples (100 µL) being suitable for paediatric research.

During the past decade, there was increased the importance of trace element chemistry in biological systems. This awareness was stimulated by the rising concern in industrialized nations of man's impact on his environment and its biological effect on him. Of primary importance is the role played by trace elements and their beneficial or harmful effects on the biochemistry of man. Whether an element is essential or toxic to human metabolism, will depend to a large extent on its concentration level in the organism.[1] However, some elements which are present at fairly constant concentrations in all healthy tissues of all living beings are considered to be essential trace elements[2]. The elements fulfilling these requirements are Cr, Co, Cu, F, Fe, I, Mn, Mo, Ni, Se, Si, Sn, V, and Zn. The limiting factor in the study of the role of trace elements in biochemical metabolism has been the presence of many elements at extremely low levels,[3,4] which requires a major effort before its evaluation. Manganese and cobalt are among these elements, which are present at µgL levels in blood serum.[5]

Manganese is essential for bone and tissue formation, carbohydrate metabolism, reproductive processes, and lipid metabolism.[6] Human metabolism of manganese has been extensively studied with radiactive tracer techniques,[7,8] and its inclusion for patients on intravenous feeding is recommended. Literature values for manganese in blood decreased over the years.[1] In 1940 it was reported as high as 10 mg/L, but recent reports indicate only 0.06 mg L.[1] The same tendency has been observed with the manganese values in blood serum, e.g. : methods involving furnace A.A.S. have given, to date, higher values for normal levels than the most careful work based on neutron activation analysis and catalysis.[9] Disagreement over values for normal levels of manganese in serum[5] shows that there are still many problems involved in this measurement.

Cobalt is also a vital element that is required in the normal diet of man in the form of the cyanocobalamin complex, vitamin B_{12}. In the case of iron-deficiency anaemia, inorganic cobalt may be added to the diet (with iron) to increase the rate of haemogolobin synthesis,[10,11] however, cobalt in doses of about 5 mg per day can be toxic to man.[12] Over 24 papers have been published on the determination of cobalt in either whole blood, plasma or serum,[13] usually in connection with medical studies in which an observed difference in the cobalt level has been usefully attributed to a clinical condition. Values for cobalt in blood serum as high as 370[14] and as low as 0.072 μg L[15] have been reported. It appears that the unexpectedly large variation observed in the cobalt serum values arises primarily from the difficulties caused by an actual μg/L level of this element. Neutron-activation analysis has been the most popular method more recently, but the results still vary by a factor of at least 100.[13]

Flow injection analysis (FIA) is based on the remarkably reproducible behaviour of fluid streams under fixed geometrical arrangements and constant flow rates.[16] Hence, the repeated injection of volumes of sample into an inlet carrier stream will yield reproducible response curves,[17] This principle combined with several methods, such as chemiluminescence,[18,19] colorimetry,[20] fluorimetry,[21] atomic absorption,[22,23] and enzymaiic methods[24] has produced useful solutions to a broad range of protblems.

FIA-AAS has been applied to the determination of Li,[25] Zn,[26] Cu,[26] Ca,[27,29], Mg,[27,28], Na,[22] and K.[22] To the author's best knowledge, studies of the determination of Co and Mn by a FIA-AAS system have not yet been carried out. Thus, this paper describes a combination of FIA and AAS for the direct determination of cobalt and manganese in serum. A continuous analytical stream is aspirated through the injection part into the atomic absorption spectrometer nebulizer at a constant rate, and the sample is injected into the stream. The transient analytical signal is recorded. A similar technique has been applied to the analysis of Ca, Mg, Na, and K in serum.[22,28]

EXPERIMENTAL

Reagents. The chemicals were of analytical grade. The water was deionised and then twice distilled. Cobalt chloride ($CoCl_2 \cdot 4H_2O$, Merck) and manganese chloride ($MnCl_2 \cdot 4H_2O$, BDH) were used to prepare primary 1000 ppm cobalt and manganese standard solutions, respectively. Secondary standard solutions were prepared daily. All standards were prepared in

20% (V/V) glycerol, and 3500, 30, 3600, 33 and 5500 mg/L of sodium, phosphate, chloride, sulphate and human albumin, respectively. All glassware, pipettes, syringes and sample tubes were cleaned with 20% (V/V) nitric acid and thoroughly rinsed with water before use.

Sample collection. The blood samples analyzed in the present study were collected by means of disposable polystyrene syringes with rubber plungers and to which platinum needles were adapted. The blood was transferred into acid-washed polystyrene tubes (with polyethene stoppers), allowed to clot for 30 min and then centrifuged into the same tubes. Serum was separated and stored in polystyrene tubes at —20°C. Aliquots of the trace elements were analyzed within one month. Before analysis, the frozen serum was allowed to come to room temperature and homogenized by mixing with a plastic rod.

Instrumentation. A Varian-Techtron 1475-BD atomic absorption spectrometer was used under the operating conditions shown in Table 1, for the measurements of cobalt and manganese signals. Absorbance-time signals were recorded with a Varian-Techtron 9176 potentiometric chart recorder. Hamilton syringes of 10, 100, 200 and 500 μL capacity were used. Fig. 1 shows a diagram of the FIA-AAS system. The atomic absorption spectrometer nebulizer tubing was connected to the outlet part of the sample injector which was held in a clamp mounted on a stand at the same level with the nebulizer. The carrier solution flow rate was accurately controlled by adjustment of the valve regulating the air flow to the nebulizer. We found this system easy to install, simple to use and well reproducible. The sample was injected manually with the correspondingly microsyringe through the self-sealing septum of the sample injector previously described.[29] The microsyringe needle should be inserted through

Table 1

Atomic absorption spectrophotometer settings

	Cobalt	Manganese
Wavelength (nm)*	240.7	279.5
Lamp current(mA)	7	3
Slit width (nm)	0.2	0.5
Burner	Single slot type	
Flame	Air/Acetylene	
Air (L/min)	8.5	8.5
Acetylene (L/min)	1.5	1.5
Burner height (cm below axis)	1.0	1.0
Response (s)	0.5	0.5
Recorder range(mV)	50	50
Working range (μg/mL)	0.001—0.18	0.008—0.1

* Single element hollow cathode lamps.

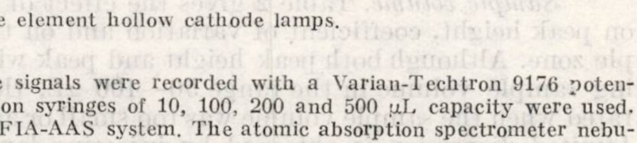

Fig. 1. — FIA system for determination of cobalt and manganese. *C* — container of the carrier solution; *S* — syringe containing the sample; *I* — sample injector unit; *D* — dispersion tube; *N* — nebulizer; *AAS* — atomic absorption spectrometer (settings as in Table 1); *R* — chart recorder.

the septum and pushed into the sample injector unit as far as the barrel of the syringe will allow. The piston is then gently pushed to expel the sample into the carrier stream in ca. 2s. With a little practice a precise and reproducible rate of injection is easily achieved. The resulting peak will appear on the chart recorder in about 3 seconds and during this time the syringe is left in the sample injector so as not to disturb the carrier flow until after the recorder will return to base line in about 6 seconds, after which repeatedly injections may be performed. An injection rate of Ca 1 sample per minute is in this way easily achieved.

RESULTS

The introduction of a discrete amount of sample into our FIA-AAS system gives a peak response or a transient signal as shown in Fig. 2. When a sample is injected into the carrier solution and is swept through the dispersion tube towards the nebulizer in a laminar fashion the height, width, and shape of the signals will be affected by three interrelated factors : sample volume, tube length, and flow rate. In order to optimize the sensitivity and precision of the method we investigate these variables.

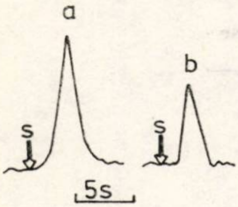

Fig. 2. — Typical FIA-AAS signals: a: 0.2µg Co mL^{-1}; b: 0.08 µg Mn mL^{-1}. 100µL sample volume. Other conditions as in Table 1.

Sample volume. Table 2 gives the effect of different sample volumes on peak height, coefficient of variation and on the dispersion of the sample zone. Although both peak height and peak width increase with increasing sample volume in the range 50—400 µL, the reproducibility deteriorated when the sample volume was too small or as it increased over 100 cm. Limited dispersion is obtained by injecting larger sample volumes. The

Table 2

Effect of sample volume on peak heights, reproducibility and sample dispersion

Sample volume (µL)	h_0(mm)		CV(%)		D	
	Co	Mn	Co	Mn	Co	Mn
50	8.0	8.0	10.0	9.6	2.4	2.5
100	11.3	13.1	3.5	3.0	1.7	1.5
200	11.5	14.1	7.4	3.5	1.63	1.4
300	17.8	16.2	13.4	4.9	1.06	1.3
400	17.8	18.3	14.2	10.0	1.04	1.0

h_0 = peak height; CV = coefficient of variation; D = dispersion coefficient defined as previously reported (28).

sample volume selected for subsequent work was found to be a good compromise between analytical sensitivity, reproducibility and sample dispersion.

Dispersion tube length and carrier solution flow rate. Table 3 shows the effect of tubing length on carrier solution flow rate, sensitivity (peak height), coefficient of variation and on the dispersion. As the tubing length increased the carrier flow rate decreased. Both variables influence the sensitivity, reproducibility and sample dispersion, therefore a compromise must be made. A dispersion tube of 10 cm, which allowed a carrier flow rate of 6.0 μmL/min, was found to be a good compromise for the system tested for both elements, cobalt and manganese.

Table 3

Effect of dispersion tube length on carrier flow rate, peak heights, reproducibility and sample dispersion

Tubing length (cm)	Carrier solution flow rate (mL/min)	h_0 (mm)		$CV(\%)$		D	
		Co	Mn	Co	Mn	Co	Mn
5	12.0	13.0	35.0	5.3	11.0	2.5	2.0
10	6.0	11.3	20.4	3.5	5.0	1.7	1.5
18	5.1	10.4	18.2	7.7	8.2	1.6	1.6
30	1.8	6.8	13.1	14.0	11.0	1.5	1.3

Interferences. In the present work the effect of physiological concentrations of zinc, copper, iron, calcium, magnesium, potassium, sodium, phosphate, chloride, carbonate, sulphate and human albumin in the determination of cobalt and manganese by the FIA-AAS method was studied. Added ions – zinc, copper, iron, calcium, magnesium and potassium – cause no changes in cobalt and manganese signals, except sodium and albumin which enhanced the cobalt and manganese signals in about 50 and 40% respectively, whereas added phosphate, chloride and sulphate depressed the cobalt and manganese signals (in about 6, 10 and 15%, respectively).

In order to eliminate the described interferences, solutions containing physiological amounts of sodium, chloride, sulphate, human albumin, phosphate and sulphate were included in the standards. Glycerol 20% (V/V) was added to adjust viscosity.

Cobalt and manganese determination. Under the atomic absorption spectrophotometer conditions given in Table 1, and the optimized FIA conditions (100 μL sample volume, 10-cm dispersion tubing length and 6.0 mL/min carrier flow rate), the maximum peak heights increased linearly with the concentration for both metal ions, as expressed by the equations: $A_{Co} = 0.001 + 0.151 \ X_{Co}$ ($r = 0.999$), and $A_{Mn} = 0.001 + 0.745 \ X_{Mn}$($r = 0.996$), where A_{Co} and A_{Mg} represent peak height (in millimeters) and X_{Co}(1.0–180.0 μg/L) and X_{Mn}(8.0–100.0 μg/l) represent cobalt and manganese concentration, respectively.

Analytical precision and recovery. The results (Table 4) show that the FIA-AAS system used here has similar precision when compared with the standard addition method. [30] The serum, cobalt and manganese values found in this work (Table 4) are in good agreement with those obtained previously in our working team for 70 healthy people. [4] As well, our results are in good agreement with values from some other different centres. [2,5] Moreover, it is a direct, fast and simple method for analysis of microsamples containing cobalt and manganese.

Table 4

Precision of various assay procedures for Co and Mn

Element	Method	Within-batch			Between-batch		
		$\overline{X}$	*SD*	*CV*, %	$\overline{X}$	*SD*	*CV*, %
Cobalt[a]	Standard addition[b]	27.8	1.3	4.7	28.8	1.8	6.3
		56.0	1.1	1.9	59.1	1.4	2.4
		37.5	1.0	2.7	40.0	1.4	3.5
		35.2	1.2	3.4	36.0	1.4	3.9
		28.3	0.9	3.2	31.1	1.2	3.9
		24.9	1.5	6.0	26.0	1.4	5.4
	FIA-AAS[c]	28.3	1.0	3.5	28.8	1.0	3.5
		55.1	0.8	1.5	56.0	0.9	1.6
		36.0	0.9	2.5	38.0	0.9	2.4
		32.0	1.1	3.4	34.0	1.0	2.9
		27.2	0.9	3.3	28.2	0.9	3.2
		26.1	1.2	4.6	28.0	1.2	4.3
Manganese[b]	Standard addition[b]	19.0	0.9	4.7	20.2	0.9	4.5
		33.0	0.9	2.7	34.5	1.0	2.9
		28.0	1.0	3.6	28.9	1.0	3.5
		27.5	1.5	5.5	29.2	1.7	5.8
		32.1	1.2	3.7	33.5	1.4	4.2
		30.1	0.8	2.7	32.0	0.9	2.8
	FIA-AAS[c]	19.9	0.7	3.5	19.8	0.8	4.0
		32.4	0.9	2.8	34.0	0.9	2.6
		25.7	0.8	3.1	27.0	0.9	3.3
		28.9	1.2	4.2	29.2	1.0	3.4
		31.0	1.0	3.2	32.1	1.1	3.4
		30.2	0.5	1.7	32.4	0.8	2.5

[a] In µg/L ; [b, c] 1.0 and 0.1 mL sample volume, respectively, $n = 12$.

Recovery of both trace metals was calculated by analysing serum samples before and after the addition of a known quantity of cobalt or manganese to a serum of low cobalt or manganese content. The results of this study are shown in Table 5. Each result is the mean of 10 determinations. The average percentage recovery was 100.2 and 100.0.

Table 5

Analytical recoveries by the FIA-AAS method

	μg/L added	μg/L found	% recovery
Cobalt	10.0	10.2	102
	20.0	20.0	100
	30.0	29.1	97
	40.0	37.6	94
	50.0	49.5	99
		MEAN=	98.4
Manganese	15.0	14.4	96
	20.0	18.8	94
	25.0	24.7	99
	30.0	30.3	101
	35.0	35.4	101
		MEAN=	98.2

CONCLUSIONS

In our attempts we found a simple, fast, direct and precise method for the determination of cobalt and manganese in micro-volumes of serum, ideally suited for use with children. The proposed method takes less time to perform and gives similar precise results with the standard addition method. The introduction of this FIA-AAS method should help in achieving a greater appreciation of the role of cobalt and manganese in nutrition and disease, the literature for which is somewhat clouded by suspect analytical data.

ACKNOWLEDGEMENTS. The authors express their gratitude to Mr. Cergio Rivas of the Department of Chemistry, Faculty of Science, University of Los Andes, Mérida, for his technical assistance. Thanks are also due to the C.D.C.H.T. of the University of Los Andes for its financial support (Project TC—05—83).

REFERENCES

[1] G. M. Morrison, *CRC Crit. Rev. in Anal. Chem.*, **8**, 287 (1979).
[2] H. J. M. Bowen, in: "Trace Elements in Biochemistry", Academic Press, London, 1966.
[3] J. D. Winefordner and T. J. Vickers, *Anal. Chem.*, **46**(5), 192 R (1974).
[4] J. L. Burguera, M. Burguera and O. M. Alarcón, Unpublished work.
[5] J. Versieck and R. Cornelis, *Anal. Chim. Acta*, **116**, 217 (1980).
[6] R. M. Leach and M. S. Lilburn, *World Rev. Nutr. Diet.*, **32**, 123 (1978).
[7] G. C. Cotzias, K. Horinchi, S. Fuenzalida and I. Mena, *Neurology*, **18**, 376 (1968).
[8] J. P. Mahoney and W. J. Small, *J. Clin. Invest.*, **47**, 643 (1968).
[9] D. J. Halls and G. S. Fell, *Anal. Chim. Acta*, **129**, 205 (1981), and references therein.
[10] M. J. Harp and F. I. Scoular, *J. Nutr.*, **47**, 67(1952).
[11] R. J. Rohn and W. H. Bond, *Lancet*, **73**, 317 (1953).
[12] H. Kesteloot, J. Roelandt, J. Willems, J. H. Claes and J. V. Joossens, *Circulation*, **37**, 854 (1968).

[13] R. A. Barfoot and J. G. Pritchard, *Analyst* (*London*), **106**, 551 (1980), and references therein.

[14] R. N. Nugmanova, I. K. Musabaev, D. M. Guseva and I. G. Mukhamedova, *Uzbeksk, Khim. Zh.*, **7**, 20 (1953).

[15] R. E. Thiers, J. F. Williams and J. H. Yoe, *Anal. Chem.*, **27**, 1725 (1955).

[16] W. E. Van der Linden, *Trends in Anal. Chem.*, **1**, 188 (1982).

[17] C. B. Ranger, *Anal. Chem.*, **53**, 21 (1981).

[18] J. L. Burguera, A. Townshend and S. Greenfield, *Anal. Chim. Acta*, **114**, 209 (1980).

[19] J. L. Burguera, *Anal. Proc.* (London), **17**, 43 (1980).

[20] J. L. Burguera and M. Burguera, *Anal. Chim. Acta*, **153**, 207 (1983).

[21] J. L. Burguera, M. Burguera and M. Gallignani, *Acta Cient. Venezolana*, **33**, 99 (1982).

[22] J. L. Burguera, M. Burguera and M. Gallignani, *An. Acad. Bras. Cienc.*, **55**, 209 (1983).

[23] L. Nord and B. Karlberg, *Anal. Chim. Acta*, **145**, 151 (1983).

[24] H. A. Mottola, *Anal. Chim. Acta*, **145**, 27 (1983).

[25] B. F. Rocks, R. A. Sherwood and C. Riley, *In. Chem.*, **28**, 440 (1982).

[26] B. F. Rocks, R. A. Sherwood, L. M. Bayford and C. Riley, *Ann. Clin. Biochem.*, **19**, 338 (1982).

[27] T. Uchida, C. S. Wei, C. Iida and H. Wada, *Nagoya Kogyo Daigaku Gakuho*, **33**, 97 (1982).

[28] J. L. Burguera, M. Burguera, M. Gallignani and O. M. Alarcón, *Clin. Chem.*, **29**, 569 (1983).

[29] B. F. Rocks, R. A. Sherwood and C. Riley, *Ann. Clin. Biochem.*, **21**, 51 (1984).

[30] M. Bader, *J. Chem. Educ.*, **57**, 703 (1980).

Revue Roumaine de Chimie, **31**, *3*, 361 (1986)

COMPTES RENDUS

J. SIMON and J. J. ANDRÉ, "Molecular Semiconductors. Photoelectrical Properties and Solar Cells" Springer Verlag, Berlin, 1985, hard cover, 288 pp, 174 DM.

Molecular insulators, molecular metals and molecular superconductors have all been reported. Now, after thirty years of considerable efforts, it is the turn of molecular semiconductors to be taken into account. The book of Jacques Simon, Professor at the École Supérieure de Physique et Chimie Industrielles in Paris and Jean-Jacques André, Research Director at the Centre de Recherches sur les Macromolécules in Strasbourg, is a comprehensive monograph which approaches this subject both from a chemist's and a physicist's point of view. It is devoted to the understanding of the chemical mechanisms involved in photoelectric and photovoltaic phenomena during the irradiation of organic and metallo-organic materials denoted by the generic name of "molecular semiconductors".

In the first chapter the authors present those aspects of solid-state physics necessary for understanding the behaviour of solid organic materials : dark conductivity, band theory, Fermi levels, charge migration, charge carrier trapping processes, etc. As far as it was possible, a chemical interpretation of the above phenomena has been also given. Taking into account the significant role of the chemists in this interdisciplinary field of activity, this approach proved to be very useful, despite the authors' fears that chemists' gain in intuitive understanding will be compensated by physicists' loss in precision.

The second chapter describes the photoelectrical properties of organic semiconductors : light absorption, photogeneration of charge carriers, photovoltaic effect, etc. Mechanisms involved in organic solar cells are emphasized and the factors affecting the extent of energy transfer in molecular materials are briefly recalled.

A clear distinction is made between the two main classes of molecular semiconductors : molecular crystals, available in highly purified form, but with a limited mobility on account of the small π overlap, and semiconducting polymers, with a large mobility because of the strong covalent intrachain interactions, but very hard to purify ; the authors present in the next two chapters representative examples of those two classes of compounds : phtalocyanines and polyacetylenes. Their synthesis, physico-chemical properties, dark electrical conductivity and behaviour under irradiation are discussed.

The last chapter gives an overview of the other main molecular conductors or semiconductors : aromatic hydrocarbons and graphite, metallo-organic derivatives, charge transfer systems, polysulfurnitride and polydiacetylene, polymethines, polyphenylene, polyacrylonitrile, polypyrroles, etc.

In conclusion the authors define accurately the molecular semiconductors as molecular materials which possess a reasonable mobility of charge carriers, have a band gap of the order of 1—2 eV and are able to form typical semiconductor-based devices as junctions and solar cells. Although no example of molecular semiconductor has been found up to the present time, the authors are optimistic ; no physical or theoretical considerations limit the possibility of obtaining molecular semiconductors. Once the existence of molecular semiconductors will be proven, the creation of well-behaved devices may be reasonably envisaged. The key to the problem is in the chemists' hands.

The book is well illustrated by chemical and mathematical formulas, tables, diagrams, physicochemical relationships. It has a subject index which facilitates retrieval of any desired data. The bibliography is vast, including nearly 1200 literature quotations. The quality of the printing and the clarity of formulae and diagrams are excellent.

A. Dinculescu

NOTE POUR LES AUTEURS

La Revue Roumaine de Chimie publie des articles en anglais, français, russe, allemand ou espagnol. Les auteurs sont priés d'envoyer des articles et des comptes rendus inédits.

Les manuscrits seront dactylographiés à double interligne. La bibliographie, les tableaux et la légende des figures seront placés après le texte.

Si l'article fait partie d'une série numérotée, la partie précédente sera donnée comme première référence.

Chaque article sera précédé d'un résumé comprenant quinze lignes au maximum.

Les références bibliographiques dans le texte seront faites par des exposants sans parenthèses et paraîtront à la fin de l'ouvrage.

Les publications périodiques mentionnées dans la bibliographie seront présentées suivant les prescriptions internationales : le nom de l'auteur précédé de l'initiale du prénom, le titre du périodique abrégé conformément à «Chemical Abstracts» et souligné par une ligne, le numéro du tome indiqué par des chiffres arabes et souligné par deux lignes, suivi de la première page de l'article : à la fin, l'année de la parution sera placée entre parenthèses. Le numéro de la revue ne sera pas indiqué si les pages du volume sont numérotées consécutivement.

Les textes des livres ou traités inclueront : le nom des auteurs, précédés de l'initiale du prénom, le titre du livre entre guillemets et sans être souligné, le numéro du tome précédé par l'abréviation «vol.» (ou «Bd.»), le numéro de l'édition, les éditions (the publisher), la localité de la parution du livre, l'année de la parution et la page de la référence précédée(s) par l'abréviation «p» (ou «S»).

Les brevets seront indiqués comme suit : l'auteur ou la firme, le pays et le numéro du brevet, la date de la revue (*Chem. Abstr.*). Par. ex. : M. Jones (to Union Carbide Co.). Brit. Pat. 610 238, 2 Sept. 1959 : cf. *Chem. Abstr.*, 54, 12808 (1960).

Si la référence n'a pas été lue en original, on indiquera aussi la revue de références consultée.

Les diagrammes seront tracés à l'encre de Chine sur papier calque. Les tableaux et les figures (en nombre strictement nécessaire), ainsi que les courbes dans les figures seront numérotés par des chiffres arabes. Leur explication sera donnée dans la légende des figures. Prière de ne pas inscrire les mêmes données dans les tableaux et les figures. Chaque tableau aura un titre. On indiquera dans le texte la place approximative des tableaux et des figures. Les formules chimiques seront incluses dans le text ; en outre, elles seront transcrites sur papier calque, à l'encre de Chine.

Les auteurs sont priés d'indiquer les caractères italiques (en soulignant les lettres au crayon), ainsi que tout autre caractère spécial : les préfixes, *ortho*, *meta*, *para*, *cis*, *trans*, etc. seront soulignés pour indiquer leurs caractères italiques, et ne seront jamais écrits avec des majuscules.

Aucune correction à la main ne sera admise sur le manuscrit. Les corrections seront frappées à la machine. Les lettres grecques ou d'autres symboles spéciaux seront insérés à la main à l'encre clairement.

Le manuscrit sera signé par l'auteur.

Le titre courant aura 50 lettres au maximum.

L'entière responsabilité du contenu des articles appartient aux auteurs.

Sur demande on peut obtenir une note plus complète.

PRINTED IN ROMANIA

1986 Ark 2 41

TRAVAUX PARUS AUX ÉDITIONS DE L'ACADÉMIE DE LA RÉPUBLIQUE SOCIALISTE DE ROUMANIE

V. DRĂGUTAN, A. T. BALABAN, M. DIMONIE, **Olefin Metathesis and Ring-Opening Polymerization of Cyclo-Olefins**, coédition avec John Wiley and Sons, 1985, 544 p.

C. LITEANU, I. RÎCA, **Optimizarea proceselor analitice**, 1985, 360 p.

N. PERESCU, **Chimia extracţiei cu solvenţi şi aplicaţii**, 1985, 212 p.

V. EM. SAHINI, M. HILLEBRAND, **Chimie cuantică în exemple şi aplicaţii**, 1985, 378 p.

GH. MARCU, **Chimia compuşilor coordinativi**, 1984, 415 p.

E. CORDOŞ, C. MANOLIU, **Spectrometria de absorbţie şi fluorescenţă atomică**, 1984, 178 p.

C. BODEA, **Tratat de biochimie vegetală**, p. II, vol. 5, 1984, 438 p.

ELENA CEAUŞESCU, **Cercetări în chimia şi tehnologia polimerilor**, 1983, 519 p.

N. ASANDEI, A. GRIGORIU, **Chimia şi structura fibrelor**, 1983, 395 p.

N. IONESCU, M. CĂLDĂRARU, **Oxidarea catalitică a olefinelor inferioare**, 1983, 178 p.

C. CAŞCAVAL, **Studiul polimerilor prin piroliză şi cromatografie de gaze**, 1983, 220 p.

C. I. SIMIONESCU, F. DANEŞ, **Originea vieţii**, 1983, 110 p.

C. BODEA (sous la direction), **Tratat de biochimie vegetală**, p. II, vol. IV, 1982, 408 p.

I. G. MURGULESCU, RODICA VÎLCU, **Introducere în chimia fizică. Vol. III, Termodinamica chimică**, 1982, 624 p.

I. G. MURGULESCU, J. PĂUN, **Introducere în chimia fizică. Vol. I. 3. Nucleul atomic, reacţii nucleare, particule elementare**, 1982, 606 p.

ELENA CEAUŞESCU, **Noi cercetări în domeniul compuşilor macromoleculari**, 1981, 536 p.

I. G. MURGULESCU, TATIANA ONCESCU, E. SEGAL, **Introducere în chimia fizică, Vol. II, 2, Cinematică chimică şi cataliză**, 1981, 1024 p.

LYDIA-MARIA VAICUM, **Epurarea apelor uzate cu nămol activ. Bazele biochimice**, 1981, 218 p.

I. GĂLĂŢEANU, **Procese şi metode radiochimice în energetica nucleară**, 1981, 234 p.

O. IORDACHE, **Procese polistocastice aplicate în fenomenele de transfer**, 1981, 186 p.

CR. SIMIONESCU, VALERIA GORDUZA, **Polimeri biocompatibili şi biologic activi**, 1980, 479 p.

ELENA CEAUŞESCU, **Polimerizarea stereospecifică a izoprenului**, 1979, 307 p.

C. GH. MACAROVICI, **Analiza chimică cantitativă anorganică**, 1979, 457 p.

M. FLORESCU, **Metode ştiinţifice în dezvoltarea industriei chimice moderne**, 1979, 256 p.

A. T. BALABAN, I. GĂLĂŢEANU, G. GEORGESCU, LIGIA SIMIONESCU, **Compuşi marcaţi şi radiofarmaceutici cu aplicaţii în medicina nucleară**, 1979, 495 p.

I. G. MURGULESCU, E. SEGAL, **Introducere în chimia fizică. Vol. II. 1. Teoria molecular-cinetică a materiei**, 1979, 1036 p.

S. STERNBERG, FL. DANEŞ, **Termodinamica chimică aplicată** 1978, 400 p.

I. G. MURGULESCU, V. EM. SAHINI, **Introducere în chimia fizică. Vol. I. 2. Structura şi proprietăţile moleculelor**, 1978, 604 p.

I. ZUGRĂVESCU, MAGDA PETROVANU, **N-ylid chemistry**, coédition avec McGraw-Hill International Book Company, U.S.A., 1977, 396 p.

I. G. MURGULESCU, **Introducere în chimia fizică. Vol. I. 1. Atomi, molecule, legătură chimică**, 1976, 560 p.

ELENA CEAUŞESCU, **Research work on synthesis and characterization of macromolecular compounds, Contributions**, 1974, 251 p.

CR. SIMIONESCU, VIORICA RUSAN, V. POPA, **Chimia algelor marine**, 1974, 212 p., 1 pl.

ISSN 0035—3930

c. 1733—I.P. INFORMAŢIA

43 423

Lei 40

$ 80 (pour un abonnement annuel)

F 1103

~~94~~ ~~66~~

ACADÉMIE DE LA RÉPUBLIQUE SOCIALISTE DE ROUMANIE

REVUE ROUMAINE DE CHIMIE

~~R~~ 1986 MA'J 6

MO

REFERALVA

TOME 31

N° 4

Avril 1986

Rev. Roumaine Chim.

RRCHAX, 31, 4, p. 363–458 (1986), Bucarest

EDITURA ACADEMIEI REPUBLICII SOCIALISTE ROMÂNIA

ACADÉMIE DE LA RÉPUBLIQUE SOCIALISTE DE ROUMANIE

COMITÉ DE RÉDACTION

Rédacteur en chef :

I. G. MURGULESCU, membre de l'Académie de la République Socialiste de Roumanie

Rédacteurs en chef adjoints :

A. T. BALABAN et V. EM. SAHINI, membres correspondants de l'Académie de la République Socialiste de Roumanie

Collège de rédaction :

EM. BRATU, ELENA CEAUȘESCU, ECATERINA CIORĂNESCU-NENITZESCU, CR. SIMIONESCU, membres de l'Académie de la République Socialiste de Roumanie ; P. SPACU, membre correspondant de l'Académie de la République Socialiste de Roumanie : M. BANCIU, M. D. GHEORGHIU, I. HAIDUC, D. I. MARCHIDAN, G. NIAC et D. SĂNDULESCU

La Revue Roumaine de Chimie paraît 10 fois par an. Toute commande de l'étranger sera adressée à ROMPRESFILATELIA — sectorul Export-Import Presă, P. O. Box, 12—20 1,télex10376, prsfi r 78104 Bucarest, Calea Griviței nr. 64—66, Roumanie

Les manuscrits, les livres et les revues proposés en échange, ainsi que toute correspondance seront envoyés à la rédaction

REVUE ROUMAINE DE CHIMIE

125, Calea Victoriei, 79717 Bucarest, Roumanie, téléphone 50 76 80

EDITURA ACADEMIEI REPUBLICII SOCIALISTE ROMÂNIA
125, Calea Victoriei, 79717 Bucarest, Roumanie, téléphone 50 76 80

ORSZÁGOS MŰSZAKI INFORMÁCIÓS KÖZPONT ÉS KÖNYVTÁR 1883

REVUE ROUMAINE DE CHIMIE

Tome 31, N° 4 **Avril, 1986**

E. I. GEORGESCU, FLORENTINA GEORGESCU, M. D. GHEORGHIU, P. FILIP and MAGDA PETROVANU, Dipolar derivatives in the quinazoline series. V. Inactivation of quinazolinium-ylids ; a new approach towards novel pyrrolo[1,2-c]quinazoline derivatives (in French) . . . . **365—369**

GHEORGHE SURPĂŢEANU, PIERRE GRANDCLAUDON and ALAIN LABLACHE COMBIER, Theoretical study of the reactivity of benzo[b]-thiophenes with heterocyclic amines and their anions (in French) . . . **371—374**

IOAN SĂNDULESCU, VASILE PÂRVULESCU, ELENA SZABO, ALEXANDRU POPA and IOAN V. NICOLESCU, Styrene hydrogenation on supported Pd and Pd-Co/γ-Al_2O_3 catalysts . . . . **375—385**

ABDEL MOMEN A. EL-KHAMRY, MOHAMED E. SHABAN and MOHAMED M. HABASHY, Synthesis and reactions of 6-aryl-4,5-dihydropyridazin-3-(2H)-ones . . . . **387—392**

M. M. ISMAIL and M. S. MOHAMED, Cyclization of ethyl cyanoacetate and 3,5-dichlorosalicylaldehyde with ketones by means of ammonium acetate . . **393—402**

R. BACALOGLU, L. COTARCĂ, ANABELA IŞFAN and C. IŞFAN, High-performance liquid chromatography of 2,4,6-haloalkyl-1,3,5-triazines . . . **403—409**

E. BEZAK, Studies on 4-alkylpyridines usability for extraction of Co(II), Ni(II), Cu(II), Zn(II) and Cd(II) complexes from nitrate solutions . . . . . . **411—418**

EVELINE POPOVICI, MIHAI CRUCEANU, MIHAELA GRECU, AURELIA VASILE and MARIA ALEXANDROAEI, Synthetic zeolites for detergent conditioning. II. On zeolite — surfactant — bleaching agent systems **419—424**

SPIRIDON OPREA, EMIL DUMITRIU, VASILE HULEA and KAYED YOUSEF, Activity and selectivity of neodymium exchanged zeolites in the alkylation reaction of toluene with methanol . . . . **425—429**

S. STERNBERG, T. VIŞAN, VALERIA PETRESCU and ADINA COTÂRŢĂ, Electrochemical reactions of cupric and cupreous ions in lithium chloride-potassium chloride eutectic. III . . . . **431—442**

J. ZSAKÓ, J. DEMETER-VODNÁR, I. BÂLDEA and CS. VÁRHELYI, Kinetics and mechanism of substitution reactions of complexes. LVIII. Hg(II) assisted aquation of *cis*-$[Co(en)_2Br(\gamma\text{-picoline})]^{2+}$ . . . . **443—449**

AL. CECAL, D. CIOBANU and I. SANDU, Use of beta-rays back-scattering in the study of corrosion process of some carbon steel samples in acid solutions . . . . **451—456**

BOOK REVIEWS . . . . **457—458**

[Rev. Roumaine Chim.] **31, *4*,** 363—458 (1986), Bucarest

Revue Roumaine de Chimie, **31**, *4*, 365–369 (1986)

DÉRIVÉS DIPOLAIRES EN SÉRIE QUINAZOLINIQUES. V[1]

L'INACTIVATION DES QUINAZOLINIUM-YLURES, UNE NOUVELLE VOIE POUR L'OBTENTION DE NOUVEAUX DÉRIVÉS PYRROLO[1,2-c]QUINAZOLINIQUES

E. I. GEORGESCU[a], FLORENTINA GEORGESCU[a], M. D. GHEORGHIU[b], P. FILIP[c] et MAGDA PETROVANU[d]

[a]Centre de Recherches, Rîmnicu Vîlcea, Rue Uzinei 1, Roumanie
[b]Institut Polytechnique, Bucarest, Roumanie
[c]Centre de Chimie Organique, Bucarest, Roumanie
[d]Institut Polytechnique, Jassy, Roumanie

Reçu le 15 novembre 1985

On a établi que par l'inactivation des quinazolinium-3-phénacyleylures (**1**) on obtient des dérivés pyrrolo[1,2-c]quinazoliniques avec la structure **2**. Ce fait représente une manière originale d'inactivation des produits N-yluriques et offre une voie simple pour la synthèse des derivés pyrrolo[1,2-c]quinazoliniques **2**. Dans le travail on propose un mécanisme pour expliquer la formation des composés **2**.

By the inactivation of the quinazolinium-3-phenacylylides (**1**), the pyrrolo[1,2-c]quinazoline derivatives with structure **2** are obtained. This represents a singular mode of inactivating of the N-ylides compounds and offers a simple way for the synthesis of pyrrolo [1,2-c]quinazoline derivatives **2**. A new mechanism for explaining the compounds **2** formation is suggested in the paper.

Les quinazolinium-ylures sont des produits très réactifs. Aussi bien qu'au cas des autres N-ylures hétérocycliques,[2] si dans le milieu réactionnel on ne trouve pas de réactants appropriés, les quinazolinium-ylures subissent un processus d'inactivation à la suite duquel ils se transforment en des produits stables par la modification de la structure moléculaire, sans l'intervention visible d'un réactant externe. À la différence des autres N-ylures hétérocycliques, la réactivité des quinazolinium-3-phénacylylures **1** est augmentée, fait dû à l'existence d'un fort déficit d'électrons dans la position 4, ce qui fait que cette position soit très sensible à l'attaque des réactants nucléophiles.

Comme nous l'avons déja montré,[1,3,4] les essais d'isoler les quinazolinium-3-phénacylylures **1** ont échoué, mais leur formation comme intermédiaires a été mise en évidence par les produits des réactions de cycloaddition 3 + 2 dipolaire avec des acéthylènes et des défines activées. Dans tous les essais d'isolement des quinazolinium-3-phénacylylures **1** on a séparé des produits d'inactivation très stables.

Les mêmes produits d'inactivation ont été obtenus lorsque pour la réalisation des réactions de cycloaddition on a essayé l'utilisation des bases anorganiques ou des amines tertiaires comme agent pour générer des ylures en partant des sels quaternaires.

Dans ce travail on présente la structure des produits d'inactivation et on propose un mécanisme pour expliquer la formation de ces produits.

Dans la classe de N-ylures hétérocycliques on connait, en général, deux types d'inactivation qui sont en fait des réactions de dimérisation [2] (schéme 1). Le premier type (I) et le plus connu se produit par une réaction de cycloaddition 3 + 3 dipolaire entre deux molecules d'ylures et conduit à des dimères avec une structure pyrazinique. En quelques-uns des cas on a obtenu ces dimères déhydrogénés.[2,5] Le deuxième type d'inactivation (II) se produit grâce aux intermédiaires carbéniques et conduit à des dimères avec une liaison éthylenique. En quelques-uns des cas on a remarqué les deux types d'inactivation, en obtenant un mélange d'isomères.[2]

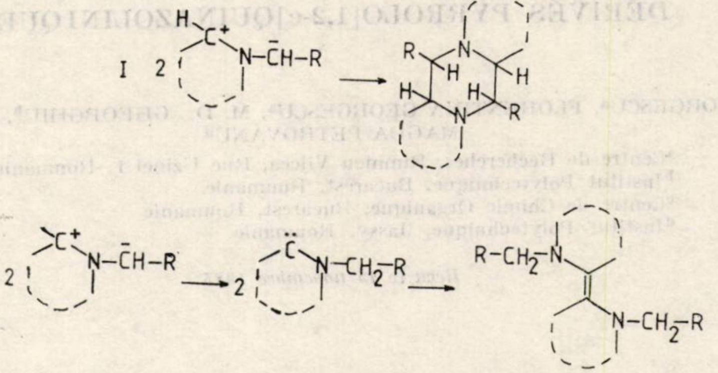

Dans le cas de quinazolinium-3-phénacylylures **1** le processus d'inactivation ne se produit par aucun de ces mécanismes et il constitue un type singulier d'inactivation dans la classe de N-ylures hétérocycliques. Ainsi, tenant compte des données des analyses élémentaires, des spectres IR, ^{1}H-RMN et des spectres de masse nous avons établi les structures de pyrrolo [1,2-c] quinazoline **2 a-g** pour les produits d'inactivation des quinazolinium-3-phénacylylures **1 a-g**.

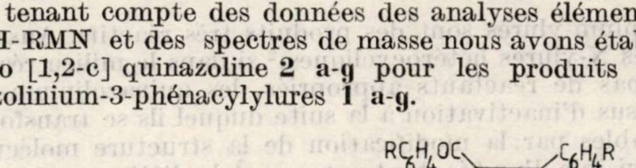

1 2

a : R=H
b : R=OCH$_3$
c : R=F
d : R=Cl
e : R=Br
f : R=NO$_2$
g : R=CN

Le mécanisme proposé pour cette transformation suppose l'attaque du carbanion ylurique sur le centre positif de la position 4 d'une autre molécule d'ylure ou même d'une molécule du sel quaternaire,[6] suivie par l'élimination d'une molécule de quinazoline, l'élimination de l'eau et cyclisation.

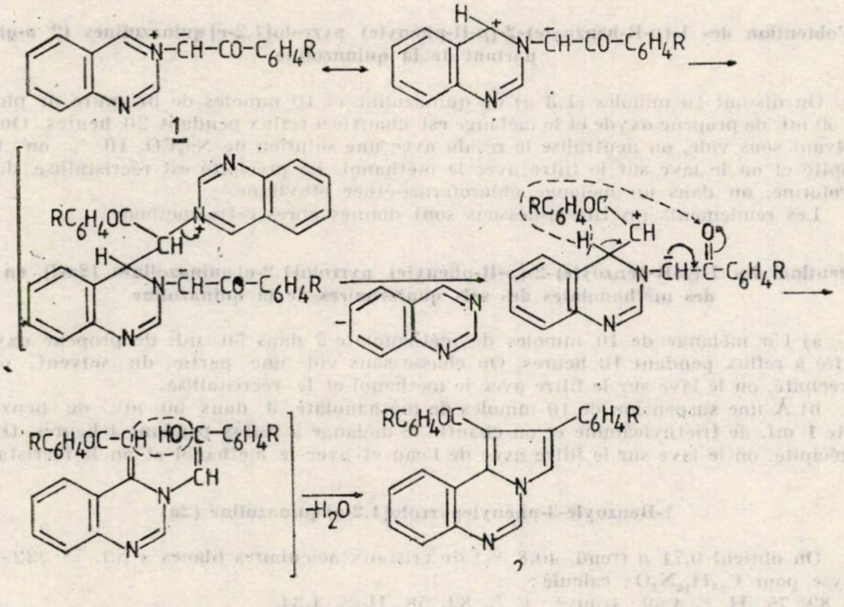

La présence de la quinazoline dans la solution résultée après la séparation des produits d'inactivation a été mise en évidence par la chromatographie en phase gazeuse.

L'obtention des pyrrolo [1,2-c]quinazolines **2** par l'inactivation des quinazolinium-3-phénacylylures offre une voie simple pour la synthèse de ces produits. Les dérivés pyrrolo[1,2-c]quinazoliniques **2** peuvent être obtenus d'une manière relativement simple par le chauffage de la quinazoline avec le bromure de phénacyle respectif dans un époxide. De même, ces dérivés peuvent être obtenus par le chauffage des méthanolates des sels quaternaires de quinazolinium [6] dans divers solvants en présence des bases anorganiques ou organiques, ou par le chauffage des méthanolates dans un époxide.

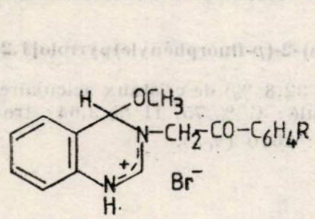

3

PARTIE EXPÉRIMENTALE

Les méthanolates **3** ont été obtenus par la méthode décrite dans un travail antérieur.[6] Les spectres IR ont été enregistrés sur un spectromètre Perkin Elmer 621 A, les spectres ^{1}H-RMN sur un spectromètre Varian EM 360—L et les spectres de masse sur un spectromètre DP—102. L'analyse chromatographique a été effectuée sur un gazchromatographe Shimadzu GC—1C.

Les points de fusion ne sont pas corrigés.

L'obtention des 1-(*p*-R-benzoyle)-2-(*p*-R-phényle) pyrrolo[1,2-c] quinazolines (2 a-g) en partant de la quinazoline

On dissout 10 mmoles (1,3 g) de quinazoline et 10 mmoles de bromure de phénacyle dans 50 mL de propène oxyde et le mélange est chauffé à reflux pendant 20 heures. On chasse le solvant sous vide, on neutralise le résidu avec une solution de Na_2CO_3 10 %, on filtre le précipité et on le lave sur le filtre avec le méthanol. Le précipité est récristallisé dans du chloroforme, ou dans un mélange chloroforme-éther éthylique.

Les rendements inscrits ci-dessous sont donnés après cette méthode.

L'obtention des 1-(*p*-R-bénzoyle)-2-(*p*-R-phényle) pyrrolo[1,2-c] quinazolines (2a-f) en partant des méthanolates des sels quaternaires de la quinazoline

a) Un mélange de 10 mmoles de méthanolate 3 dans 50 mL de propène oxyde est chauffé à reflux pendant 10 heures. On chasse sous vide une partie du solvent, on filtre le précipité, on le lave sur le filtre avec le méthanol et le récristallisé.

b) À une suspension de 10 mmoles de méthanolate **3** dans 50 mL de benzène on ajoute 1 mL de triéthyleamine et on chauffe le mélange à reflux pendant 4 heures. On filtre le précipité, on le lave sur le filtre avec de l'eau et avec le méthanol et on le récristallise.

1-Benzoyle-3-phénylepyrrolo[1,2-c] quinazoline (2a)

On obtient 0,71 g (rend. 40,8 %) de cristaux aciculaires blancs à p.f. = 222—223°C. Analyse pour $C_{24}H_{16}N_2O$; calculé :
C % 82, 75, H % 4,59 ; trouvé : C % 82, 58, H % 4,34.

Spectre IR(KBr, cm^{-1}) : 1,608 (ν_{CO}).

Spectre ^{1}H-RMN($CDCl_3$, δ, ppm) : 6,95—7,41 m (9H), 7,50—7,83 m (4H), 7,95—8,33m (2H), des protons aromatiques ; 10,08 s (1H), H—5.

Spectre de masse* : M^+ = 348(100) ; 319(30) ; 271(25,3) ; 174(12,9) ; 77(8,0).

1-(-*p*Méthoxybenzoyle)-2-(*p*-méthoxyphényle)pyrrolo[1,2-c] quinazoline (2b).

On obtient 0,73 g (rend. 35,8 %) de cristaux aciculaires blancs à p.f. = 229—230°C. Analyse pour $C_{26}H_{20}N_2O_3$; calculé : C % 76,47, H % 4,90 ; trouvé : C % 76,23, H % 4,64.

Spectre IR (KBr, cm^{-1}) : 1609 (ν_{CO}).

Spectre ^{1}H—RMN(TFA-d$_1$, δ, ppm) : 3,94 et 3,98, 2 s (6H), les protons du groupement carbométhoxy ; 6,83—7,20 m (4H), 7,31—7,58 d (2H), 7,66—7,91 m (3H), 8,00—8,28 m (3H), des protons aromatiques ; 8,46—8,73, m (1H), H—10 ; 11, 20, s (1H), H—5.

Spectre de masse : M^+ = 408(100) ; 379(21,8) ; 300(23,5) ; 135(18,2).

1-(*p*-Fluorbenzoyle)-2-(*p*-fluorphényle)pyrrolo[1,2-c] quinazoline (2c).

On obtient 0,63 g (rend. 32,8 %) de cristaux aciculaires blancs p.f. = 264—266°C. Analyse pour $C_{24}H_{14}N_2O_2F_2$; calculé : C % 75, H % 3,64 ; trouvé : C % 75,22, H % 3,71.

Spectre IR(KBr, cm^{-1}) : 1610 (ν_{CO}).

---

* Dans toute la partie expérimentale les intensités sont données en pour cent (entre parenthèses).

Spectre ^{1}H—RMN(TFA-d_1, δ, ppm) : 6,60—7,78 m (9H), 7,78—8,21 m (3H), des protons aromatiques ; 8,26—8,60 m (1H), H—10 ; 11,02 s (1H), H—5.

Spectre de masse : M^+ = 384(100) ; 355(27,3) ; 289(32,4) ; 123(11,4).

1-(*p*-Chlorobenzoyle)-2-(*p*-chlorophényle)pyrrolo[1,2-c] quinazoline (2d).

On obtient 0,77 g (rend. 37 %) de cristaux aciculaires blancs à p.f. = 277—278°C. Analyse pour $C_{24}H_{14}N_2O_2Cl_2$; calculé : C % 69,23, H % 3,36 ; trouvé : C % 69,08, H % 3,25.

Spectre IR(KBr, cm^{-1}) : 1604 (ν_{CO}).

Spectre ^{1}H-RMN (TFA-d_1, δ, ppm) : 7,00—7,77 m (9H), 7,83—8,20 m (3H), des protons aromatiques ; 8,23—8,56 m (1H), H—10 ; 11, 01 s (1H), H—5.

Spectre de masse : M^+ = 416 (100) ; 389 (18,4) ; 305 (29,1) ; 243 (23,2) ; 139 (17,3) ; 111 (12,6).

1-(*p*-Bromobenzoyle)-2-(*p*-bromophényle)pyrrolo [1,2-c] quinazoline (2e).

On obtient 0,8 g (rend. 31,6 %) de cristaux aciculaires blancs à p.f. = 284—285°C. Analyse pour $C_{24}H_{14}N_2OBr_2$; calculé : C % 56,91 ; H % 2,76 ; trouvé : C % 56,82, H % 2,66.

Spectre IR(KBr, cm^{-1}) : 1610 (ν_{CO}).

Spectre ^{1}H-RMN(TFA, δ, ppm) : 7,08—7,58, m (8H), 7,70 s (1H), 7,95—8,25 m (3H), des protons aromatiques ; 8,38—8,66 m (1H), H—10 ; 11,20 s (1H), H—5.

Spectre de masse : M^+ = 506 (100) ; 4,77(21) ; 270(31,2) ; 242(19,2).

1-(*p*-Nitrobenzoyle)-2-(*p*-nitrophényle)pyrrolo[1,2-c] quinazoline (2f).

On obtient 0,8 g (rend. 31,6 %) de cristaux jaunes pâle à p.f. = 316—319°C. Analyse pour $C_{24}H_{14}N_4O_5$; calculé : C % 65,75, H % 3,19 ; trouvé : C % 65,70, H % 3,31.

Spectre IR(KBr, cm^{-1}) : 1615 (ν_{CO}).

Spectre ^{1}H-RMN(TFA, δ, ppm) : 7,60—8,41m (12H), des protons aromatiques ; 8,55—8,88 m (1H), H—10 ; 11,45 s (1H), H—5.

Spectre de masse : M^+ = 438(100) ; 408(12, 8) ; 316(31,7) ; 270(9,3) ; 103(5,6).

1-(*p*-Cyanobenzoyle)-2-(*p*-cyanophényle) pyrrolo [1,2-c] quinazoline (2g) :

On obtient 0,58 g (rend. 29 %) de cristaux jaunes à p.f. = 332—334°C. Analyse pour $C_{26}H_{14}N_4O$: calculé : C % 78,39, H % 3,51 ; trouvé : C % 77,92, H % 3,66.

Spectre IR(KBr, cm^{-1}) : 1605 (ν_{CO}) ; 2210 (ν_{CN}).

Spectre ^{1}H—RMN(^{1}TFA-d_1, δ, ppm) : 7,33—7,86 m (9H), 7,93—8,50 m (3H), des protons aromatiques ; 8,35—8,68 m (1H), H—10 ; 11,06 s (1H), H—5.

Spectre de masse : M^+ = 398(100) ; 369(23,8) ; 297(39,7) ; 268(17.7) : 102(12.7).

BIBLIOGRAPHIE

[1] Quatrième partie : E. I. Georgescu, F. Georgescu, M. Gheorghiu, E. G. Georgescu et M. Petrovanu, *Rev. Roumaine Chim.*, **30**, 611—615 (1985).

[2] I. Zugrăvescu and M. Petroveanu, « N-Ylid Chemistry », Ed. Academiei, Bucharest and McGraw-Hill Internat. Book Co., New York, 1976, chap. 6.2.2.

[3] E. I. Georgescu, I. Druţă et M. Petrovanu, *Rev. Roumaine Chim.*, **26**, 109(1981).

[4] E. I. Georgescu, I. Druţă et M. Petrovanu, *Bul. Inst. Politehnic Iaşi*, **27**, fasc. 3—4, 81 (1981).

[5] M. Petrovanu, E. Ştefănescu et I. Druţă, *Rev. Roumaine Chim.*, **16**, 1107 (1971).

[6] E. I. Georgescu, F. Georgescu, F. Chiraleu et M. Petrovanu, *Rev. Roumaine Chim.*, **28**, 841 (1983).

Revue Roumaine de Chimie, **31**, 4, 371—374 (1986)

ÉTUDE THÉORIQUE SUR LA RÉACTIVITÉ DE BENZO[b]THIOPHÈNES AVEC DES AMINES HÉTÉROCYCLIQUES ET LEURS ANIONS

GHEORGHE SURPĂŢEANU*, PIERRE GRANDCLAUDON** et
ALAIN LABLACHE COMBIER **

* Département de Chimie Organique, Institut Polytechnique, Iaşi, Splai Bahlui Stg. 71, 6600, Iaşi, Roumanie

**. Laboratoire de Chimie Organique Physique, L.A. du C.N.R.S., 351, 59655 Villeneuve d'Ascq Cédex, France

Reçu le 27 avril 1985

Using the perturbation theory and the MO—CNDO/2 procedure method, the 2-position in benzo[b]thiophenes has been shown to be more reactive than the 3-position in their reactions with heterocyclic amines.

Deux types de réaction du benzo[b]thiophène avec un nucléophile dérivé d'une amine ont été décrits.[1,2] Dans les deux cas, l'acte primaire est l'addition de l'azote du nucléophile sur le carbone C_2 du benzo[b]thiophène. La réaction évolue ensuite différemment suivant les conditions expérimentales pour donner soit un dérivé dihydro du benzo [b]thiophène,[1] soit une ouverture électrocyclique du noyau thiophènique.[2]

Nous avons développé, dans ce travail, une étude théorique sur la réactivité du benzo[b]thiophène (**1**) et du méthyl-3 benzo[b]thiophène (**2**) vis-à-vis de trois amines cycliques (pyrrolidine **3**, pipéridine **4**, morpholine **5**) et de leurs anions (**3a**, **4a**, **5a** respectivement). La théorie des perturbations généralisées nous a paru bien d'interaction entre deux systèmes moléculaires A et B, par leurs atomes a_i et b_j respectivement, comme la somme de trois termes T_1, T_2, T_3.[3,4]

Le premier terme $T_1 = -\sum_{ij} (q_i + q_j)\, \beta_{ij} \cdot S_{ij}$, terme répulsif, n'a de valeur significative que dans la comparaison de l'interaction entre un atome b_j et des atomes a_i de nature différente.

Le second terme $T_2 = \sum_{a_i<b_j} \dfrac{Q_{a_i} \cdot Q_{b_j}}{\varepsilon R_{a_i b_j}}$ correspond à la répulsion ou à l'attraction coulombienne entre les atomes a_i et b_j qui réagissent.

Le troisième terme T_3 est appelé soit délocalisation, soit stabilisation par transfert de charge. On peut admettre que les réactions étudiées sont de type donneur (amine ou anion de l'amine) — accepteur (benzo [b]thiophène ou méthyl-3 benzo[b]thiophène). Dans ce cas, l'interaction des orbitales frontières représente la contribution la plus importante au terme T_3.

$$T_3 = \frac{2}{b_\nu^{BV} - a_\mu^{HO}} A_\mu^{HO} \cdot B_\nu^{BV} \cdot \beta_{ij}\ 2$$

a_μ^{HO} est l'énergie de l'orbitale moléculaire la plus haute occupée du donneur et b_ν^{BV} l'énergie de l'orbitale moléculaire la plus basse vacante de l'accepteur.

A_μ^{HO} est le coefficient de l'orbitale atomique p_z de l'atome d'azote dans l'orbitale moléculaire HO du donneur et B_ν^{BV} le coefficient de l'orbi-

Tableau 1

Composé		Orbitale frontière	Energie eV	Coefficients des orbitales atomiques A, B et charge atomique Q des atomes:		
				C_2:	C_3:	N:
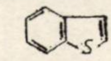	(1)	H.O. B.V.	—11.09454 + 2.34034	B : —0.0825 B : —0.1464 Q : —0.0379	B : +0.1378 B : —0.0439 Q : +0.0322	— — —
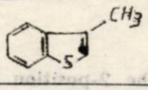	(2)	H.O. B.V.	—10.81315 + 2.37175	B : —0.2130 B : +0.4348 Q : —0.0596	B : —0.3489 B : —0.3913 Q : +0.0740	— — —
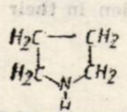	(3)	H.O. B.V.	—11.56262 + 4.77272	— — —	— — —	A : +0.4505 A : —0.0283 Q : —0.2333
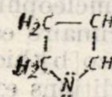	(3a)	H.O. B.V.	— 1.75000 +11.20827	— — —	— — —	A : —0.8726 A : +0.0451 Q : —0.5682
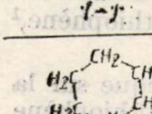	(4)	H.O. B.V.	—13.09715 + 6.87038	— — —	— — —	A : +0.6836 A : +0.1596 Q : —0.1989
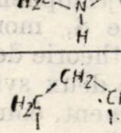	(4a)	H.O. B.V.	— 2.39610 +12.88521	— — —	— — —	A : +0.6564 A : +0.0300 Q : —0.5419
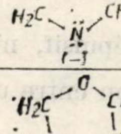	(5)	H.O. B.V.	—12.22525 +6.98638	— —	— —	A : —0.7498 A : —0.0435 Q : —0.1781
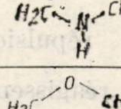	(5a)	H.O. B.V.	— 2.19405 +13.14920	— —	— —	A : —0.7498 A : —0.0780 Q : —0.5418

tale atomique $2p_z$ de l'atome de carbone C_2 ou C_3 dans l'orbitale moléculaire BV de l'accepteur.

β_{ij} est l'intégrale de résonance entre les orbitales atomiques i et j qui réagissent. Les énergies des orbitales frontières, les charges atomiques totales et les coefficients des orbitales atomiques des atomes centres de réaction présentés dans le tableau 1, ont été calculés selon la méthode MO–CNDO/2 [5].

Les différences de charge atomique totale sur les atomes C_2 et C_3 des deux benzo[b]thiophènes ne sont pas significatives. Il est donc difficile d'en déduire la position la plus réactive de ces hétérocycles vis-à-vis de nucléophile. C'est pourquoi il est préférable de comparer la valeur des composants du terme T_3 rassemblés dans le tableau 2.

Tableau 2

Donneur-Accepteur	$b_\nu^{BV} - a_\mu^{HO}$ (eV)	Atomes qui réagissent	$(A_\mu^{HO} \cdot B_\nu^{BV})^2 \cdot 10^{-3}$
Pyrrolidine **3**—Benzo [b]thiophène **(1)**	13.90296	N—C_2	4.3498
		N—C_3	0.3911
Anion de la pyrrolidine **3a**—Benzo [b] thiophène **(1)**	4.09034	N—C_2	16.3197
		N—C_3	1.4674
Pyrrolidine **3**—Méthyl—3-benzo [b] thiophène **(2)**	13.93437	N—C_2	38.3679
		N—C_3	31.0748
Anion de la pyrrolidine **3a**—Méthyl—3-benzo[b] thiophène (2)	4.12175	N—C_2	143.9492
		N—C_3	116.5869
Pipéridine **4**—Benzo [b]thiophène **(1)**	15.43749	N—C_2	10.0158
		N—C_3	0.9006
Anion de la pipéridine **4a**—Benzo[b]thiophène **(1)**	4.73644	N—C_2	9.2346
		N—C_3	0.8303
Pipéridine **4**—Méthyl—**3**-benzo[b]thiophène **(2)**	13.93437	N—C_2	88.3451
		N—C_3	71.5522
Anion de la pipéridine **4a**—Méthyl—3-benzo[b] thiophène **(2)**	4.76785	N—C_2	81.4547
		N—C_3	65.9715
Morpholine **5**—Benzo [b]thiophène **(1)**	14.56559	N—C_2	7.4835
		N—C_3	0.6729
Anion de la morpholine **5a**—Benzo[b] thiophène**(1)**	4.53439	N—C_2	12.0496
		N—C_3	0.1083
Morpholine **5**—Méthyl—3-benzo [b]thiophène **(2)**	14.59700	N—C_2	66.0095
		N—C_3	53.4622
Anion de la morpholine **5a**—Méthyl—3-benzo [b] thiophène **(2)**	4.5658	N—C_2	106.2844
		N—C_3	86.0816

Du point de vue énergétique, (composante $b_\nu^{BV} - a_\mu^{HO}$), les interactions avec les anions des amines sont beaucoup plus favorisées que celles avec les amines correspondantes. Si l'on compare la valeur du produit des coefficients des orbitales atomiques des atomes N des nucléophiles et des atomes C_2 ou C_3 des benzo[b]thiophènes étudiés, dans les deux cas la position C_2 apparaît plus réactive que la position C_3.

Toutefois, la différence de réactivité est plus marquée dans le cas du benzo[b]thiophène (**1**) que dans celui du méthyl-3 benzo[b]thiophène (**2**).

Nous avons pu vérifier expérimentalement que les amines seules ne réagissaient pas avec les deux benzo[b]thiophènes (**1**) et (**2**), mais que la présence d'anion de l'amine suffisait pour rendre la réaction efficace.[1] Ces résultats sont en bon accord avec les conclusions théoriques présentées. Dans ce type de réaction, tous les produits obtenus confirment le fait que la position C_2 de l'hétérocycle est beaucoup plus réactive que la position C_3.[1,2] Dans le cas du méthyl-3-benzo[b]thiophène (**2**), où les différences sont moins marquées, l'effet stérique dû au groupement méthyle en position 3 peut s'ajouter pour favoriser la position 2.

NOTES ET BIBLIOGRAPHIE

[1] P. Grandclaudon et A. Lablache-Combier, *J. Org. Chem.*, **43**, 4379 (1978).

[2] A.E.M. Beyer et H. Kloosterziel, *Rec. Trav. Chim. Pays-Bas*, **96**, 178 (1977).

[3] G. Klopman, « Chemical Reactivity and Reaction Paths », J. Wiley, New York, 1974.

[4] Les composantes des termes T_1, T_2, T_3, qui n'ont pas été détaillées, sont celles habituellement utilisées dans la littérature [3].

[5] J. A. Pople et D. L. Beveridge, « Approximate Molecular Orbital Theory », McGraw-Hill, New York, 1970.

[6] La géométrie des anions est conservée identique à celle des amines correspondantes. Elles ont été déterminées d'après [7]. Dans le cas des benzo[b]thiophènes **1** et **2**, les approximations suivantes ont été utilisées :

- la géométrie du noyau benzénique est conservée,
- distance des liaisons, $C-S$: 1,72 Å ; C_2-C_3 : 1,33 Å ; C_3-C_{3a} : 1,35 Å ; C_3-CH_3 : 1,50 Å,
- angles, $C-S-C$: 92° ; $S-C_2-C_3$: 106° ; $C_2-C_3-C_{3a}$: 117°.

Les calculs ont été effectués sur un ordinateur FELIX C 256 à l'Université de Iași (Roumanie).

[7] C. Rerat, *Acta Crystallogr.*, **13**, 72 (1960) ; T. Sundaresan et S. C. Wallwork, *Acta Crystallogr.*, **B28**, 491 (1972).

Revue Roumaine de Chimie, **31**, *4*, 375—385 (1986)

STYRENE HYDROGENATION ON SUPPORTED Pd AND Pd-Co/γ-Al_2O_3 CATALYSTS

IOAN SĂNDULESCU*, VASILE PÂRVULESCU*, ELENA SZABO**,
ALEXANDRU POPA*** and IOAN V. NICOLESCU*
* National Institute of Chemistry, Department of Chemical Technology, Bucharest, Romania
** Institute of Geology and Geophysics
*** Institute of Physics and Technology of Radiation Apparatus

Received June 3, 1985

In order to arrive at an interpretation of the way in which cobalt and palladium on γ-Al_2O_3 support may interact with each other, we have investigated the styrene hydrogenation reaction in chromatographic pulse. The kinetics of the hydrogenation reaction, as influenced by addition of cobalt to palladium, has also been investigated. Likewise some correlations have been established between selectivity and electronic properties as determined by magnetic susceptibility measurements. The changes of metal distribution on carrier have been determined with a view to correlating them with catalytic activity. For bicomponent catalysts, the activity and selectivity depend on the number of interaction centers which appear between cobalt and palladium.

Elsewhere we have mentioned the practical and theoretical imporance of the hydrogenation of styrene. [1-3]

In this interesting process, the way in which the catalyst directs the hydrogenation reaction — depending on the nature of the active metal— becomes apparent.

In the case of Pd/γ-Al_2O_3 catalysts (used also on industrial scale) the hydrogenation of sytrene proceeds selectively to ethylbenzene.[4,5]

As for transitional metals, Mn, Co, Fe, Cu/γ-Al_2O_3 the hydrogenattion proceeds unselectively, occurring both the hydrogenation of the vinyl group and that of the aromatic ring, by parallel or subsequent reactions resulting in ethylbenzene and the respective ethylcyclohexane.

It is very interesting to note the behaviour of the bimetallic Pd-Me catalyst with transitional Me of the IV-th period depending on the position of Me in the period therefore on its electronic structure.

The behaviour of Pd/γ-Al_2O_3 and Pd-Mn/γ-Al_2O_3 has been presented. [6]

In the present paper we are interested in the activity, selectivity and kinetics of styrene hydrogenation on Pd-Co/γ-Al_2O_3 catalysts as a function of palladium concentration and conditions of reaction.

Certain hypotheses are put forward concerning the interaction Pd-Co on the γ-Al_2O_3 surface.

EXPERIMENTAL

The Pd/γ-Al_2O_3 catalysts preparation was described.[2]

Cobalt deposition on the above mentioned catalysts was carried out by impregnation with solution of cobalt nitrate, followed by drying, calcination and hydrogen reduction at 500 °C.

The following catalysts were prepared: Co(1.0%)/γ-Al_2O_3; Pd(0.1%)—Co(1.0%)/γ-Al_2O_3; Pd(0.3%)—Co(1.0%)/γ-Al_2O_3 and Pd(0.5%)—Co(1.0%)/γ-Al_2O_3.

Styrene hydrogenation was carried out in chromatographic pulse in a microreactor under the same conditions as in the reactions on Pd/γ-Al_2O_3 and Pd-Mn/γ-Al_2O_3:[6]

— weight of the catalyst:	0.140 g;
— temperature of styrene vaporization:	240°C;
— temperature of reaction:	50—80°C;
— hydrogen flow rate:	50—130 mL/min;
— volume of pulse:	0.5—4.0 μL

The electronic properties of the catalysts were determined by magnetic susceptibility measurements, with a magnetic balance by the Faraday method.

To get the surface images and the metal distribution on the surface, a Stereoscan 180 scanning electron microscope, coupled with a Link-type spectrometer for the analysis of energy dispersion of X-rays, was used. Images "with elemental contrast" were obtained; they monitor the metal distribution on the analysed surfaces.

RESULTS

In the chromatographic pulse reaction for styrene hydrogenation, the styrene/hydrogen molar ratio and the contact time have been varied by varying the hydrogen flow. The influence of the hydrogen flow on the activity, depending on the catalyst nature, is shown in fig. 1.

As shown in fig. 1 *a*, for Pd/γ-Al_2O_3 catalysts, styrene conversion is diminished, by increasing the hydrogen flow. However, at any flow the increase of conversion with the increase of paladium concentration is maintained in the same order. It should be noted that the great jump in conversion is found when palladium concentration increases from 0.1 to 0.3 %.

A comparison of the activity of one and two component catalysts shows that cobalt presence leads to the formation of ethylcyclohexane, and by this, hydrogenation is not selective. The influence of the flow is more significant for the 0.5 % Pd/γ-Al_2O_3 catalyst, and less significant for bimetallic catalysts.

One should remark the influence of cobalt on the activity of the 0.1 % Pd-1.0 % Co catalysts, in comparison with 0.1 % Pd. Also, not so much the activity, but especially the much more increased selectivity with respect to ethylbenzene in the case of the catalyst of 0.1 % Pd-1.0 % Co in comparison with 0.3 % Pd-1.0 % Co (and even more, in comparison with 0.5 % Pd—1.0 % Co) would not have been expected.

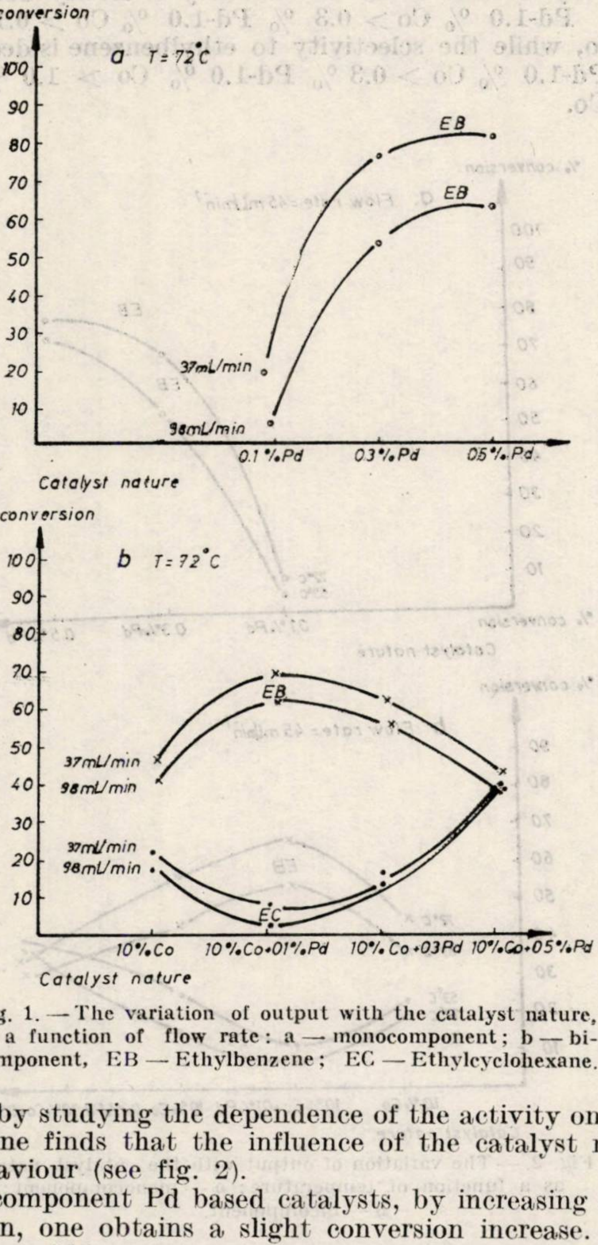

Fig. 1. — The variation of output with the catalyst nature, as a function of flow rate: a — monocomponent; b — bicomponent, EB — Ethylbenzene; EC — Ethylcyclohexane.

Further, by studying the dependence of the activity on the reaction temperature, one finds that the influence of the catalyst nature shows the same behaviour (see fig. 2).

In monocomponent Pd based catalysts, by increasing the temperature of reaction, one obtains a slight conversion increase.

In the case of bicomponent catalysts, we have found that the 0.1 % Pd catalyst is much more selective than those with 0.3 % and 0.5 % Pd, at all the investigated temperatures.

From the experimental data one concludes that, for the Pd/γ-Al_2O_3 monocomponent catalysts, the conversion is increasing with the amount of Pd, while the selectivity to ethylbenzene remains practically 100 %.

For catalysts with cobalt the activity is slowly decreasing in the order 0.5 % Pd-1.0 % Co > 0.3 % Pd-1.0 % Co > 0.1 % Pd-1.0 % Co > 1.0 % Co, while the selectivity to ethylbenzene is decreasing in the order 0.1 % Pd-1.0 % Co > 0.3 % Pd-1.0 % Co > 1.0 % Co > 0.5 % Pd − 1.0 % Co.

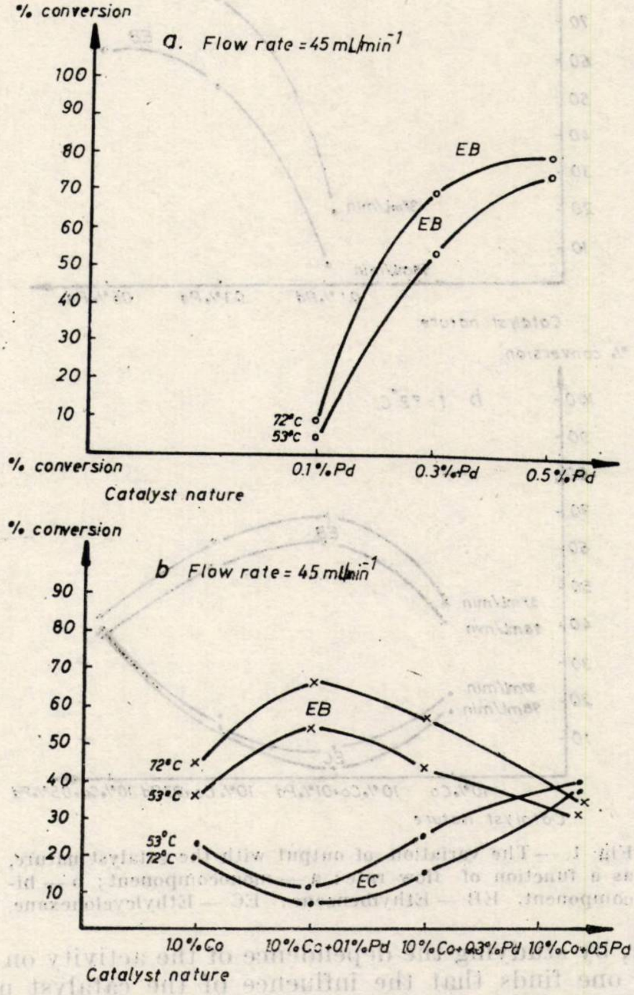

Fig. 2. — The variation of output with the catalyst nature, as a function of temperature: a — monocomponent; b — bicomponent.

Kinetical data and discussions

The reactions have followed a kinetics which is specific for the conditions of chromatographic pulse. [7–9]

From the experimental data, a first order reaction kinetics has been obtained for the Pd/γ-Al_2O_3 catalysts.

A comparison of the determined adsorption heats and apparent activation energies (fig. 3) shows that, for Pd/γ-Al_2O_3 catalysts there is a marked variation when the paladium concentration increases from 0.3 to 0.5 percents.

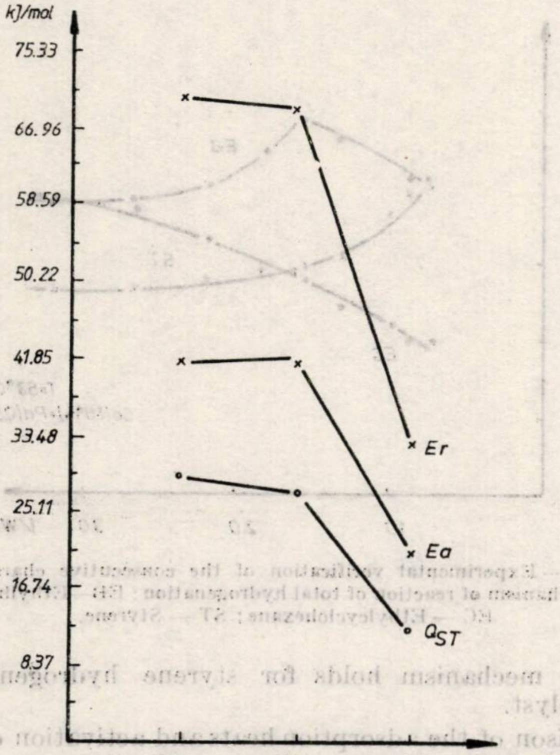

Fig. 3. — Adsorption heat (0) and activation energy (x) for styrene on Pd catalyst/support
E_r — real activation energy; E_a — — activation energy; Q — adsorption heat.

The adsorption heat is higher at lower palladium concentrations because of a higher dispersion of the metal.

The fact that the catalysts with 0.1 and 0.3 percents of Pd (which have, approximately, the same real activation energy) show a great difference of activity would be explained by the difference between the calculated preexponential factors and the velocity constants.

In the case of the bicomponent catalysts, Pd-Co/γ-Al_2O_3 the styrene hydrogenation follows two successive stages, first a hydrogenation to ethylbenzene, and then the hydrogenation of ethylbenzene to ethylcyclohexane.

$$\mathrm{PhCH = CH} \xrightarrow[K_1]{H_1} \mathrm{PH{-}Et} \xrightarrow[K_2]{H_2} \mathrm{C_6H_{11}{-}Et}$$

Both these stages have verified a second order kinetics. This mechanism has also been verified on the shape of the curves (typical for consecutive reactions) representing the variation of the concentration of reagents and the reaction products (see fig. 4) versus contact time.

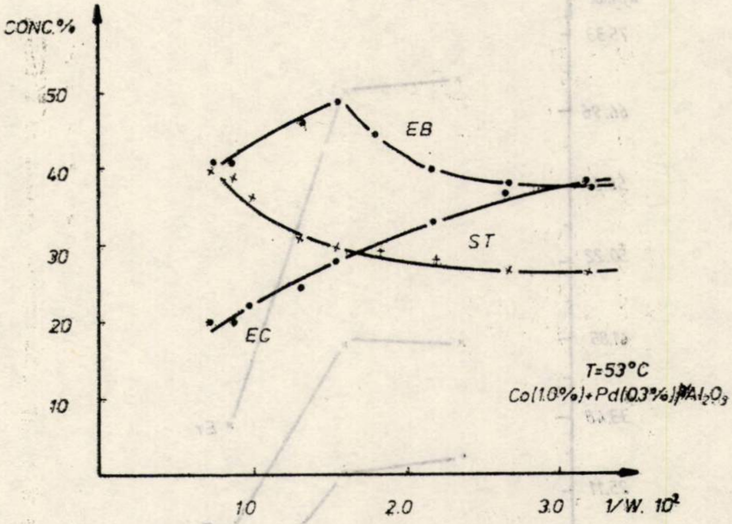

Fig. 4. — Experimental verification of the consecutive character of the mechanism of reaction of total hydrogenation : EB—Ethylbenzene ; EC — Ethylcyclohexane ; ST — Styrene.

The same mechanism holds for styrene hydrogenation on the $Co/\gamma\text{-}Al_2O_3$ catalyst.

A comparison of the adsorption heats and activation energies (fig. 5) for the first stage of hydrogenation shows small differences. The real energy is decreasing slightly from the $Co/\gamma\text{-}Al_2O_3$ catalyst to bicomponent catalysts, and the decrease is progressing with the increase of the palladium concentration. The velocity constants show the opposite behaviour, and this would explain the close conversion obtained with bicomponent catalysts.

The second stage of hydrogenation, however, leads to obvious differences between the catalysts, concerning the ethylbenzene adsorption heat and the activation energy for the reaction of hydrogenation to ethylcyclohexane. The 0.1 % Pd-1.0 % Co catalyst stands appart with a smaller adsorption heat and a higher activation energy.

For this stage the experimental data have been processed on the equation for consecutive reactions in chromatographic pulse.[10]

A system of transcedental equations has been obtained. A graphical solution has firstly been evaluated, and then the solution has been improved by the Newton method. The velocity constants k_2 have been calculated, and they have been used to calculate the activation energies.

It is obvious that cobalt incorporated to Pd/γ-Al$_2$O$_3$ catalysts leads to increased activity, but this effect is decreasing significantly with the increase in the amount palladium.

The observed differences of activity and selectivity for these catalysts can be accounted for by the interaction of the two metals. In the case of the Pd/γ-Al$_2$O$_3$ catalysts, a chemisorption on metal through the vinyl group by a $d - \pi$ interaction is likely to happen. We consider that the increase of activity with the amount of palladium is a result of the decrease of dispersion and the formation of palladium agglomeration.

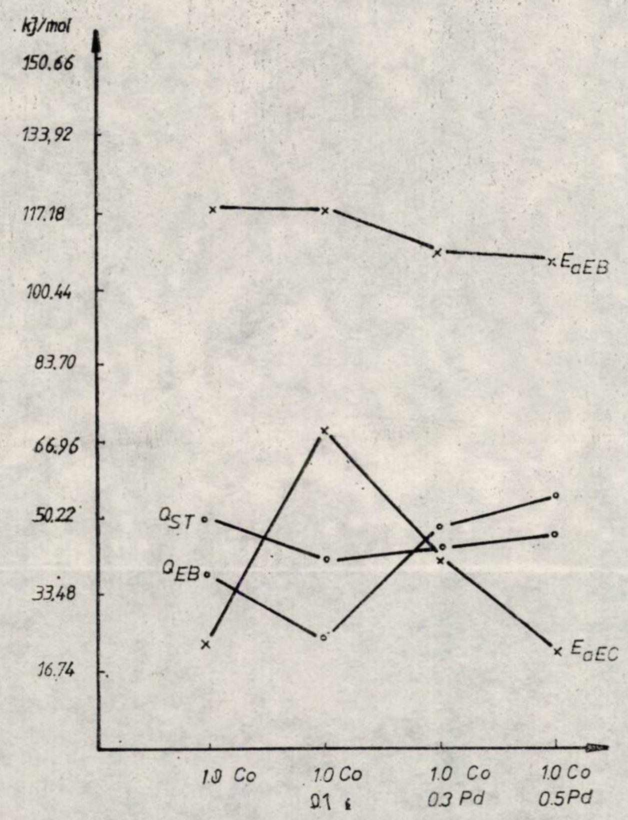

Fig. 5. — Adsorption heat (0) and activation energy (x) for styrene and ethylbenzene, as a function of the palladium concentration in Pd-Co catalysts
E_a — activation energy; Q — adsorption heat; EB — Ethylbenzene; ST — Styrene.

In the case of the cobalt as well as in that of manganese there is the possibility of a $d - \pi$ interaction both with the vinyl group, and with the benzene ring and this explains the non-selective character of the hydrogenation.

The cobalt, both in the monocomponent catalyst 1.0 %Co/γ-Al_2-O_3 and in the bicomponent catalysts Co-Pd shows a high degree of dispersion and uniformity, as can be seen in the images obtained by electronic microscope, figure 6.

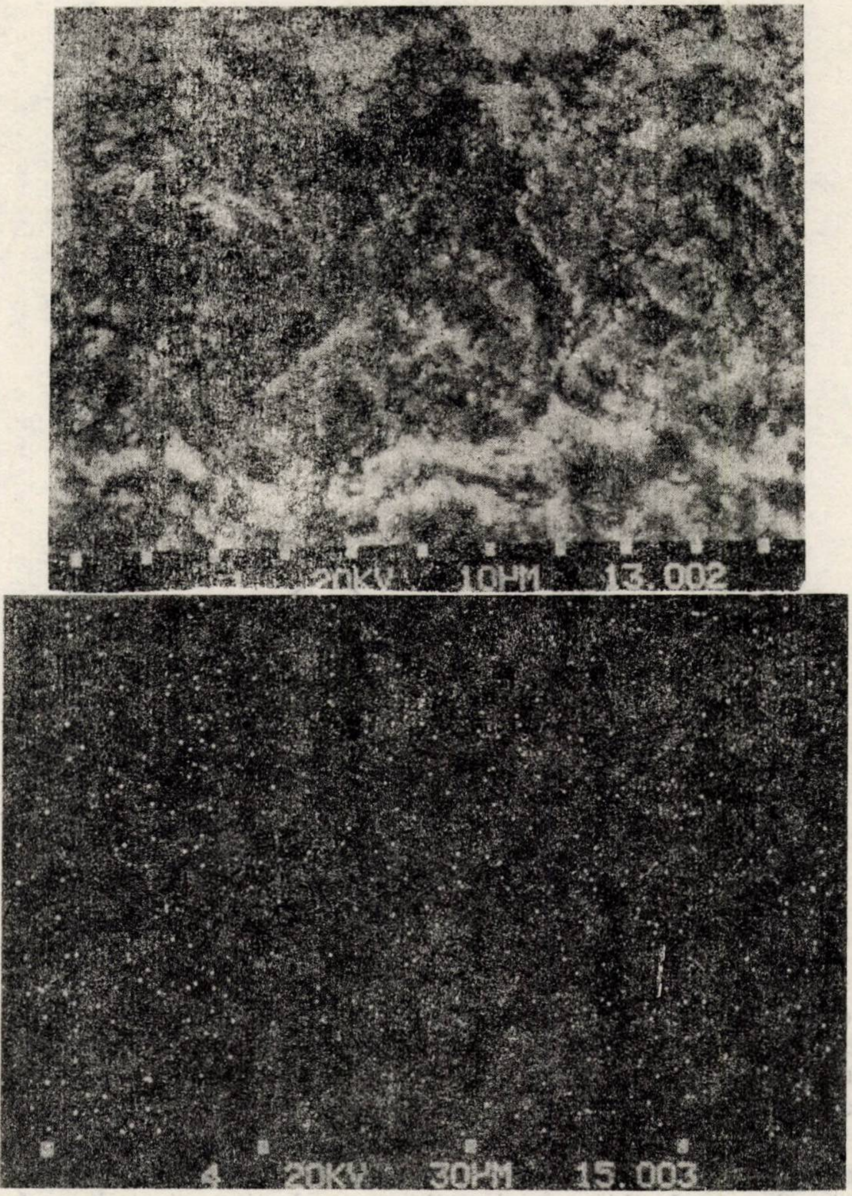

Fig. 6. — Electron microscopy pictures and analysis of X-ray energy dispersion : a — picture of the surface ; b — dispersion of cobalt.

As shown previously at the monocomponent catalysts, of the type Pd/γ-Al_2O_3 the increase of Pd concentration from 0.1 to 0.3 % produces the appearance of Pd agglomerations that is clusters. [6]

From the data given by other authors,[11-13] obtained in investigations of magnetical properties, one has concluded that an electronic interaction between cobalt and palladium is possible, and this could be defined as a chemisorption of cobalt on palladium. At the same time, the cobalt is regarded as a poison for platinic metals.[14-16]

Establishing the oxidation states of cobalt at such concentrations is very difficult. The common methods such as X-ray, RPE, cannot give the necessary information required for cobalt supported on γ-Al_2O_3. Consequently, the magnetic susceptibility measurements were used. The results for the monocomponent Pd/γ-Al_2O_3 catalyst were published.[1]

The magnetic susceptibility data for bicomponent Pd-Co/γ-Al_2O_3 catalysts are shown in Table 1.

Although it is very likely to exist cobalt oxides, the magnetic susceptibilities indicate the presence of cobalt mostly as reduced.

In atomic state cobalt has an (Ar)$3d^7 4s^2$ configuration and 1.73 free electron number. The 1.0 % Co/γ-Al_2O_3 catalyst has a paramagnetism corresponding to 1.20 free electron number, thus very close to that of free cobalt.

The magnetic susceptibilities for bicomponent catalysts Pd-Co/γ-Al_2O_3 are a result of both the contributions of palladium and cobalt and of contributions of Pd-Co interactions; these contributions are not additive.

The temperatures in preparation stages of the catalysts do not favour the formation of intermetallic Pd-Co compounds.

Table 1

Magnetic properties of the catalysts

Catalytic system	Magnetic susceptibility χ—10^{-6}CGS	Free electrons in *d* band
1 % Co	169.03	1.20
1 % Co—0.1 % Pd	—0.86	—
1 % Co—0.3 % Pd	6.72	—
1 % Co—0.5 % Pd	160.29	—
Co^{2+}	30	—
metallic Co	—	1.73

A decreased magnetic susceptibility with decreasing of palladium concentration suggests less free electrons, thus an advanced interaction of the two metals.

The magnetic susceptibility determinations confirm the possible interaction between the aromatic ring or the vinyl group and the bicomponent supported clusters.

The high dispersion of the palladium for 0.1 % Pd nucleates the highest amount of cobalt, and leads to the highest number of bimetallic centers.

This would explain the high increase of activity (from 8 % for 0.1 % Pd to 73 % for 0.1 % Pd – 1.0 % Co at 72°C and 54 mL/ /minute) and a selectivity higher than 92 % with respect to ethylbenzene.

The formation of a small amount of ethylcyclohexane can be accounted for by a $d - \pi$ interaction of the free cobalt with the aromatic ring.

This explains why this catalyst has a very small ethylbenzene adsorption heat (23.61 kJ/mol), which is smaller than for styrene, but close to the ethylbenzene adsorption heat for the 0.1 % Pd/γ-Al_2O_3 catalyst; besides, the hydrogenation to ethylcyclohexane on the bicomponent catalyst has a high activation energy.

As an increase of the amount of palladium from 0.3 to 0.5 % leads to formation of palladium agglomerations, the amount of cobalt which interacts with the palladium grows smaller and smaller hence also the number of bimetallic active formations will be smaller.

It results that, for bimetallic catalysts with 0.3 and 0.5 % Pd the amount of free cobalt is in the same order (i.e. in increasing order). Hence, due to the interaction with the aromatic nucleus, the selective behaviour with respect to ethylbenzene is significantly decreasing.

This explains the high ethylbenzene adsorption heat for these catalysts, with respect to monocomponent catalysts (48.98 kJ/mole for 0.3 % Pd – 1.0 % Co with respect to 14.86 kJ/mole for 0.3 % Pd; 55.10 kJ/mole for 0.5 % Pd – 1.0 % Co with respect to 13.4 kJ/mole for 0.5 % Pd) and they are close to the styrene adsorption heat for the same catalysts (43.5 kJ/mole for 0.3 % Pd – 1.0 % Co and 46.88 kJ/ /mole for 0.5 % Pd – 1.0 % Co); also the activation energy for ethylcyclohexane formation much smaller than for ethylbenzene (42.36 with respect to 108.96 kJ/mole with the 0.3 % Pd – 1.0 % Co catalyst and 21.22 with respect to 106.45 kJ/mole with the 0.5 % Pd-1.0 % Co catalyst).

Cobalt deposition does not change the surface topography of the catalysts of the type Pd/γ-Al_2O_3 – which was shown in [6] – as cobalt distribution is uniform and similar to that of manganese for all palladium concentrations.

CONCLUSIONS

One can estimate that, in Pd/γ-Al_2O_3 single component catalysts, the increase of activity in the styrene hydrogenation reaction to ethylbenzene depends on the magnitude of the palladium formations dispersed on the alumina surface.

Addition of cobalt to palladium catalysts results in a significant increase of activity, while keeping a high ethylbenzene selectivity, but only at small palladium concentration.

The high dispersion of palladium on γ-Al_2O_3 enables the formations of a great number of active centers by cobalt addition.

Besides, the cobalt leads to a total hydrogenation of styrene by consecutive reactions.

REFERENCES

[1] I. V. Nicolescu, V. Pârvulescu, Xu Yandong and I. Săndulescu, Proc. V-th Intern. Symp. Heterogeneous Catalysis, Varna, Part. I, 321, 1983.
[2] I. Săndulescu, Xu Yandong and V. Pârvulescu, *Rev. Chim.* (Bucureşti) **34**, 311 (1983).
[3] I. Săndulescu and V. Pârvulescu, Communication at the "2nd National Conference of Chemistry and Engineering Chemistry", Bucharest, 1983.
[4] I. Săndulescu and V. Pârvulescu, *Rev. Chim. (Bucureşti)*, **30**, 1086 (1979).
[5] I. Săndulescu, V. Pârvulescu and S. Neagu, communication at the "2nd National Congress of Chemistry", Bucharest, 1981.
[6] I. Săndulescu, I. V. Nicolescu, Xu Yandong and V. Pârvulescu, *Rev. Roumaine Chim.*, **28**, 669 (1983).
[7] A. G. Gaziev, B. I. Filinovskii and M. I. Yanovskii, *Kinetika Kataliz.*, **5**, 688 (1983).
[8] G. Z. Roghinskii and A. L. Rosental, *Doklady Akad. Nauk. SSSR*, **146**, 152 (1962).
[9] M. I. Yanovskii and A. D. Berman, *Uspekhi Khim.*, **42**, 147 (1973).
[10] Y. Murakami and T. Nattorri, *J. Catalysis*, **10**, 114 (1968).
[11] F. W. Constant, *Phys. Rev.*, **36**, 786, 1654 (1930).
[12] G. Grube, *Angew Chem.*, **146**, 714 (1935).
[13] H. Remy and H. Connington, *Z. Anorg. Chem.*, **148**, 279 (1925).
[14] D. E. Maxted, *Adv. Catalysis*, **3**, 129 (1951).
[15] G. C. Bond, "Catalysis by Metals", Academic Press, London, 24, 1962.
[16] P. H. Leftin and W. E. Stern, *J. Catalysis*, **6**, 337 (1966).

Revue Roumaine de Chimie, **31**, 4, 387—392 (1986)

SYNTHESIS AND REACTIONS OF 6-ARYL-4,5-DIHYDROPYRIDAZIN-3-(2H)-ONES

ABDEL MOMEN A. EL-KHAMRY, MOHAMED E. SHABAN and MOHAMED M. HABASHY
Ain Shams University, Faculty of Science, Chem. Dep., Abassia, Cairo, Egypt

Received March 23, 1985

The hitherto unknown β-aroylpropionic acids and their α-phenyl analogues (**1 a—f**) were synthesized *via* Friedel-Crafts reactions of *o*-haloanisoles and succinic or phenylsuccinic anhydride. 6-Aryl-4,5-dihydropyridazin-3-(2H)-ones (**2 a-l**) were obtained by the reactions of hydrazines with (**1**). The pyridazinones (**2**) were found to respond to : i) The base catalysed condensation with benzaldehyde, ii) Grignard reagents and iii) Hydroxymethylation and Mannich reaction. The structures assigned to the obtained products were established by different analytical tools.

The present investigation has been carried out aiming to synthesize some 6-arylpyridazin-3-(2H)-ones containing a halogen atom in the aryl group and to study their behaviour towards some nucleophiles and electrophiles. The importance of this type of compounds arose, as it has been reported[1] that analogous compounds possess a significant physiological activity.

β-Aroylpropionic acids and their α-phenyl analogues (**1 a-f**) were obtained upon treating *o*-haloanisoles with succinic or phenylsuccinic anhydride under the condition of Friedel Crafts reaction. The structure of (**1**) was substantiated from analytical and spectral data. Their IR spectra (Table 1) show the stretching frequency absorptions consistent with aroyl

Table 1

Characterization of compounds **1**

Compd.	X	R_1	M.p. °C	Formula/ M.wt.	Analysis Calcd % (Found)			IR		
					C	H	X	ν >C=O	ν >C=O	—OH
1a	Cl	H	196—8^{a}	$C_{11}H_{11}ClO_4$ (242.5)	54.43 54.58	4.53 4.45	14.63 14.70	1670	1695	3430
1b	Cl	C_6H_5	204—6^{a}	$C_{17}H_{15}ClO_4$ (318.5)	64.05 64.29	4.70 4.64	11.14 11.15	1675	1710	3420
1c	Br	H	208—10^{a}	$C_{11}H_{11}BrO_4$ (287)	45.99 46.08	3.83 4.10	27.87 28.34	1670	1690	3410
1d	Br	C_6H_5	212—14^{b}	$C_{17}H_{15}BrO_4$ (363)	56.19 56.22	4.13 4.11	22.03 22.44	1670	1700	3450
1e	I	H	222—24^{a}	$C_{11}H_{11}IO_4$ (334)	39.52 39.70	5.29 3.26	38.02 38.04	1670	1700	3400
1f	I	C_6H_5	229—31^{a}	$C_{17}H_{15}IO_4$ (410)	49.75 60.15	3.65 3.54	30.97 31.08	1675	1695	3450

^{a} Crystallised from acetic acid ; ^{b} Crystallised from acetic acid/H_2O mixture.

and carboxyl carbonyl groups,[2] beside the interbonded hydroxyl absorption at the 3μ region. The α-phenyl structure was assigned to **1 b**, **d** and **f** since, Friedel-Crafts reactions involving phenyl-succinic anhydride were reported [3] to yield predominatly the α-phenyl rather than the β-phenyl isomer.

6-Aryl-4,5-dihydropyridazin-3(2H)-ones and their 2- and 4-substituted analogues **(2 a-l)** were obtained in a fairly good yield *via* the reaction of hydrazines with **(1 a-f)**. The structure of **(2)** was inferred from analytical and spectral data. Thus, their IR spectra (Table 2) show strong absorptions consistent with νC = O of cyclic amides.[4] Moreover, compounds **(2a, b, e, f, i and j)** exhbiit broad bands at the 3μ region attributable to ν NH. The structure of **(2 a)** was further supported by its ^{1}H-NMR spectrum which shows from low to high field, the signals of : aromatic (multiplet), methoxyl (singlet), and methylenes (multiplet) protons, with the integrated proton areas of 3 :3 :2 :2, respectively. The disappearance of

Table 2

Characterization of compounds 2

Compd.	X	R$_1$	R$_2$	M.p. °C	Formula/ M.wt.	Analysis Calcd % (Found)				ν C=O	νNH,
						C	H	X	N		
2a	Cl	H	H	208−10^a	$C_{11}H_{11}ClN_2O_2$ (238.5	55.34 55.65	4.61 4.53	14.88 14.99	11.74 11.96	1670	3210
2b	Cl	C_6H_5	H	198−200^b	$C_{17}H_{15}ClN_2O_2$ (314.5)	64.86 64.59	4.76 4.69	11.28 11.40	8.90 8.97	1670	3200
2c	Cl	C_6H_5	CH_3	162−4^a	$C_{18}H_{17}ClN_2O_2$ (328.5)	65.75 66.37	5.17 5.30	10.80 10.91	8.52 8.77	1665	—
2d	Cl	C_6H_5	C_6H_5	126−7^a	$C_{23}H_{19}ClN_2O_2$ (390.5)	70.67 70.90	4.87 5.03	9.10 9.41	7.17 7.33	1665	—
2e	Br	H	H	176−77^a	$C_{11}H_{11}BrN_2O_2$ (283)	46.64 46.95	3.88 3.70	28.26 28.48	9.89 10.02	1670	3220
2f	Br	C_6H_5	H	204−6^b	$C_{17}H_{15}BrN_2O_2$ (359)	56.82 57.10	4.17 4.20	22.29 22.34	7.78 7.92	1670	3200
2g	Br	C_6H_5	CH_3	149−150^a	$C_{18}H_{17}BrN_2O_2$ (373)	57.90 58.09	4.55 4.81	21.44 21.80	7.50 7.77	1665	—
2h	Br	C_6H_5	C_6H_5	136−8^a	$C_{23}H_{19}BrN_2O_2$ (435)	63.44 63.66	4.37 4.18	18.39 18.50	6.43 6.57	1670	—
2i	I	H	H	190−2^c	$C_{11}H_{11}IN_2O_2$ (330)	40.00 39.87	3.33 3.41	38.48 38.59	8.48 8.53	1680	3230
2j	I	C_6H_5	H	211−12^c	$C_{17}H_{15}IN_2O_2$ (406)	50.24 50.60	3.69 3.89	31.28 31.57	6.89 6.99	1675	3250 3100
2k	I	C_6H_5	CH_3	157−9^a	$C_{18}H_{17}IN_2O_2$ (420)	51.42 51.36	4.04 4.29	30.23 30.50	6.66 6.85	1670	—
2l	I	C_6H_5	C_6H_5	220−22^d	$C_{23}H_{19}IN_2O_2$ (482)	57.26 57.54	3.94 3.88	26.34 26.60	5.81 5.99	1670	—

[a] Crystallised from ethanol ; [b] Crystallised from benzene ; [c] Crystallised from benzene/ethanol mixture ; [d] Crystallised from benzene/light pet. 60−80°.

the acidic — NH proton signal is normal [5] and is attributed to the intermolecular hydrogen bonding with the solvent.

Base-catalysed condensation of **(2-d, g, h** and **k)** with benzaldehyde gave the corresponding 6-aryl-5-benzylidene-4-phenyl-4,5-dihydropyridazin-3-(2H)-ones **(3)**. The structure of **(3)** has been elucidated from : i) Their IR spectra (Table 3) which show close similarity to the parent pyridazin-3-(2H)-ones **(2)**. The ^{1}H-NMR spectrum of **(3c)**, which shows from low to high field the signals of: aromatic and olefinic (multiplet), methoxyl (singlet), N-methyl (singlet) and the hetero-ring methine (singlet) protons, with the integrated proton areas of 14 :3 :3 :1, respectively.

Table 3

Characterization of compounds **3**

Compd.	X	R_1	R_2	M.p. °C	Formula/M.wt.	Analysis Calcd % (Found)			
						C	H	X	N
3a	Cl	C_6H_5	C_6H_5	174–6[a]	$C_{30}H_{23}ClN_2C_2$ (478.5)	75.23 75.50	4.80 5.02	7.41 7.70	5.85 6.09
3b	Br	C_6H_5	C_6H_5	168–70[a]	$C_{30}H_{23}BrN_2O_2$ (523)	68.83 69.10	4.39 4.46	15.30 15.52	5.35 5.29
3c	Br	C_6H_5	CH_3	218–20[b]	$C_{25}H_{21}BrN_2O_2$ (461)	65.07 65.36	4.56 4.49	17.35 17.60	6.07 6.26
3d	I	C_6H_5	CH_3	228–30[b]	$C_{25}H_{21}IN_2O_2$ (508)	59.06 58.89	4.13 4.27	25.00 25.30	5.51 5.48

[a] Crystallised from ethanol ; [b] Crystallised from benzene.

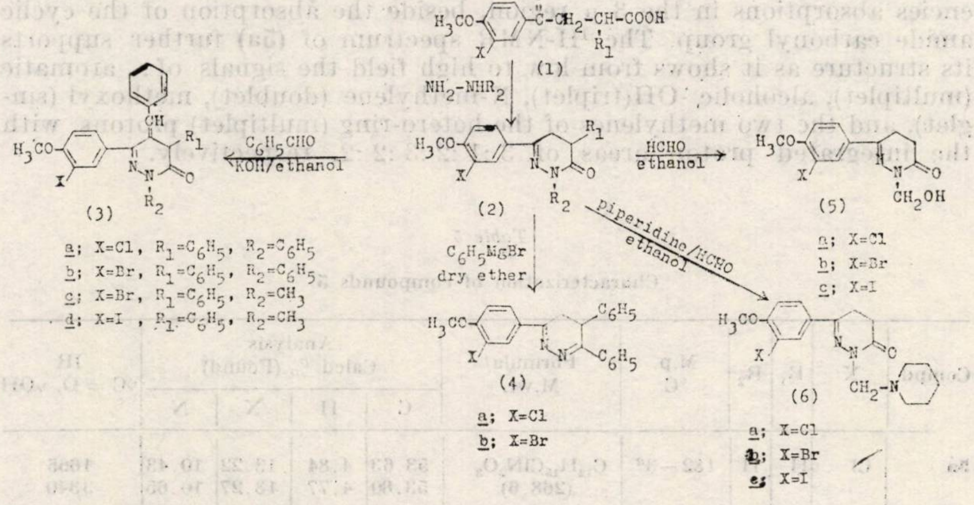

(1)
NH₂-NHR₂
(2)
C₆H₅CHO
KOH/ethanol
(3)
a; X=Cl, R₁=C₆H₅, R₂=C₆H₅
b; X=Br, R₁=C₆H₅, R₂=C₆H₅
c; X=Br, R₁=C₆H₅, R₂=CH₃
d; X=I , R₁=C₆H₅, R₂=CH₃
HCHO
ethanol
(5)
a; X=Cl
b; X=Br
c; X=I
C₆H₅MgBr
dry ether
(4)
a; X=Cl
b; X=Br
piperidine/HCHO
ethanol
(6)
a; X=Cl
b; X=Br
c; X=I

2)	a	b	c	d	e	f	g	h	i	j	k	l
X	Cl	Cl	Cl	Cl	Br	Br	Br	Br	I	I	I	I
R_1	H	C_6H_5	C_6H_5	C_6H_5	H	C_6H_5	C_6H_5	C_6H_5	H	C_6H_5	C_6H_5	C_6H_5
R_2	H	H	CH_3	C_6H_5	H	H	CH_3	C_6H_5	H	H	CH_3	C_6H_5

(1)	a	b	c	d	e	f
X	Cl	Cl	Br	Br	I	I
R_1	H	C_6H_5	H	C_6H_5	H	C_6H_5

Treatment of **(2 b** and **2 f)** with phenylmagnesium bromide gave the respective 6-aryl-3,4-diphenyl-4,5-dihydropyridazin-3(2H)-ones **(4a-b)** (Table 4). The structure of **(4)** was constructed from analytical data and IR spectra which lack any absorption related to the carbonyl or -NH or -OH groups. Furthermore, the ^{1}H-NMR spectrum of **(4a)**, which shows from low to high field the signals of aromatic (multiplet), methoxyl (singlet), methine and methylene of hetero-ring (multiplet) protons, with the integrated proton areas of 13 :3 :3, respectively supported firmly the assigned structure.

Table 4

Characterization of compounds **4**

Compd.	X	R_1	R_2	M.p. °C	Formula/M.wt.	Analysis Calcd % (Found)			
						C	H	X	N
4a	Cl	C_6H_5	H	$233-5^{+}$	$C_{23}H_{19}ClN_2O$ (374.5)	73.69 73.88	5.07 5.25	9.48 9.60	7.48 7.66
4b	Br	C_6H_5	H	$220-22^{+}$	$C_{23}H_{19}BrN_2O$ (419)	65.87 66.01	4.53 4.20	19.09 18.87	6.68 6.59

6-Aryl-2-hydroxymethyl-4,5-dihydropyridazin-3(2H)-ones **(5a-c)** were obtained by the action of formaldehyde on the corresponding pyridazinones **(2 a,e** and **i)**. The structure of **(5)** was confirmed from analytical data and IR spectra (Table 5) which exhibit strong stretching frequencies absorptions in the 3 μ region, beside the absorption of the cyclic amide carbonyl group. The ^{1}H-NMR spectrum of **(5a)** further supports its structure as it shows from low to high field the signals of: aromatic (multiplet), alcoholic -OH(triplet), N-methylene (doublet), methoxyl (singlet), and the two methylenes of the hetero-ring (multiplet) protons, with the integrated proton areas of 3 :1 :2 :3 :2 :2, respectively.

Table 5

Characterization of compounds **5**

Compd.	X	R_1	R_2	M.p. °C	Formula/ M.wt.	Analysis Calcd % (Found)				IR $\nu C = O$, νOH
						C	H	X	N	
5a	Cl	H	H	$182-3^{a}$	$C_{12}H_{13}ClN_2O_3$ (268.6)	53.63 53.80	4.84 4.77	13.22 13.27	10.43 10.65	1665 3340
5b	Br	H	H	$193-5^{a}$	$C_{12}H_{13}BrN_2O_3$ (313)	46.00 45.98	4.15 4.30	25.56 25.68	8.94 9.13	1660 3330
5c	I	H	H	$207-9^{b}$	$C_{12}H_{13}IN_2O_3$ (360)	40.00 39.79	3.61 3.57	35.28 35.37	7.78 7.99	1670 3310

[a] Crystallised from ethanol ; [b] Crystallised from acetic acid/H_2O.

Reaction of **(2)** with formaldehyde and piperidine afforded 6-aryl-2-piperidylmethyl-4,5-dihydropyridazin-3(2H)-ones (**6a-c**) whose structure was established by analytical, spectral and chemical evidence. Thus, their IR spectra (Table 6) show νC=O of cyclic amides and lack of any absorption in the 3 μ region, and the ^{1}H-NMR spectrum of (**6a**) shows from low to high field the signals of : aromatic (multiplet), N-methylene (singlet), methoxyl (singlet), two hetero-ring methylene (triplet) and piperidyl methylenes (two separated multiplet) protons, with the integrated proton areas of 3 :2 :3 :4 :6, respectively. The easy conversion of (**5 a-c**) into (**6 a-c**) on their treatment with piperidine, provided a further chemical support to the suggested structure.

Table 6
Characterization of compounds **6**

Compd.	X	R_1	R_2	M.p. °C	Formula/M.wt.	Analysis Calcd % (Found)				IR
						C	H	X	N	νC=O
6a	Cl	H	H	141–3^a	$C_{17}H_{22}ClN_3O_2$ (335.5)	60.80 61.15	6.56 6.56	10.58 10.79	12.50 12.58	1680
6b	Br	H	H	84–6^b	$C_{17}H_{22}BrN_3O_2$ (380)	53.68 53.90	5.79 5.96	21.05 21.00	11.55 11.59	1670
6c	I	H	H	195–7^a	$C_{17}H_{22}IN_3O_2$ (427)	47.78 47.99	5.15 5.31	29.74 30.00	9.83 10.00	1670

^{a} Crystallised from benzene ; ^{b} Crystallised from pet. ether 80–100°.

EXPERIMENTAL

All melting points are uncorrected. Infrared spectra were measured on a Pye Unicam SP 200 G as KBr wafer technique. ^{1}H-NMR spectrum was taken on a Varian EM 360 instrument operating at 60 MHz in a solution of dimethyl sulphoxide containing tetramethylsilane as an internal standard with chemical shift (δ) expressed in ppm. downfield from TMS.

(1) β-*Aroylpropionic acids and their* β-*phenylanalogues* **(1 a-f).** Succinic anhydride or phenylsuccinic anhydride (0.1 mole), haloanisole (0.1 mole) and fresh powder anhydrous aluminium chloride (0.11 mole) were stirred in acetylene tetrachloride, on a water bath for 3 hrs. After removal of solvent, the reaction mixture was taken up in ether. The ethereal fraction was treated with sodium carbonate (10%) solution, from which the acid was precipitated as colourless solid after acidification. The solid was crystallised from the suitable solvent.

(2) 6-*Aryl*-4,5-*dyhydropyridazin*-3(2H)-*ones***(2a-l)**

The aroylacids **(1)** (0.01 mole) were refluxed with the corresponding hydrazine derivative (0.01 mole), in ethanol (10 mL per 1g. acid) on a water bath for 4 hrs. After removal of alcohol, the residual colourless solid was crystallised from the suitable solvent.

(3) 6-*Aryl*-4-*benzylidene*-2,5-*diphenyl*-4,5-*dihydropyridazin*-3(2H)-*ones and their* 2-*methyl*-5-*phenyl analogues* **(3a-d)**

A mixture of the pyridazinone **(2)** (0.01 mole) and benzaldehyde (0.01 mole) in ethanol (20 mL) was treated with 4 % ethanolic sodium hydroxide solution (25 mL) and the whole mixture was refluxed for 3 hrs. A colourless solid was formed after cooling and acidification. The product was crystallised from a suitable solvent.

(4) 6-*Aryl*-3,5-*dihydropyridazin*-3(2H) *ones* (**4 a** *and* **b**)

A solution of phenylmagnesium bromide (0.02 mole) in dry ether (20 mL) was added dropwise to a solution of the pyridazinone (**2**) (0.01 mole) in dry benzene (40 mL). The reaction mixture was refluxed for 8 hrs. on boiling water bath. After being left overnight, the reaction mixture was decomposed with ice-cold ammonium chloride solution. The ethereal--benzene layer was separated, washed and dried over anhydrous sodium sulphate. After removal of most of solvents, the colourless solid formed was filtered off and crystallised from the suitable solvent.

(5) 6-*Aryl*-2-*hydroxymethyl*-4,5-*dihydropyridazin*-3(2H)-*ones* (**5 a-c**)

A solution of 6-aryl-4,5-dihydropyridazin-3(2H) ones (**2 a, e** and **i**) (1 g) in methanol (20 mL) was treated with formaldehyde, and the reaction mixture was refluxed for 4 hrs. A colourless solid was precipitated after cooling, filtered off and dried. The solid product was recrystallised from a suitable solvent.

(6) 6-*Aryl*-2-*piperidylmethyl*-4,5-*dihydropyridazin*-3(2H)-*ones* (**6a-c**)

A solution of 6-aryl-4,5-dihydropyridazin-3(2H) ones (**2 a, e, i** or **i**) (0.01 mole), piperidine (0.01 mole) and formaldehyde (5 mL) in 30 mL ethanol, were refluxed for 6 hrs. A colourless solid was formed after removal of the solvent, and was recrystallised from a suitable solvent.

REFERENCES

[1] R. Buchman, J. A. Scozzie and R. D. Heilman, *J. Med. Chem.*, **23**, 389 (1980).

[2] L. J. Bellamy, "The Infrared Spectra of Complex Molecules", John Wiley, New York, second edition, 1958.

[3] L. S. El-Assal and A. H. Shehab, *U.A.R. J. Chem.*, **13**, 169 (1970).

[4] F. G. Baddar, M. H. Nosseir and N. L. Doss, *J. Chem. Soc.*, 3878 (1972).

[5] R. M. Silverstein and G. C. Bassler, "Spectrometric Identification of Organic Compounds" New York—London—Sydney, 1968.

Revue Roumaine de Chimie, 31, 4, 393—402 (1986)

CYCLIZATION OF ETHYL CYANOACETATE AND 3,5-DICHLOROSALICYLALDEHYDE WITH KETONES BY MEANS OF AMMONIUM ACETATE

M.M. ISMAIL* and M. S. MOHAMED
Department of Organic Chemistry, Faculty of Pharmacy,
Cairo University, Cairo, Egypt

Received April 27, 1985

Various substituted 7,9-dichloro-6-oxabenzo[f]isoquinolines were prepared by the condensation of ethyl cyanoacetate and 3,5-dichlorosalicylaldehyde with aliphatic or aromatic ketones in the presence of ammonium acetate. On the other hand, condensation with cyclic ketones such as cyclopentanone and cyclohexanone gave 8,10-dichloro-7-oxa-benzo[f]cyclopent[c] isoquinolines and 9,11-dichloro-8-oxa-benzo[k]phenanthridines respectively.

The syntheses of various nitrogen-containing heterocyclic compounds by condensation of active methylene compounds such as ethyl cyanoacetate,[1] ethyl acetoacetate,[2] malononitrile,[3] and benzoylacetonitrile[4] with ketones[1] or aldehydes[5] in the presence of ammonium acetate were reported. Furthermore, the condensation of 3-carbethoxycoumarin with ketones in the presence of ammonium acetate or amines was reported[6] to afford benzoisoquinolone derivatives. The present work will deal with the synthesis of 7,9-dichloro-6-oxa-benzo[f]isoquinoline; 8,10-dichloro-7-oxa-benzo[f]-2,3-dihydro-1H-cyclopent[c]isoquinoline; and 9,11-dichloro-8-oxa-1,2,3,4-tetrahydrobenzo[k]phenanthridine derivatives by the condensation of ethyl cyanoacetate, 3,5-dichlorosalicylaldehyde, and a variety of ketones in the presence of ammonium acetate.

The reaction of ethyl cyanoacetate and 3,5-di-chlorosalicylaldehyde with ketones was carried out by heating a mixture of ester, aldehyde, ketone, and ammonium acetate (molar ratio 1 :1 :1 :1 —1.5) in ethanol. In this case (Scheme 1), the dehydration of the amino group of I and the carbonyl group of ketone, cyclization between the methyl or methylene group of the ketone and the 4-position of the coumarin ring, and subsequent dehydrogenation took place to form 2- or 1,2-disubstituted-4-amino 7,9-dichloro-5-oxo-6-oxabenzo[f]isoquinolines (II).

When 3,5-dichlorosalicylaldehyde was heated with ethyl cyanoacetate and ammonium acetate in ethanol for a few minutes, a crystalline product was obtained. Its infrared spectrum exhibited no characteristic absorption for a C≡N group. When dissolved in dilute hydrochloric acid, this substance afforded pale yellow needles. This compound was confirmed as the hydrochloride salt of 6,8-dichloro-3-amidinocoumarin (I) on the basis of elemental anaylsis and its infrared spectrum. Furthermore, when heated with ketones and ammonium acetate in ethanol, crude I gave compounds of the types II and V.

---

* The author to whom correspondence should be addressed.

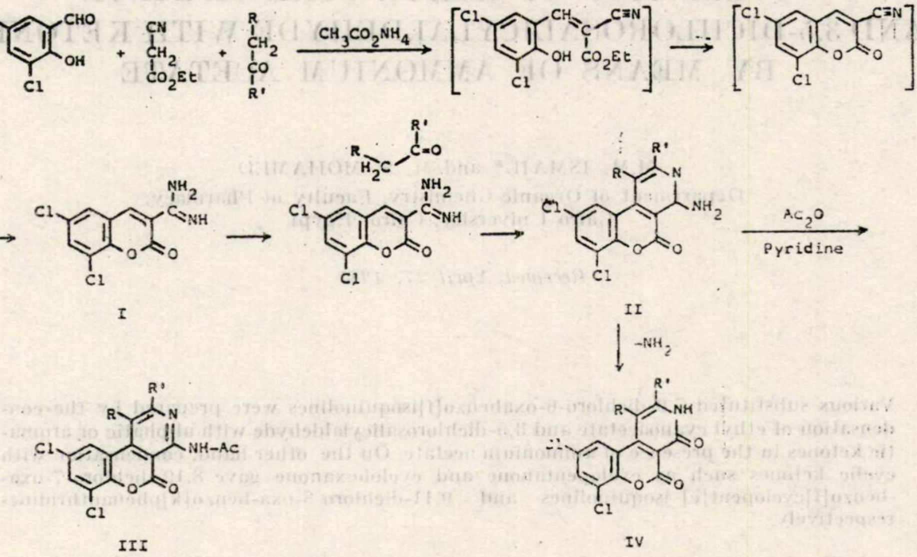

Scheme 1

The cyclization reaction in the present study, therefore, can reasonably be explained in terms of a two-step condensation. Ethyl cyanoacetate and 3,5-dichlorosalicylaldehyde condensed to give 6,8-dichloro-3-cyanocoumarin, which in turn converts readily to 6,8-dichloro-3-amidinocoumarin. Then, the 3-amidinocoumarin condenses with ketones to give heterocyclic compounds of the types II, IV, and V. The structural assignment of these products was based on the infrared and ^{1}H-NMR spectra (Tables 3 and 5). For example, the ^{1}H-NMR spectrum of IIa (prepared when acetone was employed as the ketone reactant) showed only a methyl singlet at δ 2.8 ppm corresponding to three protons in a higher field position than the aromatic ring region. This fact indicated that one methyl group of acetone was involved in this cyclization.

In the infrared spectra of II, carbonyl and amino stretching bands were shifted to slightly lower frequencies owing to the intramolecular C=O . . . . H$_2$N bonding.

The structure of the type II was further supported by the fact that the compound obtained by the condensation of 6,8-dichloro-3-amidinocoumarin (I) and methyl-*n*-propyl ketone in the presence of ammonium acetate was found to be IId by a comparison of their melting points and by infrared and elemental analyses. When methyl ethyl ketone was employed as the ketone reactant, two products, melting at 198–200° and

248—250°C, were isolated. Their elemental analyses indicated the formula of $C_{14}H_{10}O_2N_2Cl_2$, ^{1}H-NMR spectrum of the former (mp 198—200°C) exhibited a triplet corresponding to three protons (CH_3) and a quartet corresponding to two protons (CH_2). On the other hand, the latter (mp 248—250°C) showed only a singlet corresponding to six protons (CH_3). On the basis of these data, it seemed reasonable to assume the two structures of IIb and IIc for them. The ratio of the formation of IIb to IIc was about 1 :0.5 (Scheme 2).

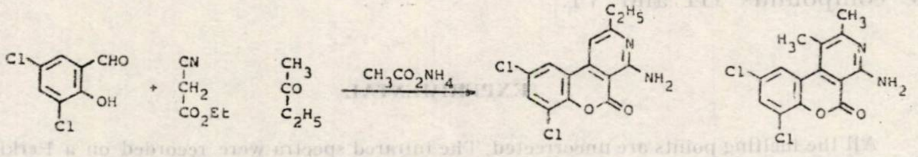

Scheme 2

Reaction with cyclic ketones (Scheme 3) resembles the reaction with the straight-chain ketones described above. In this case, cyclization occurred between the methylene group adjacent to the carbonyl group of

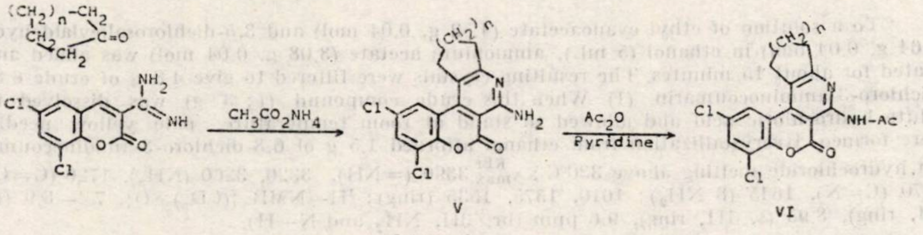

Scheme 3

the ketone and the 4-position of the coumarin ring to form 5-amino-8,10-dichloro-6-oxo-7-oxabenzo[f]-2,3-dihydro-1H-cyclopent[c]isoquinoline (Va) (from cyclopentanone) and 6-amino-9,11-dichloro-7-oxo-8-oxa-1,2,3,4-tetrahydrobenzo[k]phenanthridine (Vb) (from cyclohexanone). These structures were supported by a study of the infrared and ^{1}H-NMR spectra (Tables 3 and 5). In addition, a product obtained by the condensation of I and cyclohexanone was identified as Vb.

Reaction with methyl aryl ketones (Scheme 1) gave 4-amino-7,9-dichloro-2-aryl-5-oxo-6-oxabenzo[f]isoquinolines (IIg-i). On the other hand, the use of acetophenone or *p*-methoxyacetophenone as the ketone reactant afforded 2-aryl-7,9-dichloro-5-oxo-6-oxabenzo[f]-1(2H)-isoquinolones (IVa-b) as the main product under the same reaction conditions. The infrared spectra of IVa-b have strong bands at about 1750 and 1640 cm^{-1}. The former band is shifted to frequencies higher by 50 to 60 cm^{-1} than those of the compounds II. This fact shows the absence of intramolecular hydrogen bonding in the structure of the type IV, since the latter band (1640 cm^{-1}) can be attributed to the carbonyl group (4-position) of the quinolone type.

The reaction of ethyl cyanoacetate and 3,5-di-chlorosalicylaldehyde with propiophenone gave 4-amino-7,9-dichloro-1-methyl-5-oxo-2-phenyl-

-6-oxabenzo[f]isoquinoline (IIi). The ^{1}H-NMR spectrum revealed only a singlet corresponding to three protons (CH_3) in the high field. It is clear that the cyclization occurred between the methylene group of the ketone and the coumarin ring.

The acetylation of the compounds of the types II and V, when treated with acetic anhydride in pyridine, afforded monoacetyl derivatives III and VI respectively (Table 2), while a diacetylamino derivative was obtained from IIi under the same reaction conditions as those producing the compounds III and VI.

EXPERIMENTAL

All the melting points are uncorrected. The infrared spectra were recorded on a Perkin-Elmer Model 521 spectrophotometer by means of potassium bromide pellets. The ^{1}H-NMR spectra were obtained using a JNM-C-60 spectrometer; the peak positions are reported in δ values (parts per million downfield from tetramethylsilane). The mass spectra were determined on Finniganmat 312 mass spectrometer.

Reaction of ethyl cyanoacetate and 3,5-dichlorosalicylaldehyde

To a solution of ethyl cyanoacetate (4.52 g, 0.04 mol) and 3,5-dichlorosalicylaldehyde (7.64 g, 0.04 mol) in ethanol (5 mL), ammonium acetate (3.08 g, 0.04 mol) was added and heated for about 15 minutes. The resulting crystals were filtered to give 4.8 g of crude 6,8-dichloro-3-amidinocoumarin (I). When this crude compound (I; 3 g) was dissolved in dilute hydrochloric acid and allowed to stand at room temperature, pale yellow needles were formed. Recrystallization from ethanol afforded 1.5 g of 6,8-dichloro-3-amidinocoumarin hydrochloride melting above 330°C; ν_{max}^{KBr} 3390 (=NH), 3320, 3200 (NH_2), 1720 (C=O), 1670 (C=N), 1645 (8 NH_2); 1610, 1575, 1535 (ring); ^{1}H—NMR {$(CD_3)_2SO$}, 7.4—8.9 (m, 2H, ring), 8.95 (s, 1H, ring), 9.6 ppm (br, 3H, NH_2 and N—H).

Found: C, 41.0; H, 2.5; N, 8.9; Cl, 36.4

Calcd. for $C_{10}H_6O_2N_2Cl_2.HCl$: C, 40.91; H, 2.40; N, 9.54; Cl, 36.23%.

Reaction of 6,8-dichloro-3-amidinocoumarin (I) and methyl n-propyl ketone

A mixture of I, (2 g), methyl n-propyl ketone (1 g), and ammonium acetate (1 g) in ethanol (3 mL) was heated for 1 hr. After cooling, the resulting precipitate was collected and recrystallized from ethanol-glacial acetic acid to give 1.1 g of colourless needles, m.p 203—204°C. This substance was found to be identical with IId by elemental analyses and a study of the infrared spectral data.

Reaction of 6,8-dichloro-3-amidinocoumarin (I) and cyclohexanone

A mixture of I (2 g), cyclohexanone (1 g), and ammonium acetate (1 g) in ethanol (3mL) was heated for 1 hr. A pale yellow crystalline matter precipitated out during the reaction; this was collected and recrystallized from glacial acetic acid to afford 0.8 g of pale yellow crystals, m.p 265—267°C. This substance was proved to be identical with Vb by a study of their infrared spectra and by the results of elemental analyses.

Reaction of ethyl cyanoacetate and 3-5-dichlorosalicylaldehyde with ketones

To a mixture of ethyl cyanoacetate (0.01 mol), 3,5-dichlorosalicylaldehyde (0.01 mol), and ketone (0.01 mol) in ethanol (3 mL), ammonium acetate (0.01—0.02 mol) was added, and the new mixture was refluxed for 0.5—2 hr. A crystalline compound precipitated out during the reaction or after the reaction mixture had been allowed to stand at room temperature. The experimental results and spectral data are summarized in tables 1, 3 and 5. The mole-

Table 1

4-Amino-7,9-dichloro-5-oxo-6-oxabenzo[f]isoquinoline derivatives and related compounds

Compd	R	R′	m.p°C	Yield %	Molecular formula	Analysis %		
							Calcd	Found
IIa	H	CH_3	271–171	33	$C_{13}H_8O_2N_2Cl_2$	C H N	52.90 2.73 9.49	52.7 2.6 9.3
IIb	H	C_2H_5	198–200	13	$C_{14}H_{10}O_2N_2Cl_2$	C H N	54.39 3.26 9.06	54.4 3.3 9.0
IIc	CH_3	CH_3	248–250	7	$C_{14}H_{10}O_2N_2Cl_2$	C H N	54.39 3.26 9.06	54.2 3.3 9.1
IId	H	n-C_3H_7	203–204	24	$C_{15}H_{12}O_2N_2Cl_2$	C H N	55.74 3.74 8.66	55.5 3.6 8.5
IIe	H	n-C_4H_9	177–178	22	$C_{16}H_{14}O_2N_2Cl_2$	C H N	56.99 4.18 8.30	56.7 4.0 8.3
IIf	H	iso-C_4H_9	185–186	27	$C_{16}H_{14}O_2N_2Cl_2$	C H N	56.99 4.18 8.30	56.8 4.3 8.4
IIg	H	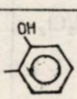	335–336	32	$C_{18}H_{10}O_2N_2Cl_2$	C H N	57.93 2.70 7.50	57.8 2.7 7.5
IIh	H	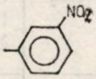	293–296	48	$C_{18}H_9O_4N_3Cl_2$	C H N	53.75 2.25 10.44	53.8 2.3 10.5
IIi	CH_3	Ph	272–273	17	$C_{19}H_{12}O_2N_2Cl_2$	C H N	61.47 3.25 7.54	61.5 3.3 7.3
IVa	H	Ph	302–303	38	$C_{18}H_9O_3NCl_2$	C H N	60.52 2.82 7.84	60.3 2.8 7.9
IVb	H	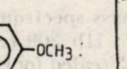	330–331	35	$C_{19}H_{11}O_4NCl_2$	C H N	58.78 2.85 3.60	58.6 2.7 3.5
Va	H	n = 1	280–281	20	$C_{15}H_{10}O_2N_2Cl_2$	C H N	56.09 3.10 8.72	56.2 3.1 9.0
Vb	H	n = 2	268–270	18	$C_{16}H_{12}O_2N_2Cl_2$	C H N	57.33 3.60 8.35	57.5 3.6 8.5

Table 2

4-Acetamino-7,9-dichloro-5-oxo-6-oxabenzo[f]isoquinoline derivatives and related compounds

Compd	R	R′	M.p°C	Yield %	Molecular formula	Analysis %		
							Calcd	Found
IIIa	H	CH_3	283—285	64	$C_{15}H_{10}O_3N_2Cl_2$	C H N	53.43 2.98 8.30	53.5 3.0 8.3
IIIb	H	C_2H_5	230—233	42	$C_{16}H_{12}O_3N_2Cl_2$	C H N	54.72 3·44 7.97	54.5 3.2 8.0
IIIc	CH_3	CH_3	260—263	64	$C_{16}H_{12}O_3N_2Cl_2$	C H N	54.72 3.44 7.97	55.0 3.5 8.1
IIId	H	n-C_3H_7	246—247	64	$C_{17}H_{14}O_3N_2Cl_2$	C H N	56.08 3.84 7.64	56.2 4.0 7.8
IIIe	H	n-C_4H_9	247—249	87	$C_{18}H_{16}O_3N_2Cl_2$	C H N	57.00 4.25 7.38	57.0 4.4 7.0
IIIf	H	iso-C_4H_9	254—256	87	$C_{18}H_{16}O_3N_2Cl_2$	C H N	57.00 4.25 7.38	57.3 4.4 7.5
IIIg	H	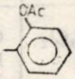	261—263	67	$C_{22}H_{14}O_5N_2Cl_2$	C H N	57.78 3.08 6.12	58.0 3.2 6.0
IIIh	H	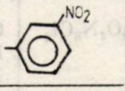	335—337	92	$C_{20}H_{11}O_5N_3Cl_2$	C H N	54.07 2.49 9.45	54.2 2.6 9.7
VIa	H	n = 1	260—262	74	$C_{17}H_{12}O_3N_2Cl_2$	C H N	56.21 3.33 7.71	56.0 3.5 8.0
VIb	H	n = 2	281—282	65	$C_{18}H_{14}O_3N_2Cl_2$	C H N	57.31 3.74 7.42	57.0 4.0 7.5

cular weight, as determined by means of high-resolution mass spectrometry, exhibited the following values: IIa 295 (calcd for $C_{13}H_8O_2N_2Cl_2$, 295.125); IIb 309 (calcd for $C_{14}H_{10}O_2N_2Cl_2$, 309.152); IIc 309 (calcd for $C_{14}H_{10}O_2N_2Cl_2$, 309.152); IId 323 (calcd for $C_{15}H_{12}O_2N_2Cl_2$, 323.179); IIg 373 (calcd for $C_{18}H_{10}O_3N_2Cl_2$, 373.195); IIh 402 (calcd for $C_{18}H_9O_4N_3Cl_2$, 402.193), IVa 357 (calcd for $C_{18}H_9O_3NCl_2$, 357.196); IVb 388 (calcd for $C_{19}H_{11}O_4NCl_2$, 388.206); Vb 335 (calcd for $C_{16}H_{12}O_2N_2Cl_2$, 335.174).

Acetylation of compounds II and V by acetic anhydride in pyridine

To a solution of II or V (0.001 mol) dissolved in pyridine (2—4 mL), acetic anhydride (4—6 mL) was added, after which, the mixture was refluxed for 2—4 hr. After being cooled,

Table 3

Infrared spectral data for 4-amino-7,9-dichloro-5-oxo-6-oxabenzo[f]isoquinoline derivatives and related compounds (cm^{-1})

Compd	νNH_2	$\nu C=O$	δNH_2	Aromatic ring	δCH
IIa	3420, 3265, 3120	1700	1630	1610, 1600, 1585, 1550	790
IIb	3420, 3260, 3120	1700	1630	1610, 1600, 1590, 1560	785
IIc	3500, 3380	1680		1610, 1595, 1585, 1535	790
IId	3420, 3280, 3130	1700	1630	1610, 1600, 1580, 1550	780
IIe	3410, 3270, 3150	1705	1625	1610, 1600, 1580, 1545	785
IIf	3400, 3260, 3130	1695	1630	1610, 1600, 1585, 1550	780
IIg	3430, 3300	1705	1630	1615, 1600, 1585, 1550	775
IIh	3440, 3360	1700		1610, 1600, 1580, 1525, 1530, 1350, (νNO_2)	790
IIi	3410, 3270, 3150	1710	1630	1610, 1590, 1550, 1540	780
IVa		1760, 1640		1615, 1590, 1540, 1510	788
IVb		1740, 1630		1610, 1590, 1575, 1535, 1520	780
Va	3470, 3350	1675		1600, 1590, 1580, 1545	790
Vb	3420, 3260, 3130	1690	1620	1610, 1550	790

the deposited precipitate was collected and washed with dilute methanol. The experimental results and spectral data are summarized in tables 2, 4 and 6.

Acetylation of IIi

Acetic anhydride (7 mL) was added to a solution of IIi (0.5 g) dissolved in pyridine (4 mL), after which the mixture was refluxed for 4 hr. After cooling, ice water was added to the reaction mixture to afford a crystalline precipitate. The precipitate was collected, washed with cold dilute methanol, and dried. Recrystallization from glacial acetic acid gave 0.6 g of 4,4-diacetylamino-7,9-dichloro-1-methyl-5-oxo-2-phenyl-6-oxabenzo[f]isoquinoline, m. p. 245—247°C ; ν_{max}^{Kbr} 1740 (O—C=O), 1710, 1695 (CH_3—C=O), 1610, 1590, 1560, 1530 (hetero ring and phenyl), 775, 705 (δ CH) ; ^1H—NMR (CF_3CO_2H) peaks at 2.35, 2.65 (s, 3H each, CO—CH_3), 3.0 (s, 3H, CH_3), 7.5—8.0 and 8.55—8.8 ppm (m, 7H, ring).

Table 4

Infrared spectral data for 4-Acetamino-7,9-dichloro-5-oxo-6-oxabenzo[f]isoquinoline derivatives and related compounds (cm^{-1})

Compd	νNH	Ring C=O, NH−C=O	Aromatic ring	δ CH
IIIa	3240	1695, 1665	1610, 1595, 1560, 1525	790
IIIb	3260	1700, 1675	1610, 1595, 1555	785
IIIc	3240	1675	1605, 1595, 1565, 1550, 1500	790
IIId	3250	1700, 1665	1615, 1595, 1555, 1520, 1500	790
IIIe	3250	1695, 1665	1615, 1595, 1555, 1520, 1500	788
IIIf	3250	1700, 1670	1615, 1595, 1550, 1515	775
IIIg	3260	1760, 1700, 1675 (O−Ac)	1610, 1595, 1550, 1520	780
IIIh	3240	1700, 1670	1610, 1595, 1530, 1520, 1550, 1350 (NO_2)	780
VIa	3230	1670	1605, 1595, 1570, 1550, 1500	790
VIb	3240	1700, 1670	1590, 1570, 1550	790

Table 5

^{1}H-NMR spectral data* for 4-Amino-7,9-dichloro-5-oxo-6-oxabenzo[f]isoquinoline derivatives and related compounds

Compd	CH_3	OCH_3	CH_2	$-\overset{\vert}{C}H-$	Ring−CH=	NH
IIa	2.8 (s, 3H)				7.5−8.5 (m, 4H)	8.9−9.7 (br, 1H)
IIb	1.55 (t, 3H)		3.1 (q, 2H)		7.5−8.7 (m, 4H)	8.9−9.6 (br, 1H)
IIc	2.8 (s, 6H)				7.5−8.0 (m, 2H)	8.5 (br, 1H) 8.65 (br, 1H)

* Parts per million downfield from tetramethylsilane in CF_3CO_2H;
s = singlet, d = doublet, t = triplet, q = quartet, m = multiplet, br = broad.

Table 5 (continued)

Compd	CH_3	OCH_3	CH_2	$-\overset{\vert}{C}H-$	Ring—CH=	NH
IIf	1.15 (d, 6H)		2.9 (d, 2H)	2.0—2.5 (m, 1H)	7.4—8.4 (m, 4H)	8.9—9.7 (br, 1H)
IIh					7.5—9.0 (m, 7H)	9.3—9.9 (br, 1H)
IIi	2.8 (s, 3H)				7.5—8.1,8.5—8.8 (m, 7H)	
IVb		4.07 (s, 3H)			7.2—8.6 (m, 7H)	
Va			2.3—2.9 (m, 2H) 3.1—3.9 (m, 4H)		7.5—8.9 (m, 3H)	10.9 (s, 1H)
Vb			2.3—2.9 (m, 4H) 3.1—3.9 (m, 4H)		7.5—8.9 (m, 3H)	10.9 (s, 1H)

Table 6

^{1}H-NMR spectral data* for 4-acetamino-7,9-dichloro-5-oxo-6-oxabenzo[f]isoquinoline derivatives and related compounds

Compd	CH_3	NH—CO—CH_3	CH_2	Ring—CH=	NH
IIIa	2.98 (s, 3H)	2.66 (3, 3H)		7.5—8.5 (m, 3H)	12.6 (br, 1H)
IIId	1.2 (t, 3H)	2.67 (s, 3H)	2.05 (sx, 2H) 3.23 (t, 2H)	7.5—8.5 (m, 3H)	12.55 (br,1H)
IIIg		2.72 (s, 3H) 2.45 (O—CO—CH_3, s, 3H)		7.5—8.6 (m, 7H)	12.67 (br, 1H)
VIa		2.7 (s, 3H)	2.3—2.9 (m, 2H) 3.3—4.1 (m, 4H)	7.2—8.1 (m, 2H)	12.75 (br, 1H)

---

* Parts per million downfield from tetramethylsilane in CF_3CO_2H; s = singlet, t = triplet, sx = sextet, m = multiplet, br = broad.

Found: C, 61.0; H, 3.7; N, 6.0.

Calcd for $C_{23}H_{16}O_4N_2Cl_2$: C, 60.67; H, 3.54; N, 6.15%.

The molecular weight, as determined by high resolution mass spectrometer gave a value of 455 (calcd 455.297).

REFERENCES

[1] A. Sakurai and H. Midorikawa, *Bull. Chem. Soc. Japan*, **40**, 1680 (1967).

[2] A. Sakurai and H. Midorikawa, *Bull. Chem. Soc. Japan*, **41**, 165 (1968).

[3] A. Sakurai and H. Midorikawa, *Bull. Chem. Soc. Japan*, **41**, 430 (1968).

[4] A. Sakurai and H. Midorikawa, *Bull. Chem. Soc. Japan*, **42**, 220 (1969).

[5] A. Sakurai and H. Midorikawa, *J. Org. Chem.*, **34**, 3612 (1969).

[6] A. Sammour and M. Alkady, *Indian J. Chem.*, **12**, 51 (1974).

Revue Roumaine de Chimie, 31, 4, 403—409 (1986)

HIGH-PERFORMANCE LIQUID CHROMATOGRAPHY OF 2,4,6-HALOALKYL-1,3,5-TRIAZINES

R. BACALOGLU*, L. COTARCĂ*, ANABELA IŞFAN** and C. IŞFAN**
* Polytechnic Institute "Traian Vuia" Timişoara, Department of Organic Chemistry, str. Bocşa no. 6, Timişoara 1900, Romania
** ICECHIM—CCMP "Solventul" Timişoara 1900, Romania

Received March 23, 1985

A fast and simple HPLC method was developed for the separation of 2-alkyl-4,6-bis (trichloromethyl)-1,3,5-triazines and 2,4,6-haloalkyl-1,3,5-triazines. Procedures for the determination of reversed phase column performance, by using the Barber and Carr graphical method and Bristow-Knox algorithm were evaluated. A computer program in Basic has been built for the calculations of the relevant chromatographic parameters from experimental data. The elution order and chromatographic behaviour of nine triazine compounds suggested a structure-retention relationship.

INTRODUCTION

1,3,5-Triazine derivatives are used mainly in agriculture as herbicides, but they have also fungicidal properties and some of them are utilized as pharmaceuticals. Recently, very effective 1,3,5-triazine flame retardants for urethane foams are reported.[1]

Because this chemical class consists of a great number of structurally closely related compounds for which it is difficult to use classical analytical procedures for identification and quantitative assay, chromatographic methods (GL, TLC and HPLC) predominate at present for their determination.[2-5]

High-pressure liquid chromatography (HPLC) has been found to offer a rapid method for the analysis of a large number of 1,3,5-triazines.[6-8] Apparently there is no published information describing HPLC separation of 2,4,6-haloalkyl-1,3,5-triazines or 2-alkyl-1,3,5-triazines.

This paper reports a HPLC method of analysis suitable for a wide range of 2,4,6-haloalkyl-1,3,5-triazines that can be performed with minimum sample preparation. The method has been developed in order to follow the 2,4,6-haloalkyl-1,3,5-triazine synthesis by the acid catalyzed cyclotrimerization of the corresponding haloalkane nitriles.[9] Moreover, it has been found that chromatographic retention-electronic and steric structure relationships exist making possible the prediction of the structure of 1,3,5-triazines by using retention time, polar substituent (Taft) constants and steric substituent constants assigned to each substituent group on the triazine ring.

EXPERIMENTAL

A Waters 244 LC instrument with a 6000 high-pressure pump, a Rheodyne 7125 loop injector and a Varian 5020 LC instrument (automated Valco loop injector) with UV detectors operating at a wavelength of 254 nm were used. A Varian 9176 dual channel recorder and a Control Data System CDS 111 L were used. Chromatographic separations were accomplished by using a RP—18 Brownlee cartridge (10 cm × 4 mm i.d.). Experiments concerning kinetic efficiency of RP column in the separation of a standard triazine have been carried out on Varian 5020 LC instrument equipped with MicroPak MCH—10 (Varian) column (30 cm × 4 mm i.d.).

The best separations for all compounds and the best compromise between resolution and analysis time were obtained with water-acetonitrile mobile phase, when the linear gradient was adjusted from 55 % MeCN to 100 % MeCN, at a flow rate of 1.2 mL/min. The column pressure was maximum 1500 psi. The injection volumes were 20 and 10 microliters, respectively.

Acetonitrile (Merck) which was better than methanol for resolving these compounds) was of UV spectrograde distilled-in-glass. Water was kalium permanganate treated and double distilled-in-glass. Solvents were on line filtered before use.

2,4,6-Haloalkyl-1,3,5-triazines have been synthetized by acid catalyzed cyclotrimerization of the corresponding alkane or haloalkane nitriles and were purified by recrystallization from ethanol or fractional distillation under reduced pressure. [9] 2,4,6-tris(Dichloromethyl) -1,3,5-trianzine was obtained by chlorination of 2,4,6-trimethyl-1,3,5-triazine. [10] The physica and spectral properties are shown in Table 1.

Table 1

Physical and spectral properties of alkyl- and haloalkyl-1,3,5-triazines

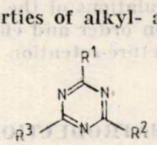

No.	R^1	R^2	R^3	B.P.,°C/mmHg	M.P.,°C(solv)	UV (MeOH) λ_{max}, nm(ϵ)
1	Me	CCl_3	CCl_3		96—97 (EtOH)	220 (1925) 280 (945)
2	Et	CCl_3	CCl_3	160—163/10	33—35 (EtOH)	222 (1775) 279 (575)
3	n-Pr	CCl_3	CCl_3	175—178/15		221 (1824) 279 (660)
4	n-Bu	CCl_3	CCl_3	160—163/5		218 (1825) 276 (614)
5	n-$C_{15}H_{31}$	CCl_3	CCl_3	205—207/5		219 (1810) 275 (650)
6	CCl_3	CCl_3	CCl_3		92—93 (EtOH)	220 (2595) 289 (945)
7	$ClCH_2CH_2$	CCl_3	CCl_3		65—67 (EtOH)	244 (3324)
8	$ClCH_2CH_2$	$ClCH_2CH_2$	CCl_3		60—62 (EtOH)	241 (3156)
9	Cl_2CH	Cl_2CH	Cl_2CH		81—83 (EtOH)	230 (3156)

RESULTS AND DISCUSSION

Figures 1 and 2 show the separation of 2-alkyl-4,6-bis(trichloromethyl)-1,3,5 triazines and 2,4,6-haloalkyl-1,3,5-triazines, respectively, on microparticulate reversed phase column (Brownlee RP—18) by using acetonitrile-water mobile phase gradient. Table 2 gives relative retention times for the 1,3,5-triazines investigated. The sensitivity limits were in the 80-120 ng range by UV detection at 254 nm.

Several experiments have been done for the actual kinetic efficiency determination of the HPLC column (MicroPak-MCH—10). The main chromatographic parameters of the standard compound, 2-methyl-4,6-bis(trichloromethyl)-1,3,5-triazine were calculated according to the graphical method described by Barber and Carr[11] and by using the author's

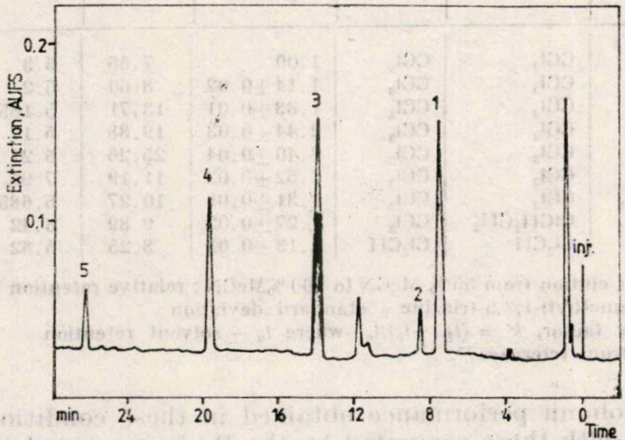

Fig. 1. — HPLC separations of 2-alkyl-4,6-bis(trichloromethyl)-1,3,5-triazines. Waters 244 LC instrument, RP—18 Brownlee SPHERI 5 cartridge ; MeCN-water (55 %—100 %) ; flow rate 1.2 mL/min, UV 254 nm detection (for the compound numbers and structures see table 1).

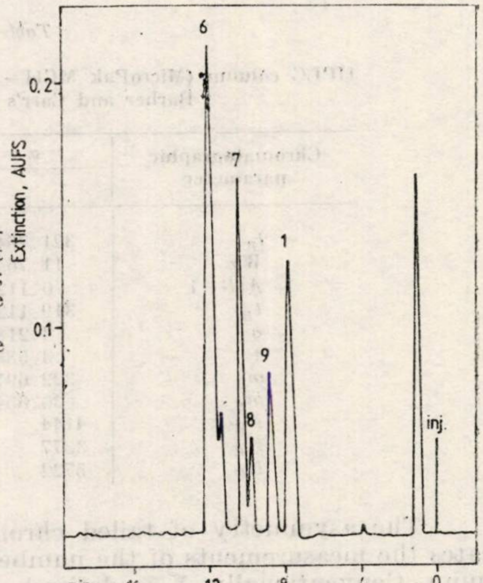

Fig. 2. — HPLC separation of 2,4,6-haloalkyl-1,3,5-triazines. Waters 244 LC instrument RP—18 Brownlee SPHERI 5 cartridge; MeCN — water (55 % — 100 %), flow rate 1.2 mL/min, UV 254 nm detection (for the compoud numbers and structures see table 1).

Table 2

Relative retentions of the investigated 1,3,5-triazines

No.	R^1	R^2	R^3	t_{Ri}/t_{Ro} a)	k' b)	$\Sigma\sigma^*$ c)	ΣE_s c)
1	Me	CCl_3	CCl_3	1.00	7.56	5.3	−4.12
2	Et	CCl_3	CCl_3	1.14±0.02	8.60	5.2	−4.19
3	n-Pr	CCl_3	CCl_3	1.83±0.01	13.71	5.185	−4.48
4	n-Bu	CCl_3	CCl_3	2.44±0.03	19.88	5.17	−4.51
5	n-$C_{15}H_{31}$	CCl_3	CCl_3	3.40±0.04	25.26	5.21	−4.33
6	CCl_3	CCl_3	CCl_3	1.52±0.02	11.19	7.95	−6.18
7	$ClCH_2CH_2$	CCl_3	CCl_3	1.31±0.01	10.27	5.685	−5.02
8	$ClCH_2CH_2$	$ClCH_2CH_2$	CCl_3	1.27±0.02	9.89	3.42	−3.86
9	Cl_2CH	Cl_2CH	Cl_2CH	1.13±0.03	8.25	5.82	−4.62

a) Gradient elution from 55 % MeCN to 100 %MeCN ; relative retention times to 2-methyl-4,6-bis(trichloromethyl)-1,3,5-triazine ± standard deviation

b) Capacity factor, $k' = (t_{Ri} - t_0)/t_0$, where t_0 — solvent retention

c) Taken from reference [17].

tables. The column performance obtained in these conditions (Table 3) was identical with those computed by the Basic program built for a microcomputer MC—18 (Table 4). This program is based on the Bristow-Knox standardized testing procedures which convert the experimental parameters into relevant chromatographic parameters, and is the most popular method for checking the efficiency of a HPLC column.[12–14]

Table 3

HPLC column (MicroPak MCH—10) performance determined by Barber and Carr's graphical method

Chromatographic parameter	$\alpha = 0.5$		$\alpha = 0.1$	
		s%		s%
t_p	321.7647	0.53	321.7647	0.50
$W\alpha$	11.7647	3.10	23.5294	2.90
$A/B-1$	0.1122	4.20	0.1860	3.90
t_R	319.1120	0.74	319.2113	0.71
σ	4.2186	3.04	4.6374	3.00
τ	3.5858	5.10	3.2462	4.70
m_1	322.6978	0.48	322.4575	0.47
$\overline{m}_2$	30.6544	3.70	32.0435	0.30
$N_{W\alpha}$	4144	0.75	3876	1.25
N_K	3377	9.76	3231	8.31
N_G	5722	6.30	4738	5.91

The asymmetry of tailed chromatographic peaks usually complicates the measurements of the number of theoretical plates (N) on a column. Conventionally N is defined as :

$$N_K = \frac{t_p^2}{\overline{m}_2} \qquad (1)$$

Table 4

Chromatographic parameters for the separation of 2-methyl-4,6-bis(trichloromethyl)-1,3,5-triazine on MicroPak MCH—10 column, determined by the computer standardized testing program

Parameter		Parameter	
Plate number:	4.14404 E 03	Reduced H:	7.23930 E 00
HETP :	7.23930 E 01 μm	Resistance:	3.67816 E 02
Linear velocity:	4.99999 E 00 mm/s		
Permeability:	2.71874 E−13 m²		
Performance: index	1.66786 E 03/Bar s		
Knox-Parcher:	5.33333 E 00	Total porosity:	2.65383 E−01
Reduced velocity:	6.32910 E 01		
Separation impedance:	1.92763 E 04	Column capacity: factor	4.36274 E 00

where t_p and $\overline{m}_2$ are the retention time (i.e., time of appearance of the peak maximum) and the variance (i.e., second central moment) of the peak, respectively.[15] The equivalent expression for a pure Gaussian is:

$$N_G = \frac{t_R^2}{\sigma^2} \tag{2}$$

where t_R is not only the peak apex but also is the center of gravity (first statistical moment, m_1) and σ is the standard deviation of the Gaussian profile. The most common method for estimating plate counts (N) is given by the following equation:

$$N_{W0.5} = \left(\frac{t_p}{W_{0.5}}\right)^2 \cdot 5.54 \tag{3}$$

where $W_{0.5}$ is the peak width at half-height.

The most commonly used model of a tailed peak is the so-called exponentially modified Gaussian equation:

$$\frac{h(t)}{h_{\max}} = \left(\frac{\pi}{2}\right)^{1/2} \frac{\sigma}{\tau} \cdot \exp\left(\frac{-\sigma}{2\tau}\left[\frac{t-t_R}{\sigma} - \frac{\sigma}{\tau}\right]\right) \operatorname{erf}\left(\frac{1}{2^{1/2}}\left[\frac{t-t_R}{\sigma} - \frac{\sigma}{\tau}\right]\right) \tag{4}$$

where $h(t)$ is the height of the chromatographic peak as a function of time in arbitrary units, $h_{\max}$ is the maximum height that the peak would have if it were perfect Gaussian, and τ is the time constant of the exponential peak modifier. Equation (4) indicates that all relative (to t_R) temporal properties of a peak expressed in units of σ will be a function only of the ratio τ/σ. The τ/σ ratio, if the peak is well fit by an exponentially modified Gaussian model is more useful for describing the relative peak asymmetry than A/B ratio, graphically measured as shown in Figure 3.

This dependence on only the ratio of σ/τ is the basis of Barber and Carr's graphical method for obtaining measures of N, σ, τ, t_R, m_1 and $\overline{m}_2$.[11]

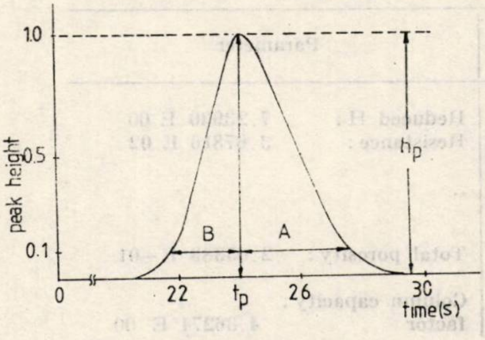

Fig. 3. — Example of the measurements required for the graphical method; $W_\alpha = A + B$. The value of α is 0.1 and for $A/B - 1 = 0.11$, τ/σ ratio is 0.55.

As shown in Table 3, $N_{W\,0.5}$ can be measured with better accuracy and precision than either N_G or N_K at either α equal to 0.5 or 0.1. $N_{W\,0.5}$ is given also by the more complex standardized testing program. The main point of the graphical method is to show that it is possible to obtain fundamental chromatographic parameters such as t_R, m_1, $\overline{m}_2$, σ, τ, and various estimates of system efficiency such as N_G and N_K with or without automated data aquisition systems or on-line computers.

All the kinetic efficiency experiments were carried out under isocratic elution, after the conversion of gradient elution conditions to the isocratic mobile phase, keeping constant the k' values.[16]

Retention-structure relationships

Retention times could be used to predict the structure of investigated compounds. A multiple linear regression equation analogous to the Taft equation[17] can be deduced relating the relative retention, electronic and steric effect of substituents:

$$\log \frac{t_{Ri}}{t_{R0}} = a_0 + a_1 \sum \sigma^* + a_2 \sum E_s \qquad (5)$$

Thus, a_1 and a_2 parameters can be interpreted as a measure of the electronic and steric sensitivity, respectively, of the particular 1,3,5-triazine series for resolution on the specified chromatographic column under stated elution conditions. t_{Ri} and t_{R0} are the retention times of the substituted and reference 1,3,5-triazines. As reference 1,3,5-triazine 2-methyl-4,6-bis(trichloromethyl)-1,3,5-triazine was selected.

The obtained equation coefficients for the 2-alkyl-4,6-bis(trichloromethyl)-1,3,5-triazines series (compounds 1—5 from Table 2) and 2,4,6-haloalkyl-1,3,5-triazines series (compounds 6—9 from Table 2) are given in Table 5.

No pretention to theoretical rigor has been made in this study since the object was only to develop a methodology which would allow quanti-

Table 5

Structure-retention relationships for alkyl- and haloalkyl-1,3,5-triazines

Triazines	a_0	a_1	a_2	r
2-Alkyl-4,6-bis(trichloromethyl)--1,3,5-triazines (compounds 1—4)	4.380	−1.210	−0.491	0.947
2,4,6-Haloalkyl-1,3,5-triazines (compounds 1,6—9)	−0.345	−0.0753	−0.180	0.976

tative analysis and resonable qualitative prediction of a variety of substituted 1,3,5-triazines. The identification of a particular compound by this method is very useful in the absence of a mass spectrometer.

REFERENCES

R. Bacaloglu, N. Mircu, L. Cotarcă, I. Iorga, A. Târnăveanu, N. Pop, C. Işfan and S. Rist Rom. Pat. 76577 (1981).

[2] C. E. Parker, C. A. Haney, D. J. Horvan and J. R. Hass, *J. Chromatogr.*, **242**, 247 (1982).

[3] "EPA Manual of Chemical Methods for Pesticides and Devices", Beltsville, 1983.

[4] E. Matisová and J. Krupčik, *J. Chromatogr.*, **142**, 597 (1977).

[5] W. P. Cochrane and R. Purkayastha, *Toxicol. Envir. Chem. Rev.*, **1**, 137 (1973).

[6] P. Dufek, V. Paćaková and E. Tesařová, *J. Chromatogr.*, **191**, 115 (1980).

[7] H. Jork and B. Roth , *J. Chromatogr.*, **144**, 39 (1977).

[8] E. Smolková Jr. and V. Paćaková, *Chromatographia*, **11**, 698 (1978).

[9] L. Cotarcă and R. Bacaloglu, *Bul. şt. şi tehnic al I. P. Timişoara*, **30** (44), 93(1985).

[10] F. C. Schalfer and J. H. Ross, *J. Org. Chem.*, **29**, 1527 (1964).

[11] W. E. Barber and P. W. Carr, *Anal. Chem.*, **53**, 1939 (1981).

[12] P. A. Bristow and J. H. Knox, *Chromatographia*, **10**, 279 (1977).

[13] R. W. A. Oliver and J. Sugden, *Chromatographia*, **12**, 620 (1979).

[14] L. Cotarcă, D. Ciubotariu, S. Holban and M. Cotarcă, *Rev. Chim.*, **36**(3), 252 (1985).

[15] L. R. Snyder and J. J. Kirkland, "Introduction to Modern Liquid Chromatography", 2nd ed., Wiley, New York, 1979, p. 28.

[16] L. R. Snyder , "Gradient Elution" in C. Horváth (ed.), "High-Performance Liquid Chromatography. Advances and Perspectives", vol. 1, Academic Press, New York, 1980, p. 208.

[17] J. E. Leffler and E. Grunwald, "Rates and Equilibria of Organic Reactions", Wiley, New York, 1963, p. 222.

Table 5

Structure-retention relationships for alkyl- and haloalkyl-1,3,5-triazines

Triazines	a_0	a_1	a_2	
2-Alkyl-4,6-bis(trichloromethyl)-1,3,5-triazines (compounds 1—4)	4.380	−1.210	−0.401	0.947
2,4,6-Haloalkyl-1,3,5-triazines (compounds 1,5—9)	−0.345	−0.0763	−0.180	0.970

tative analysis and resonable qualitative prediction of a variety of substituted 1,3,5-triazines. The identification of a particular compound by this method is very useful in the absence of a mass spectrometer.

REFERENCES

[1] H. Bărdoglu, N. Marin, L. Cotarcă, E. Iorga, A. Tărnăveanu, N. Pop, G. Istan and S. Rist, Rom. Pat. 76577 (1981).
[2] G. E. Parker, G. A. Hanley, D. J. Horvan and J. B. Hess, *J. Chromatogr.*, **242**, 247 (1982).
[3] "EPA Manual of Chemical Methods for Pesticides and Devices", Beltsville, 1983.
[4] E. Matisová and J. Krupčík, *J. Chromatogr.*, **142**, 597 (1977).
[5] W. P. Cochrane and R. Purkayastha, *Toxicol. Envir. Chem. Rev.*, **1**, 137 (1973).
[6] P. Dufek, V. Pacáková and E. Tesařová, *J. Chromatogr.*, **191**, 115 (1980).
[7] H. Jork and B. Roth, *J. Chromatogr.*, **144**, 39 (1977).
[8] E. Smolková Jr. and V. Pacáková, *Chromatographia*, **11**, 698 (1978).
[9] L. Cotarcă and H. Sacaloglu, *Bul. şt. şi tehnic al I. P. Timişoara*, **30** (44), 93 (1985).
[10] P. G. Schaffer and J. H. Ross, *J. Org. Chem.*, **29**, 1527 (1964).
[11] W. E. Barber and P. W. Carr, *Anal. Chem.*, **53**, 1939 (1981).
[12] P. A. Bristow and J. H. Knox, *Chromatographia*, **10**, 279 (1977).
[13] B. W. A. Oliver and J. Sugden, *Chromatographia*, **12**, 620 (1979).
[14] L. Cotarcă, O. Ghibotaşu, S. Holban and M. Cotarcă, *Rev. Chim.*, **36**(3), 232 (1985).
[15] L. R. Snyder and J. J. Kirkland, "Introduction to Modern Liquid Chromatography", 2nd ed., Wiley, New York, 1979, p. 28.
[16] L. R. Snyder, "Gradient Elution" in C. Horváth (ed.), "High-Performance Liquid Chromatography, Advances and Perspectives", vol. 1, Academic Press, New York, 1980, p. 208.
[17] J. E. Leffler and E. Grunwald, "Rates and Equilibria of Organic Reactions", Wiley, New York, 1963, p. 222.

Revue Roumaine de Chimie, **31**, *4*, 411–418 (1986)

STUDIES ON 4-ALKYLPYRIDINES USABILITY FOR EXTRACTION OF Co(II), Ni(II), Cu(II), Zn(II) and Cd(II) COMPLEXES FROM NITRATE SOLUTIONS

E. BEZAK
Institute of Chemistry, Pedagogical University, 25–020 Kielce, Poland

Received January 21 1984
Revised October 4, 1985

The extraction of the Co(II), Ni(II), Cu(II), Zn(II) and Cd(II) complexes pf 4-alkylpyridines with several solvents has been studied. The extraction percent E, and partition coefficients D, characterizing the extraction, have been shown to correlate well with the formatipn degrees α_n, of the same complexes. Based on the dependence $D = f(\alpha_n \nu)$, the distribution constants P_n of the successive complexes passing to the organic phase during extraction have been determined.

Nitrates of the following metals M : Ni(II), Zn(II), Cd(II), Co(II) and Cu(II) can coordinate pyridine bases in aqueous solutions with a formation of series of $[M/H_2O/_{6-n} L_n]$ — type complexes. The complexes are formed by a substitution of H_2O ligands within the coordination sphere of metal by pyridine base molecules.[1-3] An increase in the number of attached heterocyclic ligand is acompanied by the growth in complex ion size and by decrease of complex solubility in water. Consequently, a displacement of the complex from aqueous to organic phase should be facilitated during further extraction.[4]

The extraction of the above mentioned metal complexes with 4-methyl- or -4-ethylpyridine has been described in our previous articles.[5,6] The purpose of this study is to discuss the details of extraction course if 4-butylpyridine is used as a ligand in $[M/H_2O/_{6-n} L_n]$— type complexes. The selection of 4-butylpyridine has been done in order to understand better the role which a large hydrophobic substituent, bounded in position 4 of pyridine ring, can play in the extractability of the complex by the substituent influence on the number of extractable complexes and the values of their individual distribution constants P_n.

EXPERIMENTAL

Both reagent preparation and extraction procedure were identical to those described elsewhere.[5,7]

Before an organic phase was added, aqueous phase had contained the following amounts of p.a. reagents in 1 dm^3 of the solution :

corresppnding metal nitrate —0.02 mole
nitric acid — 0.025 mole
potassium nitrate in sufficient amuont to fix the ionic strength equal to 0.5

Organic phase was comppsed of 4-butylpyridine dissplved either in 2-butanol pr 2-pentanol. Cyclohexanol had been also used as solvent of pyridine base when the extraction of Cp(II)—complexes was to be examined.

RESULTS AND DISCUSSION

Extraction process was quantitatively characterized by the utilization of two previously defined [5] quantities : partition coefficient D and extraction percentage E. The values of both quantities, corresponding to a given concentration of 4-butylpyridine, were calculated from the experimental data. The free base concentration $[L]$ was calculated from the equation :

$$[L] = \frac{K_a\, C_{\mathrm{HNO_3}}}{[\mathrm{H}^+]}$$

where $C_{\mathrm{HNO_3}}$ and $[\mathrm{H}^+]$ are the concentrations of nitric acid and hydrogen ion, respectively, and K_a is the dissociation constant of the con'ugate acid of pyridine derivative.

Non-thermodynamic dissociation constant K_a has been expressed by concentrations rather than activities, so that its value had to depend on acid-base concentrations in considered $4.2 + 6.0$ pH range, as is seen from Fig. 1. This diagram was then used for K_a estimation after prior measurement of pH value in the solution investigated.

The $D = f(\mathrm{pH})$ functions for all systems studied are shown in Fig. 2. All the curves but those corresponding to Zn(II) complexes exhibit a rapid growth of distribution constants as pH is raised. Such a shape of curves is understandable in the light of the fact that an increase in the pH value in aqueous phase is accompanied by an increase in the concentration of free 4-butylpyridine, and this is tantamount to the growth of concentration of extractable complexes.

A dissimilar shape of extraction curves for Zn(II) — 4-butylpyridine — solvent system is probably conditioned by further detailed differences in the mechanism of Zn(II) — complexes extraction.

The correlations $E = f([L])$, for two choice system shown in Figs. 3, 4, has been presented together with the diagrams of the degrees α_n of successive complex formation.

The α_n is defined as :

$$\alpha_n = \frac{\beta_n\,[L]^n}{\sum\limits_{n=0}^{n=N} \beta_n [L^n]}$$

The values of cumulative stability constants β_n, required for α_n calculation, were taken from Ref. [8].

The diagrams illustrating the extraction of copper, cobalt and nickel complexes exhibit that an explicit correlation exists between extraction percent values and the values of free ligand concentration in aqueous phase. Additionally, these plots resemble to some extent the diagrams of the degree of the successive complexes. This is particularly noticeable for Cu(II) complexes extraction diagrams, in which the curves corresponding to the both used alcohols (2-butanol and 2-pentanol) run closely and are very similar in shape to the curve representing the degree of formation complexes α_2. One may hence conclude that copper complexes containg two coordinated 4-butylpyridine molecules have passed to the organic phase.

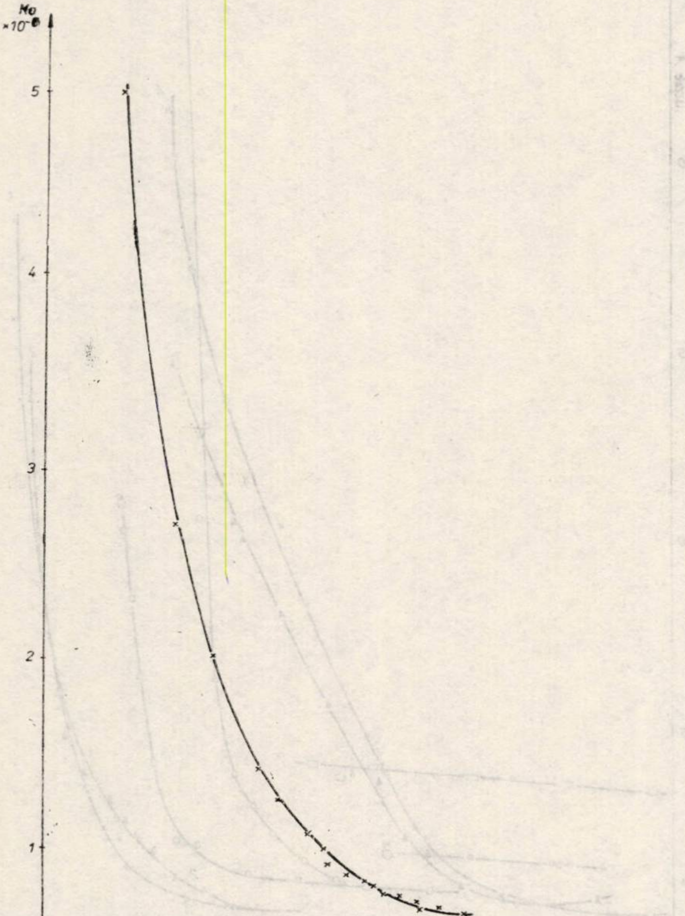

Fig. 1. — Dissociation constant of the conjugate acid of 4-butylpyridine as a function of pH.

The $E = f([L])$ function for Zn(II) complexes is unlike in shape to the functions of other considered complexes, being a straight line almost parallel to the free ligand concentration axis; this reveals that Zn^{2+} ion

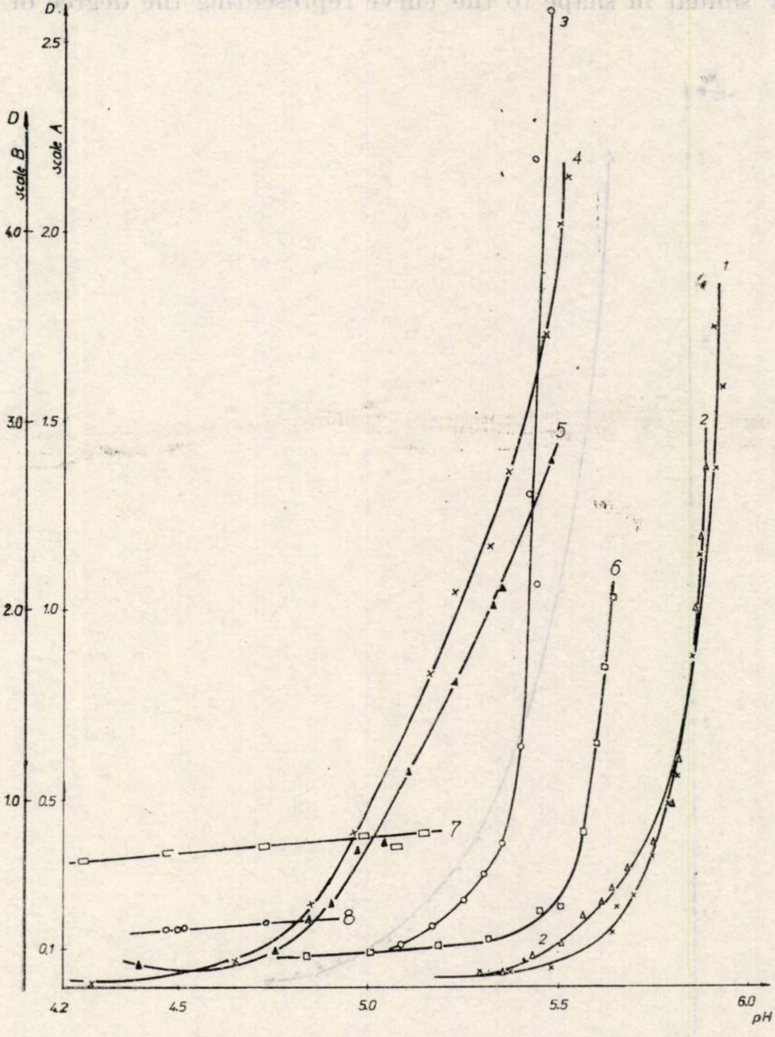

Fig. 2. — Plots of the function $D = f(\text{pH})$. Scale A : *1* — Cd(II) — 4-butylpyridine — 2-butanol; *2* — Co(II) — 4-butylpyridine — cyclohexanol; *3* — Ni(II) — 4-butylpyridine — 2-pentanol. Scale B : *4* — **Cu(II)** — 4-butylpyridine — 2-pentanol; *5* — Ni(II) — 4-butylpyridine — 2-butanol, curves; *6* — Zn(II) — 4-butylpyridine — 2-butanol; *7* — Zn(II) — 4-butylpyridine — 2-pentanol; *8* — Cu(II) — 4-butylpyridine — 2-butanol.

displacement to the organic phase is independent of pyridine base concentration. Because of small values of stability constants $\beta_n(\beta_1 = 25{,}1;\ \beta_2 = 600)$, the complexes: Zn(II) — alcohol, compete with the complexes: Zn(II) — 4-butylpyridine, perhaps due to greater stability of the former ones. Metal ion and oxonium extractant concentrations, which were maintained constant at considered conditions, would decide then for the extraction yield.

The next task of this work was to determine the composition of the complexes that are able to pass from aqueous to organic phase. In order

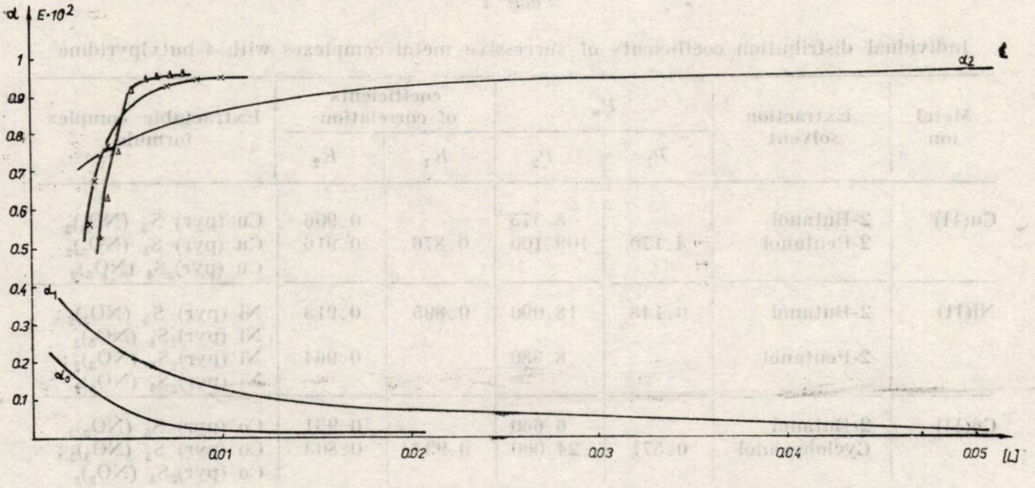

Fig. 3. — $E = f(L)$ in the system Cu(II) — 4-butylpyridine together with the degrees of fprmation α_0, α_1, α_2 pf successive complexes. ××× — 2-butanol; ΔΔΔ — 2-pentanol.

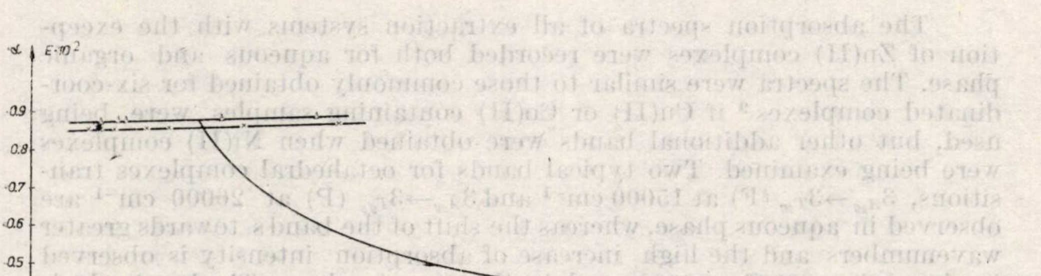

Fig. 4. — $E = f(L)$ in the system Zn(II) — 4-butylpyridine together with the degrees of formation α_0, α_1, α_2 of successive complexes. ××× — 2-pentanol; ΔΔΔ — 2-butanol.

to attain this goal the method of determination of individual distribution constants has been employed. It was based on the dependence $D = \alpha_1 P_1 + \alpha_2 P_2 + \ldots + \alpha_n P_n$; the computation details were previously described.[5] The series of P_n values counted in this way are listed in Table 1 which indexes individual distribution coefficients given for the number of molecules of 4-butylpyridine in complex which undergoes extraction. In relation to system under consideration, the complex containing both 1 and 2 of 4-butylpyridine molecules, will be extractable.

Table 1

Individual distribution coefficients of successive metal complexes with 4-butylpyridine

Metal ion	Extraction solvent	P_n		coefficients of correlation		Extractable complex formula
		P_1	P_2	K_1	K_2	
Cu(II)	2-Butanol		5.375		0.906	Cu (pyr) S_5 $(NO_3)_2$
	2-Pentanol	4.170	109.100	0.876	0.916	Cu (pyr) S_5 $(NO_3)_2$ Cu $(pyr)_2S_4$ $(NO_3)_2$
Ni(II)	2-Butanol	0.148	18.090	0.895	0.913	Ni (pyr) S_5 $(NO_3)_2$; Ni $(pyr)_2S_4$ $(NO_3)_2$
	2-Pentanol		8.880		0.964	Ni $(pyr)_2S_4$ $(NO_3)_2$; Ni $(pyr)_2S_4$ $(NO_3)_2$
Co(II)	2-Butanol		6.660		0.931	Co (pyr) S_5 $(NO_3)_2$
	Cyclohexanol	0.571	24.000	0.934	0.803	Co (pyr) S_5 $(NO_3)_2$; Co $(pyr)_2S_4$ $(NO_3)_2$

Abbreviation : pyr = 4-butylpyridine

The absorption spectra of all extraction systems with the exception of Zn(II) complexes were recorded both for aqueous and organic phase. The spectra were similar to those commonly obtained for six-coordinated complexes [9] if Cu(II) or Co(II) containing samples were being used, but other additional bands were obtained when Ni(II) complexes were being examined. Two typical bands for octahedral complexes transitions, $3_{A_{2g}} \to 3_{T_{2g}}$ (F) at 15000 cm^{-1} and $3_{A_{2g}} \to 3_{T_{g_2}}$ (P) at 26000 cm^{-1} are observed in aqueous phase, whereas the shift of the bands towards greater wavenumbers and the high increase of absorption intensity is observed in the region 20000±22000 cm^{-1} in the organic phase. The band which is known as characteristic for four-coordinated Ni(II) complexes appears in this wavenumber region.[10,11] The obtained absorption band shape suggests the presence of both six-coordinated and four-coordinated complexes in organic phase. Taking into account, on the basis of absorption spectra, either six-coordinated or four-coordinated structure of metal sphere, and including into considerations the fact of partial replacement of H_2O within the sphere by heterocyclic ligand or solvent molecule, the probable composition of extractable complexes could be established (Table 1). For the Ni(II) complexes, where configurational octahedron-suare or octahedron-tetrahedron equilibrium can be readily established in organic phase, the two formulas for both complexes, expected to exist in organic phase, have been given.

The comparison of stability constant values for 4-methyl, 4-ethyl-[8] and 4-butyl-pyridine complexes of considered metals allows to state that an increase in size of the substituent attached to pyridine ring is accompanied by the decreasing number of the complexes formed. Free ligand concentration in aqueous solution can be so high, if easily soluble pyridine derivatives are used, that this enables the formation of four successive complexes. For example, four complexes described by β_1, β_2, β_3 and β_4 constants appear in Cu(II) — 4-methyl-pyridine solution. Only two of the successive complexes are present, however, in Cu(II) — 4-butylpyridine solutions on account of lower solubility of the heterocyclic base in water. The numbers and the structure of these coordinated compounds which are present in aqueous phase explicitly affect the extraction, or to be more exact, the composition of extractable complexes.

When to extract 4-methylpyridine complexes, the prevailing complexes in organic phase are those with three or four pyridine ligands (Table 2). If the extraction of 4-ethylpyridine complexes was performed all complexes with 1, 2, 3 or 4 organic ligands coexisted in organic solvent On the other hand, the displacement of only two first successive complex. es, characterized by P_1 and P_2, e.g. containing one and two molecules of organic base, has been observed when the M — 4-butylpyridine system was examined (Table 3).

Table 2

Selected P_n values for various ligands

Metal ion	Extraction solvent	Ligand	Individual distribution coefficients			
			P_1	P_2	P_3	P_4
Cd(II)	Cyclohexanol	4-Methylpyridine	—	—	13.80	8.82
Co(II)	2-Pentanol	4-Ethylpyridine	43.50	2.50	—	—
Ni(II)	2-Pentanol	4-Ethylpyridine	—	—	85.70	—
Ni(II)	Cyclohexanol	4-Butylpyridine	0.571	24.00	—	—

Table 3

Selected stability constants for Ni(II) complexes with different ligands

Metal ion	Ligand	1	2	3
Ni(II)	4-Methylpyridine	130.0	6600	64600
Ni(II)	4-Ethylpyridine	81.3	2190	10500
Ni(II)	4-Butylpyridine	95.5	8710	—

Thus, the conclusion can be drawn from the above considerations that under established equilibrium between aqueous and organic phases, these complexes exist in organic phase which were previously existing (even if their concentration was negligible) in aqueous phase.

REFERENCES

[1] M. S. Sun. and D. G. Brever, *Can. J. Chem.*, **45**, 2729 (1967).
[2] B. Lenarcik and Z. Warnke, *Rocz. Chem.*, **43**, 457 (1969).
[3] B. Lenarcik and M. Rzepka, *Pol. J. Chem.*, **52**, 447 (1978).
[4] Jeżowska-Trzebiatowska, S. Kcpacz and T. Mikulski, *Pierwiastki rzadkie*, *PWN*, *1976*, 119.
[5] B. Lenarcik and E. Bezak, *Sep. Sci. Techn.*, **16**, 505 (1981).
[6] E. Bezak and B. Lenarcik, *Pol. J. Chem*, in press.
[7] B. Lenarcik and E. Bezak, *Rev. Roumaine Chim.*, **26**, 229 (1981).
[8] B. Lenarcik and M. Rzepka, *Pol. J. Chem.*, (in press).
[9] Jörgensen "Absorption Spectra and Chemical Bonding in Complexes", Pergamon Press, 1962
[10] H. B. Gray and C. J. Ballhausen ; *J. Am. Chem. Soc.*, **85**, 260 (1963).
[11] D. M. L. Goodgame, J. Am. Chem. Soc., **83**, 4161, (1961).

Revue Roumaine de Chimie, 31, 4, 419—424 (1986)

SYNTHETIC ZEOLITES FOR DETERGENT CONDITIONING. II

ON ZEOLITE – SURFACTANT – BLEACHING AGENT SYSTEMS

EVELINE POPOVICI, MIHAI CRUCEANU, MIHAELA GRECU *, AURELIA VASILE
and MARIA ALEXANDROAEI

Department of Chemical Technology, Polytechnic Institute, Splai Bahlui, 71, Jassy, Romania, 6600

* ICECHIM, Bucharest, Splaiul Independenţei, 202, Romania, 77208

Received April 27, 1985

Taking into account the fact that, in detergents, zeolites act alongside of active substances and bleaching agents, this paper deals with the zeolite (ZPI—12 and HAB-A40)——bleaching agent (sodium percarbonate) and zeolite-surfactant systems (sodium alkylarylsulphonate, sulphated fatty alcohols, sulphated nonylphenol-ethoxylate with 8 moles ethylene oxide). The experimental results show that the employed surfactants exhibit a stabilizing action over zeolite suspension. Catalytic action of the iron ions over decomposition of bleaching agents depends on their concentration and location in zeolite structure or in washing liquor. The maximum admissible concentration of iron in zeolite, established experimentally is about 200 γ Fe/g.

INTRODUCTION

Production of laundry detergents in which tripolyphosphate is replaced partially with synthetic zeolites is an up-to-date problem that opens large possibilities in both manufacture and use of zeolites.[1-10] An important factor that makes zeolites to be utilized in laundry detergents is, besides their rapid kinetics and high ion exchange capacity against calcium, their resistance to the sedimentation in washing liquor during the washing cycle.[4,5,9]

Taking into account the fact that, in the detergency process, zeolites work together with surfactants and bleaching agents, the experiments to be discussed in this paper were especially designed to the problem of stability of several zeolite-surfactant and zeolite-bleaching agent systems.

Because on world market there are several types of zeolites proper for laundry detergents manufacture the results are presented comparatively with HAB–A40, Degussa product.

EXPERIMENTAL

The investigated zeolites are from both Degussa Company, HAB-A40 (17.71% Na_2O, 29.42% Al_2O_3, 35.61% SiO_2, 17.26% H_2O and 142 γ Fe/g) and Polytechnic Institute of Jassy, ZPI—12 (14.90% Na_2O, 26.46% Al_2O_3, 40.62% SiO_2, 18.00% H_2O and 59 γFe/g).

Systems were prepared by dispersing dry zeolites in aqueous surfactants solutions. The main surfactants studied are sodium alkyl (C_{15}—C_{18}) arylsulphonate (SAAS), fatty alcohols (C_{15}—C_{18}) sulphated (FAS) and nonylphenolethoxylated with 8 moles ethylene oxide (NF_8). Their concentration in the system ranged from 0.048 to 0.220 g/L and zeolite concentration in suspension was 2 g/L. Hardness of water was in between 0.00 and 33.6 degrees. In these systems the remnant hardness *versus* time was determined, concentration of calcium ions being determined complexometrically[9,12].

In order to determine the stability of dispersed zeolites in aqueous solutions of known hardness in the presence of different amounts of surfactant, nephelometrical measurements of suspension recording their transmittance against time of aging were performed.

Stability of sodium percarbonate in the presence of iron impurified zeolites and iron ions in washing water, at 22°C was studied. The content of sodium percarbonate was determined permanganometrically.[11] The content of iron ions in zeolites and washing waters colorimetrically with orthophenanthroline was determined.[12]

RESULTS AND DISCUSSION

Stability of zeolite dispersion, S, determined nephelometrically, was estimated quantitatively by reciprocal value of system transmittance and represented against aging time in Figures 1 and 2. The experimental

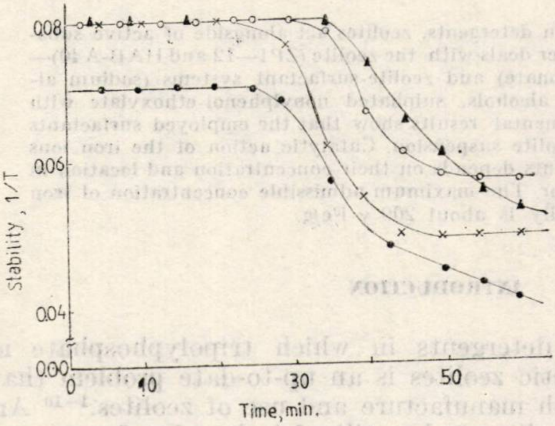

Fig. 1. — Stability of the HAB-A40 — hard water — surfactant systems against time. D_i = 16.0°G ; 2 g zeolite/L ; 0.048 g tensioactive substance/L ; ● HAB-A40 — hard water ; × HAB-A40 — hard water — SAAS ; ○HAB-A40 — hard water — FAS ; ▲HAB-A40 — hard water — NF_8.

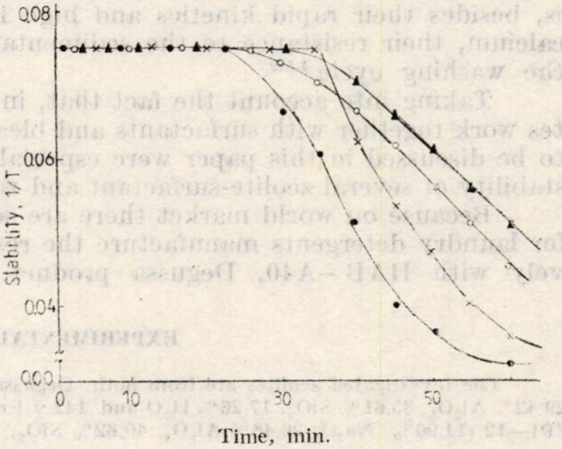

Fig. 2. — Stability of the ZPI—12 — hard water — surfactant systems against time. D_i= 16°G ; 2 g zeolite/L ; 0.048 g tensioactive substance/L ; ● ZPI—12 — hard water ; × ZPI—12 — hard water — SAAS ; ○ ZPI—12 — hard water — FAS ; ▲ ZPI—12 — hard water — NF_8.

data set out in Figures 1 and 2 show that, in the presence of surfactants, stability of system is much improved in comparison with its stability in hard water without surfactant. This phenomenon can be explained by interaction of submicellar or micellar associations, corresponding to operating critical micellar concentration [4,5] with hydroxylic groups preexistent or formed by hydrolysis on the surface of zeolite fine granules. In both cases, the stabilizing action of surfactants is situated in the order :

$$NF_8 > FAS > SAAS$$

Investigation of surfactant influence on separation of calcium ions in the zeolite-hard water and zeolite-hard water-surfactant systems exhibited a diminishing retention capacity against calcium ions, which also are situated in the order mentioned above (Figs. 3 and 4).

The phenomenon is due to the difficult mobility of exchanging ions in the presence of micellar associations which screen their access in and from cavities and to the negative influence of sodium ions which come from either surfactant hydrolysis or zeolite hydrolysis [9].

In laundry detergents a special importance has the possible presence of impurities, heavy metals ions, which influence stability of the products because cause catalytical decomposition of the bleaching agents (Fig. 5).

Curves *1* and *2* show the stability of sodium percarbonate in the presence of the ZPI—12 and HAB—A40 products with a content of 59 γFe/g and 142 γFe/g, respectively, added in washing liquor, corresponding to a concentration of 2 g/L.

Curves *3* and *4* were obtained for the same systems under the conditions in which in washing liquor was added an amount of 560 γFe/L, as $FeCl_3$ solution, thus reaching an overall concentration of 619, respectively 844 γ Fe/L.

It has been found that stability of sodium percarbonate decreases with increase of iron ions concentration, which is in good agreement with the data in literature.[8,9] A more satisfactory behaviour of ZPI—12 product comparatively with HAB—A40 one is noticed, showing at the same time a better agreement as regards the importance of zeolite products purity.

Curves *5* and *6* were obtained for the systems in which the increasing zeolite concentration, the same overall concentration of 844 γ Fe/L was realized by the entire amount of iron ions coming from the zeolite mass only. It was found a weaker decreasing effect over stability of bleaching agent studied, what shows that the influence of iron ions concentration must not be looked over only globally, but also taking into acount the localization of their ions in zeolite mass or in washing liquor. At the same overall concentration of iron ions (curves *4*, *5* and *6*) the decreasing effect of sodium percarbonate stability is stronger when the iron ions are brought by washing water, in comparison with the case in which the iron ions come from the zeolite mass. This fact comes to point out the role of diffusion process of iron ions from zeolite structure, over the percarbonate ion stability.

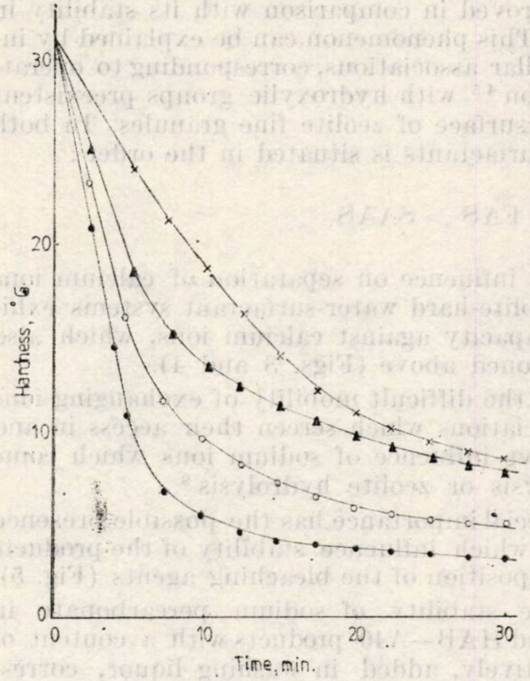

Fig. 3.—Variation of remanent hardness *versus* time; initial hardness — 33.6°G; 0.048 g tensioactive substance/L; t = = 22°C; ● ZPI—12 — hard water; ○ ZPI—12 — hard water — SAAS; ▲ ZPI—12 — hard water — FAS; × ZPI—12 — hard water — NF_8.

Fig. 4. — Variation of remanent hardness *versus* time; initial hardness = = 33.6°G; 0.048 g tensioactive substance/L; t = 22°C: ● HAB-A40 — — hard water; ○ HAB-A40 — hard water — SAAS; ▲ HAB-A40 — hard water — FAS; × HAB-A40 — hard water — NF_8.

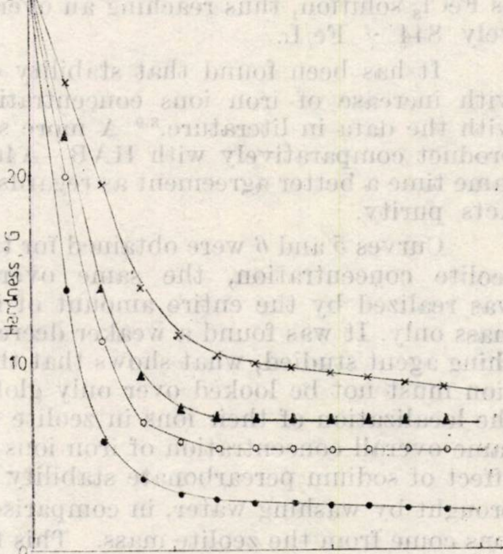

In order to evidence the limit concentration up to which, under the washing conditions at 22°C, the iron ions come from zeolite do not influence significantly the stability of bleaching agent, the dependence of this stability on iron ions concentration in zeolite was studied. As it comes out from Figure 6, the maximum limit of iron concentration in zeolite is about 200 γ Fe/g.

Fig. 5. — Stability of the sodium percarbonate in the zeolite-iron ions systems: *1* — ZPI — 12 ... 59 γ Fe/g; *2* — HAB-A40 ... 142 γ Fe/g; *3.* — ZPI—12 + $FeCl_3$sol ... 619 γ Fe/L; *4.* — HAB-A40 + $FeCl_3$sol. ... 844γ Fe/L; *5.* — ZPI—12 ... 844 γ Fe/L; *6.* — HAB-A40 ... 844 γFe/L.

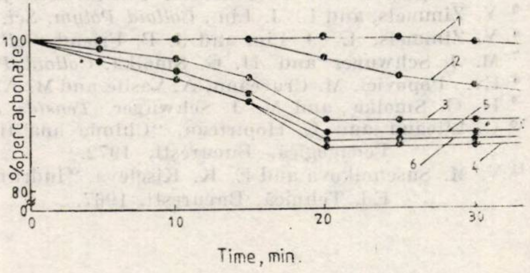

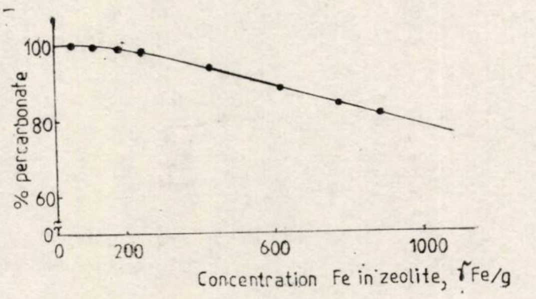

Fig. 6. — Stability of sodium percarbonate against concentration of iron ions in zeolite.

CONCLUSIONS

Study of the ZPI—12 — surfactant, HAB—A40 — surfactant and zeolite—sodium percarbonate systems presented above, led to the following conclusions:

1. The employed surfactants exhibit a stabilizing action on zeolite suspension situated in the order:

$$NF_8 > FAS > SAAS$$

2. The investigated surfactants diminish the retention capacity of zeolite against calcium ions from washing liquor, troubling their transport phenomenon, by access of screen effect in and from zeolite cavities;

3. Catalytic action of the iron ions on decomposition of sodium percarbonate depends on their concentration and initial location in zeolite structure or in washing liquor;

4. The maximum admissible concentration of iron ions in zeolite, established experimentally, is about 200 γ Fe/g.

REFERENCES

[1] M. Sittig, *Chemical Technology Review*, 129 (1979)

[2] P. Berth, *J. Am. Oil Chemist. Soc.*, **55**, 1 (1978).

[3] R. Despotovic and co., *Croat. Chem. Acta*, **48**, 683 (1976).

[4] R. Despotovic and Z. Grabaric, *Tenside Detergent.*, **8**, 313 (1971).

[5] Y. Zimmels, and L. J. Lin., *Colloid Polym. Sci.*, **252**, 594 (1974).

[6] Y. Zimmels, L. J. Lin, and J. P. Friend, *Colloid Polym. Sci.*, **253**, 404 (1975).

[7] M. J. Schwuger and H. G. Smolka, *Colloid Polym. Sci.*, **256**, 1014 (1978).

[8] Ev. Popovici, M. Cruceanu, A. Vasile and M. Alexandroaei, Buletin I.P. Jassy (in print.).

[9] H. G. Smolka and M. J. Schwuger, *Tenside Detergent.*, **14**, 222 (1977).

[10] C. Liteanu and E. Hopirtean, "Chimie analitică cantitativă. Volumetrie", Ed. Did. şi Pedagogică, Bucureşti, 1972.

[11] V. M. Susennikova and E. K. Kiseleva, "Îndrumător pentru prepararea soluţiilor titrate", Ed. Tehnică, Bucureşti, 1967.

Revue Roumaine de Chimie, **31**, *4*, **425**—429 (1986)

ACTIVITY AND SELECTIVITY OF NEODYMIUM EXCHANGED ZEOLITES IN THE ALKYLATION REACTION OF TOLUENE WITH METHANOL

SPIRIDON OPREA, EMIL DUMITRIU, VASILE HULEA and KAYED YOUSEF
Department of Organic Chemical Technology, Faculty of Chemical Technology, Jassy 6600, Romania

Received April 1, 1985

The alkylation reaction of toluene with methanol in the presence of HNdY zeolite was studied. The influence of the temperature, contact time, molar ratio of reagents and partial pressure of organic phase on the activity and selectivity was investigated. A correlation between the ionic radius of the cations from the lanthanum series and the selectivity increase was stated.

In a forthcoming period, the alkylation of toluene with methanol seems to be a valuable method for the production of xylenes. This assertion is based on the fact that methanol is an efficient alkylation agent, it is also relatively cheap as raw material, while the synthetic zeolites (especially the modified zeolites) have proved their catalytic properties for this reaction.

Though recently this way of toluene conversion has exhibited a real interest, however the data on the alkylation of toluene with methanol are relatively few.

Taking into account the data of literature [1-3] and our previously reported data [4-7] we conclude that the introduction of the rare earth cations, by ionic exchange, in the Y zeolites enhances the catalytic properties of zeolites. Starting from this point of view we studied here the catalytic properties of neodymium exchanged zeolite (HNdY) and, on the other hand, we tried to establish a correlation between the nature of exchanged cations (from the lanthanum series) and the catalytic properties.

EXPERIMENTAL

Reagents. Methanol and toluene were purified by the common methods.

Catalyst. The catalyst was prepared on the basis of NaY zeolite (LZ-Y52 extrudates, VENTRON) which had the following characteristics: 66.5 % SiO_2, 20.8 % Al_2O_3, 10.4 %Na_2O, 0.23 % Fe_2O_3 and 0.33 % CaO (by weight); specific area is about 800 m^2g^{-1}, the grain dimensions are 1.5 × 1—2 mm. NaY zeolite was firstly subjected to a partial exchange with NH_4NO_3 when about 52 % Na^+ ions were substituted by NH_4^+. Then NH_4NaY was calcinated in a dry air stream at 500°C obtaining the deaminated form HNaY. The next stage was another ionic exchange with $Nd(NO_3)_3$ when 38 % from residual natrium ions were substituted by Nd^{3+} ions. The final product HNdY was checked in respect of its crystallinity and this was kept unchanged during the treatment.

Apparatus and procedure. The experiments were carried out on an integral fixed-bed reactor isothermal operated at the atmospheric pressure. The reagents were fed at constant rate by means of a calibrated syringe pump. Nitrogen was used as carrier gas and diluent. The reaction product was collected into a cooled trap (—30°C).

Analysis. The condensable products were analysed on a GC using a column with bentone 34 and dinonyl phthalate on Chromosorb W.

RESULTS AND DISCUSSION

As above mentioned, the choice of HNdY as catalyst for toluene alkylation was made on the basis of the results obtained when modified zeolites with La^{3+}, Ce^{3+} and Pr^{3+} were used. This study comes to complete the earlier investigations on the zeolites exchanged with cations from the lanthanum series and, at the same time, it allows a correlation of the catalytic properties with the ionic radius of the exchanged cations.

At the beginning we studied the influence of temperature on the alkylation process. The experiments were carried out in the temperature range between 250—450°C and at a mole ratio of reagents of 1/1. Figure 1 shows that as the temperature rises the conversion of reagents to xylenes and trimethylbenzenes is also increased. An interesting aspect consists in the analysis of the reaction product distribution, see Figure 2, when a certain selectivity for *p*-xylene can be observed. It should be noticed that it is for the first time when such a selectivity for the *para* isomer is observed, for a large range of temperature, in the series of the zeolite catalysts modified with lanthanides.

The fact that the proportion of *m*-xylene increases at the same time with temperature, whereas the *p*-xylene content diminishess, is not a proof of the selectivity decrease but an increase of the isomerization reaction of *p*-xylene to *m*-xylene occurs. This was experimentally proved when, in the same reaction conditions, the pure *p*-xylene was fed (see Figure 3).

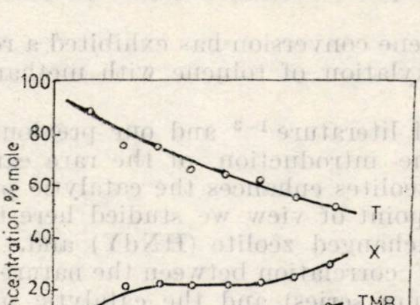

Fig. 1. — The distribution of reaction products *vs.* temperature; $W/F = 40$ g.h.mol^{-1}, T/MeOH = = 1 /1 (mole). $N_2/F = 5/1$; T = toluene; X = xylene; TMB = trimethylbenzene.

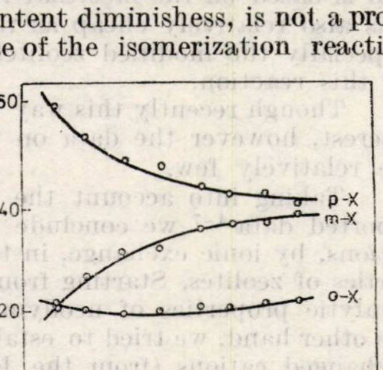

Fig. 2. — The influence of temperature on the distribution of xylenes.

From these data results that the electrophile attack to the aromatic ring occurs rather in the *para* position than at the *ortho* position and the *meta* isomer results from the isomerization reaction occurring subsequently or simultaneously. Moreover, from the graphs of selectivity *vs.* time factor (Figure 4) we can observe that at short contact times, *p*-xylene is mainly obtained but as the contact time is increased the *p*-xylene isomerization to *m*-xylene is favoured. It can be also mentioned that according to our expectations, the contact time rise is accompanied by a significant increase of the reagents conversion.

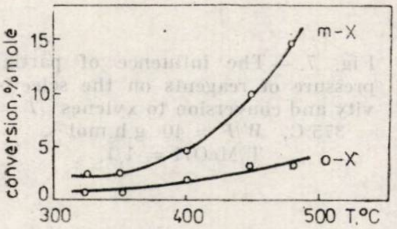

Fig. 3. — The influence of temperature on the *p*-xylene isomerization to *m*- and *o*-xylene.

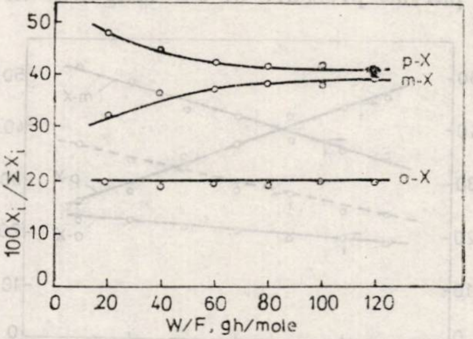

Fig. 4. — The influence of contact time on the selectivity with respect to *p*-xylene; $T = 375°C$.

One of the most important secondary reactions, which is strongly affected by the temperature and contact time rising, consists in the subsequent alkylation of toluene to trimethylbenzene. An interesting aspect can be pointed out whether the distribution of C_9 hydrocarbons is analysed.

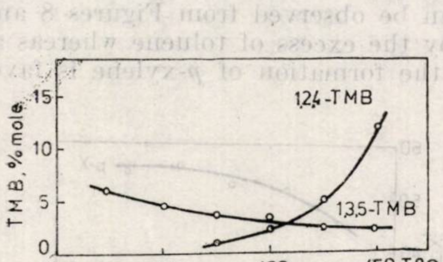

Fig. 5. — The distribution of trimethylbenzenes *vs.* reaction temperature.

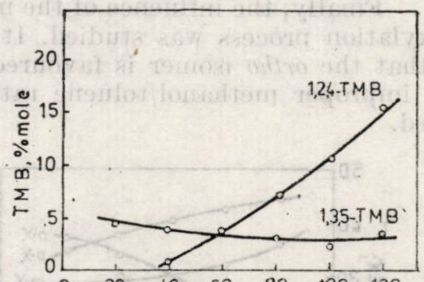

Fig. 6. — The distribution of trimethylbenzenes *vs.* contact time, $T = 375°C$.

As it is observed from Figures 5 and 6 the amount of 1,2,4-trimethylbenzene is increased as the temperature and contact time rise, whereas the amount of 1,3,5-trimethylbenzene is decreased. If these data are correlated with those obtained from the thermodynamic calculations, when an increase of the equilibrium constant for 1,3,5-trimethylbenzene to 1,2,4-trimethylbenzene isomerization reaction is observed, [8] we can assert that, though from the point of view of the electronic density the alkylation of toluene at 3,5 position is not favoured, however from the steric reasons, 1,3,5-trimethylbenzene is mainly formed during the subsequent alkylation and this can isomerise to 1,2,4-trimethylbenzene in the favourable reaction conditions.

As it was already shown, all experiments were performed using nitrogen as diluent and carrier gas. Therefore the problem of the influence of partial pressure of the reagents on the alkylation process appears.

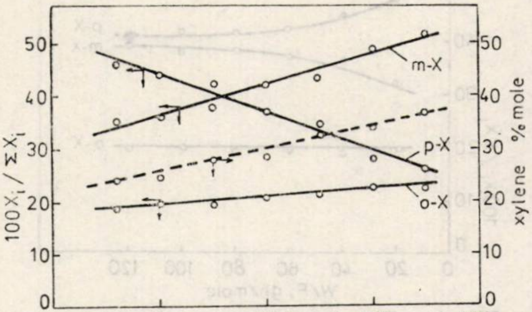

Fig. 7. — The influence of partial pressure of reagents on the selectivity and conversion to xylenes; $T = 375°C$, $W/F = 40$ g.h.mol^{-1}, T/MeOH = 1/1.

The experimental data from Figure 7 show, on the one hand, that the conversion increases as the partial pressure of reagents is increased (the dotted line), but, on the other hand, the distribution of xylenes is significantly affected by this parameter. One can observe that the proportion of *m*-xylene is considerably increased as the partial pressure of the organic phase is risen whereas the content of *p*-xylene in the reaction mixture is decreased.

Finally, the influence of the molar ratio between the reagents on the alkylation process was studied. It can be observed from Figures 8 and 9 that the *ortho* isomer is favoured by the excess of toluene whereas at an improper methanol/toluene ratio the formation of *p*-xylene is favoured.

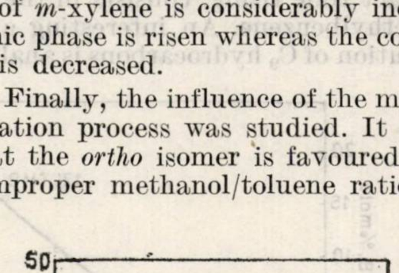

Fig. 8. — The influence of mole ratio of the reagents on the selectivity; T/MeOH ⩾ 1.

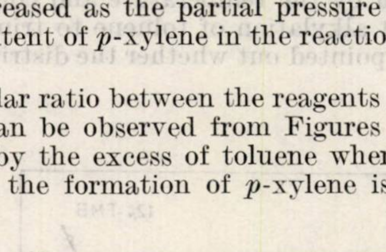

Fig. 9. — The influence of mole ratio of the reagents on the selectivity; MeOH/T ⩾ 1.

Taking into account the above data we can conclude that HNdY zeolite has a good activity for the catalytic alkylation of toluene with methanol and this catalyst exhibits a considerable selectivity for *p*-xylene. On the basis of this study and those previously reported, two aspects of the catalytic properties of the rare earth exchanged zeolites can be emphasized :

(1) — the activity of the catalysts decreases as follows :

$$\text{HLaY} > \text{HCeY} > \text{HPrY} > \text{HNdY}$$

(2) — the selectivity with respect to the *p*-xylene increases as the ionic radius of the cations is increased :

$$\text{Nd}^{3+} > \text{Pr}^{3+} > \text{Ce}^{3+} > \text{La}^{3+}$$

The last conclusion can be correlated with the volume modifications which occur in the zeolite supercavities when Na^+ cations are replaced by the rare earth cations. The modifications in the distribution of the electric charges can be also taken into account.

REFERENCES

[1] T. Yashima, H. Ahmed, K. Yamazaki, M. Katsuta and N. Hara, *J. Catalysis*, **16**, 273 (1970).

[2] S. Zielinski and Z. Sarbok, *Reac. Kinet. Catal. Lett.*, **16**, 119 (1981).

[3] K. J. Parasiewicz, *Przem. Chem.*, **221**, 197 (1977).

[4] K. Yousef, Sp. Oprea and Em. Dumitriu, Symposium "Scientific Contributions in Chemistry", Cluj-Napoca, 1982, p. 108.

[5] K. Yousef, Sp. Oprea and Em. Dumitriu, *Rev. Chim. (București)*, **35**, 906 (1984).

[6] Em. Dumitriu, Sp. Oprea and K. Yousef, *Rev. Chim. (București)*, **36**, 29 (1985).

[7] K. Yousef, Sp. Oprea and Em. Dumitriu, Symposium "Zeolits in Modern Technology", Jassy, 1983, p. 272.

[8] K. Yousef, Dissertation. Polytechnic Institute of Jassy, 1985.

Revue Roumaine de Chimie, 31, 4, 431–442 (1986)

ELECTROCHEMICAL REACTIONS OF CUPRIC AND CUPREOUS IONS IN LITHIUM CHLORIDE - POTASSIUM CHLORIDE EUTECTIC. III[1]

CYCLIC VOLTAMMETRY

S. STERNBERG, T. VIȘAN, VALERIA PETRESCU and ADINA COTÂRȚĂ *

Laboratory for Applied Physical Chemistry, Faculty of Chemical Technology, The Polytechnic, Bucharest, Romania

* Institute of Chemical and Biochemical Energetics, Bucharest, Romania

Received April 1, 1985

Cyclic voltammetric measurements were performed in LiCl—KCl—$CuCl_2$—CuCl melts at 500°C using a graphite electrode. Voltammograms recorded at different scan rates have a symmetric shape owing to the cathodic reduction of Cu^{2+} and anodic oxidation of Cu^+ ion. The deposition and dissolution of metallic copper were also studied. It is shown that the redox Cu^{2+}/Cu^+ couple was mainly controlled by diffusion. However, the peak separations ΔE_p, measured on cyclovoltammograms were used to estimate standard rate constant, k°; the exchange currents are also determined.

INTRODUCTION

In course of investigating the possibility of the implementation of high-capacity molten salt batteries based on redox couple Cu^{2+}/Cu^+, we have recently made a comprehensive study of LiCl–KCl–$CuCl_2$–CuCl systems by galvanostatic [2] and steady-state potentiostatic [1] techniques. These studies have pointed out that in molten LiCl–KCl eutectic containing both copper ions, two consecutive processes corresponding to $Cu^{2+} \rightarrow Cu^+ \rightarrow Cu$ reduction are observed at cathodic polarization. At anodic polarization in the same melt, the $Cu^+ \rightarrow Cu^{2+}$ oxidation and chlorine evolution appear as two distinct processes. We mention that Timchenko et al.[3] have also confirmed the existence of two successive cathodic steps of cupric ion reduction in molten alkali halides.

In this paper we present the results of cyclic voltammetry measurements in LiCl–KCl–$CuCl_2$–CuCl melts; cyclic voltammetry was chosen as experimental technique, since it was conveniently used to investigate the redox couples and to estimate the diffusion coefficients as well as the kinetic parameters. This technique has not yet been employed for the study of Cu^{2+}/Cu^+ redox couple in chloride melts.

Earlier method of "oscillographic polarography" has been exclusively applied to determine the diffusion coefficient of Cu^+ ion; thus, the value obtained by Schmidt[4] was $D_{Cu^+} = 4.3 \times 10^{-5}$ cm²/s in LiCl-KCl eutectic at 450°C, whereas Naryshkin and co-workers [5-7] studied the Cu^+/Cu reduction at Pt microelectrodes in NaCl—KCl [5] and LiCl—KCl [6] melts. Furthermore, the latter workers used the oscillopolarographic method to study the temperature dependence of D_{Cu^+} in LiCl—KCl.[7] We have recently employed the cyclic voltammetry technique in dilute molten systems LiCl—KCl—$CuCl_2$ and LiCl—KCl—CuCl using metallic (Pt and W) electrodes. [8]

EXPERIMENTAL TECHNIQUE

A detailed description of solutions preparation and of electrochemical cell has been reported elsewhere.[1,2] Table 1 shows the systems investigated in this work, with cupric and cupreous ions in an equimolecular ratio. Firstly, either Cu^{2+} or Cu^+ ion was introduced in the eutectic melt (see also Table 1).

Table 1

The composition of molten systems investigated by cyclic voltammetry (t = 500°C)

System	$c_{CuCl_2} \times 10^5$, mol/cm^3	$c_{CuCl} \times 10^5$, mol/cm^3	Electrode
initial solution	—	8.57	graphite
system (A)	8.38	8.57	graphite, Pt
initial solution	—	16.9	graphite
system (B)	16.57	16.9	graphite
initial solution	32.3	—	graphite
system (C)	32.3	32.3	graphite, Pt
system (D)	61.9	59.4	graphite
initial solution	—	76.02	graphite
system (E)	75.0	76.02	graphite
system (F)	88.9	88.8	graphite

The working electrode was made of spectral graphite with a 0.25 cm^2 constant surface area; regeneration of its surface was achieved by repolishing. Some experiments were carried out using Pt electrode as working electrode. The counterelectrode was a carbon rod with a large surface area. The reference compartment contained a 0.1 mol/kg solution of AgCl in LiCl-KCl eutectic; the reference electrode was a silver wire immersed in this melt and all potential values are quoted relative to Ag/Ag^+ (0.1 M) electrode.

Cyclic voltammetry measurements were performed with a P.A.R. Model 173 potentiostat/galvanostat connected to a low frequency triangular pulse generator; voltammetric curves were recorded on an XY recorder. Potential scan rates were within the range 0.01—0.5 V/s. All experiments were carried out at constant temperature of 500°C.

RESULTS AND DISCUSSION

The electrode processes which appear in our experiments are depicted schematically in the voltammogram of Figure 1. It is remarked the difference of about 1 V between the electrochemical couples Cu^{2+}/Cu^+ and Cu^+/Cu as well as the vicinity and thus the possible superposition of Cu^+ ion oxidation and chlorine evolution processes. A cyclovoltammogram yielded in the base electrolyte (LiCl-KCl eutectic melt) shows only the existence of lithium deposition at very negative potentials beginning from about -2 V and the evolution of chlorine gas at more $+1$ V anodic potentials (dashed line in Fig. 1). The background current on graphite electrode was < 1 mA in the potential range -2 V to $+1$ V, at 0.5V/s scan rate.

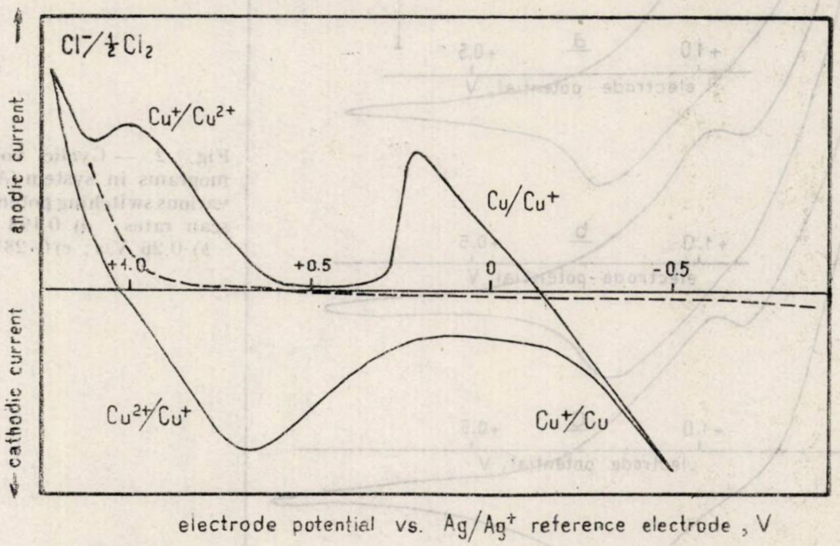

Fig. 1. — Schematical representation of all involved processes on graphite electrode: solid line — LiCl—KCl—$CuCl_2$—CuCl systems; dashed line — LiCl—KCl background electrolyte.

As can be seen in the following, the main attention in this paper is given to redox electrochemical process, described by the equilibrium

$$Cu^{2+} + e \rightleftharpoons Cu^+ \qquad (1)$$

Cyclic voltammograms were recorded for each solution presented in Table 1 at different potential scan rates.

In Figures 2 *a-c* are successively shown some voltammograms obtained in dilute system (A), by extending the potential range in anodic direction. Firstly, the existence of a redox couple is clearly shown in Fig. 2-*a*; the $i - E$ curve is plotted for a cycle beginning with a cathodic polarization followed by an anodic polarization. The cathodic peak which appears at *cca* $+0.75 \div +0.8$ V is assigned to the reduction reaction of equilibrium (1). Along the anodic half-cycle, a smooth peak is obtained within the potential region $+1 \div +1.2$ V, corresponding to Cu^+/Cu^{2+} oxidation reaction. At more positive potentials (Figs. 2-*b* and 2-*c*) one observes a subsequent increase of the current due to the evolution of chlorine on graphite surface. It is also observed that the position and the peak currents of Cu^{2+}/Cu^+ redox process remained unchanged in all voltammograms from Figures 2.*a-c*.

Figure 3 shows the multi-sweep voltammograms obtained in system (B). After continuous cycling a steady-state situation is achieved, in which further potential cycling resulted in superposed traces (for exam-

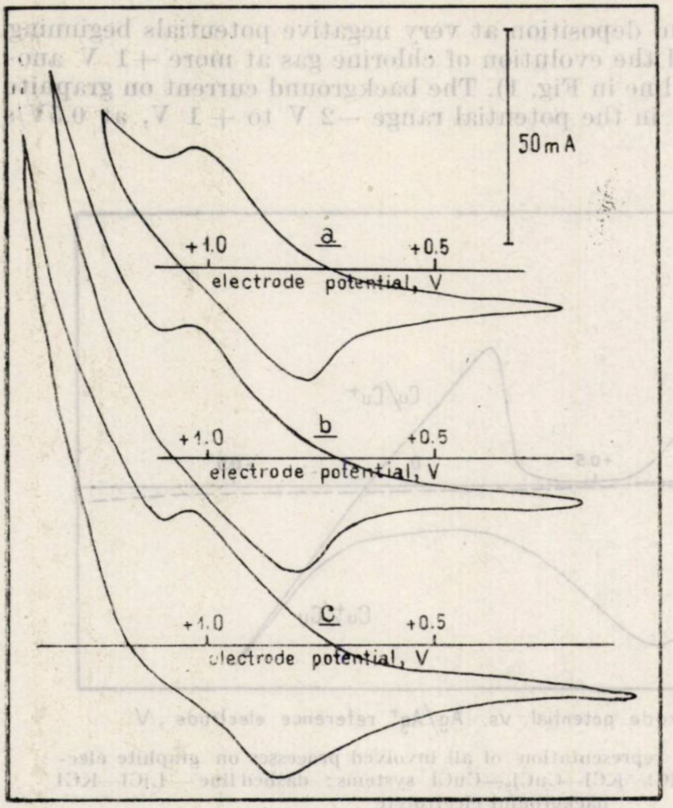

Fig. 2. — Cyclic voltammograms in system (A) for various switching potentials; scan rates: *a*) 0.198 V/s; *b*) 0.26 V/s; *c*) 0·28V/s.

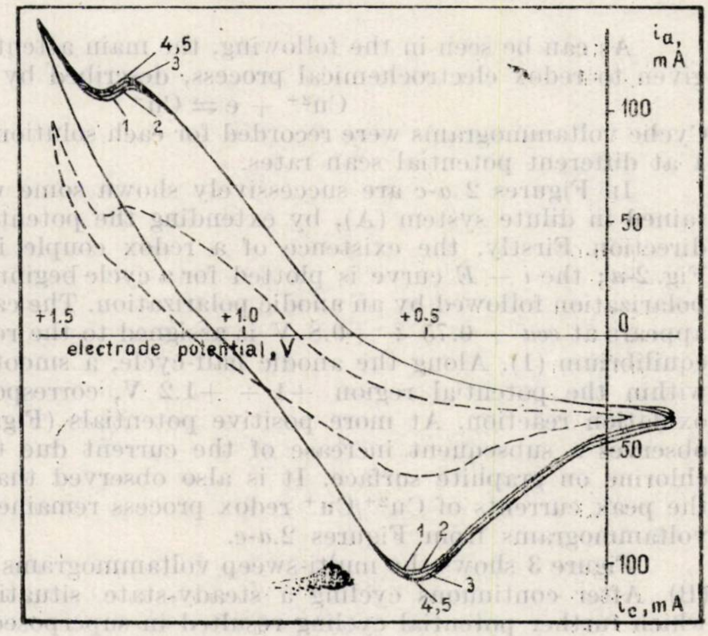

Fig. 3.—Progressive cyclic voltammograms in system (*B*) at 0.228 V/s scan rate. The numbers indicate the cycles. Dashed lines — LiCl — KCl—CuCl partial solution(B) at v=0.228 V/s.

ple the cycles 4,5 . .). In this system the anodic process is more clearly outlined than in the case of solution (A). In comparison with the voltammogram for LiCl—KCl—CuCl partial system, also presented in Fig. 3 (dashed line), the addition of Cu^{2+} ion resulting from solution (B), increases substantially both cathodic and anodic currents, the scan-rates being approximately equal.

Figure 4 illustrates the effect of varying scan-rate for the same concentration of copper ions (system B). It is known that the relevant quantities to be measured from each voltammogram are the peak currents (i_{p_c} and i_{p_a}, respectively) and the separation in peak potentials, $\Delta E_p = E_{p_a} - E_{p_c}$. The properties of such voltammograms from Fig. 4 can be summarized as follows : a) the ratio i_{p_c}/i_{p_a} is nearly unity and i_{p_c}, i_{p_a} values increase as potential scan-rate, v, increases ; b) E_{p_c} potential becomes more cathodic and E_{p_a} potential more anodic, that is the difference ΔE_p increases.

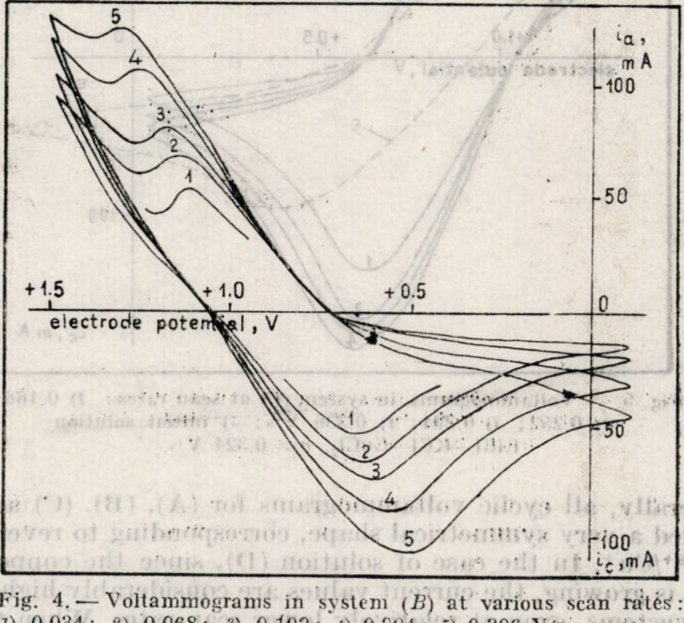

Fig. 4. — Voltammograms in system (B) at various scan rates: 1) 0.034; 2) 0.068; 3) 0.102; 4) 0.204; 5) 0.306 V/s.

Figure 5 clearly shows the modification which was produced between voltammograms of system (C) and those of the initial system LiCl—KCl—$CuCl_2$ from Table 1. For comparison, curves *4* and *5* in this Figure are necessary to be examined, both recorded at approximately equal scan-rates. In the case of partial solution LiCl—KCl—$CuCl_2$ (curve *5*) the oxidation reaction $Cu^+ \rightarrow Cu^{2+}$ has a slightly outlined peak, in fact only a shoulder. That seems to be naturally explained by the existence of a very low concentration of cupreous ion, resulting from the disproportionation reaction :

$$CuCl_2 = CuCl + 1/2\ Cl_2 \qquad (2)$$

The voltammograms recorded for solution (C) were found to increase in anodic peak current, thus verifying an increase in the quantity of oxidized Cu^+ ion. Regarding the cathodic half-cycle of voltammogram in solution (C), the cathodic currents became considerably enlarged in the presence of both Cu^{2+} and Cu^+ ions.

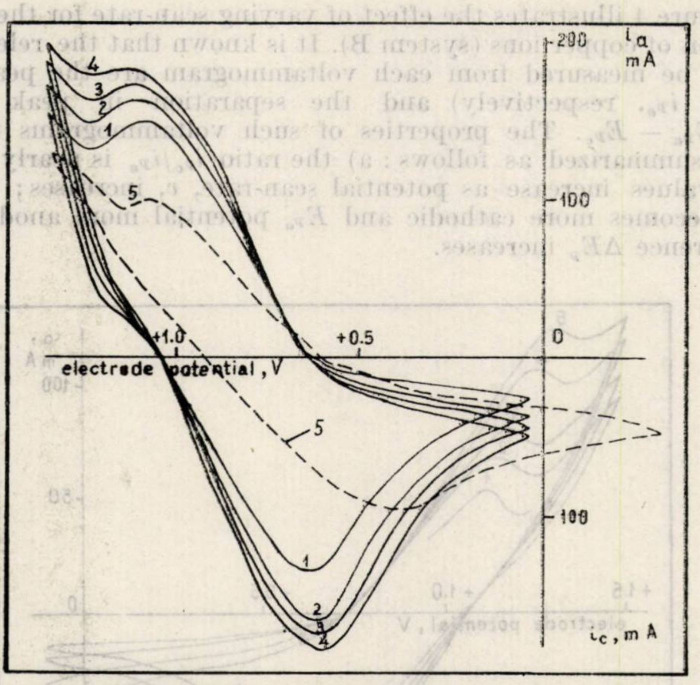

Fig. 5. — Voltammograms in system (*C*) at scan rates: *1*) 0.168; *2*) 0.252; *3*) 0.294; *4*) 0.336 V/s; *5*) initial solution LiCl—KCl—$CuCl_2$, $v = 0.324$ V/s.

Generally, all cyclic voltammograms for (A), (B), (C) and (D) systems showed a very symmetrical shape, corresponding to reversible redox couple Cu^{2+}/Cu^+. In the case of solution (D), since the copper ions concentration is growing, the current values are considerably higher than the foregoing systems, even at relatively lower scan-rates. When the concentration of dissolved electroactive species is still increasing, the above described features were again observed. The voltammograms for (E) and (F) systems show that the addition of $CuCl_2$ to LiCl—KCl—CuCl concentrated solution also caused a strong increase of the reduction peak, but its evidence is diminished, especially at higher scan-rates. The return sweep exhibits a broad current peak or rather a shoulder, which in the case of system F is poorly defined.

It is worth noticing that the shape of anodic half-cycle is quite different on metallic electrodes, for example on Pt sheet or W wire. As can be seen from Figure 6, in the case of system (A) using metallic electrodes, at anodic polarization firstly the oxidation of Cl^- ion occurs, resulting the main anodic peak and, by reversing the potential, also a second anodic peak appears, due to $Cu^+ \rightarrow Cu^{2+}$ oxidation reaction. This voltammogram is very similar in shape to those previously obtained by us on Pt or W electrodes for LiCl—KCl—CuCl and LiCl—KCl—$CuCl_2$ melts.[8] In the case of more concentrated systems, for example the system (C) also presented in Fig. 6, the unexpected second peak (of Cu^+/Cu^{2+} reaction) was not observed, the oxidation of cupreous ion being completely masked by chlorine evolution.

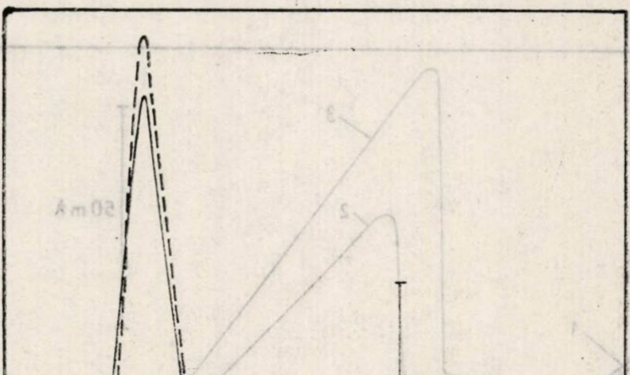

Fig. 6. — Voltammograms of a Pt electrode ($A = 1$ cm^2) in system (A) (curve *1*, $v = 0.0288$ V/s) and in system (C) (curve *2*, $v = 0.038$ V/s).

To get more information about the reduction of cupreous ion to metallic copper, some voltammograms were taken in the range of negative potentials, where this process occurs. Figure 7 shows the $i - E$ curves corresponding to Cu^+/Cu couple. From the successive voltammograms presented in this figure, all obtained at the same potential sweep, it follows that as the cathodic reversal potential was increased to -0.2V or higher cathodic values, the deposition of metallic copper as a straight line occurs, giving a little hysteresis of the half-cycle. Consequently, a return anodic peak of copper redissolution, due to the stripping process on graphite, is obtained. One observes that the anodic peak has a characteristic shape of stripping, namely, with a very clear breakdown of the current. If the cathodic reversal potential was extended, the electric charge, Q_a, contained in this stripping peak area, becomes substantially higher and the breakdown potential shifts to more positive values (see curves *2, 3* in Fig. 7). This shift of stripping peak is probably difficult to explain, being related to the nucleation effect that undoubtedly occurs in the electrochemical process, or rather, to the morphology of deposited copper layer onto the graphite surface.

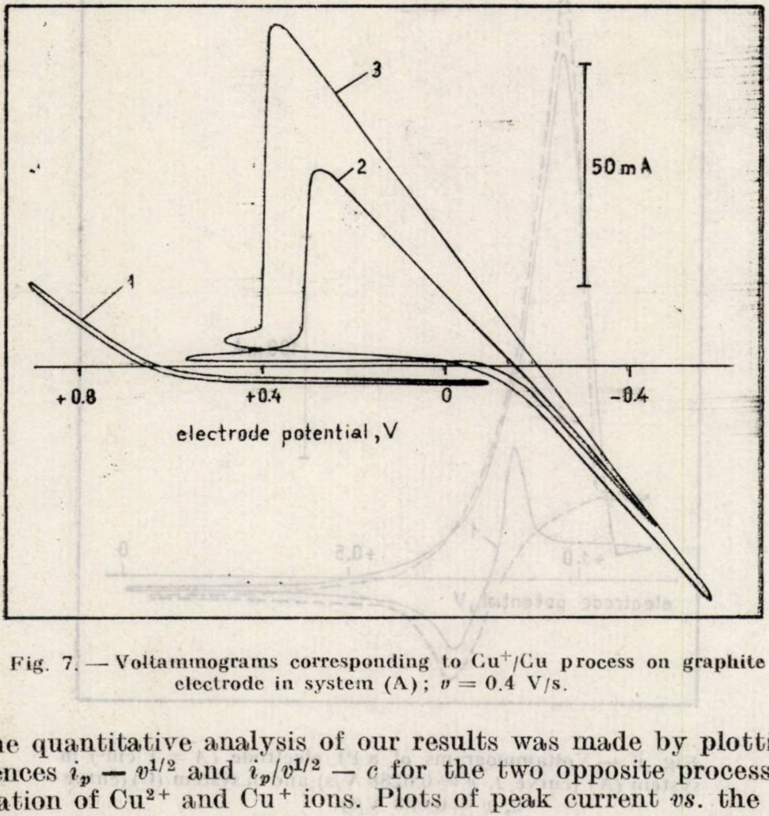

Fig. 7. — Voltammograms corresponding to Cu^+/Cu process on graphite electrode in system (A); $v = 0.4$ V/s.

The quantitative analysis of our results was made by plotting the dependences $i_p - v^{1/2}$ and $i_p/v^{1/2} - c$ for the two opposite processes with participation of Cu^{2+} and Cu^+ ions. Plots of peak current *vs.* the square root of the scan-rate at various cupric (cupreous) ion concentrations seem to be linear (see for example Fig. 8). Correspondingly, the quotients $i_p/v^{1/2}$ plotted *versus* the concentration give a straight line, passing through the origin. From these findings, we can deduce that the redox Cu^{2+}/Cu^+ couple is mainly diffusion controlled, the current function $i_p/(v^{1/2} \cdot c)$ being almost constant at a mean value of 771 A. cm^3/(V$^{1/2}$. mol).

An evaluation of the diffusion coefficient $D_{Cu^{2+}}$ is approximate because of the uncertainty of surface area of graphite electrode. Accordingly, using a plausible value of $D_{Cu^{2+}} = 2 \times 10^{-5}$ cm^2/s (from the value $D = 1.2 \times 10^{-5}$ cm^2/s at 450°C determined galvanostatically[2]), a geometrical area $A = 0.25$ cm^2 of electrode and the relation :

$$i_p = \frac{0.447(\mathrm{nF})^{3/2} D^{1/2} c v^{1/2} A}{(RT)^{1/2}}, \tag{3}$$

the current function $i_p/(v^{1/2} \cdot c) = 187$ A.cm^3/(V$^{1/2}$ · mol) was calculated ($t = 500$°C). In the above expression very much used in cyclic voltammetry, R and T have their usual meanings and n is the number of electrons

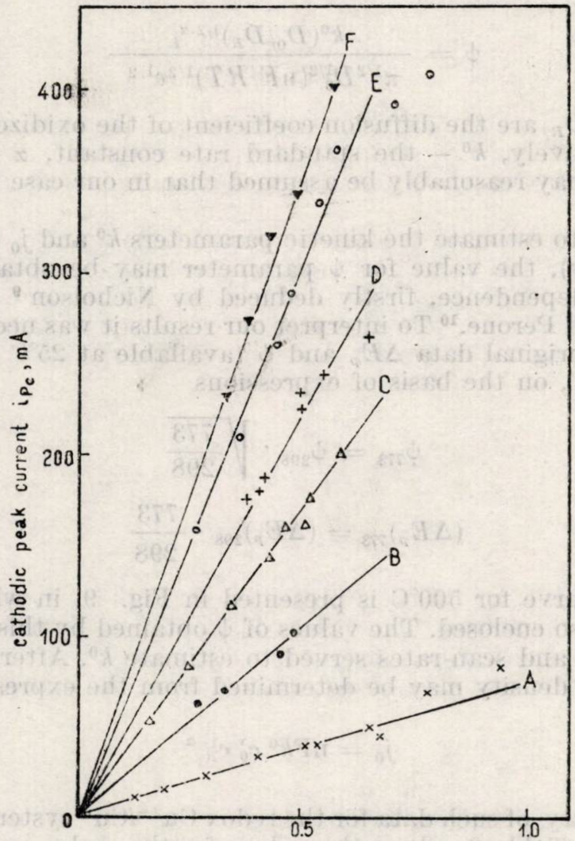

Fig. 8—. Plots of i_p *versus* $v_p^{1/2}$ for cathodic reduction $Cu^{2+} \rightarrow Cu^+$. The letters denote LiCl—KCl—$CuCl_2$—CuCl melts, according to Table 1.

participating in the electrochemical reaction (n = 1) ; certainly, i_p refers to cathodic as well as to anodic reaction, the ratio i_{p_c}/i_{p_a} being near unity. The obtained result for the current function proves that the true (real) working area of graphite electrode was about 4 times larger than its apparent geometrical area.

A further point of interest involves the analysis of the reversibility of redox Cu^{2+}/Cu^{+} process in LiCl-KCl. It is well known that the decrease in reversibility causes a substantial dependence of the peak separation ΔE_p on the scan rate. As can be seen from Figures 2—5 all ΔE_p values measured on voltammograms exceeded the theoretical value 2.3 $RT/\mathrm{n}F$ (that is 153 mV at 500°C), thus confirming that the redox process $Cu^{2+}/$ $/Cu^{+}$ is not truly reversible. By solving the appropriate equations in cyclic voltammetry conditions, Nicholson [9] has established a correlation between the peak potential separation ΔE_p, and a dimensionless function ψ defined by

$$\psi = \frac{k^0(D_0/D_R)^{1/2\cdot\alpha}}{\pi^{1/2}D_0^{1/2}(\mathrm{n}F/RT)^{1/2}v^{1/2}} \tag{4}$$

where D_0 and D_R are the diffusion coefficient of the oxidized and reduced species, respectively, k^0 — the standard rate constant, α — the transfer coefficient. It may reasonably be assumed that in our case $D_0 = D_R$ and $\alpha = 0.5$.

In order to estimate the kinetic parameters k^0 and j_0 (the exchange current density), the value for ψ parameter may be obtained from the ΔE_p — log ψ dependence, firstly deduced by Nicholson [9] and improved with the data of Perone.[10] To interpret our results it was necessary the extrapolation of original data ΔE_p and ψ (available at 25°C in Nicholson's paper) at 500°C, on the basis of expressions

$$\psi_{773} = \psi_{298} \cdot \sqrt{\frac{773}{298}} \tag{5}$$

$$(\Delta E_p)_{773} = (\Delta E_p)_{298} \cdot \frac{773}{298} \tag{6}$$

The working curve for 500°C is presented in Fig. 9, in which the curve for 25°C was also enclosed. The values of ψ obtained by this procedure for different melts and scan-rates served to estimate k^0. Afterwards, the exchange current density may be determined from the expression

$$j_0 = \mathrm{nF}k^0\, c_0^{\alpha}\, c_R^{1-\alpha} \tag{7}$$

A summary of such data for the redox Cu^{2+}/Cu^{+} system in LiCl—KCl is collected in Table 2, where the values for the molar exchange current density, $J_0 = \mathrm{n\,F}\,k^0$ were also presented. Good agreements between all kinetic parameters obtained for different scan-rates and concentrations were observed. We mention that these results of voltammetric measurements are very similar to those obtained by us in previous steady-state potentiostatic studies.[1] The orders of magnitude, $k^0 = 10^{-3}$ cm/s and $J_0 = 10^2$ A. cm^2/mol, are typical of many electrochemical systems in molten salts.[11]

The results obtained in this work indicate a behaviour of Cu^{2+}/Cu^{+} redox process in LiCl-KCl melt with higher electron transfer rates than the redox processes in aqueous solutions.

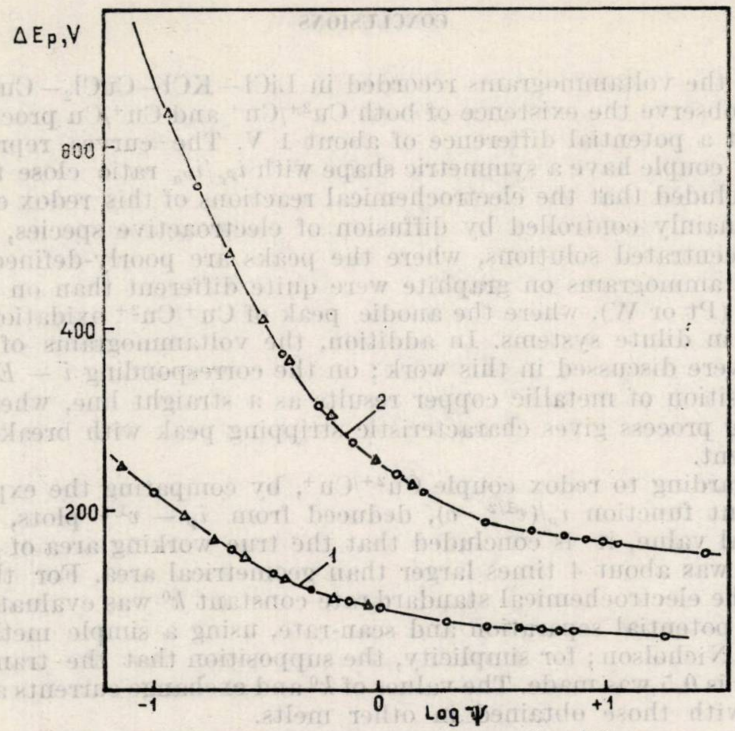

Fig. 9. — Semilogarithmic plot of peak separation ΔE_p *vs.* parameter ψ; *1)* $T = 298$ K; *2)* $T = 773$ K; O — Nicholson's data [9] ($\alpha = 0.5$); Δ — Perone's data [10] ($\alpha = 0.53$).

Table 2

Values of kinetic parameters for Cu^{2+}/Cu^+ couple in LiCl—KCl eutectic melt using graphite electrodes ($t = 500$ °C)

System	ΔE_p, mV	Scan rate v, V/s	Parameter ψ	$k^0 \times 10^3$, cm/s	$j_0 \times 10^3$, A/cm²	J_0, $\frac{A.cm}{mol}$
(A)	450	0.018	0.25	1.29	10	124
(B)	500	0.034	0.2	1.13	18.2	109
	640	0.068	0.12	0.96	15.5	92.6
	700	0.102	0.09	0.90	14.3	87
(C)	500	0.168	0.2	2.5	78	241
	570	0.252	0.15	2.3	71	220
	580	0.294	0.14	2.3	71	220
(D)	450	0.032	0.25	1.38	80	133
	520	0.064	0.18	1.4	81	135
	600	0.096	0.125	1.19	69	114
				Mean value: 1.53×10^{-3} cm/s		Mean value: $147 \frac{A.cm}{mol}$

CONCLUSIONS

On the voltammograms recorded in $LiCl-KCl-CuCl_2-CuCl$ melts one can observe the existence of both Cu^{2+}/Cu^{+} and Cu^{+}/Cu processes, situated at a potential difference of about 1 V. The curves representing Cu^{2+}/Cu^{+} couple have a symmetric shape with i_{p_c}/i_{p_a} ratio close to unity. It is concluded that the electrochemical reactions of this redox equilibrium are mainly controlled by diffusion of electroactive species, even at very concentrated solutions, where the peaks are poorly-defined.

Voltammograms on graphite were quite different than on metallic electrode (Pt or W), where the anodic peak of Cu^{+}/Cu^{2+} oxidation appears only in dilute systems. In addition, the voltammograms of Cu^{+}/Cu process were discussed in this work; on the corresponding $i - E$ curves, the deposition of metallic copper results as a straight line, whereas the dissolving process gives characteristic stripping peak with breakdown of the current.

Regarding to redox couple Cu^{2+}/Cu^{+}, by comparing the experimental current function $i_p/(v^{1/2} \cdot c)$, deduced from $i_p - v^{1/2}$ plots, with a theoretical value, it is concluded that the true working area of graphite electrode was about 4 times larger than geometrical area. For the same system, the electrochemical standard rate constant k^0 was evaluated from the peak potential separation and scan-rate, using a simple method initiated by Nicholson; for simplicity, the supposition that the transfer coefficient α is 0.5 was made. The values of k^0 and exchange currents are comparable with those obtained in other melts.

REFERENCES

[1] Part. II. S. Sternberg, T. Vişan and A. Cotârţă, *Rev. Roumaine Chim.*, **29**, 699 (1984)

[2] S. Sternberg, V. Petrescu, T. Vişan and A. Cotârţă, *Rev. Roumaine Chim.*, **28**, 565 (1983).

[3] A. P. Timchenko, *Ukr. Khim. Zhur.*, **44**, 768 (1978); A. P. Timchenko and A. V. Gorodyskyi, "Fiz. Khim. Elektrokhim. Raspl. Tverd. Elektrolytov, Tezisy Dokl. Vses. Konf. Fiz. Khim. Ionnykh. Raspl. Tverd. Elektrolytov, 7-th" 1979, 2, p. 138.

[4] E. Schmidt, *Electrochim. Acta*, **8**, 23 (1963).

[5] I. I. Naryshkin, V. P. Yurkinskyi and B. S. Yavich, *Elektrokhimiya*, **2**, 864 (1966).

[5] I. I. Naryshkin, V. P. Yurkinskyi and P. T. Stangrit, *Elektrokhimiya*, **5**, 1476 (1969).

[7] I. I. Naryshkin and V. P. Yurkinskyi, *Elektrokhimiya*, **5**, 871 (1969).

[8] S. Sternberg and T. Vişan, "III-rd International Conference on Molten Salt Chemistry—Proceedings, Wroclaw – Karpacz, Poland, May 28 – June 1", 1976 p. 293–304.

[9] R. S. Nicholson, *Analyt. Chem.*, **37**, 1351 (1965).

[10] S. P. Perone, *Analyt. Chem.*, **38**, 1158 (1966).

[11] G. E. Blomgren in "Physical Chemistry "vol. IX B, ed. H. Eyring, D. Henderson, W. Jost, Academic Press, New York, 1970, p. 589; Yu. K. Delimarskyi, "Ionnye Rasplavy", 2, Naukova Dumka, Kiev, 1974 p. 3; Yu. K. Delimarskyi, "Elektrokhimiya Ionnykh Rasplavov", Metallurgizdat, Moskva, 1978.

Revue Roumaine de Chimie, **31**, *4*, 443—449 (1986)

KINETICS AND MECHANISM OF SUBSTITUTION REACTIONS OF COMPLEXES. LVIII[1].

Hg(II) ASSISTED AQUATION OF *cis*-$[Co(en)_2Br(\gamma\text{-picoline})]^{2+}$

J. ZSAKÓ, J. DEMETER-VODNÁR, I. BÂLDEA and CS. VÁRHELYI
Faculty of Chemical Technology, "Babeş-Bolyai University",
3400—Cluj-Napoca, Arany János str. No. 11, Romania

Received April 27, 1985

The presence of Hg(II) shifts completely the aquation equilibrium of $[Co(en)_2Br(\gamma\text{-picoline})]^{2+}$(I) towards the formation of $[Co(en)_2(H_2O)(\gamma\text{-picoline})]^{3+}$(II) and increases the reaction rate by several orders of magnitude. The spectrophotometric study of the kinetics of the Hg(II) assisted aquation showed that several processes occur, *viz.* the non-assisted aquation, and aquations accelerated by the molecular species Hg^{2+}, $HgBr^+$, $HgBr_2$ and $HgBr_3^-$. The assisted aquation reactions are of first order with respect to (I) and of first order with respect to the accelerating species. Second order rate constants are derived for the reactions accelerated by Hg^{2+}, $HgBr^+$ and $HgBr_2$ at 25°. These rate constants decrease with increasing number of the Br atoms in the accelerating molecular species.

INTRODUCTION

In the last 80 years the accelerating effect of some metal ions (Ag^+, Hg^{2+}, Pb^{2+}, Fe^{3+}, Tl^{3+}, Au^{3+}, Pt^{4+}, etc.) upon the rate of solvation (substitution of ligands for solvent molecules) of complexes containing halide, pseudohalide or N_3^- ions was observed and studied by many authors.[2–26] Most attention was paid to the solvation of acido-complexes of Co(III) and Cr(III) in aqueous solutions in the presence of Hg(II).

At the beginning the process was considered to be a catalytic reaction, but actually Hg^{2+} is not a catalyst. According to the theory of soft and hard acids and bases, the process can be given as[12]

$$M_1X + M_2L \rightleftarrows M_1L + M_2X$$

where M_1 and M_2 are Lewis acids, L and X are Lewis bases. Such reactions can be expected to be fast ones, if M_1 and L are hard, M_2 and X are soft and the complexes M_2L and M_2X are labile. This is the case e.g. for $X = Cl^-$, Br^-, NCS^-, $L = H_2O$, M_1X complex of Co(III), Cr(III), M_2L complex of Hg(II). As seen, the above reaction is not the aquation only of M_1X, but it leads also to the formation of M_2X. Thus, it is more correct to call this reaction Hg(II) assisted aquation and not catalysis.

Kinetic studies showed these aquations to be generally second order reactions, *viz.* of first order with respect to the complex and first order with respect to Hg^{2+}.[20]

Concerning the mechanism, both mono- and bimolecular pathways may occur. Thus, in the case of the Hg(II) assisted aquation of $[Co(NH_3)_5X]^{2+}$, the existence of the intermediate $[Co(NH_3)_5]^{3+}$ could be evidenced, but the complete absence of this intermediate was observed if the aquation occurred without Hg(II)[8]. Consequently, the Hg(II) assisted aquation is monomolecular in this case.

The following bimolecular pathway

$$MX^{n+} + Hg^{2+} \overset{fast}{\rightleftarrows} MXHg^{(n+2)+} \xrightarrow[H_2O]{slow} M(H_2O)^{(n+1)+} + HgX^+$$

was reported for the aquation of $[Cr(H_2O)_5(NCS)]^{2+}$. From the kinetic measurements both the equilibrium constant for the formation of the binuclear intermediate and the rate constant of the slow aquation could be derived.[25]

In the case of $[Co(en)_2ACl]^{n+}$ type complexes the mechanism of the spontaneous non-assisted aquation depends on the nature of the ligand A. Electron repulsing ligands as OH, Cl, NCS, favour the monomolecular pathway and the electron withdrawing ligands as NH_3, H_2O, NO_2, favour the bimolecular mechanism.[23]

The study of the aquation of $[Co(DH)_2Cl_2]^-$

$$[Co(DH)_2Cl_2]^- \xrightarrow{H_2O} [Co(DH)_2Cl(H_2O)] \xrightarrow{H_2O} [Co(DH)_2(H_2O)_2]^+$$

where DH_2 stands for dimethylglyoxime, showed the Hg(II) assisted reaction to be the sum of four parallel processes, in both successive aquation stages.[26] Reaction (I) is the spontaneous, non-assisted aquation, reactions (II), (III) and (IV) are the aquations assisted by different Hg(II) species, *viz.* $HgCl_2$, $HgCl^+$ and Hg^{2+}, respectively. Thus, by taking the aquation for a first order reaction with respect to the complex, the overall rate constant can be given as

$$k = k_{I} + k_{II}[HgCl_2] + k_{III}[HgCl^+] + k_{IV}[Hg^{2+}]$$

By comparing the Hg(II) assisted aquation of analogous complexes, containing Cl and Br, respectively, generally the reaction is found to be much faster in the case of the bromo-complex, as compared to the chloro one.[20]

In the present paper the aquation reaction

$$[Co(en)_2Br(\gamma\text{-picoline})]^{2+} + H_2O \rightarrow [Co(en)_2(H_2O)(\gamma\text{-picoline})]^{3+} + Br^- \quad (1)$$

was studied.

The spontaneous, non-assisted aquation (1) was studied in our previous paper.[27] At room temperature this reaction is very slow, but in the presence of Hg(II) it becomes rather fast. Since the initial complex (I) is red-violet and the colour of the product (II) is yellow, the aquation can be observed easily. After adding the Hg(II) solution, the initially red-violet colour turns yellow in less than one minute. This colour change enables us to follow the aquation reaction spectrophotometrically. These measurements were performed at 358 nm since the spectra of the complexes showed the difference between the absorptions to be the most important between 350 and 360 nm.

EXPERIMENTAL

cis-$[Co(en)_2Br(\gamma\text{-picoline})](NO_3)_2$. 0.1 mole of *trans*-$[Co(en)_2Br_2]Br$, completely acid-free, are dissolved in 150 mL water and 0.11 mole of γ-picoline are added dropwise. The yellow-green solution becomes gradually violet-red. After standing for about 12 hrs, the solution is filtered and mixed with a concentrated aqueous solution of 100 g $NaNO_2$. After a short time a brilliant reddish-violet precipitate, consisting of irregular plates, appears. The substance is filtered, washed with ice water and dried in air.

Analysis: Co calcd. 12.38, found 12.32, NO_3 calcd. 26.05, found 26.10.

The *cis* configuration of the complex was established on the basis of IR spectral data.

The Hg(II) salt used was $Hg(ClO_4)_2$ obtained by dissolving HgO in perchloric acid.

Visible and UV absorption spectra were recorded in aqueous solution by using a Specord spectrophotometer.

In the kinetic measurements performed at 358 nm a VSU—1, Carl Zeiss, Jena spectrophotometer was used, to which a G—1, B—1 universal recorder was adopted as well as a special thermostated compartment for the cell. The kinetic runs were performed in a quartz cell. In the cell were introduced 4 mL of solution containing the complex (I) and $NaClO_4$ to ensure the needed ionic strength. After starting of the recorder, 1 mL of Hg(II) solution was injected by means of a syringe. The Hg(II) solutions contained 5×10^{-2} mole/L $Hg(ClO_4)_2$, $HClO_4$ in excess, in order to prevent basic hydrolysis, and NaBr, allowing us to vary the relative amount of the molecular species Hg^{2+}, $HgBr^+$, $HgBr_2$, $HgBr_3^-$. All the measurements were made at 25° and at a constant ionic strength of 0.1 M.

RESULTS AND DISCUSSIONS

According to our earlier data reaction (1) leads to an equilibrium.[27] Our first aim was to test the Hg(II) assisted aquation from thermodynamic point of view. For this purpose two samples were prepared, an aqueous solution of (I), and an aqueous solution of (I) to which an excess amount of $AgNO_3$ was added. The concentration of (I) was the same in both samples, and in the second one the ratio Ag :Br was higher than 10. After boiling them several minutes, both samples were kept at room temperature for a couple of days, in order to allow the first sample to reach the equilibrium. In the second sample the presence of Ag^+ shifts completely the equilibrium towards the formation of (II). Spectrophotometric measurements showed the absorption at 358 nm of the two samples to be different, in agreement with the above mentioned data. In a third sample the concentration of (I) was the same as in the before mentioned ones, but it contained also Hg^{2+} ions. The absorption at 358 nm decreased rapidly and its limiting value was identical with the absorption of the sample in which (I) was boiled with an excess of $AgNO_3$. Consequently, in the presence of Hg(II) reaction (1), becomes total, i.e. its equilibrium is shifted completely towards the right side.

In the kinetic runs from the absorption data the concentration of (I) can be derived. The reaction order with respect to (I) can be determined by performing a plot of $\log \frac{\mathrm{d}E}{\mathrm{d}t}$ *vs.* $\log (E - E_\infty)$, where E and E_∞ stand for the actual and for the limiting value of the extinction, respectively, the last one corresponding to $t \to \infty$. $\mathrm{d}E/\mathrm{d}t$ values are obtained by graphical derivation of the experimentally recorded E *vs.* t curve. As seen from fig. 1. the plot is linear and from the slope the reaction order $n = 1$ is obtained.

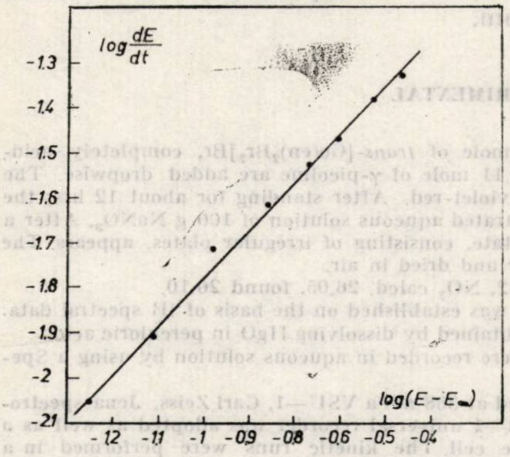

Fig. 1. — Derivation of reaction order with respect to (I).

Since the reaction is of the first order, the plot of $\log (E - E_\infty)$ *vs.* t allows us to derive apparent first order rate constants for different conditions.

In the samples both the initial concentration of (I) and the overall concentration of the Hg(II) species was equal to $a = 10^{-2}$ M. By adding NaBr, a complex formation equilibrium is established, leading to the formation of the following species $HgBr^+$, $HgBr_2$, $HgBr_3^-$ and $HgBr_4^{2-}$. Let us denote the stability constants of these species by β_1, β_2, β_3 and β_4. The concentrations of the Hg(II) species can be given in the following form:

$$[Hg^{2+}] = \frac{a}{1 + \beta_1[Br^-] + \beta_2[Br^-]^2 + \beta_3[Br^-]^3 + \beta_4[Br^-]^4}$$

$$[HgBr^+] = \beta_1[Br^-][Hg^{2+}]; \quad [HgBr_2] = \beta_2[Br^-]^2[Hg^{2+}]; \tag{2}$$

$$[HgBr_3^-] = \beta_3[Br^-]^3[Hg^{2+}]; \quad [HgBr_4^{2-}] = \beta_4[Br^-]^4[Hg^{2+}].$$

The concentration of the free Br^- ions can be obtained from the relation:

$$b = [Br^-] + (\beta_1[Br^-] + 2\beta_2[Br^-]^2 + 3\beta_3[Br^-]^3 + 4\beta_4[Br^-]^4)\ [Hg^{2+}] \tag{3}$$

where b stands for the overall concentration of Br^-.

In the kinetic runs a number of six different concentrations b were used. The log $(E - E_\infty)$ *vs.* t plots showed a good linearity, as seen from fig. 2. From the slopes apparent first order rate constants were derived. These k_{obs} values are presented in Table 1. The same Table contains also the concentration of the Hg(II) species and of the free Br^- ions, calculated by means of Eqs. (2) and (3). In these calculations the following stability constant values were used $\log \beta_1 = 8.94$; $\log\beta_2 = 16.88$, $\log \beta_3 = 19.15$; $\log \beta_4 = 20.90$. [28]

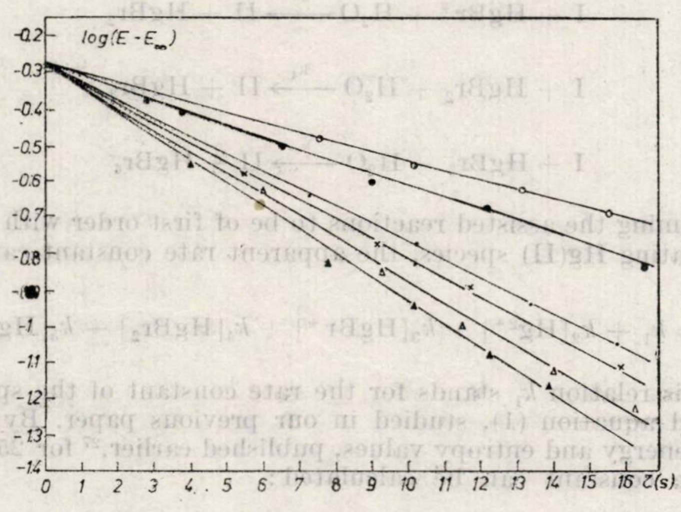

Fig. 2. — Derivation of apparent first order rate constants. $a = 10^{-2}$ M, $T = 25°C$, ionic strength : 1 M.

Table 1

Concentration (mole/L) of different molecular species and the apparent rate constant of reaction (1)

($a = 10^{-2}$ M, $t = 25°C$, ionic strength : 1 M)

$b \cdot 10^3$	$[Br^-] \cdot 10^{10}$	$[Hg^{2+}] \cdot 10^8$	$[HgBr^+] \cdot 10^3$	$[HgBr_2] \cdot 10^5$	$[HgBr_3^-] \cdot 10^{10}$	k_{obs}, s^{-1}	k_{calc}, s^{-1}
1	1.906	8.575	1.399	2.563	0.0109	0.150	0.151
3	5.446	6.702	3.145	15.22	0.1620	0.144	0.141
5	10.68	4.981	4.588	43.05	0.8786	0.122	0.132
10	41.06	1.730	6.094	217.8	16.87	0.110	0.109
15	167.2	0.283	3.984	573.3	81.93	0.085	0.084
19	1080.5	0.005	0.541	945.2	$1.1 \cdot 10^4$	0.067	0.065

As seen from Table 1, the k_{obs} values decrease with increasing b. The dependence of k_{obs} upon b indicates that besides reaction (1) in the system other parallel reactions occur, presumably the following ones:

$$I + Hg^{2+} + H_2O \xrightarrow{k_2} II + HgBr^+ \qquad (4)$$

$$I + HgBr^+ + H_2O \xrightarrow{k_3} II + HgBr_2 \qquad (5)$$

$$I + HgBr_2 + H_2O \xrightarrow{k_4} II + HgBr_3^- \qquad (6)$$

$$I + HgBr_3^- + H_2O \xrightarrow{k_5} II + HgBr_4^- \qquad (7)$$

Presuming the assisted reactions to be of first order with respect to the accelerating Hg(II) species, the apparent rate constant can be written as

$$k_{obs} = k_1 + k_2[Hg^{2+}] + k_3[HgBr^+] + k_4[HgBr_2] + k_5[HgBr_3^-] \qquad (8)$$

In this relation k_1 stands for the rate constant of the spontaneous non-assisted aquation (1), studied in our previous paper. By using the activation energy and entropy values, published earlier,[27] for 25°C the following rate constant can be calculated:

$$k_1 = 2.36 \times 10^{-6}\ s^{-1}$$

Since k_{obs} decreases with increasing b and the only Hg(II) species which has a decreasing concentration with increasing b, is Hg^{2+}, the hypothesis that $k_2 > k_3 > k_4 > k_5$ seems to be reasonable. As seen from Table 1, $[HgBr_3^-]$ is vanishing as compared to the concentration of the other Hg(II) sepcies and thus, in the conditions of our kinetic runs, in Eq. (8) the last term of the right hand side can be neglected.

By using the experimental k_{obs} values presented in Table 1, an attempt was made to derive the value of k_2, k_3 and k_4. For this purpose a curve fitting method was used by performing the minimization of the standard deviation of the experimental data from the calculated ones. The calculations performed by means of a Felix 256 computer, the following rate constants were derived:

$$k_2 = 15.5\ L\,mole^{-1}s^{-1};\ k_3 = 11.2\ L\,mole^{-1}s^{-1};$$

$$k_4 = 6.0\ L\,mole^{-1}s^{-1}$$

As seen, the second order rate constants decrease with increasing number of the halide ligand in the accelerating Hg(II) species. This is in perfect agreement with the literature data concerning the Hg(II) assisted aquation of
$[Co(en)_2(R-NH_2)Cl]^{2+}$ type complexes.[20]

The overall rate constants calculated by means of Eq. (8), by using the above given k_1, k_2, k_3 and k_4 values, are presented in the last column of table 1. As seen, the calculated values are in good agreement with the experimental ones.

REFERENCES

[1] Part LVII. J. Zsakó, I. Gănescu, Cs. Várhelyi and G. Brînzan, *Z. physik. Chem. (Leipzig)*, **265**, 1001 (1984).

[2] A. Werner and A. Gubser, *Ber. dtsch. chem. Ges.*, **39**, 1828 (1906).

[3] J. N. Brönsted and C. E. Teeter, *J. Phys. Chem.*, **28**, 583 (1924).

[4] J. N. Brönsted and R. Livingstone, *J. Amer. Chem. Soc.*, **49**, 435 (1927).

[5] G. Schwarzenbach, *Helv. chim. Acta*, **32**, 1845 (1949).

[6] S. Asperger and D. Pavlovic, *J. Chem. Soc.*, **1955**, 1449.

[7] R. Travagli, *Gazz. chim. ital.*, **87**, 682 (1957).

[8] T. A. Posey and H. A. Taube, *J. Amer. Chem. Soc.*, **79**, 255 (1957).

[9] R. Dyke and W.C.E. Higginson, *J. Chem. Soc.*, **1959**, 1620.

[10] W. C. E. Higginson and M. P. Hill, *J. Chem. Soc.*, **1960**, 1998.

[11] S. Kosky and R. Anentaraman, *J. Amer. Chem. Soc.*, **82**, 1574 (1960).

[12] R. G. Pearson, *J. Amer. Chem. Soc.*, **85**, 3533 (1963).

[13] A. M. Sargeson and G. H. Searle, *Nature*, **200**, 356 (1963).

[14] D. M. Sargeson, *Austr. J. Chem.*, **16**, 352 (1963); **17**, 385 (1964).

[15] J. H. Espenson, *Inorg. Chem.*, **4**, 527 (1965).

[16] J. H. Espenson and S. R. Hubbard, *Inorg. Chem.*, **5**, 586 (1966).

[17] D. A. Loeslinger and H. A. Taube, *Inorg. Chem.*, **5**, 1376 (1966).

[18] W. L. Johnson and M. M. Jones, *Inorg. Chem.*, **5**, 1345 (1966).

[19] M. D. Alexander and D. H. Busch, *J. Amer. Chem. Soc.*, **88**, 1130 (1966).

[20] S. C. Chan and S. F. Chan, *J. Chem. Soc.*, **1969 A**, 202.

[21] S. Asperger, J. Murati and D. Pavlovic, *J. Chem. Soc.*, **1969 A**, 2044.

[22] S. P. Tanna and W. C. E. Higginson, *J. Chem. Soc.*, **1969 A**., 1164.

[23] G. C. Lalor and S. D. Rustard, *J. inorg. nucl. Chem.*, **31**, 3219 (1969).

[24] M. D. Archer and M. Spiro, *J. Chem. Soc.*, **1970**, 68, 73, 78.

[25] J. N. Armor and A. Haim, *J. Amer. Chem. Soc.*, **93**, 867 (1971).

[26] V. I. Belevantsev, E. I. Evdohimova and B. I. Peshevitsky, *Izv. Sib. Otd. Akad. Nauk*, **1978**, 38.

[27] J. Zsakó, Cs. Várhelyi and S. Bleoca, *Acta Chim. Acad. Sci. Hung.*, **70**, 175 (1971).

[28] L. G. Sillén, "Stability constants of Metal-ion Complexes", The Chemical Society, London, 1964.

Revue Roumaine de Chimie, 31, 4, 451—456 (1986)

USE OF BETA-RAYS BACK-SCATTERING IN THE STUDY OF CORROSION PROCESS OF SOME CARBON STEEL SAMPLES IN ACID SOLUTIONS

AL. CECAL*, D. CIOBANU** and I. SANDU*
* Faculty of Chemical Technology, Polytechnic Institute of Iaşi, Romania
** Faculty of Physics, "Al. I. Cuza" University of Iaşi, Romania

Received September 3, 1984

The present paper deals with the investigation of the corrosion process of samples of OL—37 and OL—60 carbon steel in HNO_3, H_2SO_4 and $H_2C_2O_4$ solutions, in the absence and in the presence of benztriazole, as inhibitor. In order to follow the variation in time of iron ions concentration passing from metal into the corrosive solution, the radioanalytical method based on the β-rays back-scattering has been employed. The precision of the proposed method for the study of metal corrosion kinetics was checked up by means of potentiometric titration of iron ions resulting in solution due to anodic dissolution of these steel samples.

INTRODUCTION

Radioactive tracers have been successfully used in the study of metal corrosion and corrosion protection processes.[1-7]

Close and Hines[8] first subjected steels to neutron activation obtaining ^{59}Fe and ^{51}Cr radioisotopes. These tracers were used afterwards in following the corrosion process of the very steel samples immersed in different aggresive solutions. Horanyi and coworkers[9] used marked atoms in order to study the double electric layer properties appearing at the interface of noble metals and corrosive media.

In order to establish the rate of corrosion reactions of some metals under the influence of oxygen, Jesenak and Tölgyessy[10] used an experimental device, determining the emission of noble radioactive gases (Kr and Xe) previously confined to the surfaces of given metals. Kiss and others[11] employed a radiotracer technique to determine the development in time of metal corrosion, establishing afterwards the oxygen amounts adsorbed on the solid surfaces immersed in different corrosive solutions.

The present paper is carrying on some previous studies regarding radioisotopes use in the kinetic investigation of metal corrosion process.[12-23] In this respect OL—37 and OL—60 carbon steel samples were taken and they were immersed in HNO_3, H_2SO_4 and $H_2C_2O_4$ solution in the absence and in the presence of benztriazole as corrosion inhibitor. To follow the development in time of corrosion process of given samples, the β-rays back-scattering technique was employed.

EXPERIMENTAL

From OL—37 and OL—60 carbon steel bars (0 = 3 cm) ring samples with about equal dimensions were cut out. These samples were firstly ground, then washed with water and cleaned with methanol and acetone, after which they were introduced into a $CaCl_2$ desiccator.

The composition of the two steels used in this study is given in table 1.

Table 1

Chemical composition of the OL—37 and OL—60 carbon steel samples. (The rest to 100% is iron)

Sample	C(%)	Mn(%)	Si(%)	P(%)	S(%)
OL—37	0.23	0.68	0.27	0.016	0.015
OL—60	0.39	1.15	0.25	0.016	0.019

18 Erlenmayer flasks of 250 mL were taken and they were divided into two series. Into each glass of both series 150 mL from one of the corrosive acid solutions were introduced: HNO_2 (1 N), H_2SO_4 (1 N), $H_2C_2O_4$ (1 N), HNO_3 (0.1 N), H_2SO_4 (0.1 N), $H_2C_2O_4$ (0.1 N) and 145 mL HNO_3 (1 N)+ + 5 mL benztriazole (0.1 M), 145 mL-H_2SO_4 (1 N) + 5 mL benztriazole (0.1 M) and 145 mL $H_2C_2O_4$ (1 N) + 5 mL benztriazole (0.1 M). Then, in the first series of 9 flasks an OL—37 steel sample was introduced in each, while in the other series an OL—60 steel sample in each one. Benztriazole was dissolved in DMF.

At the moment each metal sample was immersed in the solution, the respective corrosion process started.

In order to follow the development in time of the corrosion process, by means of variation of iron ions concentration passing from the metal sample into aggressive solution, the radioanalytical method based on the β-rays back-scattering was chosen. With the advance of the corrosion process, the activity of β-rays back-scattered became greater and greater, because the iron ions concentration increased in that aggresive medium.

The device used (Fig. 1) is made up of 3 CTC-6 detectors set in parallel (*a*) under which there is a lead hose (*b*), in which an active ^{204}Tl source (*c*) with specific activity of $5 \cdot 10^6$ Bq/g is placed. The solution containing iron ions producing the back-scattering of β-rays emitted by the respective source, was set in the capsule (*d*). The CTC-6 detectors were connected to an electronic scaler VSP—1961.

At given time intervals, the whole solution content in each Erlenmayer flask was introduced into the capsule (*d*) in order to measure the activity of β-rays back-scattered. After 3 activity measurements lasting about 3 minutes each, out of which an average value was calculated, the solution was introduced back into the Erlenmayer flask so that the corrosion process previously commenced be continued.

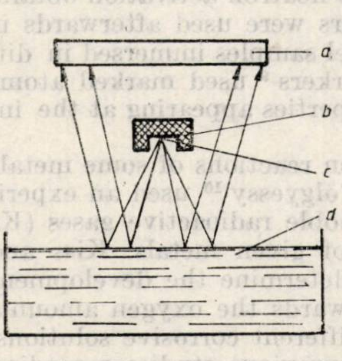

Fig. 1. — Experimental device for β-rays back-scattering measurements.

From the mean activity $\bar{R}$ (cpm) everytime the activity of device background (with water) R_f (cpm) was subtracted, so that:

$$R = \bar{R} - R_f \tag{1}$$

The mean net activity (R) of back-scattered β-rays corrected for the decay of emitter, was proportional to the total iron content of the solution. To increase the activity measurements precision it is recommended to use pure β-radioisotope, having a decay time as long as possible and β-rays energy greater than 0.5 MeV. At the same time the respective β-sources should have a greater activity so that it should be overcome by cosmic rays. Thus, the following radioisotopes are suggested: ^{90}Sr and ^{204}Tl.

In order to confirm the accuracy of the suggested method by β-rays back-scattering, in the study of metal corrosion kinetics, a well known comparative method was employed, the potentiometric titration. In this respect three OL—37 and three OL—60 carbon steel samples were immersed in corrosive media: HNO_3 (1 N), H_2SO_4 (1 N) and $H_2C_2O_4$ (1 N) in the corcrosive solution, was done by means of an ILM Labor-Titrimeter TM—3, with two electrodes : Platinum/Calomel.

RESULTS AND DISCUSSION

The process of carbon steel corrosion may be rendered by the successive reactions :[24-26]

— anodic dissolving of iron

$$Fe \rightarrow Fe^{2+} + 2\,e^-$$

— cathodic reduction of hydrogen ions with depolarisation role :

$$2\,H^+ + 2\,e^- \rightarrow H_2$$

Other possible reactions can be met :

$$1/2\,O_2 + H_2O + 2\,e^- \rightarrow 2\ OH^-$$

$$Fe^{2+} + 2\,OH^- \rightarrow Fe(OH)_2$$

$$2\,Fe^{2+} + 1/2\,O_2 + H_2O \rightarrow 2\,Fe^{3+} + 2\,OH^-$$

Corrosion reactions of metal samples in these aggressive media may be considered to be subjected to a I order reaction, i.e. :

$$\ln(c - x) = kt \tag{2}$$

Here $(c - x)$ represents the iron ions concentration in corrosive medium at a time t, while k is the constant of the studied corrosive reaction rate.

Due to the corrosion process in aggressive solution, the iron ions concentration by these ions will consequently increase. Therefore one may conclude that there is a proportionality between the activity of β-rays back-scattered and the iron ions concentration in that solution, i.e. :

$$R = f([Fe^{2+}] + [Fe^{3+}]) \tag{3}$$

Hence, relation (2) may be rendered as follows :

$$\ln R = k\,t, \tag{4}$$

If relation (4) is plotted : $\ln R = f(t)$, a straight line results, whose slope makes it possible to calculate the rate constant of corrosion reaction, which in fact also characterizes the development of the respective process under certain experimental conditions.

Figures 2 and 3 render the experimental data obtained by measuring in time the activity of β-rays back-scattered by iron ions in corrosive solution appeared after anodic dissolution of OL—37 and OL—60 carbon steel samples, immersed in acid media. In these figures the corrected activity according to relation (2) *vs* time was drawn out.

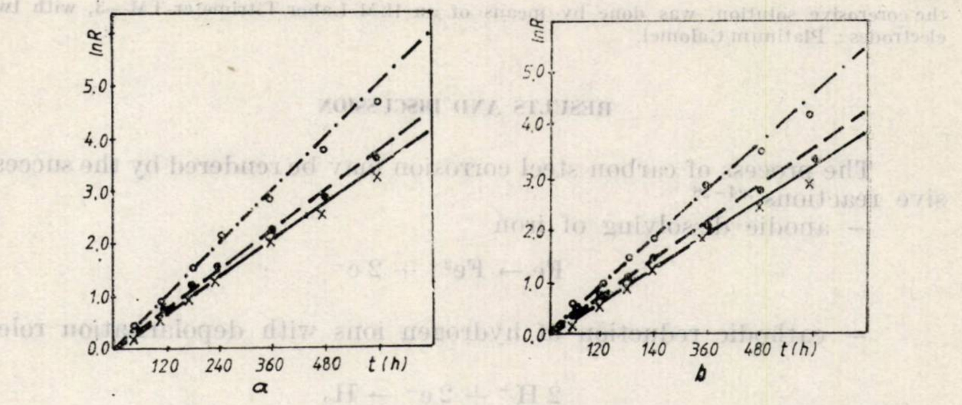

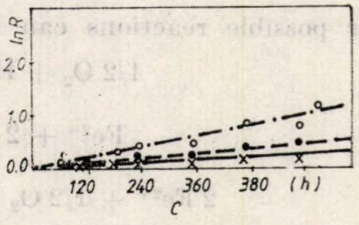

Fig. 2.—Dependence of activity of back-scattered β-rays *vs.* contact time between the OL—37 carbon steel and aggressive solution : *a*—in HNO_3 solution ; *b* — in H_2SO_4 solution ; *c* — in $H_2C_2O_4$ solution ; ○ acid solution 1N ; ● acid solution 0.1 N ; × — mixture of solution of corresponding 1 N acid and benztriazole (0.1 M).

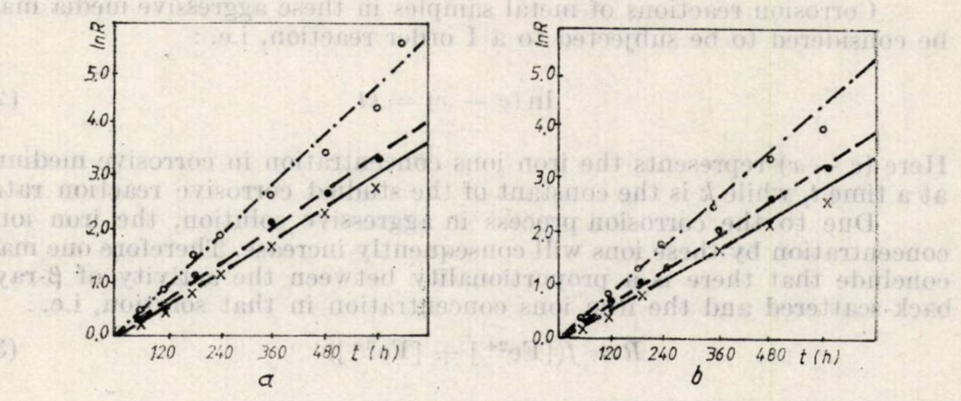

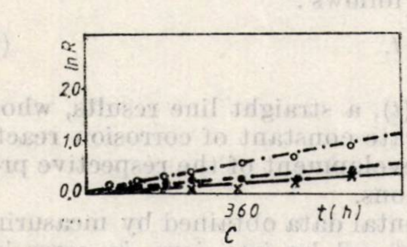

Fig. 3. — Dependence of activity back-scattered β-rays *vs.* contact time between the OL-60 carbon steel and aggressive solution : *a* = in HNO_3 solution ; *b* — in H_2SO_4 solution ; *c* — in $H_2C_2O_4$ solution ; ○ acid solution 1 N ; ● — acid solution 0.1 N ; × — mixture of solution of corresponding 1 N acid and benztriazole (0.1 M).

In the next figures 4 and 5, the experimental data obtained by means of potentiometric titration, in the coordinates: $\ln[Fe^{2+}] = f(t)$ were plotted.

Reaction rate constants for the corrosive systems under study calculated from the straight lines slopes previously plotted, are presented in Table 2.

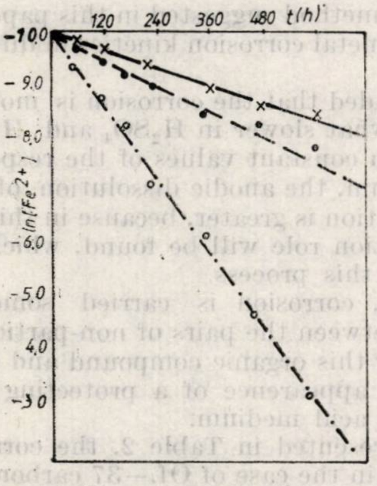

Fig. 4. — Dependence of Fe^{2+}-ions concentration on the corrosion time for the OL—37 carbon steel established by means of potentiometric method: O — HNO_3 solution 1 N, ● — H_2SO_4 solution 1 N, × — $H_2C_2O_4$ solution 1 N.

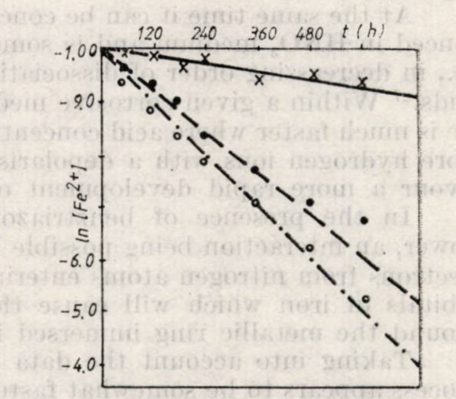

Fig. 5. — Dependence of Fe^{2+}-ions concentration on the corrosion time for the OL—60 carbon steel established by means of potentiometric method; O — HNO_3 1 N solution, ● — H_2SO_4 solution 1 N, × — $H_2C_2O_4$ solution 1 N.

Table 2

Rate constant values of corrosion reactions under study

Steel sample	Corrosive medium	k (h^{-1}) β-rays back-scattering	k (h^{-1}) Potentiometric titration
OL—37	HNO_3 (1 N)	$8.4.10^{-3}$	$9.2.10^{-3}$
	HNO_3 (0.1 N)	$6.2.10^{-3}$	—
	HNO_3 (1 N) + benztriazole (0.1 M)	$5.8.10^{-3}$	—
	H_2SO_4 (1 N)	$7.7.10^{-3}$	$7.4.10^{-3}$
	H_2SO_4 (0.1 N)	$5.9.10^{-3}$	—
	H_2SO_4 (1 N) + benztriazole (0.1 M)	$5.4.10^{-3}$	—
	$H_2C_2O_4$ (1 N)	$1.6.10^{-3}$	$1.2.10^{-3}$
	$H_2C_2O_4$ (0.1 N)	$8.3.10^{-4}$	—
	$H_2C_2O_4$ (1 N) + benztriazole (0.1 M)	$5.6.10^{-4}$	—
OL—60	HNO_3 (1 N)	$8.0.10^{-3}$	$8.6.10^{-3}$
	HNO_3 (0.1 N)	$5.7.10^{-3}$	—
	HNO_3 (1 N) + benztriazole (0.1 M)	$5.1.10^{-3}$	—
	H_2SO_4 (1 N)	$7.3.10^{-3}$	$6.7.10^{-3}$
	H_2SO_4 (0.1 N)	$5.6.10^{-3}$	—
	H_2SO_4 (1 N) + benztriazole (0.1 M)	$4.7.10^{-3}$	—
	$H_2C_2O_4$ (1 N)	$1.5.10^{-3}$	$1.3.10^{-3}$
	$H_2C_2O_4$ (0.1 N)	$6.8.10^{-4}$	—
	$H_2C_2O_4$ (1 N) + benztriazole (0.1 M)	$4.9.10^{-4}$	—

It can be observed a good concordance between the values of rate constants determined by β-rays back-scattering method and potentiometrically for the corrosive reaction of OL—37 and OL—60 carbon steel samples immersed in 1 N acid solutions.

These data clearly show that the method suggested in this paper can be successfully applied in the study of metal corrosion kinetics in different aggresive solutions.

At the same time it can be concluded that the corrosion is more advanced in HNO_3 medium and is somewhat slower in H_2SO_4 and $H_2C_2O_4$, i.e., in decreassing order of dissociation constant values of the respective acids.[27] Within a given corrosive medium, the anodic dissolution of sample is much faster where acid concentration is greater, because in this case more hydrogen ions with a depolarisation role will be found, which will favour a more rapid development of this process.

In the presence of benztriazole, corrosion is carried somewhat slower, an interaction being possible between the pairs of non-participant electrons from nitrogen atoms entering this organic compound and d free orbitals of iron which will cause the appearence of a protecting layer around the metallic ring immersed in acid medium.

Taking into account the data presented in Table 2, the corrosion process appears to be somewhat faster in the case of OL—37 carbon steel as compared to OL—60 carbon steel, due probably to a different amount of manganese, with a passivation effect.

REFERENCES

[1] K. Schwabe, *Chem. Techn.*, **13**, 275 (1961).

[2] J. G. N. Thomas, *Werkst. Korr.*, **19**, 957 (1968).

[3] K. H. Lieser, O. Kalvenes and S. Compostella, *Corros. Sci.*, **4**, 51 (1964).

[4] J. Vehlow, *Werkst. Korr.*, **26**, 338 (1975).

[5] J. Vehlow, *Werkst. Korr.*, **31**, 167 (1980).

[6] G. Reinhard, *Isotopenpraxis*, **18**, 41 (1982).

[7] G. Reinhard, *Isotopenpraxis*, **18**, 157 (1982).

[8] H. J. Close and D. B. Hines, *Isotop. Radiat. Technol.*, **7**, 404 (1970).

[9] G. Horanyi, S. Solt and F. Nagy, *J. Electroanal. Chem.*, **31**, 87 (1971).

[10] V. Jesenak and J. Tölgyessy, *Radiochem. Radioanal. Letters*, **19**, 267 (1974).

[11] L. Kiss, A. I. Molodov, L. M. Vassany, G. N. Markosyan, J. Farkas, V. V. Losev, L. Sziroky and A. I. Safrinova, *Zastch. metall.*, **16**, 99 (1980).

[12] Al. Cecal, N. Calu and P. Harabor, *Bull. Soc. Chim. France*, **1975**, 1076.

[13] Al. Cecal and St. Reșu, *Radiochim. Acta*, **23**, 20 (1976).

[14] Al. Cecal and D. Ciobanu, *Radiochim. Acta*, **28**, 171 (1981).

[15] Al. Cecal, *Isotopenpraxis*, **17**, 328 (1981).

[16] Al. Cecal and V. Stan, *Z. phys. Chem. (Leipzig)*, **263**, 117 (1982).

[17] Al. Cecal and D. Ciobanu, *Radiochem. Radioanal. Letters*, **51**, 9 (1982).

[18] Al. Cecal, *Rev. Roumaine Chim.*, **28**, 91 (1983).

[19] Al. Cecal, *Electrochim. Acta*, **28**, 681 (1983).

[20] Al. Cecal, *Metalurgia (București)*, **35**, 190 (1983).

[21] Al. Cecal, *Isotopenpraxis*, **20**, 9 (1984).

[22] Al. Cecal and N. Mihai, *Rev. Roumaine Chim.*, **29**, 315 (1984).

[23] Al. Cecal, *Isotopenpraxis*, **20**, 259 (1984).

[24] H, H. Uhlig, "The Corrossion Handbook", J. Wiley, New York, 1948.

[25] J. O'M. Bockris, A.K.N. Reddy, "Modern Electrochemistry", Vol. I, Mc. Donald, London 1970.

[26] M. G. Fontana and R. W. Staehle, "Advances in Corrosion Science and Technology", Plenum Press, New York, 1970.

[27] "Handbook of Chemistry and Physics", 55th Edition 1974—1975, CRC Press Inc., Cleveland 1974.

Revue Roumaine de Chimie, **31**, *4*, 457—458 (1986)

COMPTES RENDUS

"Cation Ordering and Electron Transfer" (edited by J. B. Goodenough and C. K. Jørgensen), "Structure and Bonding" [vol. 61, Springer-Verlag, 1985. Hard cover, DM 98.00, ISBN 3—540—15446—9.

The book presents an interesting assortment of two purely inorganic chemical reviews and of an application of X-ray photoelectron spectroscopy (XPS) for monitoring the oxidation state of sulphur in sulphur-containing amino-acids of intact or degraded proteins.

G. Gleitzer and J. B. Goodenough review mixed valence iron oxides with reference to model systems: *magnetite* (Fe_3O_4) with spinel-related structure, *hexagonal ferrites* (magnetoplumbites), with mixed Fe^{2+}/Fe^{3+} valence and considerable technical interest because they are ferrimagnetic semiconductors, *wüstite* ($Fe_{1-x}O$) with random defects and clustering which is the dominant phase in the blast furnace, and *perovskite* ($CaFeO_3$) with partial replacement of calcium by strontium or lanthanide cations, where Fe—O—Fe interactions lead to semiconductivity. Of these, ferrospinels are the most thoroughly studied. The importance of iron oxides can hardly be overestimated since they were the first (natural) compasses, their direction of magnetization gives important geological clues, and they have been used by living organisms (e.g. homing pigeons) for navigational systems. Theoretical data are presented in terms of itinerant electrons, polarons, etc. and of Néel's theory of ferrimagnetism.

M. O'Keefe and B. G. Hyde's chapter is entitled "An alternative approach to non-molecular crystal structures with emphasis on the arrangements of cations". The authors are inverting the traditional approach and consider a packed array of cations into whose interstices the anions are inserted. Actually, the terms "cation" and "anion" imply rather the distinction between more electropositive and more electronegative atoms, respectively, and does not represent a commitment to ionic bonds, encompassing also silicates and other oxides. Even physically, this approach gives a useful description of crystal structures: some structures have their own antitypes; in silicates, silicon "cations" have larger radii than oxygen "anions". Analogies between binary alloys and oxides can be made (oxides may be viewed as stuffed alloys). A detailed review, with many illustrations of structures (infinite arrays of cations) constitutes the main part of the chapter, including perovskites, spinels, barium sulfate (which has not been satisfactorily described), etc. Thus, interatomic distances and structural parameters can be quantitatively described, e.g. for spinel, garnet, rutile, zircon, bixbyite, scheelite, calcite, pyrochlore, etc. Finally, the effect of pressure on structure may be understood for the phase transitions that are not accompanied by an increase in primary coordination number at increased pressure, e.g. for olivine → spinel, or zircon → scheelite transitions.

The last review by U. Weser discusses redox reactions of sulphur-containing amino-acid residues in proteins and metalloproteins, a study by X-ray photoelectron spectroscopy (XPS). For differentiating between oxidation states of sulphur or selenium (e.g. between RS^- or RSSR), XPS is ideally suited. In lapis lazuli or ultramarines, the polysilicates contain mainly S(VI). In bovine serum albumin there are 4 methionine residues, 17 disulfide bridges and one cysteine residue; the bands in the S_{2p} region of the XPS data at —150° indicate around 163 eV these sulphur atoms as one intense maximum with smaller maxima at 168 eV due to S(VI) formed by oxidation. Cu_2Zn_2-superoxide dismutase, used as a marker enzyme in studies of the biochemistry of ageing, shows only one signal at 163 eV when its preparation was free of oxidation products, but on standing (even in freeze-dried samples), the appearance of S(VI) signals at 168 eV is noted. Selenoenzymes such as glutathione peroxidase can also reveal the oxidation state of selenium. The method is very sensitive and fast (one S or Se atom per 20 000 daltons may be detected) and allows the study of S- or Se-containing aminoacids in native or degraded biopolymers.

The volume is almost error-free (on p. 106 one should replace *not* by *note*); inorganic chemists as well as chemists interested in XPS or in protein chemistry will profit from the three outstanding reviews.

Alexandru T. Balaban

J. V. Kissin, "Isospecific Polymerization of Olefins with Heterogeneous Ziegler — Natta Catalysts" (Polymers: Properties and Applications, vol. 9), Springer-Verlag, New York — Berlin — Heidelberg — Tokyo, 1985. 439 pp, XIV, 165 figs., hard cover, DM 450, ISBN 3—540—96105—4.

The entire book is devoted to problems associated with the special olefin polymerization mechanism under the action of heterogeneous catalysts (organic derivatives of transition metals such as $RTiCl_3$). Such active centers have the ability to order spatially the growing polymer chain, leading to stereoregular polymers. K. Ziegler first demonstrated experimentally how such catalysts can be obtained, while G. Natta analysed theoretically and experimentally the stereochemical features of polymers.

The five book chapters are as follows:

1. Kinetics of olefin polymerization with heterogeneous Ziegler—Natta catalysts.
2. Heterogeneous Ziegler — Natta catalysts: chemistry and kinetics of the formation and functioning of active centers.
3. Stereospecificity of heterogeneous Ziegler — Natta catalysts.
4. Inhomogeneity of active centers of heterogeneous Ziegler — Natta catalysts.
5. Mechanism of isospecific olefin polymerization.

Each chapter has a separate bibliography, totalling almost one thousand recent references. As indicated in the author's preface, the number of publications following the Nobel Prize award to Ziegler and Natta in 1963 reached a maximum in the 1960's, then declined, although the flux of patents continued unabated. This illustrates the practical use of fundamental discoveries which goes on for long periods. Then in the beginning of 1980's commercial companies discovered very active supported isospecific catalysts, leading to a recent revival of academic and applied research interest.

An advantage of the book is the fact that it gives a comprehensive survey of the world's recent relevant literature, including Western, Soviet, and Japanese papers. Few patents are cited, however (without *Chemical Abstracts* correspondence). The book does not have a historical outlay: although many of Natta's papers are quoted, it seems that no paper of Ziegler's is cited. Neither in the sections dealing with modifications of $TiCl_3$-$AlEtCl_2$ systems, nor in the chapter on the reaction mechanism is there any mention of the controversy between Ziegler and the Nenitzescu — Huch group, or of the Romanian procedure using pentylsodium instead of $AlEtCl_2$.

The book presents an in-depth analysis of stereochemical features of polymers, including methods for analyzing polyolefin isotacticity (mainly IR, ^{1}H-NMR and especially ^{13}C-NMR), and statistical methods for correlation between isotacticity parameters. Again, owing to the fact that historical aspects are not stressed, Katritzky's early papers (cf. *Chem. Brit.* 1976, **12**, 45) are not mentioned. No mention of two-dimensional *J*-correlated NMR spectra (cf. L. W. Jelinski, *Chem. Eng. News*, **62**, No. 45, 1984) or of optically active polymers appears in the book (cf. G. Wulff et al., *Nouv. J. Chim.*, 1982, **6**, 681; Y. Okamoto et al., *J. Am. Chem. Soc.*, 1979, **101**, 4763; 1981, **103**, 6971; *J. Org. Chem.*, 1984, **49**, 557).

Thorough reviews on kinetic models for olefin polymerization, on poisoning effects, on the function and formation of isospecific polymerization centers, on the inhomogeneity of Ziegler-Natta catalysts (including modern supported catalysts such as $MgHal_2$ first patented in Belgium, which enhance 100 times the activity of the catalyst) and on factors affecting the reactivity of olefins and of catalytic centers are particular assets of the book. The author has obtained permission to reproduce many figures and data from periodicals or books, so that the reading is easy. The critical evaluation of data, including theoretical calculations of the catalytic center and of the insertion step is very useful for those who are not yet familiar with the literature.

A new concept of catalyst isospecificity (stereospecificity) is presented on the basis of the author's earlier papers. The intimate mechanism of the olefin insertion reaction and the steric factors around the organometallic center with one or two vacancies explains how the catalyst promotes regio- and stereoregularity of the growing coil of polymer (however, the explanation of chemical shift nonequivalence for the diastereotopic methyls in 2,4,6-trimethylheptane on pp. 407—408 is too brief).

The book has a subject but no author index. It is very informative and its literature coverage is up-to-date. It will be very useful to polymer chemists working as scientists or engineers in teaching, research or development, either in universities or in industry. Owing to its self-consistency, the book will also be useful to advanced students.

Alexandru T. Balaban

NOTE POUR LES AUTEURS

La Revue Roumaine de Chimie publie des articles en anglais, français, russe, allemand ou espagnol. Les auteurs sont priés d'envoyer des articles et des comptes rendus inédits.

Les manuscrits seront dactylographiés à double interligne. La bibliographie, les tableaux et la légende des figures seront placés après le texte.

Si l'article fait partie d'une série numérotée, la partie précédente sera donnée comme première référence.

Chaque article sera précédé d'un résumé comprenant quinze lignes au maximum.

Les références bibliographiques dans le texte seront faites par des exposants sans parenthèses et paraîtront à la fin de l'ouvrage.

Les publications périodiques mentionées dans la bibliographie seront présentées suivant les prescriptions internationales : le nom de l'auteur précédé de l'initiale du prénom, le titre du périodique abrégé conformément à « Chemical Abstracts » et souligné par une ligne, le numéro du tome indiqué par des chiffres arabes et souligné par deux lignes, suivi de la première page de l'article : à la fin, l'année de la parution sera placée entre parenthèses. Le numéro de la revue ne sera pas indiqué si les pages du volume sont numérotées consécutivement.

Les textes des livres ou traités incluront : le nom des auteurs, précédés de l'initiale du prénom, le titre du livre entre guillemets et sans être souligné, le numéro du tome précédé par l'abréviation « vol. » (ou « Bd. »), le numéro de l'édition, les éditions (the publisher), la localité de la parution du livre, l'année de la parution et la page de la référence précédée(s) par l'abréviation « p » (ou « S »).

Les brevets seront indiqués comme suit : l'auteur ou la firme, le pays et le numéro du brevet, la date de la revue *(Chem. Abstr.)*. Par. ex. : M. Jones (to Union Carbide Co.). Brit. Pat. 610 238, 2 Sept. 1959 : cf. *Chem. Abstr.*, **54**, 12808 (1960).

Si la référence n'a pas été lue en original, on indiquera aussi la revue de références consultée.

Les diagrammes seront tracés à l'encre de Chine sur papier calque. Les tableaux et les figures (en nombre strictement nécessaire), ainsi que les courbes dans les figures seront numérotés par des chiffres arabes. Leur explication sera donnée dans la légende des figures. Prière de ne pas inscrire les mêmes données dans les tableaux et les figures. Chaque tableau aura un titre. On indiquera dans le texte la place approximative des tableaux et des figures. Les formules chimiques seront incluses dans le texte ; en outre, elles seront transcrites sur papier calque, à l'encre de Chine.

Les auteurs sont priés d'indiquer les caractères italiques (en soulignant les lettres au crayon), ainsi que tout autre caractère spécial : les préfixes *ortho*, *meta*, *para*, *cis*, *trans*, etc. seront soulignès pour indiquer leurs caractères italiques, et ne seront jamais écrits avec des majuscules.

Aucune correction à la main ne sera admise sur le manuscrit. Les corrections seront frappées à la machine. Les lettres grecques ou d'autres symboles spéciaux seront insérés à la main à l'encre clairement.

Le manuscrit sera signé par l'auteur.

Le titre courant aura 50 lettres au maximum.

L'entière responsabilité du contenu des articles appartient aux auteurs.

Sur demande on peut obtenir une note plus complète.

PRINTED IN ROMANIA

TRAVAUX PARUS AUX ÉDITIONS DE L'ACADÉMIE DE LA RÉPUBLIQUE SOCIALISTE DE ROUMANIE

V. DRĂGUŢAN, A. T. BALABAN, M. DIMONIE, **Olefin Metathesis and Ring-Opening Polymerization of Cyclo-Olefins**, coédition avec John Wiley & Sons, 1985, 544 p.

C. LITEANU, I. RÎCA, **Optimizarea proceselor analitice**, 1985, 360 p.

N. PERESCU, **Chimia extracţiei cu solvenţi şi aplicaţii**, 1985, 212 p,

V. E. SAHINI, M. HILLEBRAND, **Chimie cuantică în exemple şi aplicaţii**, 1985, 378 p.

GH. MARCU, **Chimia compuşilor coordinativi**, 1984, 415 p.

E. CORDOŞ, C. MANOLIU, **Spectrometria de absorbţie şi fluorescenţă atomică**, 1984, 178 p.

C. BODEA, **Tratat de biochimie vegetală**, p. II, vol. 5, 1984, 438 p.

ELENA CEAUŞESCU, **Cercetări în chimia şi tehnologia polimerilor**, 1983, 519 p.

N. ASANDEI, A. GRIGORIU, **Chimia şi structura fibrelor**, 1983, 395 p.

N. IONESCU, M. CĂLDĂRARU, **Oxidarea catalitică a olefinelor inferioare**, 1983, 178 p.

C. CAŞCAVAL, **Studiul polimerilor prin piroliză şi cromatografie de gaze**, 1983, 220 p.

C. I. SIMIONESCU, F. DANEŞ, **Originea vieţii**, 1983, 110 p.

C. BODEA (sous la direction), **Tratat de biochimie vegetală**, 2 partie, t. IV, 1982, 408 p.

I. G. MURGULESCU, RODICA VÎLCU, **Introducere în chimia fizică. Vol. III, Termodinamica chimică**, 1982, 624 p.

I. G. MURGULESCU, J. PĂUN, **Introducere în chimia fizică. Vol. I. 3. Nucleul atomic, reacţii nucleare, particule elementare**, 1982, 606 p.

ELENA CEAUŞESCU, **Noi cercetări în domeniul compuşilor macromoleculari**, 1981, 536 p.

I. G. MURGULFSCU, TATIANA, ONCESCU, E. SEGAL, **Introducere în chimia fizică, Vol. II, 2, Cinematică chimică şi cataliză**, 1981, 1024 p.

LYDIA-MARIA VAICUM, **Epurarea apelor uzate cu nămol activ. Bazele biochimice**, 1981, 218 p.

I. GĂLĂŢEANU, **Procese şi metode radiochimice în energetica nucleară**, 1981, 234 p.

O. IORDACHE, **Procese polistocastice aplicate la fenomenele de transfer**, 1981, 186 p.

CR. SIMIONESCU, VALERIA GORDUZA, **Polimeri biocompatibili şi biologic activi**, 1980, 479 p.

ELENA CEAUŞESCU, **Polimerizarea stereospecifică a izoprenului**, 1979, 307 p.

C. GH. MACAROVICI, **Analiza chimică cantitativă anorganică**, 1979, 457 p.

M. FLORESCU, **Metode ştiinţifice în dezvoltarea industriei chimice moderne**, 1979, 256 p.

A. T. BALABAN, I. GĂLĂŢEANU, G. GEORGESCU, LIGIA SIMIONESCU, **Compuşi marcaţi şi radiofarmaceutici cu aplicaţii în medicina nucleară**, 1979, 495 p.

I. G. MURGULESCU, E. SEGAL, **Introducere în chimia fizică. Vol. II. 1. Teoria molecular-cinetică a materiei**, 1979, 1036 p.

S. STERNBERG, FL. DANEŞ, **Termodinamica chimică aplicată**, 1978, 400 p.

I. G. MURGULESCU, V. EM. SAHINI, **Introducere în chimia fizică. Vol. I. 2. Structura şi proprietăţile moleculelor**, 1978, 604 p.

I. ZUGRĂVESCU, MAGDA PETROVANU, **N-ylid chemistry**, coédition avec McGraw-Hill International Book Company, U.S.A., 1977, 396 p.

I. G. MURGULESCU, **Introducere în chimia fizică. Vol. I. 1. Atomi, molecule, legătură chimică**, 1976, 560 p.

ELENA CEAUŞESCU, **Research work on synthesis and characterization of macromolecular compounds, Contributions**, 1974, 251 p.

CR SIMIONESCU, VIORICA RUSAN, V. POPA, **Chimia algelor marine**, 1974, 212 p., 1 pl.

ISSN 0035—3930

1986 MAJ 2 2

c. 2009–I.P. INFORMAŢIA

43 426

Lei 40

$ 80 (pour un abonnement annuel)

F 1103

66

ACADÉMIE DE LA RÉPUBLIQUE SOCIALISTE DE ROUMANIE

REVUE ROUMAINE DE CHIMIE

TOME 31

N° 5

Mai 1986

Rev. Roumaine Chim.

RRCHAX, 31, 5, p. 459–564 (1986), Bucarest

EDITURA ACADEMIEI REPUBLICII SOCIALISTE ROMÂNIA

ACADÉMIE DE LA RÉPUBLIQUE SOCIALISTE DE ROUMANIE

COMITÉ DE RÉDACTION

Rédacteur en chef:

I. G. MURGULESCU, membre de l'Académie de la République Socialiste de Roumanie

Rédacteurs en chef adjoints:

A. T. BALABAN et V. EM. SAHINI, membres correspondants de l'Académie de la République Socialiste de Roumanie

Collège de rédaction:

EM. BRATU, ELENA CEAUȘESCU, ECATERINA CIORĂNESCU-NENITZESCU, CR. SIMIONESCU, membres de l'Académie de la République Socialiste de Roumanie, S. SPACU, membre correspondant de l'Académie de la République Socialiste de Roumanie; M. BANCIU, M. D. GHEORGHIU, I. HAIDUC, D. I. MARCHIDAN, G. NIAC et D. SĂNDULESCU

La Revue Roumaine de Chimie paraît 10 fois par an. Toute commande de l'étranger sera adressée à « ROMPRESFILATELIA » — sectorul Export-Import Presă, P.O. Box 12—201, télex 10376 prsfi r 78104, Calea Griviței, nr. 64—66, București, Roumanie.

Les manuscrits, les livres et les revues proposés en échange, ainsi que toute correspondance seront envoyés à la rédaction :

REVUE ROUMAINE DE CHIMIE

125, Calea Victoriei, 79717 Bucarest, Roumanie, téléphone 50 76 80

EDITURA ACADEMIEI REPUBLICII SOCIALISTE ROMÂNIA
125, Calea Victoriei, 79717 Bucarest, Roumanie, téléphone 50 78 60

REVUE ROUMAINE DE CHIMIE

Tome 31, N° 5 **Mai, 1986**

VALENTINA LĂZĂRESCU, O. RADOVICI and M. VASS, Cyclic voltammetry studies on oxygen/silver system 461–471

VIOREL BRÂNZOI, AHMED KABIR and MIHAI CIOPEC, Corrosion kinetics of Armco iron in aqueous solution of citric acid 473–480

ROBERT SCHWARTZ, ANIKÓ JUHÁSZ and PETRONELA COLŢEA, Comparative study of the IR spectra of some B-nor and natural steroids . . 481–488

NARENDRA NATH and L.P. SINGH, Kinetics and mechanism of osmium(VIII) catalysed oxidation of benzyl alcohol and benzylamine by alkaline hexacyanoferrate(III) ion 489–496

KERIMAN GÜNAYDIN and ÜLKÜ OYMAN, Investigation of dehydration products of aryl and arylalkyl cyclododecanols 497–501

M. BANCIU, DANA ELIAN, M. ELIAN, LIGIA STĂNESCU and ECATERINA CIORĂNESCU, 4b,10b-dihydrochrysene, a new dibenzo$(CH)_{10}$ hydrocarbon 503–506

MICHAELA STĂNESCU, FLORIN BADEA and GHEORGHE MIHAI, The acetolysis of ditosylates with a bicyclo[4.4.0]decane skeleton 507–518

EMERIC BARTHA, ZSOLT ARVAY and ALEXANDRU C. RĂZUŞ, Synthesis of benzospiro[2,4]heptane derivatives 519–524

C.I. CHIRIAC, Amides from N-acylphthalimides and aliphatic amines 525–527

B.T. THAKER and PURNIMA B. THAKER, Synthesis and characterization of mixed ligand Schiff base complexes formed by template method . . . 529–532

M.M. ISMAIL and M.S. MOHAMED, Synthesis of certain substituted benzopyranopyridine and pyrimidine ring systems 533–539

N. A. SHAMS, A. A. HAMED, S. G. DONIA and S. A. SHAKER, Synthesis of 4-aroyl-4,5-dihydro-2(3H)-furanones and their reactions with some nucleophiles 541–546

MIHAI TALABĂ, Computer use of nitrophosphate fertilizers. Computer-aided analysis of the nitric decomposition of phosphatic raw materials . . . 547–564

Rev. Roumaine Chim. **31**, 5, 459–564 (1986), Bucarest

Revue Roumaine de Chimie, **31**, *5*, 461–471 (1986)

CYCLIC VOLTAMMETRY STUDIES ON OXYGEN/SILVER SYSTEM

VALENTINA LĂZĂRESCU*, O. RADOVICI** and M. VASS*
* ICECHIM — Center of Physical Chemistry, Spl. Independenţei 202, Bucharest 79611, Romania
**IPB — Faculty of Chemical Technology, Chemistry Department, Bucharest, Romania

Received April 13, 1985

Cyclic voltammetry has been used to investigate the anodic oxidation of silver in alkaline solutions. Particular attention has been given to the Ag(I) region. The influence of the potential sweep rate and the potential sweep anodic limit as well as the effects of alkali concentration and chloride ions addition have been examined. The experimental results have shown that after the dissolution of silver(I) hydroxy complexes, two layers of Ag_2O, a subsurface one and a surface one, were formed.

INTRODUCTION

The interaction between oxygen and silver has long been a favourite subject for both gas — solid and electrolyte — solid interface studies. The interest for this system, shown by technologists and academic workers, is due to the silver quality as unique catalyst for ethylene epoxidation, on the one hand, or as cathodic material in primary and secondary batteries, on the other hand.

The most modern methods of the surface physics (XPS, LEED, IS, HREELS) have been used for the characterization of the oxygen adsorbed on silver. Three different species have been identified[1–4] : a diatomic oxygen, stable only at $T \leqslant 173$ K, a monoatomic chemisorbed (in fourfold coordination) oxygen and a monoatomic subsurface oxygen.

Although extensively studied,[5–17] the anodic oxidation of silver in alkaline solutions is not however, well understood. Anodic oxidation performed by appropriate electrochemical techniques (galvanostatic,[5,9] cyclic voltammetry,[5,9–12,14,16] ac — impedance,[12–14,16] rotating — disk electrode[15] coupled with X — ray diffraction and electron microscopic investigations[8] revealed two well-defined oxides : Ag (I) oxide ($E^\circ = 0.338$ V[18]) and a higher oxide formulated Ag (I) Ag (III) O_2 ($E^\circ = 0.599$ V[19]). However, there are other two anodic processes occurring before the formation of these oxides : a minor one, usually ignored[10,11,15,16] and a more important one, which, for various reasons, was assigned as AgOH formation[5,10], H_{ads} desorption[7], Ag_2O[14,15] or silver dissolution.[16,17]

It is the aim of this paper to investigate these two processes taking place on the silver electrode in the first stage of its anodic oxidation in KOH solutions.

EXPERIMENTAL

The measurements were performed in potassium hydroxyde (Chemapol pro analyse reagent) aqueous solutions in the presence or absence of chloride ions. The concentration range was 0.1 M — 1 M in KOH and 0.01 M — 1 M in KCl, in 1 M KOH.

A polycrystalline silver 0.1 mm sheet (Goodfellow Metals 99.95 % purity) with a geometric surface area of 1.1 cm^2 has been used as test electrode. The silver electrode was washed prior to each experiment in a mixture of $H_2O_2 : NH_3 : H_2O$ (1 :1 :3) and rinsed several times with twice distilled water. The experiments were carried out in a conventional two-compartments glass cell at room temperature.

A saturated calomel electrode (SCE) connected via a Luggin cappilary to cell was used as reference. The cyclic voltammograms were carried out with sweep rates ranging from 10 mV/s to 550 mV/s. For this purpose, a Tacussel Bipotentiostat (type BIPAD) coupled with a Tacussel function generator (GSTP — 2 Al) was used. The voltammograms were recorded with a X—Y Hewlett-Packard recorder.

RESULTS

The anodic oxidation of silver in KOH solutions is characterized by a voltammogram similar to those reported previously in literature.[11,16] Figure 1 shows a typical current-potential curve for the silver electrode, recorded in 1 M KOH at a sweep rate, v, of 10 mV/s.

A careful examination of this plot points out four distinct processes A, B, C and D before the oxygen evolution.

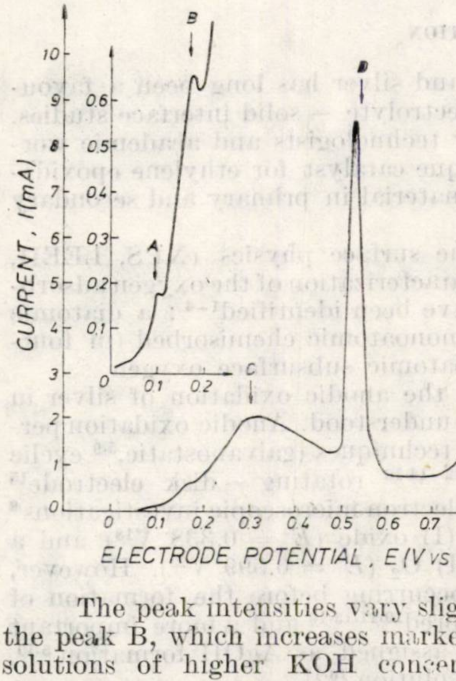

Fig. 1. — Current — potential curve for Ag oxidation in 1 M KOH at $v = 10$ mV/s pointing out the four anodic processes (A, B, C, D).

The peak intensities vary slighty during the first sweeps, except for the peak B, which increases markedly in the second run, particularly for solutions of higher KOH concentrations (Fig. 2). A decrease of the charge corresponding to peak C and an increase of that corresponding to peak B are also observed. However, after 4—5 cycles, all the peaks become superimpossable.

In order to obtain more information concerning the electrode processes preceding the Ag_2O formation phase, the effects of the sweep rate and sweep anodic limit variations, as well as the influence of KOH concentration and KCl addition have been investigated. As it has been already mentioned, particular attention is given in the present study to the silver oxidation to Ag_2O. Therefore, only the results referring to the first three anodic peaks will be presented.

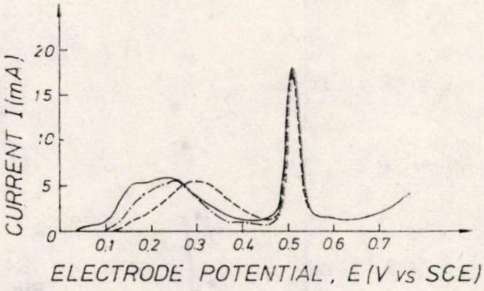

Fig. 2. — Current — potential curves for Ag oxidation in 5 M KOH at $v = 10$ mV/s recorded in the 1st run (- -), the 2nd run (- .), the 4th run and the following ones (—).

Sweep rate effects

The increase of the sweep rate results in an increase of all the anodic peak intensities, as it has been observed for other systems too.[20,21] The peak intensities, I_p, increase with the sweep rate regardless of the nature of the electrode processes. However, according to the theoretical approaches of the method, this increase is proportional to v for processes controlled by the charge transfer step[22] and to $v^{1/2}$ for those limited by diffusion.[23,24] Therefore, establishing the functional dependence $I_p = f(v)$, we have an important criterion to find out what kind of electrode process is involved.

The most convenient exploration of this relation is in the logarithmic form. A plot log I_p *vs* log v yields a straight line in both cases, but the slope will be 1 for the charge transfer controlled processes and 0.5 for those limited by diffusion. Figure 3 shows this dependence for the three anodic processes occurring in the first stage of the oxidation of the silver surface.

Values of $\delta \log I_p / \delta \log v$ show that processes A and B are going in conditions near to those of charge transfer, respectively mass transport control. Only process C does not integrate itself with the simple patterns presented, having more complex kinetics.

Other differences between these three anodic processes are revealed by the comparison of the sweep rate induced changes on the coulombic charges, as can be seen in figure 4.

Q_A increases slighty only at $v \geqslant 200$ mV/s, while Q_B and Q_C decrease pronouncedly with v rise, emphasizing the distinction between the first process, independent of HO^- diffusion in solution and the other two ones, considerably influenced by this phenomenon.

The slight increase of Q_A observed at high sweep rate values is due to the increased capacity contribution of the current.

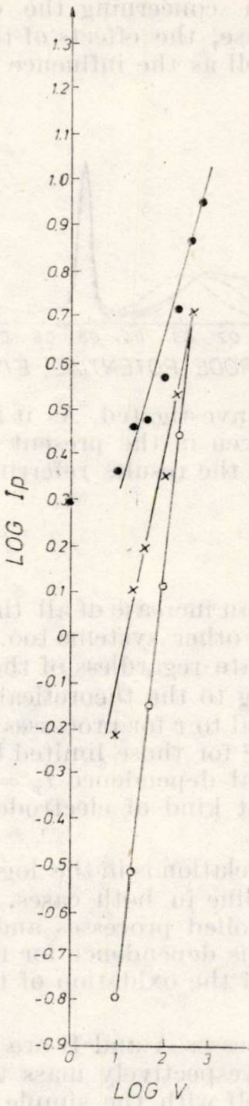

Fig. 3. — Dependence of peak current (I_p) on sweep rate (v) for anodic peaks: A(○), B(×) and C(●) ($\text{tg}\,\alpha^A = 0.95$; $\text{tg}\,\alpha^B = 0.52$; $\text{tg}\,\alpha^C = 0.32$).

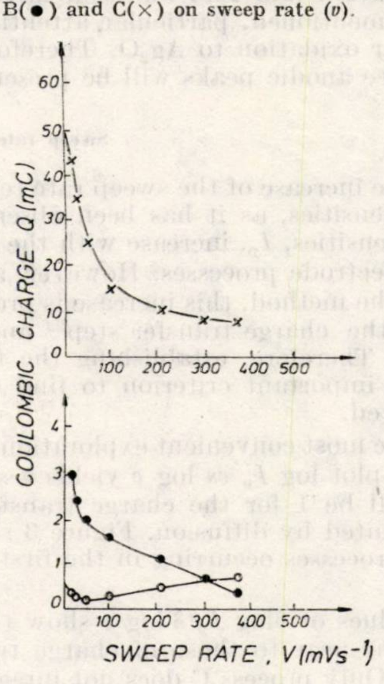

Fig. 4. — Dependence of coulombic charge (Q) corresponding to peaks: A(○), B(●) and C(×) on sweep rate (v).

Influence of KOH concentration

The potentiodynamic profile of silver in KOH solution is also strongly dependent on the KOH concentration, c. As KOH concentration increases, rises of coulombic charges and shiftings towards less positive values take place for all the anodic peaks, as is seen in figure 5.

The three anodic processes do not however behave in the same way. As is shown in figure 6, charges under the first two peaks have practically constant values in lower KOH concentrations (⩽ 1 M), increasing only in the concentrated solutions. The charge involved in process C is, on the contrary, increasing in diluted solutions and less affected by the changes in the higher KOH concentrations.

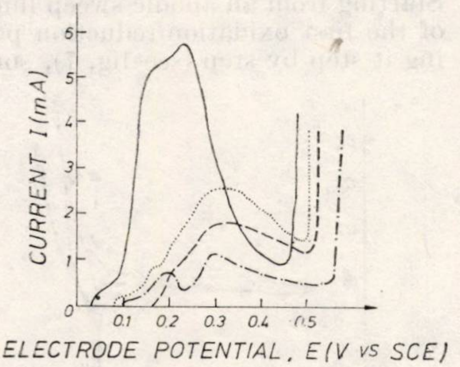

Fig. 5. — Current — potential curves for Ag oxidation in 0.1 M KOH (-.), 0.5 M KOH (--), 1 M KOH (...) and 5 M KOH (—) at $v = 10$ mV/s.

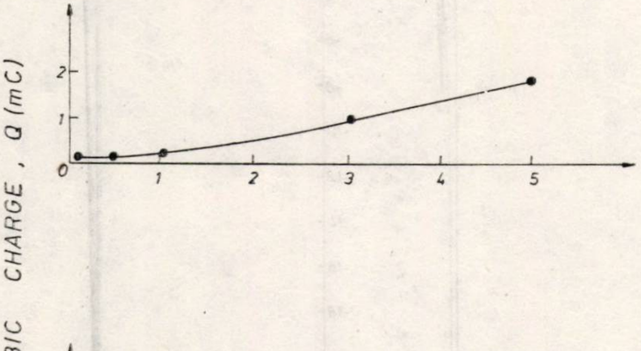

Fig. 6. — Dependence of coulombic charge (Q) corresponding to peaks: A(●), B(○) and C(×) on KOH molarity.

Sweep anodic limit variation

The technique of the sweep anodic limit variation may provide further information concerning the processes developing on the electrode surface. Starting from an anodic sweep limit which is convenient for the isolation of the first oxidation/reduction process on the silver surface and increasing it step by step (see fig. 7), some features are to be reported.

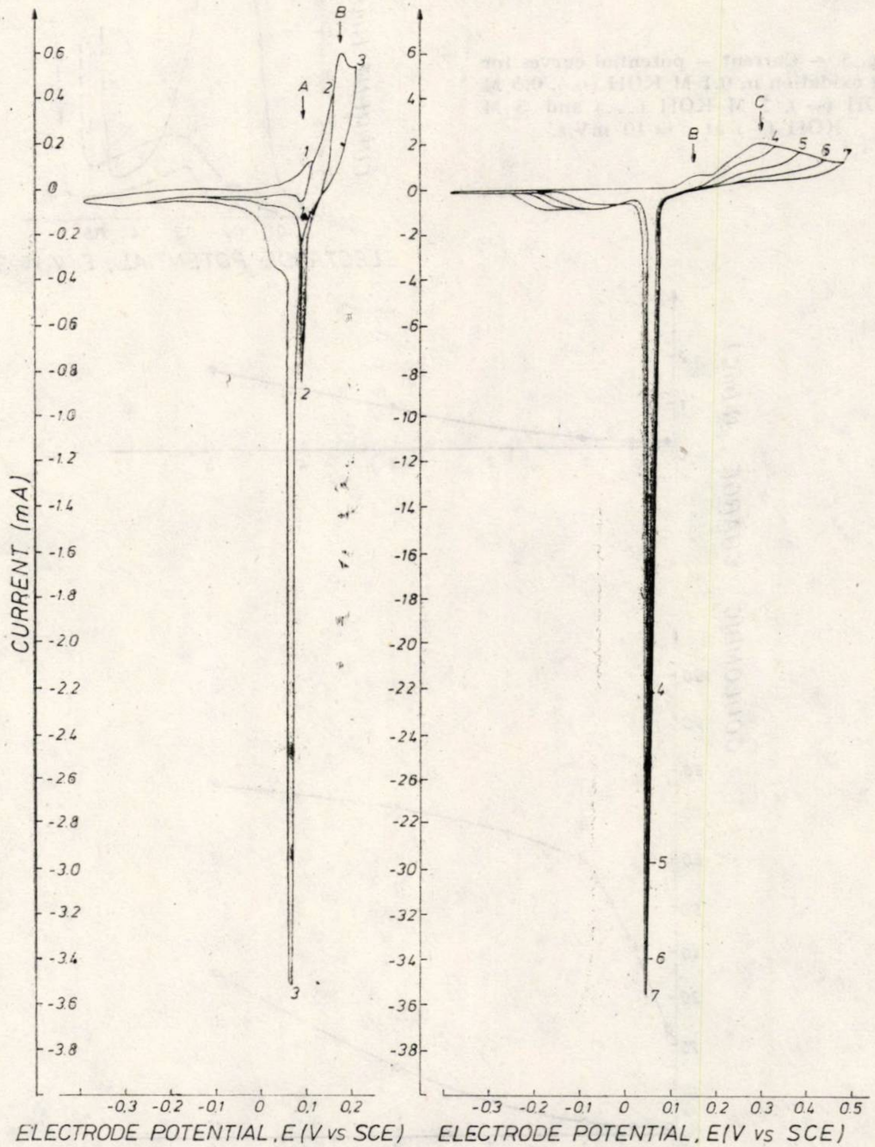

a. b.

Fig. 7. — Cyclic voltammograms of Ag electrode in 1 M KOH at $v = 10$ mV/s illustrating the effect of varying the anodic potential sweep limit from 0.1 to 0.2 V(SCE); *a* — sweeps 1 ÷ 3 and from 0.2 to 0.5 V (SCE); *b* — sweeps 4 ÷ 7.

It can be seen that the reduction of the species resulted in the three anodic processes concerned interfere strongly, occurring in a narrow potential range. Peaks B and C have obviously, a commun cathodic correspondent. A pronounced difference between the anodic and cathodic branches of the process A have been also observed. This difference is no longer maintained however, at higher sweep rate values (see fig. 8), which suggests formation of a soluble product diffusing away in solution when there is enough time for it (slow sweeps).

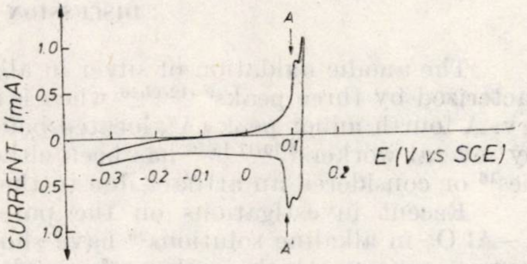

Fig. 8. — Cyclic voltammogram of Ag electrode in 1 M KOH at $v = 100$ mV/s with the anodic sweep limit $E_a = 0.1$ V (SCE).

Effects of Cl⁻ addition

Addition of potassium chloride to the base electrolyte brings about some modifications of the voltammogram shape. In fact, we observed only changes of the peak to peak ratio and no other electrode processes. The effects of Cl^- addition were examined in solutions 0.01 M and 0.1 M KCl in 1 M KOH. As can be seen in figure 9, in solution of lower Cl^- concentration, areas of peaks A and B increase while that of peak C decreases. Consequently, the coulombic charges involved in the first two processes increase from 0.3 mC to 1 mC (A), respectively from 3 mC to 21 mC (B) and that associated to peak C decreases from 51.6 mC to 36.3 mC. Repeated scans, especially the slower ones, result in a pronounced rise of the peak B.

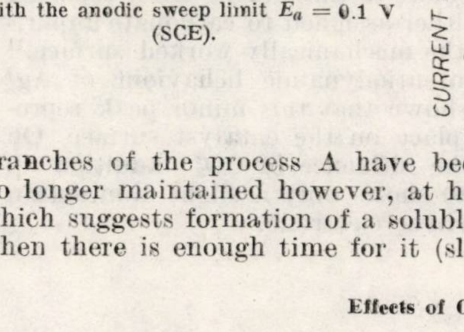

Fig. 9. — Current — potential curves for Ag oxidation in 1 M KOH (...), 0.01 M KCl in 1 M KOH (—) and 0.1 M KCl in 1 M KOH (— .) at $v =$ $= 10$ mV/s.

In the higher Cl^- concentration (1 M KCl), an increase of all the anodic peaks is observed, but the most striking one is that of the first peak : the charge is raised from 0.3 mC (in 1M KOH) to 84.7 mC. In addition, all the peaks become higher and higher from scan to scan, as a result of a developing surface roughening brought about by an important dissolution process.

DISCUSSION

The anodic oxidation of silver in alkaline solutions is generally characterized by three peaks[9-12,14,16] when is investigated by cyclic voltammetry. A fourth minor peak (A), located before to these three ones, reported by several workers[6,10,11,15,16] has been either assigned to carbonate impurities[16] or considered an artifact due to the mechanically worked surface.[11]

Recent investigations on the potentiodynamic behaviour of Ag/ $\alpha-Al_2O_3$ in alkaline solutions[25] have shown that this minor peak represents a process which is also taking place on the catalyst surface. On the other hand, the examination of the influence of CO_3^{2-} addition up to 10% in KOH solution (see fig. 10) shows only a slight diminution of the potentiodynamic peaks of the silver electrode.

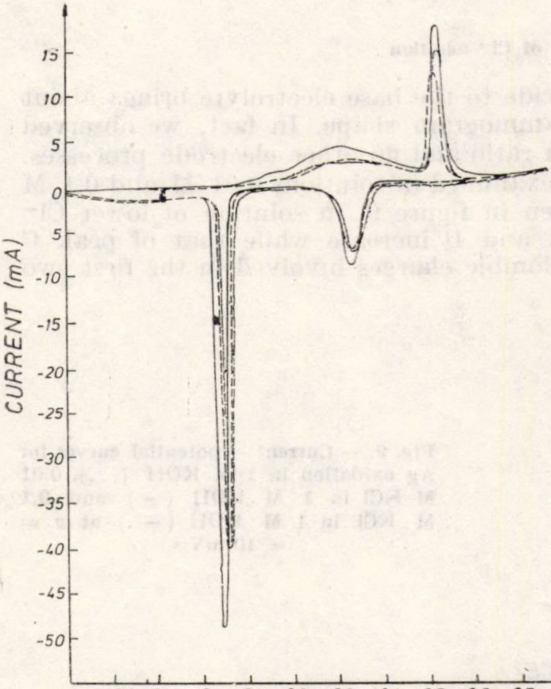

Fig. 10. — Cyclic voltammograms of Ag electrode in 1 M KOH (--), 5% K_2CO_3 in 1 M KOH (- .) and 10% K_2CO_3 in 1 M KOH (- -) at $v = 10$ mV/s.

The process that seems to be the best fitted to the features pointed out, is silver dissolution, taking place in three steps : silver atom ionization

$$Ag \rightarrow Ag^+ + e^- \tag{1}$$

followed by the fast complexation reaction (2) resulting in negative silver hydroxy complexes

$$Ag^+ + x\,HO^- \rightleftharpoons Ag(HO)_x^{1-x} \qquad (2)$$

that would leave the electrode surface by diffusion or discharge themselves in the subsequent step. Evidences have been found that $Ag(OH)_2^-$ ions are predominating in concentrated KOH solutions (5M).[26]

The increase of the corresponding coulombic charge, Q_A, in the presence of the chloride anions, particularly in higher concentration, strengthens our assumptions. The higher chloride concentration enhances the silver tendency to form complex anions:[27]

$$Ag^+ + n\,Cl^- \rightleftharpoons AgCl_n^{1-n} \qquad (3)$$

as well as the higher alkali concentrations[15,28], when an increase of Q_A has been also observed (see fig. 6). According to a simple estimation, in 1 M KOH the amount of dissolved silver, evaluated from Q_A, is no greater than 1.5 monolayers of silver atoms (approx. 1.8×10^{15} Ag atoms). Therefore, unimportant changes are expected. However, when 0.1 M KCl is added to the base electrolyte, about 4×10^3 monolayers of silver atoms leave the electrode surface as $AgCl_n^{1-n}$ and a pronounced surface roughening is expected to develop. The marked increase of all the anodic peaks, higher and higher on repeated scans, supports our assumptions. These are also in a good agreement with both the thermodynamic approaches[29] according to which the metal dissolution has to precede the formation of the lowest oxide and the Faradaic impedance studies certifying the presence of soluble species as $Ag(OH)_2^-$ before the Ag_2O monolayer phase formation[14] on the electrode surface.

The next anodic process, represented by peak B, is the first step of the silver oxidation to Ag_2O, which is generally accepted to be characterized by two potentiodynamic peaks.[12,14,16] However, although there is an agreement regarding the significance of the more anodic peak (C), the formation of a thick layer of Ag_2O,[6,10,12,14,16] divergences referring to the former process are still persisting.[4,7,10,14–17]

We suggest that this first step may be represented by the thin dense firstly formed layer of Ag_2O (clearly observed in X-ray diffraction and electron microscopy studies[8]) beside the thick, porous Ag_2O deposit subsequently formed. A rough estimation of the charge required by the formation of an Ag_2O monolayer leads, considering each 0 atom bound by two Ag atoms, to a value of 0.2 mC/cm^2. Therefore, taking into account the charge under peak B, the corresponding oxide thickness is evaluated at about 15 monolayers, in agreement with our assumptions.

The formation of this first dense layer of Ag_2O has to be related to the well-known possibility of 0 atom to penetrate the silver lattice. All the recent studies on the oxygen adsorption on silver[1–4] agree on the existence of a subsurface oxygen, which besides, seems to play an important role in ethylene epoxidation.[30,31]

In view of all these facts, the first stage of the silver oxidation to Ag_2O may be considered as taking place in the following steps: HO^- diffusion towards the electrode, discharge reaction of HO^- ions:

$$2\ Ag + 2\ HO^- \rightarrow Ag_2O + H_2O + 2\ e^- \tag{4}$$

and, concomitantly, that of $Ag(OH)_2^-$ ions remaining in the electrode neighbourhood:

$$Ag + Ag(OH)_2^- \rightarrow Ag_2O + H_2O + e^- \tag{5}$$

and O^{2-} ion diffusion in silver lattice.

The second stage, formation of the thick porous layer of Ag_2O occurs, as we have shown, differently. Indeed, the process C is dependent but not controlled by HO^- diffusion and leads to a thick deposit estimated at about 300 monolayers. Careful galvanostatic and potentiostatic transient studies[9,12] have shown that the anodic oxidation of silver in this step is limited by Ag^+ diffusion / migration through the firstly formed dense layer.

During the reverse sweep, besides the oxide reduction:

$$Ag_2O + H_2O + 2\ e^- \rightarrow 2\ Ag + 2\ HO^- \tag{6}$$

the oxide dissolution is also taking place:

$$Ag_2O + H_2O + 2\ e^- \rightarrow 2\ Ag(OH)_2^- \tag{7}$$

as it has been shown in a coupled potential sweep and ac-impedance study of the silver oxides.[16] Moreover, the solubility of Ag_2O was found to increase with the increase of KOH molarity.[15,28] Therefore, changes of surface roughness and surface area are expected in the first runs, until a stationary "reacting surface" is attained, especially in the more concentrated solutions. The enhanced dissolution of silver in the presence of Cl^- ions has the same effect. An increased surface roughness is associated with a higher density of defects making easier the Ag lattice penetration for O^{2-} ions. Indeed, pronounced increases of Q_B are observed in the higher KOH concentrations, on repeated scans and when KCl is added to the base electrolyte. The higher values of Q_B mean however, a thicker dense firstly formed oxide layer which is a barrier for Ag^+ ions in their way to surface. For that reason, every time when Q_B increases, a decrease of Q_C is observed.

CONCLUSION

The first process of the anodic oxidation of silver in alkaline solutions is the metal dissolution as $Ag(OH)_2^-$. These complex anions diffuse away into solution or/and discharge themselves together with HO^- ions in the next anodic process. The O^{2-} ions resulted penetrate the silver lattice forming a dense thin oxide layer. The development of a thick porous Ag_2O layer limited by Ag^+ diffusion/migration through the dense layer ends the first stage of the anodic oxidation of silver.

REFERENCES

[1] R. W. Joyner and M. W. Roberts, *Chem. Phys. Lett.*, **60**, 459 (1979).

[2] C. Backx, C. P. M. De Groot and P. Biloen, *Surf. Sci.*, **104**, 300 (1981).

[3] G. Rovida, F. Pratesi and E. Ferroni, *Appl. Surf. Sci.*, **5**, 121 (1980).

[4] W. M. H. Sachtler, C. Backx and R. A. Van Santen, *Catal. Rev.*, **23**, 127 (1981).

[5] A. Hickling and D. Taylor, *Disc. Faraday Soc.*, **1**, 277 (1947).

[6] T. P. Dirkse and D. B. De Vries, *J. Phys. Chem.*, **63**, 107 (1959).

[7] T. G. Clarke, N. A. Hampson, J. B. Lee, J. R. Morley and B. Scanlon, *Can. J. Chem.* **46**, 3437 (1968).

[8] G. W. D. Briggs, M. Fleishmann, D. J. Lax and H. R. Thirsk, *Trans. Faraday Soc.*, **64**, 3120 (1968).

[9] M. Fleishmann, D. J. Lax and H. R. Thirsk, *Trans. Faraday Soc.*, **64**, 3128, 3137 (1968).

[10] P. Stonehart, *Electrochim. Acta*, **13**, 1789 (1968).

[11] P. Stonehart and F. P. Portante, *Electrochim. Acta*, **13**, 1805 (1968).

[12] Z. Takehara, Y. Namba and S. Yoshizawa, *Electrochim. Acta*, **13**, 1395 (1968).

[13] R. D. Giles, J. A. Harrison and H. R. Thirsk, *J. Electroanal. Chem.*, **22**, 375 (1969).

[14] R. D. Giles and J. A. Harrison, *J. Electroanal. Chem.*, **27**, 161 (1970).

[15] B. Miller, *J. Electrochem. Soc.*, **117**, 491 (1970).

[16] B. V. Tilak, R. S. Perkins, H. A. Kozlowska and B. E. Conway, *Electrochim. Acta*, **17**, 1447 (1972).

[17] B. G. Pound, D. B. Macdonald and J. W. Tomlinson, *Electrochim. Acta*, **25**, 563 (1980).

[18] T. P. Dirkse, *J. Chem. Eng. Data*, **6**, 538 (1961).

[19] T. P. Dirkse, *J. Electrochem. Soc.*, **109**, 173 (1962).

[20] J. P. Carr and N. A. Hampson, *J. Electrochem. Soc.*, **118**, 536 (1971).

[21] D. D. Macdonald and D. Owen, *J. Electrochem. Soc.*, **120**, 317 (1973).

[22] S. Srinivasan and E. Gileadi, *Electrochim. Acta*, **11**, 321 (1966).

[23] P. Delahay, "New Instrumental Methods in Electrochemistry", Ch. 6, Interscience, New York, 1954.

[24] D. D. Macdonald, "Transient Techniques in Electrochemistry", Ch. 4, Plenum Press, New York, 1977.

[25] V. Lăzărescu, M. Vass, O. Radovici, C. Dașoveanu, M. Stanciu and M. Tolan, *Rev. Roumaine Chim.*, **30**, 933 (1985).

[26] P. J. Antikainen, S. Hietanen and L. G. Sillén, *Acta Chem. Scand.*, **14**, 95 (1960).

[27] R. D. Giles, *J. Electroanal. Chem.*, **27**, 11 (1970).

[28] R. F. Amlie and P. Ruetschi, *J. Electrochem. Soc.*, **108**, 813 (1961).

[29] B. G. Pound, D. D. Macdonald and J. W. Tomlinson, *Electrochem. Acta*, **24**, 929 (1979).

[30] C. Backx, J. Moolhuysen, P. Geenen and R. A. Van Santen, *J. Catal.*, **72**, 364 (1981).

[31] R. Haul, D. Hoge, G. Neubauer and U. Zeeck, *Surf. Sci.*, **122**, L622 (1982).

Revue Roumaine de Chimie, **31**, *5*, 473–480 (1986)

CORROSION KINETICS OF ARMCO IRON IN AQUEOUS SOLUTION OF CITRIC ACID

VIOREL BRÂNZOI*, AHMED KABIR** and MIHAI CIOPEC**

* Department of Physical Chemistry and Electrochemical Technology, Polytechnic Institute, Bucharest, Romania

** Department of Chemistry, Institute of Petroleum and Gas, Blvd. Bucureşti, No. 39, 2000 Ploieşti, Romania

Received April 29, 1985

Using potentiostatic method, corrosion of iron Armco was studied in aqueous solution of citric acid as well as in the mixture of citric acid, sodium citrate and water, keeping constant either hydrogen ions or citrate ions. Kinetic parameters of corrosion determined from the polarisation curves suggest a mechanism of dissolution of the Bockris-Kelly type, similar to those of the aqueous inorganic acids. Increase of acid concentration has the following effect:

— displacement of the polarisation curves towards more negative potentials;
— increase of corrosion rate:
— increase of limiting current densities of diffusion.

At high over voltage and at concentrations of citric acid greater than 0.1 M lead to the appearance of active-passive transition. Appearance of passivity is due to the formation of some sparingly soluble citrates of the metal, which dissolve and cover the surface hindering from the progress of the processes at the interface metal/liquid phase.

INTRODUCTION

Study of corrosion of iron Armco in aqueous solution of citric acid has got a special importance in connection with the utilisation of this solution for washing initially the installations of crude oil refinery.

Citric acid, $C_6H_8O_7$, is a tricarboxylic monohydroxyacid and is a solvent of protic character in nature.[1–5] It contains a few or more hydrogen atoms of acid character, unlike the aprotic solvents which do not contain hydrogen atoms of acid character. Solutions of protic solvents and water behave similarly to the solutions of inorganic acids in water, which means that from the physico-chemical point of view corrosion in such media belongs to the field of the processes that take place at the interface metal/liquid phase. So, corrosion of the iron Armco in aqueous solution of citric acid follows an electrochemical mechanism, which means that the transfer of charge between the aggresive agent and metal takes place.

In the present work, polarisation behaviour of iron Armco in aqueous solution of citric acid, similarly to the mixture of citric acid, sodium citrate and water (keeping constant either the concentration of hydrogen ions or citrate ions) with a view to establishing the mechanism of the reaction were studied.

EXPERIMENTAL PART

The polarisation curves were traced by using the potentiostatic method. Electrical fittings used in this scope and also in working cell were described in a previous work.[6] In all experiments accomplished, electrochemical polarisation was started after approximately 30 minutes from the immersion of the working electrode in electrolyte to allow sufficient time to stablize the static potential. Potential of the working electrode was varied gradually and the corresponding current that appeared in the external circuit was represented graphically as a function of the applied potential. It is to mention that potential of the working electrode was always measured in comparison with saturated calomel electrode.

To reduce the potential fall due to resistance, a single compartmental cell was used in which the working electrode placed in the centre of the cell was surrounded by an auxiliary electrode, made of platinum net. This sort of arrangement of the two electrodes creates an intense and uniform electric field at the time of anodic and cathodic polarisation.

To reduce ohmic drop of potential to a minimum, reference electrode and the working cell was connected through capillary Habber-Luggin and the solution was stirred continuously through bubbling of purified argon introduced at the bottom of the cell, through a glass tube fused at the cell wall with a provision of net at the end for the assurance of the uniform distribution of argon through the solution.

Working electrode of surface area 1 cm^2 was prepared fom iron Armco and was placed in the center of the cell. Before each determination, working electrode was polished mechanically with sand papers of different dimensions, degreased in boiling benzene for 5 minutes to give away the fats and polishing powder left on the surface after polishing. At last the working electrode was subjected to electropolishing to a current density of 85 mA/cm^2 for two minutes in a 4 :1 mixture of $HClO_4$ and CH_3COOH. After electropolishing, working electrode was washed with bidistilled water and then with the experimental solution and only after that it was introduced and fixed in the cell for electrochemical polarisation.

Previously, the experimental solution was deaerated with argon for one hour and deaeration was continued for all the time of determinaton. It is to mention that all the substances used were of purity p.a., and the solvent utilised was bidistilled water. With the help of the thermostat UM 210, the temperature of the experimental solution in the cell was kept constant as desired.

Registration of the polarisation curves was always done starting from the mixed potential of the static state. For each solution several determination swere done until a good reproductible result is obtained. During tracing of the polarisation curves we considered the fact that prolonged anodic polarisation may give rise to the modification of the electrode surface[7,8] which will lead to the modification of Tafel slopes. This aspect may be avoided by tracing the cathodic and after that the anodic polarisation curves. This method was also used by us in the present work.

RESULTS AND DISCUSSIONS

Polarisation curves of iron Armco in the aqueous solutions of citric acid of different concentrations are presented in figure 1a and 1b; Table 1 gives the kinetic parameters. Analysis of these polarisation curves shows that at low over voltage, the dissolution process is controlled by activation. Increase in concentration of citric acid has got the effect of displacement of the curves towards a more negative potential, increase of corrosion rate and the values of the limitting current densities. At

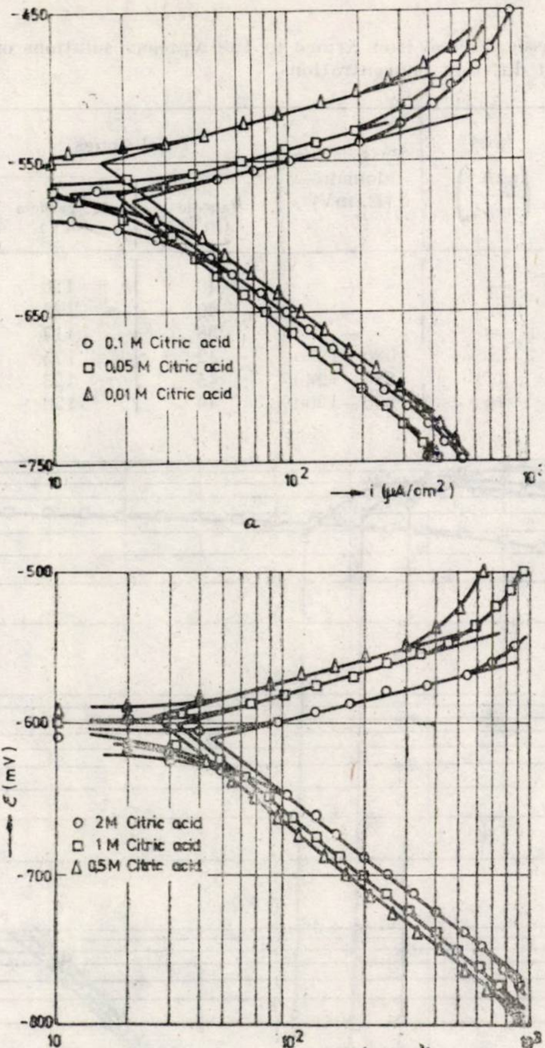

Fig. 1.a and b. — Polarisation curves of iron Armco in the aqueous solutions of citric acid of different concentrations.

high over voltage (Fig. 2) and a concentration of citric acid greater than 0.1 M, active-passive transitions appear. Passive domain increases with the increase of acid concentrations and passivation current densities decrease with increase of acid concentrations. Appearance of passivity is due to the formation of sparingly soluble citrate of the metal which dissolves and covers the surface hindering from the progress of the processes at the interface metal/liquid phase.

In continuation, cathodic and anodic polarisation curves of iron Armco in citric acid solution, sodium citrate and water are treated. In this case, the concentrations of the citrate ions are either varied keeping

Table 1

Kinetic parameters for corrosion and passivation of iron Armco in the aqueous solutions of citric acid of different concentrations

Concentration of the acid (M)	i_{corr} $\left(\frac{\mu A}{cm^2}\right)$	$-\varepsilon_{corr}$ (mV)	i_{pass} $\left(\frac{\mu A}{cm^2}\right)$	Passivation domain (E, mV)	Tafel slopes	
					b_{anodic} (mV)	$-b_{cathdic}$ (mV)
0.01	16	550	—	—	40	120
0.05	19	570	—	—	40	125
0.10	22	575	—	—	38	117
0.50	26	595	20	1020—1250	42	125
1.00	32	600	17	880—1240	45	125
2.00	45	610	15	800—1200	40	120

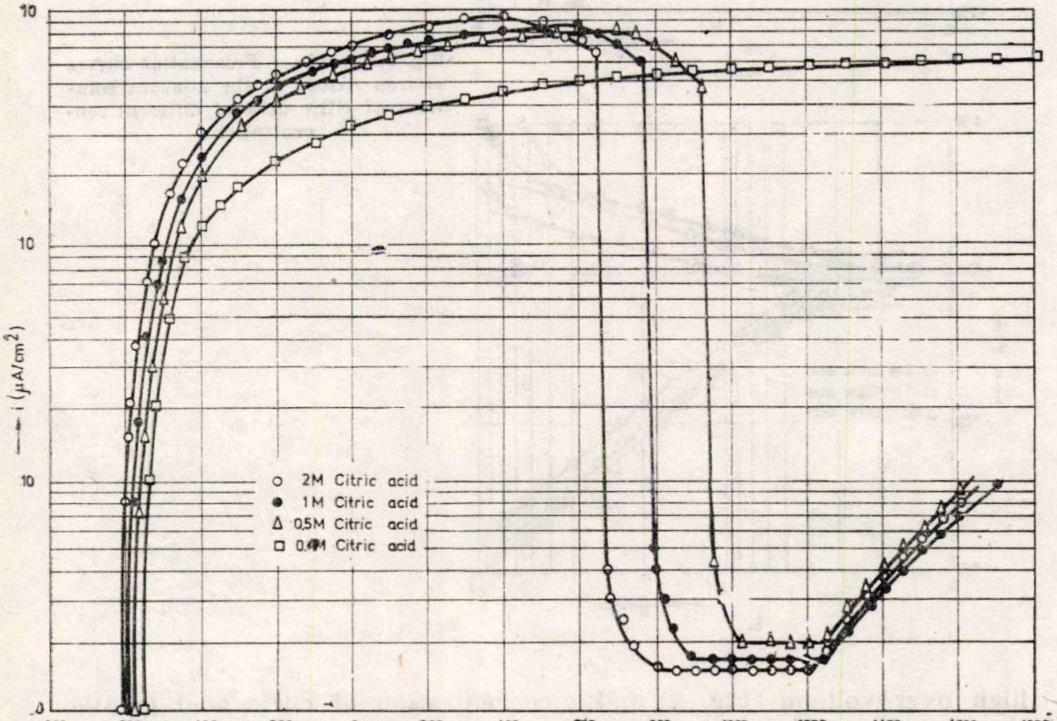

Fig. 2. — Displacement of the polarisation curves of iron Armco in the aqueous solutions of citric acid of increased concentrations.

the concentration of hydrogen ions constant or inversely. In figure 3 and 4 are presented cathodic and anodic polarisation curves obtained in these conditions and in tables 2 and 3 are presented kinetic parameters calculated from these curves. Analysing figure 3 and table 2 it is possible

Table 2

Kinetic parameters for corrosion of iron Armco in the aqueous solutions of citric acid and sodium citrate keeping the concentration of hydrogen ions constant (1 ion gram/dm^3)

Concentration (moles/dm^3)	i_{corr} (μA/cm^2)	Tafel slopes		$-E_{corr}$ (mV)
		b_{anodic} (mV)	$-b_{cathodic}$ (mV)	
0.4 citric acid 0.2 sodium citrate	29	45	120	610
0.4 citric acid 0.4 sodium citrate	31	45	120	620
0.4 citric acid 0.6 sodium citrate	33	45	120	620
0.4 citric acid 0.8 sodium citrate	39	40	120	630

to say that, increase in concentration of citrate ions, keeping constant the hydrogen ions concentration to 0.4 M, has the following effects:

— increase of corrosion rate represented by the corrosion current density;

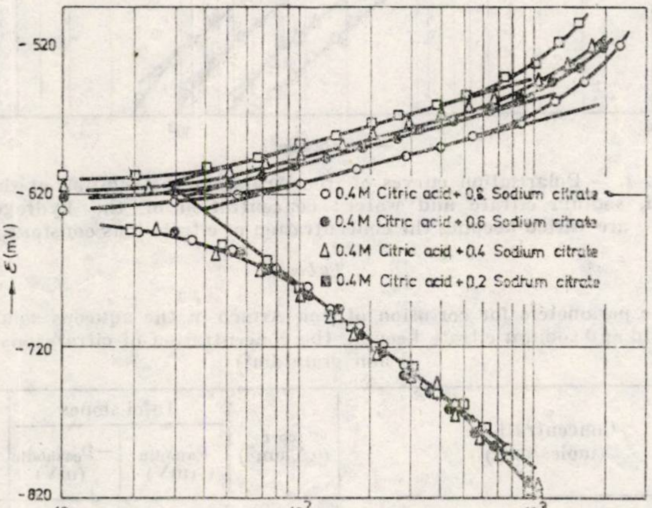

Fig. 3. — Polarisation curves of iron Armco in the solution of the citric acid, sodium citrate and water: concentration of the citrate ions is varied keeping the concentration hydrogen ions constant.

— overlapping of all cathodic curves demonstrates the fact that only hydrogen ions participate to the cathodic reduction reaction. When hydrogen ions concentration is kept constant, overlapping of the cathodic polarisation curves is a natural consequence of this fact;

- increase of limitting current densities of diffusion with increase of citrate ions concentration;
- anodic Tafel slopes are approximately 40 mV and cathodic Tafel slopes have got the usual values[9] of approximately 120 mV.

In figure 4 and table 3 is presented the reverse case of that presented in figure 3 and table 2, which means that keeping constant the citrate ions concentration to 1 M, hydrogen ions concentration was varied. In this case it is seen that corrosion rate is increased with the increase of hydrogen ions concentration and displacement of corrosion potentials

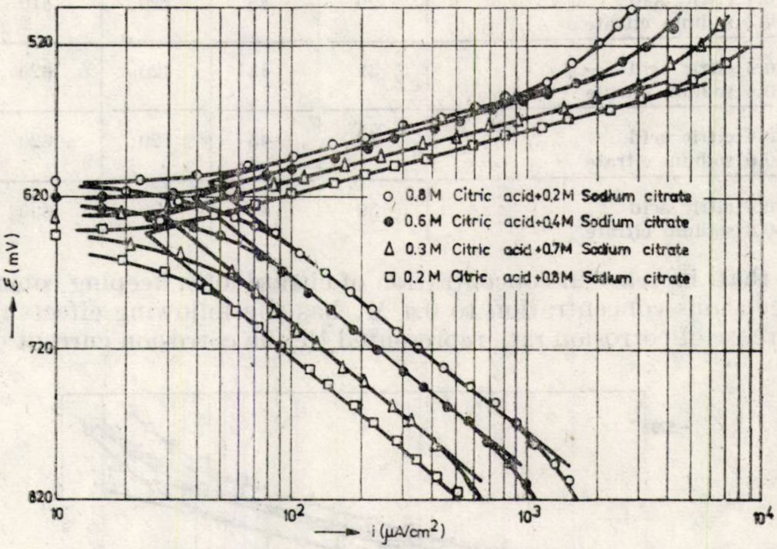

Fig. 4. — Polarisation curves of iron Armco in the solution of the citric acid, sodium citrate and water: concentration of the hydrogen ions are varied keeping the concentration of citrate ions constant.

Table 3

Kinetic parameters for corrosion of iron Armco in the aqueous solutions of citric acid and sodium citrate keeping tbe concentration of citrate ions constant (1 ion gram/dm³)

Concentration (moles/dm³)	i_{corr} (μA/cm²)	Tafel slopes		$-E_{corr}$ (mV)
		b_{anodic} (mV)	$-b_{cathodic}$ (mV)	
0.8 citric acid 0.2 sodium citrate	44	40	120	610
0.6 citric acid 0.4 sodium citrate	38	42	125	620
0.3 citric acid 0.7 sodium citrate	29	45	125	630
0.2 citric acid 0.8 sodium citrate	24	42	125	645

towards more positive values. This phenomenon is explained taking into consideration the fact that ε_{coor} has got the intermediate value between reversible potential of the reaction of hydrogen ions discharge and reversible potential of the reaction of metal dissolution. Similarly, anodic Tafel slopes and cathodic Tafel slopes are ascertained to be approximately 40 mV and 120 mV respectively.

Evaluation of the reaction order with respect to hydrogen ions is presented in figure 5. In the domain of anodic potential − 570 mV and − 545 mV and cathodic potential − 770 mV and − 720 mV, the reaction order is ± 1. The results obtained by us for the order of reaction, anodic and cathodic Tafel slopes correspond with the values obtained by other authors [9,10] for anorganic acid systems.

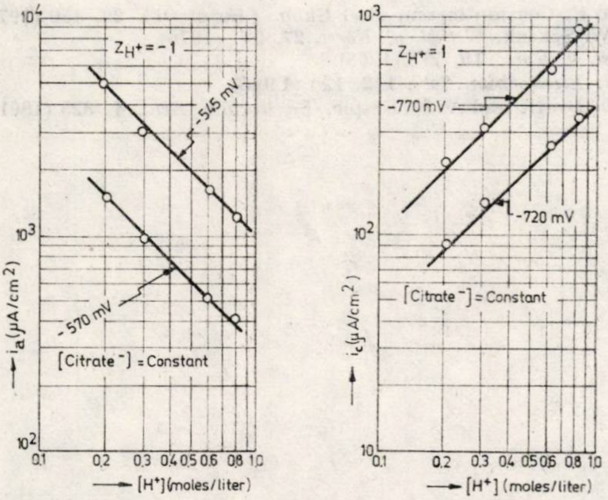

Fig. 5. — Evaluation of the reaction order between iron Armco and aqueous solutions of citric acid with respect to hydrogen ions.

On the basis of the kinetic parameters of corrosion determined by us for the system iron Armco in the aqueous solution of citric acid, it is possible to consider that in the said medium dissolution process of iron takes place through the mechanism of the type proposed by Bockris-Kelly, which follows :

$$Fe + H_2O \rightleftharpoons Fe \cdot H_2O_{ads}$$

$$Fe \cdot H_2O_{ads} \rightleftharpoons FeOH^-_{ads} + e^-$$

$$FeOH^-_{ads} \rightleftharpoons FeOH_{ads} + e^-$$

$$FeOH_{ads} \rightarrow FeOH^+ + e^- \quad \text{(rate determining step)}$$

$$FeOH^+ + H^+ \rightleftharpoons Fe^{++} + H_2O.$$

In conclusion it is possible to say that the polarisation behaviour of iron Armco in the aqueous solution of citric acid is similar to that of aqueous inorganic acids.

REFERENCES

[1] E. Price, "The chemistry of nonaqueous solvents" vol. 1, Academic Press, New York, 1966, p. 67, edited by J. J. Lagowski.

[2] H. Huber, "Titrations in nonaqueous solvents", Akad. Verlagages, Frankfurt, 1964, p. 327.

[3] R. G. Bates, "The chemistry of nonaqueous solvents", ed. by J. J. Lagowski, vol. 1, Academic Press, New York, 1966, p. 97.

[4] H. Strehlow, "The chemistry of nonaqueous solvents", edited by J .J. Lagowski, vol. 1, Academic Press, New York, 1966, p. 129.

[5] L. G. Gidin, W. A. Kasakowa and I. N. Putilova, *Doklady Akad. Nauk S.S.S.R.*, **80**, 777 (1951).

[6] V. Brânzoi and E. Constantinescu, *Rev. Chim. (Bucureşti)*, **29**, 450 (1978).

[7] E. Heitz and W. Schenk, *Werkst. u. Korr.*, **27**, 241 (1976).

[8] E. Heitz, *Werst. u. Korr.*, **19**, 773 (1968).

[9] E. J. Kelly, *J. Electrochem. Soc.*, **112**, 124 (1 965).

[10] J. O'Bokris, D. Drazic and A. R. Despic, *Electrochim. Acta*, **4**, 325 (1961).

Revue Roumaine de Chimie, **31**, *5*, 481–488 (1986)

COMPARATIVE STUDY OF THE IR SPECTRA OF SOME B-NOR AND NATURAL STEROIDS

ROBERT SCHWARTZ, ANIKÓ JUHÁSZ and PETRONELA COLȚEA
Chemical and Pharmaceutics Research Institute, Str. Fabricii No. 126, 3400 Cluj-Napoca, Romania

Received May 13, 1985

The B-ring contraction of the steroid molecule causes some changes in the spectral behaviour of the obtained B-nor-derivatives. We compared the IR spectra of some B-nor-steroids with those of the corresponding derivatives of the natural series. The essential differences between the IR spectra of the B-nor and the natural series in the stretching vibration range of the double bonds : $\nu C = C$, $\nu = C - H$ and $\nu C = O$ were observed.

INTRODUCTION

The steroid molecule is a quite rigid system which may be used as an "ideal" model for stereochemical studies. The B-nor-steroids are more suited for these studies since their molecules contain two six-membered and two five-membered rings. We can expect that the B-ring contraction may yield significant stereochemical consequences. In order to investigate the influence of the conformational changes on the spectral properties of these substances we compared the IR spectra of some B-nor-steroids with those of the corresponding derivatives of the natural series.

EXPERIMENTAL

The investigated substances of both series (excepting diosgenin) were prepared by our collective.[1–6] The IR spectra were recorded with a Specord 75R, C. Zeiss spectrophotometer.

The characteristic vibration bands of some B-nor and corresponding natural steroids are presented in Table 1 and 2.

RESULTS AND DISCUSSION

The essential differences between the IR spectra of the B-nor and the natural steroids are located in the stretching vibration range of the double bonds : $\nu C = C$, $\nu = C - H$ and $\nu C = O$.

The $C = C$ stretching vibration band of isolated double bond appears in the range 1620 –1675 cm^{-1}, its intensity being usually low.[7–9] A determinative factor of the band intensity is the symmetry of the double

Table 1

Characteristic IR stretching vibrations of some B-nor- and natural steroid derivatives

No.	Derivatives	Characteristic IR stretching vibrations				
		ν = C–H	νC–H	νC=C	Others ν	
1a	Diosgenin (KBr)	3025 vw	2980, 2923, 2900, 2862, 2837 s	—	3480 m	OH
1b	B-nor-Diosgenin (KBr)	3037 m	2961, 2935, 2862 s	1718 w, 1680 w 1637 m	3410 m	OH
2a	O-Acetyl-diosgenin (KBr)	3055 vw	2966, 2920, 2900, 2850 s	—	1725 s 1239 s	CO C–O–C
2b	O-Acetyl-B-nor-diosgenin (KBr)	3060 w	2960, 2890 s	1665 w	1729 s 1260 s	CO C–O–C
3a	O-Acetyl-pseudodiosgenin (KBr)	—	2962, 2943, 2906, 2875, 2852, 2826 s	1687 m	1725 s 1280 s	CO C–O–C
3b	O-Acetyl-B-nor-pseudodiosgenin (KBr)	3037 w	2950, 2935, 2906, 2850 s	1681 m	1723 s 1237 s	CO C–O–C
4a	5-Pregnene-3β-ol-20-one (KBr)	3025 w	2950, 2937, 2918, 2900, 2847, 2822 s	—	3500 m 1668 s	OH CO
4b	B-nor-5-Pregnene-3β-ol-20-one (KBr)	3031 w	2962, 2925, 2852 s	1626 w	3450 m 1687 s	OH CO
5a	3β-Acetoxy-5-pregnene-20-one (KBr)	3025 w	2937, 2900, 2877, 2865 s	—	1718, 1688 s 1230 s	CO C–O–C
5b	3β-Acetoxy-B-nor-5-pregnene-20-one (KBr)	3037 w	2941, 2925, 2907, 2877, 2848 s	1625 vw	1718, 1688 s 1225 s	CO C–O–C
6a	3β-Acetoxy-5,16-pregnadiene-20-one (KBr)	3037 w	2962, 2941, 2900, 2860 s	1575 s	1718, 1650 s 1237 s	CO C–O–C
6b	3β-Acetoxy-B-nor-5,16-pregnadiene-20--one (KBr)	3062 w	2962, 2937, 2912, 2850, 2825 s	1568 s	1718, 1653 s 1237 s	CO C–O–C
7a	3β-Acetoxy-5,16-pregnadiene-20-oxime ($CHCl_3$)	—	2952, 2916, 2868 s	—	1726 s 1252 s	CO C–O–C
7b	3β-Acetoxy-B-nor-5,16-pregnadiene-20--oxime ($CHCl_3$)	3032 w	2924, 2864 s	1580 w	1630 w 1720 s 1240 s	 CO C–O–C
8a	3β-Acetoxy-5-androstene-17-one (KBr)	—	2948, 2900, 2862, 2843 s	1662 w	1737, 1725 s 1237 s	CO C–O–C
8b	3β-Acetoxy-B-nor-androstene-17-one (KBr)	3026 m	2937, 2900, 2856, 2837 s	1623 w	1737, 1725 s 1237 s	CO C–O–C

9a	5-Androstene-3β-ol-17-one (KBr)	3037 w	2961, 2943, 2900, 2860, 2823 s	—	3500, 3462 s 1725 s	OH CO
9b	B-nor-Androstene-3β-ol-17-one (KBr)	3025 m	2975, 2937, 2925, 2912, 2875, 2843 s	1618 w	3456 s 1718 s	OH CO
10a	17α-Ethyl-5-androstene-3β, 17β-diol-3β-acetate ($CHCl_3$)	—	2944, 2908, 2870 s	—	3598, 3450 m 1720 s 1240 s	OH CO C—O—C
10b	17α-Ethyl-B-nor-5-androstene-3β,17β-diol-3β-acetate ($CHCl_3$)	3020 w	2940, 2862 s	1632 w	3600, 3460 m 1722 s 1252 s	OH CO C—O—C
11a	3-(3β, 17β-dihydroxy-5-androstene-17α-yl) propanoic acid lactone ($CHCl_3$)	3030 w	2940, 2900, 2856, 2825 s	1666 w	3600, 3460 m 1754 s	OH CO
11b	3-(3β, 17β-dihydroxy-B-nor-5-androstene-17α-yl) propanoic acid lactone ($CHCl_3$)	3035 w	2945, 2930, 2866 s	1624 w	3600, 3464 m 1756 s	OH CO
12a	5-Cholestene-3β-ol (KBr)	3040 vw	2945, 2900, 2870, 2850 s	—	3445 m	OH
12b	B-nor-5-Cholestene-3β-ol (KBr)	3030 w	2950, 2925, 2865 s	1640 m	3430 m	OH
13a	3β-Acetoxy-5-cholestene (KBr)	3020 vw	2960, 2950, 2930, 2900, 2880, 2872, 2850, 2820 s	—	1730 s 1250 s	CO C—O—C
13b	3β-Acetoxy-B-nor-5-cholestene (KBr)	3040 w	2960, 2935, 2920, 2870, 2855 s	1640 w	1740 s 1248 s	CO C—O—C
14a	5-Cholestene chloride (UBr)	3030 vw	2960, 2940, 2910, 2870, 2855 s	—	1480, 1390 m	
14b	B-nor-5-Cholestene chloride (UBr)	3035 m	2960, 2935, 2900, 2865 s	1642 m	1480, 1450, 1440, 1385, 1390 s	
15a	3β-Caproyloxy-5-cholestene (UBr)	3030 vw	2950, 2880, 2868 s	—	1730 s, 1250 m, 1469, 1375, 1170 s	
15b	3β-Caproyloxy-B-nor-5-cholestene (UBr)	3030 m	2950, 2920, 2860 s	1625 w	1730 s, 1240 m, 1470, 1430, 1380, 1340 m, 1175 s	

Table 2

Characteristic IR stretching vibrations of the studied 4-ene-3-one derivatives

No	Derivatives	Characteristic IR stretching vibrations					
		νO–H	ν=C–H	ν C–H; CH_2	$\nu CO_{conj.}$	νC=C	Others ν
1a	4-Cholestene-3-one	—	3025 m	2950, 2876 s	1660 s	1614 m	—
1b	B-nor-4-Cholesten-3-one	—	3030 w	2940, 2876 s	1652 s		—
2a	4-Diosgenin-3-one	—	3025 w	2960, 2885 s	1662 s	1614 m	—
2b	B-nor-Diosgenin-3-one	—	3030 w	2965, 2932, 2880 s	1652 s		—
3a	4-Androstene-3,17-dione	—	3035 m	2958, 2900, 2868 s	1660 s	1616 m	1732 s $C\overset{17}{=}O$
3b	B-nor-Androstene-3,17-dione	—	3042 m	3034, 2982, 2946, 2872 s	1652 s		1734 s $C\overset{17}{=}O$
4a	Lactone of 3-(4-androstene-3-one-17β-ol-17α-yl) propanoic acid	—	3025 w	2960, 2872, 2848 s	1658 s	1616 m	1764 s C=O lactone
4b	Lactone of 3-(B-nor-4-androstene-3-one-17β-ol-17α-yl) propanoic acid	—	3040 m	2936, 2874 s	1652 s		1764 s C=O lactone
5a	Testosterone	3624, 3464 m	3025 w	2972, 2952, 2845 s	1660 s	1612 m	—
5b	B-nor-Testosterone	3630, 3456 m	3035 w	2962, 2946, 2878 s	1654 s		—
6a	17α-Methyl-testosterone	3620, 3454 m	3030 w	2965, 2956, 2878 s	1660 s	1614 m	—
6b	17α-Methyl-B-nor-testosterone	3620, 3468 m	3035 w	2970, 2940, 2878 s	1652 s		—
7a	17α-Ethynyl-testosterone	3610 m	3025 w	2965, 2956, 2808 s	1662 s	1616 m	3316 m C≡C
7b	17α-Ethynyl-B-nor-testorone	3614 m	3030 w	2960, 2954, 2944, 2874 s	1650 s		3316 m C≡C
8a	17α-Allyl-testosterone	3470 m	3030 w	2962, 2940, 2870 s	1650 s	1614 m	3080 m $=CH_2$ asym. 1732 s C=C allyl
8b	17α-Allyl-B-nor-testostererone	3568, 3460 m	3040 m	2956, 2940, 2874 s	1650 s		3080 m $=CH_2$ asym 1708 w C=C allyl
9a	Testosterone benzoate	—	3036 w	2950, 2890, 2860 s	1660 s	1614 m	1708 s C=O 1280 m C–O–C
9b	B-nor-Testosterone benzoate	—	3045 m	2942, 2864 s	1650 s		1710 s C=O 1276 m C–O–C
10a	Progesterone	—	3026 w	3000, 2940, 2880, 2850 s	1652 s	1610 m	1690 s $C\overset{21}{=}O$
10b	B-nor-progesterone	—	3030 w	3000, 2964, 2930, 2874, 2850 s	1648 s		1692 s $C\overset{21}{=}O$

bond.[8] In the steroid skeleton the isolated double bond may appear as : *cis*-disubstituted, trisubstituted and tetrasubstituted. The symmetrical tetrasubstituted double bond yields a very low-intensity νC = C band which is difficult to distinguish. The trisubstituted less symetrical double bond yields a low-intensity but distinguishable νC = C band in the case of more unsaturated steroids.

The investigated substances of both series contain the less symmetrical trisubstituted double bond between the carbon atoms C_5 and C_6 of the B ring. A constant concentration of the samples was used in order to compare the band intensities (5% in $CHCl_3$ solution and 0.3% in KBr pellets). The detection of the νC = C band failed for almost all derivatives of the natural series at these concentrations. Working at the same concentration it was possible to identify in the spectra of the B-nor-steroids the C = C stretching vibration band, as a low-intensity band between 1615 –1680 cm^{-1} (Fig. 1). The easier distinguishability of the C = C stretching vibration band of the B-nor-derivatives may be explained as a consequence of the presence of the more strained five-membered **B** ring.

A determinative factor of the position (and also of the intensity) of the νC = C band is the ring strain; with increasing of the strain, the band of the endocyclic double bond is shifted to lower frequencies.[9]

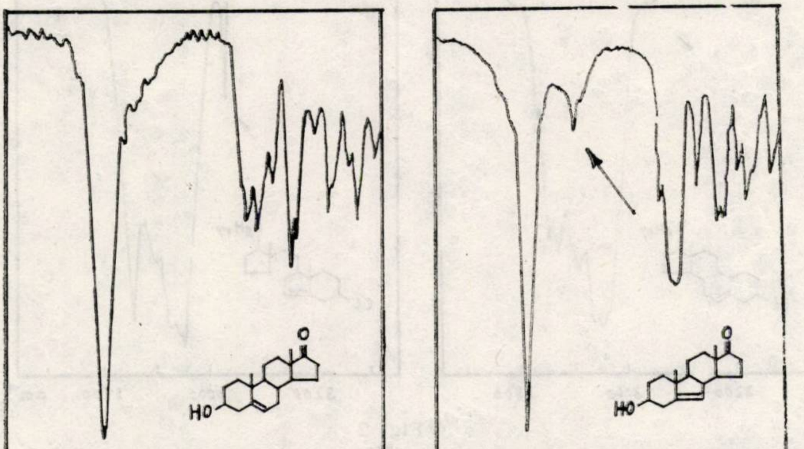

Fig. 1

Based on this general remark we may expect the IR spectra of B-nor-steroids – these containig the double bond in the five-membered more strained ring – to have the C = C stretching vibration band at lower frequencies than the derivatives of natural series. For the above-mentioned reason we used the literature data[10–14] as terms of comparison for the natural series. As a matter of fact in the case of B-nor-derivatives a shift of the C = C stretching vibration band to lower frequencies, with 20 –30 cm^{-1}, was observed (see some examples in table 3).

Table 3

Comparative data for C=C stretching vibration of natural steroides (literature data 11, 12, 14), with corresponding B-nor-steroides

Natural series	ν C=C cm^{-1}	B-nor series	νC=C cm^{-1}
3β-Acetoxy-5-androstene-17-one	1660	3β-Acetoxy-B-nor-5-androstene-17-one	1623
5-Androstene-3β-ol-17-one	1669	B-nor-5-Androstene-3β-ol-17-one	1618
3β-Acetoxy-5-cholestene	1660	3β-Acetoxy-B-nor-5-cholestene	1640
5-Cholestene-3β-ol	1660	B-nor-5-Cholestene-3β-ol	1640

In addition to this, a double bond may be recognized by a variable intensity band (generally a low-intensity one) present between 3000—3150 cm^{-1} which is due to the stretching vibration of the hydrogens attached to the double bond.[15] In the case of the natural series the IR spectra showed for $\nu = C-H$ a very low-intensity band (3025—3040 cm^{-1}), generally a simple shoulder on the very strong band of saturated C—H bonds. The IR spectra of all B-nor-derivatives showed a sharp band of medium or low-intensity between 3030—3050 cm^{-1}(Fig. 2).

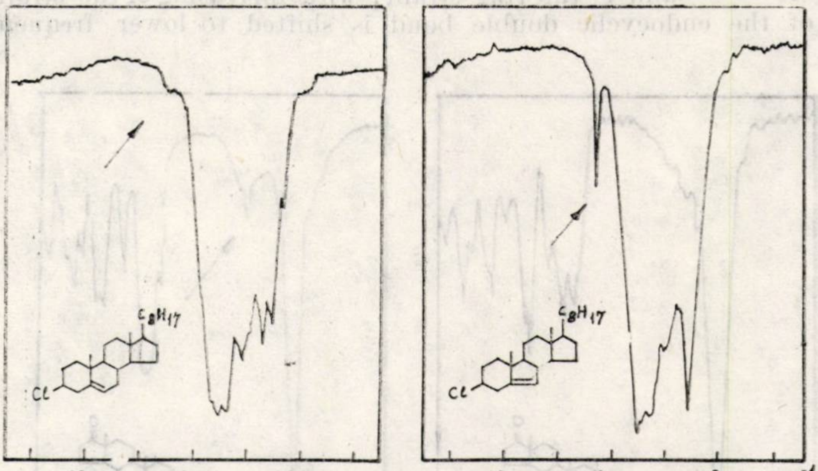

Fig. 2

The difference of intensities and the shift of the $\nu = C-H$ band to higher frequencies in the case of B-nor-steroids is due to the more strained five-membered B ring.[12]

All observations showed above concerning the $\nu = C-H$ vibrations refer to the spectra recorded with the potassium bromide pellet technique. The spectra of chloroform-dissolved materials give no clear bands which should permit to differentiate the two series.

Studying the IR spectra (in chloroform solution) of the 3-oxo-4-ene-B-nor-steroids as compared with the spectra of conjugated ketones of the natural series we made the following observations.

The α, β-unsaturated ketones give in the range of the C=C stretching vibration a more intense band shifted to lower frequencies as the band of the compounds with isolated double bond.[7,9] This fact was also observed in the case of enones of the natural series, whose spectra, as a result of the conjugation, show the νC=C band already detectable between 1610—1616 cm^{-1}, being thus shifted with 50—60 cm^{-1} to lower frequencies as compared with the frequencies of the isolated double bond. The vibration band of the double bond is followed by that of the keto-group between 1652—1662 cm^{-1}. If the molecule contains another keto-groups its stretching vibration band is well resolved and is visible between 1690—1760 $\mathrm{cm.}^{-1}$

The spectra of the investigated B-nor-enones differ much from the spectra of the enones of the natural series. The B-nor-enones give between 1645—1655 cm^{-1} a single intense band. The fusing of the two well resolved bands (νC = C and νC = O) may be explained by the presence of the five-membered B ring which causes an additional strain in A ring. This additional strain determines the shift of the C = C stretching vibration band to higher frequencies up to the range of the stretching vibrations of the isolated double bond and the overlapping with the vibration band of the keto-group (Fig. 3).

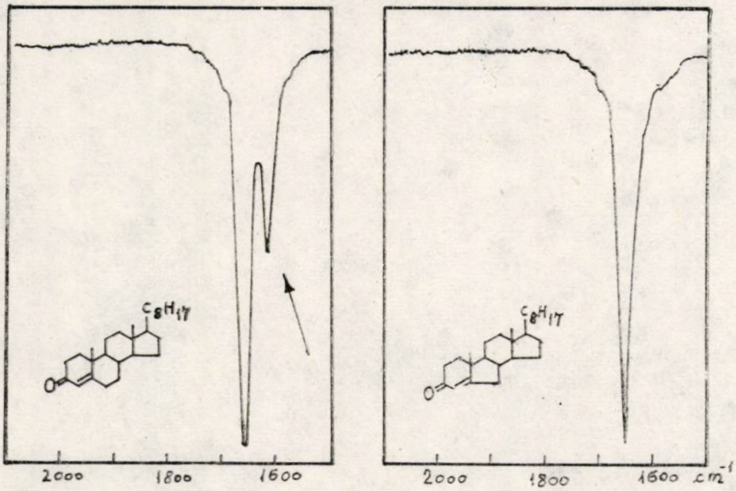

Fig. 3

These spectral data suggest that in the case of the α, β-unsaturated B-nor-ketones the conjugation is to some extent hindered. It is interesting to note that the UV spectra of B-nor-enones do not support this assumption. Both the B-nor and the natural enones show a maximum absorption band at 240 —245 nm.

ACKNOWLEDGEMENT. We wish to thank Dr. doc. F. Hodoșan for helpful discussions. We express also our thanks to Miss Rodica Grecu who recorded the IR (KBr) spectra.

REFERENCES

[1] R. Schwartz, A. Juhász and S. Selinger, *Rev Chim. (Bucureşti)*, **31**, 1196 (1980).

[2] R. Schwartz and A. Juhász, *Rev. Chim. (Bucureşti)*, **32**, 685 (1981).

[3] R. Schwartz, A. Juhász, S. Selinger and L. Moraru, *Rev. Roumaine Chim.*, **28**, 499 (1983).

[4] R. Schwartz, A. Juhász and P. Colţea, *Rev. Roumaine Chim.* **29**, 755 (1984).

[5] R. Schwartz and A. Juhász, *Rev. Chim. (Bucureşti)*, **35**, 992 (1984).

[6] R. Schwartz and A. Juhász, *Rev. Chim. (Bucureşti)*, **36**, 500 (1985).

[7] M. Avram and C. H. Mateescu, "Spectroscopia in infraroşu. Aplicaţii în chimia organică", Ed. Tehnică, Bucureşti, 1966, Part. III, Cap. 1, Cap. 6.

[8] F. Hodoşan and H. Mantsch, *St. Cerc. Chim.*, **13**, 1116 (1965).

[9] F. Hodoşan and H. Mantsch, *St. Cerc. Chim.*, **14**., 411 (1966).

[10] R. N. Jones, P. Humphries, E. Packard and K. Dobriner, *J. Amer. Chem. Soc.*, **72**, 86 (1950).

[11] R. N. Jones, P. Humphries, E. Packard and K. Dobriner, *J. Amer. Chem. Soc.*, **74**, 80 (1952).

[12] P. Baldon, J. M. Fabian, H. B. Henbest, H. P. Koch and G. W. Wood, *J. Chem. Soc.*, **1951**, 2402.

[13] R. E. Schaub and H. J. Weiss, *Chem and Ind.*, **1961**, 2003.

[14] W. Neudert and H. Röpke, "Steroid-Spektrenatlas. Atlas of Steroid Spectra", Springer-Verlag, 1965.

[15] F. Hodoşan and H. Mantsch, *St. Cerc. Chim.*, **14**, 465 (1966).

Revue Roumaine de Chimie, 31, 5, 489–496 (1986)

KINETICS AND MECHANISM OF OSMIUM(VIII) CATALYSED OXIDATION OF BENZYL ALCOHOL AND BENZYLAMINE BY ALKALINE HEXACYANOFERRATE(III) ION

NARENDRA NATH* and L. P. SINGH**

* Department of Chemistry, Gorakhpur University, Gorakhpur (India)

Received March 8, 1985

Kinetics of oxidation of benzylalcohol and benzylamine by hexacyanoferrate(III) ion in the presence of Os(VIII) catalyst has been carried out. The reaction follows zero order kinetics with respect to hexacyanoferrate(III) ion concentration and first order kinetics at lower concentrations of hydroxyl ion and organic substrates showing a decreasing trend at their higher concentrations. All the reactions have been carried out at constant ionic strength. The energy of activation and entropy of activation for the reactions have been calculated. A probable mechanism explaining all the experimental results has been postulated.

Solymosi[1] found that osmium(VIII) is an effective catalyst with alkaline hexacyanoferrate(III) ion but no kinetics was reported. This gave impetus to many workers to carry out the kinetic studies of osmium(VIII) catalysed oxidation of organic substrates by alkaline ferricyanide. There have been quite a good number of investigations [2,3] concerning osmium(VIII) catalysed oxidation of aliphatic compounds with alkaline ferricyanide. However, the investigations concerning the kinetics of the catalysed oxidation of aromatic compounds are still lacking and a lot of work is needed in this direction to decide the role of the catalyst. The present work is an attempt in this direction.

EXPERIMENTAL

Materials and the progress of the reaction: The standard solution of benzyl alcohol (B.D.H.) and benzylamine (Riedel-Dehaenagseelze Hannover) were prepared by dissolving the known amount of the samples in distilled water. The osmium tetroxide (Johnson-Matthey and Co. Ltd.) solution was prepared by dissolving a known amount of sample in aqueous sodium hydroxide. The final strength of sodium hydroxide was kept at 8.92×10^{-2} M and that of OsO_4 was 3.93×10^{4} M. Sodium hydroxide and potassium chloride used were of G.R. (S. Merck) and A. R. (BDH) potassium hexacyanoferrate(III) of A.R. (B.D.H.) grade was used.

The kinetic experiments were followed by adding the required quantity of the organic substrate solutions of potassium hexacyanoferrate(III), sodium hydroxide and osmium tetroxide kept in a reaction bottle at the same temperature. The temperature of the reaction mixture was kept constant with an electrically operated thermostat with an accuracy of ± 0.1°C.

** Address for correspondence, Dr. L. P. Singh, Department of Chemistry, R.H.S. Degree College, Singramau, Jaunpur (U.P.) India

The progress of the reaction was followed by estimating the amount of hexacyanoferrate(II) ion produced after a definite time interval with a standard solution of ceric(IV), sulphate using ferroin as a redox indicator.[4] This method always gave reproducible results.

Stoichiometry and product analysis: The number of moles of hexacyanoferrate(III) ion consumed by one mole of benzyl alcohol and benzylamine was determined by taking a number of reaction mixtures in which the concentrations of hexacyanoferrate(III) ion was kept ten times larger than the organic substrate concentration. After completion of the reaction, the remaining hexacyanoferrate(III) ion were estimated in different sets of experiments and at varying concentrations of NaOH. In each set it was found that one mole of benzyl alcohol and benzylamine required two moles of hexacyanoferrate(III) ion. The reaction product on analysis was found to be benzaldehyde.

RESULT SAND DISCUSSION

The order of reaction with respect to each reactant, namely, the oxidant, the organic substrates, the alkali and the catalyst were determined. The order with respect to hexacyanoferrate (III) ion was determined in the presence of a large excess of organic substrate so that Ostwald's isolation method for the determination of the order of reaction may be valid. The results were found to be the same for both the organic substrates benzyl alcohol and benzylamine.

The order with respect to hexacyanoferrate (III) ion was found to be zero (Tables 1 and 2). Standard zero order rate constant *ks* have beer calculated by multiplyng $k_0 \left(= \frac{\Delta x}{\Delta t} \right)$ by $\frac{x}{V}$ where x is the strength of ceric (IV) sulphate and V is the volume of aliquot taken.

Table 1

Temp. 35°C

[NaOH] $= 2.00 \times 10^{-1}$M

[Benzylalcohol] $= 1.00 \times 10^{-2}$M

[OsO_4] $= 7.32 \times 10^{-6}$M

μ $= 1.20$M

$K_3Fe(CN)_6 \times$ $\times 10^3$ (M)	$k_s \times 10^5$ mole^{-1} min^{-1}
1.0	2.108
2.0	2.328
3.00	2.440
4.0	2.128
5.0	2.280
6.0	2.240
8.0	2.234

Table 2

Temp. 35°C

[NaOH] $= 2.00 \times 10^{-1}$M

[Benzylamine] $= 1.00 \times 10^{-2}$M

[OsO_4] $= 3.66 \times 10^{-6}$M

μ $= 1.20$M

$K_3Fe(CN)_6 \times$ $\times 10^3$ (M)	$K_s \times 10^5$ mole^{-1} min^{-1}
2.00	4.180
3.00	4.144
4.00	3.984
5.00	4.250
6.00	4.180
8.00	4.220
10.00	4.320

The plot of $\left(-\frac{dc}{dt} \right)$ against the respective substrate concentration showed that the reaction followed the first order kinetics with respect to both benzyl alcohol and benzylamine at their lower concentrations. At higher concentrations a retarding trend in the first order velocity constants was observed (Fig. 1).

The hydroxide ion variation on the reaction rate showed that the rate followed first order kinetics at its lower concentrations, showing a tendency towards zero order kinetics at higher hydroxyl ion concentration (Fig. 2).

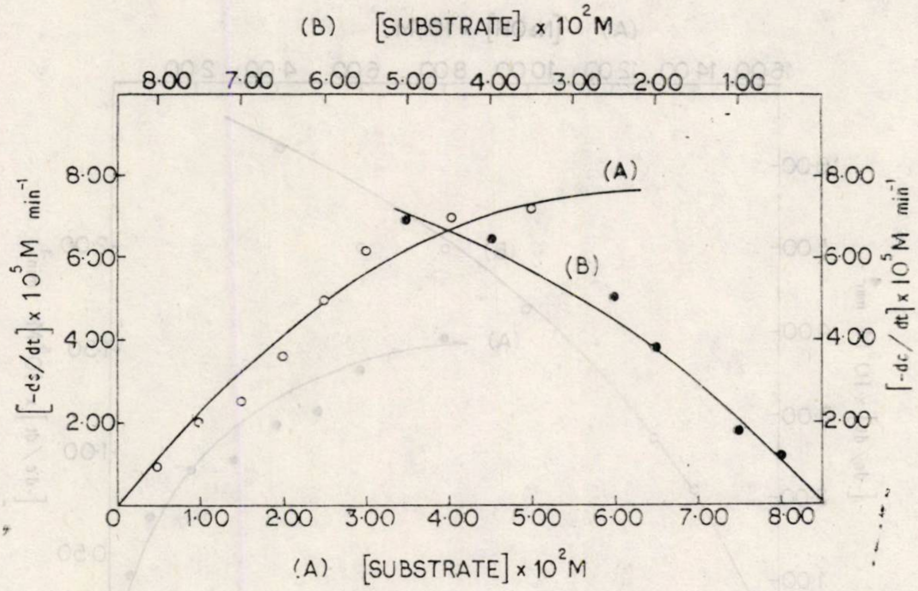

FIG. 1. EFFECT OF VARIATION OF SUBSTRATE ON THE REACTION RATE.
(A) (BENZYL ALCOHOL)·$[K_3Fe(CN)_6] = 3{\cdot}00 \times 10^{-3}$ M, $[NaOH] = 2{\cdot}00 \times 10^{-1}$ M, $[OsO_4] = 7{\cdot}32 \times 10^{-6}$ M, μ = 1·20 M, TEMPERATURE 35°C.

(B) (BENZYL AMINE)·$[K_3Fe(CN)_6] = 2{\cdot}00 \times 10^{-3}$ M, $[NaOH] = 2{\cdot}00 \times 10^{-1}$ M, $[OsO_4] = 3{\cdot}66 \times 10^{-6}$ M, μ = 1·20 M, TEMPERATURE 35°C.

Finally, the effect of variation of osmium tetroxide, the catalyst on the reaction rate was studied. The results for benzylamine and benzyl alcohol have been shown in Table 3 and Table 4 respectively. In each table the values of $ks/[OsO_4]$ assume nearly a constant value, indicating the first order deependence of the reaction rate on the catalyst concentration.

The value of energy of activation for benzyl alcohol and benzylamine have been found to be 66.42 kJ mol^{-1} and 74.03 kJ mol^{-1} respectively. The values of entropy of activation at 35° have been found to be -126.26 J mol^{-1} k^{-1} and -98.56 J mol^{-1} k^{-1} respectively.

On the basis of the experimental results the rate law proposed at lower concentration of both the organic substrates and hydroxide ion concentration would be

$$-\frac{d[Fe(CN)_6]^{3-}}{dt} = k[S][OH^-][Os(VIII)]$$

Where S represents the organic substrate.

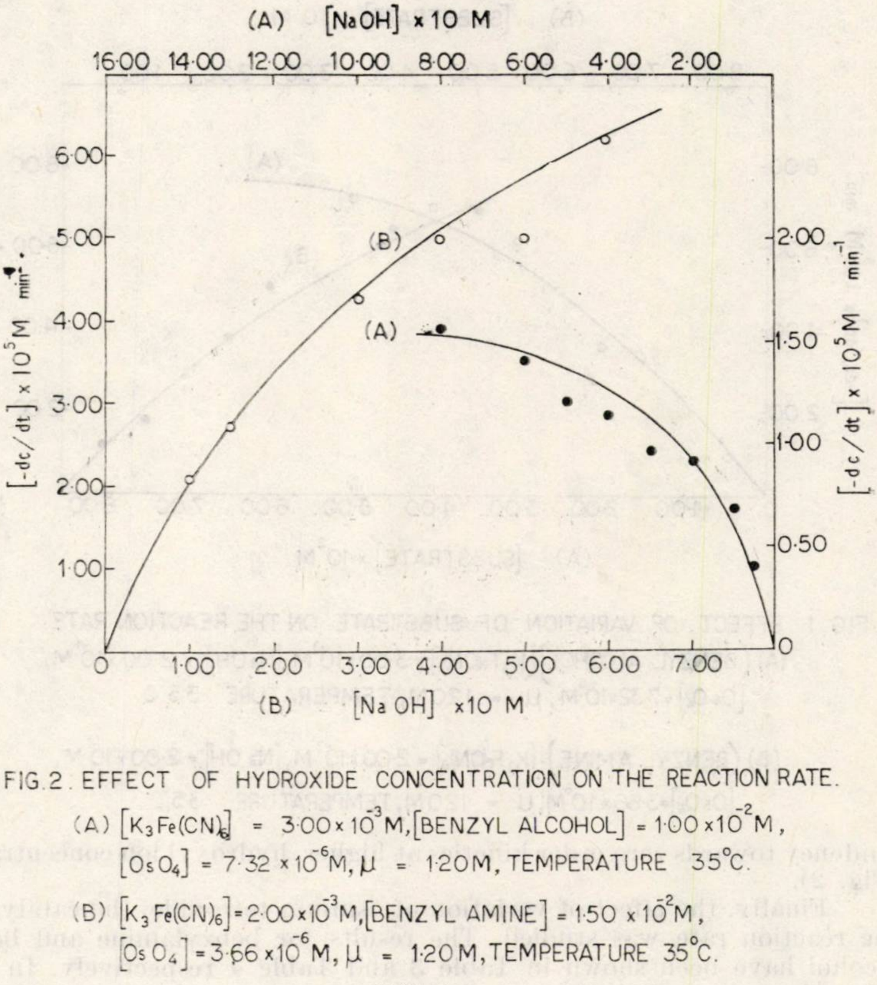

FIG. 2. EFFECT OF HYDROXIDE CONCENTRATION ON THE REACTION RATE.

(A) $[K_3Fe(CN)_6] = 3{\cdot}00 \times 10^{-3}$ M, [BENZYL ALCOHOL] $= 1{\cdot}00 \times 10^{-2}$ M, $[OsO_4] = 7{\cdot}32 \times 10^{-6}$ M, $\mu = 1{\cdot}20$ M, TEMPERATURE 35°C.

(B) $[K_3Fe(CN)_6] = 2{\cdot}00 \times 10^{-3}$ M, [BENZYL AMINE] $= 1{\cdot}50 \times 10^{-2}$ M, $[OsO_4] = 3{\cdot}66 \times 10^{-6}$ M, $\mu = 1{\cdot}20$ M, TEMPERATURE 35°C.

Table 3

Temp. 35°C

$[K_3Fe(CN)_6] = 3.00 \times 10^{-3}$M ; $[NaOH] = 2.00 \times 10^{-1}$M

[Benzylamine] $= 1.00 \times 10^{-2}$M ; $\mu = 1.20$ M

$[OsO_4] \times 10^6$ M	1.83	2.928	3.66	5.49	7.320	9.150	10.98	14.640
$K_s \times 10^5$ mole^{-1}min^{-1}	1.610	3.040	4.144	6.78	8.000	10.548	11.620	15.840
$\frac{k_s}{[OsO_4]}$ min^{-1}	8.79	10.38	11.30	12.35	10.92	11.53	10.58	10.81

Table 4

Temp. 35°C

$[K_3Fe(CN)_6] = 3.00 \times 10^{-3}M$; $[NaOH] = 2.00 \times 10^{-1}M$

$[\text{Benzylalcohol}] = 1.00 \times 10^{-2}$ M ; $\mu = 1.20$ M.

$[OsO_4] \times 10^6 M$	3.66	7.32	10.98	14.64	18.30	21.96	25.62	29.28
$K_s \times 10^5$ mole^{-1}min^{-1}	0.880	2.444	2.730	3.884	4.828	5.732	6.363	7.624
$\frac{K_s}{[OsO_4]}$ min^{-1}	—	2.40	3.34	2.48	2.65	2.64	2.60	2.46

Griffith[5] suggested that in alkaline medium osmium-tetroxide gives the octahedral complexes of the form *trans*$[OsO_4(OH)_2]^{2-}$ and $[OsO_4(OH)(H_2O)]^{1-}$. It seems justified to assume that $[OsO_4(OH)(H_2O)]^{1-}$ species at lower hydroxide ion concentration takes the form of $[OsO_4(OH)_2]^{2-}$ at higher hydroxide ion concentration as shown in the following equation :

$$OsO_4 + OH^- + H_2O \rightleftharpoons [OsO_4(OH)(H_2O)]^{1-}$$

(at low hydroxide ion concentration)

$$[OsO_4(OH)(H_2O)]^{1-} + OH^- \rightleftharpoons [OsO_4(OH)_2]^{2-} + H_2O$$

(at higher hydroxide ion concentration)

However, the formation of species $[OsO_4(OH)_2]^{2-}$ for OH^- ion is shown below.[6]

$$OsO_4 + 2OH^- \rightleftharpoons [OsO_4(OH_2)]^{2-}$$

Singh and coworkers[7] have assumed that the species $[OsO_4(OH)(H_2O)]^{1-}$ exists in equilibrium with the species $[OsO_4(OH)_2]^{2-}$ and it is $[OsO_4(OH)_2]^{2-}$ which acts as an effective catalyst.

In the light of the above discussion, the probable mechanism may be postulated as the formation of an intermediate complex between the reactive Os(VIII) species and the organic substrate (S) in an equilibrium step. The intermediate complex decomposes in a rate determining step to give intermediate Os(VI) species which is finally converted to Os(VIII) in subsequent fast steps by oxidation with hexacyanoferrate(III) ion leading to zero order dependence with respect to the oxidant. The postulated mechanism involves the following step

$$[OsO_4(H_2O)(OH)]^{1-} + OH^- \overset{K_1}{\rightleftharpoons} [OsO_4(OH)_2]^{2-} + H_2O \qquad \text{(I)}$$

$$[OsO_4(OH)_2]^{2-} + S\ K_2 \overset{K_2}{\rightleftharpoons} \text{Intermediate complex} \qquad \text{(II)}$$

$$\text{Intermediate complex} \xrightarrow[\text{slow}]{k} [OsO_2(OH)_4]^{2-} + \text{Reaction product} \qquad \text{(III)}$$

$$[OsO_2(OH_4)]^{2-} + 2OH^- + 2\,[Fe(CN)_6]^{3-} \xrightarrow{\text{fast}} [OsO_4(OH)_2]^{2-} + 2H_2O + 2\,[Fe(CN)_6]^{4-} \qquad \text{(IV)}$$

The third step being the rate determining step, the rate of oxidation would be

$$-\frac{\mathrm{d}[\mathrm{Fe(CN)_6}]^{3-}}{\mathrm{d}t} = k\,[\text{Intermediate complex}]$$

$$= kK_2\,[\mathrm{OsO_4(OH)_2}]^{2-}\,[\mathrm{s}] \qquad (1)$$

At any instant out of the total osmium(VIII) concentration $[\mathrm{Os(VIII)}]_T$, a part of it exists in the form of complex and the rest remains free.

$$[\mathrm{Os(VIII)}]_T = [\mathrm{Os(VIII)}]\ \text{Free} + [\text{Intermediate complex}]$$

$$= [\mathrm{OsO_4(OH_2)}]^{2-} + [\mathrm{OsO_4(OH)\,(H_2O)}]^{-1} + [\text{Intermediate complex}]$$

Making use of first and second steps equilibrium :

$$[\mathrm{OsO_4}](\mathrm{OH})_2]^{2-} = \frac{K_1[\mathrm{OH^-}][\mathrm{Os(VIII)}]_T}{1 + K_1([\mathrm{OH^-}] + K_1K_2[\mathrm{S}][\mathrm{OH^-}]} \qquad (2)$$

where the equilibrium constant K_1 includes the H_2O concentrations, and substituting the value of $[\mathrm{OsO_4\,(OH)_2}]^{2-}$ in equation (1), the rate expression takes the form

$$-\frac{\mathrm{d}[\mathrm{Fe(CN)_6}]^{3-}}{\mathrm{d}t} = \frac{kK_1K_2[\mathrm{S}][\mathrm{OH^-}][\mathrm{Os(VIII)}]_T}{1 + K_1[\mathrm{OH^-}] + K_1K_2[\mathrm{S}][\mathrm{OH^-}]} \qquad (3)$$

The rate expression (3) shows zero order kinetics with respect to hexacyanoferrate(III) ion, the oxidant and first order kinetics with respect to Os(VIII), the catalyst. It also explains the observed kinetic features of the reaction rate with respect to the substrate and hydroxyl ion concentration.

Rate expression (3) is rearranged as

$$-\frac{\mathrm{d}[\mathrm{Fe(CN)_6}]^{3-}}{\mathrm{d}t} = \frac{kK_1K_2[\mathrm{S}][\mathrm{OH}][\mathrm{Os(VIII)}]_T}{1 + K_1[\mathrm{OH^-}]\,(1 + K_2[\mathrm{S}])} \qquad (4)$$

At lower substrate concentration, the inequality $1 \gg K_2[\mathrm{S}]$ can be safely assumed to hold good and the rate law (4) under this condition becomes :

$$-\frac{\mathrm{d}[\mathrm{Fe(CN)_6}]^{3-}}{\mathrm{d}t} = \frac{kK_1K_2[\mathrm{S}][\mathrm{OH^-}][\mathrm{Os(VIII)}]_T}{1 + K_1[\mathrm{OH^-}]} \qquad (5)$$

Thus the rate law (5) confirms the observed first order kinetics at lower substrate concentrations. Further, at lower concentrations of hydroxyl ions, the inequality $1 \gg K_1[\mathrm{OH^-}]$ can be assumed to hold good and therefore, expression (5) reduces to

$$-\frac{\mathrm{d}[\mathrm{Fe(CN)_6}]^{3-}}{\mathrm{d}t} = kK_1K_2[\mathrm{S}][\mathrm{OH^-}][\mathrm{Os(VIII)}]_T \qquad (6)$$

This rate law is again in agreement with the observed first order kinetics at lower concentration of hydroxyl ions. However, at higher

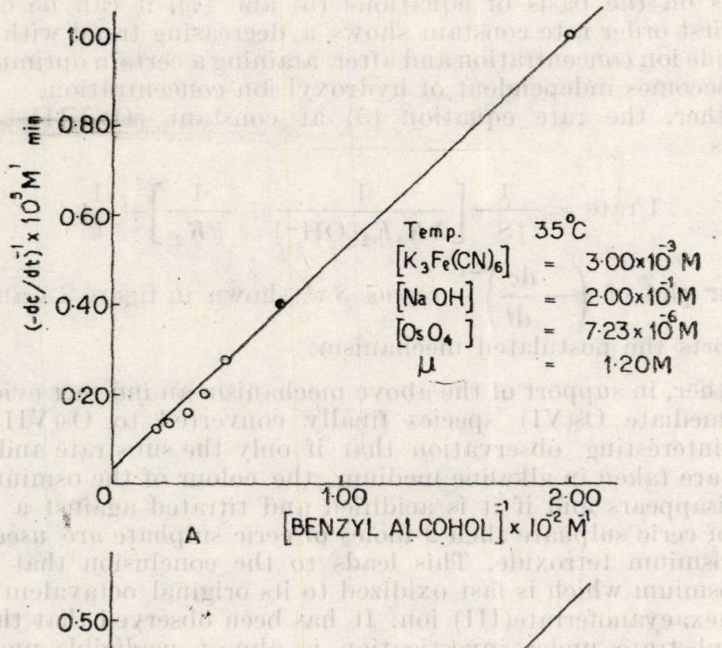

Fig. 3. The linear plot of $\left(-\frac{dc}{dt}\right)^{-1}$ *versus* $[S]^{-1}$.

hydroxyl ion concentration the inequality $K_1[OH^-] \gg 1$ may be assumed to hold good and under this condition expression (5) may be written as

$$-\frac{d[Fe(CN)_6]^{3-}}{dt} = kK_2[S]Os[(VIII)]_T \tag{7}$$

Thus on the basis of equations (5) and (7), it can be concluded that the first order rate constant shows a decreasing trend with increase in hydroxide ion concentration and after *ataining a certain optimum value,* the rate becomes independent of hydroxyl ion concentration.

Further, the rate equation (5) at constant $[\mathrm{Os(VIII)}]_T$ can be written as

$$1/\mathrm{rate} = \frac{1}{[\mathrm{S}]}\left[\frac{1}{kK_1K_2[\mathrm{OH}^-]} + \frac{1}{kK_2}\right] + \frac{1}{k} \tag{8}$$

The linear plot of $\left(-\frac{dc}{dt}\right)^{-1}$ *versus* S^{-1} shown in figure 3A and Figure 3B, *supports the postulated* mechanism.

Further, in support of the above mechanism an indirect evidence for *the intermediate* Os(VI) species finally converted to Os(VIII) exists. It is an interesting observation that if only the substrate and osmium tetroxide are taken in alkaline medium, the colour of the osmium immediately disappears and if it is acidified and *titrated against a standard* solution of ceric sulphate then 2 moles of ceric sulphate are used for one mole of osmium tetroxide. This leads to the conclusion that it is the reduced osmium which is fast oxidized to its original octavalent state by alkaline hexacyanoferrate(III) ion. It has been observed that the oxidation of substrate under *investigation is almost negligible* under these conditions and therefore it is probable that the intermediate Os(VI) formed during the course of reaction is finally oxidized to Os(VIII) rapidly by hexacyanoferrate(III) ion.

ACKNOWLEDGEMENT. One of the authors (Dr. L. P. Singh) is grateful to the U.G.C. New Delhi for the award of financial assistance under minor research scheme.

REFERENCES

[1] F. Solymosi, *Naturwissenschaften.*, **44**, 374 (1957).

[2] N. P. Singh, V. N. Singh and M. P. Singh, *Anst. J. Chem.*, **21**, 2913 (1969).

[3] V. N. Singh and B.B.L. Saxena, *J. Amer. Chem. Soc.*, **91**, *2643 (1969).*

[4] I. M. Kolthoff, "Volumetric analysis" Vol. III, Inter Science Publishers, Inc. New York, pp. 273–275.

[5] W. P. *Griffith, Q. Rev.*, **19**, 254 (1965).

[6] F. A. Cotton and G. Wilkinson, "Advanced Inorganic Chemistry" Wiley Eastern Pvt. Ltd., New Delhi, 1007, 1960.

[7] M. P. Singh and Coworkers, *Ind. J. Chem.*, **13**, 112 (1975).

Revue Roumaine de Chimie, 31, 5, 497–501 (1986)

INVESTIGATION OF DEHYDRATION PRODUCTS OF ARYL AND ARYLALKYL CYCLODODECANOLS

KERIMAN GÜNAYDIN and ÜLKÜ OYMAN

Istanbul Technical University, Department of Chemistry, Yeni Levent-Istanbul-Turkey

Received April 24, 1985
Revised October 20, 1985

In this research, aryl and arylalkyl cyclododecanols were synthesized with Grignard reactions, then their dehydration products were investigated. For the dehydration process in liquid phase three dehydration agents were used: H_3PO_4 in toluene, $SOCl_2$ in pyridine, H_2SO_4 (85 %) without solvent. In addition, when t-cyclododecanols were applied on Silicone OV-17, 3% GLC column at 240°C injection temperature, it was observed that pyrolitic elimination products were obtained.

Dehydration of alcohols is readily carried by using different dehydration reagents in homogeneous or in heterogeneous media. For homogeneous reactions, dehydration occurs under strongly acidic conditions. A range of acidic reagents such as Brönsted or Lewis acids, iodine, acid anhydrides and halogen compounds can be used. Under heterogeneous conditions, dehydration can be performed by passing the alcohol vapours over heated catalysts such as metal oxides or anhydrous metal sulfates.[1]

In this research, first some *t*-cyclododecanols were synthesized, then their dehydration products were investigated. For the synthesis of *t*-cyclododecanols were used Grignard reagents and cyclododecanone. For instance, 1-phenylcyclododecanol (**1**) is prepared from phenyl-magnesium bromide and cyclododecanone[2]:

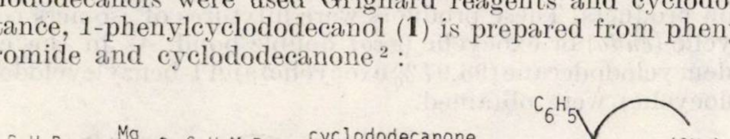

By this way, 1-phenylmethylcyclododecanol (**2**); 1-phenylethylcyclododecanol (**3**) and 1-phenylpropylcyclododecanol (**4**) were synthesized.[2]

For the dehydration process in liquid phase three dehydration agents were used: H_3PO_4 in toluene[3]; $SOCl_2$ in pyridine[4]; H_2SO_4(85 %) without solvent.[5,6] In addition, when **1**, **2**, **3** and **4** are applied on Silicone OV-17, 3% GLC column at 240°C injection temperature, it is observed that pyrolitic elimination products are obtained. In this study, the percentage composition of the compounds obtained with different dehydration reagents was calculated by GLC analysis. In the procedure, a

Schimadzu model GC-5A gas chromatograph equipped with a flame ionization detector and 1/8 × 12 ft stainless steel column packed with Silicone OV-17, 3% was used. In *operating conditions the column temperature* was 190°C, the injection and detector temperature was 240°C. The optimum flow rate of N_2 gas was 100 mL/min.

The dehydration products obtained from H_3PO_4 in toluene, $SOCl_2$ in pyridine, and pyrolitic elimination on the chromatographic column are listed in Table 1.

Table 1

Partition of endocyclic (*endo*) and exocyclic (*exo*) isomers (%)

Carbinols	H_3PO_4		$SOCl_2$: Py		Silicone OV-17	
	endocyclic	exocyclic	endocyclic	exocyclic	endocyclic	exocyclic
1	98.26	—	—	—	99.9	—
2	3	96.97	33.64	58.25	9.5	90.5
3	71.26	27.2	89.12	9	76.16	23
4	52.1	34	66.34	27.34	53	47

In the reactions performed with H_3PO_4 in toluene, the hydroxyl group of alcohol is converted into a better leaving group ($\overset{+}{O}H_2$) and it was suggested[1] that the reaction involved two steps : a slow ionization, followed by fast loss of a proton from the resulting carbocation. The number of elimination products is dependent on the type of β-hydrogens of the carbinols. For instance, **1** gives only one elimination product, 1-phenylcyclododecene-1 (**5**) because it contains only four equivalent β-hydrogens:

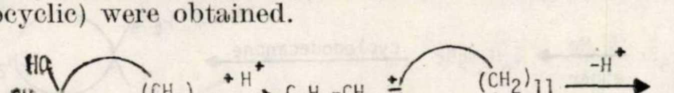

The carbinols that involve two different β-hydrogens gave two different elimination products. These products were mixtures of isomers containing an endocyclic (*endo*) or exocyclic (*exo*) double bond. As in the case of **2**, 1-benzylidencyclododecane (96.97 % exocyclic) and 1-benzylcyclododecene-1 (3 %, endocyclic) were obtained.

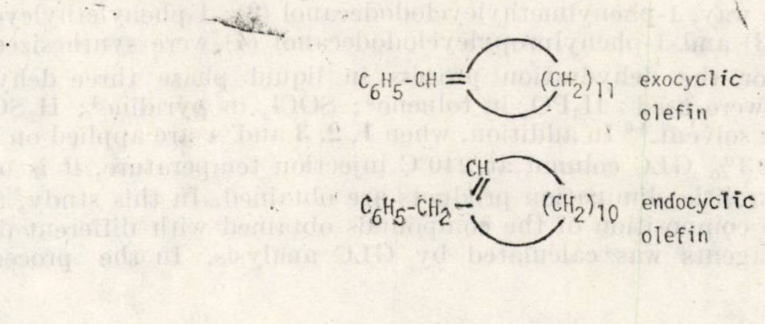

In acidic media, **3** gave 1-phenylethylidencyclododecane (27.20 %, exocyclic) and 1-phenylethylcyclododecene-1 (71.26 %, endocyclic) too. From **4**, 1-phenylpropylidencyclododecane (38 %, exocyclic) and 1-phenyl-propylcyclododecene-1 (52.16 %, endocyclic) were obtained. In addition spiro[cyclododecane-1 :1′-tetralin] (**9**) 13.8 % was found as cyclodehydration product in the mixture. The convenient GLC analysis of the olefin distribution in conjunction with the ^{1}H-NMR integrated spectrum allows the structural assigments to be made for the endocyclic and exocyclic isomers. The endocyclic isomers have rather characteristic GLC retention time, as well as they show in the ^{1}H-NMR spectra a signal at δ3.4 for the isolated benzylic methylene group and a signal at δ5.4 for the olefinic proton. On the other hand, the ^{1}H-NMR spectral data for the conjugated exocyclic olefins show a signal at δ6.5 for the olefinic proton. Table 2 cites the GLC and pertinent ^{1}H-NMR data for endocyclic and exocyclic olefin mixtures prepared from **2**, **3** and **4** carbinols.

Table 2

GLC and ^{1}H-NMR data for **2**, **3** and **4** carbinol

Carbinols	endocyclic olefin			exocyclic olefin	
	GLC	^{1}H-NMR δ(CCl_4)ppm		GLC	^{1}H-NMR δ(CCl_4)ppm
	R.T. (min)	$>C{=}CH-$	$Ar-CH_2-$	R.T. (min)	$Ar-CH=$
2	13.70	5.42	3.4	11.55	6.6
3	18.03	5.4	3.5	15.99	6.8
4	25.76	5.35	3.5	21.72	6.1

In the reactions that were made with $SOCl_2$ in pyridine, the OH group is converted into OSOCl to cleave easily. The ester intermediates produced during reaction, decompose either unimolecularly (E_1) or bimolecularly (E_2) or thermally and give the elimination products.[1,4]

Compound **1**, unlike arylalkyl cyclododecanol, gave 1-phenyl-1-chloro-cyclododecane (**6**) a substitution product. That is, $SOCl_2$ reacted as a halogenation agent. The reaction is formulated as following :

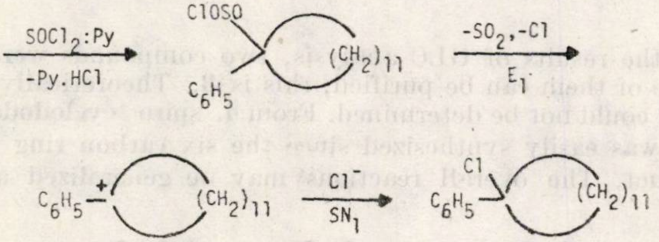

According to E_1 mechanism, unstable ester intermediates easily converts into the carbocation and the chloride ion attacks as a strong nucleophille. Ultimately, chlorination occurs before the transfer of β-hydrogen.

The dehydration products obtained from **2**, **3** and **4** with $SOCl_2$ in pyridine were similar to the dehydration products obtained from the same reactants with H_3PO_4 in toluene but their endocyclic to exocyclic *olefin ratio* values are different (Table 1). The ester intermediates, obtained from these carbinols according to E_2 mechanism are converted into the elimination products with the separation of β-hydrogen and leaving group (OSOCl) simultaneously. For instance from **2**, endocyclic and exocyclic isomers are synthesized according to the following reactions :

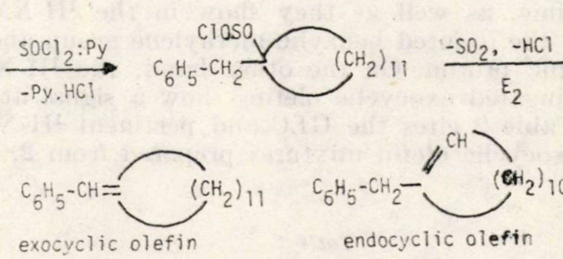
SOCl2:Py
-Py.HCl
ClOSO
C6H5-CH2
(CH2)11
-SO2, -HCl
E2
C6H5-CH=
(CH2)11
exocyclic olefin
C6H5-CH2-
CH
(CH2)10
endocyclic olefin

In the dehydration reactions carried out in H_2SO_4 (85%) *cyclodehydration products* were only obtained from **3** and **4**.

As a result of the reactions shown below, cyclododecane [1, 2, 1′, 2′] tetralin (**7**) and spiro [cyclododecane-1 :1′-indane] (**8**) can be expected to occur from **3** :

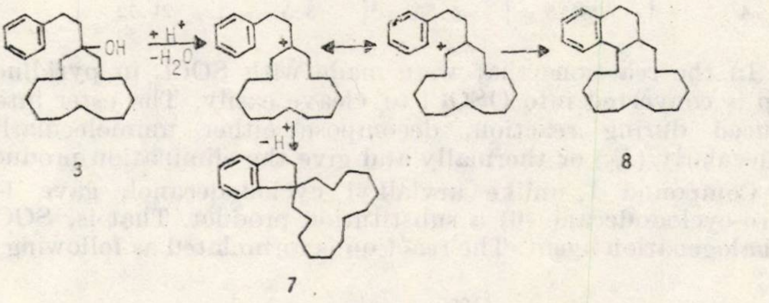
OH
+H+
-H2O
+
+
-H+
3
8
7

From the results of GLC analysis, two compounds were detected, but only one of them can be purified, this is **8**, Theoretically expected, compound **7** could not be determined. From **4**, spiro [cyclododecane-1 :1′-tetralin] **9** was easily synthesized since the six carbon ring is a highly stable product. The overall reactions may be generalized as follows :

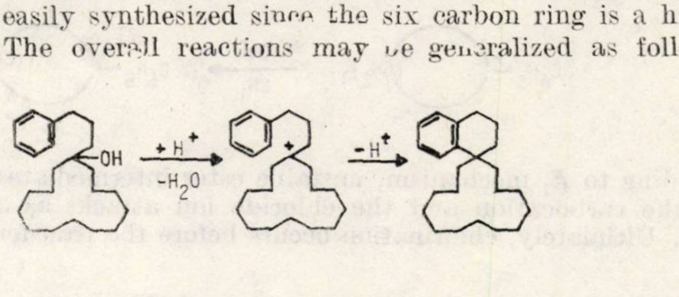

The spectra data of compounds **5**, **6**, **8**, **9** are registered in Table 3.

Table 3

Spectral data for compounds **5**, **6**, **8**, **9**

Compounds	IR data (νcm^{-1})	^{1}H-NMR data (δ ppm)
5	3000 3100 2930 2850 1640 1600 1590	7.1 (C_6O_5-, 5H) ; 5.4($> C=CH-$, 1H) 2−2.6 ($-CH_2-$, 4H) ; 1.35($-CH_2-$, 16H)
6	3000 3100 2850 2995 1600 650	7.6(C_6H_5-,5H) ; 2.4($-CH_2-$,4H) ; 1.5(CH_2-, 18H)
8	3050 3000 2650 1940 1900 1790 1700 1595 1570 1580 1560 1440 1340 1240 1140 1100 1020 830 780 710	6.5−7(C_6H_4-, 4H) ; 2.8($ArCH_2$, 2H) 1.2−1.6($-CH_2-$26H)
9	3100 3060 3025 2950 2850 1600 1580 1490 1470 1440 1340 1300 1280 1275 1250 1220 1140 1060 1040 850 815 760 740 720 700	7(C_6H_4-, 4H) 2.84($ArCH_2-$, 2H) ; 1.1−1.9 ($-CH_2-$, 26H) ;

Furthermore, when the carbinols **1**, **2**, **3**, **4** were applied on the column (Silicone OV-17, 3% at 240°C injection temperature) the chromagrams of these carbinols were found to be the same as the chromatograms obtained from dehydration products of the carbinols in homogeneous phase. This result may be attributed to the occurrence of the dehydration in the column. The catalytic activity of the column packed with Silicone OV-17, 3% should be taken into account, since the column containing SiO-bonds and the metal oxides are well-known catalysts in dehydration procesess. As shown in Table 1 the partitions of endocyclic and exocyclic olefins were similar to the dehydration products obtained in acidic condition. So, it may be assumed that this reaction in the column proceeds according to E_1 mechanism.

REFERENCES

[1] H. William, J. R. Saunders and F. E. Anthony, "Mechanism of Elimination", Wiley-Interscience, New York, 1973.

[2] Ü. Oyman, *Chimica Acta Turcica*, 2 (1974).

[3] A. A. Kaevskii, A. D. Treboganov, T. D. Marieva, G. V. Varnikova and W. A. Probrazhenskii, *Zh. Org. Chim.*, **3**, 441 (1967).

[4] J. Casanova and B. Weagell, *Bull. Soc. Chim. Fr.*, **4**, 1289 (1971).

[5] H. Christol, A. Gaven, Y. Pietrasanta and J. L. Vernet, *Bull. Soc. Chim., Fr.*, **21**, 4510 (1971).

[6] D. Perlman, D. Davidson and M. T. Bogert, *J. Org. Chem.*, **1**, 300 (1936).

[7] R. G. Newkome, J. W. Allen and M. G. Anderson, *J. Chem. Educ.*, **50**, 372 (1973).

Revue Roumaine de Chimie, **31**, *5*, 503–506 (1986)

4b, 10b-DIHYDROCHRYSENE, A NEW DIBENZO$(CH)_{10}$ HYDROCARBON

M. BANCIU,[a] DANA ELIAN,[a] M. ELIAN,[b] LIGIA STĂNESCU[b]
and ECATERINA CIORĂNESCU[a,b]

[a] Laboratory of Organic Chemistry, The Polytechnic, TCH, Spl. Independenţei 313, 76206 Bucharest, Romania

[b] Centre of Organic Chemistry — ICECHIM, Spl. Independenţei 202B, 78100 Bucharest, Romania

Received December 10, 1985

The title hydrocarbon, **1**, a new dibenzo$(CH)_{10}$ hydrocarbon, was obtained by flow-vacuum pyrolysis of the adduct **2** between benzobarrelene and benzyne.

The valence isomers of annulenes as well as their benzoannelated derivatives present a continuing theoretical and experimental interest in recent years.[1] There exist 102 possible dibenzoderivatives of valence isomers of [10]annulene (79 of which being not *o*-quinonoid); all were tabulated,[2] but only nine such hydrocarbons were synthesized until now.[1,2b] In continuation of our investigations concerning dibenzo$(CH)_{10}$ hydrocarbons[3] we report here the synthesis and characterization of a new isomer, namely 4b, 10b-dihydrochrysene (**1**).

The starting material for the synthesis of **1** was dibenzo[*c*,*i*] tetracyclo $[4.4.0.0^{2,8}.0^{5,7}]$ deca-3,9-diene (**2**), a dibenzo$(CH)_{10}$ hydrocarbon which was described briefly in 1967[4] and has received no attention until now.

When hydrocarbon **2**, obtained from benzobarrelene and benzyne,[4b] was flow-vacuum pyrolysed at temperatures between 350° and 600° (retention times about 0.1 s) the reaction product contained two new hydrocarbons (A and B) along with unreacted starting material **2**. We assigned the structures of 4b, 10b-dihydrochrysene (**1**) for A and chrysene (**3**) for B on the basis of physico-chemical data presented below.

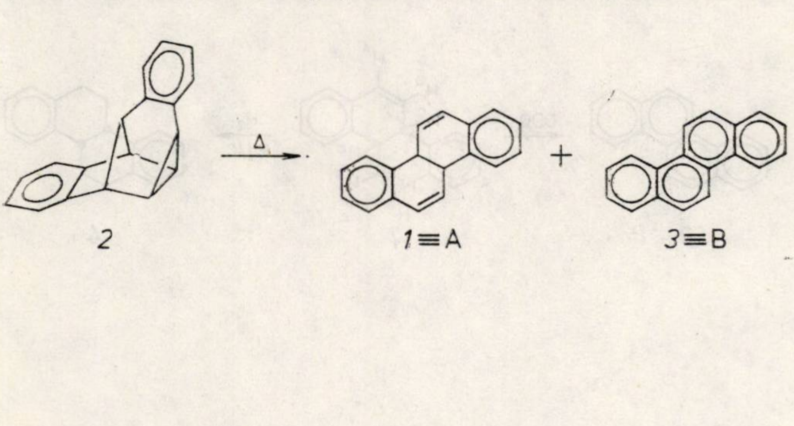

The distribution of the reaction products as a function of temperature was studied gas-chromatographically and the results are plotted in fig. 1.

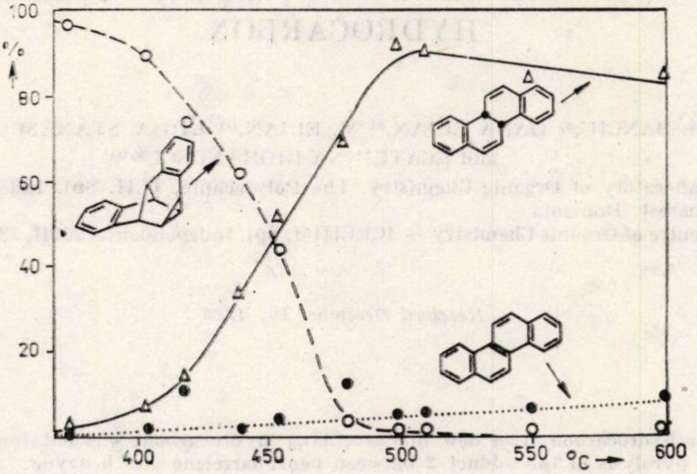

Fig. 1. — Product distribution in the flow-vacuum pyrolyses of **2**.

Preparative pyrolysis performed at 500° at which temperature a maximum amount of **1** (91%) is reached, permitted the isolation of the new hydrocarbon. Separation from small quantities of **3** (about 5%) was effected through fractional crystallization from ethanol. Hydrocarbon **1**, m.p. 95—97°, corresponds to $C_{18}H_{14}$ formula and presents a characteristic ^{1}H-NMR spectrum : $\delta = 3.83$ ($2H^C$, singlet) 5.63 ($2H^B$; doublet); 6.47 ($2H^A$; doublet) and 6.9 — 7.3 ppm (H_{aryl}). Further confirmation of the structure **1** resulted from : (a) the favourable comparison of its ^{1}H-NMR spectrum with those of Z-4b,-8a-dihydrophenanthrene,[5] the monobenzo(CH)$_{10}$ hydrocarbon corresponding to **1** and (b) dehydrogenation with dichloro-dicyanobenzoquinone (DDQ) in benzene at room temperature, affording chrysene (**3**). Because the ^{1}H-NMR spectrum does not permit the assignment of Z-or E-stereochemistry of ring juncture in **1**, this hydrocarbon was hydrogenated catalytically. The product of hydrogenation proved to be identical (m.p., UV and ^{1}H-NMR-spectra) with the known[6] Z-4b, 5, 6, 10b, 11, 12-hexahydrochrysene (**4**), demonstrating thus the Z-stereochemistry of **1** :

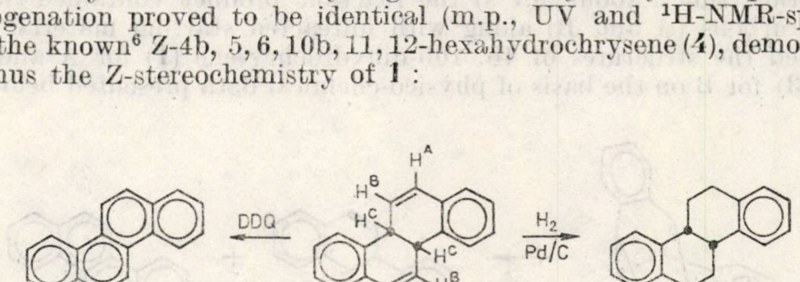

The chrysene structure of the minor pyrolysis product, B ≡ **3** was proved by its m.p. = 254 – 5°, UV- and ^{1}H-NMR spectra identical with those of an authentic sample.[7]

An attractive rationale (including thermally allowed reactions) explaining the formation of **1** during the pyrolysis of **2** (Scheme 1) includes the intermediacy of Z-6a,12a-dihydro-benzo[a]-anthracene (**5**). This could be formed from **2**, either directly (through a retrodiene reaction) or indirectly, *via* dibenzo [10] annulene (**6**) formed in a retro [2 + + 2 + 2] cycloaddition; electrocyclic reaction of **6** affords also **5**. A [1.5] sigmatropic reaction in **5** allows the formation of dihydrochrysene (**1**), whereas elimination of two Z-hydrogen atoms from **5** and **1** gives rise to benzo [*a*] anthracene (**7**) and chrysene (**3**) respectively. A proof in confirmation of the above suggested mechanism was brought by v.p.c. identification of small amounts (~1 %) of benzo[*a*]anthracene (**7**) in the crude pyrolysates of **2**.

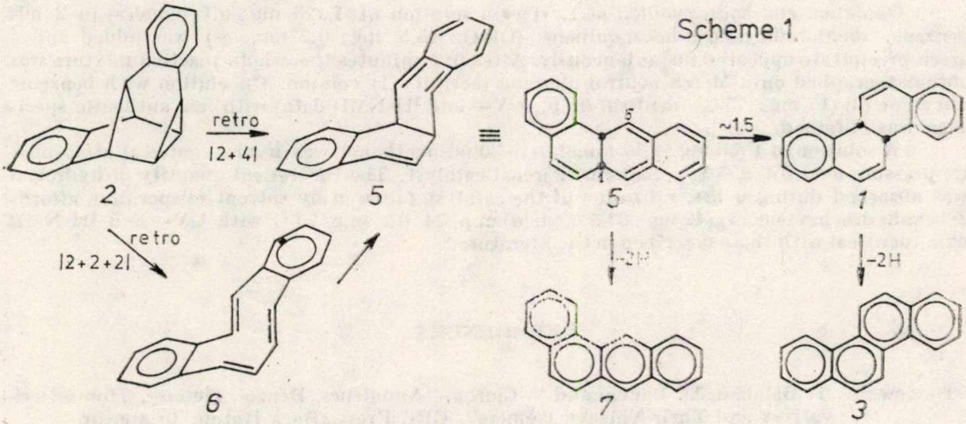

It should be noted also that hydrocarbon **1** (as well as **5**) were suggested by us[3b] as intermediates in the pyrolyses of other dibenzo (CH)$_{10}$ hydrocarbons but could not be isolated (probably due to higher temperatures and/or longer contact times used in those experiments)

EXPERIMENTAL

Melting points are uncorrected. IR spectra : UR 20 — C. Zeiss. UV spectra : SPECORD UV—VIS — C. Zeiss. ^{1}H-NMR : Varian A—60 A (TMS) as internal standard). V.p.c. analyses : CARLO ERBA model 2450, flame ionisation detector, integrator SPECTRA PHYSICS, capillary glass column (20 m, with methyl silicone SE 30), temperature programming between 100—270° with 10°/min, hydrogen flow-rate 1 mL/min.

Dibenzo[c, i]*tetracyclo* [4.4.0.0^{2,8},0^{5,7}] *deca*-3,9,*diene* (**2**) was obtained after Friedman[4b] from benzobarrelene and benzyne (generated from diazoanthranilic acid with propene oxide) in 1,2-dichloroethane solution ; 3 hrs at reflux temperature. The crude product was purified by chromatography on Merck neutral alumina (activity I) column affording pure **2** with m.p. 154—155° (lit. m.p. 154°,[4a] 154—155° [4b]) and spectral data (UV, ^{1}H-NMR) identical with those reported.[4a]

Flow-pyrolyses of dibenzo[c,i]*tetracyclo*$[4.4.0.0^{2,8}.0^{5,7}]$*deca-3,9-diene* (**2**). All the pyrolyses were performed in a vertical quartz tube of 10 mm internal diameter filled with quartz chips for 200 mm. The heating was realized with an electrical oven, the temperatures being determined by means of a chromel-copel thermocouple. Pyrolyses were conducted at 0.5 Torr in inert argon atmosphere (flow rate 1—2 mL/min). The pyrolysis products, crystallized in the lower cooled part of the quartz tube, were dissolved in chloroform and subsequently v.p.c. analysed. The results of pyrolyses of **2** (samples of 30 mg ; 99.5 % purity) at different temperatures are presented in Fig. 1.

4b,10b-Dihydrochrysene (**1**) *through preparative pyrolysis of* **2**. A sample of **2** (200 mg ; 0.87 mmoles) was flow-pyrolysed at 500° as described above and the crude solid product obtained (180 mg : 90 % yield) was dissolved in 10 mL hot ethanol then cooled and filtered rapidly affording 7 mg (3.7 %) chrysene (**3**), m.p. 254—5°, with UV— and ^{1}H-NMR spectra identical with the reported ones.[7] The filtrate affords on further cooling a first crop of **1** as a white solid, m.p. 93—94° (80 mg ; 40 %) then a second crop of 40 mg (20 %) **1** with. mp. 88—95°. The pure **1** has m.p. 95—97° (from ethanol). Calcd. for $C_{18}H_{14}$: C, 93.91 ; H, 6.09 ; Found : C, 94.25 ; H, 6.27.

UV spectrum (methanol) λ max (ε max) : 218.5 (35300) ; 225 (34500) 256 (15900) ; 266.5 (shoulder, 13400) and 298.5 nm (1700). *^{1}H-NMR spectrum*, see text.

Oxidation and hydrogenation of **1**. Over a solution of **1** (23 mg ; 0.1 mmoles) in 2 mL benzene, dichlorodicyano-*p*-benzoquinone (DDQ : 45.5 mg ; 0.2 mmoles) was added and a green precipitate appeared instantaneously. After five minutes the whole reaction mixture was chromatographed on a Merck neutral alumina (activity I) column. On elution with benzene, chrysene (**3**) (17 mg ; 75 %) identical (m.p., UV— and ^{1}H-NMR data) with an authentic specimen was obtained.

A solution of **1** (50 mg ; 2.17 mmoles) in 30 mL methanol was hydrogenated at atmospheric pressure over 0.1 g 5 %-palladium/charcoal catalyst. The theoretical quantity of hydrogen was absorbed during 6 hrs. Filtration of the catalyst followed by solvent evaporation affords *Z*-hexahydrochrysene (**4**) (42 mg ; 83.5 % yield) m.p. 74° (lit. m.p. 75°[6]) with UV— and ^{1}H-NMR data identical with those described in the literature.[6]

REFERENCES

[1] Review : A. T. Balaban, M. Banciu and V. Ciorba, "Annulenes, Benzo-, Hetero-, Homo-Derivatives and Their Valence Isomers", CRC Press, Boca Raton, to appear.

[2] a) A. T. Balaban, *Rev. Roumaine Chim.*, **19**, 1185 (1974) ; b) review : M. Banciu and A. T. Balaban, *Chem. Scr.*, **22**, 188 (1983).

[3] a) M. Banciu, M. Elian, E. Ciorănescu and C. D. Nenitzescu, *Tetrahedron Letters*, **1972**, 2573 ; b) M. Elian, M. Banciu, L. Stănescu and E. Ciorănescu, *Rev. Roumaine Chim.*, **21**, 89 (1976) ; c) M. Banciu, M. Elian, Phan Le Thuy, C. Drăghici and E. Ciorănescu, *ibid.*, **27**, 19 (1982).

[4] a) M. Stiles, U. Burckhardt and G. Freund, *J. Org. Chem.*, **32**, 3718 (1967) ; b) L. Friedman, *J. Amer. Chem. Soc.*, **89**, 3071 (1967).

[5] L. A. Paquette, M. J. Kukla and J. C. Stowell, *J. Amer. Chem. Soc.*, **94**, 4920 (1972).

[6] a) G. R. Ramage and R. Robinson, *J. Chem. Soc.*, **1933**, 607 ; b) F. A. Askew, *ibid.*, **1935**, 512 ; c) R. G. Harvey, *J. Org. Chem.*, **36**, 3306 (1971).

[7] a) E. Clar, „Aromatische Kohlenwasserstoffe. Polycyclysche Systeme", Springer, Berlin, 1941, p. 107 ; b) N. F. Chamberlain, "The Practice of NMR Spectroscopy", Plenum Press, New York, London, 1974, p. 391, 206.

Revue Roumaine de Chimie, **31**, *5*, 507–518 (1986)

THE ACETOLYSIS OF DITOSYLATES WITH A BICYCLO[4.4.0]DECANE SKELETON

MICHAELA STĂNESCU,[a] FLORIN BADEA[b] and GHEORGHE MIHAI[a]

[a] Centre of Organic Chemistry, Bucharest, Romania
[b] Department of Organic Chemistry, Polytechnic Institute, Bucharest, Romania

Received May 27, 1985

The acetolysis of *cis*-1,6-bis(β-tosyloxyethyl)-bicyclo[4.4.0]deca-3,8-diene (3a) and the corresponding saturated derivative was performed. The unsaturated compound undergoes acetolysis, yielding only bridged compounds, by direct participation of the double bonds in the ionisation (π-route). Rate measurements were performed. At 110°, k_U/k_S is 935 for the first ionisation step and 87 for the second step. An isokinetic relationship (β = 378°) between the activation parameters determined in this work and other activation parameters, recorded in literature for similar π-route reactions, was established.

In a series of papers of our laboratory[1] we studied the competition, in solvolyses, between the participation in ionisation of neighbouring aromatic ring (phenonium route) and the anchimeric assistance of a neighbouring double bond (π-route). Thus, in tosylates with general formula **1**, the weight of the π-route pathway is determined by: a) an electronic control, determined by the nucleophilicity of the double bond and of the aromatic ring (the electronic effects of X and Y groups); b) a geometric control, determined by the distance of the double bond to the reaction site, in the most favourable conformation; c) a conformational control, determined, on one hand, by the rigidity of the system which constrains the median ring to remain in the necessary conformation for double bond participation and, on the other hand, by the other stable conformations of the side chain, which may reduce the weight of the conformation presenting the proper distance of the double bond to the reaction centre.

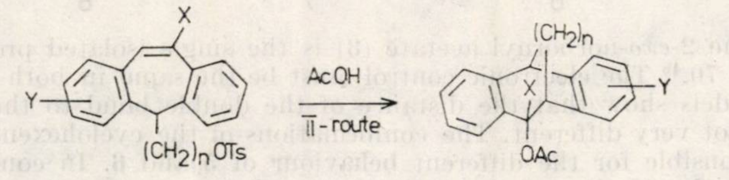

1 2
n = 1, 2

From our results, as well as from the data recorded in the literature,[2–4] it seems that the conformational control is decisive in the double bond participation in ionisation reactions.

In the present work, initiated in 1968 by professor Ecaterina Ciorănescu, we have synthesized the ditosylates **3a** and **4**, in order to study the behaviour of a system having two double bonds and two ionisable groups.

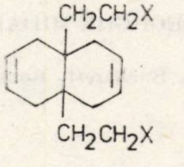

3a ; X = OTs

3b ; X = Br

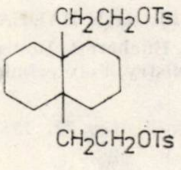

4

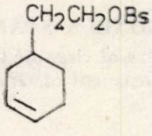

5

Indeed, in the acetolysis of cyclohexenylethyl brosylate **5**, Winstein and Carter[2] noticed only a small anchimeric acceleration, due to the presence of the double bond in molecule ($k_U/k_S = 4$)*, the unrearranged acetate being formed beside the bridged acetate. In contrast to **5**,[2,3] the cyclopentenyl arenesulphonate **6** undergoes acetolysis practically only by a π-route participation.

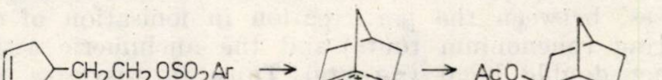

6 7 8

The 2-*exo*-norbornyl acetate (**8**) is the single isolated product and $k_U/k_S = 70$.[4b] The electronic control must be the same in both **5** and **6**, and models show that the distance of the double bond to the reaction site is not very different. The conformations of the cyclohexene ring can be responsible for the different behaviour of **5** and **6**. In contrast to **6**, the ditosylate **3a** has a lower flexibility of the two cyclohexene rings and each reaction centre may present a better chance to be assisted in ionisation by a double bond. We hoped therefore to observe a high reactivity of **3a** as compared either to the saturated analog **4** or to the much simpler arenesulphonate **5**.

During the progress of this work, Paquette and coworkers[5] have determined the products formed from the dibromide **3b**, on treatment with silica gel, in petroleum ether, at room temperature. Only bridged products are formed, in agreement with our own results. The present paper will mainly deal with the kinetic of the acetolysis of **3a**, not studied for **3b** by the afore-mentioned author.

---

* k_U stands for the rate of the unsaturated compound and k_S for that of the analogous saturated system.

RESULTS

The synthesis of **3a** and **4** is given in Scheme.

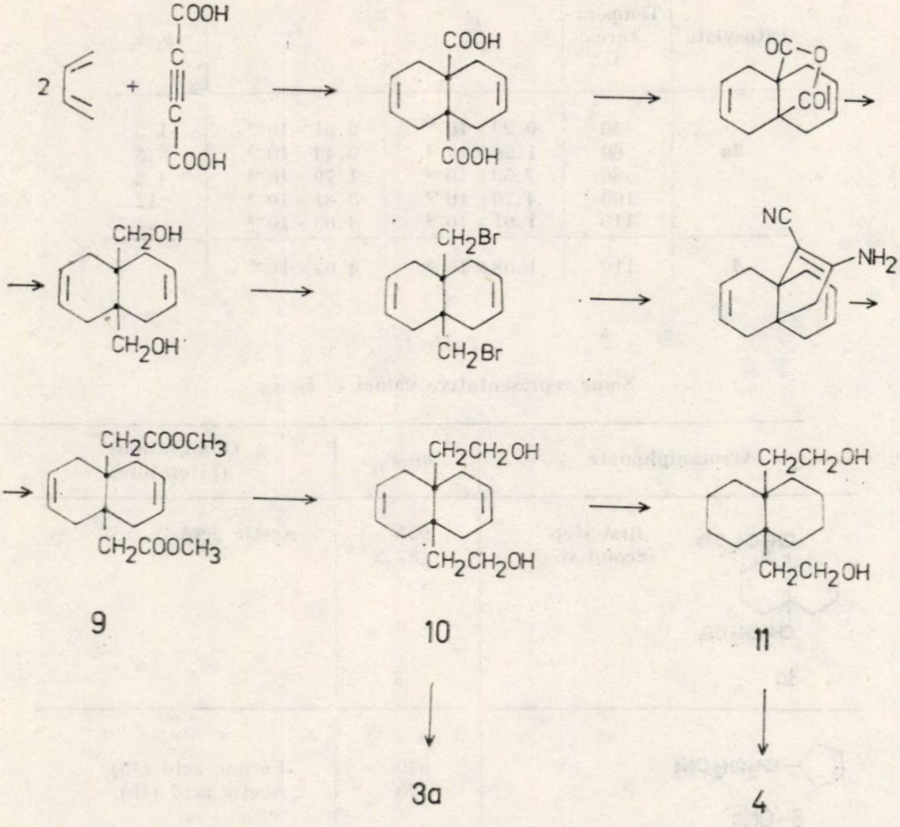
COOH
2
+
C
C
COOH
COOH
COOH
OC
O
CO
CH2OH
CH2OH
CH2Br
CH2Br
NC
NH2
CH2COOCH3
CH2COOCH3
CH2CH2OH
CH2CH2OH
CH2CH2OH
CH2CH2OH
9
10
11
3a
4

For the preparation of the diester **9** we used the method described by Ginsburg.[6] The products derived from ditosylate **3a**, in acetolysis, after treatment with $LiAlH_4$, have been analysed by gas-chromathography, which indicated the presence of four hydrocarbons (5 – 7%), seven unsaturated secondary alcohols (35%) and three diols (60%). The 1H-NMR spectra of products ruled out the occurrence, even in traces, of a primary alcohol group CH_2-CH_2OH, indicating that the solvolysis proceeds exclusively by a π-route mechanism. A full account of the isolation and identification of the reaction products will be given in a forthcoming paper.

KINETIC MEASUREMENTS

The progress of the acetolysis was followed by the titration of *p*-toluenesulphonic acid formed during the reaction. The solvolyses of ditosylates **3a** and **4** are examples of two first-order consecutive reactions :

$$A \xrightarrow{k_1} B \xrightarrow{k_2} C$$

Table 1

Rate constants in the acetolyses of ditosylates **3a** and **4**

Ditosylate	Temperature °C	k_1 s^{-1}	k_2 s^{-1}	k_1/k_2
3a	40	9.23×10^{-6}	6.01×10^{-6}	1.5
	60	1.20×10^{-4}	3.44×10^{-5}	3.5
	80	7.53×10^{-4}	1.79×10^{-4}	4.2
	100	4.70×10^{-3}	3.81×10^{-4}	12
	110	1.01×10^{-2}	4.03×10^{-4}	25
4	110	1.08×10^{-5}	4.62×10^{-6}	

Table 2

Some representative values of k_U/k_S

Arenesulphonate		k_U/k_S	Observations (Literature)
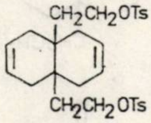 3a	first step second step	935 87.2	Acetic acid
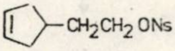 6-ONs		640 70	Formic acid (4b) Acetic acid (4b)
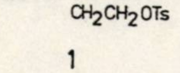 5		10 4	Formic acid (2) Acetic acid (2)
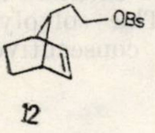 1		17	Acetic acid (1)
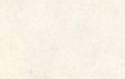 12		10^5	Acetic acid (8)

where k_1 and k_2 have the same order of magnitude. By known procedures,[7] the experimental data can be used to compute both rate constants, k_1 and k_2. Table 1 lists for **3a** the computed values of k_1 and k_2 at five different temperatures, and for **4**, at 110°.

Table 2 gives the values of k_U/k_S, determined by us for the two steps in the solvolysis of **3a** (110°), together with other representative values of this ratio for alicyclic compounds having in the side-chain a primary arenesulphonate group, $CH_2-CH_2-OSO_2Ar$.

The values of k_U/k_S determined by us are among the highest ratios observed in solvolyses proceeding by a π-route mechanism. The ratio for the first step ($k_U/k_S = 935$) is even larger than the ratio determined by Bartlett,[5b] in the formolysis of **6**-ONs. In the latter case, both the high ionisation power of formic acid (Y = + 2,054) and the better leaving group ability of nosylate group ($Ns = p-O_2N-C_6H_4SO_2$) with respect to the tosylate group ($Ts = p-CH_3-C_6H_4SO_2$) enhance double bond participation, increasing k_U/k_S. At 100° the rate of acetolysis of **3a** is about ten times faster in the first step than the acetolysis of **6**-OTs, the latter having about the same rate with that determined by us for the second step in the solvolysis of **3a** (see Table 3).

Table 3

Rate constants and activation parameters in solvolyses implying a π-route mechanism

No.	Compound	Temp. °C	k s^{-1}	ΔH* kcal/mol	ΔS* e.u.	Lit.
	3a first step	100	4.70×10^{-3}			
1.		25	1.34×10^{-6}*	23.12	−7.59	
2.	second step	100	3.81×10^{-4}	16.05	−30.87	
	4 first step	110	1.08×10^{-5}	—	—	
	second step	110	4.62×10^{-6}	—	—	
	5 in HOAc	75	7.40×10^{-6}			(2)
	in HOOCH	75	4.0×10^{-4}			(2)
3.	in HOAc	100	4.2×10^{-4}	21.72	−16.77	(4b)
	6-OTs	25	1.33×10^{-7}*			
4.	in HOOCH	25	7.13×10^{-5}	13.58	−32.20	(4b)
5.	**6**-ONs in HOAc	25	2.49×10^{-6}*	20.45	−17.56	(4b)
6.	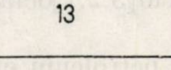 13	25	3.41×10^{-8}*	21.32	−21.63	(4b)
7.	**12** in HOAc	25	9.10×10^{-4}	16.3	−17.0	(8)

* Extrapolated values.

Table 3 includes constant rates and activation parameters of some solvolyses related to the reaction studied in this work. The most active compound, presenting also the highest value k_U/k_S, is the brosylate **12**[8] ($Bs = p - Br - C_6H_4SO_2$).

DISCUSSIONS

1. The π-route in the acetolysis of 3a

As expected, the ditosylate **3a** presents a high reactivity in both steps of the acetolysis. In order to compare its rate constants with the rate constant determined by Winstein and Carter[3] in the acetolysis of **5** at 75°, the values of k_2 (second step) were extrapolated to 75° ($k_2 = 1.32 \cdot 10^{-4} s^{-1}$) and, a correction factor $k_{ROBs}/k_{ROTs} = 3.5$ was applied.[9] It can be thus appreciated that even in the second step of the solvolysis, the compound **3a** is 60 times more reactive than the cyclohexenylethyl arenesulphonate **5**. The reactivity of the former compound surpasses by far, in the first step, the reactivity of cyclopentenylethyl tosylate **6**-OTs and is merely the same in the second step of the reaction (see Table 3). Clearly the rigidity of the skeleton and probably the geometric and conformational factors are responsible for the high reactivity observed by us in both steps of the reaction of **3a**.

The absence of either a primary alcohol group (CH_2CH_2OH), or of a vinyl group ($CH{=}CH_2$), in the acetolysis products, after treatment with $LiAlH_4$, is a confirmation of a π-route mechanism in the solvolysis of **3a**. Theoretically, by double bond participation in the ionisation of **3a** may result three types of isomeric diols :

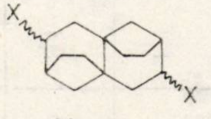

14a ; X = OH

14b ; X = Br

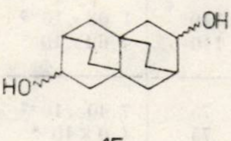

15

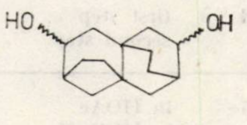

16

— a pair of diastereoisomeric diols **14a**, having two fused bicyclo[3.2.1]octane systems;

— a pair of diastereoisomeric diols **15**, having two fused bicyclo[2.2.2]octane systems;

— diastereoisomeric diols **16**, having a bicyclo[3.2.1]octane system fused with a bicyclo[2.2.2]octane system.

The dibromide **3b** treated with silica gel in petroleum ether, gave with high yield (83%) only the dibromide **14b**.[6] In order to explain this high selectivity in isomerisation, the authors suggested that the assisted ionisation of the two 2-bromoethyl groups occur simultaneously, leading to the dication **17** :

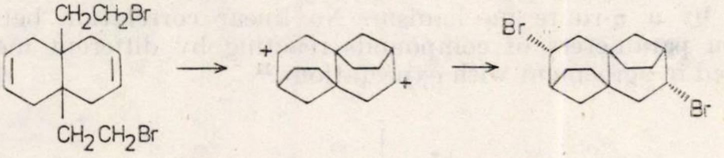

3b 17 14b

However, in the acetolysis of **3a**, the main reaction products (60%) are three diols, which on oxidation form at least two different ketones. That proves that the initial diols are also structurally different and that different ways of cyclisation have occurred. Thus, our results agree incompletely with the results obtained, in different conditions, by Paquette and coworkers.[5] They are in perfect agreement with the fact that both double bonds have participated in ionisation, but differ strinkingly in the outcome of this participation.

The inspection of Dreiding models shows that in the most stable conformation of compounds **3**,[12] the synchronous pathway is possible and cannot be ruled out. In the intermediate **18**, the attack of the bromide ion from the tight ion pair may be symmetric, yielding preferentially the dibromide **14b** :

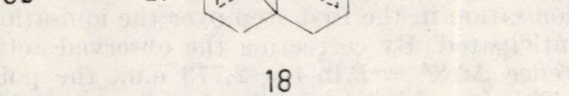

18

However, in acetic acid, the solvent is involved in ionisation. In petroleum ether only tight ion pairs **18** may exist. On the contrary, in acetic acid, tight ion pairs may be in equilibrium with different solvated ion pairs and even dissociated ions, each of these species having a different reactivity towards the nucleophilic reagent.[10] Thus, **3a** undergoes a stepwise ionisation of the two primary tosylate groups, as the kinetic data of Table 1 prove it, determining the formation of at least two polycyclic systems.

2. The isokinetic relationship

Representing the values of Table 3 in a plot ΔH^* *vs* ΔS^*, the points corresponding to **6**-OTs and **6**-ONs, both in acetic (3, 5)* and formic (4) acid and the second step in the solvolysis of **3a** (2) fall on a straight line with the slope $\beta = 380°$ (Fig. 1). The other three points (1, 6, and 7) are scattered with respect to the correlation line determined by the other four points. The deviation of nosylate **13** from the correlation line is easily explained. The saturated arenesulphonate **13** undergoes only a solvent assisted solvolysis, whereas the unsaturated derivatives **6** and **3a** react by a π-route mechanism. No linear correlation between the activation parameters of compounds reacting by different mechanisms is observed in agreement with expectations.[11]

---

* These and the following bracketed numbers correspond to the numbers from Table 3 and figure 1.

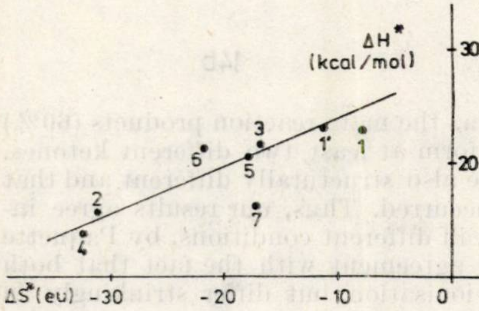

Fig. 1. — Solvolyses of some arenesulphonates : **3a** — first step (HOAc) — 1, 1′ ; **3a** — second step (HOAc) — 2 ; **5** (HOAc) — 3 ; **6**-ONs (HCOOH) — 4 ; **6**-ONs (HOAc) — 5 ; **13** (HOAc) — 6 ; **12** (HOAc) — 7.

The point corresponding to the first step in the reaction of **3a** presents a higher activation entropy than would have been predicted from its activation enthalpy on the basis of the isokinetic relationship. In figure 2 some of the possible conformations of **3a** are depicted. In the most stable conformation, chair-chair (A), each leaving group points only towards one of the double bonds, whereas in the *syn*-boat-boat conformation (B) the two ionisation centres of **3a** may be equally assisted by the two double bonds. A statistical factor of 2 and 4, respectively, favouring the ionisation in the first step over the ionisation in the second step, can be anticipated. By correcting the observed activation entropy with the difference $\Delta\Delta S^* = R \ln 4 = 2.773$ e.u., the point falls on the isokinetic line. This fact does not imply that **3a** reacts in the *syn*-boat-boat conformation (B). Indeed, it is well-known that such systems[12] have two easily interconvertible chair-chair conformations, symmetrizing the orientation of the substituents with respect to the cyclohexane rings. Models show that the same equilibration is also possible for **3a**. The rapid interconversion of the two equivalent chair-chair conformations will have the same result upon the reaction rates as it will have been observed if **3a** had reacted from the *syn*-boat-boad conformation. Moreover models show that in the chair-chair conformation the distance from the double bond to the reaction centre is the shortest possible one (Fig. 2).

The ratios k_1/k_2 recorded in Table 1 sustain only in part this conclusion. At the lowest temperature used in determinations (40°), the ratio is about 2 and increases at about 4 at 80°. The observed variation may reflect that at 40° the acetolysis is faster than the conformer interconversion, the latter exceeding the rate of solvolysis at the higher temperature. However, over 80°, the ratio increases rapidly, and is about 25 at 110°. The behaviour of the ditosylate **3a** in the second step will be discussed in the following section. For the moment, it must be retained that the correlation noticed by us for compounds **6** and **3a** demonstrates that they react by a similar pathway. The large reactivity of **3a** in both steps of the acetolysis and the low reactivity of **5** are sufficient proofs that the conformational control in π-route reactions is essential in determining the reactivity in cyclohexenylethyl compounds.

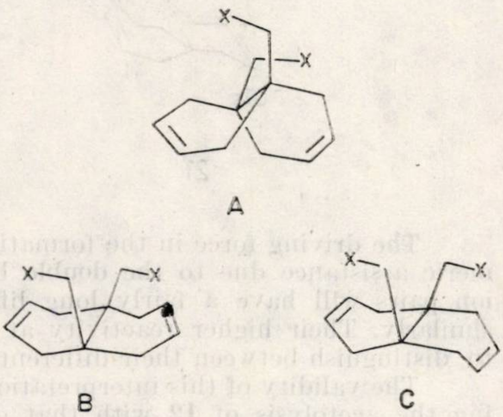

Fig. 2. — Some conformations of compounds **3** : A — chair-chair conformation ; B — *syn*-boat-boat conformation ; C — *anti*-boat-boat conformation.

3. Ion pair return

There are two more observations that need some further comment. One of them is the large increase of the k_1/k_2 ratio with increasing temperature, observed in this work, and the other one is the behaviour of brosylate **12** studied by Bly and coworkers.[8]

Indeed, considering only conformer equilibration at higher temperatures, k_1/k_2 must remain fairly constant with a mean value of about 4. Another plausible explanation could be that at lower temperatures in the first step of the reaction, the acetate **19** is formed having a bicyclo[3.2.1]octane system and at higher temperatures results the isomer **20**, with a bicyclo[2.2.2]octane system, reacting more sluggishly than the former.

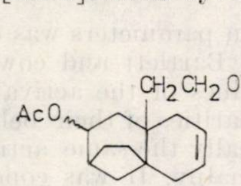

19

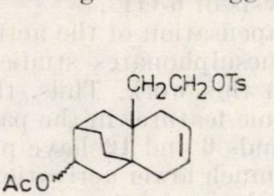

20

However, we estimated from Dreiding models that the distance from the double bond to the reaction centre is the same in both **19** and **20**.

Another explanation for the steep increase of k_1/k_2 over 80° is that ion pair return in the ionisation of **19** (or **20**) is more important than it is in the first step of the acetolysis of **3a**. It is well argumented in the literature[13] that the more crowded the ion pair, the more important will be their collapse to the covalent species. It is easily seen that in the ion pair **22** the tosylate ion has a smaller opportunity to be moved away than it has in ion pair **21**.

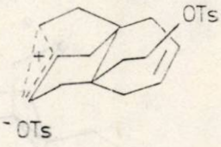

21

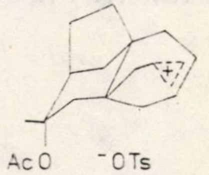

22

The driving force in the formation of both **21** and **22** is the anchimeric assistance due to the double bond. At lower temperatures these ion pairs will have a fairly long life-time in order to behave quite similarly. Their higher reactivity at the higher temperatures will allow to distinguish between their different tendency to ion pair return.

The validity of this interpretation seems to be confirmed by comparing the acetolysis of **12** with that of **19** (or **20**). In the solvolysis of the former compound, about 40% from the total reaction represents an ion pair return to the saturated brosylates **23** and **24** :[8]

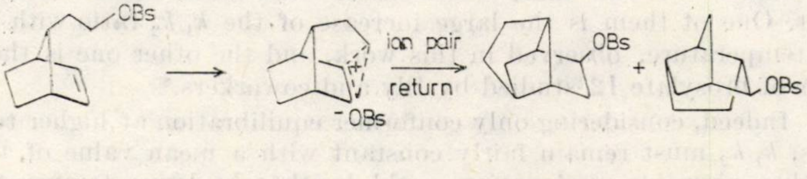

12 25 23 24

Clearly, ion pair **25** is more crowded than is the ion pair resulted in the solvolysis of **6**-OTs.

No compensation of the activation parameters was observed, either with the arenesulphonates studied by Bartlett and coworkers,[4] or with **19** studied in this work. Thus, the values of the activation parameters can reveal some features in the particularities of their behaviour in solvolysis. Compounds **6** and **12** have practically the same activation entropy, but **12** has a much lower activation enthalpy. It was concluded[8] that the difference in the activation enthalpies reflects the higher nucleophilicity of the double bond in a norbornene system, as compared to the reactivity of the double bond in a cyclopentene ring. However, theoretically, the two compounds cannot have the same opportunity for double bond assistance and thus their identical activation entropy is due to the compensation between the favourable conformation for π-route in **12** with an unfavourable factor, present in **12** and absent in **6**. We think that this factor must be the ion pair return in the more crowded brosylate **12**. On the other hand, **12** presents the same activation enthalpy as **19** (or **20**), but **12** differs largely from **19** (or **20**) in their activation entropy (see Table 3). Clearly, there is one single stable conformation in **12**, favourable for double bond participation and a large number of conformations for **19** (or **20**), from which only a few are suitable for a π-route reaction. On the other hand, from models we estimate that the distance between the double bond and the reaction centre in **19** is about 2.35 – 2.40 Å, practically the same as was appreciated in brosylate **12**.[8] In compounds **6** this distance is about 3.2Å, sensibly longer than in **12** and **19**. We conclude that in **12** and **19** the same activation enthalphy is the result of the shorter distance of the double bond to the reaction centre, in agreement with the conclusion of Bly *et al.*[8] of a high nucleophilicity of the double bond in **12**, as compared with the compounds **6**. However, this higher nucleophilicity is determined by the geometrical control (shorter distance between the reacting centres), rather than by the strain of the double bond in systems such as **12**.

The data reported herein confirm the overwhelming role of the conformational and geometric factors in determining the π-route reactions of cyclohexenylethyl derivatives, as compared to the cyclopentenylethyl derivatives.

EXPERIMENTAL

Melting points are uncorrected. IR spectra were recorded with a double beam UR-20 spectrophotometer.

cis-1,6-Bis (β-hydroxyethyl)bicyclo [4.4.0] deca-3,8-diene (10)

A solution of 31 g (113 mmoles) dimethyl ester **9**,[1] in 50 mL anhydrous dimetoxyethanol was added, dropwise, with mechanical stirring, to a suspension of $LiAlH_4$ (10g ; 263 mmoles in 100 mL of the same solvent. The mixture was refluxed for 20 hrs. After the usual workup 20 g (80 %) of alcohol **10**, white solid, m.p. 151 – 2° (ethanol), was obtained. (Found : C, 75.50 ; H, 10.0. $C_{14}H_{22}O_2$ requires : C, 75.63 ; H, 9.98 %). *IR spectrum* (KBr ; cm^{-1}) : 654 s, 661 s, 1008 s, 1040 vs, 1441 m, 1449 m, 1464 w, 1642 w, 3022 m.

The tosylate **3a** was prepared from the alcohol **10** with p-toluenesulphochloride in pyridine ; 86 % yield, m.p. 118° (methanol). (Found : C, 63.28 ; H, 6.48 ; S, 11.93. $C_{28}H_{34}O_6S_2$ requires : C, 63.30 H, 6.40 ; S, 12.10 %) *IR spectrum* (KBr ; cm^{-1}) : 1173 vs, 1188 s, 1363 vs

cis-1,6-Bis(β-hydroxyethyl)bicyclo [4.4.0] decane (11)

11.1 g (50 mmoles) alcohol **10**, in 100 mL methanol, was hydrogenated (catalyst 10 % Pd/C), at 50° and 10 atm. After the usual workup, 10 g (90 % yield) of alcohol **11** was obtained, m.p. 126 – 7°. (Found : C, 74.55 ; H, 11.82. $C_{14}H_{26}O_2$ requires : C, 74.28 ; H, 11.63 %). *IR spectrum* (KBr ; cm^{-1}) : 1016 s, 1043 s, 1054 m, 1451 m, 1476 m.

From the saturated alcohol **11**, the tosylate **4** was prepared in the usual manner ; m.p. 116 – 7° (methanol). (Found : C, 63.12 ; H, 7.45 ; S, 11.46. $C_{28}H_{38}O_6S_2$ requires : C, 62.90 ; 7.22 ; S, 11.99 %). *IR spectrum* (KBr ; cm^{-1}) : 1172 vs, 1185 s, 1360 vs.

For the kinetic determinations the ampoule technique was used.

The p-toluenesulphonic acid formed in the reaction was determined by titration with 0.05 M NaOAc/HOAc solution.

The acetic acid and the sodium acetate solutions were obtained as generally described. For recordings, a potentiograph A Metrohm, model E336, with platinum electrode and graphite capillary electrode, was used.

The rate constants were obtained by analytical integration of the kinetic equations derived from the reaction scheme mentioned before :

$$\begin{array}{l} A \xrightarrow{k_1} B + \text{TsOH} \\ \xrightarrow{k_2} C + \text{TsOH} \end{array}$$

A computer program was devised to obtain the best fit (least squares method) between calculated and experimental data.

ACKNOWLEDGEMENT. Thanks are expressed to Dr. M. Elian for helpful discussions.

REFERENCES

[1] E. Ciorănescu, A. Bucur, M. Elian, M. Banciu, M. Voicu and C. D. Nenitzescu, *Rev. Roumaine Chim.*, **10**, 161 (1965); E. Ciorănescu, M. Banciu, R. Jelescu, M. Rentzea, M. Elian and C. D. Nenitzescu, *Rev. Roumaine Chim.*, **14**, 911 (1969); M. Voicu, F. Badea and A. Voicu, *Rev. Roumaine Chim.*, **18**, 131 (1973); M. Stănescu, G. Mihai, L. Stănescu and E. Ciorănescu, *Rev. Roumaine Chim.*, **24**, 197 (1979).

[2] S. Winstein and P. Carter, *J. Amer. Chem. Soc.*, **83**, 4485 (1961).

[3] R. G. Lawton, *J. Amer. Chem. Soc.*, 83, 2399 (1961).

[4] a. P. D. Bartlett and S. Bank, *J. Amer. Chem. Soc.*, **83**, 2591 (1961); b. P. D. Bartlett, S. Bank, P. J. Crawford and G. H. Schmid, *J. Amer. Chem. Soc.*, **87**, 1288 (1965).

[5] H. Park, P. F. King and L. A. Paquette, *J. Amer. Chem. Soc.*, **101**, 4773 (1979).

[6] J. Altman, E. Babad, J. Pucknat, N. Reshef and D. Ginsburg, *Tetrahedron*, **24**, 975 (1968).

[7] S. W. Benson, *The Foundations of Chemical Kinetics*, Mc Graw-Hill, New York, 1960, p. 33–36.

[8] R. S. Bly, R. K. Bly, A. O. Badenbaugh and O. R. Vail, *J. Amer. Chem. Soc.*, **89**, 880 (1967).

[9] S. Winstein, B. K. Morse, E. Grunwald, K. C. Schreiber and J. Corse, *J. Amer. Chem. Soc.*, **74**, 1113 (1952).

[10] S. Winstein, E. Clippinger, A. H. Fainberg, R. Heck and G. C. Robinson, *J. Amer. Chem Soc.*, **78**, 328 (1956).

[11] J. E. Leffler and E. Grunwald, *Rates and Equilibria of Organic Reactions*, Wiley, New York, 1963, chapter 7.

[12] R. Bucourt, *Bull. Soc. Chim. France*, **1963**, 1983; *ibid.*, **1964**, 1262.

[13] P. v. R. Schleyer, *J. Amer. Chem. Soc.*, **86**, 1853 (1964); H. C. Brown (with comments by P.v.R. Schleyer) *The Nonclassical Ion Problem*, Plenum Press, New York. 1977, chapter 8.

Revue Roumaine de Chimie, 31, 5, 519–524 (1986)

SYNTHESIS OF BENZOSPIRO[2,4]HEPTANE DERIVATIVES

EMERIC BARTHA, ZSOLT ARVAY and ALEXANDRU C. RĂZUŞ
Centre of Organic Chemistry, Spl. Independenţei 202B R-78100, Bucharest, Romania

Received May 11, 1985

A method of preparing spirocyclopropaneindanols (1A—3A) by reducing the corresponding ketones (1B—3B) is reported. Improved and new procedures for the synthesis and purification of these ketones are described. The route requires cycliacylation of cyclopropanated phenylalkanoic acids or the oxidation of spirocyclopropaneindene.

In continuation of synthetic and mechanistic work in the field of the cyclopropanecarbinylic derivatives[1a–d], it seemed to us of interest to study some spirocyclopropanecarbinols with spirocyclopropaneindanic framework. The starting materials used in our studies are spiro[cyclopropane-1,2′-[2H]inden]-1′[3′H]-ol (**1A**), spiro[cyclopropane-1,1′-[1H]inden]-3′[2′H]-ol (**2A**) and spiro[cyclopropane-1,1′-[1H] inden]—2′[3′H]-ol (**3A**) whose forerunners are the respective ketones **1B**, **2B** and **3B**.

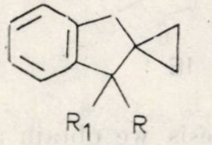

1

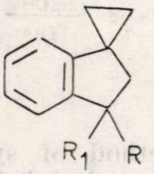

2

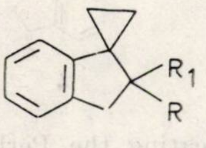

3

A: R=H ; R_1= OH
B: R + R_1= O

In fact, the alcohol synthesis by reduction of the corresponding ketones occurs readily and with almost quantitative yields. The difficulties reside in the obtention of these ketones.

In order to obtain the first ketone, namely spiro[cyclopropane-1,2′-[2H]inden]-1′[3′H]-one (**1B**), Fraisse-Julien and Fréjaville[2] started from ethyl α-benzylacrylate whose cyclopropanation was accomplished by treatment with diazomethane followed by irradiation. After saponification of the ester thus obtained, the resulting 1-benzylcyclopropanecarboxylic acid was cyclised to the ketone **1B**. An alternative synthesis, proposed for obtaining the ketone **1B** started from the readily available 1-indanone as a starting material.[3] The condensation of indanone with formaldehyde and piperidine hydrochloride leads to 2-(piperidinomethyl)-1--indanone hydrochloride which is pyrolysed to 2-methylene-1-indanone. The double bond is cyclopropanated *via* the pyrazolic intermediate which is also subjected to pyrolysis.

Perkins and co-workers[4] have obtained spiro[cyclopropane-1,1'-[1H]inden]-3[2'H]-one (**2B**) by cyclization of 1-phenylcyclopropaneacetyl chloride in the presence of $AlCl_3$ at −5°C.

The ketone **3B** has been unknown till now.

Both, the great number of steps and their poor yields make these synthetical methods unsuitable for obtaining larger amounts of ketones and it was necessary to develop new methods.

In order to obtain the ketone **1B**, we have employed two different syntheses. The first method is an improvement of the synthesis proposed by Fraisse-Julien.[2] We observed that cyclopropanation of ethyl benzylacrylate with methylene iodide in the presence of Zn-Cu couple takes place with improved yields and the resulted product has an advanced purity. Another modification refers to cycliacylation of benzylcyclopropanecarboxylic acid to ketone **1B**. The ketone **1B** results in a quantitative yield starting from the acid *via* acid chloride cyclization in the presence of $AlCl_3$ at low temperature.

The second method consists in the cyclopropanation of 1-indanone in a single step. The reaction was developed in a phase transfer catalysis : the indanone (**4**) reacts with ethylene dibromide (**5**) in the presence of benzyltriethylammonium chloride (TEBA) and a concentrated solution of sodium hydroxide.

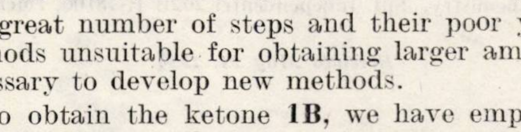

Repeating the Perkin's method of synthesis we obtain a small quantity of ketone **2B**, the major product being the ethylidene ketone **7**.

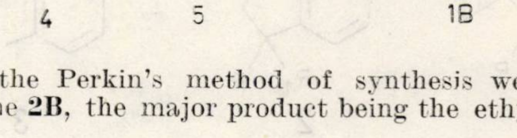

We observed that in this cyclization the initial reaction temperature and the ratio $AlCl_3$: acid chloride are very important. Thus, working at a temperature below −18°C and using a 1 :1 molar ratio, the spiroketone **2B** is the major product. The starting material in the synthesis, 1-phenylcyclopropaneacetic acid (**6**), was obtained by Wilt and co-workers from the nitril of the 1-phenylcyclopropanecarboxylic acid.[5] We have prepared the acid **6** by the oxidation of the alcohol **9**, obtained from the unsaturated alcohol **8** in a Simmons-Smith reaction, and the total yield was greater than 70%.

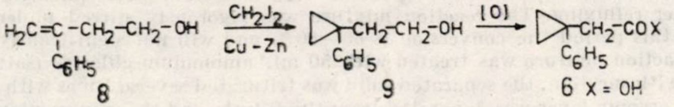

We have obtained the unknown spiro[cyclopropane-1,1′-[1H] inden]-2′[3′H]-one (**3B**) in a two-stage reaction, starting from indene.

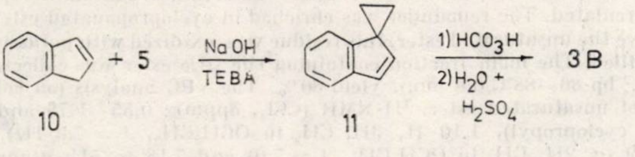

We carried out the cyclopropanation of indene in a phase transfer catalysis using dimethyl sulfoxide (DMSO) as co-solvent. In these conditions the conversion was about 50% and the yield almost quantitative. In the subsequent step, the spiran **11** was oxidized with performic acid, followed by the hydrolysis of the intermediately formed formate with sulfuric acid. Steam distillation leads to ketone **3B** with 60% yield and a purity greater than 98%.

As it was mentioned above, the alcohols **1A**, **2A** and **3A** were obtained by reducing the corresponding ketones with almost quantitative yields.

The separation and isolation of the ketones and alcohols was performed by liquid chromatography. Structural assignments for the alcohols and ketones are based on ^{1}H-NMR spectral data. The spectral data revealed interesting aspects and are under investigation in our laboratory.

In summary, our new synthetic methods appear to be more convenient and effective than the reported methods.

EXPERIMENTAL

All melting and boiling points are uncorrected. ^{1}H-NMR spectra were recorded with a Varian A 60-A spectrometer, using TMS as internal standard. IR spectra were recorded on a UR-10 Carl Zeiss Jena spectrophotometer. The VPC analyses were performed on a Willy Giede model 18−3 gas chromatograph using a flame ionisation detector and two different columns, column A : 3m×4mm packed with 15% ethylene glycol succinate and 5% silicon QF$_1$ on chromosorb W silanized (60−80 mesh) and column B : 1m × 4mm packed with 13% ethylene glycol succinate and 7% carbowax 20M on chromosorb W silanized (60−80 mesh).

Spiro[cyclopropane-1,2′-[2H] inden] -1′-(3′H)-one, (1B)

Method A : The cyclization of the 1-benzylcyclopropanecarboxylic acid chloride.

Ethyl α-benzylacrylate was prepared according to Fraisse-Julien.[2] The VPC analysis (column A) indicates a purity greater than 98%, bp 160−170°C/30−40 mm (lit.[2] bp 75−80°C/0.6 mm). ^{1}H-NMR (CCl_4, δppm) : 1.21 (t, 3H, CH_3 in OCH_2CH_3), 3.58 (s, 2H, CH_2 benzylic), 4.11 (q, 2H, CH_2 in OCH_2CH_3, J=7.0 Hz), 5.36 and 6.16 (2s, 2H, olefinic protons from=CH_2) and 7.18 (s, 5H, aromatics).

Ethyl 1-benzylcyclopropanecarboxylate. The Cu—Zn couple for the cyclopropanation was prepared according to Rowson[6] from 26.5 g (0.4 atg) Zn and 40 g (0.4 moles) CuCl in 60 mL ether, under inert atmosphere. To this couple 19 g (0.1 moles) α-bezylacrylic ester and 53.6 g (0.2 moles) methylene iodide (in which 0.2 g iodine were dissolved) were quickly added, maintaining the ether refluxing. The reaction mixture was vigorously stirred under reflux for 6—8 hours. After this period the conversion is 60—80% and will not significantly rise further in time. The reaction mixture was treated with 50 mL ammonium chloride (saturated solution) and filtered with suction, the separated solid was triturated several times with ether and then filtered. The organic layer was separated from the filtrate and the aqueous layer was extracted two times with 50 mL ether. The organic layer and the ether washings were treated twice with a 10% sodium hydroxide solution and with brine to neutral. After drying over anhydrous sodium sulfate, the ether was removed in vacuo and the oily residue was fractionated on a 50 cm Vigreux column with a 1 :5 reflux ratio. The distillate containing up to 60% unreacted ester was recirculated. The remainder was enriched in cyclopropanated ester (up to 90%). In order to remove the unsaturated ester, this residue was oxidized with potassium permanganate[2] and then distilled. The main fraction containing the title ester was collected, bp 130—140°C/2—3 mm (lit.[2] bp 86—88°C/0.6 mm), yield 80%. The VPC analysis (on column A) indicated the absence of unsaturated ester. ^{1}H-NMR (CCl_4, δppm) : 0.55—1.78 and 1.03—1.26 (A_2B_2 system, 4H, cyclopropyl), 1.10 (t, 3H, CH_3 in OCH_2CH_3, J = 7.0 Hz), 2.93 (s, 2H, CH_2 benzylic), 3.99 (q, 2H, CH_2 in OCH_2CH_3, J = 7.0) and 7.18 (s, 5H, aromatics).

1-*Benzylcyclopropanecarboxylic acid* was obtained from its ester by saponification with potassium hydroxide in ethanol, mp 99—100°C, the yield was 91%. Recrystallization from hexane gave a pure product, mp 104°C (lit.[2] 104°C). ^{1}H-NMR ($CDCl_3$, δppm) : 0.70—1.03 and 1.13—1.47 (A_2B_2 system, 4H, cyclopropyl), 2.95 (s, 2H, CH_2), 7.23 (s, 5H, aromatics) and 10.91 (s, large, 1H, COOH).

1-*Benzylcyclopropanecarboxylic acid chloride* was usually prepared by reaction of the corresponding acid with thionyl chloride in benzene, bp 120—125°C/2—3 mm. The yield was 90%. ^{1}H-NMR (CCl_4 δppm) : 0.73—1.09 and 1.31—1.66 (A_2B_2 system, 4H, cyclopropyl), 2.96 (s, 2H, CH_2 benzylic) and 7.14 (s, 5H, aromatics).

Cyclization of the acid chloride. To a stirred and cooled suspension of 32 g (0.24 moles) $AlCl_3$ in 125 mL methylene chloride, 38.9 g (0.2 moles) 1-benzylcyclopropanecarboxylic acid chloride in 100 mL methylene chloride were added dropwise so that the temperature might be maintained between —5°C and 0°C The reaction mixture was stirred at 0—5°C for additional 30 minutes, and then was poured into a solution of brine and ice. The organic layer was separated and the aqueous solution was extracted twice with 50 mL methylene chloride. The combined organic solutions were washed with water, with a saturated solution of sodium bicarbonate and again with water, then dried over anhydrous sodium sulfate and finally the methylene chloride was evaporated in vacuo. The residue, 31.6 g (almost quantitative yield), after crystallization from hexane, gave 27.7 g pure spiro [cyclopropane-1,2′-[2H]inden]-1′-[3′H]-one (**1B**). VPC analysis on column B, mp 54—55°C (lit.[2] 56°C). ^{1}H-NMR (CCl_4, δppm) : 0.86—1.15 and 1.21—1.46 (A_2B_2 system, 4H, cyclopropyl), 3.13 (s, 2H, CH_2 in indanone), 7,25—7.56 (m, 3H, aromatics), 7.71 (dd, 1H, aromatic adjacent to carbonyl group, $J_0 = 7.5$ Hz, $J_m = 2.0$ Hz).

Method B : The cyclopropanation of the 1-indanone. TEBA (0.3 g) was suspended in 20 mL of 50% NaOH solution and a mixture of 5.4 g (0.04 moles) 1-indanone, 9.4 g (0.05 moles) 1,2-dibromoethane and 4 mL DMSO were added dropwise to this suspension within 10 minutes, the temperature rising from 30° to 45°C. The reaction mixture was stirred 30 minutes at 45—50°C, cooled to 30°C and then 9.4 g (0.05 moles) 1,2-dibromoethane were dropped within 5 minutes. As no exothermal effect was observed, 0.2 g TEBA was additionaly added and the heating was continued for 30 minutes at 45—50°C. The supplementary addition of TEBA and ethylene dibromide was repeated twice and the final reaction mixture was diluted with 25 mL water and extracted three times with 25 mL ether. The ethereal solutions were washed with brine to neutral, dried on anhydrous sodium sulfate and the solvent distilled in vacuo. The ^{1}H-NMR spectrum of the raw product showed the presence of 90—95% spiroindanone **1B**, 5—10% 1-indanone (**4**) along with a quantity of indanone polymers. The product was chromatographed on 40 g neutral alumina with petroleum ether : ethylic ether 5 :1. The first fraction contained 4.1 g product, mp 40—46°C and the second contained 1 g crystalline indanone dimer. The crystallization of the first fraction from hexane gave 3.2 g (50% yield) pure ketone **1B** (VPC analysis on column B), mp 54—55°C (lit.[2] 55—56°C). The ^{1}H-NMR spectrum was identical with that obtained at method A.

Spiro[cyclopropane-1,1′-[1H]inden]-3[2′H]-one, 2B

3-Phenyl-3-buten-1-ol was prepared by saponification of 3-phenyl-3-buten-1-yl acetate with alcoholic potassium hydroxide, bp 120—123°C/2—3 mm (lit.[5] 130—131°C/13 mm). ^{1}H-NMR (CCl_4, δppm) : 2.65 (t, 2H, $=CH_2$, J = 7.0 Hz), 3.58 (t, 2H, CH_2 at OH), 3.68 (2, 1H, OH), 5.01 and 5.26 (2 m, 2H, olefinics) and 7.03—7.40 (m, 5H, aromatics).

2-(1-Phenylcyclopropyl)-ethanol. To the couple Zn-Cu prepared from 54 g (0.8 atg) Zn, 80 g (0.8 mol) CuCl and 120 mL ether, 30 g (0.2 moles) 3-phenyl-3-buten-1-ol were quickly added under inert atmosphere and 107.2 g (0.4 moles) methylene iodide (containing 0.4 g iodine) were dropped so that the ether might be slowly refluxed. After 6 hours the reaction was completed and the reaction mixture was worked up in a manner similar to that mentioned for ethyl 1-benzylcyclopropanecarboxylate. The obtained oily product (31.8 g) was distilled in vacuo. The main fraction, 23.6 g (72% yield), was the title product, bp 120—130°C/2—3mm. ^{1}H-NMR (CCl_4, δppm) : 0.68 (m, 4H, cyclopropyl), 1.7 (t, 2H, CH_2 bounded by cyclopropyl, J = 7.0 Hz), 3.28 (s, 1H, OH), 3.4 (t, 2H, CH_2 at OH) and 6.95—7.30 (m, 5H, aromatics).

1-Phenylcyclopropaneacetic acid was prepared by oxidation of 2-(1-phenylcyclopropyl)-ethanol with chromic anhydride in acetic acid. To 23 g (0.14 moles) cyclopropanated alcohol dissolved in 100 mL acetic acid, a solution of 23 g (0.23 moles) chromic anhydride dissolved in a mixture of 25 mL water and 200 mL acetic acid was added under stirring so that the temperature be kept below 30°C (it was necessary a weak cooling with water). The resulted solution was stirred for three hours at room temperature, poured into 600 mL water and extracted five times with 100 mL methylene chloride. The organic solutions were washed twice with 100 mL water and the solvent was removed in vacuo. To the residue, an aqueous alcoholic solution of NaOH was added and the mixture was refluxed for three hours. The ethanol was distilled in vacuo, the alkaline water was extracted three times with 50 mL ether and 9.2 g alcohol was this way recovered. The aqueous solution acidified with hydrochloric acid led to 15 g raw material. After trituration with hexane were obtained 11.7 g (78% yield) pure acid, mp 45—50°C (lit.[5] mp 52°C). ^{1}H-NMR ($CDCl_3$, δppm) : 0.90 (s, large, 4H, cyclopropyl), 2.58 (s, 2H, CH_2), 7.25 (m, 5H, aromatics) and 10.06 (s, large, 1H, COOH).

1-Phenylcyclopropaneacetyl chloride was usually prepared in benzene with thionyl chloride in excess, bp 105—110°C/4—5 mm (80% yield). ^{1}H-NMR ($CDCl_3$, δppm) : 0.88 (m, 4H, cyclopropyl), 3.06 (s, 2H, CH_2) and 7.25 (s, 5H, aromatics).

Cyclization of the acid chloride. To a stirred suspension of 3.5 g (0.026 moles) $AlCl_3$ in 20 mL methylene chloride cooled at —19 . . . —20°C, 4.86 g (0.025 moles) 1-phenylcyclopropaneacetyl chloride in 12 mL methylene chloride were quickly added dropwise, while the temperature rose spontaneously to —5°C. The reaction mixture was stirred for 10 minutes, the exothermic reaction ceased and the temperature fallen down to — 15°C. The mixture was poured into ice and salt, the aqueous layer was separated and extracted twice with 25 mL methylene chloride. The combined organic layers were twice washed with water, once with saturated sodium bicarbonate solution and again with water. After drying and removing the solvent in vacuo, the residue weights 3.8 g (yield 96%). The product was contaminated with variable quantities of unsaturated ketone. In order to remove them, the product was oxidized with potassium permanganate[2] and the obtained mixture was chromatographed on the neutral alumina (eluent petroleum ether : diethyl ether 10 :1), to give the crystalline pure ketone **2B**, yield 55%, mp 37—41°C (lit. [4] 44°C). ^{1}H-NMR ($CDCl_3$, δppm) : 1.13 (s, 4H, cyclopropyl), 2.63 (s, 2H, CH_2 in indanone), 6.90 (d, 1H, aromatic proton adjacent to the cyclopropyl), 7.03—7.55 (m, 2H, aromatics), and 7.66 (dd, 1H, aromatic proton adjacent to carbonyl, $J_\theta =$ $= 7.0$ Hz, $J_m = 1.5$ Hz).

Spiro[cyclopropane-1,1′-[1H]inden]-2′[3′H]-one, 3B

Spiro [cyclopropane-1,1′-indene], **11**. To a solution of 2 g TEBA in 144 mL 50% sodium hydroxide solution, a mixture of 36 g (0.30 moles) fresh distilled indene, 87.5 g (0.465 moles) 1,2-dibromoethane and 60 mL DMSO was added dropwise. The reaction was strongly exothermic and the temperature rose rapidly at 50—55°C and it was maintained at this value by external cooling in the course of dropping. The reaction mixture was stirred at 60°C for three hours, then was poured into 150 mL cold water. The organic layer was separated and the aqueous layer was extracted twice with 100 mL ether. The organic solution was washed with water to neutral, dried on anhydrous sodium sulfate, the solvent was removed in vacuo and the residue was distilled. The fraction between 100 and 150°C was collectde (34.6 g). This colourless product containing mainly indene and spiroindene **11**, was fractioned on a Vigreux column. The first fraction (12.2 g, bp 105—130°C/30—40 mm) contained mainly indene (20—30% spiroindene). The major fraction (20 g, bp 130—140°C/20—30 mm) was pure spiroindene **11**. The total yield was 70%. ^{1}H-NMR (CCl_4, δppm): 1.38 (s, 4H, cyclopropyl), 5.95 and 6.71 (2d, AB system, 2H olefinic, $J = 5.5$ Hz), and 6.58—7.41 (m, 4H, aromatics).

Oxidation of spiro[cyclopropane-1,1'-indene]. To a magnetically stirred mixture of 35 mL 80% formic acid and 7 mL hydrogen peroxide 30%, 7.1 g (0.05 moles) spiroindene **11** were added dropwise with a weak external cooling so that the reaction temperature might not exceed 40°C. The spiroindene was dissolved in the reaction medium as soon as it is reacting. After finishing the dropping, the reaction mixture was stirred further for 1—2 hours at room temperature, then was poured into 100 mL water and was extracted three times with 25 mL ether. The ethereal solutions were washed with water and with saturated solution of sodium bicarbonate and finally the solvent was removed in vacuo. To the residue 150 mL sulfuric acid (7% in volume) were added and the ketone **3B** was steam distilled. The solid ketone was filtered in vacuo and dried in desiccator. The ketone **3B** resulted in high purity (over 98%). The yield was 60%, mp 78—80°C (VPC analysis on column B). The extraction of the filtrate gave more 0.5 g ketone **3B**, having 85—90% purity, mp 70—74°C. ^{1}H-NMR ($CDCl_3$, δppm): 1.05—1.76 (m, 4H, A_2B_2 system, cyclopropyl), 3.43 (s, 2H, CH_2 in indene), 6.70 (m, 1H, aromatic adjacent to cyclopropyl) and 7.00—7.46 (m, 3H, aromatics).

Spiro[cyclopropaneindanylic] alcohols

The alcohols **1A**, **2A** and **3A** corresponding to the ketones **1B**, **2B** and **3B** were obtained from these ketones by reduction with an excess of sodium borohydride in aqueous methanol, with almost quanitative yields.

Spiro [cyclopropane-1,2'-*[2H] inden]*-1'*[3'H]-ol*, **1A**, mp 58—59°C (hexane), ^{1}H-NMR ($CDCl_3$, δppm): 0.40—1.06 (m, 4H, cyclopropyl), 2.48 (s, 1H, OH), 2.65 and 3.00 (AB system, 2H, CH_2 in indene), 4.48 (s, 1H, CH at α-OH) and 6.98—7.31 (m, 4H, aromatics).

Spiro [cyclopropane-1,1'-[1H] inden]-3'[2'H]-ol, **2A**, mp 41°C (ethanol-water), ^{1}H-NMR (CCl_4, δppm): 0.58—1.06 (m, 4H, cyclopropyl), 1.88 and 2.08 (AB fragment of ABX system, 2H, CH_2 in indene $J_{AB}=13.0$ Hz, $J_{AX}=8.0$ Hz and $J_{BX}=6.0$ Hz), 4.83 (s, 1H, OH), 5.08 (m, X fragment of ABX system, 1H, CH adjacent to OH), 6.50 (m, 1H, aromatic adjacent to cyclopropyl), and 6.86—7.40 (m, 3H, aromatics).

Spiro [cyclopropane-1,1'-[1H] inden]-2'[3'H]-ol, **3A**, mp 88—89°C (methanol-water), ^{1}H-NMR ($CDCl_3$, δppm): 0.63—1.40 (m, 4H, cyclopropyl), 1.98 (s, 1H, OH), 2.93 and 3.33 (AB fragment of ABX system, 2H, CH_2 in indene, $J_{AB}=17.0$ Hz, $J_{AX}=6.0$ Hz and $J_{BX}=3.0$ Hz), 4.03 (dd, X fragment of ABX system, 1H, CH adjacent to OH), 6.70 (m, 1H, aromatic adjacent to the cyclopropyl) and 6.95—7.33 (m, 3H, aromatics).

REFERENCES

[1] a) A. C. Răzuş, V. Wertheimer, F. Badea and A. M. Glatz, *Tetrahedron Letters*, **1975**, 1799; b) V. Wertheimer, A. M. Glatz and A. C. Răzuş, *Rev. Roumaine Chim.*, **22**, 1505 (1977); c) F. Badea, A. M. Glatz and A. C. Răzuş, *ibid.*, **26**, 629 (1981); d) A. C. Răzuş, E. Bartha, Zs. Arvay and A. M. Glatz, *ibid.*, **29**, (1984).

[2] R. Fraisse-Julien and C. Fréjaville, *Bull. Soc. Chim. France*, **1970**, 219.

[3] R. O. Loutfy and P. Yates, *J. Amer. Chem. Soc.*, **101**, 4694 (1979).

[4] M. J. Perkins, N. B. Peynircioglu and B. V. Smith, *Tetrahedron Letters*, **1975**, 4165.

[5] J. W. Wilt, L. L. Moravetz and J. F. Zawazki, *J. Org. Chem.*, **31**, 3018 (1966).

[6] R. J. Rowson and J. T. Harrison, *J. Org. Chem.*, **35**, 2075 (1970).

Revue Roumaine de Chimie, 31, 5, 525–527 (1986)

AMIDES FROM N-ACYLPHTHALIMIDES AND ALIPHATIC AMINES

C. I. CHIRIAC
"P. Poni" Institute of Macromolecular Chemistry, Aleea Gr. Ghica-Vodă 41 A — Jassy — Romania

Received June 3, 1985

Various amides are prepared in high yields from N-acylphthalimides and aliphatic amines in pyridine as solvent at 75—85° for 4—5 hours.

In 1981, C. Palomo[1] presented the first direct synthesis of N-acylphthalimides from phthalimide and free carboxylic acid in the presence of diphenyl chlorophosphate as reagent. He tried to use the N-acylphthalimides as reagents for acylation of amines, but he obtained a mixture of compounds in which the presence of the corresponding amid was not detected.

RESULTS AND DISCUSSIONS

In a previous paper,[2] we showed that the N-acylphthalimides react with phenols, affording the corresponding esters in high yields.

We tried to use the N-acylphthalimides for the acylation of amines. We obtained pure products only in the reactions with aliphatic amines and impure products with aromatic amines. The aliphatic amines (strong nucleophylic reagents) can react with the acyl group at low temperatures (70–80°). The aromatic amines react at higher temperatures (120–130°), when, probably, these compounds destroy the imidic cycle, resulting impure products, without importance for our subject. In the case of reaction between benzoyl phthalimide and cyclohexylamine, we obtained benzoylcyclohexylamine, in high yields, in different solvents such as : pyridine, dioxane or tetrahydrofurane at 75–85°. Acetyl- or propionylphthalimide reacts with aliphatic amines just at room temperature.

The high reactivity of the N-acylphthalimides with aliphatic amines at low temperature, can be explained by the influence of these three acyl groups at the same nitrogen atom the first acyl group being the most reactive. A similar case is that of tribenzoylamines, when the first benzoyl group reacts with amines at low temperature, the second and the third reacting at higher temperatures. This progressive reactivity is also known in other cases, e.g. at triacylphosphites,[3] diacylphenylphosphites[4] and other reactive compounds with phosphorus, but it is unknown until now for nitrogen.

The reaction takes place, after the following mechanism :

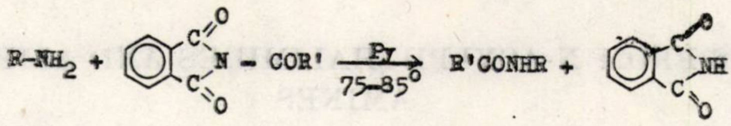

(I) (II) (III)

The reaction involves a nucleophylicat tack of the amine(I) at the carbonyl group from the acylphthalimide (II), which can be presented as a four-centred transition state (IV), known in many other similar cases.[5,6]

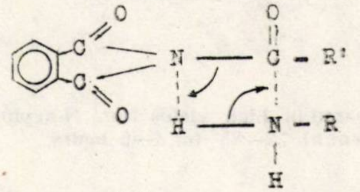

(IV)

Table 1

Amides from acylphthalimides and amines

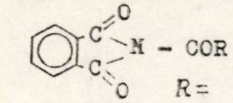 R=	Amines	Amides[a]		
		Yield[b] %	M.p.[c] °C	Literature m.p.[d] °C
CH_3	cyclohexylamine	75	64—66	65—66[7]
CH_3	benzylamine	68	59—61	60—61
C_2H_5	cyclohexylamine	73	88—91	88—90
C_2H_5	benzylamine	71	40—42	42—43[8]
C_6H_5	cyclohexylamine	91	145—147	146—147[9]
C_6H_5	benzylamine	88	105—107	106[10]
C_6H_5	pyperidine	79	49—51	49—50[11]
p $CH_3O—C_6H_4$	cyclohexylamine	93	158—160	159—161[9]
p-$CH_3O—C_6H_4$	benzylamine	86	131—133	131—132[8]
p-$Cl—C_6H_4$	benzylamine	77	164—166	164—165[10]

[a] The products were identified by comparison of m.p. and IR spectra with authentic samples.

[b] Yields calculated on acylphthalimide employed.

[c] After recrystallization.

[d] From "Beilstein Handbuch der Organischen Chemie".

As we see in this reaction phthalimide results as by-product, and can be easy recovered and used for the synthesis of the acylphthalimide (II).

A general procedure for the synthesis of the amides by this method consists in the addition under stirring of one mole of (I) to a solution of one mole of (II) in dried pyridine, followed of a feeble heating. Table 1 shows the amides (III) obtained by this procedure.

The yields ranged from 68% to 93% (Table 1).

In conclusion, we have found that the N-acylphthalimides can be used as reagents for the acylation of aliphatic amines at low temperatures, the corresponding amides resulting in high yields.

EXPERIMENTAL

Benzoylcyclohexylamine

A solution of 2.51 g(0.01 mole) benzoylphthalimide[1] and 1.1 mL (0.01 mole) cyclohexylamine in 7 mL dried pyridine was heated, under stirring, at 75—85° for 4—5 hours, At the end of reaction, the obtained solution was slowly poured into 40—50 mL water with ice, when the desired product precipitated. Then the mixture was treated with 8% NaOH solution till pH = 9—10 and the product was collected by filtration, washed three times with 5—10 mL water and dried under vacuum at 60—70°. Benzoylcyclohexylamine (1.85 g) was obtained with m.p. 145—147° (after recrystallization from ethanol) Mixed m.p. with pure product undepressed.

Yield 91% calculated on benzoylphthalimide employed.

Anal. Found: C, 76.31; H, 8.12; N, 6.57%. Calculated for: $C_{13}H_{17}ON$; C, 76.84; H, 8.37; N, 6.89%.

Under similar conditions, the other amides (presented in table 1) were prepared from acylphthalimides and aliphatic amines.

REFERENCES

[1] C. Palomo, *Synthesis*, **1981**, 993.
[2] C. L. Chiriac, *Rev. Roumaine Chim.*, **30**, 753 (1985)
[3] C. I. Chiriac, *Rev. Roumaine Chim.*, **24**, 609 (1979).
[4] C. I. Chiriac, *Rev. Roumaine Chim.*, **26**, 1001 (1981).
[5] H. O. Becker and K. F. Funk, *J. prakt. Chem.*, **14**, 55 (1961).
[6] W. Gerrard and J. A. Cade, *J. Chem. Soc.*, **1954**, 2034.
[7] G. Fouge, *Ann. Chim.*, **15**, 291 (1921); *Chem. Abstr.*, **15**, 4004 (1921).
[8] O. C. Dermer and J. King, *J. Org. Chem.*, **8**, 168 (1943); *Chem. Abstr.*, **37**, 3733 (1943).
[9] G. W. Cannon, *J. Org. Chem.*, **18**, 516 (1953); *Chem. Abstr.* **48**, 3927 (1954).
[10] T. Shingaki, *Nippon Kagaku Zasshi*, **80**, 55 (1959); *Chem. Abstr.* **55**, 4408 (1961).
[11] K. Kindler, *Chem. Ber.*, **95**, 1992 (1962).

Revue Roumaine de Chimie, **31**, *5*, 529–532 (1986)

SYNTHESIS AND CHARACTERIZATION OF MIXED LIGAND SCHIFF BASE COMPLEXES FORMED BY TEMPLATE METHOD

B. T. THAKER* and PURNIMA B. THAKER
* Department of Chemistry, South Gujarat University, Surat-395007
Chemistry Department, P.T. Sarvajanic College of Science, Athwalines, Surat-395001

Received January 28, 1985

Template synthesis of Schiff base complexes has been carried out with coordinated ethylene diamine or propylene diamine in the mixed ligand complexes [(cat) M-en or Pn] and [(naph) M-en or Pn] where M = Cu(II) or Ni(II), cat = catechol and naph = 2,3-dihydroxynaphthalene. The resulting mixed ligand complexes retain catechol or 2,3-dihydroxynaphthalene moiety. The Schiff base formed by the condensation of 2-hydroxy-1-naphthaldehyde with coordinated en or Pn is a bidentate ligand, while the OH groups of the Schiff base N, N′-ethylene or propylene bis(2-hydroxy-1-naphthylmethyleneamine) remain uncoordinated. This has been confirmed by molar conductance, magnetic and spectral studies.

The template synthesis has been very well known since Curtis[1] described the formation of macrocyclic metal complexes of considerable stability by the reaction of metal diamine complexes with aliphatic aldehyde and ketone. Bhattacharya et al.[2,3] have prepared Schiff base complexes of bidentate ligands through template reaction. In this reaction the coordinated amine is either en or Pn and it reacts with 2-hydroxy-1-naphthaldehyde; there is a formation of tetradentate Schiff base (TSB) disposed in the square planar way around the metal ion.

Similar reactions have however not been carried out with large molecules (such as 2-hydroxy-1-naphthaldehyde) and coordinated diamines in the mixed ligand complexes. An attempt was therefore made to study such reactions with 2-hydroxy-1-naphthaldehyde in order to confirm whether it behaves as salicylaldehyde in TSB.

The mixed ligand complexes 1. [(naph) Ni-en], 2. [(naph) Ni-Pn], 3. [(cat) Ni-Pn], 4. [(naph) Cu-Pn] and 5. [(cat) Cu-Pn] were synthesized according to reported procedure[4].

Analysis 1. [(naph) Ni-en] : Found : C, 52.14 ; H, 5.15 ; N, 10.21 Ni, 21.12 %. calculated for $C_{12}H_{14}O_2N_2Ni$: C, 52.04 ; H, 5.05 ; N, 10.11 ; Ni, 21.21%. 2. [(naph) Ni-Pn] Found : C, 53.50 ; H, 5.45, N, 9.65 ; Ni 20.25%. calculated for $C_{13}H_{16}O_2N_2Ni$: C, 53.66 ; H, 5.50 ; N, 9.63 ; Ni 20.19 %. 3. [(cat) Ni-Pn] Found : c, 45.01 ; H, 5.90 ; N, 11.50 ; Ni 24.50 %. calculated for $C_9H_{14}O_2N_2Ni$: C, 44.86 ; H, 5.81 ; N, 11.63 ; Ni, 24.39% 4.

[(naph) Cu-Pn] Found : Cu, 52.80 ; H, 5.50 ; N, 9.50 ; Cu 21.55%. calculated for $C_{13}H_{16}O_2N_2$ Cu : C, 52.78 ; H, 5.41 ; N, 9.47 ; Cu, 21.49%. 5. [(cat) cu-Pn] Found : C, 44.05 ; H, 5.85 ; N, 11.55 ; Cu, 25.95. % calculated for $C_9H_{14}O_2N_2$ Cu : C, 43 .98 ; H, 5.70 ; N, 11.40 ; Cu 25.87 %.

The reactions of the above compounds have been carried out with 2-hydroxy-1-naphthaldehyde. Exact weight of the substance was mixed with an excess ethanolic solution of 2-hydroxy-1-naphthaldehyde. The reaction mixture was refluxed for 4 hrs. When the solid dissolved and it became homogeneous, the solution was evaporated to reduce the volume. To this was added an excess of ether. Reddish solid in the case of Ni(II) complexes and violet in the case of Cu(II) complexes, separated out. The compounds were washed with ether and ethanol to remove excess 2-hydroxy-1-naphthaldehyde and they were recrystallized from chloroform solution and were analysed for C, H, N and metal contents.

The homogeneity of all metal mixed complex preparation was confirmed by TLC analysis. The molar conductance of all Cu(II) and Ni(II) mixed ligand Schiff base complexes in chloroform show them to be non electrolytes.

Table 1

Magnetic moments, electronic spectral band and elemental analysis of mixed ligand Schiff base complexes of Cu(II) and Ni(II)

Complexes	Found %				Calculated %				Electronic spectral bank λ_{max}	Magnetic moment μeff. B.M.
	Cu/Ni	C	H	N	Cu/Ni	C	H	N		
1. [L_1 Ni TSB-1]	10.10	69.86	4.52	4.80	10.04	69.77	4.44	4.78	540	Diamagnetic
2. [L_1 Ni TSB-2]	9.85	70.02	4.80	4.65	9.80	70.15	4.67	4.67	540	-do-
3. [L_2 Ni TSB-2]	10.72	67.82	4.65	5.15	10.69	67.79	4.73	5.10	540	-do-
4. [L_1 Cu TSB-2]	10.62	69.63	4.75	4.50	10.52	69.58	4.63	4.63	570	1.79
5. [L_2 cu TSB-2]	11.50	67.35	4.78	5.15	11.47	67.20	4.69	5.05	570	1.81

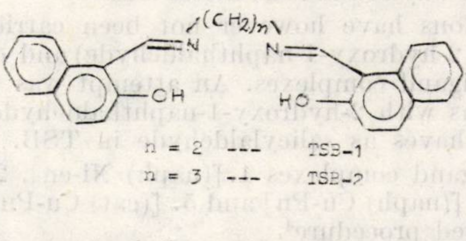

The magnetic moment of the compounds was determined by using the Gouy method at room temperature. Ni(II) complexes are found to be diamagnetic. The Cu(II) complexes show magnetic moment values between 1.73 to 1.82 B.M. (Table 1).

The visible spectra of the compounds in chloroform solution weres obttined in the region 400—800 nm using neotronics visible spectrophotometer. Ni(II) complexes show a band at ~ 540 nm. In the case of Cu(II) complexes one band is obtained at ~570 nm.

The IR spectra of the above mixed ligand Schiff base ~ compounds were obtained in form of KBr pellets.

The reaction of performed mixed ligand complexes having coordinated diamine with 2-hydroxy-1-naphthaldehyde gave product [L_1 Ni TSB-1], [L_1 Ni TSB-2], [L_2 Ni TSB-2], [L_1 Cu TSB-2] and [L_2 Cu TSB-2] where, (TSB-1) = N, N′-ethylene bis (2-hydroxy-1-naphthylmethyleneamine), (TSB-2) = N,N′-Propylene bis (2-hydroxy-1-naphthylmethyleneamine),

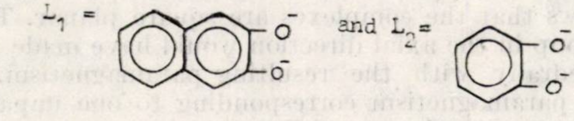

Thus it is observed from the composition of the complexes that catechol or 2,3-dihydroxy naphthalene are retained in the structure and the coordinated diamine (en or Pn) in mixed ligand complexes, on reaction with 2-hydroxy-1-naphthaldehyde, undergoes condensation resulting in the formation of the tetradentate Schiff base. The reaction schemes proposed are as follows :

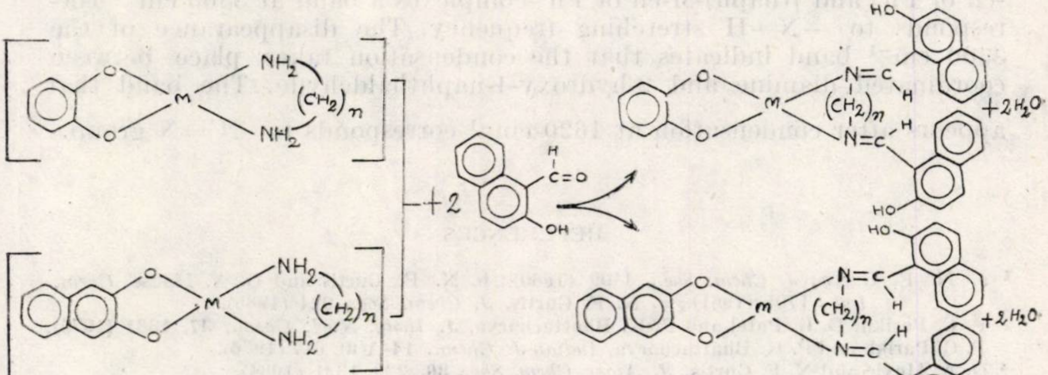

where n = 2 or 3.

If the reaction is carried out by mixing of 1 :1 :1 metal salt, catechol or 2,3-dihydroxy naphthalene and TSB-1 or TSB-2, there is a formation of [M-TSB-1] or [M-TSB-2]. This indicates that the coordination tendency of free TSB-1 or TSB-2 is greater because TSB-1 and TSB-2 are more basic hence they can liberate H from hydroxyl groups more easily than the corresponding catechol or 2,3-dihydroxynaphthalene.

It is observed that after recrystallization the composition of the complexes remains unchanged thus the catechol or 2,3-dihydroxy-naphthelene is in the coordination sphere and not in the crystal lattice. The reaction is similar to that observed in the case of bis ethylenediamine complexes.[1-a,4] However in that case the resulting Schiff base acts as a quadridentate ligands. Thus the Schiff base has two negative charges. In the present case the resulting complexes are neutral, because they have the catecholate or 2,3-dihydroxy naphthalate ions with two negative charges. This indicates that the $-$OH groups of the Schiff base formed by 2-hydroxy-1-naphthaldehyde remain undissociated. There can be also explained that the Schiff base with a double bond cannot occupy two equatorial and two axial positions.[5,6] If the $-$OH groups would have coordinated, loosing the proton, the complex would have been ionic. But it is observed that the compounds are insoluble in water and soluble in organic solvents. The conductivities of their solutions show them to be nonelectrolytes.

The structure is supported by diamagnetism of Ni(II) complexes. This clearly shows that the complexes are square planar. The coordination of $-$OH group in the axial direction would have made the complex distorted octahedrally with the resulting paramagnetism. The Cu(II) complexes have paramagnetism corresponding to one unpaired electron as expected for square planar configuration.

The visible spectra of the Cu(II) and Ni(II) complexes are like the characteristic square planar structure.[7]

The IR spectra of mixed ligand Schiff base complexes i.e. [L_1-M-TSB-1 or 2] and [L_2-M-TSB-1 or 2] show a broad band in the range 3600$-$3300, corresponding to $-$OH stretching frequency, indicating the undissociated hydrogen of OH groups of TSB-1 and TSB-2. In [(cat)-M-en or Pn] and [(naph)-M-en or Pn]-complexes a band at 3300 cm^{-1} corresponds to $-$N$-$H stretching frequency. The disappearance of the 3300 cm^{-1} band indicates that the condensation takes place between coordinated diamine and 2-hydroxy-1-naphthaldehyde. The band that appears after condensation at 1620 cm^{-1} corresponds to $>$C$=$N group.

REFERENCES

[1] a. N. F. Curtis, *J. Chem. Soc.*, 4409 (1960); b. N. F. Curtis and D. A. House, *Chem. Ind.*, 1708 (1961); c. N. F. Curtis, *J. Chem. Soc.*, 924 (1965).

[2] P. C. Parikh, D. C. Patel and P. K. Bhattacharya, *J. Inorg. Nucl. Chem.*, **37**, 1381 (1975).

[3] P. C. Parikh and P. K. Bhattacharya, *Indian J. Chem.*, **14-A(8)**, 617 (1976).

[4] D. A. Hovie and N. F. Curtis, *J. Amer. Chem. Soc.*, **86**, 223, 1331 (1964).

[5] F. A. Cotton, "Progress in Inorganic Chemistry", Vol. $-$7, (Ed. by F. A. Cotton) Interscience Publishers, New York, 108, 193 (1966).

[6] R. L. Carlin, "Transition Metal Chemistry", **4**, 281 (1968).

[7] R. S. Drags, "Physical Methods in Inorganic Chemistry", Reinhold, New York, 179 (1968).

Revue Roumaine de Chimie, **31**, 5, 533–539 (1986)

SYNTHESIS OF CERTAIN SUBSTITUTED BENZOPYRANOPYRIDINE AND PYRIMIDINE RING SYSTEMS

M. M. ISMAIL* and M. S. MOHAMED
Department of Organic Chemistry, Faculty of Pharmacy, Cairo University, Cairo, Egypt

Received April 27, 1985

Various 1-substituted benzopyranopyridines were prepared by the condensation of ethyl cyanoacetate and 3,5-dichlorosalicylaldehyde with aliphatic aldehydes in the presence of ammonium acetate. On the other hand, condensation with aromatic aldehydes gave 2-aryl-benzopyranopyrimidines.

Benzopyranopyridines were prepared by Villani *et al.*[1] from phenoxypyridine carboxylic acids *via* polyphosphoric acid cyclization. On the other hand, benzopyranopyrimidines could be synthesized by the cyclization of 4-oxo-4H-[1] benzopyran-3-carboxylic acids,[2] esters,[3] and carboxaldehydes[3-5] with guanidine. In an analogous work,[6] the synthesis of 2- or 1,2-disubstituted benzopyranopyridines by the condensation of ethyl cyanoacetate, and 3,5-dichlorosalicylaldehyde with ketones in the presence of ammonium acetate has been reported.

The present paper deals with the synthesis of 1-alkylbenzopyranopyridines (from aliphatic aldehydes) and 2-arylbenzopyranopyrimidines (from aromatic aldehydes) by the reaction of ethyl cyanoacetate and 3,5-dichlorosalicylaldehyde with various aldehydes in the presence of ammonium acetate. The reaction of ethyl cyanoacetate and 3,5-dichlorosalicylaldehyde with aliphatic aldehydes was carried out by refluxing a mixture of the ester, 3,5-dichlorosalicylaldehyde, aliphatic aldehyde, and ammonium acetate (molar ratio 1 :1 :1 :1–1.5) in ethanol. In this case, (Scheme 1) the condensation of the amino group of 6,8-dichloro-3-amidino-coumarin[6] (I) with the carbonyl group of the aldehyde, cyclization between the methylene group adjacent to the aldehyde carbonyl and the 4-position of the coumarin ring, and subsequent dehydrogenation took place to form 1-alkyl-4-amino-7,9-dichloro-5-oxo-[1] benzopyrano[3,4-c] pyridines (II). The ^{1}H-NMR spectrum (in CF_3CO_2H) of IIa (from propionaldehyde) showed only a methyl singlet at δ 2.9 ppm, while IIb (from *n*-butyraldehyde) showed a methyl triplet at 1.5 ppm and a methylene quartet at 3.3 ppm in a higher field than the aromatic-ring region. These facts indicated

---

* The author to whom correspondence should be addressed

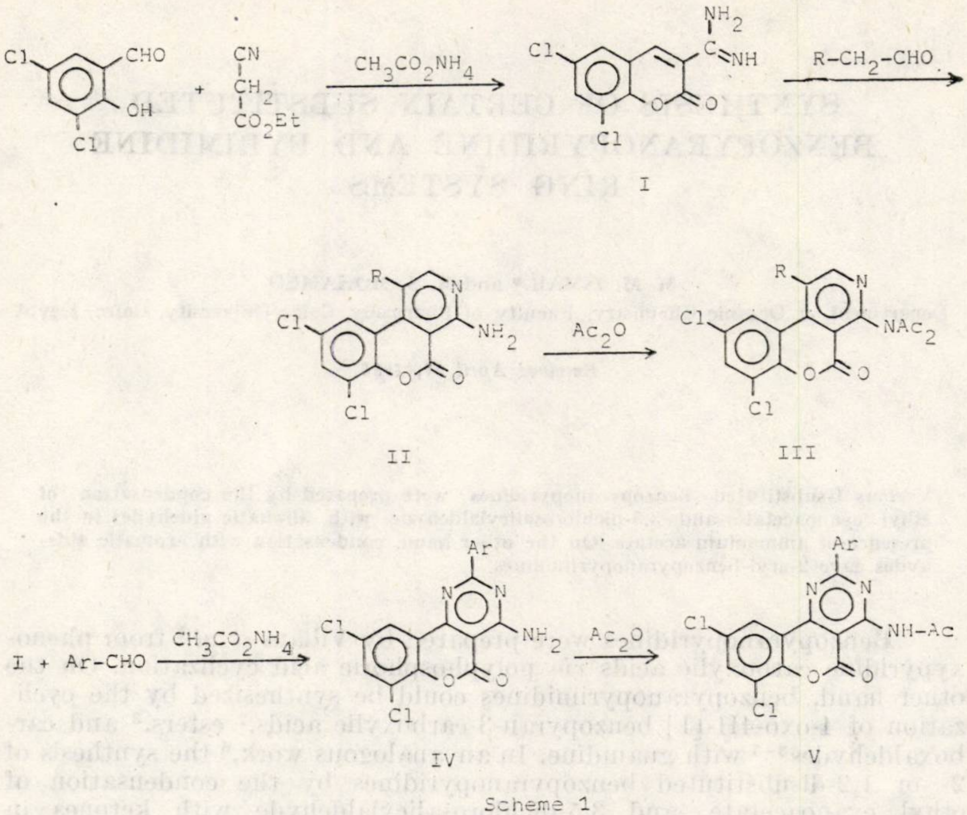

Scheme 1

that the methylene group adjacent to the aldehyde carbonyl was involved in this cyclization. On the other hand, the condensation with aromatic aldehydes (benzaldehyde or its derivatives) gave 2-aryl-4-amino-7,9-dichloro-5-oxo-[1] benzopyrano[4,3-d]pyrimidines (IV). In this case, one mole each of ethyl cyanoacetate, 3,5-dichlorosalicylaldehyde, and

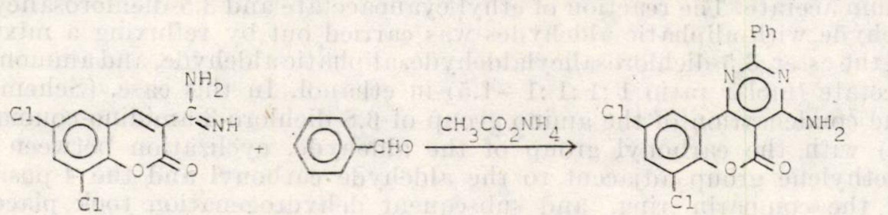

Scheme 2

benzaldehyde (or its derivaties) reacted with two mols of ammonia to give (IV), with the elimination of one mole of ethanol and two mols each of water and hydrogen. In all cases, 6,8-dichloro-3-amidinocoumarin (I) is an essential intermediate. Compound IVa was also obtained by the condensation of 6,8-dichloro-3-amidino-coumarin with benzaldehyde in the presence of ammonium acetate (Scheme 2). The infrared spectra of

IV revealed slightly lower shifted absorption bands for a primary amino group at about 3400 and 3300 cm^{-1} and at about 1700 cm^{-1} for a coumarin-type carbonyl group. This shows the presence of intramolecular C=O--H_2N bonding.

When heated with acetic anhydride in pyridine, compounds of the type IV were converted to their corresponding monoacetylated derivatives (V). On the other hand, compounds (II) gave diacetylated derivatives III under the same reaction conditions. In the infrared spectra of (III), carbonyl stretching bands are shifted to higher frequencies by 20 to 30 cm^{-1} than those of the compounds (II). However, the carbonyl bands of (V) appeared in the region nearly the same as or slightly lower than those of the compounds (IV), and the imino stretching band always appeared at 3250 cm^{-1}. These data, therefore, can reasonably be explained by the presence of intramolecular hydrogen bonding in the compounds (II) and (IV).

EXPERIMENTAL

All the melting points are uncorrected. The infrared spectra were recorded on a Perkin-Elmer Model 521 spectrophotometer by means of potassium bromide discs. The ^1H-NMR spectra were determined in trifluoroacetic acid using a JNM-C-60 spectrometer, using tetramethylsilane as internal standard. The chemical shifts are reported as parts per million downfield from TMS.

Reaction of Ethyl Cyanoacetate and 3,5-Dichlorosalicyl-aldehyde with Aldehydes

A mixture of ethyl cyanoacetate (0.03 mol), 3,5-dichlorosalicylaldehyde (0.03 mol), aldehyde (0.03 mol), and ammonium acetate (0.04 mol) in ethanol (10 mL) was refluxed for 0.5—1.5 hr. A pale yellow crystalline matter precipitated out during the reaction. The experimental results and spectral data are summarized in tables 1, 3, 5, 6, 8 and 10.

Table 1

1-Alkyl-4-amino-7,9-dichloro-5-oxo-[1]benzopyrano[3,4-c] pyridine (II)

Compd No.	R	M.p., °C	Yield %	Mol. formula	Analysis %	
					Calcd	Found
IIa	CH_3	261—262	34	$C_{13}H_8O_2N_2Cl_2$	C 52.90	53.2
					H 2.73	3.0
					N 9.49	9.7
IIb	C_2H_5	247—249	19	$C_{14}H_{10}O_2N_2Cl_2$	C 54.39	54.5
					H 3.26	3.5
					N 9.06	9.0
IIc	n-C_3H_7	226—227	20	$C_{15}H_{12}O_2N_2Cl_2$	C 55.74	56.0
					H 3.74	3.7
					N 8.66	8.5

Reaction of 6,8-Dichloro-3-amidinocoumarin (I) and Benzaldehyde

A mixture of (I, 2.8 g), benzaldehyde (1.5 g), and ammonium acetate (1.5 g) in ethanol (5 mL) was refluxed for 0.5 hr. A crystalline precipitate was formed during the reaction; this was collected, and washed with ethanol and then with water. Recrystallization from

Table 2

1-Alkyl-4,4-diacetamino-7,9-dichloro-5-oxo-[1]benzopyrano[3,4-c] pyridine (III)

Compd No.	R	M.p., °C	Yield %	Mol. formula	Analysis %	
					Calcd	Found
IIIa	CH_3	210—213	55	$C_{17}H_{12}O_4N_2Cl_2$	C 53.84 H 3.18 N 7.38	54.0 3.0 7.5
IIIb	C_2H_5	172—175	86	$C_{18}H_{14}O_4N_2Cl_2$	C 54.98 H 3.58 N 7.12	55.0 3.7 7.0
IIIc	n-C_3H_7	144—148	88	$C_{19}H_{16}O_4N_2Cl_2$	C 56.03 H 3.96 N 6.87	56.0 4.0 6.5

Table 3

Infrared spectral data for the compounds II (cm^{-1})

Compd No.	ν NH_2	νC=O	δ NH_2	Aromatic ring	δ CH
IIa	3430, 3270, 3150	1700	1625	1610, 1590, 1570, 1545	760
IIb	3420, 3260, 3130	1690	1620	1610, 1590, 1565, 1540	755, 745
IIc	3410, 3270, 3130	1700	1625	1610, 1590, 1570, 1545	765, 750

Table 4

Infrared spectral data for the compounds III (cm^{-1})

Compd No.	νO—C=O	νN—C=O	Aromatic ring	δ CH
IIIa	1725	1700	1610, 1590, 1575, 1540	770
IIIb	1735	1715	1600, 1590, 1570, 1540	770
IIIc	1735	1720	1610, 1590, 1570, 1540	770

Table 5

^{1}H-NMR spectral data* for the compounds II and III

Compd No.	CH_3	OCH_3	CH_2	Ring—CH=
IIa	2.9 (s, 3H)			7.5—7.7 (m, 2H), 8.0—8.3 (m, 1H)
IIb	1.5 (t, 3H)		3.3 (q, 2H)	7.5—7.7 (m, 2H), 8.0—8.3 (m, 1H)
IIc	1.2 (t, 3H)		1.9 (sx, 2H), 3.2 (t, 2H)	7.5—7.7 (m, 2H), 8.0—8.4 (m, 1H)
IIIb	1.6 (t, 3H) 2.4, 2.7 (s, 3H each)	2.7 (s, 3H each)	3.5 (q, 2H)	7.5—7.7 (m, 2H), 8.4—8.8 (m, 1H)

* Parts per million downfield from tetramethylsilane in CF_3CO_2H; s = singlet, t = triplet, q = quartet, sx = sextet, m = multiplet.

Table 6

2-Aryl-4-amino-7,9-dichloro-5-oxo-[1] benzopyrano[4,3-d] pyrimidine (IV)

Compd No.	Ar	M.p., °C	Yield %	Mol. Formula	Analysis % Calcd	Analysis % Found
IVa	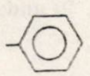	306—308	20	$C_{17}H_9O_2N_3Cl_2$ H 2.53	C 57.00 H 2.53 N 11.73	57.3 2.5 11.6
IVb	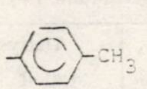	317—320	13	$C_{18}H_{11}O_2N_3Cl_2$	C 58.08 H 2.97 N 11.28	58.2 3.0 11.4
IVc	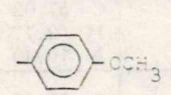	302—304	11	$C_{18}H_{11}O_3N_3Cl_2$	C 55.69 H 2.85 N 10.82	55.5 3.0 11.0
IVd	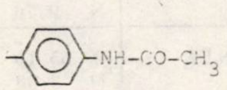	330	17	$C_{19}H_{12}O_3N_4Cl_2$	C 54.95 H 2.91 N 13.49	55.2 3.0 13.5
IVe	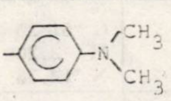	294—296	6	$C_{19}H_{14}O_2N_4Cl_2$	C 56.87 H 3.51 N 13.96	57.0 3.5 14.2
IVf	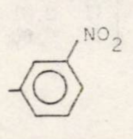	295—297	25	$C_{17}H_8O_4N_4Cl_2$	C 50.64 H 2.00 N 13.89	50.8 2.3 13.5
IVg	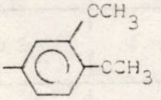	287—288	12	$C_{19}H_{13}O_4N_3Cl_2$	C 54.56 H 3.13 N 10.04	50.5 3.0 10.0
IVh	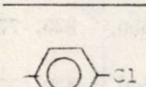	315—318	20	$C_{17}H_8O_2N_3Cl_3$	C 52.00 H 2.05 N 10.70	52.3 2.0 11.0
IVi	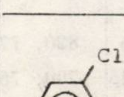	312—315	18	$C_{17}H_8O_2N_3Cl_3$	C 52.00 H 2.05 N 10.70	52.0 2.3 10.5

pyridine afforded 0.9 g of pale yellow crystals; m.p. 305—308°C. By the infrared spectra and the results of elemental analyses, this compound was identified as IVa.

Reaction of Compounds II and IV with Acetic Anhydride

To a solution of II or IV (0.001 mol) dissolved in pyridine (3—5 mL), acetic anhydride (5—8 mL) was added, the mixture was then refluxed for 2—4 hs. After standing overnight at room temperature, the crystalline precipitate thus formed was washed with dilute methanol. The experimental results and spectral data are summarized in tables 2, 4, 7, 9, and 10.

Table 7

2-Aryl-4-acetamino-7,9-dichloro-5-oxo-[1] benzopyrano[4,3-d]pyrimidine (V)

Compd No.	Ar	M.p., °C	Yield %	Mol. Formula	Analysis % Calcd		Analysis % Found
Va	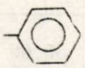	292—293	87	$C_{19}H_{11}O_3N_3Cl_2$	C H N	57.02 2.77 10.49	57.2 3.0 10.5
Vb	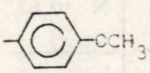	297—300	88	$C_{20}H_{13}O_4N_3Cl_2$	C H N	55.83 3.04 9.76	56.0 3.0 9.5
Vc	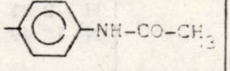	330	77	$C_{21}H_{14}O_4N_4Cl_2$	C H N	55.15 3.08 12.25	55.0 3.0 12.5
Vd	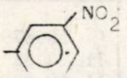	300—303	88	$C_{19}H_{10}O_5N_4Cl_2$	C H N	51.25 2.26 12.58	51.5 2.1 12.5
Ve	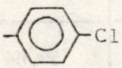	330	75	$C_{19}H_{10}O_3N_3Cl_3$	C H N	52.40 2.31 9.66	52.5 2.5 9.7

Table 8

Infrared spectral data for the compounds IV (cm^{-1})

Compd No.	ν NH_2	ν C = O	δ NH_2	Aromatic ring	δ CH
IVa	3480, 3360	1705	1630	1615, 1595, 1555, 1535	765, 700
IVb	3430, 3330	1695	1630	1615, 1605, 1580, 1550, 1540	825, 770
IVc	3430, 3330	1695	1625	1615, 1600, 1580, 1540	830, 775
IVd	3420, 3290, 3200	1710, 1680	1640	1615, 1600, 1550, 1530	825, 775
IVe	3420, 3345	1700	1625	1615, 1600, 1565, 1545	820, 775
IVf	3450, 3340	1705	1625	1610, 1600, 1555, 1545	790, 750
IVg	3420, 3290	1705	1630	1615, 1605, 1590, 1555	820, 770
IVh	3480, 3380	1705	1625	1610, 1590, 1560, 1535	770

Table 9

Infrared spectral data for the compounds V (cm^{-1})

Compd No.	ν NH	ν O—C=O, NH—C=O	Aromatic ring	δ CH
Va	3250	1700, 1685	1610, 1600, 1590, 1570	765, 700
Vb	3250	1700, 1680	1610, 1600, 1590, 1570	825, 780
Vc	3360, 3250	1700, 1680	1615, 1600, 1580, 1550	830, 775
Vd	3250	1700, 1690	1610, 1590, 1575, 1550	830, 780
Ve	3250	1700, 1695	1610, 1590, 1575	820, 780

Table 10

^{1}H-NMR spectral data* for the compounds IV and V

Compd No.	CH_3	OCH_3	Ring—CH=	NH
IVa			7.5—8.9 (m, 8H)	9.7 (br, 1H)
IVc		4.0 (s, 3H)	7.1—8.7 (m, 7H)	9.6 (br, 1H)
IVd	2.5 (s, 3H)		7.6—8.8 (m, 7H)	9.3, 9.7 (s, 1H each)
IVe	3.6 (s, 6H)		7.6—8.1, 8.5—8.8 (m, 7H)	9.8 (br, 1H)
IVg		4.1 (d, 6H)	7.2—8.8 (m, 6H)	9.6 (br, 1H)
Va	2.7 (s, 3H, $CO—CH_3$)		7.5—8.9 (m, 7H)	12.2 (br, 1H)

*Parts per million downfield from tetramethylsilane in CF_3CO_2H;
s = singlet, d = doublet, m = multiplet, br = broad.

REFERENCES

[1] I. Villani, *J. Med. Chem.*, **18** 1, (1975).
[2] C. K. Ghosh, and K. K. Mukhopadhay, *Synthesis*, **10**, 779, (1978).
[3] C. K. Ghosh, and S. Khan, *Indian J. Chem.*, *Sect. B.* **18**, 128, (1979).
[4] U. Petersen and H. Heitzer, *Justus Liebigs Ann. Chem.*, **3**, 1663 (1976).
[5] C. Pene and H. M. Hubert, *J. Heterocycl. Chem.*, **17**, 329, (1980).
[6] M. M. Ismail and M. S. Mohamed, Submitted for Publication in *Rev. Roumaine Chim.*

Revue Roumaine de Chimie, **31**, *5*, 541–546 (1986)

SYNTHESIS OF 4-AROYL-4,5-DIHYDRO-2(3H)-FURANONES AND THEIR REACTIONS WITH SOME NUCLEOPHILES

N. A. SHAMS, A. A. HAMED, S. G. DONIA and S. A. SHAKER
Chemistry Department, Faculty of Science, Ain Shams University, Cairo, Egypt

Received May 13, 1985

Hydroxyalkylation of 3-aroylpropanoic acids (**1a**, **b**) using either formaldehyde or acetaldehyde in sodium hydroxide solution gave two products, 4-aroyl-4,5-dihydro-2(3H)-furanones (**2a-d**), and butenoic or pentanoic acid derivatives (**3a-d**). Reaction of the title compounds with different molar ratios of hydrazine hydrate and with phenylmagnesium bromide was investigated.

The present investigation deals with the interaction of 3-(*p*-phenoxybenzoyl) (**1a**)[1] and 3-(3,4-dimethylbenzoyl) (**1b**)[2] propanoic acids with formaldehyde or acetaldehyde in dilute sodium hydroxide solution in a molar ratio 1 :1.1 :1.1, respectively, to give two products, in each case, 4-aroyl-4,5-dihydro-2(3H)-furanones (**2a-d**) (major product) and 3-aroyl-3-butenoic acids (**3a**, **b**) or 3-aroyl-3-pentenoic acids (**3c** and **3d**) (minor product).

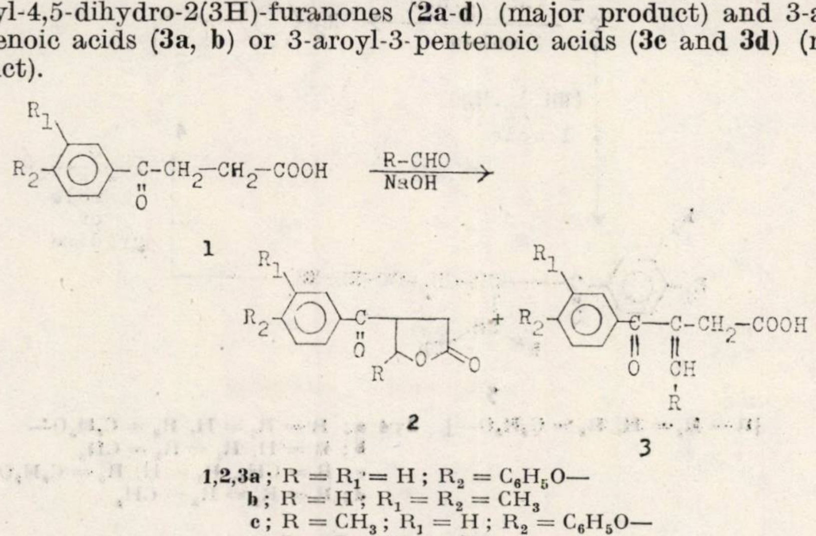

1,2,3a ; $R = R_1 = H$; $R_2 = C_6H_5O—$
b ; $R = H$; $R_1 = R_2 = CH_3$
c ; $R = CH_3$; $R_1 = H$; $R_2 = C_6H_5O—$
d ; $R = R_1 = R_2 = CH_3$

The structure of the products **2** and **3** was inferred from : (i) analytical data, (ii) the infrared spectra which show absorption bands characteristic of $\nu C=O$ (aroyl and lactone for **2** and aroyl and carboxylic groups for **3**).

In addition the infrared spectra of **3** show $\nu C{=}C$ at $\simeq 1640$ cm^{-1} an (iii) the ^{1}H-NMR spectrum of (**2b**) shows signals at δ 4.73 — 4.0 (m, 3H, CH, CH_2O); 3.24 — 2.82 (m, 2H, $CH_2.CO$) while the ^{1}H-NMR spectrum of (**3b**) shows signals at δ 9.68 (br s, 1H, COOH); 6.22 + 5.79 (2 apparent s, 2H, $C{=}CH_2$); 3.58 (s, 2H, CH_2COOH).

The reaction of 4-aroyl (**2a**, **b**) and 4-aroyl-5-methyl (**2c**, **d**)-4,5-dihydro-2(3H) furanones with hydrazine hydrate (98 % 1 :2 molar ratio) at room temperature up to three hours, gave exclusively one product, in each case, to which structure **4** was assigned. The infrared spectra of the products indicate absorption due to C=O at 1650—1670 cm^{-1} and to NH at 2800—3600 cm^{-1}, very similar to the corresponding bands which appeared in the spectra of 4,5-dihydropyridazin-3 (2H)-ones.[4] The electronic spectra showed maximum absorption at 285—298 nm (log $\epsilon_{max} \simeq 4.38$ — — 4.47) which is very similar to those of tetrahydropyridazinones.[5] This result confirms that the reaction of **2a-d** with hydrazine hydrate in 1 :2 molar ratio, irrespective of reaction time, affords the corresponding 6-aryl-4,5-dihydro-5-hydroxyalkylpyridazin-3(2H)-ones (**4a-d**).

However, when **2a** was allowed to react with hydrazine hydrate (1 :1 molar ratio) at room temperature or even in boiling ethanol or *n*-butanol (as high boiling point solvent) up to three hours, it yielded 4-hydroxy-3-*p*-phenoxybenzoyl butanoic acid hydrazide (**5**) as a sole product in 92 % yield.

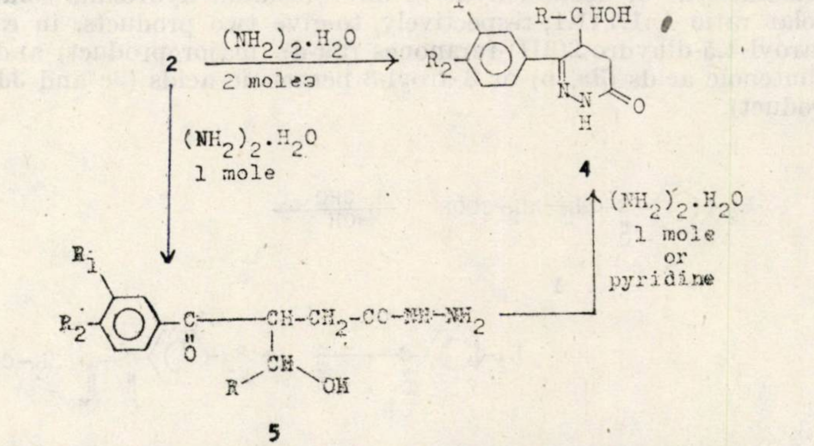

[R = R_1 = H, R_2 = C_6H_5O—]   **2**; **4** **a**; R = R_1 = H, R_2 = C_6H_5O—
b; R = H, R_1 = R_2 = CH_3
c; R = CH_3, R_1 = H, R_2 = C_6H_5O —
d; R = R_1 = R_2 = CH_3

The structure assigned to product **5** was consistent rather than elemental analysis, with its infrared spectrum which displays absorption bands characteristic for the stretching frequencies of C=O (both aroyl and hydrazide groups), NH and OH groups (Table 1). This fact tempted us to investigate whether the nature of the product controlled mainly by lactone/hidrazine hydrate molar ratio or merely by the bazicity of

Table 1

Characterisation of Compounds **1—7**

Compound	Solvent*	M.p. (°C)	Yield (%)	Formula	Analytical data Found/Required %			IR(cm^{-1})				Electronic spectrum $\lambda^{nm}_{(max)}$	$\log\varepsilon_{(max)}$
					C	H	N	ν C = O	ν C=C	ν NH	ν OH		
2a	B	101—2	82	$C_{17}H_{14}O_4$	72.66 72.33	5.21 5.00		1760 1675				262	4.05
2b	B	93—4	79	$C_{13}H_{14}O_3$	71.88 71.54	6.81 6.47		1780 1678				259	3.90
2c	T	107—8	76	$C_{18}H_{16}O_4$	72.73 72.96	5.64 5.44		1775 1670				266	4.10
2d	B	102—3	72	$C_{14}H_{16}O_3$	72.81 72.39	6.64 6.94		1778 1675				264	4.20
3a	L.P	78—9	14	$C_{17}H_{14}O_4$	72.72 72.33	5.06 5.00		1700 1678	1635				
3b	L.P	71—2	17	$C_{13}H_{14}O_3$	72.01 71.54	6.77 6.47		1710 1678	1640				
3c	.P L	85—6	20	$C_{18}H_{16}O_4$	73.23 72.96	5.33 5.44		1708 1675	1640				
3d	L.P	98—9	22	$C_{14}H_{16}O_3$	72.12 72.39	7.23 6.94		1700 1670	1638				
4a	B	153—4	78	$C_{17}H_{16}N_2O_3$	69.00 68.90	5.48 5.44	9.75 9.45	1670		3270	2890 (sh)	296	4.37
4b	B	148—9	69	$C_{13}H_{16}N_2O_2$	67.64 67.22	7.02 6.94	12.43 12.06	1678		3086	2900 (sh)	285	4.38
4c	B	160—1	70	$C_{18}H_{18}N_2O_3$	69.92 69.66	5.94 5.85	9.42 9.03	1663		3077	2874 (sh)	298	4.47
4d	B	172—3	74	$C_{14}H_{18}N_2O_2$	68.11 68.21	7.20 7.31	11.27 11.37	1672		3058	2970 (sh)	289	4.45
5	L.P	141—2	81	$C_{17}H_{18}N_2O_4$	65.32 64.95	6.01 5.77	9.33 8.91	1645 1675		3190	2920		
6a	B	137—8	30	$C_{35}H_{32}O_4$	81.49 81.37	6.45 6.24					3115		
6b	B	154—5	29	$C_{31}H_{32}O_3$	81.89 82.27	7.27 7.13					3110		
7a	L.P	168—9	55	$C_{35}H_{28}O_2$	87.88 87.47	5.89 5.87			1630				
7b	L.P	182—3	57	$C_{31}H_{28}O$	88.94 89.33	7.03 6.78			1625				

*B = Benzene, T = Toluene, L.P = light petrol (b.p. 60—80°)

sh. = sharp

the medium. Thus, treatment of **5** with pyridine (1 :1 molar ratio) in ethanol at room temperature for one hour yields exclusively the pyridazinone **4a**, indicating that ring closure of **5** to **4a** was effected only by the basicity of the medium.

In continuation of our investigation on the ring opening reactions of 4-aroyl-4,5-dihydro-2(3H) furanones with some nucleophiles, we report that the reaction of (**2a, b**) with phenylmagnesium bromide (1 :3 molar ratio) yielded two products in each case namely 1-aryl-1,4,4-triphenyl-2-hydroxymethylbutane-1,4-diol (**6a, b**) and 2,2-diphenyl-4(aryl phenylmethylene)-tetrahydrofuran (**7a, b**).

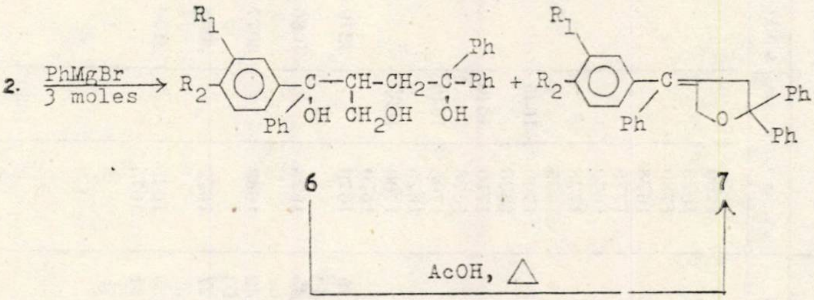

6; **7** **a**; $R_1 = H$; $R_2 = C_6H_5O—$
b; $R_1 = R_2 = CH_3$

The structural assignment for compounds **6** was confirmed by elemental analysis and by their infrared spectra which show absorption bands in the 3 μ region characteristic of νOH. In addition, Zerewitinoff and Tschugaev's method indicates that each product of strucure **6** has three OH groups. On the other hand, the infrared spectra of (**7a,b**) lack any band characteristic of OH and C=O stretching frequencies, but exhibit νC=C at about 1630 cm^{-1}. Moreover the ^{1}H-NMR spectrum of **7a** shows signals at δ3.1; (s, $CH_2-C\begin{smallmatrix}Ph\\Ph\end{smallmatrix}$) and δ 3.6 (s, $-CH_2O-$), which indicate that the product derived from 1,2-addition to the aroyl group undergoes cleavage, under the influence of the nucleophile to give the corresponding acyclic ketone, which in turn reacts with another molecule of the reagent followed by elimination of two molecules of water. The structure of compounds **7** was rigidly established by the following facts : (i) their ethanolic solution decolourises potassium permanganate solution and (ii) **7a** is identical in all respects to the product obtained when **6a** was refluxed in glacial acetic acid for two hours.

EXPERIMENTAL

Melting points are uncorrected. A Pye-Unicam SP 1200 infrared spectrophotometer was used to take infrared spectra using KBr Wafer technique. Electronic spectra were carried out on a Perkin-Elmer Specord Model 4000 A spectrophotometer using ethanol as solvent.

^{1}H-NMR spectra were obtained on a Varian A-60 A spectrophotometer using solutions in hexadeuterio-dimethylsulfoxide with tetramethylsilane as internal standard. Elemental analyses were carried out at the microanalytical units of Cairo University and Drug Control and Research Center, Cairo, Egypt.

Action of formaldehyde and acetaldehyde on 3-aroylpropanoic acids : Synthesis of 2a-d and 3a-d

37 % Formaldehyde (8.91 g ; 1.1 mole) or acetaldehyde (4.8 g 1.1 mole) is added to a stirred solution of 3-*p*-phenoxybenzoylpropanoic acid (**1a**, 27 g, 1 mole) or 3-(3,4-dimethyl)-benzoylpropanoic acid (**1b** ; 20.6 g, 1 mole) in 0.5N sodium hydroxide (220 mL) (molar ratio of **1**/aldehyde/NaOH=1 :1.1 :1.1]. After one hr. at room temperature, the mixture is acidified with concentrated hydrochloric acid (about 30 mL) and stirred for additional 12 hrs. The semi-solid product which separates, in each case, is triturated with diethyl ether (250 mL) to give 4-aroyl (**2a**, **b**) or 4-aroyl-5-methyl (**2c**, **d**) 4,5-dihydro-2(3H)-furanones, respectively.

The ether-soluble fraction is chromatographed on silicagel (elution with benzene/acetone (95 :5) ; there are collected in succession (**2a-d**) in small yield and either 3-aroyl-3-butenoic acids (**3a**, **b**) or 3-aroyl-3-pentenoic acids (**3c**, **d**), respectively.

Action of hydrazine hydrate on 4-aroyl (2a, b) and 4-aroyl-5-methyl-4,5-dihydro-2(3H)-furanone

After a mixture of 4-*p*-phenoxybenzoyl (**2a**, 28.2 g, 1 mole), 4-(3,4-dimethyl) benzoy (**2b**, 21.8 g, 1 mole), 4-*p*-phenoxybenzoyl-5-methyl (**2c**, 29.6 g,1 mole) or 4-(3,4- dimethyl)benzoyl-5-methyl (**2d**, 23.7 g, 1 mole) 4,5-dihydro-2(3H)furanones in ethanol (100 mL) and hydrazine hydrate (98 %, 10.012 g, 2 moles) was kept at room temperature for two hours, the resulting solution was placed on a watch glass and allowed to evaporate to dryness in a current of air. The residue thus obtained was recrystallised from a suitable solvent to yield 6-aryl-4,5-dihydro-5-hydroxyalkylpyridazin-3(2H)-ones (**4a-d**) as colourless crystals.

Synthesis of 4-hydroxy-3-*p*-phenoxybenzoylbutanoic acid hydrazide (5)

A solution of (**2a**, 2.82 g, 0.01 mole) in ethanol or *n*-butanol (10 mL) was treated with hydrazine hydrate (98 %), 0.5 g, 0.01 mole) at room temperature and under reflux up to 3 hrs. The mixture was treated as described in the aforementioned procedure. Filtration yielded 2.55 g (81.2 %) of crude **5**, m.p. 132—136°C, and recrystallisation from light petrol (b.p. 60—80°) afforded the pure compound as colourless needles, m.p. 141—2°C.

Synthesis of 4a *via* cyclisation of 5

Compound **5** (3.14 g, 0.01 mole) in ethanol (25 mL) was treated with either hydrazine hydrate (0.5 g, 0.01 mole) or pyridine (0.79 g, 0.01 mole) and the reaction mixture was left at room temperature for one hr. After concentration and cooling, the solid product obtained, in each case, was filtered off, washed with water and crystallised from benzene to give 2.65 g of 4,5-dihydro-5-hydroxymethyl-6-*p*-phenoxyphenyl pyridazin-3-(2H)-one, m.p. 153—4°C, yield 89.5 %.

Action of phenylmagnesium bromide on 4-aroyl-4,5-dihydro-2(3H)-furanones (2a, b)

To 3.6 g of magnesium turnings (0.15 g atom) in 100 mL of dry ether was added dropwise 15.7 mL (23.55 g, 0.ε5 mole) of brombenzene. After the reaction had subsided, **2a** (8.46 g, 0.03 mole) or **2b** (6.54 g, 0.03 mole) dissolved in 100 mL dry benzene was added in portions over one hr period. The mixture was heated under reflux for an additional 3 hrs and then decomposed with saturated ammonium chloride solution (20 %). The ether-benzene layer was washed with water and dried over anhydrous sodium sulphate. Concentration of the ether-benzene mixture yielded a colourless solid, which on recrystallisation from benzene afforded 1-aryl-1,4,4-triphenyl-2-hydroxymethylbutane-1,4-diol (**6a**, **b**).

Evaporation of the filtrate recovered from **6** gave an oily residue. Trituration of the oil with light petrol (b.p. 40—60°) and concentration of the triturant yielded 2,2-diphenyl-4--(arylphenylmethylene)-tetrahydrofuran (**7a**, **b**).

Conversion of 6a to 7a

A mixture of **6a** (0.5 g) and glacial acetic acid (10 mL) was heated on a steam bath for one hr. Pouring on ice cold water caused the precipitation of 0.3 g of **7a**, m.p. 158—163°C. Recrystallization from light petrol (60—80°) raised the m.p. to 168—9°C.

REFERENCES

[1] M. Huang, *J. Amer. Chem. Soc.*, **68**, 2487 (1946).
[2] W. P. Campbell and M. D. Soffer, *J. Amer. Chem. Soc.*, **64**, 417 (1942).
[3] G. Cignarella, G. Grella and M. M. Curzu, *Synthesis*, **1980**, 825.
[4] F. G. Baddar, A. El-Habashi and A. K. Fateen, *J. Chem. Soc.*, **1965**, 3342.
[5] A. K. Fateen and N. A. Shams, *J. Chem. U.A.R.*, **11**, 301 (1968).

Revue Roumaine de Chimie, **31**, *5*, 547–564 (1986)

COMPUTER USE OF NITROPHOSPHATE FERTILIZERS

COMPUTER-AIDED ANALYSIS OF THE NITRIC DECOMPOSITION OF PHOSPHATIC RAW MATERIALS

MIHAI TALABĂ

Department of Chemical Technology, Polytechnic Institute, Splai Bahlui Stînga 71,
Iaşi, Romania

Received May 5, 1985

The use of computer-aided analysis, employing mathematical models of mass balance of the phosphatic raw materials nitric decomposition by the Norks-Hydro procedure was justified, and the mathematical models of mass balance for each of the four component processes which ensures the phosphonitric solutions obtaining were established. The peculiarities of the matter under study were taken into account in establishing the logical diagram of calculation. Computer aided analysis correlations were determined between the nitric acid required — through D_R ratio — and the composition of phosphatic raw materials, as well as between the same ratio and L, S, R_D, A and W ratios, characterizing quantitatively the process flow rates. Thus, qualitatively and quantitatively stable phosphonitric solutions were obtained irrespective of the phosphatic raw material used.

1. THE OPPORTUNITY OF COMPUTER-AIDED ANALYSIS

The increase of fertilizer consumption determined by the development of agriculture is correlated with the possibility of recovering the potential of arable soils as quick as possible.

The main role in this direction is played by the NPK complex fertilizers whose weight of above 60 % of the overall fertilizer production satisfies both quantitatively and qualitatively the requirement.[1–3,6]

Under the particular conditions of sulphur price increase on the world market,[4] especially in the 'seventies, in the countries with a deficit of this material but possessing natural gas sources instead, the nitrophosphate industry has developed in various technological variants,[3,6] among which the Norks-Hydro procedure has a head place.

The operation scheme of nitrophosphate obtained by Norks-Hydro procedure is given in Fig. 1.

In this process the nitric decomposition of phosphatic raw materials as well as working of phosphonitric solutions for the partial separation of calcium nitrate by crystallization at temperatures below 0°C were carried out. By subsequent ammoniation, concentration and granulation nitrophosphates of desired composition are obtained.[3,6] If the Ca/P mass ratio

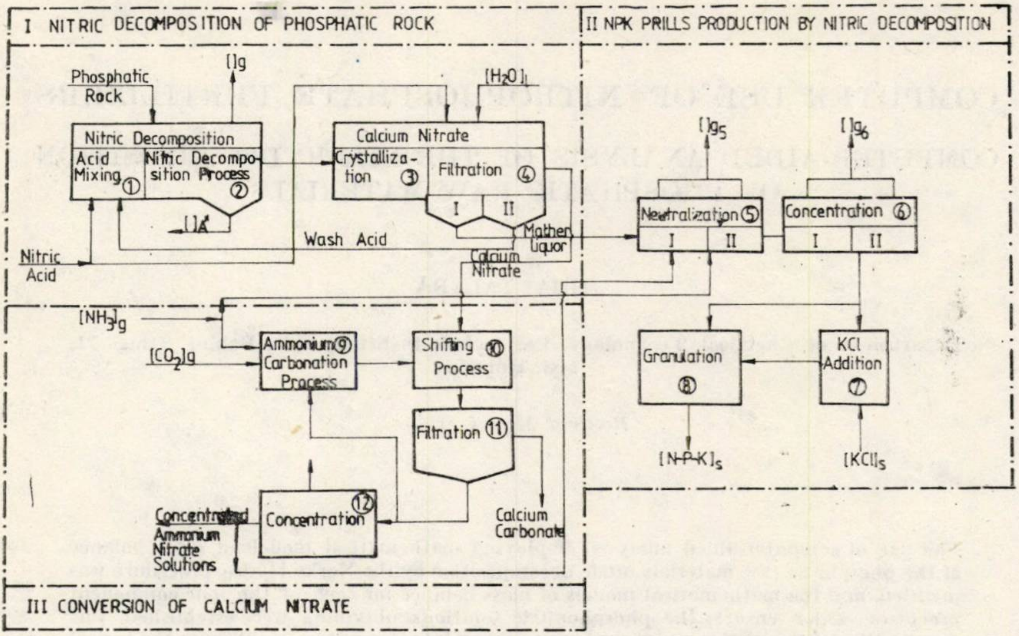
I NITRIC DECOMPOSITION OF PHOSPHATIC ROCK
II NPK PRILLS PRODUCTION BY NITRIC DECOMPOSITION
III CONVERSION OF CALCIUM NITRATE
Phosphatic Rock
[ ]g
Nitric Decomposition
Acid Mixing ①
Nitric Decomposition Process ②
[ ]A
Nitric Acid
Wash Acid
[H2O]l
Calcium Nitrate
Crystallization ③
Filtration ④
I
II
Mother Liquor
Calcium Nitrate
[ ]g5
[ ]g6
Neutralization ⑤
Concentration ⑥
KCl Addition ⑦
Granulation ⑧
[N-P-K]s
[KCl]s
[NH3]g
[CO2]g
Ammonium ⑨ Carbonation Process
Shifting ⑩ Process
Filtration ⑪
Concentration ⑫
Concentrated Ammonium Nitrate Solutions
Calcium Carbonate

Fig. 1. — Block diagram of Norks-Hydro procedure.

Table 1

Chemical composition of some types of phosphorite and apatite

	Type of Phosphatic Raw Material	Chemical composition (% weight)										Mass ratio	
		P_2O_5	CaO	F	CO_2	Al_2O_3	Fe_2O_3	SiO_2	MgO	K_2O	SO_3	CaO/P_2O_5	P_2O_5/F
PHOSPHORITE	KARATAU (USSR)	28.2	43.8	2.6	5.4	0.9	0.9	11.3	2.0			1.553	10.846
	EGOREVSK (USSR)	28.5	43.5	2.9	5.0	1.5	5.0	5.0				1.526	9.827
	FLORIDA (USA)	33 - 36	46-50	3.3 - 4	1.5-4.4	0.7-1.1	0.7-2.6	7.3-9.8	max 0.5	max 0.6	0.3 - 1.5	1.166	8.25
	TENNESSEE (USA)	30 36	42 49	3.2 - 3.9	1.0-2.0	1.2-3.1	2.2-3.4	3.9-4.4	max 0.3	0.1 - 0.3	0.7 - 2.7	1.166-1.531	7.692
	SYRIA	31.84	50.34	3.5	5.07	0.82	0.5	1.5	0.18			1.581	9.097
	MOROCCO	35.11	53.0	4.24	4.12	0.45	0.12	0.86	0.16	1.19	1.40	1.509	8.28
	EGYPT	31.05	48.74	3.21	4.11	0.38	1.28	3.81	0.35	1.00	2.7	1.569	9.672
	TOGO	36.18	51.20	3.87	2.0	1.0	1.5	3.76	0.15	0.2	0.43	1.415	9.348
APATITE	KOLA (USSR)	39.4	52.0	2.8-3.1		0.5-0.9	0.1-0.3	0.2-1.5	0.1-0.2			1.319	12.7-14.07
	KOLA concentrate	35.4	53.5	1.1-2.8	2.9-7	0.7-1.8			0.5-2.5			1.511	12.64-32.18
	KHRENBERG (Thuringia)	40.3	42.3	2.52			3.11		7.54			1.054	15.992
	JIWAARY (Finland)	40.9	51.6	1.83			0.14		1.06	1.24		1.261	22.349
	JORDAN	32.46	49.9	3.7	3.8	0.44	0.44	5.13				1.537	8.773

is $\leqslant 0.35$ in the phosphonitric solution before ammoniation, a nitrophosphate containing up to 85 % P_2O_5 soluble in water is obtained.

In the present economic circumstances, the countries in which phosphatic raw materials are imported, are frequently forced to purchase various sorts of raw materials during relatively short periods sometimes a few months, as a function of furnisher's offers.

The large variety of chemical composition of phosphatic raw materials depending on the geographical zone they come from can be seen in Table 1.[1-3]

The frequent change of the sorts of phosphatic raw materials in the same industrial equipment diminishes the productivity due to the time consumption for adopting the process parameters to the new conditions imposed by the change of material sort. At the same time, the quality of the obtained nitrophosphates is uncertained since very often the fertilizer type is determined by the quality of the raw material used.

In this situation, during the nitric decomposition of phosphatic raw material the correlation between the nitric acid (including the excess) and washing acid, recycled from the filtration of calcium nitrate, becomes necessary so that to permit the obtention of a constant chemical composition of the phosphonitric solution resulted after the calcium nitrate separation (known as "mother liquor"). Thus the stability of the subsequent processes as well as the obtaining of desired nitrophosphate type are assured.

Given the significant role of nitric decomposition stage as a governing step of the overall process, depending on the phosphatic raw material available, the existence of an adequate chemical engineering literature becomes quite necessary.

The rigorously scientific approach of technological problems implies the computer-aided analysis of the process of nitric decomposition of phosphatic raw material employing of mathematical models of mass balance. The possibility is taken into account of obtaining a "mother liquor" of stable chemical composition no matter which sort of phosphatic raw material is to be used.

2. MATHEMATICAL MODELS OF MASS BALANCE

According to the scheme in Fig. 1 the "mother liquor" results after working the phosphatic raw materials and the phosphonitric solutions in the first four component processes: acid mixing, nitric decomposition, crystallization and filtration of tetrahydrated calcium nitrate.

The general procedure for obtaining the mathematical models of mass balance for each component process,[8] consists in establishing the elementary processes of conversion from which, based on qualitative and quantitative criteria, the independent conversion processes are selected. Then the relations for the conversion degrees as a function of valuable components for all components implied in the independent processes are established, and on their basis the primary mass balance on components and phases is derived.

By substituting the conversion degrees by the corresponding measurable amounts the secondary mass balance model is obtained and the measurable amounts are settled.

Using this procedure the mathematical mass balance models are established for each of the four component processes.

Process of acid mixing

The process can be symbolically expressed by the following characteristic equation:

$$[HNO_3 + H_2O]^0_{l_1} + [HNO_3 + H_3PO_4 + Ca(NO_3)_2 + A_1'' + H_2O]_{f_{II}} \rightarrow$$
$$\rightarrow [HNO_3 + H_3PO_4 + Ca(NO_3)_2 + A_1'' + H_2O]^0_l$$

Table 2

Mass balance equations — Mixing of acids

INPUT			OUTPUT		
Phase	Chemical composition $[\bar{x}^0_{A_i}]$	Mass balance [Kg/hour]	Phase	Chemical composition $[\bar{x}^0_{A_i}]$	Mass balance [Kg/hour]
$[\,]^0_{l_1}$	$\bar{x}^0_{HNO_3[\,]_1}$	$m^0_{HNO_3[\,]_{l_1}} = m^0_{[\,]_{l_1}} \bar{x}^0_{HNO_3[\,]_{l_1}}$	$[\,]^0_l$	$\bar{x}^0_{N[\,]_l} = \bar{x}_{N_{f_{II}}} + R^0_L(\bar{x}^0_{N[\,]_{l_1}} - \bar{x}_{N_{f_{II}}})$	$m^0_{HNO_3[\,]_l} = 4.5\, m^0_{[\,]_l}(\bar{x}^0_{N[\,]_l} - 0.7\bar{x}^0_{Ca[\,]_l})$
	$\bar{x}^0_{H_2O[\,]_{l_1}}$	$m^0_{H_2O[\,]_{l_1}} = m^0_{[\,]_{l_1}}(1 - \bar{x}^0_{HNO_3[\,]_{l_1}})$		$x^0_{P[\,]_l} = (1 - R^0_L)\, x_{P_{f_{II}}}$	$m^0_{H_3PO_4[\,]_l} = 3.161\, m^0_{[\,]_l} \bar{x}^0_{P[\,]_l}$
		$m_{[\,]_{l_1}} = \sum m^0_{Ai[\,]_{l_1}} = R_D R^0_L m^0_{[\,]s}$		$\bar{x}^0_{Ca[\,]_l} = (1 - R^0_L)\bar{x}_{Ca_{f_{II}}}$	$m^0_{Ca(NO_3)_2[\,]_l} = 4.1\, m^0_{[\,]_l} \bar{x}^0_{Ca[\,]_l}$
$[\,]_{f_{II}}$	$\bar{x}_{N\,f_{II}}$	$m_{HNO_3 f_{II}} = 4.5\, m_{f_{II}}(\bar{x}_{N_{f_{II}}} - 0.7\bar{x}_{Ca_{f_{II}}})$		$\bar{x}^0_{A_1} = (1 - R^0_L)\bar{x}_{A_1 f_{II}}$	$m^0_{A_1[\,]_l} = m^0_{[\,]_l} \bar{x}^0_{A_1}$
	$\bar{x}_{P\,f_{II}}$	$m_{H_3PO_4\,f_{II}} = 3.161\, m_{f_{II}} \bar{x}_{P_{f_{II}}}$		$\bar{x}^0_{H_2O[\,]_l} = \bar{x}_{H_2O_{f_{II}}} + R^0_L(\bar{x}^0_{H_2O_{[\,]_{l_1}}} - \bar{x}_{H_2O\,f_{II}})$	$m^0_{H_2O[\,]_l} = m^0_{[\,]_l} \bar{x}^0_{H_2O[\,]_l}$
	$\bar{x}_{Ca\,f_{II}}$	$m_{Ca(NO_3)_{2f_{II}}} = 4.1\, m_{f_{II}} \bar{x}_{Ca\,f_{II}}$			
	$\bar{x}_{A_1 f_{II}}$	$m_{A_{1f_{II}}} = m_{f_{II}} \bar{x}_{A_{f_{II}}}$			
	$\bar{x}_{H_2O_{f_{II}}} = 1 - \sum \bar{x}_{A_{i-1}f_{II}}$	$m_{H_2O_{f_{II}}} = m_{f_{II}} \bar{x}_{H_2O f_{II}}$			
		$m_{f_{II}} = \sum m_{Ai f_{II}} = R_D(1 - R_L)\, m^0_{[\,]s}$			$m^0_{[\,]_l} = m^0_{[\,]_{l_1}} + m^0_{f_{II}} = R_D m^0_{[\,]s}$

In the process the physical mixing of two miscible nonreacting liquids takes place which simplifies the procedure due to the lack of elementary conversion processes.

The mass balance equations for this process are given in Table 2.

As can be seen in Table 2 the experimentally measurable amounts, giving the chemical composition of phases, are expressed as mass fraction of fictitious components ($\bar{x}_N$, $\bar{x}_P$ for instance etc.). The mass balance equation for the real components in the corresponding phase, made also evident in the characteristic equations, are obtained by means of conversion factors.

To calculate the composition of acid mixture the mixing ratio of the two liquid phases, R^0_L, was defined as:

$$R^0_L = \frac{m^0_{[\,]_{l_1}}}{m^0_{[\,]_{l_1}} + m_{f_{II}}} = \frac{D_R - A\bar{x}^0_{HNO_3}}{R_D \bar{x}^0_{HNO_3}}$$

where: $\bar{x}^0_{HNO_3}$ — denotes the mass fraction of HNO_3 in the mixtures of nitric acid from fresh acid desaggregation and acid washing on filters of $[Ca(NO_3)_2 4H_2O]_s$;

D_R = specific consumption of nitric acid;

R_D = decomposition phase ratio;

A = phase ratio for acid washing on calcium nitrate filters.

The relations for calculating these ratios in measurable amounts are given together with the mass balance models of the respective processes.

$D_R = N + E$, where N is the stoichiometric or experimental quota and E is the excess of nitric acid; all of them are measured in $[\mathrm{t}\ 100\ \%\ \mathrm{HNO_3/t[\,]^0_s}]$.

Nitric decomposition process

The characteristic equation of the process can be written as:

$$[\mathrm{Ca_3(PO_4)_2 + CaF_2 + CaCO_3} + A_2'']^0_s + [\mathrm{HNO_3 + H_3PO_4 + Ca(NO_3)_2} +$$

$$+ A_1'' + \mathrm{H_2O}]^0_1 \rightarrow [\mathrm{H_3PO_4 + Ca(NO_3)_2 + HNO_3 + HF} + A_3'' + \mathrm{H_2O}]_{l_2} +$$

$$+ [A_4'']_{s_2} + [\mathrm{CO_2 + HF + H_2O}]_{g_2}$$

The phosphatic raw material is symbolically represented by the main real components since the $\mathrm{CaO/P_2O_5}$ ratio varies for the most types of phosphorite and apatite (Table 1), and differs from the mole ratio $\mathrm{Ca_3(PO_4)_2/CaF_2} \neq 3/1$ or the mass ratio $\mathrm{CaO/P_2O_5} \neq 11.21$, corresponding to fluoroapatite mineral $\mathrm{Ca_5(PO_4)_3F}$[1,2].

A_2'' — The impurities in phosphatic raw material (usually the compounds less than 1 %) are divided into $A''_{3[\,]l_2}$, as soluble impurities, and $A''_{4[\,]s_2}$ as insoluble impurities (especially $\mathrm{SiO_2}$, $\mathrm{SiO_2 \cdot nAl_2O_3}$).

The independent conversion processes, corresponding to the characteristic equation are the following:

$$\mathrm{Ca_3(PO_4)_2 + 6\,HNO_3 = 2\,H_3PO_4 + 3\,Ca(NO_3)_2} \tag{1}$$

$$\mathrm{CaF_2 + 2\,HNO_3 = 2\,HF + Ca(NO_3)_2} \tag{2}$$

$$\mathrm{CaCO_3 + 2\,HNO_3 = Ca(NO_3)_2 + CO_2 + H_2O} \tag{3}$$

$$\mathrm{CO}_{2[\,]_1} \rightleftharpoons \mathrm{CO}_{2[\,]_g} \tag{4}$$

$$\mathrm{HF}_{[\,]_1} \rightleftharpoons \mathrm{HF}_{[\,]_g} \tag{5}$$

$$\mathrm{H_2O}_{[\,]_1} \rightleftharpoons \mathrm{H_2O}_{[\,]_g} \tag{6}$$

By using the above described procedure the mass balance equations listed in Table 3 were derived.

To correlate the liquid and solid phase flow rates obtained in the process of nitric decomposition with the supply of phosphatic raw mate-

Table 3

Mass balance equations — Nitric decomposition

INPUT			OUTPUT		
Phase	Chemical composition $[\bar{X}^{0}_{A_i}]$	Mass balance [kg/hour]	Phase	Chemical composition $[\bar{X}_{A_i}]$	Mass balance [kg/hour]
$[\,]^{0}_{s}$	$\bar{X}^{0}_{P_2O_5[\,]s}$ $\bar{X}^{0}_{CaO[\,]s}$ $\bar{X}^{0}_{F[\,]s}$ $\bar{X}^{0}_{CO_2[\,]s}$ $\bar{X}^{0}_{A'_3[\,]s}=$ $=\bar{X}^{0}_{A''_{1s}}+\bar{X}^{0}_{A''_s}$	$m^{0}_{Ca_3(PO_4)_2}=2.183m^{0}_{[\,]s}\bar{X}^{0}_{P_2O_5[\,]s}$ $m^{0}_{CaF_2}=2.052m^{0}_{[\,]s}\bar{X}^{0}_{F[\,]s}$ $m^{0}_{CaCO_3}=2.272m^{0}_{[\,]s}\bar{X}_{CO_2[\,]s}$ $m^{0}_{A'_2}=m^{0}_{[\,]s}\bar{X}^{0}_{A'_2[\,]s}$	$[\,]s$	$\bar{X}_{P_2O_5[\,]s_2}$ $\bar{X}_{F[\,]s_2}$ $\bar{X}_{CO_2[\,]s_2}$ $\bar{X}_{A''_3[\,]s_2}$	$m^{2}_{Ca_3(PO_4)_2}=2.183m_{[\,]s_2}\bar{X}_{P_2O_5[\,]s_2}$ $m^{2}_{CaF_2}=2.052m_{[\,]s_2}\bar{X}_{F[\,]s_2}$ $m^{2}_{CaCO_3}=2.272m_{[\,]s_2}\bar{X}_{CO_2[\,]s_2}$ $m^{2}_{A''_4}=m_{[\,]s}\bar{X}_{A''_4[\,]s}=m^{0}_{[\,]s}\bar{X}^{0}_{A''_i[\,]s}$
		$m^{0}_{[\,]s}=\sum m^{0}_{A_i[\,]s}$			$m_{[\,]s_2}=\sum m_{A_i[\,]s_2}=R_S m^{0}_{[\,]s}$
$[\,]^{02}_{l}$	$\bar{X}^{02}_{N[\,]_l}=\bar{X}^{0}_{N[\,]_l}$ $\bar{X}^{02}_{P[\,]_l}=\bar{X}^{0}_{P[\,]_l}$ $\bar{X}^{02}_{Ca[\,]}=\bar{X}^{\bullet}_{Ca[\,]_l}$ $\bar{X}^{02}_{A''[\,]_l}=\bar{X}^{0}_{A''_2[\,]_l}$ $\bar{X}^{02}_{H_2O[\,]_l}=1-$ $-\sum\bar{X}^{02}_{A_{i-1}[\,]_l}$	$m^{02}_{HNO_3}=4.5m^{02}_{[\,]}(\bar{X}^{02}_{N[\,]_l}-0.7\bar{X}^{02}_{Ca[\,]_l})$ $m^{02}_{H_3PO_4}=3.161m^{02}_{[\,]_l}\bar{X}^{02}_{P[\,]_l}$ $m^{02}_{Ca(NO_3)_2}=4.1m^{02}_{[\,]_l}\bar{X}^{02}_{Ca[\,]_l}$ $m^{02}_{A''_1}=m^{02}_{[\,]_l}\bar{X}^{02}_{A[\,]_l}$ $m^{02}_{H_2O}=m^{02}_{[\,]_l}\bar{X}^{02}_{H_2O[\,]_l}$	$[\,]_{l_2}$	$\bar{X}_{N[\,]_{l_2}}$ $\bar{X}_{P[\,]_{l_2}}$ $\bar{X}_{Ca[\,]_{l_2}}$ $\bar{X}_{F[\,]_{l_2}}$ $\bar{X}_{CO_2[\,]_{l_2}}$ $\bar{X}_{A''_3[\,]_{l_2}}$ $\bar{X}_{H_2O[\,]_{l_2}}=$ $=1-\sum\bar{X}_{A_{i-1}[\,]_{l_2}}-$	$m^{2}_{H_3PO_4}=3.161m_{[\,]_l}\bar{X}_{P[\,]_{l_2}}$ $m^{2}_{HNO_3}=4.5m_{[\,]_{l_2}}(\bar{X}_{N[\,]_{l_2}}-0.7\bar{X}_{Ca[\,]_{l_2}})$ $m^{2}_{Ca(NO_3)_2}=4.1m_{[\,]_{l_2}}\bar{X}_{Ca[\,]_{l_2}}$ $m^{2}_{HF}=1.052m_{[\,]_{l_2}}\bar{X}_{[\,]_{l_2}}$ $m^{2}_{CO_2}=m_{[\,]_{l_2}}\bar{X}_{CO_2[\,]_{l_2}}$ $m^{2}_{A''_3}=m_{[\,]_{l_2}}\bar{X}_{A''_3[\,]_{l_2}}$ $m^{2}_{H_2O}=m_{[\,]_{l_2}}X_{H_2O[\,]_{l_2}}$
					$m_{[\,]_{l_2}}=\sum m^{2}_{A_i}=R_L m^{0}_{[\,]s}$
			$[\,]g_2$	$\bar{X}_{HF[\,]g_2}$ $\bar{X}_{CO_2[\,]g_2}$ $\bar{X}_{H_2O[\,]g_2}$	$m^{2}_{HF[\,]g}=1.052m^{0}_{[\,]s}(\bar{X}^{0}_{F[\,]s}-R_S\bar{X}_{F[\,]s_2}-R_L\bar{X}_{F[\,]_{l_2}})$ $m^{2}_{CO_2[\,]g}=m^{0}_{[\,]s}(\bar{X}^{0}_{CO_2[\,]s}-R_S\bar{X}_{CO_2[\,]s_2}-R_L\bar{X}_{CO_2[\,]_{l_2}})$ $m^{2}_{H_2O[\,]g}=m^{0}_{[\,]s}[R_D\bar{X}^{02}_{H_2O[\,]_l}+0.408(\bar{X}^{0}_{CO_2[\,]s}-R_S\bar{X}_{CO_2[\,]s_2})-R_L\bar{X}_{H_2O[\,]_{l_2}}]$
		$m^{02}_{[\,]_l}=\sum m^{02}_{A_i}=R_D m^{0}_{[\,]s}$			$m_{[\,]g}=\sum m^{2}_{A_i[\,]g}$

rial, the following phase ratios were defined:

$$R_L=\frac{m_{[\,]_{l_2}}}{m^{0}_{[\,]_s}}=\frac{(L+S)(\overline{x}^{I}_{P[\,]_1})^2-0.43657\,\overline{x}^{0}_{P_2O_5[\,]_s}\overline{x}_{P[\,]_{s^*_4}}}{\overline{x}^{I}_{P[\,]_1}(\overline{x}^{I}_{P[\,]_1}-\overline{x}_{P[\,]_{s^*_4}})}.$$

$$R_S=\frac{m_{[\,]_{s_2}}}{m^{0}_{[\,]_s}}=\overline{x}^{0}_{A''_{2[\,]_s}}\quad\text{is}$$

$L=\dfrac{m^{I}_{[\,]_1}}{m^{0}_{[\,]_s}}$, is the phase ratio between "mother liquor" and phosphatic raw material;

$S = \dfrac{m^{I}_{[]_{s*}}}{m^{0}_{[]_{s}}}$, is the phase ratio between washed calcium nitrate separated on filters and phosphatic raw material.

The relations for calculating the two ratios will be given later.

The requirement of nitric acid defined by D_R ratio is established experimentally or by stoichiometric calculation, as a function of the sort of phosphatic raw material used and the nitrophosphate obtained; in the Norks-Hydro procedure this ratio can be varied between 1.4 and 1.6 [t 100 % $HNO_3/t[]^0_s$].

The reagent phase ratio, $R_D = (m^0_{[]_{l_1}} + m_{f_{II}})/m^0_{[]_s}$, is calculated by the relation:

$$R_D = \frac{R_L \bar{x}_{N[]_{l_2}} \bar{x}_{Pf_{II}} - (R_L \bar{x}_{P[]_{l_2}} - 0.4366 \bar{x}^0_{P_2O_5[]_s})(\bar{x}_{Nf_{II}} - 0.2222 \bar{x}^0_{HNO_3})}{0.2222 \bar{x}^0_{HNO_3} \bar{x}_{Pf_{II}}}$$

The gas output in the nitric decomposition process can be calculated by the ratio:

$$G = \frac{m_{[]_{g_2}}}{m^0_{[]_s}} = 1 + D_R/\bar{x}^0_{HNO_3} + F - R_L - A$$

Process of calcium nitrate crystallization

The characteristic equation of the process is the following:

$$[H_3PO_4 + Ca(NO_3)_2 + HNO_3 + HF + A''_3 + H_2O]_{l_2} \rightarrow$$

$$\rightarrow \{[H_3PO_4 + HNO_3 + Ca(NO_3)_2 + HF + A''_3 + H_2O]_{l_3} + [Ca(NO_3)_2\, 4\, H_2O]_{s_3}\}$$

In agreement with this characteristic equation the crystallization process is determined by a single independent conversion process:

$$Ca(NO_3)_2 + 4\, H_2O \rightleftharpoons Ca(NO_3)_2\, 4\, H_2O_{[]_s}$$

The crystallization of tetrahydrated calcium nitrate is determined by the technological conditions specific to the Norks-Hydro process[3,6]: excess of nitric acid larger than 10 % HNO_3 in the nitric decomposition of phosphatic raw material and cooling of phosphonitric solution below 0°C for separating the calcium nitrate (between −5°C and −10°C). These conditions were established after studies on liquid-solid equilibrium by means of the double-exchange quaternary diagrams.[9–12]

The mass balance equations for the crystallization process are listed in Table 4.

Table 4

Mass balance equations — Crystallization of calcium nitrate

INPUT			OUTPUT			
Phase	Chemical composition $\bar{x}^{03}_{A_{i[]_{l_1}}}$	Mass balance [kg/hour]	Phase		Chemical composition $\bar{x}^{3}_{A_i}$	Mass balance [Kg/hour]
$[]^{o}_{l_3}$	$\bar{x}^{03}_{N_{[]_{l_1}}} = \bar{x}_{N_{[]_{l_2}}}$ $\bar{x}^{03}_{Ca_{[]_{l_1}}} = \bar{x}_{Ca_{[]_{l_2}}}$ $\bar{x}^{03}_{P_{[]_{l_1}}} = \bar{x}_{P_{[]_{l_2}}}$ $\bar{x}^{03}_{F_{[]_{l_1}}} = \bar{x}_{F_{[]_{l_2}}}$ $\bar{x}^{03}_{CO_{2[]_{l_1}}} = \bar{x}_{CO_{2[]_{l_2}}}$ $\bar{x}^{03}_{A_{3[]_{l_1}}} = \bar{x}_{A_{3[]_{l_2}}}$ $\bar{x}_{H_2O_{[]_{l_1}}} = 1 - \sum \bar{x}^{03}_{A_{i-1[]_{l_1}}}$	$m^{03}_{HNO_3} = 4.5\, m^{03}_{[]_{l_1}} (\bar{x}^{03}_{N_{[]_{l_1}}} - 0.7\bar{x}^{03}_{Ca_{[]_{l_1}}}$ $m^{03}_{H_3PO_4} = 3.161\, m^{03}_{[]_{l_1}}\ \bar{x}^{03}_{P_{[]_{l_1}}}$ $m^{03}_{Ca(NO_3)_2} = 4.1\, m^{03}_{[]_{l_1}}\ \bar{x}^{03}_{Ca_{[]_{l_1}}}$ $m^{03}_{HF} = 1.052\, m^{03}_{[]_{l_1}}\, x^{03}_{F_{[]_{l_1}}}$ $m^{03}_{CO_2} = m^{03}_{[]_{l_1}}\, \bar{x}^{03}_{CO_{2[]_{l_1}}}$ $m^{03}_{A_3} = m^{03}_{[]_{l_1}}\, \bar{x}^{03}_{A_{3[]_{l_1}}}$ $m^{03}_{H_2O} = m^{03}_{[]_{l_1}}\, \bar{x}^{03}_{H_2O_{[]_{l_1}}}$	Slurry from crystallization	$[]_{l_3}$	$\bar{x}_{P_{[]_{l_3}}}$ $\bar{x}_{N_{[]_{l_3}}}$ $\bar{x}_{Ca_{[]_{l_3}}}$ $\bar{x}_{F_{[]_{l_3}}}$ $\bar{x}_{CO_{2[]_{l_3}}}$ $\bar{x}_{H_2O_{[]_{l_3}}}$ $\bar{x}_{A_{3[]_{l_3}}}$	$m^{3}_{H_3PO_4} = 3.161\, m^{03}_{[]_{l_1}}\, x^{03}_{P_{[]_{l_1}}}$ $m^{03}_{HNO_3} = 4.5\, m^{03}_{[]_{l_1}} (\bar{x}^{03}_{N_{[]_{l_1}}} - 0.7\bar{x}^{03}_{Ca_{[]_{l_1}}})$ $m^{3}_{HF} = 1.052\, m^{03}_{[]_{l_1}}\, \bar{x}^{03}_{F_{[]_{l_1}}}$ $m^{3}_{Ca(NO_3)_2} = 4.1\, m_{[]_{l_3}}\, \bar{x}_{Ca_{[]_{l_3}}}$ $m^{3}_{CO_2} = m^{03}_{[]_{l_1}} \cdot \bar{x}^{03}_{CO_{2[]_{l_1}}}$ $m^{3}_{H_2O} = m^{03}_{[]_{l_1}} (\bar{x}^{03}_{H_2O_{[]_{l_1}}} - 1.8\bar{x}^{03}_{Ca_{[]_{l_1}}}) + 1.8\, m_{[]_{l_3}}\, \bar{x}_{Ca_{[]_{l_3}}}$ $m^{3}_{A_3} = m^{03}_{[]_{l_1}}\, x_{A_{3[]_{l_1}}}$ $m_{[]_{l_3}} = m^{03}_{[]_{l_1}} \dfrac{1 - 5.9\,\bar{x}^{03}_{Ca_{[]_{l_3}}}}{1 - 5.9\,\bar{x}_{Ca_{[]_{l_3}}}}$
		$m^{03}_{[]} = \sum_{i=1}^{7} m^{03}_{A_i}$		$[]_{s_3}$	$\bar{x}_{Ca_{[]_{s_3}}}$ $\bar{x}_{N_{[]_{s_3}}}$ $\bar{x}_{H_2O_{[]_{s_3}}}$	$m^{3}_{Ca(NO_3)_2 \cdot 4H_2O} = 5.9\, m^{03}_{[]_{l_1}} \dfrac{\bar{x}^{03}_{Ca_{[]_{l_1}}} - \bar{x}_{Ca_{[]_{l_3}}}}{1 - 5.9\,\bar{x}_{Ca_{[]_{l_3}}}}$ $m_{[]_{s_3}} = m^{3}_{Ca(NO_3)_2 \cdot 4H_2O}$

Filtering and washing process of calcium nitrate

This process is accomplished in two stages :

First filtration stage — Separation of "mother liquor" from tetrahydrated calcium nitrate in solid phase.

The characteristic equation is the following:

$$\{[H_3PO_4 + HNO_3 + Ca(NO_3)_2 + HF + A_3'' + H_2O]_{l_3} + [Ca(NO_3)_2\ 4\,H_2O]_{s_3}\} \rightarrow$$

$$\rightarrow [H_3PO_4 + HNO_3 + HF + Ca(NO_3)_2 + A_4'' + H_2O]_{l_I} +$$

$$+ \{[Ca(NO_3)4\,H_2O]_{s_4} + [H_3PO_4 + HNO_3 + Ca(NO_3)_2 + A_1'' + H_2O]_{l_3^\bullet}\}_{s_4^\bullet}$$

Second filtration stage — Washing of tetrahydrated calcium nitrate with fresh nitric acid for recovering the phosphoric acid carried out with the solid in the first filtration stage followed by washing with water for recovering the nitric acid retained as moisture by the solid.

In the second stage the washing acid, which is recycled to acid mixing, $[]_{f_{II}}$, as well as washed, moistened tetrahydrated calcium nitrate, $[]_{s_I^\bullet}$, are obtained.

The characteristic equation is the following :

$$\{[\mathrm{Ca(NO_3)_2\,4\,H_2O}]_{s_4} + [\mathrm{H_3PO_4 + HNO_3 + Ca(NO_3)_2} + A_1'' + \mathrm{H_2O}]_{l_3}^{\bullet}\}_{s_4}^{\bullet} +$$

$$[\mathrm{HNO_3 + H_2O}]_{l_2}^{0} + [\mathrm{H_2O}]_{l_3}^{0} \rightarrow \{[\mathrm{Ca(NO_3)_2\,4\,H_2O}]_{s_I} + [\mathrm{H_2O}]_{l}^{\bullet}\}_{s_I}^{\bullet} +$$

$$+ [\mathrm{HNO_3 + H_3PO_4 + Ca(NO_3)_2} + A_1'' + \mathrm{H_2O}]_{f_{II}}$$

In the two characteristic equations $[\;]_{l_3}^{\bullet}$ and $[\mathrm{H_2O}]_{l^{*}}$ represent the liquid phases found as moisture in solid phases while $[\;]_{s_4}^{\bullet}$ and $[\;]_{s_I}^{\bullet}$ are the humid solid phases.

In deriving the mass balance equations listed in Table 5 the partial dissolution of tetrahydrated calcium nitrate during washings of the second filtration stage was taken into account.

To correlate the liquid and solid outputs with the supply of raw material the following ratios have been defined :

$$L = \frac{m^{I}_{[]_{l}}}{m^{0}_{[]_{s}}} = \frac{0.4366\,\overline{x}^{0}_{P_2O_5[]_s}}{\overline{x}^{I}_{P[]_l}}$$

$$S = \frac{m^{I}_{[]_{s^*}}}{m^{0}_{[]_{s}}} = \frac{0.7142\,\overline{x}^{0}_{CaO[]_s}\cdot\overline{x}^{I}_{P[]_l} - 0.4366\,\overline{x}^{0}_{P_2O_5[]_s}\overline{x}^{I}_{Ca[]_l}}{\overline{x}^{I}_{P[]_l}\cdot\overline{x}^{I}_{Ca[]_{s^*}}}$$

$$F = \frac{m_{f_{II}}}{m^{0}_{[]_{s}}} = \frac{(R_L - L - S)\cdot\overline{x}^{I}_{P[]_l}}{\overline{x}_{Pf_{II}}}$$

$$A = \frac{m^{0}_{[]_{l_2}}}{m^{0}_{[]_{s}}} = \frac{F}{0.2222\,\overline{x}^{0}_{HNO_3}}\left[\overline{x}_{Nf_{II}} - 0.7\,\overline{x}_{Caf_{II}} - \frac{\overline{x}_{Pf_{II}}}{\overline{x}^{I}_{P[]_l}}(\overline{x}^{I}_{N[]_l} - 0.7\,\overline{x}^{I}_{Ca[]})_l\right] +$$

$$+ \frac{S}{0.2222\,\overline{x}^{0}_{HNO_3}}(\overline{x}^{I}_{N[]_{s^*}} - 0.7\,\overline{x}^{I}_{Ca[]_{S^*}})$$

$$W = \frac{m^{0}_{[]_{l_3}}}{m^{0}_{[]_{s}}} = F\,\frac{\overline{x}^{I}_{P[]_l} - \overline{x}_{Pf_{II}}}{\overline{x}^{I}_{P[]_l}} - A$$

In the mass flux sketched in Fig. 2 the place of phasical ratios previously defined is indicated so as to offer a more suggestive representation of their significance.

Table 5

Mass balance equations — Filtration and washing of calcium nitrate

INPUT				OUTPUT			
Phase		Chemical composition $\bar{x}^{04}_{A_i}$	Mass balance [kg/hour]	Phase		Chemical composition $\bar{x}_{A_i}$	Mass balance [kg/hour]
FIRST STAGE FILTRATION	$[]^{04}_l$	$\bar{x}^{04}_{P[]_l} = \bar{x}_{P[]_{l_3}}$ $\bar{x}^{04}_{N[]_l} = \bar{x}_{N[]_{l_3}}$ $\bar{x}^{04}_{Ca[]_l} = \bar{x}_{Ca[]_{l_3}}$ $\bar{x}^{04}_{F[]_l} = \bar{x}_{F[]_{l_3}}$ $\bar{x}^{04}_{F[]_l} = \bar{x}_{F[]_{l_3}}$ $\bar{x}^{04}_{CO_2[]_l} = \bar{x}_{CO_2[]_{l_3}}$ $\bar{x}^{04}_{A''_3[]_l} = \bar{x}_{A''_3[]_{l_3}}$ $\bar{x}^{04}_{H_2O[]_l} = \bar{x}^3_{H_2O[]_l}$	$m^{04}_{H_3PO_4} = m^3_{H_3PO_4}$ $m^{04}_{HNO_3} = m^3_{HNO_3}$ $m^{04}_{HF} = m^3_{HF}$ $m^{04}_{Ca(NO_3)_2} = m^3_{Ca(NO_3)_2}$ $m^{04}_{CO_2} = m^3_{CO_2}$ $m^{04}_{A''_3} = m^3_{A''_3}$ $m^{04}_{H_2O} = m^3_{H_2O}$ $m^{04}_{[]_l} = m_{[]_{l_3}}$	FIRST STAGE FILTRATION	$[]^I_l$	$\bar{x}^I_{P[]_l}$ $\bar{x}^I_{N[]_l}$ $\bar{x}^I_{Ca[]_l}$ $\bar{x}^I_{F[]_l}$ $\bar{x}^I_{CO_2[]_l}$ $\bar{x}^I_{A''_4[]_l}$ $\bar{x}_{H_2O} = 1 - \sum A^I_{i-1}$	$m^I_{H_3PO_4} = 3.161\, m^I_{[]_l}\, \bar{x}^I_{P[]_l}$ $m^I_{HNO_3} = 4.5\, m^I_{[]_l} (\bar{x}^I_{N[]_l} - 0.7\bar{x}^I_{Ca[]_l})$ $m^I_{HF} = 1.052\, m^I_{[]_l}\, \bar{x}^I_{F[]_l}$ $m^I_{CO_2} = m^I_{[]_l}\, \bar{x}^I_{CO_2[]_l}$ $m^I_{A''_4[]_l} = m^I_{[]_l}\, x^I_{A''_4[]_l}$, $m^I_{Ca(NO_3)_2} = 4.1\, m^I_{[]_l}\, \bar{x}^I_{Ca[]_l}$ $m^I_{H_2O} = m^I_{[]_l}\, \bar{x}^I_{H_2O[]_l}$ $m^I_{[]_l} = m^{03}_{[]_l}(1 - 5.9 \frac{\bar{x}^I_{P[]_l}(\bar{x}^{03}_{Ca[]_l} - \bar{x}^I_{Ca[]_l})}{(1 - 5.9\bar{x}^I_{Ca[]_l})(\bar{x}^I_{P[]_l} - \bar{x}_{P[]^*_{s_4}})}$ $m^I_{[]_l} = 0.4366\, m^o_{[]s} \frac{\bar{x}^o_{P_2O_5[]s}}{\bar{x}^I_{P[]_l}}$
	$[]^{04}_s$	$\bar{x}^{04}_{Ca} = \bar{x}_{Ca[]s_3}$ $\bar{x}^{04}_{N} = \bar{x}_{N[]s_3}$	$m^{04}_{[]s} = m_{[]s_3}$		$[]^*_{s_4}$	$\bar{x}_{P[]s^*_4}$ $\bar{x}_{N[]s^*_4}$ $\bar{x}_{Ca[]s^*_4}$	$m^*_{[]s_4} = 5.9\, m^{03}_{[]_l} \frac{\bar{x}^I_P(\bar{x}^{03}_{Ca[]_l} - \bar{x}^I_{Ca[]_l})}{(1 - 5.9\bar{x}^I_{Ca[]_l})(\bar{x}^I_{P[]_l} - \bar{x}_{P[]s^*_4})}$ $m^*_{[]s_4} = m^o_{[]s}(R_L - 0.4366 \frac{\bar{x}^o_{P_2O_5[]s}}{\bar{x}^I_{P[]_l}}$
SECOND STAGE FILTRATION	$[]^o_{l_2}$	$\bar{x}^o_{HNO_3[]_l}$ $\bar{x}^o_{H_2O[]_{l_2}} = 1 - \bar{x}^o_{HNO_3[]_l}$	$m^o_{HNO_3[]_l} = m^o_{[]}\, \bar{x}^o_{HNO_3[]_{l_2}}$ $m^o_{H_2O[]_{l_2}} = m^o_{[]_{l_2}}(1 - \bar{x}^o_{HNO_3[]_{l_2}})$ $m^o_{[]_{l_2}} = m^o_{[]s}\left(\frac{D_R}{\bar{x}^o_{HNO_3}} - R_D R^o_L\right)$	SECOND STAGE FILTRATION	$[]_{f_{II}}$	$\bar{x}_{P_{f_{II}}}$ $\bar{x}_{N_{f_{II}}}$ $\bar{x}_{Ca_{f_{II}}}$ $\bar{x}_{A''_{f_{II}}}$ $\bar{x}_{H_2O_{f_{II}}} = 1 - \sum \bar{x}_{A_{i-1} f_{II}}$	$m^f_{H_3PO_{4f_{II}}} = 3.161\, m_{f_{II}}\, \bar{x}_{P_{f_{II}}}$ $m_{HNO_{3f_{II}}} = 4.5\, m_{f_{II}}(\bar{x}_{N_{f_{II}}} - 0.7\bar{x}_{Ca_{f_{II}}})$ $m_{Ca(NO_3)_{2f_{II}}} = 4.1\, m_{f_{II}}\, \bar{x}_{Ca_{f_{II}}}$ $m_{A''_{f_{II}}} = m_{f_{II}}\, \bar{x}_{A'_{f_{II}}}$ $m_{H_2O_{f_2}} = m_{f_{II}}\, \bar{x}_{H_2O_{f_{II}}}$ $m_{f_{II}} = m^o_{[]s} \frac{\bar{x}_{P[]s^*_4}}{\bar{x}_{P_{f_{II}}}}\left(R_L - 0.4366 \frac{\bar{x}^o_{P_2O_5[]s}}{\bar{x}^I_{P[]_l}}\right)$
	$[]^o_{l_3}$		$m^o_{[]_{l_3}} = m^I_{[]_l}\, \bar{x}^I_{H_2O[]_l} + m^I_{[]s^*}\, \bar{x}^I_{H_2O[]s^*} - (m^o_{[]_{l_1}} + m^o_{[]_{l_2}})(1 - \bar{x}^o_{HNO_3})$		$[]_s$	$\bar{x}^I_{Ca[]s^*}$ $\bar{x}^I_{N[]s^*}$	$m^I_{[]s^*} = m^o_{[]s}\left(0.7142 \frac{\bar{x}^o_{CaO[]s}}{\bar{x}^I_{Ca[]s^*}} - 0.4366 \frac{\bar{x}^o_{P_2O_5[]s}\, \bar{x}^I_{Ca[]_l}}{\bar{x}^I_{P[]_l}\, \bar{x}_{Ca[]s^*}}\right)$

Obs: $\bar{x}^I_{H_2O} = 1 - 3.161\bar{x}^I_{P[]_l} - 4.5\bar{x}^I_{N[]_l} - 0.95\bar{x}^I_{Ca} - \bar{x}^I_{F[]} \cdot 1.052 - \bar{x}^I_{CO_2[]_l} - \bar{x}^I_{A''_4[]_l}$

$\bar{x}^I_{H_2O[]s^*} = 1 - 0.95\bar{x}^I_{Ca[]s^*} - 4.5\bar{x}^I_{N[]s^*}$

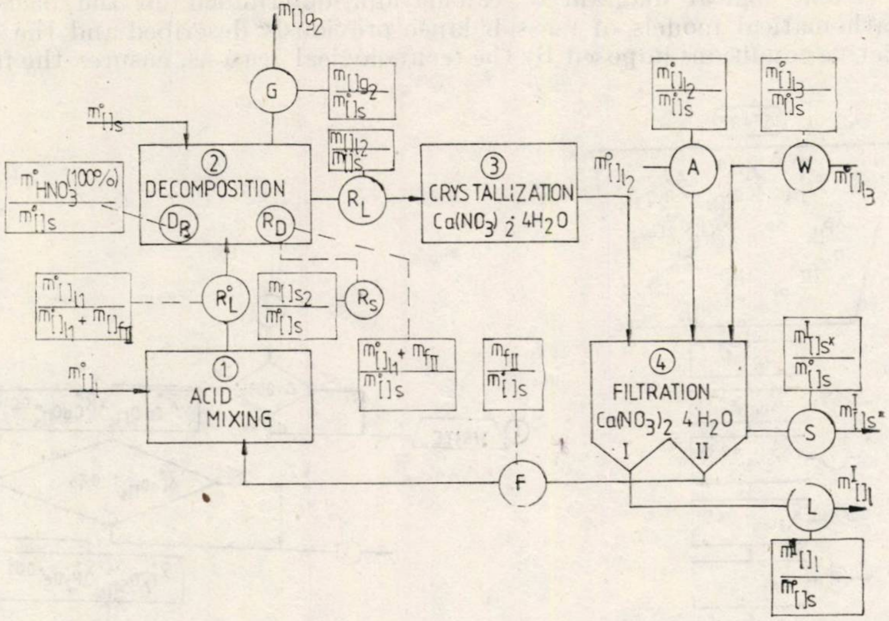
m[]g2
G
m[]g2 / m°[]s
m°[]s
m[]l2 / m°[]s
②
DECOMPOSITION
m°HNO3(100%) / m°[]s
DB
RD
RL
③
CRYSTALLIZATION
Ca(NO3)2 · 4H2O
m°[]l2
A
m°[]l2 / m°[]s
W
m°[]l3 / m°[]s
m°[]l3
m°[]l1 / m°[]l1 + m[]fII
R°L
m[]s2 / m°[]s
RS
m°[]l1 + mfII / m°[]s
mfII / m°[]s
①
ACID MIXING
m°[]l1
④
FILTRATION
Ca(NO3)2 4H2O
I
II
F
mI[]s* / m°[]s
S
mI[]s*
mI[]l
L
mI[]l / m°[]s

Fig. 2.—Material flux-phase ratios in the nitric decomposition of phosphatic raw material.

3. LOGICAL DIAGRAM OF CALCULATION [13,14]

In plotting the logical diagram of calculation in Fig. 3 the peculiarities of the process of nitric decomposition of phosphatic raw materials in the Norks-Hydro procedure for obtaining nitrophosphates were taken into account.

Thus in the "mother liquor", the Ca/P mass ratio has to be maximum 0.35 while the phosphorus content should be constant (implicitly the water content).

At the same time the water content in phosphonitric solution from nitric decomposition is correlated with the water content in "mother liquor" and also with the content of water of crystallization in $[Ca(NO_3)_2\,4\,H_2O]_s$. Since the water content in the calcium nitrate crystal is of about 31% the maintenance of about the same content in the solution from nitric decomposition ($\pm 1\%$) ensures the obtention of a "mother liquor" with the same water content.

In this way in the industrial equipments, minimum volumes of solutions are to be handled, the overloading of evaporators for nitrophosphate suspensions due to the excessive dilution of phosphonitric solutions being thus avoided. In the process only the washing water found as moisture in the solid phase after filtering calcium nitrate is introduced.

To accomplish the correlation for the water content in phosphonitric solutions from decomposition in the logical diagram, a monitoring key was introduced : $|\bar{x}_{H_2O[]_{l_2}} - \bar{x}^{I}_{H_2O[]_{l}}| \leqslant 0.002$

The logical diagram of calculation, determined on the basis of mathematical models of mass balance previously described and the restrictive conditions imposed by the technological reasons, ensures the find-

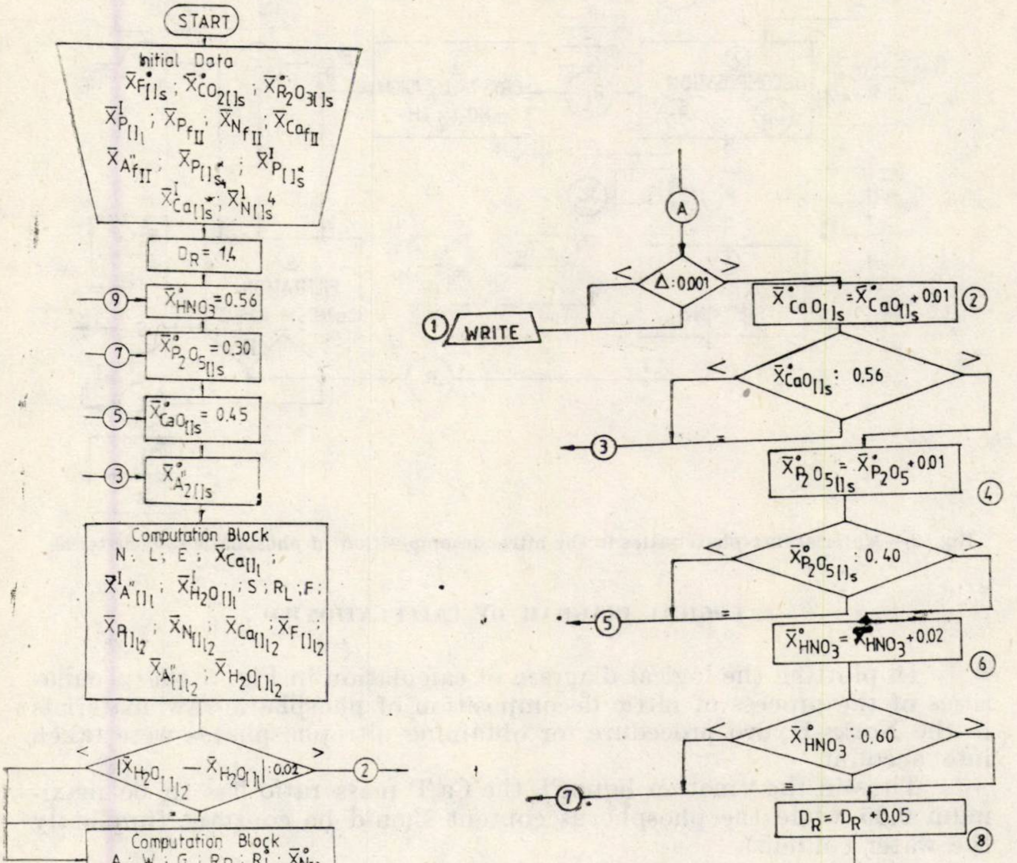
START
Initial Data
$\overline{X}^{\circ}_{F[\,]s}$; $\overline{X}^{\circ}_{CO_2[\,]s}$; $\overline{X}^{\circ}_{R_2O_3[\,]s}$
$\overline{X}^{I}_{P[\,]_l}$; $\overline{X}_{P_{fII}}$; $\overline{X}_{N_{fII}}$; $\overline{X}_{Ca_{fII}}$
$\overline{X}_{A''_{fII}}$; $\overline{X}_{P[\,]_{s4}}$; $\overline{X}^{I}_{P[\,]s}$
$\overline{X}^{I}_{Ca[\,]s}$; $\overline{X}^{I}_{N[\,]s}$
$D_R = 1.4$
9
$\overline{X}^{\circ}_{HNO_3} = 0.56$
7
$\overline{X}^{\circ}_{P_2O_5[\,]s} = 0.30$
5
$\overline{X}^{\circ}_{CaO[\,]s} = 0.45$
3
$\overline{X}^{\circ}_{A''_2[\,]s}$
Computation Block
N ; L ; E ; $\overline{X}_{Ca[\,]_l}$;
$\overline{X}^{I}_{A''[\,]_l}$; $\overline{X}^{I}_{H_2O[\,]_l}$; S ; R_L ; F ;
$\overline{X}_{P[\,]_{l2}}$; $\overline{X}_{N[\,]_{l2}}$; $\overline{X}_{Ca[\,]_{l2}}$; $\overline{X}_{F[\,]_{l2}}$;
$\overline{X}_{A''[\,]_{l2}}$; $\overline{X}_{H_2O[\,]_{l2}}$
<
$|\overline{X}_{H_2O[\,]_{l2}} - \overline{X}_{H_2O[\,]_l}| : 0.02$
>
2
=
Computation Block
A ; W ; G ; R_D ; R'_L ; $\overline{X}^{\circ}_{N[\,]_l}$
$\Delta = 1 + D_R / \overline{X}_{HNO_3} + W - L - S - G$
A
A
<
$\Delta : 0.001$
>
1
WRITE
$\overline{X}^{\circ}_{CaO[\,]s} = \overline{X}^{\circ}_{CaO[\,]s} + 0.01$
2
<
$\overline{X}^{\circ}_{CaO[\,]s}$: 0.56
>
3
=
$\overline{X}^{\circ}_{P_2O_5[\,]s} = \overline{X}^{\circ}_{P_2O_5} + 0.01$
4
<
$\overline{X}^{\circ}_{P_2O_5[\,]s}$: 0.40
>
5
=
$\overline{X}^{\circ}_{HNO_3} = \overline{X}_{HNO_3} + 0.02$
6
<
$\overline{X}^{\circ}_{HNO_3}$: 0.60
>
7
=
$D_R = D_R + 0.05$
8
<
D_R : 1.60
>
STOP
9
=

Fig. 3. — Logical diagram of calculation.

ing of correlations between the composition of phosphatic raw materials, expressed by mass fractions, $\overline{x}^0_{P_2O_5[\,]_s}$ and $\overline{x}^0_{CaO[\,]_s}$, initial concentration $\overline{x}^0_{HNO_3}$ and the excess of nitric acid, D_R, respectively. At the same time the phasical ratios connected to the chosen variables are calculated.

The initial data are listed in Table 6. The relations for calculating the mass fractions given in this table were settled from the balance equations of the corresponding components for the phases they are involved in.

Table 6

Measured amounts — initial data

Phase	Measurable amounts — Initial data
Phosphatic Raw Materials $[\,]_s$	$\bar{x}^{\bullet}_{P_2O_5[\,]_s} = 0.3-0.4$; $\bar{x}^{\bullet}_{CaO[\,]_s} = 0.45-0.56$ $\bar{x}^{\bullet}_{F[\,]_s} = 0.035$; $\bar{x}^{\bullet}_{CO_2[\,]_s} = 0.01$; $\bar{x}^{\bullet}_{R_2O_3[\,]_s} = 0.02$ $\bar{x}^{\circ}_{A''_4[\,]_s} = 1-2.183\cdot\bar{x}^{\bullet}_{P_2O_5[\,]_s} = 2.052\cdot\bar{x}^{\bullet}_{F[\,]_s} - 2.272\cdot\bar{x}^{\bullet}_{CO_2[\,]_s} - \bar{x}^{\bullet}_{R_2O_3}$
Nitric Acid Solution $[\,]^{\bullet}_{l_1}$ $[\,]^{\bullet}_{l_2}$	$\bar{x}^{\bullet}_{HNO_3} = 0.56-0.60$
Mother liquor $[\,]_{l_1}$	$\bar{x}^{I}_{P[\,]_{l_1}} = 0.10$; $\bar{x}^{I}_{Ca[\,]_{l_1}} = 0.35\,\bar{x}^{I}_{P[\,]_{l_1}}$; $\bar{x}^{I}_{A'_4[\,]_{l_1}} = 0.9\cdot\bar{x}^{\circ}_{A''_2[\,]_s}/L$; $\bar{x}^{I}_{N[\,]_{l_1}} = (E\cdot\bar{x}^{I}_{P[\,]_{l_1}} + 1.375\bar{x}^{\bullet}_{P_2O_5[\,]_s}$ $\bar{x}^{I}_{Ca[\,]_{l_1}})/1.9647\cdot\bar{x}^{\bullet}_{P_2O_5[\,]_s}$
Nitric Decomposition Solution $[\,]_{l_2}$	$D_R = 1.4-1.6$; $N = 2.25\cdot\bar{x}^{\bullet}_{CaO[\,]_s} + 3.034\cdot\bar{x}^{\bullet}_{R_2O_3[\,]_s}$ $\left\lvert\bar{x}_{H_2O[\,]_{l_2}} - \bar{x}_{H_2O[\,]_{l_1}}\right\rvert \leqslant 0.002$, $E = D_R - N$ $\bar{x}_{P[\,]_{l_2}} = (0.4366\cdot\bar{x}^{\bullet}_{P_2O_5[\,]_s} + F\cdot\bar{x}_{PfII})/R_L$ $\bar{x}_{N[\,]_{l_2}} = (0.2222\cdot D_R + 0.7F\cdot\bar{x}^{\circ}_{CafII})/R_L$ $\bar{x}_{Ca[\,]_{l_2}} = (0.7142\cdot\bar{x}^{\bullet}_{CaO[\,]_s} + F\cdot\bar{x}_{CafII})/R_L$
Recirculated Wash Acid $[\,]_{fII}$	$\bar{x}_{PfII} = 0.03$; $\bar{x}_{NfII} = 0.10$ $\bar{x}_{CafII} = 0.035$; $\bar{x}_{AfII} = 0.025$
Humid Solid 1-st step filtration $[\,]^{*}_{s_4}$	$\bar{x}_{P[\,]_{s_4^*}} = 0.0175$
Humid Washed Solid $[\,]^{I}_{s^*}$	$\bar{x}_{P[\,]_{s^*}} = 0$; $\bar{x}_{Ca[\,]_{s^*}} = 0.153$; $\bar{x}_{N[\,]_{s^*}} = 0.111$.

4. RESULTS AND DISCUSSION

By running on computer the program based on the logical diagram in Fig. 3 and the initial data listed in Table 6, particularly significant data for the scientific management of nitric decomposition process of phosphatic raw materials could be obtained.

The obtained data are presented both in graphical form and in tables.

Thus Table 7 lists the data evidencing the dependence of decomposition ratio, D_R, on the composition of phosphatic raw materials. The fact deserves mention that D_R increases with increasing P_2O_5 and CaO content and the number of sorts of phosphatic raw material which can be worked in the decomposition process decreases.

A more suggestive representation of the correlation between D_R and composition of phosphatic raw materials is offered by Fig. 4 : the data required for plotting were taken from Table 7. The study on this diagram leads to the following conclusions :

— To a sort of phosphatic raw material of a given composition, a certain D_R value corresponds that is a certain amount of 100 % HNO_3. For instance a sort of raw material of $\overline{x}^0_{CaO[]_s} = 0.53$ is worked with $D_R = 1.46$, for $\overline{x}^0_{P_2O_5} = 0.34$ and $\overline{x}^0_{P_2O_5} = 0.36$ D_R's of 1.50 and 1.56 respectively are needed ;

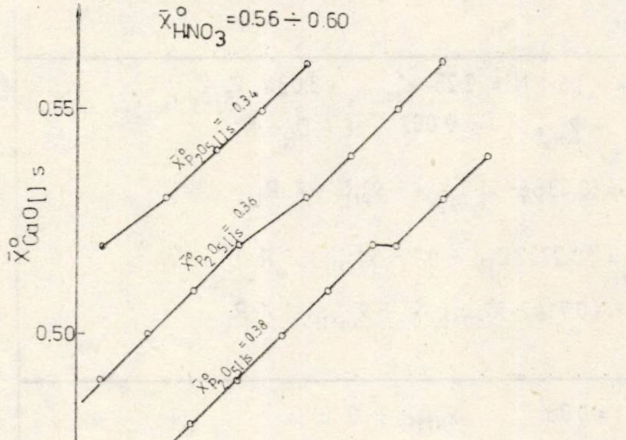

Fig. 4. — The correlation between D_R and composition of phosphatic raw materials.

— At the same D_R only sorts of phosphatic raw materials with certain P_2O_5 and CaO contents, respectively can be worked. Thus at $D_R = 1.50$ the sorts having $\overline{x}^0_{P_2O_5}$ of 0.34, 0.36 and 0.38 and $\overline{x}^0_{CaO}$ of 0.56, 0.53 and 0.505, respectively can be worked ;

Table 7

Correlation between D_R and composition of phosphatic raw materials

Chem. Composition \ D_R			$m^{\circ}_{HNO_3(100\%)}/m^{\circ}_{[]_5}$																				
			1.40	1.41	1.42	1.43	1.44	1.45	1.46	1.47	1.48	1.49	1.50	1.51	1.52	1.53	1.54	1.55	1.56	1.57	1.58	1.59	1.60
Phosphatic Raw Materials	$\bar{X}^{\circ}_{P_2O_5[]_5}$	0.30																					
		0.31		××× ● ▼ ▮																			
		0.32	○○○ ● ▼ ▮		●●● ● ▼ ▮		△△△ ● ▼ ▮	⊙⊙⊙ ● ▼ ▮															
		0.33		△△△ ● ▼ ▮		××× ● ▼ ▮				○○○ ● ▼ ▮													
		0.34		○○○ ● ▼ ▮			○○○ ● ▼ ▮		△△△ ● ▼ ▮		▭▭▭ ● ▼ ▮		◐◐◐ ● ▼ ▮										
		0.35	△△△ ● ▼ ▮		△△△ ● ▼ ▮		▭▭▭ ● ▼ ▮			⊙⊙⊙ ● ▼ ▮		▭▭▭ ● ▼ ▮		××× ● ▼ ▮		◐◐◐ ● ▼ ▮							
		0.36		◐◐◐ ● ▼ ▮		○○○ ● ▼ ▮		××× ● ▼ ▮		△△△ ● ▼ ▮			▭▭▭ ● ▼ ▮		××× ● ▼ ▮		△△△ ● ▼ ▮		▭▭▭ ● ▼ ▮				
		0.37	××× ● ▼ ▮		⊙⊙⊙ ● ▼ ▮		●●● ● ▼ ▮		▭▭▭ ● ▼ ▮		△△△ ● ▼ ▮		○○○ ● ▼ ▮	⊙⊙⊙ ● ▼ ▮		▭▭▭ ● ▼ ▮		◐◐◐ ● ▼ ▮		○○○ ● ▼ ▮		△△△ ● ▼ ▮	
		0.38		▭▭▭ ● ▼ ▮		△△△ ● ▼ ▮		○○○ ● ▼ ▮		××× ● ▼ ▮		⊙⊙⊙ ● ▼ ▮		△△△ ● ▼ ▮		○○○ ● ▼ ▮	◐◐◐ ● ▼ ▮		××× ● ▼ ▮		▭▭▭ ● ▼ ▮		××× ● ▼ ▮
		0.39		⊙⊙⊙ ● ▼ ▮	××× ● ▼ ▮		⊙⊙⊙ ● ▼ ▮		◐◐◐ ● ▼ ▮		○○○ ● ▼ ▮		△△△ ● ▼ ▮		○○○ ● ▼ ▮		⊙⊙⊙ ● ▼ ▮		△△△ ● ▼ ▮	⊙⊙⊙ ● ▼		○○○ ● ▼ ▮	
		0.40					××× ● ▼ ▮	△△△ ● ▼ ▮		◐◐◐ ● ▼ ▮		○○○ ● ▼ ▮		◐◐◐ ● ▼ ▮		××× ● ▼ ▮		▭▭▭ ● ▼ ▮		◐◐◐ ● ▼ ▮		▭▭▭ ● ▼ ▮	▲▲▲ ● ▼ ▮
	$\bar{X}^{\circ}_{CaO[]_5}$	0.45		⊙⊙⊙ ● ▼ ▮	××× ● ▼ ▮		××× ● ▼ ▮	△△△ ● ▼ ▮															
		0.46		▭▭▭ ● ▼ ▮			⊙⊙⊙ ● ▼ ▮			◐◐◐ ● ▼ ▮													
		0.47	××× ● ▼ ▮			△△△ ● ▼ ▮			◐◐◐ ● ▼ ▮			○○○ ● ▼ ▮											
		0.48			⊙⊙⊙ ● ▼ ▮			○○○ ● ▲ ▮			○○○ ● ▲ ▮			◐◐◐ ● ▲ ▮									
		0.49		◐◐◐ ● ▼ ▮			●●● ● ▼ ▮			××× ● ▼ ▮			△△△ ● ▼ ▮			××× ● ▼ ▮							
		0.50	△△△ ● ▼ ▮			○○○ ● ▼ ▮			▭▭▭ ● ▼ ▮			⊙⊙⊙ ● ▼ ▮			○○○ ● ▼ ▮			▭▭▭ ● ▼ ▮					
		0.51			△△△ ● ▼ ▮			××× ● ▼ ▮			△△△ ● ▼ ▮			△△△ ● ▼ ▮			⊙⊙⊙ ● ▼ ▮			◐◐◐ ● ▼ ▮			
		0.52		○○○ ● ▼ ▮			▭▭▭ ● ▼ ▮			△△△ ● ▼ ▮			○○○ ● ▼ ▮	⊙⊙⊙ ● ▼ ▮		○○○ ● ▼ ▮	◐◐◐ ● ▼ ▮		△△△ ● ▼ ▮	⊙⊙⊙ ● ▼ ▮		▭▭▭ ● ▼ ▮	▲▲▲ ● ▼ ▮
		0.53		△△△ ● ▼ ▮			○○○ ● ▼ ▮			⊙⊙⊙ ● ▼ ▮			▭▭▭ ● ▼ ▮			▭▭▭ ● ▼ ▮			××× ● ▼ ▮			○○○ ● ▼ ▮	
		0.54	○○○ ● ▼ ▮			××× ● ▼ ▮			△●△ ● ▼ ▮			▭▭▭ ● ▼ ▮			××× ● ▼ ▮			◐◐◐ ● ▼ ▮			▭▭▭ ● ▼ ▮		
		0.55			●◐● ● ▼ ▮			⊙⊙⊙ ● ▼ ▮			▭▭▭ ● ▼ ▮			××× ● ▼ ▮			△△△ ● ▼ ▮			○○○ ● ▼ ●			××× ● ▼ ▮
		0.56		××× ● ▼ ▮			△△△ ● ▼ ▮			○○○ ● ▼ ▮			◐◐◐ ● ▼ ▮			◐◐◐ ● ▼ ▮			▭▭▭ ● ▼ ▮			△△△ ● ▼ ▮	

● - $\bar{X}^{\circ}_{HNO_3} = 0.56$ ▼ - $\bar{X}^{\circ}_{HNO_3} = 0.58$ ▮ - $\bar{X}^{\circ}_{HNO_3} = 0.60$

— Within the 56 % — 60 % HNO_3 range the initial composition of the nitric acid solution does not influence the correlation between D_R and composition of phosphatic raw material.

The governing function of the process of nitric decomposition in the overall process for obtaining nitrophosphates, materialized in obtaining qualitatively and quantitatively stable "mother liquor", under the conditions of variable qualities of phosphatic raw material, is very well made evident by the plots in Fig. 5. As can be seen in Fig. 5 for a given chemical composition (Table 6), L ratio, characterizing quantitatively the "mother liquor", depends only on $\overline{x}^0_{P_2O_5[]_s}$, being invariable with respect to the initial concentration $\overline{x}^0_{HNO_3}$ and the excess of nitric acid, D_R.

For the other product of this technological stage, $[Ca(NO_3)_2\,4\,H_2O]_s$, the S ratio increases with increasing both $\overline{x}^0_{P_2O_5[]_s}$ and D_R, due to the corresponding increase of $\overline{x}^0_{CaO[]_s}$ as results from Table 7 and Fig. 4, respectively.

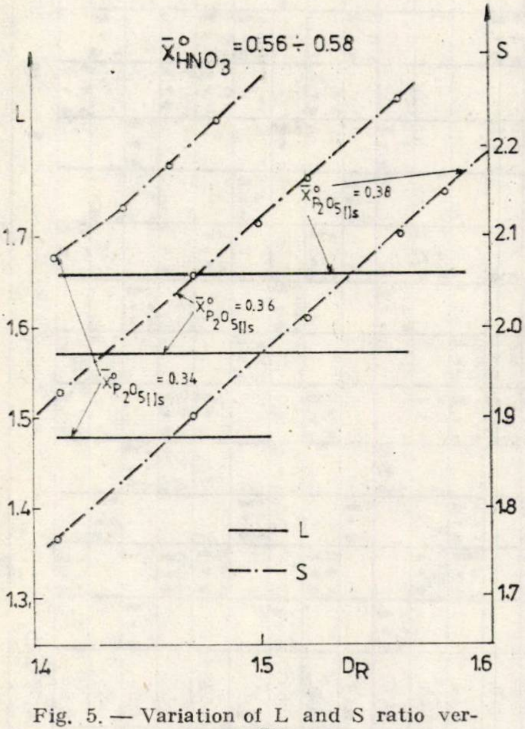

Fig. 5. — Variation of L and S ratio versus D_R.

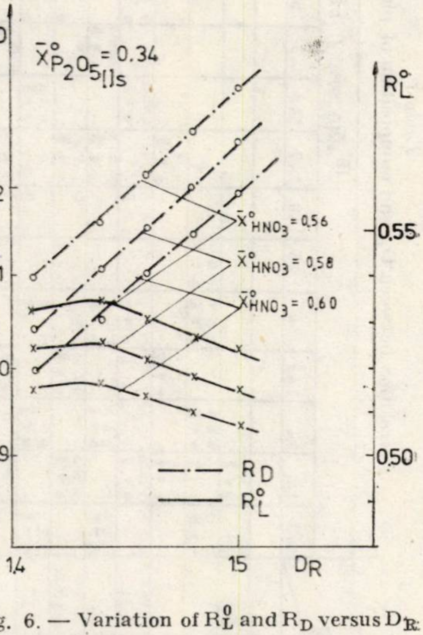

Fig. 6. — Variation of R^0_L and R_D versus D_R.

The stability of L ratio with respect to the variation of composition and supply of phosphatic raw material and of composition of initial nitric acid is given by the corresponding variation of nitric aid, recycled washing acid and water, characterized by R^0_L, R_D, A and W ratios. The direction of variation of these ratios is depicted in Fig. 6 and Fig. 7.

As a characteristic of these ratios, their variation with the composition of initial nitric acid $\overline{x}^0_{HNO_3}$ deserves mention.

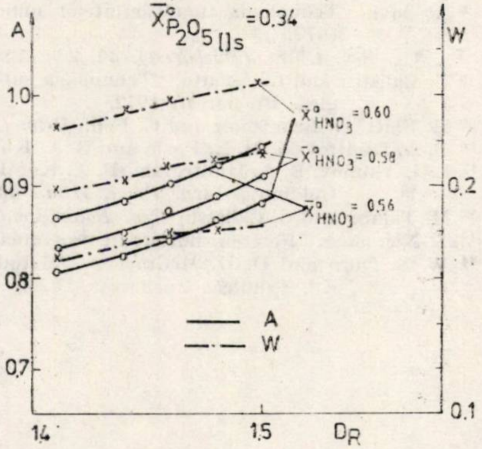

Fig. 7. — Variation of A and W ratio versus D_R and $x^0_{HNO_3}$.

Computer-aided analysis based on the program given in this paper offers the possibility of establishing all the correlations between chosen variables required by the technological needs.

NOTATIONS

$[\,]^0_k$ — Initial phase symbol (prior to the development of a process)
$[\,]_k$ — Final phase symbol;
$m^0_{[]_k}$ — Initial flowrate of k phase, [t/hour];
$m_{[]_k}$ — Final flowrate of k phase, [t/hour];
m^0_{Ai}, m_{Ai} — Initial and final output of Ai component, [t/hour];
$k = 1$ — liquid, s — solid, g — gaseous;
$\overline{x}^0_{Ai[]_s}$ — mass fraction of Ai component in phosphatic raw material;
$\overline{x}_{Ai[]_{l_2}}$ — mass fraction of Ai component in the solutions from nitric decomposition;
$\overline{x}_{Aif_{II}}$ — mass fraction of Ai component in the recycled washing acid;
$\overline{x}^0_{A_s[]_s}$ — mass fraction of insoluble impurities in phosphatic raw material;
$\overline{x}_{Ai[]s^*_4}$ — mass fraction of Ai component in humid solid before washings with fresh nitric acid and water;
$\overline{x}_{Ai[]_{s^*}}$ — mass fraction of Ai component in humid washed solid.

REFERENCES

[1] I. Moldovan, N. Popovici and G. Chivu, "The Technology of Mineral Fertilizers", The British Sulphur Co. Lts., London 1969.

[2] D. Davidescu, Z. Borlan, V. Davidescu and C. Hera "Fosforul în agricultură", Ed. Academiei R.S.R., Bucharest, 1974.

[3] C. Calistru, C. Leonte, C. Hagiu, I. Siminiceanu and O. Popa "Tehnologia îngrăşămintelor minerale" vol. 2, Ed. Tehnică, Bucharest, 1984.

[4] * * * — *Rev. Chim. (Bucharest)*, **31**, 1018 (1980).

[5] * * * — "Conjunctura economiei mondiale", *Rev. Economică*, Bucharest, 1980.

[6] A. Iovi, "Tehnologia îngrăşămintelor minerale", Ed. Didactică şi Pedagogică, Bucharest, 1977.

[7] * * * *Rev. Chim. (Bucharest)*, **34**, 269 (1983).

[8] C. Calistru and C. Leonte, "Tehnologia substanţelor anorganice", Ed. Didactică şi Pedagogică, Bucharest, 1972.

[9] R. Flatt, G. Brunisholz and G. Fell, *Helv. Ch. Acta*, **37**, 607 (1954); **39**, 473 (1956).

[10] B. A. Dmitrevski, M. E. Pozin and B. A. Kopjlev, *Jurn. Prikl. Him.*, **44**, 1934 (1971).

[11] L. I. Akimov, B. A. Dmitrevski, B. A. Kopjlev, A. P. Siskanov, Θ. B. Abramov, and A. L. Goldinov, *Jurn. Prikl. Him.*, **49**, 1677 (1976).

[12] M. Talabă and C. Calistru, *Rev. Roumaine Chim.*, **30**, 491 (1985).

[13] S. Niculescu, "Fortran, iniţiere în programarea structurală", Ed. Tehnică, Bucharest, 1973.

[14] W. S. Dorn and D. D. McCracken, "Metode numerice cu programe în Fortran", vol. IV, Ed. Tehnică, Bucharest, 1976.

INDUSTRIAL CENTRAL OF REFINERY
AND PETROCHEMICAL PRODUCTS PLOIEŞTI, ROMANIA
telephone : 53121 (Ploieşti), telex : 19343

"BRAZI"

PETROCHEMICAL WORKS

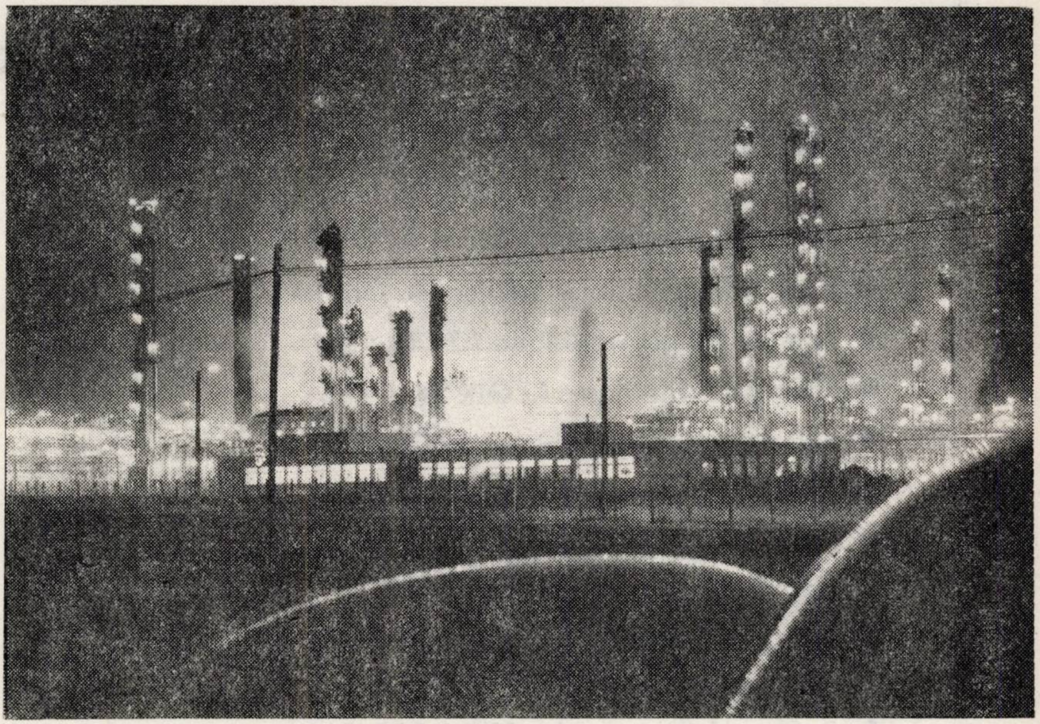

"Brazi" Petrochemical Works is a complex unit, having high-efficiency installations and equipment that afford advanced technological processing.

- Refines in installations in the refinery section the crude oil by secondary processes, mainly catalytical ones. The petrochemical section ensures the overall processing of pyrolysis products and crude oil materials.
- Supplies fuels, gas, liquefied gas, aromatic hydrocarbons and petrochemical products such as : ethylene oxide, glycols, polyethylene, synthetic rubber, phthalic and maleic anhydrides, dimethyl terephthalate, ethanolamine, choline chloride, ethyl methyl ketone, acetylene.

AZOMUREȘ

TÎRGU MUREȘ

Str. Gh. Doja No 300 Telex 065–264 Roumanie

L'usine de

matériaux PHOTOSENSIBLES azo

produit et offre:

- Film microscopie électronique **AZO-AME**
- Film radiographique médical **AZOIX RXR-2**
- Film cinéangiographique **AZOIX AX-1**
- Film sériographique **AZOIX SX-1**
- Film sérioangiographique **AZOIX ASX-1**
- Film micro-radio-photo **AZOIX MX-1**
- Film négatif pour reproductions photographiques des documents **AZOCOPY DN-3**
- Film positif pour reproductions photographiques des documents **AZOCOPY DP-1**
- Papier dérivatographe **AZOGRAF ID-2**
- Films phototechniques, papiers photographiques noir et blanc et en couleurs, pellicules cinématographiques négatives, positives, réversibles, etc...

HE SYNTHETIC FIBERS PLANTS

"SĂVINEȘTI"

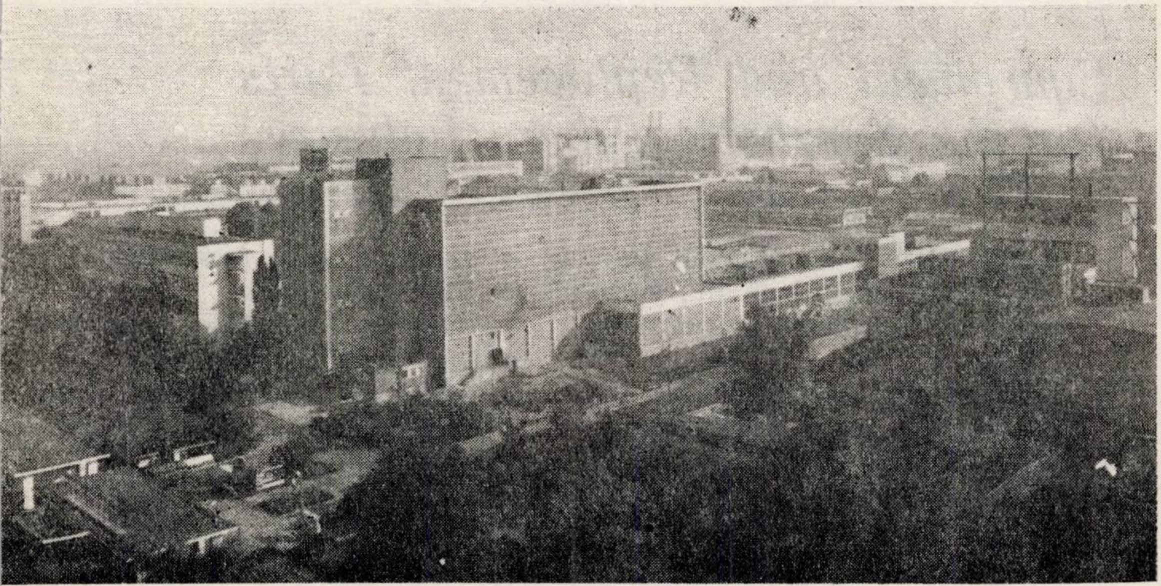

PRODUCE AND DELIVER:

ynthetic Fibers and Yarns

- **Melana® acrylic fibers**
- **Relon® polyamidic fibers**
- **Relon® textile polyamidic yarns**
- **Relontex® rug polyamidic yarns**
- **Relon® cords and technical polyamidic yarns**
- **String brushes**

Chemical Products

- Caprolactam
- Adipic acid
- Tetrachlorethane
- Cyanuryl chloride—Savicid®
- Dibenzyldiisocyanate
- Polyethyleneglycoladipate
- Relon® polyamidic pellets for plastics
- Relon® polyamidic bars and plates

Equipment and Replacement Parts for the Synthetic Fibers Industry

- Complete technological lines for synthetic fibers and yarns
- Spinning pumps for synthetic fibers
- Cleaning forcing pumps for vessels in the chemical industry
- Winding yarn machines
- Spool machines
- Spindles for textile machines
- Cutting fiber machines
- Different replacement parts in the chemical fibers industry

PRODUCER:

THE SYNTHETIC FIBERS
PLANTS "SĂVINEŞTI"
PIATRA NEAMŢ
Telex: 025221—222;
Telegraph CFS Săvineşti

EXPORTERS:

Synthetic fibers and yarns:
I.C.E. DANUBIANA BUCUREŞTI
Bl. Republicii nr. 10—12
sector 4 Bucureşti
telex 11184
Danaz

Equipment and replacement parts:
I.C.E. INDUSTRIALEXPORT-IMPORT
BUCUREŞTI
Str. Scaune 1—3
telex 10052—10930
PO Box/—764

AZOMUREŞ®
TÎRGU MURES

AZO

manufactures and delivers:

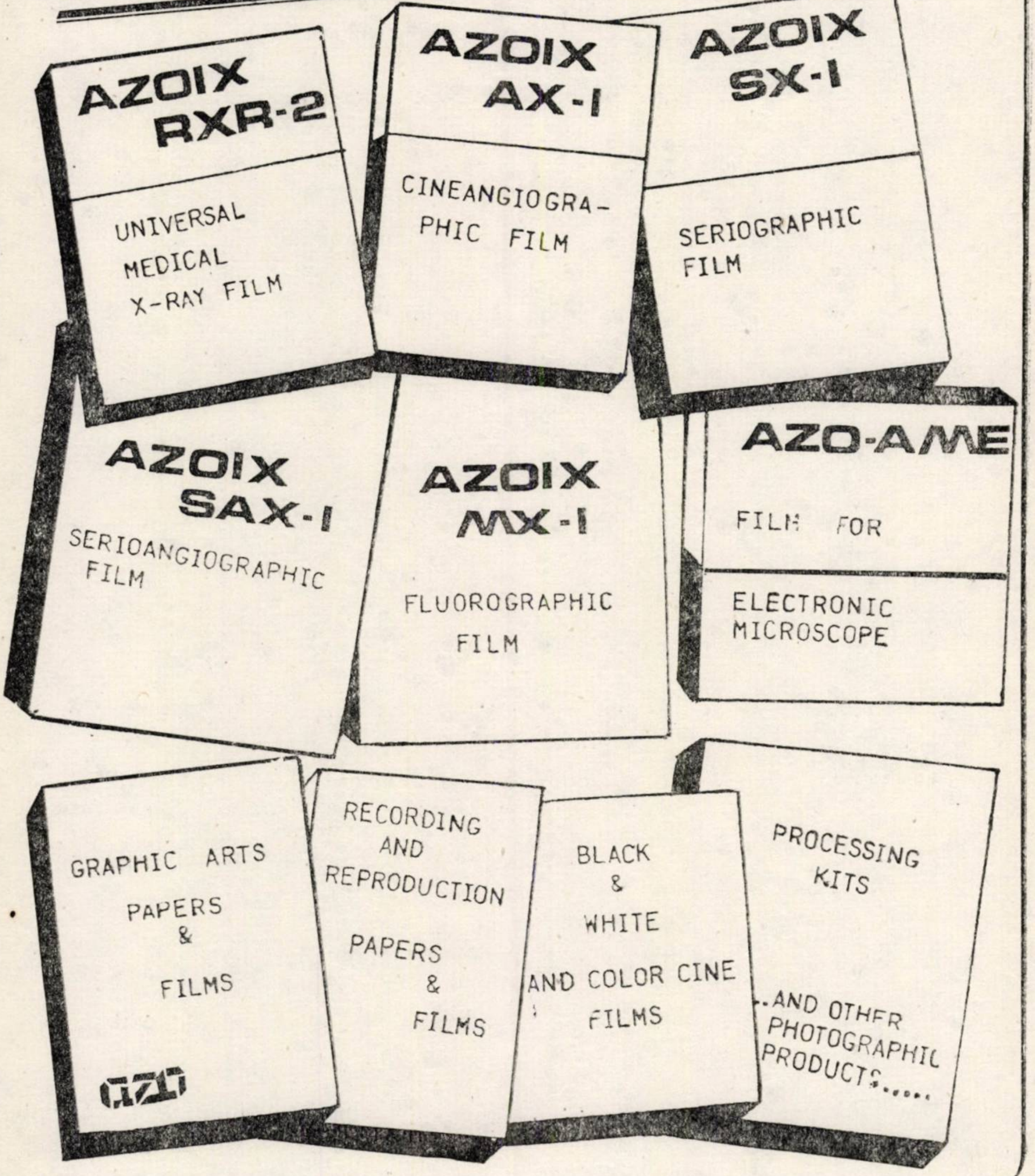
AZOIX
RXR-2
UNIVERSAL
MEDICAL
X-RAY FILM
AZOIX
AX-I
CINEANGIOGRA-
PHIC FILM
AZOIX
SX-I
SERIOGRAPHIC
FILM
AZOIX
SAX-I
SERIOANGIOGRAPHIC
FILM
AZOIX
MX-I
FLUOROGRAPHIC
FILM
AZO-AME
FILM FOR
ELECTRONIC
MICROSCOPE
GRAPHIC ARTS
PAPERS
&
FILMS
AZO
RECORDING
AND
REPRODUCTION
PAPERS
&
FILMS
BLACK
&
WHITE
AND COLOR CINE
FILMS
PROCESSING
KITS
...AND OTHER
PHOTOGRAPHIC
PRODUCTS.....

NOTE POUR LES AUTEURS

La Revue Roumaine de Chimie publie des articles en anglais, français, russe, allemand ou espagnol. Les auteurs sont priés d'envoyer des articles et des comptes rendus inédits.

Les manuscrits seront dactylographiés à double interligne. La bibliographie, les tableaux et la légende des figures seront placés après le texte.

Si l'article fait partie d'une série numérotée, la partie précédente sera donnée comme première référence.

Chaque article sera précédé d'un résumé comprenant quinze lignes au maximum.

Les références bibliographiques dans le texte seront faites par des exposants sans parenthèses et paraîtront à la fin de l'ouvrage.

Les publications périodiques mentionnées dans la bibliographie seront présentées suivant les prescriptions internationales : le nom de l'auteur précédé de l'initiale du prénom, le titre du périodique abrégé conformément à « Chemical Abstracts » et souligné par une ligne, le numéro du tome indiqué par des chiffres arabes et souligné par deux lignes, suivi de la première page de l'article ; à la fin, l'année de la parution sera placée entre parenthèses. Le numéro de la revue ne sera pas indiqué si les pages du volume sont numérotées consécutivement.

Les textes des livres ou traités incluront : le nom des auteurs, l'initiale du prénom, le titre du livre entre guillemets et sans être souligné, le numéro du tome précédé par l'abréviation « vol. » (ou « Bd. », le numéro de l'édition, les éditions (the publisher), la localité de la parution du livre, l'année de la parution et la page de la référence précédée(s) par l'abréviation « p. » (ou « S. »).

Les brevets seront indiqués comme suit : l'auteur ou la firme, le pays et le numéro du brevet, la date et la revue (*Chem. Abstr.*). Par. ex. : M. Jones (to Union Carbide Co), Brit. Pat. 601 238, 2 Sept. 1959 ; *cf. Chem. Abstr.*, 54, 12808 (1960).

Si la référence n'a pas été lue en original, on indiquera aussi la revue de référence consultée.

Les diagrammes seront tracés à l'encre de Chine sur papier calque. Les tableaux et les figures (en nombre strictement nécessaire) ainsi que les courbes dans les figures seront numérotés par des chiffres arabes. Leur explication sera donnée dans la légende des figures. Prière de ne pas inscrire les mêmes données dans les tableaux et les figures. Chaque tableau aura un titre. On indiquera dans le texte la place approximative des tableaux et des figures. Les formules chimiques seront incluses dans le texte ; en outre, elles seront transcrites sur papier calque, à l'encre de Chine.

Les auteurs sont priés d'indiquer les caractères italiques (en soulignant les lettres au crayon), ainsi que tout autre caractère spécial ; les préfixes *ortho*, *meta*, *para*, *cir*, *trans*, etc. seront soulignés pour indiquer leurs caractères italiques et ne seront jamais écrits avec des majuscules.

Aucune correction à la main ne sera admise sur le manuscrit. Les corrections seront tapées à la machine. Les lettres grecques ou d'autres symboles spéciaux seront insérés à la main à l'encre clairement.

Le manuscrit sera signé par l'auteur.

Le titre-courant aura 50 lettres au maximum.

L'entière responsabilité du contenu des articles appartient aux auteurs.

Sur demande on peut obtenir une note plus complète.

PRINTED IN ROMANIA

TRAVAUX PARUS AUX ÉDITIONS DE L'ACADÉMIE DE LA RÉPUBLIQUE SOCIALISTE DE ROUMANIE

V. DRĂGUŢAN, A. T. BALABAN, M. DIMONIE, **Olefin Metathesis and Ring-Opening Polymerization of Cyclo-Olefins**, Coédition avec John Wiley and Sons, 1985, 544 p.
C. LITEANU, I. RÎCĂ, **Optimizarea proceselor analitice**, 1985, 360 p.
N. PERESCU, **Chimia extracţiei cu solvenţi şi aplicaţii**, 1985, 212 p.
V. E. SAHINI, M. HILLEBRAND, **Chimie cuantică în exemple şi aplicaţii**, 1984, 378 p.
GH. MARCU, **Chimia compuşilor coordinativi**, 1984, 415 p.
E. CORDOŞ, C. MANOLIU, **Spectrometria de absorbţie şi fluorescenţă atomică**, 1984, 178 p.
C. BODEA, **Tratat de biochimie vegetală**, p. II, vol. 5, 1984, 438 p.
ELENA CEAUŞESCU, **Cercetări în chimia şi tehnologia polimerilor**, 1983, 519 p.
N. ASANDEI, A. GRIGORIU, **Chimia şi structura fibrelor**, 1983, 395 p.
N. IONESCU, M. CĂLDĂRARU, **Oxidarea catalitică a olefinelor inferioare**, 1983, 178 p.
C. CAŞCAVAL, **Studiul polimerilor prin piroliză şi cromatografie de gaze**, 1983, 220 p.
C. I. SIMIONESCU, F. DANEŞ, **Originea vieţii**, 1983, 110 p.
C. BODEA (sous la direction). **Tratat de biochimie vegetală**, 2^{e} partie, t. IV, 1982, 408 p.
I. G. MURGULESCU, RODICA VÎLCU, **Introducere la chimia fizică. Vol. III. Termodinamica chimică**, 1982, 624 p.
I. G. MURGULESCU, J. PĂUN, **Introducere în chimia fizică. Vol. I.3. Nucleul atomic, reacţii nucleare, particule elementare**, 1982, 606 p.
ELENA CEAUŞESCU, **Noi cercetări în domeniul compuşilor macromoleculari**, 1981, 536 p.
I. G. MURGULESCU, TATIANA ONCESCU, E. SEGAL, **Introducere în chimia fizică. Vol. II, 2, Cinematică chimică şi cataliză**, 1981, 1024 p.
LYDIA-MARIA VAICUM, **Epurarea apelor uzate cu nămol activ. Bazele biochimice**, 1981, 218 p.
I. GĂLĂŢEANU, **Procese şi metode radiochimice în energetica nucleară**, 1981, 234 p.
O. IORDACHE, **Procese polistocastice aplicate în fenomenele de transfer**, 1981, 186 p.
CR. SIMIONESCU, VALERIA GORDUZA, **Polimeri biocompatibili şi biologic activi**, 1980, 479 p.
ELENA CEAUŞESCU, **Polimerizarea stereospecifică a izoprenului**, 1979, 307 p.
C. GH. MACAROVICI, **Analiza chimică cantitativă anorganică**, 1979, 457 p.
M. FLORESCU, **Metode ştiinţifice în dezvoltarea industriei chimice moderne**, 1979, 256 p.
A. T. BALABAN, I. GĂLĂŢEANU, G. GEORGESCU, LIGIA SIMIONESCU, **Compuşi marcaţi şi radiofarmaceutici cu aplicaţii în medicina nucleară** 1979, 495 p.
I. G. MURGULESCU, E. SEGAL, **Introducere în chimia fizică, Vol. II. 1. Teoria molecular-cinetică a materiei**, 1979, 1036 p.
S. STERNBERG, FL. DANEŞ, **Termodinamica chimică aplicată**, 1978, 400 p.
I. G. MURGULESCU, V. EM. SAHINI, **Introducere în chimia fizică. Vol. I. 2. Structura şi proprietăţile moleculelor**, 1978, 604 p.
I. ZUGRĂVESCU, MAGDA PETROVANU, **N-ylid chemistry**, coédition avec McGraw Hill International Book Company U.S.A., 1977, 396 p.
I. G. MURGULESCU, **Introducere în chimia fizică. Vol. I. 1. Atomi, molecule, legătură chimică**, 1976, 560 p.
ELENA CEAUŞESCU, **Research work on synthesis and characterization of macromolecular compounds, Contributions**, 1974, 251 p.
CR. SIMIONESCU, VIORICA RUSAN, V. POPA, **Chimia algelor marine**, 1974, 212 p. 1 pl.

1986 JUN 2 4

ISSN 0035–3930

c. 2066 – I.P. INFORMAŢIA

43426

Lei 40
$ 80 (pour un abonnement annuel)

F 1103

~~04~~

ACADÉMIE DE LA RÉPUBLIQUE SOCIALISTE DE ROUMANIE

06

REVUE ROUMAINE DE CHIMIE

TOME 31
N° 6
Juin 1986

Rev. Roumaine Chim. RRCHAX, 31, *6*, p. 555–646 (1986), Bucarest
EDITURA ACADEMIEI REPUBLICII SOCIALISTE ROMÂNIA

ACADÉMIE DE LA RÉPUBLIQUE SOCIALISTE DE ROUMANIE

COMITÉ DE RÉDACTION

Rédacteur en chef :

I. G. MURGULESCU, membre de l'Académie de la République Socialiste de Roumanie

Rédacteurs en chef adjoints :

A. T. BALABAN et V. EM. SAHINI, membres correspondants de l'Académie de la République Socialiste de Roumanie

Collège de rédaction :

EM. BRATU, ELENA CEAUŞESCU, ECATERINA CIORĂNESCU-NENITZESCU, CR. SIMIONESCU, membres de l'Académie de la République Socialiste de Roumanie; P. SPACU, membre correspondant de l'Académie de la République Socialiste de Roumanie; M. BANCIU, M. D. GHEORGHIU, I. HAIDUC, D. I. MARCHIDAN, G. NIAC et D. SĂNDULESCU.

La Revue Roumaine de Chimie paraît 10 fois par an. Toute commande de l'étranger sera adressée à ROMPRESFILATELIA — sectorul Export-Import Presă, P. O. Box 12—201, télex 10376, prsfi r 78 104 Bucarest, Calea Griviţei nr. 64—66, Roumanie

Les manuscrits, les livres et les revues proposés en échange, ainsi que toute correspondance seront envoyés à la rédaction

REVUE ROUMAINE DE CHIMIE

125, Calea Victoriei, 79717 Bucarest, Roumanie, téléphone 50 76 80

EDITURA ACADEMIEI REPUBLICII SOCIALISTE ROMÂNIA
125, Calea Victoriei, 79717 Bucarest, Roumanie, téléphone 50 76 80

REVUE ROUMAINE DE CHIMIE

Tome 31, N° 6 Juin 1986

N. DOCA and E. SEGAL, Dehydrogenation kinetics of low aliphatic alcohols on copper catalysts. II. Preparation, stabilisation and catalytic activity of Cr—O—Cu and Mn—O—Cu systems . . . . 567—570

VIOREL BRÂNZOI, AHMED KABIR and MIHAI CIOPEC, Corrosion of steel C-95 in aqueous hydrochloric acid in the presence and absence of organic inhibitors . . . . 571—579

SAROJ SHARMA, S. K. HAWA, S. P. MATHUR and M. SATAKE, Spectrophotometric determination of palladium(II) with N-naphthyl-N′-pyridylthiourea . . . . 581—583

R. K. AGARWAL and S. K. GUPTA, Magnetic and spectral studies of lanthanide perchlorate complexes of 2-ethoxycarbonylamino-pyridine-N-oxide . 585—588

MĂRIUCA GARTNER and M. VASS, Ellipsometric spectroscopy of pure and CO covered gold films . . . . 589—596

J. HERNÁNDEZ MÉNDEZ, A. ALONSO MATEOS and E. J. MARTÍN MATEOS, Gravimetric determination of mercury and cadmium *via* formation of ion pairs $[(C_4H_9)_4N]_2[HgI_4]$ and $[(C_4H_9)_4N]_2[CdI_4]$ (in Spanish) 597—604

ELIZA-MANUELA VASILESCU and DUMITRU SĂNDULESCU, Molecular compounds with some alkyl aryl ethers. I . . . . 605—614

A. N. OSMAN, M. M. ISMAIL and M. A. BARAKAT, Synthesis and biological activity of certain nicotinic acid derivatives . . . . 615—624

C. I. CHIRIAC, Synthesis of aromatic thioureas . . . . 625—627

O. M. O. HABIB, A. M. KHALIL, E. M. KANDEEL and E. B. ABDALLA, Syntheses and reactions of some new 4-(*p*-substituted cinnamoyl)phenyl-3′4′-xylene sulphonates of expected potential biological activity . . . . . . 629—635

OLGA PÉREZ DE MÁRQUEZ, Mechanistic and synthetic aspects of the anodic oxidation of the 1,4-dimethoxybenzene (in Spanish). . . . . 637—645

Rev. Roumaine Chim. **31**, *6*, p. 565—646 (1986), Bucarest

Revue Roumaine de Chimie, **31**, *6*, 567–570(1986)

DEHYDROGENATION KINETICS OF LOW ALIPHATIC ALCOHOLS ON COPPER CATALYSTS. II[1]

PREPARATION, STABILISATION AND CATALYTIC ACTIVITY OF Cr—O—Cu AND Mn—O—Cu SYSTEMS

N. DOCA* and E. SEGAL**

* Chemical Research Center, Bd. Mihai Viteazul 24, Timişoara, Romania

** Chair of Physical Chemistry and Electrochemical Technology, Faculty of Chemical Engineering, Polytechnical Institute of Bucharest, Bulevardul Republicii 13, Bucharest, Romania

Received June 10, 1985

Metalic copper catalysts with 0.5, 0.0 and 1.5 at. % of Cr and Mn oxides respectively, were prepared by hydrogen reduction of impregnated CuO, and were stabilised against reoxidation by adsorption of inert gases (N_2 and CO_2). The presence of MeO/Cu junction increases the catalyst stability in the dehydrogenation reaction. Generally, the apparent activation energy determined by the chromatographic pulse technique, decreases in the presence of MeO/Cu catalysts, and on the same catalyst increases as follows : EtOH i-PrOH n-PrOH 2-BuOH n-BuOH.

In a previous paper, [1] the results concerning the kinetics of dehydrogenation reactions of low aliphatic alcohols on freshly prepared pure copper catalyst were presented.

In order to find the rate equation and to determine the kinetic parameters, the chromatographic pulse technique was used.

This paper deals with the results obtained by using Cr—O—Cu and Mn—O—Cu catalysts for the same reactions.

CATALYST PREPARATION AND CHARACTERISATION

The desired compositions were of 0.5, 1.0 and 1.5 at. % Cr and Mn respectively. To a certain amount of CuO powder (prepared according to ref.[1]), the necessary volume of $Cr(NO_3)_3$ or $Mn(NO_3)_2$ 0.1 N solution was added. After 2 hours impregnation followed by 5 hours drying at 95–100° and 5 hours calcination at 250°, the catalysts were ready for reduction and stabilisation.

Information about the CuO—MO system in the presence of hydrogen is available from the calculated variation of free enthalpy *vs*. temperature for the reaction :

$$M_xO_y + yH_2 \rightleftarrows xM + yH_2O \qquad (1)$$

Using the wellknown equation of thermodynamic functions as well as the tables of thermodynamic data,[2] the values given in Table 1 were obtained. According to these values, CuO is completely reduced to metal, while Cr_2O_3 and MnO remain unreduced. Thus, these reduced catalysts are considered as metal oxides deposited on metalic copper. [3]

The equipment and procedure for reduction and stabilisation were the same as in the previous paper[1] and the experimental conditions were: hydrogen flow 0.5 cm^3/s for 10 g catalysts; heating rate up to $400° \simeq \simeq 3°/min$; reduction time=7h at 400°. The temperature *vs.* time diagram of stabilisation was the same as that for copper catalyst[1] and the main characteristics of the catalysts are listed in table 2.

Table 1

Calculated variation of free enthalpy for metal oxide reduction with hydrogen

Oxide	ΔG_T^0, kJ/mol				
	$T=473$	573	673	773	873K
CuO	—79.0	—77.3	—75.3	—72.9	—70.4
$Cr_2O_3^*$	153.5	151.0	140.0	128.5	117.0
MnO	125.5	122.3	118.5	115.0	112.0

$^*\Delta G_T^0$ is calculated for one gram-atom of Cr

Table 2

Main characteristics of the stabilised catalysts

Catalyst	Added element	Amount of add. metal at. %*	Extrapol. red. beg. temp.°	Stability,° for**	
				CO_2	N_2
C_1	Cr	0.49	207	135	250
C_2	Cr	0.97	209	135	240
C_3	Cr	1.47	215	130	275
C_4	Mn	0.48	206	140	210
C_5	Mn	1.02	208	130	145
C_6	Mn	1.46	210	125	195

* determined in nitric solution with a Pye Unicam SP 1900 spectrophotometer, in air— C_2H_2 flame and wave lengths of 324.8, 357.9 and 279.48 nm for Cu, Cr and Mn respectively.

** comparatively with pure copper limits of 200° and 270° for CO_2 and N_2 respectively.[1]

The presence of Cr and Mn oxide increases the reduction starting temperature (which was 174° for pure copper), but it was not possible to establish a significant and clear variation of these temperatures *vs.* compositions. The stability limits of the catalysts were strongly decreased by the added metal oxide, but remained higher by stabilisation with nitrogen.

KINETICS OF ALCOHOLS DEHYDROGENATION

The kinetics of ethyl, *n*-propyl, *i*-propyl, *n*-butyl and 2-butyl alcohols dehydrogenation on C_1-C_6 catalysts was determined by the chromatographic pulse technique. Firstly, the stability of the catalyst activity during the dehydrogenation reaction was determined as in our previous paper.[1] The catalysts containing Cr or Mn had a lower initial activity as compared with pure copper, but the stability during the dehydrogenation was better (see for example figure 1).

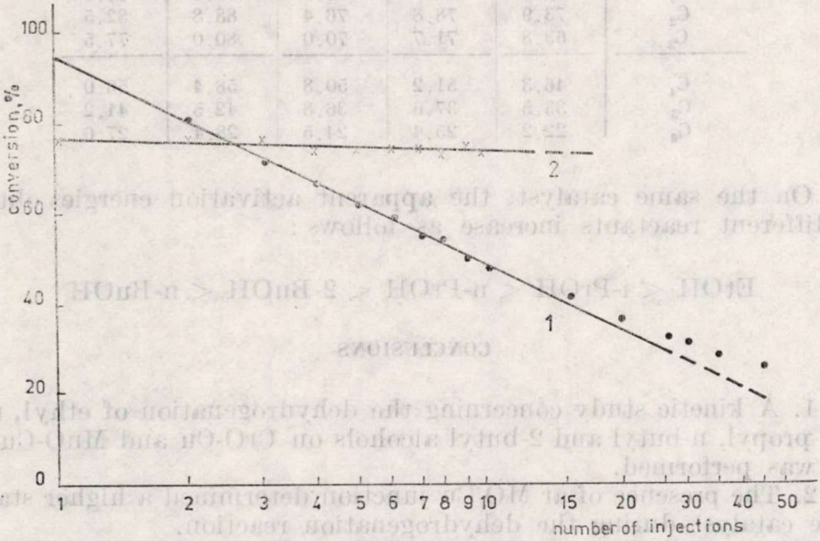

Fig. 1. — Conversions *vs.* number of injections for pure copper catalyst (1) and C_1 catalyst respectively (2); reactant i-Pr OH, eluent flow 60 μL/min, reaction temperature 200°.

The copper catalyst deactivation was explained by the formation of a thin layer of copper oxide gradually covering the active surface. The *a priori* formation of an MO/Cu junction increases the electron work function through the free metal surface,[3] determining a high stability of the uncovered copper surface.

The values of the apparent activation energy (see ref.[1]) presented in Table 3 were determined in the following conditions : catalyst weight — 0.150 g ; catalyst bed volume $V_c = 0.065$ cm^3 ; volume of injected alcohol — 2 μL ; catalyst bed temperature — 200, 240 and 280° ; eluent flow rates — 60, 90 and 120 cm^3 N_2/min.

Generally, for the same alcohol, the apparent activation energy decreases in the presence of the added metal oxides, as compared with the pure copper catalyst (see ref.[1]). The addition of MnO is more efficient than of Cr_2O_3. The increase of added metal concentration determined a corresponding decrease of the apparent activation energy, excepting EtOH on C_1-C_3 catalysts.

Table 3

Apparent activation energy (E_{ap}), kJ/mol

Catalyst	Reactant				
	EtOH	n-PrOH	i-PrOH	n-BuOH	2-BuOH
C_1	65.7	81.2	76.8	95.1	86.5
C_2	73.9	78.8	76.4	88.8	82.5
C_3	63.8	71.7	70.0	80.0	77.5
C_4	46.3	51.2	50.8	58.4	56.0
C_5	33.5	37.6	36.8	42.5	41.2
C_6	22.2	25.4	24.5	28.4	27.6

On the same catalyst, the apparent activation energies obtained for different reactants increase as follows:

$$\text{EtOH} < \text{i-PrOH} < \text{n-PrOH} < \text{2-BuOH} < \text{n-BuOH}$$

CONCLUSIONS

1. A kinetic study concerning the dehydrogenation of ethyl, n-propyl, i-propyl, n-butyl and 2-butyl alcohols on CrO-Cu and MnO-Cu catalysts was performed.

2. The presence of ar MO/Cu junction determined a higher stability of the catalyst during the dehydrogenation reaction.

3. The added metal oxide generally decreases the apparent activation energy. The particular values of E_{ap} depend on both added metal concentration and reactant nature.

REFERENCES

[1] N. Doca and E. Segal, *Rev. Roumaine Chim.*, **30**, 949(1985).

[2] M. H. Karapetyants, "Khimiceskaia Termodinamika", Goskhimizdat, Moskva, 1953.

[3] F. F. Volkenstein, "Fiziko-Khimia poverkhnosti poluprovodnikov", Izd. Nauka, Moskva, 1973.

Revue Roumaine de Chimie, 31, 6, 571–579(1986)

CORROSION OF STEEL C-95 IN AQUEOUS HYDROCHLORIC ACID IN THE PRESENCE AND ABSENCE OF ORGANIC INHIBITORS

VIOREL BRÂNZOI*, AHMED KABIR** and MIHAI CIOPEC**

* Department of Physical Chemistry and Electrochemical Technology, Polytechnical Institute, Bucharest, Romania

** Department of Chemistry, Institute of Petroleum and Gas, Blvd. București, No. 39, 2000 Ploiești, Romania

Received April 29, 1985

Corrosion of steel C-95 was studied in aqueous solutions of HCl of different concentrations in the presence and absence of organic inhibitors. Kinetic parameters determined from the polarisation curves suggest a dissolution mechanism of the type McCafferty-Hackerman. Use of some of the organic inhibitors led to a considerable reduction of corrosion process. At 25°C hexamethylene tetramine got the maximum efficiency, on the other hand at 70°C inhibitor 4 got the highest efficiency. Increase of temperature from 25°C to 70°C led to the intensification of the corrosion process as well as reduction of the efficiency of the inhibitors used.

INTRODUCTION

Today when consumption of energy and raw materials is continually increasing, dealing with the intensification of hydrocarbon extraction has become a major interest. To this end, 15% and 28% hydrochloric acid solutions are deliberately used in drilling with a view to make a better hydrodynamic communication between the protective layer of earth and the drilling pipe.[1-4] In this way, considerable increase in flow or crude oil and gas is obtained in the well in production and betterment of the receptivity of injected water in the deposit. Use of concentrated hydrochloric acid leads to the intensification of corrosion processes in the installations of extractive industries. For the protection of these installations, a large number of procedures against corrosion based on utilisation of inhibitors, anticorrosion coatings, cathodic protection etc. are developed and being used simultaneously.

In recent years new methods have been developed, namely covering of the interior of the pipe and utilisation of nonmetals, yet for the protection of installations for crude oil extraction against corrosion, the most convenient method was based on the utilisation of inhibitors. The advantage of this procedure is that the inhibitors can be easily introduced in the installations and can reach any part of the metallic surfaces where agressive fluids circulate.

Organic inhibitors, called inhibitors of adsorption, control corrosion acting either on the anodic or cathodic reaction or influencing both of them. Since they usually affect the entire metallic surfaces when sufficient amounts are present, it is not possible to ascertain whether they act anodically or cathodically. Inhibition in this case is the result of adsorption of organic compound on the metallic surface with the formation of an invisible thin layer of film of some molecules. [5] This type of inhibitors are especially used in acid medium.

In the present work, corrosion of steel C-95 was studied in the solution of hydrochloric acid in the presence and absence of organic inhibitors.

EXPERIMENTAL PART

Using the potentiostatic method, inhibition action was studied through tracing the polarisation curves. Calculation of kinetic parameters of corrosion in the case of solutions, with inhibitors, especially the corrosion current densities, and their comparison with the kinetic parameters of the solution without inhibitors were the basis of the study of efficiency of these inhibitors.

Electrochemical installation and the cell for the electrochemical polarisation were presented in a previous work.[6] It is worth mentioning that before each experimental determination, the working electrode with a surface area of 1 cm^2 was mechanically polished, degreased in boiling benzene and washed with acetone. At last the working electrode was subjected to electropolishing in a solution prepared from perchloric acid and glacial acetic acid in a proportion of 4 : 1, to a potential of 25 – 30 V and a current density of 8.5 A/dm^2 for a period of two minutes. After electropolishing, the electrodes were washed with distilled water and the solution for experiment and only after that it was fixed in the cell for electrochemical polarisation. Tracing of the polarisation curves was always started from the static potential, which, similarly to all other potentials were measured in comparison with the saturated calomel electrode. The electrode was always polarised first cathodically and then anodically.

With the help of the thermostat UM-210, the temperature of the solution in the cell was kept constant. Several determinations were made for each solution, until a good reproducible result was obtained.

RESULTS AND DISCUSSION

Polarisation curves of steel C-95 in varied concentrations of hydrochloric acid solution in water are presented in figure 1. Increase in concentration of the acid leads to the displacement of the curves towards a more negative potential and also increases the corrosion current density and the corrosion rate respectively. Analysis of the polarisation curves shows that does not exist any active-passive transition even at high current densities. This phenomenon may be explained by the presence of chloride ions which hinder the formation of passive film and accelerate the anodic dissolution with a greater rate, as the concentration of chloride ions is increased. It is supposed that chlorine ions participate to the reactions from the interface metal/electrolyte through competitive adsorption, for the formation of chemisorbed films which satisfy the affinity of the metallic surfaces for the atom of oxygen or water molecule[7,8]. E. McCafferty and N. Hackerman showed that in the concentrated hydrochloric acid solutions exist a synergetic effect between the chloride ions chemisorbed on the metallic surface and hydrogen ions from the solutions, which are attracted electrostatically by the chloride anions that cover the metallic surface and catalyze the dissolution reaction. In this way the increase of corrosion rate with the increase of acid concentration is explained (see figure 1 and table 1).

Polarisation parameters presented in table 1 are in concordance with the experimental results the two authors[9] found out for the dissolution of iron Mallinkrodt in concentrated HCl solutions. It can be said that steel C-95, whose composition is given in table 2, dissolves in hydrochloric the acid solution studied by us (6 % HCl; 8 % HCl; 10 % HCl; 12.5 % HCl; and 15 % HCl) after a mechanism proposed by McCafferty-Hackerman, valid for the concentrated hydrochloric acid solutions.

In continuation, influence of organic inhibitors upon corrosion of steel C-95 in the solution of 15 % hydrochloric acid was studied at 25°C. Inhibition action of these substances was studied through tracing of the polarisation curves, using potentiostatic method and calculation of kinetic parameters of corrosion (especially the corrosion current densities)

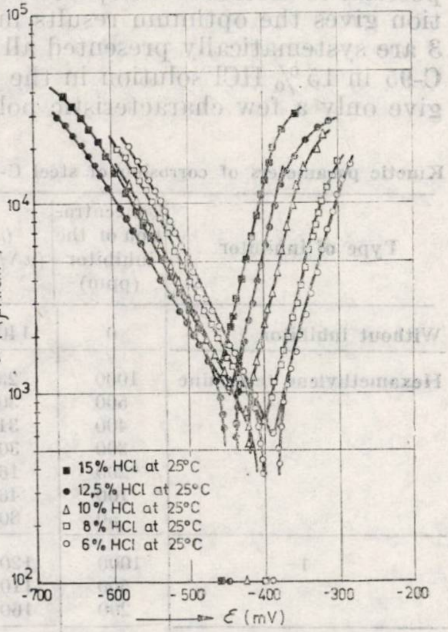

Fig. 1. — Polarisation curves of steel C-95 in varied concentrations of hydrochloric acid solution in water, at 25°C.

Table 1

Corrosion parameters of steel C-95 in HCl solution in varied concentrations at 25°C

Concentration of hydrochloric acid (%)	i_{cor} (μA/cm^2)	b_a (mV)	$-b_c$ (mV)	$-\varepsilon_{cor}$ (mV)
6	590	70	117	390
8	680	60	125	405
10	760	57	127.5	425
12.5	973	60	125	450
15	1400	65	130	460

Table 2

Composition of steel C-95

Type of steel	Components, in %									
C-95	C	Mn	Si	P	S	Cr	Ni	Mo	V	Ti
	0.28	1.07	0.25	0.024	0.005	0.54	—	—	—	0.02

and comparing them with the kinetic parameters without inhibitors. Likewise, efficiency of different inhibitors was calculated so that it is possible to ascertain with precision which inhibitor and at what concentration gives the optimum results in the respective medium. Thus in table 3 are systematically presented all kinetic parameters of corrosion of steel C-95 in 15 % HCl solution in the presence of inhibitors. Figures 2 and 3 give only a few characteristic polarisation curves.

Table 3

Kinetic parameters of corrosion of steel C-95 in the 15 % HCl solution + inhibitors at 25°C

Type of inhibitor	Concentration of the inhibitor (ppm)	i_{cor} (μA/cm²)	P_{mm} (mm/year)	R_{mpy} (millinch/year)	K_g $\left(\frac{g}{m^2 \cdot h}\right)$	Efficiency (%)
Without inhibitor	0	1400	16.42	653	14.58	—
Hexamethylene tetramine	1000	230	2.69	107	2.39	83.6
	500	300	3.50	140	3.21	78.6
	400	310	3.63	144	3.23	77.8
	300	300	3.50	140	3.12	78.6
	*200	160	1.87	74	1.66	88.6
	100	460	5.39	214	4.79	67.1
	50	800	9.38	373	8.33	42.8
1	1000	1200	14.07	560	12.50	14.3
	500	1100	12.90	513	11.45	21.4
	200	1600	18.76	746	16.66	—
2	1000	400	4.69	186	4.16	71.4
	500	500	5.61	205	4.58	68.6
	400	500	5.86	233	5.20	64.3
	300	670	7.85	312	6.97	52.1
	200	1000	11.73	466	10.41	28.6
	100	1400	16.42	653	14.58	—
3	500	600	7.03	280	6.24	57.1
	300	600	7.03	280	6.24	57.1
	200	850	9.97	396	8.85	39.3
	100	1200	14.07	560	12.50	14.3
4	1000	420	4.92	195	4.37	70.0
	500	340	3.98	158	3.53	75.7
	400	380	4.45	177	3.95	72.8
	*300	340	3.98	158	3.53	75.7
	200	700	8.21	326	7.29	50.0
	100	1000	11.73	466	10.41	28.6
Aniline	1000	1400	16.42	653	14.58	—
	500	1400	16.42	653	14.58	—
	400	1400	16.42	653	14.58	—
	300	1400	16.42	653	14.58	—
	200	1400	16.42	653	14.58	—
	100	1400	16.42	653	14.58	—
***o*-Phenylene diamine**	1000	3000	35.19	1399	31.25	—
Orthanilic acid	1000	3000	35.19	1399	31.25	—
	500	3000	35.19	1399	31.25	—

* The most efficient doses of the inhibitors

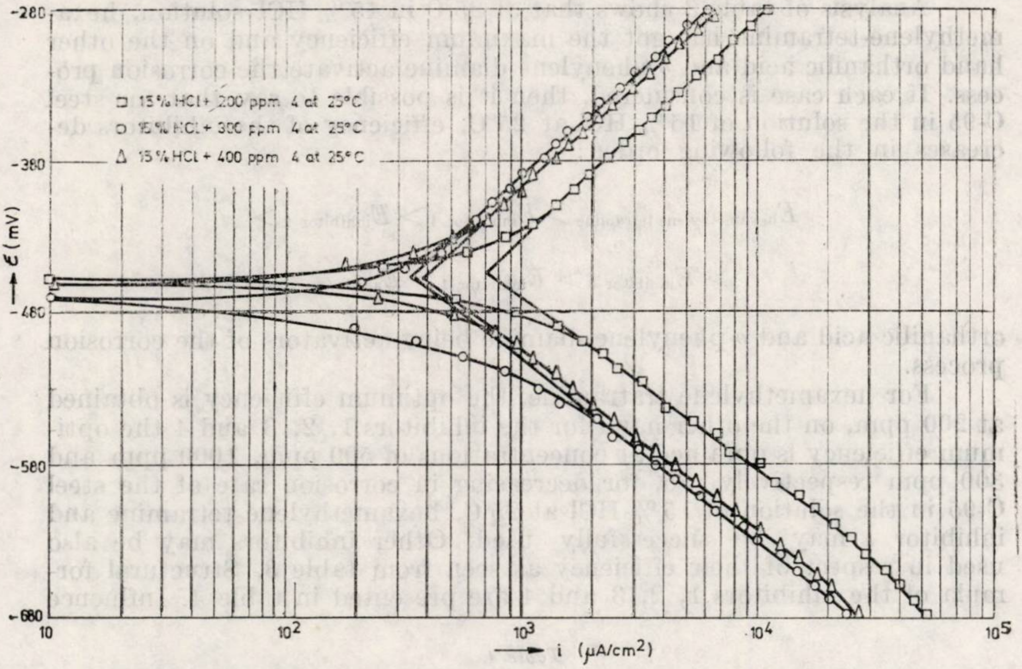

Fig. 2. — Polarisation curves of steel C-95 in 15% HCl solution in the presence of different quantities of inhibitor 4, at 25°C.

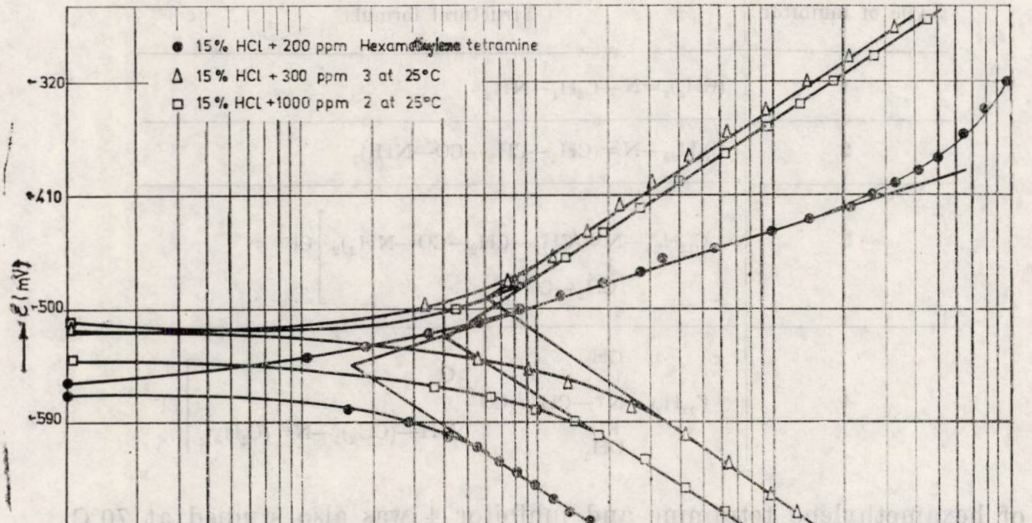

Fig. 3. — Characteristic polarisation curves of steel C-95 in 15% HCl solution in the presence of different inhibitors.

Analysis of table 3 shows that at 25°C in 15 % HCl solution, hexamethylene-tetramine has got the maximum efficiency and on the other hand orthanilic acid and *o*-phenylene diamine activate the corrosion process. If each case is considered, then it is possible to say that for steel C-95 in the solution of 15 % HCl at 25°C, efficiency of the inhibitors decreases in the following order:

$$E_{\text{hexamethylene tetramine}} > E_{\text{inhibitor 4}} > E_{\text{inhibitor 2}} >$$

$$> E_{\text{inhibitor 3}} > E_{\text{inhibitor 1}} > E_{\text{aniline}},$$

orthanilic acid and *o*-phenylene diamine being activators of the corrosion process.

For hexamethylene tratramine, the optimum efficiency is obtained at 200 ppm, on the other hand for the inhibitors 1, 2, 3 and 4 the optimum efficiency is obtained at concentrations of 500 ppm, 1000 ppm and 300 ppm respectively. So, for decreasing in corrosion rate of the steel C-95 in the solution of 15 % HCl at 25°C, hexamethylene tetramine and inhibitor 4 may be successfully used. Other inhibitors may be also used in respect of their efficiency as seen from table 3. Structural formula of the inhibitors 1, 2, 3 and 4 are presented in table 4. Influence of hexamethylene tetramine and inhibitor 4 was also studied at 70°C, taking into consideration that these inhibitors gave greater efficiency at 25°C.

Table 4

Structural formula of the inhibitors 1, 2, 3 and 4

Type of inhibitor	Structural formula
1	$(CH_3)_2=N-C_6H_4-NH_2$
2	$C_{12}H_{25}-N=(CH_2-CH_2-CO-NH_2)_2$
3	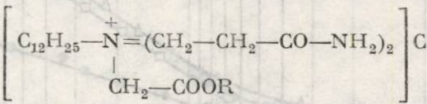 $\left[C_{12}H_{25}-\underset{\substack{\vert\\ CH_2-COOR}}{\overset{+}{N}}=(CH_2-CH_2-CO-NH_2)_2\right]Cl^-$
4	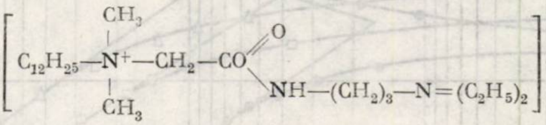 $\left[C_{12}H_{25}-\underset{\substack{\vert\\ CH_3}}{\overset{\substack{CH_3\\ \vert}}{N^+}}-CH_2-CO\begin{matrix}\nearrow O\\ \searrow NH-(CH_2)_3-N=(C_2H_5)_2\end{matrix}\right]Cl^-$

In figures 4 and 5 are presented polarisation curves at 70°C and in table 3 are given systematically all kinetic parameters of corrosion of steel C-95 in the solution of 15 % HCl at 70°C.

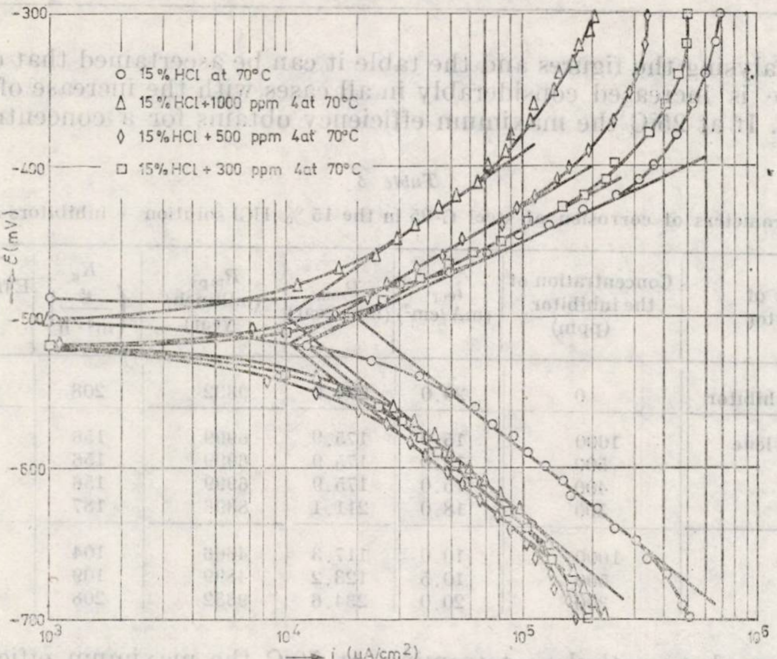

Fig. 4. — Polarisation curves at 25°C of steel C-95 in 15% HCl solution, at 70°C, without inhibitor and with inhibitor 4 in different quantities.

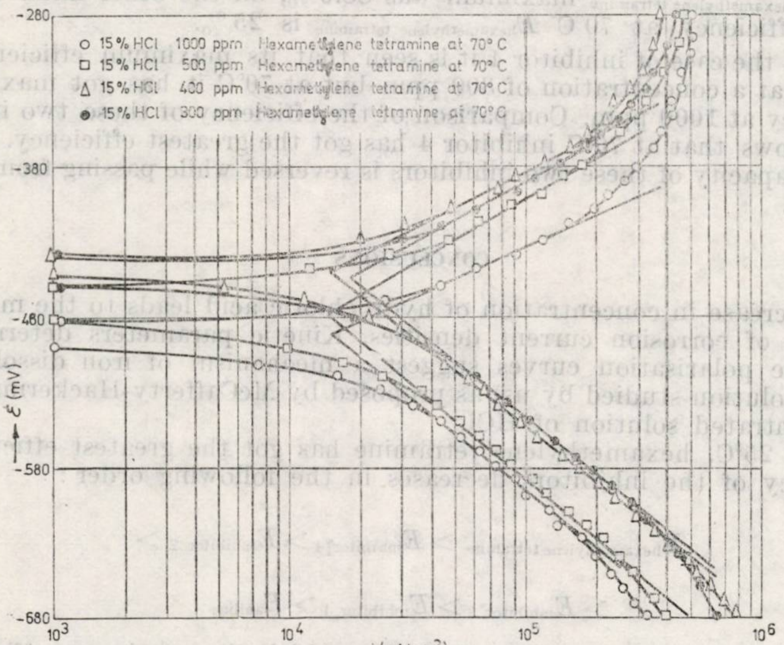

Fig. 5. — Characteristic polarisation curves of steel C-95 in 15% HCl solution in the presence of hexamethylene tetramine as inhibitor, at 70°C.

Analysing the figures and the table it can be ascertained that corrosion rate is increased considerably in all cases with the increase of temperature. If at 25°C the maximum efficiency obtains for a concentration of 200 ppm hexamethylene tetramine, at 70°C the maximum efficiency obtains for a concentration of 400 ppm hexamethylene tetramine (for example :

Table 5

Kinetic parameters of corrosion of steel C-95 in the 15 % HCl solution + inhibitors at 70°C

Type of inhibitor	Concentration of the inhibitor (ppm)	i_{cor} (mA/cm^2)	P_{mm} (mm/year)	R_{mpy} (millinch/year)	K_g $\left(\frac{g}{m^2 \cdot h}\right)$	Efficiency (%)
Without inhibitor	0	20.0	234.6	9332	208	—
Hexamethylene tetramine	1000	15.0	175.9	6999	156	25
	500	15.0	175.9	6999	156	25
	400	15.0	175.9	6999	156	25
	300	18.0	211.1	8398	187	10
4	1000	10.0	117.3	4666	104	50
	500	10.5	123.2	4899	109	48
	300	20.0	234.6	9332	208	—

$E_{\text{hexamethylene tetramine}}$ maximum was 88.6 %, on the other hand maximum efficiency at 70°C $E_{\text{hexamethylene tetramine}}$ is 25 %.

In the case of inhibitor 4 it is seen that its maximum efficiency is at 25°C at a concentration of 300 ppm but at 70°C it has got maximum efficiency at 1000 ppm. Comparison of the efficiency of these two inhibitors shows that at 70°C inhibitor 4 has got the greatest efficiency. Inhibition capacity of these two inhibitors is reversed while passing from 25°C to 70°C.

CONCLUSIONS

Increase in concentration of hydrochloric acid leads to the marked increase of corrosion current densities. Kinetic parameters determined from the polarisation curves suggest a mechanism of iron dissolution (in the solution studied by us) as proposed by McCafferty-Hackerman[9] in a concentrated solution of HCl.

At 25°C, hexamethylene tetramine has got the greatest efficiency. Efficiency of the inhibitors decreases in the following order :

$$E_{\text{hexamethylene tetramine}} > E_{\text{inhibitor 4}} > E_{\text{inhibitor 2}} >$$

$$> E_{\text{inhibitor 3}} > E_{\text{inhibitor 1}} > E_{\text{aniline}}$$

Concentrations of the inhibitors at which the maximum efficiency is obtained at 25°C and also the order of the inhibition capacity are modified at 70°C. In all cases corrosion rates are higher at 70°C than at 25°C.

REFERENCES

[1] Al. Constantinescu, S. Socol, D. C. Crăciun and P. Constantinescu, "Protecţia anticorosivă în industria extractivă de petrol şi gaze", Ed. Tehnică, Bucharest, 1978.
[2] H. H. Uhlig, "Corrosion et protection", Ed. Dunod, Paris, 1970.
[3] A. A. Gonik, *Korroziia i zashcita v neftegkazovoi promyshlennosti*, **4**, 3(1972).
[4] C. C. Wright, "Materials protection and performance", NACE, Houston, 1972.
[5] * * * "NACE Basic Corrosion Course", Second edition, NACE, Houston, 1971.
[6] V. Brânzoi and S. Sternberg, *Rev. Chim. (Bucureşti)*, **34**, 148 (1983).
[7] N. D. Stolica and H. H. Uhlig, *J. Electrochem. Soc.*, **112**, 124 (1965).
[8] E. J. Kelly, *J. Electrochem. Soc.*, **115**, 1215 (1968).
[10] E. McCafferty and N. Hackerman, *J. Electrochem. Soc.*, **119**, 146 (1972).

Revue Roumaine de Chimie, **31**, *6*, 581–583 (1986)

SPECTROPHOTOMETRIC DETERMINATION OF PALLADIUM(II) WITH N-NAPHTHYL-N′-PYRIDYLTHIOUREA

SAROJ SHARMA, S. K. HAWA, S. P. MATHUR and M. SATAKE*
Research Laboratories, Govt. College, Beawar, 305901, India
* Faculty of Engineering, Fukui University, Fukui, Japan

Received June 10, 1985

Palladium(II) forms an intense yellow complex with N-naphthyl-N′-pyridylthiourea with a maximum absorbance at 390 nm. The molar absorptivity of the palladium complex is 3.4×10^4 L.mol^{-1}.cm^{-1} at 390 nm and Beer's law is obeyed over the concentration range 1.2–12 ppm. The sensitivity of the reaction is 0.0096 μg Pd(II) cm^{-1} for 0.001 absorbance. The slope ratio method and Job's method suggest that a 1 : 2 (metal :ligand) complex is formed in the system. Tolerance of diverse ions has also been discussed.

INTRODUCTION

The analytical applications of substituted thioureas and their analogues have extensively been studied and reported from our laboratories.[1-5] Thiourea and its substituted derivatives are found to react with many cations and anions to give colour reactions of analytical importance. Survey of the literature reveals that pyridyl substituted thioureas have not been investigated in detail. Of the several methods available for palladium dibenzyl-dithiooxamide,[6] 3-quinoxalinedithiol,[7] 2-(mercapto-acetamido)-pyridine,[8] 2-mercaptoacetamide[9] are more favoured. The present communication describes a sensitive and selective photometric method for the determination of palladium(II) with N-naphthyl-N′-pyridylthiourea.

EXPERIMENTAL

Preparation of reagent* : N-naphthyl-N′-pyridylthiourea has been prepared by the method of Mathur[10] by reacting equimolecular quantities of naphthylisothiocyanate and 2-aminopyridine in ethanol. The purity of the compound was checked by TLC, elemental analysis and IR spectroscopy.

***Reagent solution* : 0.25 % (W/V) solution of the reagent in 70 % ethanol was prepared fresh each time.**

***Standard palladium chloride solution* : Approximately 1 g of reagent grade palladium chloride was dissolved in a little water containing 5mL of hydrochloric acid and volume was made to one Litre. The palladium content was determined by using dimethylglyoxime. It was diluted to give a solution containing 40 ppm of palladium.**

Solution of diverse ions : The reagent grade soluble salts, usually chlorides, nitrates or sulphates were employed for the preparation of solutions of inorganic ions. The solutions were diluted in such a way that they contained 1 mg of the metallic element per mL.

Instruments : All absorbance measurments were made with a Beckmann quartz spectrophotometer, model DU. pH measurments were made with an expanded scale pH meter (ECModel).

RESULTS AND DISCUSSION

Spectral characteristics of palladium(II) complex : 5 mL of standard palladium solution containing 40 ppm of palladium were pipetted into a 25 mL flask and 5mL of 0.25 % reagent and hydrochloric acid were added so that pH after final dilution was about 2.5. Volume was made up to the mark and absorbance was measured after 5 minutes at different wavelengths using reagent solution as blank. The absorbance peak is at 390 nm, it then steadily falls and shows a flat region between 420—480 nm.

Reagent ratio for full absorbance : A series of solutions were prepared as described and varying amounts of equimolecular solutions of the reagent were added such that mole ratio of palladium to reagent was 1 : 1 to 1 : 3. Absorbance was measured after 5 minutes at 390 nm. The absorbance is found to be constant at 1 : 20 ratio of palladium to reagent.

The system obeys Beer's law over the concentration range of 1.3—12 ppm and molar absorptivity of the palladium complex is 3.4×10^4 $\mathrm{L.mol^{-1}.cm^{-1}}$. Sandellds sensitivity is 0.0096 μg Pd(II) $\mathrm{cm^{-1}}$ absorbance. The slope ratio method[11] and Job's method[12] suggest that 1 : 2 (metal : ligand) complex is formed in the system.

Recommended procedure : Palladium solution containing 40 ppm of the metal was taken into 25 mL volumetric flask and a suitable quantity of hydrochloric acid was added to bring the pH of the solution between 2.0 and 2.5. 5 mL of 0.25 % reagent solution were taken and added and volume made up to the mark. Absorbance was measured at 390 nm using reagent as blank.

Tolerance of diverse ions : Tolerance of diverse ions was studied by developing the colour as outlined under recommended procedure. pH between 2.0 and 2.5 was used to increase the selectivity of the reagent.

Table 1 summarises the tolerance of diverse ions. Silver(I), lead(II) and gold(III) interfere the estimation. The reaction may be partially masked by tartrate and completely by fluoride. Tungstate and phosphate interfere, below pH 3.5 Zn(II), Mn(II), Fe(II), Al(III), Fe(III), Cr(III), Hg(II), Cd(II), Sb(III), As(III), Sn(II), Ti(IV), Zirconyl(II), Uranyl(II), alkali and alkaline earth metals and common anion do not give any colour reaction with the reagent and thus they are not likely to interfere in the direct photometric determination of palladium.

Precision : The precision of the method was determined for a set of ten samples of solutions containing 3 ppm of palladium and 1 ppm each of rhodium, ruthenium, iridium and platinum. The standard deviation was 0.035 ppm palladium.

ACKNOWLEDGEMENT. Thanks are expressed to the University grants commission of India for awarding financial assistance for the project.

Table 1

Tolerance of diverse ions (3 ppm Pd)

Ions	Added as	Conc.ppm.
Mn(II)	Sulphate	1000
Zn(II)	Sulphate	1000
Co(II)	Sulphate	80
Ni(II)	Sulphate	140
Cu(II)	Sulphate	26
Fe(II)	Sulphate	90
Fe(III)	Sulphate	48
Al(III)	Sulphate	40
Pt(IV)	Chloride	20
Rh(III)	Chloride	20
Ir(IV)	Na_2IrCl_6	35
Ru(III)	Chloride	25

REFERENCES

[1] S. P. Mathur and M. R. Bhandari, *Chem. Ind.*, **17**, 745 (1976).

[2] S. P. Mathur, R. S. Thakur, C. S. Bhandari and N. C. Sogani, *Talanta*, **25**, 592 (1978).

[3] S. P. Mathur, *An. quim.*, **74**, 1020 (1978).

[4] S. P. Mathur, R. S. Thakur, C. S. Bhandari and N. C. Sogani, *J. Macromol. Sci. Chem.*, **A 12**, 1965 (1978).

[5] S. P. Mathur, R. S. Thakur, C. S. Bhandari and N. C. Sogani, *Afinidad*, **36**, 499 (1979).

[6] W. D. Jacobs, *Anal. Chem.*, **33**, 1279 (1961).

[7] G. H. Ayres and R. W. Mc Crory, *Anal. Chem.*, **36**, 133 (1964).

[8] S. P. Mathur, *Chemia Analityczna*, **22**, 819 (1977).

[9] S. P. Mathur, K. K. Jain and C. S. Bhandari, *Nat. Appl. Sc. Bull.*, **29**, 69 (1977).

[10] S. P. Mathur, *J. Inst. Chemists*, **46**, 300 (1976).

[11] Harvey and Manning, *J. Am. Chem. Soc.*, **72**, 4488 (1950).

[12] P. Job, *Ann. Chim.*, **9**, 113 (1928).

Revue Roumaine de Chimie, **31**, *6*, 585–588 (1986)

MAGNETIC AND SPECTRAL STUDIES OF LANTHANIDE PERCHLORATE COMPLEXES OF 2-ETHOXYCARBONYL-AMINO-PYRIDINE-N-OXIDE

R. K. AGARWAL and S. K. GUPTA
Department of Chemistry, Lajpat Rai Post-Graduate College,
Sahibabad-201 005 (Ghaziabad), India

Received June 3, 1985

Addition compounds of lanthanide perchlorate with 2-ethoxycarbonylamino-pyridine-N-oxide (ECAPO) with composition $Ln(ClO_4)_3.6ECAPO$ were prepared and characterized by molecular weight, molar conductance, magnetic and infrared studies. In all the compounds ECAPO acts as monodentate ligand. The possible coordination number six is assigned to lanthanides in these complexes.

INTRODUCTION

In recent years West et al. [1-4] have investigated a number of 2-substituted pyridine N-oxide complexes of metal ions. More recently, we have reported the complexes of 2-ethoxycarbonylamino N-oxide (ECAPO) with zirconium(IV)[5], thorium(IV)[6], uranium(VI),[7] zinc(II),[8] cadmium (II),[8] nickel(II),[9] cobalt(II)[9] and copper(II).[9] In all these cases ECAPO bonded to the metal ions *via* both the N-oxide and carbonyl functions and thereby acted as a bidentate ligand. It is somewhat surprising that in the case of lanthanide perchlorates ECAPO acts as monodentate and is bonded only through N-oxygen. Thus in the present study we have prepared and characterized the lanthanide perchlorate complexes of ECAPO derived from 6 : 1 ligand-metal ion molar ratios and report our findings here.

EXPERIMENTAL

Materials

All the solvents and reagents were of good quality products and were used as received. Lanthanide oxides were obtained from Rare Earth Products Ltd. India and were treated with 30 % perchloric acid, filtered and evaporated to dryness. The ligand ECAPO was prepared from 2-aminopyridine as reported earlier. [10]

Preparation of the complexes

Hydrated lanthanide perchlorate was dissolved in a small quantity of ethanol and treated with an ethanolic solution of the ligand (molar ratio 1 : 6, with a small excess). The mixture was treated with an excess of 2,2′-dimethoxy propane and maintained in a desiccator

over calcium chloride. The crystals obtained, after one or two days were filtered, washed with ethanol and 2,2′-dimethoxypropane and dried in vacuo, over anhydrous calcium chloride.

The metals were estimated as their oxides, while others, by physico-chemical measurements on the complexes, were made as reported previously.[11]

RESULTS AND DISCUSSIONS

The analytical data of the newly synthesised complexes are summarised in Table 1. All the complexes have the general formula $M(ClO_4)_3 \cdot 6ECAPO$ (M = La, Ce, Pr, Nd, Sm, Gd, Tb, Dy and Ho). The compounds are non-hygroscopic quite stable and can be stored for long periods.

Table 1

Analytical data of ECAPO complexes of lanthanide perchlorates

Complex	Found (Calcd.) %				Ωm (ohm^{-1} cm^2 mole^{-1})	Average mol wt. in $PhNO_2$	Formula weight	μeff. B.M.
	Metal	N	C	H				
$La(ClO_4)_3.6ECAPO$	9.12 (9.08)	11.10 (10.98)	37.53 (37.65)	3.86 (3.92)	78.6	385	1529.5	Diamag.
$Ce(ClO_4)_3.6ECAPO$	9.20 (9.14)	10.89 (10.97)	37.50 (37.63)	3.87 (3.92)	77.9	386	1530.5	2.61
$Pr(ClO_4)_3.6ECAPO$	9.29 (9.20)	10.88 (10.96)	37.50 (37.61)	3.85 (3.91)	76.9	389	1531.5	3.72
$Nd(ClO_4)_3.6ECAPO$	9.46 (9.38)	10.86 (10.94)	37.42 (37.53)	3.85 (3.91)	78.2	390	1534.5	3.62
$Sm(ClO_4)_3.6ECAPO$	9.87 (9.73)	10.82 (10.90)	37.29 (37.39)	3.84 (3.89)	80.1	392	1540.5	1.62
$Gd(ClO_4)_3.6ECAPO$	10.24 (10.14)	10.78 (10.85)	37.12 (37.22)	3.83 (3.87)	78.9	395	1547.5	7.92
$Tb(ClO_4)_3.6ECAPO$	10.41 (10.26)	10.76 (10.84)	37.06 (37.17)	3.81 (3.87)	80.9	1396	1549.5	9.21
$Dy(ClO_4)_3.6ECAPO$	10.61 (10.46)	10.71 (10.81)	37.02 (37.08)	3.80 (3.86)	79.3	398	1553.0	10.82
$Ho(ClO_4)_3.6ECAPO$	10.81 (10.60)	10.64 (10.80)	36.91 (37.02)	3.80 (3.85)	79.9	399	1555.5	10.45

The compounds are fairly soluble in common organic solvents. The values of molar conductance of these complexes in nitrobenzene determined at room temperature are given in Table 1. These complexes dissociate in this solvent and behave as 1 : 3 electrolytes. The molecular weight data (Table 1) also support the similar electrolytic behaviour of the complexes.

The magnetic moments of these complexes recorded in Table 1, show little deviation from the Van Vleck values[12,13] indicating thereby that 4f-electrons do not participate in bond formation in these chelates. Thus, the magnetic moments of these complexes are within the range predicted and observed in the complexes of lanthanide ions.[14,15]

Infrared spectra

Table 2 records important IR bands for the ligand and the complexes. The N-O stretching frequencies in free ligand occur as strong bands at 1265 and 1245 cm^{-1}, which show red shifts on complexation. This lowering of the frequency of N-O vibrational mode is due to the shift of electron density[16,17] from oxygen to metal ions. The N-O bending[2-5] in the free ligand observed at 840 cm^{-1} exhibits a small shift in the spectra of the metal complexes as expected. The N—H stretching frequencies occur at 3220 and 3060 cm^{-1} in the free ligand, and there is no appreciable change in these frequencies after complexation.

Table 2

Partial IR spectral data (cm^{-1}) of ECAPO and its metal complexes

Complex	ν(NH)	ν(C=O)	ν(N—O)	δ(N—O)	ν(M—O)
$La(ClO_4)_3$.6ECAPO	3220m 3060m	1725vs	1265vs 1245s	840m	—
$Ce(ClO_4)_3$.6ECAPO	3220m 3090m	1727vs	1240s 1225s	830m	380m
$Pr(ClO_4)_3$.6ECAPO	3210m 3060m	1725s	1240s 1230s	832m	375m
$Nd(ClO_4)_3$.6ECAPO	3215m 3055m	1727vs	1245s 1225s	830m	372m
$Sm(ClO_4)_3$.6ECAPO	3220m 3060w	1725s	1242s 1220s	825m	370m
$Gd(ClO_4)_3$.6ECAPO	3220m 3060m	1722s	1245s 1220s	828m	365m
$Tb(ClO_4)_3$.6ECAPO	3220m 3070m	1725s	1240s 1220s	835m	362m
$Dy(ClO_4)_3$.6ECAPO	3215m 3065m	1725s	1245s 1218s	832m	365m
$Ho(ClO_4)_3$.6ECAPO	3210m 3060w	1725s	1240s 1218s	835m	360m

The carbonyl stretching frequency of the $COOC_2H_5$ moiety is a strong band at 1725 cm^{-1} in the free ligand. Contrary to our previous observations,[5-9] in the present metal ion complexes the band is not shifted appreciably. Absorptions associated with CH out-of-plane deformation modes, as expected, undergo a slight positive shift due to tightening of the aromatic ring on complexation.[13,17] The overall IR spectral evidences suggest that ECAPO acts as a mondentate ligand and coordinates only through N-oxygen.

We have assigned a band in the 360—380 cm^{-1} region to ν(M-O) and assume it to be indicative of N-oxide bonding to the lanthanide ions. The absorption is comparable with the work of West et al.[1-4] on various 2-substituted pyridine N-oxide complexes of lanthanides.

Soundararajan[18] and Vicentini et al.[19] have investigated a large number of lanthanide perchlorate complexes of various ligands. In the present studies the 1 : 3 electrolytic behaviour of the perchlorate complexes in nitrobenzene and molecular weight determination in solvent showing the presence of four species reveal the non-coordinating nature of the perchlorate groups. The occurrence of two bands at 1100—1085 cm^{-1} (ν_3) and *ca.* 625 cm^{-1} (ν_1) indicate the retention of the T_d symmetry of the perchlorate ion in these complexes and the presence of perchlorate groups outside the coordination sphere in these complexes.

In conclusion, the trivalent metal ions are bounded by six oxygens from the N-oxide functions of the six ligands.

ACKNOWLEDGEMENT. The authors wish to express their gratitude to the Council of Scientific and Industrial Research, New Delhi for their financial support of this work. They are also thankful to Dr. G.D. Sharma, Principal, Lajpat Rai Post Graduate College, Sahibabad for taking keen interest in the work.

REFERENCES

[1] S. A. Boyel, R. E. Kohrman and D. X. West, *Inorg. Nucl. Chem. Letters*, **12**, 603 (1976).

[2] D. X. West and C. A. Frank, *J. Inorg. Nucl. Chem.*, **41**, 49 (1979)

[3] D. X. West and R. E. Kohrman, *J. Inorg. Nucl. Chem.*, **41**, 1569 (1979).

[4] D. X. West and C. L. Bielinski, *J. Inorg. Nucl. Chem.*, **42**, 229 (1980).

[5] A. K. Srivastava, Mahesh Srivastava and R. K. Agarwal, *Nat. Acad. Sci. Letters*, **4**, 473 (1981).

[6] R. K. Agarwal and S. C. Rastogi, *Thermochim. Acta.*, **62**, 379 (1983).

[7] R. K. Agarwal, J. R. Chopra and S. C. Rastogi, *J. Indian Chem. Soc.*, (in Press).

[8] R. K. Agarwal, Gyanendra Singh and S. C. Rastogi, *Nat. Acad. Sci. Letters*, (in Press).

[9] M. Srivastava, A. K. Srivastava and R. K. Agarwal, *Polish J. Chem.* (in Press).

[10] A. R. Katritzky, *J. Chem. Soc.*, 2064 (1956).

[11] R. K. Agarwal, P. C. Jain, Veena Kapur, Sunita Sharma and A. K. Srivastava, *Transition Met. Chem.*, **5**, 237 (1980).

[12] D. M. Yost, H. Russel and C. S. Garner, "The Rare Earth Elements and Their Compounds", Chp. 2, Wiley, New York.

[13] A. K. Garga, "Physico-Chemical Studies on Some Rare Earth Complexes with Nitrogen Containing Ligands", Ph. D. Thesis (1975), Meerut University, India.

[14] N. M. Karayannis, C. M. Mikulski, L. L. Pytlewski and M. M. Labes, *J. Less Common Metals*, **20**, 29 (1970).

[15] M. C. Jain, R. K. Sharma, A. K. Srivastava and P. C. Jain, *J. Inorg. Nucl. Chem.*, **41**, 1305 (1970).

[16] N. M. Karayannis, *Coord. Chem. Revs.*, **11**, 93 (1973).

[17] N. M. Karayannis, A. N. Speca, D. E. Chasen and L. L. Pytlewski, *Coord. Chem. Revs.*, **20**, 37 (1976).

[18] S. Soundararajan, "Studies in the Coordination Chemistry of the Rare Earth", *Proc. Chem. Symp.*, **1**, 203 (1970).

[19] L. B. Zinner and G. Vicentini, *Inorg. Nucl. Chem. Letters*, **7**, 967 (1971).

Revue Roumaine de Chimie, 31, *6*, 589–596 (1986)

ELLIPSOMETRIC SPECTROSCOPY OF PURE AND CO COVERED GOLD FILMS

MĂRIUCA GARTNER and M. VASS
ICECHIM — Center of Physical Chemistry, Spl. Independenţei 202, Bucharest, Romania 77208

Received June 10, 1985

Ellipsometric measurements were carried out on gold films deposited by vacuum evaporation on quartz substrate. The determined optical (dielectric) constants were used for indexing the interband transitions in the visible region. The variations of these constants with the temperature of the substrate and with the adsorption of CO at 77 K are also reported.

INTRODUCTION

Ellipsometry, a sensitive and non-destructive technique, suitable for gas adsorption experiments, allows the determination of the optical constants and implicitly gives information on the band structure of the system.

The number of published papers in this field is continuously increasing but rather a few[1-3] are dealing with gas adsorption on 1–B group metals.

Ellipsometric response due to carbon monoxide adsorbed on copper and silver was investigated by Merkt and Wissmann[4,5] in the visible range and by Dignam [6] and Watanabe [7] in the infrared range.

Merkt and Wissmann[8] are also the only ones who have studied the system carbon monoxide-gold film in the visible range of the spectrum.

Carbon monoxide adsorption on gold is of a weak type, with heats of adsorption between 37.7 kJ/mol [9] and 56.9 kJ/mol. [10] Carbon monoxide adsorbed on gold behaves like a positively charged layer.[11] Some hypotheses[10-13] were advanced to account for this positively charged layer. The most likely one[12] is that the adsorbate penetrates below the mean electronic plane of the metal surface. The negatively polarized molecule induces an extra positive polarization of the ions near the surface which makes the resultant surface potential positive.

Infrared studies[14] suggest that CO adsorption on 1–B group metals can be visualized *via* a mechanism involving a bond formation by electron donation on carbon into vacant orbitals of the metal atoms, but also by a back donation of electrons from filled d orbitals of the metal[14] into antibonding orbitals of the carbon monoxide molecules which tends to stabilize the metal-carbon bond. Contribution of the gold excited states $5d^96s^2$ and $5d^86s^2p$ to the surface bond was also suggested[14].

The aim of this work is the determination of the interband transitions in the visible range for clean gold films and the study of the modifications of the energy spectrum produced by carbon monoxide adsorption. The ellipsometric spectroscopy method was used for these purposes.

EXPERIMENTAL

The ellipsometric measurements have been performed in high vacuum at 293 K using a photoelectric null-ellipsometer of the type P — C — S — A (polarizer-compensator-sample-analyser). The apparatus, built by IPTRD* (Romania) allowed a reading accuracy of 1 minute for both azimuthal angles P and A (of the polarizer and analyzer respectively) and for the angle of incidence.

The light source was a SP-500 mercury lamp coupled with a monochromator. The compensator C was a $\lambda/4$ achromatic retarder of the Fresnel type, made of suprasil quartz. The incident angle was $\varnothing = 70^{\circ}$ and the range of wavelengths 400 — 600 nm .

The measuring cell (Fig. 1) connected to a bakable high vacuum line was made of glass, with optically polished quartz windows. The substrate on which the gold films were deposited was also of optically polished quartz and it formed the basis of an L-shaped test tube.

The substrate could be heated or cooled by introducing in the cavity C either a heater or liquid nitrogen.

The films were deposited at room temperature in 10^{-8} torr residual gas pressure using a collimated evaporation source (Johnson-Matthey spectrographically standardized gold). The films were annealed after the evaporation for half an hour at 353 K.

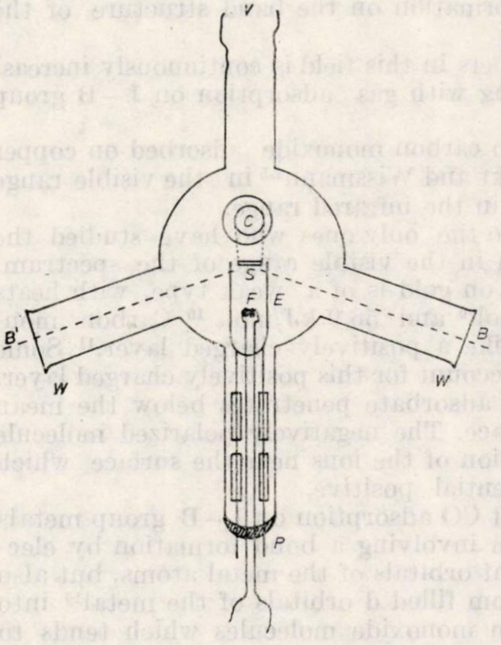

Fig. 1. — Evaporation cell. BB′ — optical axis ; W-quartz windows ; V-connection to the vacuum pump ; P-pinch ; F-evaporation source ; E-protection screen ; S-substrate ; C-cavity for introducing a heater or liquid nitrogen, one of its walls is the substrate itself.

---

* IPTRD — Institute for Physics and Technology of Radiation Devices.

High purity carbon monoxide (B.O.C. grade) was introduced by using a bakable Granville Phillips leak-valve.

During the gas adsorption experiments the vacuum pumps were isolated using a magnetically operated glass-ball valve.

CALCULATION PROCEDURE

It is well known[15] that the ellipsometric angles Δ and ψ within the Maxwell theory are related to the optical constants (n and k) of an absorbing material. The complex refractive index $\bar{N} = n - ik$ is related to the complex dielectric constants $\varepsilon = \varepsilon_1 - i\varepsilon_2$ by the relation $\bar{N}^2 = \varepsilon$ or equivalently :

$$\begin{cases} \varepsilon_1 = n^2 - k^2 \\ \varepsilon_2 = 2nk \end{cases} \tag{1}$$

On the other hand, ε gives information about the excitation of the medium under an electromagnetic perturbation. It contains phononic contributions as well as inter and intraband electronic excitations.

Nevertheless, in the visible range of the spectrum only the interband transitions are important. The energy band structure is contained in the expression of ε_2 as follows[16,17];

$$\varepsilon_2 \sim \frac{1}{\omega^2} M_{vc}^2 \cdot J_{vc}(\omega) \tag{2}$$

where : M_{v_c} — is the matrix element for the transition considered and usually is slowly varying with ω.

J_{vc} — is the joint density of states (the number of pairs of states $E_c(\vec{k})$, $E_v(\vec{k})$, one in the conduction band, the other in the valence band, both having the same quasi-momentum k with $E_c(\vec{k}) - E_v(\vec{k})$ belonging to an infinitesimal energy interval (ω, $\omega + d\omega$)).

The peculiar features of $J_{v_c}(\omega)$ at the critical points of $E(\vec{k})$, the so-called Van Hove singularites, are included in the expressions of $\varepsilon_1(\omega)$ and $\varepsilon_2(\omega)$.

In the presence of an adsorbed layer, Δ and ψ have deviations, $\delta\Delta$ and $\delta\psi$, from the clean surface values and these depend on the wavelength of the incident light, angle of incidence, n and k of the substrate and especially on the optical constants and thickness of the layer. In this case a direct evaluation of the parameters of interest from Δ and ψ is impossible and therefore McCrackin's FORTRAN program was used.[18]

THE OPTICAL PROPERTIES OF CLEAN GOLD FILMS

The optical (dielectric) constants were obtained from a set of 22 pairs of ellipsometric parameters Δ and ψ. In Fig. 2 the optical constants are plotted against the wavelength for a typical gold film (85 nm thickness).

The value given by Schulz [19] (for a 60 nm gold film deposited in 10^{-5} torr) and by Atkinson[1] (for a 10 nm gold film deposited in 10^{-7} torr) are also plotted. In spite of the different conditions of preparation the results show a good agreement.

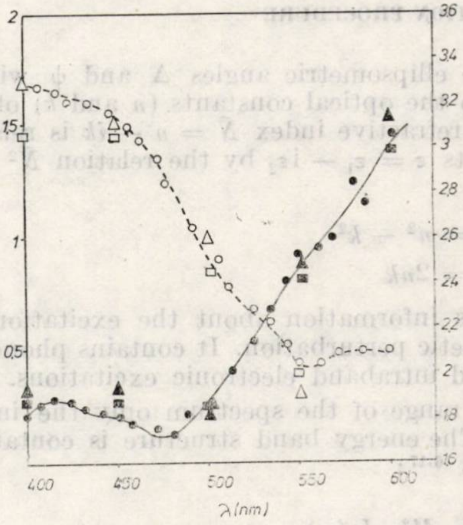

Fig. 2. — n and k *vs* λ for clean gold film (n-dashed curve; k-continuous curve; our data for n-o ; our data for k-● ; data published by Shulz[5] — □, ▩ ; data published by Atkinson[1] — Δ, ▲).

In Fig. 3 the dielectric constants *vs* the frequency of the incident light were plotted. A comparison with the results of Merkt and Wissmann[8] (for a 35 nm gold film deposited at 3.10^{-10} torr), Aspness[20] and with theoretical calculations [17] show a good agreement too.

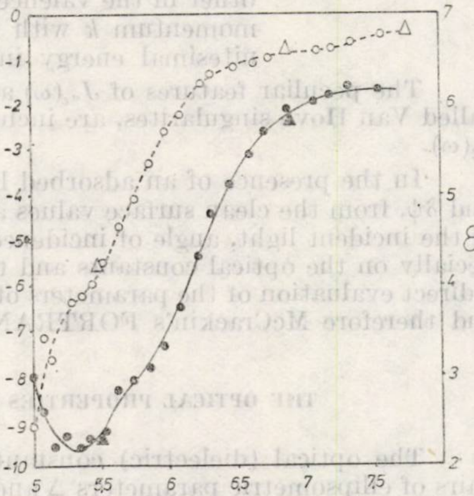

Fig. 3. — ε_1 and ε_2 *vs* ν for clean gold films (ε_1-dashed curve; ε_2-continuous curve; our data for ε_1-o ; our data for ε_2-● ; data published by Merkt and Wissmann[8] —Δ, ▲).

In order to identify the critical points we plotted the imaginary part of the inverse dielectric constants against the wavelength (Fig. 4).

The positions of the maxima are 2.17 eV and 2.59 eV.

Buckman and Bashara[21] obtain the transition $L_{32} \rightarrow L'_2$ at 2.1 eV by means of the modulated ellipsometry.

Lasser and Smith[22] find two other transitions at 2.5 eV and 3 eV respectively as being due to transitions from the highest level of the d-states (band number 5) to the s and p states (band number 6) just above the Fermi level.

Christensen and Seraphin[17] taking into account relativistic effect in their band structure calculations find for the transition $(Q_3 + Q_4)^5 \rightarrow E_F(Q_3 + Q_4)^6$ a value of 2.6 eV.

Therefore, our results are consistent with the energy bands of gold as reported in the literature.[17,21,22]

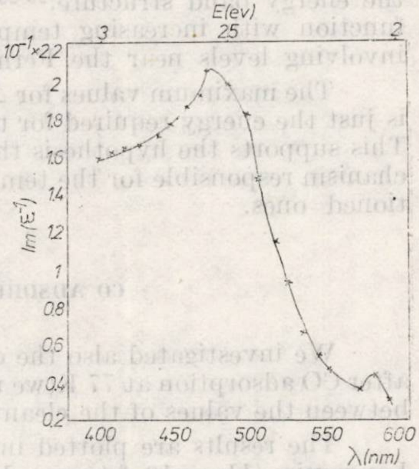

Fig. 4. — Imaginary part of the inverse dielectric constant *vs* the energy (wavelength).

THE TEMPERATURE DEPENDENCE OF THE OPTICAL CONSTANTS

In order to investigate the support temperature dependence of the optical constants we performed the measurements at 293 K and 77 K and calculated the following differences:

$$\begin{cases} \Delta_T \varepsilon_1 = \varepsilon_1(77\text{K}) - \varepsilon_1(293\text{K}) \\ \Delta_T \varepsilon_2 = \varepsilon_2(77\text{K}) - \varepsilon_2(293\text{K}) \end{cases} \tag{3}$$

The results are shown in Fig. 5 as a function of frequency.

Several mechanisms may account for these temperature shifts as pointed out by Merkt and Wissmann[5]: the thermal expansion of the

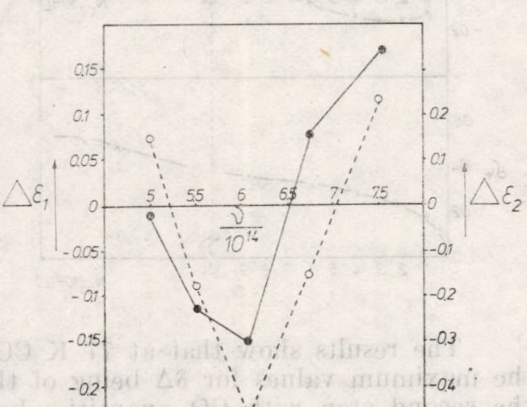

Fig. 5. — The variation of $\Delta\varepsilon_1$ and $\Delta\varepsilon_2$ *vs* ν in the temperature range 77—300 K ($\Delta\varepsilon_1$-dashed curve; $\Delta\varepsilon_2$-continuous curve).

lattice, the strains induced by the difference between the thermal expansion coefficients of the glass and the gold film, which in their turn influence the energy band structure,[23-25] the increase of Boltzmann tail of Fermi function with increasing temperature, which modifies[24] the transitions involving levels near the Fermi energy etc.

The maximum values for $\Delta_T \varepsilon_1$ and $\Delta_T \varepsilon_2$ were found at 2.59 eV, which is just the energy required for the interband transition to the Fermi level. This supports the hypothesis that, at least for this energy range, the mechanism responsible for the temperature shift is the last of the above mentioned ones.

CO ADSORPTION ON GOLD FILMS

We investigated also the changes $\delta\Delta$, $\delta\psi$ of the ellipsometric angles after CO adsorption at 77 K(we used their usual definition as the difference between the values of the clean film and the values for CO covered film).

The results are plotted in Fig. 6 against the amount of gas (N) in Langmuirs ($1\text{L} = 10^{-6}$ torr.s). It may be seen that $\delta\Delta = f(N)$ curve tends to oscillate, especially for low N.

The experiment of Fig. 6 was performed in two steps :

1) In the first one, the ellipsometric measurements on the CO adsorbed layer were made after pumping the gas excess.

2) In the second step, the glass-ball valve was closed towards the vacuum line, that means it was higher pressure.

Twice as higher values of $\delta\Delta$ and $\delta\psi$ were observed in this case.

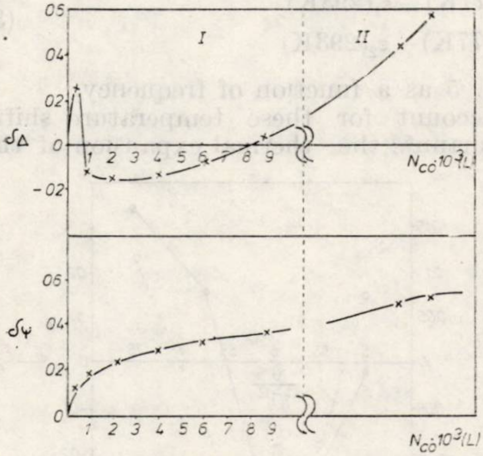

Fig. 6. — $\delta\Delta$, $\delta\psi$ *vs* CO dose (N).

The results show that at 77 K CO/Au adsorption is a weak one, the maximum values for $\delta\Delta$ being of the order of 0.2°. Working as in the second step with CO quantities between 10^3L and 2.10^6L we get greater $\delta\Delta$ values, which increase with the amount of admitted gas.

Plotting $\delta\Delta_{max} = f(\lambda)$ (Fig. 7) (where $\delta\Delta_{max}$ is the value of $\delta\Delta$ for the maximum quantity of carbon monoxide admitted in the system) a sharp peak was observed around 2.59 eV (corresponding to one of the known interband transitions of gold). Therefore it seems that the adsorption only intensifies the transition without modifying the energetic spectrum.

The checking of our data against the theoretical models available in the literature turned out to be very difficult. For instance, the model of Mayer and Bootsma [26,27] originally proposed for semiconductors, requires $\delta\Delta \sim 1/\lambda$ and $\delta\psi \lesssim 0$ over the whole range of wavelengths. Neither our results for carbon monoxide adsorbed on gold nor other systems of gas adsorbed on metals [4,5,28] satisfy these relations.

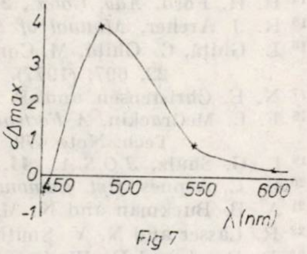

Fig. 7 — The variation of $\delta\Delta_{max}$ with wavelength (energy).

The effective layer model of Bruggemann, [29] which gives fairly good results for oxygen-copper system, [30,31] could not be applied for our system CO/Au, due to the absence of reliable data concerning the optical constants of a carbon monoxide layer.

CONCLUSIONS

The data reported in this paper emphasize a good agreement between the optical (dielectric) constants of our gold films and band structure energies available in the literature.

The influence of temperature on the ellipsometric parameters in 400 — 600 nm wavelength range is maximum at 2.59 eV — the value corresponding to the interband transition.

It was also found that the CO adsorption on the gold films is of a weak type; however a small charge transfer pointed out by an increased maximum of 2.59 eV transition is involved.

ACKNOWLEDGEMENTS. We are indebted to Dr. C. Ghiţă, Dr. L. Ghiţă and Dr. M. Constantinescu from IPTRD (Romania) for valuable suggestions and discussions.

REFERENCES

[1] R. Atkinson, P. H. Lissberger and I. W. Salter, *Short Report*, Queen's Univ., Belfast, (1979).
[2] D. E. Aspnes, E. Kinsbron, D. D. Bacon, *Phys. Rev. B*, **21**, 3290 (1980).
[3] I. Ohlidal and F. Lukes, *Thin Solid Films*, **85**, 181 (1981).
[4] U. Merkt and P. Wissmann, *Thin Solid Films*, **57**, 65 (1979).
[5] U. Merkt and P. Wissmann, *Surf. Sci.*, **96**, 529 (1980).
[6] M. J. Dignam, *Appl. Spectroscopy Rev.*, **14**, 249 (1979).
[7] M. Watanabe, *Surf. Sci.*, **138**, 95 (1984).
[8] U. Merkt and P. Wissmann, *Vakuum Technik*, **2**, 41 (1980).
[9] D. O. Hayward and B. M. W. Trapnell, *Chemisorption*, London, Butterworths (1964).

[10] N. A. Surplice and W. Brearley, *Surf. Sci.*, **52**, 62 (1975).

[11] R. Smoluchowski, *Phys. Rev.*, **60**, 661 (1941).

[12] R. Ch. Burshtein and N. A. Shurmoskaya, *Surf. Sci.*, **2**, 210 (1964).

[13] N. A. Surplice and J. Müller, *Thin Solid Films*, **28**, 179 (1975).

[14] R. R. Ford, *Adv. Catal.*, **21**, 51 (1970).

[15] R. J. Archer, *Manual of Ellipsometry*, Gaertner Sci. Corp., Chicago (1968).

[16] L. Ghiţă, C. Ghiţă, M. Constantinescu, I. Baltog and T. Velula, *Rev. Roumaine Phys.* **22**, 697, (1977).

[17] N. E. Christensen and B. O. Seraphin, *Solid State. Commun.*, **8**, 1221 (1970).

[18] F. L. McCrackin, *A Fortran Program for Analysis of Ellipsometric Measurements, N.B.S.* Tech. Note 479, U S. Govt. Printing Office, Washington, D. C. (1969).

[19] L. G. Shulz, *J.O.S.A.*, **44**, 357 (1954).

[20] D. E. Aspnes, *Opt. Commun.*, **8**, 222 (1973).

[21] A. B. Buckman and N. M. Bashara, *Phys. Rev.*, **174**, 719 (1968).

[22] R. Lasser and N. V. Smith, *Solid State Commun.*, **37**, 507 (1981).

[23] R. Rosei and D. W. Lynch, *Phys. Rev. B.* **5**, 3883 (1972).

[24] G. Joos and A. Klopfer, *Z. Physik*, **138**, 251 (1954).

[25] P. Winsemius, F. F. van Kampen, H. P. Lengkeek and C. G. van Wenz, *J. Phys. F. (Metal Phys.)*, **6**, 1583 (1976).

[26] G. A. Bootsma and F. Meyer, *Surf. Sci.*, **14**, 52 (1969).

[27] F. Meyer, *Surf. Sci.*, **56**, 37 (1976).

[28] C. Mc. Elhiney, H. Papp and J. Pritchard, *Surf. Sci.*, **54**, 617 (1976).

[29] D. A. G. Bruggemann, *Ann. Physik (Leipzig)*, **24**, 636 (1935).

[30] F. H. P. M. Habraken, E. Ph. Kieffer and G. A. Bootsma, *Surf. Sci.*, **83**, 45 (1979).

[31] M. Gartner, N. Stănică and M. Vass, *to be published.*

Revue Roumaine de Chimie, 31, 6, 597–604 (1986)

DETERMINACIÓN GRAVIMÉTRICA DE MERCURIO Y CADMIO MEDIANTE FORMACIÓN DE LOS PARES IÓNICOS $[(C_4H_9)_4N]_2[HgI_4]$ Y $[(C_4H_9)_4N]_2[CdI_4]$

J. HERNÁNDEZ MÉNDEZ, A. ALONSO MATEOS y E.J. MARTÍN MATEOS
Departamento de Química Analítica, Facultad de Química,
Universidad de Salamanca, España

Recibido: el 13 de Mayo de 1985

Los complejos Hg(II)—I^- y Cd(II)—I^- forman con el ion tetrabutilamonio compuestos de asociación iónica insolubles en agua. En las condiciones experimentales óptimas, estos compuestos presentan estequiometrías definidas, $[(C_4H_9)_4N_2][HgI_4]$ y $[(C_4H_9)_4N][CdI_4]$; por esto, pueden servir para la determinación gravimétrica de mercurio y cadmio. El factor gravimétrico para el primer compuesto, 0.1675, es sensiblemente más favorable que los encontrados en bibliografía para mercurio, mientras que el del segundo, 0.1024, es del mismo orden que los más favorables para cadmio; permiten determinar cantidades de mercurio y cadmio superiores a 4 mg con errores inferiores al 0.6%.

Hg(II)-I^- and Cd(II)-I^- complexes form water-insoluble ionic-association compounds with the tetrabutylammonium ion. These compounds show definite stoichiometric compositions, $[(C_4H_9)_4N]_2[HgI_4]$ and $[(C_4H_9)_4N]_2[CdI_4]$ in the optimal deduced conditions. Thus these compounds can be used for the gravimetric determination of mercury and cadmium. The experimental gravimetric factor of the first compound, 0.1675, is sensibly more favourable than the others reported elsewhere for the determination of Hg; the factor of the compound of cadmium, 0.1024, is in the same order that the most favourable factors above reported for Cd. They enable us to determine at least 4 mg of Hg or Cd with errors smaller than 0.6%

INTRODUCCION

Los procedimientos para la determinación gravimétrica de mercurio pueden clasificarse [1] en tres grupos, en el primero de los cuales se engloban los procedimientos basados en la reducción a Hg^0, empleando diversos agentes reductores, como ácido ascórbico, hipofosfito, hidracina, hidroxilamina o formaldehido; en el segundo se agrupan los procedimientos basados en la formación de compuestos de Hg(I), como son, cloruro, yodato, cromato, molibdato, vanadato, oxalato o cupferronato, que, por lo general, presentan factores gravimétricos poco favorables.

Por último, en le tercer grupo se sitúan los procedimientos basados en la formación de compuestos de Hg(II), entre otros, las obtenciones de peryodato, antranilato, arseniato o yoduro de Hg(II), así como los mercuritiocianatos de Zn(II) o Co(II); pero quizás, en cuanto al factor gravimétrico más favorable que presentan, deben mencionarse el reineckato de Hg(II) o los compuestos que forma dicho catión con el complejo tetraamin-cadmio (II) o con el dietilendiamin-cobre(II), en presencia de yoduro en ambos casos, así como el compuesto formado con piridina y dicromato Más interés aún tiene, aunque sólo sea por su relación con el presente trabajo, la precipitación con yoduro de trimetilfenilamonio en medio yodurado. [2]

En cuanto a los métodos para la determinación gravimétrica de cadmio, se pueden clasificar,[1] igualmente en tres grupos, el primero de los cuales se fundamenta en la deposición electrolítica del metal; como es natural, es el que presenta factor gravimétrico menos favorable y, además, está sometido a numerosas interferencias. En el segundo grupo se hallan los procedimientos basados en la precipitación con reactivos inorgánicos, entre los que puede citarse la precipitación como hidróxido y posterior calcinación a óxido, ó como sulfato ó como sulfuro y posterior transformación en sulfato, asi como la precipitación con fosfato en presencia de sales amónicas, desecando posteriormente a temperatura ambiente hasta $CdNH_4PO_4 \cdot H_2O$ ó calcinando por encima de 700°C hasta $Cd_2P_2O_7$. Especial mención merece la reacción con hidracina en medio yodurado, así como con triyodomercuriato en medio amoniacal.

Finalmente, el tercer grupo lo constituyen procedimientos basados en la precipitación con reactivos orgánicos. Entre estos pueden citarse los compuestos obtenidos por reacción con oxina, con los ácidos quinaldinico o antranílico, con mercaptobenzotiazol en medio amoniacal, con piridina (o piperazina) y tiocianato, con el complejo etilendiamino-cobre(II) en medio yodurado o con el yoduro de trimetilfenilamonio también en medio yodurado. [3] Por último, puede mencionarse el compuesto obtenido por reacción con tioureay sal de Reinecke.

En el presente trabajo se estudia la formación de pares iónicos entre los complejos yodurados de Hg(II) y Cd(II) y el catión $But_4\,N^+$ a fin de determinar las condiciones experimentales óptimas en cada caso. Tras obtener y desecar los precipitados en estas condiciones, presentan composiciones estequiométricas definidas, siendo posible proponer procedimientos experimentales para la determinación gravimétrica de mercurio y cadmio en márgenes definidos y con precisiones adecuadas.

PARTE EXPERIMENTAL

Reactivos

Todas las soluciones se prepararon en agua desionizada y bidestilada; a menos que se especifique lo contrario, los reactivos eran de calidad Reactivo Análisis.

Se prepararon soluciones de Hg(II) en HNO_3 diluido a partir de $Hg(NO_3)_2$ sólido, comprobando la concentración mediante reducción con ácido ascórbico hasta el estado metálico. Se prepararon soluciones de Cd(II) a partir del sólido $Cd(NO_3)_2 \cdot H_2O$, y determinando posteriormente su concentración precipitando con fosfato en medio amoniacal, calcinando a 800°C y pesando finalmente como $Cd_2P_2O_7$. Soluciones 0.10 y 0.050 M de tetrabutilamonio preparadas a partir del reactivo $But_4N^+I^-$ sólido puro (BDH). Soluciones de KI así como el reactivo sólido. Acidos nítrico y sulfárico y amoníaco diluídos. Tolueno. Para los ensayos cualitativos y el estudio de interferencias, se prepararon soluciones de diversos cationes metálicos a partir de sales inorgánicas solubles en medio acuoso de diferentes firmas comerciales. Debe hacerse especial mención de las soluciones de Cu(II), Au(III) y Pt(IV), preparadas a partir de los metales sólidos con purezas del 99,88 %, 99.99 % y 99.9 %, respectivamente.

Aparatos

Se utilizó una termobalanza STANTON mod. TR-01.

Procedimiento

Sobre las soluciones de mercurio(II) ó cadmio(II), al pH adecuado, se adiciona KI en exceso y posteriormente $But_4N^+I^-$, con lo que se obtienen precipitados que se filtran, lavan y desecan hasta peso constante.

Ensayos cualitativos

Al añadir un exceso de yoduro de tetrabutilamonio sobre las soluciones incoloras de los complejos yodurados de mercurio(II) ó cadmio(II), se observa la formación de los correspondientes pares iónicos insolubles de color blanquecino. El aspecto físico de estos precipitados, al menos aparentemente, no es muy favorable y para mejorarlo es necesario efectuar la precipitación a bajas temperaturas (inferiores a 10°C), agitando vigorosamente durante algunos minutos para facilitar la aglomeración de las partículas del sólido. Las partículas de precipitado son tan finas que es necesario utilizar crisoles de vidrio de porosidad nº 5 para retenerlas. Asímismo se comprueba que es necesario un franco exceso de yoduro y de sal de amonio cuaternario para la obtención de los precipitados.

En principio, la variación en el valor del pH no parece afectar a la formación de los pares iónicos hasta prácticamente 8 ó 9; para pH muy ácido (del orden de 1 o menor), si se mantienen los precipitados en digestión algún tiempo, se aprecia la aparición de un color amarillento que pardea, debido a la formación de I_2 en dicho medio. Esta es la razón por la que es conveniente lavar los precipitados con tolueno. En la práctica, la precipitación se efectúa a un pH próximo a 5.

Experimentalmente se comprueba que conviene trabajar con pequeño volumen de solución (del orden de 50—60 ml), debido a la relativa solubilidad de los precipitados.

RESULTADOS Y DISCUSION

Influencia de la temperature de secado

A soluciones de mercurio(II) o cadmio(II) conteniendo 56.80 ó 26.52 mg de los metales respectivos, se les adiciona exceso de yoduro potásico (1.5—2.0 g del producto sólido) y se ajusta el pH a un valor próximo a 5; la precipitación se lleva a cabo con exceso de yoduro de tetrabutilamonio (20—25 ml de la solución 0.10 M). Los precipitados así obtenidos se filtran, lavan y desecan hasta peso constante a temperaturas comprendidas entre 20 y 90°C. Se deduce un comportamiento similar al de otros pares iónicos objeto de anteriores trabajos de los autores,[4-6]; la descomposición del catión amonio cuaternario a partir de temperaturas próximas a 60°C hace que los precipitados deban ser desecados a 40—50°C. Los sólidos resultantes, dejados a temperatura ambiente en contacto con la atmósfera, no aumentan apreciablemente de peso, por lo que se puede considerar que no son higroscópicos.

Influencia de la concentración de H^+ sobre la precipitación

En distintas series de soluciones conteniendo una de ellas 56.80 mg de Hg en cada muestra y 26.52 mg de Cd en cada una de las integrantes de la segunda serie, junto con exceso de KI (1.5—2.0 g), se ajusta el valor del pH entre 1 y 10, para las distintas experiencias y, finalmente, se adicionan 20—25 ml de solución 0.10 M de $But_4N^+I^-$, obteniendo los pares iónicos respectivos. Se comprueba que, desde pH 1 hasta 8, aproximadamente, el peso de sólido obtenido tras el tratamiento térmico, no varía de modo apreciable (Figura 1). Para pH entre 1 y 2, al lavar los precipitados con tolueno se detecta la presencia de I_2 adsorbido sobre el precipitado, como consecuencia de la oxidación del I^- por el oxigeno atmosférico; no obstante, este fenómeno sólo se aprecia si la digestión del precipitado es muy prolongada. La disminución del peso de precipitado obtenido a valores de pH superiores a 8 se debe a la degradación de la sal de amonio cuaternario, observándose, sobre todo en el compuesto de Hg(II), una transformación en la morfología y coloración de los precipitados, que se transforman en oxiyoduros. En experiencias posteriores se trabaja a pH próximo a 5.

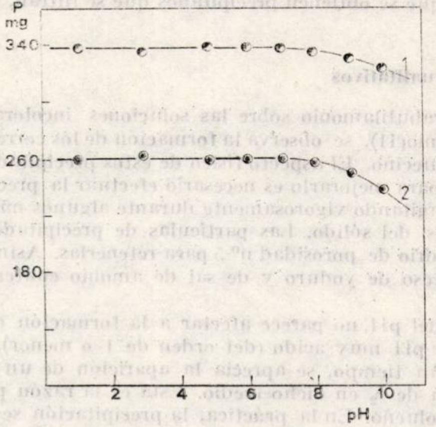

Fig. 1. — Influencia del pH del medio: 1 — Hg: puesto: 56.80 mg; 2 — Cd: puesto: 26.52 mg.

Influencia de la concentración de But_4N^+ sobre la precipitación

En distintas series de soluciones conteniendo una de ellas 56.80 mg de mercurio(II) (0.283 mmol) y la otra 26.52 mg de cadmio(II) (0.236 mmol), a pH ~ 5, se adiciona exceso de KI (1.5—2.0 g) y diferentes cantidades de la solución 0.10 M de la sal de amonio cuaternario, de modo que la cantidad de But_4N^+ en milimoles varíe aproximadamente desde

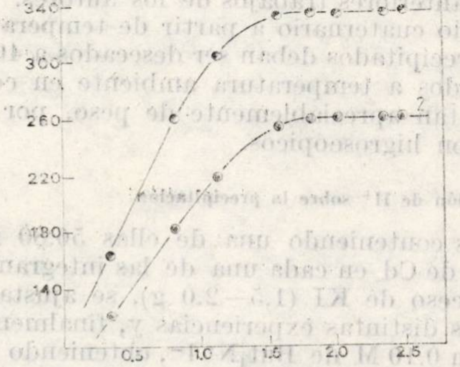

Fig. 2. — Influencia de la concentración de But_4N^+: 1 — Hg: puesto: 56.80 mg (0.283 mmol); 2 — Cd: puesto: 26.52 mg (0.236 mmol).

1.5 hasta 8 veces el número de milimoles del elemento metálico respectivo. En ambos casos, no se obtiene constancia en el peso de los pares iónicos respectivos hasta un valor al menos de 5 para la relación molar But_4N^+/ ion metálico (Figura 2). Sin embargo, un exceso mucho mayor de la sal de tetrabutilamonio no resulta conveniente porque, además de la contaminación de los precipitados, produce un cambio indeseable en la morfología de los mismos, que se vuelven más ,,pastosos''.

Influencia de la concentración de I^- sobre la precipitación

Sobre diferentes soluciones conteniendo 56.80 mg de mercurio(II) (0.283 mmol) ó 26.52 mg de cadmio(II) (0.236 mmol), a pH próximo a 5, se adicionan 25 ml de solución 0.10 M de la sal de amonio cuaternario y distintas cantidades de KI, desde 1 hasta 9 mmol (desde 3 hasta casi 30 veces el número de mmol del metal formador del complejo yodurado, teniendo en cuenta el I^- que acompaña al catión amonio cuaternario). Los resultados, que se representan en la Figura 3, muestran que, para conseguir la cuantitatividad de la precipitación, es necessario añadir exceso de complejante.

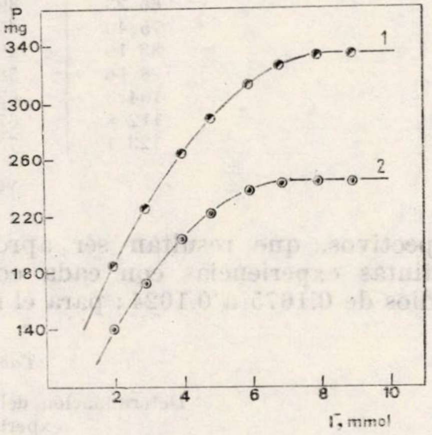

Fig. 3. — Influencia de la concentración de I^- : 1 — Hg : puesto : 56.80 mg (0.283 mmol) ; 2 — Cd : puesto : 26.52mg (0.236 mmol) ;

En todas las experiencias realizadas, el aspecto físico y el color de los precipitados es idéntico para cada metal, lo que parece indicar que el par iónico obtenido en cada caso presenta la misma estequiometría, para las concentraciones de yoduro estudiadas. Además, un exceso de yoduro superior al considerado como óptimo no afecta al peso final de los sólidos ni a su morfologia.

Condiciones óptimas. Determinación de los factores gravimétricos

Las condiciones óptimas para la precipitación son : pH entre 1 y 8 (se trabaja a pH$\sim$5), KI entre 1.5 y 2.0 g (para un volumen total de 50—60 ml) y 20—25 ml de solución 0.10 M de $But_4N^+I^-$, para las cantidades estudiadas de los respectivos elementos metálicos.

En estas condiciones experimentales se precipitan soluciones de mercurio(II) conteniendo desde 38.12 hasta 123.1 mg y de cadmio(II) desde 26.52 hasta 101.1 mg. A partir de los pesos de los sólidos obtenidos (Tablas 1 y 2), se calculan los valores de los factores gravimétricos respectivos, que resultan ser aproximadamente coincidentes para las distintas experiencias con cada compuesto, pudiendo calcular valores medios de 0.1675 a 0.1024 ; para el mercurio, dicho factor es más favorable, en cuanto a sensibilidad, que los de los restantes procedimientos aparecidos en bibliografía, mientras que el factor para el cadmio es del mismo orden que los de los más sensibles. Estos factores gravimétricos experimentales corresponden a compuestos cuyas composiciones estequiométricas son $[(C_4H_9)_4N]_2[HgI_4]$ y $[(C_4H_9)_4N]_2[CdI_4]$.

Tabla 1

Determinación del factor gravimétrico experimental

Hg (mg)	Precipitado (mg)	Factor Gravimétrico
38.12	226.1	0.1686
47.30	283.2	0.1670
56.80	337.3	0.1684
66.23	394.2	0.1680
75.40	451.8	0.1669
83.19	494.6	0.1682
98.16	589.5	0.1665
104.3	625.7	0.1667
112.8	671.8	0.1679
123.1	737.1	0.1670

valor medio = 0.1675

Tabla 2

Determinación del factor gravimétrico experimental

Cd (mg)	Precipitado (mg)	Factor Gravimétrico
26.52	257.5	0.1030
33.13	323.9	0.1023
39.40	387.0	0.1018
48.70	471.9	0.1032
54.13	527.6	0.1026
61.06	602.8	0.1013
77.23	749.1	0.1031
85.53	846.0	0.1011
96.20	933.9	0.1030
101.14	985.8	0.1026

Valor medio = 0.1024

Márgenes de aplicabilidad, precisión y exactitud de los métodos

Se ha llevado a cabo la determinación gravimétrica sobre muestras conteniendo cantidades diferentes de mercurio (entre 1.63 y 53.08 mg) y cadmio (de 1.01 a 44.18 mg). De los resultados obtenidos se deduce que pueden determinarse cantidades de ambos del orden de 3—4 mg, con errores del orden del 0.6 %, si bien, por encima de los 20 mg el error medio es del orden del 0.3—0.4 %.

Al realizar las determinaciones sobre sendas series de 12 muestras conteniendo cada una de ellas 56.80 mg de mercurio ó 26.52 mg de cadmio, se obtienen valores medios de 56.85 mg de Hg y 26.56 mg de Cd, calculando desviaciones estándar relativas de 0.17 % y 0.31 %, respectivamente.

Procedimientos propuestos

Las muestras a analizar deben contener más de 3 mg de Hg ó Cd, o bien se toma una alícuota adecuada de la solución preparada a partir de las muestras; es conveniente trabajar con el menor volumen posible de solución (50—60 ml puede resultar adecuado). Se ajusta el valor de pH aproximadamente a 5, si bien puede trabajarse en el margen de pH de 1 a 8; se adicionan entre 1.5 y 2 g de KI sólido y se agita. Se enfrían las soluciones de los complejos de coordinación obtenidos por debajo de 10°C, se añaden entre 20 y 25 ml de solución 0.10 M de yoduro de tetrabutilamonio, agitando durante algunos minutos y dejando posteriormente en digestión durante 30—60 minutos. Los precipitados se filtran a través de crisol de vidrio poroso del n°5 y se lavan con varias porciones de 10 ml de agua fría, a menos que se trabaje a pH muy ácido o que se añada un exceso muy considerable de sal de amonio cuaternario, casos en que conviene lavar los precipitados en primer lugar con dos porciones de 5—10 ml de tolueno, para evitar la contaminación por I_2 o por $But_4N^+I^-$ en exceso. Los precipitados se desecan hasta peso constante a 50°C. Los factores gravimétricos experimentales son 0.1675 para mercurio y 0.1024 para cadmio.

Interferencias

Por tratamiento de los complejos yodurados de algunos cationes metálicos con yoduro de tetrabutilamonio, se observa el enturbiamiento de la solución dando,en algunos casos, precipitados de aspecto granulado que se depositan lentamente. Así, además de los citados Hg(II) y Cd(II), también Ag(I) da un precipitado blanquecino (en presencia de una concentración muy elevada de I^-, al menos 5 M), Tl(I) da lugar a un precipitado de color blanco amarillento y Pb(II) (tambien para concentraciones elevadas de I^-) da lugar en principio a un precipitado amarillento, que se transforma poco después en blanco de aspecto algodonoso, que se deposita con facilidad en el fondo de los recipientes. También originan pares iónicos insolubles parecidos Bi(III) (naranja), Au(III) (pardo rojizo), Pd(II) (pardovioleta) y Pt(IV) (rojo granate).

Todos estos elementos interfieren la determinación gravimétrica propuesta tanto para mercurio como para cadmio. Las cantidades mínimas de dichos elementos determinables gravimétricamente en las condiciones esperimentales mencionadas, se encuentran en el orden de 3—5 mg (similares al mínimo determinable de Hg(II) ó Cd(III)), con errores relativos del orden del 1 %.

A partir de una muestra conteniendo 10.0 mg de Hg se obtienen 59.7 mg del correspondiente par iónico; la presencia de 3.0 mg de Cd(II), Bi(III), Pb(II), Ag(I), Tl(I), Au(III), Pd(II) ó Pt(IV) origina errores positivos en torno al 25 %, excepto en los casos de la presencia de Cd ó Pd en que el error se situá en un 50 %. La determinación a partir de 10.0 mg de Cd conduce a 97.7 mg del par iónico correspondiente; la presencia de 3.0 mg de alguno de los elementos mencionados provoca errores en torno al 15 %, excepto en el caso del Pd, en que el error se situá ligeramente por encima del 30 %. Todos estos valores deben considerarse con las precauciones inherentes al bajo valor de los pesos.

Al aumentar la cantidad de cualquiera de los elementos interferentes citados, el error aumenta proporcionalmente al peso de los pares iónicos respectivos, en relación con los de los pares iónicos de Hg(II) ó Cd(II) y, en definitiva, con el contenido de cada uno de los metales respectivos. No obstante, para cantidades más pequeñas de los metales interferentes, resulta muy dificil evaluar los errores, debido a que la precipitación ya no es cuantitativa.

BIBLIOGRAFIA

[1] L. Erdey, „Gravimetric Analysis", part II. 1ª Ed. Pergamon Press, Oxford, 1965.
[2] W. W. White y J. P. Zuber, *Anal. Chem.*, **39**, 258 (1967).
[3] A. Pass y A. M. Ward, *Analyst.* **58**, 667 (1933).
[4] J. Hernandez-Mendez, A. Alonso-Mateos, E. J. Martin-Mateos, y C. Garcia de Maria, *Rev. Roum. Chim.*, **27**, 981 (1982).
[5] J. Hernandez-Mendez, A. Alonso-Mateos, E. J. Martin-Mateos, y C. Garcia de Maria, *Studia Chemica.*, En prensa.
[6] J. Hernandez-Mendez, A. Alonso-Mateos, E. J. y E. J. Martin-Mateos, *Afinidad.*, En prensa.

Revue Roumaine de Chimie, 31, 6, 605–614 (1986)

MOLECULAR COMPOUNDS WITH SOME ALKYL ARYL ETHERS. I

CHARGE TRANSFER COMPLEXES

ELIZA-MANUELA VASILESCU and DUMITRU SĂNDULESCU
I.P.G. Ploiești, Bd. București 39, Romania

Received September 30, 1985

The possibility of some alkyl aryl ethers (AAE) to participate in the formation of charge-transfer (CT) complexes is investigated by electronic spectra. The thermodynamic functions are measured and some structure-property relationships are derived.

1. INTRODUCTION

The study of the properties of molecular complexes of alkyl aryl ethers (AAE) is important theoretically, especially in connexion with other aromatic compounds (hydrocarbons or ethers) as well as practically, AAE being potentially useful as plasticizers or antioxidants.

A large number of reports on investigations of electron donor-acceptor complexes in which aromatic derivatives function as electron-donors have appeared in the last twenty years.[1-16] In contrast to them, the relatively new compounds, AAE[17-19] have not yet been studied.

Mulliken,[12-14] theoretically, or Voight[3] and Orgel,[15] by experimentation, have proved that some aromatic derivatives show well defined charge-transfer absorption bands. These bands are assigned to one electron transition of the highest and the next occupied donor orbital to the lowest unoccupied molecular orbital of the acceptor. The two CT bands are associated with two isomer conformations of the complex.

The capacity of the partner for interaction in electron-donor complexes is dependent on both the electron donating ability of a specific atom and the molecular environment. There are reported in literature numerous relationships between the structure of donor-acceptor and the CT properties, some of them having an empirical quantitative character.[5,6,16]

Beside the investigations of the CT properties of AAE, the present paper is also devoted to the study of the influence of various electronic and steric elements on the magnitude of the donor-acceptor interaction.

2. EXPERIMENTAL

a). AAE, prepared in Organic Chemistry Laboratory, Pharmacy Department, IMF Bucharest,[17–19] 98–99 % purity, belong to the following groups:

A.

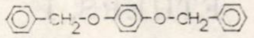

B.

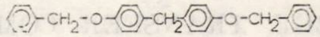

C.

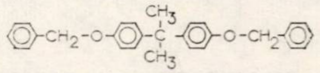

D.

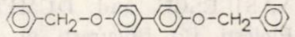

E.

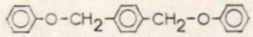

F.

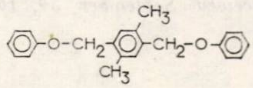

In each group, the compounds differ by the position and the number of the substituents. The ethers were characterized by melting point, elemental analysis as well as IR,[20], UV[21] and ^{1}H-NMR spectra.[21]

b) The CT complexes were made evident by electronic spectra, through the new CT absorption bands which arise beyond the absorption range of the pure partners. Tetracyane ethylene (TCNE) or tetrachlorobenzoquinone (chloranil – CHL) were used as acceptors.

The donor (D) concentration (10^{-1}–10^{-3} mol/L) was limited by its solubility in CH_2Cl_2 solvent as well as by the conditions of simplification imposed by the Benesi-Hildebrand equation.[1]

The acceptor (A) concentration (10^{-3} mol/L) was the lowest for which the intensity of CT band was adequate for thermodynamics calculations.

By the Job [22] and Briegleb [1] methods we proved that in this range of concentration for D and A, only one complex was present in solution with the donor/acceptor ratio 1/1.

The Benesi-Hildebrand [1] equation (1) was employed for the calculation of equilibrium constant, K:

$$\frac{C_A^0}{\bar{D}_i} = \frac{1}{\Sigma_c K_c} \cdot \frac{1}{C_D^0} + \frac{1}{\Sigma_c} \tag{1}$$

C_A^0, C_D^0 – the initial acceptor concentration and the initial donor concentration; $\bar{D}_i$ – the absorbance calculated from the values of differential absorptions by matrix method.[23] The differential absorption is obtained by measuring the absorptions of the complex relative to the sum of the absorptions of the individual components rather than to the absorption of the solvent as in the usual case; K_c, Σ_c – equilibrium constant and absorptivity, were obtained by regression method from equation (1). From the values of K at several temperatures, the values of enthalpy ($\Delta H°$), entropy ($\Delta S°$) and the free enthalpy ($\Delta G°$) characteristic of complexation equilibrium are calculated.

The K experimental error (± 3–5 %) amplified by the error from simplification of the Benesi-Hildebrand equation (± 10 %) corresponds with ± 0.25 kcal/mol error for the thermodynamics properties.

Electronic spectra were recorded on the UV-VIS spectrophotometer with thermostat device (Carl Zeiss-Jena, DDR) with the accuracy ± 50 cm^{-1}.

The values of wave number ($\tilde{\nu}_{CT}$), equilibrium constant and thermodynamics functions were measured on the CH_2Cl_2 solutions. The influence of the solvent upon the CT properties was measured on the solutions in CCl_4, $CHCl_3$ and CH_3NO_2 (all the solvents used were of a spectral grade).

c) The ionization potentials were calculated as functions of the transition energy ($h\nu_{CT}$) by means of empirical equations reported by Farrel [11] and Kuboyama [25] for related compounds (aromatic derivatives).

d) Hückel molecular orbital (HMO) method was used to calculate the transition energies (for ethers with maximum 24 atoms in molecule, without the hydrogen atoms). The calculations were carried out on the FORTRAN program.[25]

3. RESULTS AND DISCUSSION

a. Number and position of CT bands

As one can see in Tables 1 and 2 the number of AAE-CT bands in electronic spectra is different as a function of structure of the donors or the nature of the acceptor. For TCNE, a stronger acceptor, the two CT bands are well defined for almost all ethers, so that we discuss the phenomenon in this case.

The two CT absorption bands of A_1 complex (unsubstituted ether) change in a band and a shoulder in the complex of A_2 (one methyl substituent on the benzene terminal ring). The effect of substitution becomes more pronounced in the spectrum of A_4 complex (two *ortho* methyl substituents). On the contrary, all the ethers of the group E (methylenic group attached to the central ring and the etheric oxygen to the terminal aromatic ring) exhibit two well defined absorption bands, except for the compounds with two substituents adjoining methoxy group (E_4, F_2 ethers) which exhibit only one broad absorption band.

Furthermore, the values of transition energy and the values measured for the equilibrium constant prove that the methylene substituents increase the donor capacity of ether. In the spectrum of the complex of ether D_1 (two central benzene rings) arises only a CT band; the great rigidity of this molecule was proved by the values of chemical shifts in

Table 1

The values of calculated energies by HMO method and experimental transition energies

Ether	$HFMO_{heteroatom}$		$HFMO_{hyperconjugation}$		ν_{CT}Tcne/10^{-3} cm^{-1}/		ν_{CT}CHL/10^{-3} cm^{-1}/	
	I	II	I	II	I	II	I	II
GROUP A								
$A_1(-)$	0.30181	0.32732	0.86159	0.90592	17.1	25.76	—	25.24
$A_2(p^*)$	0.28441	0.50590	0.84523	0.87288	18.0(Sh)	25.28	—	24.78
$A_3(m)$	0.280402	0.50596	0.39778	0.86466	18.0(Sh	24.91	—	24.38
$A_4(0,0)$	0.26121	0.50558	0.44445	0.60635	—	22.64	—	23.00
GROUPS E AND F								
$E_1(-)$	0.06886	0.61634	0.10835	0.44116	20.00	25.80	20.30	23.64
$F_1(-)$	0.06806	0.60926	0.10793	0.44016	19.90	25.64	20.26	23.06
$F_2(m)$	0.03925	0.59891	0.09427	0.44018	18.96	23.60	20.02	23.32
$E_4(0,m)$	0.03917	0.59807	0.08625	0.43872	—	22.88	—	24.34
$F_3(0,m)$	0.03905	0.59738	0.08234	0.43067	—	22.72	—	23.98
$F_5(0,p)$	0.03850	0.59255	0.08196	0.43127	18.00	22.00	19.96	23.24
$F_6(m,m)$	0.03927	0.59087	0.08195	0.42876	19.72	21.20	19.93	23.20
$E_2(pCl)$	—	—	0.74479	0.83763	20.00	27.6(Sh)	—	25 .90

* The methyl substituents are situated on the terminal aromatic nucleus in the indicated positions.

^{1}H-NMR spectra, listed in Table 2. The break of conjugation (B, C groups) permits the free rotation of the two moieties of the molecule and then two CT bands appear in spectrum at the lowest values of frequencies.

Table 2

The transition energies for CT Complexes and the ^1H-NMR shifts for the unsubstitued ethers from different groups

Ether	TCNE ν_{CT_I} (10^3 cm^{-1})	TCNE $\nu_{CT_{II}}$ (10^3 cm^{-1})	CHL $\nu_{CT_{II}}$ (10^{3}cm^{-1})	$-CH_2-$ δ (ppm)
A_1	17.10	25.76	25.24	5.00
B_1	19.60	25.52	24.64	4.92
C_1	18 40	25.22	24.22	4.86
D_1	—	26.00	—	5.13
E_1	20.00	25.80	23.64	5.04

Consequently, the number of CT bands is mainly determined by steric effects, although the energetic factors as the nature of the substituents appear as a possible explanation (comparison of A_3 and F_2 ethers) for this fact.

The second CT band is not due to the presence of some impurities; the elemental analysis and the appearance of the second band with the change of acceptor (CHL → TCNE) are arguments for this assertion. Furthermore, the experimental determination of the stoichiometry of the complex indicates only one kind of complex in solution.

Let us now examine the position of charge transfer absorption bands. The position of CT bands or the difference between the bands are criteria to estimate the electron-donating ability of the compounds in the charge-transfer process.[2,3,6,15,24]

The values $h\nu_{CT}$ listed in Tables 1, 2 clearly demonstrate the influence of nature, number or position of the substituents of the terminal benzene ring. For the A and E, F group ethers, for which the reaction sites in the electron-donor and acceptor remain the same (the terminal benzene ring, see 3.b), we try to correlate the transition energy of CT_{II} band with Hammett's constant, σ, of the substituents (or with the sum of the constants for more substituents).

We use the equation due to Argentar[5]:

$$pE_T = pE_T^0 + \rho\sigma \qquad (2) \qquad \text{in which:}$$

σ — is Hammett's constant

ρ, pE_T — are the slope and respectively the intercept, calculated by regression analysis.

pE_T — is the "extrathermodynamic function" of the transition energy, E_T

$$E_T = \frac{E_{CT}}{2.3\ RT} \qquad (3)$$

T is the absolute temperature
R is the constant of gases
E_{CT} is the CT transition energy per mole of the complex, readily obtained by spectroscopic measurements using the relationship (4):

$$E_{\mathrm{CT}} = N_0 h \nu_{\mathrm{CT}} \qquad (4)$$

N_0 is Avogadro's number
h is Planck's constant
ν_{CT} is the frequency at which the differential absorption of the complex is maximum. We establish the equation:

$$\text{Ethers group A: } pE_T = 1.74 + 0.23\,\sigma;\ r = 0.85 \qquad (5)$$

$$\text{Ethers group E, F: } pE_T = 1.72 + 0.18\,\sigma;\ r = 0.89 \qquad (6)$$

The experimental values for compounds with three adjoining substituents (A_4 or E_4, F_3 ethers) are larger than those E_T calculated by equations (5) and (6) (see the figure 1); the reason for this might be some steric hindrance effect which is not included in Hammett's constant. Probably, the same effect causes, as we pointed out above, only one CT band, instead of two, in electronic spectra. Furthermore, Trofimov[27] which has studied the effects of structure of ethers on the ionization potential, indicated a ~10% contribution of hyperconjugation effects against the inductive and mesomeric effects of substituents. The value pE_T, of ether E_3 (substituent NO_2) was excluded (a test for outliers [27] — 95% confidence interval). The exceptional behaviour of this derivative can be interpreted by formation of one extended molecular orbital between unshared electrons of the nitrogen atom and π electrons of the benzene ring; the electronic spectrum of E_3 ether[21] being essentially different as compared with the spectra of other ethers, support this explanation.

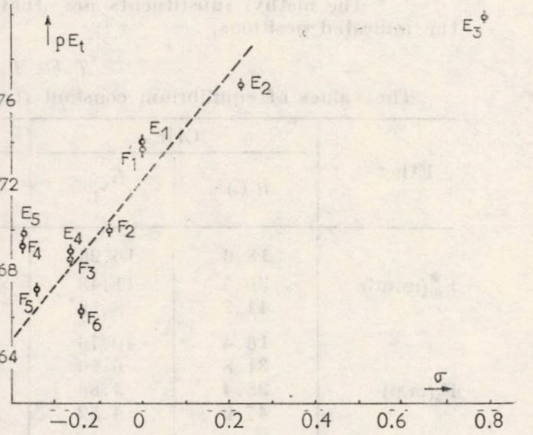

Fig. 1. — Transition energy dependence of the CT complexes (group E,F) on Hammett's constant.

In Table 1 we reproduce the values calculated for transition energies by Huckel's method[25] which are in fair agreement with the experimentally found values.

b. The structure of the complex

For alkyl aryl ethers, acting as donors in molecular complexes, two hypotheses are possible: the electron involved in transition is given by oxygen atom or by π system of one of aromatic rings (terminal or central).

Table 3

The values of equilibrium constants or the AAE complexes with CHL (at room temperature)

Ether	$\nu_{CT} \times 10^3 (cm^{-1})$		$K_{\nu_{II}}$	Ether	$\nu_{CT} \times 10^3 (cm^{-1})$		$K_{\nu_{II}}$
	I	II	(L/mol)		I	II	(L/mol)
$A_1(-)$	—	25.24	0.62	$E_1(-)$	20.30	23.64	0.98
$A_2^*(p)$	—	24.78	1.41	$F_1(-)$	20.26	23.60	1.26
$A_3(m)$	—	24.38	2.24	$F_2(m.CH_3)$	20.02	23.32	5.68
$E_4(0,m)$	—	23.34	2.40	$F_5(m,p)$	19.96	23.29	10.00
$E_5(0,p)$	—	24.28	2.45	$F_6(m,m)$	19.93	23.20	15.90
$F_3(0,m)$	—	23.98	3.15	—	—	—	—
$F_4(0,p)$	—	23.72	5.31	—	—	—	—

* The methyl substituents are situated on the terminal aromatic rings in the indicated positions.

Table 4

The values of equilibrium constant (L/mol) at different temperatures

Ether	CHL		TCNE		
	$t(°C)$	$K_{\nu_{II}}$	$t(°C)$	K_{ν_I}	$K_{\nu_{II}}$
$F_6^*(m,m')$	18.6	16.96	15.2	—	47.7
	30.5	11.48	28.2	—	26.5
	41.7	8.18	41.8	—	15.1
$F_5(m,p)$	16.4	10.76	15.7	20.0	16.2
	31.8	6.96	27.4	13.5	11.5
	38.4	5.86	40.8	9.5	7.5
	47.9	4.52	—	—	—
$F_2(m)$	18.2	6.46	12.1	9.10	9.10
	32.8	4.41	28.0	5.78	5.80
	48.3	3.05	41.8	4.09	4.07
$F_4(0,p)$	15.6	5.97	16.2	5.43	6.25
	31.5	4.81	27.4	4.31	4.94
	49.3	4.17	40.8	3.34	3.82
$E_5(0,p)$	20.8	2.45	12.7	4.81	5.86
	37.6	2.50	27.2	3.59	4.38
	46.8	1.86	40.8	2.80	3.42
$E_1(-)$	16.9	1.06	15.0	4.21	5.70
	31.7	0.89	25.2	3.45	4.67
	46.9	0.75	40.6	2.62	3.54
$A_1(-)$	13.6	0.67	—	—	—
	22.4	0.60	—	—	—
	36.4	0.52	—	—	—

* The methyl substituents are situated on the terminal aromatic rings in the indicated positions.

The solid complexes (obtained by evaporation of the saturated solution of complex under atmosphere of vapours of solvent) were examined by IR, UV, ^{1}H-NMR spectroscopy and also by X-ray diffraction.

The results of elemental analysis of the solid complexes lead to a ratio of one molecule donor to one molecule acceptor, in agreement with the data obtained for CT complex in solution.

The spectra of solid complexes as against the spectra of each of partners indicate as reaction sites one of terminal benzene rings. So, in IR spectra, in the region assigned to β_{C-H} vibration of aromatic nucleus ($800-1000\ cm^{-1}$) a considerable change in number, position and intensity of the bands arises.

This conclusion can be also drawn by the unaltered position and intensity of ν_{asym} C—O—C band, although very sensitive to the changes of electronic environment.

The substituents of the central aromatic nucleus have smaller influence than the substituents of the terminal ring upon the electron-donating properties of the ethers (see Table 1, $h\nu_{CT}$ values or Tables 3 — 6, K, ΔH° values).

Table 5

The thermodynamic properties determined for the equilibrium AAE+CHL

	$-CH_3$*	Number of CT bands	$-\Delta H$ (kcal/mol)	$-\Delta G^0_{298}$ (kcal/mol)	$-\Delta S$ (u.e.)	$\nu_{CT\ II}$ $\times 10^3\ cm^{-1}$
E_1	—	2	2.12	1.60	1.75	25.64
F_2	m	2	4.62	2.62	6.70	23.32
F_5	m,p	2	4.97	2.88	7.00	23.24
F_6	m,m	2	5.76	3.18	8.66	23.20
A_1	—	1	1.89	1.31	1.95	25.24
E_5	o,p	1	2.19	1.94	0.84	24.28
F_4	o,p	1	2.37	2.14	0.78	23.72

* The methyl substituents are situated on the terminal aromatic rings in the indicated positions.

Table 6

The thermodynamic properties determined for the equilibrium AAE+TCNE

$-CH_3$*	ν_I CT Bands			ν_{II} CT Bands				
	$-\Delta H$ (kcal/mol	$-\Delta G^0_{298}$	$-\Delta S^\circ$ (u.e.)	$-\Delta H$ (kcal/mol)	$-\Delta G^0_{298}$	$-\Delta S^\circ$ (u.e)	CT II $\times 10^3$ (cm^{-1})	$\Delta_{\nu_{I-II}}$ $10^3(cm^{-1}$
E_1—	3.32	2.36	3.2	3.36	2.53	2.65	25.80	5.80
E_5o,p	3.43	2.40	3.4	3.40	2.51	3.05	23.44	5.60
F_4o,p	3.57	2.51	3.5	3.51	2.59	3.22	23.10	5.42
F_2m	4.80	2.71	7.0	4.82	2.71	7.00	23.60	4.60
F_5m,p	5.34	3.22	7.1	5.31	3.10	7.52	22.00	4.00
F_6m,m	—	—	—	7.80	3.67	13.8	21.00	1.28

* The methyl substituents are situated on the terminal aromatic rings in the indicated positions.

All the signals of protons in a solid complex (the ^{1}H-NMR spectrum) are shifted to the stronger field (deshielding) comparatively to the signals of protons in uncomplexed ether ; this points out why the formation of D_2A complex is not favoured.

The measurements by X-rays diffraction indicate one singular (individual) compound, with weak linkages with a parallel positions of the molecules of donor and acceptor ; the last condition is required for the existence of the two isomeric configurations, described by Voight[3] and associated with the two CT bands.

c. The estimation of equilibrium constants and thermodynamic properties

In Tables 3 and 4 we list the values obtained for the equilibrium constants of molecular complexes of ethers with CHL or TCNE, and in Tables 5 and 6 we present the thermodynamic values. These values, *K*, ΔH°, Δ*G*° have a good correlation with the frequencies of CT absorption bands or with the difference between the two bands. One example is given in figure 2, the other properties have analogous variations. One can

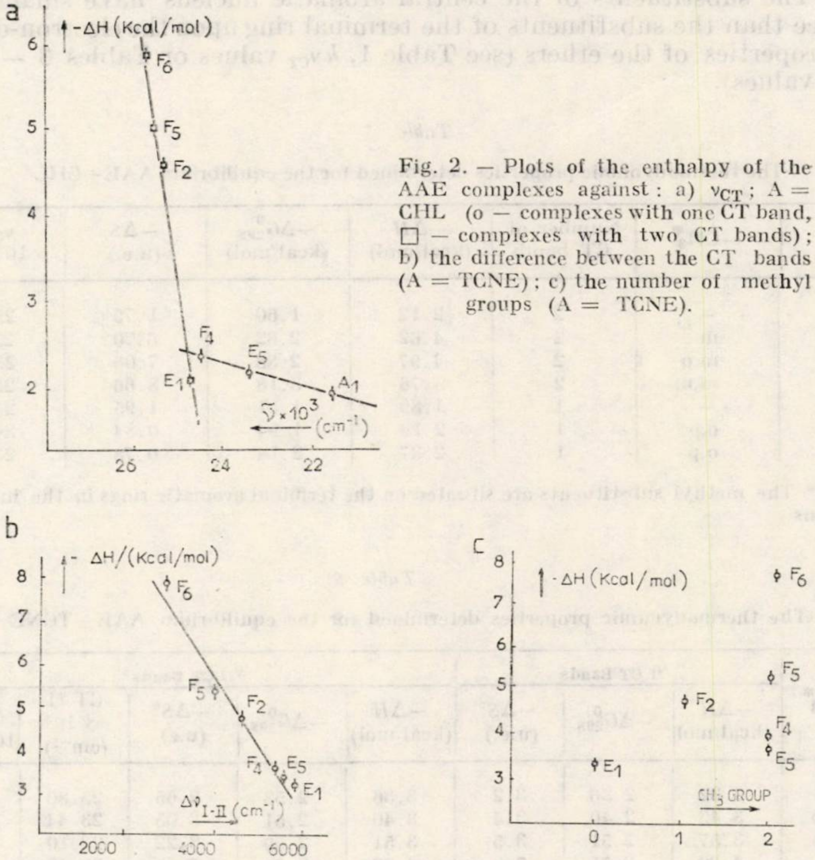

Fig. 2. — Plots of the enthalpy of the AAE complexes against : a) ν_{CT} ; A = CHL (o — complexes with one CT band, □ — complexes with two CT bands) ; b) the difference between the CT bands (A = TCNE) ; c) the number of methyl groups (A = TCNE).

observe the existence of two trends of variation as a function of the number of CT bands. The plots of thermodynamic properties, ΔH°, ΔG°, ΔS°, against the number of methyl groups of the terminal nucleus reflect, as in the previous discussion, the effect of steric hindrance of the *ortho* substituents. The photoelectron spectra [28] of the derivatives of anisol proved the decrease of interpenetration of the molecular orbital between unshared electrons of oxygen atom and π electrons (which is maximal in phenol or anisol) in the compounds with *ortho* substituents, as against methoxy group. This fact involves the constraint of the methoxy group outside the plane and the decrease of donating properties for these derivatives.[5,9,10]

The values obtained for K and ΔH°, ΔG°, ΔS° are in good agreement with the other data previously reported by different authors.[4,6,9,10,16,24]

The assignment for one terminal benzene nucleus, as reaction site of donor, is also supported by the fair agreement between equation (7) (which gives the variation of ΔG° as a function of ionization potential of ethers) and equation (8) reported by Merrifield [16] for methylbenzenes. In both cases the acceptor was the same, TCNE.

$$-\Delta G^\circ = 0.0510\ I_D - 11.25(\text{kcal}) \tag{7}$$

$$-\Delta G^\circ = 0.053\ I_D - 13.57(\text{kcal}) \tag{8}$$

d. The influence of the solvent upon the properties of CT complexes

With the increase of dielectric constant, D, of the solvent, and with the decrease of refractive index, n, the charge transfer bands shift to higher values of the wavenumbers. We established the following equation:

$$pE_T = 2.45 - 2.92\frac{n^2-1}{n^2+2} + 0.054\frac{D-1}{D+2} \tag{9}$$

This equation has a similar form to the equation for the complexes $n \to v$ reported by Argentar, [5] but coefficients of equation (9) have smaller values. This is not a surprising fact because the shifts of the CT bands are smaller in the complexes of AAE($\pi-\pi$ complexes) than in the case of strong complexes. The values determined for the parameters of equation (9) prove that the refractive index term is of primary importance in determination of the transition energies of CT complexes.

REFERENCES

[1] G. Briegleb, "Electron Donor — Acceptor Komplexe", Springer Verlag, Berlin, Göttingen, 1962, S. 98.
[2] A. R. Lepley, *Tettrahedron Letters*, **1968**, 2823.
[3] E. M. Voight, *J. Amer. Chem. Soc.*, **86**, 3611 (1964).
[4] W. Weschke, *J. Prakt. Chem.*, **321**, 605 (1979).
[5] H. Argentar, *J. Research. Nat. Brev. Standards*, **80A**, 173 (1976).
[6] A. Giurgiu, A. Truţia and V. Vântu, *Bull. Inst. Petrol Gaze*, **18**, 15 (1972).
[7] J. Bendig and B. Doleslav, *Z. phys. Chem. (Leipzig)*, **258**, 297 (1977).
[8] J. Bendig, *Z. phys. Chem. (Leipzig)*, **258**, 699 (1977).
[9] S. Santini, *J. Chem. Soc., Perkin II.*, 1956 (1974).

[10] J. W. Jones, *J. Chem. Soc., Farad. Trans. I.*, **70**, 1908 (1974).
[11] P. G. Farrell and J. Newton, *J. Phys. Chem.*, **69**, 3506 (1965).
[12] R. S. Mulliken, *J. Phys. Chem.*, **56**, 801 (1952).
[13] R. S. Mulliken, *J. Amer. Chem. Soc.*, **74**, 811 (1952).
[14] R. S. Mulliken, *Ann. Rev. Phys. Chem.*, **73**, 107 (1962).
[15] L. E. Orgel, *J. Chem. Phys.*, **23**, 1352 (1955).
[16] R. E. Merrifield and W. D. Phillips, *J. Amer. Chem. Soc.*, **80**, 2779 (1958).
[17] M. Iovu and F. Ispas, *Rev. Chim. (București)*, **30**, 841 (1979).
[18] M. Iovu. *Rev. Roumaine Chim.*, **16**, 1223 (1971).
[19] M. Iovu. *Rev. Roumaine Chim.*, **17**, 1261 (1972).
[20] M. Iovu and E. M. Vasilescu, *Rev. Roumaine Chim.*, **27**, 629 (1982).
[21] M. Iovu, F. Chiraleu and E. M. Vasilescu, *Rev. Roumaine Chim.*, **25**, 1383 (1980).
[22] P. Job., *Ann. Chim. (France)*, **9**, 113 (1928).
[23] M. Ciureanu, Thesis, Fac. Chimie, Univ. Buc., 1977.
[24] F. Kuboyama, *Nippon Kagaku Kaishi*, **12**, 2269 (1973).
[25] A. Căilean and C. Mandravel, *Bul. Inst. Politeh. Buc., Chimie-Metalurgie*, **53**, 65 (1980).
[26] B. A. Trofimov, *Izvest. Akad. Nauk S.S.SR. Ser. Kim.*, **12**, 2731 (1970).
[27] P. D. Lark, B. R. Craven and R. C. L. Bosworth, "The Handling of Chemical Data", Pergamon Press, Oxford, 1968, p. 153–6.
[28] P. S. Dewar and J. R. Gilmore, *Tetrahedron*, **30**, 2455 (1974).

Revue Roumaine de Chimie, 31, 6, 615–624 (1986)

SYNTHESIS AND BIOLOGICAL ACTIVITY OF CERTAIN NICOTINIC ACID DERIVATIVES

A.N. OSMAN, M.M. ISMAIL and M.A. BARAKAT*
Organic Chemistry and Biochemistry* Departments, Faculty of Pharmacy,
Cairo University, Egypt

Received April 27, 1985

A simple procedure for the synthesis of 3-ethoxycarbonyl-4,6-dimethyl-2-pyridone (I) is described. The reaction of I with $NaOC_2H_5$ affords the corresponding sodio derivative II, which reacts readily with certain alkyl and acyl halides to give exclusively the O-alkyl and O-acyl derivatives III. Structures of the reaction products were determined using both chemical and spectroscopic methods. Biological screening of some of the newly synthesized compounds revealed that they exhibit antihyperlipidaemic activity.

INTRODUCTION

Nicotinic acid was originally used in the treatment of pellagra and circulatory disorders as it produces short but marked dilatation of blood vessels; in addition it reduces the serum triglyceride and cholesterol levels.[1,2] Out of a large number of nicotinic acids substituted in the pyridine ring the 5-chloro, the 2-hydroxy and the 2-methylnicotinic acids inhibited the fatty acid and cholesterol biosynthesis and showed greater

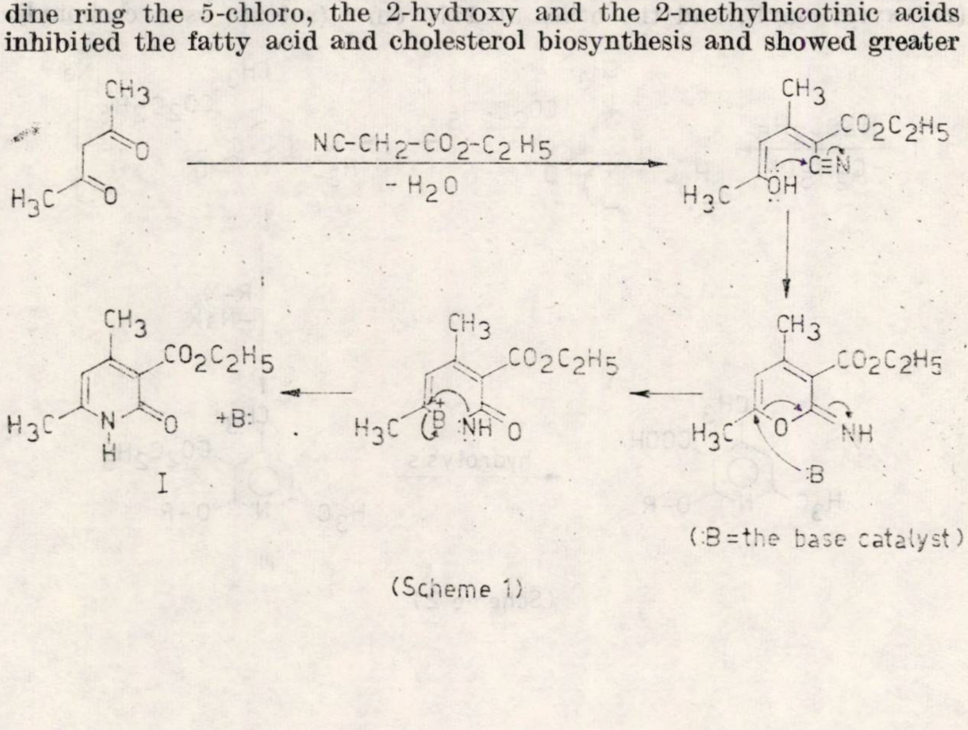

(Scheme 1)

activity than the unsubstituted nicotinic acid.[3-6] Consequently we decided to synthesize certain nicotinic acid derivatives devoid of drawbacks of nicotinic acid and evaluate them as antihyperlipidaemic agents.

DISCUSSION

Although the synthesis of 3-ethoxycarbonyl-4,6-dimethyl-2-pyridone (I) has been reported earlier,[7] the procedure described therein was however tedious and hence it is simplified in the present work by using ethanol as a solvent and triethylamine as base catalyst to obtain I in the same reported yield. Thus the condensation of acetylacetone and ethyl cyanoacetate might involve a base-catalysed intramolecular rearrangement of an imidol form to the expected more stable amidic structure.

Pyridone I reacts with $NaOC_2H_5$ to afford sodium salt II, which behaves as ambident anion. According to Kornblum et al.,[8] the negative charge in such an ambident nucleophile will be more resident on the oxygen atom, not only in consequence of the greater electronegativity of oxygen than the nitrogen atom, but also because this maximizes the aromatic character of the heterocyclic nucleus. The reaction of salts of 2-pyridones with alkyl and acyl halides has been reported to afford only the O-derivatives[8-10] or a mixture of N- and O-derivatives.[11-13]

However in the present work the reaction of II with certain alkyl and acyl derivatives led to the production of the corresponding O-derivatives (Scheme 2); no N-derivatives could be detected using TLC and IR spectroscopy.

The IR spectra of the ethyl nicotinate derivatives IIIb-d showed one carbonyl absorption band at 1725 cm^{-1} which is assignable to the ester carbonyl. Diester IIIa showed two intense carbonyl bands : one at 1725cm^{-1} (ethoxycarbonyl), and the other at 1770 cm^{-1} (acetate ester carbonyl).

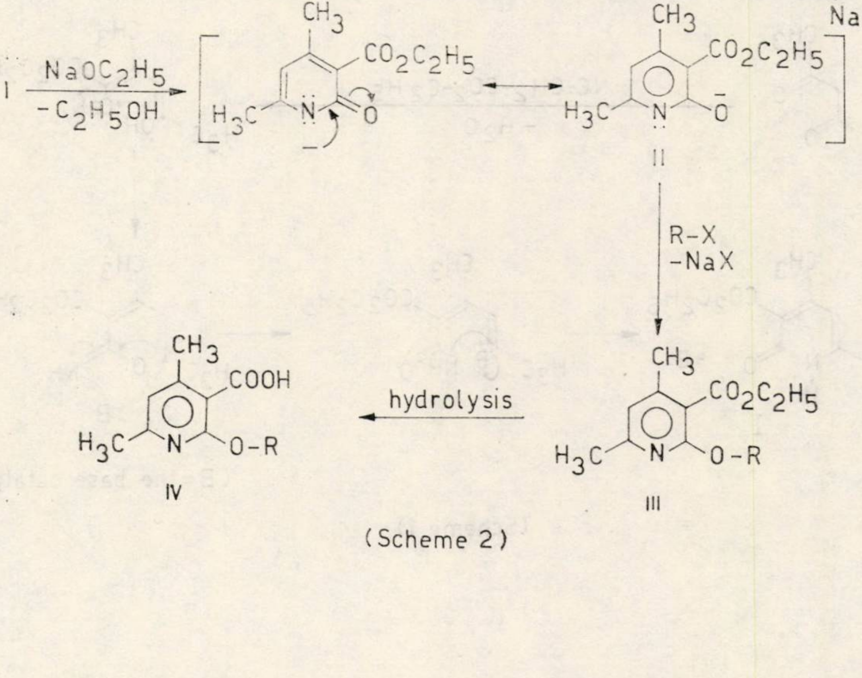

(Scheme 2)

At the same time NH and/or the OH bands in the IR spectra of the compounds III were absent.

The ^{1}H-NMR spectra of III(a-d) showed the following general signals: δ 1.35 ppm (triplet, CH_3, $J = 7.5$ Hz); δ 2.25 ppm (singlet, CH_3 at 6-position); δ 2.45 ppm (singlet, CH_3 at the 4-position); δ 4.35 ppm (quartet, CH_3, $J = 7.5$ Hz), and δ 6.9 ppm (singlet, CH at the 5-position). The acetyl group protons in the diester IIIa appeared as a singlet at δ 2.35 ppm. The latter chemical shift value was assigned to the CH_3 group of 2-acetoxypyridines rather than the N-acetyl isomers.[11] The off resonance ^{13}C-NMR spectrum of IIIa exhibited six singlets, a doublet, a triplet and four quartets as illustrated in table 1.

Table 1

The ^{13}C-NMR spectrum or IIIa

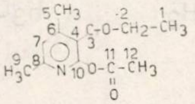

Chemical shift (δ), ppm.	Assignment	Signal multiplicity
168.78	C–3	singlet
165.28	C–11	singlet
159.42	C–10	singlet
155.75	C–4	singlet
150.80	C–6	singlet
124.25	C–7	doublet
118.49	C–8	singlet
61.49	C–2	triplet
23.93	C–12	quartet
20.99 20.93	C–5, C–9	quartets
14.22	C–1	quartet

Reaction of II with epichlorohydrin ended with the formation of propanol-2 derivative Va, but neither the epoxide Vb, nor the halogen compound Vc could be detected even when equimolecular amounts of reactants were used. This may be ascribed to the large nucleophilicity of II (Scheme 3).

The IR spectrum of the reaction product Va showed a doublet band at about 1710 cm^{-1} ($COOC_2H_5$), and a broad OH absorption at 3350 cm^{-1}. Its ^{1}H-NMR spectrum showed the following signals: δ 1.40 ppm. (triplet, 6H, 2 CH_3-CH_2-, $J = 7$ Hz); δ 2.25 ppm. (singlet, 6H, 2 CH_3-attatched at the 6-position of the pyridine ring); δ 2.45 ppm. (singlet, 6H, 2 CH_3-attached at the 4-position of the pyridine ring); δ 3.3 ppm. (multiplet, 1H, $-\overset{|}{C}H-$); δ 4.20 ppm. (doublet, 4H, 2-CH_2-O); δ 4.35 ppm. (quartet, 4H, 2 CH_3-CH_2-, $J=7$ Hz); δ 5.30 ppm. (broad signal, 1H, OH) and δ 6.05 ppm. (singlet, 2H, pyridine hydrogens at the 5-position). The broad signal at δ 5.30 ppm. disappeared upon deuteration.

The mass spectrum of compound Va showed the molecular ion peak at m/e 446. The prominent peaks may be outlined by the following frag-

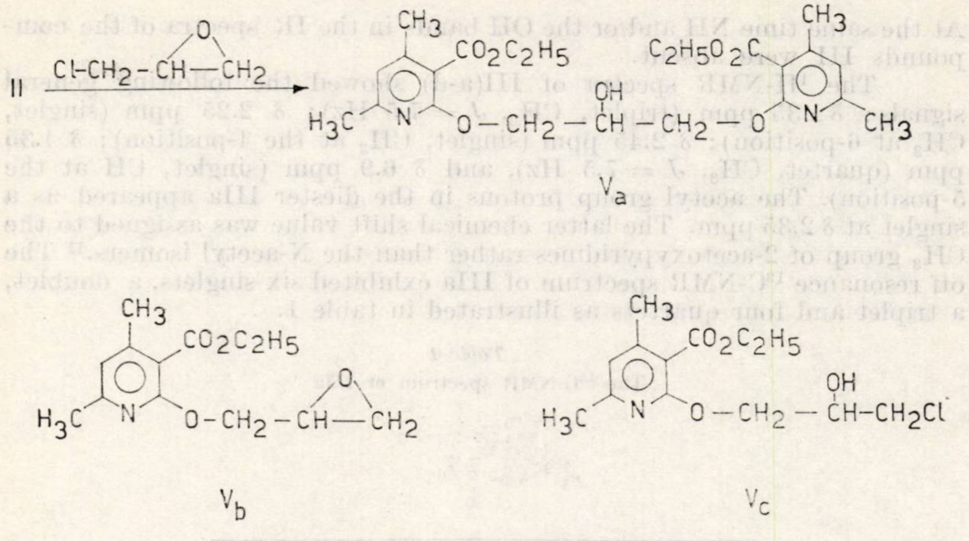
II
Cl-CH2-CH—CH2
Va
Vb
Vc

(Scheme 3)

mentation scheme :

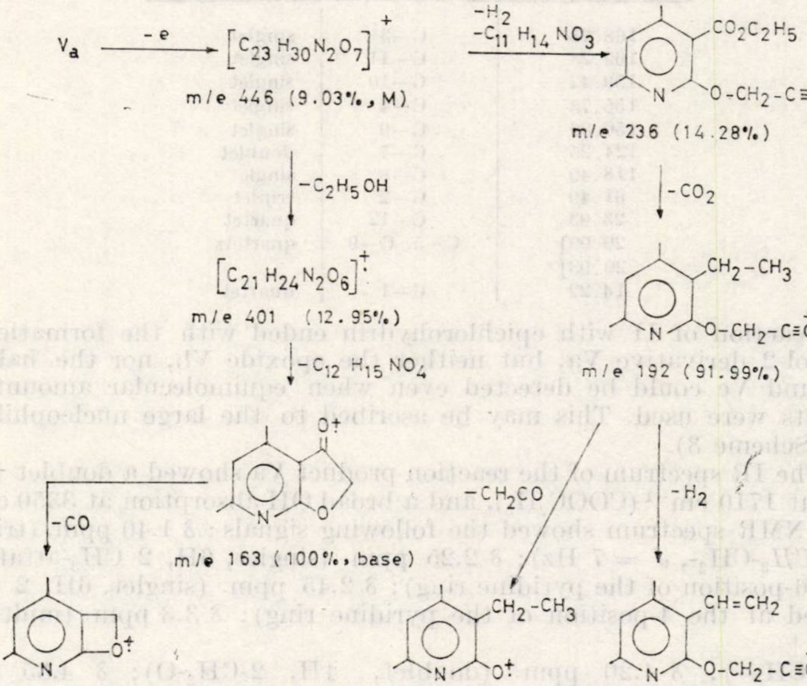
Va
- e
[C23 H30 N2 O7]+
m/e 446 (9.03%, M)
-H2
-C11 H14 NO3
m/e 236 (14.28%)
-C2H5OH
[C21 H24 N2 O6]+
m/e 401 (12.95%)
-CO2
m/e 192 (91.99%)
-C12 H15 NO4
-CO
-CH2CO
-H2
m/e 163 (100%, base)
m/e 135 (10.03%)
m/e 150 (55.3%)
m/e 190 (28.68%)

(Scheme 4)

Hydrolysis of the esters IIIb-d and Va by hydroalcoholic KOH did afford the corresponding carboxylic acids IVb-d and Vd respectively.

BIOLOGICAL ACTIVITY

Evaluation of reducing power of mixed hyperlipidaemia

Mixed hyperlipidaemia is a collective term, used to describe the human condition when elevated concentrations of lipids are present in the blood plasma. Since this condition is strictly related to atherosclerosis, the development of antihyperlipidaemic agents is a major aim of medical research at present. [3]

Induction of hyperlipidaemia

Mature male rats weighing 140—160 g were fed for 80 days on hyperlipidaemic diet (7 g of this diet for each rat daily).[14−18] The latter consisted of : casein 10%, hydrogenated oil 22%, carbohydrate 60% (sucrose and starch in equal amounts), cholesterol 2%, sodium cholate 1%, choline chloride 0.3%, vitamin mixture 2% and salt mixture 3%.[18] Rats were maintained at constant environmental conditions throughout the whole experimental period.

Design of the experimental work

A group of rats were decapitated on the 35th day to ascertain the existence of hyperlipidaemia, the remainder were divided into five groups : groups I—IV were given an oral dose of 3 mg/200 g. body weight of nicotinic acid, IIIa (AM-1), IIIb (AM-2), and IIIc (AM-3) respectively. Group V was injected subcutaneously with isotonic saline solution (on the 35th day of feeding the hyperlipidaemic diet) for 45 days and served as hyperlipidaemic control.

A group of rats was fed on normal diet consisting of : bread, vegetables and milk, and served as normal control. Each group comprised six mature male rats.

Tissue sampling

Rats were decapitated after fasting overnight, blood samples were collected in centrifuge tubes containing heparin, and then centrifuged at 2000 r.p.m. for 15 minutes. The separated plasma was transferred with a Pasteur pipette into another tube for subsequent lipid analysis.

Lipid analysis

Total phospholipids,[19,20] cholesterol and its esters,[21] triglycerides[22,23] and nonesterified fatty acids (NEFA)[24] were analysed using the reported methods. The summation of these lipid fractions afforded the total lipids. Statistical analysis and comparison of the effect of the tested compounds on lipids in hyperlipidaemic animals are shown in Table 2 and Fig. 1 respectively.

RESULTS

1. Hyperlipidaemic diet caused a significant increase in total lipids, phospholipids, cholesterol esters, free cholesterol and triglycerides.

2. Nicotinic acid treated animals showed a significant decrease in lipid fractions except NEFA (which was significantly increased) as compared with hyperlipidaemia but were still significantly higher than normal controls. AM-3 showed more or less similar results to nicotinic acid.

Table 2

Effect of hyperlipemia, nicotinic acid and nicotinic acid derivatives (AM-1, AM-2 and AM-3) on plasma total phospholipids, cholesterol, cholesterol esters, triglycerides, non-esterified fatty acids and total lipids (mg /100 mL plasma ± S.E.)

Groups / Lipids	Total phospholipids	Cholesterol	Cholesterol esters	Triglycerides	NEFA	Total lipids
Normal control	0.92 ± 0.02	0.19 ± 0.01	0.43 ± 0.02	0.71 ± 0.03	0.19 ± 0.004	2.44 ± 0.04
Hyperlipemic control	$1.78 \pm 0.04^{*}$	$0.36 \pm 0.02^{*}$	$0.82 \pm 0.03^{*}$	$1.88 \pm 0.04^{*}$	0.20 ± 0.01	$4.56 \pm 0.29^{*}$
Nicotinic acid	$1.10 \pm 0.07^{*}_{**}$	$0.24 \pm 0.01^{*}_{**}$	$0.52 \pm 0.03^{*}_{**}$	$1.21 \pm 0.05^{*}_{**}$	$0.23 \pm 0.01^{*}_{**}$	$3.31 \pm 0.08^{*}_{**}$
AM-1	$1.78 \pm 0.03^{*}$	$0.19 \pm 0.01^{*}_{**}$	$0.41 \pm 0.01^{*}_{**}$	$0.71 \pm 0.01^{*}_{**}$	$0.11 \pm 0.01^{*}_{**}$	$3.20 \pm 0.02^{*}_{**}$
AM-2	$1.73 \pm 0.03^{*}$	$0.25 \pm 0.02^{*}_{**}$	$0.57 \pm 0.01^{*}_{**}$	$0.91 \pm 0.01^{*}_{**}$	0.18 ± 0.01	$3.64 \pm 0.04^{*}_{**}$
AM-3	$1.43 \pm 0.04^{*}_{**}$	$0.27 \pm 0.01^{*}_{**}$	$0.72 \pm 0.03^{*}_{**}$	$0.84 \pm 0.03^{*}_{**}$	0.20 ± 0.01	$3.46 \pm 0.06^{*}_{**}$

N.B. : Mean values out of six ± S.E.
* Significant difference from control. ($P < 0.05$).
** Significant difference from hyperlipemia ($P < 0.05$)

3. The AM-1 treated rats showed normalization of cholesterol (free and esterified), triglycerides but total phospholipids was not affected as compared with the control hyperlipidaemic groups.

4. The AM-2 showed results similar to nicotinic acid except that the total phospholipids were not affected as compared with the hyperlipidaemic animals.

DISCUSSION

The condition of hyperlipidaemia has been extensively studied along with dietary and drug treatment of hyperlipoproteinemia.[25–29] In the present work, the hyperlipidaemia, induced by feeding caused marked alteration in certain aspects of lipid metabolism in rat tissues, and this result is fully compatible with literature.[30–32] Thus the elevation in plasma cholesterol in hyperlipidaemic rats could be attributed to sodium cholate, which facilitates the absorption of cholesterol,[33] and drains sulphur which in turn is essential for bile acids in the form of taurocholates.[34] Also it could be attributed to ingested dietary cholesterol [35] and the dietary fat which stimulates acetate incorporation into cholesterol. [36]

Seskind et al.[37] found that the predominance of saturated fat in the diet and addition of cholesterol with cholates increase cholesterol esterification of serum lipids. In addition the dietary sucrose is another factor for elevation of serum lipids,[38] and triglycerides.[39] The increased plasma phospholipids by hyperlipidaemic diet might be explained by increased tissue and liver phospholipid synthesis. [40]

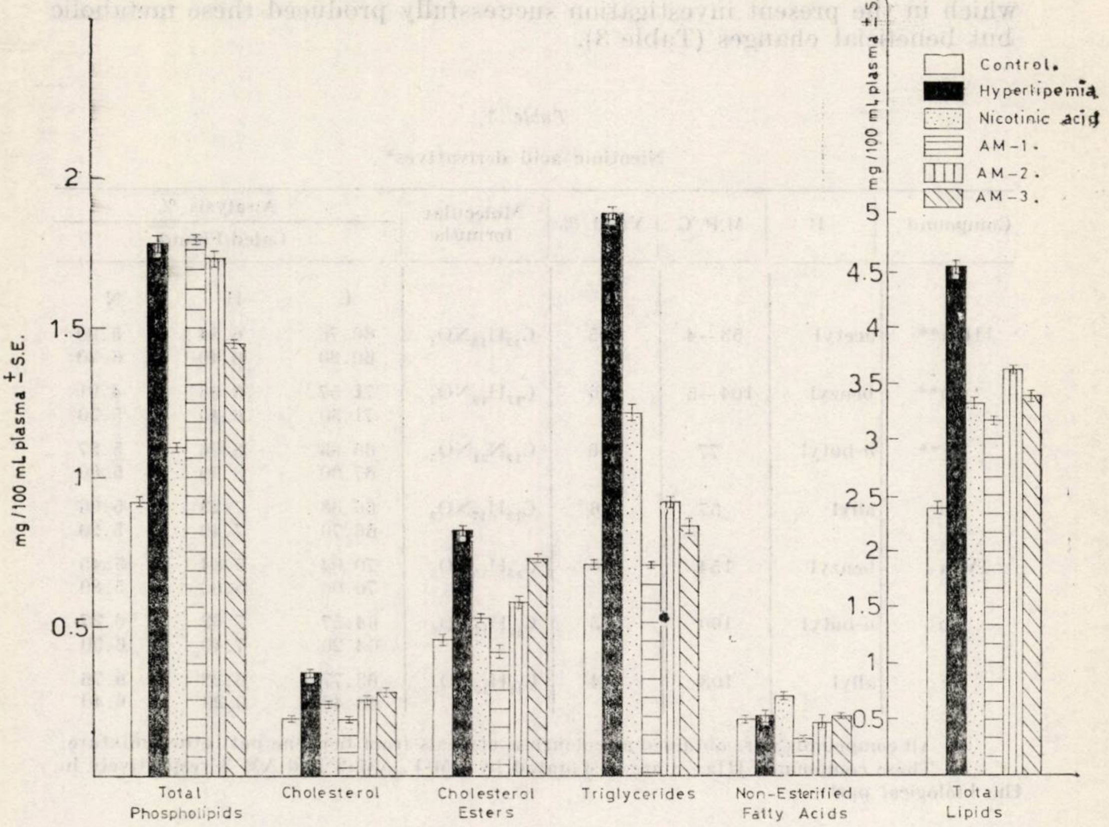

Fig. 1. — Effect of hyperlipidemia, nicotinic acid and its derivatives AM-1, AM-2, AM-3 on total lipids as well as differential lipids (mg/100 mL plasma ±S.E.).

Reduction of hyperlipidaemia by nicotinic acid and its derivatives was reported, and interpreted by the raised steroid excretion and inhibition of cholesterol synthesis from active acetate.[41-42] In addition nicotinic acid showed marked antilipolytic action[14] by preventing the release of NEFA and glycerol from fatty tissues, and decreases the synthesis and release of VLDL-TG from the liver.[3] May the antihyperlipidaemic effect, shown in the present work by the newly synthesized compounds (AM-1, AM-2 and AM-3), be produced by the same mechanism of action or not, this is a subject which requires further investigation.

CONCLUSIONS

Compounds AM-1, AM-2 and AM-3 showed reduction in the dietary-induced hyperlipidaemia in rats. Out of these compounds AM-1 seemed to be the best effective in reducing hyperlipidaemia to the normal lipid pattern extent. However, further studies are in progress concerning the toxicological, pharmacological and other biological activities of AM-1, which in the present investigation successfully produced these metabolic but beneficial changes (Table 3).

Table 3

Nicotinic acid derivatives*

Compound	R	M.P.°C	Yield %	Molecular formula	Analysis % Calcd/Found		
					C	H	N
III a**	acetyl	53—4	95	$C_{12}H_{15}NO_4$	60.76 60.80	6.54 6.40	5.90 6.20
b**	benzyl	104—5	36	$C_{17}H_{19}NO_3$	71.57 71.50	6.66 6.40	4.91 5.20
c**	*n*-butyl	77	56	$C_{14}N_{21}NO_3$	66.93 67.00	8.36 8.50	5.57 5.80
d	allyl	57	36	$C_{13}H_{17}NO_3$	66.38 66.70	7.23 7.40	5.96 5.90
IV a	benzyl	154	98	$C_{15}H_{15}NO_3$	70.04 70.00	5.84 5.60	5.45 5.80
b	*n*-butyl	160	85	$C_{12}H_{17}NO_3$	64.57 64.20	7.62 7.40	6.27 6.50
c	allyl	108	94	$C_{11}H_{13}NO_3$	63.77 63.40	6.28 6.20	6.76 6.40

* All compounds were obtained as colourless crystals from benzene/pet. ether mixture.

** These compounds IIIa—c are designated by AM-1, AM-2 and AM-3 respectively in the biological part.

EXPERIMENTAL

All mps are uncorrected and determined by the open capillary method. IR spectra are recorded with a Pye Unicam Sp 1100 spectrophotometer using KBr discs. The ^{1}H-NMR spectra were recorded on EM-390 90 MHz ^{1}H-NMR spectrometer using 5% deuterochloroform solution and TMS as internal standard. Mass spectra were determined on Finnigan Mat 312 mass spectrometer. ^{13}C-NMR-spectrum was carried out using Varian FT-80 ^{1}H-NMR-spectrometer using $CDCl_3$ solution (1%), and TMS as internal standard.

3-Ethoxycarbonyl-4,6-dimethyl-2-pyridone(I)

Ethyl cyanoacetate (22 g, 0.195 mole), acetylacetone (20 g, 0.20 mole) and triethylamine (2 mL) were dissolved in absolute ethanol (40 mL), and the resulting mixture was heated under reflux for 10 hours on a steam bath. Ethanol was distilled under diminished pressure and the residue was cooled to yield I as pale-yellow needles. It was washed with ether and recrystallized from ethanol. Yield 17 g (44.7%), m.p. 136°C (reported[7] : yield 44.7%, m.p. 135—6°C).

IR spectrum : 1650 cm^{-1} (pyridone carbonyl) ; 1725 cm^{-1} (ester carbonyl) ; 3150 and 3300 cm^{-1} NH and/or OH stretch).

^{1}H—NMR spectrum : δ 1.5 ppm (triplet, CH_3—CH_2—, $J = 7.5$ Hz) ; δ 2.4 ppm (singlet, 3H, CH_3 at 4-position) ; δ 2.45 ppm (singlet, CH_3 at the 6-position) ; δ 4.5 ppm (quartet, 2H, CH_3—CH_2—, $J = 7.5$ Hz) ; δ 6.1 ppm (singlet, 1 H at the 5-position) ; and δ 13.8 ppm (broad signal, disappears by deuteration, 1 H, NH or OH).

3-Ethoxycarbonyl-4,6-dimethyl-2-pyridone sodium salt II

5.0 g of the ester I (0.025 mole) was dissolved in 50 mL of absolute ethanol. Sodium ethoxide (1.70 g, 0.025 mole) in 25 mL of absolute ethanol was gradually added with stirring to the ester solution. Upon cooling a white crystalline precipitate of the sodium salt II separated out, which was filtered off and washed several times with absolute ethanol. Yield 5.4 g (almost quantitative), m.p. 198—200°C.

Ethyl 2-acetoxy-4,6-dimethylnicotinate IIIa

The mixture of 2 g of sodium salt II (0.01 mole), 2 mL of acetyl chloride (0.02 mole) and 20 mL of dry benzene was heated under reflux for 30 minutes, then cooled and filtered. Benzene was distilled off from the filtrate and the solid residue was recrystallized (Table 3).

Ethyl 2-alkoxy-4,6-dimethylnicotinates IIIb-d

A mixture of the sodium salt II (2 g, 0.01 mole), the suitable alkyl (or aralkyl) bromide (0.01 mole) and dimethylformamide (10 mL) was heated under reflux on a steam-bath for 2 hours. After cooling, the reaction mixture was poured into 50 mL of ice-cold water, and then extracted three times with benzene. The combined benzene extract was washed twice with water then dried over anhydrous Na_2SO_4. Benzene was distilled off under vacuum, and residue was recrystallized (Table 3).

2-Substituted-4,6-dimethylnicotinic acids IVb-d

Esters IIIb-d (0.02 mole) were hydrolyzed by heating under reflux with 20 mL of 20% (w/v) hydroalcoholic KOH solution for 2 hours (or till clear solution). After cooling and filtration, the clear filtrate was acidified with dil. HCl till pH = 4. The white precipitate thus produced was filtered off and recrystallized (Table 3).

1,3-bis(3-ethoxycarbonyl-4,6-dimethyl-2-pyridyloxyl)propan-2-ol Va

4.0 g of the sodium salt II (0.02 mole), 10 mL of dimethylformamide and 1.2 mL (0.01 mole) of epichlorohydrin were stirred well at room temperature for 3 hours. The reaction mixture was then poured into 60 mL of ice cold water, the white precipitate was collected and recrystallized from benzene/petroleum ether mixture to yield 2.1 g (94%)), m.p. 150°C.

Analysis. Calcd. for $C_{23}H_{30}N_2O_7$: C, 61.43 ; H, 6.72 ; N, 6.28
found : C, 61.40 ; H, 6.40, N, 6.50%

1,3-bis(3-carboxy-4,6-dimethyl-2-pyridyloxy)propan-2-ol Vd

This compound was prepared by hydrolysis of the corresponding ester Va, applying the same general procedure used for the preparation of the acids IVb-d, and was recrystallized from aqueous ethanol. Yield. 92%, m.p. 246°C (eff.).

Analysis. Calcd for $C_{19}H_{22}N_2O_7$: C, 58.46 ; H, 5.64 ; N, 7.18
found : C, 58.40 ; H, 6.50 ; N, 6.80%

REFERENCES

[1] R. Altshul, A. Hoffer and J. D. Stephen, *Arch. Biochem., Biophys.*, **54**, 558 (1966).

[2] W. B. Parsons, R. W. Archor and K. G. Berge, *Meet. Mayo Clin.*, **31**, 377 (1956); D. Bronx and O. Selvaag, *Acta Med. Scand.*, **182**, 437 (1967); N. Svedmyr, *Acta Pharmacol. Toxicol.*, **25**, 29 (1968): H. Kitagama, K. Higo., T. Naruke and T. Irikura, *Chem. Pharm. Bull.*, **19**, 552 (1971).

[3] G. P. Ellis and G. B. West, "Progress in Medicinal Chemistry", 11 North-Holland Publishing Company Amsterdam, Oxford, 1975, p. 124.

[4] A. R. Sarker and M. K. De, *Calcutta Med. J.*, **77**, 40—7, (1980).

[5] N. Mitchell, W. T. Robinson, D. Jean and D. Duscan, *Biochem. Pharmacol.*, **28**, 1163—7, (1979).

[6] N. E. Stjernstrom, *Acta Pharm. Suecica*, **9**, 221 (1972).

[7] J. L. Simonson and M. Nayak, *J. Chem. Soc.*, **107**, 792–8 (1915).

[8] N. Kornblum, R. A. Smiley, R. K. Blackwood and D. C. Iffland, *J. Amer. Chem. Soc.*, **77**, 6269 (1955).

[9] P. A. Singgih and M. J. Janssen, *Tetrahedron Letters*, **1971**, 4223–4.

[10] A. E. Tschitschibabin and P. G. Szokow, *Ber. dtsch. chem., Ges.* **58**, 2650 (1925).

[11] A. Mckillop, M. J. Zelesko and E. C. Taylor, *Tetrahedron Letters*, **1968**, 4945.

[12] D. Y. Curtin and L. L. Miller, *J. Amer. Chem., Soc.*, **89**, 637 (1967).

[13] M. T. Bogert and H. A. Sell, *J. Amer. Chem. Soc.*, **29**, 517 (1907).

[14] L. A. Carlson, *Progr. Biochem. Pharmacol.*, **3**, 151 (1967).

[15] J. J. Vitale, P. L. White, M. Nakamura, D. M. Hegsted, M. Zamacheck and E. E. Hellerstin, *J. Exptl. Med.*, **106**, 757 (1957).

[16] W. F. Cuthbertson, P. V. Elcoate, D. M. Ireiand, D. C. Mills, and P. Shearley, *Brit. J. Nutrition*, **13**, 227 (1959).

[17] H. M. Shue and E. L. Hove, *J. Nutrition*, **71**, 303 (1960).

[18] W. A. Thomas and W. S. Hartroft, *Circulation*, **19**, 65 (1959).

[19] R. M. Broekhuyse, *Biochemica et Biophysica Acta*, **152**, 307 (1968).

[20] C. H. Fiske and Y. Subbarow, *J. Biol. Chem.*, **66**, 375 (1925).

[21] D. Webster, *Clin. Chim. Acta*, **7**, 277 (1962).

[22] M. J. Fletcher, *Clin. Chim. Acta*, **22**, 393 (1968).

[23] L. B. Foster and R. T. Dunn, *Clin. Chem.*, **19**, 388 (1973).

[24] W. G. Duncombe, *Biochem. J.*, **88**, 7 (1963).

[25] L. H. Krut, *Brit. J. Clin. Pract.*, **22**, 517 (1968).

[26] D. F. Davies, *J. Atherosclerosis Res.*, **10**, 253 (1969).

[27] H. Selye, "Experimental Cardiovascular Diseases", Springer Verlag, New York (1970).

[28] R. J. Havel, *Mod. Med.*, **40**, 78 (1972).

[29] D. Kritchevski "Search for New Drugs", p. 261 (1972).

[30] C. Carroll, *J. Nutrition*, **79**, 93 (1963).

[31] P. Vijayagopalan and P. A. Kurup, *Atherosclerosis*, **11**, 257 (1970).

[32] P. Vijayagopalan and P. A. Kurup, *Atherosclerosis*, **15**, 215 (1972).

[33] M. D. Siperstein, "Current Topics In Cellular Regulation" Vol. 2, p. 65, Academic Press, London (1970).

[34] L. C. Fillios, S. B. Andrus, G. N. Mann and F. J. Stare, *J. Exptl. Med.*, **104**, 539 (1956).

[35] I. L. Chaikoff, *J. Biol. Chem.*, **191**, 407 (1952).

[36] K. K. Carroll, *J. Amer. Chem. Soc.*, **44**, 607 (1967).

[37] C. R. Seskind, *Proc. Soc. Exptl. Biol. Med.*, **102**, 90 (1969).

[38] A. M. Cohen, *Biochem. Biophys. Acta*, **279**, 129 (1972).

[39] D. J. Naismith, *Nutr. Metab.*, **16**, 295 (1974).

[40] C. Mukherjee, *J. Nutrition* **101**, 713 (1971).

[41] T. A. Miettinen, *Clin. Chim. Acta* **20**, 43 (1968a).

[42] T. A. Miettinen, *Scand. J. Clin. Lab., Inves.*, **21**, suppl. **101**, 20 (1968b).

Revue Roumaine de Chimie, **31**, *6*, 625–627 (1986)

SYNTHESES OF AROMATIC THIOUREAS

C.I. CHIRIAC
"P. Poni" Institute of Macromolecular Chemistry, Aleea Ghica-Vodă 41 A, Jassy, Romania

Received February 25, 1985

Aromatic thioureas are prepared in good yields through reaction of aromatic amines and carbon disulfite in the presence of dimethylchloroformiminium chloride prepared *in situ* (from dimethylformamide and thionyl chloride). The reaction proceedes in pyridine solution at 40–50° for 5–6 hours.

Reactions of carbon dioxide or carbon disulfide with amines have been studied extensively from the biochemical point of view using different reagents with phosphore,[1] dicyclohexylcarbodiimide [2] etc. For the syntheses of thioureas from amines and carbon disulfide, phenyldichlorophosphite was used as reagent. [3]

RESULTS AND DISCUSSION

A precious communication from this laboratory showed that ethylene chlorophosphite is a useful reagent in syntheses of thioureas.[4]

Dimethylchloroformiminium chloride (DMCFC), prepared from dimethylformamide (DMF) and thionyl chloride, has many applications for syntheses of isonitriles from formamides, [5] of nitriles from amides, [6] for the formylation of dimethylaniline, [7] etc. In this work we have investigated a new application of DMCFC as reagent in synthesis of aromatic thioureas from aromatic amines and carbon disulfide. At the beginning we used pure DMCFC, [8] but in order to simplify the procedure we prepared DMCFC *in situ* from thionyl chloride and DMF. [5] Thus by heating at 40–50° for 5–6 hours, one mole of carbon disulfide with two moles of aniline in pyridine as solvent and a solution formed from 1 mole + + 10 % excess thionyl chloride in DMF as reagent, diphenylthiourea resulted with 70 % yield (a small excess of reagent improves the yield). The same yield is obtained when the reaction takes place at room temperature for 24 hours. With aliphatic amines, impure products resulted.

We suppose that this reaction involves the following mechanism :

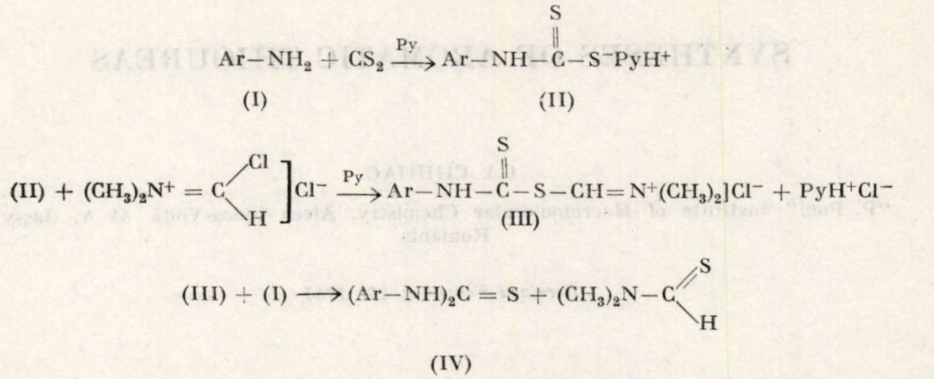

$$\mathrm{Ar{-}NH_2} + \mathrm{CS_2} \xrightarrow{\mathrm{Py}} \mathrm{Ar{-}NH{-}}\overset{\overset{\mathrm{S}}{\|}}{\mathrm{C}}\mathrm{{-}S^{-}PyH^{+}}$$

(I) (II)

$$\mathrm{(II)} + \left[\mathrm{(CH_3)_2N^{+}=C}\begin{matrix}\mathrm{Cl}\\ \mathrm{H}\end{matrix}\right]\mathrm{Cl^{-}} \xrightarrow{\mathrm{Py}} \mathrm{Ar{-}NH{-}}\overset{\overset{\mathrm{S}}{\|}}{\mathrm{C}}\mathrm{{-}S{-}CH=N^{+}(CH_3)_2]Cl^{-}} + \mathrm{PyH^{+}Cl^{-}}$$

(III)

$$\mathrm{(III)} + \mathrm{(I)} \longrightarrow \mathrm{(Ar{-}NH)_2C=S} + \mathrm{(CH_3)_2N{-}C}\begin{matrix}\mathrm{S}\\ \mathrm{H}\end{matrix}$$

(IV)

Therefore, by reaction between (I) and carbon disulfide in the presence of pyridine as a base, dithiocarbamic acid pyridinium salt (II) results, similar to other cases. [9,10] In the second stage (II) reacts with DMCFC prepared *in situ*, resulting a reactive compound (III) and $\mathrm{PyH^{+}Cl^{-}}$ as a by-product. In many other cases, [5,11] DMCFC gives reactive intermediates having similar structures with the compound (III). The reaction between (III) and (I), affording the final product (IV), involves a four-centred transition state (V), characteristic for many nucleophylic substitutions. [12,13]

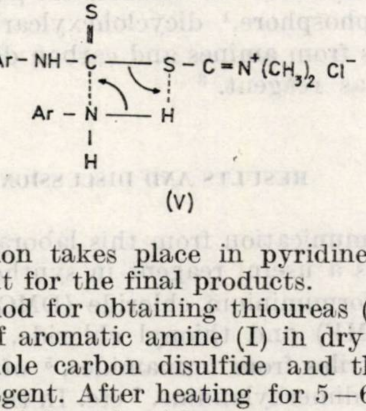

(V)

The above reaction takes place in pyridine, which is a suitable base and a good solvent for the final products.

The general method for obtaining thioureas (IV) consists, thus, in dissolving two moles of aromatic amine (I) in dry pyridine followed by the addition of one mole carbon disulfide and then a solution of one mole + 10 % excess reagent. After heating for 5–6 hours at 40–50° the final product was precipitated with water.

Table 1 shows that the yields ranged from 62 to 70 %.

In conclusion, we present in this work a new application of DMCFC (prepared *in situ*) for the synthesis of aromatic thioureas.

EXPERIMENTAL

Dimethylchloroformiminium chloride (DMCFC) prepared in situ

To 3 mL dry DMF in a dropping funnel, 1.5 mL (0.02 moles + 10 % excess) thionyl chloride was added very slowly under shaking. This solution was kept for 1 hour at room temperature in the funnel closed by a stopper.

Table 1

Aromatic thioureas obtained from aromatic amines and CS_2 in the presence of DMCFC/Py as reagent

$(Ar-NH)_2C=S$[a] Ar	Yield[b] %	M.p.[c] °C	M.p. from literature[d] °C
C_6H_5	70	153–155	154–155
β-naphthyl	66	191–193	192–193
p-$CH_3-C_6H_4$	71	177–179	178–179
p-$Cl-C_6H_4$	62	173–175	173–174
p-$CH_3O-C_6H_4$	68	183–185	184–185
α-naphthyl	65	206–208	206–207
p-$Br-C_6H_4$	63	187–189	188–189

[a] The products were identified by comparison of m.p. and IR spectra with those of authentic samples.

[b] Yields determined by isolation of the crude products.

[c] After recrystallisation.

[d] From "Beilstein Handbuch der Organischen Chemie".

Diphenylthiourea

To 10 mL dry pyridine, 1.8 mL (0.02 moles) aniline and then 1.2 mL (0.02 moles) carbon disulfide were added under stirring. After 30 minutes, the solution of DMCFC prepared as above, was added from the dropping funnel very slowly under stirring and cooling. This solutions was stirred for 1 hour at room temperature, then 1.8 mL (0.02 moles) aniline were added. The obtained solution was stirred for 5–6 hours at 40–50° or for 24 hours at room temperature. At the end of reaction, the solution was poured into 70–100 mL of water with ice, when the diphenylthiourea precipitated. The solution was treated with 10 % HCl solution till pH = 1–2. The desired product was colected by filtration, washed with 40–50 mL 5 % NaOH solution and three times with 20–30 mL water.

After drying under vacuum at 100–120° and recrystallisation from ethanol, 3.2 g diphenylthiourea with m.p. 153–155° were obtained (mixed m.p. with pure diphenylthiourea undepressed). Yield 70 % (calculated on aniline employed).

Anal. calculated for: $C_{13}H_{12}N_2S$; C, 68.41; H, 5.21; N, 12.28 %. Found; C, 68.21; H, 5.37; N, 12.43 %.

In similar conditions, the other aromatic thioureas presented in table 1 were prepared

REFERENCES

[1] N. Yamazaki and F. Higashi, *Tetrahedron Lett.*, **1974**, 1191.

[2] T. Kobayassi and H. Ogura, *Synthesis*, **1978**, 394.

[3] T. Tomioka and F. Higashi, *Bull. Chem. Soc., Japan*, **49**, 3106 (1976).

[4] C. I. Chiriac, *Rev. Roumaine Chim.*, **29**, 329 (1984).

[5] H. W. Walborsky and G. E. Niznik, *J. Org. Chem.*, **37**, 187 (1972).

[6] E. A. Lawton and D. D. McRitchie, *J. Org. Chem.*, **24**, 26 (1959).

[7] H. H. Bosshard and H. Zollinger, *Helv. Chim. Acta.*, **42**, 1659 (1959).

[8] J. S. Roth and F. Doda, *J. Org. Chem.*, **34**, 1629 (1969).

[9] J. C. Jochims, *Chem. Ber.*, **101**, 1749 (1968).

[10] F. Craig and W. L. Davidson, *J. Polymer Sci.*, **8**, 312 (1952).

[11] P. A. Stadler, *Helv. Chim. Acta.*, **61**, 1075 (1978).

[12] H. O. Becker and K. F. Funk, *J. prakt. Chem.*, **14**, 55 (1961).

[13] B. Iselin and W. Rittel, *Helv. Chim. Acta*, **40**, 373 (1957).

Revue Roumaine de Chimie, **31**, *6*, 629–635 (1986)

SYNTHESIS AND REACTIONS OF SOME NEW 4-(*p*-SUBSTITUTED CINNAMOYL)PHENYL-3′,4′-XYLENE SULPHONATES OF EXPECTED POTENTIAL BIOLOGICAL ACTIVITY

O.M.O. HABIB, A.M. KHALIL, E.M. KANDEEL and E.B. ABDALLA
Chemistry Department, Faculty of Science, Mansoura University, Mansoura, Egypt

Received September 23, 1985

Condensation of 4-acetylphenyl-3′,4′-xylene sulphonate (I) with aromatic aldehydes gave chalcones (II). Reaction of IIa-d with hydrazine hydrate, phenylhydrazine, hydroxylamine hydrochloride, piperidine, morpholine and thiophenol has been studied. Michael condensation of IIa-d with ethyl acetoacetate, acetylacetone and ethyl cyanoacetate has also been investigated.

It has been reported in literature that chalcones and their analogues could be used as bactericides,[1,2] germicides,[3,4] cardiovascular sedative[5] and fertility[6] agents. It is also well known that the aromatic esters of aromatic sulphonic acids exhibit high biological activity.[7–9]

These facts have encouraged us to synthesize some new products containing both the chalcone and the sulphonate moieties and study their reactions with different reagents, hoping that structural variations will bring the corresponding modification in the properties of chalcones, which would, in turn, influence the biological activity.

This idea was followed by treating 3,4-xylene sulphonyl chloride with 4-hydroxyacetophenone in the presence of aqueous sodium hydroxide to give 4-acetylphenyl-3,4-xylene sulphonate (I). The structure of I has been established from the analytical data and IR spectrum which showed stretching frequencies at 1660 and 1340 cm^{-1} characteristic of the C=O and $SO_2 \cdot O$ groups, respectively.

Some new 4-(*p*-substituted cinnamoyl)phenyl-3′,4′-xylene sulphonates (II) were synthesized in the present work by the Claisen-Schmidt condensation of the 4-acetylphenyl-3′,4′-xylene sulphonate (I) with the appropriate aromatic aldehydes. The IR spectrum of IIa showed bands at 1675, 1668 and 1340 cm^{-1} attributable to the α, β-unsaturated ketones and the $SO_2 \cdot O$ groups, respectively.

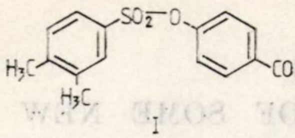

I

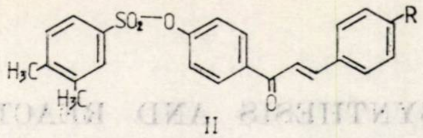

II

a $R = H$ c $R = Br$

b $R = OCH_3$ d $R = Cl$

It has been previously reported that treatment of α, β-unsaturated ketones with hydrazines in boiling ethanol[10,11] or benzene : ethanol mixture[12] affords the corresponding pyrazolines. Thus, compounds IIa-d were treated with hydrazine hydrate and with phenylhydrazine in benzene-ethanol mixture (1 : 1) to give the pyrazoline derivatives IIIa-g.

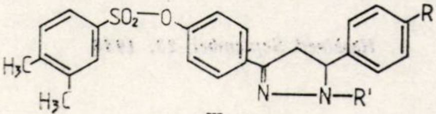

III

a $R = H$; $R' = H$

b $R = Br$; $R' = H$

c $R = Cl$; $R' = H$

d $R = H$; $R' = C_6H_5$

e $R = OCH_3$; $R' = C_6H_5$

f $R = Br$; $R' = C_6H_5$

g $R = Cl$; $R' = C_6H_5$

The IR spectra of compounds IIIa and IIId are in agreement with the proposed structures and showed the absence of the $C=O$ stretching frequency, but revealed bands at 1630–1620, 3300 and 1340 cm^{-1} attributable to the $C=N$, NH and SO_2-O groups, respectively.

On the other hand, condensation of the chalcones IIa-d with hydroxylamine hydrochloride in pyridine afforded the corresponding isoxazoline derivatives IVa-c. The IR spectra of IVa showed a band at 1640 cm^{-1} characteristic of the $C=N$ group.

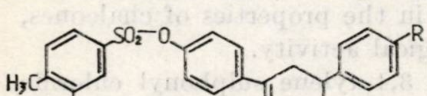

IV

a $R = H$

b $R = OCH_3$

c $R = Br$

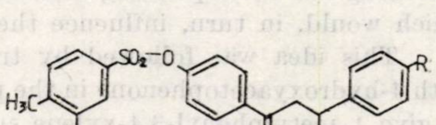

a $R = H$ V $R' = NC_5H_{10}$

b $R = OCH_3$ VI $R' = NC_5H_8O$

c $R = Br$ VII $R' = SC_6H_5$

d $R = Cl$

Reactions of α, β-unsaturated ketones with secondary amines[13] and mercaptans[14] lead to the formation of the corresponding hydrocinnamoyl derivatives. Thus, in the present work, compounds IIa-d were treated with piperidine, morpholine or thiophenol to give 4-(β-piperidino, β-morpholino, or thiophenyl-hydrocinnamoyl) phenyl-3,4′-xylene sulphonates (V), (VI) and (VII), respectively.

The IR spectra of these compounds showed bands at 3060, 1675 and 1340 cm^{-1} attributable to the enolized carbonyl, C=O and SO_2-O groups, respectively.

It has been previously reported that condensation of α, β-unsaturated ketones with ethylacetoacetate or acetylacetone yields the corresponding cyclohexenone derivatives.[15] Thus, compounds IIa-d were condensed with these two reagents in the presence of piperidine as a base to give 4-(4″-ethoxycarbonyl-3-oxo-5-aryl-1-cyclohexene-1-yl)phenyl-3,4-xylene sulphonates (VIIIa-c) and 4-(4″-acetyl-3-oxo-5-aryl-1-cyclohexene-1-yl) phenyl-3,4-xylene sulphonates (IXa-c). These products were characterised by analytical data and IR spectra revealing bands at 1755, 1660, 1650 and 1590 cm^{-1} characteristic of the acetyl, ester, six membered carbonyl and the C=C groups, respectively.

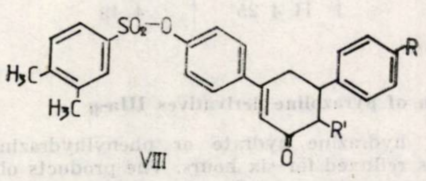

VIII

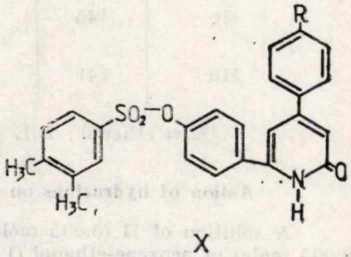

X

VIII R′ = $CO_2C_2H_5$
a R = H
b R = OCH_3
c R = Br

IX R′ = $COCH_3$
a R = H
b R = Br
c R = Cl

a R = H
b R = OCH_3
c R = Br
d R = Cl

On the other hand, it is known that pyridone derivatives are synthesized *via* the condensation of α, β-unsaturated ketones with ethyl cyanoacetate.[16] Thus, compounds IIa-d were condensed with this reagent in the presence of excess ammonium acetate to yield 4-(4″-aryl-3″-cyano-2″-oxo-pyridine)phenyl-3′,4′-xylene sulphonates (Xa-d).

The structure of Xa-d has been established by analyses and IR spectra which showed bands at 3090, 2200 and 1660 cm^{-1} attributable to the NH, C≡N and CONH groups, respectively.

EXPERIMENTAL

IR spectra were measured with a Unicam SP 1100-Spectrophotometer using KBr wafer technique. Elemental analyses were determined by the microanalytical unit, Mansoura University. All melting points are uncorrected.

Preparation of 4-acetylphenyl-3′,4′-xylene sulphonate (I)

This compound was prepared according to the general method described by Dale and Hennis.[17] It was crystallised from methanol as white crystals; m.p. 63°C; (yield 40 %). Found: C, 63.42; H. 5.16; S, 10.12; $C_{16}H_{16}O_4S$, required: C, 63.14; H, 5.30; S, 10.53 %.

Preparation of 4-(p-substitued cinnamoyl)phenyl-3'4'-xylene sulphonates (IIa-d)

To a mixture of I(0.03 mole) and the appropriate aldehyde (0.03 mole) in ethanol (25 mL), 6 mL of 10 % sodium hydroxide were added. The reaction mixture was refluxed for 30 minutes and the solid product which separated on cooling was filtered and crystallised from the suitable solvent to give IIa-d (Table 1).

Table 1
Characterisation of compounds IIa-d

Compound	m.p.(°C)	Solvent* Yield (%)	Formula	Analysis (%) Found	Required
IIa	116	E 50	$C_{23}H_{20}O_4S$	C 70.11 H 4.96	70.39 5.14
IIb	102	E 50	$C_{24}H_{22}O_5S$	C 68.08 H 5.07	68.23 5.25
IIc	145	B/E 64	$C_{23}H_{19}O_4BrS$	C 58.21 H 4.00	58.61 4.06
IId	141	B/E 70	$C_{23}H_{19}O_4ClS$	C 64.51 H 4.25	64.71 4.49

*E = ethanol ; B/E = benzene/ethanol

Action of hydrazines on IIa-d. Formation of pyrazoline derivatives IIIa-g

A solution of II (0.005 mole in each case), hydrazine hydrate or phenylhydrazine (0.005 mole) in benzene-ethanol (1 : 1 ; 60 mL) was refluxed for six hours. The products obtained after concentration and cooling were crystallised from benzene-ethanol to give the pyrazoline derivatives IIIa-g (Table 2).

Table 2
Characterisation of compounds IIIa–g

Compound	m.p.(°C)	Solvent* Yield (%)	Formula	Analysis (%)	
				Found	Required
IIIa	81	B/E 40	$C_{23}H_{22}N_2O_3S$	C 67.64 H 5.12	67.94 5.45
IIIb	151	B/E 41	$C_{23}H_{21}N_2O_3BrS$	C 56.60 H 4.00	56.90 4.36
IIIc	85	B/E 60	$C_{23}H_{21}N_2O_3ClS$	C 62.31 H 4.42	62.63 4.80
IIId	145	B/E 63	$C_{29}H_{26}N_2O_3S$	C 71.99 H 4.99	72.17 5.43
IIIe	61	B/E 63	$C_{30}H_{28}N_2O_4S$	C 70.45 H 5.20	70.28 5.50
IIIf	130	B/E 61	$C_{29}H_{25}N_2O_3BrS$	C 61.73 H 4.21	62.02 4.49
IIIg	148	B/ED 55	$C_{29}H_{25}N_2O_3ClS$	C 66.99 H 4.52	67.35 4.87

* B/E = benzene/ethanol.

Action of hydroxylamine hydrochloride on IIa-c. Formation of isoxazole derivatives IVa-c

A mixture of IIa-c (0.005 mole in each case), hydroxylamine hydrochloride (0.005 mole) and pyridine (50 mL) was heated under reflux for six hours. The reaction mixture was diluted with water and the products obtained were crystallised from ethanol to give the isoxazole derivatives IVa-c (Table 3).

Table 3

Characterization of compounds IVa—c

Compound	m.p.(°C)	Solvent* Yield(%)	Formula	Analysis (%) Found	Required
IVa	184	E 40	$C_{23}H_{21}NO_4S$	C 67.62 H 5.01	67.78 5.19
IVb	139	E 42	$C_{24}H_{23}NO_5S$	C 65.70 H 5.00	65.89 5.30
IVc	168	E 45	$C_{23}H_{20}NO_4BrS$	C 56.50 H 3.90	56.79 4.14

* E = ethanol

Addition of piperidine or morpholine to chalcones IIa-d. Formation of V and VI

A solution of IIa-d (0.005 mole in each case) and piperidine or morpholine (0.005 mole) in dry benzene (50 mL) was stirred and heated at 60°C for 30 minutes. The reaction mixture was allowed to stand overnight at room temperature, after which light petroleum ether 40—60°C was added. The precipitates were crystallised from the appropriate solvent to give yellow crystals of Va-d and VIa-d (Tables 4 and 5).

Table 4

Characterisation of compounds Va—d

Compound	m.p.(°C)	Solvent* Yield (%)	Formula	Analysis (%) Found	Required
Va	108	E 50	$C_{28}H_{31}NO_4S$	C 70.50 H 6.20	70.40 6.54
Vb	110	E 50	$C_{29}H_{33}NO_5S$	C 68.43 H 6.40	68.61 6.55
Vc	149	E 68	$C_{28}H_{30}NO_4BrS$	C 60.61 H 5.44	60.42 5.43
Vd	135	B/M 60	$C_{28}H_{30}NO_4ClS$	C 65.32 H 5.53	65.67 5.90

*E = ethanol ; B/M = benzene/methanol.

Table 5

Characterisation of compounds VIa—d

Compound	m.p.(°C)	Solvent* Yield (%)	Formula	Analysis (%) Found	Required
VIa	112	E 50	$C_{27}H_{29}NO_5S$	C 67.99 H 6.24	67.61 6.09
VIb	108	E 50	$C_{28}H_{31}NO_6S$	C 66.39 H 6.25	65.98 6.13
VIc	138	B/E 48	$C_{27}H_{28}NO_5BrS$	C 58.28 H 5.34	58.06 5.05
VId	135	E 50	$C_{27}H_{28}NO_5ClS$	C 63.39 H 5.18	63.08 5.49

* ethanol ; B/E = benzene/ethanol.

Addition of thiophenol to chalcones IIa-d. Formation of VIIa-d.

To a mixture of chalcones IIa-d (0.005 mole in each case), thiophenol (0.005 mole) and benzene (50 mL). 0.5 mL of piperidine was added and the mixture was stirred with heating at 60°C for 30 minutes. After standing overnight at room temperature, light petroleum ether 40—60°C was added. The separated solid products were filtered and crystallised from the proper solvent to give VIIa-d (Table 6).

Table 6

Characterisation of compounds VIIa—d

Compound	m.p.(°C)	Solvent * Yield (%)	Formula	Analysis (%)	
				Found	Required
VIIa	123	M 50	$C_{29}H_{26}O_4S_2$	C 69.54 H 5.45	69.30 5.21
VIIb	108	M 45	$C_{30}H_{28}O_5S_2$	C 67.99 H 5.07	67.65 5.30
VIIc	136	B/M 57	$C_{29}H_{25}O_4BrS_2$	C 60.11 H 4.55	59.89 4.33
VIId	120	B/M 50	$C_{29}H_{25}O_4ClS_2$	C 64.52 H 4.31	64.85 4.69

* M = methanol ; B/M = benzene/methanol.

Condensation of IIa-d with ethyl acetoacetate or acetylacetone. Formation of VIIIa-c and IXa-c

A solution of IIa-c (0.01 mole in each case), ethyl acetoacetate or acetylacetone (0.01 mole) in *n*-butanol (50 mL) containing 1.0 mL of piperidine, was refluxed for 8 hrs. The reaction mixture was added to dilute hydrochloric acid, and the formed products were filtered and crystallised from the suitable solvent to give VIIIa-c and IXa-c (Tables 7 and 8).

Table 7

Characterisation of compounds VIIIa—c

Compound	m.p.(°C)	Solvent * Yield(%)	Formula	Analysis (%)	
				Found	Required
VIIIa	124	E 42	$C_{29}H_{28}O_6S$	C 69.63 H 5.41	69.03 5.59
VIIIb	125	B/E 45	$C_{30}H_{30}O_7S$	C 67.63 H 5.91	67.40 5.66
VIIIc	138	B/E 42	$C_{29}H_{27}O_6BrS$	C 59.36 H 4.31	59.69 4.66

* E = ethanol ; B/E = benzene/ethanol.

Table 8

Characterisation of compounds IXa—c

Compound	m.p.(°C)	Solvent* Yield(%)	Formula	Analysis (%)	
				Found	Required
IXa	159	B/E 40	$C_{28}H_{26}O_5S$	C 71.02 H 5.31	70.86 5.52
IXb	85	B/E 42	$C_{28}H_{25}O_5BrS$	C 60.53 H 4.21	60.76 4.55
IXc	95	B/E 42	$C_{28}H_{25}O_5ClS$	C 66.34 H 5.01	66.07 4.95

*B/E = benzene/ethanol.

Condensation of IIa-d with ethyl cyanoacetate. Formation of Xa-d

A mixture of IIa-d (0.01 mole in each case), ethyl cyanoacetate (0.01 mole) and ammonium acetate (0.08 mole) in *n*-butanol (10 mL) was refluxed for 10 hrs. The solids that were obtained after cooling were filtered and washed successively with water and ethanol. Crystallisation from acetic acid gave Xa-d (Table 9).

Table 9

Characterisation of compounds Xa – d

Compound	m.p.(°C)	Solvent* Yield (%)	Formula	Analysis (%)	
				Found	Required
Xa	258	A	$C_{26}H_{20}N_2O_4S$	C 68.11	68.39
		45		H 4.21	4.41
Xb	213	A	$C_{27}H_{22}N_2O_5S$	C 66.32	66.64
		42		H 4.20	4.56
Xc	265	A	$C_{26}H_{19}N_2O_4BrS$	C 58.00	58.31
		45		H 3.21	3.58
Xd	258	A	$C_{26}H_{19}N_2O_4ClS$	C 63.29	63.59
		45		H 3.52	3.90

*A = acetic acid.

REFERENCES

[1] M. El-Deek, M. A. I. Salem, A. A. Hamed and M. Samaan, *Rev. Roumaine Chim.*, **26**, 775 (1981).
[2] S. S. Misra and Bhola Nath, *Indian J. Appl. Chem.*, **34**, 200 (1971).
[3] S. S. Misra and A. Labdev, *J. Sci. Tech.* (India), **8**, 152 (1971).
[4] S. C. Kushwaha and J. B. Lal. *Indian J. Chem.*, **5**, 82 (1967).
[5] S. S. Misra and S. Dinkar, *J. Indian Chem. Soc.*, **52**, 556 (1975).
[6] S. S. Misra and S. C. Kushwaha, *J. Indian Chem. Soc.*, **52**, 564 (1975).
[7] L. Geppson, *J. Econ. Entomot.*, **44**, 823 (1951).
[8] J. M. Barners, *J. Econ. Entomol.*, **41**, 672 (1951).
[9] K. Marshall, *Canad. J. Chem.*, **3**, 598 (1954).
[10] A. Essawy, M. El-Garby Younes, M. M. Badran and A. Z. M. Heikal, *Rev. Roumaine Chim.*, **26**, 245 (1981).
[11] A. Abdel Maksoud, G. Hosni, O. Hassan and S. Shafik, *Rev. Roumaine Chim.*, **23**, 1541 (1978).
[12] E. M. Afsah, F. A. Amer and H. Etman, *Z. Naturforsch., B : Anorg. Chem., Org. Chem.* **34**B, 502 (1979).
[13] N. Cromwell and J. Burch, *J. Amer. Chem. Soc.*, **66**, 872 (1944).
[14] A. Sammour and M. Elkassaby, *U.A.R J. Chem.*, **13**, 243 (1970).
[15] A. Sammour, A. Marei and M. H. M. Hussein, *J. Chem. U.A R.*, **12**, 451 (1969).
[16] I. I. Abd El-Gawad, A. M. Kaddah, A.m. Khalil, O. M. O. Habib and H. Al-Rifai, *Indian J. Chem.*, **21B**, 37 (1982).
[17] W. J. Dale and H. E. Hennis, *J. Amer. Chem. Soc.*, **78**, 2543 (1956).

Revue Roumaine de Chimie, **31**, *6*, 637–645 (1986)

ASPECTOS MECANISTICOS Y SINTETICOS DE LA OXIDACION ANODICA DEL 1,4-DIMETOXIBENCENO

OLGA PÉREZ de MÁRQUEZ
Facultad de Ciencias
Departamento de Química
Laboratorio de Electroquímica
Universidad de Los Andes
Mérida, Venezuela

Recibido: el 3 de Junio de 1985

The electrochemical oxidation of 1,4-dimethoxyebenzene at platinum electrode with dry acetonitrile and tetrabulylammonium tetrafluoroborate as electrolytic medium is considered. The voltammetric, chronoamperometric and Specular Modulated Reflectance Spectroscopy results, show ECE mechanism behavior with a reversible first electron transference leading to a cation radical, which undergoes a further nucleophilic attack by the acetonitrile. A second electron transference occurs, and a further hydrolysis produces 2,5-dimethoxybenzyl acetamide as the main reaction product. The use of pulsing electrolysis, in conjunction with a cationic exchange resin, increases the yield of the acetamide which reaches a value of 34% with respect to the starting material concentration.

En este trabajo se hace un estudio mecanístico amplio de la oxidación electroquímica del 1,4-dimetoxibenceno sobre electrodo de platino en acetonitrilo seco/tetrafluoroborato de tetra-n-butil amonio como medio electrolítico. Los resultados voltamétricos, cronoamperométricos y de espectroscopía de Reflectancia Especular Modulada, muestran el seguimiento de un mecanismo del tipo EQE por este compuesto en la oxidación electroquímica, con transferencia reversible del primer electrón y conducente a la formación de un radical catión, el cual posteriormente sufre una reacción química nucleofílica, lenta, de ataque por el solvente acetonitrilo. Una segunda transferencia electrónica y la hidrólisis posterior, permiten la obtención de la 2,5-dimetoxibencilacetamida como producto principal. La utilización conjunta del método de electrólisis por pulsos y de una resina de intercambio catiónico, permiten un incremento considerable en el rendimiento material de la acetamida, la cual alcanza un valor de 34% con respecto al material de partida.

INTRODUCCION

Los compuestos alcoxiaromáticos han sido ampliamente estudiados por métodos electroquímicos,[1–13] quizás por el efecto estabilizante de los grupos electrodonantes sobre los radicales cationes, lo cual ha permitido la propuesta de varios esquemas de reacción. En particular, el 1,4-dimetoxibenceno produce las especies intermediarias más estables en esta serie, por lo cual presenta condiciones apropiadas para un detallado estudio mecanístico.

La cianuración, metoxilación y acetoxilación de metoxibencenos han sido extensamente estudiadas,$^{1-3,14-17}$ y en todos estos casos se ha propuesto la formación del radical catión como la especie primaria producida sobre el electrodo. También hay coincidencia en cuanto a que la oxidación anódica de metoxibencenos puede seguir un mecanismo del tipo EQE^{14,18} y a que el decaimiento del radical catión ocurre por ataque nucleofílico y no por pérdida de un protón.

La conjunción sobre un mismo estudio de diversas técnicas electroquímicas, acoplado a un análisis preciso de los productos formados, permiten una mayor confiabilidad en las conclusiones que de allí se deriven. Desde el punto de vista sintético, la comercialización de las mismas por métodos electroquímicos continúan siendo un reto, y se hace necessario por ello, en cada uno de estos estudios, el considerar diversos aspectos de interés sintético, que amplíen la información existente en esta importante área de la electroquímica moderna.

EXPERIMENTAL

Reactivos

Acetronitrilo de fisons, grado UV se destiló sobre P_2O_5 a presión atmosférica. El destilado se recogió sobre $KMnO_4$ y fué redestilado a 5 ml/min y almacenado sobre alúmina neutra Woelm grado super.

El Tetrafluoroborato de tetra-n-butilamonio se preparó por un procedimiento modificado de Claru, Fleishmann y Pletcher[19]. El sulfato ácido de tetra-n-butilamonio (339 gr) se disolvió en 2 lt de agua tridestilada y se mezcló con 1 lt de solución acuosa de 110 gr. de tetrafluoroborato de sodio. El precipitado formado (fluorobrato de tetra-n-butilamonio) se filtró y disolvió en 200 ml de diclorometano y esta solución se lavó con tres porciones de 300 ml de agua tridestilada, la solución de diclorometano se filtró y vertió sobre éter. Los cristales precipitados de $Bn_4{}^nNBF_4$ fueron finalmente doble purificados por disolución en dicloroetano, lavado con agua tridestilada y posteriormente vertida en éter. El precipitado se secó al vacío a 80°C por 48 horas.

Equipo

Los experimentos de voltametría cíclica se realizaron utilizando un potenciostato Hi-Teck modelo DT 2101 y un generador de functiones H-Teck tipo PPR1. Los voltamogramas se registraron, directamente en un registrador X—Y de la Hewlett Packard modelo 7015-B a velocidades de barrido de potencial lentos, o utilizando un osciloscopio de memoria digital 054100 de la Gould Advance a velocidades de barrido superiores a los 0,7 $V.s^{-1}$.

En los experimentos cronoamperométricos se utilizó el mismo equipo que fuera utilizado en los experimentos de voltametría cíclica a velocidades altas de barrido del potencial.

Los experimentos de coulombimetría preparativa utilizaron adicionalmente un integrador de corriente, de construcción en el laboratorio.

En los experimentos, ópticos la fuente de luz la constituyó un arco Hg-Xe de 200 watts (Engelhard Hanovia 901-B1) colocada en una caja especial (oriel optical comp. 6165) con un ventilador incorporado. La lámpara se acopló con un monocromador de la Baush y Lamb. Los rayos de salida del monocromador y entrada e al detector se enfocaron con lentes de distancia focal 2,5 cm de thermal syndicate Ltd. Un fotomultiplicador EM1625613, y un fotodiodo UDT500 se utilizaron como detectores. Los componentes ópticos se montaron sobre un banco óptico de la longitud requerida, y el detector sobre un banco óptico independiente y perpendicular al primero. El arreglo óptico, con excepción de la lámpara y el monocromador estuvieron ubicados en el interior de una caja negra.

Celdas y Electrodos

En los experimentos de voltametría cíclica y cronoamperimétricos, se utilizó una celda de tres electrodos y dos compartimientos. El electrodo de trabajo lo constituyó un alambre de platino con 0,2 cm^2 de área geométrica. El electrodo secundario lo constituyó un cilindro de malla de platino que rodeó al electrodo de trabajo, permitiendo un arreglo altamente simétrico. El electrodo de referencia la constituyó un electrodo de $Ag/AgNO_3$ (0,01M) en solución de acetonitrilo-Bn_4 $^nNBF_4$ (0,1M), y un capilar luggin separó el electrodo de referencia del compartimiento del electrodo de trabajo.

Los experimentos de coulombimetría preparativa se realizaron con la utilzación de una celda de tres compartimientos. Los electrodos de trabajo y contraelectrodo fueron en este caso mallas planas y paralelas de platino con áreas geométricas de 2 cm^2, cada uno, separadas entre sí por dos discos de vidrio sinterizado Nº 3 que minimizaron la mezcla del anolito y catolito. El anolito estuvo permanentemente agitado y con burbujeo de gas inerte (N_2), se usó una resina catiónica (DOWEK 500 W-X8, 100—200 mesh) en el compartimiento de trabajo durante la electrólisis para atrapar el intermediario y simplificar la reacción. Se utilizó la misma referencia que en los experimentos anteriormente señalados.

Los experimentos ópticos se realizaron utilizando una celda óptica típica, construída con vidrio pyrex, excepto las ventanas ópticas, hechas con discos de ,,spectrosil''. El electrodo de trabajo lo constituyó un espejo de platino en forma de disco, montado sobre el émbolo de una jeringa. El electrodo secundario fué un disco de platino, paralelo al electrodo de trabajo y a una distancia de 3 cm del mismo. La referencia, al igual que en los otros experimentos la constituyó el electrodo de $Ag/AgNO_3$. El ángulo de incidencia del rayo de luz sobre el electrodo de trabajo fué de 45°. El electrodo de trabajo se pulió con alúmina de grados decrecientes, se le hizo un tratamiento químico con mezcla 1 : 1 de $HNO_3(c)/H_2SO_4(c)$ en caliente, lavado con agua tridestilada y secado al vacío a 30°C.

Las celdas y el material de vidrio utilizado se trataron con acetona, agua destilada, mezcla 1 : 1 de $HNO_3(c)/H_2SO_4(c)$ en caliente, agua tridestilada en ebullición y secado al vacío a 100°C previo a su destilación.

RESULTADOS

Voltametría cíclica

La fig. 1 nos muestra voltamogramas tipo obtenidos para el 1,4-dimetoxibenceno en las condiciones allí especificadas. Un incremento en la velocidad de barrido del potencial permitió observar la reversibilidad del voltamograma (Tabla I). Se construyeron las curvas de trabajo teóricas para un mecanismo del tipo EQE (Fig. 2) siguiendo el procedimiento descrito en las referencias,[20,21] e la curva experimental se determinó la constante de velocidad de pseudo primer orden, kf, para el paso químico acoplado (Tabla II).

Tabla I

Datos voltamétricos para la oxidación anódica del 1,4-dimetoxibenceno

Ep(v)	Ep/2(v)	Ep-Ep/2(v)
+ 1,00	+ 0,94	+ 0,06

Tabla II

Oxidación anódica del 1,4-dimetoxibenceno. Valores determinados para la constante de velocidad de pseudo primer orden

Técnica	Potencial base(v)	Altura del pulso(v)	λ(nm){ε(M^{-1} cm^{-1})}	$k_f(S^{-1})$
Voltametría Cíclica	—	—	—	0,7
Cronoampermetría	+0,750	+0,375	—	0,8
Espectroscopía de reflectancia especular modulada	+0,750	+0,375	550{3135}	0,9

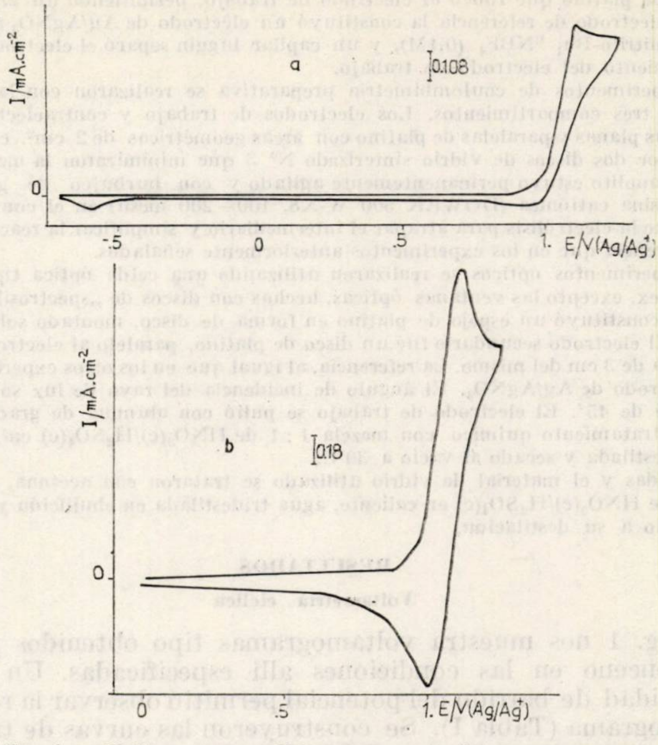

Fig. 1. — Voltamograma Ciclico para el 1,4-dimetoxibenceno (5mM) en CH_3CN-$Bu^n_4NBF_4$(0,1M), Et = Pt : *a* — ν = 0,01 vs^{-1}; *b* — ν = 0,3 vs^{-1}

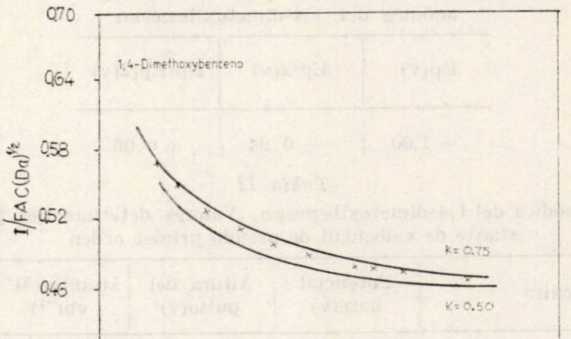

Fig. 2. — Curvas de trabajo voltamétricas para la determinación de la constante de veclocidad Kf. × × ×: experimental ; ——— : teoría.

Cronoamperometría

Se registraron los transitorios I-t en las condiciones especificadas en la sección experimental y, a partir de ellos, se construyeron los gráficos I vs$t^{-1/2}$ del tipo mostrado en la fig. 3. Se construyeron curvas de trabajo teóricas siguiendo el procedimiento descrito en [22] para varios valores de kf, asumiendo difusión lineal semiinfinita y un proceso total con n = 2. Por ello las condiciones de frontera correspondieron a la transferencia de un electrón (kf = 0), y de dos electrones (kf = ∞) respectivamente. Los puntos experimentales se fijaron en el gráfico determinándose así el valor de la constante de velocidad de pseudo ler. orden (Tabla II).

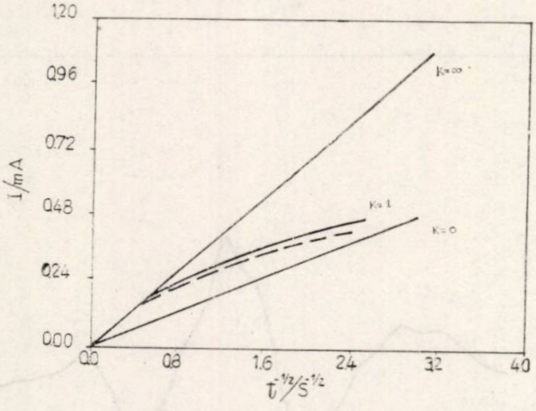

Fig. 3. — Curvas de trabajo cronoamperométricas para la determinación de la constante de velocidad Kf. : ---------- experimental ; ——— : teoria.

Espectroscopía de Reflectancia Especular Modulada

La Fig. 4 muestra el espectro obtenido para el 1,4-dimetoxybenceno a temperatura ambiente, en acetonitrilo seco y $Bu^n_4NBF_4$. La tabla III muestra las características del espectro obtenido. Se registraron los

Tabla III

Espectroscopía de reflectancia especular modulada. Características espectrales en la región UV-visible para el 1,4-dimetoxibenceno

Rango de modulación voltios	Frecuencia H_z	Longitud de onda de las líneas espectrales, n.m		
		λ_1	λ_2	λ_3
+0,800 — +1,200	80	(560 — 600)	(460 — 430)	330

cambios normalizados de reflectancia $\Delta R/R$ en función del tiempo a una longitud de onda correspondiente al radical catión producido en la primera transferencia electrónica. El transitorio teórico, asumiendo que el radical catión es estable[23] está dado por:

$$\Delta R/R = \frac{4\varepsilon CA(Dt)^{1/2}}{(1/2)\ \mathrm{Cos}\ \theta}$$

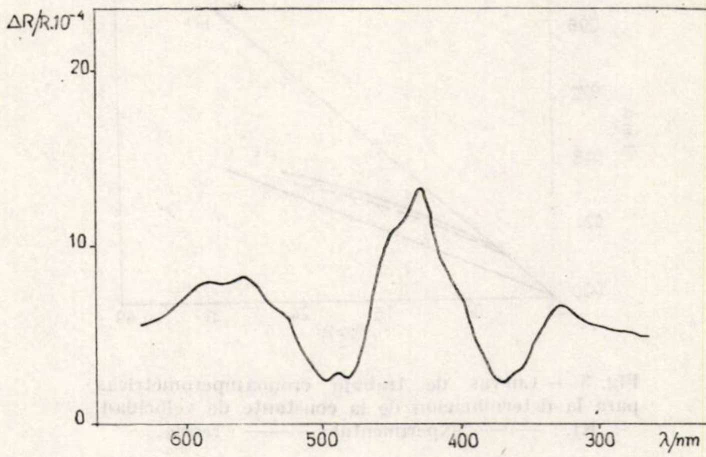

Fig. 4. — Espectro de reflectancia especular modulada para el 1,4-dimetoxibenceno.

En la zona lineal del gráfico $\Delta R/R$ Vs $t^{1/2}$ (Fig. 5) y del valor de la pendiente, es posible calcular el valor para ε (Coeficiente de extinción). La constante k_f para el decaimiento del catión radical, puede calcularse a partir de la gráfica 5, de acuerdo al método desarrollado por Bewick y colaboradores[22].

Coulombimetría preparativa

Las electrólisis preparativas se realizaron en presencia de resina (2 gr) y utilizando la técnica de activación por pulsos. Se electrolizaron 35 mg ($2{,}53 \times 10^{-4}$ mol) de 1,4-dimetoxibenceno en acetonitrilo por modulación del potencial entre +0,80 volts y + 1,00 volt con una onda cuadrada simétrica de 2 Hz.

La corriente inicial fue de 95 mA, deteniéndose la electrólisis cuando alcanzó un valor de 3 mA. El residuo extraído (14,3 mg) se disolvió en éter dietílico y fué analizado por RMN, IR y GLC acoplado con espectrómetro de masa. Los resultados de este análisis sugirieron la formación de 2,5-dimetoxibencilacetamida con un rendimiento del 34 % respecto de material de partida.

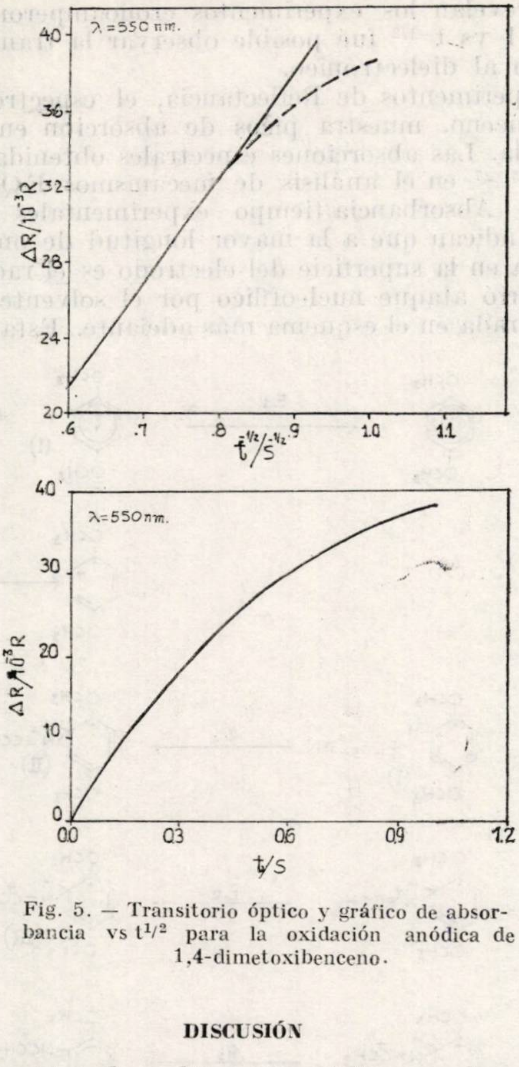

Fig. 5. — Transitorio óptico y gráfico de absorbancia vs $t^{1/2}$ para la oxidación anódica de 1,4-dimetoxibenceno.

DISCUSIÓN

Los experimentos de voltametría cíclica revelaron que la altura de los picos voltamétricos para la oxidación del 1,4-dimetoxibenceno muestran una proporcionalidad lineal simple con la raíz cuadrada de la velocidad de barrido del potencial en el rango de velocidades de barrido utilizados. A partir de la función de corriente $Ip/v^{1/2}$ vs. v, la velocidad de barrido, se obtuvo información cualitativa utilizando el criterio-diagnóstico presentado por Nicholson y Shain [20,24]. Se observó una región donde la función de corriente permanece independiente de la velocidad de barrido, indicando una transferencia electrónica simple controlada por difusión (Transferencia del primer electrón para formar el radical catión). A velocidades de barrido inferiores, la función corriente no fué más independiente de la velocidad de barrido, indicando que sobre esta escala de tiempo el radical catión sufre una reacción química. Los mismos resultados nos los revelan los experimentos cronoamperométricos. A partir de los gráficos I vs $t^{-1/2}$ fué posible observar la transición del proceso monoelectrónico al dielectrónico.

En los experimentos de Reflectancia, el espectro obtenido para el 1,4 dimetoxibenceno, muestra picos de absorción en tres regiones de longitud de onda. Las absorciones espectrales obtenidas concuerdan con la literatura [21,25–27] en el análisis de mecanismos EQE. Las formas de los transitorios Absorbancia/tiempo experimentales a diferentes longitudes de onda indican que a la mayor longitud de onda la especie primaria producida en la superficie del electrodo es el radical catión (tabla III) el cual sufrió ataque nucleofílico por el solvente para producir la especie(II) mostrada en el esquema más adelante. Esta especie sufre una

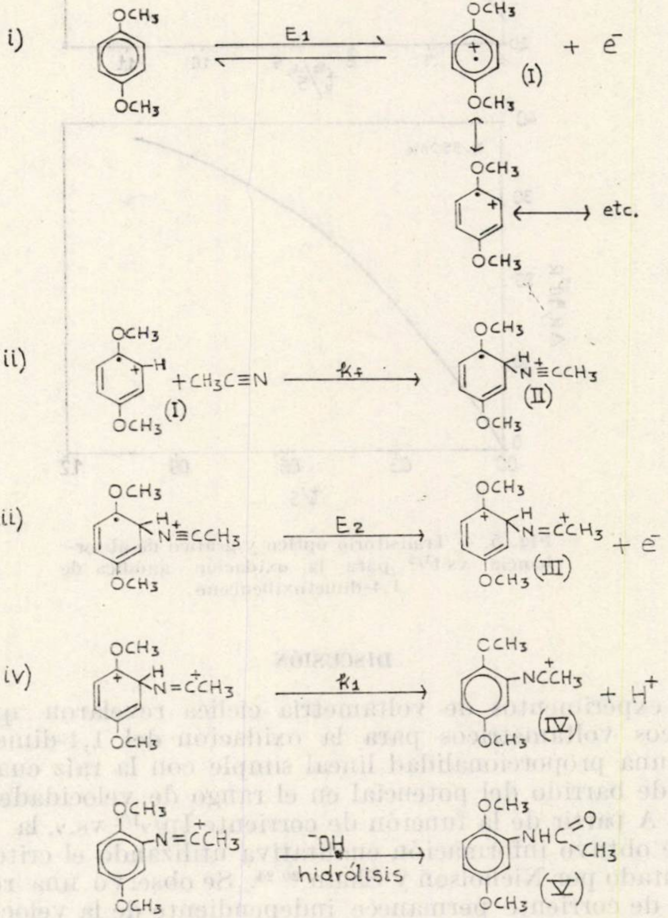

nueva transferencia electrónica seguida por la pérdida de un potrón aromático para dar orígen a la especie (IV), la cual por hidrólisis produce finalmente la 2,5-dimetoxibencilacetamida(V), producto principalemente formado en la electrólisis.

Los experimentos coulombimétricos y electrolíticos mostraron considerables mejoras desde el punto de vista sintético con la utilización de una resina catiónica (la cual permitió, el intercambio del ión metálico con el protón de la resina originando un incremento en la selectividad y favoreciendo la formación de la 2,5-dimetoxibencilacetamida) acoplada a un procedimiento de pulsos de potencial el cual parece contribuír al establecimiento de condiciones apropiadas para el atrapamiento por la resina de intermediarios, minimizando la posibilidad de reacciones colaterales que puedan conducir a la formación de especies adsorbibles contaminantes.

Los resultados obtenidos muestran claramente que las variaciones sintéticas químicas observadas se deben principalmente a la estructura y estabilidad de la especie radical catión producida inicialmente al ocurrir la primera transferencia electrónica. Los factores importantes son claramente el tiempo de vida del radical catión antes de su decaimiento por pérdida de un protón (relacionado a su fuerza como ácido) y su susceptibilidad hacia el ataque nucleofílico, (determinado por la distribución de carga en el ión).

REFERENCIAS

[1] S. Andreades y E. W. Zahnow, *J. Am. Chem. Soc.*, **91**, 4181 (1969).
[2] K. Yoshida, M. Shigi, T. Kanbe y T. Fueno, *J. Org. Chem.*, **40**, 3805 (1975).
[3] B. Bellean y N. L. Weimberg, *J. Am. Chem. Soc.*, **85**, 2525 (1963).
[4] K. Yoshida, M. Shigi y T. Fueno, *J. Org. Chem.*, **40**, 63 (1975).
[5] M. Rokoutz, D. Michelet, B. Brassaro y J. Varagnat, *Tet. Letters*, **39**, 3723 (1979).
[6] M. J. Manning, D. R. Henton y J. S. Swenton, *Tet. Letter*, 1679 (1977).
[7] W. T. Dixon y D. Murphy, *J. Chem. Soc. Perkin II*, 1823 (1976).
[8] L. Eberson y B. Helgee, *Acta. Chem. Scand*, **B29**, 151 (1975).
[9] L. Eberson y B. Helgee, *Chem. Scripta*, **5**, 47 (1974).
[10] B. Grant, N. J. Clekac, M. Oxsen, A. Jaffe y G. S. Keller, *J. Org. Chem.*, **45**, 702 (1980).
[11] P. D. Sullivan, J. R. Bolton y W. E. Geier Jr, *J. Am. Chem. Soc.*, **92**, 4176 (1970).
[12] D. R. Henton, R. L. McGreery y J. S. Swenton, *J. Org. Chem.*, **45**, 369 (1980).
[13] A. Laurent, E. Laurent y P. Locher, *Electrochim. Acta.*, **30**, 857 (1975).
[14] L. Eberson, M. Baizer, ,,Ed. Organic. Electrochemistry", Dekker, New York (1973).
[15] N. L. Weinberg y B. Bellean, *Tetrahedron Letters*, **29**, 279 (1973).
[16] L. Eberson y B. Helgee, *Acta. Chem. Scand*, **B32**, 313 (1978).
[17] K. Yoshida y S. Nagase, *J. Am. Chem. Soc.*, **101** : 15, 4268 (1979).
[18] L. Eberson y K. Nyberg, *Acc. Chem.*, **6**, 106 (1973).
[19] M. Fleishman y D. Pletcher, *Tetraheron Letters*, **60**, 6255 (1968).
[20] R. S. Nicholson y I. Shain, *Anal. Chem.*, **37**, 178 (1965).
[21] B. S. Pons. PhD. Thesis. Southampton University (1979).
[22] A. Bewick, J. M. Mellor and B. S. Pons. *Electrochim. Acta*, **25**, 931 (1980).

NOTE POUR LES AUTEURS

La Revue Roumaine de Chimie publie des articles en anglais, français, russe, allemand ou espagnol. Les auteurs sont priés d'envoyer des articles et des comptes rendus inédits.

Les manuscrits seront dactylographiés à double interligne. La bibliographie, les tableaux et la légende des figures seront placés aprés le texte.

Si l'article fait partie d'une série numérotée, la partie précédente sera donnée comme première référence.

Chaque article sera précédée d'un résumé comprenant quinze lignes au maximum.

Les références bibliographiques dans le texte seront faites par des exposants sans parenthèse et paraîtront à la fin de l'ouvrage.

Les publications périodiques mentionnées dans la bibliographie seront présentées suivant les prescriptions internationales : le nom de l'auteur précédé de l'initiale du prénom, le titre du périodique abrégé conformément à « Chemical Abstract » et souligné par une ligne, le numéro du tome indiqué par des chiffres arabes et souligné par deux lignes, suivi de la première page de l'article : à la fin, l'année de la parution sera placée entre parenthèses. Le numéro de la revue ne sera pas indiqué si les pages du volume sont numérotées consécutivement.

Les textes des livres ou traités inclueront : le nom des auteurs, précédés de l'initiale du prénom, le titre du livre entre guillemets et sans être souligné, le numéro du tome précédé par l'abréviation « vol. » (ou « Bd. »), le numéro de l'édition, les éditions (the publisher), la localité de la parution du livre, l'année de la parution et la page de la référence précédée(s) par l'abréviation « p » (ou « S »).

Les brevets seront indiqués comme suit : l'auteur ou la firme, le pays et le numéro du brevet, la date de la revue (*Chem. Abstr.*). Par ex. : M. Jones (to Union Carbide Co.). Brit. Pat. 610 238, 2 Sept. 1959 : cf. *Chem. Abstr.*, **54**, 12808 (1960).

Si la référence n'a pas été lue en original, on indiquera aussi la revue de références consultée.

Les diagrammes seront tracés à l'encre de Chine sur papier calque. Les tableaux et les figures (en nombre strictement nécessaire), ainsi que les courbes dans les figures seront numerotés par des chiffres arabes. Leur explication sera donnée dans la légende des figures. Prière de ne pas inscrire les mêmes données dans les tableaux et les figures. Chaque tableau aura un titre. On indiquera dans le texte la place approximative des tableaux et des figures. Les formules chimiques seront incluses dans le text ; en outre, elles seront transcrites sur papier calque, à l'encre de Chine.

Les auteurs sont priés d'indiquer les caractéres italiques (en soulignant les lettres au crayon), ainsi que tout autre caractère spécial : les préfixes, *ortho*, *meta*, *para*, *cis*, *trans*, etc. seront soulignés pour indiquer leurs caractères italiques, et ne seront jamais écrits avec des majuscules.

Aucune correction à la main ne sera admise sur le manuscrit. Les correction seront frappées à la machine. Les lettres grecques ou d'autres symboles spéciaux seront insérés à la main à l'encre clairement.

Le manuscrit sera signé par l'auteur.

Le titre courant aura 50 lettres au maximum.

L'entière responsabilité du contenu des articles appartient aux auteurs.

Sur demande on peut obtenir une note plus complète.

PRINTED IN ROMANIA

TRAVAUX PARUS AUX ÉDITIONS DE L'ACADÉMIE DE LA RÉPUBLIQUE SOCIALISTE DE ROUMANIE

V. DRĂGUȚAN, A. T. BALABAN, M. DIMONIE, **Olefin Metathesis and Ring-Opening Polymerization of Cyclo-Olefins**, coédition avec John Wiley and Sons, 1985, 544 p.
T. ONCESCU, S. G. IONESCU, **Conversie fotochimică și stocare de energie solară**, 1985, 272p.
C. LITEANU, I. RÎCA, **Optimizarea proceselor analitice**, 1985, 360 p.
N. PERESCU, **Chimia extracției cu solvenți și aplicații**, 1985, 212 p.
V. EM. SAHINI, N. HILLEBRAND, **Chimie cuantică în exemple și aplicații**, 1985, 378 p.
GH. MARCU, **Chimia compușilor coordinativi**, 1984, 415 p.
E. CORDOȘ, C. MANOLIU, **Spectrometria de absorbție și fluorescență atomică**, 1984, 178 p.
C. BODEA, **Tratat de biochimie vegetală**, p. II, vol. 5, 1984, 438 p.
ELENA CEAUȘESCU, **Cercetări în chimia și tehnologia polimerilor**, 1983, 519 p.
N. ASANDEI, A. GRIGORIU, **Chimia și structura fibrelor**, 1981, 395 p.
N. IONESCU, M. CĂLDĂRARU, **Oxidarea catalitică a olefinelor inferioare**, 1983, 178 p.
C. CAȘCAVAL, **Studiul polimerilor prin piroliză și cromatografie de gaze**, 1983, 220 p.
C. I. SIMIONESCU, F. DANEȘ, **Originea vieții**, 1983, 110 p.
C. BODEA (sous la direction), **Tratat de biochimie vegetală**, p. II, IV, 1982, 408 p.
I. G. MURGULESCU, RODICA VÎLCU, **Introducere în chimia fizică. Vol. III. Termodinamica chimică**, 1982, 624 p.
I. G. MURGULESCU, J. PĂUN, **Introducerea în chimia fizică. Vol. I. 3. Nucleul atomic, reacții nucleare, particule elementare**, 1982, 606 p.
ELENA CEAUȘESCU **Noi cercetări în domeniul compușilor macromoleculari**, 1981, 536 p.
I. G. MURGULESCU, TATIANA ONCESCU, E. SEGAL, **Introducere în chimia fizică. Vol.II. 2. Cinematică chimică și cataliză**, 1981, 1024 p.
LYDIA-MARIA VAICUM, **Epurarea apelor uzate cu nămol activ. Bazele biochimice**, 1981, 218 p.
I. GĂLĂȚEANU, **Procese și metode radiochimice în energetica nucleară**, 1981, 234 p.
O. IORDACHE, **Procese polistocastice aplicate în fenomenele de transfer**, 1981, 186 p.
CR. SIMIONESCU, VALERIA GORDUZA, **Polimeri biocompatibili și biologie activi**, 1980, 479 p.
ELENA CEAUȘESCU, **Polimerizarea stereospecifică a izoprenului**, 1979, 307 p.
C. GH. MACAROVICI, **Analiza chimică cantitativă anorganică**, 1979, 457 p.
M. FLORESCU, **Metode științifice în dezvoltarea industriei chimice moderne**, 1979, 256 p.
A. T. BALABAN, I. GĂLĂȚEANU, G. GEORGESCU, LIGIA SIMIONESCU, **Compuşi marcați și radiofarmaceutici cu aplicații în medicina nucleară**, 1979, 495 p.
I. G. MURGULESCU, E. SEGAL, **Introducere în chimia fizică. Vol. II. 1. Teoria molecular-cinetică a materiei**, 1979, 1036 p.
S. STERNBERG, FL. DANEȘ, **Termodinamica chimică aplicată**, 1978, 400 p.
I. G. MURGULESCU, V. EM. SAHNI, **Introducere în chimia fizică. Vol. I. 2. Structura și proprietățile moleculelor**, 1978, 604 p.
I. ZUGRĂVESCU, MAGDA PETROVANU, **N-ylid chemistry**, coédition avec McGraw-Hill International Book Company, U.S.A., 1977, 396 p.
I. G. MURGULESCU, **Introducere în chimia fizică. Vol. I. 1. Atomi, molecule, legătură chimică** 1976, 560 p.
ELENA CEAUȘESCU, **Research work on synthesis and characterization of macromolecular compounds, Contributions**, 1974, 251 p.
CR. SIMIONESCU, VIORICA RUSAN, V. POPA, **Chimia algelor marine**, 1974, 212 p., 1 pl.

ISSN 0035-3930

I.P.INFORMAȚIA, c. 2155

43 426

Lei 40

$ 80 (pour un abonnement annuel)

F 1103

04

ACADÉMIE DE LA RÉPUBLIQUE SOCIALISTE DE ROUMANIE

REVUE ROUMAINE DE CHIMIE

TOME 31

N° 7

Juillet 1986

Rev. Roumaine Chim.

RRCHAX, 31, 7, p. 647–738 (1986), Bucarest

EDITURA ACADEMIEI REPUBLICII SOCIALISTE ROMÂNIA

ACADÉMIE DE LA RÉPUBLIQUE SOCIALISTE DE ROUMANIE

COMITÉ DE RÉDACTION

Rédacteur en chef :

I. G. MURGULESCU, membre de l'Académie de la République Socialiste de Roumanie

Rédacteurs en chef adjoints :

A. T. BALABAN et V. EM. SAHINI, membres correspondants de l'Academie de la République Socialiste de Roumanie

Collège de rédaction :

EM. BRATU, ELENA CEAUŞESCU, ECATERINA CIORĂNESCU-NENITZESCU, CR. SIMIONESCU, membres de l'Académie de la République Socialiste de Roumanie; P. SPACU, membre correspondant de l'Académie de la République Socialiste de Roumanie; M. BANCIU, M. D. GHEORGHIU, I. HAIDUC, D. I. MARCHIDAN, G. NIAC et D. SĂNDULESCU

La Revue de Chimie paraît 10 fois par an. Toute commande de l'étranger sera adressée à ROMPRESFILATELIA — sectorul Export-Import, Presă, P.O. Box 12—201, télex 10376 prsfi r, 78104 Bucarest, Calea Griviței nr. 64—66, Roumanie.

Les manuscrits, les livres et les revues proposés en échange, ainsi que toute correspondance seront envoyés à la rédaction.

REVUE ROUMAINE DE CHIMIE

125, Calea Victoriei, 79717 Bucarest, Roumanie, téléphone 50 76 80

EDITURA ACADEMIEI REPUBLICII SOCIALISTE ROMÂNIA
125, Calea Victoriei 79717 Bucarest, Roumanie, téléphone 50 76 80

REVUE ROUMAINE DE CHIMIE

Tome 31, N° 7 **Juillet, 1986**

MIHAELA HILLEBRAND and V. EM. SAHINI, Electronic spectra of some heteroaromatic cation-radicals 649–656

RODICA VÎLCU, VASILE BĂRBÎNȚĂ, IOAN GĂINAR and DUMITRU SAVA, Estimation of chemical nonhomogeneity of polymers using the interrelation structure-entropy-information. I. The use of the tracer method 657–660

VALERIA GORDUZA, I. COCÂRLĂ, C. GHIRVU, LUMINIȚA WAGNER and VIANORA PESCARU, Studies on the reactivity of benzimidazolone derivatives, based on the electronic spectra and molecular diagrams 661–670

N.I. IONESCU, M. S. CHIRCA and D.I. MARCHIDAN, Thermal effect and oscillations in the catalytic oxidation of methanol 671–677

ALEXANDRU T. BALABAN, Chemical Graphs. Part. 44. Isomer enumeration for substituted saturated polyhedral valence isomers of annulenes. 679–694

ALEXANDRU T. BALABAN, Chemical Graphs. Part 45. Edge-labelled graphs as unsaturated valence isomers of annulenes ; applications of Pólya's theorem 695–708

RUBÉN SÁNCHEZ-OBREGÓN, HÉCTOR BARRIOS, BENJAMÍN ORTÍZ and FRANCISCO YUSTE, Diels-Alder reaction of *trans, trans*-1,4-diacetoxy-1,3-butadiene and 1,2-pentadien-4-one 709–710

OLGA PÉREZ DE MÁRQUEZ, Anodic oxidation of alkylbenzenes in dry acetonitrile 711–718

K. N. THIMMAIAH and V. C. SEKHAR, Hydrazine carbothioamide-2-[(4-hydroxy-3-methoxy phenyl) methylene] as a sensitive reagent for rapid spectrophotometric determination of palladium(II) and copper(II) : analysis of alloys and minerals 719–726

I. CAYRE, C. ARIAS and C. RUEDA, Rheological characteristics of sodium carboxymethylcellulose solutions at low shear rate. The evaluation of parameters thermodynamics. The effects of the dextran's addition (in Spanish) 727–735

BOOK REVIEWS 737

Rev. Roumaine Chim. **31**, 7, 647–738 (1986), Bucarest

Revue Roumaine de Chimie, 31, 7, 649–656 (1986)

ELECTRONIC SPECTRA OF SOME HETEROAROMATIC CATION-RADICALS

MIHAELA HILLEBRAND and V. EM. SAHINI
Department of Physical Chemistry, Polytechnic Institute, Blvd. Republicii 13,
Bucharest, Romania

Received January 15, 1986

Mo calculations of the electronic structure of the cation-radicals provided by some anthracene heteroanalogs (phenoxathiin, phenoxaselenine, thianthrene, phenothiazine) were performed by the restricted SCF semiempirical method of Longuet-Higgins and Pople. The electronic transitions were calculated considering the configurational interaction of the ground and 31 excited doublet states. The results account well for the visible spectra of the ions and reflect some experimental features observed in the UV range.

The electronic spectra of the ion-radicals were rarely investigated as compared with the collection of the data referring to the hyperfine splittings and other ESR parameters. This difference is more apparent when we consider the applications of the theoretical approaches.[1,2] Thus, while the spin distribution in ion-radicals has been the subject of extensive and successful calculations, the theoretical methods dealing with the electronic excited states were less applied and not always with encouraging results.

Last years more attention has been paid to test the validity of open shell calculations and to obtain reliable data with the experimental electronic transitions.[3–12] These works are especially concerned with hydrocarbon and substituted anion- and neutral-radicals and only few of them refer to cation-radicals. This is generally explained by the more complex and reactive environment in which the cation-radicals are produced. In sulfuric acid a number of intermediates, protonated and associated forms were noticed making the assignments of the experimental bands very difficult.

The cation-radical provided by some anthracene heteroanalogs were found interesting to investigate as their visible spectra were carefully

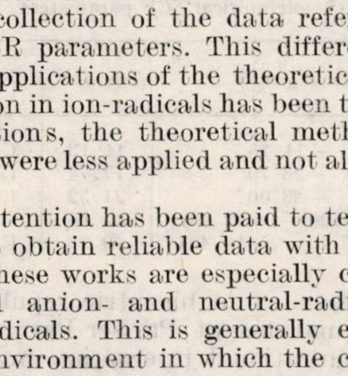

I X = O; Y = S; II X = O; Y = Se; III X = Y = S

IV - X = S; Y = NH

analysed.[13-16] On the other side, a set of heteroatomic parameters which led to an adequate description of the neutral molecules was previously established and can be used as a starting point.

In this paper we report the results obtained by one of the restricted methods described for open shell systems, the version of Longuet-Higgins and Pople, [2] including the configurational interaction in the formalism of Ishitani and Nagakura[3] and Carsky and Zahradnik. [9]

MO CALCULATIONS

A previous study on the neutral compounds containing oxygen revealed that oxygen atom has a little influence on the last occupied mo's, the most implied in the ionization process and the electronic spectra. Therefore the oxygen W_0 parameter was kept constant through all calculations. Although the electronic structures of the neutral compounds were well described using $W_S = -20.00$ eV and $W_{Se} = -17.40$ eV, in the present calculations these parameters were changed in the ranges (−20.00 eV)−(−22.00 eV) and (−17.40 eV)−(−19.40 eV) respectively, in order to account for the effect of ionization. All the parameters used are collected in Table 1.

Table 1

Semiempirical SCF parameters

X	W_X (eV)	γ_{XY} (eV)	X−Y	β_{X-Y} (eV)
C	−11.16	11.13	C−C	−2.30
N	−26.70	17.74	C−N	−2.30
O	−33.00	21.52	C−O	−1.99
S	(−20.00)−(−22.00)	11.86	C−S	−0.92
Se	(−17.40)−(−19.40)	9.28	C−Se	−0.92

The bielectronic mono- and bicentric repulsion integrals were estimated by the approximations of Pariser-Parr and Nishimoto-Mataga, respectively. The configurational interaction was limited to the ground (G) and 31 monoexcited doublet states of the A, B, C_α, C_β type, including all the transitions between the $m-3$ and $m+4$ orbitals (m labells the odd electron orbital). The calculations were performed at the computational Center of the Polytechnic Institute of Bucharest using a program written in Fortran IV.

RESULTS AND DISCUSSION

The molecular orbitals can be classified in symmetrical and antisymmetrical with respect to a plane passing through the heteroatoms of the central ring. Differing from the case of the neutral compounds the MO energies are less influenced by the change of the sulfur or selenium parameters (*i.e.* the change of W_S from (−20.00 eV) to (−22.00 eV) determines for I only a decrease of about 0.20 eV in the energy of the odd electron

Table 2

Molecular orbital energies (eV) and heteroatomic coefficients ($W_S = -20.25$ eV; $W_{Se} = -17.65$ eV)

		I			II			III		IV		
i	Sim	ε_i	c_O	c_S	ε_i	c_O	c_{Se}	ε_i	c_S	ε_i	c_N	c_S
1	S	−19.17	0.791	0.064	−18.96	0.788	0.059	−16.82	0.215	−18.76	0.653	0.127
2	A	−16.73	0	0	−16.58	0	0	−16.52	0	−16.73	0	0
3	S	−16.15	−0.403	0.283	−15.98	−0.406	0.243	−14.26	−0.363	−15.88	−0.457	−0.385
4	S	−14.49	0.009	−0.599	−14.20	−0.021	0.550	−14.20	−0.465	−14.69	0.030	0.543
5	A	−13.75	0	0	−13.62	0	0	−13.56	0	−13.74	0	0
6	A	−13.66	0	0	−13.55	0	0	−13.50	0	−13.67	0	0
7	S	−13.18	0.250	−0.375	−12.99	−0.278	0.367	−12.76	0.509	−12.88	0.27	−0.437
8	S	−10.79	−0.298	−0.628	−10.59	−0.073	−0.686	−10.53	0.561	−10.08	−0.421	−0.547
9	A	− 4.69	0	0	− 4.53	0	0	− 4.43	0	− 4.78	0	0
10	A	− 4.35	0	0	− 4.22	0	0	− 4.17	0	− 4.35	0	0
11	S	− 4.29	−0.045	0.154	− 4.16	−0.039	0.152	− 4.14	0.142	− 4.15	0.014	−0.18
12	S	− 4.03	−0.210	0.030	− 3.89	−0.211	0.039	− 4.08	0.085	− 3.80	−0.289	0.07
13	A	− 1.55	0	0	− 1.40	0	0	− 1.34	0	− 1.54	0	0
14	S	− 1.36	−0.119	0.068	− 1.22	−0.121	0.066	− 1.26	−0.071	− 1.25	−0.165	0.09

orbital). The theoretical energies are listed in Table 2. Table 2 contains also the coefficients of the heteroatoms in order to evidence the degree of delocalization of each molecular orbital.

It can be seen that, as for the neutral compounds, the antisymmetrical bonding orbitals, labelled $i = 2, 5, 6$ have no contribution from the heteroatoms, presenting a benzenic character ; this determines fairly constant energies for all the investigated ions, similar to those obtained for the anthracene positive ion. The odd electron orbitals present a high degree of delocalization on the sulfur or selenium atoms in I, II and IV, while in III the last two occupied molecular orbitals are influenced by the sulfur atoms.

The calculated charge distribution in all the cation-radicals points out that the sulfur and selenium atoms are the most implied in the ionization process, the oxygen atom and the benzenic positions being less affected. The increase of sulfur W_S parameter enhanced this effect, i.e. the sulfur charge density in I decreased from 1.76 for $W_S = -22.00$ eV to 1.52 for $W_S = -20.00$ eV.

The molecular diagrams calculated for $W_S = -20.25$ eV and $W_{Se} = -17.65$ eV (the values which led to the best agreement for the electronic visible bands, see below) are presented in Fig. 1.

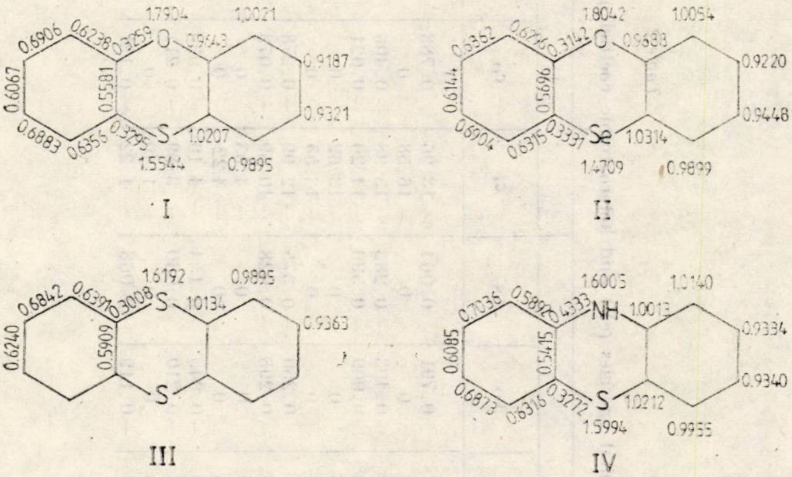
1.7904
1.0021
0.6906
0.6238
0.3259
O
0.9643
0.9187
0.6067
0.5581
0.9321
0.6883
0.6356
0.3295
S
1.0207
1.5544
0.9895
1.8042
1.0054
0.6362
0.6796
0.3142
O
0.9638
0.9220
0.6144
0.5696
0.9448
0.6904
0.6315
0.3331
Se
1.0314
1.4709
0.9899
1.6192
0.9895
0.6842
0.6391
0.3008
S
1.0134
0.9363
0.6240
0.5909
S
1.6005
1.0140
0.7036
0.5892
0.4333
NH
1.0013
0.9334
0.6085
0.5415
0.9340
0.6873
0.6316
0.3272
S
1.0212
1.5994
0.9955

I

II

III

IV

Fig. 1. — The molecular diagrams of the cation-radicals I— IV.

The π bond orders are increased as compared to those in the neutral parent compounds, reflecting an enhancement of the conjugation in the ion-radicals. Secondly, an alternating double band character is evident in the benzenic rings, while in the neutral molecules the bond orders were almost equal.

All the cation-radicals, prepared by dissolution of the parent neutral compounds in sulfuric acids, are strongly coloured exhibiting bands in the range of 450—600 nm. As phenoxathiin and thianthrene present only a single band in this range, located at 578 and 546 nm, respectively, its assignment to the cationic species is unambigous.[13,14] For phenoxaselenine characterised by the presence of two bands (462 nm, 584 nm) a previous work ascribed the longest wavelength to the cation-radical.[15] The analysis made by Hansom and Norman[16] of the complex electronic spectrum of phenothiazine, which is known to undergo in sulfuric acid different secondary reactions led to the assignment of the 516 nm maximum to the phenothiazine cation-radical IV. All the experimental maxima are presented in Table 3.

Table 3

Experimental and theoretical energies for the visible bands (eV)

Cation-radical	$h\nu_{(exp)}$	$h\nu_{(calc)}$	Assignment
I	2.14	2.13	$A(6-8)$
II	2.12	2.20	$A(6-8)$
III	2.27	2.32	$A(6-8)$
IV	2.40	2.67	$A(6-8)$

The calculated energies of the lowest excited states, assigned generally to the visible bands are significantly dependent on the value of W_S, W_{Se} parameters, decreasing as W_x decreased, but only slightly influenced by the configurational interaction; consequently the correspondent doublet functions belong to nearly pure (87 percent) A $(i - m)$ type configurations, i labelling a double occupied mo and m the odd electron orbital (*i.e* $A(7-8)$, $A(6-8)$, $A(5-8)$). The first possible assignment for the visible bands would be to the transition from the ground (G) to the $A(7-8)$ state. This is unlikely for two reasons: firstly, because the energies of these transitions are situated in the near I R range, and secondly the calculated transition moments are too small. We interpreted therefore the visible bands of all the cation-radicals in terms of transitions to the second excited states, namely the $G - A$ $(6-8)$ transition (As the $i = 5$, $i = 6$ molecular orbitals are quasi degenerate, the energies of the $A(6-8)$ and $A(5-8)$ doublet configurations are very close; the larger values of the transition moments for the $G - A$ $(6-8)$ transitions as against those corresponding to the $G - A$ $(5-8)$ transition justify the assignment made). The best agreement between the experimental and calculated energies was reached for $W_S = -20.25$ eV and $W_{Se} = -17.65$ eV, that is for values fairly different from those established for the neutral compounds; the results are presented in Table 3.

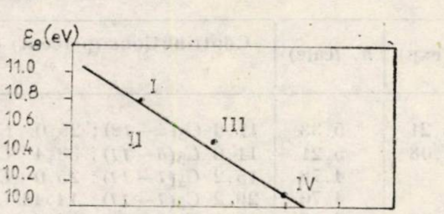

Fig. 2. — The correlation of the experimental energies (eV) with the calculated ε_8 energies (eV).

Besides the agreement between the experimental and calculated energies, another fact that could be considered consistent with this assignment is the linearity found between the observed transition energies and the calculated ε_m energies (Fig. 2).

This correlation implies that the transition responsible for the visible band is not influenced by the "starting" orbital; this is possible only for a transition involving the $i = 5$, $i = 6$ orbitals, which were seen to have constant energy for all the ions.

The *G*---*A* *(6—8)* transitions are characterised by a significant charge transfer from the benzenic rings toward the central heteroatoms in order to compensate the large positive charges on the sulfur or selenium atoms in the ground states of the radicals (Table 4).

Table 4

Charge densities in the ground (*G*) and excited $A(5-8)$ states ($W_S = -20.25$ eV)

Radical	q_μ \ μ	1	2	3	4	5	6	7	8
I	(*G*)	1.790	0.964	1.002	0.919	0.932	0.989	1.021	1.554
	(A_{6-8})	1.843	0.952	0.997	0.809	0.863	0.995	0.973	1.941
III	(*G*)	1.620	1.013	0.990	0.936	0.936	0.990	1.013	1.620
	(A_{6-8})	1.935	0.958	0.992	0.831	0.831	0.992	1.958	1.935

The UV spectra are more difficult to interpret owing to the experimental incertitudes raised by the presence in solution of unoxidised parent compounds, protonated species or by-products; from a theoretical point of view there is a multitude of very close calculated energies obtained by the inclusion of the 32 doublet configurations, the real spectrum being certainly a superposition of all these. The results obtained for the same parameters as for the visible spectra are listed in Tables 5—8, but the assignments are only temptative. However, inspection of Tables 5—8 points out that the theoretical results reflect some features of the experimental spectra.

Table 5

UV experimental and calculated transition energies (eV) for the phenoxathin cation-radical

$h\nu$ (exp)	$h\nu$ (calc)	Contributions (percent) of the different configurations to the excited states*
5.21	5.33	11.6 $C_\beta(5-12)$; 25.0 $C_\alpha(7-9)$: 21.2 $B\,(8-10)$; 11.6 $C_\alpha(7-10)$;
5.08	5.21	11.0 $C_\beta(6-11)$; 38.4 $C_\alpha(7-9)$; 11.6 $B\,(8-10)$;
	4.78	15.2 $C_\alpha(7-11)$; 25.0 $C_\alpha(5-9)$; 20.2 $C_\beta(5-9)$; 20.2 $C_\alpha(6-10)$;
	4.70	29.2 $C_\beta(7-11)$; 14.46 $C_\beta(5-9)$; 26.01 $C_\alpha(5-10)$;
4.49	4.57	16.0 $C_\alpha(7-9)$; 14.4 $C_\beta(7-9)$; 25.0 $C_\beta(5-11)$;
	4.49	15.2 $C_\beta(6-9)$; 50.0 $B\,(8-11)$;
	3.81	11.6 $C_\beta(6-11)$; 12.96 $C_\alpha(7-9)$; 20.25 $B\,(8-9)$; 29.16 $B\,(8-10)$;
4.04	3.65	22.1 $C_\beta(7-12)$; 16.81 $C_\beta(7-12)$; 16.81 $C_\beta(6-9)$; 18.5 $C_\beta(5-10)$; 17.0 $B\,(8-12)$

* Contributions below 10 percent were not considered

Table 6

UV experimental and calculated transition energies (eV) for the phenoxaselenine cation-radical

$h\nu$ (exp)	$h\nu$ (calc)	Contributions (percent) of the different configurations to the excited states *
5.19	5.31	13.7 $C_\beta(6-11)$; 38.44 $C_\alpha(7-8)$; 11.0 B $(8-10)$;
5.08	5.19	17.6 $C_\alpha(7-11)$; 22.1 $C_\alpha(5-9)$; 19.4 $C_\beta(5-9)$; 18.5 $C_\alpha(6-10)$
	4.75	22.1 $C_\beta(7-11)$; 13.7 $C_\beta(5-9)$; 18.5 $C_\beta(5-10)$
	4.69	22.1 $C_\alpha(7-9)$; 13.7 $C_\beta(7-9)$; 11.7 B $(8-10)$; 20.25 $C_\beta(5-11)$
4.56	4.52	13.0 $C_\beta(7-11)$; 16.0 $C_\beta(6-9)$: 11.6 $C_\beta(5-10)$; 44.5 $B(8-11)$
	4.45	22.1 B $(8-9)$; 24.0 B $(8-10)$; 19.4 $C_\beta(7-10)$
	3.74	26.0 $C_\beta(7-12)$; 13.7 $C_\beta(6-9)$; 19.4 $C_\beta(5-10)$; 25.0 B $(8-12)$
3.97	3.59	16.0 $C_\beta(5-12)$; 37.2 B $(8-9)$: 16.0 $C_\beta(7-9)$; 14.4 $C_\beta(7-10)$

* Contributions below 10 percent were not considered

Table 7

UV experimental and calculated transition energies (eV) for the thianthrene cation-radical

$h\nu$ (exp)	$h\nu$ (calc)	Contributions (percent) of the different configurations to the excited states*
4.71	4.78	22.10 $C_\alpha(7-12)$; 19.4 $C_\beta(7-12)$; 16.81 $C_\beta(6-9)$; 18.5 $C_\beta(5-10)$ 22.1 B $(8-11)$
	4.70	13.7 $C_\beta(5-12)$; 23.04 B $(8-9)$ 31.4 $C_\alpha(7-10)$; 23.04 $C_\beta(7-10)$
4.59	4.58	30.2 $C_\alpha(7-11)$; 14.4 $C_\beta(7-11)$ 13.0 $C_\alpha(5-9)$; 25.0 $B(8-12)$
4.40	4.30	56.2 $C_\alpha(7-9)$; 22.1 $C_\beta(7-9)$;
	4.17	19.4 $C_\beta(6-11)$; 15.21 $C_\beta(5-12)$; 46.24 B $(8-9)$; 13.6 $C_\beta(7-10)$
4.27	4.15	15.2 $C_\alpha(7-12)$; 25.0 $C_\beta(6-9)$; 23.0 $C_\beta(5-10)$; 31.4 B $(8-11)$

* Contributions below 10 percent were not considered

Table 8

Experimental and calculated transition energies (eV) for the phenothiazine cation-radical

$h\nu$ (exp)	$h\nu$ (calc)	Contributions (percent) of the different configurations to the excited states *
	4.77	36.0 $C_\alpha(7-11)$; 34.8 $C_\beta(5-10)$
	4.70	38.4 $C_\beta(7-10)$; 10.0 $C_\alpha(7-9)$; 10.0 C_α $(7-10)$
4.59	4.27	11.6 $C_\beta(6-10)$; 64.0 B $(8-11)$
	4.14	20.25 $C_\alpha(7-9)$; 10.0 $C_\beta(7-9)$: 53.3 B $(8-10)$;
	3.82	10.0 $C_\beta(5-9)$; 10.0 $C_\beta(7-12)$; 17.6 $C_\beta(6-9)$; 10.2 $C_\beta(5-10)$
2.83	3.41	72.25 $B(8-9)$; 46.2 B $(8-10)$

* Contributions below 10 percent were not considered

The first UV maxima in the spectra of I and II are similar to those of the neutral compounds; the assignments given in Tables 5 and 6 for these two bands point out a reduced contribution of the doublet configurations involving the odd electron orbitals (the most implied in the ions) and explain therefore the constant values of the energies as compared to those of the neutral compounds.

On the other side, the absorption peak located for all the sulfur containing radicals at 4.40 – 4.59 eV, which is also present in the spectrum of the thioxanthilium ion and not observed in the spectra of the neutral molecules, must be correlated with the excited states containing substantial contributions of the B type transitions, what is really found.

From Tables 5 – 8 it can also be noted that the theoretical values for the longest wavelength transitions reflect the bathochromic shift experimentally observed for the sequence III > I > II > IV; The assignment of these bands points out their correlation with the longest wavelength bands in the neutral compounds ascribed to the $m \rightarrow m + 1$, $m \rightarrow m + 2$ transitions.

From the present results it can be seen that the method of Longuet-Higgins and Pople leads to a good agreement for the visible spectra of the cation-radicals, pointing out a significant charge transfer character of the visible band. Considering the UV range, the calculations account well for some similitudes and differences experimentally observed between the cation-radicals or the cation-radicals and the parent neutral compounds.

REFERENCES

[1] C. C. J. Roothaan, *Rev. Mod. Phys.*, **32**, 179 (1960).

[2] H. C. Longuet-Higgins and J. A. Pople, *Proc. Phys. Soc.*, **A 68**, 591 (1956).

[3] A. Ishitani and S. Nagakura, *Theoret. Chim. Acta*, **4**, 236 (1966).

[4] T. Shida and S. Iwata, *J. Phys. Chem.*, **75**, 2591 (1971).

[5] P. Carsky and R. Zahradnik, "Topics in Current Chemistry. New Concepts III", Springer-Verlag, Berlin, p. 1.

[6] T. Shida and S. Iwata, *J. Chem. Phys.*, **56**, 2858 (1972).

[7] T. Shida and S. Iwata, *J. Amer. Chem. Soc.*, **95**, 3473 (1973).

[8] D. A. Lowitz, *J. Chem. Phys.*, **46**, 4698 (1967).

[9] R. Zahradnik and P. Carski, *J. Phys. Chem.*, **74**, 1235 (1970).

[10] M. A. Ali and R. J. Wratten, *Mol. Phys.*, **13**, 233 (1967).

[11] M. Kamiya, T. Mitsui and J. Akahori, *Bull. Chem. Soc. Jap.*, **46**, 1577 (1973).

[12] J. Fajer, B. H. J. Bielski and R. H. Felton, *J. Phys. Chem.*, **72**, 1281 (1968).

[13] B. Lamotte and G. Berthier, *J. Chim. Phys.*, **63**, 369 (1966).

[14] Mihaela Hillebrand, O. Maior, V. Sahini and Elena Volanschi, *J. Chem. Soc.*, **(1969)**, 755.

[15] Mihaela Hillebrand, O. Maior and V. Sahini, *Rev. Roumaine Chim.*, **16**, 1489 (1971).

[16] P. Hanson and R. O. C. Norman, *J. Chem. Soc. P.T.II.*, **(1973)**, 264.

Revue Roumaine de Chimie, 31, 7, 657–660 (1986)

ESTIMATION OF CHEMICAL NONHOMOGENEITY OF POLYMERS USING THE INTERRELATION STRUCTURE-ENTROPY-INFORMATION. I.

THE USE OF THE TRACER METHOD

RODICA VÎLCU, VASILE BĂRBÎNȚĂ, IOAN GĂINAR and DUMITRU SAVA
Department of Physical-Chemistry, Polytechnical Institute, Bucharest, Romania

Received July 20, 1985

The polymer characterization in terms of the chemical nonhomogeneity requires the overcoming of the difficulties generated by the coprecipitation of fractions at equilibrium during fractioning, as well as the interpretation of the data as a function of the structure-functionality relation. In order to evaluate the mass transfer at equilibrium, the tracer method has been used.

I. INTRODUCTION

Due to the complex character of the macromolecular synthesis, the structure of a polymer is characterized by a polydispersion concerning its length, composition, defects and stereoregularity degree.[1]

Furthermore, the nonhomogeneity degree for copolymers is considerably increased owing to their distribution upon composition and sequences.[2,3]

The experimental and theoretical methods currently used to characterize the nonhomogeneity of polymers do no longer fulfil the present standard.

The polymer fractioning upon composition and structure by fraction separation at separation equilibrium is quite difficult due to the transport process.[4] The theoretical limit of this method is given by thermodynamical theory concerning the fraction separation at phase equilibrium.

Better results were obtained with methods other than synthesis, the present results being expressed as a distribution of sequences.

In this case we note a limitation due to the resolution of the equipment used to determine the length of the sequences. Besides the research method, even the quantitative way to express the nonhomogeneity degree as variation of composition around a mean value or using the sequence distribution is not sufficiently clear. This aspect is obvious for a polymer having a higher degree of complexity : to establish a given structure specific for a certain property involves a lot of data regarding the distribution of the sequences.

II. METHOD

The aim of the present paper is to describe a new way to define the concept of chemical nonhomogeneity of the polymers, using the logical correlation between thermodynamics and information theory. We have tried to make this, based on a rigorous scientific justification of the computing procedure, owing to the fact that the incorrect use of information theory frequently leads to worse results than those obtained by classical methods.[4]

From the thermodynamic point of view, the studied system can be regarded as a distribution of microstates, determined by the nature of the compounds and by the characteristic state parameters.

For copolymers, there may occur structures during the conversion, which are dependent on copolymerization constants and the changes in the conditions of synthesis. The tendency to copolymerize is achieved by a certain specific fractioning determined by the chemical potentials of the monomers, this process being different from a random distribution specific for a maximum entropy.[5]

As any conditioning, this leads to the lowering of the state probability and therefore to the lowering of entropy value. This entropy change constitutes a measure of the information which may be obtained from the analysis of the "message" transmitted by the fractioning of mers in polymers.

Each reaction stage is, in this way, characterized by another probability to form a given chemical structure. During the separation of frac. tions, this will be disposed upon structures of different lengths, compositions or sequences. The separation of the whole ensemble into fractions becomes, therefore, practically impossible.

At this point we introduce the first element of originality : based on the relationships existent between the structure of the formed polymer and the kineticprocess of polymerization, one reconstitutes the structure of the whole polymer, using a single fraction, quantitatively determined.[6] This fraction, the richest or the poorest in what a certain component is concerned, can be quantitatively determined using the tracer method, the one capable to estimate the mass transfers at equilibrium, the limits of the classical thermodynamics being thereby avoided. In order to check this original idea, five copolymers were synthesized, all of them having the vinylidene chloride in common, which offers the possibility to label the fraction with Cl^{36}.

As a common solvent, cyclohexanone was used, to which specific solvents of the other components (styrene, methyl metacrylate, acrylonitrile) : dioxane, benzene, chloroform, dimethyl formamide were added.

By a repeated precipitation with petroleum ether the richest in vinylidene chloride fraction is separated. This fraction obtained by repeated refracting operations is structurally pure, but it cannot be considered as quantitatively "pure", due to the lost by coprecipitation at the separation equilibrium botween fractions.

In order to obtain quantitatively the same pure fraction, it is labelled by isotope echange with $AlCl_3^{36}$. The labelled fraction is mixed with unfractionated polymer. It is then solved in the solvent mixture and the same fractioning operations are repeated. The losses which accompany the refracting operations of diffusion into other fractions can be determined by studying a new equilibrium of the labelled fractions.[7] The integral value of the fraction can be determined because the added portion of labelled fraction participates to all mass transfers between fractions and constitutes, therefore, a control of such processes.

The real mass of the extracted fraction can be obtained with the law of isotopic dilution [8] :

$$m_x = \left(\frac{\lambda_1}{\lambda_f} - 1\right) m_x^* \tag{1}$$

where :

m_x — is the real mass of extracted fraction
m_x^* — the labelled portion of m_x added to the initial sample
λ_1 — the specific activity of m_x^* fraction and
λ_f — the final one.

Details concerning the experimental and computing procedures are reported elsewhere.[9]

In what the quantitative treatment of the chemical nonhomogeneity degree at polymer fractioning is concerned, both the variations in the molar fractions and the variation of homohetero ratio may be used.

With respect to the nonhomogeneity determined by variation in molar composition, it must be taken into account that the nonhomogeneity upon composition is a continuous function of conversion degree.

This nonhomogeneity may vary within large limits between the first and the last conversion degree which may be of two orders.

For this reason, even in the case where the nonhomogeneity is expressed as the deviation around the mean value, the copolymer composition expressed in terms of fractions determined by the summation of conversion degree is incorrect from the analytical point of view.

If the composition at various conversion degrees causes different deviations, i.e. different nonhomogeneities, they must be computed by weighted summation at the same deviation.[10] This constitutes the second original idea of this paper. In order to express the composition not in terms of conversion degree which are quantitatively equal but unequal in what the homogeneity is concerned but in terms of fractions quantitatively unequal and equal with respect to homogeneity, one may use as the measure of homogeneity degree of the fractions, the homogeneity of the first conversion degree α, because under these conditions the molar fractions of the reagents do vary to a little extent. Based on this principle, the formation process of the fractions during the conversion, becomes

$$\begin{aligned} f_1 &= M_0 \cdot \alpha \\ f_2 &= (M_0 - f_1)\,\alpha = M_0\,(1 - \alpha)\cdot \alpha \\ f_3 &= [M_0 - (f_1 + f_2)]\cdot \alpha = M_0\,[\alpha - (2\alpha^2 + \alpha^3)] \\ &\cdots\cdots\cdots\cdots\cdots\cdots \\ f_n &= \left[M_0 - \sum_{i=1}^{n-1} f_n\right]\cdot \alpha = M_0\{\alpha - [(n-1)\alpha^2 + \\ &+ (n-2)\alpha^3 + \ldots 3\alpha^{n-2} + 2\alpha^{n-1} + \alpha^n]\} \end{aligned} \tag{2}$$

where f_n represents the fraction arisen from the n-th conversion degree.
α — stands for the first conversion degree
M_0 — the initial number of moles
According to equations (2), the quantitative ratios between two i and j fractions corresponding to the i-th and j-th conversion degree, become

$$\frac{f_i}{f_j} = \frac{\alpha - [(i-1)\alpha^2 + (i-2)\alpha^3 + \ldots + 3\alpha^{i-2} + 2\alpha^{i-1} + \alpha^i]}{\alpha - [(j-1)\alpha^2 + (j-2)\alpha^3 + \ldots + 3\alpha^{j-2} + \alpha^{j-1} + \alpha^j]} \qquad (3)$$

The calculation of the contribution of each conversion degree is therefore made through the weighted average of conversion degree upon $\alpha_x(x = i, j, \ldots, k)$. The α_x values are calculated as a function of conversion degrees α chosen as homogeneity unity

$$\alpha_x = \alpha - [(x-1)\alpha^2 + (x-2)\alpha^3 + \ldots + 2\alpha^{x-1} + \alpha^x] \qquad (4)$$

Based on this criterion of homogeneity, quantitative estimations can be made only in the case of the same polymer, because the relation to one of the conversion degrees of the polymer sample is relative.

Because the nonhomogeneity of the fractions is not only due to the variation of mole number but also to the homo-/heterosequence ratio it is necessary to consider a second criterion of homogeneity, given by the information entropy.

To establish the fractions which define the polymer structure based on the new criterion, this means the cumulation of the relative fractions (obtained with α_x values) in such a way that the homo-/heterosequence ratio become equal for each fraction.

The information treatment based on the relationship functionality-property-structure achieves the correlation between the properties of the polymers and their specific structures. The polymer refraction by the information principle means in our view the polymer characterization by equientropic fractions. We have immagined and made for this aim a computing program which has been tested on a number of copolymers with three and four-components, the common one being the vinylidene chloride.

The results of the calculation and their interpretation will be published in a subsequent note.

The authors express their thanks to International Atomic Energy Agency of Vienna for financial support of this work.

REFERENCES

[1] P. J. Flory, "Statistical Mechanics of Chain Molecules", Interscience, New York, 1969.
[2] C. Tosi, *European Polymer J.*, **6**, 17 (1970).
[3] C. Tosi, *European Polymer J.*, **4**, 237 (1968).
[4] M. L. Huggins, "Polymer Fractionation", Academic Press, New-York, 1967.
[5] P. Corradini, C. Tosi, *European Polymer J.*, **4**, 227 (1968).
[6] International Atomic Energy Agency (Vienna), Agency Research Contract No. 1825/RB.
[7] G. Ayrey, *Chem. Rev.*, **63**, 645 (1963).
[8] G. Ayrey, *Adv. Polymer Sci.*, **6**, 128 (1969).
[9] E. C. Buruiană, V. T. Bărbinţă, A. A. Caraculacu, *European Polymer J.*, **13**, 311 (1977).
[10] International Atomic Energy Agency (Vienna), Agency Research Contract No. 1826/R2/RB.

Revue Roumaine de Chimie, **31**, 7, 661–670 (1986)

STUDIES ON THE REACTIVITY OF BENZIMIDAZOLONE DERIVATIVES, BASED ON THE ELECTRONIC SPECTRA AND MOLECULAR DIAGRAMS

VALERIA GORDUZA, I. COCÂRLĂ, C. GHIRVU, LUMINIȚA WAGNER * and VIANORA PESCARU

Polytechnical Institute, Spl. Bahlui 71, Iași 6600, Romania

*ICECHIM, Research Center for Dyestuffs, Spl. Independenței 202, Bucharest 77208, Romania

Received December 9, 1985

Reactivity studies were undertaken on four benzimidazolone derivatives, used in the synthesis of heterocyclic azo-pigments on the basis of the electronic spectra and molecular diagrams. The recorded absorption bands, assigned to the π → π*, n → π* and charge transfer transitions were explained on the basis of the halo and solvochromy effects. The O. M. Hückel type calculation for the transitions between frontier orbitals has indicated a good agreement between the theoretical and experimental transition energies.

The utilization of 5-aceto-acetyl-amino-benzimidazolon-2 in the synthesis of certain high quality heterocyclical azo-pigments has aroused the interest in the study of the structure and reactivity of benzimidazolone derivatives (I–IV).

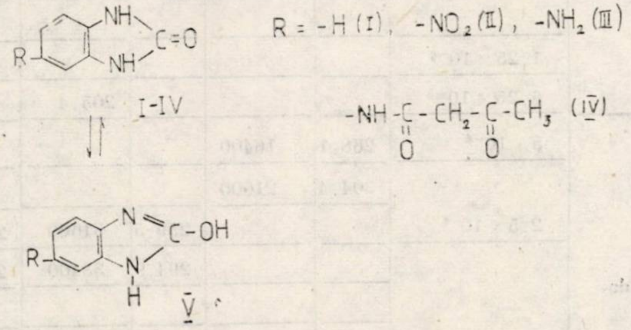

Being an o-phen ylene-urea, benzimidazolone-2 takes part in a tautomeric equilibrium, shifted in the direction of the (I) form, taking into account the value of the basicity constant ($pK_b = 11.56$).

The double reactivity of the benzimidazolone derivatives was correlated with the amphoteric character and their susceptibility to react in the undissociated (I) or ionized state.

Table

The spectral parameters for the UV

Substance	Concentration mol. dm^{-3}	Solvent $HC(=O)-N(CH_3)_2$		C_2H_5OH		CH_3OH	
		λ$_{max}$.	ε	λ$_{max}$.	ε	λ$_{max}$.	ε
Benzimidazolone-2	5×10^{-4}	288	18600	280	20400		
				228	18000		
	2.5×10^{-4}					280.6	30400
						227	28000
	6.25×10^{-5}			206	67200	207	192000
5-Nitro-benzimidazolone-2	5×10^{-4}	290	2080				
		347	3680				
	2.5×10^{-4}			200	33600	204	42400
				224	33600	223	48800
				250	27600	251.3	39600
				340	18400	341	25200
5-Amino-benzimidazolone-2	5×10^{-4}	318	8200				
	2.5×10^{-4}			304.4	25600	305.8	19200
	1.25×10^{-4}						
	6.25×10^{-5}				205.4		128000
5-Aceto-acetyl-amino-benzimidazolone-2	5×10^{-4}	268.1	16400				
		304.4	21000				
	2.5×10^{-4}			259.5	31600	260	44800
				294.9	38400	295.6	49200
	1.25×10^{-4}						
	6.25×10^{-5}			215.2	130000	216.7	188800

Note : The units of measure for the spectral parameters (λ$_{max}$, ε) are : nm and dm^{-3}mol^{-1}cm^{-1} respectively.

1

absorption in benzimidazolone derivatives

CH_3OH HCl 0.1 N		CH_3OH HCl 1 N		CH_3OH HCl 10 N		CH_3OH NaOH 0.1 N		CH_3OH NaOH 0.2 N	
$\lambda_{max.}$	ε	$\lambda_{max.}$	ε_{ν}	$\lambda_{max.}$	ε	λ_{max}	ε	λ_{max}	ε
282	12210	282	11400	276	7600	287	6105	287.4	4440
226	shoulder	226	shoulder	269	7621	245	shoulder	248.8	2424
				206	20630	214	16630	220.8	6340
204	112800	204	50526						
201.4	14526	202.8	11157			212	13684		
222.6	16631	222.8	14947	221.6	21052	236.2	12210	236.2	9834
251	13263	251.7	11790	244.3	12210	269.7	13263	270	11370
340	9052	341	8000	324.4	9473	403.7	16631	403.8	17000
286.8	7157	286.1	6530	278.8	5470	307	6736	306.7	9620
		230.9	3790	228.2	5680	250	shoulder	250.5	shoulder
				207.5	25680	216	24200	218.9	25470
208.4	19790	208.8	56000						
207	89600								
260	10105	259	5890	279.1	4630	256.6	6950	250	shoulder
269.9	10530	291.4	8000	340	7578	314	14105	310.8	13470
				220.8	28421	217.7	17050	220	11790
				209	24842				
214.9	23580	206.8	21890						

When the cation is formed, the proton gets fixed at the oxygen atom from the structure (I) with the transfer of the positive charge to the nitrogen atom from the imidazole cycle, the system coplanarity being maintained.[1]

EXPERIMENTAL

Benzimidazolone-2 (I), obtained by the condensation of the o-phenylenediamine with urea in a molar ratio (1 : 2), in aqueous medium [2] was purified by the recrystallization in ethanol (m.p. 308°C). 5-Nitrobenzimidazolone-2 (II) was prepared by nitration with sulphonitric mixture[3] (m.p. 305°C) after its recrystallization from water. 5-Aminobenzimidazolone-2 (III) was obtained by catalytic hydrogenation of the nitroderivative, m.p. 340°C (from ethanol : ethyl-ether 1 : 1).[4] 5-Aceto-acetylamino-benzimidazolone-2 (IV) (m.p. 246°C) was prepared by means of an original method,[5] i.e. by the acylation of the ammino-derivative with acetylacetate, in chlorbenzene, in the presence of dimethyl formamide and triethanolamine at low pressure, in inert atmosphere.

The electronic spectra of the benzimidazolone derivatives have been registered by means of a Specord Carl--Zeiss Jena spectrophotometer, for concentrations ranging between 6.25×10^{-5} M and 5×10^{-4} M, using different solvents (ethyl alcohol, methyl alcohol, N, N'-dimethyl formamide) and different pH's (NaOH 0.1N and 0.2 N and HCl, 0.1 N : 1 N and 10 N respectively)

RESULTS AND DISCUSSION

Correlations between the Electronic Spectra and the Reactivity of the Benzimidazolone Derivatives

The electronic spectrum of the benzimidazolone-2 is characterized by three absorption bands situated, depending on the solvent polarity, at 280.6—288 nm, 206—207 nm and 226—227 nm, respectively and assigned to the $\pi \rightarrow \pi^*$ and $n \rightarrow \pi^*$ transitions respectively.

An extended conjugated system is realized in benzimidazolone, due to the carbonyl group polarizability, the electrodonor character of the nitrogen atoms from the ureidic rest and the presence of the phenyl ring. It is possible to differentiate the absorption bands on the basis of the solvochromic effect.[6]

By stabilizing the excited state more than the fundamental state, the polar solvents determine a bathochromic effect on the $\pi \rightarrow \pi^*$ transition and a hypsochromic effect on the $n \rightarrow \pi^*$ transition, correlated with the lower polarity of the $n\ \pi^*$ excited state (Table 1).

The registration of the electronic spectra in methanol in the presence of NaOH 0.1 N and 0.2 N respectively gave similar curves, but with a more evident batchochromic shift at the maximum alkaline concentration, i.e. at higher energy transitions. Simultaneously a hypochromic effect, maximum for the $n \rightarrow \pi^*$ transition, was seen.

At an acid pH, a hypsochromic effect was seen, more evident at the maximum acid concentration. It is also worth noticing the disappearance of the maximum corresponding to the $n \rightarrow \pi^*$ transition and the alteration of the shape of the high wavelength maximum. While at a low acid concentration only a bathochromic shift was seen, at high concentration a double absorption maximum was noticed (276 and 269 nm), correlated with the appearance of the ionic structure, involved in the electrophilic substitution reaction of the benzimidazolone.

5-Nitro-benzimidazolone-2

Due to the presence of the nitro chromophore, grafted on a heterocyclic system, 5-nitro-benzimidazolone-2 has four absorption bands.

The absorption band correlated with the $n \rightarrow \pi^*$ transition of the carbonyl group from the benzimidazolone is again hypsochromic shifted at 223—224 nm (Table 1). The absorptions in the ranges 251.3 ÷ 290 and 341 ÷ 347 nm are significant, they being accounted for, by the charge transfer from the aromatic ring to the nitric group.

The alkalinization determines significant bathochromic effects (17 ÷ ÷ 61.8 nm), a bathochromic shift of the band corresponding to the $n \rightarrow \pi^*$ transition of the carbonyl group being seen, smaller than in the case of benzimidazolone, while the hypochromic effects are comparable.

The registration of the absorption spectra in methanol at acid pH resulted for by the protonization of the nitric groups.

5-Amino-benzimidazolone-2

The possibility of the $p - \pi$ conjugation in the heteroaromatic ammines results in the decrease of the bonding orbital energy and the increase of the nonparticipant orbital energy, so that to reduce the $n \rightarrow \pi^*$ transition energy. On the other side, by the protonization at nitrogen, a halochromic effect was noticed revealed by a hypsochromic spectral shift (Table 1).

The absorption band characteristic for the 5-amino-benzimidazolone-2, situated at 304.4 ÷ 318 nm, depending on the solvent polarity shows a significant hypsochromic shift, coupled with a hypochromy in the acid medium.

It is interesting that by acidulation or alkalinization the absorption band corresponding to the $n \rightarrow \pi^*$ transition of the carbonyl group (226 nm) reappears, shifted and altered under the form of a peak at 228—231 nm (acid medium) and at 250—250.5 nm (basic medium).

5-Aceto-Acetylamino-benzimidazolone-2

The disturbance of the carbonyl bonding orbitals due to the interaction with the non-participant orbital of the nitrogen and the effect of the acetyl group results in a bathochromic shift of the $\pi - \pi^*$ transition corresponding to the aromatic system where the 5-aceto-acetylamino group (215 nm) is grafted (Table 1).

Beside this intense band, a low intensity absorption band is registered (294.9—304.4 nm), correlated with a $\pi - \pi^*$ transition.

The absorption band at 259.5 ÷ 268.1 nm can be a band with a charge transfer that may be influenced by the hydrogen bond association.

At high acid concentrations, bathochromic, shifts were registered as well as a double maximum at 216.7 nm, resulting in the registration of two absorption maxima at 209 and 220.8 nm. The above mentioned spectral shift is accounted for by the double reactivity of the aceto-acetyl-aminic rest correlated with the possibility of generating the conjugated bases of the enolic and ketonic forms :

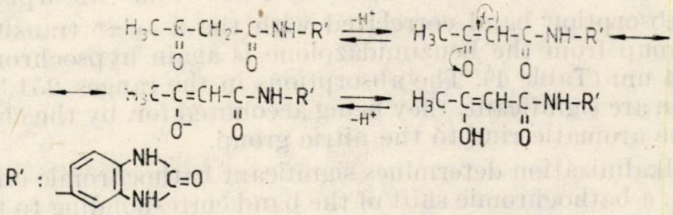

At alkaline pH, a hypsochromic shift is seen of the charge transfer band, associated with the hypochromy strengthening by the increase of the alkaline concentration, as well as a bathochromic shift of the maximum wavelength absorption.

Electronic Structure-Reactivity Correlations Based on the Calculation of the Molecular Orbitals

Some aspects of the theoretical interpretation of theexperimental results presented in the preceding paragraph can be obtained on the basis of the quantum orbital theory. Thus, OM calculations have been made on the Hückel type,[7] using the following parameters, suggested or adopted from the literature[8-10]: $h_{NH_2} = 1.8$; $h_{NH} = 1.4$; $h_{O(C=O)} = 0.7$; $h_{N(NO_2)} = 1.7$; $h_{O(NO_2)} = 0.4$; $k_{C-NH_2} = 0.6$; $k_{C-NH} = 0.8$: $k_{C=O} = 1$; $k_{C-NO_2} = 0.6$; $k_{C-CO} = 0.6$; $k_{N-O} = 0.9$.

The molecular diagrams are presented in Figure 1.

The diagrams of the molecular electronic structure in the fundamental state shows an increase of the electrophylic reactivity of the constitutive benzene ring and unsignificant alterations of the electronic structure of the carbonyl group in the substituted benzimidozolone compounds. Comparable probabilities will result for showing the tautomeric equilibrium I for the investigated cases.

In order to interpret the electronic spectra it was admitted that the absorption bands made evident experimentally may be assigned to some $\pi \rightarrow \pi^*$ transitions, above them the $n \rightarrow \pi^*$ and charge transfer transitions being overlapped.

Accordingly, it was suggested that within the simple Hückel method, the most important transitions implied in the radiation absorption process are those between the frontier orbitals, as Figure 2 shows.

To simplify, we shall use the band notation suggested by Clar for the aromatic hydrocarbons.[11]

The electronic configurations implied in the radiation absorption process, according to the transitions indicated in Figure 2, are :

$$\psi = |\varphi_1 \overline{\varphi}_1 \varphi_2 \overline{\varphi}_2 \cdots \varphi_m \overline{\varphi}_m| \quad (1)$$

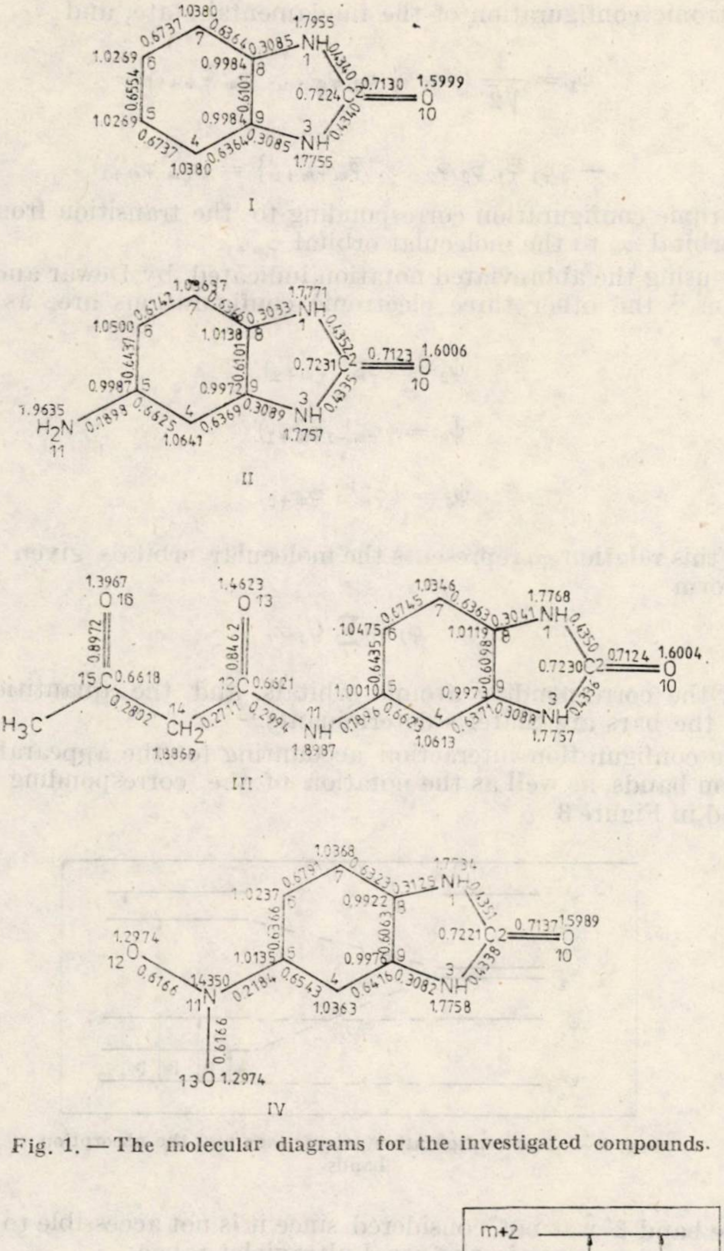
1.0380
0.6737
7
0.6364
0.3085
NH
1.7955
1.0269
6
0.9984
8
1
0.4340
0.7130
1.5999
0.6554
0.6101
0.7224
C2
O
10
1.0269
5
0.9984
9
3
0.4340
0.6737
4
0.6364
0.3085
NH
1.0380
1.7755
I
1.05637
1.7771
NH
0.3033
1.0500
6
7
1.0138
8
1
0.7123
1.6006
0.6437
0.6101
0.7231
C2
O
10
0.9987
5
0.9972
9
3
0.4335
1.9635
H_2N
0.1893
0.6625
4
0.6369
0.3089
NH
11
1.0641
1.7757
II
1.3967
O 16
0.8972
15 C 0.6618
0.2802
H_3C
14
CH_2
1.8869
1.4623
O 13
0.8462
12 C 0.6621
0.2711
0.2994
11
NH
1.8987
1.0346
0.6745
7
0.6363
0.3041
1.7768
NH
1
1.0475
6
1.0119
8
0.6435
0.6098
0.7124
1.6004
0.7230
C2
O
10
1.0010
5
0.9973
9
3
NH
0.1896
0.6629
4
0.6371
0.3088
1.0613
1.7757
III
1.0368
0.6791
7
0.6323
0.3129
1.7734
NH
1
1.0237
6
0.9922
8
0.6366
0.6063
0.7137
1.5989
0.7221
C2
O
10
1.2974
O
12
1.0135
5
0.9976
9
3
0.4338
0.6166
1.4350
N
11
0.2184
0.6543
4
0.6416
0.3082
NH
1.0363
1.7758
0.6166
13 O 1.2974
IV

Fig. 1. — The molecular diagrams for the investigated compounds.

Fig. 2. — The transitions between the frontier orbitals.

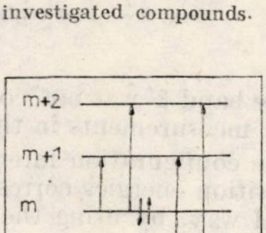

the electronic configuration of the fundamental state, and

$$\psi_1 = \frac{1}{\sqrt{2}} \{ | \varphi_1 \overline{\varphi}_1 \varphi_2 \overline{\varphi}_2 \ldots \varphi_m \overline{\varphi}_{m+1} | - \\ - | \varphi_1 \overline{\varphi}_1 \varphi_2 \overline{\varphi}_2 \ldots \overline{\varphi}_m \varphi_{m+1} | \} = (\varphi_m^{-1} \varphi_{m+1}) \tag{2}$$

the electronic configuration corresponding to the transition from the molecular orbital φ_m to the molecular orbital φ_{m+1}.

By using the abbreviated notation indicated by Dewar and Longuet — Higgins,[11] the other three electronic configurations are as follows:

$$\psi_2 = (\varphi_m^{-1} \varphi_{m+2}) \tag{3}$$

$$\psi_3 = (\varphi_{m-1}^{-1} \varphi_{m+1}) \tag{4}$$

$$\psi_4 = (\varphi_{m-1}^{-1} \varphi_{m+2}) \tag{5}$$

In this relation φ_j represents the molecular orbitals given under the LCAO form

$$\varphi_j = \sum_r C_{jr} \varkappa_r \tag{6}$$

$\varkappa_r$ being the corresponding atomic orbitals, and the quantities written between the bars are Slater's determinants.[12]

The configuration interaction accounting for the appearance of the absorption bands, as well as the notation of the corresponding bands are presented in Figure 3.

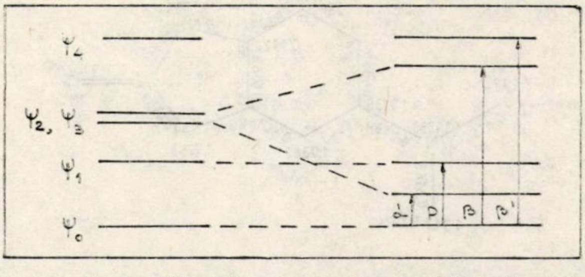

Fig. 3. — The configuration interactions and the absorption bands.

The band β' was not considered since it is not accessible to the experimental measurements in the usual ultraviolet range.

The configuration interaction was considered for the calculation of the transition energies corresponding to the α, p and β bands, in a semiempirical way, by using the benzimidazolone molecule as standard, i.e.

$$\Delta E_{\text{exp.}(\alpha,\, p,\, \beta)} = \Delta E_{\text{teor.}(\alpha,\, p,\, \beta)} \tag{7}$$

On the other side,

$$\Delta E_{\text{theor.}(\alpha,p,\beta)} = \Delta n \beta_{\alpha,\ p,\ \beta} \tag{8}$$

Where Δn is the variation of the Coulomb parameter coefficients for the molecular orbitals implied in the transition. By using the experimental values for the transition energy and relation (8), one can calculate three parameters useful in the calculation of the transition energy of the other molecules.

The quantity Δn corresponding to different transitions was calculated as follows;

$$\Delta n_{(p)} = n_{m+1} - n_m \tag{9}$$

$$\Delta n(\alpha,\beta) = \frac{1}{2}\left[(n_{m+2} - n_m)(n_{m+1} - n_{m-1})\right] \tag{10}$$

The electronic spectra registered in ethanol were used as experimental data to determine the positions of the absorption bands. Thus the following values of the parameters were obtained:

$$\beta_\alpha = 2.51\ \text{eV},\ \beta_p = 3.52\ \text{eV};\ \beta_\beta = 3.41\ \text{eV} \tag{11}$$

The comparison between the calculated and the experimental data is given in Table 2. We used for the comparison $\Delta(\Delta E)$, i.e. the difference between the calculated and the experimental value of ΔE.

Table 2

The calculated transition energies and their comparison with the experimental data

Molecule	Band	Δn	ΔE, eV Exp.	ΔE, eV Theor.	$\Delta(\Delta E) = \lvert\Delta E_{\text{exp.}} - \Delta E_{\text{theor}}\rvert$
$R-H$	α	1.7645	4.43	4.43	0
	p	1.5472	5.44	5.44	0
	β	1.7645	6.02	6.02	0
$R-NH_2$	α	1.7528	4.07	4.40	0.33
	p	1.5227	5.00	5.35	0.35
	β	1.7528	6.04	5.98	0.06
$\mathrm{R{-}NH{-}\underset{\underset{O}{\parallel}}{C}{-}CH_2{-}\underset{\underset{O}{\parallel}}{C}{-}CH_3}$	α	1.5333	4.18	3.85	0.33
	p	1.3194	4.78	4.64	0.14
	β	1.5333	5.76	5.23	0.53
$R-NO_2$	α	1.1564	3.63	2.90	0.72
	p	0.7583	4.90	2.67	2.24
	β	1.1564	5.54	3.95	1.49
			6.20		2.25

R:
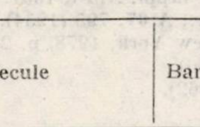

As can be seen from Table 2, the agreement between the theoretical and the experimental values is quite satisfactory, excepting the compound containing the nitro group.

It is well known that the nitro-group strongly interacts with the benzene ring, resulting in the appearance of an intense charge transfer band.[13,14] There is, hence, the possibility that the bands situated at 253 nm (4.90 eV) of 342 nm (3.63 eV) should be charge transfer bands and thus they should not correctly integrate in the computing scheme we adopted. Anyhow, the simultaneous presence of the nitro and carbonyl groups in a molecular system makes difficult the interpretation of the electronic spectra, since three types of bands are superimposed in the range 250—360 nm, that can exist in this case. Moreover, the excited electronic configurations can be highly polarized, which determines the incompatibility of the conficuration interactions with the scheme proposed here. This type of researches is carried on in our laboratory.

REFERENCES

1 L. S. Efros and A. V. Eltsov, *Zhur. Obsch. Khim.*, **27**, 684 (1957).
2 L. S. Efros, B. A. Porai-Koshitz and S. G. Farbenstein, *Zhur. Obsch. Khim.*, **23**, 1691 (1953).
3 L. S. Efros and A. V. Eltsov, *Zhur. Obsch. Khim.*, **26**, 127 (1956).
4 R. L. Clark, and A. A. Pessolano, *J. Amer. Chem. Soc.*, **80**, 1657 (1958).
5 V. Gorduza, L. Wagner and L. Stănescu, *Rev. Chim. (Bucharest)*, **35**, 888 (1984).
6 C. N. R. Rao, "Ultraviolet and Visible Spectroscopy. Chemical Applications", 1967, Butterworths, London, p. 17.
7 E. Hückel, *Z. Phys.*, **70**, 204 (1931) ; **76**, 628 (1932).
8 A. Streitwieser, Jr., "Molecular Orbital Theory for Organic Chemistry", Wiley, 1961.
9 A. Julg and O. Julg, "Exercices de Chimie Quantique", Dunod, Paris, 1967.
10 W. P. Purcell and J. A. Singer, *J. Chem. Eng. Data.*, **12** (2), suppl. April, 1967.
11 M. J. S. Dewar, and H. C. Longuet-Higgins, *Proc. Phys. Soc.*, **A 67**, 795 (1954).
12 M. Weissbluth, "Atoms and Molecules", Academic Press, New York, 1978, p. 240.
13 J. Tanaka and S. Nagakura, *J. Chem. Phys.*, **24**, 1274 (1956).
14 J. E. Bloor and F. Paradejordi, *Theoret. Chim. Acta.* **1**. 83 (1962).

Revue Roumaine de Chimie, **31**, 7, 671—677 (1986)

THERMAL EFFECT AND OSCILLATIONS IN THE CATALYTIC OXIDATION OF METHANOL

N. I. IONESCU, M. S. CHIRCA and D. I. MARCHIDAN

ICECHIM — Center of Physical Chemistry, Spl. Independenței 202, Bucharest 79611, Romania

Received July 20, 1985

The methanol oxidation on Pd and Pt supported catalysts was studied in a dynamic calorimeter. The thermal effect in steady state conditions was influenced by the type of the catalyst, the flow rate of the oxygen, the methanol concentration and the reaction temperature. Regular oscillations of the catalyst temperature with very high amplitude (110 K) were detected.

The methanol, oxidation on noble metal catalysts of the platinum group produces only carbon dioxide and water, but it generates interest because in certain conditions regular oscillations of the catalyst temperature were detected.[1-3]

The aim of this paper is to evidence that a dynamic calorimeter may be a useful tool in order to compare the activity of various catalyst samples and also in the detection of the thermal oscillations in heterogeneously catalytic oxidation of methanol.

EXPERIMENTAL

The main part of the installation used for studying the thermal effect in the catalytic oxidation of methanol was the dynamic calorimeter, whose schema is presented in fig. 1. The reaction cell was similar with those presented by Kral[4] and by Jaeger,[1,3] but it differed by the position of the thermocouple-catalyst support system, by the direction of the gases flow which permitted a better contact with the catalyst and by the introduction of a thermocouple which allowed to measure the temperature of the ambient gases at 5 mm above the catalyst. Also, in order to avoid any possible catalytic effect, the catalyst support was made from a tantalum plate 0.2 mm thick. The large area of the support permitted the distribution of the very finely divided catalyst sample (up to 50 mg) in a uniform thin layer, so that the entire quantity of the catalyst took part in the reaction and the catalyst support acquired instantaneously the catalyst sample temperature.

The temperature of the gaseous mixture and the difference between this temperature and those of the catalyst sample was measured by a differential system of chromel-alumel thermocouples. The e.m.f. values were read on digital voltmeters E 0303 (IAEMI — Bucharest) and the temperature difference was continuously recorded on a Speedomax XL 681 recorder (LNI — Italy).

The reaction cell was kept at a constant temperature (353—373 K) by circulating ethyleneglycol with a U 10 thermostat (G.D.R.)

The catalytic oxidation of methanol was studied both with air and with oxygen. A serie of needle valves Unitra ZD 200 (Poland) was used in order to assure a very precise flow o the gases. A three-way valve permitted to switch the gases either directly through the reaction cell or first through the methanol saturator, kept at the temperature needed to achieve a certain content of methanol in the reaction mixture.

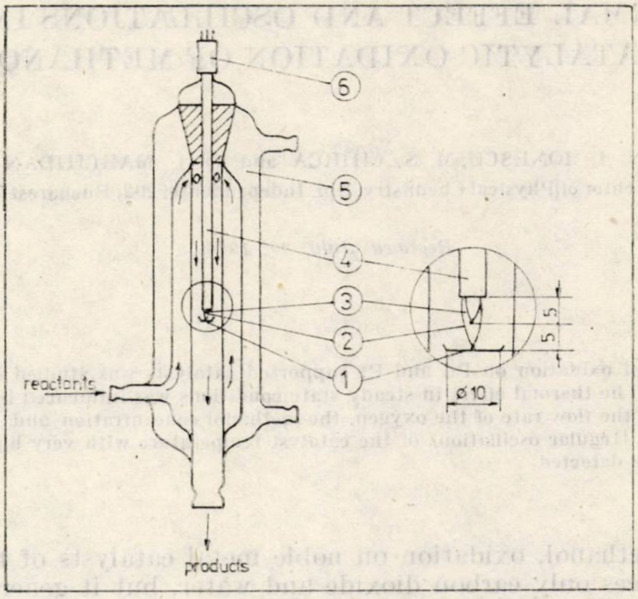

Fig. 1. — The dynamic calorimeter used for studying the catalytic oxidation of methanol (1 — catalyst sample support ; 2 — differential thermocouple ; 3 — reference thermocouple ; 4 — ceramics tube ; 5 — thermostated mantel ; 6 — thermocouples connection).

The catalysts studied in the reaction of methanol oxidation were 0.5% $Pd/LiAl_5O_8$ (Bayer), 0.5% Pt/Al_2O_3 (Vega) and 0.38% Pt/Al_2O_3 (Octafining). The granulation of the catalyst samples was 0.08—0.11 mm and their weight varied between 18 and 30 mg.

In order to analyse the gaseous products, a 104 model Pye Unicam chromatograph was used, fitted with two glass columns filled with Porapak Q and with molecular sieves 5 Å respectively. Carbon dioxide was identified as the main product, which proved that the total oxidation of methanol took place.

RESULTS AND DISCUSSION

The rise of the catalyst temperature comparative with the temperature of the gaseous reaction mixture evidenced the high exothermicity of the methanol oxidation reaction. Usually, an equilibrium temperature difference, ΔT_e, is attained, but in some special conditions the reaction may reach an oscillatory regime.

The dynamic calorimeter used in our experiments permitted to establish that the magnitude of the equilibrium temperature difference, ΔT_e, and the rate of its attainment are affected by a large number of parameters such as : the type and the weight of the catalyst sample, the type and the flow rate of the oxidizing agent (air or oxygen), the methanol content in the reaction mixture and the temperature of the reaction cell. Among these parameters the most important seems to be the flow rate of oxygen or air. In fig. 2 a typical experiment is presented in which the oxygen flow rate was increased progressively. It results that the rate of the attainment of the equilibrium temperature difference, ΔT_e, increases with the oxygen flow rate. For a flow rate of oxygen higher than 40 mL/min, the temperature difference ΔT presents a sudden jump at the moment of establishing the new oxygen flow rate. In these cases the ΔT_e value reaches first a rapid maximum and then descends to the equilibrium value, since in the catalyst layer the equilibrium temperature is attained sooner than in the ambient gaseous mixture.

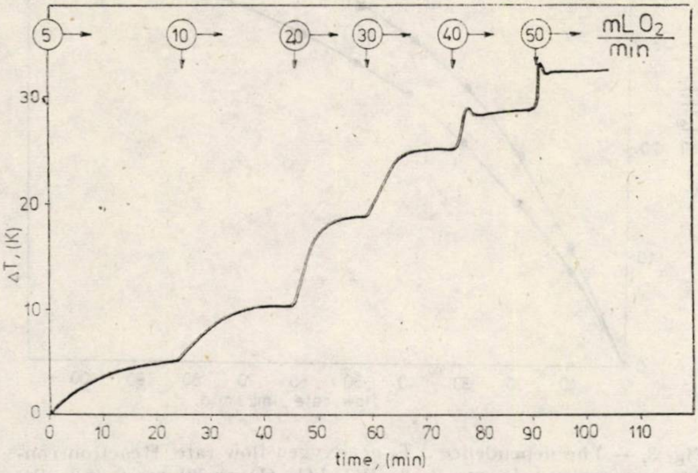

Fig. 2. — The rise of the catalyst temperature at different oxygen flow rates. Reaction conditions: catalyst 18 mg 0.5% Pt/Al_2O_3; cell temperature 353 K; methanol concentration 2.3% *V*.

From fig. 2 it can be also seen that the ΔT_e value is greater at greater oxygen flow rates. The dependence ΔT_e *vs.* the oxygen flow rate is presented in fig. 3 for two experiments which differ by the type and the weight of the catalysts used. For oxygen flow rates below 20 mL/min this dependence is quite liniar, but it seems that at very high oxygen flow rates a limit ΔT_e, value is attained. This fact may be regarded as due either to the cooling of the catalyst support at a higher flow of gases, or more probably to the fact that a higher reactants flow rate is similar with a lower contact time, so that in these conditions the catalyst sample does not participate entirely at the reaction.

The methanol concentration also seems to influence the ΔT_e value, as is presented in fig. 4, for an experiment in which the temperature of the methanol saturator was gradually increased.

Another factor which influences the ΔT_e value is the temperature of the reaction cell, properly the temperature of the gaseous reactants at the entrance in the reaction chamber. This dependence is presented in fig. 5.

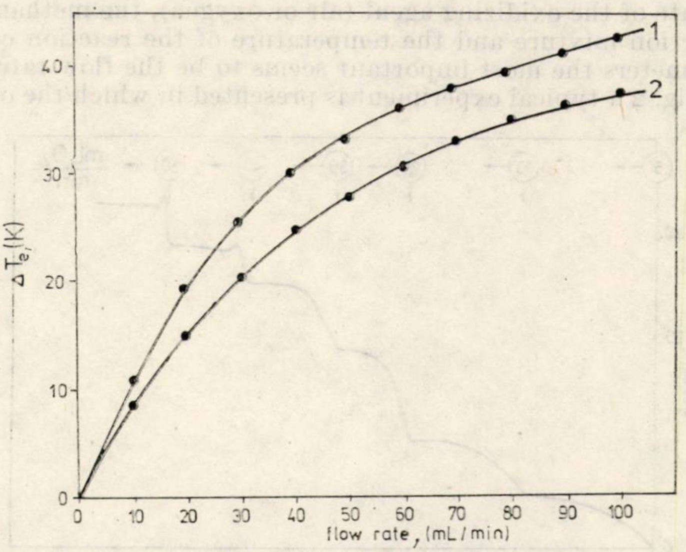

Fig. 3. — The dependence ΔT_e *vs.* oxygen flow rate. Reaction conditions: catalyst 18 mg 0.5% Pt/Al_2O_3 (1) or 30 mg 0.38% Pt/Al_2O_3 (2); cell temperature 353 K; methanol concentration 2.3% *V*

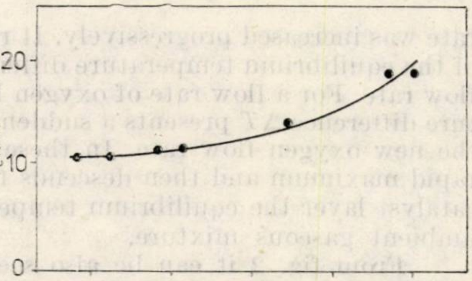

Fig. 4. — The dependence ΔT_e *vs.* methanol concentration. Reaction conditions: catalyst 30 mg 0.5% $Pd/LiAl_5O_8$; cell temperature 365 K; air flow rate 11 mL/min.

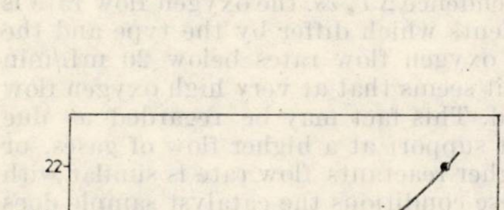

Fig. 5. — The dependence ΔT_e *vs.* cell temperature. Reaction conditions: catalyst 30 mg 0.5% Pt/Al_2O_3; methanol concentration 3.9% *V*; air flow rate 11 mL/min.

The data presented till now indicate that in the experimental area studied for the catalytic oxidation of methanol the ΔT_e value is greater when either the reaction (cell) temperature, the methanol concentration in gases or the oxygen flow rate grows. In these conditions, keeping constant all the above mentioned parameters it is possible to use the dynamic calorimeter in order to compare the activity of different catalysts. This direction for the utilization of the dynamic calorimeter was already presented by Kral,[4] who tested some catalysts for hydrogen oxidation at 20°C. The data here presented in fig. 3 may thus be used to compare the activity of the two catalysts used (0.5% Pt and 0.38 % Pt respectively supported on alumina) in the methanol oxidation at 353 K. Since the ΔT_e value is greater for the first catalyst it seems that it has a better activity. This was confirmed by the gas-chromatographic analysis of the gaseous products, which showed a 1.2 time higher conversion of methanol on 0.5 % Pt/Al_2O_3.

Though in the greatest range of experimental conditions a steady state, respectively a constant ΔT value is attained, in certain conditions regular oscillations of the catalyst temperature may be detected. The main factors which determine the appearance of the thermochemical oscillations in the catalytic oxidation of methanol are the type of the catalyst, the oxygen flow rate and the methanol concentration. In order to determine the appropriate oxygen flow rate, Jaeger, Plath and van Raaij[3] continuously increased it till a sudden jump of the catalyst temperature is detected. As it can be seen from fig. 3, in certain experimental conditions this jump is not attained. In order to determine the appropriate methanol content for the appearance of the thermal oscillations, the continuous increase of the methanol concentration in gases, at a constant oxygen flow rate was realised, till a very high jump of the catalyst temperature was detected (fig. 6). At a methanol concentration close to the value corresponding to the ΔT jump, by smoothly varying the oxygen flow rate, regular thermal oscillations may be obtained.[5]

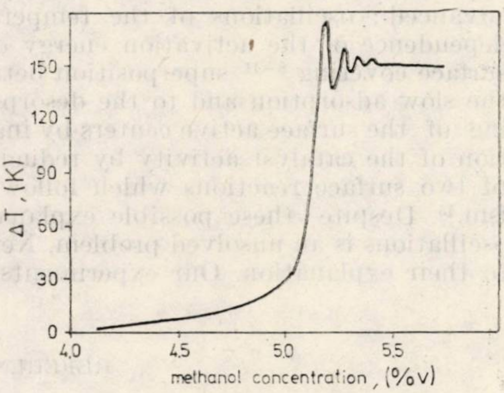

Fig. 6. — The establishment of the methanol concentration at which chemical oscillations can appear. Reaction conditions: catalyst 18 mg 0.5% Pd/$LiAl_5O_8$; cell temperature 353 K; oxygen flow rate 95 mL/min.

The opportunity of the reference thermocouple (fig. 1), which permits to measure the temperature of the ambient gases, is evidenced by the fact that one could determine that the real amplitude of the catalyst temperature oscillations is far greater than those already reported in literature.[1-3] Because the registred ΔT value represents the difference between the catalyst temperature and those of the gases at the reference point (T_g), the real amplitude of the thermal oscillations may reach 110 K, as presented in fig. 7.

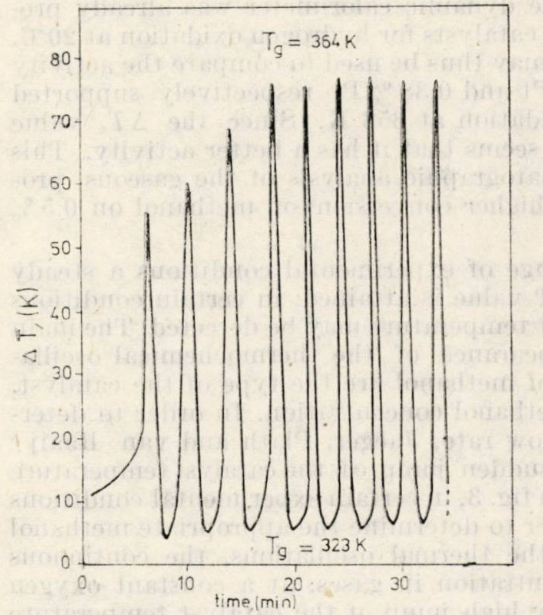

Fig. 7.—Thermal oscillations in the catalytic oxidation of methanol T_g denotes the temperature of the ambient gaseous mixture. Reaction conditions: catalyst 20 mg 0.5% Pd/LiAl$_5$O$_8$; cell temperature 353 K; methanol concentrantion 4.95% V; oxygen flow rate 6 mL/min.

The mechanism which generates thermochemical oscillations in heterogeneous catalytic systems is not known. In order to explain the apperance of the oscillations in these systems, many hypothesis have been advanced: oscillations of the temperature of the catalyst surface [6,7]; dependence of the activation energy or of the adsorption heat on the surface covering [8-11] superposition between multiple steady states due to the slow adsorption and to the desorption of an inert compound,[12] blocking of the surface active centers by inactive oxygen species and regeneration of the catalyst activity by reducing these species,[13,14] superposition of two surface reactions which follow a Langmuir-Hinshelwood mechanism.[15] Despite these possible explanations, the nature of the chemical oscillations is an unsolved problem. New experimental data may be useful to their explanation. Our experiments are in progress.

REFERENCES

[1] N. I. Jaeger, P. J. Plath and E. van Raaij, Proceedings of the 4-th International Symposium on Heterogeneous Catalysis, vol. 2, Varna, 1979, p. 15.

[2] N. I. Jaeger, P. J. Plath and E. van Raaij, *Ber. Bunsenges. Phys. Chem.*, **84**, 417 (1980).

[3] N. I. Jaeger, P. J. Plath and E. van Raaij, *Z. Naturforsch.*, **36 a**, 195 (1981).

[4] H. Kral, *G-I-T, Fachzeitschrift für das Laboratorium*, **11**, 699 (1967).

[5] N. I. Ionescu, M. Chirca and D. I. Marchidan, *React. Kinet. Catal. Lett.*, (in press).

[6] R. Dagonnier and J. Nuyts, *J. Chem. Phys.*, **65**, 2061 (1976).

[7] R. E. Lagos, B. C. Sales and H. Suhl, *Surf. Sci.*, **82**, 325 (1976).

[8] M. Sheintuch and R. A. Smitz, *A.C.S. Symp. Ser.*, 165, 487 (1978).

[9] M. Sheintuch and R. A. Smitz, *Catal. Rev. Sci. Eng.*, **15**, 107 (1977).

[10] M. G. Slinko and M. M. Slinko, Catal. Rev. Sci. Eng., **17**, 119 (1978).

[11] C. A. Pikios and D. Luss, *Chem. Eng. Sci.*, **32**, 191 (1977).

[12] G. Einberger, *Chem. Eng. Sci.*, **31**, 1263 (1978).

[13] E. Wicke, P. Kummann, W. Keil and J. Schiefler, *Ber. Bunsenges. Phys. Chem.*, **84**, 315 (1980).

[14] R. A. Schitz, *Proc. J.A.C.C.*, **2**, 21 (1979).

[15] B. C. Sales, J. E. Turner and M. B. Maple, *Surf. Sci.*, **114**, 3815 (1982).

Revue Roumaine de Chimie, **31**, 7, 679—694 (1986)

CHEMICAL GRAPHS. Part 44.[1]

ISOMER ENUMERATION FOR SUBSTITUTED SATURATED POLYHEDRAL VALENCE ISOMERS OF ANNULENES

ALEXANDRU T. BALABAN
Polytechnic Institute, Department of Organic Chemistry, 76206 Bucharest, Roumania

Received November 19, 1985

By using Pólya's enumeration theorem together with symmetry operations involving either only proper rotation axes or also the improper rotation axes, enumerations of all isomers or only of constitutional isomers were carried out for substituted saturated regular or semiregular polyhedral $(CH)_n$ valence isomers I—VI, IX, XII—XV as well as for XVI, perhomocubane ($C_{20}H_{32}$) which is a hydrocarbon related to cubane.

INTRODUCTION

Enumeration of valence isomers of [*n*]annulenes using graph theoretical formulas[2] afforded numbers of connected and disconnected cubic multigraphs.[1] From the former, the planar connected cubic multigraphs are relevant because they correspond to chemically feasible [*n*]annulene valence isomers.[3] An algorithm for constructing such structures has been developed earlier;[4] the numbers of these structures for various *n* values agree for the two different approaches. A book reviewing annulenes and their valence isomers is in press,[5] and several reviews were recently published.[6]

Lately, spectacular experimental successes rewarded the prolonged effort towards the synthesis of several polyhedral valence isomers such as pentaprismane, IV (Eaton and coworkers),[7] and dodecahedrane, VI (Paquette and coworkers)[8]. Cubane, III, had been prepared earlier by Eaton *et al.*[9] The last of the Platonic regular polyhedra which corresponds to a cubic graph, tetrahedrane, I, is too unstable, when unsubstituted, to be isolated.[10] However, tri- and tetra-substituted tetrahedranes were prepared by Masamune et al.[11] and by Maier et al.[12] Tetra-t-butyltetrahedrane (Maier and coworkers[13]) is especially stable owing to the "straightlace effect (Korsett-Effekt)". The remaining two regular polyhedra, the octahedron and icosahedron, cannot correspond to $(CH)_n$ hydrocarbons because their graphs have vertices of degree 4 and 5, respectively, whereas CH groups have three free valencies. A C_6 molecule with an octahedral arrangement of six covalently bonded carbon atoms would have a huge strain because all valencies of each carbon would have 60° angles on a single side of a plane.

Semiregular polyhedra which are regular graphs of degree three and which could represent valence isomers of annulenes are the truncated tetrahedron V, $(CH)_{12}$ with four triangular faces and with four hexagonal faces, symbol (3,6, 6) indicating numbers of sides for polygonal faces meeting at each vertex; truncated cube VII, $(CH)_{24}$ with eight triangular and six octogonal faces, symbol (4,6,6); truncated octahedron VIII, $(CH)_{24}$ with eight hexagonal and six square faces, symbol (4,6,6); truncated icosahedron $(CH)_{60}$ with 12 pentagonal and 20 hexagonal faces, symbol (5,6,6); truncated dodecahedron $(CH)_{60}$ with 20 triangular and 12 decagonal faces, symbol (3,10,10). It can be noted that the last four semiregular polyhedra form two complementary (dual) pairs. There exist also two semiregular polyhedra with vertex degree three which have three types of faces: the truncated cuboctahedron, symbol (4,6,8) with six octogonal, eight hexagonal and twelve square faces; and the truncated icosidodecahedron with twelve decagonal, twenty hexagonal and thirty square faces, symbol (4,6,10).

A carbon atom cluster C_{60} with the probable structure of a truncated icosahedron was detected experimentally by laser-vaporization of graphite in a high-pressure supersonic nozzle; a lanthanum complex $C_{60}La$ with a caged metal atom was also found by Smalley and co-workers.[14] Theoretical predictions of this C_{60} molecule (called "Buckminsterfullerane" or "Buckyball" by Smalley's group at Rice University, Houston, Texas) had been made earlier by Stankevich, Nikerov and Bochvar, who argued on the basis of HMO calculations that it might be aromatic and stable.[14]

The prisms are also semiregular polyhedra representing cubic graphs; triprismane (benzprismane) II, is a highly strained $(CH)_6$ valence isomer,[15] but pentaprismane IV, $(CH)_{10}$ is stable, despite the strain in the four-membered rings.[7]

Other polyhedral $(CH)_n$ systems are cuneane,[16] IX, $(CH)_8$ which is formed from cubane III in the presence of silver(I) salts; other $(CH)_8$ valence isomers which are formed from III and IX and rhodium(I) salts are the cyclobutadiene dimer X and semibullvalene XI, respectively; two of the $(CH)_{12}$ valence isomers are XII and hexaprismane XIII; two triangular and square polyhedra with pentagonal side-faces are XIV, $(CH)_{12}$ and XV, $(CH)_{16}$, respectively. A final polyhedral molecule XVI is not an annulene valence isomer; it is derived from cubane by inserting in each C—C bond a CH_2 group.

The present paper describes the application of Pólya's theorem[17] in adapted form to the calculation of the number of isomers for substituted saturated polyhedral valence isomers I — VI, i.e. $(CH)_n$ with $n \leqslant 20$ (Fig. 1). Earlier work in this field includes:

1) Application of Pólya's theorem for calculating the number of isomers of benzprismane,[18] adamantane[19] and polymantanes.[20]

2) Ruch's double coset formalism[21] applied to computing the numbers of isomers of substituted adamantane derivatives. A review in book form is available.[22]

3) De Bruijn,[23] as well as Harary and Palmer[2,24] used the power group theorem for isomer enumeration.

Davidson[25] made use of all these approaches for molecular stereoanalysis. A recent review on isomer enumeration contains details and examples.[26]

However, no consistent treatment exists for predicting the numbers of stereoisomers and constitutional isomers by suitable choice of the symmetry operations inherent in the application of Pólya's theorem.

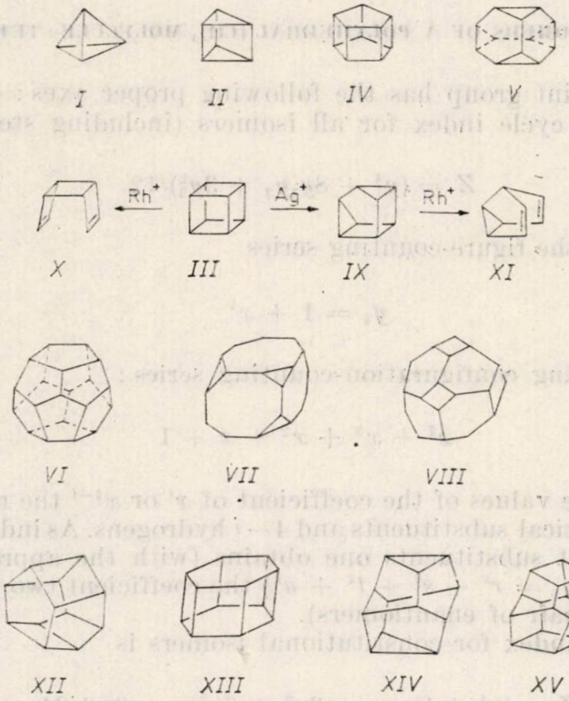

Fig. 1. — Polyhedral valence isomers of annulenes from which I—VI, IX, XII—XV will be discussed here.

Whenever we discuss substituted isomers of these polyhedral valence isomers of annulenes, we have in mind either H-labelled or C-labelled derivatives (wherein the label may be isotopic, or a substituent replacing the hydrogen) but not both at the same time. However, the latter alternative may be considered if the figure-counting series is suitably chosen ($y_k = x^k + z^k + x^k z^k$) but this will not be developed here; see ref.[27]

It was shown that for obtaining the numbers of all isomers including stereoisomers (counting separately the enantiomers) only the proper symmetry axes have to be taken into account in the cycle index;[19] for ignoring stereoisomers (i.e. for enumerating all constitutional isomers, counting an enantiomeric pair as one constitutional isomer), one has to include, in addition, improper rotation-reflection axes and reflection planes into the cycle index formula;[19] a symmetry plane is equivalent to an improper S_1 axis. The number of improper symmetry operations equals that of proper symmetry operations; the latter include the identity operation which is translated by y_1^n in the cycle index Z.

Finally, for counting geometrical *(cis-trans)* isomers but not the enantiomers, one has to modify the constitutional graphs in certain ways, as it was shown for substituted cycloalkanes[19,28] and for adamantane.[19]

The present paper indicates the cycle indices Z and number of isomers for constitutional and steric isomers. These numbers are presented as coefficients of configuration-counting series (isomer-counting series).

1. SUBSTITUTED ISOMERS OF A POLYHEDRAL $(CH)_4$ MOLECULE : TETRAHEDRANE (I)

The T_d point group has the following proper axes : $4C_3$ and $3C_2$; accordingly the cycle index for all isomers (including stereoisomers) is

$$Z = (y_1^4 + 8y_1y_3 + 3y_2^2)/12 \tag{1}$$

Substitution of the figure-counting series

$$y_k = 1 + x^k \tag{2}$$

gives the following configuration-counting series :

$$x^4 + x^3 + x^2 + x + 1 \tag{3}$$

indicating by the values of the coefficient of x^i or x^{4-i} the number of isomers with i identical substituents and $4-i$ hydrogens. As indicated in ref.[18] for four different substituents one obtains (with the appropriate figure counting series $y_k = r^k + s^k + t^k + u^k$) the coefficient two for the stereoisomers *rstu* (a pair of enantiomers).

The cycle index for constitutional isomers is

$$Z = (y_1^4 + 8y_1y_3 + 3y_2^2 + 6y_1^2y_2 + 6y_4)/24 \tag{4}$$

because there are $3S_4$ axes coinciding with the C_2 axes, and $6S_1$ (symmetry planes through two vertices); it leads to the same configuration-counting series ; however, for four different substituents one obtains the coefficient 1 for the corresponding term.

2. SUBSTITUTED ISOMERS OF A POLYHEDRAL $(CH)_6$ MOLECULE : BENZPRISMANE (TRIPRISMANE), (II)

The molecule has a ternary proper C_3 axis and three binary C_2 axes, therefore the cycle index for all isomers (including stereoisomers) is

$$Z = (y_1^6 + 2y_3^2 + 3y_2^3)/6 \tag{5}$$

By substituting into this cycle index, according to Pólya's theorem, the "figure-counting series" (2) and by developing algebraically the resulting polynomial one obtains the so-called "configuration-counting series" whose coefficients indicate the numbers of isomers :

$$x^6 + x^5 + 4x^4 + 4x^3 + 4x^2 + x + 1 \tag{6}$$

Thus there are four di-, tri- and tetra-substituted isomers. For more complicated substitution patterns (other partitions of the six possible substituents) ref. 18 should be consulted.

The molecule has one symmetry plane parallel to the triangular faces and three symmetry planes containing two CH groups each, orthogonal to the triangular faces. Hence the cycle index for constitutional isomers is

$$Z = (y_1^6 + 2y_3^2 + 4y_2^3 + 3y_1^2y_2^2 + 2y_6)/12 \tag{7}$$

and the resulting configuration-counting series is

$$x^6 + x^5 + 3x^4 + 3x^3 + 3x^2 + x = 1 \tag{8}$$

Fig. 2 presents for (8) the three constitutional isomers each of the di- and tri-substituted benzprismane. An asterisk marks the chiral isomer in each series, therefore counting separately the enantiomers one obtains four isomers (including stereoisomers) as required by (6).

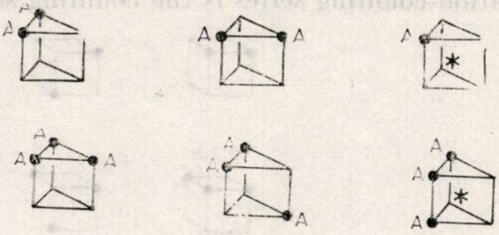

Fig. 2. — Di- (upper row) and tri-substituted constitutional isomers of benzprismane II (lower row). Substituents are indicated as black cycles, and the asterisk indicates a chiral compound.

Hexaprismane is so strained that it isomerizes explosively to benzene in a reaction forbidden by the Woodward-Hoffmann rules.

It was shown in ref. 18 that the cycle index (7) is common also to benzene derivatives; it was also mentioned that the equality in numbers of isomers for benzprismane (ignoring stereoisomerism) and benzene led to a long historical discussion between Ladenburg and Kekulé. Such molecules having the same cycle index are called *coisomeric.*

3. SUBSTITUTED ISOMERS OF POLYHEDRAL $(CH)_8$ MOLECULES

3A. Cubane (III)

According to its O_h point group the cube has the following proper axes : $3C_4$ coinciding with $3C_2$, $4C_3$ passing through two antipodal vertices, and $6C'_2$. As a consequence, the cycle index for all substituted isomers of cubane (including stereoisomers) is :

$$Z = (y_1^8 + 6y_4^2 + 8y_1^2y_3^2 + 9y_2^4)/24 \tag{9}$$

Substitution of the same figure-counting series (2) yields the configuration-counting series

$$x^8 + x^7 + 3x^6 + 3x^5 + 7x^4 + 3x^3 + 3x^2 + x + 1 \qquad (10)$$

Taking into account also the reflection-inversion (improper) axes $3S_4$, $4S_6$, S_2 (inversion centre) and the S_1 axes (six symmetry planes passing through four vertices and the three symmetry planes parallel to the square faces) one obtains the cycle index for constitutional isomers :

$$Z = (y_1^8 + 12y_4^2 + 8y_1^2y_3^2 + 13y_2^4 + 6y_1^4y_2^2 + 8y_2y_6)/48 \qquad (11)$$

The corresponding configuration-counting series is :

$$x^8 + x^7 + 3x^6 + 3x^5 + 6x^4 + 3x^3 + 3x^2 + x + 1 \qquad (12)$$

Fig. 3 indicates the six constitutional isomers of tetrasubstituted cubane, and the asterisk denotes the unique chiral isomer. Here, as in the preceding and subsequent cases, the difference between the two configuration-counting series is the counting series for chiral isomers.

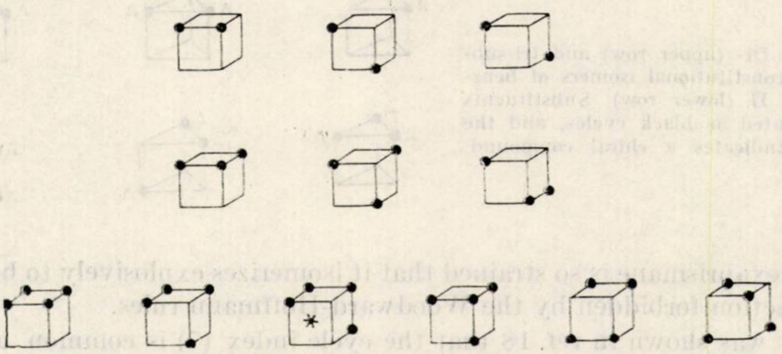

Fig. 3. — Constitutional isomers of di- (upper row), tri- (middle row) and tetra-substituted cubane III (lower row) ; see Fig. 2 for explanations.

Owing to its steric strain, cubane is less stable thermodynamically than both cuneane (see following paragraph) and tricyclo[4.2.0.0^{2,6}] octa-3,7-diene (the *syn*-dimer of cyclobutadiene), X ; in the presence of Rh(I), cubane isomerizes into the former, and the presence of Ag(I) into the latter,[16] in reactions forbidden thermally by the Woodward-Hoffmann rules. In turn, cuneane is isomerized by Rh(I) into semibullvalene (XI), a fluctuating molecule.

3B. Cuneane (IX)[16]

The molecule IX has a proper C_2 axis and two symmetry planes which intersect along it and which pass through two vertices each. The cycle index for all isomers of cuneane (including stereoisomers) is :

$$Z = (y_1^8 + y_2^4)/2 \qquad (13)$$

leading by the substitution (2) to the following isomer counting series :

$$x^8 + 4x^7 + 16x^6 + 28x^5 + 38x^4 + 28x^3 + 16x^2 + 4x + 1 \qquad (14)$$

By including the two improper symmetry operations one obtains the cycle index for constitutional isomers :

$$Z = (y_1^8 + y_2^4 + 2y_1^2 y_2^3)/4 \qquad (15)$$

leading to the following isomer counting series :

$$x^8 + 3x^7 + 10x^6 + 17x^5 + 22x^4 + 17x^3 + 10x^2 + 3x + 1 \qquad (16)$$

Fig. 4 illustrates the three monosubstituted constitutional isomers (indicating by an asterisk the unique chiral one) and the ten disubstituted constitutional isomers of cuneane indicating by asterisks the six chiral ones.

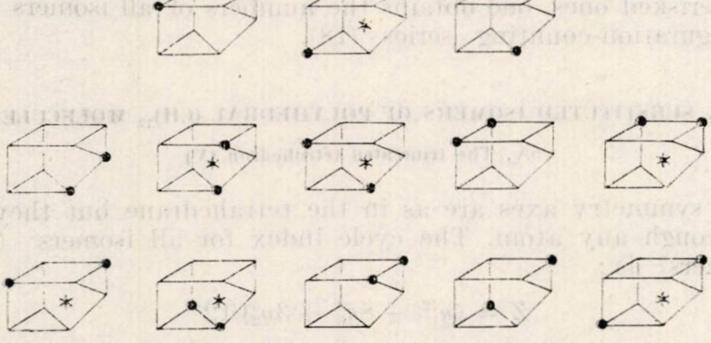

Fig. 4. — Constitutional isomers of monosubstituted (upper row) and disubstituted cuneane (IX). For explanations see Fig. 2.

4. SUBSTITUTED ISOMERS OF A POLYHEDRAL $(CH)_{10}$ MOLECULE : PENTAPRISMANE (IV)

The molecule IV has one proper C_5 axis and five C_2 proper axes. With rotations of 72°, 144°, 216°, and 288° one obtains for the former axis four fivefold permutations, and with rotations of 180° one obtains for the latter axes five twofold permutations, hence the cycle index for all isomers, including stereoisomerism, is :

$$Z = (y_1^{10} + 4y_5^2 + 5y_2^5)/10 \qquad (17)$$

By substituting the figure-counting series (2) one obtains the configuration-counting series :

$$x^{10} + x^9 + 7x^8 + 12x^7 + 26x^6 + 26x^5 + 26x^4 + 12x^3 + 7x^2 + x + 1 \quad (18)$$

Taking into account that the molecule has one reflection plane parallel to the pentagonal faces and five reflection planes (which contain two vertices) orthogonal to it, the cycle index for constitutional isomers is :

$$Z = (y_1^{10} + 4y_5^2 + 6y_2^5 + 5y_1^2y_2^4 + 4y_{10})/20 \tag{19}$$

Substitution of the figure counting series (2) yields the configuration-counting series :

$$x^{10} + x^9 + 5x^8 + 8x^7 + 16x^6 + 16x^5 + 16x^4 + 8x^3 + 5x^2 + x + 1 \tag{20}$$

It was shown in ref. 18 that the cycle index (20) is common both to the constitutional isomers of pentaprismane and to planar substituted cyclodecapentane ignoring its conformational problems and instability; these two compounds are coisomeric, like benzene and benzprismane.

Fig. 5 presents the 5, 8, 16 and 16 constitutional isomers of di-, tri-, tetra- and penta-substituted pentaprismane : an asterisk indicates the chiral ones. By adding the numbers of the constitutional isomers and of the asterisked ones, one obtains the numbers of all isomers shown by the configuration-counting series (18).

5. SUBSTITUTED ISOMERS OF POLYHEDRAL $(CH)_{12}$ MOLECULES

5A. The truncated tetrahedron (V)

The symmetry axes are as in the tetrahedrane but they pass no longer through any atom. The cycle index for all isomers (including stereoisomers) is :

$$Z = (y_1^{12} + 8y_3^4 + 3y_2^6)/12 \tag{21}$$

leading to the following configuration-counting series :

$$x^{12} + x^{11} + 7x^{10} + 21x^9 + 45x^8 + 66x^7 + 86x^6 + 66x^5 + 45x^4 + \ldots \tag{22}$$

By including the three S_4 axes and the six reflection planes S_1 passing each through two CH groups one obtains the cycle index for constitutional isomers :

$$Z = (y_1^{12} + 8y_3^4 + 3y_2^6 + 6y_4^3 + 6y_1^2y_2^5)/24 \tag{23}$$

leading to the following configuration-counting series :

$$x^{12} + x^{11} + 5x^{10} + 13x^9 + 27x^8 + 38x^7 + 48x^6 + 38x^5 + 27x^4 + \ldots \tag{24}$$

Fig. 6 represents the five disubstituted constitutional isomers; there are two chiral isomers denoted by asterisks.

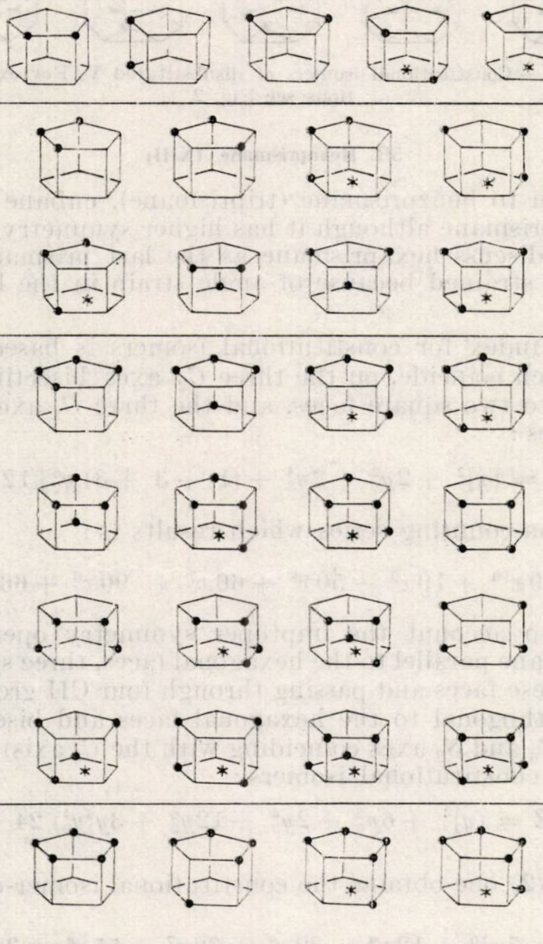

Fig. 5. — Constitutional isomers of di- (upper row), tri- (next rows), tetra- (next rows) and penta-substituted pentaprismane IV (lowest rows). For explanations see Fig. 2.

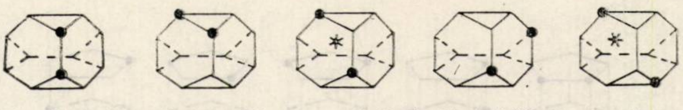

Fig. 6. — Constitutional isomers of disubstituted V. For explanations see Fig. 2.

5B. Hexaprismane (XIII)

In addition to benzprismane (triprismane), cubane (which may be viewed as tetraprismane although it has higher symmetry) and pentaprismane, we shall discuss hexaprismane as the last prismane; higher prismanes are more strained because of angle strain in the larger polygonal faces.

The cycle index for constitutional isomers is based on the C_6, C_3 and C_2 axes which coincide, on the three C_2 axes bisecting the six C—C bonds common to two square faces, and the three C_2 axes orthogonal to the square faces:

$$Z = [y_1^{12} + 2y_6^2 + 2y_3^4 + (1 + 3 + 3)\, y_2^6]/12 \qquad (25)$$

The configuration-counting series which results is:

$$x^{12} + x^{11} + 9x^{10} + 19x^9 + 50x^8 + 66x^7 + 90x^6 + 66x^5 + \ldots \qquad (26)$$

Taking into account the improper symmetry operations ($S_2 = i$, one symmetry plane parallel to the hexagonal faces, three symmetry planes orthogonal to these faces and passing through four CH groups, three symmetry planes orthogonal to the hexagonal faces and bisecting the C—C bonds, and the S_6 and S_3 axes coinciding with the C_6 axis) one obtains the cycle index for constitutional isomers:

$$Z = (y_1^{12} + 6y_6^2 + 2y_3^4 + 12y_2^6 + 3y_1^4y_2^4)/24 \qquad (27)$$

By substituting (2) one obtains the constitutional isomer-counting series:

$$x^{12} + x^{11} + 7x^{10} + 12x^9 + 32x^8 + 38x^7 + 55x^6 + 38x^5 + \ldots \qquad (28)$$

Fig. 7 illustrates the seven disubstituted isomers of hexaprismane, two of which (marked by asterisks) are chiral.

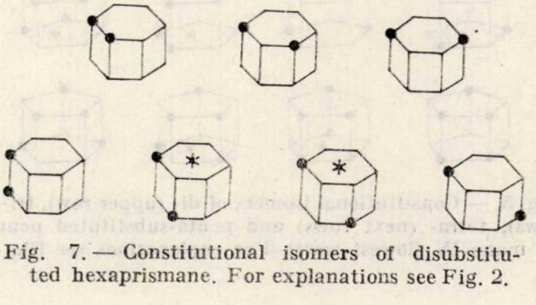

Fig. 7. — Constitutional isomers of disubstituted hexaprismane. For explanations see Fig. 2.

5C. A heptacyclododecane $(CH)_{12}$ valence isomer (XII)

The graph corresponding to this molecule is related to the K_4 graph representing tetrahedrane and the graph representing cubane, in representations with hamiltonian circuits (denoted by prime symbols).

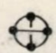

I′

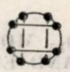

III′

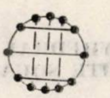

XII′

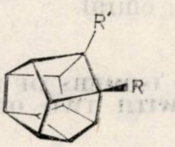

The molecule has as symmetry elements a proper C_2 axis coinciding with an improper S_2 axis, two mutually orthogonal reflection planes intersecting on the above axes and passing through two CH groups, and two more C_2 axes. The cycle index for all isomers (including stereoisomers) is

$$Z = (y_1^{12} + 3y_2^6)/4 \tag{29}$$

leading to the following isomer-counting series :

$$x^{12} + 3x^{11} + 21x^{10} + 55x^9 + 135x^8 + 198x^7 + 246x^6 + 198x^5 + \ldots \tag{30}$$

The cycle index for constitutional isomers is

$$Z = (y_1^{12} + 3y_2^6 + 2y_4^3 + 2y_1^2y_2^5)/8 \tag{31}$$

leading to the following isomer-counting series :

$$x^{12} + 2x^{11} + 12x^{10} + 30x^9 + 72x^8 + 104x^7 + 128x^6 + 104x^5 + \ldots \tag{32}$$

There exist therefore two constitutional monosubstituted isomers of XII : a chiral one with R $\neq$ H and R′ = H, and an achiral one with R = H and R′ $\neq$ H.

5D. A polyhedral $(CH)_{12}$ valence isomer with two opposite triangular and six pentagonal faces (XIV)

The molecule has a C_3 axis which coincides with an S_6 axis, three C_2 axes parallel to the triangular faces and three reflection planes perpendicular to those faces, passing through four CH groups.

The cycle index for all isomers is :

$$Z = (y_1^{12} + 2y_3^4 + 3y_2^6)/6 \tag{33}$$

leading to the following isomer-counting series :

$$x^{12} + 2x^{11} + 14x^{10} + 38x^9 + 90x^8 + 132x^7 + 166x^6 + 132x^5 + \ldots \tag{34}$$

The cycle index for constitutional isomers is :

$$Z = (y_1^{12} + 2y_3^4 + 4y_2^6 + 2y_6^2 + 3y_1^4y_4^2)/12 \tag{35}$$

leading to the following isomer-counting series :

$$x^{12} + 2x^{11} + 10x^{10} + 24x^{9} + 54x^{8} + 76x^{7} + 96x^{6} + 76x^{5} + \ldots \quad (36)$$

There exist therefore ten disubstituted constitutional isomers, four of which are chiral.

6. SUBSTITUTED ISOMERS OF POLYHEDRAL $(CH)_{16}$ MOLECULES. A $(CH)_{16}$ VALENCE ISOMER (XV) WITH TWO OPPOSITE SQUARE AND EIGHT PENTAGONAL FACES

The molecule has a C_4 and a C_2 axis coinciding with an S_8 axis, four C_2 axes parallel to the square faces, and four reflection planes passing through four CH groups.

The cycle index for all isomers is :

$$Z = (y_1^{16} + 2y_4^4 + 5y_4^8)/8 \qquad (37)$$

leading to the following isomer-counting series :

$$x^{16} + 2x^{15} + 20x^{14} + 70x^{13} + 246x^{12} + 546x^{11} + 1036x^{10} +$$

$$+ 1430x^{9} + 1654x^{8} + 1430x^{7} + \ldots \qquad (38)$$

The cycle index for constitutional isomers is :

$$Z = (y_1^{16} + 2y_4^4 + 5y_2^8 + 4y_8^2 + 4y_1^4y_2^6)/16 \qquad (39)$$

leading to the following isomer-counting series :

$$x^{16} + 2x^{15} + 13x^{14} + 42x^{13} + 136x^{12} + 294x^{11} + 547x^{10} +$$

$$+ 750x^{9} + 865x^{8} + 750x^{7} + \ldots \qquad (40)$$

There are therefore 13 constitutional disubstituted isomers, seven of which are chiral.

Both this and the preceding molecule are related to the subsequent one which has a much higher symmetry.

7. SUBSTITUTED ISOMERS OF A POLYHEDRAL $(CH)_{20}$ MOLECULE : DODECAHEDRANE, (VI)

In agreement with point group I_h there exist $6C_5$, $10C_3$ (passing through two antipodal vertices) and $15C_2$ proper axes, therefore the cycle index for all isomers (including stereoisomers) is :

$$Z = (y_1^{20} + 24y_5^4 + 20y_1^2y_3^6 + 15y_2^{10})/60 \qquad (41)$$

Revue Roumaine de Chimie, **31**, 7, 679—694 (1986)

CHEMICAL GRAPHS. Part 44.[1]

ISOMER ENUMERATION FOR SUBSTITUTED SATURATED POLYHEDRAL VALENCE ISOMERS OF ANNULENES

ALEXANDRU T. BALABAN

Polytechnic Institute, Department of Organic Chemistry, 76206 Bucharest, Roumania

Received November 19, 1985

By using Pólya's enumeration theorem together with symmetry operations involving either only proper rotation axes or also the improper rotation axes, enumerations of all isomers or only of constitutional isomers were carried out for substituted saturated regular or semiregular polyhedral $(CH)_n$ valence isomers I—VI, IX, XII—XV as well as for XVI, perhomocubane ($C_{20}H_{32}$) which is a hydrocarbon related to cubane.

INTRODUCTION

Enumeration of valence isomers of [*n*]annulenes using graph theoretical formulas[2] afforded numbers of connected and disconnected cubic multigraphs.[1] From the former, the planar connected cubic multigraphs are relevant because they correspond to chemically feasible [*n*]annulene valence isomers.[3] An algorithm for constructing such structures has been developed earlier;[4] the numbers of these structures for various *n* values agree for the two different approaches. A book reviewing annulenes and their valence isomers is in press,[5] and several reviews were recently published.[6]

Lately, spectacular experimental successes rewarded the prolonged effort towards the synthesis of several polyhedral valence isomers such as pentaprismane, IV (Eaton and coworkers),[7] and dodecahedrane, VI (Paquette and coworkers)[8]. Cubane, III, had been prepared earlier by Eaton *et al.*[9] The last of the Platonic regular polyhedra which corresponds to a cubic graph, tetrahedrane, I, is too unstable, when unsubstituted, to be isolated.[10] However, tri- and tetra-substituted tetrahedranes were prepared by Masamune et al.[11] and by Maier et al.[12] Tetra-t-butyltetrahedrane (Maier and coworkers[13]) is especially stable owing to the "straightlace effect (Korsett-Effekt)". The remaining two regular polyhedra, the octahedron and icosahedron, cannot correspond to $(CH)_n$ hydrocarbons because their graphs have vertices of degree 4 and 5, respectively, whereas CH groups have three free valencies. A C_6 molecule with an octahedral arrangement of six covalently bonded carbon atoms would have a huge strain because all valencies of each carbon would have 60° angles on a single side of a plane.

Semiregular polyhedra which are regular graphs of degree three and which could represent valence isomers of annulenes are the truncated tetrahedron V, $(CH)_{12}$ with four triangular faces and with four hexagonal faces, symbol (3,6, 6) indicating numbers of sides for polygonal faces meeting at each vertex; truncated cube VII, $(CH)_{24}$ with eight triangular and six octogonal faces, symbol (4,6,6); truncated octahedron VIII, $(CH)_{24}$ with eight hexagonal and six square faces, symbol (4,6,6); truncated icosahedron $(CH)_{60}$ with 12 pentagonal and 20 hexagonal faces, symbol (5,6,6); truncated dodecahedron $(CH)_{60}$ with 20 triangular and 12 decagonal faces, symbol (3,10,10). It can be noted that the last four semiregular polyhedra form two complementary (dual) pairs. There exist also two semiregular polyhedra with vertex degree three which have three types of faces: the truncated cuboctahedron, symbol (4,6,8) with six octogonal, eight hexagonal and twelve square faces; and the truncated icosidodecahedron with twelve decagonal, twenty hexagonal and thirty square faces, symbol (4,6,10).

A carbon atom cluster C_{60} with the probable structure of a truncated icosahedron was detected experimentally by laser-vaporization of graphite in a high-pressure supersonic nozzle; a lanthanum complex $C_{60}La$ with a caged metal atom was also found by Smalley and co-workers.[14] Theoretical predictions of this C_{60} molecule (called "Buckminsterfullerane" or "Buckyball" by Smalley's group at Rice University, Houston, Texas) had been made earlier by Stankevich, Nikerov and Bochvar, who argued on the basis of HMO calculations that it might be aromatic and stable.[14]

The prisms are also semiregular polyhedra representing cubic graphs; triprismane (benzprismane) II, is a highly strained $(CH)_6$ valence isomer,[15] but pentaprismane IV, $(CH)_{10}$ is stable, despite the strain in the four-membered rings.[7]

Other polyhedral $(CH)_n$ systems are cuneane,[16] IX, $(CH)_8$ which is formed from cubane III in the presence of silver(I) salts; other $(CH)_8$ valence isomers which are formed from III and IX and rhodium(I) salts are the cyclobutadiene dimer X and semibullvalene XI, respectively; two of the $(CH)_{12}$ valence isomers are XII and hexaprismane XIII; two triangular and square polyhedra with pentagonal side-faces are XIV, $(CH)_{12}$ and XV, $(CH)_{16}$, respectively. A final polyhedral molecule XVI is not an annulene valence isomer; it is derived from cubane by inserting in each C—C bond a CH_2 group.

The present paper describes the application of Pólya's theorem [17] in adapted form to the calculation of the number of isomers for substituted saturated polyhedral valence isomers I — VI, i.e. $(CH)_n$ with $n \leqslant 20$ (Fig. 1). Earlier work in this field includes:

1) Application of Pólya's theorem for calculating the number of isomers of benzprismane,[18] adamantane [19] and polymantanes.[20]

2) Ruch's double coset formalism [21] applied to computing the numbers of isomers of substituted adamantane derivatives. A review in book form is available.[22]

3) De Bruijn,[23] as well as Harary and Palmer [2,24] used the power group theorem for isomer enumeration.

Davidson[25] made use of all these approaches for molecular stereoanalysis. A recent review on isomer enumeration contains details and examples.[26]

However, no consistent treatment exists for predicting the numbers of stereoisomers and constitutional isomers by suitable choice of the symmetry operations inherent in the application of Pólya's theorem.

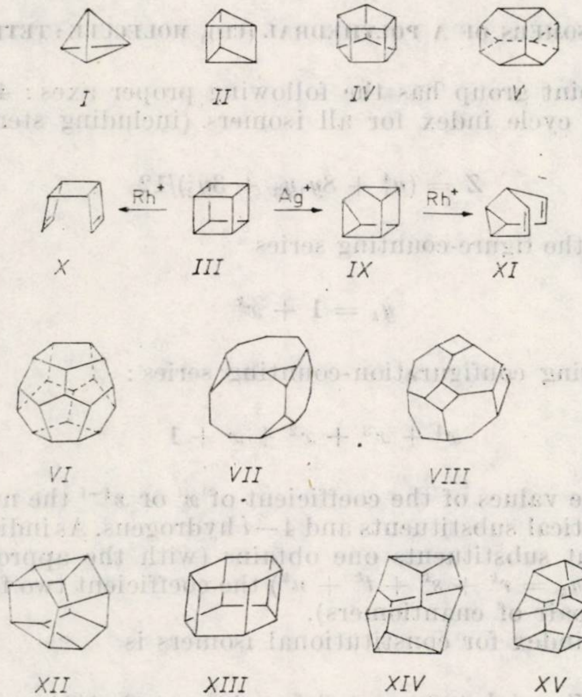

Fig. 1. — Polyhedral valence isomers of annulenes from which I—VI, IX, XII—XV will be discussed here.

Whenever we discuss substituted isomers of these polyhedral valence isomers of annulenes, we have in mind either H-labelled or C-labelled derivatives (wherein the label may be isotopic, or a substituent replacing the hydrogen) but not both at the same time. However, the latter alternative may be considered if the figure-counting series is suitably chosen ($y_k = x^k + z^k + x^k z^k$) but this will not be developed here; see ref.[27]

It was shown that for obtaining the numbers of all isomers including stereoisomers (counting separately the enantiomers) only the proper symmetry axes have to be taken into account in the cycle index; [19] for ignoring stereoisomers (i.e. for enumerating all constitutional isomers, counting an enantiomeric pair as one constitutional isomer), one has to include, in addition, improper rotation-reflection axes and reflection planes into the cycle index formula; [19] a symmetry plane is equivalent to an improper S_1 axis. The number of improper symmetry operations equals that of proper symmetry operations; the latter include the identity operation which is translated by y_1^n in the cycle index Z.

Finally, for counting geometrical *(cis-trans)* isomers but not the enantiomers, one has to modify the constitutional graphs in certain ways, as it was shown for substituted cycloalkanes [19,28] and for adamantane.[19]

The present paper indicates the cycle indices Z and number of isomers for constitutional and steric isomers. These numbers are presented as coefficients of configuration-counting series (isomer-counting series).

1. SUBSTITUTED ISOMERS OF A POLYHEDRAL $(CH)_4$ MOLECULE : TETRAHEDRANE (I)

The T_d point group has the following proper axes : $4C_3$ and $3C_2$; accordingly the cycle index for all isomers (including stereoisomers) is

$$Z = (y_1^4 + 8y_1y_3 + 3y_2^2)/12 \tag{1}$$

Substitution of the figure-counting series

$$y_k = 1 + x^k \tag{2}$$

gives the following configuration-counting series :

$$x^4 + x^3 + x^2 + x + 1 \tag{3}$$

indicating by the values of the coefficient of x^i or x^{4-i} the number of isomers with i identical substituents and $4-i$ hydrogens. As indicated in ref.[18] for four different substituents one obtains (with the appropriate figure counting series $y_k = r^k + s^k + t^k + u^k$) the coefficient two for the stereoisomers *rstu* (a pair of enantiomers).

The cycle index for constitutional isomers is

$$Z = (y_1^4 + 8y_1y_3 + 3y_2^2 + 6y_1^2y_2 + 6y_4)/24 \tag{4}$$

because there are $3S_4$ axes coinciding with the C_2 axes, and $6S_1$ (symmetry planes through two vertices) ; it leads to the same configuration-counting series ; however, for four different substituents one obtains the coefficient 1 for the corresponding term.

2. SUBSTITUTED ISOMERS OF A POLYHEDRAL $(CH)_6$ MOLECULE : BENZPRISMANE (TRIPRISMANE), (II)

The molecule has a ternary proper C_3 axis and three binary C_2 axes, therefore the cycle index for all isomers (including stereoisomers) is

$$Z = (y_1^6 + 2y_3^2 + 3y_2^3)/6 \tag{5}$$

By substituting into this cycle index, according to Pólya's theorem, the "figure-counting series" (2) and by developing algebraically the resulting polynomial one obtains the so-called "configuration-counting series" whose coefficients indicate the numbers of isomers :

$$x^6 + x^5 + 4x^4 + 4x^3 + 4x^2 + x + 1 \tag{6}$$

Thus there are four di-, tri- and tetra-substituted isomers. For more complicated substitution patterns (other partitions of the six possible substituents) ref. 18 should be consulted.

The molecule has one symmetry plane parallel to the triangular faces and three symmetry planes containing two CH groups each, orthogonal to the triangular faces. Hence the cycle index for constitutional isomers is

$$Z = (y_1^6 + 2y_3^2 + 4y_2^3 + 3y_1^2y_2^2 + 2y_6)/12 \tag{7}$$

and the resulting configuration-counting series is

$$x^6 + x^5 + 3x^4 + 3x^3 + 3x^2 + x = 1 \tag{8}$$

Fig. 2 presents for (8) the three constitutional isomers each of the di- and tri-substituted benzprismane. An asterisk marks the chiral isomer in each series, therefore counting separately the enantiomers one obtains four isomers (including stereoisomers) as required by (6).

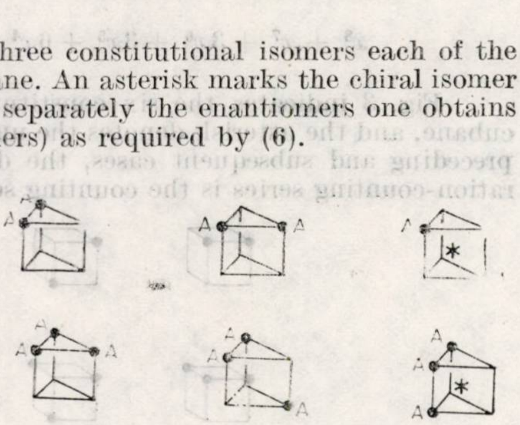

Fig. 2. — Di- (upper row) and tri-substituted constitutional isomers of benzprismane II (lower row). Substituents are indicated as black cycles, and the asterisk indicates a chiral compound.

Hexaprismane is so strained that it isomerizes explosively to benzene in a reaction forbidden by the Woodward-Hoffmann rules.

It was shown in ref. 18 that the cycle index (7) is common also to benzene derivatives; it was also mentioned that the equality in numbers of isomers for benzprismane (ignoring stereoisomerism) and benzene led to a long historical discussion between Ladenburg and Kekulé. Such molecules having the same cycle index are called *coisomeric*.

3. SUBSTITUTED ISOMERS OF POLYHEDRAL $(CH)_8$ MOLECULES

3A. Cubane (III)

According to its O_h point group the cube has the following proper axes : $3C_4$ coinciding with $3C_2$, $4C_3$ passing through two antipodal vertices, and $6C'_2$. As a consequence, the cycle index for all substituted isomers of cubane (including stereoisomers) is :

$$Z = (y_1^8 + 6y_4^2 + 8y_1^2y_3^2 + 9y_2^4)/24 \tag{9}$$

Substitution of the same figure-counting series (2) yields the configuration-counting series

$$x^8 + x^7 + 3x^6 + 3x^5 + 7x^4 + 3x^3 + 3x^2 + x + 1 \qquad (10)$$

Taking into account also the reflection-inversion (improper) axes $3S_4$, $4S_6$, S_2 (inversion centre) and the S_1 axes (six symmetry planes passing through four vertices and the three symmetry planes parallel to the square faces) one obtains the cycle index for constitutional isomers :

$$Z = (y_1^8 + 12y_4^2 + 8y_1^2y_3^2 + 13y_2^4 + 6y_1^4y_2^2 + 8y_2y_6)/48 \qquad (11)$$

The corresponding configuration-counting series is :

$$x^8 + x^7 + 3x^6 + 3x^5 + 6x^4 + 3x^3 + 3x^2 + x + 1 \qquad (12)$$

Fig. 3 indicates the six constitutional isomers of tetrasubstituted cubane, and the asterisk denotes the unique chiral isomer. Here, as in the preceding and subsequent cases, the difference between the two configuration-counting series is the counting series for chiral isomers.

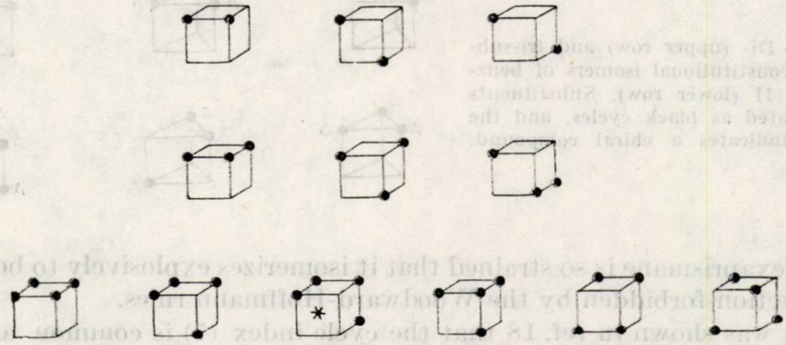

Fig. 3. — Constitutional isomers of di- (upper row), tri- (middle row) and tetra-substituted cubane III (lower row) ; see Fig. 2 for explanations.

Owing to its steric strain, cubane is less stable thermodynamically than both cuneane (see following paragraph) and tricyclo[4.2.0.0^{2,6}] octa-3,7-diene (the *syn*-dimer of cyclobutadiene), X ; in the presence of Rh(I), cubane isomerizes into the former, and the presence of Ag(I) into the latter, [16] in reactions forbidden thermally by the Woodward-Hoffmann rules. In turn, cuneane is isomerized by Rh(I) into semibullvalene (XI), a fluctuating molecule.

3B. Cuneane (IX)[16]

The molecule IX has a proper C_2 axis and two symmetry planes which intersect along it and which pass through two vertices each. The cycle index for all isomers of cuneane (including stereoisomers) is :

$$Z = (y_1^8 + y_2^4)/2 \qquad (13)$$

leading by the substitution (2) to the following isomer counting series :

$$x^8 + 4x^7 + 16x^6 + 28x^5 + 38x^4 + 28x^3 + 16x^2 + 4x + 1 \qquad (14)$$

By including the two improper symmetry operations one obtains the cycle index for constitutional isomers :

$$Z = (y_1^8 + y_2^4 + 2y_1^2y_2^3)/4 \qquad (15)$$

leading to the following isomer counting series :

$$x^8 + 3x^7 + 10x^6 + 17x^5 + 22x^4 + 17x^3 + 10x^2 + 3x + 1 \qquad (16)$$

Fig. 4 illustrates the three monosubstituted constitutional isomers (indicating by an asterisk the unique chiral one) and the ten disubstituted constitutional isomers of cuneane indicating by asterisks the six chiral ones.

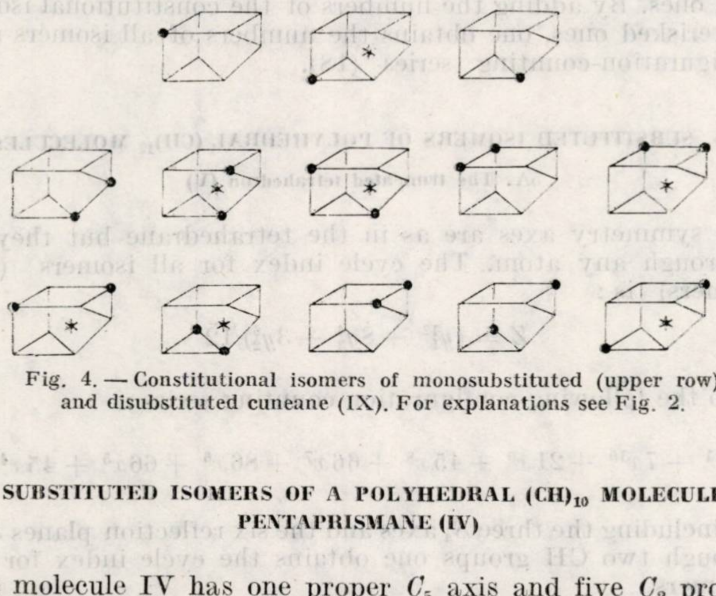

Fig. 4. — Constitutional isomers of monosubstituted (upper row) and disubstituted cuneane (IX). For explanations see Fig. 2.

4. SUBSTITUTED ISOMERS OF A POLYHEDRAL $(CH)_{10}$ MOLECULE : PENTAPRISMANE (IV)

The molecule IV has one proper C_5 axis and five C_2 proper axes. With rotations of 72°, 144°, 216°, and 288° one obtains for the former axis four fivefold permutations, and with rotations of 180° one obtains for the latter axes five twofold permutations, hence the cycle index for all isomers, including stereoisomerism, is :

$$Z = (y_1^{10} + 4y_5^2 + 5y_2^5)/10 \qquad (17)$$

By substituting the figure-counting series (2) one obtains the configuration-counting series :

$$x^{10} + x^9 + 7x^8 + 12x^7 + 26x^6 + 26x^5 + 26x^4 + 12x^3 + 7x^2 + x + 1 \qquad (18)$$

Taking into account that the molecule has one reflection plane parallel to the pentagonal faces and five reflection planes (which contain two vertices) orthogonal to it, the cycle index for constitutional isomers is :

$$Z = (y_1^{10} + 4y_5^2 + 6y_2^5 + 5y_1^2y_2^4 + 4y_{10})/20 \tag{19}$$

Substitution of the figure counting series (2) yields the configuration-counting series :

$$x^{10} + x^9 + 5x^8 + 8x^7 + 16x^6 + 16x^5 + 16x^4 + 8x^3 + 5x^2 + x + 1 \tag{20}$$

It was shown in ref. 18 that the cycle index (20) is common both to the constitutional isomers of pentaprismane and to planar substituted cyclodecapentane ignoring its conformational problems and instability; these two compounds are coisomeric, like benzene and benzprismane. Fig. 5 presents the 5, 8, 16 and 16 constitutional isomers of di-, tri-, tetra- and penta-substituted pentaprismane : an asterisk indicates the chiral ones. By adding the numbers of the constitutional isomers and of the asterisked ones, one obtains the numbers of all isomers shown by the configuration-counting series (18).

5. SUBSTITUTED ISOMERS OF POLYHEDRAL $(CH)_{12}$ MOLECULES

5A. The truncated tetrahedron (V)

The symmetry axes are as in the tetrahedrane but they pass no longer through any atom. The cycle index for all isomers (including stereoisomers) is :

$$Z = (y_1^{12} + 8y_3^4 + 3y_2^6)/12 \tag{21}$$

leading to the following configuration-counting series :

$$x^{12} + x^{11} + 7x^{10} + 21x^9 + 45x^8 + 66x^7 + 86x^6 + 66x^5 + 45x^4 + \ldots \tag{22}$$

By including the three S_4 axes and the six reflection planes S_1 passing each through two CH groups one obtains the cycle index for constitutional isomers :

$$Z = (y_1^{12} + 8y_3^4 + 3y_2^6 + 6y_4^3 + 6y_1^2y_2^5)/24 \tag{23}$$

leading to the following configuration-counting series :

$$x^{12} + x^{11} + 5x^{10} + 13x^9 + 27x^8 + 38x^7 + 48x^6 + 38x^5 + 27x^4 + \ldots \tag{24}$$

Fig. 6 represents the five disubstituted constitutional isomers; there are two chiral isomers denoted by asterisks.

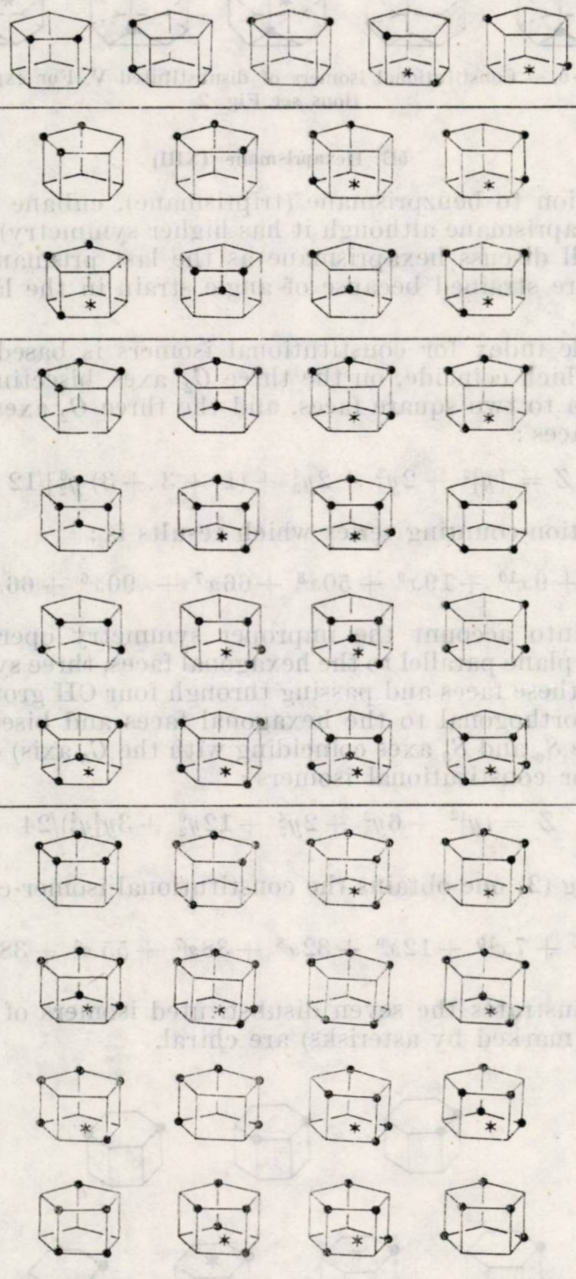

Fig. 5. — Constitutional isomers of di- (upper row), tri- (next rows), tetra- (next rows) and penta-substituted pentaprismane IV (lowest rows). For explanations see Fig. 2.

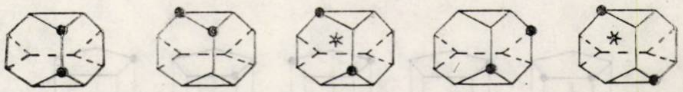

Fig. 6. — Constitutional isomers of disubstituted V. For explanations see Fig. 2.

5B. **Hexaprismane (XIII)**

In addition to benzprismane (triprismane), cubane (which may be viewed as tetraprismane although it has higher symmetry) and pentaprismane, we shall discuss hexaprismane as the last prismane; higher prismanes are more strained because of angle strain in the larger polygonal faces.

The cycle index for constitutional isomers is based on the C_6, C_3 and C_2 axes which coincide, on the three C_2 axes bisecting the six C—C bonds common to two square faces, and the three C_2 axes orthogonal to the square faces:

$$Z = [y_1^{12} + 2y_6^2 + 2y_3^4 + (1 + 3 + 3)\, y_2^6]/12 \tag{25}$$

The configuration-counting series which results is:

$$x^{12} + x^{11} + 9x^{10} + 19x^9 + 50x^8 + 66x^7 + 90x^6 + 66x^5 + \ldots \tag{26}$$

Taking into account the improper symmetry operations ($S_2 = i$, one symmetry plane parallel to the hexagonal faces, three symmetry planes orthogonal to these faces and passing through four CH groups, three symmetry planes orthogonal to the hexagonal faces and bisecting the C—C bonds, and the S_6 and S_3 axes coinciding with the C_6 axis) one obtains the cycle index for constitutional isomers:

$$Z = (y_1^{12} + 6y_6^2 + 2y_3^4 + 12y_2^6 + 3y_1^4y_2^4)/24 \tag{27}$$

By substituting (2) one obtains the constitutional isomer-counting series:

$$x^{12} + x^{11} + 7x^{10} + 12x^9 + 32x^8 + 38x^7 + 55x^6 + 38x^5 + \ldots \tag{28}$$

Fig. 7 illustrates the seven disubstituted isomers of hexaprismane, two of which (marked by asterisks) are chiral.

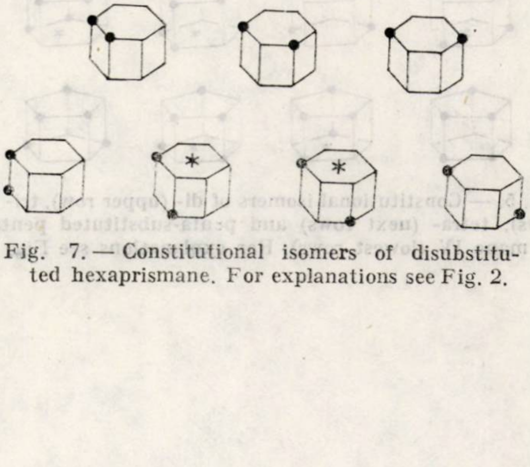

Fig. 7. — Constitutional isomers of disubstituted hexaprismane. For explanations see Fig. 2.

5C. A heptacyclododecane $(CH)_{12}$ valence isomer (XII)

The graph corresponding to this molecule is related to the K_4 graph representing tetrahedrane and the graph representing cubane, in representations with hamiltonian circuits (denoted by prime symbols).

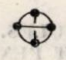

I′

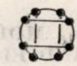

III′

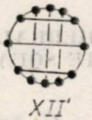

XII′

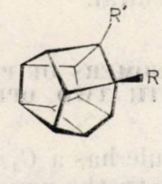

The molecule has as symmetry elements a proper C_2 axis coinciding with an improper S_2 axis, two mutually orthogonal reflection planes intersecting on the above axes and passing through two CH groups, and two more C_2 axes. The cycle index for all isomers (including stereoisomers) is

$$Z = (y_1^{12} + 3y_2^6)/4 \tag{29}$$

leading to the following isomer-counting series :

$$x^{12} + 3x^{11} + 21x^{10} + 55x^9 + 135x^8 + 198x^7 + 246x^6 + 198x^5 + \ldots \tag{30}$$

The cycle index for constitutional isomers is

$$Z = (y_1^{12} + 3y_2^6 + 2y_4^3 + 2y_1^2y_2^5)/8 \tag{31}$$

leading to the following isomer-counting series :

$$x^{12} + 2x^{11} + 12x^{10} + 30x^9 + 72x^8 + 104x^7 + 128x^6 + 104x^5 + \ldots \tag{32}$$

There exist therefore two constitutional monosubstituted isomers of XII : a chiral one with $R \neq H$ and $R' = H$, and an achiral one with $R = H$ and $R' \neq H$.

5D. A polyhedral $(CH)_{12}$ valence isomer with two opposite triangular and six pentagonal faces (XIV)

The molecule has a C_3 axis which coincides with an S_6 axis, three C_2 axes parallel to the triangular faces and three reflection planes perpendicular to those faces, passing through four CH groups.

The cycle index for all isomers is :

$$Z = (y_1^{12} + 2y_3^4 + 3y_2^6)/6 \tag{33}$$

leading to the following isomer-counting series :

$$x^{12} + 2x^{11} + 14x^{10} + 38x^9 + 90x^8 + 132x^7 + 166x^6 + 132x^5 + \ldots \tag{34}$$

The cycle index for constitutional isomers is :

$$Z = (y_1^{12} + 2y_3^4 + 4y_2^6 + 2y_6^2 + 3y_1^4y_4^2)/12 \tag{35}$$

leading to the following isomer-counting series :

$$x^{12} + 2x^{11} + 10x^{10} + 24x^{9} + 54x^{8} + 76x^{7} + 96x^{6} + 76x^{5} + \dots \quad (36)$$

There exist therefore ten disubstituted constitutional isomers, four of which are chiral.

6. SUBSTITUTED ISOMERS OF POLYHEDRAL $(CH)_{16}$ MOLECULES. A $(CH)_{16}$ VALENCE ISOMER (XV) WITH TWO OPPOSITE SQUARE AND EIGHT PENTAGONAL FACES

The molecule has a C_4 and a C_2 axis coinciding with an S_8 axis, four C_2 axes parallel to the square faces, and four reflection planes passing through four CH groups.

The cycle index for all isomers is :

$$Z = (y_1^{16} + 2y_4^4 + 5y_4^8)/8 \quad (37)$$

leading to the following isomer-counting series :

$$x^{16} + 2x^{15} + 20x^{14} + 70x^{13} + 246x^{12} + 546x^{11} + 1036x^{10} +$$

$$+ 1430x^{9} + 1654x^{8} + 1430x^{7} + \dots \quad (38)$$

The cycle index for constitutional isomers is :

$$Z = (y_1^{16} + 2y_4^4 + 5y_2^8 + 4y_8^2 + 4y_1^4y_2^6)/16 \quad (39)$$

leading to the following isomer-counting series :

$$x^{16} + 2x^{15} + 13x^{14} + 42x^{13} + 136x^{12} + 294x^{11} + 547x^{10} +$$

$$+ 750x^{9} + 865x^{8} + 750x^{7} + \dots \quad (40)$$

There are therefore 13 constitutional disubstituted isomers, seven of which are chiral.

Both this and the preceding molecule are related to the subsequent one which has a much higher symmetry.

7. SUBSTITUTED ISOMERS OF A POLYHEDRAL $(CH)_{20}$ MOLECULE: DODECAHEDRANE, (VI)

In agreement with point group I_h there exist $6C_5$, $10C_3$ (passing through two antipodal vertices) and $15C_2$ proper axes, therefore the cycle index for all isomers (including stereoisomers) is :

$$Z = (y_1^{20} + 24y_5^4 + 20y_1^2y_3^6 + 15y_2^{10})/60 \quad (41)$$

The configuration-counting series obtained by means of relationship (2) is:

$$x^{20}+x^{19}+6x^{18}+21x^{17}+96x^{16}+262x^{15}+681x^{14}+1302x^{13}+$$
$$+2157x^{12}+2806x^{11}+3158x^{10}+2806x^{9}+\dots \qquad (42)$$

The improper axes are $6S_{10}$ coinciding with the fivefold axes, $10S_6$ coinciding with the threefold axes, $1S_2$ (inversion centre) and $15S_1$ axes (symmetry planes passing through four vertices). The cycle index for constitutional isomers is:

$$Z=(y_1^{20}+24y_5^4+20y_1^2y_3^6+16y_2^{10}+24y_{10}^2+$$
$$+20y_2y_6^3+15y_1^4y_2^8)/120 \qquad (43)$$

and it affords the following configuration-counting series:

$$x^{20}+x^{19}+5x^{18}+15x^{17}+58x^{16}+149x^{15}+371x^{14}+693x^{13}+$$
$$+1135x^{12}+1466x^{11}+1648x^{10}+1466x^{9}+\dots \qquad (44)$$

There are four achiral and one chiral disubstituted isomers; the latter is marked with an asterisk in Fig. 8. [27a]

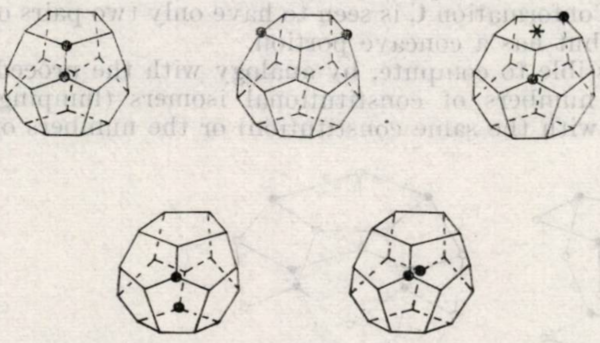

Fig. 8. — Constitutional isomers of disubstituted dodecahedrane VI. For explanations see Fig. 2.

8. A $C_{20}H_{32}$ HYDROCARBON (XVI)

Finally, a last C_{20} *polyhedral hydrocarbon* (XVI) will be discussed, although it is not an annulene valence isomer; it is derived from cubane similarly to the derivation of adamantane from tetrahedrane, namely by inserting a CH_2 group into each C—C bond of cubane. One obtains perhomocubane $(CH)_8(CH_2)_{12}$ i.e. $C_{20}H_{32}$.

The cycle index for all isomers (including stereoisomers) has to be calculated separately for C-labelled and H-labelled derivatives; the proper symmetry axes are the same as for cubane but the C_2 axes passing through the centres of faces (coinciding with the C_4 axes) lead to a different term in the cycle index from the C_2 axes passing through the middle of cubane edges, i.e. through two CH_2 carbons. The cycle index for C-labelled derivatives is :

$$Z = (y_1^{20} + 6y_4^5 + 8y_1^2y_3^6 + 6y_1^2y_2^9 + 3y_2^{10})/24 \tag{45}$$

and it leads to the following figure-counting series :

$$x^{20} + 2x^{19} + 12x^{18} + 54x^{17} + 224x^{16} + 666x^{15} + 1665x^{14} + 3282x^{13} + \\ + 5335x^{12} + 7068x^{11} + 7806x^{10} + 7068x^9 + \ldots \tag{46}$$

For H-labelled derivatives the cycle index is :

$$Z = (y_1^{32} + 6y_4^8 + 8y_1^2y_3^{10} + 9y_2^{16})/24 \tag{47}$$

and it gives rise to the following counting series :

$$x^{32} + 2x^{31} + 27x^{30} + 210x^{29} + 1552x^{28} + 8394x^{27} + \ldots \tag{48}$$

There is no strain-free conformation of this hydrocarbon although there exist three conformations which have no angular strain. These three conformations with conflicting proximity of hydrogen atoms are shown in Fig. 9; conformation **A** has two practically planar cyclooctane rings with the conflicting hydrogens indicated on the figure; conformation **B** is a portion of the dodecahedrane molecule whose missing C—C bonds are replaced by front-on colliding hydrogen atoms (only one of the two C—H bonds appended to the CH_2 groups symbolized by the open circles is shown in XVI—**B**). Conformation **C** is seen to have only two pairs of overlapping C—H bonds, but has a concave portion.

It is possible to compute, by analogy with the procedure described earlier,[28] the numbers of constitutional isomers (lumping together all stereoisomers with the same constitution) or the numbers of diastereoiso-

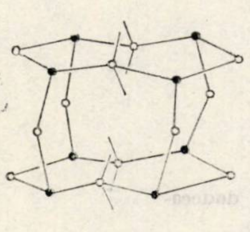

XVI-A

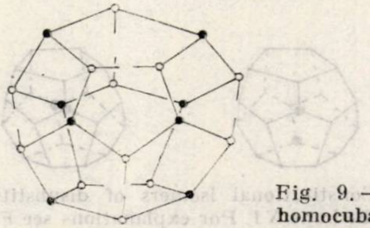

XVI-B

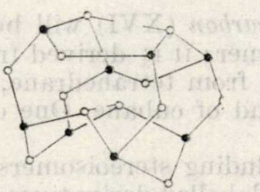

XVI-C

Fig. 9.— Hydrocarbon XVI (perhomocubane) $C_{20}H_{32}$ and three conformations (A, B, and C) with no angle strain but with overlapping hydrogen atoms; black points represent CH groups, and white points CH_2 groups.

mers (lumping together all enantiometric pairs), by choosing suitably modified graphs and finding their cycle indices by the use of the symmetric alternating groups (or pair groups). For instance the hydrogen-labelled graph excluding enantiomerism but including diastereomerism is XVII and the graph for constitutional H-labelled isomer is XVIII where each point represents a hydrogen atom (black points refer to CH groups, and white points to CH_2 groups). Since the cycle indices are quite complicated (e.g. whereas for H-labelled adamantanes including all isomers the cycle index Z has three terms, the cycle index for H-labelled adamantanes including diastereomers but excluding enantiomers has five terms, and the cycle index for constitutional isomers has 24 terms!), we shall not give the cycle indices for constitutional isomers of XVII and XVIII.

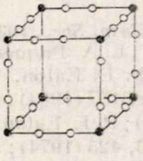

XVII

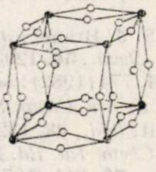

XVIII

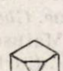

XIX

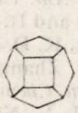

XX

NOTE ON NOMENCLATURE AND REVIEWS

The cumbersome von Baeyer — IUPAC nomenclature for polyhedral hydrocarbons (reviewed by Moyano, Serratosa *et al.* [29]) made it necessary to coin trivial names such as cubane. A more general proposal is due to Paquette *et al.* :[30] cubane III is called $[4^6]$ hexahedrane, pentaprismane IV is called p-$[4^3 : 5^2]$ heptahedrane, etc. According to this last nomenclature, benzprismane II is p-$[3^2 : 4^3]$pentahedrane, hexaprismane XIII is p-$[4^6 : 6^2]$octahedrane, and XII is S_2 - $[4^4 : 5^4]$octahedrane. Another fairly general nomenclature for systems XIX and XX related to XIV and XV, respectively, is due to Garratt and White :[31] XIX is called [3]peristylane, and XX which was prepared by Paquette *et al.*[30] is called accordingly [4]peristylane; originally, XIX had been prepared by Nickon and Pandit [32] who has called it triaxane; the *Chemical Abstracts* nomenclature for XIX was at variance with the IUPAC name, therefore trivial names seemed the obvious way out.

A review on regular and semiregular polyhedral hydrocarbons was published by Schultz.[33] Polyquinanes (hydrocarbons having condensed five-membered rings as faces of planar, non-planar, or polyhedral systems) were reviewed by Jacobsen.[34] The syntheses and rearrangements of cage molecules related to cubane were reviewed by Jefford;[35] basketene, snoutene, triquinacene, hypostrophene, diademane, pentaprismane, and various homocubanes are included in this review.

REFERENCES

[1] Part 43, A.T. Balaban, R. Vancea, S.Holban and I. Moţoc, *J. Chem.Inf. Comput. Sci.* (in press)

[2] F. Harary and E. M. Palmer, "Graphical Enumeration", Academic Press, New York, 1973.

[3] A. T. Balaban, *Rev. Roum. Chim.*, **11**, 1097 (1966).

[4] A. T. Balaban, *Rev. Roum. Chim.*, **15**, 463 (1970) ; **17**, 865 (1972).

[5] A. T. Balaban, M. Banciu and V. Ciorba, "Annulenes, Benzo-, Homo-, Hetero-Derivatives and Their Valence Isomers", CRC Press, Boca Raton, Florida (in press).

[6] A. T. Balaban and M. Banciu, *J. Chem. Educ.*, **61**, 766 (1984) ; M.Banciu and A. T. Balaban, *Chem. Scripta*, **22**, 188 (1983) ; M. Banciu, C. Popa and A. T. Balaban, *ibid.* **24**, 28 (1984).

[7] P. E. Eaton, Y. S. Or and S. J. Brance, *J. Am. Chem. Soc.*, **103**, 2134 (1981).

[8] L. A. Paquette, *Pure Appl. Chem.*, **50**, 1291 (1978) ; L. A. Paquette and D. W. Balogh, *J. Am. Chem. Soc.*, **104**, 774 (1982) ; see also P. E. Eaton, *Tetrahedron*, **35**, 2189 (1979).

[9] P. E. Eaton and T. W. Cole, *J. Am. Chem. Soc.*, **86**, 3157 (1964) ; see also J. C.Barborak, L.Watts and R. Pettit, *ibid.*, **88**, 1328 (1966) ; P. E. Eaton, *Tetrahedron*, **35**, 2189 (1979)

[10] Reviews : G. Maier, *Angew Chem. Int. Ed. Engl.*, **13**, 425 (1974) ; J. F. Liebman and A. Graen-. berg, *Chem. Rev.*, **76**, 311 (1976) ; N. S. Zefirov, A. S. Kozmin and A. V. Abramenkov, *Russ. Chem. Rev.* **47**, 163 (1978) ; for a possible experimental evidence see P. S. Shevlin and A. P. Wolf, *J. Am. Chem. Soc.*, **92**, 406, 3250, 5291 (1970).

[11] S. Masamune and M. Kato, *J. Am. Chem.Soc.*, **87**, 4190 (1965) ; **88**, 610 (1966).

[12] G. Maier, S. Pfriem, U. Schäfer and R. Matusch, *Angew. Chem. Int. Ed. Engl.*, **17**, 520 (1978).

[13] G. Maier, S. Pfriem, U. Schäfer, K. D. Malsch and R. Matusch, *Chem . Ber.*, **114**, 3965 (1981).

[14] J. R. Heath, S. C. O'Brien, Q. Zhang, Y. Liu, R. F. Curl, H. W. Kroto, F. K. Tittel and R. E. Smalley, *J. Am. Chem. Soc.*, **107**, 7779 (1985) and further references therein ; I. V. Stankevich, M. V. Nikerov and D. A. Bochvar, *Russ. Chem. Rev.*, **53**, 640 (1985) ; R. M. Baum, *Chem. Eng. News*, Dec. 23, p. 20 (1985).

[15] K. E. Wilzbach and L. Kaplan, *J. Am. Chem. Soc.*, **87**, 4004 (1965) ; T. J. Katz and N. Acton, *ibid.*, **95**, 2738 (1973).

[16] L. Cassar, P. E. Eaton and J. Halpern, *J. Am. Chem. Soc.*, **92**, 63366 (1970).

[17] G. Pólya, *Z. Kristal.* (*A*) **93**, 415 (1936); *Acta Math.*, **68**, 145 (1937).

[18] A. T. Balaban, *Rev. Roum. Chim.*, **19**, 1323 (1974).

[19] A. T. Balaban, E. M. Palmer and F. Harary, *Rev. Roum. Chim.*, **22**, 517 (1977) ; two corrections are necessary in this paper : In Table 1 (p. 519) the number of H-labelled adamantanes excluding enantiomerism but including diastereomerism is 13 instead of 16. On p. 522, second line from bottom, 48 $y_1^2 y_2^3 y_4$ should be replaced by $48 y_1^2 y_2^3 y_4^2$

[20] A. T. Balaban and V. Baciu, *Math. Chem.*, **4**, 131 (1978).

[21] E. Ruch, W. Hässelbarth and B. Richer, *Theoret. Chim. Acta.*, **19**, 288 (1970).

[22] J. Brocas, M. Gielen and R. Willem, "The Permutational Approach to Dynamic Stereochemistry", Mc Graw-Hill, New York, p. 268 (counting constitutional isomers by double cosets).

[23] N. G. de Bruijn, *J. Comb. Theory*, **2**, 418 (1967).

[24] F. Harary and E.M. Palmer, *J. Comb. Theory*, **1**, 157 (1966).

[25] R. A. Davidson, *J. Am. Chem. Soc.*, **103**, 312 (1981) ; Ph. D. Thesis, Pennsylvania State Univ. (1976).

[26] A. T. Balaban, chapter reviewing Isomer Enumeration, in press.

[27] A. T. Balaban, D. Fărcaşiu and F. Harary, *J. Labelled Comp.*, **6**, 211 (1970).

[27a] In a recent paper, J. Brocas (*J. Amer. Chem. Soc.*, **108**, 1135 (1986)) used double cosets for supplementing data on the numbers of isomeric substituted dodecahedranes obtained earlier by L.A. Paquette, R.J. Ternanski, D.W. Balogh and W.J. Taylor (*ibid*'. **105**, 5441 (1983)). These numbers agree with those presented here.

[28] A. T. Balaban, *Croat. Chem. Acta*, **51**, 35 (1978).

[29] A. Moyano, F. Serratosa, P. Camps and J. M. Drudis, *J. Chem. Educ.*, **59**, 126 (1982).

[30] L. A. Paquette, A. R. Browne, C. W. Doecke and R. V. Williams, *J. Am. Chem. Soc.*, **105**, 4113 (1983), footnote 4.

[31] P. J. Garratt and J. F. White, *J. Org. Chem.*, **42**, 1733 (1977), footnote 8.

[32] A. Nickon and G. D. Pandit, *Tetrahedron Lett.*, 3663 (1968).

[33] H. P. Schultz, *J. Org. Chem.*, **30**, 1361 (1965).

[34] T. Jacobson, "Polyquinanes. Studies on the Synthesis of Compounds Containing Accumulated Pitzer Strain", Ph. D. Thesis, Lund, 1973 ; *Acta Chem. Scand.*, **21**, 2235 (1967) ; **26**, 2477 (1972) ; *Chem. Scripta*, **2**, 121 (1972) ; **2**, 127 (1972).

[35] C. W. Jefford, *J. Chem. Educ.*, **53**, 477 (1976).

Revue Roumaine de Chimie, **31**, 7, 695—708 (1986)

CHEMICAL GRAPHS. Part 45.[1]

EDGE-LABELLED GRAPHS AS UNSATURATED VALENCE ISOMERS OF ANNULENES; APPLICATIONS OF PÓLYA'S THEOREM

ALEXANDRU T. BALABAN
Polytechnic Institute, Department of Organic Chemistry, Splaiul Independenţei 313, 76206 Bucharest, Roumania

Received January 15, 1986

On applying Pólya's theorem to the cycle index based on the rotation group of polyhedra (tetrahedron, cube, dodecahedron, triangular prism) one obtains counting series for edge-labelled polyhedra; if the labelling is the insertion of a CH=CH group one obtains unsaturated polyhedral $(CH)_n$ valence isomers. Numbers of substituted isomers of such systems are obtained by applying Pólya's theorem to the cycle index of the vertex rotation group of these unsaturated systems.

I. INTRODUCTION

In the previous part,[1] Pólya's theorem[2] was used for computing the numbers of substituted isomers of saturated polyhedral valence isomers of annulenes $(CH)_n$. Among unsaturated $(CH)_n$ systems, polyhedral hydrocarbons may be derived from lower saturated or unsaturated polyhedral homologues on replacing a C—C bond by a C—CH=CH—C bond sequence. In order to obtain all possible isomers derived from given saturated polyhedral hydrocarbon by such single or multiple replacement, we present here the adaptation of Pólya's theorem[2] to counting "edge-labelled graphs", including or excluding stereoisomerism. Then a few selected examples of polyhedral unsaturated hydrocarbons will be discussed as in the preceding part.[1]

II. COUNTING EDGE-LABELLED GRAPHS AS UNSATURATED VALENCE ISOMERS OF ANNULENES

The obvious thought that comes to mind in the attempt to apply Pólya's theorem to the title problem is to convert a graph G into the corresponding line graph $L(G)$ for applying then Pólya's theorem to counting vertex-labelled line graphs[3] which should be equivalent to counting corresponding edge-labelled graphs. Actually this approach does not work: whenever the initial graph G has triangular faces the line graph $L(G)$ makes no discrimination between the case when (i) three edges of G meet at the same vertex of degree three ; and (ii) G has a triangular face. In both cases $L(G)$ will have a triangular face and it will generally be impossible to find which case was present in order to reconstruct G from $L(G)$.

Therefore the correct solution is to find the cycle index for the edge rotation group, then to apply Pólya's theorem to this cycle index. Four examples will illustrate this solution.

II.1. Numbers of edge-labelled benzprismanes

Taking into account the trigonal C_3 axis and the three digonal C_2 axes, the cycle index for proper axes (all isomers being considered, including stereoisomers) is

$$Z = (y_1^9 + 2y_3^3 + 3y_1y_2^4)/6 \tag{1}$$

An automorphism involving each of the three digonal axes permutes four pairs of edges and preserves one edge (incident with the C_2 axis) even though the rotation interchanges the endpoints of that edge : this is the origin of the term $3y_1y_2^4$.

By applying Pólya's theorem one substitutes

$$y_k = 1 + x^k \tag{2}$$

and one obtains the isomer-counting series

$$x^9 + 2x^8 + 8x^7 + 17x^6 + 24x^5 + 24x^4 + 17x^3 + 8x^2 + 2x + 1 \tag{3}$$

If instead of counting all isomers one wishes to count only the constitutional isomers, the cycle index must also consider the improper symmetry axes (rotation-reflection, including S_2 centrosymmetric operations and S_1 reflection). With the reflection plane parallel to the triangular faces, the three reflection planes orthogonal to the three square faces, and the S_3 axis, the new cycle index is

$$Z = (y_1^9 + 2y_3^3 + 3y_1y_2^4 + 4y_1^3y_2^3 + 2y_3y_6)/12 \tag{4}$$

and the resulting constitutional isomer-counting series is

$$x^9 + 2x^8 + 6x^7 + 12x^6 + 16x^5 + 16x^4 + 12x^3 + 6x^2 + 2x + 1 \tag{5}$$

There are therefore two isomeric single-edge-labelled benzprismanes (both achiral), six constitutional isomers with two labelled edges (two of which are chiral), twelve with three labelled edges (five of which are chiral), and sixteen with four labelled edges (eight of which are chiral). The number of chiral systems is the difference between the above two counting series (5) and (3).

In fig. 1 the edges are "labelled" by the insertion of a double bond, and chiral systems are marked with an asterisk. Some of the corresponding

$(CH)_n$ hydrocarbons with at least two double bonds may undergo Cope rearrangements. Thus from the disubstituted systems of Fig. 1, the first two may be interconverted by such a rearrangement; all remaining ones but the last may undergo automerization by degenerate Cope rearrangements (such systems were analyzed in an earlier part of this series [4]); the third "edge-dilabelled" benzprismane corresponds to hypostrophene (**11**) which indeed presents evidence for such automerization.[5]

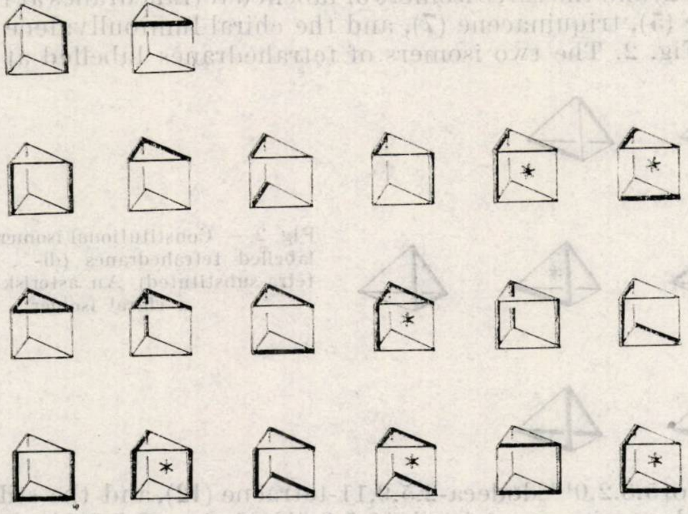

Fig. 1. — Constitutional isomers of edge-labelled benzprismanes: upper row, monosubstituted; next row, disubstituted; lowest two rows, trisubstituted. An asterisk denotes chiral systems.

II.2. Numbers of edge-labelled tetrahedra

The four threefold axes and the three twofold axes give rise to the following cycle index for the rotation group of edges in a tetrahedron:

$$Z = (y_1^6 + 8y_3^2 + 3y_1^2y_2^2)/12 \tag{6}$$

On applying Pólya's theorem the following configuration-counting series results for all isomers (including stereoisomers):

$$x^6 + x^5 + 2x^4 + 4x^3 + 2x^2 + x + 1 \tag{7}$$

If the improper symmetry axes are also taken into account the cycle index is:

$$Z = (y_1^6 + 8y_3^2 + 9y_1^2y_2^2 + 6y_2y_4)/24 \tag{8}$$

and the corresponding constitutional isomer counting series is :

$$x^6 + x^5 + 2x^4 + 3x^3 + 2x^2 + x + 1 \qquad (9)$$

Thus there are : one single-edge-labelled tetrahedrane (i.e. benzvalene), two isomers of labelled tetrahedranes at two edges (i.e. **1** and semibullvalene **2**) and the three isomers of labelled tetrahedranes at three edges : bullvalene (**5**), triquinacene (**7**), and the chiral lumibullvalene (**9**) as indicated in Fig. 2. The two isomers of tetrahedranes labelled at four edges

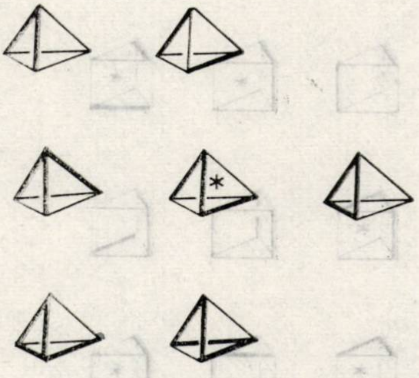

Fig. 2. — Constitutional isomers of edge-labelled tetrahedranes (di- , tri-, and tetra-substituted). An asterisk indicates a chiral isomer.

are tricyclo[5.3.2.0^{4,8}]dodeca-2,5,9,11-tetraene (**12**), and the still unknown $(CH)_{12}$ valence isomer tricyclo[5.5.0.0^{4,10}]dodeca-2,5,9,11-tetraene (**13**).

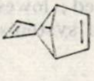
1

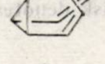
2

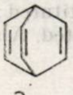
3

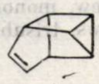
4

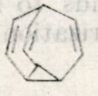
5

≡

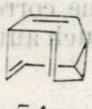
5A

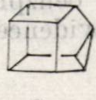
6

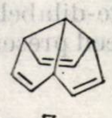
7

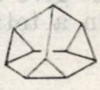
8

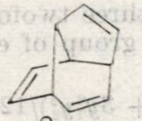
9

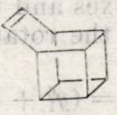
10

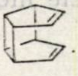
11

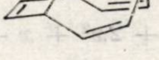
12

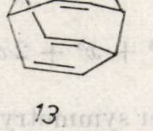
13

The unique tetrahedrane labelled at five edges and the unique tetrahedrane labelled at each of its six edges with one —CH=CH— group are still unknown and will not be discussed further here.

II.3. **Numbers of edge-labelled cubanes**

When applied to edge permutations, the three tetragonal C_4 axes coinciding with C_2 axes, then the four C_3 axes passing through two opposite vertices and the six C_2 axes passing through two opposite edges (the latter yielding the term $6y_1^2y_2^5$) furnish the cycle index for all isomers (including stereoisomers) :

$$Z = (y_1^{12} + 8y_3^4 + 6y_1^2y_2^5 + 3y_2^6 + 6y_4^3)/24 \qquad (10)$$

Application of substitution (2) according to Pólya's theorem affords the counting series :

$$x^{12} + x^{11} + 5x^{10} + 13x^9 + 27x^8 + 38x^7 + 48x^6 + 38x^5 + \ldots \qquad (11)$$

If only constitutional isomers are to be considered, the improper axes have to be considered too : the three mutually orthogonal reflection planes cutting (and therefore preserving in the permutation) four edges, the six planes containing (and preserving) two opposite edges, the centrosymmetric operation, the four S_6 axes pasing through opposite vertices, and the three S_4 axes. The cycle index is :

$$Z = (y_1^{12} + 8y_3^4 + 12y_1^2y_2^5 + 4y_2^6 + 12y_4^3 + 8y_6^2 + 3y_1^4y_2^4)/48 \qquad (12)$$

and the constitutional isomer counting series is

$$x^{12} + x^{11} + 4x^{10} + 9x^8 + 18x^7 + 24x^6 + 30x^5 + 24x^4 + \ldots \qquad (13)$$

There exist therefore : one edge-monolabelled (the cube is edge-transitive), four edge-dilabelled (one of which is chiral), nine trilabelled cubes (four of which are chiral), etc., where the label is attached to an edge. In Fig. 3 this label is a double bond and an asterisk indicates the chiral systems.

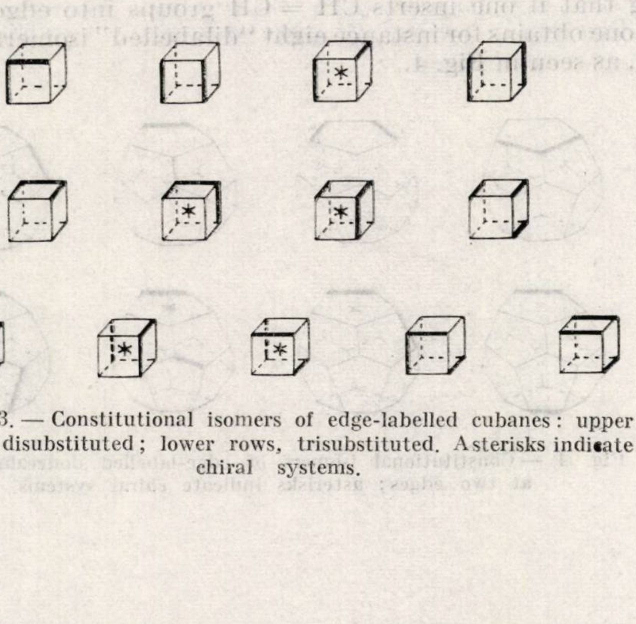

Fig. 3. — Constitutional isomers of edge-labelled cubanes : upper row, disubstituted ; lower rows, trisubstituted. Asterisks indicate chiral systems.

The mono-edge-labelled system is known as basketene, **10**; both basketene and the four edge-dilabelled systems **14**—**17** will be discussed here, but not the other systems with more than two labelled edges.

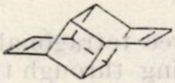

14

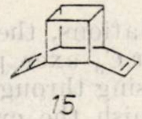

15

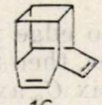

16

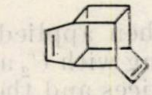

17

II.4. Numbers of edge-labelled dodecahedranes

The cycle index for the rotation group of edges takes into account the six C_5 axes, ten C_3 axes, and $15C_2$ axes passing through two edges; for all isomers (including enantiomers) the index is:

$$Z = (y_1^{30} + 24y_5^6 + 20y_3^{10} + 15y_1^2y_2^{14})/60 \tag{14}$$

and it leads to the following counting series:

$$x^{30} + x^{29} + 11x^{28} + 78x^{27} + 483x^{26} + 2423x^{25} + 10025x^{24} + \\ + 34112\,x^{23} + 97890^{22} + \ldots \tag{15}$$

For enumerating only constitutional isomers the cycle index takes into account the six S_{10} axes, ten S_6 axes, 15 symmetry planes passing through four edges and one inversion centre.

$$Z = (y_1^{30} + 24y_5^6 + 20y_3^{10} + 15y_1y_2^{14} + y_2^{15} + 24y_{10}^3 + 20y_6^5 + 15y_1^4y_2^{13})/120 \tag{16}$$

The constitutional isomer counting series is:

$$x^{30} + x^{29} + 8x^{28} + 46x^{27} + 262x^{26} + 1257x^{25} + \\ + 5113\,x^{24} + 49270\,x^{23} + \ldots \tag{17}$$

indicating that if one inserts CH = CH groups into edges of the dodecahedron one obtains for instance eight "dilabelled" isomers, three of which are chiral, as seen in Fig. 4.

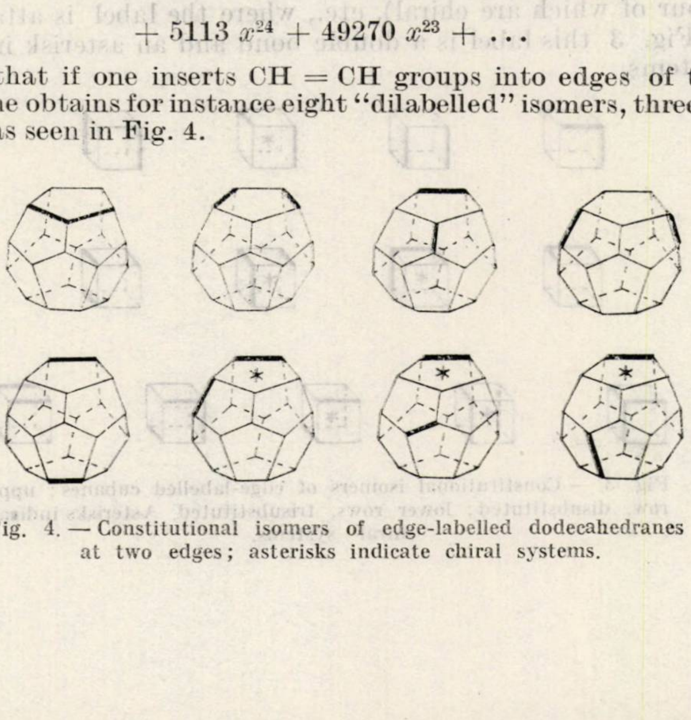

Fig. 4. — Constitutional isomers of edge-labelled dodecahedranes at two edges; asterisks indicate chiral systems.

II.5. Numbers of edge-labelled pentaprismanes

Since the situation parallels closely the case II.1 of triprismane (benzprismane) we indicate only the cycle index for all isomers

$$Z = (y_1^{15} + 4y_5^3 + 5y_1y_2^7)/10 \tag{18}$$

leading to the isomer-counting series

$$x^{15} + 2x^{14} + 14x^{13} + 49x^{12} + 147x^{11} + 312x^{10} + \\ + 518x^9 + 661x^8 + 661x^7 + \ldots \tag{19}$$

The cycle index for constitutional isomers is

$$Z = (y_1^{15} + 4y_5^3 + 5y_1y_2^7 + y_1^6y_2^5 + 4y_5y_{10} + 5y_1^3y_2^6)/20 \tag{20}$$

and the corresponding isomer counting series is:

$$x^{15} + 2x^{14} + 10x^{13} + 31x^{12} + 85x^{11} + 174x^{10} + 282x^9 + 357x^8 + 357x^7 + \ldots \tag{21}$$

There exist thus two achiral single-edge labelled pentaprismanes, ten isomers labelled at two edges, four of which are chiral, etc. One of the two single-edge labelled isomers is the known **18**; the other one, **19**, is still unknown and will not be discussed here.

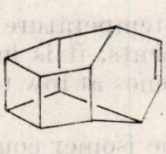
18

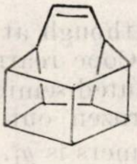
19

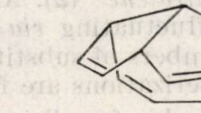
20

III. APPLICATIONS TO POLYHEDRAL UNSATURATED $(CH)_n$ HYDROCARBONS

From now on, Pólya's theorem will be applied for the figure-counting series and cycle index referring to vertex-labelled graphs (symmetry operations of the rotation group for graph vertices). In a previous paper, the numbers of substituted isomers of benzvalene and Dewar-benzene were discussed.[6] The present paper will discuss other unsaturated $(CH)_n$ polyhedral valence isomers.

III.1. Polyhedral valence isomers of $(CH)_8$ unsaturated hydrocarbons

A. *Barrelene* [7](**3**). The cycle index for all isomers (including stereoisomers) takes into account the C_3 axis passing through two vertices and the three C_2 axes. The cycle index is :

$$Z = (y_1^8 + 2y_1^2y_3^2 + 3y_2^4)/6 \tag{22}$$

and the isomer counting series is :

$$x^8 + 2x^7 + 7x^6 + 10x^5 + 16x^4 + 10x^3 + 7x^2 + 2x + 1 \tag{23}$$

The cycle index for constitutional isomers takes also into account the three symmetry planes passing through four vertices, the symmetry plane bisecting the double bonds, and the S_3 axis. The cycle index is :

$$Z = (y_1^8 + 2y_1^2y_3^2 + 4y_2^4 + 3y_1^4y_2^2 + 2y_2y_6)/12 \tag{14}$$

and the corresponding counting series for constitutional isomers is :

$$x^8 + 2x^7 + 6x^6 + 8x^5 + 12x^4 + 8x^3 + 6x^2 + 2x + 1 \tag{25}$$

These counting series show that there are six disubstituted isomers, one of which is chiral (Fig. 5).

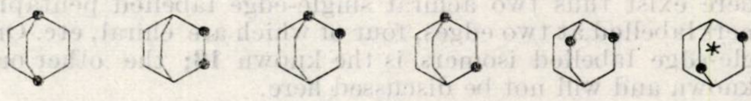

Fig. 5. — Constitutional isomers of disubstituted barrelenes. An asterisk denotes a chiral isomer. For simplicity, double bonds were omitted.

B. *Semibullvalene* [8] (**2**). Although at room temperature semibullvalene is rapidly fluctuating *via* Cope rearrangements, it is interesting to compute the numbers of substituted semibullvalenes at low temperatures when the automerizations are frozen out.

The cycle index for all isomers is y_1^8, and the isomer counting series is the binomial $(x + 1)^8$. The cycle index for constitutional isomers takes into account the unique symmetry element, a reflection plane :

$$Z = (y_1^8 + y_1^2y_2^3)/2 \tag{26}$$

The constitutional isomer counting series is therefore :

$$x^8 + 5x^7 + 16x^6 + 31x^5 + 38x^4 + 31x^3 + \ldots \tag{27}$$

indicating that there are five monosubstituted isomers, three of which (with the substituent linked to a carbon atom off the symmetry plane) are chiral. It was shown earlier [6] that semibullvalene **2** is coisomeric with another known $(CH)_8$ valence isomer, tetracyclo$[3.3.0.0^{2,4}.0^{3,6}]$oct-7-ene[9] (**4**).

C. *The* $(CH)_8$ *valence isomer* **1**, *tricyclo*$[3.3.0.0^{2,6}]$*octa-3,7-diene*.[10] There exist a C_2 axis coinciding with an S_4 axis, two other C_2 rotations and two symmetry planes passing through four vertices. The cycle index for all isomers is :

$$Z = (y_1^8 + 3y_2^4)/4 \tag{28}$$

leading to the configuration-counting series :

$$x^8 + 2x^7 + 10x^6 + 14x^5 + 22x^4 + 14x^3 + 10x^2 + 2x + 1 \tag{29}$$

The cycle index for constitutional isomers is :

$$Z = (y_1^8 + 3y_2^4 + 2y_1^4y_2^2 + 2y_4^2)/8 \tag{30}$$

leading to the isomer counting series :

$$x^8 + 2x^7 + 7x^6 + 10x^5 + 15x^4 + 10x^3 + 7x^2 + 2x + 1 \tag{31}$$

These two series indicate that there exist seven disubstituted, isomers, three of which are chiral (Fig. 6).

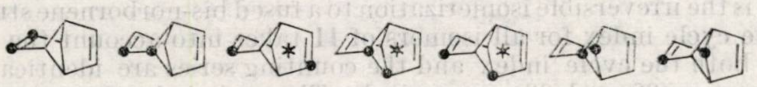

Fig. 6. — Constitutional isomers of disubstituted derivatives of **1**. Asterisks indicate chiral isomers.

D. *Tetracyclo*$[3.3.0.0^{2,4}.0^{3,6}]$*oct-7-ene* [9] (**4**) is one of the two possible single-edge labelled benzprismanes (the other one has not yet been prepared). Compund **4**, coisomeric with **2**, has only one symmetry plane therefore its cycle index for all isomers is $(x + 1)^8$ and the isomer counting series has binomial coefficients ; the constitutional isomers are determined by the cycle index (26), i.e. $(y_1^8 + y_1^2y_2^3)/2$, and the corresponding isomer counting series is (27) i.e. $x^8 + 5x^7 + 16x^6 + 31x^5 + 38x^4 + 31x^3 + \ldots$ indicating that there exist five monosubstituted isomers, three of which are chiral.

III.2. Polyhedral unsaturated $(CH)_{10}$ valence isomers

E. *Basketene* [11] (**10**). The molecule **10** has only one proper C_2 axis, hence the cycle index for all isomers is

$$Z = (y_1^{10} + y_2^5)/2 \tag{32}$$

leading to the isomer-counting series

$$x^{10} + 5x^9 + 25x^8 + 60x^7 + 110x^6 + 126x^5 + 110x^4 + \dots \qquad (33)$$

The cycle index for constitutional isomers takes also into account the two mutually orthogonal symmetry planes (one of which passes through six vertices).

$$Z = (y_1^{10} + 2y_2^5 + y_1^6 y_2^2)/4 \qquad (34)$$

and the resulting constitutional isomer counting series is :

$$x^{10} + 4x^9 + 18x^8 + 38x^7 + 69x^6 + 76x^5 + 69x^4 + \dots \qquad (35)$$

There are therefore four monosubstituted isomers, one of which is chiral (the substituent is linked to the unique vertex which is not situated on any of the two symmetry planes).

The silver-ion catalyzed isomerization of basketene into snoutene, discovered serendipitously by Furstoss and Lehn,[11] was to have far-reaching consequences by opening the way to metal-ion catalyzed isomerizations.[11a]

F. *Hypostrophene* (**11**). At low temperature the molecule **11** does not fluctuate, but at higher temperatures (0°) it undergoes automerization *via* a Cope rearrangement ;[5] however, at still higher temperature, the main reaction is the irreversible isomerization to a fused bis-norbornene structure.

The cycle index for all isomers of **11** takes into account the unique C_2 axis ; both the cycle index and the counting series are identical to the preceding ones (32) and (33), respectively. The cycle index for constitutional isomers considers also the two symmetry planes one of which passes through two carbon atoms :

$$Z = (y_1^{10} + 2y_2^5 + y_1^2 y_2^4)/4 \qquad (36)$$

and the resulting constitutional isomer counting series is :

$$x^{10} + 3x^9 + 15x^8 + 32x^7 + 60x^6 + 66x^5 + 60x^4 + \dots \qquad (37)$$

G. *Bullvalene* (**5**). The $(CH)_{10}$ hydrocarbon **5** whose automerization at elevated temperature (100°) leads to complete equivalence of all ten CH groups was predicted to behave thus by Doering[12] before it was prefared by Schröder.[13] In the absence of fluctuating bonds, the cycle index opr allisomers is based on the ternary axis passing through one vertex :

$$Z = (y_1^{10} + 2y_1 y_3^3)/3 \qquad (38)$$

leading to the isomer counting series :

$$x^{10} + 4x^9 + 15x^8 + 42x^7 + 72x^6 + 84x^5 + 72x^4 + \dots \qquad (39)$$

The cycle index for constitutional isomers takes also into account the three symmetry planes which pass through four vertices

$$Z = (y_1^{10} + 2y_1y_3^3 + 3y_1^4y_2^3)/6 \tag{40}$$

and the resulting isomer counting series is :

$$x^{10} + 4x^9 + 12x^8 + 29x^7 + 47x^6 + 54x^5 + 47x^4 + \ldots \tag{41}$$

It was shown previously [6] that bullvalene **5** is coisomeric with a saturated $(CH)_{10}$ valence isomer, **6** ; the relationship is more easily seen if bullvalene is drawn as **5A**, indicating how **6** is obtained by theoretical conversion of three double bonds of **5A** into three new single bonds of **6**.

H. *Triquinacene* [14] (**7**). Just as for bullvalene, the cycle index for all isomers is (38) and the resulting isomer counting series is (39). However, for constitutional isomers the cycle index takes into account the three symmetry planes which pass only through two vertices, therefore :

$$Z = (y_1^{10} + 2y_1y_3^3 + 3y_1^2y_2^4)/6 \tag{42}$$

and the constitutional isomer counting series is :

$$x^{10} + 3x^9 + 10x^8 + 25x^7 + 41x^6 + 48x^5 + 41x^4 + \ldots \tag{43}$$

The monosubstituted triquinacene with the substituent attached to a double bond is chiral.

It was shown earlier [6] that triquinacene **7** and the saturated $(CH)_{10}$ valence isomer **8** (diademane, mitrane)[15] are coisomeric ; indeed, Ag^+-catalysts convert the latter into the former compound.[11,15] In turn, diademane is formed photochemically from snoutene, [11,15] and reverts to it in the presence of Rh(I) catalysts.

III.3. Valence isomers of $(CH)_{12}$ hydrocarbons

I. *Pentacyclo*[*6.4.0.0*^{2,7}.*0*^{3,10}.*0*^{4,9}]*dodeca-5,11-diene* (**14**). The molecule has three C_2 axes, neither of which passes through any vertex.

$$Z = (y_1^{12} + 3y_2^6)/4 \tag{44}$$

and the resulting isomer counting series is

$$x^{12} + 3x^{11} + 21x^{10} + 55x^9 + 135x^8 + 198x^7 + 246x^6 + \\ + 198\,x^5 + \ldots \tag{45}$$

If one takes into account the three symmetry planes and the inversion centre, the cycle index for constitutional isomers is

$$Z = (y_1^{12} + 5y_2^6 + y_1^4y_2^4 + y_1^8y_2^2)/8 \tag{46}$$

and the corresponding counting series is :

$$x^{12} + 3x^{11} + 17x^{10} + 39x^{9} + 91x^{8} + 126x^{7} + \\ + 158x^{6} + 126x^{5} + \ldots \qquad (47)$$

All three monosubstituted systems are achiral but four from the seventeen disubstituted ones are chiral.

J. *Pentacyclo[6.4.0.0*$^{2.7}$*.0*$^{3.12}$*.0*$^{6.9}$*]dodeca-4-10-diene* (**15**). The molecule has a C_2 axis and therefore the cycle index for all isomers is

$$Z = (y_1^{12} + y_2^{6})/2 \qquad (48)$$

The isomer counting series is

$$x^{12} + 6x^{11} + 36x^{10} + 110x^{9} + 255x^{8} + 396x^{7} + \\ + 472x^{6} + 396\,x^{5} + \ldots \qquad (49)$$

The cycle index for the constitutional isomers (considering also the two symmetry planes) is

$$Z = (y_1^{12} + 3y_2^{6})/4 \qquad (50)$$

The resulting counting series is

$$x^{12} + 3x^{11} + 21x^{10} + 55x^{9} + 135\,x^{8} + 198x^{7} + \\ + 246\,x^{6} + 198\,x^{5} + \ldots \qquad (51)$$

Therefore the three monosubstituted systems are chiral but only 15 of the 21 disubstituted systems are chiral. The molecule fulfills the structural condition for presenting a degenerate Cope rearrangement.[4]

K. *Pentacyclo[6.4.0.0*$^{2.5}$*.0*$^{3.12}$*.0*$^{4.11}$*]dodeca-6,9-diene* (**16**). The molecule has only one symmetry plane, therefore the cycle index for all isomers is y_1^{12} and the counting series is the binomial $(x+1)^{12}$. The cycle index for constitutional isomers is :

$$Z = (y_1^{12} + y_1^{4}y_2^{4})/2 \qquad (52)$$

and the counting series is

$$x^{12} + 8x^{11} + 38x^{10} + 120x^{9} + 263x^{8} + 416x^{7} + \\ + 484x^{6} + 416x^{5} + \ldots \qquad (53)$$

Therefore from the eight constitutional isomers, four are chiral.

L. *Pentacyclo[6.4.0.0^{2,5}.0^{3,10}.0^{4,9}]dodeca-6,11-diene* (ansaradiene)[16] (**17**). Again the cycle index for all isomers is y_1^{12} and the counting series is $(x+1)^{12}$. The molecule has an improper rotation axis, therefore the cycle index for constitutional isomers is the same as (48); the counting series is (49). The molecule fulfills the structural condition for presenting a degenerate Cope rearrangement.[4]

The molecule has six pairs of constitutionally equivalent CH groups; all six monosubstituted systems are chiral; from the 36 disubstituted systems, 30 are chiral.

M. *Hexacyclo[6.4.0.0^{2,7}.0^{3,6}.0^{4,12}.0^{5,9}]dodec-10-ene*[17] (**18**). The molecule is one of the two possible pentaprismanes labelled at one edge. There is just one proper binary axis, therefore the cycle index for all isomers is (48) and the isomer counting series is (49). For constitutional isomers one has to take into account the two symmetry planes, one of which passes through four CH groups. The cycle index is

$$Z = (y_1^{12} + 2y_2^6 + y_1^4 y_2^4)/4 \qquad (54)$$

and the constitutional isomer counting series is

$$x^{12} + 4x^{11} + 22x^{10} + 60x^9 + 139x^8 + 208x^7 + \\ + 252x^6 + 208x^5 + \dots \qquad (55)$$

Therefore there exist four monosubstituted isomers, two of which are chiral (i.e. those whose substituent is not attached to the CH group lying on a symmetry plane).

N. *Hexacyclo[5.5.0.0^{2,6}.0^{3,12}.0^{4,11}.0^{5,8}]dodec-9-ene* (**19**). The second pentaprismane labelled at one edge, **19**, has no proper axis, therefore its cycle index for all isomers is $(x+1)^{12}$. There exists one symmetry plane, therefore the cycle index for constitutional isomers is:

$$Z = (y_1^{12} + y_1^2 y_2^5)/2 \qquad (56$$

leading to the counting series:

$$x^{12} + 7x^{11} + 36x^{10} + 115x^9 + 255x^8 + 406x^7 + 472x^6 + \dots \qquad (57)$$

There are thus seven monosubstituted isomers, five of which are chiral (whose substituent is not attached to any of two carbon atoms lying on the symmetry plane).

O. *Tricyclo[5.3.2.0^{4,8}]dodeca-2,5,9,11-tetraene*[18] (**12**). The molecule has only one symmetry plane which passes through four CH groups, therefore the cycle index for all isomers is $(x+1)^{12}$ and the cycle index for constitutional isomers is (52). The counting series for all isomers has as coefficients the binomial series C_{12}^i ($i = 0, 1, 2, \dots, 12$) and the constitutional isomer counting series is (53), indicating that from the eight monosubstituted isomers, four are chiral (those whose substituent is not bonded to any of the CH groups lying on the symmetry plane).

P. *Tricyclo*[*5.4.1.0*^{4,12}]*dodeca-2,5,8,10-tetraene*[19] (**20**). This molecule has also only one symmetry plane passing through two CH groups, and is therefore coisomeric with **19**.

CONCLUSION

It was shown that one can apply Pólya's theorem for counting edge-labelled isomers if the cycle index is calculated on the basis of the rotation group of edges. By taking as the label a CH=CH grouping, one can convert polyhedra of degree three into unsaturated $(CH)_n$ valence isomers. Then Pólya's theorem was applied to enumerating isomers of some of these valence isomers.[20]

REFERENCES

[1] Part 44, preceding paper in this issue.

[2] G. Pólya, *Z. Kristal.* (A) **93**, 415 (1936) ; *Acta Math.*, **68**, 145 (1937).

[3] Each vertex of the line graph *L*(*G*) corresponds to an edge of G, and each edge of *L*(*G*) connects two vertices of *L*(*G*) corresponding to adjacent edges of G ; see F. Harary, "Graph Theory", Addison-Wesley, Reading, Mass., 1969, p. 71.

[4] A. T. Balaban, *Rev. Roum. Chim.*, **17**, 883 (1972).

[5] J. S. McKennis, L. Brener, J. S. Ward and R. Pettit, *J. Am. Chem. Soc.*, **93**, 4957 (1971) ; L. A. Paquette, R. F. Davis and D. J. James, *Tetrahedron Lett.*, 1615 (1974).

[6] A. T. Balaban, *Rev. Roum. Chim.*, **19**, 1323 (1974).

[7] H. E. Zimmerman and H. M. Paufler, *J. Am. Chem. Soc.*, **82**, 1514 (1960) ; H. E. Zimmerman G. L. Grunewald, H. M. Paufler and M. A. Shervin, *ibid.*, **91**, 2330 (1969).

[8] H. E. Zimmerman and G. L. Grunewald, *J. Am. Chem. Soc.*, **88**, 183 (1966).

[9] G. W. Klumpp and J. Stapersma, *Tetrahedron Lett.*, 747 (1977).

[10] J. Meinwald and H. Tsuruta, *J. Am. Chem. Soc.*, **91**, 5879 (1969).

[11] S. Masamune, H. Cuts and M. G. Hogben, *Tetrahedron Lett.*, 1017 (1966) ; R. Furstoss and J. M. Lehn, *Bull. Soc. Chim. France*, 2497 (1966) : W. G. Dauben, C. H. Schallhorn and D. L. Whalen, *J. Am. Chem. Soc.*, **93**, 1446 (1971).

[11a] L. A. Paquette, *Acc. Chem. Res.*, **4**, 280 (1971) ; C. W. Jefford, *J. Chem. Educ.*, **53**,477 (1976)

[12] W. von E. Doering and W. R. Roth, *Tertrahedron*, **19**, 715 (1963) ; *Angew. Chem.*, **75**, 27 (1963).

[13] G. Schröder, *Angew Chem.*, **75**, 722 (1963) ; *Chem. Ber.*, **97**, 3131, 3140 (1964).

[14] R. B. Woodward, T. Fukunaga and R. C. Kelly, *J. Am. Chem. Soc.*, **86**, 3162 (1964) ; L. A. Paquette, *Topics Curr. Chem.*, **79**, 41 (1979) ; **119**, 1 (1984) ; D. Bosse and A. de Meijere, *Chem. Ber.*, **111**, 2223, 2243 (1978) ; L. A. Paquette, F. R. Kearney, A. F. Drake, and S. F. Mason, *J. Am. Chem. Soc.*, **103**, 5064 (1981) ; M. J. Wyvratt and L. A. Paquette, *Tetrahedron Lett.*, 2433 (1974) ; C. Mercier, P. Souci, W. Rosen and P. Deslongchamps, *Synth. Commun.*, **3**, 161 (1973) ; I. T. Jacobson, *Acta Chem. Scand.*, **21**, 2235 (1967) ; **26**, 2477 (1972) ; *Chem. Scripta*, **2**, 121, 127 (1972).

[15] A. de Meijere, D. Kaufmann and O. Schallner, *Angew. Chem.*, **83**, 404 (1971) ; H. Prinzbach and D. Stusche, *Helv. Chim. Acta*, **54**, 755 (1971).

[16] H. D. Martin and P. Pfoehler, *Angew. Chem.*, **90**, 901 (1978).

[17] E. Le Goff and S. Oka, *J. Am. Chem. Soc.*, **91**, 5665 (1969).

[18] J. N. Labows, J. Meinwald, H. Röttele and G. Schröder, *J. Am. Chem. Soc.*, **89**, 612 (1967)

[19] L. A. Paquette, M. J. Kukla, S. V. Ley and S. G. Traynor, *J. Am. Chem. Soc.*, **99**, 4756 (1977).

[20] A. T. Balaban, M. Banciu and V. Ciorba, "Annulenes, Benzo-, Homo-, Hetero-Derivatives and Their Valence Isomers", CRC Press, Boca Raton, Florida, in press ; A. T. Balaban and M. Banciu, *J. Chem. Educ.*, **61**, 766 (1984) ; M. Banciu and A. T. Balaban, *Chem. Scripta*, **22**, 188 (1983) ; M. Banciu, C. Popa and A. T. Balaban, *ibid.*, **24**, 28 (1984).

Revue Roumaine de Chimie, **31**, 7, 709—710 (1986)

DIELS-ALDER REACTION OF *trans*, *trans*-1,4-DIACETOXY-1,3-BUTADIENE AND 1,2-PENTADIEN-4-ONE

RUBÉN SÁNCHEZ-OBREGÓN *, HÉCTOR BARRIOS, BENJAMÍN ORTÍZ
and FRANCISCO YUSTE
**Instituto de Química, Universidad Nacional Autónoma de México, Ciudad Universitaria,
Circuito Exterior, Coyoacán, 04510, México, D. F.**

Received September 16, 1985

The Diels-Alder adduct of *trans, trans*-1,4-diacetoxy-1,3-butadiene and 1,2-pentadien-4-one undergoes a [3,3] sigmatropic shift followed by elimination of acetic acid to produce 2′-acetoxymethylacetophenone.

The Diels-Alder cycloaddition reactions involving allenic ketones as dienophiles have received little attention.[1] In the course of a study directed to the synthesis of piquerol A,[2] we have investigated the Diels-Alder addition of *trans*, *trans*,-1,4-diacetoxy-1,3-butadiene **1** to 1,2-pentadien-4-one **2.** In this paper we reported the results obtained in the above reaction.

Condensation of **1** with acetylallene **2** was attempted under a large variety of conditions. Unfortunately in none case, the expected Diels-Alder adduct could be obtained and the only isolated product was acetophenone **3** in 20 % yield. The formation of **3** can be explained by a [3,3] sigmatropic rearrangement on the initial adduct [3] and subsequent elimination of acetic acid.

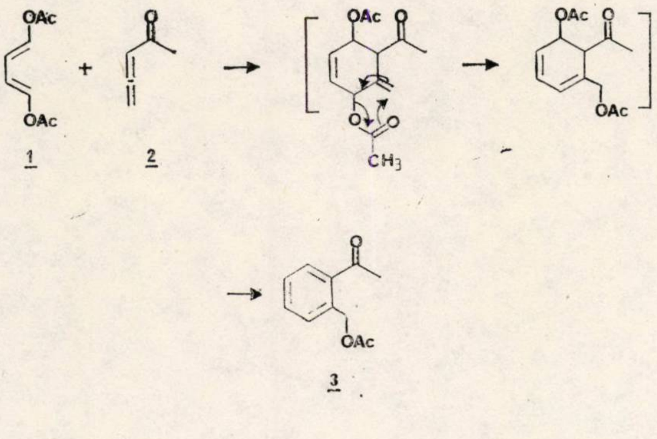

3

EXPERIMENTAL

Infrared spectra were taken on a Perkin-Elmer 283b or Nicolet 55X instruments. ^1H and ^{13}C-NMR-spectra were obtained with a Varian FT-80A spectrometer with tetramethylsilane as an internal reference. Mass spectra were recorded on a Hewlett-Packard 5985-b spectrometer at 70 eV.

trans, trans-1,4,*Diacetoxy-1-3-butadiene* **1**. This compound was prepared according to the method of Carlson and Hill[4] : mp 99—101°C (lit. [4] 102—104°C) ; IR ($CHCl_3$) 1752 (br), 1625 cm^{-1} ; ^1H-NMR ($CDCl_3$, δ ppm), 2.12 (s, 6H), 5.95 (mm, 2H), 7.35 (m, 2H) ; MS m/e(relative intensity) 170 (M^+, 8), 86 (67), 57 (20), 43 (100).

(E/Z)-4-Bromo-3-penten-2-one. This mixture (ca. 9/1 ^1H-NMR) was prepared using the procedure of Piers *et al.* [5] : bp 45—46°C/8 torr (lit. [6] 47—48°C/8 torr).

1,2-Pentadien-4-one **2**. The allenic ketone **2** was obtained following the method of Buono[6] : bp 60—62°C C/80 torr (lit.[6] 62°C/80 torr) ; IR (film) 1960, 1935, 1685, 860 cm^{-1} : ^1H-NMR ($CDCl_3$, δ ppm) 2.25 (s, 3H), 5.22 (d, J = 7Hz, 1H), 5.70 (t, J = 7Hz, 1H) ; ^{13}C-NMR ($CDCl_3$, δ ppm) 217.29 (s, C-2), 197.32 (s, C-4) 97.22 (d, C-3), 79.25 (t, C-1), 26.42 (q,C-5) ; MS m/e (relative intensity) 82 (M^+8), 51 (13), 50 (9), 43 (100).

2.Acetoxymethylacetophenone **3**. A solution of 0.189 g (1.11 mmol) of **1** and 0.186 g (2.26 mmol) of **2** in 2 mL of deaerated toluene was heated at 100°C for 48 h in a Pyrex tube which had been sealed under nitrogen. After cooling, the tube was opened and the solution evaporated to dryness. The residue was chromatographed in two 20 × 20 × 0.2 cm silica gel plates. The plates were developed with hexane-ethyl acetate (70 : 30) and the product was recovered with acetone to give 0.043 g (20%) of 3.[7] IR (film) 1745, 1685 cm^{-1} ; ^1H-NMR ($CDCl_3$, δ ppm), 2.12 (s, 3H), 2.60 (s, 3H), 5.42 (s, 2H), 7.20—7.55 (m, 3H), 7.65—7.85 (m, 1H) ; MS, m/e (relative intensity) 192 (M^+, 3) 150 (51), 149 (89), 135 (70), 131 (100), 77 (41), 43 (40).

REFERENCES

[1] M. Bertrand and J. Le Gras, *Bull. Soc. Chim. Fr.*, **1967**, 4336.

[2] J. Romo, A. Romo de Vivar, L. Quijano, T. Rios, and E. Diaz, *Rev. Latinoamer. Quim.*, **1**, 72 (1970).
M. Soriano-Garcia, M. Jiménez, M. González, A. Hernández, M. Schatz and C. Campana, *Chem. Lett.*, **1983**, 617.

[3] T. L. Gilchrist and R. C. Storr, "Organic Reactions and Orbital Symmetry", 2nd ed. ; Cambridge University Press, Cambridge, 1979, p. 280.

[4] M. Carlson and R. K. Hill, *Org. Synth.*, **50**, 24 (1970).

[5] E. Piers., J. R. Grierson, C. K. Lau and I. Nagakura, *Can J. Chem.*, **60**, 210 (1982).

[6] G. Buono, *Synthesis*, **1981**, 872.

[7] T. Mitsui, M. Kitahara, and T. Nagase, *J. Sci. Res. Inst., Tokyo*, **50**, 65 (9156) ; *Chem.Abstr.* **51**, 8658e (1957).

Revue Roumaine de Chimie, 31, 7, 711—718 (1986)

ANODIC OXIDATION OF ALKYLBENZENES IN DRY ACETONITRILE

OLGA PÉREZ DE MÁRQUEZ
Universidad de Los Andes, Facultad de Ciencias, Departamento de Química, Mérida 5101, Venezuela

Received September 9, 1985

The anodic oxidation of a series of alkylbenzenes in dry acetonitrile is discussed. Electrochemical techniques, assisted by analysis of the products, were used to determine mechanistic aspects. An ECE sequence is proposed for the oxidation of the aromatics under study. Hexaethylbenzene was taken as an example to explain the mechanism for the oxidation of alkylbenzenes. A reversible oxidation wave was observed for hexaethylbenzene in dry acetonitrile and tetrabutylammonium tetrafluoroborate. All the other compounds oxidized irreversibly under the same conditions. Decay of the cation radical of the alkylbenzenes occurs due to a side chain proton loss.

INTRODUCTION

When a solution containing an aromatic hydrocarbon is oxidized, a great number of reactions can take place as a function of the structure of the aromatic compound and the environmental conditions.

The most common reaction observed in anodic oxidation of aromatic compounds has been classified as : side chain substitution, addition and dimerization. Typical examples have been given by the authors.[1-4] If the experimental conditions are suitably chosen, the course of the oxidation could be shifted to favour any of these processes. Many cases are known to undergo reaction with the solvent to form stable compounds : Nyberg and co-workers,[5] working with hexamethylbenzene in acetonitrile obtained the N-benzylacetamide.

More interesting studies have been made about the oxidation of alkylbenzenes[6,7] leading to functionalized derivatives. Bewick *et al.*[7-9] have studied the mono and polyfunctionalization of alkylbenzenes.

In this paper, the functionalization of longer chain substituted alkylbenzenes in acetonitrile will be described.

EXPERIMENTAL

Cyclic voltammetry experiments were performed using a Hi-Teck potentiostat type DT 2101 and Hi-Teck waveform generator type PPR1. The voltammograms were recorded either directly on a Hewlett Packard 7015B X-Y recorder at slow sweep rates or *via* Gould Advance 054100 Digital storage oscilloscope/waveform Digitizer at those sweep rates higher than 0.7 V/S.

Oxidation of the hydrocarbons was carried out in a voltammetric cell consisting of a platinum wire working electrodes surrounded by a platinum mesh counter electrode. The reference electrode was in a separate compartment connected to the working compartment by a fine Luggin capillary brought close to the working electrode. All measurements were taken against a silver wire held in an acetonitrile — $Bu_4^nNBF_4$ (0.1M) solution containing silver nitrate (0.01M). For quantitative studies, only the first sweep was recorded, being the working electrode flamed before each run. Concentrations of substrates were between 5×10^{-3} and 1×10^{-3}M and background currents were measured for cyclic voltammetry and for coulometry.

Preparative coulometry experiments were performed using a three compartment electrolysis cell. Both the working and the secondary electrodes were 2 cm^2 geometrical area platinum gauzes. The anolyte was continously stirred. A cationic resin (Dowex 500 w-X8, 100—200 mesh) was added to the working electrode compartment before the start of the electrolysis to trap the intermediate and to simplify the reaction. The product was extracted from the resin and hydrolyzed with NaOH solution.

For the separation and analysis of the products, thin layer chromatography (TLC) were run on 20 × 20 glass plates with 1 mm thick silica gel crat. Mass spectra were carried out in a Kratos MS 30 mass spectrometer.

RESULTS

Figure 1 shows the hexaethylbenzene cyclic voltammogram at two different sweep rates. Except for the tert-butylbenzene, which showed a second wave at 2.16 V, all the compunds showed only one peak within the

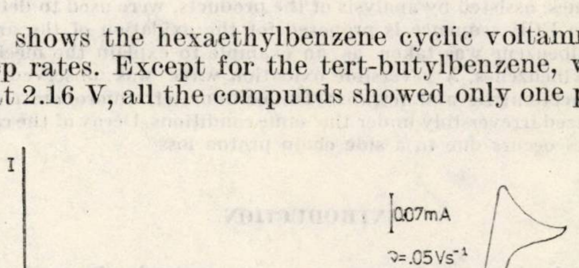

Fig. 1: — Cyclic voltammograms of hexaethylbenzene (1 mM) in CH_3CN on a 0.16 cm^2 platinum electrode.

range of potential +1.84 — +1.94 volts. Those values of potential were found to be much higher than those observed for hexaethylbenzene.

All the compounds showed a broad reverse peak at −0.60 V which disappeared at high sweep rates. It has been reported [10] that such wave is due to the reduction of hydrogen ion. Table 1 shows the voltammetric data for all the hydrocarbons under study taken at a sweep rate of 0.2 V/S.

Table 1

Voltammetric data for anodic oxidation of hydrocarbons

Substrate	E_p(V)	$Ep/2$(V)	E_p—$Ep/2$(V)
Hexaethylbenzene	1.360	1.300	0.060
1-Phenyloctane	1.920	1.820	0.100
1-Phelylnonane	1.850	1.770	0.080
n-Propylbenzene	1.900	1.800	0.100
tert-Butylbenzene	1.940	1.840	0.080

From the voltammetric studies carried out at several sweep rates, theoretical working curves were constructed and the best fit[11,12] for a pseudo-first order rate constant was found to be within a range of $1.0\times\times10^3$ and $1.5\times10^3\,s^{-1}$, except for the hexaethylbenzene with a rate constant of $0.75\ s^{-1}$ (Figs. 2 and 3).

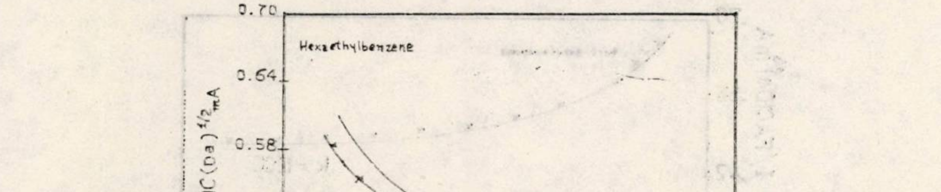

Fig. 2. — Cyclic voltammetric working curves for the determination of the pseudo-first order homogeneous rate constant : — theoretical ; x x x experimental.

Table 2 shows the values of K_f obtained for the homogeneous reaction coupled with the two electron transferences.

Pulsing potential electrolyses were performed under the conditions showed in Table 3. A list of the products is given in Table 4.

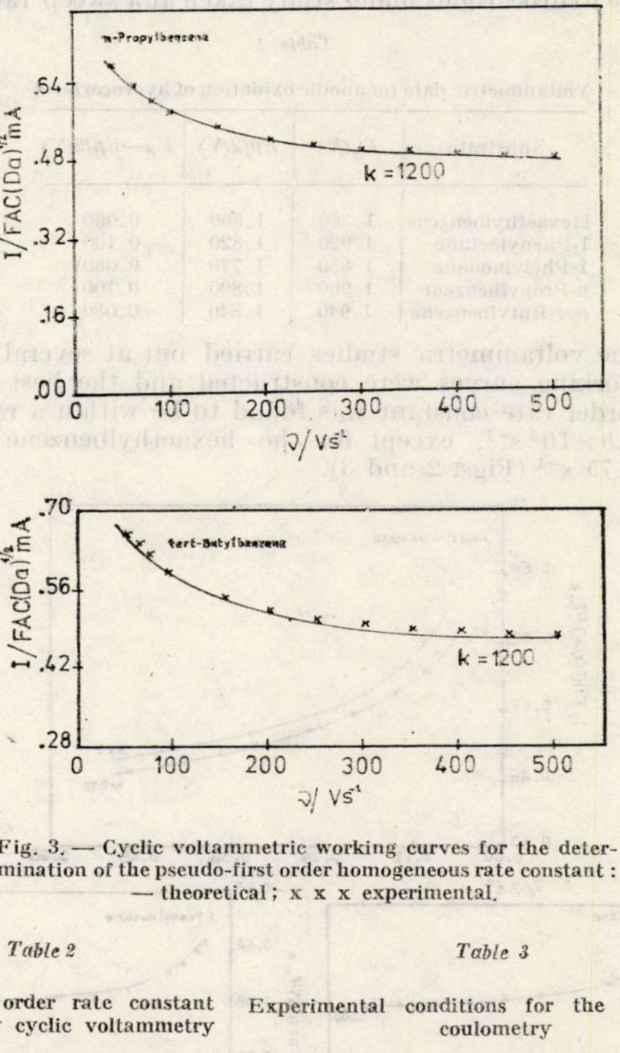

Fig. 3. — Cyclic voltammetric working curves for the determination of the pseudo-first order homogeneous rate constant : — theoretical ; x x x experimental.

Table 2

Pseudo-first order rate constant calculated by cyclic voltammetry

Substrate	$k_f 1$ (s^{-1})
Hexaethylbenzene	0.75
1-Phenyloctane	1000
1-Phenylnonane	1000
n-Propylbenzene	1200
tert-Butylbenzene	1200

Table 3

Experimental conditions for the preparative coulometry

Substrate	Base potential (V)	Pulseheight (V)
Hexaethylbenzene	1.200	0.300
1-Phenyloctane	1.500	0.520
1-Phenylnonane	1.700	0.320
n-Propylbenzene	1.600	0.500
tert-Butylbenzene	1.600	0.540

Table 4

Anodic oxidation of alkylbenzenes in dry acetonitrile at platinum. The mass spectra data to support these structures are shown in the appendix

Starting material	Organic yield (%)	Product
Hexaethylbenzene	71.3	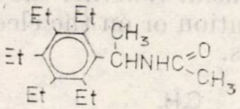
1-Phenyloctane	56.0	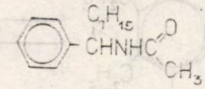
1-Phenylnonane	51.2	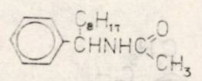
n-Propylbenzene	50.6	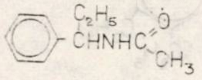
tert-Butylbenzene	20.4	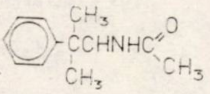

DISCUSSION

The cyclic votammetric oxidation peak heights for all the members of this series did not show linear proportionality to the square root of the sweep rates. For the data processing, an ECE type of mechanism has been assumed. From the current function $Ip/\nu^{1/2}$, as a function of scan rate, qualitative information was obtained : at high sweep rates an electron transference occurs to form the cation radical; at lower sweep rates the current function was not independent of the sweep rate, indicating that over that time scale the cation radical was undergoing a chemical reaction. At even slower velocities the transference of the second electron was observed for all, except the hexaethylbenzene where the data were possibly affected by convection at the very slow sweep rates required. For convenience of presentation, only the data concerned with the transference of the first electron and the coupled chemical reaction are included in the graphs.

Hexaethylbenzene behaved quite differently than the others : the cation radical was very stable : its lifetime was found to be 10 times longer than those for the other hydrocarbons, obtained from cyclic voltammetry.

From the working curves it could be observed that at very short times, for all the hydrocarbons, the behaviour approached that for a one electron oxidation, while at long times, the current function reached values which were indicative of a two-electron behaviour. A crossover region between the two extreme situations was exhibited by all the aromatics, so it can be concluded that the anodic oxidation of hexaethylbenzene, 1-phenyloctane, 1-phenylnonane and *tert*-butylbenzene, follow an ECE type of mechanism. Whether the second electron transference occurs in the bulk of the solution or on the electrode surface, it cannot be predicted by these techniques.

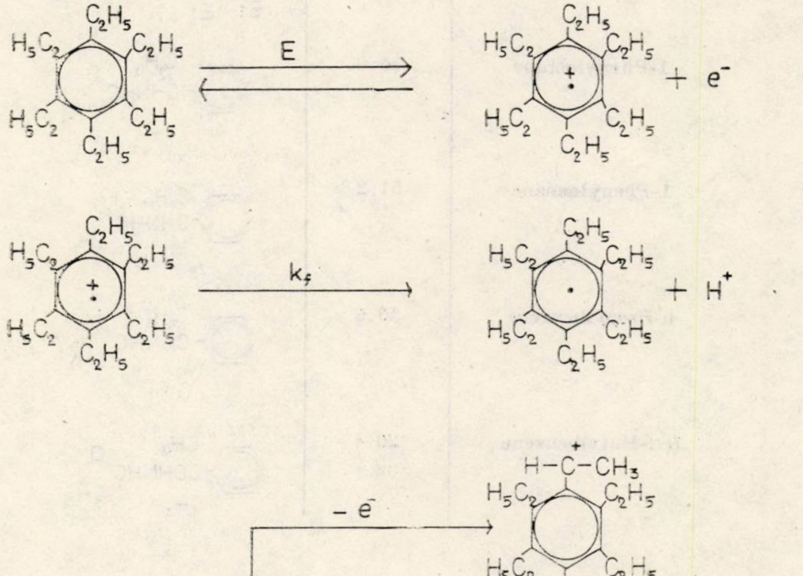

The results presented for preparative electrolyses of the hydrocarbons showed that they are oxidized in dry acetonitrile to give functionalized products, the acetamide being the main product, under conditions of pulsing electrolysis.

Using the hexaethylbenzene as an example, and from the results of this work, the scheme shown below can be suggested for the production of the acetamide.

If the transference of the second electron is taking place on the electrode surface, the carbonium ion is produced through reaction (a), whilst if it occurs in the bulk of the solution, it will follow path (b). In any case, the production of the nitrilium ion takes place by nucleophylic attack of the acetonitrile.

NOTATIONS

Symbol	*Description*	*Unity*
E_p	Voltammetric peak potential	V
$E_{p/2}$	Voltammetric half peak potential	V
Kf	Pseudo-first order homogeneous rate constant	S
ν	Sweep rate	V/S
ECE	Electron transference — Chemical reaction Electron transference	

ACKNOWLEDGEMENTS. I would like to thank Dr. A. Bewick and Dr. J. Mellor at Southampton University, Chemistry Department Southampton, England, where this work was carried out.
I would also like to thank the Universitdad de Los Andes, Mérida, Venezuela, for financial support.

APPENDIX

1. Mass spectrum for the product of oxidation of hexaethylbenzene. This spectrum shows mainly a mixture of the mono- and di-amide (M. W. of the monoamide: 303 and the diamide: 360).

Fractions	Loss of
303—360	Mono and diamide, respectively
261—318	$—CH_2CO$
260—317	$—COCH_3$
246—303	$—NCOCH_3$
244	$2(—NHCOCH_3)$
245—302	$—NHCOCH_3$
234—291	$—CNCOCH_3$
232—289	$—COCH_3, C_2H_4$
220—277	$—CONHC—, C_2H_4$
217—274	$COCH_3, C_2C_4, CH_3$
216—273	$NHCOCH_3, C_2H_5$

2. Mass spectrum for the product of oxidation of 1-Phelyloctane.

Fractions	Loss of
232	$—CH_3$
220	$—NHCO$
218	$—C_2H_5$
217	$2(—CH_3)$
204	$—C_3H_7$
190	$—C_4H_9$
189	$—NHCOCH_3$
176	$—C_5H_{11}$
174	$—CH_3, NHCOCH_3$
162	C_6H_{13}
148	C_7H_{15}
135	$CH(C_7H_{15})$
90	$C_7H_{15}, NHCOCH_3$
77	$(—C_7H_{15})CHNHCOCH_3$

3. Mass spectrum for the product of oxidation of 1-phenylnonane.

Fractions	Loss of
246	$—CH_3$
231	$2(—CH_3)$
218	$—C_3H_7$
204	$—C_4H_9$
203	$—NHCOCH_3$
190	$—C_5H_{11}, —CHNCOCH_3$
176	$—C_6H_{13}$
162	$—C_7H_{15}$
148	$—C_8H_{17}$
135	$—CH(C_8H_{17})$
77	$—CH(C_8H_{17})NHCOCH_3$

4. Mass spectrum for the product of oxidation of n-propylbenzene.

Fractions (M.W.)	Loss of
162	$—CH_3$
148	$—C_2H_5$
147	$2(—CH_3)$
135	$—CHC_2H_5$
134	$—COCH_3$
119	$—NHCOCH_3$
106	$—CHNHCOCH_3$
105	$—C_2H_5, —COCH_3$
77	$CH(C_2H_5)NHCOCH_3$ or $NHCOCH_3, CHC_2H_5$

5. Mass spectrum for the product of oxidation of *tert*-butylbenzene.

Fractions (M.W.)	Loss of
176	$—CH_3$
161	$2(—CH_3)$
148	$—COCH_3$ or $—NHCO$
146	$3(—CH_3)$
133	$—NHCOCH_3$
119	$—CH_2NHCOCH_3$
107	$—CCH_2NHCOCH_3$
103	$—NHCOCH_3, 2(—CH_3)$
92	$—CCH_2NHCOCH_3, —CH_3$
77	$—CCH_2NCOCH_3, 2(—CH_3)$ or $—C(CH_3)_2CH_2NHCO\,CH_3$

REFERENCES

[1] L. Eberson and B. Oloffsson, *Acta Chem. Scand.*, **23**, 2355 (19699).
[2] M. Leug, J. Leung, J. Herz and H. M. Salzberg, *J. Org. Chem.*, **30**, 310 (1965).
[3] H. Lund, *Acta Chem. Scand.*, **11**, 1323 (1957).
[4] Y. D. Parker and R. N. Adams, *Tetrahedron Lett.*, 1721 (1969).
[5] R. Nyberg and A. Trojanek, *Coll. Czech, Chem., Comm.*, **40**, 526 (1975).
[6] M. Baizer, "Organic Electrochemistry", Dekker, New York 1973.
[7] A. Bewick, G. Edwards and J. Mellor, *Electrochim. Acta*, **21**, 1101 (1976).
[8] A. Bewick, G. Edwards and J. Mellor, *J. Chem. Soc. Perkins Trans.*, **2**, 1952 (1977).
[9] A. Bewick, J. M. Mellor and S. B. Pons, *Electrochim. Acta*, **25**, 931 (1980).
[10] R. Nicholson J. Shain, *Anal. Chem.*, **36**, 706 (1964).
[11] R. Nicholson and J. Shain, *Anal . Chem.*, **37**, 178 (1965).
[12] G. Alberts and J. Shain, *Anal. Chem.*, **35**, 1859 (1963).

Revue Roumaine de Chimie, **31**, 7, 719—726 (1986)

HYDRAZINE CARBOTHIOAMIDE-2-[(4-HYDROXY-3-METHOXY PHENYL) METHYLENE] AS A SENSITIVE REAGENT FOR RAPID SPECTROPHOTOMETRIC DETERMINATION OF PALLADIUM(II) AND COPPER(II): ANALYSIS OF ALLOYS AND MINERALS

K. N. THIMMAIAH *[a] and V. C. SEKHAR *
Department of Chemistry, The University of Texas at El Paso, El Paso, Texas
79968—0513 USA

Received September 2, 1985

Hydrazine carbothioamide-2-[(4-hydroxy-3-methoxy phenyl) methylene], (HCHMM), is proposed as a sensitive reagent for the rapid spectrophotometric determination of palladium(II) and copper(II). The reagent forms 1 : 2 yellow coloured complex with palladium(II) in hydrochloric acid — sodium acetate buffer medium and an orange yellow coloured complex with copper(II) in potassium dihydrogen phosphate — sodium hydroxide buffer medium instantaneously at room temperature. The palladium(II) — HCHMM complex has an absorption maximum at 368 nm with a molar absorptivity of 2.52×10^4 l mol^{-1} cm^{-1}. The copper(II) — HCHMM complex exhibits maximum absorbance at 410 nm with a molar absorptivity of 1.23×10^4 l mol^{-1} cm^{-1}. Beer's law is obeyed in the 0.04—2.4 ppm range for palladium(II) and in the 0.1—3.2 ppm range for copper(II) complexes. Molar excess of 38-fold and 45-fold of the reagent is required for palladium(II) and copper(II) respectively. The effects of pH, alkali, time, order of addition of reagents, temperature, reagent concentration and diverse ions are reported. These methods have been successfully used for the determination of palladium and copper in alloys and minerals.

INTRODUCTION

Hydrazine carbothioamide, 2-[(4-hydroxy-3-methoxyphenyl) methylene] (HCHMM) was used as a retarder for photographic emulsion, tuberculostatic,[2–4] and as antirheumatic agent.[5] Guha-Sircar et al.[6] have prepared HCHMM and used it as a reagent for the detection of a few metal ions. A survey of chemical literature has shown that no attempt has been made to use HCHMM as a spectrophotometric reagent for determination of palladium(II) or copper(II). The present investigation deals with the study of the colour reaction of HCHMM with palladium(II) and copper(II) for the rapid spectrophotometric determination of both palladium and copper.

---

[a] Visiting scholar (on leave) from University of Mysore, Mysore, India.

EXPERIMENTAL

Reagents and Equipment

Palladium(II) Solution

A stock solution of palladium(II) was prepared by dissolving about 1g of palladium(II) chloride (Johnson Mathey Chemicals Ltd.) in 1 Litre of 0.1M hydrochloric acid and standardised gravimetrically by the dimethylglyoximemethod. [7]

Copper(II) Solution

A stock solution of copper(II) was prepared by dissolving requisite amount of copper(II) chloride (analar) and standardised gravimetrically by the thiocyanate method[8].

HCHMM solution

HCHMM was prepared by the reaction of hydrazine carbothioamide with vanilline and purified by the recommended method.[9] A stock solution of 0.3% (m/v) HCHMM in 85% ethanol (v/v) was prepared.

Buffer Solutions

Solutions of hydrochloric acid — sodium acetate buffer (Walpole buffer), potassium dihydrogen phosphate — sodium hydroxide buffer (Britton and Walford buffer) and foreign ions of suitable concentrations were prepared by using analytical grade reagents. The Walpole buffer was prepared by mixing 50 mL of 1M sodium acetate solutions with 10—100 mL of 1M hydrochloric acid. This mixture was diluted to 250 mL to give solutions of pH 0.65—5.2. The Britton and Walford buffer was prepared by mixing 100 mL of 0.2N potassium dihydrogen phosphate with 5—100 mL of 0.2N sodium hydroxide to give solutions of pH 5.86—12.27.

Apparatus

A Beckman spectrophotometer model DB with matched 1 cm pathlength silica cells was used for absorbance measurements.

Recommended Procedure

Aliquots of the stock solutions containing 1—60 μg of palladium(II) or 2.5—80 μg of copper(II) were transferred into a series of 25 mL calibrated flasks. 5 mL of hydrochloric acid — sodium acetate buffer of pH 3.65 for paladium(II) or 5 mL of potassium dihydrogen phosphate — sodium acetate buffer of pH 11.98 for copper(II), 6 mL of doubly distilled ethanol and 4mL of 0.3% HCHMM solution were added to each flask and diluted to the mark with doubly distilled water. The solutions were thoroughly mixed and absorbance measurements at 368 nm for palladium(II) solutions and at 410 nm for copper(II) solutions were done against the corresponding reagent blank prepared similarly. The amount of palladium(II) or copper I(II) was then deduced from the standard calibration curve.

Determination of Copper in Brass, Bronze and Copper-Nickel Alloy

An accurately weighed amount of copper alloy (approximately 0.1 g) was transferred into a covered 50 mL beaker and treated with 3 mL of analar concentrated nitric acid. The solution was gently heated to dissolve the alloy and 6 mL of analar concentrated hydrochloric acid was carefully added in 2 mL portions. The solution was evaporated to dryness after each addition on a steam bath. The resulting residue was dissolved and diluted with doubly distilled water a 500 mL calibrated flask. Aliquots of this solution were used for reaction with HCHMM as described in the procedure for the determination of copper. Absorbance measurements were done at 410 nm and copper concentration read from the calibration graph. The relevent results are shown in Table 1.

Table 1

Determination of copper in its alloys

Sample	Certified Composition * %	Copper content of solution ppm	
		Certified value	Found**
Brass	Cu, 70.03 ; Zn, 29.97	0.5	0.51
		1.0	1.00
		1.5	1.49
		2.0	2.02
		3.0	3.04
Bronze	Cu, 89.62 : Sn, 1.38	1.0	0.99
		1.5	1.48
		2.0	2.01
		2.5	2.52
		3.0	2.97
Copper--Nickel Alloy	Cu, 74.85 ; Ni, 25.15	0.5	0.49
		1.0	1.01
		2.0	2.03
		2.5	2.48
		3.0	3.03

* Values provided by the suppliers of the samples

** Average value of five determinations on each solution

Determination of Palladium and Copper in Synthetic Mixtures Corresponding to Alloys and Minerals

Alloy samples of jewellery alloy (95.5% palladium and 4.5% ruthenium), palladium — gold (50% palladium), steel backed copper — lead automative bearings (2% copper, 8% tin and 90% lead), high tin babitts (8.5% copper, 87.5% tin and 4% antimony) and the minerals, stibiopalladinite (75% palladium and 25% antimony) and chalcopyrites (50% copper and 50% iron) were not available for analysis. Hence, synthetic mixtures containing the metal ions corresponding to the composition of alloys and minerals are prepared. The palladium and copper contents are determined by the procedures mentioned above and the results obtained are given in Table 2.

RESULTS AND DISCUSSION

HCHMM readily forms light yellow coloured complex with palladium(II) and an orange yellow coloured complex with copper(II) in hydrochloric acid, sulphuric acid, acetic acid, Walpole buffer or Britton and Walford buffer medium instantaneously at room temperature (27°C). The study of palladium — HCHMM complex in hydrochloric acid, sulphuric acid, acetic acid or Britton and Walford buffer medium, and copper — HCHMM complex in hydrochloric acid, sulphuric acid, acetic acid or Walpole buffer medium is not recommended because they are less stable ($<$ 5 min.) and least sensitive. Therefore, Walpole buffer medium for palladium — HCHMM complex and Britton and Walford buffer medium for copper — HCHMM complex are selected for further investigations. Maximum colouration takes place in the effective pH range 2.9 --4.1 and

9.3–11.6 for palladium – HCHMM complex and copper – HCHMM complex respectively. Outside these pH ranges maximum absorbance is not obtained. Hence all studies were confined to pH 3.55 and 11.2 for palladium – HCHMM and copper – HCHMM complexes respectively. The effective ethanolic concentration is found to be 24–52 % (v/v) for palladium – HCHMM complex and 24–64 % (v/v) for copper – HCHMM complex. Below these ranges turbidity is observed and above these ranges, maximum absorbance is not attained.

Table 2

Determination of palladium and copper in synthetic mixtures corresponding to alloys and minerals

Mixtures	Metal taken ppm			Metal ion added ppm					Metal found* ppm	
	Pd	Cu	Ru	Sb	Au	Sn	Fe	Pb	Pd	Cu
Jewellery alloy	0.50	—	0.023	—	—	—	—	—	0.49	—
	1.00	—	0.046	—	—	—	—	—	1.02	—
	1.50	—	0.069	—	—	—	—	—	1.50	—
	1.75	—	0.081	—	—	—	—	—	1.77	—
	2.00	—	0.092	—	—	—	—	—	2.02	—
Palladium-Gold-alloy	0.50	—	—	—	0.50	—	—	—	0.51	—
	1.00	—	—	—	1.00	—	—	—	1.00	—
	1.50	—	—	—	1.50	—	—	—	1.48	—
	2.00	—	—	—	2.00	—	—	—	1.97	—
	2.20	—	—	—	2.20	—	—	—	2.21	—
Steel backed copper-lead automative bearings	—	0.50	—	—	—	2.0	—	22.50	—	0.50
	—	1.00	—	—	—	4.0	—	45.00	—	1.02
	—	1.50	—	—	—	6.0	—	67.50	—	1.48
	—	2.00	—	—	—	8.0	—	90.00	—	2.02
	—	3.00	—	—	—	12.0	—	135.00	—	3.01
High tin babbits	—	1.00	—	0.50	—	10.75	—	—	—	0.99
	—	1.50	—	0.75	—	16.10	—	—	—	1.50
	—	2.00	—	1.00	—	21.50	—	—	—	2.02
	—	2.50	—	1.25	—	26.85	—	—	—	2.53
	—	3.00	—	1.50	—	32.15	—	—	—	3.01
Chalco-pyrites	—	0.50	—	—	—	—	0.50	—	—	0.50
	—	1.00	—	—	—	—	1.00	—	—	1.02
	—	2.00	—	—	—	—	2.00	—	—	2.02
	—	2.50	—	—	—	—	2.50	—	—	2.48
	—	3.00	—	—	—	—	3.00	—	—	3.02
Stibio-palladinite mineral	0.50	—	—	0.165	—	—	—	—	0.50	—
	1.00	—	—	0.330	—	—	—	—	1.02	—
	1.50	—	—	0.495	—	—	—	—	1.51	—
	2.00	—	—	0.660	—	—	—	—	1.98	—
	2.20	—	—	0.726	—	—	—	—	2.22	—

* Average of five determinations

Absorption Spectra

The absorption spectra of the palladium – HCHMM complex, copper – HCHMM complex, reagent blanks, palladium(II) and copper(II) solutions are shown in Fig. 1. The palladium – HCHMM complex (pH

3.55) exhibits maximum absorbance at 366—370 nm and copper — HCHMM complex (pH 11.2) at 408—412 nm. The absorption spectra of palladium (II) and copper (II) solutions and reagent blanks show little absorbance at these wavelengths. All subsequent studies were made at 368 nm and 410 nm for palladium — HCHMM complex and copper — HCHMM complex respectively.

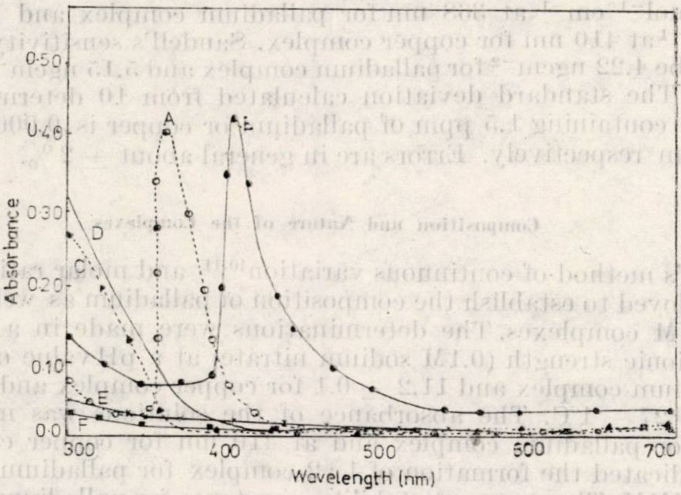

Fig. 1. — Absorption spectra of palladium(II) — HCHMM complex copper(II) — HCHMM complex, palladium(II) and copper(II) solutions, and, reagent blanks: A—Pd(II) — HCHMM complex, pH 3.55, [Pd(II)]=1.5 pp and [HCHMM]=3.99×10^{-2} M; B — Cu (II) — HCHMM complex, pH 11.2, [Cu(II)] = 1.5 ppm and [HCHMM]= 5.3×10^{-2} M; C — Reagent blank 3.99×10^{-2} M at pH 3.55; D—Reagent blank 5.3×10^{-2} M at pH 11.2; E—[Pd (II)]=1.5 ppm, pH 3.55 and F — [Cu (II)] = 1.5 ppm, pH 11.2.

Effect of Experimental Variables

Investigations on the variation of the absorbance, due to palladium — HCHMM complex and copper — HCHMM complex with the reagent concentration were carried out by measuring the absorbance of the solutions containing 1.5 μg/mL of palladium at 368 nm (pH 3.55) and solutions containing 1.5 μg/mL of copper (II) at 410 nm (pH 11.2) with varying amounts of HCHMM. A 38-fold molar excess of the reagent over palladium and a 45-fold molar excess of the reagent over copper were required for the full developement of the colour intensity.

The maximum absorbance is obtained instantaneously after mixing the reagents. The palladium (II) — HCHMM and copper(II) — HCHMM complexes are stable for 45 minutes and 75 minutes in the respective buffer media respectively. There is no appreciable change in the absorbance of the complexes if the order of addition of the reagents was varied. The absorbance values are not affected by temperature in the 4—55°C range for palladium complex and 7—47°C range for copper complex. At higher temperatures the absorbance gradually decreases.

Calibration Curve, Range and Sensitivity

Beer's law is valid over the concentration range 0.04 – 2.4 ppm for palladium complex and 0.1 – 3.2 ppm for copper complex. The optimum concentration range for effective spectrophotometric determination, evaluated by Ringbom's method is 0.2 – 2.3 ppm for palladium and 0.2 – 3.1 ppm for copper. The molar absorptivities were determined to be $2.52 \times \times 10^4$ L mol^{-1} cm^{-1} at 368 nm for palladium complex and 1.23×10^4L mol^{-1} cm^{-1} at 410 nm for copper complex. Sandell's sensitivity was determined to be 4.22 ngcm^{-2} for palladium complex and 5.15 ngcm^{-2} for copper complex. The standard deviation calculated from 10 determinations on a solution containing 1.5 ppm of palladium or copper is 0.0066 ppm and 0.0017 ppm respectively. Errors are in general about ± 2 %.

Composition and Nature of the Complexes

Job's method of continuous variation[10,11] and molar ratio[12] methods were employed to establish the composition of palladium as well as copper – HCHMM complexes. The determinations were made in a medium of constant ionic strength (0.1M sodium nitrate) at a pH value of 3.55 ±0.1 for palladium complex and 11.2 ± 0.1 for copper complex and at a temperature of 27 ± 1°C. The absorbance of the solutions was measured at 368 nm for palladium complex and at 410 nm for copper complex. The results indicated the formation of 1 : 2 complex for palladium and copper with HCHMM. The apparent stability constants for palladium and copper complexes were calculated from the absorbance data using mole ratio method. The log *K* value for palladium complex is found to be 6.55, whereas the copper complex has a log *K* value of 6.30.

The electrolytic nature of two complexes was found by ion – exchange experiments. When 25 mL of a 10^{-5} M solution of the palladium or copper complex was passed through Dowex 50 W – X8 cation exchange resin column (30 × 1.4 cm) the yellow colour was completely adsorbed and the eluent was colourless. When Dowex 1 – X8 anionic resin column was used, the eluent was yellow coloured, indicating that the complexes are cationic in nature.

Effect of Diverse Ions

In order to assess the analytical application of HCHMM complexes of palladium and copper, the effect of some foreign ions that often accompany palladium or copper is examined. For these studies different amounts of ionic species are added to the sample solution containing 37.5 μg of palladium(II) or copper(II) in 25 mL calibrated flasks and the colour is developed as outlined in the standard procedure. An error of ±2 % in the absorbance readings is considered tolerable. Many cations and anions do not interfere. Interference from platinum metals and iron can be reduced by using phosphate, fluoride and EDTA as masking agents. The interference due to silver(I) can be eliminated by removing it as silver chloride using sodium chloride (Table 3).

Table 3

Interference of foreign ions in the determination of palladium and copper

Ion added	Tolerance limit of ion ppm		Ion added	Tolerance limit of ion ppm	
	Determination of 1.5 ppm of Pd(II)	Determination of 1.5 ppm of Cu(II)		Determination of 1.5 ppm of Pd(II)	Determination of 1.5 ppm of Cu(II)
Cu (II)	0.1	—	Pd (II)	—	0.5
Cu (II)	3*	—	Pd (II)	—	2.0*
Zn (II)	690	20	Au (III)	4	5
Zn (II)	—	28**	U (VI)	75	30
Ba (II)	3600	10	Te(VI)	19	31
Ca(II)	2100	10	Sb (III)	10	6
Fe (III)	60	6	Zr (IV)	60	15
Fe (III)	—	24*	Bi (III)	12	6
Co (II)	920	0.5	Na (I)	5600	9400
Co (II)	—	4.0*	K (I)	8800	9200
Ni (II)	1200	0.5	Ti (IV)	2	1.5
Ni (II)	—	1.0*	Sn (II)	38	27
Al (III)	650	14	Sn (II)	—	52**
Al (III)	—	36**	Sn (IV)	48	32
As (III)	280	104	Sn (IV)	—	47**
Pb (II)	1600	24	Cr (IV)	12	1.5
Pb (II)	—	140*	SO_4^{2-}	2400	9000
Ag (I)	6	3	NO_3^-	8800	10400
Ag (I)	—	5*	PO_4^{3-}	2480	3600
Mn (II)	400	100	$S_2O_3^{2-}$	80	10400
Mg (II)	360	24	Oxalate	85	80
W (VI)	267	2500	Citrate	120	7200
Mo (VI)	20	80	Tartrate	210	7200
Ru (III)	1	1	EDTA	580	160
Ru (III)	—	3***	F^-	160	9000
Rh (III)	3	1	Cl^-	5600	9400
Rh (III)	—	3*	Br^-	8800	9200
Os (VI)	1	1	I^-	600	860
Os (VIII)	12	12	Acetate	80	10400
Ir (III)	4	13			
Ir (III)	8**	—			
Pt (IV)	2	2.5			
Pt (IV)	3*	—			

* EDTA
** Phosphate
*** Fluoride

HCHMM is more sensitive towards palladium as compared to 2-chlorophenothiazine,[13] phenyl urea,[14] diacetylmonoxime,[15] and 2,2′-diquinolylketoxime.[16] It is also a more sensitive reagent for copper than 3-thianaphthenoyl trifluoroacetone,[17] ferrozine,[18] 6-methyl-2-pyridyl-hydrazine[19] and acetoacetanilide[20] which can be used for copper determination.

CONCLUSIONS

The proposed methods could be used for the rapid spectrophotometric determination of palladium and copper in their alloys and minerals. The results shown in Table 1 indicate that zinc, tin and nickel present in the alloys of copper do not interfere in the estimation of copper.

REFERENCES

[1] K. Murobushi, K. Kawaguchi and E. Ashikawa, *J. Chem. Soc. Japan, Ind. Chem. Sect.*, **56,** 373 (1953).

[2] E. Hoggarth, A. R. Martin, N. E. Storey and E. H. P. Young, *Brit. J. Pharmacol.*, **4,** 248 (1949).

[3] R. Donovick, F. Pansy, G. Stryker and J. Bernstein *J. Bact.*, **59,** 667 (1950).

[4] J. Bernstein, H. L. Yale, K. Losee, M. Holsing, J. Martins and W. A. Lott, *J. Am. Chem. Soc.*, **73,** 906 (1951).

[5] S. Casadio and V. Casadio, *Ball. Chem. Farm.*, **91,** 138 (1952).

[5] S. S. Guha-Sircar and S. Satpathy, *J. Ind. Chem. Soc.*, **31,** 450 (1954).

[7] A. I. Vogel, "A Text-book of Quantitative Inorganic Analysis", Third Edition, The Elbs and Longmans, London, 1975, p. 512.

[8] A. I. Vogel, "A Text-book of Quantitative Inorganic Analysis", Third Edition, The Elbs & Longmans, London, 1975, p. 497.

[9] J. Bernstein, H. I. Yale, K. Losee, M. Holsing, J. Martins and W. A. Lott, *J. Am. Chem. Soc.*, **73,** 906 (1951).

[10] P. Job, *Justus Liebigs Ann. Chem.*, **9,** 113 (1928).

[11] H. Irving and T. B. Pierce, *J. Chem. Soc.*, 2565 (1959).

[12] J. H. Yoe and A. L. Jones, *Ind. Engng. Chem. Anal. Ed.*, **16,** 111 (1944).

[13] H. S. Gowda and K. N. Thimaiaj, *Z. Anal. Chem.*, **279,** 208 (1976).

[14] S. P. Patil and V. M. Shinde, *Mikrochim. Acta*, 853 (1974).

[15] P. K. Paria and S. K. Majumdat, *Z. Anal. Chem.*, **275,** 205 (1975).

[16] S. Stupavasky and W. J. Holland, *Mikrochim. Acta*, 122 (1972).

[17] J. R. Johnston and W. J. Holland, *ibid.*, 126 (1972).

[18] S. K. Kundra, M. Katyal and R. P. Singh, *Anal. Chem.*, **46,** 1605 (1974).

[19] L. L. Stookey, *Talanta*, **17,** 644 (1970).

[20] A. K. Sarkar and J. J. Das, *J. Ind. Chem. Soc.*, **48,** 817 (1971).

Revue Roumaine de Chimie, 31, 7, 727—735 (1986)

CARACTERÍSTICAS REOLÓGICAS DE LA CARBOXIMETILCELULOSA SÓDICA A BAJOS GRADIENTES DE VELOCIDAD. ESTUDIO ENERGÉTICO. INFLUENCIA DE LA ADICIÓN DE DEXTRANO

I. CAYRE, C. ARIAS y C. RUEDA
Departamento de Físico-Química y Técnicas Instrumentales, Facultad de Farmacia, Universidad Complutense, Ciudad Universitaria, 28040 Madrid, Spain

Recibido: el 3 de septiembre de 1984
Revisto: el 10 de febrero de 1986

These aqueous solutions are not particularly stable. They presented a tendency to associate and reached an equilibrium state after a certain time. The analyses presented in this study for C.M.C. solutions were based on the use of the Ellis model. The viscosity *vs.* low shear rate behaviour of the solutions was determined with a rotational viscometer. As will be shown, the critical characteristic of the rheological model includes the transition from newtonian behaviour. We also noted a wide range of conformational changes where different temperatures were applied to the system. The properties of the Na-CMC system were also investigated in the presence of dextran.

Debido a la tendencia que tienen estas sustancias a multimerizarse realizamos un análysis en función del tiempo. Basándonos en el modelo de Ellis [1] realizamos un estudio de la viscosidad a bajos gradientes de velocidad, comprobando que se produce un cambio en el comportamiento de la Carboximetilcelulosa sódica. Igualmente se han observado una serie de cambios conformacionales al ser sometida a diferentes temperaturas. Posteriormente vemos la influencia que puede tener en las propiedades de la Carboximetilcelulosa sódica la adición de dextrano.

INTORDUCCIÓN

La importancia que la Carboximetilcelulosa sódica tiene en la Industria Farmacéutica se ha puesto de manifiesto en numerosos estudios. [2]

Se ha publicado mucho sobre las propiedades de la Carboximetilcelulosa sódica pero tan solo de forma parcial, por lo que en este trabajo completamos algunos aspectos del estudio reológico.

Según Newman y colb.[3] este tipo de sustancias tienen gran tendencia a multimerizarse llevado a la formación de agregados de elevada masa molecular. Además la posibilidad de formación de estructuras helicoidales que se situarían paralelamente según el modele de Meyer y Misch,[4] favorece la formación de estructuras cristalinas estabilizadas por puente de hidrógeno, que serían similares a las obtenidas por Burchard y colb.[5] con poliolefinas isotácticas. Bouret [6] comenta en un trabajo similar con Agarosa, que la formación de dicha estructura helicoidal es un proceso lento.

Estudiando el modelo de Ellis, comentado por Duda y colb[1]., basado en el comportamiento que tienen las macromoléculas a bajos gradientes de velocidad, vemos que a inferiores de $10s^{-1}$ existe un comportamiento newtoniano, produciéndose una transición a no-newtoniano a velocidades más elevadas. En nuestro trabajo revisamos estos aspectos y los relacionamos con el estudio energético de las mismas.

METODOLOGÍA

El aparato de medida utilizado es el Rheomat 15 que dispone de gradientes de velocidad comprendidos entre $1{,}262s^{-1}$ y — $702{,}3s^{-1}$, trabajando nosotros entre $2{,}180\ s^{-1}$ y $702{,}3\ s^{-1}$.

Las disoluciones de Carboximetilcelulosa sódica se llevan a cabo en tampón AcH/AcNa a pH = 4 con un valor de fuerza iónica $\mu = 0{,}5725$ y con tres concentraciones diferentes: 2 %, 3 %, 4 %. Las medidas se realizan a siete temperaturas diferentes entre 26°C y 55°C y a un tiempo de 24 horas.

La adición de dextrano se realiza según las siguientes relaciones de [Na—CMC]/[Dextrano] iguales a 1,17, 1,56, 12,5 manteniendo constante en todas ellas la concentración de Carboximetilcelulosa sódica al 4 %.

RESULTADOS Y DISCUSIÓN

Para realizar un estudio del tiempo en función de la concentración y del gradiente de velocidad, se presentan las curvas reológicas (fig. 1) obtenidas para una concentración de Na—CMC de 2 % a diferentes tiem-

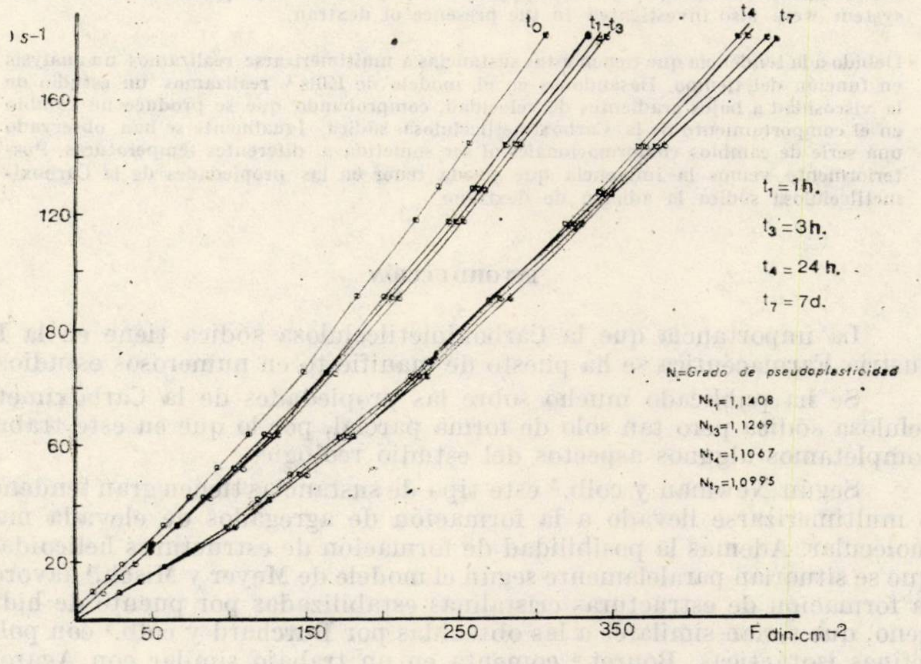

Fig. 1. — Curvas reológicas de la Na—CMC al 2 % para diferentes tiempos. $T = 26°C$

pos. Estas curvas características de un flujo pseudoplástico se ajustan a la ecuación de Ostwald [7]:

$$F^N = \eta' \frac{dv}{dx}$$

siendo F la fuerza de cizalla, η' el coeficiente de viscosidad aparente y dv/dx el gradiente de velocidad D (s^{-1}). Donde $N > 1$, el número estructural, indica el grado de pseudoplasticidad (los valores de N se indican en la figura 1).

Observamos una evolución lenta, ya que inicialmente la solución se mantiene estable durante un período de 3 horas, determinándose un tiempo de equilibrio final de 24 horas. De igual manera suceda para una concentración del 4 %, como corresponde a soluciones que tienen gran tendencia a multimerizarse. Utilizando otros métodos de trabajo, Kunh y colb.[8] determinan para el mismo compuesto un tiempo de equilibrio entre 30 a 50 horas.

Inicialmente existe un período de latencia de 180 min. (3 horas) a partir del cual se produce un aumento de la viscosidad. Este aumento se atribuye al período correspondiente a la formación de estructuras helicoidales según el modelo de Meyer y Misch citado por Ellis y Warwicken[4].

El tiempo de equilibrio o tiempo que necesitarían las soluciones para estabilizarse correspondería a la formación deagregados de unidades helicoidales paralelas, estabilizadas — por puente de hidrógeno entre los grupos hidroxilo intramoleculares responsables de la estabilización de la estructura.[9] Este tiempo ha sido fijado en 24 horas y es independiente de la concentración así como del gradiente de velocidad utilizado, como se observa en la citada gráfica.

Realizando un estudio de la viscosidad en función del gradiente de velocidad (fig. 2) observamos una disiminución de este parámetro al aumentar el gradiente. La solución inicial, hasta aproximadamente el tiempo dado para la formacón de la estructura helicoidal, presenta un comportamiento pseudoplástico clásico. A tiempos superiores a 180 min., la solución de concentración 2 % a partir de un gradiente de velocidad de 5,5 s^{-1} tiene un ligero aumento de la viscosidad, que puede explicarse como un espesamiento del medio como consecuencia de un fenómeno de asociación de hélices.

En consecuencia el estudio reológico se ha efectuado al tiempo de equilibrio, es decir, a las 24 horas para evitar en lo posible la influencia de la variable tiempo.

Para la concentración del 4 % (fig. 3) se observa un comportamiento típicamente pseudoplástico, mientas que para la del 2 % y 3 % esta conducta está ligada al gradiente de velocidad y para los inferiores a 6 s^{-1} se produce en ambas una disminución de la viscosidad. A continuación obtenemos una zona comprendida entre 6—28 s^{-1} en la cual la solución adopta un comportamiento newtoniano que coincide con el modelo de Ellis presentado por Duda y colb.[1] Una explicación de este comportamiento radicaría en que en estas condiciones el número de grupos hidroxilo es menor está menos fevorecida la formación de enlaces de hidrógeno intramoleculares

Fig. 2. — Curvas de viscosidad de la Na—CMC al 2 % para diferentes tiempos. $T = 26°C$.

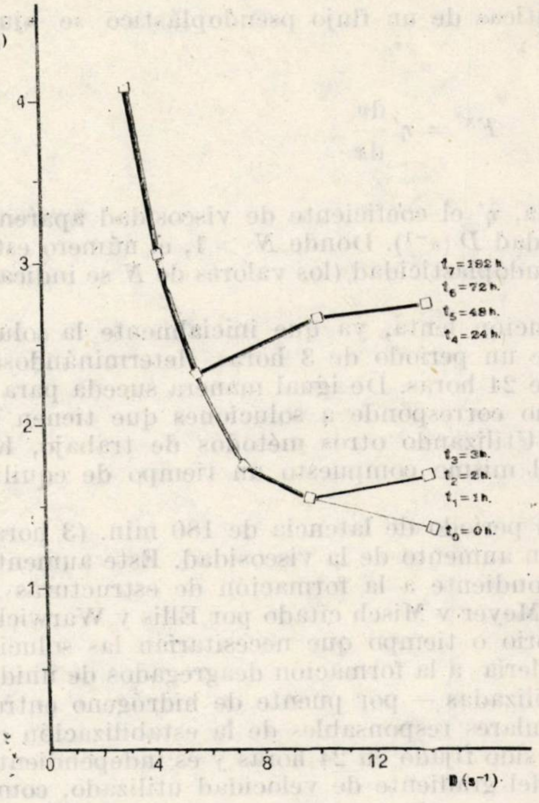

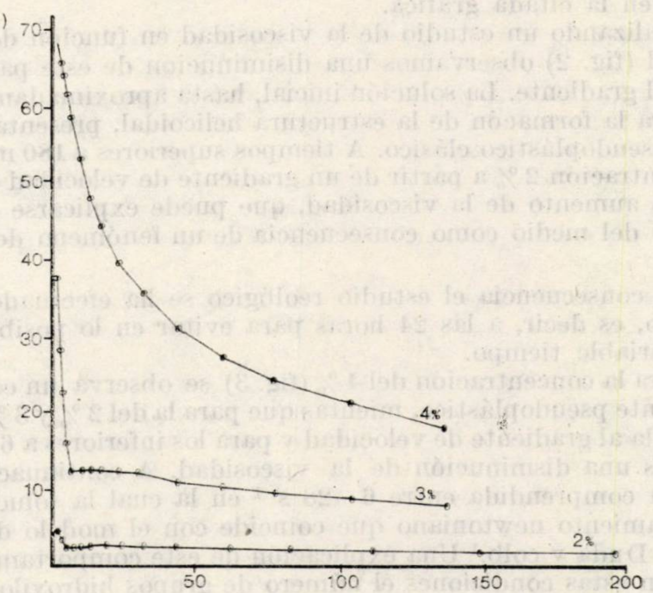

Fig. 3.—Curves de viscosidad de la Na—CMC al tiempo de equilibrio $T = 26°C$.

y asociaciones. Para gradientes de velocidad superiores a $28 s^{-1}$ se observa una ligerísima disminución de la viscosidad, siendo menos acentuada a la concentración del 2 %, por lo que pensamos que a concentraciones muy diluidas se obtenga un comportamiento newtoniano.

El carácter tixotrópico de estas sluciones nos indica la rotura o formación de puente de hidrógeno que conlleva a una destrucción o recuperación de la estructura macromolecular, siendo máas acentuado a la concentración del 4 % y prácticamente despreciable a la del 2 %. Mediante este resultado podemos afirmar la influencia de la concentración en el grado de tixotropía, aumentando el área de la curva de histéresis con la concentración.

Es de especial interés el estudio de la temperatura debido a que pequeñas diferencias de ésta van a reflejarse en los valores de viscosidad, pudiendo sufrir las macromoléculas en solución como consecuencia del aumento de agitación térmica cambios estructurales, que afectan a sus propiedades principales. Para ello realizamos un estudio reológico de las diferentes concentraciones a las temperaturas de 26°C, 31°C, 35°C, 40°C, 45°C, 50°C y 55°C, observándose en general una disminución de la viscosidad de estas soluciones y del carácter pseudoplástico con la temperatura (fig. 4).

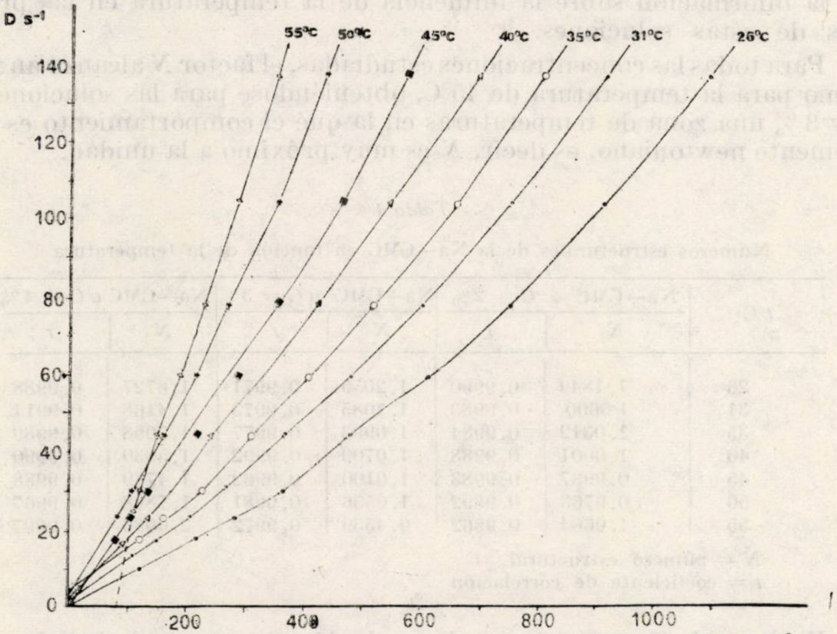

Fig. 4. — Curvas reológicas de la Na—CMC al 3 % a diferentes temperaturas.

Para la concentración del 4 % a 50°C y 55°C y para la del 3 % a 55°C se observa un cambio de comportamiento, presentando a estas temperaturas propiedades plásticas propias de un cuerpo de Bingham para la concentración del 3 % o de Casson en la del 4 %. Una explicación a este cambio producido la dan Saunders y colb.,[10] que consideran que el aumento del movimiento browniano, como consecuencia de la elevación de la temperatura, produce una rotura de los diferentes agregados que constituyen el sistema macromolecular, formándose así un mayor número de partículas. Si seguimos elevando la temperatura, la distancia entre la superficie de éstas se reduciría y existirá la posibilidad de formación de enlaces entre ellas, obteniéndose una estructura rígida tipo sólido, que explicaría este carácter plástico. A mayor concentración, el número de partículas será más elevado y en consecuencia es de esperar que el carácter de cuerpo de Bingham corresponda a una temperatura menor. La fuerza umbral o esfuerzo cortante determinado ha sido de $f_0 = 80$ dinas. cm^{-2}. El carácter plástico o la rigidez del sistema aumenta con la temperatura y a 55°C la fuerza umbral es de $f_0 = 200$ dinas. cm^{-2}. La igualdad de este parámetro a diferentes concentraciones, pensamos que debe corresponder a la red tridimensional rígida más pequeña que puede formarse para la Carboximetilcelulosa sódica y no ser función de la concentración.

El análisis de los números estructurales N en función de la temperatura calculados a partir de la ecuación de Ostwald [7] (tabla 1), por el método de regresión lineal a partir de las pendientes de las curvas log $D = f$ (log F) con buenos coeficientes de correlación r, nos permite ampliar la información sobre la influencia de la temperatura en las propiedades de estas soluciones.

Para todas las concentraciones estudiadas, el factor N alcanza un valor mínimo para la temperatura de 45°C, obteniéndose para las soluciones del 2 % y 3 % una zona de temperaturas en la que el comportamiento es aparentemente newtoniano, es decir, N es muy próximo a la unidad.

Tabla 1

Números estructurales de la Na—CMC en función de la temperatura

t°C	Na—CMC a $C = 2\%$		Na—CMC $a\ C = 3\%$		Na—CMC $a\ C = 4\%$	
	N	r	N	r	N	r
26	1,1849	0,9990	1,2059	0,9971	1,6727	0,9988
31	1'0600	0,9983	1,1085	0,9973	1,4168	0,9914
35	1,0312	0,9984	1,0993	0,9977	1,7098	0,9989
40	1,0001	0,9988	1,0709	0,9992	1,5330	0,9990
45	0,9987	0,9983	1,0100	0,9962	1,4769	0,9988
50	0,9763	0,9892	1,0556	0,9981	1,7898	0,9967
55	1,0664	0,9962	0,4539	0,9972	2,0086	0,9997

N = número estructural
r = coeficiente de correlación

En la tabla 2, presentamos la evolución de estas propiedades a las concentraciones y temperaturas estudiadas. A temperaturas inferiores a 40°C todas las soluciones presentan un carácter pseudoplástico $N > 1$, mientras que a superiores a 50°C se observa una cierta tendencia hacia un comportamiento de plástico puro o de Casson. En la zona de transición entre ambas propiedades se observa un comportamiento aparentemente newtoniano $N \simeq 1$.

Determinamos la existencia de una temperatura de 45°C en la que la agitación térmica es lo suficientemente elevada para producir un máximo grado de rotura en la macromolécula, obteniéndose el mayor número de partículas posibles. Estos fragmentos macromoleculares tendrán forma esferoidal, dado el comportamiento aparentemente newtoniano de estas soluciones. El aumento de la temperatura, aumenta el movimiento browniano de las moléculas elevándose la frecuencia del número de choques entre las partículas formadas, estableciéndose la posibilidad de nuevos enlaces entre ellas, que para concentraciones superiores al 2 % evolucionan a la formación de una estructura rígida que explica el comportamiento plástico.

Tabla 2

Evolución del comportamiento reológico de las soluciones de Na—CMC en función de la concentración y de la temperatura

T°C	$C = 2\%$	$C = 3\%$	$C = 4\%$
26°C	Pseudoplástico	Pseudoplástico	Pseudoplástico
31°C			
35°C			
40°C	Aparentemente Newtoniano		
45°C		Apartemente Newtoniano	
50°C	Pseudoplástico	Cuerpo de Bingham-Casson	Duerpo de Bingham-Casson
55°C			

El número de fragmentos moleculares a la temperatura de 45°C será para al concentración del 4 % superior a las anteriores, aumentando las posibilidades de agregación con el gradiente de velocidad, que traduce la ausencia de un comportamiento newtoniano.

Basándonos en la ecuación de Eyring [11] y para bajos gradientes de velocidad de acuerdo con las condiciones de la citada teoría, se lleva a cabo un estudio energético mediante el cálculo de las entalpías y entropías de activación. Los valores obtenidos se muestran en la tabla 3 y se puede ver que los resultados de ΔH^* son todos positivos lo cual es característico de un sistema endotérmico y propio de un medio líquido. Existe una elevación de la energía de activación al aumentar la concentración, que puede explicarse como un aumento de las fuerzas de interacción entre las macromoléculas. Por otro lado, los valores de B igualmente aumentan con la concentración loque indicaría un restablecimiento del orden del sistema, es decir, una disminución de los valores de entropía de activación con la concentración. Ambos resultados son perfectamente compatibles con le evolución presentada en general por nuestras soluciones, de un comportamiento pseudoplástico a plástico sea cuerpo de Bingham o Casson.

La influencia del Dextrano se analiza a partir de las curvas de histéresis (fig. 5), observándose que la adición de éste disminuye la viscosidad de la Carboximetilcelulosa sódica. Para les relaciones de concentración

Tabla 3

Entalpías y entropías de activiación para este proceso

Concentraciones	*B*	ΔH^* *en calorías*	*r*
Na—CMC a $C = 2\%$	$-5,1483$	7624, 003	0, 9979
Na—CMC a $C = 3\%$	$-4,7102$	7902, 388	0, 9953
Na—CMC a $C = 4\%$	$-4,4254$	8348, 217	0, 9954

B = factor entrópico
ΔH^* = variación entálpica del proceso
r = coefficiente de correlación

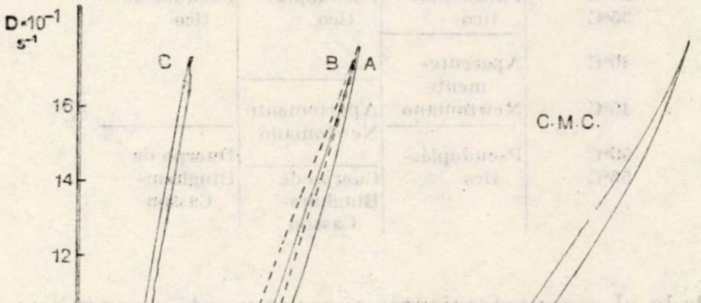

Fig. 5. — Bucles de histéresis de las mezclas de Na—CMC al 4% con diferentes concentraciones de Dextrano. $T = 26°C$. C.M.C. — bucle correspondiente a la Na—CMC, A = bucle correspondiente a [Na—CMC]/[Dextrano] = 12, 5, B = bucle correspondiente a [Na—CMC]/[Dextrano] = 1, 56, C = bucle correspondiente a [Na—CMC]/[Dextrano] = 1, 17.

de 12,5 y 1,56, se ve un comportamiento pseudoplástico similar al de la Carboximetilcelulosa sódica, aunque la consistencia del medio es inferior. Para [Na—CMC]/[Dextrano] = 1,56 hay un grado de tixotropía más elevado que en los otros casos, indicando la rotura o formación de nuevas estructuras, aspecto que queda confirmado al obtener para [Na—CMC]/[Dextrano] = 1,17 un cambio en el comportamiento reológico de estas soluciones. Aspecto confirmado mediante el cálculo de los números estructurales (tabla 4). La Carboximetilcelulosa sódica tiene un valor de $N = 1,672$ y la adición de Dextrano disminuye este valor hasta parala concentración más alta de las utilizadas, donde se obtiene un número calaremente inferior a la unidad $N = 0,7831$. Esto indicaría una inversión del comportamiento pseudoplástico, lo que lleva a pensar que a esta concentración se produce una pseudodilatación como consecuencia de un predominio de la estructura del Dextrano sobre la de la Carboximetilcelulosa sódica. Este comportamiento reológico es de suponer se mantendría para las concentraciones superiores de Dextrano.

Tabla 4

Números estructurales de las mezclas de Na—CMC y Dextrano

Concentrationes		*B*	*N*	*r*
Na—CMC al 4% + + Dextrano al	3,42%	—0,0397	0,7831	0,9966
Na—CMC al 3% + Dextrano + Dextrano al	2,56%	—1,5548	1,1886	0,9969
Na—CMC al 2% + + Dextrano al	0,32%	—1,6769	1,2224	0,9965

B = factor entrópico
N = número estructural
r = coeficiente de correlación

BIBLIOGRAFÍA

[1] J. L. Duda y colb., *Ind. Eng. Chem., Fundam.*, **22**, 299 (1983).
[2] J. Izutsu y colb., *J. Texture Stud.*, **12**, 259 (1981).
[3] S. Newman, W. R. Krigbaum y D. K. Carpenter, *J. Phys. Chem.*, **60**, 648, (1956).
[4] K. C. Ellis y J. O. Warwicken, *J. Polymer. Sci.*, **56**, 339 (1962).
[5] W. Burchard, y E. Husemann, *Makromol Chem.*, **44—46**, 358, (1971).
[5] E. Bourret y L. Bardet, *Inter. J. of Pharm.*, **9**, 81, (1981).
[7] L. Bardet, "Eléments de Calcul Statistique et de Physique —Appliquée", Ed. U. Montpellier I, 1982.
[8] W. Kunh y colb., *Helv. Chim. Acta*, **44**, 770, (1961).
[9] J. Mann y H. J. Marrinan, *J. Polym., Sci.*, **32**, 357, (1958).
[10] F. L. Saunders, J. Col. Int. Sci., **23**, 230 (1967).
[11] M. Alain, F. Pharmacie. These Universite de Montpellier I, (1973).

Revue Roumaine de Chimie, **31**, 7, 737 (1986)

COMPTES RENDUS

'Polymer Membranes" (Advance in Polymer Science, vol. 64) Springer, Berlin, 1985, 155 pages, 98 DM (hard-cover).

This volume containes three contributions.

"Polymeric Monolayers and Liposomes as Models for Biomembranes" is the first article written by H. Bader, K. Dorn, B. Hupfer and H. Ringsdorf. The chemical understanding of membrane structures has been obtained through the investigation of models, most of which are based on the reconstruction of the lipid bilayer part. The synthetic biomembranes are not stable in time in contrast to natural membranes. This article deals with the stabilization of membrane model systems. The desired biological functionalization of these stabilized polymeric membranes is possible *via* incorporation of proteins. Cell-cell recognition can be mimicked with polymeric vesicles carring sugar headgroups.

"Polyamides as Barrier Materials" written by H. Sumimoto and K. Hashimoto, the next paper in the volume, presents various polyamides and their analogues as barrier materials for membranes. It is important for the molecular design, as the authors emphasize, to take into account the balance and distribution of hydrophilic and hydrophobic microdomains as well as the stiffness and flexibility of a macromolecule, in order to place the subject on the fundamental understanding of the interactions among solvents, solutes and macromolecules.

"Membranes with Non-Homogeneous Sorption and Transport Properties" written by J. H. Petropoulos is the last review. Inhomogeneities at the microscopic level affect sorption and transport properties. This is exemplified by dual mode gas sorption and diffusion in glassy polymers. Non-homogeneity at the microscopic level is exemplified by the gas permeability of composite membranes. Finally, membranes exhibiting macroscopically nonhomogeneous sorption and diffusion properties are considered. These properties are characterized by means of transient-state measurements.

The articles are highly readable and presented systematically; attention is drawn on the understanding of the basic phenomena. Like all the other volumes in the series "Advances in Polymer Science" edited by the Springer Verlag, this book is excellently printed. It is a main source of fundamental knowledge of synthetic membranes design and transport properties

Ursula Bologa

"Actinides — Chemistry and Physical Properties" (Structure and Bonding, vol. 59/60), Springer, Berlin, 1985, 164 DM (hard-cover).

This volume attempts to give an overview of the up-to-date information available on the solid state physics of actinides. It contains six chapters:

i) "Actinide Solids: 5*f* Dependence of Physical Properties" by J. M. Fournier and L. Manes;

ii) "The Preparation of High Purity Actinide Metals and Compunds", by W. Müller and J. —C. Spirlet;

iii) "Structural and Thermodynamic Properties of Actinide Solids and Their Relation to Bonding" by L. Manes and U. Benedict;

iv) "Magnetic Properties of Actinide Solide" by J. M. Fournier;

v) "Localization and Hybridization of 5*f* States in the Metallic and Ionic Bond as Investigated by Photoelectron Spectroscopy" by J. R. Naegele and J. Ghijsen:

vi) "The Theory of 5*f* Bonding in Actinide Solids" by M. S. S. Brooks.

The aim of the book is not to be comprehensive in all aspects but to present a coherent picture of the chemistry and physical properties of actinides. In the general introduction of the volume attention is focused on the organization of the material.

It is the merit of the editor to publish in one volume articles concerned with actinide chemistry and their physical properties which are explained by the specific electronic structure. The reader, if (s)he is a beginner in this research field, is able to get a very fast understanding of the basic aspects of these 5*f* transition metals. Specialists will find out developments of actinide chemistry. The authors are authorities, with long experience in this field. Tables, diagrams and figures are drawn clearly. Suggestive illustrations of the crystalline actinide compounds are given in each paper.

Ursula Bologa

Revue Roumaine de Chimie, 31, 7, 787 (1986)

COMPTES RENDUS

"Polymer Membranes" (Advances in Polymer Science, vol. 64) Springer, Berlin, 1985, 156 pages, 88 DM (hard-cover).

This volume contains three contributions.

"Polymeric Monolayers and Liposomes as Models for Biomembranes" is the first article written by H. Bader, K. Dorn, B. Hupfer and H. Ringsdorf. The chemical understanding of membrane structures has been obtained through the investigation of models, most of which are based on the reconstruction of the lipid bilayer part. The synthetic biomembranes are not stable in time in contrast to natural membranes. This article deals with the stabilization of membrane model systems. The desired biological functionalization of these stabilized polymeric membranes is possible via incorporation of proteins. Cell-cell recognition can be mimicked with polymeric vesicles carrying sugar head groups.

"Polyamides as Barrier Materials" written by H. Sumimoto and K. Hashimoto, the next paper in the volume, presents various polyamides and their analogues as barrier materials for membranes. It is important for the molecular design, as the authors emphasize, to take into account the balance and distribution of hydrophilic and hydrophobic microdomains as well as the stiffness and flexibility of a macromolecule in order to place the subject on the fundamental understanding of the interactions among solvents, solutes and macromolecules.

"Membranes with Non-Homogeneous Sorption and Transport Properties" written by J. G. Petropoulos is the last review. Inhomogeneities at the microscopic level affect sorption and transport properties. This is exemplified by dual mode gas sorption and diffusion in glassy polymers. Non-homogeneity at the macroscopic level is exemplified by the gas permeability of composite membranes. Finally, membranes exhibiting macroscopically nonhomogeneous sorption and diffusion properties are considered. These properties are characterized by means of transient-state measurements.

The articles are highly readable and presented systematically; attention is drawn on the understanding of the basic phenomena. Like all the other volumes in the series "Advances in Polymer Science" edited by the Springer Verlag, this book is excellently printed. It is a major source of fundamental knowledge of synthetic membranes' design and transport properties.

Ursula Bologa

"Actinides — Chemistry and Physical Properties" (Structure and Bonding, vol. 59/60), Springer, Berlin, 1985, 164 DM (hard-cover).

This volume attempts to give an overview of the up-to-date information available on the solid state physics of actinides. It contains six chapters:

i) "Actinide Solids: 5f Dependence of Physical Properties" by J. M. Fournier and L. Manes;

ii) "The Preparation of High Purity Actinide Metals and Compounds", by W. Müller and J. C. Spirlet;

iii) "Structural and Thermodynamic Properties of Actinide Solids and Their Relation to Bonding" by L. Manes and U. Benedict;

iv) "Magnetic Properties of Actinide Solids" by J. M. Fournier;

v) "Localization and Hybridization of 5f States in the Metallic and Ionic Bond as Investigated by Photoelectron Spectroscopy" by J. R. Naegele and J. Ghijsen;

vi) "The Theory of 5f Bonding in Actinide Solids" by M. S. S. Brooks.

The aim of the book is not to be comprehensive in all aspects but to present a coherent picture of the chemistry and physical properties of actinides. In the general introduction of the volume attention is focused on the organization of the material.

It is the merit of the editor to publish in one volume articles concerned with actinide chemistry and their physical properties which are explained by the specific electronic structure. The reader, if (s)he is a beginner in this research field, is able to get a very fast understanding of the basic aspects of these 5f transition metals. Specialists will find out developments of actinide chemistry. The authors are authorities, with long experience in this field. Tables, diagrams and figures are drawn clearly. Suggestive illustrations of the crystalline actinide compounds are given in each paper.

Ursula Bologa

NOTE POUR LES AUTEURS

La Revue Roumaine de Chimie publie des articles en anglais, français, russe, allemand ou espagnol. Les auteurs sont priés d'envoyer des articles et des comptes rendus inédits.

Les manuscrits seront dactylographiés à double interligne. La bibliographie, les tableaux et la légende des figures seront placés après le texte.

Si l'article fait partie d'une série numérotée, la partie précédente sera donnée comme première référence.

Chaque article sera précédé d'un résumé comprenant quinze lignes au maximum.

Les références bibliographiques dans le texte seront faites par des exposants sans parenthèses et paraîtront à la fin de l'ouvrage.

Les publications périodiques mentionnées dans la bibliographie seront présentées suivant les prescriptions internationales : le nom de l'auteur précédé de l'initiale du prénom, le titre du périodique abrégé conformément à « Chemical Abstracts » et souligné par une ligne, le numéro du tome indiqué par des chiffres arabes et souligné par deux lignes, suivi de la première page de l'article : à la fin, l'année de la parution sera placée entre parenthèses. Le numéro de la revue ne sera pas indiqué si les pages du volume sont numérotées consécutivement.

Les textes des livres ou traités incluront : le nom des auteurs, précédés de l'initiale du prénom, le titre du livre entre guillemets et sans être souligné le numéro du tome précédé par l'abréviation « vol. » (ou « Bd. »), le numéro de l'édition, les éditions (the publisher), la localité de la parution du livre, l'année de la parution et la page de la référence précédée (s) par l'abréviation « p » (ou « S »).

Les brevets seront indiqués comme suit : l'auteur ou la firme, le pays et le numéro du brevet, la date de la revue *(Chem. Abstr.)*. Par. ex. : M. Jones (to Union Carbide Co.). Brit. Pat. 610 238, 2 Sept. 1959 ; *cf. Chem. Abstr.*, **54**, 12808 (1960).

Si la référence n'a pas été lue en original, on indiquera aussi la revue de références consultée.

Les diagrammes seront tracés à l'encre de Chine sur papier calque. Les tableaux et les figures (en nombre strictement nécessaire), ainsi que les courbes dans les figures seront numérotés par des chiffres arabes. Leur explication sera donnée dans la légende des figures. Prière de ne pas inscrire les mêmes données dans les tableaux et les figures. Chaque tableau aura un titre. On indiquera dans le texte la place approximative des tableaux et des figures. Les formules chimiques seront incluses dans le texte ; en outre, elles seront transcrites sur papier-calque, à l'encre de Chine.

Les auteurs sont priés d'indiquer les caractères italiques (en soulignant les lettres au crayon), ainsi que toute autre caractère spécial : les préfixes *ortho, meta, para, cis, trans.* etc. seront soulignés pour indiquer leurs caractères italiques, et ne seront jamais écrits avec des majuscules.

Aucune correction à la main ne sera admise sur le manuscrit. Les corrections seront frappées à la machine. Les lettres grecques ou d'autres symboles spéciaux seront insérés à la main à l'encre clairement.

Le manuscrit sera signé par l'auteur.

Le titre courant aura 50 lettres au maximum.

L'entière responsabilité du contenu des articles appartient aux auteurs.

Sur demande on peut obtenir une note plus complète .

PRINTED IN ROMANIA

TRAVAUX PARUS AUX ÉDITIONS DE L'ACADÉMIE DE LA RÉPUBLIQUE SOCIALISTE DE ROUMANIE

T. ONCESCU, S. G. IONESCU, **Conversie fotochimică şi stocare de energie solară**, 1985, 272 p.

V. DRĂGUŢAN, A. T. BALABAN, M. DIMONIE, **Olefin Metathesis and Ring-Opening Polymerization of Cyclo-Olefins**, coédition avec John Wiley and Sons, 1985, 544 p.

C. LITEANU, I. RÎCA, **Optimizarea proceselor analitice**, 1985, 360 p.

N. PERESCU, **Chimia extracţiei cu solvenţi şi aplicaţii**, 1985, 212 p.

V. E. SAHINI, M. HILLEBRAND, **Chimie cuantică în exemple şi aplicaţii**, 1985, 378 p.

GH. MARCU, **Chimia compuşilor coordinativi**, 1984, 415 p.

E. CORDOŞ, C. MANOLIU, **Spectrometria de absorbţie şi fluorescenţă atomică**, 1984, 178 p.

C. BODEA, **Tratat de biochime vegetală**, p. II, vol. 5, 1984, 438 p.

ELENA CEAUŞESCU, **Cercetări în chimia şi tehnologia polimerilor**, 1983, 519 p.

N. ASANDEI, A. GRIGORIU, **Chimia şi structura fibrelor**, 1983, 395 p.

N. IONESCU, M. CĂLDĂRARU, **Oxidarea catalitică a olefinelor inferioare**, 1983, 178 p.

C. CAŞCAVAL, **Studiul polimerilor prin piroliză şi cromatografie de gaze**, 1983, 220 p.

C. I. SIMIONESCU, F. DANEŞ, **Originea vieţii**, 1983, 110 p.

C. BODEA (sous la direction), **Tratat de biochimie vegetală**, 2 partie, t. IV, 1982, 408 p.

I. G. MURGULESCU, RODICA VÎLCU, **Introducere în chimia fizică. Vol. III, Termodinamica chimică**, 1982, 624 p.

I. G. MURGULESCU, J. PĂUN, **Introducerea în chimia fizică. Vol. I, 3. Nucleul atomic, reacţii nucleare, particule elementare**, 1982, 606 p.

ELENA CEAUŞESCU, **Noi cercetări în domeniul compuşilor macromoleculari**, 1981, 536 p.

I. G. MURGULESCU, TATIANA, ONCESCU, E. SEGAL, **Introducere în chimia fizică. Vol. II. 2. Cinematică chimică şi cataliză**, 1981, 1024 p.

LYDIA-MARIA VAICUM, **Epurarea apelor uzate cu nămol activ. Bazele biochimice**, 1981, 218 p.

I. GĂLĂŢEANU, **Procese şi metode radiochimice în energetica nucleară**, 1981, 234 p.

O. IORDACHE, **Procese polistocastice aplicate la fenomenele de transfer**, 1981, 186 p.

CR. SIMIONESCU, VALERIA GORDUZA, **Polimeri biocompatibili şi biologic activi**, 1980, 479 p.

ELENA CEAUŞESCU, **Polimerizarea stereospecifică a izoprenului**, 1979, 307 p.

C. GH. MACAROVICI, **Analiza chimică cantitativă anorganică**, 1979, 457 p.

M. FLORESCU, **Metode ştiinţifice în dezvoltarea industriei chimice moderne**, 1979, 256 p.

A. T. BALABAN, I. GĂLĂŢEANU, G. GEORGESCU, LIGIA SIMIONESCU, **Compuşi, marcaţi şi radiofarmaceutici cu aplicaţii în medicina nucleară**, 1979, 495 p.

I. G. MURGULESCU, E. SEGAL, **Introducere în chimia fizică. Vol. II, 1. Teoria molecular-cinetică a materiei**, 1979, 1036 p.

S. STERNBERG, FL. DANEŞ, **Termodinamica chimică aplicată**, 1978, 400 p.

I. G. MURGULESCU, V. EM. SAHINI, **Introducere în chimia fizică. Vol. I. 2. Structura şi proprietăţile moleculelor**, 1978, 604 p.

I. ZUGRĂVESCU, MAGDA PETROVANU, **N-ylid chemistry**, coédition avec McGraw-Hill International Book Company, U.S.A., 1977, 396 p.

I. G. MURGULESCU, **Introducere în chimia fizică. Vol. I. 1. Atomi, molecule, legătură chimică**, 1976, 560 p.

ELENA CEAUŞESCU, **Research work on synthesis and characterization of macromolecular compounds. Contributions**, 1974, 251 p.

CR. SIMIONESCU, VIORICA RUSAN, V. POPA, **Chimia algelor marine**, 1974, 212 p. 1 pl.

ISSN 0035–3930

1986 JUL 29

I.P. INFORMAŢIA, c. 2219

43 426

Lei 40

$ 80 (pour un abonnement annuel)

C.C. F 1103 04

ACADÉMIE DE LA RÉPUBLIQUE SOCIALISTE DE ROUMANIE

REVUE ROUMAINE DE CHIMIE

TOME 31

N° 8

Août 1986

| Rev. Roumaine Chim. | RRCHAX, 31, *8*, p. 739–836 (1986), Bucarest

EDITURA ACADEMIEI REPUBLICII SOCIALISTE ROMÂNIA

ACADÉMIE DE LA RÉPUBLIQUE SOCIALISTE DE ROUMANIE

COMITÉ DE RÉDACTION

Rédacteur en chef:

I. G. MURGULESCU, membre de l'Académie de la République Socialiste de Roumanie

Rédacteurs en chef adjoints:

A. T. BALABAN et V. EM. SAHINI, membres correspondants de l'Académie de la République Socialiste de Roumanie

Collège de rédaction:

EM. BRATU, ELENA CEAUŞESCU, ECATERINA CIORĂNESCU-NENITZESCU, CR. SIMIONESCU, membres de l'Académie de la République Socialiste de Roumanie, P. SPACU, membre correspondant de l'Académie de la République Socialiste de Roumanie; M. BANCIU, M. D. GHEORGHIU, I. HAIDUC, D. MARCHIDAN, G. NIAC et D. SĂNDULESCU

La Revue Roumaine de Chimie paraît 10 fois par an. Toute commande de l'étranger sera adressée à « ROMPRESFILATELIA » — sectorul Export-Import Presă, P. O. Box 12—201, télex 10376 prsfi r 78104, Calea Griviţei, nr. 64—66, Bucureşti, Roumanie.

Les manuscrits, les livres et les revues proposés en échange, ainsi que toute correspondance seront envoyés à la rédaction:

REVUE ROUMAINE DE CHIMIE

125, Calea Victoriei, 79717 Bucarest, Roumanie, téléphone 50 76 80

EDITURA ACADEMIEI REPUBLICII SOCIALISTE ROMÂNIA
125, Calea Victoriei, 79717 Bucarest, Roumanie, téléphone 50 76 80

ORSZÁGOS MŰSZAKI INFORMÁCIÓS KÖZPONT ÉS KÖNYVTÁR

REVUE ROUMAINE DE CHIMIE

Tome 31, N° 8 **Août 1986**

RODICA VÎLCU, VASILE BĂRBÎNȚĂ, IOAN GĂINAR and DUMITRU SAVA, Estimation of chemical nonhomogeneity of polymers using the interrelation structure-entropy-information. II. Computing program and results 741–751

EUGENIA SAVIUC and A. CĂLUȘARU, Rate constants and activation energies of Cr(II) to Cr(III) oxidation reaction by hydroxylamine in normal and heavy water 753–760

D. P. KHURANA, A. D. TANEJA and J. S. TYAGI, Spectroscopic determination of enethiol content of substituted pyridyl-thioureas in different solvents 761–771

BERNARD VIDAL and CHRISTIAN DUPRET, Enlargement of transitions and relative order of band heights. Application to incidence of remote interactions and solvation on the UV spectra of some phenylalkylamines (in French) 773–785

OLCAY ANAÇ, Some observations on the catalytic and direct photolytic reactions of *cis*-cyclodecene and *cis*-bicyclo[3.3.0]oct-2-ene with dimethyldiazomalonate 787–793

ALEXANDRU T. BALABAN, Chemical graphs. Part 46. Enumeration of valence isomers of adamantane using Pólya's theorem 795–810

LUMINIȚA PATRON, ADRIANA CONȚESCU, G. MUNTEANU, MARIA BREZEANU and E. SEGAL, Coordination compounds as raw materials for mixed oxides. III. Trinuclear, oxo-centered, carboxylate compounds containing Fe(II, III, III) 811–818

CRISTINA MANDRAVEL, MELANIA GUȚUL and MARGARETA TOMESCU, Synthesis and characterization of the Pd(II), Cd(II) and Hg(II) complex compounds with carbazole derivatives 819–822

VICTOR DAVID and DAN CIOMÂRTAN, On the spectral analytical measuring processes regarded as information processes 823–831

BOOK REVIEWS 833–836

Rev. Roumaine Chim. **31**, *8*, 739–836 (1986), Bucarest

Revue Roumaine de Chimie, **31**, *8*, 741—751 (1986)

ESTIMATION OF CHEMICAL NONHOMOGENEITY OF POLYMERS USING THE INTERRELATION STRUCTURE-ENTROPY-INFORMATION. II[1]

COMPUTING PROGRAM AND RESULTS

RODICA VÎLCU, VASILE BĂRBINȚĂ, IOAN GĂINAR and DUMITRU SAVA
Department of Physical-Chemistry, Polytechnical Institute of Bucharest, Romania

Received July 20, 1985

The results concerning the synthesis of copolymer as well as the data about the resulting copolymer have been expressed in terms of information theory. A fraction which is quantitatively determined by tracer method, allows to build the structure of the whole polymer using the existent correlation between the structure of the obtained polymer and the kinetic equations of the polymerization process. The computing program developed to this purpose based on the structure-entropy-information interrelation allows to obtain the data necessary to characterize the polymers in a new fashion.

I. INTRODUCTION

The aim of the present paper can be briefly summarized, as follows:

1. To reconstitute the polydisperse structure of the polymer given the average composition of the sample and the data concerning the extracted fraction.[1]

2. The fractions f_j of equal weights but different homogeneity degrees are regrouped into fractions of equal homogeneity degrees but different weights.

Such a regrouping is achieved by two criteria of homogeneity.

a) homogeneity as variations in molar fractions, using the weight factor α_j of each fraction f_j instead of factor α_0

b) equientropic homogeneity, the fractions f_j being regrouped in such a way that the ratio homo/hetero-sequences remains constant.

II. NOTATIONS

Let be a mixture of monomers

$$M_1, M_2, \ldots, M_j, \ldots, M_n \tag{1}$$

where the component concentrations are expressed as molar fractions.

During the polymerization reaction, copolymers result where the monomers are found in concentrations other than in the original mixture, due to the different reactivities of monomers

$$m_1, m_2, \ldots, m_j, \ldots m_n \tag{2}$$

The concentrations are also expressed as molar fractions. Note that the monomer concentrations in the reaction mixture and in copolymers are time-dependent, *i.e.* they are dynamically changed during the polymerization-reaction. One may imagine the following scheme of this process :

1-st stage (the first conversion degree or multiple or submultiple of this quantity)

— mixture of monomers

$$M_1^1, M_2^1, M_3^1, \ldots, M_x^1, \ldots M_n^1 \tag{3}$$

— monomers contained by copolymer, which constitute the fraction f_1 :

$$m_1^1, m_2^1, m_3^1, \ldots, m_x^1, \ldots, m_n^1 \tag{4}$$

2-nd stage (second conversion degree)

$$M_1^2, M_2^2, M_3^2, \ldots, M_x^2, \ldots, M_n^2 \tag{5}$$

fraction $f_2 : m_1^2, m_2^2, m_3^2, \ldots, m_x^2 \ldots m_n^2$ (6)

. . . .

j-th stage (j-th conversion degree)

$$M_1^j, M_2^j, M_3^j, \ldots, M_x^j, \ldots, M_n^j \tag{7}$$

fraction f_j :

$$m_1^j, m_2^j, m_3^j, \ldots, m_x^j, \ldots, m_n^j \tag{8}$$

. . . .

n-th stage (n-th conversion degree)

$$M_1^n, M_2^n, M_3^n, \ldots, M_x^n, \ldots, M_n^n \tag{9}$$

fraction f_n :

$$m_1^n, m_2^n, m_3^n, \ldots, m_x^n, \ldots, m_n^n \tag{10}$$

III. THE RELATIONSHIP BETWEEN QUANTITIES

1. The molar concentrations of monomers in copolymer may be calculated after each stage of the process, if the molar concentrations of monomers in the reaction mixture are known, according to the equation [2]:

$$m_x = M_x Q_x \sum_{i=1}^{n} M_i Q_i \exp(-e_x e_i) \Big/ \sum_{\substack{i=1\\j=1}}^{n} M_i Q_i \cdot M_j Q_j \exp(-e_i \cdot e_j) \qquad (11)$$

where Q_i and e_i are the specific constants dependent on the chemical character of the monomers (Q_i is a reactivity constant and e_i a polarity constant).

2. Let us consider as known the monomer composition of a reaction mixture which leads to the formation of the j-th fraction of copolymer:

$$M_1^j, M_2^j, M_3^j, \ldots, M_x^j, \ldots, M_n^j$$

After the formation of the j-th fraction, the mixture of monomers will have another composition, which at its turn will be modified by the formation of (j + 1) fraction.

The monomer composition corresponding to the two subsequent stages will be:

$$M^{j+1} = \frac{M_1^j - \alpha_j \cdot m_1^j}{1 - \alpha_j}, M^{j+1} = \frac{M_2^j - \alpha_j \cdot m_2^j}{1 - \alpha_j}, \ldots, M_n^{j+1} = \frac{M_n^j - \alpha_j M_n^j}{1 - \alpha_j} \qquad (12)$$

3. The estimation of indices used to regroup the fractions f_j into equientropic fractions F_x

a) The evaluation of weight factors α_j (*i.e.* to express the homogeneity by equal changes in molar fractions)

$$\alpha_j = \alpha_0 - (j-1)\alpha_0^2 - (j-2)\alpha_0^3 - , \ldots, - \alpha_0^j \qquad (13)$$

where α_0 is the number of conversion degrees (either multiple or submultiple of it).

This quantity is determined from the quantitative contribution of an extracted fraction which is used to determine the entire polydispersion.[3]

b) Homogeneity expressed in equientropic F_x fractions which shows the constant ratio of homosequences with respect to heterosequences.

The calculation of information entropy is carried out using Tosi's relationships.[4] In the case of copolymers where the number of components is greater than 2, the ratio between homo- and hetero-sequences can be expressed by means of other indices determined also by Tosi.[5,6]

$$
\begin{aligned}
\Lambda_1 &= \frac{M_1}{r_{11}} + \frac{M_2}{r_{12}} + \ldots + \frac{M_x}{r_{1x}} + \ldots + \frac{M_n}{r_{1n}} \\
\Lambda_2 &= \frac{M_1}{r_{21}} + \frac{M_2}{r_{22}} + \ldots + \frac{M_x}{r_{2x}} + \ldots + \frac{M_n}{r_{2n}} \qquad (14) \\
&\ldots\ldots\ldots\ldots\ldots\ldots \\
\Lambda_n &= \frac{M_1}{r_{n1}} + \frac{M_2}{r_{n2}} + \ldots + \frac{M_x}{r_{nx}} + \ldots + \frac{M_n}{r_{nn}}
\end{aligned}
$$

where

$$r_{ij} = Q_i/Q_j \cdot \exp[-e_i(e_i - e_j)] \qquad (15)$$

The indices S_i corresponding to the information entropy are determined :[2]

$$S_1 = \frac{\Lambda_1 - M_1}{\Lambda_1},\ S_2 = \frac{\Lambda_2 - M_2}{\Lambda_2},\ \ldots,\ S_n = \frac{\Lambda_n - M_n}{\Lambda_n} \qquad (16)$$

By means of $S_1, S_2, \ldots, S_n$ values, the general parameter of the fraction is determined :

$$S_T = m_1S_1 + m_2S_2 + \ldots + m_nS_n \qquad (17)$$

Each fraction f_j is characterized by an information index S_T and the variation ΔS_T given by

$$\Delta S_T = (S_T)_j - (S_T)_{j+1} \qquad (18)$$

We have adopted the convention that the last index should be equal to the forelast one.

The term $\sum_{j=1}^{n} \Delta S_T/n_f = \Delta S_k$, defines the interval of each fraction F_x. If the sum $\sum_{j=1}^{i} (\Delta S_T)_j > \Delta S_k$, the last fraction f_j is divided into the fractions F_k and F_{k+1}, using the weight factors D_k and B_{k+1} which must fulfill the condition $D_k + B_{k+1} = 1$.
There results that

$$D_k = \frac{\Sigma\Delta S_T - \Delta S_k}{\Sigma\Delta S_T},\ B_k = 1 - D_{k-1},\ B_1 = 0,\ D_{n_f} = 0 \qquad (19)$$

4. The regrouping way of the fractions f_j into F_x fractions. This operation which is essential for our study, is made under the following conditions :

a) The transition from f_j to F_x fractions is made using the weight factors α_j (equation 13);

b) The regrouping of f_j into F_x fractions is made using the relation which defines the interval proper to each fraction F_x.

c) The weight of each F_x fraction existent between the fraction f_i and f_l is calculated from the expresion

$$\frac{B_k\cdot\alpha_i + \sum_{j=i+1}^{l-1}\alpha_j + D_k\cdot\alpha_l}{\sum_{j=1}^{n}\alpha_j} \tag{20}$$

IV. INPUT DATA

1. Experimental data

a) The composition of extracted fractions (molar fractions in monomers):

$$m_1, m_2, m_3, \ldots, m_x, \ldots m_n$$

b) The amount of extracted fraction is used to estimate the weight of each fraction and α_0 respectively.

c) the averaged composition of analyzed copolymer given as ratios of averaged composition

$$\frac{\overline{m_1}}{m_2}, \frac{\overline{m_1}}{m_3}, \frac{\overline{m_1}}{m_4}, \ldots, \frac{\overline{m_1}}{m_x}, \ldots, \frac{\overline{m_1}}{m_n}.$$

Besides these values, the mean composition of fractions calculated for a given number of stages must be considered. These values are obtained with analytical methods applied to the determination of composition of the sample.

2. Characteristic constants of the synthesis process of copolymer: Q_i, e_i, r_{ij}.

3. Maximum admitted errors.

a) $\Delta_m < \varepsilon_1$ — involved in the subroutine used to evaluate the quantities M_i if m_i values are known.

The value Δm means the deviation involved in the calculation of mass balance.

b) $\Delta_m < \varepsilon_2$ — represents the condition imposed to the limit deviation admitted to the determination of the position of extracted fraction relative to the richest or poorest fraction in what the constant of monomer with highest or lowest reactivity is concerned.

c) $\overline{m} - \frac{\Sigma m\cdot\alpha_x}{\Sigma\alpha_x} = \Delta_m < \varepsilon_3$, is the limit deviation admitted to the calculus of f_x fractions.

COMPUTING SCHEME

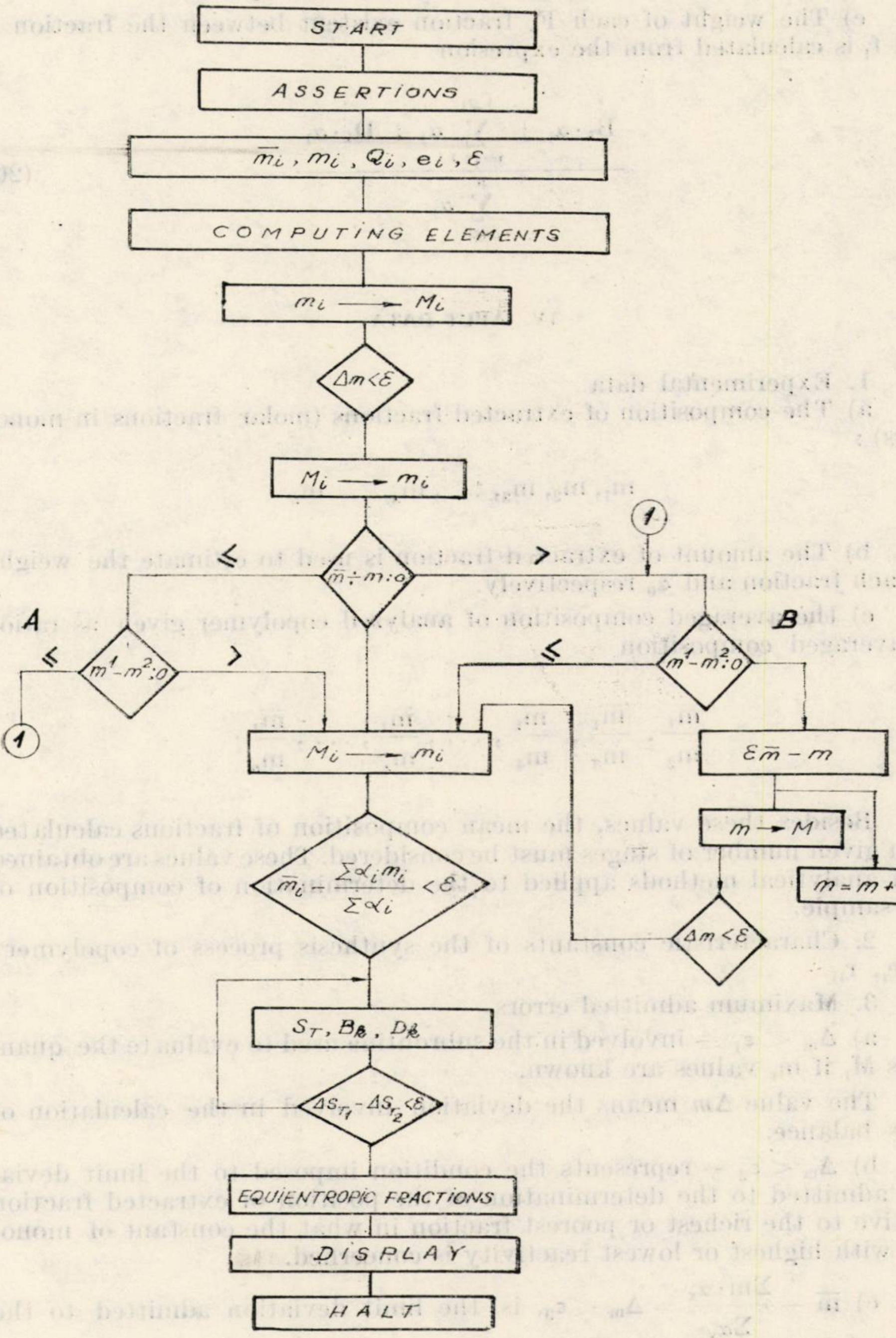
START
ASSERTIONS
$\overline{m}_i, m_i, Q_i, e_i, \mathcal{E}$
COMPUTING ELEMENTS
$m_i \longrightarrow M_i$
$\Delta m < \mathcal{E}$
$M_i \longrightarrow m_i$
$\leqslant$
$>$
$\overline{m}_i - m_i : 0$
1
A
$\leqslant$
$>$
$m^1 - m^2 : 0$
1
B
$\leqslant$
$m^1 - m^2 : 0$
$M_i \longrightarrow m_i$
$\mathcal{E}\overline{m} - m$
$m \rightarrow M$
$m = m + \Delta$
$\overline{m}_i - \frac{\sum \alpha_i m_i}{\sum \alpha_i} < \mathcal{E}$
$\Delta m < \mathcal{E}$
S_T, B_k, D_k
$\Delta S_{T_1} - \Delta S_{T_2} < \mathcal{E}$
EQUIENTROPIC FRACTIONS
DISPLAY
HALT

V. PROGRAMMED OPERATIONS

1. Estimation of concentration of the monomer mixture which is used in the obtention of extracted fraction.

For this purpose, the following set of values

$$m_1^i, m_2^i, m_3^i, \ldots, m_x^i, \ldots, m_n^i \tag{20}$$

representing the composition of extracted fraction is used. These values are used together with equation (11) and the subroutine "reciprocal calculation" to obtain the searched values:

$$M_1^i, M_2^i, M_3^i, \ldots, M_x^i, \ldots, M_n^i \tag{21}$$

The mentioned subroutine makes the calculation of trial and error type: a set of trial values for the quantities (21) are put in, by means of which the corresponding composition of the fraction is calculated. The obtained values are compared with the set of real values (20), the operation being repeated until self consistency of condition 3a.

2. The position of the extracted fraction in the distribution upon the composition of a copolymer.

By means of the data previously obtained (V.1) and equations (11) and (13) the first conversion degrees are calculated. The position of the fraction in copolymer is then tested (if the extracted fraction represents the richest or poorest in the required monomer, or if it is formed at the beginning or at the end of the polymerization process).

The following situations can occur during the check of fraction position

$$\text{a) } m_x^i > m_x^{i+1} \begin{cases} m - m_x^1 < 0 & \text{initial fraction} \\ m - m_x^1 > 0 & \text{final fraction} \end{cases}$$

$$\text{b) } m_x^i < m_x^{i+1} \begin{cases} m - m_x^1 < 0 & \text{final fraction} \\ m - m_x^1 > 0 & \text{initial fraction} \end{cases}$$

c) $m_x^i = m_x^{i+1}$. This situation can occur in that case where the imposed exactness for the calculation of $(m_x^i - m_x^{i+1})$ difference is not sufficiently large and requires further steps in the programme, until $m_x^i \neq m_x^{i+1}$.

3. Calculation of the fractions of composition upon the place of the extracted fraction in polydispersion.

a) For the initial fractions, the calculation is performed using the set of values (21) and expressions (11) and (13), until condition IV-c is fulfilled.

b) For the final fractions, the calculation is performed by means of "reciprocal calculation" subroutine starting from the relationship

$$m_x^0 = 2\overline{m}_x - m_x^1$$

When the set of values (21) under the error $\Delta m < \varepsilon_2$ is obtained, the computation is followed as shown in V—3 a.

4. The calculation of f_j fractions and of the indices useful for the conversion to F_x fractions from the set of values (21) and relationships

(11) and (13), the f_j fractions are calculated under the condition

$$\sum_{x=1}^{n}\left| m_x - \frac{\sum_{i=1}^{n} m_x^i \cdot \alpha_i}{\sum_{i=1}^{n} \alpha_i} \right| < \varepsilon_3$$

With the data concerning the f_j fractions, the indices S_T, D_k and B_k may then be estimated.

5. Copolymer refraction by means of the new criteria of homogeneity. In order to get an explicit unitary view about the way to present the final data of the calculation, we shall give below a detailed scheme of the composition of the fractions F_x: [7]

$$m_1 = \frac{\sum_{j=1}^{i-1} \alpha_j \cdot m_1^j + D_1 \cdot \alpha_i \cdot m_1^i}{\sum_{j=1}^{i-1} \alpha_j + D_1 \cdot \alpha_i}$$

. . . .

$$m_n = \frac{\sum_{j=1}^{i-1} \alpha_j \cdot m_n^j + D_1 \cdot \alpha_i \cdot m_n^i}{\sum_{j=1}^{i-1} \alpha_j + D_1 \cdot \alpha_i}$$

F_2

$$m_1 = \frac{B_2 \cdot \alpha_i \cdot m_1^i + \sum_{j=i+1}^{l-1} \alpha_j \cdot m_1^j + D_2 \cdot \alpha_l \cdot m_1^l}{B_2 \cdot \alpha_i + \sum_{j=i+1}^{l-1} \alpha_j + D_2 \cdot \alpha_l}$$

. . . .

$$m_n = \frac{B_2 \cdot \alpha_i \cdot m_n^i + \sum_{j=i+1}^{l-1} \alpha_j \cdot m_n^j + D_2 \cdot \alpha_l \cdot m_n^l}{B_2 \cdot \alpha_i + \sum_{j=i+1}^{l-1} \alpha_j + D_2 \cdot \alpha_l}$$

$F = n_f$

$$m_1 = \frac{B_{n_f} \cdot \alpha_k \cdot m_1^k + \sum_{j=k+1}^{n} \alpha_j \cdot m_1^j}{B_{nf} \cdot \alpha_k + \sum_{j=k+1}^{n} \alpha_j}$$

$$m_n = \frac{B_{n_f} \cdot \alpha_k \cdot m_n^k + \sum_{i=k+1}^{n} \alpha_j \cdot m_n^j}{B_{n_f} \cdot \alpha_k + \sum_{j=k+1}^{n} \alpha_j}$$

EXPERIMENTAL

The experimental data summarized in Tables 1—3 give the fractioning of the three-component polymers obtained with methyl methacrylate, acrylonitrile and vinylidenechloride.

Since one starts from different values of the mean composition and of extracted fraction, a variation in the fraction distribution as a function of composition of the chosen sample is obtained. Copolymer (3) is not fractionated with the same homogeneity degree and does not contain the same number of fractions as copolymers (1) and (2). They cannot, therefore, be discussed from the same information point of view.

Table 1

The Copolymer MM—NA—CVd

$m_1 = 49.65$	$\overline{m}_1 = 50.70$	$Q_1 = 0.76$	$e_1 = 0.40$
$m_2 = 28.95$	$\overline{m}_2 = 28.87$	$Q_2 = 0.57$	$e_2 = 1.18$
$m_3 = 21.40$	$\overline{m}_3 = 20.44$	$Q_3 = 0.18$	$e_3 = 0.50$

F	P %	m_1	m_2	m_3
1	11.53	51.39	28.62	19.99
2	18.30	51.07	28.74	20.19
3	12.28	50.77	28.85	20.38
4	16.73	50.55	28.93	20.52
5	12.62	50.26	29.04	20.70
6	15.76	50.02	29.13	20.85
7	12.77	49.72	29.23	21.04

The data contained in Tables 1 and 2 refer, however, to the fractioning of the same polymer, starting from the same mean composition but from different extracted fractions.

The data summarized clearly show the logical consistency of the new method herein presented as well as the coherence of the proposed computing program, which allows, in the case of the same polymer taken as a sample, irrespective of the extracted fraction, in such a way the same structure for the whole polymer with minimum errors to be obtained.

The same conclusion is drawn from the analysis of data concerning the fractioning of four-component polymers (Table 4, 5): styrene-methyl methacrylate-acrylonitrile-vinylidenechloride.

Table 2

The copolymer MM—NA—CVd

$m_1 = 41.57$	$\overline{m}_1 = 50.70$	The parameters Q_i, e_i are the same as in Table 1
$m_2 = 31.35$	$\overline{m}_2 = 28.87$	
$m_3 = 27.08$	$\overline{m}_3 = 20.44$	

F	P %	m_1	m_2	m_3
1	11.53	51.30	28.62	19.99
2	18.30	51.07	28.74	20.19
3	12.28	50.77	28.85	29.38
4	16.73	50.55	28.93	20.52
5	12.62	50.26	29.04	20.70
6	15.76	50.02	29.13	20.85
7	12.77	49.72	29.23	21.04

Table 3

The copolymer MM—NA—CVd

$m_1 = 61.80$	$\overline{m}_1 = 56.30$
$m_2 = 23.80$	$\overline{m}_2 = 26.70$
$m_3 = 14.40$	$\overline{m}_3 = 17.00$

F	P %	m_1	m_2	m_3
1	21.03	60.70	24.31	14.99
2	20.92	59.51	24.82	15.68
3	20.31	58.22	25.35	16.43
4	19.32	56.87	25.90	17.23
5	18.42	55.43	26.47	18.10

Table 4

The copolymer S—MM—NA—CVd

$m_1 = 43.85$	$\overline{m}_1 = 42.75$	$Q_1 = 1.00$	$e_1 = -0.75$
$m_2 = 25.96$	$\overline{m}_2 = 26.42$	$Q_2 = 0.76$	$e_2 = 0.40$
$m_3 = 24.35$	$\overline{m}_3 = 24.45$	$Q_3 = 0.57$	$e_3 = 1.18$
$m_4 = 5.84$	$\overline{m}_4 = 7.38$	$Q_4 = 0.18$	$e_4 = 0.50$

F	P%	m_1	m_2	m_3	m_4
1	13.26	43.97	26.26	24.55	5.22
2	13.58	43.73	26.42	24.61	5.36
3	13.12	43.39	26.57	24.65	5.51
4	12.96	43.03	26.74	24.70	5.68
5	12.61	42.61	26.91	24.74	5.86
6	15.40	42.09	27.11	24.79	6.09
7	19.07	41.41	27.45	24.90	6.43

Table 5

The copolymer S—MM—NA—CVd

$m_1 = 40.78$	$\overline{m}_1 = 42.75$
$m_2 = 27.63$	$\overline{m}_2 = 26.42$
$m_3 = 24.91$	$\overline{m}_3 = 24.45$
$m_4 = 6.68$	$\overline{m}_4 = 7.38$

F	P%	m_1	m_2	m_3	m_4
1	13.41	43.99	26.16	24.39	5.47
2	13.59	43.74	26.31	24.44	5.61
3	13.16	43.42	26.46	24.48	5.77
4	12.92	43.06	26.61	24.52	5.94
5	12.61	42.65	26.77	24.56	6.12
6	15.35	42.15	26.97	24.60	6.36
7	18.91	41.51	27.29	24.71	6.70

Finally, one concludes that this refractioning based on the polymer calculation allows the identification of the macromolecules, irrespective of fractioning way, and allows also to estimate the whole complexity by a single index only.

The authors wish to express their gratitude to the International Atomic Energy Agency in Vienna for the subvention supplied in fullfilling the present research work.

REFERENCES

[1] R. Vîlcu, V. Bărbinţă and I. Găinar, *Rev. Roumaine Chim.*, **31**, 657 (1986).

[2] J. A. Seiner, *J. Polymer Sci.*, **A3**, 2401 (1965).

[3] R. Vîlcu, V. Bărbinţă and I. Găinar, Internatioal Atomic Energy Agency (Vienna) Agency Research Contract No. 1826/Rl/RB.

[4] P. Corradini and C. Tosi, *European Polymer J.*, **4**, 227 (1968).

[5] C. Tosi, *European Polymer J.*, **6**, 16 (1970).

[6] C. Tosi, *European Polymer J.*, **4**, 237 (1968).

[7] R. Vîlcu, V. Bărbinţă and I. Găinar, International Atomic Energy Agency (Vienna), Research Contract, No. 1826/R2/RB.

Revue Roumaine de Chimie, **31**, *8*, 753—760 (1986)

RATE CONSTANTS AND ACTIVATION ENERGIES OF Cr(II) TO Cr(III) OXIDATION REACTION BY HYDROXYLAMINE IN NORMAL AND HEAVY WATER

EUGENIA SAVIUC * and A. CĂLUȘARU **

* Department of Inorganic and Analytical Chemistry, Polytechnical Institute, Iași, Romania

** Institute of Chemical Research, Bucharest, Romania

Received August 28, 1985

In the present paper the rate constants and activation energies were determined in normal and heavy water for the Cr(II) to Cr(III) oxidation reaction in the presence of hydroxylamine. In this system Cr(III) forms a kinetic wave owing to the superimposition of the chemical oxidation reaction of Cr(II) by hydroxylamine on the diffusion Cr(III) polarographic wave. For the rate constants the following values were determined : $k_{\mathrm{H},\,25°\mathrm{C}} = 2.74 \times 10^2$ L mol^{-1} s^{-1} and $k_{\mathrm{D},\,25°\mathrm{C}} = 1.68 \times 10^2$ L mol^{-1} s^{-1} with the corresponding isotope effect $k_\mathrm{H}/k_\mathrm{D} = 1.63$. In the case of the activation energies the values are : $E_\mathrm{H} = 9.74$ kcal mol^{-1} and $E_\mathrm{D} = 12.4$ kcal mol^{-1} with the ratio $E_\mathrm{H}/E_\mathrm{D} = 0.785$. By using the Arrhenius equation the ratio of the preexponential factors was determined : $A_\mathrm{H}/A_\mathrm{D} = 1.63$. This value shows that the origin of the kinetic isotope effect is the variation of the collision frequency of molecules involved in the chemical oxidation reactions.

An important case of polarographic study of the kinetic currents in the case of chemical reactions superimposed on an electron transfer process (catalysed process) is represented by the systems : low valence metal ion/hydroxylamine. The most studied is the oxidation of Ti(III) resulted by electrochemical reduction of Ti(IV) by normal [1] and deuterated hydroxylamine.[2] Other studies were afterwards carried out.[3] In the case of Cr(II) to Cr(III) oxidation reaction systematic studies were published in a series of papers.[4–6]

The general feature is that these couples are an effective source of $\cdot\mathrm{NH_2}$ or $\cdot\mathrm{NH_3^+}$ radicals, depending on the pH of the solution. These radicals play an important role in a series of interesting organic reactions, widely applied in practice. It has been shown[3,7,8] that the ammino or ammoniumyl radicals can act by hydrogen atom abstraction with a series of suitable substrates or by addition with alkenes and their derivatives. In these cases the continuous flow ESR (electron spin resonance) spectroscopy was used in an attempt to detect the radicals formed in these reactions and hence to study the selectivity with which $\cdot\mathrm{NH_3^+}$ or $\cdot\mathrm{NH_2}$ attack different hydrogen atoms or other reactive sites in a variety of substrates.[9]

An advantage of polarographic[1-5,10] or pulse polarographic[8] methods is the possibility to determine both the rate constants and activation energies of the chemical oxidation reaction superimposed in the electron transfer reaction. As is well known for the catalysed processes, the polarographic kinetic currents allow to determine the rate constants, without knowing the equilibrium constants of the involved reactions.[11] At the same time, as has been already shown, [2] the polarographic method is sensitive to the hydrogen isotope effect of the reactions in which $\cdot NH_2$ or $\cdot NH_3^+$ radicals participate in form of $\cdot ND_2$ or $\cdot ND_3^+$ radicals. In this way a valuable tool is available for the deeper understanding of the reaction mechanism.

In the present paper the rate constants and activation energies of the Cr(II) to Cr(III) oxidation reaction by hydroxylamine in both normal hydrogen and deuterium media are studied. Using the data on the kinetic isotope effects, a reaction mechanism of the Cr(II) oxidation by hydroxylamine is proposed.

EXPERIMENTAL

The polarograms were recorded in inert atmosphere using an LP 60 type polarograph. The anodic part of the polarographic cell was an SCE electrode and the cathodic room a double-wall vessel for keeping constant the temperature.

The solutions of hydroxylamine hydrochloride were calibrated iodometrically. The deuterated hydroxylamine was provided by VEB-Chemie Berlin Adlershoff.

The triethanolamine was transformed into hydrochloride and purified by several recrystallizations with alcohol. The dried salt was then dissolved in heavy water and the water excess removed by evaporation ; this operation was repeated for four times. In this way the hydrogen atoms from the hydroxylic groups only were substituted by deuterium. It is important to emphasize that deuteration of the active groups only is the most suitable, since a complete deuteration should introduce a supplementary mass effect which modifies the intrinsic isotope effect.

The deuterated sodium hydroxide was obtained by the reaction of metallic sodium with water. The solutions of chromic nitrate were obtained by the solubilisation of the dried product in the normal or heavy water correspondingly.

EXPERIMENTAL RESULTS

In the presence of hydroxylamine the triethanolamine chromium(III) complexes in alkaline medium form a limiting current, whose kinetic character is produced by the superimposition of a Cr(II) to Cr(III) chemical oxidation reaction by hydroxylamine on the electron transfer of Cr(III) reduction. The oxidation reaction is typically bimolecular since two components participate in it : Cr(II) and hydroxylamine. When a large excess of hydroxylamine is used as compared with Cr(II) formed by electron transfer, the oxidation reaction becomes pseudo-monomolecular and the polarographic data can be used for the calculation of the corresponding rate constant.

1. Effect of D_2O concentration on the kinetic limiting current

In so far as normal water is substituted by the heavy one, the polarographic kinetic current of Cr(II) to Cr(III) oxidation reaction by hydroxylamine decreases considerably. The decrease in the case of chromium is higher as compared with titanium[2] or iron.[12] This effect can be explained by a more important role played by the water molecules in the structure of the chromium complexes

In is interesting to note that within a wide range of heavy water content (70 volume percent) there is a linear relationship between the current ratio i_l/i_d (i_l is the kinetic current and i_d the diffusion current corresponding to Cr(III) reduction) as a function of the volume percent of heavy water added in solution, as it is shown in Fig. 1. The same variation has been also found in the case of other low valence metal ions, such as Ti(III)[2] and Fe(II).[12]

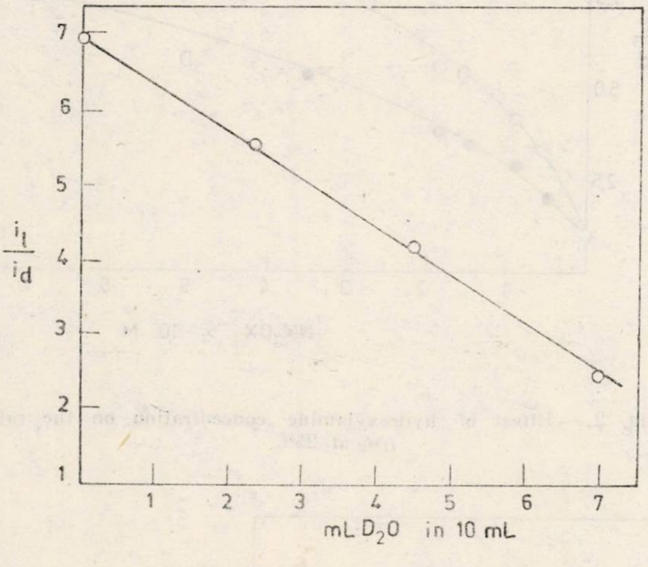

Fig. 1. — Ratio i_l/i_d as a function of D_2O content.

2. Effect of hydroxylamine concentration in normal and heavy water

We have already emphasized the role of the excess of hydroxylamine in considering the bimolecular reaction as a pseudo-monomolecular one. Only in this case the quantitative treatment for the calculation of the rate constant is available using the polarographic currents.[13]

The effect of hydroxylamine concentration of the Cr(II) to Cr(III) oxidation reaction is shown in Fig. 2 for both normal hydrogen (H) and deuterium (D) systems. Two very different curves were obtained for each system. But in both cases in so far as the hydroxylamine concentration is increased, the curves tend to a limiting value, corresponding to the pseudo-monomolecular character of the Cr(II) oxidation reaction. The limiting value is reached faster for the slower reaction (Fig. 2, D) as compared with the more rapid one (Fig. 2, H). Comparing again this system with other ones in which the metal is at a lower valency state (Ti[2] and

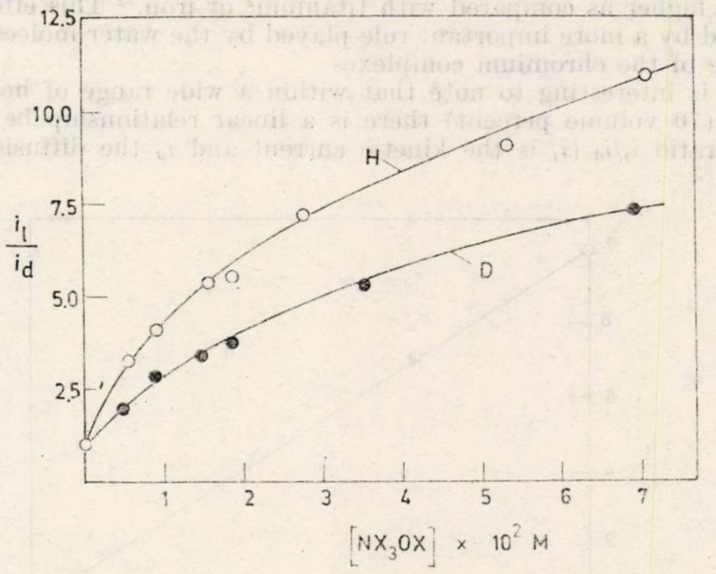

Fig. 2. — Effect of hydroxylamine concentration on the ratio i_l/i_d at 25°C.

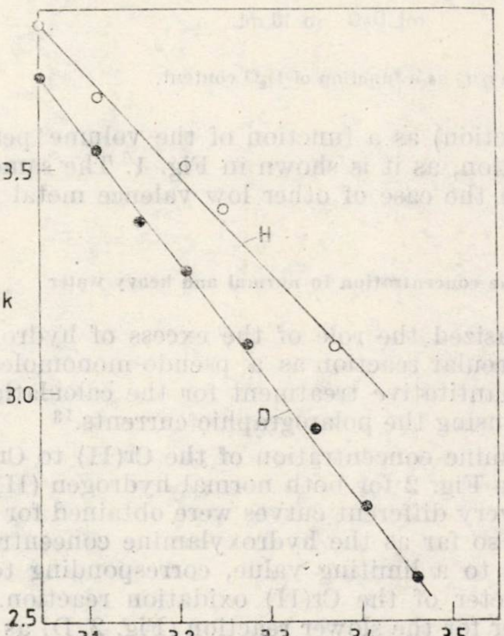

Fig. 3. — Logarithm of the rate constant as a function of i/T in hydrogen (H) and deuterium (D) systems.

Fe[12]) we can conclude that this behaviour appears as a general feature of these systems.

3. Effect of the temperature on the kinetic current

In contrast with the diffusion currents, the limiting kinetic ones are considerably more influenced by the temperature changes owing to the strong variation of the reaction rate constant as a function of the temperature. Keeping constant the composition of the solution and at the same work parameters, the temperature was modified in order to calculate the corresponding rate constants for both normal hydrogen and deuterium systems. With the values obtained, log $k_{X,T}$ was plotted as a function of the reciprocal value of the temperature. $k_{X,T}$ is the rate constant for H or D at a defined temperature. As is shown in Fig. 3, two straight lines were obtained, which confirm the validity of an Arrhenius type equation :

$$\log k_{X,T} = -0.43\,E/RT + \text{const} \tag{1}$$

From this equation the activation energies for the Cr(II) to Cr(III) oxidation reaction in both H and D systems were calculated. The following values were obtained : $E_{H,25}$ 9.74 kcal mol^{-1} and $E_D = 12.4$ kcal mol^{-1}.

DISCUSSION

All data presented above can be correlated for the discussion of the reaction mechanism, rate constants and isotope effects.

1. Reaction mechanism

On the electron transfer reaction :

$$\mathrm{Cr(III)} + e \rightarrow \mathrm{Cr(II)} \tag{2}$$

a chemical oxidation reaction of Cr(II) by hydroxylamine is superimposed. Two kinds of radical species can result as a consequence of this reaction :

(a) the unprotonated $\cdot NX_2$ form

$$\mathrm{Cr(II)} + NX_2OX \rightarrow \mathrm{Cr(III)} + \cdot NX_2 + OX^- \tag{3}$$

and

(b) the protonated $\cdot NX_3^+$ ammoniumyl radical

$$\mathrm{Cr(II)} + NX_2OX + X^+ \rightarrow \mathrm{Cr(III)} + \cdot NX_3^+ + OX^- \tag{4}$$

In alkaline medium, reaction (3) is the most probable. Literature data[3] indicate that even in acidic media, it is NH_2OH rather than the protonated form NH_3^+OH, which reacts with the low valence metal, for instance Ti(III). By pulse radiolysis of aqueous solutions of hydroxylamine $\cdot NH_2$ or $\cdot NH_3^+$ form *via* reaction of e_{aq}^- with NH_2OH ; at the same time, the pK_a value of 6.7 was determined for the ammoniumyl radical, which confirms that the reactive species in acidic solutions is $\cdot NH_3^+$ rather than $\cdot NH_2$.

The resulted radical reacts by hydrogen-atom abstraction from a suitable substrate or by addition with alkenes and their derivatives.[9] The high reactivity of the radical $\cdot NH_3^+$ or $\cdot NH_2$ resulted by reaction with the low valence ion provides a competing mode for its combination.

In the case of an organic substrate the reaction produced is :

$$\cdot NH_3^+ + RH \rightarrow NH_3 + \cdot R + H^+ \qquad (5)$$

while in case of water the $\cdot OX$ radical results :

$$\cdot NX_3^+ + X_2O \rightarrow \cdot OX + NX_3 + X^+ \qquad (6)$$

This last radical reacts again with the low valency metal ion :

$$\cdot OX + Cr(II) \rightarrow Cr(III) + OX^- \qquad (7)$$

The following reaction is also possible :

$$Cr(II) + \cdot NX_2 + X_2O \rightarrow Cr(III) + OX^- + NX_3 \qquad (8)$$

For reaction (5) the ESR spectroscopy was used in an attempt to detect directly the radical formed and therefore to determine the selectivity of attack for different hydrogen atoms or other reactive sites in a variety of substrates. This can explain, for instance, the stereospecificity mechanism in a series of polymerisation reactions. It is interesting to note that in solid crystals of neutral substances such as NH_4ClO_4 or ND_4ClO_4 the ESR spectra show always the presence of $\cdot NH_3^+$ or $\cdot ND_3^+$ radical respectively.[14-16] The floating wave functions were also calculated for $\cdot NH_3^+$.[17]

In the case studied in the present paper, reactions (3), (6), (7) and (8) are of particular interest.

2. Rate constants

Some authors[5] consider that the overall oxidation reaction is composed by the steps (3) and (8), owing to the fact that the activation energy remains the same in different reaction media, while the rate constant is modified within an interval of an order of magnitude. That is why they conclude that the reaction mechanism is not changed by the modification of the reaction medium.

In fact for the determination of the rate constant it is important to determine the slow reaction step in order to characterize the reaction for which the rate constant is determined. It is generally accepted that the slow step is represented by reaction (3).

In the condition of a pseudo-monomolecular reaction, therefore in a high excess of hydroxylamine, the rate constant k_X can be calculated by the rigorous method proposed by Koutecky[13] on the basis of the relationship between the current ratio i_l/i_d and a function χ_1 given by the equation :

$$\chi_1 = k_X[NX_3OX]t_1 \tag{9}$$

where t_1 is the drop time and $[NX_3OX]$ the hydroxylamine concentration.

For the calculation of the rate constants of the oxidation reaction in both systems, the experimental data from Fig. 2. were used. For the system with normal water the value $k_{H,25°C} = (2.74^{+0.29}_{-0.16})10^2$ L mol^{-1}s^{-1} was obtained; the same value in deuterium system is $k_{D,\,25°C} = (1.68^{+0.12}_{-0.17})10^2$ L mol^{-1} s^{-1}. Using these values of the rate constants the function $\chi_1^{1/2}$ was calculated with equation (9). Teh relationship $i_l/i_d - \chi_1^{1/2}$ is plotted in Fig. 4, showing that the asymptotical methods can be used. [13]

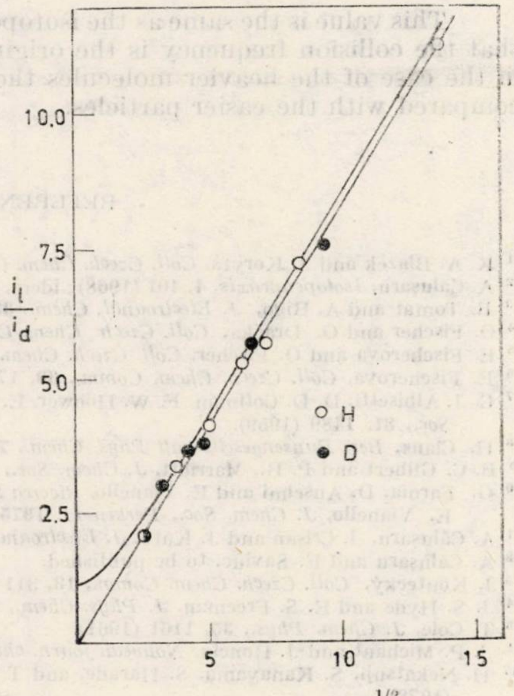

Fig. 4. — Variation of current ratio i_l/i_d as a function of $\chi_2^{1/2}$.

3. Isotope effects

The difference obtained for the rate constants $k_{H,T}$ and $k_{D,T}$ show a kinetic isotope effect of the oxidation reaction of Cr(II) to Cr(III) by hydroxylamine :

$$\frac{k_H}{k_D} = \frac{2.74 \times 10^2}{1.68 \times 10^2} = 1.63 \tag{20}$$

In the case of the activation energies we have found that $E_H < E_D$. The corresponding isotope effect is :

$$\frac{E_H}{E_D} = \frac{9.74}{12.40} = 0.785$$

Considering equation (1) in exponential form, the isotope effect, corresponding to the frequency factor A_x can be calculated :

$$\frac{A_H}{A_D} = \frac{k_H}{k_D} \frac{e^{-E_D/RT}}{e^{-E_H/RT}} = \frac{2.74 \times 10^2}{1.68 \times 10^2} \times \frac{e^{-12.4/RT}}{e^{-9.74/RT}} = 1.63 \qquad (22)$$

This value is the same as the isotope effect of rate constants, showing that the collision frequency is the origin of the isotope effect. Obviously in the case of the heavier molecules the collision frequency is smaller as compared with the easier particles.

REFERENCES

[1] K. A. Blazek and J. Koryta, *Coll. Czech. Chem. Comm.*, **18**, 326 (1953).

[2] A. Călușaru, *Isotopenpraxis*, **4**, 401 (1968) ; idem, *Uspechi Chim.* (Moscow), **58**, 221 (1979).

[3] R. Tomat and A. Rigo, *J. Electroanal. Chem.*, **35**, 21 (1972).

[4] O. Fischer and O. Dračka, *Coll. Czech Chem. Comm.*, **26**, 1505 (1961).

[5] E. Fischerova and O. Fischer, *Coll. Czech. Chem. Comm.*, **30**, 675 1965).

[6] E. Fischerova, *Coll. Czech. Chem. Comm.*, **30**, 1771 (1965).

[7] C. J. Albisetti, D. D. Coffman, F. W. Hoower, E. L. Jener and W. E. Mochel, *J. Amer. Chem. Soc.*, **81**, 1489 (1959).

[8] H. Claus, *Ber. Bunsengesellschaft Phys. Chem.*, **78**, 78 (1974).

[9] B. C. Gilbert and P. R., Marriott, *J. Chem. Soc., Perkin II*, **1977**, 978.

[10] G. Farnia, D. Anselmi and E. Vianello, *Ricerca Sci.*, **1968**, 1211 ; G. Farnia, R. Tomat and E. Vianello, *J. Chem. Soc., Perkin II*, **1975**, 763.

[11] A. Călușaru, I. Crișan and J. Kůta, *J. Electroanal. Chem.*, **46**, 51 (1973).

[12] A. Călușaru and E. Saviuc, to be published.

[13] J. Koutecký, *Coll. Czech. Chem. Comm.*, **18**, 311 (1953).

[14] J. S. Hyde and E. S. Freeman, *J. Phys. Chem.*, **65**, 1636 (1961).

[15] T. Cole, *J. Chem. Phys.*, **35**, 1161 (1961).

[16] J. P. Michaut and J. Roncin, *Nouveau journ. chim.*, **2**, 129 (1978).

[17] H. Nekatsuji, S. Kanayama, S. Harade, and T. Yonezava, *J. Amer. Chem. Soc.* **100**, 7528 (1978).

Revue Roumaine de Chimie, 31, 8, 761—771 (1986)

SPECTROSCOPIC DETERMINATION OF ENETHIOL CONTENT OF SUBSTITUTED PYRIDYL-THIOUREAS IN DIFFERENT SOLVENTS

D. P. KHURANA [a], A. D. TANEJA [b] and J. S. TYAGI [c]

[a] D. N. College, Hisar,
[b] H. A. U., Hisar
[c] Chemistry Department, Meerut College, Meerut

Received July 20, 1985

Enethiol content of N′-2-(3-hydroxy pyridyl)-N-phenyl-thiourea ; N′-2-(3-hydroxy pyridyl)-N-o-tolyl-thiourea ; N′-2-(3-hydroxy pyridyl)-N-p-tolyl-thiourea ; N′-2-(3-hydroxy pyridyl)-N-ethyl-thiourea ; N′-2-(4-methyl pyridyl)-N-phenyl-thiourea ; N′-2-(4-methyl pyridyl)-N-p-tolyl thiourea ; N′-2-(4-methyl pyridyl)-N-ethyl-thiourea ; N′-2-(6-methyl pyridyl)-N-phenyl-thiourea ; N′-2-(6-methyl pyridyl)-M-o-tolyl-thiourea ; N′-2-(6-methyl pyridyl)-N-p-tolyl-thiourea ; and N′-2-(6-methyl pyridyl)-N-ethyl-thiourea ; in acetonitrile was determined by an indirect alkali titration method at twelve hour interval till the value became constant. Relative to acetonitrile, the thiol percent in different solvents of varying polarity (Z-value) from benzene (Z.54.0) to ethylene glycol (Z. 85.1) was evaluated by the spectrophotometric method. From these values, the equilibrium constant and the free energy for tautomerization process were obtained. Equilibrium constant was found to vary approximately linearly with Z.

INTRODUCTION

Understanding of the tautomerism of heterocyclic thioureas is important due to the significant role it might play in many biochemical processes. Some atempts have been made for a detailed understanding of the tautomeric equilibrium in thiocompounds. A number of investigators have studied the existence of thione-enethiol equilibrium in thiourea.[1-8] Recently, the tautomerisms in 4-quinazolyl thioureas [9], N-substituted-N′-pyridyl-thioureas [10] and N-aryl-N′-2-(5-halo-pyridyl)-thioureas have been studied.[11] Very little has been reported in the literature on this aspect and hence we thought desirable to study the effect of solvents on the enethiolisation of some N′-2-(substituted-pyridyl)-N-substituted thioureas in different solvents of varying solvent polarity.

EXPERIMENTAL

The substituted thioureas, *viz*. N′-2-(3-hydroxypyridyl)-N-phenyl-thiourea, (HPPTuH) : N′-2-(3-hydroxypyridyl)-N-p-tolyl thiourea, (HPOTTuH) ; N′-2-(3-hydroxypyridyl)-N-p-tolyl-thiourea, (HPPTTuH) ; N′-2-(3-hydroxy pyridyl)-M-ethyl-thiourea, (HPETuH) ; N′-2-

(4-methylpyridyl)-N-phenyl-thiourea, (4MPPTuH); N′-2-(4-methylpyridyl)-N-o-tolyl-thiourea (4MPOTTuH); N′-2-(4-methyl pyridyl)-N-p-tolyl-thiourea, (4MPPTTuH); N′-2-(4-methylpyridyl)-N-ethyl-thiourea, (4MPETuH); N′-2-(6-methyl pyridyl)-N-phenyl-thiourea(6MPPTuH); N′-2-(6-methyl pyridyl)-N-otolyl-thiourea, (6 MPOTTuH); N′-2-(6-methylpyridyl)-N-p-tolyl-thiourea, (6 MPPTTuH); N′-2-(6-methyl pyridyl)-N-ethyl-thiourea, (6 MPETuH) were synthesized as outlined in our earlier paper.[12] All chemicals used were either of BDH, AnalaR or E. Merck GR quality. Acetonitrile (Riedel) was dried over calcium chloride and distilled before use. Chloroform was purified by usual methods [13] and dimethyl-sulfoxide as suggested by Kosower.[14] Other solvents used were purified by distillation after drying.[15–16] All the absorbance measurements were made on UV-Vis spectrophotometer, Carl Zeiss, Germany (Model PM Q—3).

Absorption spectra of HPPTuH, HPOTTuH, HPPTTuH, HPETuH, 4MPPTuH, 4 MPOTTuH, 4 MPPTTuH, 4MPETuH, 6 MPPTuH, 6 MPOTTuH, 6MPPTuH and 6 MPETuH were recorded in different solvents and molecular extinction coefficients ($E_{\max}$) at the absorption maxima in each solvent were calculated and the data reported in Tables 1—7. From the $E_{\max}$ thus obtained, the percentage of enol contents of these β-diketones was calculated in different solvents using the equation[17]

$$\%\ \text{thiol} = \frac{E_{\max}}{E_e} \times 100 \tag{1}$$

where $E_{\max}$ is the observed molar absorptivity and E_e is that of pure enethiol. E_e for these compounds was calculated from their $E_{\max}$ in acetonitrile and percent enethiol in the same solvent (Table 8) reported earlier[18] (taken as standard). These values of E_e, permit the evaluation of the

Table 1

Tautomeric equilibria of N′-2-(3-hydroxypyridyl)-N-phenyl thiourea (HPPTuH) in various solvents

Solvent	Z	Dielectric constant (D)	λ max (nm)	$E_{\max}$ ($\mathrm{L \cdot mol^{-1} \cdot cm^{-1}}$)	% Enethiol	K_{eq}	G ($\mathrm{cal \cdot mol^{-1}}$)
Dioxane (Diox)	—	2.21	255	20133	25.80	0.3477	625.99
Benzene (BZ)	54.0	2.28	291	18871	27.53	0.3799	573.59
Chloroform (CF)	63.2	4.81	252	17356	29.93	0.4271	504.15
Acetic acid (AcOH)	79.2	6.15	255	15016	34.60	0.5291	377.12
Dichloromethane (DM)	64.2	8.93	253	19890	26.12	0.3535	574.55
Dichloroethane (DE)	65.2	10.36	250	17782	29.21	0.4126	524.61
1-Butanol (n-BuOH)	77.7	17.51	254	26952	19.27	0.2387	848.79
2-Propanol (i-PrOH)	76.3	19.92	256	18632	27.88	0.3866	563.09
Ethyl alcohol (EtOH)	79.6	24.55	255	17860	29.09	0.4102	528.02
Methyl alcohol	83.6	32.70	252	17114	30.35	0.4358	492.14
Acetonitrile (AN)	71.3	37.50	256	17610	29.50	0.4184	516.29
Ethylene glycol (EG)	85.1	37.70	251	17325	29.99	0.4284	502.64
Dimethyl formamide (DMF)	68.5	36.71	260	13374	38.84	0.6351	268.92
Dimethyl sulfoxide (DMSO)	71.1	46.68	262	13722	37.86	0.6093	293.62

Table 2

Tautomeric equilibria of N′-2-(3-hydroxypyridyl)-N-*p*-tolyl-thiourea in various solvents (HPPTTuH)

Solvent	λ max (nm)	$E_{\max}$ ($L \cdot mol^{-1} \cdot cm^{-1}$)	% Enethiol	K_{eq}	G ($cal \cdot mol^{-1}$)
Diox	256	20224	23.95	0.3149	684.80
BZ	275	19371	25.00	0.333	651.09
CF	257	19428	24.93	0.3321	653.27
AcOH	258	16409	29.51	0.4186	516.02
DM	255	20010	24.20	0.3193	676.47
DE	256	18269	26.51	0.3607	604.29
n-BuOH	256	27490	17.62	0.2139	913.87
i-PrOH	263	18230	26.56	0.3617	602.65
EtOH	255	17650	27.44	0.3782	576.19
MeOH	260	17806	27.20	0.3736	583.42
AN	253	17482	27.70	0.3831	568.54
EG	253	18290	26.48	0.3602	605.11
DMF	263	14440	33.54	0.5047	405.23
DMSO	261	13645	35.49	0.5501	354.06

percent enethiol content of these substituted pyridyl thioureas in different solvents of varying polarity. The results are reported in Tables 1—7. From these data the values of equilibrium constant (enethiol/thione) for each compound in different solvents were calculated and $\log K_e$ was plotted as a function of Z-value.[19]

The free energy change of tautomerisation (ΔG) was calculated from the relationship

$$\Delta G = -RT \ln K_{eq} \qquad (2)$$

where R is the universal gas constant, and T the absolute temperature.

The values of K_{eq} and ΔG in various solvents are reported in Tables 1—7.

RESULTS AND DISCUSSION

The percent enethiol of HPPTuH, HPOTTuH, HPPTTuH, HPETuH, 4MPPTuH, 4MPOTTuH, 4MPPTTuH, 4MPETuH, 6MPPTuH, 6MPOTTuH, 6MPPTuH and 6MPETuH in acetonitrile at various time intervals was determined as reported in our earlier paper.[18] The enethiol, equilibrium constant (K_{eq}), free energy of tautomerisation (ΔG) in various solvents are reported in Tables 1—7. UV spectra of all these compounds show a peak in the 252 — 280 nm range[20] which has been assigned to the thiocarbonyl transition. In the thiol form this peak should have the minimum molar extinction coefficient.

There are two groups i.e. phenolic —OH and —CS— in the compounds HPPTuH, HPOTTuH, HPPTuH and HPETuH. Out of these two —CS— group gives rise to the formation of a thiol group due to the proton shift from the adjacent nitrogen to the thiocarbonyl group. The enethiol content in these compounds represents the sum of percentage of phenolic —OH group and enethiol content percent. The percentage of —OH group in these compounds was estimated and this was subtracted from the total thiol content in order to get the percent of enethiol content

Table 3

Tautomeric equilibria of N′-2-(3-hydroxypyridyl)-N-o-tolyl and N′-2-(3-hydroxypyridyl)-N-ethyl-thioureas in various solvents

Solvent	HPOTTuH					HPETuH				
	λ_{max} (nm)	E_{max} ($L \cdot mol^{-1} \cdot cm^{-1}$)	% Enethiol	K_{eq}	G ($cal \cdot mol^{-1}$)	λ_{max} (nm)	E_{max} ($L \cdot mol^{-1} \cdot cm^{-1}$)	% Enethiol	K_{eq}	G ($cal \cdot mol^{-1}$)
Diox	251	19624	26.80	0.3661	595.42	241	15312	29.47	0.4179	517.24
BZ	270	19612	26.82	0.3665	594.74	270	15012	30.06	0.4298	500.32
CF	252	19210	27.38	0.3770	578.10	253	15200	29.68	0.4221	511.10
AcOH	250	16728	32.41	0.4795	435.93	—	—	—	—	—
DM	252	19390	27.12	0.3721	585.87	256	15112	29.86	0.4257	506.06
DE	253	18491	28.44	0.3974	546.85	254	15612	28.90	0.4065	533.48
n-BuOH	256	27612	19.05	0.2353	857.25	256	24910	18.11	0.2212	893.95
i-PrOH	266	18800	27.98	0.3885	560.22	261	15810	28.54	0.3994	543.85
EtOH	252	17810	29.53	0.4190	515.47	262	16210	27.83	0.3856	564.59
MeOH	251	17916	29.36	0.4156	520.38	260	15605	28.91	0.4067	533.07
AN	250	19188	27.41	0.3776	577.14	260	19532	23.10	0.3004	712.63
EG	249	17918	29.35	0.4154	520.65	248	13870	32.53	0.4821	432.38
DMF	264	14740	35.68	0.5547	349.29	259	11441	39.44	0.6513	254.05
DMSO	261	13460	39.07	0.6412	263.33	254	10890	41.43	0.7074	205.21

Table 1

Tautomeric equilibria of N′-2-(4-methylpyridyl)-N-phenyl- and N′-2-(4-methylpyridyl)-N-p-tolyl-thioureas in various solvents

Solvent	4MPPTuH					4MPPTuH				
	λ_{max} (nm)	E_{max} ($L \cdot mol^{-1} \cdot cm^{-1}$)	% Enethiol	K_{eq}	G ($cal^{-1} mol$)	λ_{max} (nm)	E_{max} ($L \cdot mol^{-1} \cdot cm^{-1}$)	% Enethiol	K_{eq}	G ($cal\ mol^{-1}$)
Diox	252	18175	26.14	0.3539	615.48	255	18443	24.57	0.3257	664.73
BZ	273	19632	24.20	0.3193	676.47	275	20442	22.16	0.2847	744.42
CF	261	20120	23.61	0.3091	695.71	264	20853	21.73	0.2776	756.42
AcOH	263	22532	21.08	0.2671	782.21	263	23103	19.61	0.2493	836.10
DM	262	23298	20.39	0.2561	807.18	261	24414	18.56	0.2279	876.35
DE	263	22278	21.32	0.2710	773.61	266	23780	19.05	0.2353	857.25
n-BuOH	256	27160	17.49	0.2120	919.20	257	27580	16.43	0.1966	963.81
i-PrOH	266	23750	20.00	0.2500	821.50	267	22301	20.32	0.2550	809.77
EtOH	267	21821	21.77	0.2783	757.92	267	22509	20.13	0.2520	816.73
MeOH	260	21250	22.36	0.2880	737.59	263	22681	19.98	0.2497	822.19
AN	262	23083	20.58	0.2591	800.22	262	24558	18.45	0.2262	880.72
EG	260	22177	21.42	0.2726	770.20	260	22872	19.81	0.2470	828.60
DMP	268	27798	17.09	0.2061	935.84	266	29030	15.61	0.1850	1136.27
MOD	270	23620	20.11	0.2517	817.41	269	25442	17.81	0.2167	906.10

Table 5

Tautomeric equilibria of N′-2-(4-methylpyridyl)-N-o-tolyl-and N′-2-(4-methylpyridyl)-N-o-ethyl-thioureas in various solvents

Solvent	4 MPOTTuH					4 MPOTTuH				
	λ_{max} (nm)	E_{max} ($L \cdot mol^{-1} (cm^{-1})$)	% Enethiol	K_{eq}	G ($cal\ mol^{-1}$)	λ_{max} (nm)	E_{max} ($L \cdot mol^{-1}\ cm^{-1}$)	% Enethiol	K_{eq}	G ($cal\ mol^{-1}$)
Diox	253	18510	24.01	0.3160	682.61	241	19951	15.13	0.1783	1021.66
BZ	272	20139	22.06	0.2830	747.96	280	20673	14.60	0.1710	1046.49
CF	266	20740	21.42	0.2726	770.20	269	16920	17.84	0.2171	905.01
AcOH	265	23568	18.85	0.2323	863.89	265	18840	16.02	0.1908	981.55
DM	259	23770	18.69	0.2299	871.17	267	20912	14.44	0.1688	1054.13
DE	264	23675	18.77	0.2311	868.03	268	17221	17.33	0.2126	917.56
n-BuOH	262	25822	17.21	0.2079	930.66	262	21290	14.18	0.1552	1066.96
i-ProH	265	21912	20.28	0.2544	811.13	267	22544	13.39	0.1546	1106.25
EtOH	267	22912	19.39	0.2405	844.43	266	20796	14.52	0.1699	1050.31
MeOH	264	22560	19.70	0.2453	832.69	263	19500	15.48	0.1832	1005.56
AN	260	24414	18.20	0.2225	890.41	266	19886	15.18	0.1790	1019.34
EG	262	22336	19.89	0.2483	835.46	261	20350	14.83	0.1741	1035.85
DMF	267	28424	15.63	0.1863	998.88	273	27265	11.07	0.1245	1234.51
DMSO	270	24750	17.95	0.2188	900.37	274	21227	14.22	0.1658	1064.78

Table 6

Tautomeric equilibria of N′-2-(6-methylpyridyl)-N-phenyl- and N′-2-(6-methylpyridyl)-N-o-tolyl thioureas in various solvents

Solvent	6MPPTuH					6MPPTTuH				
	λ_{max} (nm)	E_{max} $(L \cdot mol^{-1} cm^{-1})$	% Enethiol	K_{eq}	G $(cal \cdot mol^{-1})$	λ_{max} (nm)	E_{max} $(L \cdot mol^{-1} \cdot cm^{-1})$	% Enethiol	K_{eq}	G $(cal \cdot mol^{-1})$
Diox	252	19746	20.84	0.2633	790.67	253	20166	20.75	0.2618	794.22
BZ	272	18686	22.02	0.2824	749.33	271	19478	21.48	0.2736	768.02
CF	263	19630	20.97	0.2653	786.32	263	19910	21.01	0.2660	784.67
AcOH	264	21658	19.00	0.2346	856.16	264	22650	18.47	0.2265	879.90
DM	262	23943	17.19	0.2076	931.47	262	23698	17.65	0.2143	912.78
DE	264	21303	19.32	0.2345	859.43	264	21960	19.05	0.2353	857.25
n-BuOH	260	25610	16.07	0.1915	979.50	256	26550	15.76	0.1871	993.28
i-PrOH	265	21041	19.56	0.2342	837.74	265	18902	22.13	0.2842	745.51
EtOH	267	22608	18.20	0.2225	890.41	267	19512	21.44	0.2729	769.52
MeOH	263	22300	18.46	0.2264	880.17	262	23700	17.65	0.2143	912.78
AN	260	20224	20.35	0.2555	808.54	262	23772	17.60	0.2136	914.69
EG	258	20392	20.18	0.2528	814.82	259	20659	20.25	0.2539	812.36
DMF	266	26494	15.53	0.1839	1003.38	265	28673	14.59	0.1708	1047.31
DMSO	268	24842	16.57	0.1986	957.81	269	23300	17.96	0.2189	900.09

Table 7

Tautomeric equilibria of N′-2-(6-methylpyridyl)-N-o-tolyl- and N′-2-(6-methylpyridyl)-N-ethyl-thioureas in various solvents

Solvent	6MPPTTuH					6MPETuH				
	λ_{max} (nm)	E_{max} $(L \cdot mol^{-1} cm^{-1})$	% Enethiol	K_{eq}	G $(cal \cdot mol^{-1})$	λ_{max} (nm)	E_{max} $(L \cdot mol^{-1} cm^{-2})$	% Enethiol	K_{eq}	G $(cal \cdot mol^{-1})$
Diox	244	19980	20.00	0.2500	821.50	241	17970	15.70	0.1862	996.15
BZ	271	19354	20.65	0.2602	797.76	276	15962	17.68	0.2148	911.42
CF	262	19540	20.46	0.2572	804.72	276	16628	18.05	0.2203	896.41
AcOH	261	22480	17.78	0.2162	807.46	263	16320	17.29	0.2090	927.65
DM	258	21843	18.30	0.2240	886.59	266	17130	16.47	0.1972	955.22
DE	262	21970	18.28	0.2237	883.27	266	17253	16.35	0.1955	967.22
n-BuOH	258	26230	15.24	0.1798	1016.61	258	19050	14.81	0.1738	1036.94
i-PrOH	264	19810	20.18	0.2528	814.82	262	18672	15.11	0.1780	1022.75
EtOH	267	19670	20.32	0.2550	809.77	267	16590	17.01	0.2050	938.98
MeOH	262	23945	16.76	0.2013	949.89	264	19500	14.47	0.1692	1052.77
AN	258	22974	17.40	0.2107	922.88	266	19064	14.80	0.1737	1037.22
EG	259	19960	20.03	0.2505	820.28	263	19042	14.82	0.1740	1036.26
DMF	266	27174	14.71	0.1725	1041.31	273	24603	11.47	0.1296	1210.77
DMSC	267	22836	17.51	0.2123	946.89	271	19874	14.20	0.1655	1065.87

due to the thiol group only. (Tables 1—3). This was found to be in the order, HPPTuH, HPPTTuH, HPOTTuH, HPETuH.

There is only one thiol group in the compounds *viz.* 4MPPTuH, 4MPPTTuH, 4MPPTTuH, 4MPETuH, 6MPPTuH, 6MPOTTuH, 6MPPTTuH and 6HPETuH and this group is formed due to the proton shift from the adjacent nitrogen to the thiocarbonyl group as represented below:

Table 8

% Enethiol, E_e and E_{max} for some N′-2-(substituted--pyridyl)-N-substitute-thioureas in acetonitrile

Compound	% Enethiol	E_{max} ($L \cdot mol^{-1} \cdot cm^{-1}$)	E_e
HPPTuH	29.50	17610	5194.95
HPPTTuH	27.70	17482	4842.51
HPOTTuH	27.41	19188	5259.43
HPETuH	23.10	19532	4511.89
4MPPTuH	20.58	23083	4750.48
4MPPTTuH	18.45	24558	4530.95
4MPOTTuH	18.20	24414	4443.35
4MPETuH	15.18	19886	2018.69
6MPPTuH	20.35	20224	4115.58
6MPPTTuH	17.60	23772	4183.87
6MPOTTuH	17.40	22974	3997.48
6MPETuH	14.89	19064	2821.47

$$R^1-NH-CS-NH-R^2$$

I

$$R^1-NH-C(SH)=N-R^2$$

II

$$R^1-N=C(SH)-NH-R^2$$

III

The enethiol content of these compounds was found to be in the order: 4MPPTuH, 6MPPTTuH, 4MPOTTuH, 6MPPTTuH, 6MPOTTuH, 4MPETuH, 6MPETuH. In this series of compounds 4MPPTuH has the maximum per cent of enethiol while 6MPETuH has the least.

The difference in enethiol content of these compounds appears to be due to the presence of the different substituents at N-atom. It is also shown that for the substituent at N-atom, the enethiol content varies as phenyl-*o*-tolyl. It was suggested by Prasad [10] and Kashyap [11] that in the process of thiolisation hydrogen was provided by —NH— group. In the thiocarbonyl group the sulphur atom is more electronegative than carbon, and this negatively charged sulphur can now accept a proton easily and hence due to the case of acceptance of a proton, the enethiol per cent is increased. Thus, the total enethiol is found to be in the order: HPPTuH, HPPTTuH, HPOTTuH, HPETuH, 4MPPTuH, 6MPPTuH, 4MPPTTuH, 4MPOTTuH, 6MPPTTuH, 6MPOTTuH, 4METuHy, 6MPETuH.

If there is a tolyl group instead of phenyl at N-position, then due to the higher electron donating power of the former, the proton shift from the nitrogen to sulphur is easier in the phenyl substituted compounds as compared to the N-tolyl substituted compounds, hence the enethiol percentage in the case of phenyl substituted compounds is greater than that corresponding to tolyl substituted compound.

The enethiol per cent in various solvents (Tables 1—7) shows that the enethiol form predominates in non-polar solvents while the thione form is more abundant in the polar solvents. This is in agreement with the results obtained by Prasad [10] and Kashyap.[11] In the case of certain thioureas, —SH— group though has only very weak hydrogen bonding is still capable of intramolecular hydrogen bonding. This presumably stabilizes the thiol form in non-polar solvents. The intramolecular hydrogen bonded species may be represented as below

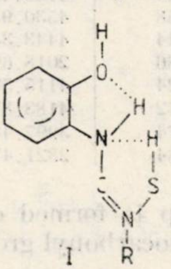

I

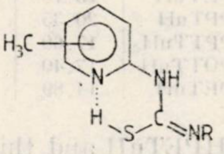

II

In general, an equilibrium involving two or more species does not respond in a simple way to the change of solvents, but the thiolisation of HPPTuH, HPOTTuH, HPPTTuH, HPETuH, 4MPPTuH, 4MPOTTuH, 4MPPTTuH, 4MPETuH, 6MPPTuH, 6MPOTTuH, 6MPPTTuH and 6MPETuH is an exception because the position of equilibrium is largel, determined by the interaction of thiol form with the solvent

$$\text{Thione} \rightleftharpoons \text{Enethiol}$$

and

$$K_{\text{eq}} = \frac{\text{enethiol}}{\text{thione}}$$

Since the thione form of a pyridyl thiourea is almost invariably more polar than the enethiol, the enethiol : thione ratio for a given pair of tautomers at equilibrium in solution depends markedly on the polarity of the solvents and this ratio tends to be greater in less polar solvents.[21] The strong interaction between the solvent and the thio-carbonyl group could reduce the extent of thiol formation in polar solvents such as dimethylformamide; it was observed by Dewar [21] that the more polar tautomer has a higher solvation energy in polar solvents, which facilitates its formation in polar solvents. Therefore, the N—CS—NH group being more polar than the group N=C(SH)—N predominantes in polar solvents. As the solubility of the thiol form relative to the thione form is much more in less polar solvents, the tendency to solvate decreases from ethylene glycol to dioxane and consequently the thiol percentage increases from ethylene glycol to dioxane. This is observed in 4MPPTuH, 4MPOTTuH, 4MPPTTuH, 4MPETuH, 6MPPTuH, 6MPOTTuH, 6MPPTTuH, and 6MPETuH, while in other compounds the trend is reverse. This is due to the intramolecular hydrogen bonding in these compounds. In less polar solvents the ability of thiol form to exist in the intramolecular hydrogen bonded configuration (I and II) is decisive as the H-bond formation reduces the polarity of the thiol form. It has been found that the plot of K_{eq} *vs* Z gave an approximately linear fit. The best straight line in each case was obtained by a least square analysis. The deviation from the regression line cannot be explained due to the large size of the molecule and the lack of data on the solvent solute interactions. This cannot be attributed to the specific solvent-solute interactions. The abnormal results in the case of DMF, BuOH and DMSO, however, may be attributed to the charge transfer complex formation between the solvents and the thione form which reduces the extent of thiolisation to some extent in the case of 4MPPTuH, 4MPOTTuH, 4MPPTTuH, 4MPRTuH, 6MPPTuH, 6MPOTTuH, 6MPPTTuH and 6MPETuH.

ACKNOWLEDGEMENT. Our thanks are due to the Principal, D. N. College, Hissar and Dr. S. K. Arora, Biochemist, Haryana Agricultural University, Hissar for providing necessary facilities to carry out the present work. Our thanks are also due to U.G.C. (New Delhi) for giving us financial assistance for completing this project.

REFERENCES

[1] B. Rathke, *Chem. Ber.*, **14**, 1776 (1881).

[2] R. Bernthson and. J. Klinger, *Chem. Ber.*, **11**, 92, (1878) ; **12**, 575 (1879).

[3] R. D. Gupta and J. B. Jha, *Indian Chem. Soc.*, **27**, 407 (1950).

[4] P. K. Mathur, *M.Sc. Thesis, Rajputana University* (1951).

[5] E. Angelescu and F. Cornea, *Analele Univ. "C. I. Parhon" București, Ser. Știint Nat.*, **15**, 87 (1957), *Chem. Abstr*, **53**, 3841 (1959).

[6] E. A. Wernet, *J. Chem. Soc.*, **1922**, 2180.

[7] T. L. Davis and H. W. Underwood, *J. Amer. Chem., Soc.*, **44**, 2595 (1922).

[8] E. Angelescu, F. Cornea and T. Brutaru, *Analele Univ. "C. I. Parhon", București Ser. Știint. Nat. Chim.*, **11**, 121 (1962) ; *Chem. Abstr.*, **60**, 13111g (1964).

[9] M. Wulf and R. Walter, *Chem. Ber.*, **106**, 471–83 (1973).

[10] C. S. G. Prasad, *Ph. D. Thesis, B.I.T.S., Pilani, India* (1973).

[11] B. C. Kashyap, *Ph. D. Thesis, B.I.T.S., Pilani, India* (1974).

[12] D. P. Khurana, J. D. Gauba, A. D. Taneja and J. S. Tyagi, *Chemical Era.*, XIV, (9), 383–86 (1978).

[13] A. I. Vogel, "Practical Organic Chemistry", 3rd Edition, Longmans, London, 1962.

[14] E. M. Kosower, *J. Amer. Chem. Soc.*, **80**, 3253 (1958).

[15] C. R. W. Strout, H. W. Wilson and M. I. Parry-Jones, "Chemical Analysis", 1962, Vol. 2, pp. 218–19, Claredon Press, Oxford.

[16] A. Weissberger, E. S. Proskaur J. Riddick and E. E. Toops Jr. "Technique of Organic Chemistry" Vol. 3, Interscience New York, 1955.

[17] A. S. M. Murthy, A. Balasubramanium and C. N. R. Rao, *Canad. J. Chem.*, **40**, 2267 (1962).

[18] O. P. Khurana, A. D. Taneja and J. S. Tyagi. *Chemical Era*, 1984 (accepted).

[19] E. M. Kosower, *J. Amer. Chem. Soc.*, **80**, 3267 (1958).

[20] O. P. Khurana, A. D. Taneja and J. S. Tyagi, *J, Chem. Soc.* (accepted).

[21] E. S. Gould, "Mechanism and Structure in Organic Chemistry", Hold Reinhart and Winston, New York, 1965.

[22] M. J. S. Dewar, "Electronic Theory of Organic Chemistry", Clarendon Press, Oxford 1949.

Revue Roumaine de Chimie, 31, *8*, 773–785 (1986)

ÉLARGISSEMENT DES TRANSITIONS ET ORDRE RELATIF DES HAUTEURS DE BANDES. APPLICATION À L'INCIDENCE DES INTERACTIONS LOINTAINES ET DE LA SOLVATATION SUR LE SPECTRE UV DE QUELQUES PHÉNYLALCOYLAMINES

BERNARD VIDAL* et CHRISTIAN DUPRET
Laboratoire de Spectroscopie de la Réactivité Chimique. Centre de Spectrochimie, UER de Chimie, Bât C2. Université des Sciences et Techniques de Lille. 59655 — Villeneuve d'Ascq Cédex, France

Reçu le 3 juin 1985

Lorsque des transitions s'élargissent sous l'influence d'une perturbation (solvatation, interaction intramoléculaire par exemple), cet élargissement provoque une diminution des coefficients d'extinction molaire, d'autant plus marquée que les transitions sont étroites. Il peut même parfois y avoir inversion dans le rapport des coefficients. L'étude est illustrée par le cas des spectres du chromophore benzène de plusieurs *n*-phénylalcoylamines et *n*-phénylalcoylammoniums. Le changement de solvent pour ces derniers (méthanol-eau) peut conduire à une perturbation en fréquence de l'ordre de grandeur de la bande 00. Nous avons pu mettre en évidence aussi que le méthanol, dans le cas de ces molécules, permet un meilleur transfert que dans l'eau des effects électroniques à longue distance de l'auxochrome terminal (NH_3^+) vers le chromophore.

The broadening of transitions under perturbations causes a decrease of their molar extinction coefficients (ε). The decrease is all the more important, for a given perturbation, as the transitions are narrower. So when considering the broadening of two transitions with $\varepsilon_1 > \varepsilon_2$, for large perturbations, if the first transition is much narrower than the second one, ε_1 may become lower than ε_2 although there is no change in the intensities. That occurrence which alters thorougly a spectrum, is illustrated with the "secondary transition" (towards 260 nm) of the benzenic chromophore in several *n*-phenylalkylamines and *n*-phenylalkylammoniums. The study of these spectra shows that under solvation effects there are inversions in some relative ε values, without intensity change. Modifying the medium may introduce a perturbation whose effect on the frequency range is as large as the width of the 00 band. We show also, by taking into account the broadening of transitions — and we explain the phenomenon — that methanol allows a better $\Phi \Leftrightarrow NH_3^+$ interaction than water.

La largeur des transitions électroniques peut avoir des origines si diverses qu'il est souvent difficile d'analyser les facteurs qui la définissent. Ces facteurs peuvent inclure : la vitesse de conversion de l'énergie relative à l'état excité en énergie vibrationnelle du substituant qui sera ensuite transmise au milieu, [1a] le recouvrement fortuit de bandes, le degré de tension dans les cycles qui peut gêner certaines vibrations.[2] Les phénomènes de solvatation souvent, en particulier pour les molécules organiques, conduisent aux effets les plus visibles.[1b] A côté de ces interactions intermoleculaires les échanges, les couplages, intramoléculaires peuvent aussi dans certains cas modifier les largeurs des bandes, par les perturbations qu'ils apportent aux niveaux électroniques. [3] La complexité du problème fait que peu d'attention lui a été porté, d'autant qe la largeur des transitions, du fait des recouvrements est parfois difficilement mesurable. Il a été possible dans certains cas d'établir des paramètres utiles pour évaluer les largeurs en termes de « structure fine ».[4-6] Les caractéristiques retenues pour le spectre UV-visible d'une molécule organique sont donc très souvent les longueurs d'onde des principales bandes, et les hauteurs des bandes ou des massifs mesurées par leurs coefficients d'extinction molaire. En théorie il vaudrait mieux disposer des intensités intégrées, des forces d'oscillateur. Toutefois l'intégration masque l'évolution d'intensité entre les différentes bandes d'une même transition. Du fait des superpositions avec les transitions voisines il faut souvent établir des corrections délicates à estimer. Le sommet des courbes lissées [7] peut aider à résoudre certains problèmes, mais il est parfois entaché de subjectivité. Aussi, les coefficients d'extinction molaire, malgré leur caractère fruste sont, dans bien des cas, ce qui permet de répérer au mieux les intensités, encore qu'il faille garder à l'esprit leurs limites même, dans la mesure où il y a à la fois contribution de la largeur des bandes et de leur hauteur à l'intensité. Nous voudrions précisément étudier ici qu'elle est l'incidence d'une élargissement éventuel sur les hauteurs relatives des différentes bandes, ou groupes de bandes, dans un spectre. Nous montrerons ce résultat surprenant, qu'un simple élargissement peut conduire à l'inversion des hauteurs relatives des pics, alors qu'aucune modification d'intensité n'est intervenue.

---

* Auteur à qui la correspondance doit être adressée.

ÉLARGISSEMENT DES TRANSITIONS

L'incidence sur une transition d'une perturbation donnée, provoquant un élargissement, ne peut être traitée de façon mathématiquement rigoureuse pour des courbes spectroscopiques d'allure gaussienne. Nous prendrons donc d'abord comme modèle pour le contour d'une transition une courbe d'allure lorentzienne. Ce contour aura la forme :

$$\varepsilon = \varepsilon_M \frac{1}{1 + \left[\dfrac{2(\nu - \nu_M)}{L}\right]^2}$$

où ε_M est la hauteur du maximum de la courbe, ν_M la fréquence à laquelle correspond ce maximum et L la largeur totale à mi-hauteur (figure 1). Posons $x = \nu - \nu_M$; l'expression ci-dessus devient :

$$\varepsilon = \varepsilon_M \frac{1}{1 + \left(\dfrac{2x}{L}\right)^2}$$

Soit une perturbation qui interdit de distinguer les fréquences au sein d'un intervalle de fréquences Δx centré sur chaque valeur de x. La valeur moyenne ε_m de la hauteur dans cet intervalle est $\varepsilon_m = \Delta S / \Delta x$ où ΔS correspond à l'intégration de la courbe entre les bornes x_1 et x_2 de l'intervalle Δx. Cette valeur ε_m peut s'exprimer ainsi :

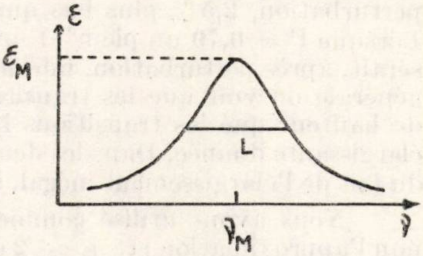

Fig. 1. — Courbe d'allure lorentzienne. ε_M : maximum de la courbe ; L : largeur totale à mi-hauteur ; ν_M fréquence correspondant au maximum de la courbe.

$$\varepsilon_m = \frac{\varepsilon_M}{\Delta x} \int_{x_1}^{x_2} \frac{\mathrm{d}x}{1 + \left(\frac{2x}{L}\right)^2}$$

cette expression se transforme après intégration en :

$$\varepsilon_m = \frac{\varepsilon_M}{\Delta x} \frac{L}{2} \left[\text{Arc tg} \frac{2x_2}{L} - \text{Arc tg} \frac{2x_1}{L} \right]$$

or $x_1 = x - \Delta x/2$ et $x_2 = x + \Delta x/2$; de plus si on considère l'évolution de hauteur du maximum, c'est-à-dire si l'on se place au point $x = 0$, la perturbation conduit à une nouvelle hauteur ε'_M :

$$\varepsilon'_M = \frac{\varepsilon_M}{\Delta x} L \,\text{Arc tg} \frac{\Delta x}{L}$$

Si on veut comparer la hauteur de deux transitions, avant et après perturbation, nous formerons les rapports :

$$\frac{\varepsilon'_{M_1}}{\varepsilon_{M_2}} = \frac{\varepsilon_{M_1}}{\varepsilon_{M_2}} \frac{L_1}{L_2} \frac{\text{Arc tg} \dfrac{\Delta x}{L_1}}{\text{Arc tg} \dfrac{\Delta x}{L_2}}$$

soit, en posant $L_1 = nL$, $L_2 = L$ et $\Delta x = m\,L$:

$$\frac{\varepsilon'_{M_1}}{\varepsilon'_{M_2}} = \frac{\varepsilon_{M_1}}{\varepsilon_{M_2}} \,\mathrm{n}\, \frac{\text{Arc tg} \dfrac{m}{n}}{\text{Arc tg}\, m}$$

Désignons par Γ le rapport des Arc tg, multiplié par n. On voit que si $n = 0{,}1$ et $m = 0{,}05$ le facteur Γ qui affecte le rapport des hauteurs est de 0,928. Si $n = 0{,}1$ et $m = 0{,}1$ $\Gamma = 0{,}788$. Dans le premier cas si le pic ε_1 est 5 % plus élevé que le pic ε_2 avant la perturbation, il sera, après perturbation, 2,5 % plus bas que ε_2. Il y aura eu dans ce cas inversion. Lorsque $\Gamma = 0{,}79$ un pic n° 1 qui serait 15 % plus haut qu'un pic n° 2 serait, après perturbation, inférieur de 9 % à ce même pic n° 2. De façon générale on voit que les transitions les plus étroites diminuent plus vite de hauteur que les transitions larges sous l'influence d'une perturbation élargissante donnée. Dans les deux cas choisis comme exemple il y a même, du fait de l'élargissement inégal, inversion des hauteurs de pics.

Nous avons utilisé comme définition de ε_m le rapport $\Delta S/\Delta x$ et non l'approximation $(\varepsilon_1 + \varepsilon_2)/2$ où ε_1 et ε_2 sont les valeurs de ε aux bornes de Δx. Pour de petites valeurs de Δx la différence n'est pas très sensible entre les deux traitements. Par contre pour de grandes valeurs le facteur correctif Γ est beaucoup trop petit. Il surestime donc les effets de la perturbation sur les rapports de hauteur. Considérons par exemple une perturbation hypothétique égale à la largeur du pic étroit. Plaçons nous au sommet de la transition. La valeur pour ce sommet sera $(\varepsilon_1 + \varepsilon_2)/2 = = \varepsilon_M/2$. Ce faisant on néglige toute la moitié supérieure de la courbe. Ainsi Γ qui prend la forme $\Gamma' = n^2(1 + m^2)/(n^2 + m^2)$ donne pour $n = 0{,}1$ et $m = 0{,}05$: $\Gamma' = 0{,}800$ au lieu de la valeur rigoureuse $\Gamma = 0{,}928$. Pour $n = 0{,}1$ et $m = 0{,}1$ on obtient $\Gamma' = 0{,}50$ au lieu de $\Gamma = 0{,}788$.

Pour modéliser une courbe d'absorption nous avons pris une lorentzienne. Comme en général les spectres électroniques en phase liquide, en particulier les spectres organiques, sont la superposition de nombreuses bandes, il importe peu de faire le calcul sur une gaussienne ou une lorentzienne pour obtenir une indication sur le sens de l'évolution du spectre. En général cependant, une transition électronique isolée tend vers un contour gaussien lorsqu'elle perd sa quantification vibrationnelle sous l'influence des perturbations. Il en est de même pour une bande de vibration isolée dans la transition électronique. Dans le cas d'une gaussienne l'intégration entre deux bornes n'est pas possible, aussi utiliserons nous un développement limité afin de montrer que l'on arrive bien au même type de résultat qu'avec une lorentzienne. Au lieu de prendre un contour : $e^{-a^2x^2}$ où $a = \dfrac{k}{L} = \dfrac{1{,}665}{L}$ nous prendrons $1 - a^2x^2 + \dfrac{a^4x^4}{2}$. Soit :

$$\varepsilon_m = \frac{\varepsilon_M}{\Delta x}\int_{x_1}^{x_2}\left(1 - a^2x^2 + \frac{a^4}{2}x^4\right)\mathrm{d}x$$

C'est-à-dire, après intégration, et pour le sommet $x = 0$ de la courbe :

$$\varepsilon'_M = \varepsilon_M\left(1 - \frac{a^2\,\Delta x^2}{12} + \frac{a^4\,\Delta x^4}{160}\right)$$

Le rapport de deux pics après perturbation sera donc en fonction des paramètres m et n :

$$\frac{\varepsilon'_{M_1}}{\varepsilon'_{M_2}} = \frac{\varepsilon_{M_1}}{\varepsilon_{M_2}} \frac{1 - \dfrac{k^2m^2}{12n^2} + \dfrac{k^4m^4}{160\,n^4}}{1 - \dfrac{k^2m^2}{12} + \dfrac{k^4m^4}{160}}$$

soit pour $m = n = 0{,}1$ un facteur de 0,82 au lieu de 0,79 obtenu pour une lorentzienne. Si $n = 0{,}1$ et $m = 0{,}05$ le facteur est de 0,947. Il était de 0,928 pour une lorentziene. L'effet sur une gaussienne est donc légèrement plus faible que sur une lorentzienne.

Le traitement que nous développons ci-dessus pourrait s'appliquer aux courbes de résonance des circuits oscillants. Ceci explique que les coefficients de surtension des circuits résonants chutent d'autant plus vite que le pic de résonance est étroit, sous l'influence d'une perturbation exercée par l'introduction d'une résistance en parallèle dans le circuit. De même si un spectre est enregistré avec des fentes dont la bande passante trop supérieure à la largeur propre des transitions, la hauteur des pics étroits est diminuée par rapport aux pics larges. D'où le danger, pour les hauteurs relatives des pics, de prendre des spectres avec des fentes asservies dont l'écartement dépend de besoins en flux lumineux du détecteur.

Nous avons pris comme exemples numériques des transitions dont les largeurs sont très différentes (rapport de 10) et une perturbation qui serait égale à la moitié de la largeur du pic étroit dans un cas, qui serait égale à la largeur du pic étroit dans l'autre cas.

On pourrait objecter qu'il est rare que des transitions de largeurs extrêmement différentes apparaissent dans un même spectre de molécule organique en solution. C'est certes exact et il s'agit là d'un cas de figure illustratif. On peut néanmoins trouver dans les spectres de la transition secondaire de dérivés du benzène des éléments pour illustrer notre propos. Le benzène est l'un des plus importants chromophores simples. Il possède par ailleurs une structure vibrationnelle très riche, sensible au milieu environnant ce qui fait un outil de choix de ce chromophore pour certaines études de solvant, soit qu'il intervienne comme molécule isolée,[17] soit qu'il s'agisse de certains de ses dérivés simples,[18-20] ou même de molécules plus grosses.[21-23] Réciproquement d'ailleurs, la généralité des phénomènes de solvatation sur les structures chimiques fait de ces phénomènes un outil dont l'intérêt va croissant,[24] et d'autre part l'intérêt du noyau Ø comme révélateur des mécanismes qui sont mis en jeu dans les systèmes moléculaires n'est plus à souligner (par ex :[25]). En ce qui nous concerne, grâce à sa richesse vibrationnelle et à la sensibilité de celle-ci il sert de sonde pour déceler les interactions intramoléculaires à distance entre groupements non liés.[3,8-10,26] Ce sont les variations des coefficients d'extinction molaire de certaines bandes qui permettent d'analyser les interactions lointaines. L'incidence d'un processus d'élargisement ne doit donc pas toujours être négligé lorsqu'on compare des hauteurs de bandes.

EXEMPLES DE VARIATIONS, À INTENSITÉ CONSTANTE, DANS LA RÉPARTITION DES HAUTEURS

La transition secondaire du chromophore benzénique se produit vers 260 nm. Elle apparaît en phase liquide comme la superposition de deux progressions vibrationnelles *A* et *B*.[3] Dans la molécule de benzène la transition est interdite du fait de la symétrie D_{6h}. Seule la progression *A* est observée. Quand on modifie le chromophore en ajoutant un substituant la symétrie s'oriente vers C_{2v} et la transition devient partiellement permise. Une deuxième progression *B* se superpose à *A*. De la superposition de toutes les bandes naît souvent un massif au sein duquel il est parfois difficile de les distinguer les unes des autres. La progression *B* cependant possède une bande 00 vers les grandes longueurs d'onde. *A* n'en possède pas. La bande 00 de *B* peut donc, si elle est assez intense, apparaître comme décalée, distincte, du massif constitué par le recouvrement de toutes les autres bandes. La bande 00 est par nature beaucoup moins large que le massif. Si une perturbation introduit un élargissement, d'après les calculs précédents, la hauteur de la bande 00 devrait être plus affectée que celle du massif, sans qu'il s'agisse d'une modification relative des intensité. Nous avons précisément montré dans un travail antérieur [11] que le spectre de l'acide *para*-fluorophénylacétique ($F-\Phi-CH_2-CO_2H$) présentait une évolution anormale de son intensité en fonction du pH. L'état de protonation de la fonction acide se répercute grâce à une interaction entre groupements non liés à travers les liaisons CH_2, sur le nuage π_Φ et modifie l'intensité de la transition. Sous l'influence d'une structure de solvatation spécifique le coefficient d'extinction molaire ε_{00} de la bande 00 décroît très fortement à pH$=$3,95 d'une part, et très fortement aussi par rapport au maximum de la transition, plus fortement que ce qu'une évolution normale en fonction de l'acidité du milieu laisserait prévoir. Nous avons montré que cela ne provenait pas d'une variation d'intensité, mais que c'était la conséquence d'un élargissement de la transition.

On peut rencontrer d'autres exemples où un élargissement rend dissemblables deux spectres quant à la répartition apparente de leurs intensités vibrationnelles. Considérons ainsi la phénylbutylamine $\Phi(CH_2)_4NH_2$ en milieu méthanol, et en milieu $H_2O + HCl$ (pH $=$ 6). On se trouve en présence dans ce dernier milieu de l'espèce $\Phi(CH_2)_4NH_3^+$. L'intensité, tout au moins sa répartition vibrationnelle, semble très différente pour les deux molécules dans les conditions signalées (Figure 2). Nous pouvons en fait montrer qu'il n'en est rien et que, largeur des bandes mises à part, les deux spectres sont très proches.

En ce qui concerne l'amine dans le méthanol, la bande 00 (système *B*) est supérieure à la première bande du système *A*. Elle est supérieure au groupe confus de bandes situé vers 39250 cm^{-1}, noté α dans ce travail, et issu entre autre du recouvrement de la troisième bande de *B* et de la troisième bande de *A*. Pour l'ammonium la bande 00 est légèrement inférieure à la première bande de *A* réduite à l'état d'épaulement. Elle est nettement inférieure au groupe α.

Nous avons effectué une moyenne mobile [3] sur le spectre de $\Phi(CH_2)_4NH_2$ (méthanol). La moyenne mobile consiste à faire la moyenne de *i* points espacés de $\delta\nu$ cm^{-1} l'un par rapport à l'autre, en décalant d'un

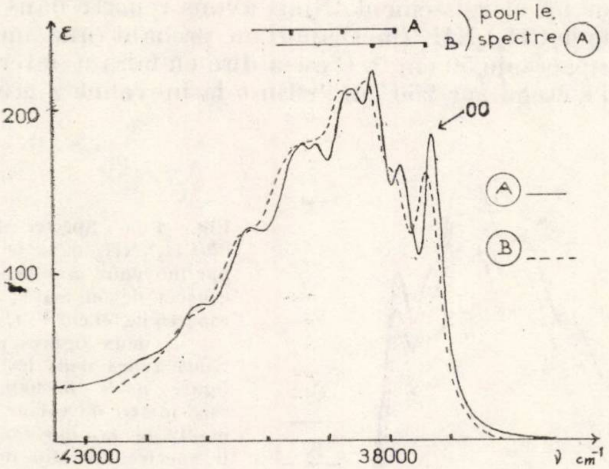

Fig. 2. — Spectres expérimentaux : A — de la phénylbutylamine $\Phi(CH_2)_4NH_3$ en milieu méthanol ($\varepsilon_{00} = 185$) ; B — de la phenylbutylamine en milieu eau + HCl (pH = 6) soit l'espèce $\Phi(CH_2)_4NH_3^+$ ($\varepsilon_{00} = 165$). Les spectres ont été retracés pour être portés en fréquences de façon à pouvoir ensuite les traiter par le procédé de la « moyenne mobile ».

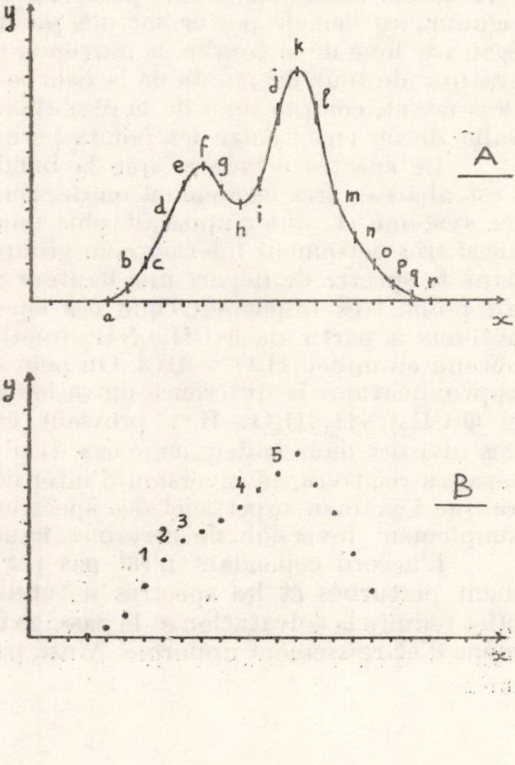

Fig. 3. — Illustration du procédé graphique d'élargissement par « moyenne mobile ». Ainsi, par exemple, le point 1 est la moyenne des points *a, b, c, d, e* ; le point 2 celle des points *b, c, d, e, f* ; le point 3 celle des points *c, d, e, f, g* ; le point 4 celle des points *f, g, h, i, j* ; le point 5 celle de *h, i, j, k, l*.

point chaque fois la moyenne obtenue (Figure 3). Ceci permet de simuler graphiquement un élargissement. Nous avons reporté dans la figure 4 en *a* le spectre de $\Phi(CH_2)_4NH_2$ (méthanol) en prenant une moyenne mobile sur 6 points espacés de 50 cm^{-1}. C'est-à-dire en faisant intervenir une perturbation qui s'étend sur 250 cm^{-1}. En *b* la moyenne a été effectuée sur 7 points espacés de 50 cm^{-1}. La perturbation s'étend donc alors sur 300 cm^{-1}. En *c* nous avons porté la moyenne de ces deux figures. Le spectre obtenu correspond donc ainsi à une perturbation simulée de 275 cm^{-1}. En toute rigueur, au lieu de porter sur des points singuliers relevés à intervalles égaux le long de la courbe, la moyenne mobile devrait porter sur une intégration de tous les points de la courbe dans l'intervalle de perturbation. Cependant, compte tenu de la résolution naturelle des spectres, un intervalle de 50 cm^{-1} entre les points permet une précision très suffisante.

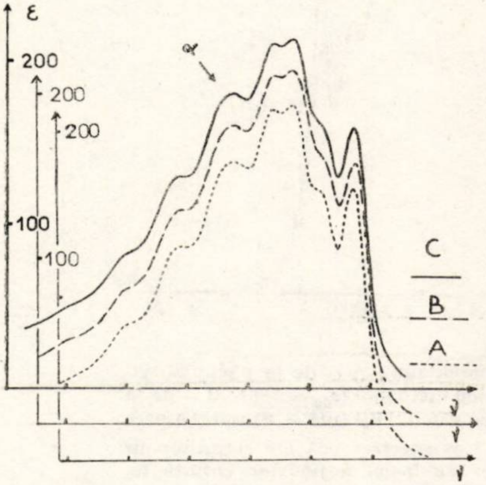

Fig. 4. — Spectre de la figure 2A ($\Phi(CH_2)_4NH_2$ dans le méthanol) traité par moyenne mobile : *A* — sur 6 points espacés de 50 cm^{-1} ; *B* — sur 7 points espacés de 50 cm^{-1} ; *C* — moyenne de ces deux figures précédentes. Nous avons dans les schémas de cette figure porté l'échelle des fréquences sans mettre de valeur. En effet le traitement de la moyenne mobile élargit le spectre 2*A* afin de la comparer au spectre 2*B*, et ne tient donc pas compte d'éventuels déplacements dûs au changement de solvant.

Le spectre *c* montre que la bande 00, du fait de l'élargissement, s'est abaissée très légèrement en dessous du niveau de la première bande du système *A*, qui n'apparaît plus que comme un épaulement. Elle est aussi très nettement inférieure au groupe des bandes α, alors qu'elle avait dans le spectre de départ une hauteur supérieure. On s'aperçoit, et c'est un point très important, que ces spectres perturbés, en particulier *c*, obtenus à partir de $\Phi(CH_2)_4NH_2$ (méthanol) sont très proches de celui obtenu en milieu $H_2O + HCl$. On peut donc en déduire que, en première approximation, la différence entre les spectres de $\Phi(CH_2)_4NH_2$ (méthanol) et $\Phi(CH_2)_4NH_3^+(H_2O+H^+)$ provient esentiellement d'un élargissement des niveaux dans le deuxième cas. Il n'y a donc pas modification des intensités relatives, ni inversion d'intensité entre les pics, contrairement à ce que l'examen superficiel des spectres pourrait laisser supposer. Il y a simplement inversion de certaines hauteurs.

L'accord cependant n'est pas parfait entre les spectres artificiellement perturbés et les spectres naturellement perturbés. On ne peut en effet réduire la solvatation et le passage de NH_2 à NH_3^+ à un simple phénomène d'élargissement uniforme. Ainsi, par exemple, la bande 00 du spectre réel se superpose mieux avec le spectre que l'on perturbe sur un intervalle de 250 cm^{-1}, alors qu'avec le même intervalle la première bande du système A présente un épaulement encore trop marqué. Cet épaulement, par contre, est mieux rendu par une perturbation de 300 cm^{-1}. La perturbation moyenne sur 275 cm^{-1} est donc un compromis. L'élargissement n'est ainsi pas uniforme d'un sous-système à un autre (A et B), ou d'une bande à une autre. On voit néanmoins que pour les faibles fréquences du spectre la perturbation est proche de 250—300 cm^{-1}.

On doit remarquer aussi, qu'une perturbation uniforme sur tout le domaine observé, lorsqu'elle donne une bonne concordance au niveau des bandes situées aux faibles fréquences, laisse apparaître le massif α, ainsi que les autres éléments du spectre situés à plus grande fréquence encore, plus distinct qu'il ne l'est dans le spectre réel. Ce massif est en fait si diffus qu'il n'apparaît que comme un point d'inflexion. Il semble donc de ce fait, et de la comparaison élaborée au paragraphe précédent entre la bande 00 de B et la première de A, que la largeur de la perturbation s'accroît au fur et à mesure que les fréquences augmentent. On peut interpréter ce phénomène sur les bases suivantes. Les bandes qui apparaissent aux fréquences élevées mettent en jeu des transitions vers des niveaux vibrationnels plus élevés que ceux impliqués dans les transitions apparaissant aux courtes fréquences. Les progressions A et B correspondent à des transitions entre les niveaux de la vibration de respiration a_{1g}. Gardons à l'esprit la courbe de potentiel d'une espèce diatomique de façon à pouvoir procéder à un raisonnement qualitatif. Dans l'état fondamental, en première approximation, on peut considérer que seul $v = 0$ est peuplé à la température ambiante où l'on opère, compte tenu de la valeur de 930 cm^{-1} pour la fréquence a_{1g}. L'amplitude entre les points d'élongation extrême est faible pour un niveau $v = 0$, d'autant que la probabilité maxima d'existence se situe entre ces points d'élongation extrême à la distance moyenne d'équilibre. La cage de solvatation dans l'état fondamental assume une géométrie qui permet cette faible amplitude d'élongation. Lorsque la molécule subit une transition vers les niveaux vibrationnels de l'état excité, elle sera d'autant plus à l'étroit dans la cage de solvatation qu'elle se trouvera créée dans des niveaux vibrationnels élevés, puisque ces niveaux mettent en jeu une amplitude d'élongation d'autant plus grande qu'ils sont élevés. En effet la cage de solvatation est, toutes autres choses étant égales, à la mesure du niveau vibrationnel de l'état fondamental. D'après le principe de Franck-Condon elle n'a pas le temps de se réarranger pour s'adapter à l'état excité pendant le très court intervalle de temps que dure la transition. Les vibrations de l'état excité, dont le nombre quantique v est élevé, seront d'autant plus gênées que la probabilité d'existence de la molécule est plus grande aux points d'élongation vibration étant gênée, l'interaction avec la cage de solvatation étant plus grande, les niveaux deviennent plus flous, plus larges.

Le résultat que nous avons obtenu en ce qui concerne la comparaison des intensités de la transition secondaire pour la phénylalcoylamine dans le méthanol, et l'ammonium correspondant dans l'eau, amène naturellement à s'interroger sur la transmission des interactions à longue distance entre l'auxochrome en bout de chaîne et le chromophore.

SOLVATATION, ÉLARGISSEMENT ET TRANSMISSION DES INTERACTIONS À LONGUES DISTANCES

La fonction NH_3^+ est plus électroattractrice que NH_2. Dans les systèmes $\Phi(CH_2)_nX$ elle diminue donc plus que ne le fait NH_2 le caractère π donneur de la chaîne aliphatique. Ce caractère π donneur s'exerce grâce au couplage σ, π de type hyperconjugatif au niveau de C_α. De ce fait la perturbation que le substituant impose au chromophore diminue. La transition devient plus interdite puisqu'on se rapproche d'une symétrie D_{6h}, et ε_{00} décroît.[3,8-13] C'est bien le cas, par exemple pour $\Phi(CH_2)_3NH_2$ et NH_3^+ où l'auxochrome terminal est plus proche de Φ, pour $\Phi(CH_2)_2NH_2$ et NH_3^+ aussi (Figure 5). Le cas de $\Phi CH_2NH_2, NH_3^+$ est spécifique dans la mesure où NH_3^+ annule totalement l'effet π donneur de CH_2 et exerce par delà celui-ci une perturbation de type π attracteur, ce qui accroît l'intensité par rapport à $\Phi\ CH_2NH_2$.[16]

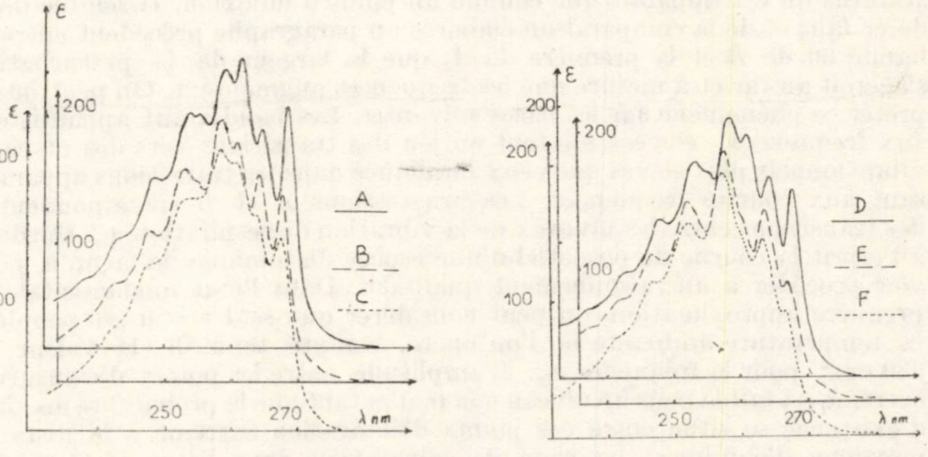

Fig. 5. — Spectres de : *A* — $\Phi(CH_2)_3NH_2$ dans le méthanol ($\varepsilon_{00} = 178$) ; *B* — $\Phi(CH_2)_3NH^2$ dans méthanol + H^+, soit $\Phi(CH_2)_3NH_3^+$ (meth.) ($\varepsilon_{00} = 135$) ; *C* — $\Phi(CH_2)_3NH_2$ dans eau + + H^+, soit $\Phi(CH_2)_3NH_3^+$ (eau) ($\varepsilon_{00} = 140$) ; *D* — $\Phi(CH_2)_2NH_2$ dans le méthanol ($\varepsilon_{00} = 145$) ; *E* — $\Phi(CH_2)_2NH_2$ dans méthanol + H^+, soit $\Phi(CH_2)_2NH_3^+$ (meth.) ($\varepsilon_{00} = 85$) ; *F* — $\Phi(CH_2)_2NH_2$ dans eau + H^+, soit $\Phi(CH_2)_2NH_3^+$ (eau) ($\varepsilon_{00} = 90$).

Si l'on se réfère à $\Phi(CH_2)_3NH_2$, l'auxochrome de $(CH_2)_4NH_2$ est plus loin, séparé par quatre chaînons du noyau aromatique. Le chromophore « ressent » donc de la présence de NH_2 en bout de chaîne un effet très faible. Ainsi la phénylbutylamine devrait avoir dans le méthanol un spectre proche de celui du *n*-butylbenzène.[14] C'est le cas. Le passage de NH_2 à NH_3^+, du fait de l'éloignement du chromophore, devrait beaucoup moins modifier l'intensité dans le cas de la phénylbutylamine que pour ses homologues inférieurs. Si l'on compare dans un même solvant $\Phi(CH_2)_4NH_2$ (methanol) et $\Phi(CH_2)_4NH_3^+$ (méthanol) (figure 6) on s'aperçoit que les spectres ont une résolution analogue et que la protonation s'accompagne d'une diminution de ε_{00} (de 185 à 160 soit 12 %) plus faible que dans le cas de $\Phi(CH_2)_3NH_2 \rightarrow NH_3^+$ (de 178 à 135 soit 24 %) (méth.) et de $\Phi(CH_2)_2NH_2 \rightarrow NH_3^+$ (méth.) (de 145 à 85 soit 41 %). Donc NH_2 a lui-même peu d'effet sur le chromophore dans la phénylbutylamine, mais le passage à NH_3^+ exerce encore une action à longue distance sur le chromophore.

Le fait que $\Phi(CH_2)_4NH_2$ (méthanol) et $\Phi(CH_2)_4NH_3^+(H_2O + H^+)$ aient, comme nous l'avons montré dans les parties précédentes, des intensités très proches, malgré des ε_{00} différents, alors que $\Phi(CH_2)_4NH_3^+$ (méthanol$+H^+$) est moins intense, montre que NH_3^+ solvaté par H_2O n'exerce pas sur Φ d'effet attracteur plus grand que NH_2 solvaté par le méthanol. Ce phénomène peut s'expliquer par le fait que l'eau, entité très polaire, hydroxylée, donc très solvatante pour les molécules étudiées ici, exerce une forte interaction avec NH_3^+, et sans doute aussi avec toute la chaîne aliphatique, inhibant ainsi partiellement l'influence attractrice de l'auxochrome. Compte tenu des positions respectives de Φ et de l'auxochrome l'incidence du passage NH_2 (méthanol) $\rightarrow NH_3^+(H_2O)$ est déjà du strict point de vue changement de caractère attracteur, faible. L'inhibition partielle de NH_3^+ par solvatation avec H_2O, qui se superpose à la faiblesse de l'effet que l'on devrait attendre, fait que l'intensité décroît très peu. Il se trouve de ce fait que coïncident de façon fortuite l'intensité des deux espèces $\Phi(CH_2)_4NH_2$ (méthanol) et $\Phi(CH_2)_4NH_3^+(H_2O + H^+)$.

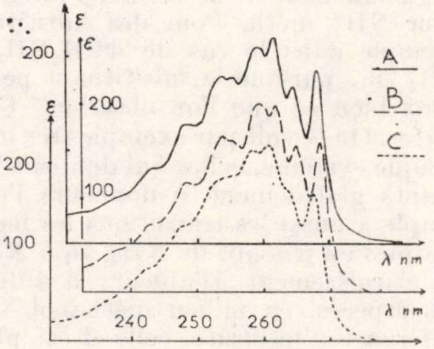

Fig. 6. — Spectres de $\Phi(CH_2)_4NH_2$. Deux de ces spectres ont déjà été reproduits dans la figure 2, mais en fréquences. Nous les retraçons ici en longueurs d'onde pour pouvoir les comparer avec ceux de la figure 5 : *A* — milieu : méthanol ($\varepsilon_{00} = 185$) ; *B* — milieu : méthanol $+ H^+$ soit $\Phi(CH_2)_4NH_3^+$ (meth) ($\varepsilon_{00} = (160)$; C — milieu : eau$+H^+$, soit $\Phi(CH_2)_4NH_3^+$ (eau) ($\varepsilon_{00} = 165$).

L'élargissement rencontré est général lorsqu'on passe aux spectres dans l'eau. Il n'est pas attribuable à la formation de $-NH_3^+$, car même avec NH_2 en milieu H_2O et OH^- il existe un élargissement analogue des niveaux.[15] L'eau du fait qu'elle est susceptible de bien solvater les molécules étudiées ici, ce qui provoque on l'a vu l'inhibition partielle du caractère attracteur de NH_3^+, forme une cage efficace autour de la molécule et peut ainsi perturber les niveaux (électroniques ou de vibration) mieux que ne le fait le méthanol.

Pour des systèmes où l'auxochrome est séparé du chromophore par moins de chaînons, la protonation provoque une plus grande perturbation. L'inhibition due au solvant ne se manifeste donc plus de façon préférentielle. Par exemple $\Phi(CH_2)_3NH_2$ (méthanol) et $\Phi(CH_2)_3NH_3^+(H_2O+H^+)$ ont des intensités très différentes, de même $\Phi(CH_2)_2NH_2$ (méthanol) et $\Phi(CH_2)_2NH_3^+(H_2O + H^+)$. Le système *B* décroît beaucoup. Sans procéder à des calculs précis on le voit à la forme générale des spectres, on le voit très facilement aussi en comparant par exemple, outre les bandes 00, la deuxième bande de *A* et la deuxième bande de *B*.

Si l'eau intervient comme inhibant le transfert des interactions attractrices par rapport au méthanol, on devrait observer que les auxochromes NH_3^+ aq sont toujours moins attracteurs que NH_3^+ méth. C'est-à-dire qu'à longueur de chaîne identique, pour des substituants fixés sur Φ globalement π donneurs, l'intensité sera plus élevée pour NH_3^+ aq que pour NH_3^+ méth. Pour des substituants globalement π attracteurs, par exemple dans le cas de $\Phi CH_2NH_3^+$, l'intensité sera moins élevée pour NH_3^+ aq. puisque le substituant perturbera moins par effet π attracteur. C'est bien ce que l'on observe.[16] Ces modifications d'intensité sont très nettes. On le voit par exemple très bien au niveau des deuxièmes bandes de chaque système, celles qui donnent lieu à ε_{max}. Notons que pour les substituants globalement π donneurs l'espèce la moins intense dans chaque couple a aussi les transitions les moins larges. La diminution de hauteur des pics en passant de NH_3^+ aq à NH_3^+ méth ne peut donc être attribuée à un élargissement. D'ailleurs la différence de largeur entre les transitions des espèces, en milieu méthanol + H^+ et eau + H^+, contribuant à la différence d'intensité, celle-ci est plus grande que ne le laisse apparaître la seule lecture des ε_{00}. On a vu en particulier que malgré des ε_{00} proches pour $\Phi(CH_2)_4NH_3^+$ dans le méthanol et l'eau, l'intensité dans l'eau était bien plus grande, semblable à celle de l'espèce non protonée dans le méthanol.

Des travaux que nous venons d'exposer il résulte que le méthanol permet à la fois une meilleure résolution que dans l'eau, phénomène déjà connu, et, ce qui est observé ici pour la première fois, un meilleur transfert que dans l'eau des effets électroniques de l'auxochrome terminal vers le chromophore.

La moyenne mobile fait intervenir un $\Delta\nu$ de 275 cm^{-1} environ pour le début du spectre. On peut évaluer grossièrement la largeur de la bande 00 dans le méthanol pour $\Phi(CH_2)_4NH_2$ à environ 220–250 cm^{-1}. Nous tenons compte pour repérer sa base du recouvrement avec le reste du massif. Ce dernier a une largeur d'environ 3000 cm^{-1}. Les valeurs numériques que nous avions retenues plus haut, pour *n* et *m*, à titre d'exemple, n'étaient donc pas irréalistes. Elles correspondaient à des cas concrets. On voit que la perturbation due au changement de solvant s'étend sur un domaine très vaste puisqu'il est de l'ordre de grandeur de la largeur de la bande 00.

CONCLUSION

L'élargissement des bandes sous l'influence d'une perturbation a une incidence très importante sur leurs rapports de hauteur, même si les intensités restent inchangées. Les coefficients d'extinction molaire sont proportionnellement d'autant plus affectés que les bandes sont étroites. Il est tout particulièrement important de tenir compte de ce facteur lorsqu'on étudie la structure vibrationnelle de spectres de molécules aromatiques en phase liquide. Les solvants en effet sont susceptibles d'induire des largeurs très différentes dans les transitions selon leur pouvoir solvatant. L'exemple concernant certaines phénylalcoylamines a souligné l'intérêt de la prise en compte de ce facteur pour étudier l'incidence du solvant sur la transmission d'interactions à longue distance.

BIBLIOGRAPHIE

[1] H. H. Jaffe, M. Orchin, « Theory and Applications of Ultraviolet Spectroscopy », Wiley, New York, 1962, a) p 252 b) p. 186.
[2] H. Rapoport et G. Smolensky, *J. Amer. Chem. Soc.*, **82**, 1171 (1960).
[3] G. Bastaert, B. Vidal et J. Brocard, *Spectrochim. Acta*, **35A**, 1043 (1979).
[4] J. E. Dubois et A. Cosse-Barbi, *Spectrochim. Acta*, **28A**, 523 (1972).
[5] A Cosse-Barbi et J. E. Dubois, *Spectrochim. Acta*, **28A**, 539 (1972).
[6] A Cosse-Barbi et J. E. Dubois, *Spectrochim. Acta.*, **28A**, 561 (1972).
[7] M. Ballester et J. Riera, *Tetrahedron*, **20**, 2217 (1964).
[8] B. Vidal, *Spectrochim. Acta*, **38A**, 367 (1982).
[9] D. Courtois et B. Vidal, *Spectroscopy Letters*, **15**, 983 (1982).
[10] D. Denis-Courtois et B. Vidal, *Spectrochim Acta*, **39A**, 735 (1983).
[11] D. Denis-Courtois et B. Vidal, *J. Chem. Phys.*, **80**. 559 (1983).
[12] J. Tournon et M. Ashraf el Bayoumi, *J. Amer. Chem. Soc.*, **93**, 6396 (1971).
[13] J. Tournon et M. Ashraf el Bayoumi, *J. Chem. Phys.*, **56**, 5128 (1972).
[14] W. W. Simons, « Sadtler Handbook of U. V. Spectra », Sadtler, Philadelphia, 1979, p. 9.
[15] G. Bastaert, Thèse, Lille, 1979.
[16] B. Vidal, *Rev. Roumaine Chim.*, **27**, 823 (1982).
[17] V. Macovei, *Rev. Roumaine Chim.*, **20**, 1413 (1975).
[18] V. Macovei, *Rev. Roumaine Chim.*, **25**, 651 (1980).
[19] V. Macovei, *Rev. Roumaine Chim.*, **21**, 193 (1976).
[20] V. Macovei, *Rev. Roumaine Chim.*, **26**, 1405 (1981).
[21] M. Răileanu, S. Florea et M. Sahini, *Rev. Roumaine Chim.*, **29**, 424 (1984).
[22] V. Macovei, *Rev. Roumaine Chim.*, **21**, 1137 (1976).
[23] B. Vidal et J. N. Murrell, *Chem. Phys. Lett.*, **31**, 46 (1975).
[24] V. Bekarek, *Coll. Czech. Chem. Comm.*, **45**, 2063 (1980).
[25] D. Isac, M. Mracec et Z. Simon, *Rev. Roumaine Chim.*, **26**, 341 (1981).
[26] A. Darry-Henaut et B. Vidal, *Spectroscopy Letters*, **17**, 463 (1984).

Revue Roumaine de Chimie, **31**, *8*, 787—793 (1986)

SOME OBSERVATIONS ON THE CATALYTIC AND DIRECT PHOTOLYTIC REACTIONS OF *cis*-CYCLODECENE AND *cis*-BICYCLO[3.3.0]OCT-2-ENE WITH DIMETHYLDIAZOMALONATE

OLCAY ANAÇ

Department of Chemistry, Technical University of Istanbul, Istanbul, Turkey

Received July 3, 1985

Catalyzed and direct photochemical reactions of dimethyldiazomalonate with *cis*-cyclodecene and *cis*-bicyclo [3.3.0]oct-2-ene were investigated. Experimental and structural details are presented and some observations on these reactions with respect to reaction rates and product distribution are given.

INTRODUCTION

Catalytically, thermally and photochemically induced decompositions of diazocompounds are well known processes[1–5] which yield carbenes and carbenoids. In recent years Wulfman and co-workers put forward many valuable data with respect to mechanistic and synthetic explanations on "Metal Salt Catalyzed Carbenoids".[6–10] Besides, they confirmed the occurrence of many unsolved problems yet to be studied.

In the photolysis of diazocompounds in the presence of olefins, two basic reactions : cyclopropane formation and C—H insertion are observed. It is generally recognized that singlet carbene is formed in direct irradiation and triplet carbene formation is predominant in sensitized irradiation. Singlet carbenes act as electrophiles in addition reactions, and stereospecific addition occurs by a synchron ous mechanism. On the other hand, triplet carbenes give non-stereospecific addition *via* a two-step mechanism. Beside addition reactions, insertion of carbenes into the C—H bonds containing the most weakly bound and the least hindered hydrogen occurred.

In the metal-salt catalyzed reactions of diazocompounds with olefins, the same products, mentioned above, and also dimers are formed at different rates. There are several mechanistic approaches to the mechanism of these reactions in the presence of homogenous copper catalysts. All these approaches can be gathered in two paths : In one model the intermediate active species involves catalyst-diazocompound complex and in the other model the intermediate is a carbenoid, carbene-catalyst complex.[8] Subsequent studies revealed that unsensitized photolysis of diazomalonic esters does not furnish solely the free carbene, [11] sometimes a pyrazoline derivative intermediate can be formed. Therefore, it seemed appropriate to study some other olefins to add more data on both catalytic and photolytic reactions.

RESULTS AND DISCUSSION

In this work two unstudied olefins, cyclodecene and cis-bicyclo [3.3.0]oct-2-ene, were allowed to react with dimethyl-diazomalonate und catalytic and photolytic conditions. The details for reactions are described in the experimental section. The general results reported here are summarized in equation (1) and in Tables 1 and 2.

As it could be seen in Tables 1 and 2, cycloaddition was predominant in great yield in catalyzed reactions, **1** 92.3 % and **7** 91.11 % whereas insertion products were formed in lower yields. Thus the cycloaddition products could be purified from the reaction mixture and were used as standards for the identification of products in the photolytic reactions where cycloaddition products **1** and **7** were in lower yields, 45.9 % and 66.56 %. Furthermore, Tables 1 and 2 reveal that dimeric products can be formed in the photolysis even if in low yields, although some workers have pointed out the difficulties of dimer formation in photolysis.[8] However it has been demonstrated by a number of workers [12,13], that it could be possible to encounter dimers in this type of reactions.

Although great importance has been attributed to the effects of catalyst concentration and species upon the reactant-product distribution, no observation of reactant consumption *versus* time could be found in the literature. This relation might yield interesting results. To test this

Table 1

Products and yields from the photolytic and catalytic reactions of dmdm with *cis*-cyclodecene

Compound	**1**	**2**	**3**	**4** + **5** + **6**
Photolytic	45.9	1.48	0.17	13.5+26.7+12.3
Catalytic	92.3	1.3	1.1	1.8+2.8+0.0

Table 2

Products and yields from the photolytic and catalytic reactions of dmdm with *cis*-bicyclo [3.3.0]oct-2-ene

Compound	**7**	**2**	**8**+**9**
Photolytic	66.56	3.67	20.05+9.79
Catalytic	91.11	0.33	4.57+3.98

idea, two different methods, quantitative IR and quantitative VPC analyses, were used in order to analyze unreacted dimethyldiazomalonate during the reaction, taking samples from the reaction mixture at various times.

Equation (1)

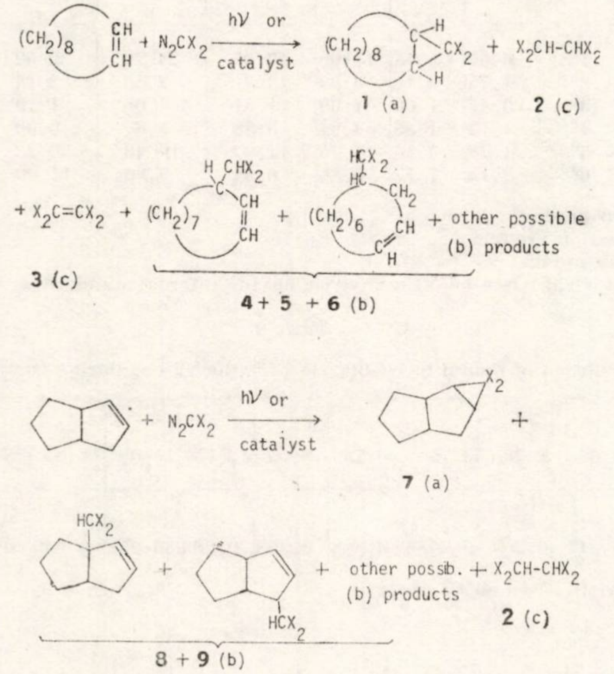

X : CO_2CH_3

a : addition product

b : insertion product

c : dimerization product

The quantitative IR technique (details were given in experimental section of the photolysis of *cis*-bicyclo[3.3.0]oct-2-ene) produced data from Table 4 and Fig. 2. Although this was easier than quantitative VPC it was not possible to analyze the products as they did not have specific peaks distinguishable from each other to calculate. But in the second technique, in addition to reactant, the product distribution *versus* time could also be determined (Table 3 and Fig. 1). As these two methods were different, the units would not be the same in Tables and Figures. But this difference would not affect the general change of curves in Figs 1 and 2. When Figs 1 and 2 for photolysis of *cis*-cyclodecene and *cis*-bicyclooct-2-ene were compared no relation between them could be found. Even a sharp contrast in the reaction rates appeared, so that after the first

Table 3

Reactant-product distribution *versus* time in the photolytic reaction of dmdm in *cis*-cyclodecene*

Time (h)		3	4.5	7.5	12	18.5	32	38	61
Unreacted dmdm		85.17	84.58	55.88	54.69	33.24	23.82	11.97	0.01
Percentage of products	**1**[a]	6.97	5.15	15.95	17.05	24.79	32.52	31.88	45.80
	2[b]	1.75	2.18	3.60	3.3	2.53	2.14	1.95	1.49
	3[b]	0.45	1.06	1.99	1.51	1.05	1.19	0.60	0.18
	4[c]	1.72	1.85	4.94	5.39	8.3	9.09	12.58	13.7
	5[c]	1.78	3.16	11.75	11.07	19.48	20.23	27.74	26.50
	6[c]	2.13	1.72	5.86	6.94	9.86	11.00	13.32	12.40

[a] Addition product
[b] Dimerization product
[c] Insertion product
* Percent yield based on VPC analysis having internal standard.

Table 4

Consumption of dmdm in *cis*-bicyclo [3.3.0]oct-2-ene during irradiation*

Time (h)	0	0.66	2.75	3.75	6.75	8.75	12.75	16.08	18.33	25	28	31.50
dmdm (M)	0.314	0.311	0.309	0.3086	0.308	0.303	0.283	0.268	0.240	0.127	0.112	0

* Molar yield based on IR analysis

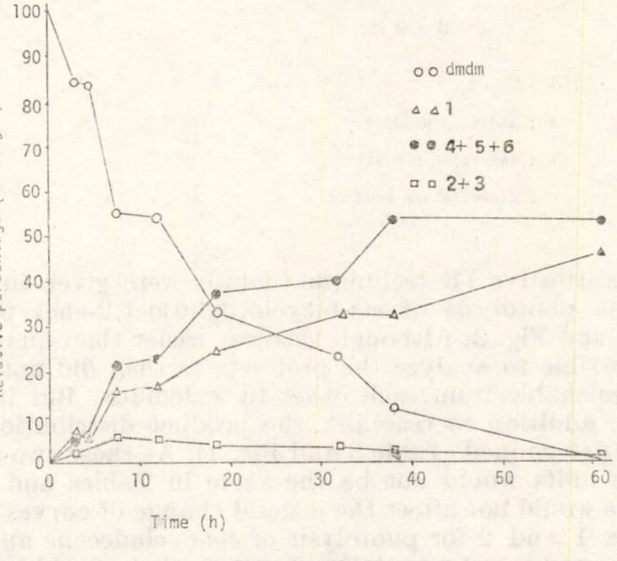

Fig. 1. — Reactant-product distribution *versus* time in the photolytic reaction of dmdm in *cis*-cyclodecene.

18 hours of the overall irradiation time for *cis*-cyclodecene the reaction rate was higher (total product yield was 66%), but at the first 9 hours of the overall irradiation time for *cis*-bicyclo-oct-2-ene no remarkable change was observed. This observation suggested that two different mechanisms were operating although their final products were similar. Generally, after absorption of a photon by a diazocompound, an excited diazocompound is formed and this excited derivative can either give a free carbene by evolving nitrogen or be transformed to a pyrazoline derivative giving subsequently the same products as had the free carbene. Of course these data are not adequate to propose definite mechanisms for both photolyses, but it seems that the photolysis in *cis*-bicyclo[3.3.3]oct-2-ene proceeds through a pyrazoline intermediate and the other through a carbene intermediate.

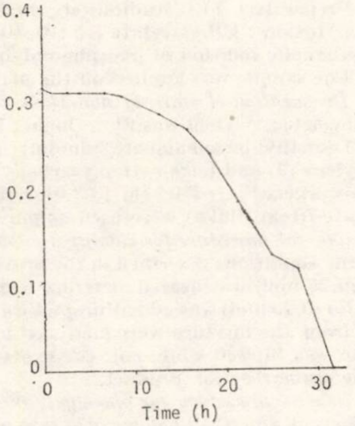

Fig. 2.—Curve of consumption of dmdm in the photolysis with *cis*-Bicyclo [3.3.0]oct-2-ene.

While examining these results it seemed that some more points were of interest :

In previous studies certain reaction times were not established for catalytic reactions. Reactions were rather kept for prolonged times in which side reactions might have occurred. For instance the catalytic reactions of *cis*-cyclodecene and *cis*-bicyclooct-2-ene in this work, occurred during very short times, in contrast to classical reaction times (12 hr or 24 hr) for some other olefins. (As these two catalytic reactions were rapid it was not possible to investigate their distribution of products *vs* reaction time).

The reaction rates *versus* time for addition, insertion and dimerization products for *cis*-cyclodecene were also ilustrated in Table 3 and Fig.1. As can be seen, no linearity for the first two reactions was observed. But the dimerization increased up to the certain reaction time and then gradually decreased during the reaction. This may be attributed to the presence of different mechanisms competing each other.

EXPERIMENTAL

Spectroscopic and gas cromatographic studies. Infrared spectra were measured on a Schimadzu IR—400 Model spectrophotometer and ^1H—NMR spectra were measured on a Varian T—60 instrument using TMS as an internal standard. Gas chromatographic studies were performed on a Schimadzu instrument, Model 5A AW, DMCS Chromosorb W 60/80 mesh. Chosen temperature programme : 5′ isothermal at 100°C ; 100° → 160°C at 10°C/min ; 160° → 190°C at 2°C/min ; 190° → 295°C at 10°C/min. Detector temperature : Injector temperature : 250°C. Carrier gas (N_2) : 0.35 L/min Integrator model : ITG—4A
Elemental analyses were performed by Hereaeus Microstandard equipment.

Preparative TLC studies were carried out using Silicagel HF_{254} layers (1mm) and CH_2Cl_2 : CCl_4 : *n*-Hexane : Ethylacetate (75 :10 :10 :5) solvent. Detection spray (for only pattern plate) : 3.5% ethanolic solution of phosphomolybdic acid. Treatment : Heat to 160° for 30 min.

The sample was applied on the plate by DESEGA Microdoser equipment.

Preparation of starting materials. p-Toluene sulphonylazide was prepared by the method of Baumgarten.[14] Yield was 91% (higher than the lierature value.[10])

Dimethyldiazomalonate (dmdm) (from *p*-toluenesulphonylazide), tetramethoxycarbonylethylene (**3**) and tetramethoxycarbonylethane (**2**) were prepared by the method of Wulfman and co-workers.[10] *cis*-Bicyclo [3.3.0]oct-2-ene, *cis*-cyclodecene and catalyst copper (II)-acetylacetonate (from Fluka) were used as purchased.

General procedure for catalyzed reactions. The catalyzed reactions were carried out under optimum conditions described in the previous work.[10] A solution of catalyst (0.14 mmol) in the olefin (0.25 mol) was heated at reflux while a solution of dimethyldiazomalonate (0.02 mol) in the olefin (0.25 mol) was added dropwise at the rate of 6 drops per minute. After addition, samples taken from the mixture were analyzed by VPC and IR. When the reaction was completed, the mixture was filtered while hot, the excess olefin recovered by vacuum distillation. The residue was the crude reaction product.

General procedure for photolysis studies. The photolysis studies were carried out under our conditions as described below : Mol rate of olefin to dmdm is 25. Appropriate solutions of olefins and dmdm were placed in a double walled, water cooled immersion well photoreactor. 125 watt medium pressure mercury lamps was used as irradiation source through pyrex vessel. All of the photolyses were carried out under nitrogen and samples taken from the continuing reaction were analyzed by VPC and IR.

Catalyzed reaction of cis-*cyclodecene with dmdm.* In the IR spectrum of a sample taken from the reaction mixture after 1 h (after the addition was complete) the azo band for dmdm at 2130 cm $^{-1}$ disappeared. VPC analysis of this sample, did not also show unreacted dmdm but represented a main product (91.4%) and four others in the lower yields. So the reaction was stopped and excess olefin was removed at 68°C/4 mm. The residue was analysed by IR and VPC. IR : 1730 cm $^{-1}$ (νs C=O) and 1635 cm $^{-1}$ (νs C=C) VPC revealed the presence of five compounds at the rates 92.3% (**1**), 1.3 (**2**) ; 1.1% (**3**) and 1.8% + 2.8% (**4** + **5**). This residue was applied on PTLC. By extraction of the main zone compound **1** was purified. NMR (CCl_4) : sharp singlet τ 6.4 (6H, $COOH_3$) and τ 7.95, τ 8.58 (18 H, ring protons). Anal. calcd. for $C_{15}H_{24}O_4$: C 67.13, H 9.01 ; found C 67.24, H 9.10. This compound was assigned structure **1** [Bicyclo [8.1.0] undecane-11.11-dicarboxylic acid dimethyl ester]. **2** and **3** were identified by comparison with the present standards.

Photolysis of cis-*cyclodecen with dmdm.* Samples taken from the solution at given times were analysed by VPC (Table 3). By comparison with the present standards, **2**, **3** and **1** (from the reaction above) were identified. After 61 hours, reaction was completed and excess olefin was removed. VPC of the residue : 45.9% (**1**), 1.48% (**2**), 0.17% (**3**) and three other compounds, 13.5, 26.7 and 12.3% (**4** + **5** + **6**) attributed to insertion products. IR : 1730 cm $^{-1}$ (νs C=O) and 1635 cm $^{-1}$ (νs C=C), ^1H-NMR (CCl_4) : multiplet τ 4.67 (vinyl protons).

Catalyzed reaction of cis-*bicyclo* [3.3.0]*oct-2-ene with dmdm.* In the IR spectrum of a sample taken from the reaction mixture when the addition was completed, azo band for dmdm at 2130 cm $^{-1}$ disappeared. Unreacted dmdm also disappeared in VPC. As the reaction was completed excess olefin was removed and the residue was analysed by IR and VPC. IR : 1735 cm $^{-1}$ (ν C=O), 1630 cm $^{-1}$ (νs C=C), VPC : 91.11% (**7**), 0.33 (**2**), 4.57 + 3.98% (**8** + **9**).

This residue was crystallized from methanol and white crystals were obtained, mp 77°C. Anal. calcd. for $C_{13}H_{16}O_6$: C 65.52, H 7.61 ; found C 65.50, H. 7.70. IR (neat) : 1735 cm $^{-1}$ (νs C=O),NMR ($CDCl_3$) (neat) : quartet at τ 6.1 (6H, $COOCH_3$, J : 6 and 8 c/s), triplet at τ8.7 (6H, J : 8 c/s, ring protons) and multiplets at τ 7.73 and τ 8.3 (one bridgehead proton and 5H, other ring protons). This compound (**7**) was assigned to be tricyclo [4.3.0.$0^{2'4}$] nonane-3.3-dicarboxylic acid dimethylester.

The methanolic filtrate from crystallization was analysed by VPC : 55% (**7**) and 45% (**8** + **9**) and traces of (**2**) were observed.

After evaporation of methanol this mixture was investigated by IR and NMR. IR : 1630 cm^{-1} (νs C=C). NMR($CDCl_3$) : τ 4.53 and τ 4.3 (vinyl protons (**8** + **9**) were attributed to insertion products.

Photolysis of cis-*bicyclo* [3.3.0]*oct-2-ene with dmdm.* Samples taken from the mixture at given times were investigated by FO5 cell (calibrated path length : 0.058 mm) at IR. The consumption of dmdm was calculated between each irradiation from IR spectra at 2130 cm^{-1} Table (4, Fig. 3).When the reaction was completed excess olefin was removed. The crude product was investigated by IR and VPC. IR : 7135 cm^{-1} (νs C=O), 1630 cm^{-1} (νs C=C) VPC : 66.56% (**7**,) 3.67% (**2**) and 20.05 + 9.79% (**8**+ **9**).

Reproductibility of results on Tables are ± 0.6% under the same conditions.

REFERENCES

[1] M. Jones, Jr., and R. A. Moss, "Carbenes", Wiley-Interscience, New York, 1973.

[2] N. S. Isaacs, "Reactive Intermediates in Organic Chemistry", Wiley-Interscience, New York, 1974, 375.

[3] M. Jones, Jr., and R. A. Moss, "Reactive Intermediates, A Serial Publication", Vol. I, Wiley-Interscience, New York, 1978, p. 69.

[4] W. Kirmse, "Carbene Chemistry, Organic Chemistry, A Series of Monographs", Academic Press, New York, 1971.

[5] E. Muller, "Houben-Weyl, Methoden der Organischen Chemie", Photochemie II, 4/5b, George Thieme Verlag, Stuttgart, 1975, p. 1158.

[6] D. S. Wulfman, N. V. Thinh, R. S. Mc. Daniel and B. W. Peace, *J. Chem. Soc. Dalton Trans.*, **1975** 522.

[7] D. S. Wulfman, *Tetrahedron*, **32**, 1231 (1976)

[8] D. S. Wulfman, R. S. Mc Daniel and B. W. Peace, *Tetrahedron*, **32**, 1241 (1976).

[9] D. S. Wulfman, B. W. Peace and R. S. Mc Daniel. Jr., *Tetrahedron*, **32**, 1251 (1976).

[10] D. S. Wulfman, B. G. Mc. Gibboney, E. K. Steffen, N. V. Thin, R. S. Mc Daniel, Jr., and B. W. Peace, *Tetrahedron*, **32**, 1257 (1976).

[11] D. S. Wulfman, B. E. Poling, and R. S. Mc Daniel, *Tetrahedron Letters*, **1975**, 4519.

[12] M. Jones Jr., W. Ando, A. Kulczycki Jr., *Tetrahedron Letters*, **(1967)** 1391.

[13] M. Jones Jr., W. Ando, M. E. Hendrick, A. Kulczycki Jr., P. M. Howley, K. F. Hummel, D. S. Malament, *J. Amer. Chem. Soc.*, **94**, 7469 (1972).

[14] H. E. Baumgarten, "Organic Synthesis", Coll. Vol. 5, Wiley, New York, 1973, 179.

Revue Roumaine de Chimie, **31**, *8*, 795–810 (1986)

CHEMICAL GRAPHS. Part 46 [1]

ENUMERATION OF VALENCE ISOMERS OF ADAMANTANE USING PÓLYA'S THEOREM

ALEXANDRU T. BALABAN
Polytechnic Institute, Department of Organic Chemistry, Splaiul Independenţei 313, 76206 Bucharest, Roumania

Received January 22, 1986

The valence isomers of adamantane $(CH)_4(CH_2)_6$ are found by a mathematically rigorous procedure, namely by applying Pólya's theorem to the cycle index of the edge rotation group of the cubic graphs $(CH)_4$ (three separable loop-graphs and two non-separable multigraphs, namely tetrahedrane and cyclobutadiene) in order to find all possible edge-labelled cubic graphs with four vertices and then by interpreting the edge labels as chains of CH_2 groups. The eleven partitions of the six CH_2 groups are assigned to eight partitions (classes *A – H* in Table 3) of the edges of $(CH)_4$ cubic graphs according to their label patterns. There exist 262 constitutional valence isomers of adamantane ("adamantaneworld") whose structural formulas are exhibited. The algorithm has the advantage that it generates all valence isomers (homeomorphic graphs) without redundancy, therefore it could be useful for implementation by means of a computer program.

1. INTRODUCTION

Since Schleyer's discovery [2] that polycyclic saturated systems may isomerize in the presence of various catalysts (e.g. $AlCl_3$ or, more recently, rhodium on carbon[3]) leading to the thermodynamically most stable isomers, a facile route towards "diamond hydrocarbons" has become available.[4,5] Indeed, owing to the absence of both angle strain (von Bayer strain) and of eclipsed bonds (Pitzer strain), adamantane, diamantane, triamantane, etc. are more stable than any of their saturated isomers and are therefore formed from them in thermodynamically-controlled reactions. The mechanisms of such reactions were investigated; [6] reaction graphs have proved to be useful in such investigations.[7]

A graph-theoretical based systematic enumeration and nomenclature was published [8] for diamond hydrocarbons.

Renewed interest in this field is apparent from the papers by Ganter and coworkers; [9,10] Ganter investigated "adamantaneland" and described interconversions between 19 isomers of adamantane. [9,10] Interestingly, it was recently reported [3] that isomerizations catalyzed by Rh/C may lead to dodecahedrane, which is neither a polymantane nor an inhabitant of "adamantaneland".

Another incentive for chemical research involving derivatives of adamantane was the discovery that adamantaneamine constituted a powerful antiviral agent and was active against Parkinsonism. This discovery triggered interest in the synthesis of many other functionalized adamantanes, or of amines of spherical molecules.

Valence isomers constitute a subclass of isomers characterized by having the same partition of vertex degrees in their molecular (constitutional) hydrogen-depleted graphs.[11] Hexane is the smallest alkane which has valence isomers : two of the five isomers of hexane, namely 2- and 3-methylpentane, are valence isomers because they share the same partition of vertex degrees : 3, 2, 2, 1, 1, 1, i.e. for both compounds, their molecular formula C_6H_{14} may be written as $(CH)(CH_2)_2(CH_3)_3$.*

The present paper reports how, by applying Pólya's theorem to edges of cubic graphs, and then by exploring systematically the partitions of the number of edges in these graphs, one can enumerate in a mathematically rigorous fashion the valence isomers of adamantane, i.e. all hydrocarbons with four tertiary and six secondary carbon atoms, $(CH)_4(CH_2)_6$. Of course, hexamethylenetetramine has exactly the same valence isomers if one replaces all CH groups by nitrogen heteroatoms.

2. CYCLE INDICES AND COUNTING SERIES FOR EDGE-LABELLED CUBIC (MULTI)GRAPHS $(CH)_4$

There exist two connected cubic graphs or multigraphs with four vertices, namely tetrahedrane and cyclobutadiene.[11]

Tetrahedrane (I) is a cubic graph of order four and cyclobutadiene (II) is an analogous multigraph. Since neither of them becomes disconnected by cutting one edge, they are both called non-separable (multi)graphs.

The cycle index for all isomers (including stereoisomers) of edge-labelled tetrahedrane was calculated in preceding parts of this series: [11,13]

$$Z = (y_1^6 + 8y_3^2 + 3y_1^2y_2^2)/12 \tag{1}$$

The corresponding constitutional isomer-counting series for up to six different edges is formed by substituting for y_k the following figure-counting series, and then by algebraic operations :

$$y_k = r^k + s^k + t^k + u^k + v^k + w^k \tag{2}$$

One obtains thus the following coefficients of terms according to the eleven partitions of the number 6 :

$$1r^6,\ 1r^5s,\ 2r^4s^2,\ 4r^3s^3,\ 3r^4st,\ 6r^3s^2t,\ 9r^2s^2t^2,\ 10r^3stu,\ 16r^2s^2tu,\ 30r^2stuv,\ 60rstuvw \tag{3}$$

---

* Schleyer and coworkers[12] used for such hydrocarbons the term *isologous:* molecules which are isomers differing in connectivity but possessing the same number of different kinds of groups such as CH_3, CH_2, CH or C.

In the above series of 11 terms were not included terms which can be deduced by any permutation between letters r, s, t, or u, e.g. $1s^6$, $1t^6$, $1rs^5$, $1r^5t$, $2r^2s^4$, etc.

The exponents of letters in each term indicate a partition of the six edges in $(CH)_4$ cubic graphs according to labels : term r^5s corresponds to partition $5 + 1$; term r^3s^2t to partition $3 + 2 + 1$; term r^3stu to partition $3 + 1 + 1 + 1$; etc. Only the first eight from the eleven terms will be useful for valence isomers of adamantane, because terms r^2s^2tu, r^2stuv or $rstuvw$ cannot correspond to any partition of six unlabelled CH_2 groups.

The cycle index for constitutional isomers of edge-labelled tetrahedrane is : [13]

$$Z = (y_1^6 + 8y_3^2 + 3y_1^2y_2^2 + 6y_2y_4 + 6y_1^2y_2^2)/24 \tag{4}$$

By substitution (2), this cycle index leads to the following coefficients terms :

$1r^6$, $1r^5s$, $2r^4s^2$, $3r^3s^3$, $2r^4st$, $4r^3s^2t$, $6r^2s^2t^2$, $5r^3stu$, $9r^2s^2tu$, $15r^2stuv$, $30rstzuvw$ (5)

The difference between the corresponding coefficients of (3) and (5) indicates how many of these constitutional isomers are chiral. Thus, there are three isomers of tetrahedrane with three labelled edges, one isomer of which is chiral, etc.

For calculating numbers of constitutional isomers of edge-labelled cyclobutadiene one has to find the cycle index on the basis of the three mutually orthogonal C_2 axes (one is perpendicular to the plane of the ring, another one bisects two single edges, and the third bisects the double bonds i.e. four edges), of the symmetry plane bisecting the single edges, and of the symmetry plane bisecting the double bonds. For expressing the complete equivalence within each pair of edges constituting a double bond, permutations of the two edges within each double bond may be performed singly or pairwise. Table 1 presents all permutations of edges in cyclobutadiene (constitutional isomerism).

The resulting cycle index is :

$$Z = (y_1^6 + 5y_1^2y_2^2 + 3y_1^4y_2 + 3y_2^3 + 2y_1^2y_4 + 2y_2y_4)/16 \tag{6}$$

and the coefficients of terms obtained on substituting y_k according to (2) are :

$1r^6$, $2r^5s$, $4r^4s^2$, $4r^3s^3$, $5r^4st$, $8r^3s^2t$, $12r^2s^2t^2$, $12r^3stu$, $17r^2s^2tu$, $27r^2stuv$, $45rstuvw$ (7)

Table 1

Permutations of edges in cyclobutadiene

Edges	Permutations
$a\ b\ c\ d\ e\ f$	y_1^6
$b\ a\ c\ d\ e\ f$	$y_1^4y_2$
$a\ b\ c\ e\ d\ f$	$y_1^4y_2$
$b\ a\ c\ e\ d\ f$	$y_1^2y_2^2$
$d\ e\ f\ a\ b\ c$	y_2^3
$d\ e\ f\ b\ a\ c$	y_2y_4
$e\ d\ f\ b\ a\ c$	y_2^3
$e\ d\ f\ a\ b\ c$	y_2y_4
$d\ e\ c\ a\ b\ f$	$y_1^2y_2^2$
$d\ e\ c\ b\ a\ f$	$y_1^2y_4$
$e\ d\ c\ a\ b\ f$	$y_1^2y_4$
$e\ d\ c\ b\ a\ f$	$y_1^2y_2^2$
$a\ b\ f\ d\ e\ c$	$y_1^4y_2$
$b\ a\ f\ d\ e\ c$	$y_1^2y_2^2$
$a\ b\ f\ e\ d\ c$	$y_1^2y_2^2$
$b\ a\ f\ e\ d\ c$	y_2^3

Table 2 presents all constitutional isomers of edge-labelled tetrahedranes and cyclobutadienes with up to three different labels, indicating chiral isomers of the former by an asterisk. It may be seen from Tables 2 and 3 that only the first eight from the eleven terms are present (classes $A-H$).

Table 3

Correspondence between the first eight terms (classes A—H) in constitutional isomer-counting series (5), (7), (9), (11), (13), partitions of edges in I—V according to labels, and partitions of CH_2 groups into chains symbolized by these labels

Class	Partition of edges by labels	Term in (5), (7), (9), (11), (13)	Partitions of the six CH_2 groups
A	6	r^6	1^6
B	5, 1	r^5s	6
C	4,2	r^4s^2	3^2
D	3,3	r^3s^3	2^3
E	4,1,1	r^4st	5,1 ; 4,2 ; $2,1^4$
F	3,2,1	r^3s^2t	$4,1^2$; $3,1^3$
G	2,2,2	$r^2s^2t^2$	$2^2, 1^2$
H	3,1,1,1	r^3stu	3,2,1

Table 2

Constitutional isomers of edge-labelled cyclobutadiene and tetrahedrane, and corresponding partitions of 6 grouped into eight classes (*A* – *H*) for obtaining valence isomers of adamantane.

Class	I	II
A	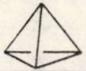	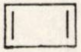
B	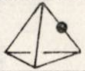	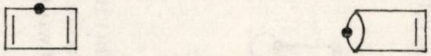
C	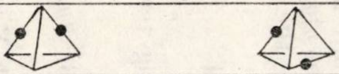	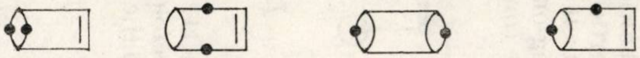
D	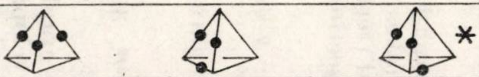	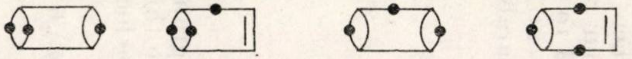
E	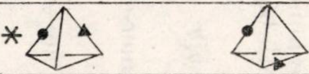	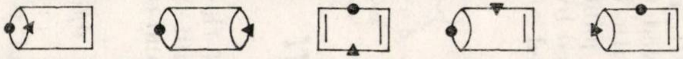
F	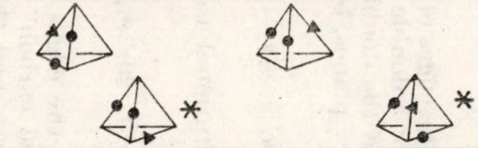	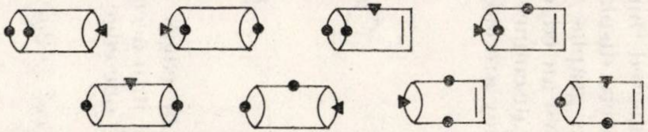
G	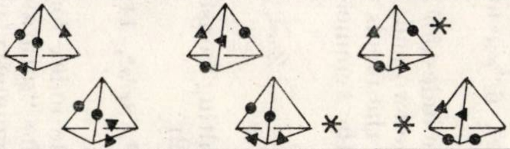	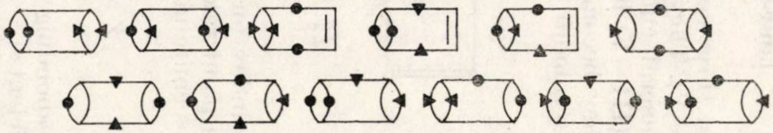
H	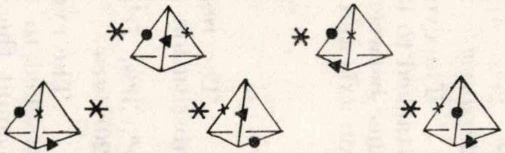	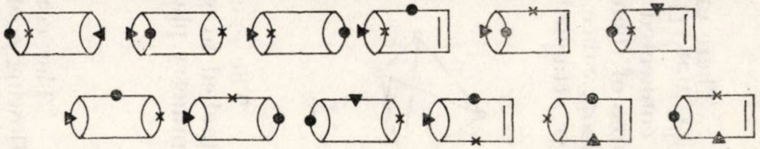

3. CYCLE INDICES AND COUNTING SERIES FOR EDGE-LABELLED CUBIC LOOP-GRAPHS WITH FOUR VERTICES

There exist three connected (multi)graphs with four vertices having loop(s)[11,13] (III—V). They were displayed when showing that the number of connected general cubic graphs with four vertices was five (I—V). Three of them (III—V) have an edge joined to itself; this edge is called a loop. Since they become disconnected by cutting one edge (namely any edge attached to a loop) they are called separable (multi)graphs.

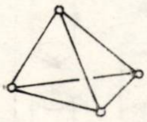

I

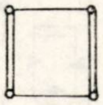

II

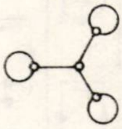

III

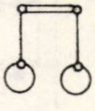

IV

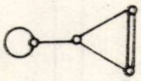

V

The cycle index for the edges of the graph III having three loops attached to one point takes into account the threefold axis and the three symmetry planes containing one edge and one loop (i.e. two edges):

$$Z = (y_1^6 + 2y_3^2 + 3y_1^2\, y_2^2)/6 \tag{8}$$

The corresponding constitutional isomer-counting terms have the following coefficients:

$1r^6$, $2r^5s$, $4r^4s^2$, $6r^3s^3$, $6r^4st$, $12r^3s^2t$, $18r^2s^2t^2$, $20r^3stu$, $32r^2s^2tu$, $60r^2stuv$, $120rstuvw$ (9)

The cycle index for the edges of the graph IV consisting of two loops attached to the two ends of a double bond takes into account the equivalence between the bonds of the double bond (term $y_1^4y_2$), the binary rotation axis and the symmetry planes, both bisecting the double bond:

$$Z = (y_1^6 + y_1^4y_2 + y_1^2y_2^2 + y_2^3)/4 \tag{10}$$

The resulting constitutional isomer-counting terms are formed by substitution (2):

$1r^6$, $3r^5s$, $7r^4s^2$, $8r^3s^3$, $11r^4st$, $20r^3s^2t$, $30r^2s^2t^2$, $36r^3stu$, $52r^2s^2tu$, $96r^2stuv$, $120rstuvw$. (11)

The cycle index for the edges of the graph V consisting of a loop attached to the "saturated carbon" of a cyclopropenyl group takes into account the symmetry plane and the equivalence between the bonds of the double bond:

$$Z = (y_1^6 + 2y_1^4y_2 + y_1^2y_2^2)/4 \tag{12}$$

The result of substituting (2) in this expression gives the coefficients of the constitutional isomer-counting series:

$1r^6$, $4r^5s$, $8r^4s^2$, $10r^3s^3$, $14r^4st$, $24r^3s^2t$, $32r^2s^2t^2$, $42r^3stu$, $58r^2s^2tu$, $102r^2stuv$, $120rstuvw$ (13)

Table 4 exhibits part of the edge-labelled cubic loop-graphs (only the first eight terms in each case) unlike Table 2 which showed all edge-labelled graphs belonging to the first eight terms. Because these edge-labelled loop-graphs are much more numerous, Table 4 contains only those systems which will be used in the next section: all systems belonging to class *A* (term r^6) corresponding to placing one CH_2 group on each edge; from class *B* (term r^5s) the structure which was retained ought to have a label on each loop (the label will correspond to a chain of six CH_2 groups) and just one structure derived from V fulfilled this condition; the same condition applies to classes *C*, *D*, *G*, *H* but in these cases more than one structure fulfills this condition. In class *C* the label is a $(CH_2)_3$ chain and in class *D* it is a $(CH_2)_2$ chain; in class *G*, one type of label is a $(CH_2)_2$ chain and the other type of label is a CH_2 group; in class *H*, the three types of label correspond to CH_2, $(CH_2)_2$ and $(CH_2)_3$ chains. The situation is more complicated in classes *E* and *F* where more than one assignment of labels is to be made. In addition to retaining all structures where each loop has a label, in these two classes one retains also those graphs having at most one loop labelled with one type of label. This type of label will correspond to a $(CH_2)_2$ chain for class *E* and to a $(CH_2)_3$ chain for class *F*; the other type of label will correspond to a HC—CH bond, and into all unlabelled edges (including the loops) one CH_2 group will be inserted. Thus the unlabelled loops will correspond to vinyl groups, and the other unlabelled edges to $CH-CH_2-CH$ chains.

4. VALENCE ISOMERS OF ADAMANTANE DERIVED FROM NON-SEPARABLE CUBIC GRAPHS I AND II

The edges of the preceding cubic graphs can be "labelled" by inserting into them CH_2 groups or chains of several CH_2 groups, for obtaining valence isomers of adamantane.

There are 11 partitions of the number 6, i.e. $p(6) = 11$. The six CH_2 groups of adamantane can therefore be grouped in eleven different fashions, indicated in abbreviated form as shown in Table 3, i.e. as 2^3 for $2 + 2 + 2$, or as 2^2, 1^2 for $2 + 2 + 1 + 1$, etc. For partition 1^6 we insert one CH_2 group into each edge corresponding to "unlabelled" cubic graph (class *A*). For partition 6 (class *B*) the unique label is a chain of six CH_2 groups, $-(CH_2)_6-$. For partition $3 + 3$, i.e. 3^2 (class *C*), each label is a chain of three CH_2 groups, $-(CH_2)_3-$. For partition *D*, 2^3, each label is a $-(CH_2)_2-$ chain. In the above cases all labels were equal, i.e. one type of label. The next partitions involve two or three different types of labels. In class *E*, for partition 5,1 one label is $(CH_2)_5$ and the other is CH_2; for partition 4,2 one label is $(CH_2)_4$ and the other is $(CH_2)_2$; the last partition belonging to this class *E* is 2, 1^4; for converting the constitutional fomulas from Table 3 corresponding to class *E* and partition 2, 1^4 of the six CH_2 groups into valence isomers of adamantane, one label is translated into a

Table 4

Constitutional isomers of edge-labelled cubic graphs of order 4 with loops (III–V), which can be converted into valence isomers of adamantane according to Table 3.

Class	III	IV	V
A	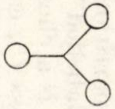	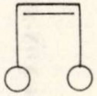	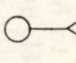
B			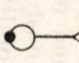
C		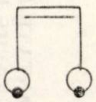	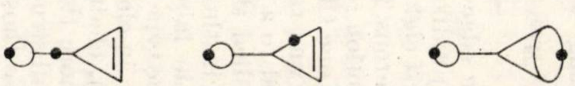
D	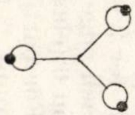	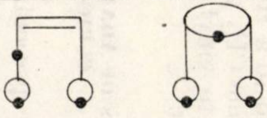	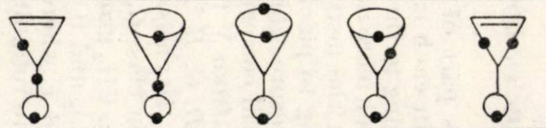
E	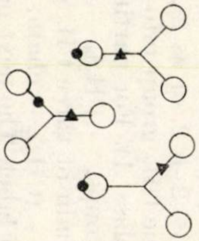	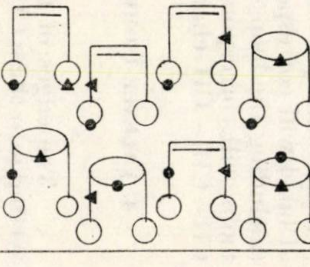	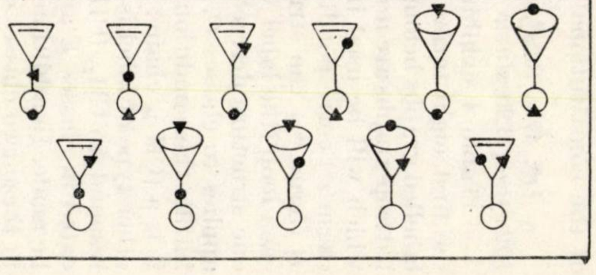

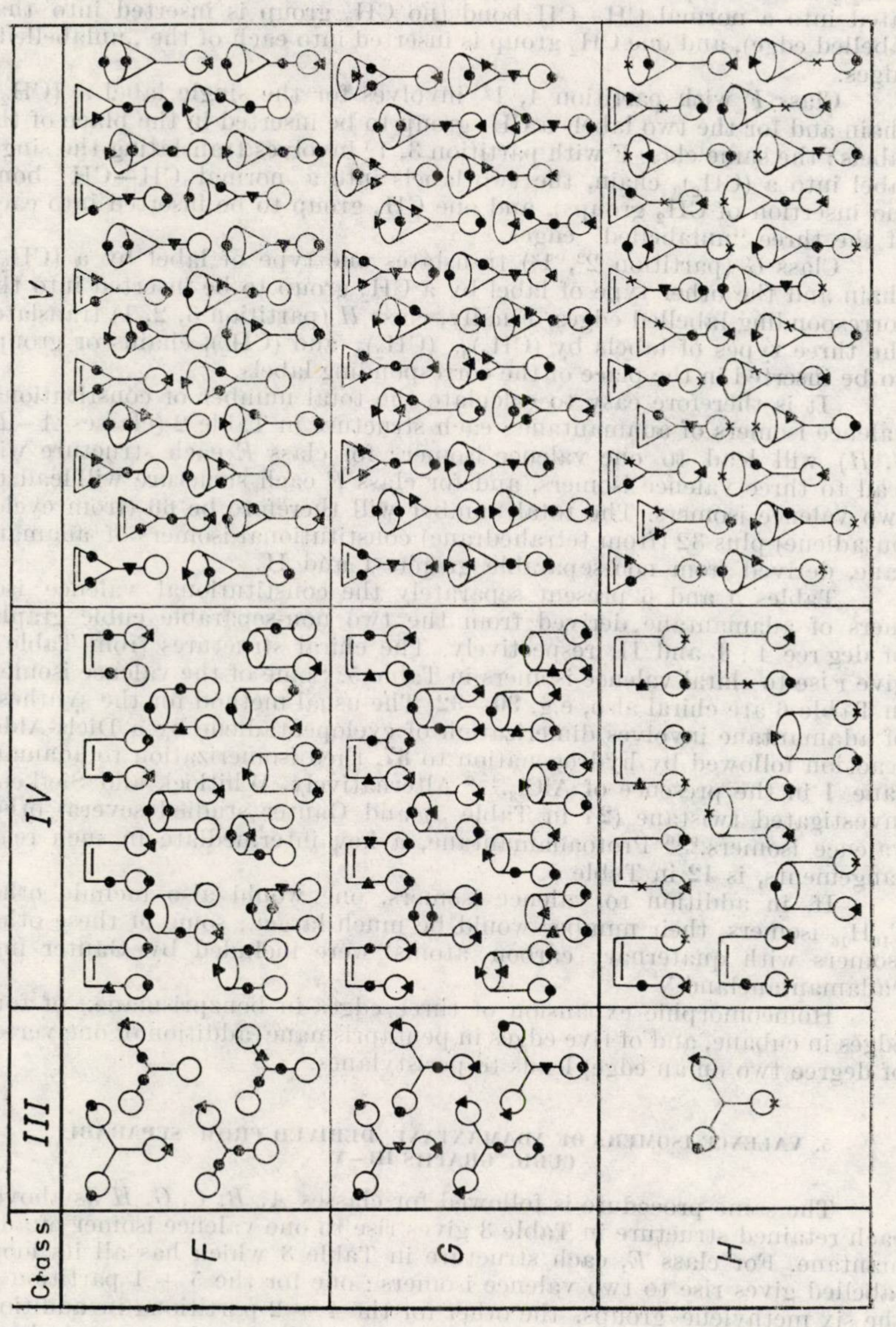
Class
III
IV
V
F
G
H

$(CH_2)_2$ chain inserted into the corresponding edge, the other label is translated into a normal CH—CH bond (no CH_2 group is inserted into that labelled edge), and one CH_2 group is inserted into each of the „unlabelled" edges.

Class *F* with partition 4, 1^2 involves for the single label a $(CH_2)_4$ chain and for the two labels a CH_2 group to be inserted in the place of the labels; the same class F with partition 3, 1^3 involves translating the single label into a $(CH_2)_3$ chain, the two labels into a normal CH—CH bond (no insertion of CH_2 groups), and one CH_2 group to be inserted into each of the three "unlabelled" edges.

Class *G* (partition 2^2, 1^2) translates one type of label by a $(CH_2)_2$ chain and the other type of label by a CH_2 group to be inserted into the corresponding labelled edges. Finally, class *H* (partition 3, 2, 1) translates the three types of labels by $(CH_2)_3$, $(CH_2)_2$ and $(CH_2)_1$ chains or groups to be inserted in the place of the corresponding labels.

It is therefore easy to calculate the total number of constitutional valence isomers of adamantane: each structure in Table 2 (classes *A*—*D*, *G*, *H*) will lead to one valence isomer; for class *E* each structure will lead to three valence isomers, and for class *F* each structure will lead to two valence isomers. The total number will therefore be 66 (from cyclobutadiene) plus 32 (from tetrahedrane) constitutional isomers of adamantane, derived from non-separable graphs I and II.

Tables 5 and 6 present separately the constitutional valence isomers of adamantane derived from the two non-separable cubic graphs of degree 4: I and II, respectively. The chiral structures from Table 2 give rise to chiral valence isomers in Table 5. Some of the valence isomers in Table 6 are chiral also, e.g. **90**—**92**. The usual method for the synthesis of adamantane involves dimerization of cyclopentadiene by a Diels-Alder reaction followed by hydrogenation to **87**, then isomerization to adamantane **1** in the presence of $AlCl_3$.[2-6] Alternatively, Whitlock and Siefken[7] investigated twistane (**24** in Table 5) and Ganter studied several other valence isomers.[9,10] Protoadamantane, a key intermediate in such rearrangements, is **12** in Table 5.

If, in addition to valence isomers, one would also include other $C_{10}H_{16}$ isomers, their number would be much larger; some of these other isomers with quaternary carbon atoms were included by Ganter into "adamantaneland".

Homeomorphic expansion of three edges in benzprismane, of four edges in cubane, and of five edges in pentaprismane (addition of one vertex of degree two on an edge) leads to peristylanes.[1]

5. VALENCE ISOMERS OF ADAMANTANE DERIVED FROM SEPARABLE CUBIC GRAPHS III—V

The same procedure is followed for classes *A*, *B*, *C*, *G*, *H* as above: each retained structure in Table 3 gives rise to one valence isomer of adamantane. For class *E*, each structure in Table 3 which has all its loops labelled gives rise to two valence isomers: one for the 5 + 1 partition of the six methylene groups, the other for the 4 + 2 partition; in addition, each of the structures with unlabelled loop(s) will give rise to one valence

Table 5
The 32 valence isomers of adamantane (constitutional formulas) derived from tetrahedrane.

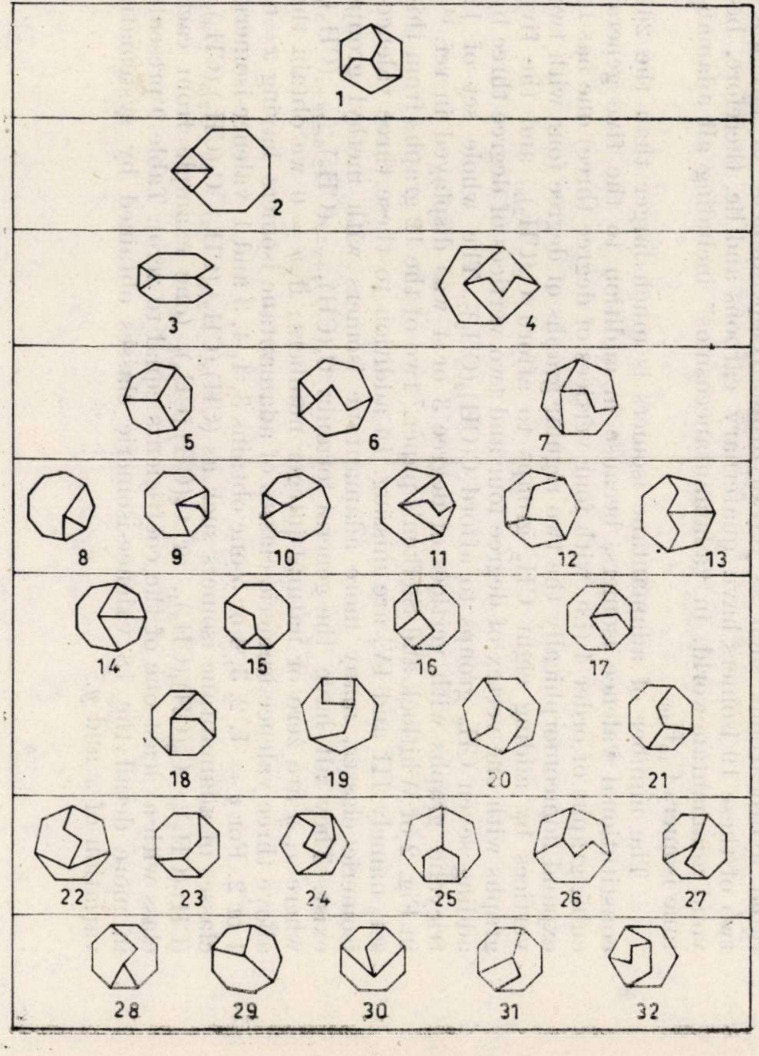
1
2
3
4
5
6
7
8
9
10
11
12
13
14
15
16
17
18
19
20
21
22
23
24
25
26
27
28
29
30
31
32

Table 6
The 66 valence isomers of adamantane (constitutional formulas, numbered in continuation of Table 5) derived from cyclobutadiene.

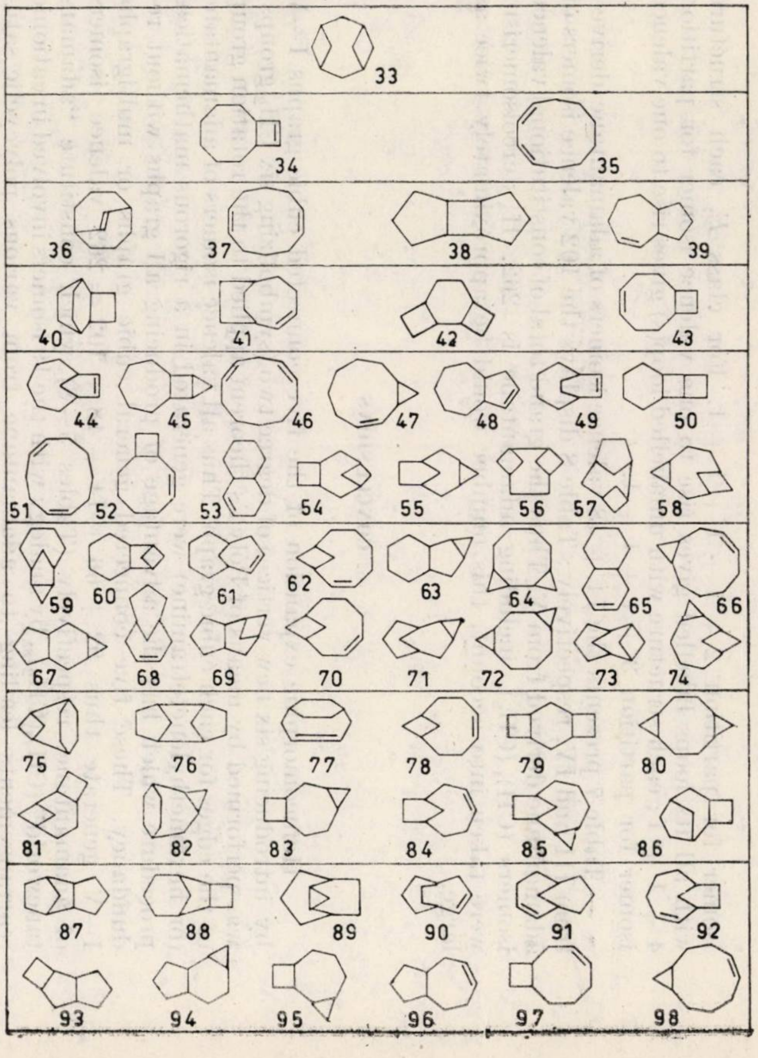
33
34
35
36
37
38
39
40
41
42
43
44
45
46
47
48
49
50
51
52
53
54
55
56
57
58
59
60
61
62
63
64
65
66
67
68
69
70
71
72
73
74
75
76
77
78
79
80
81
82
83
84
85
86
87
88
89
90
91
92
93
94
95
96
97
98

isomer for partition 2 + 1 + 1 + 1 + 1. For class *F*, each structure with all its loops labelled gives rise to one valence isomer for partition 4 + 1 + 1; each structure with unlabelled loop(s) gives rise to one valence isomer for partition 3 + 1 + 1 + 1.

Table 7 presents the 14 + 48 valence isomers of adamantane derived from III and IV, respectively; Table 8 displays the 102 valence isomers of adamantane derived from V. Thus the grand total of constitutional valence isomers $(CH)_4(CH_2)_6$ including adamantane is 262. If stereoisomerism were taken into account, this number would be approximately twice as large.

6. CONCLUSIONS

Homeomorphic expansion of the five connected cubic graphs I—V by introducing six new vertices of degree two (symbolizing six CH_2 groups) was performed by means of Pólya's theorem applied to the rotation group of the edges for each cubic graph. Thus all valence isomers of adamantane (or hexamethylenetetramine) were generated in a rigorous mathematical procedure which has the advantage of producing all graphs without redundancy. These five connected general cubic graphs or multigraphs I—V generate thus 92 + 66 + 14 + 48 + 102 = 262 valence isomers of adamantane, respectively (Tables 5—8) which constitute "adamantaneworld" $(CH)_4(CH_2)_8$, by analogy with the 19 isomers involved in cationic rearrangements leading to adamantane from various polycyclic saturated hydrocarbons such as tetrahydro-dicyclopentadiene or twistane; two of these 19 isomers have quaternary carbons and lie, therefore, beyond adamantaneworld, in "adamantanecosmos" including all adamantane isomers $C_{10}H_{16}$.

The number of adamantane isomers is much larger than the 262 constitutional valence isomers, because in addition to the five general cubic graphs of order 4 (i.e. with four vertices of degree three) one has to expand homeomorphically the two regular graphs of degree four with two vertices by adding eight CH_2 groups to afford $C_2(CH_2)_8$, and the five graphs with one vertex of degree four and two vertices of degree three by adding seven CH_2 groups to afford $C(CH)_2(CH_2)_7$. The whole set of 12 tricyclic graphs with vertices of degree 3 or 4 was displayed in ref. [14]; in Fig. 2 of Whitlock and Siefken's paper,[7] two of the 12 graphs from this set, namely III and IV, are missing. In addition to these three valence-isomeric classes, many more adamantane isomers with methyl groups exist. They all have the general formula $C_x(CH)_{4+y-x}(CH_2)_{6-2y+x}(CH_3)_y$ where x, y are zero or natural integer numbers; if $y = 0$ we obtain the above three valence-isomeric classes of adamantane isomers having $x=0$, 1 or 2. For $y = 1, 2, 3, 4$ or 5 one obtains 3, 4, 4, 3 and 1 valence-isomeric classes of adamantane isomers such as $(CH)_5(CH_2)_4(CH_3)$, $C_3(CH_2)_5(CH_3)_2$, $(CH)_7(CH_3)_3$, $C_2(CH)_4(CH_3)_4$, or $C_4(CH)(CH_3)_5$ (one example from each class with at least one of the coefficients equal to zero). Table 9 presents in more detail the 18 valence-isomeric classes obtained by systematic variation of x and y.

Table 7

Valence isomers of adamantane (constitutional formulas) derived from-graphs III and IV.

Class	*III*	*IV*
A	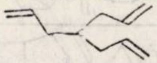	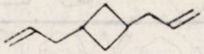
B		
C		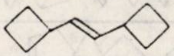
D	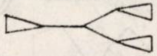	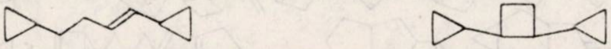
E	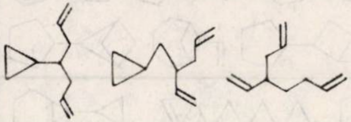	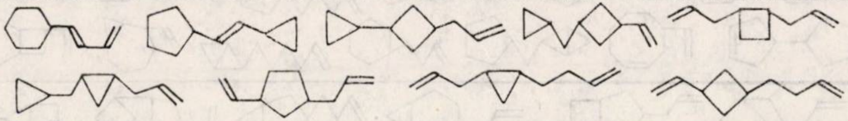
F	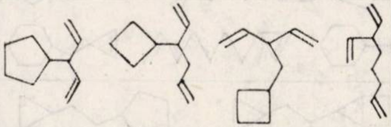	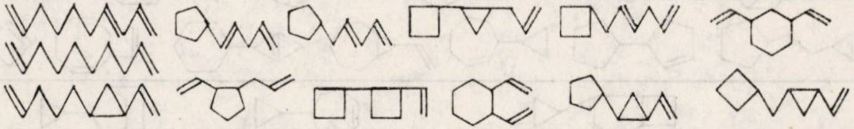
G	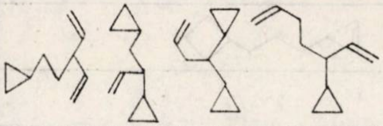	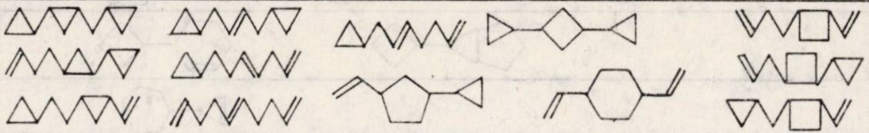
H	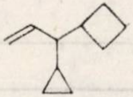	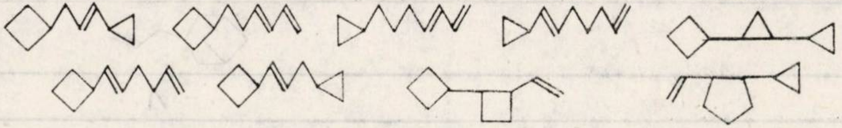

Table 8

Valence isomers of adamantane (constitutional formulas) derived from loop-graph V.

Class	V
A	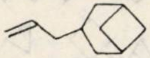
B	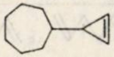
C	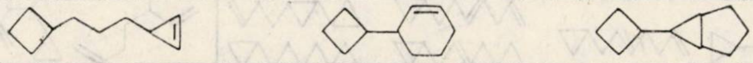
D	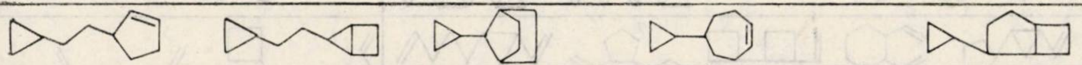
E	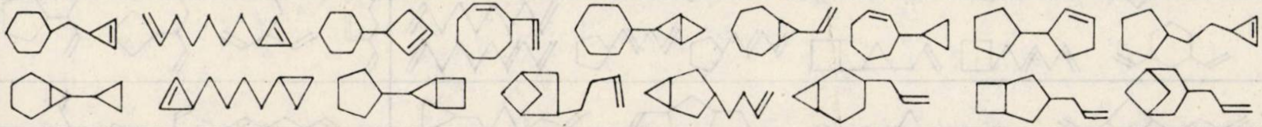
F	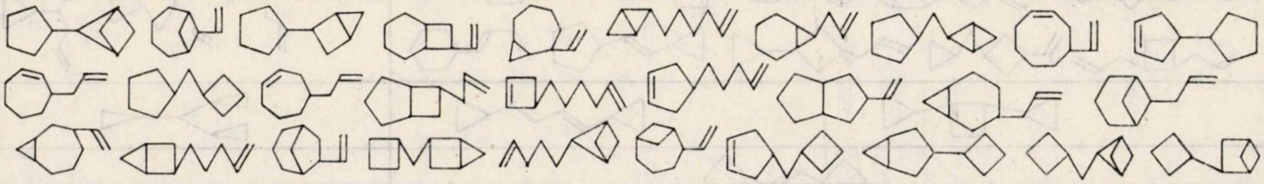
G	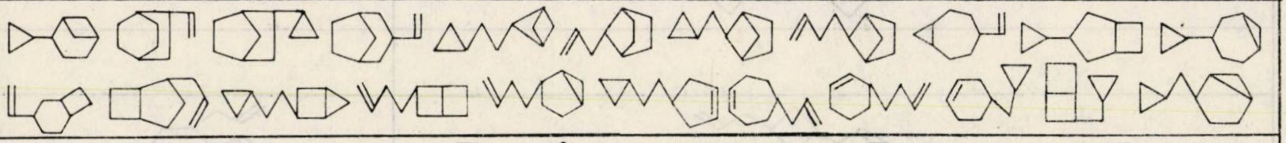
H	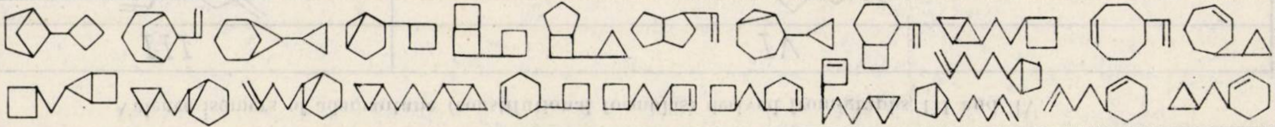

One may calculate similarly using the present method : (i) the total number of adamantane isomers (adding the systems derived homeomorphically from the other 17 classes of graphs mentioned in the preceding paragraph to the 262 constitutional valence isomers derived from I—V); (ii) the number of valence isomers of diamantane $(CH)_8(CH_2)_6$ by adding homeomorphically six points of degree two (i.e. six CH_2 groups) to the 71 general cubic graphs of order 8; (iii) any other number of isomers or valence isomers derived homeomorphically from graphs of degree 3 or 4. However, taking into account the large numbers to be manipulated, it is preferable to develop a computer program able to perform this application of Pólya's theorem to the edge rotation group followed by homeomorphic expansion ; this is a problem for the future, a theoretical challenge for programming.

Table 9

The eighteen valence-isomeric classes corresponding to adamantane isomers $C_{10}H_{16}$

$C_2(CH)_0(CH_2)_8(CH_3)_0$	$C_3(CH)_0(CH_2)_5(CH_3)_2$	$C_4(CH)_0(CH_2)_2(CH_3)_4$
$C_1(CH)_2(CH_2)_7(CH_3)_0$	$C_2(CH)_2(CH_2)_4(CH_3)_2$	$C_3(CH)_2(CH_2)_1(CH_3)_4$
$C_0(CH)_4(CH_2)_6(CH_3)_0$	$C_1(CH)_4(CH_2)_3(CH_3)_2$	$C_2(CH)_4(CH_2)_0(CH_3)_4$
	$C_0(CH)_6(CH_2)_2(CH_3)_2$	
$C_2(CH)_1(CH_2)_6(CH_3)_1$	$C_3(CH)_1(CH_2)_3(CH_3)_3$	$C_4(CH)_1(CH_2)_0(CH_3)_5$
$C_1(CH)_3(CH_2)_5(CH_3)_1$	$C_2(CH)_3(CH_2)_2(CH_3)_3$	
$C_0(CH)_5(CH_2)_4(CH_3)_1$	$C_1(CH)_5(CH_2)_1(CH_3)_3$	
	$C_0(CH)_7(CH_2)_0(CH_3)_3$	

In an earlier paper, the numbers of substituted adamantane isomers were calculated;[15] it was shown that one may obtain (with the help of Pólya's theorem and suitably chosen graphs) numbers of constitutional isomers, of all isomers, or of diastereomers (all isomers but excluding enantiomers).

Adamantyl cations are among those carbocations which undergo degenerate rearrangements,[16] as demonstrated (by means of isotopic labelling) by Schleyer and coworkers,[17] both for adamantane and for methyl-substituted adamantanes. Methyl groups are necessary for blocking the four bridgehead positions converting them into quaternary carbons (otherwise, under stable-ion conditions, the more stable tertiary 1-adamantyl cations prevail).

Whitlock and Siefken's reaction graph[7] for the isomerization of twistane (tricyclo[4.4.0.0.^{3,8}]decane) or of tetrahydrodicyclopentadiene (tricyclo[4.3.0.1^{2,5}]decane) contains 16 isomers of adamantane (two of which have a quaternary carbon) that contain all ten carbons within rings (no alkyl groups) and on three- or four-membered rings.

It would be interesting to investigate if other isomers of adamantane may rearrange to adamantane. Thus are first the acyclic systems : 3- or 4-vinyl-1,7-octadiene, 3- or 4-allyl-1,6-heptadiene (the last one, triallylmethane, is the most symmetrical) and the isomeric decatrienes : 1,3,9; 1,4,9; 1,5,9; second, butenylcyclohexenes, divinylcyclohexanes (1,2;

1, 3 ; 1, 4) and 1-cyclohexyl-1,3-butadiene ; third, allyl-vinyl-cyclopentanes (1,2 ; 1,3), 3-cyclopentyl-1,4-pentadiene, and cyclopentyl-3- or 4-cyclopentenes ; fourth, vinylcyclooctenes and allylcycloheptenes ; fifht, octahydronaphthalenes and octahydroazulenes. None of these systems (some of which are easily accessible) has appreciable angle strain but some have Pitzer strain. On the other hand, many valence isomers have three- or four-membered rings and, owing to their angle strain, they should be very prone to isomerization to the most stable isomer (thermodynamically) which is adamantane ; however, most of these are not readily accessible.

On the other hand, under carbenium ion conditions, there is no restriction against hydride migrations which may easily lead to isomeric (not valence-isomeric) systems having quaternary carbon atoms. Therefore it may be interesting to look for other starting materials for isomerization to adamantane, such as the Diels-Alder addition product of two molecules of isoprene, or other monoterpenic systems (mentadienes). This is an experimental challenge for the future.

REFERENCES

[1] Part 45. A. T. Balaban. *Rev. Roumaine Chim.*, **31**, 695 (1986).

[2] P. von R. Schleyer. *J. Am. Chem. Soc.*, **79**, 3292 (1957) ; P. von R. Schleyer and M. M. Donaldson, *ibid.*, **82**. 4645 (1960 ; M. Nomura. P. von R. Schleyer and A. A. Arz, *ibid.*, **89**. 3657 (1967) and earlier references ; R. C. Fort Jr. and P. von R. Schleyer. *Chem. Rev.*, **64**, 277 (1964).

[3] P. von R. Schleyer, personal communication ; H. Prinzbach, P. von R. Schleyer. W. R. Roth and coworkers, to appear.

[4] R. C. Fort Jr., "Adamantane. The Chemistry of Diamond Molecules". M. Dekker Inc. New York, 1976.

[5] M. A. McKervey, *Chem. Soc. Revs.*, **3**. 479 (1974).

[6] M. Fărcașiu. E. W. Hagman, E. Wenkert and P. von R. Schleyer. *Tetrahedron Lett.*, **22**. 1501 (1981) ; T. M. Gund, P. von R. Schleyer, P. H. Gund and W. T. Wipke, *J. Am. Chem. Soc.*, **97**, 743 (1975) ; E. Osawa, K. Aigami. W. Takaishi, Y. Inamoto, Y. Fujikura, Z. Majerski, P. von R. Schleyer, E. M. Engler and M. Fărcașiu, *ibid.*, **99**, 5361 (1977).

[7] H. W. Whitlock Jr. and M. W. Siefken, *J. Am. Chem. Soc.*, **90**, 4929 (1968).

[8] A. T. Balaban and P. von R. Schleyer. *Tetrahedron*, **34**, 3599 (1978).

[9] F. J. Jäggi, P. Buchs and C. Ganter, *Helv. Chim. Acta.*, **63**, 872 (1980).

[10] F. J. Jäggi and C. Ganter, *Helv. Chim. Acta*, **63**, 866 (1980) ; A. M. Klester, F. J. Jäggi and C. Ganter, *ibid.*, **66**, 1200 (1983).

[11] A. T. Balaban, *Rev. Roum. Chim.*, **11**, 1097 (1966) ; **15**, 463 (1970).

[12] E. M. Engler, J. D. Andose and P. v. R. Schleyer, *J. Am. Chem. Soc.*, **95**, 8005 (1973).

[13] A. T. Balaban, *Rev. Roum. Chim.*, **19**, 1323 (1974) ; **31**, 679 (1986).

[14] A. T. Balaban, *Rev. Roum. Chim.*, **18**, 635 (1973).

[15] A. T. Balaban, E. R. Palmer and F. Harary, *Rev. Roum. Chim.*, **22**, 517 (1977).

[16] P. Ahlberg, G. Jonsall and C. Engdahl, *Adv. Phys. Org. Chem.*, **19**, 223 (1983).

[17] Z. Majerski, P. von R. Schleyer and A. P. Wolf, *J. Am. Chem. Soc.*, **92**, 5731 (1970) ; Z. Majerski and P. von R. Schleyer, *ibid.*, **93**, 665 (1971) ; P. von R. Schleyer, D. Lenoir, P. Mison, G. Liang, G. K. S. Prakash and G. A. Olah, *ibid.*, **102**, 683 (1980).

Revue Roumaine de Chimie, **31**, *8*, 811–818 (1986)

COORDINATION COMPOUNDS AS RAW MATERIALS FOR MIXED OXIDES: III*

TRINUCLEAR, OXO-CENTERED, CARBOXYLATE COMPOUNDS CONTAINING Fe(II,III,III)

LUMINIȚA PATRON *, ADRIANA CONȚESCU *, G. MUNTEANU *, MARIA BREZEANU ** and E. SEGAL **

* Center of Physical Chemistry, Bucharest, România
** Polytechnical Institute, Bucharest, Romania

Received April 13, 1985

Trinuclear, oxo-centered, carboxylate compounds of Fe(II) – Fe(III) were isolated and characterized in order to demonstrate their role as intermediate species in the synthesis of magnetite.

Among the nonconventional methods lately employed in preparation of ferrites, an important role is played by the thermal decomposition of solid polynuclear complex compounds and the wet ferritization.[1–5]

The latter method, introduced by Japanese specialists, achieves the formation of mixed oxides of spinelic structure, directly in the reaction medium. Although it was not fully proved, the reaction mechanism advanced is based on the thermolysis of some polynuclear coordination compounds.[3,4] Consequently, the two procedures mentioned are related because both propose the polynuclear coordination compounds of Fe(III) as precursors of mixed oxides in question.

The existence of intermediate complexes in the process of wet ferritization could be conformed by isolation of these coordination compounds from the reaction medium. This contribution aimes, on the one hand, to obtain the ferrite by the wet method and, on the other hand, to isolate and characterize the precursors, the polynuclear coordination compounds which after thermal de-omposition yield the ferrite. Due to the outstanding interest it presents from theoretical and practical viewpoint we chose to study the magnetite, ($Fe_2^{III}Fe^{II}O_4$).

We have employed an original method of wet ferritization which consisted of the introduction of a complexation agent into the reaction medium.[6,7]

---

* Part II in *Rev. Roumaine Chim*, **30**, 837 (1985).

The selection of the ligand plays an important role : it must be such as to generate the metallic ion complex compounds which should be sufficiently stable to reach a high concentration and, at the same time, sufficiently unstable to decompose in the reaction medium.

The pH plays a determining role both in the obtention of mixed oxides directly in the reaction medium and in the separation of complex intermediates. Thus, at pH ranging within 8—10, from the system $Fe^{III} - Fe^{II} - L - NN_3$, where $L = HCOOH$, CH_3COOH, at a ratio $2Fe^{III} : 1\ Fe^{II}$, the magnetite separates. At acid pH (3—5), from the reaction mixture separate the intermediate coordination compounds which contain iron in two oxidation steps and which (in this pH range) are of relatively high stability. This feature has allowed their insolation as well as chemical and physico-chemical characterization.

On the basis of elemental analysis (C, H, Fe^{III}/Fe^{II} ratio) and taking account of the trend of Fe(III) ions to form polynuclear basic acetates,[8] which contain $[Fe_3O(CH_3COO_6)]^+$ cation, we advanced the following general formula for these polynuclear coordination compounds :

$$[Fe_2^{III}Fe^{II}O(RCOO)_6L_3]$$

where $R = H$; $L = HCOOH$

$$R = CH_3 ; L = H_2O$$

The literature is very rich in data concerning this type of homonuclear coordination compounds with mixed valence (Fe^{III}, Fe^{II}).[9–15] The structural formula accepted for these compounds assumes the existence in solid state of M_3O fragment with D_{3h} symmetry.[16–19] The existence of the $[(ML)_3O(RCOO)_6]$ skeleton containing common oxygen in the centre of the equilateral triangle and transition metal ions at corners is recognized ; the bridges of these ions are ensured by —O—C—O— identical groups while the *trans* positions against central oxygen atom are occupied by ligands as H_2O, Py, NH_3, HCOOH, CH_3OH, etc.[19–23] (Fig. 1).

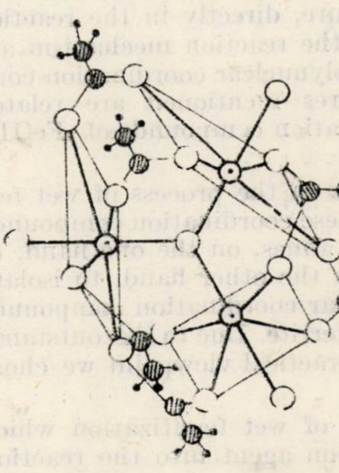

Fig. 1. — Structure of $[Fe_3O(CH_3COO)_6(H_2O)_3]$: ◉ — Fe atom ; ○ — Oxygen atom ; ▨ — carbon atom ; ● — Hydrogen atom

The conformation of this structural formula for polynuclear coordination compounds which are intermediate in the system under study, was achieved through the analysis of electronic, IR spectra, magnetic determinations and molecular electric conductivity, as well as thermogravimetric studies.

The determinations of molecular electric conductivity carried out in acetone and methanol yield values ranging between 0—16 Ω^{-1} cm^{2}mol^{-1} characteristic for nonelectrolytes (and in agreement with the formula advanced).

Interesting data concerning the structure of these polynuclear coordination compounds have been supplied by the reflectance electronic spectra at 400—1100 nm. They confirm the pseudooctahedral configuration assigned to iron atoms in both oxidation steps (Fig. 2). Thus, the band at 550 nm, in the spectra of both compounds was assigned to the spin forbidden $^6A_{1g} \rightarrow {}^4T_{1g}$ transition, in an octahedral symmetry of Fe(III), while that at 980—1020 nm, to the $^5T_{2g} \rightarrow {}^5E_g$ transition, in a high spin octahedral configuration of Fe(II). The spectra of both compounds show a relatively strong band at 790—800 nm assigned, according to literature data, [24,25] to an intervalence transfer $Fe^{II} \rightarrow Fe^{III}$.

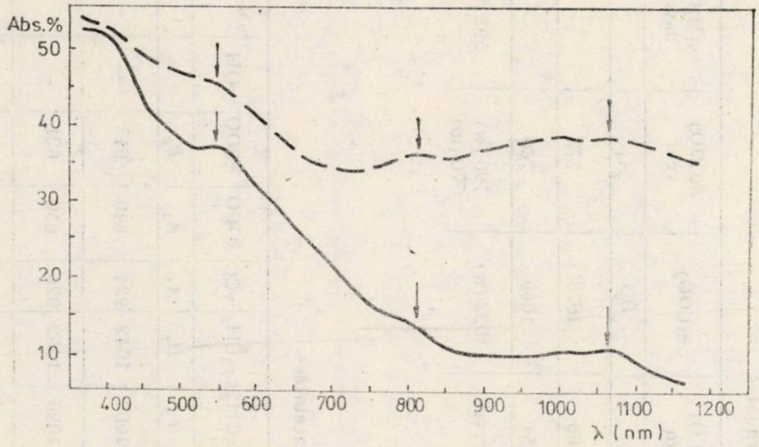

Fig. 2. — Electronic reflectance spectra of : –·–·– $[Fe_3O(CH_3COO)_6(H_2O)_3]$; ——— $[Fe_3O(HCOO)_6(HCOOH)_3]$

Useful information concerning the polynuclear coordination compounds and the way the ligands coordinate was obtained from the analysis of vibration spectra. IR spectra for coordination compounds and free ligands were recorded in the 400—4000 cm^{-1} range. Their interpretation was achieved by comparison with literature data.[22,26,27] According to these data [27] the system consists of 31 atoms with D_{3h} symmetry (if the hydrogen atoms of acetate ion is neglected and each ligand L is considered one atom). Tne separation of vibrations associated to carboxylate groups in the bridging ligands L and M_3O central fragment was shown to be possible. Tne assignments analogous to those for free ions, of the IR bands of the two compounds separated, are listed in Tables 1 and 2.

Table 1 shows that the bands assigned to ν_{sym} and ν_{asym} valence vibrations of the formiate ion are shifted to higher frequencies with respect to those of free ion, which is characteristic of its bonding as a bridge. One can also notice in this case a shift of ν_{sym} and ν_{asym} vibrations of coordinated acetate ion towards higher frequencies (Table 2).

The metal-oxygen vibrations of the M_3O fragment were assigned taking account of the vibration of M_3O planar group, independent of the perpendicular MO_4 units. It is known that the M_3O group has 4 fundamental

Table 1

Infrared absorption spectra of the formiates

	ν(CH)	ν(OCO) asym	δ(CH) asym	ν(OCO) sym	π(COO)	δ(COO) sym	$\nu(M_3O)$ asym	Ref.
	A_1	B_1	B_1	A_1	B_2	A_1		
Na^+OOCH^- (solid)	2841	1567	1377	1366	1073	772	—	26
$OOCH^-$ (aq.sol.)	2803	1585	1383	1351	1069	760	—	26
$[Fe_2^{III}Fe^{II}O(OOCH)_6(HCOOH)_3]$	2950 (sh) 2890 (w)	1620 (sh) 1600 (vs)	1410 (sh)	1370 (vs)	1052 (w)	790 (w) 770 (m)	595 (m)	—

Table 2

Infrared absorption spectra of the acetates

	νCH	νCH	νCH	νCOO as	δCH_3	δCH_3	νCOO s	δCH_3	$\rho_3 CH_3$	$\rho_3 CH_3$	νCC	δOCO	πCOO	νOH	$\nu M-OH_2$ as	νM_3O^- as
	B_1	B_2	A_1	B_1	B_1	B_2	A_1	A_1	l	B_2	A_1	A_1	B_2			
$Na^+OO\ CH_3^-$ 26 (solid)	2989	2989	2936	1578	1430	1444	1414	—	1009	1042	924	646	615	—	—	—
CH_3COO^- 26 (aq.sol.)	3011	2981	2935	1556	1429	1456	1413	1344	1020	1052	926	650	621	—	—	—
$[Fe_3O(CH_2COO)_6(H_2O)_3]$	—	—	2930	1585 vs	—	—	1420 vs	1345 m	—	1050 sh	940 w	650 s	610 sh	1030 s	550 sh	600 m

vibration modes: $\nu_{sym}(M_3O)$, $\nu_{asym}(M_3O)$, $\delta_{sym}(M_3O)$ and $\delta_{asym}(M_3O)$. Because $\nu_{asym}(M_3O)$ implies predominantly the motion of the lighter central atom it is expected that this occurs at frequencies which are considerably higher than $\nu_{sym}(M_3O)$, (which implies only the motion of heavy atoms)[20] in 500 – 700 cm^{-1} range. Such a band is easy to identify at about 600 cm^{-1} in the IR spectrum of the formiate (Table 1). The case of the acetate is more intricate because the spectrum of this compound presents two bands characteristic of coordinated acetate ion in the same range; they are assigned to $\pi(COO)$ and $\delta(OCO)$ modes. However, through analogy with literature,[28] the band at 610 cm^{-1} was assigned to $\nu_{asym}(Fe_3O)$ (Table 2).

A very interesting magnetic behaviour is assigned in the literature to oxotrinuclear coordination compounds. The study of variation of the magnetic moment with temperature has confirmed the existence of antiferromagnetic interactions between the paramagnetic metallic ions.[11,14–16]

The values of effective magnetic moments, at room temperature determined for all complex compounds of this type are lower than the single spin value. These results suggest some magnetic interactions in this system. The values of magnetic susceptibilities and effective moments at room temperature recorded for the two polynuclear coordination compounds isolated, agree with literature data.[10,21] Thus, the magnetic susceptibility determined for the oxotrinuclear acetate is $\chi_g = 19.9.10^{-6}$ which corresponds to an effective moment $\mu_{eff} = 3.09$ MB/atom Fe, while that for oxotrinuclear formite is $\chi_g = 29.00.10^{-6}$, corresponding to $\mu_{eff} = 3.67$ MB/atom Fe.

Additional data about the formation of the two oxotrinuclear coordination compounds, on the one hand, and on the other hand, about the formation of the mixed oxides as decomposition product of these compounds were obtained from their thermogravimetric analysis; this attempted to establish the decomposition steps and the intermediate products resulted.

The curves obtained show that the thermolysis of oxotrinuclear acetate and formiate occurs in three steps. Thus, the first step, the decomposition of oxotrinuclear acetate between 50 – 150°, entails a loss of $\sim 8.00\,\%$ which corresponds to elimination of three coordinated water molecules. In the second step, 200 – 450°, a loss of 52 % is recorded, corresponding to decomposition of $[Fe_3O(CH_3COO)_6]$ complex. This loss is accompanied on the DTA curve by a strong exothermic effect. On further temperature increase, no other important changes occur. The residue (39.96 %) corresponds to Fe_3O_4, which is oxidized turning into $\alpha - Fe_2O_3$. X-Ray analysis of the final product showed the characteristic lines of $\alpha - Fe_2O_3$.

The thermogravimetric analysis of these compounds was accompanied by their vacuum thermal decomposition, through mass spectrometry, to identify the gaseous products resulted. The thermogram corresponding to decomposition of the complex acetate (Fig. 3) shows loss of water in a first stage (maximum 75 %) followed by the loss of acetone in two steps (peaks at 280° and 320°) and finally elimination of CO (peak at 400°). The correlation of the results yielded by these methods with literature data [27] suggests that the following decomposition scheme of the oxotrinuclear acetate is very likely :

$$[\mathrm{Fe_2^{III}Fe^{II}O(CH_3COO)_6(H_2O)_3}] \xrightarrow[-3\mathrm{H_2O}]{50-120^\circ} [\mathrm{Fe_2^{III}Fe^{II}O(CH_3COO)_6}] \xrightarrow[\substack{-3(\mathrm{CH_3})_2\mathrm{CO}\\ -3\mathrm{CO}}]{200-400^\circ-}$$

$$\longrightarrow \mathrm{Fe_3O_4} \xrightarrow[+1/2\mathrm{O_2}]{600-700^\circ} \alpha\text{-}\mathrm{Fe_2O_3}$$

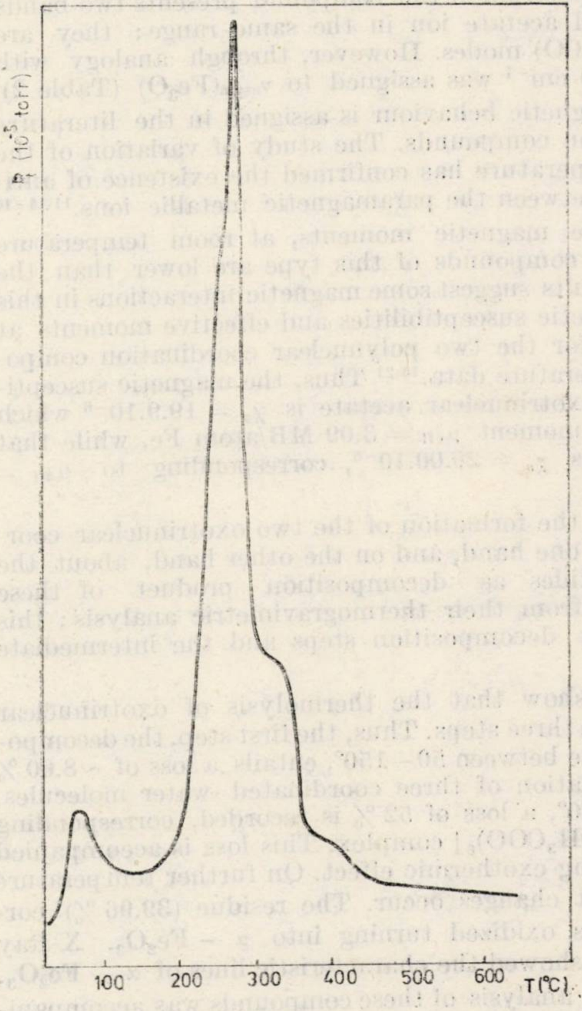

Fig. 3. — Thermal decomposition, in vacuum of $[\mathrm{Fe_3O(CH_3COO)_6(H_2O)_3}]$ $\beta = 16^\circ$/min.

Similarly, the study on decomposition of oxotrinuclear formiate supports the following scheme :

$$[\mathrm{Fe_2^{III}Fe^{II}O(HCOO)_6(HCOOH)_3}] \xrightarrow[-3\mathrm{HCOOH}]{120-250^\circ} \mathrm{Fe_2^{III}Fe^{II}O(CH_3COO)_6}] \xrightarrow[\substack{-3\mathrm{H_2O}\\ -6\mathrm{CO}}]{200-250^\circ}$$

$$\longrightarrow \mathrm{Fe_3O_4} \xrightarrow{250-300^\circ} \gamma\text{-}\mathrm{Fe_2O_3} \xrightarrow{600^\circ} \alpha\text{-}\mathrm{Fe_2O_3}$$

The thermogram corresponding to the decomposition of this compound (Fig. 4) shows the loss of HCOOH in a first stage (of two steps between 100° and 200°) followed by a gradual loss (above 200°) of HCOO radical simultaneously with fragments originating in the decomposition of this radical.

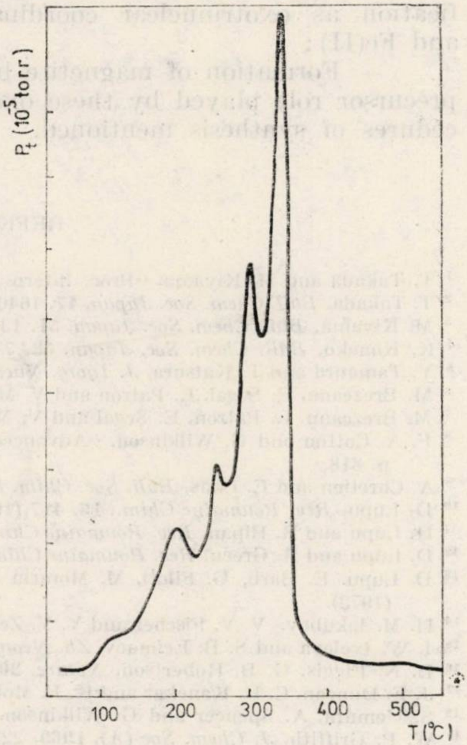

Fig. 4. — Thermal decomposition, in vacuum of $[Fe_2O(HCOO)_6(HCOOH)_3]$; $\beta = 16°/min$.

It was shown that the pH variation plays a determining role in the method of wet ferritization. Thus, while at acid pH (3—5) separation of complex oxotrinuclear intermediates could be achieved, at higher pH's (8—9) these polynuclear compounds decompose in the reaction medium and form a new phase, which in the X-ray diagram shows the lines characteristic of magnetite.

Magnetite is also obtained as a major product in the thermal decomposition of these complex precursors at temperatures lower than 250° (the lines characteristic of Fe_3O_4 are present on the X-ray diagrams of the products obtained on calcination at 220°). The X-ray analysis of the oxide obtained on calcination at 300° shows the lines characteristic of maghemite ($\gamma - Fe_2O_3$). Oxidation of magnetite to maghemite agrees in these circumstances with literature data.[18] Further calcination at 600—700° results in conversion of $\gamma - Fe_2O_3$ into $\alpha - Fe_2O_3$ modification.

On the other hand, the magnetite obtained directly in the reaction medium subjected to a calcination at 250—300°, oxidizes relatively fast to maghemite.[18] X-ray analysis confirms the formation of $\gamma - Fe_2O_3$.

CONCLUSIONS

— Some polynuclear coordination compounds which form as intermediates in the process of magnetite formation through wet ferritization, were isolated for the first time;

— Characterization of complex precursors has led to their identification as oxotrinuclear coordination compounds containing Fe(III) and Fe(II);

— Formation of magnetite by thermal decomposition confirm the precursor role played by these oxotrinuclear combinations in both procedures of synthesis mentioned.

REFERENCES

[1] T. Takada and M. Kiyama, "Proc. Intern. Conf. Ferrites", 1970, p. 69.
[2] T. Takada, *Bull. Chem. Soc. Japan*, **47**, 1646, (1974).
[3] M. Kiyama, *Bull. Chem. Soc. Japan*, **51**, 134, (1978).
[4] K. Kaneko, *Bull. Chem. Soc. Japan*, **52**, 747, (1979).
[5] Y. Tamaura and T. Katsura, *J. Inorg. Nucl. Chem.*, **43**, 671 (1981).
[6] M. Brezeanu, E. Segal, L. Patron and V. Mincu, RSR Patent, no. 77973/29.06.1981.
[7] M. Brezeanu, L. Patron, E. Segal and V. Mincu, RSR Patent no. 77972/31.08.1981.
[8] F. A. Cotton and G. Wilkinson, "Advanced Inorganic Chemistry", Interscience Publ., 1966, p. 818.
[9] A. Chrétien and E. Lous, *Bull. Soc. Chim. France*, **11**, 446 (1944).
[10] D. Lupu, *Rev. Roumaine Chim.*, **15**, 417 (1970).
[11] D. Lupu and R. Ripan, *Rev. Roumaine Chim.*, **16**, 1811, (1971).
[12] D. Lupu and R. Grecu, *Rev. Roumaine Chim.*, **16**, 43 (1971).
[13] D. Lupu, E. Barb, G. Filoti, M. Morariu and D. Tarină, *J. Inorg. Nucl. Chem.*, **34**, 2803 (1973).
[14] H. M. Iakubov, V. V. Fischer and V. V. Zelentzov, *Dokl. Akad. Nauk.*, **250**, 402, (1980).
[15] I. W. Iveleva and S. B. Ecimaev, *Zh. Neorg. Himii*, **27**, 1479, (1982).
[16] B. N. Figgis, G. B. Robertson, *Nature*, **205**, 694 (1965).
[17] J. F. Duncan, C. R. Kanekar and K. F. Mok, *J. Chem. Soc. (A)*, **1966**, 1656.
[18] S. Uemura, A. Spencer and G. Wilkinson, *J. Chem. Soc., Dalton Trans.*, **1973**, 2565.
[19] W. P. Griffith, *J. Chem. Soc (A)*, **1969**, 2270.
[20] A. Earnshaw, B. N. Figgis and J. Lewis, *J. Chem. Soc. (A)*, **1966**, 1256.
[21] B. Jezowska-Trzebiatowska and L. Pajdowski, *Rocz. Chem.*, **32**, 1061 (1958).
[22] S. T. Wilson, M. F. Bondurant, T. J. Meyer and D. J. Salok, *J. Am. Chem. Soc.*, **97**, 2285 (1972).
[23] A. B. Blake, A. Yavari and H. Kubicki, *J. Chem. Soc. Chem. Commun.*, **1981**, 796.
[24] A. B. Blake and A. Yavari, *J. Chem. Soc., Chem. Commun.*, **1982**, 1247.
[25] K. Ito and H. J. Bernstein, *Can. J. Chem.*, **34**, 170 (1956).
[26] J. J. Ziolkovski, F. Pruchnic and T. Szymanska-Buzar, *Inorg. Chim. Acta*, **7**, 473 (1973).
[27] P. Peshev and M. Pescheva, *Mat. Resch. Bull.*, **13**, 419 (1978).
[28] M. Brezeanu, L. Patron, E. Segal, V. Mincu and C. Popa, RSR Patent, no. 82631/29.06.1983.

Revue Roumaine de Chimie, 31, 8, 819—822 (1986)

SYNTHESIS AND CHARACTERIZATION OF THE Pd(II), Cd(II) and Hg(II) COMPLEX COMPOUNDS WITH CARBAZOLE DERIVATIVES

CRISTINA MANDRAVEL, MELANIA GUȚUL and MARGARETA TOMESCU
Polytechnic Institute of Bucharest, Dept. of Chemical Physics,
Bdul. Republicii 13, Bucharest, Romania

Received September 9, 1985

This paper reports elemental analysis, conductometric measurements, UV and IR spectroscopic data in order to characterize the complexes formed in systems MCl_2-N-vinylcarbazole where M=Pd(II), Cd(II), Hg(II).

INTRODUCTION

In continuation of characterization of electron-donor properties of some aromatic compounds having heteroatoms[1-3] we have studied the complex combinations formed in systems : MCl_2-N-vinylcarbazole (NVC).

In the last few years one remarks intensive works on the polymerization of N-vinylcarbazole in the presence of electron-acceptors.[4-5] is a complex phenomenon generated by different behaviour of monomer in every system monomer-solvent-catalyst or monomer-catalyst. One remarks that until now the nature and the role of active species in the NVC process of polymerization have not been elucidated.

On the other hand by comparison of charge density, obtained from HMO calculations [6,7] in carbazole and N-vinylcarbazole there results the big reactivity of vinyl group in N-vinylcarbazole and the possibility of coordination through nitrogen atoms to different metallic ions. The last mentioned property represents a starting point in explaining the active species in the polymerization process.

On the basis of the spectral determinations some authors [9,6] think of the possibility of complex compound formation between NVC and different metallic ions. Until now complex compounds of NVC have been not isolated with metallic ions.

We have attempted in the first stage to establish the conditions for isolating complex combinations of NVC with metallic ions and to characterize the presumable complex combination. From a preliminary study we have remarked the influence of the nature of cation and anion of salts on the polymerization and complexation NVC process. For the beginning we have studied only the MCl_2—NVC system.

RESULTS AND DISCUSSIONS

To establish the influence of various factors on complex compounds formation in these systems the synthesis was performed under various conditions by changing molar ratio of the components and pH of solutions.

At pH 6 – 7 and at any molar ratio of the components (see experimental part) there result definite complex combinations which on the basis of elemental analysis correspond to formulas:
$Pd(NVC)_4Cl_2$(I), $Cd(NVC)_6Cl_2$(II), $Hg(NVC)_6Cl_2$(III).
The conductometric measurements, performed in DMF solutions ($C = 10^{-3}$ m), of the new synthetized compounds lead to the following values:

$\lambda_I = 23.92$, $\lambda_{II} = 18.40$, $\lambda_{III} = 16.56\ \Omega^{-1}\ cm^2.mol^{-1}$ which indicate nonelectrolyte character for all [10].

The big number of groups round the metallic ion obtained from the elemental analysis and conductometric data indicate the possibility of coordination of the NVC already polymerized molecules (probable dimers in the case of Pd(II) and trimers in that of Cd(II) and Hg(II).[11]

The electronic reflectance spectrum was recorded for a complex combination: $Pd(NVC)_4Cl_2$. In order to ascribe the observed bands, literature data [12–14] were used on the UV spectrum of the complex ion $[PdCl_4]^{2-}$ and of carbazole derivatives.

The three bands of comparable intensity from 31,200, 27, 730 20,000 cm^{-1} were assigned to the three transitions spin allowed, d-d type. The intense band at 14,200 cm^{-1} will be provided also by d-d transition in a distortioned square-plane geometry. The large, centred at 34,000 cm^{-1} band and the intense band, at 45, 000 cm^{-1}, can be assigned to charge transfer transitions L → M.

In order to establish the coordination mode of the ligands we recorded the IR spectra in the 4,000 – 200 cm^{-1} range both for NVC and for the complex compounds (I), (II), (III).

In agreement with the literature data[15–16] in the IR spectrum of heteroaromatic ligand, absorption bands were identified which correspond to vibrational modes possible in NVC: $\nu_{,C-N}$ $\nu_{C=C}$ in aromatic ring, ν_{CH} in aromatic and vinyl compounds, ν_{C-H} wagging etc. Examination of the IR spectrum of our compounds reveals both the appearance of new bands and changes in position and intensity of the bands characteristic of two types of ligands. In the IR spectrum of the complex combination of Pd(II) the intense band at 435 cm^{-1} may be assigned, in agreement with the literature data,[3,17] to vibration $\nu_{Pd=N}$ and the weak band at 330 cm^{-1} to vibrational mode $\nu_{Pd\text{-}Cl}$ activated in a *trans* isomer.[18]

Taking into consideration both the other changes in position and the intensity of characteristic bands of heteroaromatic ligand, especially in the range (1,600 – 2,000 cm^{-1}) of summation bands of γ_{CH} out of plane of vinyl carbazolic ring one may state that the NVC is coordinated at nitrogen atom.

In IR-spectra of the Cd(II) complex a new band was observed at 390 cm^{-1}, which is found in the 280$-$420 cm^{-1} domain, predicted for frequency of vibration ν_{Cd-N} after argument from the [19] in connection with combination : [Cd(glyc)$_2$.2H$_2$O].

For complex combination $[Hg(NH_3)_2]^{2+}$ stretching mode ν_{Hg-N} is situated near 500 cm^{-1} in agreement with some calculations. [20] IR spectrum of new synthetized Hg(II) complex shows a new band which can be assigned to this vibration. The changes in the position of vibrational frequencies characteristic of carbazolic ring are more increased than in Pd(II) compound, but the identification of vibration $\nu_{3\ Hg-Cl}$ (shoulder, weak intensity) is not safe because this is coupled with a vibrational mode, characteristic of the carbazolic ring. In the range of 1.000$-$1.150 cm^{-1} the aspect of IR spectrum is distinct in the three complexes in comparison with NVC spectrum, and differentiated after the nature of the central metallic atom. This is in agreement with the literature data [16] which show this domain to be sensible to variation of the nature of the metal in complex combinations.

Examination of IR spectrum of these synthesized complex compounds brings arguments for complexation of NVC already polymerized molecules : In the range of stretching vibration ν_{C-H} one observed shifts of the maximum for existing bands in NVC ($\Delta\nu = 25-15$ cm^{-1}) and appearance of bands whose intensity increases with the number of CH$_2$ group (2.920 cm^{-1}).[16] These modifications allow that, in agreement with some authors [15,21] to indicate, the coordination of NVC molecules as dimers is possible for Pd(II) compound.

In the Cd(II) and Hg(II) compounds NVC molecules should appear as trimers, where one from the three molecules is coordinated by nitrogen atom to metal.

EXPERIMENTAL PART

Preparation of Pb(II) Cd(II) and Hg(II) complex combinations

The CdCl$_2$.H$_2$O and HgCl$_2$ were dissolved in water, PdCl$_2$ was dissolved in absolute alcohol. The molar ratios of components MX$_2$: NVC were 1 :2 ; 1 :4, 1 :6, 1 :8. NVC solutions were added to aqueous solutions of metallic salts under stirring. The formed precipitates were filtered off and washed with water and ethanol.

Analysis and apparatus

Elemental analysis for Pd, Hg, Cd, C, H, N, Cl was performed by the methods indicated in[22-24]. The results are given in table 1.

The solvent used were of spectral quality.

The conductivity measurements were performed with a Radelkis TYPE OK 102 conductometer ; the cell constant conductometer was 0.92 cm. This value was obtained by calibration with standard KCl solutions n/50 and n/100.

Electronic reflectance spectra were recorded on a Beckmann DK$-$2A spectrophotometer for pressed disks. The 100% reflectance was established for MgO powder in the 550 nm region.

IR spectra were recorded on a Perkin Elmer 571 spectrophotometer in KBr pellets. The spectrophotometer was calibrated in the 3, 750, 1,601 and 900 cm^{-1} region using appropiate polystyrene absorptions. Reproductibility was $\pm$ 2 cm^{-1}.

Table 1

Elemental analysis data

Complex compound	M%		C%		N%		H%		Cl%	
	req.	found	req.	found	req.	found	req.	found	req.	found
I $Pd(NVC)_4Cl_2$ red-brown	11.17	11.06	70.81	71.20	5.90	6.34	4.63	4.81	7.48	7.25
II $Cd(NVC)_6Cl_2$ (white)	8.71	8.70	75.14	75.08	6.20	6.50	4.90	4.79	5.30	5.10
III $Hg(NVC)_6Cl_2$ (white)	14.55	14.30	70.50	71.50	5.87	6.03	4.61	4.53	4.95	4.99

REFERENCES

[1] C. Mandravel and L. Nesfintu, *Bul. Inst. Polit. Buc.*, **6**, 33 (1979).

[2] A. Căilean, C. Mandravel and V. E. Sahini, *Rev. Roum. Chim.*, **24**, 391 (1979).

[3] C. Mandravel, G. Teodorescu, M Guţul and G. I. Teodorescu, "Proceedings of the XXII International Conference on Coordination Chemistry", Budapest, Hungary, 1982.

[4] M. Tomescu, *Materiale plastice*, **13**, 21 (1976).

[5] M. Biswas and C. Chakrawarty, *J. Macromol. Sci.*, Rec. Macrom. Chem., **7**, 189 (1972).

[6] H. Schmidt and P. Karrer, *Helv. Chim. Acta*, **29**, 537 (1946).

[7] A. Rembaum, W. Herman and R. Mnak, *J. Polym. Sci.*, **B5** 407 (1967).

[8] S. Tazuke, T. B. Tjoa and S. Okamura, *J. Polym. Sci.*, **A 1**, 191 (1967).

[9] S. Tazuke, *Adv. Polym . Sci.*, **6**, 129 (1969).

[10] W. T. Geary, *Coord. Chem. Rev.*, **7**, 811 (1971).

[11] J. P. Fachler "Progress in Inorganic Chemistry", Interscience, New York, London, 1966, 386 pp.

[12] H. P., Gray, "Transition Metal Chemistry", Willey, 1965, pp. 246.

[13] F. R. Hartley, *J. Organomet. Chem.*, **2**, 227 (1970).

[14] H. Schmidt, M. Ebnother and P. Karrer, *Helv. Chim. Acta*, **33**, 1486 (1950).

[15] N. Avram and G. D. Matteescu, "Spectroscopia in infraroşu. Aplicaţii in chimia organică", Ed. Tehnică, Bucharest, 1966 p. 243.

[16] N. B. Colthup, L. H. Daby and S.E. Wiberly, "Introduction to Infrared and Raman Spectra", Academic Press, 1975, p. 323.

[17] K. Nakamoto, "Infrared spectra of Inorganic and Coordination Compounds", Willey, 1968, p. 201.

[18] H. Peny, *Spectrochim. Acta Part A*, **23** 1137 (1967).

[19] B. H. Lew, F. L. Hirshfeld and F. N. Richards, *J. Amer. Chem. Soc.*, **81**, 442 (1959).

[20] E. P. Bertin, I. Nakagawa, S. Mizushima, T. J. Lana and J. W. Quagliano, *Spectrochim. Acta.*, **18**, 31 (1958).

[21] S. Bădilescu, M. Toader, W. Giurginca and V. Tălpuş, "Spectroscopia in infraroşu a polimerilor şi auxiliarilor", Ed. Tehnică, Bucharest, 1982, p. 81.

[22] C. Wilson and D. Wilson, "Comprehensive Analytical Chemistry. Classical Analysis" Interscience, New York, p. 684.

[23] C. Macarovici, "Chimie analitică cantitativă, Gravimetria", Ed. Tehnică, Bucharest, (1959), p. 125.

[24] C. Liteanu, "Chimia analitică cantitativă", Ed. Tehnică, Bucharest, 1959, 310 pp.

Revue Roumaine de Chimie, 31, 8, 823–831 (1986)

ON THE SPECTRAL ANALYTICAL MEASURING PROCESSES REGARDED AS INFORMATION PROCESSES

VICTOR DAVID * and DAN CIOMÂRTAN **

* Center of Protection and Hygiene, Str. Pop de Băsești, 59, Bucharest, Romania

** I.C.P.T.S.C.F., Bd. Chimiștilor, 299–301, Bucharest, Romania

Received September 16, 1985

A new analysis of spectral analytical measuring processes is developed from the information viewpoint. There are established the minimum and maximum information amounts resulting from an analytical spectral experiment, depending on the a priori to experiment probability field and on the analytical parameters such as background, standard deviation, spectral domain or resolution. New procedures are proposed for the computing of information capacity, redundant information amount and information energy amount of a spectrum.

1. INTRODUCTION

The analytical measuring process as an information process can be schematically described in the following diagram:

$$\{X_i, p_i\}_{i=1,n} \rightarrow \text{ANALYTICAL EXPERIMENT} \rightarrow \{Y_j, p'_j\}_{j=1,m(m\leqslant n)}$$
$$\{\Phi_k, q_k\}_{k=1,N}$$

Thus, from the information viewpoint, the analytical measuring process is characterized by the following fields: the a priori to the experiment probability field $\{X_i, p_i\}_{i=1,n}$, by which a certain probability p_i corresponds to each constituent (element or compound) X_i possibly to exist into the analysed sample; the probability field $\{\Phi_k, q_k\}_{k=1,N}$, specific to the spectrum, by which a probability q_k corresponds to each signal Φ_k from spectrum and by the probability field $\{Y_j, p'_j\}_{j=1,m(m\leqslant n)}$, a posteriori to the experiment. The last one characterizes the final uncertainty with regard to the sample composition on the constituent set $\{Y_j\}_{j=1,m}$ resulted from the experiment $(\{X_i\}\subset\{Y_j\})$. This representation results from the representation of communication systems, with which the analytical measuring processes are alike.[1-3]

If the analytical measuring process is represented for quantitative purposes, the concentration values or their intervals will be used instead of the compounds X_i and Y_j respectively.[4]

In this paper we propose some definitions and relations resulted by dealing with analytical measuring processes from information viewpoint, aiming at the possibility of comparing in this manner more analytical processes or more analytical physical methods.[3]

2. THE MINIMUM INFORMATION AMOUNT OF A SPECTRUM

Let a certain spectrum be for a sample consisting of n constituents, X, which have to be identified; it is made up of an aleatory noise and a background which can be stable or unstable against the wavelength λ. A signal set $\{\Phi_k(\lambda)\}_{k=1,N}$ overlaps with the background. The set $\{\lambda_k\}_{k=1,N}$ so that $\Phi_k(\lambda) = \max$ is the quantitative feature of the same sample. The shape parameters (outline), the noise level and $\Phi_k(\lambda)$ distribution half-widths depend on the parameters of the analytical measuring process.

For simplicity, let's denote by $\omega(\lambda)$ the amplitude of the background signal as against a baseline. With regard to the baseline, and to the background respectively, the signal set $\Phi_k(\lambda)$, $k = 1, N$ is characterized by the amplitudes A'_k, or A_k respectively:

$$A'_k = \max{}' \, \Phi_k(\lambda), \text{ against the baseline} \tag{1}$$

$$A_k = \max \, \Phi_k(\lambda), \text{ against the background} \tag{2}$$

Thus:

$$A_k = A'_k - \omega_k \tag{3}$$

Here it was considered the general instance of an unstable background given by the relation:

$$\omega_k = \omega_k(\lambda) \tag{4}$$

There is therefore a background value $\omega_k(\lambda)$ for $A_k(\lambda)$.

Let's denote by $I_k = \dfrac{A_k}{\omega_k}$, as a measure of signals from the set $\{\Phi_k(\lambda)\}$, $k = 1, N$.

From (3) there results that:

$$I_k = \frac{A'_k}{\omega_k} - 1 \tag{5}$$

In this manner, a probability q_k can be defined for the event of a signal from the set $\{\Phi_k\}_{k=1,N}$, by the relation:

$$q_k = \frac{I_k}{\sum\limits_{k=1}^{N} I_k} = \frac{\dfrac{A'_k}{\omega_k} - 1}{\sum\limits_{k=1}^{N} \dfrac{A'_k}{\omega_k} - N} \tag{6}$$

For a certain signal $k = 1, N$ there are the following limit relations :

$$\lim_{\substack{\omega_k \to 0 \\ \omega_k = \text{constant}}} q_k = \frac{A_k}{\sum_k A_k} \tag{7}$$

$$\lim_{\omega_k \to A'_k} q_k = 0 \tag{8}$$

$$A_k \to A'_k \text{ , as } \omega_k \to 0 \tag{9}$$

Condition (7) is achieved by measuring parameter optimization, and condition (8), e.g. is due to the physical or/and chemical matrix efects.

The information entropy or spectrum information amount, H_S, is computed using Shannon's relation[5] :

$$H_S = -\sum_{k=1}^{N} q_k \lg_2 q_k = \lg_2 \sum_{k=1}^{N} I_k - \sum_{k=1}^{N} q_k \lg_2 I_k \tag{10}$$

Jensen's inequality can be applied for changing relation (10) :

$$\sum_{k=1}^{N} q_k f(x_k) < f\left(\sum_{k=1}^{N} q_k x_k\right), \sum_{k=1}^{N} q_k = 1 \tag{11}$$

By substituting x_k for I_k and the function f for $\lg_2$, the following results :

$$-\sum_{k=1}^{N} q_k \lg_2 I_k > -\lg_2 \sum_{k=1}^{N} q_k I_k \tag{12}$$

From relations (10) and (12), the minimum of H_S is obtained :

$$\min H_S = \lg_2 \frac{\left(\sum_{k=1}^{N} I_k\right)^2}{\sum_{k=1}^{N} I_k^2} = \lg_2 \frac{\left(\sum_{k=1}^{N} \frac{A'_k}{\omega_k} - N\right)^2}{\sum_{k=1}^{N} \left(\frac{A'_k}{\omega_k} - 1\right)^2} . \tag{13}$$

According to the information theory,[2] the maximum of information entropy of a probability field is obtained for equal probabilities ; there results that the maximum information entropy of a spectrum having N signals has this formula :

$$\max H_S = \lg_2 N \tag{14}$$

The upper limit value for min H_S, if $\omega(\lambda) = \text{constant}$ and $\omega(\lambda) \to 0$, is that :

$$\max(\min H_S) = \lg_2 \frac{\left(\sum_k A_k\right)}{\sum_k A_k^2} \tag{15}$$

and the lower value for min H_S, if $\omega(\lambda) \rightarrow A'_{k,\max}$, by $A'_{k,\max}$ being noted the highest amplitude A'_k belonging to $\{A'_k\}_{k=1,N}$ set, is the next one:

$$\min(\min H_S) = 0 \tag{61}$$

For a given spectrum the information energy amount can also be computed, using Onicescu's formula[8]:

$$E_S = \sum_{k=1}^{N} q_k^2 = \frac{\sum_{k=1}^{N} \left(\frac{A'_k}{\omega_k} - 1\right)^2}{\left(\sum_{k=1}^{N} \frac{A'_k}{\omega_k} - N\right)^2} \tag{17}$$

By comparing relations (13) and (17) obtains:

$$\min H_S = \lg_2 E_S^{-1} \tag{18}$$

As a first conclusion, relations (13) and (17) prove the dependence of analytical information process upon the ratio signal/background (e.g., min H_s decreases as matrix effects encountered at spectrometric methods are potent). On the other hand, background diminution at a value $\omega' < \omega$ can involve the increase of signal number N, due to arising of M new signals Φ_k, $k = N+1, N+M$. The amplitudies of these M new signals fulfil the relation $\omega > A'_k > \omega'$, and the value of min H_S adequately increases.

3. THE INFORMATION CAPACITY OF A SPECTRAL ANALYTICAL PROCESS

The maximum information amount that can be obtained in a spectrum is called the information capacity of the spectral analytical process. This notion was initially introduced by Kaiser[9]; applied to the spectral analytical measuring process, Danzer [10] has got a relation between the information capacity and the parameters of a process. In the following we will propose a new procedure for establishing the spectral information capacity. The spectral domain, denoted by $D = \lambda_{\text{sup}} - \lambda_{\text{inf}}$, will be divided into $\frac{D}{6\sigma_\lambda}$ intervals, σ_λ being the standard deviation onto D domain; it is a function depending on resolution of measuring process. The size of an interval, $6\sigma_\lambda$, is due to the fact that every wavelength, λ, measured into the interval $\bar{\lambda} \pm 3\sigma_\lambda$ has a probability $2F_L(3) \rightarrow 1$ of being the real value $\bar{\lambda}$ ($F_L(3)$ is Laplace function. [4] The a priori probability as an interval $\alpha = 1, \frac{D}{6\sigma_\lambda}$ to exist is that:

$$p_\alpha = \frac{6\sigma_\lambda}{D}, \quad \sum_\alpha p_\alpha = 1 \qquad (19$$

Onto an interval of size $6\sigma_\lambda$ let's denote by ΔA the least spectral intensity difference that can be measured (i.e., sensibility limit), and by $[A_{\text{inf}}, A_{\text{sup}}]$ the spectral intensity domain, A_{inf} being the detection limit. Onto A-axis, $[A_{\text{inf}}, A_{\text{sup}}]$ domain can be divided into $\frac{A_{\text{sup}} - A_{\text{inf}}}{6\sigma_A}$, σ_A being the standard deviation of spectral intensities, taken as a constant value onto the whole measured domain. The a priori probability corresponding to an intensity interval of size $6\sigma_A$, measured at a certain wavelength, will be the following :

$$p_\beta = \frac{6\sigma_A}{A_{\text{sup}} - A_{\text{inf}}}, \; \beta = 1, \frac{A_{\text{sup}} - A_{\text{inf}}}{6\sigma_A} \tag{20}$$

Finally, the probability as a signal to be one of $\alpha = 1, \frac{D}{6\sigma_\lambda}$ wavelength intervals and $\beta = 1, \frac{A_{\text{sup}} - A_{\text{inf}}}{6\sigma_A}$ intensity intervals becomes :

$$p_l = p_\alpha p_\beta = \frac{36\sigma_\lambda \sigma_A}{D(A_{\text{sup}} - A_{\text{inf}})} \tag{21}$$

In this case, the probability field will be represented by $\{\Phi_l, q_l\}$, $l = 1, \frac{D(A_{\text{sup}} - A_{\text{inf}})}{36\sigma_\lambda \sigma_A}$. Its information entropy becomes :

$$\Delta H_{\text{max}} = \lg_2 \frac{(\lambda_{\text{sup}} - \lambda_{\text{inf}})(A_{\text{sup}} - A_{\text{inf}})}{36\sigma_\lambda \sigma_A} = \Delta H_{A,\text{max}} + \Delta H_{\lambda,\text{max}} \tag{22}$$

The significance of relation (22) is the following : the information capacity of a spectrum is the sum of the information capacity corresponding to the spectral intensity domain ($\Delta H_{A,\text{max}}$) and that corresponding to the spectral domain D ($\Delta H_{\lambda,\text{max}}$).

Table 1 gives several values of spectrum capacity for the visible domain and for various values of σ_λ and σ_A (Table 1).

Table 1

The bits values of visible spectrum capacity (ΔH_{max}) depending on σ_λ and $\sigma_A \cdot (\lambda_{\text{inf}} = 300$ nm ; $\lambda_{\text{sup}} = 800$ nm ; $A_{\text{sup}} = 1.000$; $A_{\text{inf}} = 0.000)$.

σ_λ \ σ_A	0.001	0.002	0.005	0.01	0.02
0.1	17.08	16.08	14.76	13.76	12.76
0.2	16.08	15.08	13.76	12.76	11.76
0.3	15.50	14.50	13.18	12.18	11.18
0.4	15.08	14.08	12.76	11.76	10.76
0.5	14.76	13.76	12.44	11.44	10.44

4. THE SPECTRAL INFORMATION REDUNDANCE

Reconsidering the set of analysed constituents $\{X_i\}_{i=1,n}$, by which a specific signal Φ_i of the set $\{\Phi_k\}_{k=1,N}$ corresponds to each constituent X_i, one obtains the set of specific signals $\{\Phi_i\}_{i=1,n}$. Consequently, the set of specific signals $\{\Phi_i\}_{i=1,n}$ taken together with their corresponding probabilities, q_i, involves a probability field, denoted by P_n, $P_n = \{\Phi_i, q_i\}_{i=1,n}$, having the following information entropy :

$$H(P_n) = -\sum_{i=1}^{n} q_i \lg_2 q_i \tag{23}$$

Where :

$$q_i = \frac{A_i}{\sum\limits_{i=1}^{n} A_i} \tag{24}$$

The remainder of signals obtained from analytical experiment $\{\Phi_k\}_{k=1,N} - \{\Phi_i\}_{i=1,n}$ is denoted by $\{\psi_j\}_{j=1,m}$ $(m = N - n)$ and it is called the set of redundant signals; these signals have intensity and specificity lower than the signals from the set $\{\Phi_i\}_{i=1,n}$. The set of signals $\{\psi_j\}_{j=1,m}$ with their corresponding probabilities q_j involves the probability field $R_m = \{\psi_j, q_j\}_{j=1,m}$. By q_{ij} there is denoted the probability of achieving the signal j in the field R_m on condition that the event i has been achieved in P_n. Then one can write :

$$q_j = \sum_{i=1}^{n} q_{ij}, \; j = l, m \tag{25}$$

Where : $q_{ij} = 0$, as signal i is not specific to X_j.

$0 < q_{ij} < 1$, as both signal i and j are specific to X_j.

The entropy of field R_m conditioned by signal i from P_n is :

$$H_m(R_m | i) = -\sum_{j=1}^{m} q_{ij} \lg_2 q_{ij} \tag{26}$$

and the entropy of field R_m conditioned by the entire field P_n becomes :

$$H_m(R_m | P_n) = \sum_{i=1}^{n} q_i H_m(R_m | i) = -\sum_{i=1}^{n}\sum_{j=1}^{m} q_i q_{ij} \lg_2 q_{ij} \tag{27}$$

This expression represents formally the redundant information entropy amount of a spectrum and it is denoted by H_R. For the two dependent fields, $P_n \times R_m$, the information entropy can be written :

$$H_{nm}(P_n \times R_m) = H(P_n) + H_R \tag{28}$$

For computing expression (28) we have to know the probabilities q_{ij}. These can be computed with the aid of q_i, thus :

$$q_{ij} = q_i \frac{A_j}{A_i} \delta_{ij} \tag{29}$$

where δ_{ij} is Kronecker's symbol and it takes the value 1 if Φ_i and $\psi_j \in X_i$, and 0 if $\Phi_i \in X_i$, $\psi_j \in X_j$. The following formula will be obtained :

$$H_R = \frac{1}{\left(\sum_{i=1}^{n} A_i\right)^2} \left[\sum_{i}^{n} \sum_{j}^{m} A_i A_j \delta_{ij} \left(\lg_2 \sum_{i=1}^{n} A_i \right) - \sum_{i}^{n} \sum_{j}^{m} A_i A_j \delta_{ij} \lg_2 A_j \right] \tag{30}$$

Acquirement of the set of specific signals of X_i, denoted by $\{\Phi_{l_i}\}_{l_i=1,N_i}$, so that $\sum_{i=1}^{n} l_i = N$, the dependence of which is expressed by formula (29), involves the existence of an a priori to experiment information amount, given by the relation :

$$H_{a \text{ priori}} = H_S - [H(P_n) + H_R] \tag{31}$$

From this point of view, H_S represents the information entropy of probability field $\{\Phi_k, q_k\}_{k=1,N}$ the signals of which are independent, and $[H(P_n) + H_R]$ represents the information entropy of the same signals the probabilities of which are dependent between them.

5. THE COMPARING PROCESS OF TWO SPECTRA

In practice, the spectrum of an unknown sample is compared with n individual spectra of constituents X_i, $i = 1, n$. In that case there are two posibilities. :

1) The lack of interferences for a set of specific signals $\{\Phi_i\}_{i=1,n}$, at wavelengths λ_i, as can be proved by the presence or the absence of constituents X_i in a sample. Afterwards, the establishment of X_i quantity (or concentration) can be made with the aid of the calibration curve :

$$A_i = f(c_i) \tag{32}$$

In this case the probability field a posteriori to analytical experiment will correspond to an empty set.

2) The presence of interferences will formally require the solving of the following equation system :

$$\sum_{i=1}^{n} f_{ik} c_i = A_k, \ k = 1, N \tag{33}$$

f_{ik} being the proportionality coefficients a priori known to the experiment by help of calibration curve.

If $n > N$, involving $H(\{X_i, p_i\}) > H(\{\Phi_k, q_k\})$, then the incompatibility of the system follows, a final uncertainty or a probability field a posteriori to the experiment on a number m from n constituents that are possibly to exist. If $n < N$, then by solving equation system (33) one can establish the qualitative and quantitative composition of an unknown sample. Hence the following important implication results :

$$\rho'_j = f(q_k) \tag{34}$$

By computing of information entropy H_i of a probability field a priori to experiment, $\{X_i, p_i\}_{i=1,n}$, and information entropy H_f of a probability field a posteriori to experiment $\{Y_j, p'_j\}_{j=1,m(m \leqslant n)}$, then the information amount ΔH is obtained :

$$\Delta H = H_i - H_f \tag{35}$$

This information amount ΔH is obtained from the sample spectrum containing H_S information amount, which fulfils the inequality :

$$\Delta H \leqslant H_S \tag{36}$$

That means that the analytical problem or the probability field a priori to experiment is entirely solved if by analytical experiment one obtains an information amount more than the information entropy of probability field a priori to experiment, $\{X_i, p_i\}_{i=1,n}$.

6. CONCLUSIONS

1. Any spectrum that removes the same uncertainty of an a priori to experiment probability field $\{\Phi_k, q_k\}_{i=1,N}$ contains a constant information amount, if the a priori to experiment probability field is invariable.

2. The entire removing of uncertainty of the a priori to experiment probability field $\{X_i, p_i\}_{i=1,n}$, is achieved if and only if the the information amount obtained by an analytical experiment is superior to the information entropy corresponding to the probability field $\{X_i, p_i\}_{i=1,n}$.

3. The maximum information amount that can be obtained from a spectrum, given by formula (22), corresponds to the analytical signal probability field $\{\Phi_l, q_l\}$, $l = 1, \dfrac{D(A_{\text{sup}} - A_{\text{inf}})}{36\,\sigma_\lambda \sigma_A}$, about which there is no information a priori to experiment. This quantity depends on parameters of analytical measuring process, and it is called spectral information capacity.

4. The replacement of the probability field $\{\Phi_l, q_l\}$, $l=1, \dfrac{D(A_{\text{sup}} - A_{\text{inf}})}{36\,\sigma_\lambda \sigma_A}$ by the probability field $\{\Phi_k, q_k\}_{k=1,N}$ $\left(N < \dfrac{D(A_{\text{sup}} - A_{\text{inf}})}{36\,\sigma_\lambda \sigma_A}\right)$ means the

acquirement of a limited number of analytical signals N instead of $\frac{D(A_{\text{sup}} - A_{\text{inf}})}{36\,\sigma_\lambda \sigma_A}$, which is the maximum number of signals that can be contained in a certain spectrum, and thus the existence of an information amount a priori to analytical experiment. The information anount corresponding to the probability field $\{\Phi_k, q_k\}_{k=1,N}$, fulfils this relation :

$$\lg_2 \frac{\left(\sum\limits_{k=1}^{N} A_k\right)^2}{\sum\limits_{k=1}^{N} A_k^2} \leqslant \Delta H \leqslant \lg_2 N$$

5. Any analytical spectral process can be characterized by a redundant information amount, H_R, given by the signal multitude of low inten-and specificity.

REFERENCES

[1] K. Eckschlager. "Information Theory as Applied to Chemical Analysis", Wiley, New York, 1979.

[2] C. Liteanu and I. Rică. "Optimizarea proceselor analitice", Ed. Academiei, București, 1985.

[3] V. David and D. Ciomârtan. *Rev. Chim. (București)* , **36**, 954 (1985).

[4] V. David and D. Ciomârtan, *Rev. Roumaine Chim.* **30**. 777 (1985).

[5] C. E. Shannon. *Bell Syst. Tech. J.*, **27**, 623 (1948).

[6] S. Guiașu and R. Theodorescu, "Matematica și informatica", Ed. Științifică, București, 1965, p. 230.

[7] S. Guiașu and R. Theodorescu. "Teoria matematică a informației", Ed. Academiei, București, 1966 p. 10.

[8] I. Petrică and V. Ștefănescu, "Aspecte noi ale teoriei informației", Ed. Academiei București, 1982, p. 20.

[9] H. Kaiser. *Pure Appl. Chem.*, **34**, 35 (1973).

[10] K. Danzer, *Z. Chem.*, **15**. 158 (1975).

Revue Roumaine de Chimie, 31, *8*, 833–836 (1986)

COMPTES RENDUS

S. Sternhell and J. R. Kalman, "Organic Structures from Spectra", Wiley, Chichester, 1986, 202 pp., soft-cover, 6.95 £

Yet another "spectra structure book"? Yes, but with certain distinctive features which make it one of the best yet published. From the authors' preface it results that this book is the outcome of a 18 years' course at the University of Sydney, Australia, for 3rd year undergraduates. A brief introduction presents the five main spectroscopic techniques (UV, IR, MS, ^{1}H—NMR, ^{13}C—NMR) at the elementary level (first-order couplings, no 2D—NMR data). After this 60-page exposition, a set of 115 problems follows. Each problem consists of a page with the five spectra in a standard format, including some additional details (sometimes information on the presence of uncommon elements, overlapping peaks, occasionally the molecular formula).

The ^{1}H—NMR data are presented as 100 MHz spectra with integral curves (sometimes with expanded insets or with 400 MHz portions of spectra), whereas the ^{13}C—NMR data are presented as 20 MHz spectra with off-resonance decoupled (SFORD) spectra. For one problem (No. 99) a whole page is sacrificed for the 400 MHz ^{1}H—NMR spectrum showing the beautiful couplings of an allylic group. The MS data and the IR data are given as spectra on which the main peaks have numerical information added : occasionally, information on metastable peaks is supplied. In keeping with the importance for structural elucidation, more than half of the page is occupied by the two NMR spectra, while the remaining three spectra occupy the remaining space (with UV data having the smallest space). This is a rather nice fashion of emphasizing the relative importance of spectral data. No answers are provided, but *bona fide* instructors may obtain the solutions by writing to the publishers.

After the set of problems, a unique feature is a collection of 16 problems concerning the interpretation of spin-spin coupling in ^{1}H—NMR spectra ; in some of these problems one is given the spectrum and one has to extract coupling information and to make assignments, being supplied the frequency at which the NMR spectrum was obtained (90, 100, or 400 MHz), or alternatively one is given coupling constants and one is requested to draw a schematic (line) representation of the pure "first-order spectrum" with a "splitting diagram".

The good assortment of structures and their relative simplicity, the standard format, the abundance of problems and the highly pedagogical order in which problems are presented make this book a favorite one of the reviewer.

Alexandru T. Balaban

M. Horváth, L. Bilitzky and J. Huttner, "OZONE", Akadémiai Kiadó, Budapest 1985, 350 p.

The monograph "Ozone" is a joint publication of Académiai Kiadó, the Publishing House of the Hungarian Academy of Sciences, and Elsevier Science Publishers B. V., Amsterdam, The Netherlands, as vol. 20 in the series "Topics in Inorganic and General Chemistry".

The emergence of numerous novel uses and technologies and partly a detailed investigation of atmospheric ozone by recent technical developments justifies the publication of this book-review. The book presents a survey on the physical and chemical properties of ozone and on its physiological effects, methods for production and storage, presence in atmosphere. The increased interest shown in ozone was reflected in the IInd International Symposium held in Montreal in 1975 to cover the production and use of ozone.

It is not very well known that the discovery of ozone is credited to F. C. Schönbein in 1840, who named the gas "ozone", after the Greek word οξειν, to smell. The new gaseous substance entered the forefront of interest of researchers who started the experiments to disclose its chemical nature. After it had become clear that the ozone molecule consisted of oxygen atoms only, experiments were initiated to investigate the structure of the substance. As the authors report, pure ozone was first produced only in 1922 and this enabled the exact determination of the physical constants and structure of the ozone molecule.

The five chapters of the monograph present : 1. The properties and analytical chemistry of ozone ; 2. Atmospheric ozone ; 3. Processes for ozone generation ; 4. Stabilization and storage of ozone ; 5. Fields of utilization of ozone. The most important methods and potential use of ozone are presented, but is not the authors' intention to discuss the traditional processes in detail as they are amply covered in the specialty literature.

After a discussion on analytical methods for determination of ozone, processes for generation, methods and generating ozone systems, storage in gaseous form under pressure, some details are referred to fields of applications, especially to its utilization for water treatment, ozone having among the oxidants the greatest redox potential, so it is capable of oxidizing practically all pollutants encountered in water.

Other fields of utilization of zone are agriculture and food industry textile industry, health protection, chemical industry and metallurgy, refreshing of air in assembly halls and in rooms accomodating large masses of people, cosmetics industry, etc. Ozon is used as an extremely efficient oxidant of fuels for rocket propulsion units, so the most recent field of application of great importance is that of rocket propulsion. Ozone is produced in extreme purity and in the liquid state for this purpose.

The monograph ends with 485 references and a final attention is called to the wide range of applications of this gas in the above reportd fields. A great number of applications will develop in the future for which only laboratory experiments have so far been carried out.

The book provides a starting point for research workers and practicing engineers by the systemization of the available results.

Margareta Craiu

"Polydiacetylenes" (Advances in Polymer Science, vol. 63), Springer, Berlin, 1984, 149 pages, 98 DM (hard-cover).

Volume 63 in this series contains three contributions dealing with polymerization of diacetylenes and the properties of the corresponding polymers.

In the foreword of the book, written by G. Wegner, it is shown that the polymerization process of diacetylenes is better understood than any other polymerization considering the formation, electronic structure and reactivity of the intermediates. The particularity of this kind of polymerization is that it proceeds within the perfect lattice and is controlled by the packing of the monomer; thus macroscopic and perfect single crystals of polymers could be prepared for the first time. Polydiacetylenes are best represented by structures with alternating single, double and triple bonds with complete electron delocalization, have one-dimensional electronic properties, and are thus interesting materials for applications in electronic devices.

The first article is written by H. Blässer ("Photopolymerization of Diacetylenes"). The main property of polydiacetylenes is that the chain is fully conjugated. The electronic structure is that of the chain (and not that of the substituents) which controls the electronic properties of the conventional polymers having σ-bonded backbones. Thus crystalline polydiacetylenes provide the closest approach to one-dimensional systems known so far, and are therefore used as models to study the effects of reduced dimensionality on optical and electronic properties. The article reviews the current state of polymerization of crystalline diacetylenes, the recent achievments regarding reaction kinetics and energies of initiation reactions and propagation. After discussing recent works on polymerization in Langmuir-Blodgett-multilayer assemblies, potential applications of polydiacetylenes are outlined.

The second article written by H. Sixl, "Spectroscopy of the Intermediate State of the Solid State Polymerization Reaction in Diacetylene Crystals" deals with electron spin resonance and optical absorption at low temperatures in order to analyse the individual reaction steps of the intermediates and kinetics of the polymerization. The reactive intermediates are diradicals, asymmetric carbenes and dicarbenes. The singlet, triplet and quintet states and their role in the polymerization process are investigated in detail. The interest of chemists and physicists in such polymers is due to the anisotropy of the optical and electrical properties expected from the regular periodic arrangement of the linear chain in the polymer single crystals.

V. Enkelmann is the author of the paper "Structural Aspects of the Topochemical Polymerization of Diacetylenes". Solid state polymerization of diacetylenes is a diffusionless, totally lattice-controlled process. As a consequence the reaction mode which requires the smallest atom displacements will be favoured. Both the crystallographic positions and the symmetry of the monomer units are retained; the symmetry of the monomer determines the symmetry of the product. The article reviews these aspects of diacetylene solid state polymerization (topochemical polymerization) considering structural properties, reaction mechanisms, growth of the macromolecule, the molecular weight and its distribution. Phase transitions are also considered.

Like all the other books edited by Springer Verlag, the printing is excellent and error-free. Figures and tables are drawn clearly.

Ursula Bologa

M. T. Pope, "Heteropoly and Isopoly Oxometalates" (Inorganic Chemistry Concepts, vol. 8), Springer, Berlin, 1983, 180 pages, 124 DM (hard-cover).

Polynuclear oxoanions of fifth- and sixth-group of transition metals are known for about 100 years and are widely used in analytical chemistry and electron microscopy. Hundreds of compounds were prepared. Two monographs and ten reviews were published in the last twenty years, but it seems that none of them treats satisfactorily this distinct class of oxygen-containing complexes.

This book is a comprehensive survey and discussion of chemistry, structures and applications of isopoly- and heteropoly anions. These two classes of compounds are represented by the general formulas $(M_mO_y)^{p-}$ and $(X_xM_mO_y)^{q-}$ where $x \leqslant m$. Polyanions result from the condensation of several simple anions with the elimination of water. These species have structures made of :

i) octahedra (polytungstates or polymolybdates) ;
ii) tetrahedra (polyphosphates) ;
iii) octahedra and/or tetrahedra.

Octahedra and tetrahedra share edges or vertices. The central atom (metallic or nonmetallic) is surrounded by six and four oxygen atoms, respectively (the oxygen is considered a ligand). Either the central atom or a ligand can be replaced. The chemistry of isopoly- and heteropolyanions has developed to the extent that the stabilities, molecular structures of these species as well as the mechanisms of their formation and interconversions are well understood.

The author stresses out that the nomenclature of the title compounds is still controversed since every atomic position must be numbered in order to recognise and to distinguish isomers. A systematic nomenclature of polyanions which appears to cope satisfactorily with these difficulties has been developed by Jeannin and Fournier (the book's Appendix).

The book contains the following eight chapters, an appendix, an author index and a subject index :

1. Introduction.
2. Preparation, Structural Principles, Properties and Applications.
3. Isopolyanions.
4. Heteropolyanions.
5. Heteropolyanions as Ligands.
6. Redox Chemistry and Heteropoly Blues.
7. Organic and Organometallic Derivatives.
8. Polyoxometalate Chemistry : Current Limits and Remaining Challenges.

It is the merit of the author to have systematized and classified the heteropoly and isopoly oxometalates such that every chemist who reads the book is able to understand their structures and chemical behavior. This up-dated monograph which contains 771 references is recommended to inorganic chemists and to analytical chemists. The book is highly readable and excellently printed. Figures representing the polyhedral forms of the complexes are very suggestive and drawn with care.

Ursula Bologa

"Siderophores from Microorganisms and Plants" (Structure and Bonding, vol. 58), Springer, Berlin, 1984, 143 pages, 86 DM (hard-cover).

This volume in the series "Structure and Bonding" is the first one devoted totally to siderophores. These compounds have become an interesting subject for study by scientists who are concerned with synthetic chemistry, organometallic chemistry or biochemistry.

"Methodology of Siderophores" written by J. B. Neilands is the first paper of the book. Siderophores, defined as iron(III) specific transport compounds, are widely distributed in aerobic and anaerobic bacterial species. As natural products, siderophores are classified conveniently as hydroxamates, catechols and "micellaneous". The article presents the methods for detection, determination, enhanced production, isolation and characterization of siderophores.

"Siderophores Mediated Absorption of Iron" written by R. C. Hider is the next paper. A brief presentation of iron chemistry is made, stressing those aspects relevant to siderophore biochemistry. Their structures and biosynthesis are described. Finally the role of siderophores in infection and their clinical potential as scavenging molecules are reviewed.

"Lysine Analogues of Siderophores" is the title of the next article written by A. Chimiak and J. B. Neilands. The latter is the author of the foreword of the volume. Considerable attention has focused on the chemical synthesis of tricatechol siderophores. The iron(III) binding ability of the tricatechols enterobactin, agrobactin and parabactin is known. This communication presents effective methods for the synthesis of di-N$^{\alpha}$,N$^{\omega}$-2,3-(dihydroxybenzoyl) lysine and di-N$^{\alpha}$,N$^{\omega}$-(2,3-dihydroxybenzoyl) lysyl-N$^{\omega}$-2,3-(dihydroxybenzoyl)lysine.

A. Liu and J. B. Neilands describe in "Mutational Analysis of Rhodotorulic Acid. Synthesis in *Rhodotorula pilimanae*" a simple system for mutagenesis of *Rhodotorula pilimanae* and for the detection of mutants defective in the biosynthesis of rhodotorulic acid.

"Phytosiderophores. Structures and Properties of Mugineic Acids and Their Metal Complexes" written by Y. Sugiura and K. Nomoto is the last article. New iron chelating substances isolated from the roots of gramineous plants, phytosiderophores, are described by contrasting them with bacterial siderophores and plant siderophores.

Volume 58 in the series "Structure and Bonding" is an important source of up-dated information in siderphore biochemistry, structure and preparation. The five articles are related to one another and complementary with regard to the aspects which are analysed. The book is error-free, and the printing is excellent.

Ursula Bologa

**MINISTERUL INDUSTRIEI
ELECTROTEHNICE
M.I.Et.
CENTRALA INDUSTRIALĂ
DE MECANICĂ FINĂ
ŞI MAŞINI TEXTILE
C.I.M.F.M.T.**

**CENTRUL DE CERCETARE ŞTIINŢIFICĂ
ŞI INGINERIE TEHNOLOGICĂ DE MAŞINI
PENTRU INDUSTRIA UŞOARĂ
C.C.S.I.T.M.I.U.**

**Exporter : C.M.T. ENTERPRISE FOR TEXTILE MACHINERY FOREIGN TRADE
70018 BUCHAREST – 3 ROMANIA, 13, Ion Ghica Street
Telephone 14 05 32, Telex 011855**

FLUIDIZED BED HEAT TREATING FURNACE

Designed to fulfill the most up-to-date requirements in heat treating. Optimum applicability is attained with an operating temperature up to 1000°C using different atmosphere compositions based on methane, air, nitrogen and ammonia. Microcomputer control of furnace parameters, safety devices, and technological functions give the most reliable operating mode.

Technical data :

- Maximum temperature : 1000°C
- Temperature uniformity : ± 5°C
- Heating rate : 5–8°/min. (depending on heating mode)
- Heating :
  1. electric resistance heating with submerged radiating tubes
  2. natural gas (internal combustion)
  3. mixed electric – gas heating
- Useful dimensions : ∅ 500/600 mm
- Fluidized medium : alumina, grain size : 0.2 mm
- Fluidizer : air, nitrogen, methane, ammonia, or their mixture
- Power supply :
  1. A.C. current 220/380 V ; 40 kW
  2. natural gas : 8 Nm^3/h
- Recommended technologies : hardening, carburizing and carbonitriding, nitrocarburizing, bright annealing, nitriding

The furnace has been developed as the result of joint research project with the "Gépipari Tehnológiai Intézet", Budapest, Hungary.

NITRION PLASMA NITRIDING INSTALLATIONS

The NITRION 10 and NITRION 30 installations have been designed to meet all the requirements of laboratory or production equipment for small parts of technological research.

The water-cooled vertical retort is to be charged from the top, on the cover plate with the cathode fixture.

The useful dimensions of the retort are of ∅ 400 × 1700 mm.

The maximum charge weight is 250 kg (providing the surface area is acceptable). The minimum pressure in the retort is 0.1 Torr. A suitable needle-valve enables manual pressure adjustment between 0.1–10 Torr to be obtained. The electrical system is 15 or 30 kW with 3 step voltage adjustment for 500, 750 and 1000 V. An electronic control prevents arc-discharge. Subminiature thermocouple built in a completely insulated form gives adequate temperature information. Temperature control is automatic within ± 5°C limits. The built-in recording instrument shows both the temperature and retort pressure variations. A separate gas generator supplies H_2 and N_2 mixture, obtained by cracking ammonia at 750–800°C. A constant flow of 200 L/h can be assured.

Power supply :	380/220V
Maximum operating temperature :	600°C
Vacuum pump :	25 m^3/h
Cooling water :	0.3 m^3/h

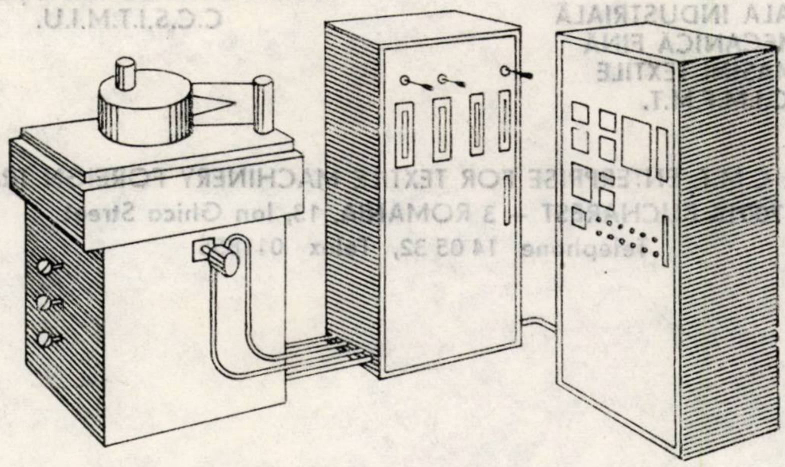

Fluidized bed heat treating furnace

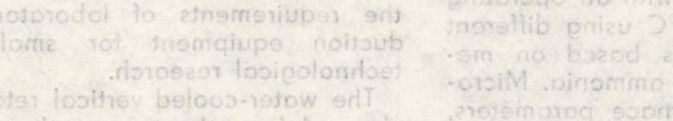

Flasma nitriding installations NITRION

„Une gamme cosmétique renée de la nature"

pell amar ®

formule 2

A. Ionescu-Călinești

Les produits PELL-AMAR – Formule 2 **contiennent** un complexe **naturel réunissant** les principes actifs des boues sapropeliques de Roumanie avec les substances contenues dans les extraits végétaux :

- des substances minérales ;
- des microéléments (Cl –, Na +, Ca ++, Mg ++, Al +++) qui règlent le ph des cellules, maintiennent l'équilibre hydrique et croissent la résistance vis-à-vis des agents pathogènes ;
- amino-acides qui interviennent dans le processus de régénération cellulaire et de révitalisation ;
- vitamines hydrosolubles (B1, B2, B6, C, PP), acide folique, qui activent la circulation du sang et préviennent les diverses affections de l'épiderme.

PELL-AMAR – ÉMULSION HYDRATANTE – nettoie les impuretés qui existent sur le visage et rétablit l'équilibre hydrique naturel.

PELL-AMAR – LOTION TONIQUE – formulé spécialement pour soigner les visages normaux et sensibles.

PELL-AMAR – CRÈME HYDRATANTE DE JOUR

- pour teint gras,
- pour teint sensible.

Protège la peau contre l'influence des agents atmosphériques en formant une pellicule lipohydrique. Constitue une base excellente pour le maquillage.

PELL-AMAR – CRÈME NUTRITIVE DE **NUIT – protective et nutritive.**

PELL-AMAR – CRÈME ÉMOLLIENTE POUR LES YEUX – pour la protection et le soin de la zone sensible autour des yeux.

PELL-AMAR – CRÈME POUR LE MASSAGE – contient une proportion optimale des substances grasses, émollientes. Refait le tonus naturel de l'épiderme.

PRODUCTEUR :
MIRAJ – Entreprise
de produits cosmétiques
BUCAREST

EXPORTATEUR :
CHIMICA – Entreprise
de commerce extérieur
BUCAREST – ROUMANIE

Première cosmétique !

ACANTHA®

formule 2

MIRAJ a créé spécialement pour vous...
«la douce comme le miel» ACANTHA

ACANTHA – Crème hydratante de jour pour teint gras

ACANTHA – Crème hydratante de jour pour teint sec

ACANTHA – Crème nutritive de nuit

La ligne cosmétique ACANTHA – formule 2 met en valeur les propriétés d'un nouveau principe actif apicole Apilarnil, substance active, extraite de larves des mâles des abeilles qui assure un riche contenu en substances nourrissantes, nécessaires à la nutrition de la peau : aminoacides, lipides, glucides, vitamines, etc. Les produits cosmétiques de la gamme ACANTHA – formule 2 contribuent au maintien de l'équilibre métabolique de la peau, ayant une action de régénération et révitalisation cellulaire.

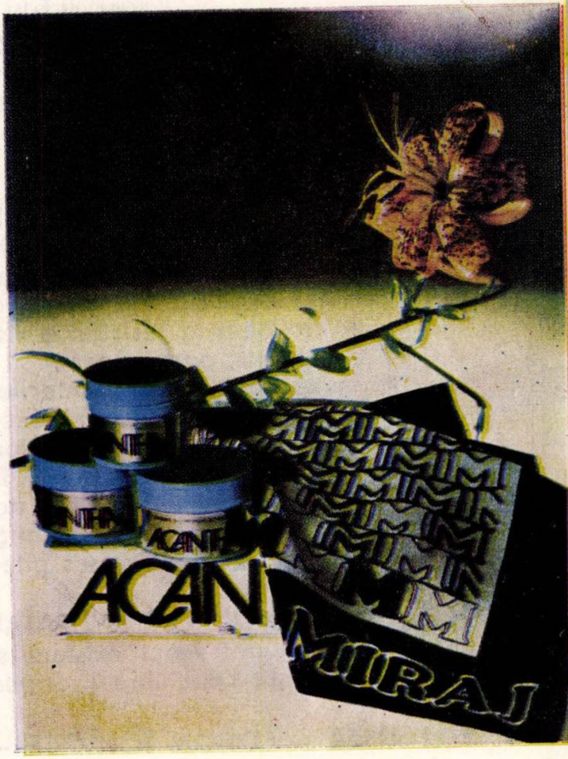

PRODUCTEUR :

**MIRAJ – Entreprise
de produits cosmétiques**
BUCAREST

EXPORTATEUR :

**CHIMICA – Entreprise
de commerce extérieur**
BUCAREST – ROMANIA

„Jeunesse • Santé • Beauté

GEROVITAL®

formule 2

Prof. Dr. A. Aslan

Les produits GEROVITAL – formule 2, une nouvelle conception supérieure, pour mettre en valeur les principes actifs naturels, associés aux produits chimiques similaires à la molecule de procaïne avec les effets suivants :

• la réglementation du métabolisme cellulaire ; • la régénération tissulaire et la prévention de l'apparition prématurée du vieillissement de la peau ; • L'activisation de la circulation sanguine périphérique ; • la réglementation du ph de l'épiderme ; • l'amélioration des propriétés physiologiques de la membrane cellulaire ; • la protection de la peau contre les radiations solaires.

GEROVITAL – LAIT DEMAQUILLANT – assure le nettoyage des impuretés, maintient la pellicule hydrique naturelle protectrice de l'épiderme. Il est recommandé le matin et le soir pour tous les types de peau.

GEROVITAL – LOTION TONIQUE – est appliquée après le démaquillage pour éloigner la pellicule grasse avec une action rafraichissante.

GEROVITAL – CRÈME HYDRATANTE DE JOUR

• pour peau grasse, • pour peau sèche. Contient des substances nutritives au rôle de filtre solaire.

Elle est hydratante et protège la peau, représentant en même temps une base excellente pour le maquillage.

GEROVITAL – CRÈME NUTRITIVE DE NUIT – hydratante, nutritive et protectrice, on l'applique le soir sur la peau démaquillée.

GEROVITAL – CRÈME ÉMOLLIENTE POUR LES YEUX – crème hydratante pour la zone sensible autour des yeux, zone exposée à la deshydratation et aux rides.

GEROVITAL – CRÈME POUR MASSAGE – crème grasse pénétrant dans la peau par un massage léger.

PRODUCTEUR :

MIRAJ – Entreprise de produits cosmétiques
BUCAREST

EXPORTATEUR :

CHIMICA – Entreprise de commerce extérieur
BUCAREST – ROUMANIE

NOTE POUR LES AUTEURS

La Revue Roumaine de Chimie publie des articles en anglais, français, russe, allemand ou espagnol. Les auteurs sont priés d'envoyer des articles et des comptes rendus inédits.

Les manuscrits seront dactylographiés à double interligne. La bibliographie, les tableaux et la légende des figures seront placés après le texte.

Si l'article fait partie d'une série numérotée, la partie précédente sera donnée comme première référence.

Chaque article sera précédé d'un résumé comprenant quinze lignes au maximum.

Les références bibliographiques dans le texte seront faites par des exposants sans parenthèses et paraîtront à la fin de l'ouvrage.

Les publications périodiques mentionnées dans la bibliographie seront présentées suivant les prescriptions internationales ; le nom de l'auteur précédé de l'initiale du prénom, le titre du périodique abrégé conformément à « Chemical Abstracts » et souligné par une ligne, le numéro du tome indiqué par des chiffres arabes et souligné par deux lignes, suivi de la première page de l'article ; à la fin, l'année de la parution sera placée entre parenthèses. Le numéro de la revue ne sera pas indiqué si les pages du volume sont numérotées consécutivement.

Les textes de livres ou traités incluerout: le nom des auteurs, l'initiale du prénom, le titre du livre entre guillemets et sans être souligné, le numéro du tome précédé par l'abréviation « vol. » (ou « Bd. ») le numéro de l'édition, les editions (the publisher), la localité de la parution du livre, l'année de la parution et la page de la référence précédée(s) par l'abréviation « p. » (ou « S. »).

Les brevets seront indiqués comme suit: l'auteur ou la firme, le pays et le numéro du brevet, la date et la revue (*Chem. Abstr.*). Par. ex. ; M. Jones (to Union Carbide Co), Brit. Pat. 601 238, 2 Sept. 1959 ; *cf. Chem. Abstr.*, 54, 12808 (1960).

Si la référence n'a pas été lue en original, on indiquera aussi la revue de référence consultée.

Les diagrammes seront tracés à l'encre de Chine sur papier calque. Les tableaux et les figures (en nombre strictement nécessaire) ainsi que les courbes dans les figures seront numérotés par des chiffres arabes. Leur explication sera donnée dans la légende des figures. Prière de ne pas inscrire les mêmes données dans les tableaux et les figures. Chaque tableau aura un titre. On indiquera dans le texte la place approximative des tableaux et des figures. Les formules chimiques seront incluses dans le texte ; en outre, elles seront transcrites sur papier calque, à l'encre de Chine.

Les auteurs sont priés d'indiquer les caractères italiques (en soulignant les lettres au crayon), ainsi que tout autre caractère spécial ; les préfixes *ortho*, *meta*, *para*, *cis*, *trans*, etc. seront soulignés pour indiquer leurs caractères italiques et ne seront jamais écrits avec des majuscules.

Aucune correction à la main ne sera admise sur le manuscrit. Les corrections seront tapées à la machine. Les lettres grecques ou d'autres symboles spéciaux seront insérés à la main à l'encre clairement.

Le manuscrit sera signé par l'auteur.

Le titre-courant aura 50 lettres au maximum.

L'entière responsabilité du contenu des articles appartient aux auteurs.

Sur demande ou peut obtenir une note plus complète.

PRINTED IN ROMANIA

1986 OKT 3

TRAVAUX PARUS AUX ÉDITIONS DE L'ACADÉMIE DE LA RÉPUBLIQUE SOCIALISTE DE ROUMANIE

V. DRĂGUŢAN, A. T. BALABAN, M. DIMONIE, **Olefin Metathesis and Ring-Opening Polymerization of Cyclo-olefins**, Coédition avec John Wiley and Sons, 1985, 544 p.
C. LITEANU, I. RÎCĂ, **Optimizarea proceselor analitice**, 1985, 360 p.
N. PERESCU, **Chimia extracţiei cu solvenţi şi aplicaţii**, 1985, 212 p.
V. E. SAHINI, HILLEBRAND, **Chimie cuantică în exemple şi aplicaţii**, 1984, 378 p.
GH. MARCU, **Chimia compuşilor coordinativi**, 1984, 415 p.
E. CORDOŞ, C. MANOLIU, **Spectrometria de absorbţie şi fluorescenţa atomică**, 1984, 178 p.
C. BODEA, **Tratat de biochimie vegetală**, p. II, vol. 5, 1984, 438 p.
ELENA CEAUŞESCU, **Cercetări în chimia şi tehnologia polimerilor**, 1983, 519 p.
N. ASANDEI, A. GRIGORIU, **Chimia şi structura fibrelor**, 1983, 395 p.
N. IONESCU, M. CĂLDĂRARU, **Oxidarea catalitică a olefinelor inferioare**, 1983, 178 p.
C. CAŞCAVAL, **Studiul polimerilor prin piroliză şi cromatografie de gaze**, 1983, 220 p.
C. I. SIMIONESCU, F. DANEŞ, **Originea vieţii**, 1983, 110 p.
C. BODEA (sous la direction), **Tratat de biochimie vegetală**, 2 partie, t. IV, 1982, 408 p.
I. G. MURGULESCU, RODICA VÎLCU, **Introducere în chimia fizică. Vol. III. Termodinamica chimică**, 1982, 624 p.
I. G. MURGULESCU, J. PĂUN, **Introducere în chimia fizică. Vol. I. 3. Nucleul atomic, reacţii nucleare, particule elementare**, 1982, 606 p.
ELENA CEAUŞESCU, **Noi cercetări în domeniul compuşilor macromoleculari**, 1981, 536 p.
I. G. MURGULESCU, TATIANA ONCESCU, E. SEGAL, **Introducere în chimia fizică. Vol. II, 2, Cinematică chimică şi cataliză**, 1981, 1024 p.
LYDIA-MARIA VAICUM, **Epurarea apelor uzate cu nămol activ. Bazele biochimice**, 1981, 218 p.
I. GĂLĂŢEANU, **Procese şi metode radiochimice în energetica nucleară**, 1981, 234 p.
O. IORDACHE, **Procese polistocastice aplicate la fenomenele de transfer**, 1981, 186 p.
CR. SIMIONESCU, VALERIA GORDUZA, **Polimeri biocompatibili şi biologic activi**, 1980, 479 p.
ELENA CEAUŞESCU, **Polimerizarea stereospecifică a izoprenului**, 1979, 307 p.
C. GH. MACAROVICI, **Analiza chimică cantitativă anorganică**, 1979 457 p.
M. FLORESCU, **Metode ştiinţifice în dezvoltarea industriei chimice moderne**, 1979, 256 p.
A. T. BALABAN, I. GĂLĂŢEANU, G. GEORGESCU, LIGIA SIMIONESCU, **Compuşi marcaţi şi radiofarmaceutici cu aplicaţii în medicina nucleară**, 1979, 495 p.
I. G. MURGULESCU, E. SEGAL., **Introducere în chimia fizică, Vol. II. 1. Teoria molecular-cinetică a materiei**, 1979, 1036 p.
S. STERNBERG, FL. DANEŞ, **Termodinamica chimică aplicată**, 1978, 400 p.
I. G. MURGULESCU, V. EM. SAHINI, **Introducere în chimia fizică. Vol. I 2. Structura şi proprietăţile moleculelor**, 1978, 604 p.
I. ZUGRĂVESCU, MAGDA PETROVANU, **N-ylid chemistry**, coédition avec McGraw-Hill International Book Company U.S.A., 1977, 396 p.
I. G. MURGULESCU, **Introducere în chimia fizică, Vol. I. 1. Atomi, molecule, legătură chimică**, 1976, 560 p.
ELENA CEAUŞESCU, **Research work on synthesis and characterization of macromolecular compounds, Contributions**, 1974, 251 p.
CR. SIMIONESCU, VIORICA RUSAN, V. POPA, **Chimia algelor marine**, 1974, 212 p. 1 pl.

ISSN 0035–3930

c. 2277—I. P. INFORMAŢIA
43 426
Lei 40
$ 80 (pour un abonnement annuel)

F 1103

ACADÉMIE DE LA RÉPUBLIQUE SOCIALISTE DE ROUMANIE

REVUE ROUMAINE DE CHIMIE

TOME 31

Nos 9—10

Septembre—Octobre 1986

| Rev. Roumaine Chim. | RRCHAX, 31, *9—10*, p. 837—918 (1986), Bucarest

EDITURA ACADEMIEI REPUBLICII SOCIALISTE ROMÂNIA

ACADÉMIE DE LA RÉPUBLIQUE SOCIALISTE DE ROUMANIE

COMITÉ DE RÉDACTION

Rédacteur en chef ;

I. G. MURGULESCU, membre de l'Académie de la République Socialiste de Roumanie

Rédacteurs en chef adjoints ;

A. T. BALABAN et V. EM. SAHINI, membres correspondants de l'Académie de la République Socialiste de Roumanie

Collège de rédaction ;

EM. BRATU, ELENA CEAUŞESCU, ECATERINA CIORĂNESCU-NENITZESCU, CR. SIMIONESCU, membres de l'Académie de la République Socialiste de Roumanie ; P. SPACU, membre correspondant de l'Académie de la République Socialiste de Roumanie ; M. BANCIU, M. D. GHEORGHIU, I. HAIDUC, D. I. MARCHIDAN, G. NIAC et D. SĂNDULESCU

La Revue Roumaine de Chimie paraît 10 fois par an. Toute commande de l'étranger sera adressée à ROMPRESFILATELIA — sectorul Export-Import Presă, P.O. Box, 12—201, télex 10376 prsfi r Bucarest, Calea Griviţei nr. 64—66, Roumanie

Les manuscrits, les livres et les proposés en échange, ainsi que toute correspondance seront envoyés à la rédaction

REVUE ROUMAINE DE CHIMIE

125, Calea Victoriei, 79717 Bucarest, Roumanie, téléphone 50 76 80

EDITURA ACADEMIEI REPUBLICII SOCIALISTE ROMÂNIA
125, Calea Victoriei, 79717 Bucarest, Roumanie, téléphone 50 76 80

REVUE ROUMAINE
DE
CHIMIE

Tome 31, N°s 9–10 **Septembre–Octobre 1986**

R. VÎLCU, V. BĂRBÎNȚĂ and I. GĂINAR, Determination of chemical non-homogeneity of polymers according to the chain length at fractionation. The use of double standardization by tracing method 839–848

B. M. BADIGER, S. A. PATIL, S. M. KUDARI and V. H. KULKARNI, Magnetic and spectral properties of cobalt(II) and copper(II) complexes with 3-substituted-4-(5′-substituted-salicylidene/2′-hydroxyacetophenoneimine)-1,2,4-triazoles 849–855

G. IVAN and MARIA GIURGINCA, Substituent and solvent effects in the absorption spectra of nitroso aromatic derivatives 857–867

RAMESH KUMARI, A. D. TANEJA and V. P. KUDESIA, Effects of solvents on the spectra of some substituted acetoacetarylamides 869–880

CAROL CRISTESCU, *as*-triazine derivatives with potential therapeutic action. XXI. Synthesis of 4-thioxo-5(fluoro-benzyl)thio-6-azauracil derivatives and their nucleosides 881–888

M. ROMÁN CEBA, J. C. JIMÉNEZ SÁNCHEZ and T. GALEANO DÍAZ, Kinetic determination of Co(II) based on its catalytic effect on atmospheric oxidation of 1,3-cyclopentandione bis(4-methylthiosemicarbazone) (in Spanish) 889–895

F. CAPITÁN, P. ESPINOSA F. MOLINA and L. F. CAPITÁN-VALLVEY, Study of metallic complexes of *Schiff* bases derived from 2-thiophenecarboxaldehyde, 2-pyridinecarboxaldehyde and o-aminobenzenethiol (in Spanish) 897–900

A. M. KHALIL, O. M. O. HABIB, I. I. ABD EL-GAWAD and H. A. ETMAN, Synthesis and reactions of some new isoquinoline-1-carbonitrile derivatives 901–908

CAROLINA HAGIU, MIHAI TALABA, VIORICA DULMAN and ANA TALABA, Ammonium polyphosphates. Obtention of ammonium polyphosphates by warm ammoniation of orthophosphoric acid 909–914

BOOK REVIEWS 915–917

Rev. Roumaine Chim. **31**, *9–10*, 837–918 (1986), Bucarest

Revue Roumaine de Chimie, **31**, *9–10*, 839–848 (1986)

DETERMINATION OF CHEMICAL NON-HOMOGENEITY OF POLYMERS ACCORDING TO THE CHAIN LENGTH AT FRACTIONATION. THE USE OF DOUBLE STANDARDIZATION BY TRACING METHOD

R. VÎLCU, V. BĂRBÎNŢĂ and I. GĂINAR
Polytechnical Institute of Bucharest, Physical Chemistry Department Bucharest, Romania

Received July 20, 1985

The paper presents two methods for applying radioactive isotopes to the determination of chemical non-homogeneity of polymers. The first method is used to prepare the standards, and the second one, named double standardization, is applied to current analysis. The method of double standardization consists in the addition to the polymer-sample of a labelled polymer synthetized from the same monomer, which at fractionation plays the role of witness for all mass transfers between fractions. Its signals give information about the mixing degree of the fractions. A mathematical model for data processing, as well as an example of application to the data delivered by IUPAC group, is also presented.

INTRODUCTION

The thermodynamic studies [1] (Flory-Schulz) concerning the polymer fractionation demonstrated the limited character of the separation procedure of fractions from the solution, because of transfer taking place between fractions. A detailed analysis of the experimental and theoretical works [2–6] shows that each polymeric fraction possesses a specific polydispersion of the molecular weight function of nonfractionated polymer (A) and the initial distribution is a linear overlap of fractions (B). According to the above mentioned remarks, the following correlation between fractions can be established:

$$C_x/(C_x^p)_i = F_1\left(\sum_1^n M_x\right) \cdot F_2\left(\sum_1^n f_i\right) \tag{1}$$

where C_x represents an x homogeneous fraction independent of the dispersion of the nonfractionated polymer, as well as of any other factors which can influence the fractionation;

$(C_x^p)_i$, represents the x heterogeneous fraction, experimentally obtained, depending both on the dispersion of the nonfractionated polymer and on the other factors affecting the fractionation;

$F_2\left(\sum_1^n M_x\right)$ is a function dependent on the dispersion of the nonfractionated polymer and

$F_z\left(\sum_1^n f_i\right)$ is a function dependent on the sum of the factors involved in the fractionation method (x).

The conclusions (A) and (B), quantitatively expressed by (1) represent two severe limitations of the possibility to compare the distribution curves of the molecular weights of the two polymers, not only in the case of different methods, but even in the frame of the same method. Modern procedures of analysis based on gel permeation chromatography, compared to the classical methods based on phase equilibrium, provide higher performances for the determination of the polymer non-homogeneity.

Nevertheless, recent works[6-7] have shown that the molecular weight distribution is affected by some factors, as the column parameters, the packing, the solvents employed and even by the weight of the sample to be tested.[8]

These deviations and especially their irregular aspect for the whole set of data representing the molecular weight distribution, have been proved by the IUPAC group, which had the task to test the same sample of polymers in various national laboratories. The results thus obtained are given in Table 1.

These mentioned aspects suggest a new way to evaluate the fraction heterogeneity, as follows : besides the separation equilibrium of the fractions, the repartition equilibrium of the labelled fractions of the standard is used as well as those of the sample to be analyzed. The use of the labelled standard sample outside and inside the analyzed sample makes the latter be a control for all the mass-transfers between fractions. The labelled standard sample is not affected by the physico-chemical factors perturbing the fraction distribution and presents the advantage to emit signals giving information about the mixing degree of the fractions.

Concretely, the use of double standardization consists in the fact that a labelled polymer P* is added to the test sample of polymer P, both obtained from the polymerization of the same monomer.

As a result of the synthesis, the specific activity of the standard polymer sample is equal for all fractions, namely in all patterns, because it is independent of the heterogeneity degree of the fractions. In the frame of the tracing method, we may regard $P^* \ll P$. Thus, after the fractionation of the polymer sample + standard, using the giving method, the concentration signals are

$$C_1^P,\ C_2^P,\ \ldots\ C_x^P,\ \ldots\ C_n^P$$

They will be accompanied by the activity signals

$$I_1^P,\ I_2^P,\ \ldots\ I_x^P,\ \ldots\ I_n^P \qquad (3)$$

for the mixture test sample + standard and by

$$I_1^E,\ I_2^E,\ \ldots\ I_x^E, \ldots\ I_n^E \qquad (4)$$

for the standard sample polymer, outside the test sample.

Table 1

Molecular weight characterization (GPC)[a]

Sample	$\overline{M}n$				$\overline{M}w$				$\overline{M}w/\overline{M}n$			
	PANARIS	RAPRA	SORVIK	BOISSEL[b]	PANARIS	RAPRA	SORVIK	BOISSEL	PANARIS	RAPRA	SORVIK	BOISSEL
I		47150	54000			175300	26400			3.72	2.80	
II	38200	39770	42000	39100	88750	86800	91300	96600	2.32	2.18	2.18	2.47
III	21500	27460	21800	21300	67000	122200	80300	74700	3.12	4.45	3.70	3.5
IV	27700	25900	27700	26000	84800	81300	91700	82900	3.03	3.14	3.30	3.2
V	27500	26940	29600	32300	64000	60180	67600	69300	2.33	2.23	2.28	2.15
VI	42000	39350	42400	43300	100000	104900	106000	96500	2.4	2.66	2.50	2.23
VII	54400	48500	47200	47200	103400	104800	108000	103300	2.5	2.16	2.28	2.2
VIII	45900	36300	46400	48800	125500	101300	115000	109700	2.73	2.79	2.49	2.25
IX	46200	43700	45600	49200	101000	103400	101000	114900	2.18	2.37	2.19	2.3

[a] Gel permeation chromatography

[b] IUPAC working party PVC defects—Cardiff September 19—22 (1978)

Since the concentration signals (2) are not real, because of the two mentioned limitations, it is suitable to apply the double standardization, for the evaluation of the fraction heterogeneity caused by the specific character of the distribution of sample molecular weight.

As a result of fraction mixture, the real value of the concentration signal for the fraction x, equal to C_x, becomes C^P, and I_x becomes I_x^P.

In the absence of the transport phenomenon between fractions occurring if the molecular weight distribution of the test sample overlapped those of the standard sample, we must have during the fraction separation :

$$I_x = I_x^P = I_x \tag{5}$$

Starting from the general equation,

$$I_x = C_x \cdot \gamma_x, \tag{6}$$

we obtain for the signal variations :

$$\frac{dI_x}{dx} = \gamma_x \frac{dC_x}{dx} + C_x \frac{d\gamma_x}{dx} \tag{7}$$

By replacing the differential quantities with finite variations, according to the relation ships

$$\begin{aligned} \Delta I_x &= I_x^E - I_x^P \\ \Delta C_x &= C_x - C_x^P \\ \Delta \gamma_x &= \gamma_x - \gamma_x^P, \end{aligned} \tag{8}$$

one obtains

$$\frac{I_x^E}{C^P} = C_x^2 - (I_x^E + I_x^P)C_x + C_x^P \cdot I_x^P = 0 \tag{9}$$

and hence

$$C_x = \frac{(I_x^E + I_x^P) \pm [(I_x^E + I_x^P)^2 - 4I_x^E \cdot I_x^E]^{1/2}}{2I_x^E/C_x^P} \tag{10}$$

Equation (10) has two solutions :

1. $C_x = C_x^P$, a solution of a particular character for which the physical meaning is the following : the test polymer sample has the same mole-

cular weight distribution as that of the standard sample polymer, i.e. the same heterogeneity degree of the fractions.

2.
$$C_x = C_x^P \cdot \frac{I_x^E}{I_x^P} \tag{11}$$

is the most general solution, valid for the case where the distribution of the test sample molecular weight does not overlap that of the standard sample, namely the heterogeneity degree of the fractions is different.

The result expressed by equation (11) is valid only for a certain group of factors which determine the fractionation and only for certain methods.

In order to emphasize the specificity of a certain chosen method, we assign the quantities occurring in equation (11) with the index "i"

$$(C_x)_i = (C_x^P)_i \cdot \frac{(I_x^E)_i}{(I_x^P)_i} \tag{12}$$

EXPERIMENTAL

Table 2 presents, comparatively, the experimental data and the solutions of equation (10). Two polymers, marked (VI) and (VII), were used; they were supplied by the international IUPAC group that dealt with the structural characterization of PVC. The caracterizations of these polymers one of which was employed as a test sample and the other as a standard sample, are given in Table 3. Table 2 presents the activity of the standard sample polymer (VI) together with its inactive form and together with the test sample polymer (VII), in order to demonstrate the influence of its own molecular distribution on the fractionation, namely on the fraction heterogeneity. Column 2 includes molecular weights for PVC fractions evidenced by the precipitate-solution equilibrium and expressed according to the data on standard sample polymer, given in Table 3.

Table 2

Activities in double standardization, for a labelled fraction/carrier fraction ratio

N_f	M_{VI} according to Rapra	I_1^{IV} (I^E) imp/min	f %	I^{VI}	$I^{VII}(I^P)$	ΔI_1^E	ΔI_2
1	2	3	4	5	6	7	8
1	$1.625.10^6$	1062	1.24	114	68	− 8	+ 38
2	$3.739.10^5$	1321	3.89	147	399	−15	− 67
3	$2.199.10^5$	7103	8.32	670	928	+40	−218
4	$1.451.10^5$	12151	14.24	1252	1289	−37	− 74
5	$0.957.10^5$	16946	19.86	1644	1504	+50	+190
6	$5.929.10^4$	17344	20.32	1699	1894	+35	−160
7	$3.754.10^4$	13722	16.08	1414	1191	−42	+181
8	$2.215.10^4$	6575	7.70	645	611	−12	+ 46
9	$1.356.10^4$	4374	5.12	429	260	+ 8	+177
10	$4.748.10^3$	2760	3.23	267	120	+ 9	+156

1. Number of fraction; 2. Molar mass; 3. The activity of fractions at the standard sample; 4. Fraction percentage; 5. The activity of the active standard sample carried away with the inactive one, in 1/10 ratio; 6. The activity of the standard sample mixed with the test sample; 7. $I_1^{VI}/10 - I^{VI}$; 8. $I_1^{VI}/10 - I^{VII}$

Table 3

Characterization of the standard and test sample polymer, according to Rapra's data

N_f	$\overline{M}$	Standard polymer (Test VI — Table 1)		Test sample (VII)	
		f %	DW/DlgM	f %	DW/DlgW
1	$2.039.10^6$	0.07	0.04		
2	$1.393.10^6$	0.19	0.11	0.15	0.06
3	$9.781.10^5$	0.31	0.19	0.24	0.15
4	$6.984.10^5$	0.63	0.42	0.43	0.29
5	$5.074.10^5$	0.86	0.64	0.83	0.63
6	$3.842.10^5$	1.53	1.25	1.36	1.10
7	$2.925.10^5$	2.58	2.26	2.26	2.29
8	$2.315.10^5$	4.12	3.90	4.40	4.05
9	$1.810.10^5$	6.28	6.09	6.83	6.59
10	$1.421.10^5$	8.67	8.71	9.45	9.45
11	$1.101.10^5$	10.72	11.09	11.66	12.01
12	$8.540.10^4$	11.84	12.39	12.69	13.21
13	$6.486.10^4$	11.66	12.20	12.29	12.80
14	$5.078.10^4$	10.32	10.73	10.63	11.00
15	$3.957.10^4$	8.36	8.60	8.24	8.43
16	$3.028.10^4$	6.42	6.51	6.19	6.25
17	$2.319.10^4$	4.78	4.76	4.45	4.41
18	$1.784.10^4$	3.50	3.46	2.94	2.89
19	$1.344.10^4$	2.48	2.40	1.97	1.91
20	$1.027.10^4$	1.73	1.67	1.18	1.13
21	$7.751.10^3$	1.16	1.10	0.74	0.65
22	$5.852.10^3$	0.77	0.71	0.38	0.35
23	$4.308.10^3$	0.47	0.42	0.28	0.25
24	$3.141.10^3$	0.29	0.25	0.05	0.04
25	$2.215.10^3$	0.19	0.16		
26	$1.550.10^3$	0.07	0.05		

Columns 3,5 and 6 contain the activities of the standard fractions, those of the labelled one carried together with its nonlabelled form and those labelled standard carried together with a polymer of different polydispersion.

The weight contribution of the fractions is calculated from the fraction activities (as well as the total one); the values obtained are given in column 4.

Apparently, the difference between the values given in columns 5 and 6 seems insignificant; if we substract the value of the standard sample fraction activities (1/10 utilized), the following facts can be noticed:

1. The differences observed with the activity measurements for the standard sample mixed with a carrier of the same molecular distribution (column 7), shows that these variations are situated within the experimental error limits.

2. The differences observed with the activity measurements, for the standard sample mixed with the test sample, therefore with a carrier of another molecular distribution, indicate significant variations compared with the experimental errors. These observations justify the necessity of introducing the ratio I^E_x/I^P_x in relationships (11, 12) as a correction able to express the differences in the behaviour of some dissimilar molecular distributions against one, taken as a reference.

The importance of expression (12) consists in the fact that it allows to express the results by means of standard sample signals $(I^E_x)_i : (I^P_x)_i = \gamma^E \cdot (C_x)_i$.

This constant is independent of the fraction,

$$(\gamma_1^E)_i = (\gamma_2^E)_i = \ldots = (\gamma_j^E)_i = \ldots = \gamma^E \tag{13}$$

and of the factors affecting the fractionation

$$(\gamma^E)_1 = (\gamma^E)_2 = \ldots = (\gamma^E)_n = \ldots = \gamma^E$$

It allows to compare the results obtained with various fractioning methods. Consequently, relationship (12) expresses the fractions independent of the test sample polymer polydispersion (the first limitation is rejected) but remains dependent on the standard sample polymer polydispersion and on the chosen method.

In order to remove the second limitation, it is necessary that the signals of the reference polymer, of the "i" chosen method, $(I_x^E)_i$, be expressed by $(I_x^E)_o$ values, of the ideal method, where the mass transfer between fractions does not exist.

The thermodynamic studies on polymer solutions lead to the conclusion that such a separation is almost impossible even if the refractionation is used. If the thermodynamic equilibrium of fraction separation overlaps a second equilibrium, the isotope equipartitioning one — without obtaining any separations — the new equilibrium gives us the necessary data for the analytical determination of the real fractions. This fact is a consequence of the special character of the tracing method and of the conclusions given below.

If we take into account the heterogeneity of the fractions at separation equilibrium, the equation of the standard sample polydispersion, for concentration and activity signals, could be written as follows:

$$\sum_1^n C_x = \sum_1^n C_{x,1} + \sum_1^n C_{x,2} + \ldots + \sum_1^n C_{x,i} + \ldots + \sum_1^n C_{x,n} \tag{15}$$

where

$$\sum_1^n C_{x,1} = (C_1)_i; \quad \sum_1^n C_{x,i} = (C_i)_i; \quad \sum_1^n C_{x.n} = (C_n)_i \tag{16}$$

and

$$\sum_1^n I_x = \sum_1^n I_{x,1} + \sum_1^n I_{x,2} + \ldots + \sum_1^n I_{x,i} + \ldots + \sum_1^n I_{x,n}$$

where

$$\sum_1^n I_{x,1} = (I_1)_i; \quad \sum_1^n I_{x,2} = (I_2)_i, \ldots, \sum_1^n I_{x,n} = (I_n)_i.$$

Signals

$$\sum_1^n I_{x,i} = (I_i)_i \tag{17}$$

represent part of the fraction $I_i(I_{ii})$ to which we add the contributions of the other fractions, $x = 1, 2, \ldots n$, indicated by the terms $I_{1,i}$; $I_{2,i}$; $\ldots$ $I_{n,i}$. The expression of the pure fraction "i", free of the other fraction contributions is rendered by the relation

$$\sum_{1}^{n} I_{i,x} \tag{18}$$

where $I_{i,i}$ represents the fraction "i" remained after separation, to which we add the contributions of fraction "i" in fractions x = 1, 2, ... n indicated by the terms

$$I_{i,2};\ I_{i,3};\ I_{i,4},\ \ldots;\ I_{i,n} \tag{19}$$

To determine the components (19) of the sum $\sum_{1}^{n} I_{i,x}$, each fraction is refractionated apart, by employing the non-labelled and non-fractionated carrier.

In this case, each fraction will be deployed on a line of the matrix

$$\left.\begin{aligned}
(I_1)_i &= \sum_{1}^{n} I_{x,1} = I_{11} + I_{21} + \ldots + I_{x,1} + \ldots + I_{n,1}\\
(I_2)_i &= \sum_{1}^{n} I_{x,2} = I_{12} + I_{22} + \ldots + I_{x,2} + \ldots + I_{n,2}\\
&\vdots\\
(I_i)_i &= \sum_{1}^{n} I_{x,i} = I_{1,i} + I_{2,i} + \ldots + I_{x,i} + \ldots + I_{n,i}\\
&\vdots\\
(I_n)_i &= \sum_{1}^{n} I_{x,n} = I_{1,n} + I_{2,n} + \ldots + I_{x,n} + \ldots + I_{n,n}
\end{aligned}\right\} \tag{20}$$

The right side of equations (20) forms the matrix for the transformation of the data, from the first equilibrium, into data characterizing the second one — the isotope equipartition equilibrium. The increase of information amount concerning the mixing of fractions helps us to pass from $(I_x)_i$ to I_x.

If we add values of each column of the matrix (20), we shall obtain the desired quantities. For instance, the first column represents

$$\sum_{1}^{n} I_{1,x} = I_1,$$

the second column

$$\sum_{1}^{n} I_{2,x} = I_2$$

and so on, and $I_1, I_2, \ldots I_n$ represent the pure fractions in a first order approximation. The approximation of "m" order expresses the number of equipartition equilibrium employed to determine the non-homogeneity of the fractions.

In order to determine the function $F_2\left(\sum_{1}^{n} f_i\right)$, we use the equipartition equilibrium of the labelled fraction also employed in the tracing method; on this basis, the ratio between concentration variations of the standard and test sample, dC_x^E/dC_x determined by the variations of the physico-chemical factors which characterize the chosen method "i", is equal to the concentration ratio :

$$\frac{dC_x^E}{dC_x} = \frac{C_x^E}{C_x} \tag{21}$$

From (13) and (14)

$$\frac{dC_x^E}{C_x^E} = \frac{dI_x^E}{I_x^E} \tag{22}$$

integrated within the limits $(C_x)_i - (C_x)_0$ for C_x and $(I_x^E)_i - (I_x^E)_0$ for I_x^E, leads to

$$C_x = (C_x)_i \, \frac{(I_x^E)_0}{(I_x^E)_i}, \tag{23}$$

which according to equation (12), becomes

$$C_x = (C_x^P)_i \cdot \frac{(I_x^E)_0}{(I_x^P)_i} \tag{24}$$

Finally, from (1) and (24), we obtain :

$$F_1\left(\sum_1^n M_x\right) = \frac{(I_x^E)_i}{(I_x^P)_i} \quad \text{and} \quad F_2\left(\sum_1^n f_i\right) = \frac{(I_x^E)_0}{(I_x^E)_i} \tag{25}$$

DISCUSSION

The paper suggests two ways of using the tracing method in order to determine the fraction heterogeneity. The first way is ideal from the theoretical point of view, but practically limited by the conditions of test sample polymer labelling and the repeated fractionation of the fractions.

These are sufficient reasons that the method becomes unsuitable in the ordinary chemical analyses, at the same time being the only way of preparing standards.

The second method, *i.e.* the double standardization, represents the main part of the paper, because it offers the possibility to be applied in common analyses. The double standardization, employing the ratio between the two signals in the fraction calculus — outside and inside test sample — offers the possibility to obtain results which do not depend on the standard sample characteristics.

Consequently, the value of the test sample polymer polydispersion becomes independent of the constant value γ^E and the distribution of the standard sample fractions.

The standard sample fractions represent only the marks which permit the correction of the polydispersion curves in the case of a given method *versus* the others or the estimation of the influence of the factors which can modify the heterogeneity of the fractions.

The prior knowledge of the standard sample and the use of the double standardization method, allows the passing from one method to another, as well as the unitary expression of the results, according to equations (24).

The knowledge of the standard sample, in a certain method, means to have the transformation matrix for the data of the given method into the real components of the standard sample. The interference of every physico-chemical factor involves certain modifications of the standard sample matrix elements. Therefore, the characterization of the methods, as regards their specific factors, is materialized by the operations effected on the matrix.

This way of representation makes easier the communication and interpretation of the various data, because it can be processed by a computer.

The practical achievement of the double standardization — which, in its principles resembles the use of double weighing in analytical chemistry — involves the use, as a standard sample, of any labelled polymer having the same chemical nature as the test sample and the addition of a detector for measuring the activity signals.

The polymer is labelled not only with radioactive isotopes but also with stable ones or even with other techniques, coulouring for instance, but using suitable detectors.

In conclusions, the two limitations of the present fractionation methods can be rejected by overlapping a second equilibrium, *i.e.* the isotope equipartition, over the separation equilibrium of the fractions.

The ways to remove the two limitations lead to the intensive property of the system, γ^E now available only by means of the tracing method. This quantity allows to express the results obtained with various methods by a unique value, independent of the fractionation method, because it maintains its value constant for any fraction or even upon the interference of physico-chemical factors affecting fractionation.

The authors wish to express their gratitude to the International Atomic Energy Agency in Vienna for the subvention supplied in fulfilling the present research work.

REFERENCES

[1] P. I. Flory, "Statistical Mechanics of Chain Molecules", Interscience, New York, 1969.
[2] C. Cotliar, *J. Polymer Sci.*, A_2, **3**, 1373 (1964).
[3] D. Feldman, C. V. Uglea, *Studii și Cercetări Chim.* Acad. R.S.R., **19**, 1051 (1970).
[4] H. Okamoto, *J. Polymer Sci.*, A_2, **8**, 3451 (1964).
[5] E. A. Haseley, *J. Polymer Sci.*, **30**, 128 (1959).
[6] G. Pezzin, G. Sinmartin, *J. Appl. Polymer Sci.*, **11**, 1539 (1967).
[7] Y. Kato, T. Hasimoto, *J. Appl. Polymer Sci.*, **18**, 4 (1974).
[8] J. V. Chiang, J. F. Johnson, *J. Appl. Polymer Sci.*, **17**, 7 (1973).

Revue Roumaine de Chimie, 31, *9–10*, 849–855 (1986)

MAGNETIC AND SPECTRAL PROPERTIES OF COBALT(II) AND COPPER(II) COMPLEXES WITH 3-SUBSTITUTED-4-(5′-SUBSTITUTED-SALICYLIDENE/2′-HYDROXY-ACETOPHENONEIMINE)-1,2,4-TRIAZOLES

B.M. BADIGER, S.A. PATIL, S. M. KUDARI and V.H. KULKARNI*
Department of Chemistry, Gulbarga University, Gulbarga – 585 106, India

Received September 2, 1985

Several complexes of cobalt(II) and copper(II) with 3-substituted-4-(5′-substituted-salicylidene/2′-hydroxyacetophenoneimine)-1,2,4-triazoles (H_2L) have been synthesized. The complexes have a stoichiometry ML. The bonding of the ligands has been inferred from IR spectroscopy. All the complexes show lower magnetic moments than required for spin only values indicating dimeric or polymeric nature of the complexes. The electronic spectra are consistent with square-planar and tetrahedral geometries of copper(II) and cobalt(II), in these complexes respectively.

INTRODUCTION

The previous paper [1] from this laboratory described the synthesis, magnetic and spectral properties of nickel(II) complexes of 3-substituted-4-(5′-substituted-salicylideneamino)-5-mercapto-1,2,4-triazoles. Magnetochemically and spectrochemically, it has been shown that in these complexes nickel(II) exhibits coordination number six and ligands exist in thiol form thus depicting tridentate behaviour. This seems to be possible in view of their displaying thione–thiol tautomerism.[2] One of the forms is retained in the complexes. Triazole nitrogens sometimes take part in coordination thus imposing a tetradentate character. This has aroused our interest in undertaking a systematic study of transition metal complexes with such ligands. The results of such efforts are the nickel(II) complexes.[1] In this paper we have chosen to report cobalt(II) and copper(II) complexes. When our work was in progress, Syamal and Niazi[3] reported copper(II) complexes with similar ligands. They have shown that the triazole Schiff bases show a divalent tridentate behaviour, in the copper(II) complexes. They have suggested dimeric structure for these complexes in view of their subnormal magnetic moments. We have taken a note of this work while authenticating our conclusions on a large series of copper(II) and cobalt(II) complexes.

In this paper we report cobalt(II) and copper(II) complexes with the following ligands.

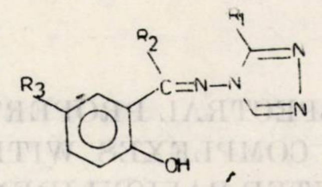

Ligand	R_1	R_2	R_3	Ligand	R_1	R_2	R_3
I	CH_3	H	H	X	C_2H_5	H	Cl
II	CH_3	H	OCH_3	XI	C_2H_5	CH_3	CH_3
III	CH_3	H	CH_3	XII	C_2H_5	CH_3	Cl
IV	CH_3	H	Cl	XIII	C_3H_7	H	H
V	CH_3	CH_3	CH_3	XIV	C_3H_7	H	OCH_3
VI	CH_3	CH_3	Cl	XV	C_3H_7	H	CH_3
VII	C_2H_5	H	H	XVI	C_3H_7	H	Cl
VIII	C_2H_5	H	OCH_3	XVII	C_3H_7	CH_3	CH_3
IX	C_2H_5	H	CH_3	XVIII	C_3H_7	CH_3	Cl

EXPERIMENTAL

The chemicals used for preparing triazoles, aldehydes and acetophenones were of reagent grade. Substituted salicylaldehydes and *o*-hydroxyacetophenones were prepared by the known methods.[4,5] 3-Substituted-4-amino-5-mercapto-1,2,4-triazoles were prepared by the reported methods.[6,7]

All the ligands were prepared according to the method reported elsewhere.[1]

General Method for preparing the complexes

Metal(II) chloride (0.01 mol) was treated with ligand (0.01 mol) in alcohol and the reaction mixture was heated under reflux for about an hour and then sodium acetate (2g) was added to the reaction mixture and heating was continued for about 3 hrs. The complex so obtained was filtered, washed with water, then with alcohol and finally dried over fused calcium chloride in vacuo.

Analysis

Copper and cobalt in the complexes were analysed as salicylaldoximate and 8-hydroxyquinolinate respectively. Sulphur was determined as $BaSO_4$ and nitrogen by Dumas' method.

Physical measurements

Magnetic susceptibilities of the complexes at room temperature were measured with a Gouy balance using $Hg[Co(SCN)_4]$ as calibrant.

Electronic spectra in DMF were taken with an ELICO-24 spectrophotometer in the region 350–900 nm.

Infrared spectra of ligands and complexes were recorded on a Perkin-Elmer-225 spectrophotometer in the region 4000–250 cm^{-1}

RESULTS AND DISCUSSION

These are intensely coloured complexes with stoichiometry 1 : 1 of the type ML (Table 1). These are insoluble in common organic solvents. However, they are soluble to a limited extent in DMF, DMSO and pyridine. Molecular weights were not determined because of their insolubility. Their insolubility and high decomposition temperature indicate dimeric or polymeric nature of the complexes.

Infrared spectra

The free ligands exist both in thiol and thione forms. A broad band around 3200 cm^{-1} due to $\nu(NH)$ indicates the thione form whereas a medium intensity broad band in the 2400 – 2300 cm^{-1} region due to $\nu(SH)$ represents the thiol form. A broad weak band with fine structure in the region 2700 – 2600 cm^{-1} is due to the intramolecular H-bonded OH. This band is absent in 3-methyl-4-(benzylideneimino)-5-mercapto-1,2,4-triazole. The high intensity band in the region 1640 – 1620 cm^{-1} is assigned to the $\nu(C=N)$ in view of the previous assignments.[1,8] It is rather difficult to locate the phenolic C–O band amidst the high intensity bands due to triazole C = N and aromatic C = C vibrations. However, taking into consideration the previous report on such band in the case of Schiff bases[9] we have assigned a band in the region 1520–1510 cm^{-1} to the phenolic C–O vibration. Another band of high intensity around 1280 cm^{-1} is assigned to the same phenolic C–O vibration. The medium intensity band in the region 760–740 cm^{-1} has been attributed to the $\nu(C=S)$.[1]

In the complexes we observe the following changes :

1. The band due to the H-bonded OH disappears and the phenolic C–O vibration appears around 1300 cm^{-1}. In copper(II) complexes the 1520–1510 cm^{-1} phenolic band shows a shift of the order of 25–35 cm^{-1}, thus offering an unambigous proof for the phenolic oxygen bridge.[9] In cobalt(II) complexes the shift is of the order of 10–15 cm^{-1}. These observations suggest that in the copper(II) complexes oxygen atom of the ligand shows bridging bidentate behaviour whereas in cobalt(II) it exhibits monodentate behaviour.

2. The $\nu(C=N)$ for these complexes appears around 1600 ± 10 cm^{-1} indicating coordination of the C=N group through nitrogen.

3. The band in the region 2400–2300 cm^{-1} due to $\nu(SH)$ disappears and the other due to $\nu(C=S)$ becomes weak and shifts to lower energy in 680–660 cm^{-1}. Thus it is evident that ligands react with these metal ions in the thiol form coordinating through azomethine nitrogen and reacting through –OH and SH groups.

Magnetic data

The observed magnetic moments for the complexes at room temperature are listed in Table 1. The copper(II) compexes show magnetic moments in the range of 1.37–1.50 B.M. significantly lower than the spin only value of 1.73 B.M.[10] The cobalt(II) complexes show magnetic moments in the range of 3.70–4.15 B.M. This value is lower than expected for tetrahedral cobalt(II) complexes *i.e.* 4.4 B.M. [10] These subnormal magnetic values suggest that the complexes may exist in polymeric form. This offers a positive support for the IR conclusions.

Table 1

Analytical, magnetic and electronic spectral data of cobalt(II) and copper(II) complexes of 3-substituted-4-(5′-substituted salicylidene(2′-hydroxyacetophenoneimine)-1,2,4-triazoles

Ligand No	Complex No	Empirical formula	Analysis (%)*			μ_{eef} B.M	λ_{max} (cm^{-1}) DMF
			M	N	S		
I	1	$C_{10}H_8ON_4SCo$	21.40 (20.26)	19.31 (19.25)	11.01 (11.00)	3.69	13510, 15620, 18180, 26320
II	2	$C_{11}H_{10}O_2N_4SCo$	18.27 (18.37)	17.52 (17.46)	9.92 (9.97)	3.84	—
III	3	$C_{11}H_{10}ON_4SCo$	19.42 (19.32)	18.47 (18.37)	10.51 (10.49)	3.90	14600, 16950, 18180, 25000
IV	4	$C_{10}H_7ON_4SClCo$	17.89 (18.11)	17.31 (17.22)	9.90 (9.84)	3.84	12820, 17240, 18180, 26320
V	5	$C_{12}H_{12}ON_4SCo$	18.52 (18.48)	17.60 (17.56)	10.02 (10.03)	3.91	—
VI	6	$C_{11}H_9ON_4SClCo$	17.42 (17.37)	16.61 (16.50)	9.44 (9.43)	3.75	—
VII	7	$C_{11}H_{10}ON_4SCo$	19.41 (19.32)	18.46 (18.37)	10.51 (10.49)	3.70	—
VIII	8	$C_{12}H_{12}O_2N_4SCo$	17.62 (17.60)	16.81 (16.72)	9.62 (9.55)	3.80	17360, 18730, 26320
IX	9	$C_{12}H_{12}ON_4SCo$	18.58 (18.48)	17.63 (17.56)	10.12 (10.03)	3.98	—
X	10	$C_{11}H_9ON_4SClCo$	17.01 (17.37)	16.61 (16.50)	9.50 (9.43)	4.14	—
XI	11	$C_{13}H_{14}ON_4SCo$	17.81 (17.70)	16.91 (16.82)	9.70 (9.61)	4.15	—
XII	12	$C_{12}H_{11}ON_4SClCo$	16.67 (16.63)	15.91 (15.81)	9.11 (9.03)	4.00	16390, 17840, 25000
XIII	13	$C_{12}H_{12}ON_4SCo$	18.56 (18.48)	17.61 (17.56)	10.14 (10.03)	4.12	—
XIV	14	$C_{13}H_{14}O_2N_4SCo$	16.91 (16.89)	16.00 (16.05)	9.16 (9.17)	3.97	13510, 14710, 18520, 25000
XV	15	$C_{13}H_{14}ON_4SCo$	17.81 (17.70)	16.92 (16.82)	9.62 (9.61)	3.98	—
XVI	16	$C_{12}H_{11}ON_4SClCo$	16.58 (16.63)	15.72 (15.81)	9.13 (9.03)	4.11	—
XVII	17	$C_{14}H_{16}ON_4SCo$	17.11 (16.98)	16.20 (16.14)	9.31 (9.22)	3.92	—
XVIII	18	$C_{13}H_{13}ON_4SClCo$	16.12 (16.04)	15.31 (15.24)	8.80 (8.71)	4.10	—
I	19	$C_{10}H_8ON_4SCu$	21.30 (21.51)	18.50 (18.95)	10.81 (10.82)	1.42	15620, 21740
II	20	$C_{11}H_{10}O_2N_4SCu$	19.30 (19.52)	17.31 (17.20)	9.79 (9.83)	1.39	15620, 21740

Ligand No	Complex No	Empirical formula	Anlysis (%)*			μ_{eef}	$\mu_{\max}$ (cm^{-1})
			M	N	S	B.M.	DMF
III	21	$C_{11}H_{10}ON_4SCu$	19.92 (20.53)	18.21 (18.09)	10.41 (10.34)	1.50	—
IV	22	$C_{10}H_7ON_4SClCu$	20.21 (19.26)	16.85 (16.97)	9.91 (9.70)	1.40	—
V	23	$C_{12}H_{12}ON_4SCu$	19.52 (19.64)	17.41 (17.31)	9.91 (9.89)	1.38	15870, 22730
VI	24	$C_{11}H_9ON_4SClCu$	18.52 (18.47)	16.40 (16.28)	9.32 (9.30)	1.49	15620, 22730
VII	25	$C_{11}H_{10}ON_4SCu$	20.61 (20.53)	19.01 (18.09)	10.51 (10.34)	1.44	15150, 23810
VIII	26	$C_{12}H_{12}O_2N_4SCu$	18.82 (18.72)	16.62 (16.50)	9.51 (9.43)	1.46	15620, 21740
IX	27	$C_{12}H_{12}ON_4SCu$	19.81 (19.64)	17.90 (17.71)	9.93 (9.89)	1.38	—
X	28	$C_{11}H_9ON_4SClCu$	18.54 (18.47)	16.38 (16.28)	9.42 (9.30)	1.37	—
XI	29	$C_{13}H_{14}ON_4SCu$	18.91 (18.83)	16.67 (16.60)	9.52 (9.48)	1.50	16130, 25000
XII	30	$C_{12}H_{11}ON_4SClCu$	17.82 (17.75)	16.71 (15.64)	9.01 (8.94)	1.47	15620, 23810
XIII	31	$C_{12}H_{12}ON_4SCu$	19.71 (19.64)	17.42 (17.31)	9.91 (9.89)	1.49	15620, 22730
XIV	32	$C_{13}H_{14}O_2N_4SCu$	17.89 (17.98)	15.90 (15.84)	9.21 (9.05)	1.39	—
XV	33	$C_{13}H_{14}ON_4SCu$	18.92 (18.83)	16.71 (16.60)	9.51 (9.48)	1.39	—
XVI	34	$C_{12}H_{11}ON_4SClCu$	17.82 (17.75)	15.65 (15.64)	8.80 (8.94)	1.42	—
XVIII	35	$C_{14}H_{12}ON_4SCu$	18.12 (18.08)	16.01 (15.93)	9.21 (9.10)	1.43	15620, 21740
XVIII	36	$C_{13}H_{13}ON_4SClCu$	17.12 (17.08)	15.10 (15.05)	8.58 (8.60)	1.50	15870, 21740

Electronic spectra

— The observed band maxima for a few of these complexes are given in Table 1.

The electronic spectra of the copper(II) complexes exhibit a broad asymmetric band in the region 16130—15150 cm^{-1} that can be attributed to the d—d transitions. In addition to this, the complexes show a high intensity band in the 25000—21740 cm^{-1} region. In view of its high intensity we have considered it to be the ligand-metal charge transfer band rather than copper-copper band.[11]

The cobalt(II) complexes exhibit a high intensity multicomponent band in the region 18730—12820 cm^{-1}. It is known that the cobalt(II) complexes having tetrahedral configuration possess a characteristic intense multicomponent band associated with $^4A_2 \rightarrow {}^4T_1(\mathrm{P})$ transition [12] in the region 16670 – 12500 cm^{-1}. Hence the band observed for these complexes may be assigned to the $^4A_2 \rightarrow {}^4T_1(\mathrm{P})$ transition. In addition to this we observe an intense band in the 26320 – 25000 cm^{-1} region. This may be due to the ligand-metal charge transfer band.

The low magnetic moments and IR data of the copper(II) complexes suggest that these complexes have oxobridge structure ; the electronic spectra imply that copper(II) has coordination number four in these complexes. Hence these complexes can have the following structure.

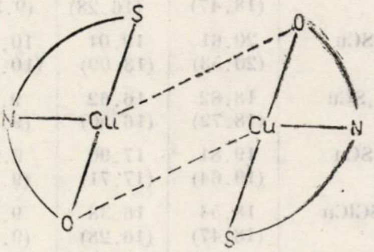

The analytical data suggest 1 : 1 stoichiometry for these cobalt(II) complexes. The IR data indicate that there is no oxobridge in these complexes. The complexes show low magnetic moments. The electronic spectra suggest that cobalt(II) in these complexes is tetrahedral. All this information directs us to propose a polymeric tetrahedrally coordinated structure for these complexes.

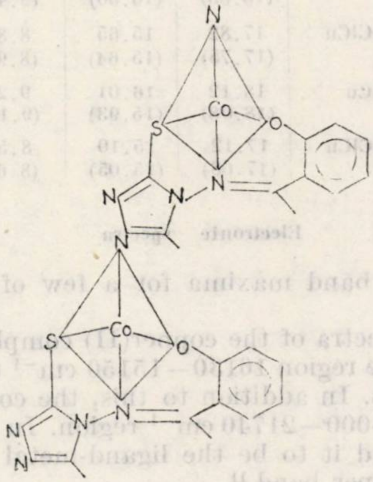

ACKNOWLEDGEMENT. The authors are grateful to Prof. S. P. Hiremath, Head of the Chemistry Department, Gulbarga University, Gulbarga for facilities and encouragement.

REFERENCES

[1] S. A. Patil, B. M. Badiger, S. M. Kudary and V. H. Kulkarni, *Trans. Met. Chem.*, **8**, 238 (1983).

[2] R. V. Gadag and M. R. Gajendragad, *Current Sci.*, **48**, 839 (1979).

[3] A. Syamal and M.A.B. Naizi, *Indian J. Chem.*, **23A**, 163 (1984).

[4] J. C. Duff, *J. Chem. Soc.*, **1941**, 547.

[5] A. I. Vogel, ''A Text Book of Practical Organic Chemistry'', ELBS 3rd Edit., Longmans Green London, 1968.

[6] L. F. Audrieth, E. S. Scott and P. S. Kipper, *J. Org. Chem.*, **19**, 733 (1954).

[7] K. S. Dhaka, J. Mohan, V. K. Chadha, and H. X. Pujari, *Indian J. Chem.*, **12**, 288 (1974).

[8] N. S. Biradar and V. H. Kulkarni, *J. Inorg Nucl. Chem.*, **33**, 2451 (1971).

[9] J. O. Miners and E. Sinn, *Synth. React. inorg. met-org. Chem.*, **2**, 231 (1972) ; J. O. Miners, E. Sinn, R. B. Cola and C. M. Harris, *J. Chem. Soc.*, Dalton, **1972**, 1149.

[10] F. A. Cotton and G. Wilkinson, ''Advanced Inorganic Chemistry'', Wiley Eastern Pvt. Ltd., New Delhi, 1969.

[11] K. Michinobu, B. Jonassen and J. C. Fanning, *Chem. Rev.*, **64**, 99 (1964).

[12] R. H. Holm, F. A. Cotton, *J. Amer. Chem. Soc.* **82**, 2979 (1960) ;
M. Goodgame, *J. Chem. Soc.*, (A), **63** (1966) ; C. K. Jorgensen, *Acta Chem. Scand.*, **8**, 1495 (1954).

Revue Roumaine de Chimie, **31**, *9—10*, 857—867 (1986)

SUBSTITUENT AND SOLVENT EFFECTS IN THE ABSORPTION SPECTRA OF NITROSO AROMATIC DERIVATIVES

G. IVAN and MARIA GIURGINCA
Research Institute for Rubber and Plastics Processing R—79628 Bucharest, Romania

Received November 11, 1986

In an attempt to understand throughly the activity of nitroso derivatives used as promoters in rubber reinforcement, some nitroso derivatives of aniline and of diphenylamine were studied. Investigation of the IR and UV spectra of these derivatives reveals the influence of the substituents on C-nitroso and N-nitroso compounds. The influence of the solvents on the absorption bands characteristic for $\pi \rightarrow \pi^*$ and $n \rightarrow \pi^*$ transitions was discussed using the Brownstein equation.

Some C-nitroso and N-nitroso aromatic derivatives are used in rubber industry in order to enhance the elastomer-filler interaction and to increase the cohesive strength of green rubber compounds. The advance in using such chemicals requests a better understanding of the structure and of the interactions in molecules of the nitroso aromatic derivatives.

EXPERIMENTAL

The substances used in the present work (Table 1) were synthetized in our laboratory (N1—N3, N7) following the methods reported in literature,[1–3] or were obtained by repeated recrystallizations from ethanol and chloroform of commercial products (N4—N6, N8). The substances used as basic structures (Table 2) were *p.a.* grade chemicals.

The ultraviolet-visible spectra from 200 to 800 nm were explored using a SPECORD-UV—VIS spectrometer (VEB Carl Zeiss, German Democratic Republic) and the infrared spectra were recorded from 4000 to 200 cm^{-1} using a PERKIN-ELMER 577 apparatus (Perkin-Elmer Co., USA). The initial solution for recording electronic spectra had the concentration 10^{-3} M; for the investigation of the infrared domain, KBr pellet technique was used for solid substances while the liquid compounds were deposited as a thin layer on KBr window.

THE INFLUENCE OF THE SUBSTITUENTS ON ELECTRONIC SPECTRA

The structure of investigated substances can be considered as constituted from one or more of the following structural units :

- a chromophore unit consisting of benzene ring and determining an absorption assigned to a $\pi \rightarrow \pi^*$ transition ;
- a chromophore unit consisting of nitroso group and determining two absorption bands assigned to $n_N \rightarrow \pi^*$ and $n_0 \rightarrow \pi^*$ transitions ;

Table 1

The studied nitroso derivatives

Symbol	Chemical structure
N_1	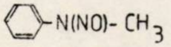
N_2	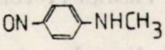
N_3	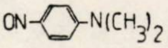
N_4	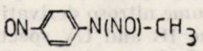
N_5	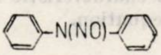
N_6	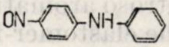
N_7	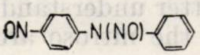
N_8	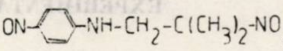

Table 2

Substances used as basic structures

Symbol	Chemical structure
E_1	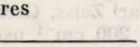
E_2	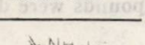
E_3	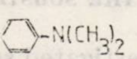

— a chromophore unit consisting of —N—NO unit present in nitrosoamines and determining an absorption assigned to an n → π* transition ;

- an auxochrome unit consisting of —NHR amine group (R — alkyl or aryl) with lone pair of electrons able to interact with π electrons of benzene ring and leading thus to the modification of the absorption characteristics of the chromophore ; is assigned to this interaction an n → π* transition [4,5].

The alteration introduced by the nitroso group in the absorption spectrum results by comparison of the obtained spectrum with the spectrum of the substance adopted as basic structure (the amine which, in principle, is the staring substance to obtain nitroso derivative) on the one hand, and, on the other hand, by comparison of the nitroso derivatives one with another providing they have a common skeleton (Table 3).

The experimental results on which the following comments are based were obtained in a mixed solvent containing 90—95 vol.% *n*-heptane and 10 — 5 vol. % ethanol.

The first group of nitroso derivatives (N1, N2, N4) can be considered as resulting from the skeleton of N-methylaniline (E1). The introduction of the nitroso group at aminic nitrogen (N1) leads to the modification of the π → π* band as well as of the n → π* band. The π → π* band is the subject of a strong hypsochromic displacement ($\Delta\lambda = -27$ nm) and a decrease of the band intensity (hypochromic modification) ; this modification may be the result of the interaction of the two chromophores (benzene ring and nitroso group) ; Nagakura and Tanaka [6,7] explained such type of interaction by an intramolecular charge transfer.

The n → π* band suffers a hypsochromic displacement ($\Delta\lambda = -19$ nm) and a significant increase of the band intensity (hyperchromic modification) proving a contribution of the nitroso group to the integral absorption taking place with the implication of the lone pair of electrons of the nitrogen atom. The —N—NO group exhibits, at the same time, an individualized absorption characterized by bands with fine structure, of low intensity.[8]

The introduction of the nitroso group in *para* position of an aromatic amine (N2) preserves the general picture of the absorption bands attributed to the π → π* and n → π* transitions of the initial amine. Some rather small displacements, hypsochromic displacement for the π → π* band ($\Delta\lambda = -2$ nm) and batochromic displacement for the n → π* band ($\Delta\lambda = +9$ nm), are accompanied by important modification of the band intensity (hypochromic modification), that may be explained by a strong interaction of the nitroso group with the aromatic cycle. The same interaction generates a new n → π* transition giving two new absorption bands at 370 and 700 nm. [9] The presence of the both N—NO and C—NO groups on the same skeleton (N4) leads to an electronic behaviour much similar to the compound containing only N-nitroso group, in respect to both transition bands (π → π* and n → π*) with participation of the aminic nitrogen as well as for the n → π* band with participation of N—NO group. The band assigned to the transition $n_0 \rightarrow \pi^*$ disappears, most probably being overlapped by the band generated by N—NO or is altered by an internal hydrogen bond.[10] The $n_N \rightarrow \pi^*$ band undergoes a strong hypsochromic effect ($\Delta\lambda = -94$ nm) demonstrating a weakening of the interaction of the aromatic ring with the nitroso group. Consequently,

Table 3

Absorption bands in the electronic spectra of the studied nitroso derivatives

Symbol	Transitions wavelength, nm absorption, L · mol^{-1} · cm^{-1}					Bands previously reported by	
						Lutskyi and coworkers[12]	Tabei[9]
	$\pi \rightarrow \pi^*$ benzenic ring	$n_N \rightarrow \pi^*$ −NO	$n_O \rightarrow \pi^*$ −NO	$n \rightarrow \pi^*$ −N−NO	$n \rightarrow \pi^*$ −NHR		
E1	247 27330				294 4245		
N$_1$	218 13000			370 100 385 98	275 9640	216 274	
N2	245 2240	700 20	370 8000		303 750		260 ; 369 690
N4	217 12000	606 10		385 220 400 230	278 7200		
E2	250 19000				298 2670		
N3	235 7000 270 ; 262 6900 ; 5500	715 56	385 30000 400 35000		303 2000 310 1900		
N8	280 10900	715 53	390 14000		303 shoulder		
E3	241 shoulder				283 23470		
N5	238 13150			400 240	294 6630	238 294	
N6	260 12760	715 60	417 25520				260 ; 400 705
N7	240 2475	715 93	330 2650	408 340	286 2600		
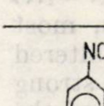 	218 ; 280 6480 ; 10330	760 40	300 5200				218 ; 280 ; 300 ; 760

Table 4

Absorption bands in infrared spectra of N1—N4 and N8 derivatives

N_1	N2	N3	N4	N8	Assignments	Literature
3420	3320	3400	3360	3240	ν_{NH}	11
3100	3120	3050	3100	3020	$\nu_{CH\ aromatic}$	11
2920 2850	2920 2850	2950 2910 2850	2920 2850	2930 2840	$\nu_{CH\ assym.}$ and $\nu_{CH\ aromatic}$	11
	1600	1600	1600		$\delta_{CH\ aromatic}$	11
1590		1585	1590	1590	ν_{C-NO} and ν_{N-NO}	13
1490	1530	1520	1530 1490	1525 1490	δ_{C-NO} ; δ_{C-NO_2} $\delta_{NO\ monomer}$	10 ; 14
1460 1430	1470 1450 1425	1470 1440	1460 1430		δ_{CH_2} $\delta_{NO\ monomer}$	5 ; 15
1390	1360 1330	1370 1350 1330	1390	1330	$\delta_{NO\ dimer}$ $\delta_{NO_2\ prim.}$	5 ; 15
1310 1290	1285	1300 1285	1320 1260	1280	$\delta_{NO\ dimer\ cis}$	5;10
1200 1095	1175 1100 1075	1210 1170 1110	1200 1175 1085	1210 1100	$\nu_{C-N\ aromatic}$ ν_{N-N}	5 ; 10
950	920	935	950		δ_{NH} ; δ_{C-NO}	5 ; 14
820 755	840 740	830 730	850 820 760	835	$\delta_{CH\ aromatic}$ and $\delta_{NO\ dimer}$	11 ; 15
685			685		δ_{N-NO}	5
	630 600	650 600			$\delta_{N=O}$	14
520	510	500	520	465	δ_{C-N} and δ_{C-NO}	5

Table 5

Absorption bands in infrared spectra of N5—N7 derivatives

N5	N6	N7	Assignments	Literature
3400	3200	3300	ν_{NH}	11
3020	3020	3020	ν_{CH} aromatic	11
1580	1580		ν_{C-NO} and ν_{N-NO}	13
1485	1530 1490		δ_{C-NO} monomer	10 ; 14 ; 15
1455 1435		1400	δ_{NO}	5
1320 1300	1340 1280	1350	δ_{NO} dimer *cis*	5
1190 1160	1215	1150	δ_{NO} and ν_{C-N}	10
1085	1100	1050	ν_{N-N} in N—NO	5
		850	δ_{NO} dimer *cis*	15
780 760	830 755	815 755	δ_{CH} aromatic	11
690		690	δ_{N-NO}	5
	650		$\delta_{-N=O}$	5

charge in the $-NO_2$ group enhancing the chance of the structure with separated charges

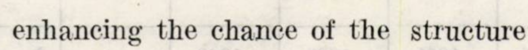

(I)

Typical vibrations for the deformation of the C—NO bond are present in the spectra of all studied compounds at 1525 ± 5 cm^{-1}.

The deformation vibration δ_{NO} for all studied N-nitroso derivatives appears at 1490 cm^{-1}.

The region 1450 — 1425 cm^{-1}, for compounds N1 — N4, is occupied by bands which may be attributed to the deformation vibration of the monomeric nitroso unit, while the bands in region 1390 — 1350 cm^{-1} were assigned [5,15] to the deformation vibration of the same unit in *cis*-dimeric form

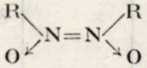

(II)

bearing in mind the low intensity of such absorptions.

For compounds N5 — N7 a few number of bands was recorded : valence vibrations of the aminic group at 3400 — 3200 cm^{-1} and deformation vibrations of the C—NO and N—NO groups at 1455—1400 cm^{-1}. This may be an indication that for N5 and N7 compounds the monomeric form is preponderant and is accompanied only by small quantities of *cis*-dimer ; for compound N6, the dimeric form is by far preponderant, as demonstrated by the intensity of the bands in the region 1350—1280 cm^{-1} and by the absence of the bands in the region 1500—1400 cm^{-1}.

THE INFLUENCE OF THE SOLVENTS ON THE ELECTRONIC TRANSITIONS

The solvatation of the nitroso derivatives was investigated in an attempt to establish the sensitivity of these compounds to the variation of the polarity of the solvent. For this purpose, solvents with various dielectric constants and different capability to realize hydrogen bonds were selected.

The solvent-solute interactions were studied following the displacements of the absorption bands, bearing in mind that these interactions are able to modify the fundamental state as well as the excited state. The polarity of the used solvents increases in the order hexane — dioxane — chloroform — acetone — ethanol — water.

The spectra recorded for various nitroso derivatives in nonpolar solvents (hexane, heptane, carbon tetrachloride) allow to observe that the $\pi \rightarrow \pi^*$ transitions are situated at the same wavelength in hexane and heptane and undergo a batochromic displacement ($\Delta\lambda \cong 16$ nm) in carbon tetrachloride in connection with the higher refractive index of this solvent.

Another effect of the interactions appearing in nonpolar solvents is the development of a fine structure observed for several of the studied substances, in region 250 — 270 nm. The difference between the maxima of the fine structure corresponds to the transition in the infrared spectrum at about 1250—1200 cm^{-1}, region assigned to the C—N valence vibration.[11] In polar solvents, the fine structure disappears, in spectrum remaining only one band covering the bands observed in nonpolar solvents.

In comparison with the same nonpolar solvents, the $n \leftarrow \pi^*$ transitions are observed at lower frequencies in carbon tetrachloride and, at the same time, an increase of the absorption intensity in domain 300—400 nm is observed accompanied by a decrease of the intensities of the bands situated in the region 700—720 nm.

In polar aprotic solvents (chloroform, acetone, dioxane), the $\pi \leftarrow \pi^*$ bands are localized at higher wavelength in proximity of the bands recorded using nonpolar solvents, *i.e.* the batochromic displacement is relatively small ($\Delta\lambda = 4-7$ nm). Such small displacements constitute an argument that the excited state of the molecule is better stabilized by solvation than the molecule in fundamental electronic state.

The bands of the $n \rightarrow \pi^*$ type allowed to observe small hypsochromic displacements ($\Delta\lambda = 5-10$ nm) supporting that for such a type of transition the fundamental state is better stabilized by solvation than the excited state. This behaviour, dissimilar for two types of transition is in fine agreement with their assignment.

In aprotic polar solvents several low intensity absorption bands were recorded which should result from some specific donor-acceptor interaction of the solvent molecules with nitroso derivatives.

Using polar solvents as ethanol and water, the hydroxyl effect was observed leading to hypsochromic displacements for some compounds and to the batochromic displacements for other compounds for the $n \rightarrow \pi^*$ bands ($\Delta\lambda = 10-37$ nm) which may be explained by the hydrogen bonds formed between solvent and solute using the lone pair of electrons of the oxygen from nitroso group (III) or of the nitrogen from aminic group

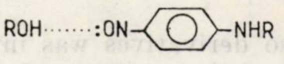
(III)

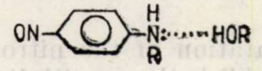
(IV)

(IV). The formation of the hydrogen bonds of the type (III) is expected to give a batochromic displacement while the type (IV) bonds should be able to bring about a hypsochromic displacement supporting, in this way, their attribution to two different $n \rightarrow \pi^*$ transitions. The rather unexpected behaviour of the $n_0 \rightarrow \pi^*$ transitions may be an indication that the excited state is more polar than the fundamental state and the transition takes place with decrease of the energy. The hipsochromic displacement observed changing the solvent from hexane to ethanol corresponds to an energy of hydrogen bond of 3–5 kcal. mol^{-1}, in agreement with literature data.[16,17]

The batochromic displacement observed for the $n_0 \rightarrow \pi^*$ transition corresponds to an energy of hydrogen bond of 3 kcal.mol^{-1} suggesting that the excitation takes place without additional energy, contributing to the stabilization of the molecule.

The dioxane used as solvent is also able to realize hydrogen bonds but only with the hydrogen atom of the aminic group

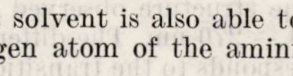
(V)

and this kind of bonds appears feasible only for C-nitroso derivatives.

A quantitative correlation of the sensitivity of the nitroso derivatives with the variation of the solvent polarity can be established using the Brownstein equation[18] where the ethanol was used (arbitrarily) as standard :

$$\bar{R} = \frac{\nu_{\text{max solv}} - \nu_{\text{max EtOH}}}{S \cdot \nu_{\text{maxEtOH}}}$$

where $\bar{R}$ is a mean constant characteristic of the sensitivity of a given solute to solvent effects ; S — a constant characteristic of any given solvent or solvent mixture (for ethanol, as standard solvent, $S = 1.0000$) ; $\nu_{\max}$ — the wavenumber (cm^{-1}) at the maximum of the band, for the given solution or for ethanolic solution. The $\bar{R}$ values for nitroso derivatives computed for the $n_0 \rightarrow \pi^*$ transition are presented in Table 6. The pre-

Table 6

$\bar{R}$ computed with Brownstein[18] equation for the studied nitroso derivatives

Symbol of nitroso derivative	$\bar{R}$
N1	0.080
N2	0.092
N3	0.263
N4	0.377
N5	0.070
N6	0.410
N7	0.330
N8	0.300

sented data allow to observe that the Ar-nitroso derivatives as well as Ar, N-dinitroso derivatives exhibit a more enhanced tendency to solvatation in comparison with N-nitroso derivatives. This fact may be partly explained by the different size of the electron density at nitrogen atom in Ar-nitroso and N-nitroso groups.

REFERENCES

[1] O. Fischer, and E. Heep, *Ber. dtsch. chem. Ges.*, **19**, 2994 (1886); **20**, 1247 (1887).

[2] S. Sabatier, *Compt. rend.*, **133**, 323 (1901).

[3] N. V. Martinov, I. I. Vaidanich, L. V. Muratova and V. S. Tlimakhova, *Khim. Prom.*, **24**, 824 (1972).

[4] O. V. Sverdlova, "Fizicheskie metody issledovanyia organicheskikh soedinenyi", Khimiyia, Leningrad, 1973.

[5] C.N.R. Rao and K. R. Bhaskar, "Spectroscopy of the Nitroso Group", Chapter 3 in "The Chemistry of the Nitro and Nitroso Groups", Part 1, by H. Feuer (Editor), Interscience, New York, 1968, p. 137.

[6] S. Nagakura and J. Tanaka, *J. Chem. Phys.*, **22**, 236 (1954).

[7] S. Nagakura and J. Tanaka, *J. Chem. Phys.*, **23**, 1441 (1955).

[8] W. A. Schroeder, *Analyt. Chem.*, **23**, 1740 (1951).

[9] K. Tabei, *Bull. Chem. Soc. Japan*, **38**, 965 (1965).

[10] T. Urbanski, *Bull. Acad. polon. Sci., Ser. Sci. chim.*, **11**, 597 (1963).

[11] M. Avram, and G. D. Mateescu, "Spectroscopia în infraroşu. Aplicaţii în chimia organică", Editura tehnică, Bucharest, 1968.

[12] A. E. Lutskyi, V. N. Konelskaya and P. M. Bugai, *Zhur. obshchei Khim.*, **30**, 3789 (1960).

[13] D. O. Hummell and F. Scholl, "Infrared Analysis of Polymers, Resins and Additives", Wiley, New York, 1971.

[14] E. J. Beleaev and L. P. Semina, *Zhur. org. Khim.*, **10**, 1721 (1974).

[15] K. Nakamoto and R. E. Rundler, *J. Amer. Chem. Soc.*, **78**, 1113 (1956).

[16] S. A. Breadley, *J. Amer. Chem. Soc.*, **77**, 4462 (1955).

[17] I. Pogany and M. Banciu, "Metode fizice în chimia organică"; Editura ştiinţifică, Bucharest, 1972, p. 150.

[18] S. Brownstein, *Canad. J. Chem.*, **38**, 1590 (1960).

Revue Roumaine de Chimie, 31, 9—10, 869—880 (1986)

EFFECTS OF SOLVENTS ON THE SPECTRA OF SOME SUBSTITUTED ACETOACETARYLAMIDES

RAMESH KUMARI[a], A. D. TANEJA[b] and V. P. KUDESIA[c]

[a] Dept. of Chemistry and Biochemistry, Haryana Agricultural University, Hissar
[b] Dept. of Plant Breeding, Haryana Agricultural University, Hissar
[c] D. N. College, Meerut

Received July 20, 1985
Revised April 20, 1986

Electronic absorption spectra of α-BrAAAH*, α-BrOAATH ,α-BrAAXH, α-BrOAAAH, α-BrPAAAH, α-BrPCAAAH, ω-BrAAAH, ω-BrOAAATH, ω-BrAAXH, ω-BrOAAAH, ω-BrPAAAH and ω-BrPCAAAH have been examined in ultraviolet region in a series of solvents covering a broad polarity range *i.e.*, from benzene (z, 54.0) to ethylene glycol (z, 85.1). Transition energies (E_T) and oscillator strengths have been calculated and E_T has been plotted against z-values, a new empirical measurement of solvent polarity. A linear relationship was observed between the transition energy and z-value for high energy Π—Π* transitions due to α, β unsaturated ketone, Π—Π* transitions and n—Π* transitions due to carbonyl group. The effect of substituent present in phenyl group on λ_{max} of a compound in te same solvent has been studied the stabilisation energy of the excited state of these ligands and hence dipole moments of the excited states have been calculated in comparison with pyridinium iodide. Solvent sensitivities of these ligands have also been calculated.

Acetoacetarylamides constitute an important class of compounds mainly because of their increasing utilisation in everyday life. Some work has been done from the stand-point of preparation,[1] adduct formation,[2] formation constant[3,4] and magnetic and spectral studies.[5,6] Survey of the literature reveals that only a little work has been reported on the spectral studies of substituted acetoacetarylamides. The purpose of the present paper is to study the effect of solvents of different solvent polarities on the electronic transitions of some substituted aromatic acetoacetamides. An attempt has been made to analyse the results of this investigation in terms of the solvent polarity parameter.

EXPERIMENTAL

Substituted aromatic acetoacetamides selected for the present studies are α-bromoacetoacetanilide (α-BrAAAH), α-bromo-*o*-acetoacetotoluidide (α-BrOAATH), α-bromoacetoacetoxylidide (α-BrAAXH), α-bromo-*o*-acetoacetanisidide (α-BrOAAAH), α-bromo-*p*-acetoacetanisidide (α-BrPAAAH), α-bromo-*p*-chloroacetoacetanilide (α-BrPCAAAH), ω-bromoacetoacetanilide (ω-BrAAAH), ω-bromo-*o*-acetoacetotoluidide (ω-BrOAATH), ω-bromo acetoacetoxylidide

---

* For notations of compounds see "Expesimental".

(ω-BrAAXH), ω-bromo-*o*-acetoacetanisidide (ω-BrOAAAH), ω-bromo-*p*-acetoacetanisidide (ω-BrPAAAH) and ω-bromo-*p*-chloroacetoacetanilide (ω-BrPCAAAH) have been synthesized. All the solvents used were either BDH, AnalaR or E. Merck GR quality. Freshly distilled solvents were used in all the experiments. All the absorbance measurements were made with UV—VIS spectrophotometer model PMQ—3 using 1 cm matched quartz cells equipped with thermoplates to stabilize the temperature of the cell compartments.

All the solutions were made just before use. The spectra of the above given compounds were obtained in a series of solvents varying in polarity from benzene (z, 54.00) to ethylene glycol (z, 85.1) at 30. C ± 0.1°C and the results are reported in Tables 1 and 2. Transition energy (E_T) was calculated by using the standard equation.

DISCUSSION

The results in Tables 1 and 2 show that α-bromo substituted aromatic acetoacetamides show three intense bands in the region 199 to 212 nm, 248—266 nm, and 278 to 306 nm and ω-bromo substituted-aromatic acetoacetamides exhibit three intense absorption maxima in the range of 199 to 212 nm, 248 to 266 nm and 276 to 310 nm. These three bands exhibited by these compounds have been assigned to (i) high energy Π—Π* transitions, (ii) Π—Π*-transitions due to carbonyl group and (iii) n — Π* transitions due to carbonyl group. These assignments are in agreement with the observation of Taneja *et al.*[6] in the case of acetoacetanilide and its derivatives. These bands exhibit a small shift in different solvents of varying polarities and is consistent with the expected spectrum of a molecule having an excited state which is more polar than the ground state.

Π—Π* Transitions

It was observed that these transitions occur in the region 246 to 265 nm in the case of α-bromo substituted acetoacetarylamides and in the region 248 to 265 nm in the case of ω-bromo substituted acetoacetarylamides.

These compounds show a blue shift on going frombenzene (*z*, 54.0) to ethylene glycol (z, 85.1). It is also observed that in general absorption maxima of α-BrPAAAH, α-BrPCAAAH, ω-BrAAXH and ω-BrPAAAH occur at a longer wavelength than other substituted aromatic acetoacetamides (Tables 1, 2). Transitions observed in each case are very similar in character and occur approximately at the same wavelength range except for FA, DMF and DMSO. There is a considerable variation in intensities of these bands. Intensities of substituted α-bromoacetoacetamides are higher in the same solvent as compared to the ω-bromo substituted aromatic acetoacetamides. The transition energies of these compounds in various solvents are plotted against z-values. The correlation between *Z* and E_T gives a scatter diagram for which the best straight line was obtained by a least square fit.

The marked difference between the calculated and actual values of transitions in FA, DMF and DMSO points to a specific solute — solvent interaction. The transitions in these solvents require lesser energy than predicted by the plot of E_T *vs Z*-value. Carbonyl oxygen and sulphur in these solvents act as good donors and form charge-transfer complexes

Table 1

Spectral data on α-bromo substituted acetoacetarylamides for

Solvent	α-BrAAAH		α-BrOAATH		α-BrAAXH		α-BrOAAAA		α-BrOAAAH		α-BrPAAAH	
	λ max	ε max	λ max	ε max	λ max	ε max	λ max	ε max	λ max	ε max	λ max	ε max
Dioxane ((Diox)	205	2152	206	1890	205	1960	205	2340	204	1993	205	1976
	256	13754	258	12650	257	12810	256	14327	260	14210	260	14001
	285	7310	286	7010	284	7180	288	8189	284	7840	286	7812
Benzene (BZ)	206	2060	207	1750	205	1860	205	2288	203	1903	205	1880
	255	13360	257	12280	258	12660	256	13940	259	13740	258	13640
	286	7220	284	6960	283	7080	287	8059	285	7720	283	7580
Carbon Tetrachloride (CT)	203	1966	204	1680	204	1710	202	2182	202	1870	203	1801
	254	12908	256	11940	256	12210	257	13432	258	13232	259	13285
	282	7110	285	6810	282	6910	285	7955	285	7602	285	7631
Chloroform (CF)	202	1884	203	1590	202	1775	203	2121	202	1786	202	1750
	252	12520	254	11820	253	11980	255	13083	257	12880	256	13120
	281	7040	285	6705	281	6870	284	7829	284	7512	284	7240
Acetic Acid (AcOH)	201	1624	205	1390	201	1520	203	2095	205	1533	200	1620
	251	10324	252	9680	252	9970	253	12650	255	11260	252	11670
	280	6624	281	6210	280	6406	282	7308	283	7301	282	7160
Dichloromethane (DM)	202	1806	202	1510	200	1808	204	2298	199	1894	201	1721
	250	11980	255	11210	253	10980	253	12678	251	12818	250	12610
	282	6910	285	6610	279	6760	283	7828	283	7520	281	7410
Dichloroethane (DE)	200	1710	200	1480	201	1760	205	2332	198	1877	199	1801
	252	11520	256	10910	252	11010	251	12457	250	12807	252	12401
	283	6818	283	6525	278	6710	282	7740	282	7440	279	7240

Table 1 (continued)

Butanol (n-BuDH)	202	1920	205	1650	199	1810	206	2360	206	1913	205	1858
	256	13152	256	12450	257	12650	255	13952	254	13695	256	13110
	285	7206	284	6910	282	7010	286	7807	285	7610	284	7501
Propanol (n-PrOH)	201	1812	204	1580	203	1704	204	2280	205	1810	206	1761
	254	12700	254	11980	256	12210	254	13600	254	13207	255	12802
	283	7110	283	6820	280	6910	284	7723	284	7420	283	7810
Ethanol(EtOH)	200	1740	204	1490	202	1620	202	2202	204	1740	206	1626
	252	12428	253	11630	255	11806	253	13260	253	12960	254	12690
	281	7024	282	6740	279	6830	283	7552	287	7310	281	7201
Methanol (MeOH)	199	1680	203	1410	202	1540	200	2110	202	1680	204	1590
	250	12096	252	11250	253	11390	252	12871	251	12660	253	12440
	278	6984	281	6670	278	6720	282	7421	280	7210	278	7040
Acetonitrite (AN)	207	2110	206	2027	204	2082	206	2382	204	2023	205	2057
	257	13660	256	12082	257	12480	258	13670	259	13877	258	13655
	285	7264	286	6982	284	7081	285	7926	286	7628	284	7830
Ethyleneglycol (EG)	202	1840	203	1787	202	1710	202	2076	200	1758	200	1907
	250	11752	251	9916	254	10120	251	11580	250	11140	252	11967
	281	6764	280	6560	279	6610	283	7420	281	7510	278	7625
Pyridine (Py)	210	1284	211	954	212	1010	209	1135	210	1196	212	1225
	—	—	—	—	—	—	—	—	—	—	—	—
	306	5740	306	5528	302	5610	304	5675	305	5590	305	5908
Dimethylformamide (DMF)	206	1904	205	1708	203	1810	205	2231	202	1769	202	1890
	266	10694	265	9680	264	9840	265	11630	265	11840	265	12420
	287	6540	288	6390	282	6480	284	7296	285	7342	288	7440
Dimethylsulphoxide (DMSO)	204	1744	204	1583	205	1620	205	2140	201	1858	201	1723
	262	12528	261	11680	264	11710	258	12139	258	12340	259	11483
	285	5560	284	5380	282	5410	282	7306	288	7404	289	7510
Formamide (FA)	202	1508	203	1410	205	1480	202	2010	203	1670	204	1844
	260	9656	261	8860	260	9410	260	11110	262	11610	261	11980
	292	5692	289	5480	285	5520	287	7410	286	7510	288	7540

Unit of λ_{max} is nm

Unit of E_{max} is 1 mol^{-1} cm^{-1}.

Table 2

Spectral data on ω-bromosubstituted acetoacetarylamides for

Solvent	ω-BrAAAH		ω-BrOAATH		ω-BrAAXH		ω-BrOAAAH		ω-BrPAAAH		ω-BrPCAAAH	
	λ max	ε max	λ max	ε max	λ max	ε max	λ max	ε max	λ max	ε max	λ max	ε max
Dioxane (Diox)	203	2131	204	1840	204	1925	204	2190	202	1928	206	1902
	253	12817	255	11670	257	11949	255	13569	257	13337	256	13297
	285	6837	283	6555	282	6696	286	7649	285	7367	291	7158
Benzene (BZ)	204	2010	205	1677	203	1829	203	2140	201	1865	204	1821
	252	12365	254	11375	255	11742	254	13227	256	12988	255	12827
	283	6861	281	6505	280	6592	285	7542	283	7221	282	6997
Carbon Tetrachloride (CT)	202	1886	204	1645	202	1768	202	2065	202	1809	203	1767
	252	12034	253	11175	254	11412	252	12887	257	12585	258	12499
	283	6772	282	6565	282	6468	284	7428	284	7119	284	6825
Chloroform (CF)	201	1827	203	1607	202	1709	204	2019	201	1758	202	1707
	251	11795	252	10825	253	11138	252	12887	255	12282	256	12169
	282	6680	281	6350	280	6393	283	7328	282	6969	283	6707
Acetic Acid (AcOH)	200	1607	200	1345	205	1475	202	1895	202	1479	200	1584
	249	9922	248	9156	350	9595	257	11248	255	10919	251	17129
	280	6257	279	5638	278	6228	277	7052	281	6669	278	6577
Dichloromethane (DM)	200	1755	201	1471	200	1719	204	2071	200	1821	201	1668
	249	11400	252	10325	248	10193	249	12212	254	12067	252	11924
	281	6585	279	6128	276	6286	278	7365	284	6910	281	6791
Dichloroethane (DE)	201	1685	202	1462	200	1625	204	2158	202	1786	201	1717
	251	10965	249	10057	250	10261	252	12074	251	11921	250	11759
	282	6419	278	6027	277	6109	277	7275	283	6890	282	6758

Table 2 (continued)

Butanol (n-BuOH)	203	1890	203	1615	204	1809	204	2187	201	1874	202	1809
	251	12776	250	11276	253	11935	254	31292	253	12997	254	12408
	284	6743	283	6248	280	6909	282	7315	282	7223	281	6950
Propanol (n-PrOH)	202	1786	204	1515	200	1669	203	2059	204	1766	204	1719
	250	12205	251	10820	252	11671	252	12919	255	12609	253	12169
	283	6610	282	6176	279	6313	281	7232	281	7090	280	6815
Ethanol (EtOH)	203	1708	205	1469	202	1579	202	1998	203	1702	203	1602
	249	11863	250	10561	252	11209	251	12685	254	12269	252	11889
	281	6539	280	6031	278	6121	280	7059	280	6913	279	6713
Methanol (MeOH)	204	1635	206	1362	201	1511	201	1959	201	1647	201	1580
	248	11519	249	10262	251	10980	250	12305	253	11823	251	11651
	280	6453	278	5923	276	6493	279	6921	279	6727	278	6578
Acetonitrile (AN)	201	1947	206	1843	206	1899	204	2189	205	1978	206	1979
	254	12673	252	11492	253	11571	254	12789	256	13186	254	12974
	276	6747	278	6457	275	6655	276	7429	278	7298	285	7229
Ethyleneglycol (EG)	200	1749	201	1671	200	1669	199	1898	198	1680	200	1773
	248	10867	248	9211	250	9479	249	11019	252	10699	250	11079
	278	6357	276	6019	275	5949	278	6912	278	6839	276	6831
Pyridine (Py)	210	1190	209	861	212	960	210	1030	210	1040	209	1105
	—	—	—	—	—	—	—	—	—	—	—	—
	306	5358	307	5035	308	4849	310	5233	306	5339	309	5479
Dimethylformamide (DMF)	202	1729	202	1589	204	1671	205	1981	202	1649	201	1730
	264	9451	266	9062	263	8967	265	10259	265	10437	265	10692
	289	5112	286	4933	288	5029	289	6439	290	6681	291	6775
Dimethylsuphomide (DMSO)	204	1659	201	1499	226	1571	202	1889	204	1715	202	1627
	258	11513	260	11126	260	10783	258	11149	260	11548	260	10529
	282	5111	280	4987	283	5099	286	6679	285	6817	287	6835
Formamide (FA)	202	1442	203	1345	203	1405	205	1768	204	1581	203	1639
	259	7876	262	8685	260	8699	260	10791	261	10990	262	10831
	286	5129	283	4881	278	4983	279	6449	282	6694	284	6755

Unit of λ_{max} is nm
Unit of E_{max} is $1 mol^{-1} cm^{-1}$.

between the solvents and the solutes. A high value of transition energy in acetonitrile (z, 71.3) may be due to the presence of polarised π-bonds which enable easy acceptance of electron from the oxygen of the enolate ion by forming a complex.[7] The small shifts in other solvents are consistent with those expected from the solvent effect on the spectrum of the single species, having an excited state which is more polar than the ground state.[8] It is also observed that ionisation process has a little effect on the spectra of these ketones.[9] Since the molecules are bulky it is difficult to achieve a fruitful relationship between Z and E_T because, as the solute molecule increases in size, the correlation becomes less precise due to specific solute — solvent interactions, self-association and distortion of cybotactic region.[10]

If we assume that the excited state dipole with the cybotactic region is directly proportional to the interaction of another somewhat larger dipole with the same solvent, then we can estimate the difference in excited state stabilisation for a transition with that found for the ground state of pyridinium iodide complex dipole. Diagram 1 is a diagramatic representation of the relationship of the ground and the excited state energy levels in benzene and ethylene glycol for transitions of one of these ligands *viz.* α-BrAAAH or ω-BrAAAH.

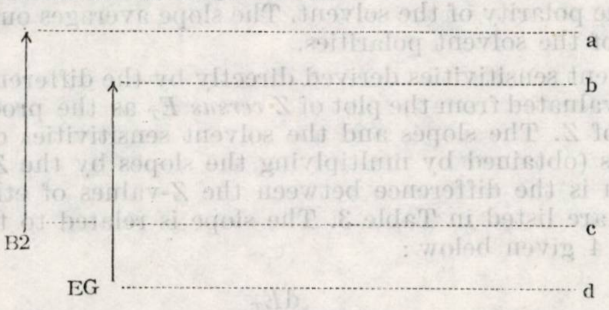

Diagram 1. Energy level diagram for $\Pi-\Pi^*$ transition in benzene (B2) and ethylene glycol, (EG)

From the diagram 1 it can be seen that

$$(a - c) = E_T \text{ (Benzene)}$$

$$(b - d) = E_T \text{ (Ethylene glycol)} \qquad (1)$$

For α-BrAAAH

$$(a - c) - (b - d) = 112.11 - 114.36 = 2.25 \text{ (see Table 1)} \qquad (2)$$

$$(a - b) = (c - d) + 2.25$$

For α-BrAAAH

$$(a - c) - (b - d) = 113.45 - 115.78 = 1.83 \text{ (see Table 2)} \qquad (3)$$

$$(a - b) = (c - d) + 1.83$$

The value of $(c - d)$ is determined by noting the shift of a particular band of α-BrAAAH or ω-BrAAAH from IR-spectra in benzene and ethylene glycol. The stabilisation of excited state dipole of α-BrAAAH and ω-BrAAAH on transfer from benzene to ethylene glycol is 4.55 and 4.05 respectively. It has been observed by Kosower that for the pyridinium iodide complex (dipole moment of 13.9 D) respectively in ethylene glycol. Using the method outlined above the minimum dipole moment for the excited states of other ligands has been calculated and was found to be 5.79 D for α-BrOAATH, 5.05 D for α-BrAAXH, 5.44 D for α-BrOAAAH, 6.85 D for, α-BrPAAAH, 6.02 D for α-BrPCAAAH, 5.063 D for ω-BrOAAAH, 4.67 D for ω-BrPAAAH and 6.78 D for ω-BrPCAAAH. The dipole moment of an excited state is of considerable interest, since it should be related to the charge-distribution within the excited molecule and might permit a more precise evaluation of certain theoretical calculations for the energies of such a state (II). The solvent sensitivities of these transitions, which are a measure of transitions response of changing the polarity of the solvent, can be obtained as an experimental measure as the difference between the transition energy of the transition in ethylene glycol (z, 85.1) highest polarity and that in benzene (z, 54.0 lowest polarity). This quantity is related to the degree to which the position of Π—Π* transitions responds to the polarity of the solvent. The slope averages out the changes over a range of the solvent polarities.

The solvent sensitivities derived directly by the difference $E_T(\mathrm{EG})-E_T(\mathrm{BZ})$ and evaluated from the plot of Z *versus* E_T as the product of slope with respect of Z. The slopes and the solvent sensitivities corresponding to these slopes (obtained by multiplying the slopes by the Z-value difference — which is the difference between the Z-values of ethylene glycol and benzene) are listed in Table 3. The slope is related to the transition energy by eq 4 given below :

$$m = \frac{\mathrm{d}E_T}{\mathrm{d}z} \tag{4}$$

Therefore, by changing the solvent polarity, the Π — Π* transition shows a trend towards blue shift. The values obtained vary between 1.74 to 3.98 and 1.77 to 3.55 in the case of α-bromoacetoacetarylamides and ω-bromoacetoacetarylamides respectively. Marked deviation from slope or from linearity of E_T *versus* Z plot may be regarded as anomaly which requires rationalisation. The solvent sensitivity of α-BrPAAAH and ω-BrPCAAAH is appreciably higher than that of other compounds. The high solvent sensitivity of α-BrOAAAH α-BrOAATH, α-BrAAXH, α-BrOAAAH, ω-BrOAATH, ω-BrAAXH, ω-BrOAAAH and ω-BrPAAH although in agreement with the increased hydrogen bonding ability is somewhat puzzling.

n—π* Transitions

These transitions fall in the region of 278 to 306 nm in the case of α-bromo substituted acetoacetarylamides and 276 to 310 nm in the case of ω-bromo substituted acetoacetarylamides. In this case also blue shifts are found passing from dioxane to acetonitrile. The plots of z vs E_T are drawn and they give a scatter diagram from which the best straight line was obtained by a least square fit. Deviation from the regression line in the case of DMF, DMSO and FA can be explained by considering the charge-transfer interactions between the carbonyl group and solvent. The deviation in the case of acetonitrile may be due to the presence of polarized π-bond in the solvent molecules as discussed earlier. These ultraviolet spectral data permit an estimate of the hydrogen bonding energy as suggested by Kosower.[7] If we consider the excited state of the transition as represented by the structure (I) and make the simple assumption that the polarisation already present in the ground state (structure II) is unaffected by the excitation, the result and dipole moment for the excited state will be very close to zero. The situation is analogous to that for the 1-alkylpyridinium iodide complex in which the destabilisation of the excited state upon the transfer of the complex dipole from one solvent to another was equal to the stabilisation of the ground state[7].

Table 3

Solvent sensitivity of α-bromo and ω-bromo substituted acetoacetarylamides for

Compound	High energy $\pi-\pi^*$ transition			$\pi-\pi^*$ transition			$n-\pi^*$ transition		
	ΔE_T^*	$E_T = mz = b$		ΔE_T^*	$E_T = mz = b$		ΔE_T^*	$E_T = mz = b$	
	(kcal/mol)	m	$m \times \Delta z^{**}$ (kcal/mol)	(kcal/mol)	m	$m \times \Delta z^{**}$ (kcal/mol)	(kcal/mol)	m	$m \times \Delta z^{**}$ (kcal/mol)
α-BrAAAH	2.75	0.0847	2.63	2.24	0.0925	2.88	1.78	0.0665	2.07
α-BrOAATH	1.93	0.0860	2.68	2.66	0.0930	2.89	1.43	0.0640	1.99
α-BrAAXH	2.07	0.0780	2.43	1.74	0.0674	2.10	2.45	0.0750	2.33
α-BrOAAAH	2.07	0.0880	2.74	2.22	0.0750	2.33	1.41	0.0425	1.32
α-BrPAAAH	2.12	0.0750	2.33	3.98	0.1270	3.95	1.43	0.0430	1.34
α-BrPCAAAH	3.49	0.0768	2.39	2.64	0.0821	2.55	1.82	0.0755	2.35
ω-BrAAAH	2.81	0.0967	3.01	1.83	0.0633	1.98	1.82	0.0755	2.35
ω-BrOAATH	2.77	0.0935	2.91	2.26	0.0820	2.55	1.84	0.0865	2.69
ω-BrAAXH	2.12	0.1160	3.61	2.25	0.1068	3.32	1.86	0.0730	2.27
ω-BrOAAAH	2.84	0.1030	3.20	2.26	0.0930	2.89	2.53	0.0820	2.55
ω-BrPAAAH	2.86	0.0724	2.25	1.77	0.0780	2.43	1.82	0.0643	2.01
ω-BrPCAAAH	2.81	0.0928	2.89	3.55	0.1145	3.56	2.20	0.0925	2 88

* Defined as the difference between ethylene glycol and benzene transition energies.

** These values should be compared with those in column ΔE_T of the same table.

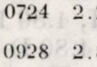
$\overset{-\ \ +}{>C{=}O}$

I

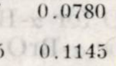
$> \overset{\delta+\ \ \delta-}{C = O}$

II

The hydrogen bonding energy is thus half of the change in the transition energy [7] from the gas phase or more simply a non-polar solvent (Bz-solution in our case) to the polar solvent. The following hydrogen bonding energy or more simply, the interaction energy have been estimated in ethylene glycol, α-BrAAAH 0.89 kcal/mole, α-BrOAATH 0.71 kcal/mole, α-BrAAXH 1.22 kcal/mole, α-BrOAAAH 0.71 kcal/mole, α-BrPAAAH 0.72 kcal/mole, α-BrPCAAAH 0.91 kcal/mole, ω-BrAAAH 0.91 kcal/mole, ω-BrOAATH, 0.92 kcal/mole, ω-BrAAXH 0.93 kcal/mole, ω-BrOAAAH 1.26 kcal/mole, ω-BrPAAAH 0.91 kcal/mole and ω-BrPCAAAH 1.10 kcal/mole.

The solvent sensitivity was measured as the difference in the excitation energies in ethylene glycol and benzene and was evaluated from the slope of regression line by using equation (4).

The solvent sensitivities evaluated from the least square plot (Table 3) show a marked difference from the previous values. This is attributed to the $Z-E_T$ correlation being only approximate in nature in the case of bulky molecules. The solvent sensitivites of these transitions in the case of α-BrAAAH, α-BrOAATH, α-BrPCAAAH, ω-BrAAAH, ω-BrOAATH, ω-BrAAX, ω-BrOAAAH, ω-BrPAAAH and ω-BrPCAAAH are higher and low in the case of α-BrAAAXH, α-BrOAAAH and α-BrPAAAH. The difference in the solvent sensitivity values is due to increasing and decreasing electron density of ground state and the excited state of the carbonyl group.

It reveals a moderately good linear relationship between the n-π* transitions and the *Z*-values.

The dipole moment of the excited state of these compounds produced by the carbonyl π−π* transitions was calculated by using eqs 2 and 3 and the values are 5.08 D for α-BrAAAH, 4.80 D for α-BrOAATH, 5.62 D for α-BrAAXH, 4.78 D for α-BrOAAAH, 4.80 D for α-BrPAAAH, 5.12 D for α-BrPCAAAH, 4.72 D for ω-BrAAAH, 4.73 D for ω-BrOAATH, 4.75 for ω-BrAAXH, 5.28 D for ω-BrOAAAH, 4.72 D for ω-BrPAAAH and 5.02 D for ω-BrPC-AAAH.

High energy π−π* transitions

High energy π−π* transitions due to α,β-unsaturated ketone are observed in these compounds in the region 199 to 212 nm in α-bromo substituted acetoacetarylamides and 199 to 212 nm in ω-bromo substituted acetoacetarylamides. The plots of *z vs* E_T are amenable to a reasonable least square fit, though the deviation from the regression line is a rule rather than the exception. The deviation from regression line cannot be explained in all cases due to the lack of knowledge of exact nature of solute-solvent interactions and due to the presence of a large and bulky substitution group in the molecule. The deviation in certain cases such as DMF, DMSO, FA and AN etc. can be explained by considering the charge-transfer interactions between the ethylenic double bond and the solvent. The solvent sensitivites are obtained as difference of the transition energies in EG and BZ. The solvent sensitivities of these transitions in the case of α-BrOAATH, α-BrAAXH, α-BrOAAAH, ω-BrAAAH, ω-BrAAXH and ω-BrOAAAH are higher and respectively low in the case of α-BrPCAAAH and ω-BrPAAAH.

The dipole of the excited state of these compounds produced by these high energy $\pi-\pi^*$ transitions has been calculated by using equations (1) and (2) and the values are 5.87 D for α-BrAAAH, 5.20 D for α-BrOAATH, 5.32 D for α-BrAAXH, 5.32 D for α-BrOAAAH, 5.36 D for α-BrPAAAH, 6.46 D for α-BrPCAAAH, 5.51 D for ω-Br-AAAH, 5.48 D for ω-BrOAATH, 4.96 for ω-BrAAXH, 5.53 D for ω-BrOAAAH, 5.55 D for ω-BrPAAAH and 5.51 D for ω-BrPCAAAH.

It is evident from the data reported in Tables 1 and 2 that the substitution on the phenyl group of the nitrogen atom does not influence much the position of maxima in the same solvent. For example the introduction of 2,4-dimethyl, 2-chloro, 2-methoxy, 2-methyl, 4-chloro or 4-methoxy group in the benzene ring of acetoacetarylamides gives a bathochromic shift of only 2 to 5 nm.

It can therefore be inferred that there is no resonance interaction between these substituents and the enolic group, thereby implying that there is a greater interaction within the group. Introduction of these groups does not impart much asymmetry in the chelated enol and so this may be taken as a support for the mobility of the hydrogen atom from $-CH_2-$ between the two carbonyl groups during enolisation and not hydrogen from -NH- group.

On the basis of the present observation it may be proposed that the difference in the λ_{max} of the bands of carbonyl group in α and ω-bromo-substituted acetoacetarylamides is due to the greater electron withdrawing ability of Br-group at α or ω-position and thereby decreasing the electron density at carbon of carbonyl group and hence decreasing electron density in the groud level and so more energy is required for the excitation and hence the position of λ_{max} is shifted to lower wavelength. The intensity of transition is also decreased for the same region.

The $n-\pi^*$ transitions are shifted to longer wavelength in the case of α-bromo substituted acetoacetarylamides than ω-bromo substituted acetoacetarylamides whereas high energy $\pi-\pi^*$ transitions also shifted to longer wavelength in the case of α-bromo substituted acetoacetarylamides. The difference in λ_{max} of the bands of α-bromoacetoacetarylamides is due to the greater electron withdrawing ability of Br-group at α-position. However, the effect is more pronounced when the bromine is at α-position than in ω-position. The electrons from the bromine substituent are donated to the carbonyl group, thereby increasing electronic density in the ground state and hence lesser energy is required for the excitation. Therefore, the position of λ_{max} is shifted to longer wavelength and intensity of the transition also increases.

REFERENCES

[1] A. D. Taneja and K. P. Srivastava, *Chimia*, **25**, 92 (1971).

[2] K. P. Srivastava and A. D. Taneja, *J. Inorg. Nuclear Chem.*, **33**, 2694 (1971).

[3] J. J. Harries, S. Savage and G. Wright, *J. Inorg. Nuclear Chem.*, **31**, 2477 (1969).

[4] A. D. Taneja, K. P. Srivastava and M. C. Gupta, *J. Inorg. Nuclear Chem.*, **36**, 2039 (1974).

[5] D. N. Sen and P. Umapathy, *Indian J. Chem.*, **6**, 516 (1968).

[6] A. D. Taneja, K. P. Srivastava and M. C. Gupta, *J. Chinese Chem. Soc.*, **20**, 95 (1973).

[7] E. M. Kosower, *J. Amer. Chem. Soc.*, **80**, 3261 (1958).

[8] E. M. Kosower and G. S. Wu, *J. Amer. Chem. Soc.*, **83**, 3142 (1961).

[9] G. S. Hammond, W. G. Borduin and G. A. Guter, *J. Amer Chem. Soc.*, **81**, 4682 (1959).

[10] E. M. Kosower, *J. Amer. Chem. Soc.*, **80**, 3253 (1958).

[11] J. W. Sidman, *J. Chem. Phys.*, **27**, 429 (1957).

[12] J. W. Sidman, *Chem. Rev.*, **58**, 689 (1958).

Revue Roumaine de Chimie, **31**, *9–10*, 881–888 (1986)

as-TRIAZINE DERIVATIVES WITH POTENTIAL THERAPEUTIC ACTION. XXI*

SYNTHESIS OF 4-THIOXO-5(FLUORO-BENZYL)THIO-6-AZAURACIL DERIVATIVES AND THEIR NUCLEOSIDES

CAROL CRISTESCU
Chemical and Pharmaceutical Research Institute
Sos. Vitan 112, 74351 Bucharest, Romania

Received February 3, 1986

Thionation with P_2S_5 in pyridine of 5(fluoro-benzyl)thio-6-azauracils at a molar ratio substance : P_2S_5 of 2 : 1 occurs selectively in position 4, yielding 4-thioxo-5(fluoro-benzyl)-thio-6-azauracils (II). The increasing amount of P_2S_5 affords the 2,4-dithioxo-derivatives (III). These compunds can be alkylated at S4 and S2,4. The S4-alkyl-derivatives react with ammonia to 5(fluoro-benzyl)thio-6-azacytosine (VI) without affecting the 5(fluoro-benzyl)thio-group. 4-Thioxo-5(fluorobenzyl)thio-6-azauridines (IX) were prepared *via* the silyl modification of the Hilbert-Johnson reaction.

In connection with the investigation on the biological activity of 4-methylthio-5-benzylthio-6-azauracil, we prepared the new 4-methyl-thio-5(substituted-benzyl)thio-derivatives. The research on 4-methylthio-5(fluoro-benzyl)thio-6-azauracils and their nucleosides was untertaken in an attempt to find substances with improved pharmacological and therapeutic properties as compared to 4-methylthio-5-benzylthio-6-azauracil. The study was stimulated by the assumption that the presence of a stronger electron-withdrawing substituent, such as the fluoro atom, on the benzylthio-group, increases the binding affinity of the benzyl-group with the biological receptor.

The selective thionation of 5-benzylthio-6-azauracil with phosphorous pentasulphide was investigated in a previous work.[1] Studies concerned with the thionation of 6-azauracil have demonstrated that the C4-position is the initial site of the reaction.[2–6] Larger amount of P_2S_5 decreased the C4-monothiated derivative and favoured the formation of the C2, C4-dithiated products. In our laboratory we examined the condition required for the C4-monothiation of 5-substituted-6-azauracils using phosphorus pentasulphide/pyridine and we found that the best results were obtained at a 5-substituted -6-azauracil/P_2S_5 molar ratio of 2 : 1 and using a pyridine with a water content of about 0.1 – 0.3%.

---

* Part XX, C. Cristescu and S. Sitaru, *Rev. Roumaine Chim.*, **30**, 233 (1985)

At the 5(fluoro-benzyl)thio-6-azauracil [7](I)/P_2S_5 2 : 1 molar ratio under similar conditions the 4-thioxo-5(fluoro-benzyl)thio-6-azauracil (II) is formed in a 55 % yield. Since II was a critical intermediate for all compounds we devised an alternate method to increase the yield of this substance. Addition of elemental sulphur [8] into the reaction medium and reversal of the I : P_2S_5 molar ratio, increases the yield of the thiolated II with about 20 % when used a pyridine with 0.3 % water. In dry pyridine (0.1 % water) and at a 2 : 4 : 0.5 (I : P_2S_5 : S_8) molar ratio, the 2,4-dithioxo-5(fluoro-benzyl)thio-6-azauracils (III) were obtained in 68—70 % field. Compounds III were also obtained from II with P_2S_5 in pyridine (0.1 % water) at a 1 : 2 molar ratio (substance : P_2S_5) in 75 % yield.

Alkylation of both monothioxo- and dithioxo-derivatives with methyl iodide leads to the corresponding methylthio-derivatives. Thus 4-thioxo-5(fluoro-benzyl)thio-6-azauracils (II a—c) in hydro-alcoholic medium and in the presence of sodium hydroxide solution (1 Ec.) lead to 4-methylthio-5(fluoro-benzyl)thio-6-azauracils (IV a—c). Similarly III a—c gives 2,4-bis(methylthio)-5(fluoro-benzyl)thio-6-azauracils (V a—c). All these reactions take place at room temperature in about 90% yield.

The lability of the C4-methylmercapto-group of derivatives IV and V, facilitates the replacement of the mercapto-groups by amino or oxo-groups. Thus IV a—c treated with ammonia in methanol at room temperature lead to 5(fluoro-benzyl)thio-6-azacytosines (VI a—c). The treatment of IV with hydrochloric acid in hydro-alcoholic media gives the starting compounds (I a—c). Similarly, when V was treated with hydrochloric acid, the C2 and C4-methylthio-groups were displaced by oxo groups to provide the starting compounds (I).

Infrared spectra of the compounds II, IV and VI showed an intensive absorption band at 1690±50 cm^{-1} ($\bar{\nu}$ CO), indicating the oxostructure of these derivatives.[9-10] In the dithioxo III and oxothioxo-derivatives II, the vibration $\bar{\nu}$ (C=S) has been found near 1100 cm^{-1}. The C=S band of II is more intensive than that of III. The methylthio-group of derivatives IV and V is absorbing in C—H stretching vibration region [11] about 2980 cm^{-1}.

The UV spectra of II and III either in acidic, neutral and alkaline media show the characteristic absorption peak of the 4-thioxoderivatives at 318 nm (acidic and neutral media) and 352 nm (alkaline medium).[12] Alkylation of the C4-thioxo-group produces a hypsochromic shift in acidic and neutral media and a bathochromic shift in alkaline medium.[2]

Treatment of II with hexamethyldisilazane in the presence of traces of chlorotrimethylsilane, under reflux, gave 2(trimethylsilyloxy)-4(trimethylsilylthio)-5(fluoro-benzyl)thio-6-azauracils (VII a—c). The condensation of VII with 1-0-acetyl-2,3,5-tri-0-benzoyl-D-ribofuranoze in dry 1,2-dichloroethane, at room temperature, in the presence of anhydrous stannic chloride, affords only the N-glycosides (VIII a—c) in 80—84 % yield. The second procedure involved the thionation of 1(2′,3′,5′-tri-O-benzoyl-β-D-ribofuranosyl)-5(fluoro-benzyl) thio-6-azauracils[7] (XI a—c) with phosphorous pentasulphide in pyridine (0.3 % water) at a 2 : 1 molar ratio (compound : P_2S_5). Usual work-up afforded a 75—80 % yield of VIII a—c, identical in all respects (TLC, UV, IR).

In the infrared spectra of compounds VIII, the intense absorption of the acyl-groups overlaps a considerable number of bands of the heterocyclic and the sugar parts of the molecule. The carbonyl groups absorb in the 1706 ± 14 cm^{-1} region. The absorption bands of the acyl-groups, linked to the ribose residue, are 1180, 1113 cm^{-1} $\tilde{\nu}$(CO.O) and 1313, 1286 cm^{-1} $\tilde{\nu}$(C.CO).

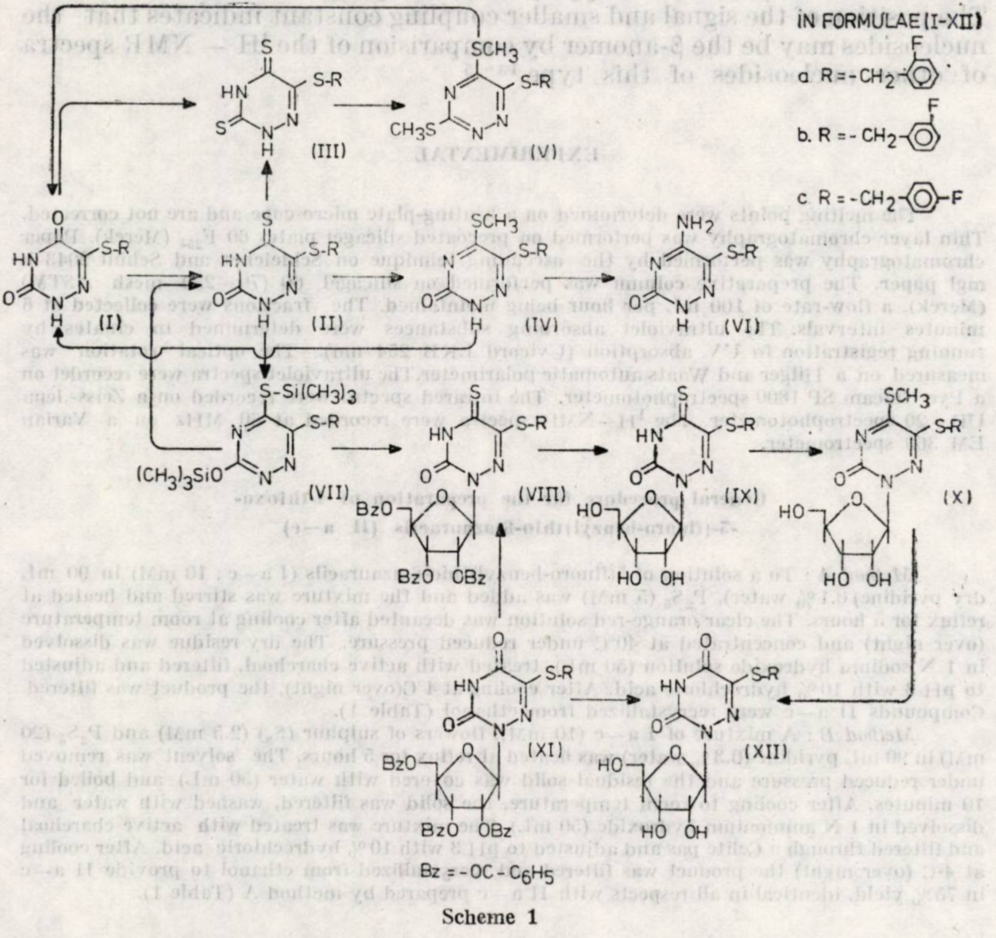
IN FORMULAE (I-XII)
a R = -CH2-C6H4-F (ortho)
b. R = -CH2-C6H4-F (meta)
c. R = -CH2-C6H4-F (para)
(I)
(II)
(III)
(IV)
(V)
(VI)
(VII)
(VIII)
(IX)
(X)
(XI)
(XII)
S-R
SCH3
NH2
S-Si(CH3)3
(CH3)3SiO
CH3S
BzO
HO
OBz
OH
Bz = -OC-C6H5

Scheme 1

Removal of the blocking groups of VIII with sodium methoxide in methanol gave 83% yield of the 4-thioxo-5(fluoro-benzyl)thio-6-azauridine (IX a–c).

The UV spectra of IX in either acidic, neutral and alkaline media show the characteristic absorption peak of 4-thioxo-6-azauridine at 326 nm (acidic and neutral media) and 334 nm (alkaline medium).

Alkylation of IX with methyl iodide in alcoholic — sodium hydroxide solution (1 Ec.) led to the 4-methylthio-5(fluoro-benzyl)-thio-6-azauridine (X a–c). Compounds X may be subjected to acidic hydrolysis to give 5(fluoro-benzyl)thio-6-azauridines (XII a—c) identical in all respects with as ample obtained *via* another method described in a previous paper.[7]

The anomeric proton of the nucleosides IX and X appear in ^{1}H-NMR spectra as a doublet at δ 5.95 ppm, with a coupling constant 2—3.5 Hz. The position of the signal and smaller coupling constant indicates that the nucleosides may be the β-anomer by comparision of the ^{1}H — NMR spectra of other nucleosides of this type.[13–15]

EXPERIMENTAL

The melting points were determined on a heating-plate microscope and are not corrected. Thin layer chromatography was performed on precoated silicagel plates 60 F_{254} (Merck). Paper chromatography was performed by the ascending tehnique on Schleicher and Schüll 2043 b mgl paper. The preparative column was performed on silicagel 60 (70—230 mesh ASTM) (Merck), a flow-rate of 100 mL per hour being maintained. The fractions were collected at 6 minutes intervals. The ultraviolet absorbing substances were determined in eluates by running registration fo UV absorption (Uvicord LKB 254 nm). The optical rotation was measured on a Hilger and Waats automatic polarimeter.The ultraviolet spectra were recordet on a Pye Unicam SP 1800 spectrophotometer. The infrared spectra were recorded on a Zeiss-Jena UR—20 spectrophotometer. The ^{1}H—NMR spectra were recorded at 60 MHz on a Varian EM 360 spectrometer.

General procedure for the preparation of 4-thioxo-5-(fluoro-benzyl)thio-6-azauracils (II a—c)

Method A : To a solution of 5(fluoro-benzyl)thio-6-azauracils (I a—c ; 10 mM) in 90 mL dry pyridine) 0.1% water), P_2S_5 (5 mM) was added and the mixture was stirred and heated at reflux for 5 hours. The clear orange-red solution was decanted after cooling at room temperature (over night) and concentrated at 40°C under reduced pressure. The dry residue was dissolved in 1 N sodium hydroxide solution (50 mL), treated with active charchoal, filtered and adjusted to pH 3 with 10% hydrochloric acid. After cooling at 4°C(over night), the product was filtered. Compounds II a—c were recrystallized from ethanol (Table 1).

Method B : A mixture of I a—c (10 mM), flowers of sulphur (S_8) (2.5 mM) and P_2S_5 (20 mM) in 90 mL pyridine (0.3% water) was heated at reflux for 5 hours. The solvent was removed under reduced pressure and the residual solid was covered with water (50 mL) and boiled for 10 minutes. After cooling to room temperature, the solid was filtered, washed with water and dissolved in 1 N ammonium hydroxide (50 mL). The mixture was treated with active charchoal and filtered through a Celite pas and adjusted to pH 3 with 10% hydrochloric acid. After cooling at 4°C (over night) the product was filtered and recrystallized from ethanol to provide II a—c in 75% yield, identical in all respects with II a—c prepared by method A (Table 1).

General procedure for the preparation of 2,4-dithioxo-5(fluoro-benzyl)thio-6-azauracils (III a—c)

Method A : 4-Thioxo-5(fluoro-benzyl)thio-6-azauracils (II a—c, 10 mM) were dissolved in pyridine (100 mL) (0.1% water) and P_2S_5(20 mM) was added at 40° C. The mixture was heated under reflux for 7 hours. The reddish-brown clear solution was decanted after standing at room temperature for 16 hours and concentrated under reduced pressure at 40°C. The dry residue was dissolved in 1 N ammonium hydroxide (50 mL), treated with active charcoal and filtered through a Celite pad. After adjusting at pH 3 with 10% hydrochloric acid, the resulting product was filtered and recrystallized from the solvent as indicated in table 1.

Method B : A mixture of 5(fluoro-benzyl)thio-6-azauracils (I a—c ; 10 mM), P_2S_5 (20 mM), and flower of sulphur (2.5 mM) in 90 mL pyridine (0.1% water) was heated at reflux for 7 hours under vigorous stirring. The reddish-brown clear solution was decanted after standing at room temperature for 16 hours. The reaction was worked up in a similar manner with that described for method A. This procedure provided III a—c identical in all respects (TLC, UV, IR) with III a—c prepared by method A.

TABLE 1 CHEMICAL AND PHYSICAL CHARACTERIZATION DATA OF THE PRODUCTS II - VI

No	mp °C	Recryst.[a] solv	Yield %	T.L.C.[b]	Paper chrom.[c]			UV Spectra λ max (log ε)			IR Spectra (KBr) cm^{-1}				Formula[d]
				A	B	C	D	EtOH	0.1N HCl	0.1N NaOH	$\tilde{\nu}$(CO)	$\tilde{\nu}$(CS)	$\tilde{\nu}$(SCH$_3$)	$\tilde{\nu}$(C=C)	
II-a	251 - 253	A	72	0.34	0.80	0.69	0.78	318(3.90)	318(3.95)	352(3.73)	1740	1140	—	1610,1490	$C_{10}H_8N_3OS_2F$
II-b	279 - 280	A	73	0.33	0.82	0.70	0.79	318(3.88)	318(3.90)	352(3.72)	1733	1133	—	1613,1510	$C_{10}H_8N_3OS_2F$
II-c	296 - 297	A	75	0.32	0.80	0.70	0.79	318(3.90)	318(3.91)	352(3.79)	1736	1133	—	1593,1500	$C_{10}H_8N_3OS_2F$
III-a	254 - 256	B	72	0.55	0.80	0.81	0.79	304(4.46)	305(4.43)	290(4.28)	—	1146	—	1600,1500	$C_{10}H_8N_3S_3F$
III-b	264 - 266	B	74	0.55	0.81	0.81	0.79	304(4.44)	305(4.41)	290(4.28)	—	1160	—	1586,1500	$C_{10}H_8N_3S_3F$
III-c	238 - 240	B	75	0.55	0.81	0.82	0.79	304(4.38)	305(4.40)	290(4.21)	—	1156	—	1583,1500	$C_{10}H_8N_3S_3F$
IV-a	199 - 201	A	82	0.74	0.81	0.76	0.82	293(3.85)	293(3.87)	335(3.85)	1653	—	2980	1573,1500	$C_{11}H_{10}N_3OS_2F$
IV-b	173 - 175	A	86	0.75	0.82	0.77	0.83	293(3.81)	293(3.83)	335(3.75)	1653	—	2968	1610,1500	$C_{11}H_{10}N_3OS_2F$
IV-c	169 - 170	A	88	0.74	0.82	0.75	0.84	293(3.87)	293(3.88)	335(3.78)	1646	—	2972	1593,1500	$C_{11}H_{10}N_3OS_2F$
V-a	66 - 68	C	85	0.73	0.88	0.87	0.91	355(3.59)	—	—	-	—	2982	1605,1480	$C_{12}H_{12}N_3S_3F$
V-b	96 - 98	C	83	0.75	0.87	0.88	0.90	355(3.59)	—	—	-	—	2980	1613,1483	$C_{12}H_{12}N_3S_3F$
V-c	101 - 102	C	85	0.75	0.87	0.88	0.89	355(3.59)	—	—		—	2976	1593,1500	$C_{12}H_{12}N_3S_3F$
VI-a	225 - 227	A	90	0.43	0.75	0.68	0.78	308(3.58)	308(3.60)	314(3.78)	1675	—	—	1610,1490	$C_{10}H_9N_4OSF$
VI-b	216 - 218	A	91	0.44	0.76	0.68	0.79	308(3.59)	308(3.61)	314(3.77)	1675	—	—	1620,1500	$C_{10}H_9N_4OSF$
VI-c	210 - 212	A	90	0.43	0.77	0.69	0.78	308(3.59)	308(3.62)	314(3.76)	1670	—	—	1623,1500	$C_{10}H_9N_4OSF$

a (A) ethanol , (B) chloroform , (C) ethanol - water (1:1)

b spots detected by UV absorption (254 nm), solvent systems (A) chloroform - methanol (8:2)

c spots detected by UV absorption (254 nm) after spraying with 0.005% fluoresceine (in ethanol), solvent systems (B) 1-butanol - acetic acid - water (4:1:1), (C) 2-propanol - conc. ammonia - water (7 1 2) (D) 1-butanol - water (86·14)

d analytical results were within ± 0.4% of the theoretical values for C,H,N,S

TABLE 2 CHEMICAL AND PHYSICAL CHARACTERIZATION DATA OF THE PRODUCTS VIII-X

No.	mp °C	Recryst.[a] solv.	Yield %	T.L.C.[b]	Paper chrom.[c]			$[\alpha]_D^{25}$	UV Spectra λ max (log ε)			IR Spectra cm^{-1}					^1H-NMR Spectra[h]	Formula[k]
				A	B	C	D		EtOH	0.1N HCl	0.1N NaOH	$\tilde{\nu}$(CO)	$\tilde{\nu}$(CS)	$\tilde{\nu}$(CO·O)	$\tilde{\nu}$(C·CO)	$\tilde{\nu}$(C=C)	$H_{1'}(J_{1',2'})$	
VIII-a	110-112	A	84	0.73	0.90	0.85	0.86	-156.3[d]	330(4.01)	—	338(3.06)	1720[f]	1113	1173,1113	1313,1286	1600,1490	6,51 (d, 3.00)[i]	$C_{36}H_{29}N_3O_8S_2F$
VIII-b	147-148	B	87	0.73	0.92	0.86	0.86	-164.2[d]	330(4.01)	—	338(3.04)	1720[f]	1113	1180,1113	1313,1286	1600,1490	6.55 (d, 2.50)[i]	$C_{36}H_{29}N_3O_8S_2F$
VIII-c	158-160	B	85	0.73	0.90	0.85	0.87	-140.6[d]	330(4,01)	—	338(3,03)	1726[f]	1115	1180,1113	1313,1286	1600,1490	6.49 (d, 2.75)[i]	$C_{36}H_{29}N_3O_8S_2F$
IX-a	189-191	B	83	0.31	0.80	0.66	0.58	- 85.5[e]	326(3.97)	326(4.00)	334 (4.03)	1700[g]	1140	–	–	1610,1490	5.97 (d, 3.25)[i]	$C_{15}H_{16}N_3O_5S_2F$
IX-b	171-173	B	88	0.31	0.80	0.66	0.61	- 99.0[e]	326(4.00)	326(3.97)	334 (3,96)	1695[g]	1142	–	–	1610,1490	5.95 (d, 3.75)[j]	$C_{15}H_{16}N_3O_5S_2F$
IX-c	121-123	B	83	0.30	0.81	0.65	0.63	-102.5[e]	326(3.96)	326(3.93)	334 (3.91)	1693[g]	1140	–	–	1600,1500	5.93 (d, 3.50)[j]	$C_{15}H_{16}N_3O_5S_2F$
X-a	152-154	B	85	0.59	0.72	0.63	0.64	- 76.5[e]	312 (3.89)	—	—	1705[g]	—	–	–	1600,1490	5.83 (d, 2.75)[j]	$C_{16}H_{18}N_3O_5S_2F$
X-b	157-159	B	84	0.61	0.76	0.64	0.65	- 70.2[e]	312 (3.87)	—	—	1700[g]	—	–	–	1600,1490	5.87 (d, 2.50)[j]	$C_{16}H_{18}N_3O_5S_2F$
X-c	161-163	B	85	0.57	0.77	0.63	0.64	- 63.5[e]	312 (3.89)	—	—	1700[g]	—	–	–	1600,1490	5.90 (d, 2.75)[j]	$C_{16}H_{18}N_3O_5S_2F$

[a] (A) 2-propanol , (B) ethanol

[b] spots detected by UV absorption (254 nm), solvent systems (A) chloroform-methanol (8:2)

[c] spots detected by UV absorption (254 nm) after spraying with 0.005% fluoresceine (in ethanol); solvent systems (B) 1-butanol-acetic acid-water (4:1:1), (C) 2-propanol-conc ammonia-water (7:1:2); (D) 1-butanol-water (86:14)

[d] C = 1% in chloroform

[e] C = 1% in methanol

[f] IR Spectra in $CHCl_3$

[g] IR Spectra in KBr

[h] chemical shifts in ppm and J values in Hz

[i] ^1H-NMR Spectra in $CDCl_3$/TMS

[j] ^1H-NMR Spectra in DMSO-d_6/TMS

[k] analytical results were within ± 0.4% of the theoretical values for C,H,N,S

General procedure for the preparation of 4-methylthio-5(fluoro-benzyl)thio-6-azauracils (IV a—c)

4-Thioxo-5(fluoro-benzyl) thio-6-azauracils (II a—c ; 5 mM) were dissolved at 40°C in ethanol (25 mL) and 1 N sodium hydroxide (5 mM). The stirred solution was cooled to room temperature and methyl iodide (5.5 mM) was added in one portion. The reaction was monitored by TLC, and when complete, the solvent was removed under reduced pressure and the residue recrystallized from the solvent as indicated in table 1.

General procedure for the preparation of 2,4-bis(methylthio)-5(fluoro-benzyl)thio-6-azauracils (V a—c)

A similar set of conditions was employed for the methylation of 2,4-dithioxo-5(fluoro-benzyl)thio-6-azauracils (III a—c). When the reaction was complete, the solvent was evaporated under reduced pressure and the residue dissolved in chloroform (50 mL). The chloroform solution was filtered and extracted with 1 N sodium hydroxide (2 × 10 mL), washed with water (2 × 20 mL), dried on sodium sulphate and evaporated. The residue was recrystallized from the solvents as indicated in table 1.

Hydrolysis of 4-methylthio-5(fluoro-benzyl)thio-6-azauracils

0.200 g of IV a—c was boiled with 10 mL ethanol and 1 mL hydrochloric acid (10 %), for 30 minutes. The solution was evaporated under reduced pressure and the residue was recrystallized from ethanol to furnish 5(fluoro-benzyl)thio-6-azauracils (I a—c) identical in all respects (m.p., TLC, UV and IR) with an authentical sample.

Hydrolysis of 2,4-bis(methylthio)-5(fluoro-benzyl)thio-6-azauracils

0.100 g of V a—c was boiled with 5 mL ethanol and 0.5 mL hydrochloric acid (10 %) for 1 hour. The solution was evaporated under reduced pressure and the residue was recrystalized from ethanol to furnish I a—c identical in all respects with an authentical sample.

General procedure for the preparation of 5(fluoro-benzyl)thio-6-azacytidine (VI a—c)

4-Methylthio-5(fluoro-benzyl)thio-6-azauracils (IV a—c ; 5.0 mM) was suspended in methanolic ammonia (10 mL, saturated at −5°C) and kept at room temperature for 3 days in a pressure bottle. During this time, the excess gases were vented and then the solvent was removed under reduced pressure. The residue was recrystallized from the solvent as indicated in table 1.

General procedure for the preparation of 1(2′, 3′,5′-tri-O-benzoyl-β-D-ribofuranosyl)-4-thioxo-5(fluoro-benzyl)thio-6-azauracils (VIII a —c)

Method A : A mixture of 4-thioxo-5(fluoro-benzyl)thio-6-azaruacils (II a—c ; 5.5 mM), hexamethyldisilazane (10 mL) and chlorotrimethylsilane (0.5 mL) was heated under reflux for 2 hours, until a clear solution was obtained. The excess of hexamethyldisilazane was removed under reduced pressure (15 mm Hg) and the viscous 2(trimethylsilyloxy)-4(trimethylsilylthio)-5(fluoro-benzyl)thio-6-azauracil (VII a—c ; 5 mM) was dissolved in dry 1,2-dichloroethane (20 mL) and added to 1—0-acetyl-2,3,5-tri-O-benzoyl-D-ribofuranose (4.5 mM) previously dissolved in dry 1,2-dichloroethane (150 mL). The mixture was stirred for 12 hours at room temperature in the presence of anhydrous stannic chloride (3.5 mM). The solution was treated with a saturated aqueous sodium hydrogen carbonate solution (2 × 50 mL) and the organic phase was filtered over Celite 535, dried on sodium sulphate and evaporated. The residue was chromatographed on a silicagel column (60 g) with chloroform. The combined collected fractions were evaporated under reduced pressure to give the pure corresponding blocked nucleosides (VIII a—c) shown in table 2.

Method B : 1(2′3′, 5′-tri-O-benzoyl-β-D-ribofuranosyl)-5(fluoro-benzyl)thio-6-azauracil [7] (XI a—c ; 2 mM) was dissolved in pyridine (0.1 % water ; 20 mL) and P_2S_5 (1 mM) was added at 50°C. The mixture was heated under reflux and stirring for 3 hours. The clear, reddish-orange solution was decanted after standing at room temperature for 16 hours and concentrated at 40° C under reduced pressure. The dry residue was dissolved in chloroform (100 mL) and washed with water and 0.2 N sodium hydrogen carbonate solution, dried (sodium sulphate) and evaporated. The residue was chromatographed on a silicagel column (40 g) with chloroform. The fractions containing the product were pooled and evaporated under reduced pressure to give the pure corresponding blocked nucleosides (VIII a—c) identical in all respects (TLC, UV, IR, and ^{1}H-NMR) with VIII a—c prepared by method A.

General procedure for the preparation of 4-thioxo-5(fluoro-benzyl)thio-6-azauridines (IX a—c)

A mixture of the blocked nucleoside VIII (2 mM), 1 N sodium methoxide (2 mL) and dry methanol (50 mL) was stirred for 4 hours at room temperature. The solvent was evaporated under reduced pressure and the resulting oil was dissolved in water (20 mL) and extracted with ethyl acetate- ether (2:1 v/v: 2 × 10 mL). The aqueous layer was treated with DOWEX 50 × 8 (H$^+$) at pH 4, filtered and evaporated. The residue was recrystallized from the solvent as indicated in table 2.

General procedure for the preparation of 4-methylthio-5(fluoro-benzyl)thio-6-azauridines (X a—c)

4-Thioxo-5-(fluoro-benzyl)thio-6-azauridines (IX a—c; 1.5 mM) were dissolved in ethanol (25 mL) and 1 N sodium hydroxide (1.5 mL) and water (5 mL) was added. The solution was cooled at 10° C and a solution of methyl iodide (3 mM) in ethanol (5 mL) was added in one portion. The mixture was stirred for 2 hours at 10°C and for 2 hours at room temperature and evaporated under reduced pressure. The dry residue was recrystallized from the solvent as indicated in table 2.

Hydrolysis of 4-methylthio-5(fluoro-benzyl)thio-6-azauridines

0.1 g X a—c was boiled with 5 mL ethanol and 0.5 mL hydrochloric acid (10%) for 30 minutes. The solution was evaporated under reduced pressure. The residue was recrystallized from 2-propanol to furnish XII a—c identical in all respects with an authentical sample.[7]

ACKNOWLEDGEMENT. The author thanks Mrs. Veronica Vişan and Mrs. Ileana Costea of the Analytical Department of our Institute for recording the IR and UV spectra, Mrs. Cornelia Ioan for the elemental analyses and Mr. D. Ionescu for NMR spectra. The author expresses his gratitude to Mrs. Anca Sava for her invaluable help.

REFERENCES

[1] C. Cristescu and V. Badea, *Rev. Roumaine Chim.*, **14**, 135 (1969).
[2] J. Gut, M. Prystas and J. Jonas, *Coll. Czech. Chem. Comm.*, **26**, 986 (1961).
[3] K. Y. Zee-Cheng and C. C. Cheng, *J. Org. Chem.*, **27**, 976 (1962).
[4] Y. Mizuno, M. Ikehara and K. A. Watanabe, *Chem. Pharm. Bull.*, **10**, 647 (1962).
[5] C. Cristescu and S. Sitaru, *Rev. Roumaine Chim.*, **16**, 135 (1971).
[6] C. Cristescu, *Rev. Roumaine Chim.*, **16**, 311 (1971).
[7] C. Cristescu, *Rev. Roumaine Chim.*, **30**, 117 (1985).
[8] U. Schmidt, A. Luttringhaus and H. Trefzgel, *Justus Liebigs Ann. Chem.*, **631**, 129 (1960).
[9] M. Horak and J. Gut, *Coll. Czech. Chem. Comm.*, **26**, 1680 (1961).
[10] M. Horak and J. Gut, *Coll. Czech. Chem. Comm.*, **28**, 3392 (1963).
[11] N. S. Ham and J. B. Wilcis, *Spectrochim. Acta*, **16**, 279 (1960).
[12] J. Johnas and J. Gut, *Coll. Czech. Chem. Comm.*, **27**, 1886 (1962).
[13] M. P. Sweizer, E. B. Banta, J. T. Witkowsky and R. K. Robins, *J. Amer. Chem. Soc.*, **95**, 3770 (1973).
[14] J. D. Stewens and H. G. Fletcher, *J. Org. Chem.*, **33**, 1799 (1968).
[15] F. E. Hruska, A. A. Grey and I. C. Smith, *J. Amer. Chem. Soc.*, **92**, 4088 (1970).

Revue Roumaine de Chimie, **31**, *9–10*, 889–895 (1986)

DETERMINACION CINETICA DE Co(II) BASADA EN SU EFECTO CATALITICO SOBRE LA OXIDACION ATMOSFERICA DEL MONOCLORHIDRATO DE LA 1,3-CICLOPENTANODIONA BIS (4-METILTIOSEMICARBAZONA)

M. ROMÁN CEBA*, J. C. JIMÉNEZ SÁNCHEZ y T. GALEANO DÍAZ
Departamento de Química Analítica. Facultad de Ciencias.
Universidad de Extremadura. 06071 Badajoz (España)

Ricibido: el 1 de april de 1985

Se propone un método cinético para la determinación de trazas de Co(II) basado en su efecto catalítico sobre la oxidación atmosférica del monoclorhidrato de la 1,3-ciclopentanodiona bis (4-methiltiosemicarbazona). La reacción se sigue espectrofotométricamente a 380 nm. Se dan los parámetros cinéticos de la reacción y se sugiere una ecuacion de velocidad. Las curvas de calibrado son lineales en el rango 0,05–0,40 µg. Co(II) $\cdot$mL^{-1}. Se estudian las interferencias de otros iones.

The present paper reports a kinetic method for the determination of traces of Co(II) based on its catalytic effect on atmospheric oxidation of 1,3-cyclopentandione bis-(4-methylthiosemicarbazone) hydrochloride. Spectrophotometrically, the reaction was followed at 380 nm. The kinetic parameters of reaction are given and a velocity equation is suggested. The calibration curves are linear within 0.05–0.40 µg. Co(II) $\cdot$ mL^{-1} range. The interferences with other ions are also studied.

INTRODUCTION

Las tiosemicarbozonas son interesantes reactivos analíticos formadores de complejos metálicos.[1–2] También presenta interés la oxidación de algunos de estos compuestos ya que ha permitido su uso en la determinación de aniones oxidantes como ClO_3^{-3} y otros.[3] Recientemente se ha ampliado el uso de estos reactivos con la determinación de iones metálicos que catalizan algunas de sus oxidaciones.[4]

Entre estos iones metálicos se encuentra el Co(II). Así, este ha sido determinado usando su efecto catalítico en la oxidación de la sal sódica de la 2-tiosemicarbazona de la 1,2-naftoquinona-4-sulfonato por H_2O_2.[5]

En el presente trabajo se propone un método cinético para la determinación de Co(II), en medio débilmente ácido, basado en su efecto catalítico sobre la oxidación atmosférica del monoclorhidrato de 1,3-ciclopentanodiona bis (4-metiltiosemicarbazona) (1,3-CPBMT.HCl) que transcurre rápidamente en medio básico, incluso en ausencia del catalizador. Un comportamiento similar se observa en el caso del monoclorhidrato de la 1,3-ciclohexanodiona ditiosemicarbazona que ha sido propuesta para la determinación cinética de Cu(II).[6]

---

* Dirección actual: Departamento de Química General. Facultad de Ciencias. Universidad de Granada. Granada (España).

PARTE EXPERIMENTAL

Aparatos. Espectrofotómetro Zeiss DMR 11 de registro automático, con cubetas de cuarzo o de vidrio de 1,0 cm de paso de luz, para UV y visible, equipado con portacubetas termostatizado.

Medidor de pH : Crison modelo digital 74, con electrodo combinado de vidrio-calomelanos.

Reactivos. El monoclorhidrato de la 1,3-ciclopentanodiona bis (4-metiltiosemicarbazona) se ha sintetizado por condensación de la 1,3-ciclopentanodiona con 4-methiltiosemicarbacida en disolución hidralcohólica de ácido clorhidricco[7], usándose disoluciones de este reactivo en agua de diferentes concentraciones. Disoluciones de Co(II) de diferentes concentraciones se prepararon por dilución de una disolución de Co(II) de 0,9898 g/l normalizada con 8-hidroxiquinoleina.[8] Todos los disolventes y reactivos son de calidad reactivo-analítico.

Procedimiento para la determinación de Co(II). A una disolución conteniendo entre 0,05 y 0,4 $\mu g \cdot Co(II) \cdot mL^{-1}$, en un matraz de 10 mL, se le añade 3 mL de DMF para evitar la aparición de turbidez, 2 mL de disolución reguladora $AcOH/AcO^-$ (pH 5,17) y 1 mL de disolución de reactivo al 0,2% en agua. Se diluye a 10 mL con agua desionizada. Inmediatamente se transfiere una porción de la mezcla de reacción a una célula de 1,0 cm termostatata a 65 ± ±0,1°C y se registra el cambio de absorbancia a 380 nm frente a blancos preparados de igual forma sin ión Co(II). Se calcula la velocidad de reacción a partir de la curva absorbancia frente a tiempo (A—t), usando el metodo de la tangente o del tiempo fijo midiendo las muestras a los 8 minutos pe preparadas.

RESULTADOS

Cuando se calientan disoluciones ligeramente ácidas de 1,3-CPBMT.HCl que contienen trazas de Co(II), adquieren un color amarillo, que presenta un espectro de absorción con un máximo a 380 nm y que se intensifica con el tiempo. Esta misma alteración ocurre de forma muy rápida y sin necesidad de calentar, en medio básico, lo que dificulta las medidas de la velocidad de reacción. La reacción se ha estudiado en medios tamponados de $AcOH/AcO^-$ en cuyo caso es fácil medir con seguridad su velocidad, que vendrá dada por la tangente a las curvas Absorbancia-tiempo (A-t) en el origen ($tg\,\alpha$). En estas condiciones se ha comprobado que la reacción es una oxidación por el O_2 disuelto, catalizada por el Co(II). Para ello se prepararon de forma simultánea cuatro disoluciones de 1,3-CPBMT.HCl de la misma concentración, dos de ellas conteniendo trazas de Co(II) en igual cantidad, estando ausente este catión en las dos restantes. Las disoluciones se calentaron a la misma temperatura y durante el mismo tiempo. Durante toda la experiencia se operó en unos casos en atmósfera inerte y en otros en presencia de O_2, tal y como se indica al pie de la figura 1, en donde están representados los espectros de absorción correspondientes.

La velocidad de reacción depende de la concentración de Co(II), 1,3-CPBMT.HCl, H_3O^+, AcOH, AcO^-, O_2 y de la temperatura. Se ha estudiado la influencia de todas estas variables, excepto la correspondiente al O_2.

Influencia de la concentración de H_3O^+, AcOH y AcO^-. Para estudiar la influencia de estas variables y calcular los órdenes de reacción con respecto a ellas, se prepararon dos series de muestra con las mismas cantidades de reactivo y Co(II) (0,5 $\mu g . mL^{-1}$ de Co(II) y $1{,}94 \times 10^{-4}$ M de 1,3-CPBMT.HCl). En la primera serie se mantuvo constante e igual a 0,2 M la concentración de AcO^- y se varió la de AcOH entre 0,01 y 0,3M con lo cual varía también la de H_3O^+. En la segunda serie se mantuvo constante e igual a 0,05 M la concentración de AcOH y se varió la de AcO^- entre 0,03 y 0,6 M, variando al mismo tiempo la concentración de KCl para mantener constante la fuerza iónica. En ambos casos las curvas A—t se registraron manteniendo la temperatura constane a 65°C.

Para la primera serie, como la concentración de todos los reactivos, salvo la de AcOH y H_3O^+, es constante, aplicando logarítmos en la expresión general de la velocidad de reacción, se llega a la expresión:

$$\log v = \log \operatorname{tg} \alpha = \log [AcOH]^m + \log [H_3O^+]^x + \text{const.}$$

Esta expresión se transforma fácilmente en la siguiente:

$$\log \frac{\operatorname{tg} \alpha}{[AcOH]^m} = -x\,pH + \text{const.}$$

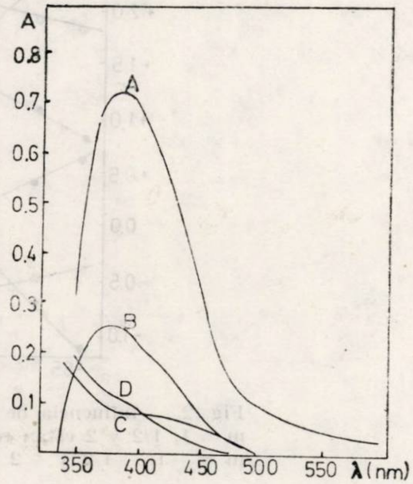

Fig. 1. — Espectros de absorción de: A — Una disolución de 1,3-CPBMT.HCl y Co(II) calentada en presencia de O_2; B — Una disolución de 1,3-CPBMT. HCl calentada en presencia de O_2; C — Una disolución de 1,3-CPBMT.HCl y Co(II) calentada en ausencia de O_2 y D — Una disolución de 1,3-CPBMT. HCl calentada en ausencia de O_2.

De forma análoga se obtiene para la segunda serie

$$\log \frac{\operatorname{tg} \alpha}{[AcO^-]^n} = -x\,pH + \text{const.}$$

Dando a m y n valores arbitrarios se obtienen las representaciones gráficas de las figuras 2 y 3. Los órdenes probables con respecto a AcOH y AcO^- serán aquellos valores sencillos de m y n que nos den valores más coincidentes para el orden de reacción con respecto a H_3O^+(x). Como se puede ver en la tabla 1, el valor más coincidente para la pendiente de las rectas (x) corresponde a un valor de m de + 1 y de n de —1/2, siendo el orden de reacción con respecto a H_3O^+ —1.

Influencia de la temperatura. Se ha estudiado la influencia de la temperatura entre 12 y 65°C, encontrándose que la velocidad de la reacción catalizada aumenta de manera exponencial con la temperatura.

Influencia de la concentracion de reactivo. El efecto de la concentración de 1,3-CPBMT.HCl en la velocidad de reacción se estudió en el rango $8.1 \times 10^{-5} - 10^{-3}$ M.

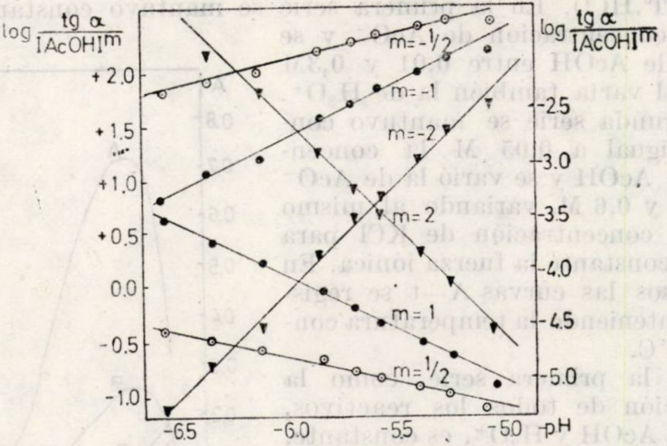

Fig. 2. — Influencia de H_3O^+ y AcOH. Las líneas rectas para m = 1, 1/2 y 2 están referidas a la ordenada izquierda y para m = —1, —1/2 y — 2 están referidas a la ordenada derecha.

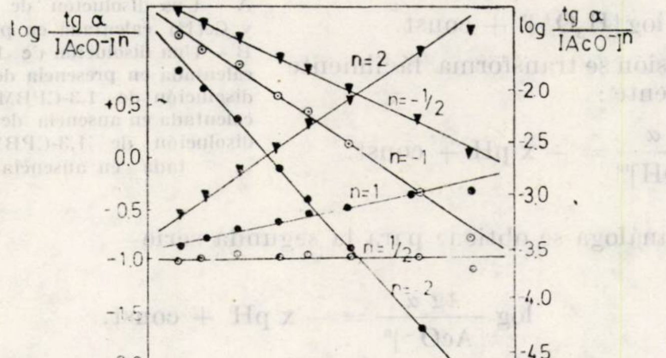

Fig. 3. — Influencia de H_3O^+ y AcO^-. Las líneas rectas para m = 1, 1/2 y 2 están referidas a la ordenada izquierda y para m = —1, —1/2 y — 2 están referidas a la ordenada derecha.

Como se puede ver en la figura 4, de la representación logarítmica se deduce un orden de reacción con respecto al reactivo de 1/2.

Influencia de la concentración de Co(II). Se han establecido las curvas de calibrado para la concentración de Co(II), usando el método de las tangentes, y el del tiempo fijo.

Tabla 1
Dependencia de la velocidad de reacción de $[H_3O^+]$, $[AcOH]$ y $[AcO^-]$

$\log tg/[AcOH]^m = -x$ (pH)		$\log tg/[AcO^-]^n = -x$ (pH)	
m	x	n	x
1/2	−0,48	1/2	0,00
2/3	−0,69	2/3	+0,15
1	−0,98	1	+0,41
3/2	−1,56	3/2	+0,88
2	−2,07	2	+1,36
−1/2	+0,48	−1/2	−0,97
−2/3	+0,65	−2/3	−1,24
− 1	+0,98	− 1	−1,40
−3/2	+1,58	−3/2	−1,87
− 2	+1,98	− 2	−2,37

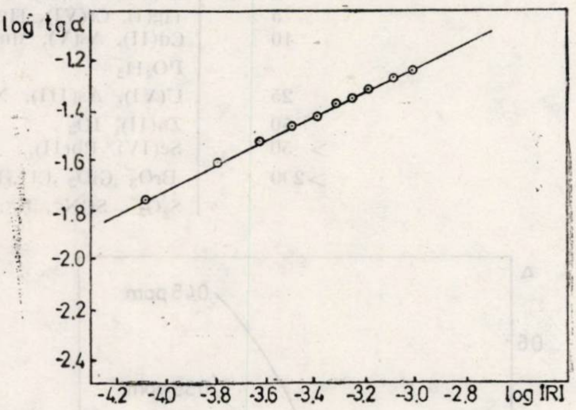

Fig. 4. — Influencia de la concentración de reactivo.

En la figura 5 se representan las curvas obtenidas. Usando el método de las tangentes el rango de concentración en el cual la curva es lineal es 0,05 — 0,4 μg·mL⁻¹ y el % de error (95 % de confianza, 11 determinaciones) es del ± 2,05 % y usando el método del tiempo fijo la curva es lineal entre 0,1 y 0,4 μg.mL⁻¹.

Interferencias. Se ha estudiado la influencia de iones extraños sobre la velocidad de reacción en presencia de 0,3 μg.mL⁻¹ de Co(II) aplicando el método de las tangentes. Los resultados se reúnen en la tabla 2.

Interfieren seriamente iones con propiedades de oxidación-reducción como Ce(IV), Fe(III) o Sn(II) y otros ligandos como AEDT. La interferencia de otros iones como Cu(II) y Os(VIII) puede ser explicada porque estos iones pueden actuar como catalizadores.

DISCUSIÓN

A partir de los estudios realizados acerca de la influencia de las diferentes variables de reacción se propone como ecuación de velocidad probable para la reacción de oxidación atmosférica del 1,3-CPBMT.HCl, catalizada por Co(II), en las condiciones de trabajo, la siguiente :

$$v = K'_c |AcOH|\ |AcO^-|^{-1/2} |H^+|^{-1} |1{,}3\text{-CPBMT}\cdot HCl|^{+1/2}\ |Co^{2+}|$$

en la cual K'_c es una constante de velocidad condicional que engloba la concentración de O_2.

Tabla 2

Efecto de iones extraños en la determinación de Co(II)

Mínima relación (en peso) interferente ión extraño/Co(II)	Iones extraños
$\leqslant 0,5$	Cu(II), V(V), Fe(II), Fe(III), Ce(IV), Cr(III), Te(IV), Os(VIII), Sn(II), Au(III), Ni(II), Ag(I), citrato, EDTA.
1	Pt(IV), Al(III), $C_2O_4^{=}$.
2	Bi(III), Pd(II), Rh(III).
5	Hg(I), Cr(VI), Hg(II).
10	Cd(II), As(V), Mn(II), tartrato, $PO_4H_2^-$.
25	U(VI), As(III), NO_2^-.
50	Zn(II), IO_3^-.
> 50	Se(IV), Pb(II).
>200	BrO_3^-, GlO_3^-, Cl^-, Br^-, I^-, $CO_3^{=}$, $S_2O_3^{=}$, SCN^-, F^-.

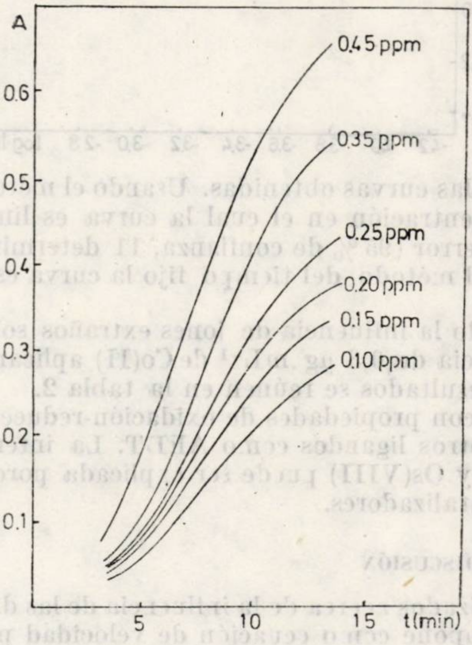

Fig. 5. — Curvas absorbancia-tiempo para diferentes concentraciones de Co(II).

El mecanismo de esta reacción catalítica no está completamente aclarado, pero parece probable que el Co(II) sirve como mediator en la transferencia electrónica. El Co(II) sería oxidado por el O_2 disuelto a

Co(III), el cual se estabilizaría formando un complejo. Este complejo de Co(III), oxidaría posteriormente al reactivo, dejando libre Co(II) que sería oxidado de nuevo. Por otra parte, no ha sido posible identificar el producto de reacción.

BIBLIOGRAFIA

[1] R. B. Singh, B. S. Gray y R. P. Singh, *Talanta*, **25**, 619 (1978).
[2] J. M. Cano Pavón, D. Pérez Bendito y M. Valcárcel, *Quim. Anal.*, **1**(**2**), 118 (1982).
[3] M. Román Ceba, J. A. Muñoz Leyva y J. J. Berzas Nevado, *Analyst*, **103**, 963 (1978).
[4] H. A. Mottola y H.B. Mark, *Analyt. Chem.*, **56**, 96R—112R (1984).
[5] R. P. Igov, M. D. Jaredic y T. G. Pecev, *Alas. Hem. Drus. Beograd.* **45** **(9)** 365 (1980).
[6] M. Román, J. C. Jiménez Sánchez y T. Galeano Diaz, *Quim.*, *Anal.*, **II**(**3**), 199 (1983).
[7] M. Román Ceba, J. C. Jiménez Sánchez y T. Galeano Díaz, *Afinidad*, En prensa.
[8] L. Erdey, "Gravimetric Analysis", Vol. 2, Primera Edición, Pergamon Press, 1965, cap. 23, p. 215.

Revue Roumaine de Chimie, **31**, *9—10*, 897—900 (1986)

ESTUDIO DE COMPLEJOS METÁLICOS DE BASES DE *SCHIFF* DERIVADAS DEL 2-TIOFENCARBOXIALDEHIDO O 2-PIRIDINCARBOXIALDEHIDO, Y o-AMINOBENCENOTIOL

F. CAPITÁN, P. ESPINOSA, F. MOLINA y L. F. CAPITÁN-VALLVEY

Departamento de Química Analítica, Facultad de Ciencias, Universidad de Granada, 18071, Granada, España

Recibido: el 13 de Julio de 1985

Se realiza un estudio de los compuestos aislados a partir de la reacción de la 2-(2-tienil) benzotiazolina y la 2-(2-piridil) benzotiazolina con diversas sales metálicas. Este estudio permite demostrar de manera clara que las complejos metálicos sintetizados son derivados de las bases de Schiff tautómeras respectivas, 2-(*o*-mercaptofeniliminometil)tiofeno y 2-(*o*-mercaptofeniliminometil)piridina.

The paper reports a study of the compounds obtained from 2-(2-thienyl) benzothiazole and 2-(2-pyridyl) benzothiazoline with different metallic salts. The results demonstarate clearly that the metallic complexes obtained are derivatives of the corresponding tautomeric Schiff bases, namely 2-(*o*-mercaptophenyliminomethyl)thiophene and 2-(*o*-mercaptophenyliminomethyl)pyridine.

INTRODUCCIÓN

La condensación de o-aminobencenotiol con un compuesto carbonílico no permite normalmente el aislamiento de una base de Schiff como cabría esperar, sino que se obtiene una tiazolina o una benzotiazolina. Esto se debe a algunas reacciones laterales que se dan en el transcurso de la condensación.

Se ha demostrado que en disolución existe un equilibrio tautomérico entre la tiazolina o benzotiazolina y la base de Schiff correspondiente, que se desplaza hacia la formación de esta última en medios muy básicos.[1,2] La reacción de una disolución de tiazolina o benzotiazolina con iones metálicos da lugar a la precipitación de los complejos metálicos de la base de Schiff tautómera. Algunos autores han postulado que el ión metálico retira a la forma base de Schiff de una mezcla de equilibrio.[3,4] Otros, sin embargo, postulan que en presencia de iones metálicos la estructura cíclica de la tiazolina o benzotiazolina se reordena para dar los quelatos metálicos de la base de Schiff de forma cuantitativa.[5,7]

A menudo, no obstante, los resultados aportados, basados fundamentalmente en estudios de IR y UV—VIS, no evidencian de forma clara cual es la naturaleza de los complejos obtenidos.

En publicaciones anteriores [8-10] hemos dado cuenta de los resultados obtenidos enel estudio de la actuación de la 2-(2-tienil)benzotiazolina* y la 2-(2-piridil)benzotiazolina* frente a iones metálicos. El objeto del presente trabajo es aportar nuevos datos que sirvan para dilucidar de una manera clara cual es la naturaleza del ligando presente en los complejos sólidos aislados.

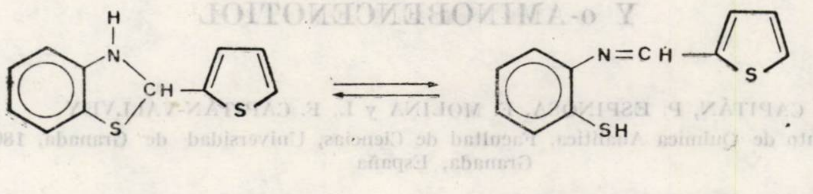

2-(2-tienil)benzotiazolina 2-(o-mercaptofeniliminometil)tiofeno

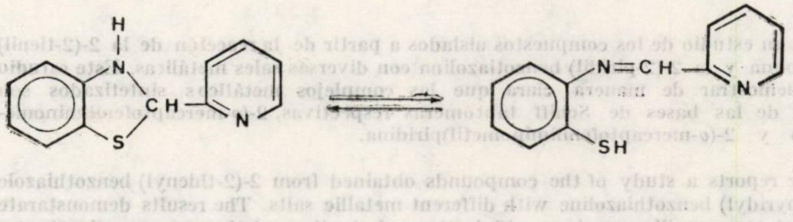

2-(2-piridil)benzotiazolina 2-(o-mercaptofeniliminometil)piridina

EXPERIMENTAL

Síntesis de los reactivos

Los reactivos se han sintetizado por condensación en etanol de 2-tiofencarboxialdehido y 2-piridincarboxialdehido con o-aminobencenotiol según los procedimientos descritos en trabajos anteriores[8,9]. La 2-(2-tienil)benzotiazolina es un sólido cristalino de color amarillo pálido (p.f. 95—96) y la 2-(2-piridil)benzotiazolina es un compuesto cristalino de color amarillo (p.f. 98.5—99).

Síntesis de los complejos

El método mas adecuado para la preparación de los complejos consiste en calentar a reflujo durante aproximadamente media hora una mezcla etanólica de la benzotiazolina y de la sal metálica correspondiente (generalmente nitrato o acetato). El sólido formado se filtra, se lava con una mezcla hidroalcohólica 50 % v/v y se deja secar a vacio sobre $CaCl_2$ y H_2SO_4. Se obtienen así los complejos metálicos con una pureza alta y con elevados rendimientos.[8,9]

---

* Esta es la forma en que normalmente aparecen nombrados estos compuestos. También pueden encontrarse en la bibliografía nombrados como 2-tiazolin-2-iltiofeno, y 2-tiazolin-2-ilpiridina.

Medidas físicas

Los espectros IR se registraron en un espectrofotómetro Beckman 4240 IR, en la región 4000−250 cm^{-1} en pastillas de KBr. Los espectros de absorción de los reactivos y de los complejos en DMSO se han registrado en un espectrofotómetro Bausch-Lomb mod. Spectronic 2000. Los espectros de ^{1}H−RMN en DMSO se han registrado en un espectrofotómetro Hitachi Perkin-Elmer mod. R−20 B usando TMS como referencia interna.

RESULTADOS Y DISCUSIÓN

El análisis de los espectros IR de los compuestos metálicos en estudio[8,9] sugiere que son quelatos metálicos de las bases de Schiff tautómeras de las benzotiazolinas. Este hecho se basa fundamentalmente en que en los espectros de los complejos se comprueba la desaparición de las bandas ν(N−H) y ν(C−S−C), presentes en los espectros de los reactivos en las regiones 3300−3200 cm^{-1} respectivamente y la aparición de una fuerte banda próxima a 1600 cm^{-1} atribuible a la vibración ν(C=N) coordinado.[11]

No obstante, resulta a veces muy difícil precisar la posición de la banda de tensión del C=N azometínico debido a la presencia en la misma zona de otras bandas intensas como las correspondientes a ν(C=C) aromáticos y ν(C=N) piridínico, así como las originadas por las vibraciones de tensión del grupo acetato en dos de los complejos aislados.

El análisis mediante espectrofotometría UV−VIS de estos compuestos pone de manifiesto lo siguiente : los espectros de los ligandos muestran dos bandas alrededor de 250 y 315 nm atribuibles a transiciones típicas de la forma cíclica benzotiazolina,[1,3,12] mientras que en los espectros de los complejos estas bandas no experimentan apenas desplazamiento si bien todos ellos exhiben una nueva vanda en la región visible (Tabla 1) atribuible a transiciones n−π* o π−π* implicando el doble enlace C=N azometínico.[12,13] Estos resultados apoyan a los anteriores respecto a que los complejos formados sean de las bases de Schiff pero sin que en ambos casos quede totalmente aclarada su naturaleza. Por ello hemos procedido a su estudio mediante ^{1}H−RMN.

Los espectros de ^{1}H−RMN de la 2-(2-tienil)benzotiazolina y de la 2-(2-piridil) benzotiazolina en DMSO constan de una señal a δ 3.30 ppm (aguda e intensa) y a 3.40 ppm (ancha, de intensidad media) respectivamente, que atribuimos al protón NH de la benzotiazolina, y multipletes complejos en la región δ 6.40−8.70 ppm que atribuimos a los protones aromáticos (Tabla 1).

En los espectros ^{1}H−RMN de los complejos se observa fundamentalmente la desaparición le la señal debida al protón NH, y la presencia de un singlete agudo en la región 8.30−8.50 ppm en el caso de los derivados tiofénicos, y en la región 9.15−9.40 ppm en el caso de los piridínicos (Tabla 1), que hemos atribuido al protón azometínico, −HC=N−, de la forma imina presente en los complejos. La forma y posición de estas señales concuerda totalmente con le de compuestos similares conteniendo todos ellos la agrupación azometina.[12,14,15] Así por ejemplo los espectros de ^{1}H−RMN en DMSO del 2-(o-hidroxifenilíminometil)tiofeno y de sus complejos (ML_2) de Zn y Cd, exhiben la señal del protón azometínico a δ 8.80, 9.10 y 8.95 ppm respectivamente.[16]

En los acetato complejos de Cd y Pb estudiados se observa la señal de los protones del grupo metilo en forma de un singlete agudo a δ 1.8 y 1.60 ppm respectivamente.

Tabla 1

Compuesto	^1H-RMN (δ ppm)			VIS	
	NH	$-HC=N-$	Aromáticos	λ (nm)	ε($l.mol^{-1}.cm^{-1}$)
$C_{11}H_9NS_2$	3.30	—	6.5−8.1	—	—
$Zn(C_{11}H_8NS_2)_2$	—	8.60	6.8−8.0	450	3.0×10^3
$Cd(C_{11}H_8NS_2)_2$	—	8.50	6.9−8.2	420	6.0×10^3
$Hg(C_{11}H_8NS_2)_2$	—	8.70	6.8−8.0	380	6.5×10^3
$Pb(C_{11}H_8NS_2)_2$	—	8.80	6.6−7.9	415	3.8×10^3
$Cd(C_{11}H_8NS_2)\ CH_3COO$	—	8.70	6.9−8.0	415	3.0×10^3
$C_{12}H_{10}N_2S$	3.40	—	6.2−8.4	—	—
$Zn(C_{12}H_9N_2S)_2$	—	9.40	6.9−8.8	520	5.0×10^3
$Cd(C_{12}H_9N_2S)_2$	—	9.15	6.9−8.7	500	6.4×10^3
$Hg(C_{12}H_9S)_2$	—	9.30	6.7−8.8	505	5.4×10^3
$Pb(C_{12}H_9N_2S)\ CH_3COO$	—	9.40	6.8−8.8	485	1.6×10^3

De los resultados anteriores se desprende pues la gran utilidad que presenta la utilización de la ^1H-RMN en estos casos. Mientras que las bandas IR que podrían servir como criterio diagnóstico se presentan solapadas en la region 1630—1480 cm^{-1}, en los espectros de ^1H-RMN se presenta una situación inversa. La señal del protón azometínico aparece claramente diferenciada de las señales de los protones aromáticos, y en una región bastante alejada de la señal de los protones metilo de los acetato complejos estudiados.

BIBLIOGRAFIA

[1] F. J. Goetz, J. *Heterocycl. Chem.*, **4**, 80 (1967) ; Ibid., **5**, 501 (1968) ; ibid., **5**, 509 (1968).

[2] L. F. Lindoy and S. E. Livingstone, *Inorg. Chim. Acta*, **1**, 365 (1967).

[3] E. Uhlemann and V. Pohl., *Z. Anorg. Allg. Chem.*, 397, 162, (1973).

[4] L. F. Lindoy, *Coord. Chem. Rev.*, **4**, 41 (1969).

[5] H. Jadamus, Q. Fernando and H. Freiser, *J. Am. Chem. Doc.*, **86**, 3056 (1964).

[6] E. I. Steifel, J. H. Waters, E. Billig and H. B. Gray, *J. Amer. Chem., Soc.*, **87**, 3016 (1965).

[7] E. Bayer and E. Breitmaier, *Chem. Ber.*, **101**, 1579 (1968) ; ibid., **102**, 728 (1969).

[8] F. Capitán, F. Salinas et L. F. Capitán-Vallvey, *Bul. Soc. Chim. France*, **1−2**, 35 (1979) ; ibid., **1−2**, 185 (1979).

[9] L. F. Capitán-Vallvey and P. Espinosa, *Polyhedron*, **2**, 1147 (1983).

[10] F. Capitán, L. F. Capitán-Vallvey, F. Molina y P. Espinosa, *Quim. Anal.*, (en prensa).

[11] E. Uhlemann and V. Pohl, *Z. Chem.*, **9**, 335 (1969) ; M. Consiglio, F. Maggio, T. Pizzno and V. Romano, *Inorg. Nucl. Chem. Lett.*, **14**, 135 (1978).

[12] R. K. Sharma, R. V. Singh and J. P. Tandon, *J. Inorg. Nucl. Chem.*, **42**, 1267 (1980).

[13] N. S. Biradar, V. H. Mahabe and V. H. Kulkarni, *Inorg. Chim. Acta*, **7**, 267 (1973).

[14] K. A. Parry, P. J. Robinson, P. J. Sainsbury and M. J. Waller, *J. Chem. Soc.* (B), 700 (1970) ; A.F.M. Iqbal, *J. Org. Chem.*, **37**, 2791 (1972).

[15] A. S. Al-Tai, D. M. Hall and A. R. Mears, J.C.S., *Perkin Trans* (II), 133 (1976) ; P.A.S. Smith and Chi Van Dang, *J. Org. Chem.*, **41**, 2013 (1976).

[16] F. Capitán, F. Molina, P. Espinosa and L. F. Capitán-Vallvey, *Acta Chimica Hungarica* (aceptado para publicación).

Revue Roumaine de Chimie, **31**, *9–10*, 901–908 (1986)

SYNTHESIS AND REACTIONS OF SOME NEW ISOQUINOLINE-1-CARBONITRILE DERIVATIVES

A. M. KHALIL, O. M. O. HABIB, I. I. ABD EL-GAWAD and H. A. ETMAN
Chemistry Department, Faculty of Science, Mansoura University, Mansoura, Egypt

Received March 8, 1985

Condensation of ethyl-α-cyano-3,4-dihydro-1-naphthylacetate with aromatic aldehydes in the presence of excess ammonium acetate afforded 2,3,4,4a,5,6-hexahydro-2-oxo-4-phenylbenz[f]isoquinoline-1-carbonitriles (I). Reactions of I with some Grignard reagents yielded 1-acetyl-4-4a,5,6-tetrahydro-4-arylbenz[f]isoquinoline-2(3H)-ones (II). Condensation of II with aromatic aldehydes gave the chalcone analogues IV which undergo further reactions to afford different products. The behaviour of I towards aminomethylation and hydroxymethylation has also been studied.

It has been reported that condensation of cyclohexanone with ethylcyclohexanylidene cyanoacetate in the presence of ammonium acetate gives the corresponding dihydropyridine derivative.[1]

As a continuation of our previous work on pyridone analogues, [2–4] we prepared a series of 2,3,4,4a,5,6-hexahydro-2-oxo-arylbenz[f]isoquinoline-1-carbonitriles (Ia–d) by treating ethyl-α-cyano-3,4-dihydro-1-naphthylacetate with aromatic aldehydes in the presence of excess ammonium acetate (molar ratios 1 : 1 : 8) at 150°C.

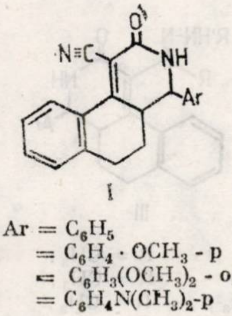

I

a Ar = C_6H_5
b = $C_6H_4 \cdot OCH_3$ - p
c = $C_6H_3(OCH_3)_2$ - o, p
d = $C_6H_4N(CH_3)_2$-p

The structures of Ia–d were confirmed from correct analytical data and from IR spectrum which revealed stretching frequencies at 2200, 1680 and 3300 cm^{-1} characteristic of C≡N, C=O and NH groups, respectively. NMR spectra of Ib showed signals at δ 3.9 and at δ 8.2 for the protons of the OCH_3 and cyclic –CONH– groups, respectively.

It has been stated [5,6] that Grignard reagents react with isoquinoline-1-carbonitriles, and that the optimum conditions were found to be four molecules of the Grignard reagent to one molecule of isoquinoline-1-carbonitrile. In the present study, addition of some Grignard reagents to I with subsequent decomposition and hydrolysis was investigated. Thus, treatment of Ia,b with methyl magnesium iodide or phenylmagnesium bromide afforded 1-acyl-4,4a,5,6-tetrahydro-4-phenylbenz[f]isoquinoline-2(3H)-ones (IIa—d).

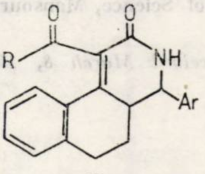

II

a Ar = C_6H_5 ; R = CH_3
b Ar = $C_6H_4 \cdot OCH_3$-p ; R = CH_3
c Ar = C_6H_5 ; R = C_6H_5
d Ar = $C_6H_4 \cdot OCH_3$-p ; R = C_6H_5

These products were characterized by elemental analyses and by IR measurements which showed stretching frequencies at 1700, 1650 and 3100 cm^{-1} for the C=O, —CONH— and —NH groups, respectively. NMR spectra of IIa,b revealed singlet at δ 2.4 for the CH_3 protons of the acetyl group.

Treatment of IIa—c with hydrazine or phenyl hydrazine gave the corresponding hydrazones IIIa—c *via* reacting with the carbonyl of the acetyl group but not with the amide carbonyl of isoquinolones. This was supported by experimental evidences which revealed that carbonitrile Ia does not react with either hydrazine or phenyl hydrazine.

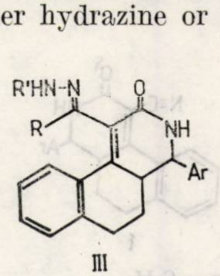

III

a Ar = C_6H_5 ; R = CH_3 ; R′ = H
b Ar = C_6H_5 R = CH_3 ; R′ = C_6H_5
c Ar = $C_6H_4 \cdot OCH_3$-p ; R = CH_3 ; R′ = H

For studying some reactions of new chalcone analogues in which one of the phenyl rings is replaced by a heterocyclic ring, the 1-cinnamoyl-4,4a,5,6-tetrahydro-4-phenylbenz[f]isoquinoline-2(3H)-one derivatives (IVa-c) were prepared. This was accomplished by the Claisen-Schmidt condensation [7,8] of aromatic aldehydes with the methyl of the acetyl group of IIa,b using ethanol as a solvent and potassium hydroxide as the condensing agent.

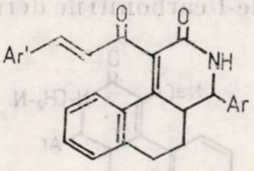

IV

a $Ar = C_6H_5$; $Ar' = C_6H_5$
b $Ar = C_6H_5$ $Ar' = C_6H_4 \cdot OCH_3\text{-p}$
c $Ar = C_6H_4 \cdot OCH_3\text{-p}$; $Ar' = C_6H_5$

The above products were identified by analyses and IR measurements showing absorption bands at 1680, 1630, and 3100 cm^{-1} for the $C{=}O$, $-CONH-$ and $-NH$ groups, respectively. ^1H-NMR showed signals at δ 7.2—7.4 and at δ 8.3 for the protons of the $-CO-CH{=}CH-$ and $-CONH-$ groups, respectively.

Furthermore, chalcone analogues IV were allowed to react with hydrazine and phenylhydrazine in ethanol to give the correspondinghydrazones which rearranged immediately to the isomeric 4,4a,5,6-tetrahidro-1--(5-aryl-2-pyrazolin-3-yl)-4-phenylbenz[f]-isoquinoline-2(3H)-one and 4,4a,5,6-tetrahydro-1-(1,5-diaryl-2-pyrazolin-3-yl)-4-phenylbenz[f]isoquinoline-2-(3H)-one derivatives (Va—c), respectively.

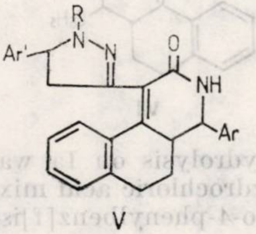

V

a $Ar = C_6H_5$; $Ar' = C_6H_5$; $R = H$
b $Ar = C_6H_5 \cdot OCH_3\text{-p}$; $Ar' = C_6H_5$; $R = H$
c $Ar = C_6H_5 \cdot OCH_3\text{-p}$; $Ar' = C_6H_5$; $R = C_6H_5$
d $Ar = C_6H_5$; $Ar' = C_6H_5$; $R = COCH_3$

Compounds Va—c were characterised by analyses and IR spectra which revealed stretching frequencies at 1600, 1630 and 3100 cm^{-1} characteristic for $-C{=}N-$, $-CONH-$ and $-NH-$ groups, respectively. ^1H-NMR spectra of Vb showed signals at δ3.4, δ7.6 and δ9.2 for the protons of the $-OCH_3$, cyclic $-CONH-$ and cyclic $N-NH$ groups, respectively. Likewise, the above pyrazolines Va—c gave the colour test for pyrazolin.[9] On the other hand, treating IVa with hydrazine in acetic acid afforded 4,4a,5,6-tetrahydro-1-(1-acetyl-5-aryl-2-pyrazolin-3-yl)-4--phenylbenz[f]isoquinolin-2(3H)one (Vd). This acetyl derivative was also obtained by refluxing Va in acetic acid and sodiumacetate.

On the other hand, the presence of cyclic —CONH-linkage in I prompted us to study their behaviour towards aminomethylation.[10] Thus treating Ia,b with piperidine and formaldehyde in methanol afforded the N-Mannich bases 2,3,4,4a,5,6-hexahydro-2-oxo-4-phenyl-3-(piperidinomethyl) benz[f]isoquinoline-1-carbonitrile derivatives (VIa, b).

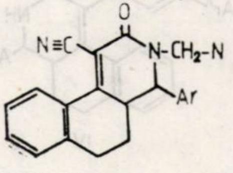

VI

a Ar = C_6H_5
b Ar = $C_6H_4 - OCH_3$-p

Product VIa was identified by elemental analysis and IR measurements which showed absorption bands at 2210, 1680 and 2925 cm^{-1} characteristic for the $-C{\equiv}N$, $C{=}O$ and $-CH_2-$ groups, respectively. The band at 3100 cm^{-1} disappeared. ^1H-NMR spectra showed a signal at $\delta 3.3$ characteristic for the protons of the $-CH_2N-$ group. When Ia was refluxed with formaldehyde in methanol, the N-hydroxymethyl derivative VII was formed. Warming VII with piperidine afforded the corresponding N-Mannich base VI.

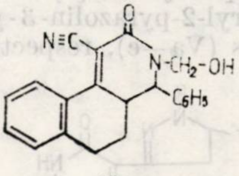

VII

The action of acid hydrolysis on Ia was also investigated. Thus heating of Ia with acetic-hydrochloric acid mixture under reflux afforded 2,3,4,4a,5,6-hexahydro-2-oxo-4-phenylbenz[f]isoquinolin-1-carboxylic acid VIII.

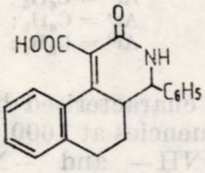

VIII

The structure of VIII was inferred from elemental analysis and IR spectra showing stretching frequencies at 1735, 1630 and 2700 cm^{-1} for the $-C{=}O$, $-CONH-$ and COOH groups, respectively. ^1H-NMR showed signals at δ 11.7 and at δ 8.8 characteristic for the protons of the COOH and $-CONH-$ groups, respectively.

EXPERIMENTAL

Melting points were uncorrected. ^{1}H-NMR spectra were obtained at 60 MHz with TMS as internal standard. IR spectra were recorded on a unicam sp 2000 spectrophotometer using potassium bromide discs ; elemental analyses were carried out at the microanalytical Unit, Faculty of Science, Mansoura University.

Preparation of ethyl-α-cyano-3,4-dihydro-1-naphthylacetate

A mixture of α-tetralone (30 mL), ethyl cyanoacetate (24 mL) and ammonium acetate (3.2 g, in a solution of acetic acid 10 mL and benzene 80 mL) was heated under reflux in a 250 mL round-bottomed flask fitted with a Dean and Stark apparatus. When the theoretical quantity of water was collected (ca. 6 hrs), the product was fractionally distilled to give ethyl-α-cyano-3,4-dihydro-l-naphthylacetate, b.p. 202–206° C/9 mm Hg.

2,3,4,4a,5,6-Hexahydro-2-oxo-4-arylbenz[f]isoquisnoline-1-carbonitrile-1-derivatives(Ia – d)

A mixture of ethyl-α-cyano-3,4-dihydro-1-naphthylacetate (0.01 mole), aromatic aldehydes (0.01 mole) and ammonium acetate (0.08 mole) was heated at 120–160°C in an oil bath for 8 hrs. The reaction product was cooled and the obtained yellow crystalline mass was filtered off, washed with ethanol and crystallized from acetic acid to give products Ia – d. The results are given in Table 1.

Table 1

2,3,4,4a,5,6-Hexahydro-2-oxo-4-arylbenz[f] isoquinoline-1-carbonitriles (Ia-d)

Compound	M.p. °C	Yield %	Colour	Formula (Mol. wt.)	Analyses %	C	H	N
Ia	300	75	Green	$C_{20}H_{16}N_2O$ (300.35)	Found Calcd	79.33 79.97	5.04 5.37	9.05 9.33
Ib	185	60	Yellow	$C_{21}H_{18}N_2O_2$ (330.37)	Found Calcd	76.12 76.34	5.13 5.49	8.88 8.48
Ic	298	65	Yellow	$C_{22}H_{20}N_2O_3$ (360.40)	Found Clacd	73.81 73.31	5.68 5.59	7.42 7.77
Id	259	**75**	Orange	$C_{22}H_{21}N_3O$ (343.41)	Found Calcd	76.42 76.94	5.63 6.16	12.02 12.23

1-Acyl-4,4a,5,6-tetrahydro-4-phenylbenz[f]isoquinoline-2(3H)-ones (IIa – d)

A suspension of Ia-d (2 g) in dry benzene (50 mL) was added dropwise to an etherial solution of methyl magnesium iodide or phenyl magnesium bromide (prepared from 0.9 g magnesium, 7.0 g methyl iodide or 8.0 g bromobenzene and 40 mL dry ether). The reaction mixture was refluxed for 3 hrs, set aside at room temperature and then decomposed with a cold solution of hydrochloric acid (10%). The solid products thus obtained were crystallized from acetic acid to give IIa – d. The results are given in Table 2.

2,3,4,4a,5,6-Hexahydro-4-phenlybenz[f]isoquinolin-l-yl methyl hydrazones III (a – c)

A mixture of IIa (0.01 mole), hydrazines (0.01 mole) and ethanol (20 mL) was refluxed for 3 hrs. The reaction mixture was cooled and the precipitated solids were collected by filtration and crystallized from acetic acid to give the corresponding hydrazones (IIIa – c). The results are presented in Table 3.

Table 2

1-Acyl-4,4a,5,6-tetrahydro-4-arylbenz[f]isoquinolin-2(3H)-ones (IIa—d)

Compound	M.p. °C	Yield %	Colour	Formula (Mol. wt.)		Analyses % C	H	N
IIa	280	65	Yellow	$C_{21}H_{19}NO_2$ (317.36)	Found Calcd	78.14 79.47	5.94 6.03	4.22 4.41
IIb	273	70	Yellow	$C_{26}H_{21}NO_2$ (379.43)	Found Calcd	82.69 82.30	5.14 5.58	4.44 3.69
IIc	178	70	Green	$C_{22}H_{21}NO_3$ (347.39)	Found Calcd	76.32 76.06	6.13 6.09	4.22 4.03
IId	187	75	Orange	$C_{27}H_{23}NO_3$ (409.45)	Found Calcd	78.88 79.20	5.32 6.56	3.53 3.42

Table 3

2,3,4,4a,5,6-Hexahydro-4-arylbenz[f]isoquinolin-1-yl methyl hydrazones (IIIa—c)

Compound	M.p. °C	Yield %	Colour	Formula (Mol wt.)		Analyses, % C	H	N
IIIa	225	70	Yellow	$C_{21}H_{21}N_3O$ (331.40)	Found Calcd	76.42 76.11	6.11 6.39	12.45 12.68
IIIb	270	65	Reddish brown	$C_{27}H_{25}N_3O$ (407.49)	Found Calcd	79.32 79.58	5.94 6.18	10.07 10.31
IIIc	210	75	Orange	$C_{22}H_{23}N_3O_2$ (361.42)	Found Calcd	72.88 73.11	6.02 6.41	11.92 11.63

Action of hydrazine on 2,3,4,4a,5,6-hexahydro-2-oxo-4-phenylbenz[f]isoquinoline-1-carbonitrile (Ia)

A mixture of Ia (0.01 mole), hydrazine hydrate or phenylhydrazine (0.01 mole) and ethanol (20 mL) was refluxed for 3 hrs. The reaction mixture was cooled and the obtained solid was crystallized from acetic acid to give unreacted I a m.p. and mixed m.p.).

1-Cinnamoyl-4,4a,5,6-tetrahydro-4-phenylbenz[f]isoquinoline-2(3H)-ones (IVa—c) :

To a solution of IIa,b (0.02 mole) in 10 % alcoholic potassium hydroxide solution, the appropiate aldehyde was added (0.02 mole). The reaction mixture was refluxed for 2 hrs, and left to stand overnight at room temperature. The solid obtained after dilution with hydrochloric acid was filtered off and crystallized from acetic acid to give (IVa—c). The results are given in Table 4.

Table 4

1-Cinnamoyl-4,4a,5,6-tetrahydro-4-phenylbenz[f]isoquinoline-2(3H)-ones (IVa—c).

Compound	M.P. °C	Yield %	Colour	Formula (Mol. wt.)		Analyses % C	H	N
IV a	279	80	Yellow	$C_{28}H_{23}NO_2$ (405.46)	Found Calcd	82.74 82.94	5.19 5.71	3.22 3.45
IV b	255	70	Orange	$C_{29}H_{25}NO_3$ (435.49)	Found Calcd	79.29 79.98	5.49 5.79	3.42 3.21
IV c	227	75	Yellow	$C_{29}H_{25}NO_3$ (435.49)	Found Calcd	79.45 79.98	5.32 5.79	3.11 3.21

Reaction of hydrazines with IV

A. In alcoholic medium : Formation of 4,4a,5,6-tetrahydro-1(5-aryl-2-pyrazolin-3-yl and 1,5-diaryl-2-pyrazolin-3-yl)-4-phenylbenz[f]-isoquinolin-2(3H)-ones (Va, b) and (Vc)

To a solution of IVa,c (0.02 mole) in ethanol (20 mL), hydrazines (0.02 mole) were added, and the mixture was refluxed for 5 hrs. The solid separated upon concentration was filtered and crystallized from ethanol to give (Va—c) (cf. Table 5).

Table 5

4,4a,5,6-Tetrahydro-1-(1-aryl-and 1,5-diaryl-2-pyrazolin-3-yl)-4-phenylbenz [f]isoquinolin-2(3H)-ones (Va, b) and (Vc)

Compound	M.p. °C	Yield %	Colour	Formula (Mol. wt.)	Analyses %			
						C	H	N
Va	300	75	Yellow	$C_{28}H_{25}N_3O$ (419.50)	Found Calcd	80.02 80.16	6.29 6.00	9.68 10.02
Vb	240	70	Orange	$C_{29}H_{27}N_3O_2$ (449.53)	Found Calcd	77.18 77.48	5.46 6.05	9.22 9.35
Vc	265	75	Orange	$C_{35}H_{31}N_3O_2$ (525.62)	Found Calcd	79.53 79.97	5.61 5.95	7.42 7.99

B. In acetic acid medium : Formation of 4,4a,5,6-tetrahydro-1-(1-acyl-5-phenyl-2-pyrazolin-3-yl)-4-phenylbenz f isoquinoline-2(3H)-one (V d)

A mixture of IVa (0.01 mole), hydrazine (0.02 mole) and acetic acid (20 mL) was refluxed for 5 hrs. The reaction mixture was cooled and the precipitated solid was filtered off and crystallized from acetic acid to give Vd, as yellow crystals, m.p. 280°C, yield 60 %.

Analysis : $C_{30}H_{27}N_3O_2$. (mol. wt. 461.57).
Found : C% 77.73, H% 5.63, N% 8.88.
Calcd : C%78.06, H% 5.89, N% 9.10.

Conversion of Va into Vd

Compound Va(1.0 g) was refluxed with acetic acid (25 mL) containing freshly fused sodium acetate (0.2 g) for 3 hrs. The reaction mixture was cooled and the obtained solid mass was crystallized from acetic acid to give N-acetyl-2-pyrazoline derivative Vd (m.p. and mixed m.p.)

Preparation of 2,3,4,4a,5,6-hexahydro-2-oxo-4-phenyl-3-piperidinomethyl benz[f] isoquinoline-1-carbonitriles (VIa, b)

To a mixture of Ia, b (0.01 mole) and piperidine (0.02 mole) in methanol, aqueous formaldehyde (35 %, 2.5 mL) was added. The reaction mixture was heated on a steam bath for five hours, left to stand overnight at room temperature, diluted with water and the obtained solid products were crystallized from ethyl alcohol to give the N-Mannich bases VIa, b. The results are given in Table 6.

2,3,4,4a,5,6-Hexahydro-2-oxo-4-phenyl-3(hydroxymethyl)benz[f]isoquinoline-1-carbonitrile VII

A mixture of Ia (1.2 g), aqueous formaldehyde (35 %, 10 mL) and methyl alcohol (50 mL) was heated under reflux for 3 hrs, cooled and the separated soli dwas crystallized from methanol to give VII as yellow crystals, m.p. 285° C, yield 70 %.

Analyses : $C_{21}H_{18}N_2O_2$ (mol. wt. 330.37).
Found : C% 76.66, H% 5.41, N% 8.22.
Calcd : C% 76.34, H% 5.49, N% 8.48.

Table 6

2,3,4,4a,5,6-Hexahydro-2-oxo-4-phenyl-3-piperidinomethyl)benz[f]isoquinoline-1-carbonitriles (VIa,b)

Compound	M.p. °C	Yield %	Colour	Formula (Mol. wt.)	Analyses %			
						C	H	N
VIa	178	60	Yellowish white	$C_{26}H_{27}N_3O$ (397.53)	Found Calcd	78.34 78.55	6.59 6.85	10.44 10.57
VIb	192	70	Yellow	$C_{27}H_{29}N_3O_2$ (427.55)	Found Calcd	75.51 75.85	6.42 6.84	9.46 9.83

Conversion of VII into VIa

To a hot solution of VII (0.01 mole) in methanol (50 mL), piperidine (0.02 mole) was added. The reaction mixture was refluxed for 2 hrs, then left to cool. The crystalline product that separated was proved to be the corresponding N-piperidinomethyl derivative VIa (m.p. and mixed m.p.).

Action of acetic-hydrochloric acid mixture on Ia

Compound Ia (1.0 g) was refluxed for 5 hrs with a mixture of glacial acetic acid (40 mL) and concentrated hydrolchloric acid (20 mL). The reaction mixture was cooled at room temperature and the obtained solid product obtained upon dilution with water was filtered and crystallized from ethanol to give VIII as grey needles, m.p. 178° C, yield 70 %.

Analyses : $C_{20}H_{17}NO_3$. (319.40)
Found : C % 74.93, H % 5.62, N % 4.49.
Calcd : C % 75.21, H % 5.37, N % 4.38.

REFERENCES

1 A. Sakurai and H. Midorikawa, *Bull. Chem. Soc. Japan*, **40**, 1680 (1967).

2 T. Zimaity, A. M. Khalil, I. I. Abd El-Gawad and S. Fouda, *J. Indian Chem. Soc.*, **54**, 623 (1977).

3 I. I. Abd El-Gawad, A. M. Khalil, T. Zimaity and S. Fouda, *J. Indian Chem. Soc.*, **54**, 626 (1977).

4 I. I. Abd El-Gawad, A. M. Khadah, A. M. Khalil, O.M.O. Habib and H. Al-Rifai, *Indian J. Chem.*, **21B**, 37 (1982).

5 R. L. Shriner and T. A. Turner, *J. Amer. Chem. Soc.*, **52**, 1267 (1930).

6 A. Sammour, Y. Akhnouk and H. Jahine, *J. Chem. UAR*, **14**, 213 (1971).

7 N. S. Vulf'son and G. M. Sukhotina, *Khim. Geterotsikl Soedin.*, (**1967**), 682 ; *Chem. Abstr.*, **68**, 39432 (1968).

8 M. Cassac and A. Boucherle, *Chim. Ther.*, **2**, 101 (1967) ; *Chem. Abstr.*, **68**, 21799 (1968).

9 V. Knorr, *Ann.*, **238**, 200 (1887).

10 F. F. Blicke, "The Mannich Reaction", vol. 1, Chapter 10, of the Organic Reactions (edited by Adams, R.), John Wiley, 1942.

Revue Roumaine de Chimie, **31**, *9–10*, 909–914 (1986)

AMMONIUM POLYPHOSPHATES. OBTENTION OF AMMONIUM POLYPHOSPHATES BY WARM AMMONIATION OF ORTHOPHOSPHORIC ACID

CAROLINA HAGIU, MIHAI TALABA, VIORICA DULMAN and ANA TALABA
Department of Chemical Technology, Polytechnic Institute, Splai Bahlui Stînga 71, Iași
Romania

Received December 20, 1985

The warm ammoniation of orthophosphoric acid was studied by experimental conditions for obtaining the ammonium polyphosphate as fertilizer. The influence of the chemical composition of orthophosphoric acid, its preheating temperature, ammoniation temperature, ammonia supply and the residence time on the composition of polyphosphate melts, through working conditions, are presented.

1. INTRODUCTION

Ammonium polyphosphate – a complex fertilizer concentrated in nitrogen and phosphorus – has a high content of active substance (10–15 % nitrogen and 55–65 % P_2O_5), is soluble in water, nonhygroscopic and nonagglomerable being able to be used for all types of cultures. The efficiency of using ammonium polyphosphates as fertilizer is determined by the high content of active substances which results in diminishing the package deposit, carriage and incorporation expenses. At the same time, the property of polyphosphates of retaining metals offers the possibility of obtaining fertiliziers with significant contents of microelements.[1] Being compatible with most of mineral fertilizers, the ammonium polyphosphates can be used in manufacture of a large scale of assortments of liquid, solid or in suspension complex fertilizers.

The researches concerning the possibilities of obtaining and using ammonium polyphosphate as fertilizer are relatively recent, the first papers in the field being reported by TVA firm.[2,3]

The literatura data,[4–7] indicate the ammonium polyphosphate, as a mixture of individual polyphosphates, to be obtained by the ammoniation of polyphosphoric and orthophosphoric acids, by thermal decomposition of ammonium orthophosphates and of the urea phosphate by the reaction between P_2O_5, gaseous NH_3 and water vapours.

Among the mentioned procedures the ammoniation of orthophosphoric acid sums the most interesting procedure, from the practical point of view, since it allows the integral use of heat of reaction and the diminution of energy consumption. The obtention of ammonium polyphosphate by the warm ammoniation of orthophosphoric acid is the object of some researches dealing especially with development of new procedures and improvement of ammoniation reactors while the investigation of chemical processes is approached in several studies.

In the present paper the results obtained in experimental studies on the ammoniation process under heating of orthophosphoric acid, aimed to settle the influences of preheating and ammoniation temperatures, of ammonia flowrate and residence time on the quality of ammonium polyphosphate are reported.

2. EXPERIMENTAL

The experimental investigation of the warm ammoniation process of orthophosphoric acid was carried out on the equipment depicted in fig. 1. The discontinuous reactor (1), of 1.6 liters capacity, is provided with a bubbling device (2), propeller stirrer (3) driven by an electromotor (4), thermometer (5), sample pipe (6) and pipe for gas removal (7), devices for gas condensing (8) and absorption (9) and drain pipe for polyphosphate melt (10). The reactor is thermostated with air (4), the heating accomplished by means of two electric resistances of 1000 W each, the homogenization of heating agent taking place by means of the turbine (11) driven by the electromotor (12). The equipment is also provided with a temperature regulator, a millivoltmeter indicating temperature in the reactor, ampermeter, operating switches as well as rotameter for measuring ammonia supply (13).

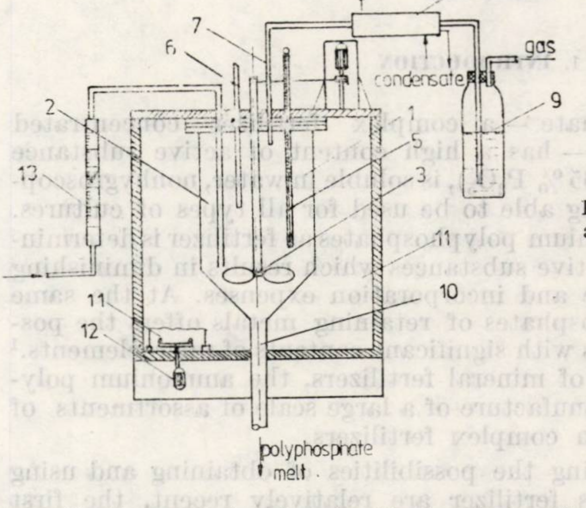

Fig. 1. — The laboratory equipment for ammonium polyphosphates obtention

For the runs technical grade orthophosphoric acid of the following composition : 49.06% P_2O_5, 1.37 % H_2SO_4, 1.01 % F, 0.56 % SiO_2 and 3 % other impurities, as well as analytical grade orthophosphoric acid with 61.58 % P_2O_5 were used. The experimental conditions varied between the following limits : preheating temperature of acid $t^{\circ} = 125^{\circ} - 230^{\circ}C$, ammoniation temperature $t = 230^{\circ} - 360^{\circ}C$, ammonia supply $V_{NH_3} = 50 - 252$ L/h and residence time $\tau = 15 - 195$ min.

The samples of melted ammonium polyphosphate were submitted to analysis for determining the overall P_2O_5 content ortho$-P_2O_5$, pyro-P_2O_5, tri- and poly-P_2O_5 and overall nitrogen. The content of overall P_2O_5 was determined gravimetrically by precipitating with quinoleine molibdate.[18] The overall nitrogen was determined by distillation with concentrated NaOH and NH_3 capture in a standard H_2SO_4 solution. The content in pyro-, tri- and poly-P_2O_5 was found by separating the components by paper chromatography and determination of orthophosphates, pyrophosphates and polyphosphates on synthesized standard samples. [19-23]

3. RESULTS AND DISCUSSION

The obtained results are listed in Tables 1 and 2.

After solidification the ammonium polyphosphate melts exhibit a glassy aspect : those obtained from pure phosphoric acid are white or transparent while those obtained from technical acid are dark-green coloured due to the presence of impurities.

Table 1

Composition of melts of ammonium polyphosphate from pure (sample 1) and and technical acid (samples $2-5$)

Working conditions				Composition of melt, % weight				
t°C	t°C	V_{N_3} (L/h)	σ(min)	P_2O_5 overall	P_2O_5 ortho-	P_2O_5 pyro-	P_2O_5 poly-	N
150	280	75	42	64.45	20.23	15.77	28.42	11.20
150	314	50	55	53.90	15.98	15.22	22.68	6.50
125	360	55	110	55.79	15.42	16.00	24.35	10.20
175	335	60	60	56.23	20.83	18.29	17.08	7.08
200	320	50	90	62.45	11.92	20.69	29.81	9.80

The nature of chemical species in ammonium polyphosphate depends on the conditions of its obtention : preheating temperature of the acid, ammoniation temperature, ammonia supply, residence time. Fig. 2 presents the chromatograms of samples with the composition given in Table 1.

The ammonium polyphosphate obtained from chemically pure orthophosphoric acid, preheated at 150°C, the temperature range being 280°C (Fig. 2,a), contains ammonium orthophosphates, pyro- and polyphosphates. The increase of preheating temperature of the ammoniation temperature results in increasing the polyphosphatic chain. Thus, ammonium polyphosphates obtained at 314°—335°C (preheating temperature 150°—175° C) contain ortho-, pyro-, tri- and tetrapolyphosphates (Fig. 2,b and c) : the increase of temperature regime to 360°C (Fig. 2, c) and of preheating temperature to 200° C (Fig. 2,e) leads to the obtaention of ammonia polyphosphates containing also pentapolyphosphates.

The influence of residence time and of ammonia supply on the composition of polyphosphates melts is depicted in Figures 3 and 4, plotted based on experimental data listed in Table 2. The overall P_2O_5 content firstly increases as a consequence of solution concentration, remaining then approximately constant. The P_2O_5 content as ammonium orthophosphates after a certain initial increase as a result of water evaporation decreases due to the formation of ammonium polyphosphates and after about 60 minutes also of tri- and polyphosphates. At higher temperatures the amount of found tri- and polyphosphates is higher. The nitrogen content increases in time up to about 150 minutes and then decreases.

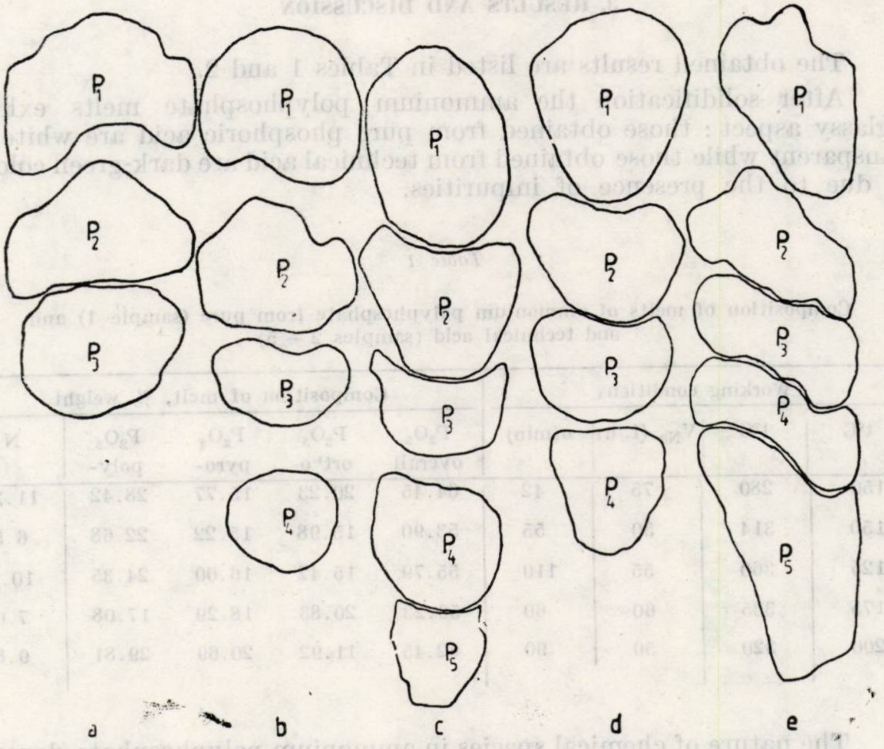

Fig. 2. — The paper chromatograms of the samples listed in Table 1.

Table 2

Variation of composition of ammonium polyphosphate melts (obtained from technical acid) with the residence time

Working conditions				Composition of melt, % weight				
t_0^0C	t° C	V_{NH_3}(L/h)	τ(min)	P_2O_5 overall	P_2O_5 ortho-	P_2O_5 pyro-	P_2O_5 poly-	N
150	230	140	15	58.40	38.40	—	—	3.28
			30	57.30	57.30	—	—	4.33
			45	54.80	40.66	14.14	—	6.85
			60	54.19	38.50	14.16	1.53	9 20
			150	54.60	24.32	20.50	6.78	13.66
			180	53.10	12.68	23.73	16.78	13.50
			195	54.20	10.52	15.94	27.74	12.80
230	230	252	15	54.80	54.80	—	—	1.46
			45	58.30	44.89	13.41	—	4.80
			60	52.30	34.83	17.42	—	5.44
			75	52.80	26.50	14.50	12.50	7.98
			90	52.40	20.57	11.26	20.57	8.32
			105	54.20	16.75	15.75	21.68	10.36

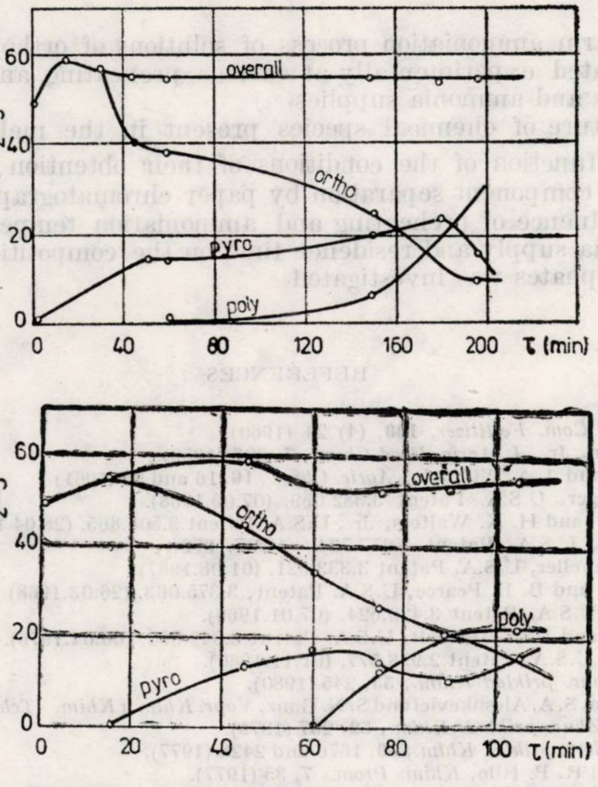

Fig. 3. — Variation of overall P_2O_5, ortho-, pyro- and poly-P_2O_5 *versus* residence time (a, Samples 1–7 ; b, Samples 8–13, Table 2).

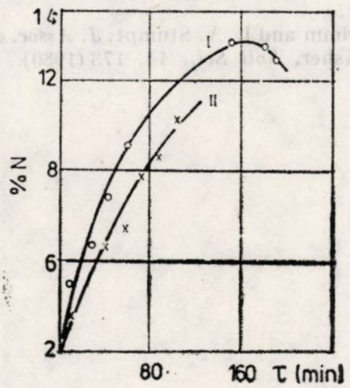

Fig. 4. — Variation of nitrogen content *versus* residence time (L, Samples 1–7 ; II, Samples 8–13, Tables 2).

The temperature increase, even under the conditions of increasing the ammonia supply, results in a diminution of nitrogen content.

4. CONCLUSIONS

The warm ammoniation process of solutions of orthophosphoric acid was investigated experimentally at various preheating and ammoniation temperatures and ammonia supplies.

The nature of chemical species present in the melts of polyphosphates, as a function of the conditions of their obtention was evidenced by means of component separation by paper chromatography.

The influence of preheating and ammoniation temperature as well as of ammonia supply and residence time on the composition of ammonium polyphosphates was investigated.

REFERENCES

1 A. V. Slack, *Com. Fertilizer*, **100**, (4) 24 (1960).
2 M. M. Striplin, Jr., *J. Agric. Food Chem.*, **7**, 623 (1959).
3 W. C. Scott and J. A. Wilbanks, *Agric. Chem.*, **16**, 16 and 93 (1961).
4 J. R. Getsinger, U.S.A. Patent 3.382.059. (07.05.1968).
5 Thad D. Farr and H. K. Walters, Jr., U.S.A. Patent 3.508.865. (28.04.1970).
6 R. L. Caroll, U.S.A. Patent 3.677.734. (18.07.1972).
7 K. O. Knollmueller, U.S.A. Patent 3.333.921. (01.08.1967).
8 J. B. Bookey and B. B. Pearce, U.S.A. Patent, 3.375.063. (26.03.1968).
9 E. B. Fitch, U.S.A. Patent 3.420.624. (07.01.1969).
10 D. C. Young and B. A. Harbolt, U.S.A. Patent 3.949.058. (06.04.1976).
11 P. G. Arvan, U.S.A. Patent 2.958.577. (01.11.1960).
12 I. P. Rilo, *Zhur. priklad Khim.*, **53**, 245 (1980).
13 N. S. Tyshkina, S. A. Aleshkevici and S. N. Ganz, *Vopr. Khim. i Khim. Tehnol.*, **54**, 6, 1979.
14 R. P. Rillo, *Zhur. priklad. Khim.*, **52**, 257 (1979).
15 R. P. Rilo, *Zhur. priklad Khim.*, **50**, 1676 and 2428 (1977).
16 I. P. Rilo and R. P. Rilo, *Khim. Prom.*, **7**, 35 (1977).
17 Yu. F. Zhdanov, N. Ya. Rezvina and N. S. Utochkina, *Khim. Prom.* **4**, 282 and **6**, 429 (1976).
18 * * * STAS 8623/3–1970.
19 Karl Kroupa, *Analyt. Chem.*, **28**, 1091 (1956).
20 H. Hettler, *J. Cromatog.*, **1**, 389 (1958).
21 T. Născuţiu, "Cromatografia pe hîrtie a substanţelor anorganice" Ed. Academiei, Bucharest, 1961.
22 J. R. Trimm and L. A. Stumpt, *J. Assoc. of Anal. Chem.*, **63**, 4.
23 L. E. Asher, *Soil Sci.*, **44**, 173 (1980).

Revue Roumaine de Chimie, **31**, *9–10*, 915–917 (1986)

COMPTES RENDUS

"Advances in Steroid Analysis '84", (S. Görök, editor), Akadémiai Kiadó, Budapest 1985, pp. 604

The volume contains the proceedings of the second Symposium on the analysis of steroids which was held in Szeged, Hungary in 1984, June 12–14.

Experts from 17 countries contributed to cover the modern conceptual, methodological and technical aspects of the steroid analysis. The published proceedings are grouped by ten sections : general aspects, protein binding and receptor binding, immunoassay (three sections), chromatography (four sections), other methods. The advantages of the association of the different analysis methods : immunoassay, gas-chromatography, high-performance liquid chromatography, mass spectrometry are presented together with their application fields. Although the programme of the symposium is focused on the methodology of the steroid analysis, new views are advanced concerning the steroid molecular biology related to the steroid structure function relationship (T. Fehér), steroid pharmacokinetics (G. Hobe), the intracellular mechanism of steroid action (J. H. H. Thijssen), etc. Besides the gonadal and adrenal steroids and their metabolites, papers describing the new progresses in the bile acids, steroid, drugs, sterols, vitamins D, cardiac glycosides, sapogenins analysis included the radioimmunoassay, gas chromatography mass spectrometry, HPLC and liquid secondary ion mass spectrometry (LSIMS). The specialists involved in the laboratory work meet in this volume some practical ways to improve the productivity and quality of the results (R. Vihko et al., A. Kage et al.). Further, the immunoassay may encounter the new radioimmunoassay (RIA) alternatives applied to the steroid hormones EIA, FIA, LIA but especially DELFIA (dissociation enhanced lanthanide fluoroimmunoassay). In this last method it is used the antibody labelling with Europium instead of the conventional fluorescent labels. For the clinical practitioners, of a particular interest is the extension of the RIA and the methods related to the measurement of the steroid hormones (endo- and exogenous) in the saliva or milk, thus minimizing the difficulties and cost of sample collection and store. On the one side, to interpret correctly a hormonal result obtained on single plasma sample may be difficult because of the circadian pronounced variation of the adrenal steroids and of the circatrigintan rhythm of the ovarian hormones. Therefore, the assay of the steroid hormones in saliva makes practical studies of the chronobiological variations using the fully automated methods. On the other side, it is be to expected that a good automation should increase precision and avoid blunders.

Concluding, the volume is of theoretical and practical interest on a large scale of fields : the human medicine (endocrinology, obstetrics-gynaecology, internal medicine, oncology, pediatrics), the sport-medicine, the veterinary medicine, the pharmaceutical industry, the industry of medical equipments and reagents.

Ligia Simionescu

"Unusual Properties of New Polymers" (Advances in Polymer Science, vol. 50), Springer, Berlin, 149 pages, 92 DM (hard-cover).

The first article "Physiological Activities of Synthetic Analogs of Polynucleotides" written by J. Pitha reviews polymers which have backbones analogous to those of plastics, and substituents analogous to those of polynucleotides. The interactions of polynucleotide analogs with natural polynucleotides and related proteins are presented.

The second paper, "Photochromic Phenomena in the Solid Phase" written by G. Smets presents the above mentioned problem for two physical properties of the polymer medium on isomerization reactions. The second part analyses the influence of conformational changes of chain segments induced by chromophore isomerization with respect to the physical behaviour of the polymer matrix.

The main article of the volume is "Polymer Square Planar Metal Chelates for Science and Industry" written by D. Wöhrle. Metal chelates where the metal atom is surrounded by one planar ligand such as porphyrin are investigated. The coordinative and covalent bonding of the chelate in a polymer chain is described in detail. Special properties such as electrical conductivity, small molecule binding, catalytic and electrolytic properties are mentioned. The author presents at the end some interesting future aspects of these special kinds of chelates.

The present volume is a useful source of up-to-date information for research workers in the field of polymer synthesis as well as for chemists interested in interdisciplinary areas related to biochemistry and inorganic chemistry.

Ursula Bologa

"Synthesis and Degradation, Rheology and Extrusion" (Advances in Polymer Science, vol. 47), Springer-Verlag, Berlin, 1982, 145 pages, 86 DM (hard-cover).

The topic of the first article "Aromatic Polybenzimidazoles. Synthesis, Properties and Applications" (author E. Neuse) is represented by all-aromatic polybenzimidazoles, which rank among the leading representatives of this class. Such materials advanced to the forefront of material technology in recent years on account of their flame retardance, radiative stability, mechanical and dielectric strength over a wide range of temperatures. Applications and performances are discussed in detail.

A. L. Bhuiyan presents in the next paper "Some Problems Encountered with Degradation Mechanisms of Addition Polymers" the most important parameters which have to be taken into consideration in deducing expressions of rate constants for thermal degradation of polyolefins. Intramolecular cyclization, intramolecular hydrogen abstraction, steric effects, and resonance effects can explain satisfactorily the yields of monomers in thermal degradation.

In "Entangled Linear, Branched and Network Polymer Systems. Molecular Theories" written by W. W. Graessley are analysed linear viscoelastic properties, macromolecular relaxation following strain, and network properties. Theoretical predictions and experimental observations are discussed for monodisperse and star-branched polymer liquids.

M. Dröscher deals with a new and important cold forming process, namely with extrusion of polymers in the solid state, in the review entitled "Solid-State Extrusion of Semicrystalline Copolymers". This procedure can be applied with success for copolymers because of the lower extrusion pressure and higher extrusion ratio used for copolymers than for homopolymers. Two types of copolymers are analysed : copoly(ethylenes) and copoly(ether/ester)s. As the author mentioned, this field of polymer science seems to be at its beginning.

One can appreciate the clearness and competence of the above reviewed articles. This volume is an example of useful up-to-date information in the field of polymer science. The books in the series "Advances in Polymer Science" edited by Springer-Verlag should be included in every library belonging to institutes which are active in the field of research and design of polymers.

Ursula Bologa

"Spectroscopy : NMR, Fluorescence, FT—IR" (Advances in Polymer Science, vol. 54), Springer-Verlag, Berlin, 1984, 166 pages, 98 DM (hard-cover).

"Self-Diffusion in Polymer Systems, Measured with Field-Gradient Spin Echo NMR Methods" is written by E. D. v. Meerwall. Nuclear magnetic resonance is used in the study of polymers not only as a tool to characterize chemical structure, but also to measure molecular motion in aggregates of polymer molecules such as solutions, melts, and entangled or crosslinked networks. This is done by measuring the width of the spectral features and characteristic NMR relaxation times (the spin-spin relaxation times and the spin-lattice relaxation times). The aim of this reviews is to familiarize chemists with field.gradient spin echo NMR methods for measuring self-diffusion and to show their applications and benefits. The methods are briefly described, and the results are mentioned in three areas : diffusion of polymers in their own melt and in concentrated solutions, diffusion of polymers in dilute and semidilute solutions, and diffusion of penetrants and diluents in high polymers host. The theoretical interpretations of these experiments are also included.

The second paper, "Photophysics of Excimer Formation in Aryl Vinyl Polymers", written by S. N. Semerak and W. Frank, deals with fluorescence technique used for obtaining details information on the structure of polymers. The objective of the present review is to concentrate on two aspects of the photophysics of synthetic polymers — excimer formation and singlet migration. The authors analyse all aromatic chromophore containing polymers but attention is paid to aryl vinyl polymers containing phenyl or naphthyl rings. Although this is a restriction, it is justified by the specificity of information obtáinable from systems containing these polymers.

"Fourier Transform Infrared Spectroscopy of Polymers" written by J. L. König is the third paper of the volume. The advent of Fourier transform infrared spectroscopy (FT—IR) has brought about a revival of interest in infrared spectroscopy as a characterization technique. The increased speed and higher signal-to-noise ratio of FT—IR relative to dispersion infrared has led to a substantially greater number of applications in polymer research. The availability of a computer, which is required for the FT—IR instrumentation, has allowed the digitized spectra to be treated by sophisticated data processing techniques and has increased the utility of the infrared spectra for qualitative and quantitative purposes. The basic theory, the sampling techniques and the spectral operations are described. The applications discussed include the study of polymer reactions, polymer structure, and dynamic effects.

The present volume continues to maintain the excellent quality of the previous numbers in this series. With the increasing amount of technical literature it has become a well-established fact that even senior scientists and technologists are no longer able to absorb the entire flow of papers, particularly those outside of their immediate field of interest. There is an accute demand to have this knowledge brought up-to-date and to learn about new concepts as they are developed. This is the aim of the Advances in Polymer Science series edited by Springer-Verlag

Ursula Bologa

NOTE POUR AUTEURS

La Revue Roumaine de Chimie publie de articles en anglais, français, russe, allemand ou espagnol. Les auteurs sont priés d'envoyer des articles et des comptes rendus inédits.

Les manuscrits seront dactylographiés à double interligne. La bibliographie, les tableaux et la légende des figures seront placés après le texte.

Si l'article fait partie d'une série numérotée, la partie précédente sera donnée comme première référence.

Chaque article sera précédé d'un résumé comprenant quinze lignes au maximum.

Les références bibliographiques dans le texte seront faites par des exposants sans parenthèses et paraîtront à la fin de l'ouvrage.

Les publications périodiques mentionnées dans la bibliographie seront présentées suivant les prescriptions internationales : le nom de l'auteur précédé de l'initiale du prénom, le titre du périodique abrégé conformément à «Chemical Abstracts» et souligné par une ligne, le numéro du tome indiqué par des chiffres arabes et souligné par deux lignes, suivi de la première page de l'article : à la fin, l'année de la parution sera placée entre parenthèses. Le numéro de la revue ne sera pas indiqué si les pages du volume sont numérotées consécutivement.

Les textes des livres ou traités inclueront : le nom des auteurs, précédés de l'initiale du prénom, le titré du livre entre guillemets et sans être souligné, le numéro du tome précédé par l'abréviation «vol.» (ou «Bd.»), le numéro de l'édition, les éditions (the publisher), la localité de la parution du livre, l'année de la parution et la page de la référence précédée*(s)* par l'abréviation «p» (ou «S»).

Les brevets seront indiqués comme suit : l'auteur ou la firme, le pays et le numéro du brevet, la date de la revue *(Chem. Abstr.)*. Par. ex. : M. Jones (to Union Carbide Co.). Brit. Pat. 610 238, 2 Sept. 1959 ; cf. *Chem. Abstr.*, **54**, 12808 (1960).

Si la référence n'a pas été lue en original, on indiquera aussi la revue de références consultée.

Les diagrammes seront tracés à l'encre de Chine sur papier calque. Les tableaux et les figures (en nombre strictement nécessaire), ainsi que les courbes dans les figures seront numérotés par des chiffres arabes. Leur explication sera donnée dans la légende des figures. Prière de ne pas inscrire les mêmes données dans les tableaux et les figures. Chaque tableau aura un titre. On indiquera dans le texte la place approximative des tableaux et des figures. Les formules chimiques seront incluses dans le texte ; en outre, elles seront transcrites sur papier-calque, à l'encre de Chine.

Les auteurs sont priés d'indiquer les caractères italiques (en soulignant les lettres au crayon), ainsi que tout autre caractère spécial : les préfixes *ortho*, *meta*, *para*, *cis*, *trans*, etc. seront soulignés pour indiquer leurs caractères italiques, et ne seront jamais écrits avec des majuscules.

Aucune correction à la main ne sera admise sur le manuscrit. Les corrections seront frappées à la machine. Les lettres grecques ou d'autres symboles spéciaux seront insérés à la main à l'encre clairement.

Le manuscrit sera signé par l'auteur.

Le titre courant aura 50 lettres au maximum.

L'entière responsabilité du contenu des articles appartient aux auteurs.

Sur demande ou peut obtenir une note plus complète.

PRINTED IN ROMANIA

PORŢELANUL

CROWN
Regent
FINE PORCELAIN
MADE IN ROMANIA
ALBA IULIA

2500 Alba Iulia, Str. Viilor nr. 128, Romania
Phone: 1 37 80; Telex: 36-240

The productions of the porcelain enterprise in Alba Iulia bear such marks as Apulum, Alba Iulia a. o. and include:

1. Houseware porcelain
   - — cups
   - — plates
   - — table sets
   - — other sets (for coffee, tea, cakes and kitchen)
2. Artware porcelain
   - — bibelots
   - — decorative pieces
3. Hotelware porcelain

The pieces are produced by highly productive manufacturing devices, or by manual procedures for limited-piece series and single pieces.

PORŢELANUL

CROWN
IMPERIAL
FINE CHINA
MADE IN ROMANIA
ALBA IULIA

2500 Alba Iulia, Str. Viilor nr. 128, Romania
Phone: 1 37 80; Telex: 36-240

The productions of the porcelain enterprise in Alba Iulia bear such marks as Apulum, Alba Iulia a. o. and include:

1. Houseware porcelain
   - cups
   - plates
   - table sets
   - other sets (for coffee, tea, cakes and kitchen)
2. Artware porcelain
   - bibelots
   - decorative pieces
3. Hotelware porcelain

The pieces are produced by highly productive manufacturing devices, or by manual procedures for limited-piece series and single pieces.

Intreprinderea de portelan
Alba Iulia
ROMANIA

MINISTERUL INDUSTRIEI CHIMICE
CENTRALA INDUSTRIALĂ DE MEDICAMENTE
COSMETICE COLORANŢI ŞI LACURI
Intreprinderea de produse cosmetice NIVEA Braşov,
Str. Karl Marx nr. 49
Telefon: 1 48 12; Telex: 61213

Cosmetics enterprise BRAŞOV delivers:

Products with therapeutical action:

BOICIL^R

antirheumatic ointment

OSSIDENTA^R

medicinal tooth paste

OSSIDENTA
pasta de dinti medicinala

Manufacturer:

Cosmetics Enterprise Braşov
Str. Karl Marx no. 49
Telephone No 14812 Telex: 61213

Sole exporter:

ICE–"CHIMIMPORTEXPORT"
POB 525, Blvd. Republicii, 10
Bucharest, Romania
Telephone No. 16. 06. 36.
Telex: 1184; 11697

A wide range of cosmetics

CORDIAL^{R}

RIPOSTA^{R}

Cosmeticals specially designed for children

Manufacturer: Cosmetics Enterprise Braşov
Str. Karl Marx no. 49
Telephone No 14812 Telex: 6123

Sole exporter: ICE – "CHIMIMPORTEXPORT"
POB 525, Blvd. Republicii, 101
Bucharest, Romania
Telephone No. 16. 06. 36.
Telex: 1184; 11697

MINISTERUL INDUSTRIEI CHIMICE
CENTRALA INDUSTRIALĂ DE MEDICAMENTE,
COSMETICE, COLORANŢI ŞI LACURI
Intreprinderea de produse cosmetice NIVEA Braşov,
Str. Karl Marx nr. 49. Telefon 1 48 12; Telex: 61213

1986 OKT 1

TRAVAUX PARUS AUX ÉDITIONS DE L'ACADÉMIE DE LA RÉPUBLIQUE SOCIALISTE DE ROUMANIE

T. ONCESCU, S. G. IONESCU, **Conversie fotochimică şi stocare de energie solară**, 1985, 272 p.
V. DRĂGUŢAN, A. T. BALABAN, M. DIMONIE, **Olefin Metathesis and Ring-Opening Polymerization of Cyclo-Olefins**, coédition avec John Wiley and Sons, 1985, 544 p.
C. LITEANU, I. RÎCĂ, **Optimizarea proceselor analitice**, 1985, 360 p.
N. PERESCU, **Chimia extracţiei cu solvenţi şi aplicaţii**, 1985, 212 p.
V. E. SAHINI, M. HILLEBRAND, **Chimie cuantică în exemple şi aplicaţii**, 1985, 378 p.
GH. MARCU, **Chimia compuşilor coordinativi**, 1984, 415 p.
E. CORDOŞ, C. MANOLIU, **Spectrometria de absorbţie şi fluorescenţă atomică**, 1984, 178 p.
C. BODEA, **Tratat de biochimie vegetală**, p. II, vol. 5, 1984, 438 p.
ELENA CEAUŞESCU, **Cercetări în chimia şi tehnologia polimerilor**, 1983, 519 p.
N. ASANDEI, A. GRIGORIU, **Chimia şi structura fibrelor**, 1983, 395 p.
N. IONESCU, M. CĂLDĂRARU, **Oxidarea catalitică a olefinelor inferioare**, 1983, 178 p.
C. CAŞCAVAL, **Studiul polimerilor prin piroliză şi cromatografie de gaze**, 1983, 220 p.
C. I. SIMIONESCU, F. DANEŞ, **Originea vieţii**, 1983, 110 p.
C. BODEA (sous la direction), **Tratat de biochimie vegetală**, 2 partie, t. IV, 1982, 408 p.
I. G. MURGULESCU, RODICA VÎLCU, **Introducere în chimia fizică. Vol. III, Termodinamica chimică**, 1982, 624 p.
I. G. MURGULESCU, J. PĂUN, **Introducere în chimia fizică. Vol. I, 3. Nucleul atomic, reacţii nucleare, particule elementare**, 1982, 606 p.
ELENA CEAUŞESCU, **Noi cercetări în domeniul compuşilor macromoleculari**, 1981, 536 p.
I. G. MURGULESCU, TATIANA ONCESCU, E. SEGAL, **Introducere în chimia fizică. Vol, II. 2. Cinematică chimică şi cataliză**, 1981, 1024 p.
LYDIA-MARIA VAICUM, **Epurarea apelor uzate cu nămol activ. Bazele biochimice**, 1981, 218 p.
I. GĂLĂŢEANU, **Procese şi metode radiochimice în energetica nucleară**, 1981, 234 p.
O. IORDACHE, **Procese polistocastice aplicate la fenomenele de transfer**, 1981, 186 p.
CR. SIMIONESCU, VALERIA GORDUZA, **Polimeri biocompatibili şi biologic activi**, 1980, 479 p.
ELENA CEAUŞESCU, **Polimerizarea stereospecifică a izoprenului**, 1979, 307 p.
C. GH. MACAROVICI, **Analiza chimică cantitativă anorganică**, 1979, 457 p.
M. FLORESCU, **Metode ştiinţifice în dezvoltarea industriei chimice moderne**, 1979, 256 p.
A. T. BALABAN, I. GĂLĂŢEANU, G. GEORGESCU, LIGIA SIMIONESCU, **Compuşi marcaţi şi radiofarmaceutici cu aplicaţii în medicina nucleară**, 1979, 495 p.
I. G. MURGULESCU, E. SEGAL, **Introducere în chimia fizică. Vol. II. 1. Teoria molecular-cinetică a materiei**, 1979, 1036 p.
S. STERNBERG, FL. DANEŞ, **Termodinamica chimică aplicată**, 1978, 400 p.
I. G. MURGULESCU, V. EM. SAHINI, **Introducere în chimia fizică. Vol. I. 2. Structura şi proprietăţile moleculelor**, 1978, 604 p.
I. ZUGRĂVESCU, MAG PETROVANU, **N-ylid chemistry**, coédition avec McGraw-Hill International Book Company, U.S.A., 1977, 396 p.
I. G. MURGULESCU, **Introducere în chimia fizică. Vol. I. 1. Atomi, molecule, legătură chimică**, 1976, 560 p.
ELENA CEAUŞESCU, **Research work on synthesis and characterization of macromolecular compounds, Contributions**, 1974, 251 p.
CR. SIMIONESCU, VIORICA RUSAN, V. POPA, **Chimia algelor marine**, 1974, 212 p. 1 pl.

ISSN 0035-3930

I. P. INFORMAŢIA, c. 2347

43 426

Lei 40
$ 80 (pour un abonnement annuel)

F 1103 04

ACADÉMIE DE LA RÉPUBLIQUE SOCIALISTE DE ROUMANIE

REVUE ROUMAINE DE CHIMIE

TOME 31

Nos 11–12

Novembre–Décembre, 1986

Rev. Roumaine Chim. RRCHAX, 31, *11–12*, p. 919–1070 (1986), Bucarest

EDITURA ACADEMIEI REPUBLICII SOCIALISTE ROMÂNIA

ACADÉMIE DE LA RÉPUBLIQUE SOCIALISTE DE ROUMANIE

COMITÉ DE RÉDACTION

Rédacteurs en chef:

I. G. MURGULESCU, membre de l'Académie de la République Socialiste de Roumanie

Rédacteur en chef adjoints:

A. T. BALABAN et V. EM. SAHINI, membres correspondants de l'Académie de la République Socialiste de Roumanie

Collège de rédaction:

EM. BRATU, ELENA CEAUȘESCU, ECATERINA CIORĂNESCU-NENITZESCU, CR. SIMIONESCU, membres de l'Académie de la République Socialiste de Roumanie ; P. SPACU, membre correspondant de l'Académie de la République Socialiste de Roumanie ; M. BANCIU, M. D. GHEORGHIU, I. HAIDUC, D. I. MARCHIDAN, G. NIAC et D. SĂNDULESCU

La Revue Roumaine de Chimie paraît 10 fois par an. Toute commande de l'étranger sera adressée a ROMPRESFILATELIA — sectorul Export-Import Presă, P. O. Box 12—201, télex 10376 prsfi r 78104 Bucarest, Calea Griviței nr. 64—66, București, Roumanie

Les manuscrits, les livres et les revues proposés en échange, ainsi que toute correspondance seront envoyés à la rédaction:

REVUE ROUMAINE DE CHIMIE

125, Calea Victoriei, 79717 Bucarest, Roumanie, téléphone 50 76 80

EDITURA ACADEMIEI REPUBLICII SOCIALISTE ROMÂNIA
125, Calea Victoriei 79717 Bucarest, Roumanie, téléphone 50 76 80

REVUE ROUMAINE DE CHIMIE

Tome 31, Nos 11 — 12 **Novembre — Décembre, 1986**

EDITORIAL . . . . 921—922

ALBERT BRUYLANTS, Early and contemporary scientific links between Romania and Belgium . . . . 923—926

K. CIBURA and A. HAAS, Reactions on tetracoordinated boron : advances in trimethyl-aminoborane-chemistry (in German) . . . . 927—933

HERBERT W. ROESKY and NASREDDINE BENMOHAMED, On reactions of tetrafluoro-1,2-ethanedisulfenyldichloride with alkynes or ketones (in German) . . . . 935—942

MARIUS ANDRUH, C. I. LEPĂDATU and MARIA BREZEANU, The position of 4,4′-bipyridyl in the spectrochemical series for nickel(II) complexes . . 943—948

G. FRITZ and K. STOLL, The cyclotetraphosphanes $(Me_3C)_3P_4H$ and $(Me_3C)_3P_4[P(CMe_3)Cl]$ (in German) . . . . 949—953

IOAN SILAGHI-DUMITRESCU and IONEL HAIDUC, The bonding in dialkyldithiophosphinato metal complexes. A molecular orbital study of bis(dimethyldithiophosphinato) nickel(II) . . . . 955—962

U. BENTRUP and L. KOLDITZ, Roëntgenographic and IR-spectroscopic investigations of the thermolysis of alkali pentafluoroaluminate hydrates (in German) . . . . 963—972

E. PINCOVSCHI and M. MERCHEŞ, Hydrothermal crystallization of zeolite Na-X . . . . 973—980

GH. MARCU, AL. BOTAR and ADRIANA NAUMESCU, Contributions to the study of cobalt(II) dioxygen complexes . . . . 981—986

D. NEGOIU, S. NEAGOE, CORNELIA CERCASOV, MARIA NEGOIU, IOANA SARAMET and C. TOMA, Complex compounds of Hg(II) with thiobenzopiperidides and thiobenzomorpholides . . . . 987—993

CRISTOFOR I. SIMIONESCU, SILVIA IOAN and BOGDAN C. SIMIONESCU, Solution properties of ultrahigh molecular weight polymers (pleistomers). 14. Solvent effect on the unperturbed dimensions of poly(butyl methacrylate) chains . . . . 995—999

MICHAELA STĂNESCU, M. ELIAN and ECATERINA CIORĂNESCU, Carbonium ion reactions. XVII. Rearrangements of dibenzobicyclo[3.2.1]-octane and dibenzobicyclo[3.2.2]nonane derivatives . . . . 1001—1011

MIHAELA BUGEANU, V. E. SAHINI, V. T. CIORBA and A. T. BALABAN, Molecular complexes with aromatic cations as electron acceptors. VII.

Spectrometric, conductimetric, and dipolar data of phenyl-substituted pyrylium salts with tetracyano-*para*-quinodimethane anions 1013–1018
M. BANCIU, M. ELIAN, ANCA BANCIU, C. DRĂGHICI and ECATERINA CIORĂNESCU, Photochemical ring contraction of 8-diazo-dibenzo[*c*,*e*]-tricyclo[5.3.0.$0^{2,10}$]deca-3,5-dien-9-one 1019–1024
ANGELA POPESCU, LUMINIȚA PÂRVULESCU, LIGIA STĂNESCU and MIRCEA D. GHEORGHIU, Synthesis of 1α, 2α- and 1β, 2β-isomers of 5,9-methano-5*H*-benzo[3,4]cyclobuta[1,2]cycloheptenes 1025–1030
MARIE-HÉLÈNE DARBIEU, Main reactions of the cobalt atom in vitamin B_{12} and in model complexes from the cobaloxime group (in French) 1031–1039
EMIL PETROVICI, EUGENIA NARTEA and GHEORGHE MARA, Criteria for nuclides ordering and observed regularities 1041–1046
N. CALU, G. BRÎNZAN and N. BÎLBĂ, IR and X-ray spectral correlations of some Reinecke type complexes (in French) 1047–1054

Author index 1055–1064
Subject index 1065–1069

Revue Roumaine de Chimie, **31**, *11–12*, 921–922 (1986)

EDITORIAL

PROFESSOR PETRU SPACU, D. Chem.

Corresponding member of the Academy of the Socialist Republic of Romania

This year Professor Petru Spacu, D. Chem., corresponding member of the Academy of the Socialist Republic of Romania celebrates the 80th anniversary of his birthday.

Born in Charlottenburg (Germany) on June 6, 1906, as the son of the well-known inorg.-chem. Gheorghe Spacu, member of the Romanian Academy, he graduated in chemistry (1929) and obtained the doctor's degree with "Magna cum laude" at the University of Cluj (1932). Between 1934 and 1937 he undertook postdoctoral research at the faculties of chemistry of the Paris and Munich Universities.

Professor Petru Spacu carried on his teaching activity at the University of Cluj between 1929 and 1937 where he was assistant-, and associate-professor at the Chair of Inorganic Chemistry ; between 1937 and 1955 he was professor of inorganic chemistry at the Polytechnic Institute of Bucharest and from 1955 to 1972 he was professor of Inorganic Chemistry at the Faculty of Chemistry, University of Bucharest. He also taught : Analytical Chemistry, Chemistry of Metals, Chemistry of Complex Compounds and between 1948–1950 Inorganic Chemistry at the Institute of Oil and Natural Gas in Bucharest.

He acted as supervisor for twenty-eight PhD theses and published 7 student handbooks.

He retired on October 1, 1972.

His rich scientific activity, carried out at the University of Cluj, Polytechnic Institute of Bucharest, University of Bucharest and the Academy of the Socialist Republic of Romania is materialized in 308 research papers (published in scientific journals in Romania and abroad) and 6 patents; this research was directed towards the following fields of investigation:

— synthesis, structural studies and stability investigations of numerous new coordination compounds, of potential importance in living cells processes, catalytic processes, and industrial applications.

— development of new chemical and physico-chemical methods for the determination and separation of several rare and dispersed elements and of some products with therapeutical action. Some of these methods are applied in drug production and analyses, in various research and industrial laboratories in Romania and abroad.

— research into the chemistry of lanthanides: mixed complex compounds of lanthanides with iron group metals and organic ligands generating mixed oxides applied in catalysis.

— industrial research (production of $SiCl_4$ from native diatomite, syntheses and properties of semiconductors, obtention of melting and degassing additives from indigenous raw materials, re-use of platinum from spent catalysts, obtention of boric acid from native ores).

Professor P. Spacu held important functions in higher-education and research institutes: deputy dean (1944–1948) and dean (1951–1955) of the Faculty of Industrial Chemistry, Polytechnic Institute of Bucharest, vice-rector of the University of Bucharest (1966–1969), head of department and head of section at the Chemical Research Centre, the Centre of Inorganic Chemistry and the Centre of Physical Chemistry of Bucharest.

In recognition of his important contribution to the chemical research, Professor Petru Spacu was elected corresponding member of the Academy of the Socialist Republic of Romania (1963), member of the Academy of Sciences in Göttingen (1970) and of the Mediterranean Academy of Sciences (Catania, 1986). During 1967–1971 he was appointed in the IUPAC committee, Section of Inorganic Chemistry.

He was awarded The Order of Labour (1964), The Star of the Socialist Republic of Romania (1966), The Order of Scientific Merit (1967).

On the occasion of the celebration of his 80th birth anniversary, the Editorial Board of Revue Roumaine de Chimie, his colleagues and students wish professor Petru Spacu many years of good health and a long and fruitful activity.

THE EDITORIAL BOARD OF REVUE ROUMAINE DE CHIMIE

Revue Roumaine de Chimie, **31**, *11–12*, 923–926 (1986)

Dedicated to Professor PETRE SPACU, corresponding member of the Romanian Academy, emeritus professor of Inorganic Chemistry at the Bucharest University and Polytechnic Institute, on the occasion of his 80th birthday.

EARLY AND CONTEMPORARY SCIENTIFIC LINKS BETWEEN ROMANIA AND BELGIUM

ALBERT BRUYLANTS
Académie Royale des Sciences, lettres et beaux-arts de Belgique

Received April 14, 1986

The 16th International Congress of History of Science, organized by the International Union of History and Philosophy of Sciences, Division of History (I U H P S/D H S), took place in Bucharest, from 26th August till 3th September, under the chairmanship of the Academician Gheorghe Mihoc. This impressive event, which gathered together about 1.200 delegates from all over the world, was patronized by Academician doctor-engineer Elena Ceaușescu, prime vice-prime Minister and Chairman of the National Council for Science and Technology. Through this congress the opportunity was granted to me to enjoy ancient and new friendly relationships with numerous Romanian scholars, more especially with colleagues chemists, namely Alexander Balaban, Ileana Necșoiu, Victor Sahini, Bogdan Simionescu and last but not least, Petre Spacu, renowed among the Romanian scientific community and outside in our learned societies.

Let me also make an account of Romanians so actively contributing to intellectual and scientific animation, at various levels in my country. In that sense, I like to mention Florentina Iona Mosora, biophysicist, nowadays associate professor at the university of Liège.

Actually, our mutual friendship is going back to the last quarter of the last century, and I feel that the anniversary issue of the *Revue Roumaine de chimie* dedicated to Professor Petre Spacu, offers a fine convenience to remember the foremost Belgian organic chemist of the 19th century, Louis Henry (1834–1913), who maintained close relationships with the Romanian scientific community, especially thanks to his colleague and friend Constantin I. Istrati (1850–1918).

Istrati was born in the historical city of Roman where, in 1859, the so-called "Union Oak" of the poet Vasile Alecsandri was set. He completed high school in Jasi, the intellectual capital of Moldavia, seat of a University founded in 1860. He had just graduated as doctor of medicine, in Bucharest in 1877, when he took part in the Independence War. Later on, he went to France and became assistant to Charles Friedel (1832—1899) under whom he doctorated in chemistry at the University of Paris, in 1885. Returning home, he was appointed professor of organic chemistry of the University of Bucharest.

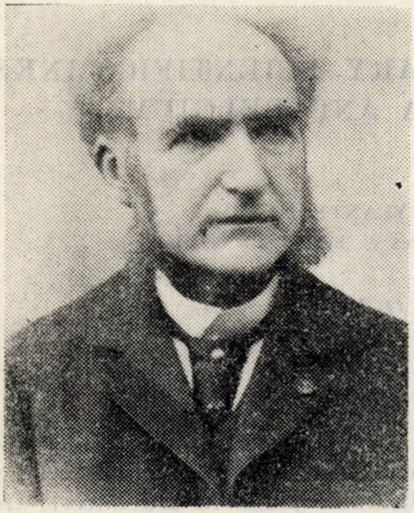

Fig. 1. — Professor Louis Henry (1837—1913). First recipient of the Belgian award "Prix Décennal des Sciences physiques et chimiques" (1899).

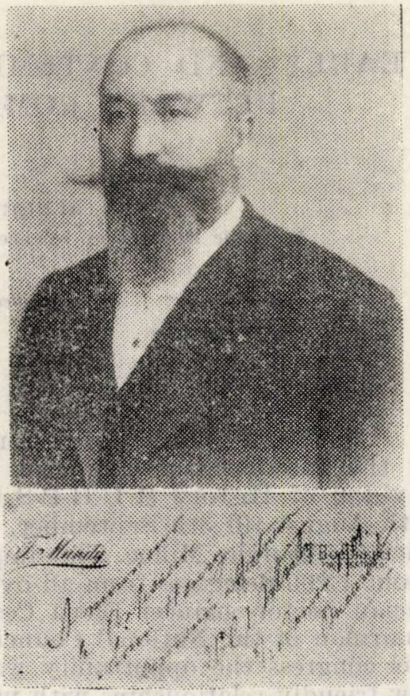

Fig. 2. — Professor Constantin I. Istrati, (1850—1918), Minister of Public Education (dedicated photograph).

Not only through his teaching and his research of the natural richness of Romania, but also through his action as lord-mayor of Bucharest and minister of public education, Istrati was a pioneer of the development of sciences in his country.

When and where Istrati and Henry met each other for the first time is not known, at least to me. It should be mentioned however that, from the Independence of Romania forth, exchanges of various kinds — culture, trade, technology — were very active between Belgium and the new kingdom.

Moreover during his stay in Paris, Istrati became acquainted with the Frenchspeaking chemical community amidst which the father of the Belgian organic chemistry was an outstanding personality. Now after the foundation by Istrati of the Romanian society of sciences, in 1890, Henry was elected honorary fellow, and later on was rewarded a 1st class medal "Benemerenti" of Romania (1900), and decorated "grand officier de la Courone de Roumanie" (1907).

On the occasion of a journey to the western countries, in October 1905, probably in connection with the General Worldfair at Bucharest in 1906 whose organizer he was, Istrati visited Henry at Louvain.

This event was seized by the Belgian chemist to plan the nomination of his visitor as a foreign member of the Royal Academy at Brussels, where a seat had remained vacant since the death of Alex. de Colnet d'Huart, in June 1905. Of this time, an undated letter of Istrati to Henry has been preserved; it was sent from Bucharest to Louvain, probably in September 1905; for the purpose of the presentation, a curriculm vitae was enclosed; cordial thanks are expressed for the nice reception within Henry's family; an invitation is extended to visit the Worldfair in Romania. This letter starts and ends with "mon cher et bon maître".

Let us now have look at Henry's scientific work.

Louis Henry had been educated successively at Louvain (1851—1855), where he graduated doctor of sciences, at Liège (1856) under Laurent de Koninck (1809—1887) and in the famous chemical laboratory, at Giessen (1857) under Heinrich Will (1812—1890), successor and former closest assistant to Liebig.

Henry's first concern and endeavour was the renovation of the teaching. In this view he published a *Précis de chimie générale élémentaire* in three volumes (1867).

Henry's original research work unfolded itself during about half a century, and is described in 400 papers almost all published in the Bulletin of the Belgian Academy, the Compte-rendus of the Sciences Academy at Paris, and in the Recueil des travaux chimiques des Pays-Bas et de la Belgique. Henry contributed to the enrichment of organic chemistry with numerous new compounds; he prepared alone, or with the help of his assistants and pupils, a lot of hydrocarbons, alcohols, and halogenated derivaties, nitro-alkanes and nitriles. One of the most amazing hand-made molecules the Belgian chemist was able to obtain is dipropargyl, or 1,5-hexadiyne, $CH\equiv C-CH_2-CH_2-C\equiv CH$, a diacetylenic hydrocarbon, Bp. 86°C, smelling sharply and highly reactive, which was the first aliphatic isomer of benzene.

In the course of his studies, Henry was eager to disclose relationships between structure and physical or chemical properties.

The volaiility of a disubstituted aliphatic compound, he expressed as a rule, *depends on the relative proximity of negative groups*; it keeps increasing in an isomer series by bringing both substituents nearer to each other. Examples are $CN-CH_2-CH_2-CH_2Cl$ (Bp. 195°C), $CN-CH_2-CHCl-CH_3$(Bp. 175°C), $CN-CHCl-CH_2-CH_3$(Bp. 145°C).

The chemical reactivities of a functionnal groups also appear to be very sensitive to the proximity of a substituent; for instance among the three hydroxybutynitrile α, β and γ, the former alone is able to react with amines substituting its alcoholic function.

According to Henry, it appears that in an organic molecule two or more substituents influence each other; the closer they are, the larger is their mutual action, a principle which he called *functionnal solidarity*; considering from a somewath antropomorphic point of view that it exists a kind of joint contribution between the different parts of a molecule to the peculiar reactivity of the compound.

In modern physical organic chemistry, functional solidarity is reflected quantitatively by the Hammett equation ($\Delta \log k = \rho\sigma$).

The chemical demonstration of the identity of the four valencies of the carbon atom needs to be mentioned among Henry's endeavours. This piece of work, first published in 1886, became a classic ; for instance Nernst in his handbook writes : "Die Frage nach der Zahl der Monosubstitution produkte ist von L. Henry systematisch in Angriff genomen ; wegen der auserordentlichen wichtigkeit, die ihr furdie Grundlage der Stereochemie zukommt sei der Weg, der deser Forscher entschlag, kurz angedeutet." Actually, Henry prepared monosubstituted methane derivaties (CH_3-X) thanks to a series of chemical reactions and in such a way that the substituent (X) should replace successively the four hydrogens (Ha, Hb, Hc, Hd). Nitromethane ($X = NO_2$) and acetonitrile ($X = CN$) were chosen for that purpose. Four samples (CXaHbHcHd) ; CHaXbHcHd) ; CHaHbHcHd ; CHaHbHcHd) of both compounds, prepared by this way, were found to be identical.

Henry also contributed to the total synthesis of natural compounds, and more specially to the t.s. of fats, in devising a glycerol synthesis based on the reaction he had discovered between nitromethane and formol. This point must be considered of interest in the light of the so-called "vitalism controversy". In 1899, Henry was awarded by the Belgian government the "Prix décennal des Sciences physiques et chimiques", which was given for the first time, in recognition of his contributions to the development of organic chemistry.

The 5th of June 1900, the very day when a formal ceremony was organized by the university of Louvain in honour of the laureate, congratulations where received not only from Belgian colleagues, friends and pupils but also from all over Europe by famous names. From Bucharest came two telegrams both signed by Istrati ; one in his capacity of Minister of Public Education and the second on behalf of the "Société roumaine des sciences" which read as follows :

> "La société roumaine des sciences qui a l'insigne honneur de compter Monsieur Henry parmi les membres d'honneur se doit de prendre la plus large part à la fête par laquelle on honore la probité, l'activité et le dévouement à la science de son illustre collègue. Vive Henry ! Vive la Belgique ! Le Secrétaire Istrati."

After the disappearance of those illustrious actors there was a low tide in the history of our mutual links which were followed by a renewal of our relationships, when Costin Nenitzescu (1902–1970), the famous professor of organic chemistry at the University and Polytechnic Institute of Bucharest, accepted our invitation to act as the main lecturer and honorary member at Louvain University, of our chemistry Congress in 1967. Ever since we may enjoy, on both sides, like on each new spring, that the flow is again keeping flowing.

Revue Roumaine de Chimie, 31, *11–12*, 927–933 (1986)

Herrn Prof. Dr. SPACU zum 80. Geburtstag gewidmet.

REAKTIONEN AM VIERFACH KOORDINIERTEN BOR: [BEITRÄGE ZUR CHEMIE DES TRIMETHYLAMINOBORANS

K. CIBURA und A. HAAS
Lehrstuhl für Anorganische Chemie II, Ruhr-Universität Bochum, Postfach 102 148, D-4630 Bochum

Eingegangen am 5. Mai 1986

Reactions of trimethylaminoborane with tetra-, tri- and di-CF_3S-substituted pyrroles (**1a-e**) as well as with pyrrole (**1f**) at 80 to 160°C give in 30 to 90% yield the corresponding monosubstituted trimethylaminoboranes (**2a-f**). In no case disubstitution was observed. The strong acid CF_3SO_3H reacts with $(CH_3)_3NBH_3$ at 20°C to yield $(CH_3)_3NBH_2OSO_2CF_3$ (**3**) and with 2 mol acid at 80°C to $(CH_3)_3NBH(OSO_2CF_3)_2$ (**6**). In benzene $Hg(EFC_3)_2$ forms with $(CH_3)_3NBH_2I$ at 20°C $(CH_3)_3NBH_2ECF_3$ (E = S, **4**; *E* = Se, **5**). IR-, ^1H-, ^{19}F-, ^{11}B- and ^{77}Se-NMR-data are provided.

Umsetzungen von Trimethylaminoboran mit tetra-, tri- und di-CF_3S substituierten Pyrrolen **1a-e**, sowie Pyrrol **1f** führen bei 80 bis 160°C zu den entsprechenden monosubstituierten Trimethylaminoboranen **2a-f** in 30 bis 90% Ausbeuten. In keinem der Fälle werden Disubstitutionen beobachtet. Die starke Säure CF_3SO_3H reagiert mit $(CH_3)_3NBH_3$ bei 20°C zu $(CH_3)_3NBH_2OSO_2CF_3$ (**3**) und mit 2 mol Säure bei 80°C zu $(CH_3)_3NBH(OSO_2CF_3)_2$ (**6**). Durch Reaktion von $(CH_3)_3NBH_2I$ mit $Hg(ECF_3)_2$ in Benzol bei 20°C entstehen $(CH_3)_3NBH_2ECF_3$ (E = S, **4**; E = Se, **5**). IR-, ^1H-, ^{19}F-, ^{11}B- und ^{77}Se-NMR-Daten werden angegeben.

Als Parahalogen hoher Ableitung[1] weist Tetrakis(trifluormethylthio) pyrrol (**1a**) ein acides Wasserstoffatom auf, das durch metallische und nichtmetallische Kationen, wie z.B. Na, K, Ag, Cu, 1/2 Hg oder NH_4, R_4M (M = N, As, Sb) und andere Oniumverbindungen, ersetzt werden kann. Zusätzlich vermag es infolge seiner halogenähnlichen Eigenschaften in z.B. MX_3[2] (M = P, As, Sb, X = Cl, Br, I) Halogene zu ersetzen. Die Substitutionen am Stickstoff in **1a** erfolgten am besten über das mesomeriefähige Anion. Aus diesem Grunde setzt man für Halogenaustauschreaktionen Elementhalogenide und das Ag- bzw. K-Salz von **1a** bevorzugt ein. Substitutionen mit Bortrihalogeniden sind bisher jedoch nicht gelungen. Im Gegensatz dazu gelingt die Bor-Funktionalisierung durch Umsetzungen von $(CH_3)_3NBH_3$ mit **1** gemäß :

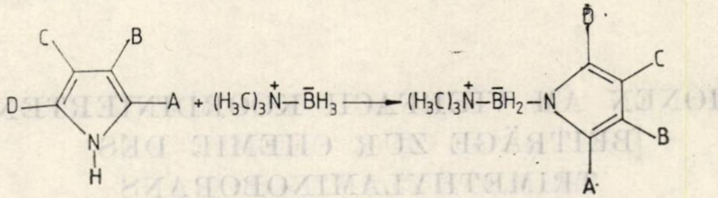
C
B
D
A
N
H
$(H_3C)_3\overset{+}{N}-\overline{B}H_3$
$(H_3C)_3\overset{+}{N}-\overline{B}H_2-N$
D
C
B
A

1 **2** (1)

1	A	B	C	D	2
a	CF_3S	CF_3S	CF_3S	CF_3S	a
b	CF_3S	CF_3S	H	CF_3S	b
c	CF_3S	CF_3S	CF_3S	H	c
d	CF_3S	H	H	CF_3S	d
e	CF_3S	H	CF_3S	H	e
f	H	H	H	H	f

Die in Gl. (1) aufgeführten Reaktionen liefen nennenswerte Ausbeuten erst oberhalb 80°C. Am Beispiel von **2a** konnte gezeigt werden, daß eine Temperatursteigerung von 80°C (Benzol), 113°C (Toluol) auf 160°C (ohne Lösungsmittel, Cariusrohr) zu einer Ausbeutenerhöhung von 46, 60 bis 65 auf 80% führt. Gleichzeitig nimmt die Reaktionsdauer in der Reihenfolge 14, 5 und 2 d ab. Auch mit abnehmender CF_3S-Substitution ist eine Reaktivitätsminderung von **1a** nach **1f** zu beobachten, so daß Pyrrol nur ohne Lösungsmittel bei 160°C mit $(CH_3)_3NBH_3$ zu **2f** reagiert. Offensichtlich wird die Reaktivität von **1** stärker durch die Acidität des NH-Wasserstoffs als durch sterische Effekte bestimmt.

Es konnte festgestellt werden, daß der am Stickstoff gebundene Wasserstoff für Substitution durch den $(CH_3)_3NBH_2$-Rest durch Substituenten am $\alpha-C$ stärker als solche am $\beta-C$ aktiviert wird. Die zunehmende Reaktivität des Substrats mit steigender Acidität konnte eindrucksvoll durch Umsetzungen von $(CH_3)_3NBH_3$ mit CF_3SO_3H aufgezeigt werden. Setzt man $(CH_3)_3NBH_3$ mit CF_3SO_3H im Molverhältnis 1 : 1 bei 20°C (3 bis 4 h) in Benzol um, so erhält man nach weiterem Rühren bei 20°C (3 d) nahezu quantitativ Trimethylamin (trifluormethylsulfonato) boran (**3**). Die geringe Acidität der instabilen Substanzen CF_3SH und CF_3SeH ist vermutlich Ursache für ihr inertes Verhalten gegenüber $(CH_3)_3NBH_3$. Die gewünschten Verbindungen Trimethylamin — (trifluormethylthio)-boran (**4**) und Trimethylamin — (trifluormethylseleno) boran (**5**) lassen sich jedoch aus $(CH_3)_3NBH_2I$ und $Hg(SeCF_3)_2$ synthetisieren, gemäß :

$$
(CH_3)_3NBH_2I \begin{array}{l} + Hg(SCF_3)_2 \rightarrow \underset{\mathbf{4}}{(CH_3)_3NBH_2SCF_3} \\ + Hg(SeCF_3)_2 \rightarrow \underset{\mathbf{5}}{(CH_3)_3NBH_2SeCF_3} \end{array} + HgI_2
$$

Das mäßig hydrolyseempfindliche **4** ist gegenüber dem sehr feuchtigkeitsempfindlichen **5** auch thermisch stabiler. Während **4** bei 20°C wochenlang stabil ist, zersetzt sich **5** bei −20°C langsam und bei 0°C rasch. Nur in benzolischer Lösung ist **5** einige Zeit haltbar. Zur Vermeidung von Nebenreaktionen und Zersetzung müssen bei der Synthese von **4** und **5** die angegebenen Reaktionszeiten streng eingehalten werden. Die ^{19}F−NMR-spektroskopisch verfolgte Zersetzung von **5** in Benzol bei 20°C (30 d) führt zu etwa 30 % $(CH_3)_3NBHF_2$ und 70 %$(CH_3)_3NBF_3$. Daneben lassen sich F_2CSe-Oligomere, $CF_3SeSeCF_3$ und ein Signal bei −150.6 ppm, das nicht zugeordnet werden konnte, identifizieren.

Eine Disubstitution des $(CH_3)_3NBH_3$ gelingt lediglich mit der sehr starken Säure CF_3SO_3H. Setzt man beide Partner im Molverhältnis 1 : 2 in Benzol um, so erfolgt bei 20°C starke H_2-Entwicklung. Zur Vervollständigung der Reaktion wird bei 80°C (3 d) gerührt. Das wenig hydrolyseempfindliche Trimethylamin-bis(trifluormethylsulfonato)boran (**6**) ist stabil und bildet sich nahezu quantitativ.

NMR-SPEKTROSKOPISCHE UNTERSUCHUNGEN

Die ^{1}H−NMR-Spektren der untersuchten Verbindungen **1** bis **6** weisen für die $(CH_3)_3N$-Gruppe δ als lösungsmittel- und konzentrationsabhängiges Singulett im Bereich von 1.4 bis 2.7 ppm auf. Die aromatischen Wasserstoffe in **2b**−**f** zeigen Verschiebungen und Kopplungen, die denen der Ausgangsverbindunge **1b**−**f** ähneln. Signale der am Bor gebundenen Wasserstoffe wurden nicht gemessen, da sie durch die Quadrupolmomente von ^{10}B und ^{11}B eine Verbreiterung von bis zu 8 ppm erfahren und somit keine analytische Bedeutung aufweisen. Die ^{19}F−NMR-Spektren von **1a**−**e** weisen δ zwischen −42 und und −46 ppm auf, wobei die am α-C-Atom gebundenen gegenüber den am β-C-Atom gebundenen CF_3S-Gruppen eine Verschiebung nach tieferem Feld von bis zu einem ppm aufweisen.

Für die Substanzen **3** und **6** liegt δ in dem für CF_3SO_2-Verbindungen zu erwartenden Bereich von etwa −70 bis −80 [3] ppm. In den zu erwartenden Bereichen von −31.5 bis −35.8 [2] bzw. −25.9 bis −31.4 [5] tritt das Signal von **4** bzw. **5** auf. In den ^{11}B-NMR-Spektren von **2a**−**c** und **2e** bzw. **3** werden $\delta(^{11}B)$ in Form von breiten Singuletts im Bereich von −2.31 bis −4.2 bzw. +3.46 pp. beobachtet. Lediglich **2d** weist ein breites nichtaufgelöstes Triplett bei 4.7 ppm auf. Gut Aufgelöste Tripletts mit einer Kopplungskonstante $J(B-H) = 107$ bis 142 Hz treten in den ^{11}B-NMR-Spektren von **2f**, **4**, **5** und **6** auf. Die Absorptionsbereiche liegen zwischen +0.09 und −4.26 ppm. Eine Erklärung für dieses unterschiedliche Verhtalen kann nicht gegeben werden. Das ^{77}Se-NMR-Spektrum von **5** weist δ bei 251.6 ppm auf. Die sich hierfür aus der Gleichung

$$\delta(^{77}Se) = 829.8 . EN - 1549^{6}$$

ergebende Elektronegativität (EN) des $(CH_3)_3NBH_2$-Restes beträgt 2.17.

BESCHREIBUNG DER VERSUCHE

IR-Spektren: Feststoffe als KBr-Preßlinge; Flüssigkeiten als Kapillarfilm zwischen KBr-Platten; Gase in einer 10 cm Gasküvette mit KBr-Platten. Gitterspektrophotometer Perkin-Elmer 325. Schwache Banden und Schultern werden nicht aufgeführt.

NMR-Spektren: Bruker WM 250 FT und Bruker HX 60/5-Spektrometer (^{19}F), interne Locksubstanz C_6D_6, ^1H-NMR: Interner Standard: $Si(CH_3)_4$; ^{19}F-NMR: C_6F_6, Werte auf $CFCl_3$ umgerechnet; ^{11}B-NMR: Äußerer Standard: $BF_3 \cdot C_2H_5OC_2H_5$, ^{77}Se-NMR: Äußerer Standard: CH_3SeCH_3. Massenspektren: Varian MAT CH5 und CH7, 70 eV, Emission 100 µA. Es werden nur M^+ aufgeführt.

Trimethylamin-(tetrakis(trifluormethylthio)pyrrol-1-yl)-boran (2a)

a) *Offenes System*

In einem 100-ml-Rundkolben, versehen mit Magnetrührstab, Rückflußkühler und $CaCl_2$-Trockenrohr, wird eine Lösung von 1 g (13.7 mmol) $(CH_3)_3NBH_3$ in 50 ml Benzol mit 3 g (6.4 mmol) **1a** versetzt. Man erhitzt unter Rühren im Rückfluß und kontrolliert alle 24 h den Reaktionsfortschritt durch Aufnahme von IR- und ^{19}F-NMR-Spektren. Alle 48 h werden weitere 0.5 g (6.9 mmol) $(CH_3)_3NBH_3$ zugegeben, um so absublimiertes Edukt zu ersetzen.

Nach 10 Tagen wird das Lösungsmittel abdestilliert, das Produkt bei 130°C i. Vak. sublimiert. Überschüssiges $(CH_3)_3NBH_3$ wird hierbei quantitativ abgetrennt. Letzte Spuren an **1a** können mit einer Hg-Diffusionspumpe bei 20°C entfernt werden. **2a** stellt einen farb- und geruchlosen, kristallinen Festkörper dar. Ausbeute: 1.6 g (46.3% d.Th., bezogen auf **1a**).

Wird Benzol durch Toluol ersetzt, läßt sich eine Ausbeutesteigerung auf 60 bis 65% d. Th. bei einer Reaktionsdauer von 5 Tagen erzielen. Die höhere Reaktionstemperatur (113°C) führt jedoch dazu, daß absublimiertes **1a** alle 12 Stunden nachgefüllt werden muß.

b) *Geschlossenes System*

Eine 110-ml-Glasbombe mit Hülse NS 14.5 wird nach Ausheizen unter Argon mit 7 g (15 mmol) **1a** und 1.1 g (15.1 mmol) $(CH_3)_3NBH_3$ beschickt. Die Vorlage wird an einer Vakuumlinie unter Kühlen mit flüssigem Stickstoff evakuiert und abgeschmolzen. Man läßt auf 20°C aufwärmen und tempert in einem Röhrenofen bei 160°C (48 h). Das farblose Reaktionsprodukt wird mit 100 ml Ether aus der Bombe gespült und nach Abziehen des Lösungsmittels i. Vak. sublimiert (s.o.).

Vorsicht! Bei beschriebenem Ansatz entsteht ein H_2-Druck von ca. 3 Atmosphären. Daher sind beim Öffnen der Bombe entsprechende Vorsichtsmaßnahmen zu treffen.

Ausbeute: 7.08 g (87.8% d. Th.). Schmp.: 71.5 bis 72°C.

$C_{11}H_{11}BF_{12}N_2S_4$ (538.3) Ber.: C 24.6 H 2.1 N 5.2 S 23.8
Gef.: C 24.5 H 2.1 N 5.1 S 23.8

^1H-NMR: $\delta = 1.45$ (s, 9H) in Benzol, 2.57 (s, 9H) in $CDCl_3$.
^{19}F-NMR: $\delta = -42.45$ (m, 6F), -42.98 (m, 6F).
^{11}B-NMR: $\delta = -3.73$ (s, br, B).
IR: 2519 (m), 2483 (m), 1484 (m), 1465 (m), 1451 (m), 1394 (m), 1198 (m), 1110 (vs), 1070 (vs), 980 (s), 832 (s), 752 (s), 730 (m), 702 (m), 665 (m), 470 (m) cm^{-1}.
MS: 538 (8) M^+.

Thermolyse von 2a

300 mg (0.55 mmol) **2a** werden 4 Tage bei 100°C auf einem offenen Uhrglas im Trockenschrank getempert.

IR-, ^{11}B-, ^{19}R-, ^1H-NMR-Spektren zeigen nur reines Ausgangsprodukt.

Trimethylamin-(2,3,5-tris(trifluormethylthio)pyrrol-1-yl)-boran 2b

3.44 g (9.4 mmol) **1b** werden mit 1.2 g (16.5 mmol) $(CH_3)_3NBH_3$ in einer Glasbombe analog zur Darstellung von **2a** bei 160°C (16 h) umgesetzt. Bei der Sublimation (90°C i. Vak.) fällt **2b** als farbloser, kristalliner Feststoff an.

Ausbeute: 3.82 g (92.9% d. Th.). Schmp.: 83.5 bis 84°C.

$C_{10}H_{12}BF_9N_2S_3$ (438.2) Ber.: C 27.4 H 2.8 N 6.4 S 22.0
Gef.: C 27.4 H 2.8 N 6.4 S 22.0

^1H-NMR: $\delta = 1.57$ (s, 9H) in Benzol, 2.73 (s, 9H) in C_6F_6;
$\delta = 7.00$ (s, 1H).
^{19}F-NMR: $\delta = -43.22$ (m, 3F), -43.89 (s, 3F), -44.09 (m, 3F).
^{11}B-NMR: $\delta = -4.3$ (s, br, ^{11}B).

IR : 2482 (m), 2456 (m), 1488 (s), 1467 (m), 1450 (m), 1389 (m), 1282 (m), 1254 (m), 1248 (m), 1201 (vs), 1159 (vs), 1130 (vs), 1107 (vs), 1068 (vs), 837 (s), 754 (s), 656 (m), 460 (m) cm^{-1}.
MS : 438 (15) M^+.

Trimethylamin-(2,3,4 tris(trifluormethylthio)pyrrol-1-yl)-boran 2c

In einem 100-ml-Rundkolben, ausgestattet mit Magnetrührstab, Rückflußkühler und Trockenrohr ($CaCl_2$), werden 3.35 g (9.1 mmol) **1c** und 1 g (13.7 mmol) $(CH_3)_3NBH_3$ in 25 ml Toluol gelöst. Die Reaktionsmischung wird im Rückfluß erhitzt und alle 48 h IR-spektroskopisch kontrolliert. Verdunstetes Toluol und $(CH_3)_3NBH_3$ wird nach Bedarf ersetzt (insgesamt ca. 10 ml Toluol und 1 g $(CH_3)_3NBH_3$). Nach 10 Tagen wird das Lösungsmittel i. Vak. abdestilliert, nicht umgesetztes **1c** und $(CH_3)_3NBH_3$ i. Vak. bei 20°C abdestilliert. Bei Erhöhung der Badtemperatur auf 90°C sublimiert farb-und geruchloses **2c**.
Ausbeute : 1.26 g (31.3 % d. Th.). Schmp. : 84°C.
$C_{10}H_{12}BF_9N_2S_3$ (438.2) Ber. : C 27.4 H 2.8 N 6.4 S 22.0
Gef. : C 27.4 H 2.8 N 6.4 S 21.7
^1H-NMR : $\delta = 2.52$ (s, 9H), $\delta = 7.46$ (s, 1H) in $CDCl_3$.
^{19}F-NMR : $\delta = -42.99$ (m, 3F), -43.47 (m, 3F), -44.53 (m, 3F).
^{11}B-NMR : $\delta = -2.31$ (s, br. ^{11}B).
IR : 2492 (m), 2442 (m), 1488 (s), 1471 (m), 1453 (m), 1427 (m), 1250 (m), 1204 (m), 1196 (s), 1068 (vs), 1068 (vs), 1031 (m), 982 (m), 839 (s), 753 (m), 737 (m), 702 (m), 478 (m) cm^{-1}.
MS : 438 (30) M^+.

Trimethylamin-(2,5-bis(trifluormethylthio)pyrrol-1-yl)-boran 2d

Eine Lösung von 5 g (18.7 mmol) **1d** und 2.05 g (28.2 mmol) $(CH_3)_3NBH_3$ in 25 ml Toluol werden in einem 50-ml-Rundkolben mit Magnetrührstab vorgelegt. Man verschließt mit einem Rückflußkühler ($CaCl_2$-Trockenrohr) und erhitzt zum Sieden. Alle 24 h wird IR-spektroskopisch der Fortschritt der Reaktion überprüft. Nach 7 Tagen filtriert man die Lösung und engt auf die Hälfte des Volumens ein. Durch Zugabe von 100 ml n-Pentan fällt das gewünschte Product aus. Zur Reinigung wird aus Ether/Hexan umkristallisiert.
Ausbeute : 2.03 g (32.1 %d. Th.). Schmp. : 131°C.
$C_9H_{13}BF_6N_2S_2$ (338.2) Ber. : C 32.0 H 3.9 N 8.3 S 19.0
Gef. : C 32.0 H 3.9 N 8.3 S 19.1
^1H-NMR : $\delta = 2.72$ (s, 9H), $\delta = 6.60$ (s, 2H) in C_6F_6.
^{19}F-NMR : $\delta = -44.83$ (s, 6F) in C_6F_6.
^{11}B-NMR : $\delta = -4.7$ (t, br, ^{11}B).
IR : 2455 (m), 1485 (m), 1467 (m), 1367 (m), 1253 (m), 1245 (m), 1161 (vs), 1152 (vs), 1130 (vs), 1118 (vs), 1104 (vs), 983 (m), 831 (s), 773 (s) cm^{-1}.
MS : 338 (18) M^+.

Trimethylamin-(2,4-bis(trifluormethylthio)pyrrol-1-yl)-boran 2e

Analog zu **2d** werden 10 g (37.5 mmol) **1e** mit 4.1 g (56.3 mmol) $(CH_3)_3NBH_3$ in 25 ml Toluol umgesetzt. Nach 11 Tagen wird überschüssiges **1e** und Lösungsmittel i. Vak. abdestilliert. Das zurückbleibende bräunliche Öl wird durch Kurzwegdestillation bei 80°C i Vak. gereinigt. Beim Erkalten verfestigt sich **2 d** zu einem farblosen Festkörper. Bei 20°C verfärbt sich die Substanz beim Aufbewahren und wird ölig.
Ausbeute : 5.77 g (45.6 % d. Th.). Schmp. : 41 bis 42°C.
$C_9H_{13}BF_6N_2S_2$ (338.2) Ber. : C 32.0 H 3.9 N 8.3 S 19.0
Gef. : C 32.0 H 3.8 N 8.2 S 19.0
^1H-NMR : $\delta = 2.48$ (s, 9H), $\delta = 7.27$ (d, 1H), $\delta = 6.86$ (d, 1H) in $CDCl_3$; J (3H, 5H) = 1.8Hz.
^{19}F-NMR : $\delta = -44.78$ (m, 3F), $\delta = -45.45$ (m, 3F).
^{11}B-NMR : $\delta = -2.62$ (s, br, ^{11}B).
IR : 1487 (s), 1467 (m), 1451 (m), 1432 (m), 1198 (s), 1080 (s), 1058 (s), 985 (m, br), 834 (s), 752 (m) cm^{-1}.
MS : 338 (31) M^+.

Trimethylamin-(pyrrol-1-yl)boran **2f**

Wie bei **2a** angegeben wird eine 110-ml-Glasbombe mit 670 mg (10 mmol) Pyrrol und 730 mg (10 mmol) $(CH_3)_3NBH_3$ beschickt und bei 160°C (72 h) im Röhrenofen getempert. Das Reaktionsprodukt wird in Ether augenommen, filtriert und and der Vakuumlinie bei 20°C vom Lösungsmittel befreit. Bei der Sublimation (80°C Badtemperatur) scheiden sich schön ausgebildete, farblose Kristalle ab. Ausbeute : 960 mg (70 % d. Th.). Schmp. : 67°C.

$C_7H_{15}BN_2$ (138.0) Ber. : C 60.9 H 11.0 N 20.3
Gef : C 61.4 H 10.4 N 20.2

^{1}H-NMR : $\delta = 1.78$ (s, 9H), $\delta = 6.40$ (t, 2H), $\delta = 6.82$ (t, 2H) ;
J(2H, 3H) = J (2H, 4H) = 1.8 Hz.

^{11}B-NMR : $\delta = +0.09$ (t, ^{11}B) ; HJ (B, H) = 107 Hz.

IR : 2423 (m), 2358 (m), 1464 (m), 1257 (m), 1250 (m), 1241 (m), 1230 (s), 1189 (m), 1162 (s), 1102 (m), 1078 (m), 1068 (m), 990(m), 981 (m), 832 (s), 745 (s), 700 (m), 679(m) cm^{-1}.

MS : 138 (10) M$^-$.

Trimethylamin-(trifluormethylsulfonato)boran **3**

In einen gut ausgeheizten 100-ml-Schlenkkolben, ausgestattet mit Magnetrührstab und Rückflußkühler ($CaCl_2$-Trockenrohr), werden 4 g (54.9 mmol) $(CH_3)_3NBH_3$ in 50 ml Benzol vorgelegt. Hierzu gibt man im Argongegestrom unter starken Rühren tropfenweise 4 g (26.7 mmol) Trifluormethansulfonsäure. Die zunächst starke Gasentwicklung (H_2) geht nach 3 bis 4 h merklich zurück. Man läßt die Lösung weitere 3 Tage bei 20°C rühren, trennt dann Benzol und nicht umgesetztes $(CH_3)_3NBH_3$ i. Vak. ab. Zurück bleibt eine farblose, bei 50°C i. Vak. nicht kondensierbare Flüssigkeit.

Ausbeute : 5.61 g (95.2 % d. Th.) Sdp.$_{10}$: $\simeq$ 144°C.

$C_4H_{11}BF_3NO_3S$ (221.0) Ber. : C 21.7 H 5.0 N 6.3 S 14.5
Gef. : C 21.7 H 4.7 N 6.3 S 14.5

^{1}H-NMR : $\delta = 2.63$ (s, 9H).

^{19}F-NMR : $\delta = -77.4$ (s, 3F).

^{11}B-NMR : $\delta = +3.46$ (s, br. ^{11}B).

IR : 3018 (m), 2961 (m), 2476 (s, br), 1488 (s), 1470 (s), 1455 (m), 1411 (m), 1373 (s, br), 1255 (s), 1245 (s), 1198 (s, br), 1181 (s, br), 1143 (s), 1108 (m), 1031 (s), 995 (s, br), 956 (s, br), 850 (s), 784 (m), 753 (m), 620 (s, br), 572 (m), 518 (m), 464 (m) cm^{-1}.

MS: 221 (11) M$^+$,

Trimethylamin-(trifluormethylthio)boran **4**

Eine Lösung von 7.44 g (37.3 mmol) $(CH_3)_3NBH_2I$ in 150 ml Benzol wird unter Argon in einem gut ausgeheizten 500-ml-Runkolben mit Schwanzhahn und Magnetrührstab hergestellt. Unter starkem Rühren werden 7.5 g (18.6 mmol) Bis (trifluormethylthio) quecksilber portionsweise zugegeben. Die farblose, klare Lösung trübt sich unter Bildung eines indischgelben Festkörpers dessen Farbe sich nach ca. 30 Sekunden schlargartig nach dunkelrot verändert. Man rührt für weitere 2 h, trennt dann durch eine Umkehrfritte vom Unlöslichen ab. Das Filtrat eine weitere Stunde nachgerührt und nochmals abgefrittet Benzol und flüchtige Nebenprodukte werden innerhalb von 48 h bei 20°C an einer Vakuumaparatur abdestilliert. **4** stellt eine gelbliche leicht bewegliche Flüssigkeit von unangenehmen Geruch dar, die bei 20°C unter Luftausschluß wochenlang beständig ist.

Ausbeute : 1.71 g (26.5 % d. Th.).

$C_4H_{11}BF_3NS$ (173.0) Ber. : C 27.8 H 6.4 N 8.1
Gef. : C 27.8 H 5.7 N 7.6

^{1}H-NMR : $\delta = 1.85$ (s, 9H).

^{19}F-NMR : $\delta = -32.7$ (s, 3F)

^{11}B-NMR : $\delta = -4.07$ (t, ^{11}B) ; J (B, H) = 119 Hz.

IR : 3010 (m), 2955 (m), 2460 (s), 2415 (s), 1486 (s), 1466 (s), 1450 (m), 1407 (m), 1252 (m), 1245 (m), 1144 (vs), 1101 (vs), 1068 (vs), 970 (m), 840 (s), 750 (m) cm^{-1}.

MS : 173 (13) M$^+$.

Trimethylamin-(trifluormethylseleno)boran **5**

Wie bei **4** angegeben werden 6 g (30.2 mmol) $(CH_3)_3NBH_2J$ mit 7.5 g (15.1 mmol) Hg $(SeCF_3)_2$ umgesetzt. Nach 1 h trennt man ausgefallenes HgJ_2 ab, rührt 30 Min. nach und frittet nochmals. Das Lösungsmittel wird i. Vak so schnel wie möglich abdestilliert. Das farblose Produkt zersetzt sich bei Temperaturen oberhalb $-20°C$ unter Verfärbung langsam, bei 20°C schnell, während in verdünnter benzolischer Lösung der Zerfall nur langsam unter Ausscheidung von gelblichem $(F_2CSe)_n$ erfolgt. **5** ist eine sehr unangenehm riechende, extrem hydrolyseempfindliche Substanz.

Ausbeute : 2.6 g (39.1 % d. Th.).
$C_4H_{11}BF_3BSe$ (219.8)
^{1}H-NMR : $\delta = 2.03$ (s, 9H).
^{19}F-NMR : $\delta = -27.99$ (s, 3F).
^{11}B-NMR : $\delta = -4.26$ (t, ^{11}B) ; H(B, H) = 122 Hz.
^{77}Se-NMR : $\delta = 251.6$ (s, ^{11}Se).
IR : 3010 (m), 2955 (m), 2472 (m), 2419(m), 1486 (s), 1464 (s), 1450 (m), 1408 (m), 1254 (m), 1247 (m), 1157 (m), 1131 (s), 1095 (vs), 1053 (vs), 1013 (m), 980(m), 842 (s), 733 (m), 686 (m) cm^{-1}.
MS : 221 (4) M^+.

Thermolyse von 5

Tempert man **5** 30 Tage bei 20°C im Dunklen, lassen sich als einzige borhaltige Produkte ca. 30 % $(CH_3)_3NBHF_2$ und 70 % $(CH_3)_3NBF_3$ nachweisen. Im ^{11}F-NMR-Spektrum findet man $CF_3SeSeCF_3$ und CF_2Se-Polymeres.

Trimethylamin-bis(trifluormethylsulfonato)boran 6

In einem 100-ml-Schlenkkolben, ausgestattet mit Magnetrührstab und Rückflußkühler ($CaCl_2$-Trockenrohr), werden unter Argon 2 g (27.5 mmol) $(CH_3)_3NBH_3$ und 50 ml Benzol vorgelegt. Unter starkem Rühren werden 8.24 g (55.0 mmol) Trifluormethansulfonsäure zugetropft. Nach Abklingen der zunächst starken H_2-Entwicklung erhitzt man mit einem Ölbad 3 Tage im Rückfluß. Das Lösungsmittel wird abdestilliert, zurück bleibt ein gelber Feststoff. Durch Sublimation bei 80°C i. Vak. erhält man farbloses, nur wenig hydrolyseempfindliches **6**.

Ausbeute : 9.68 g (95.5 % d. Th.). Schmp. : 75.5 bis 77°C.
$C_5H_{10}BF_6NO_6S_2$ (369.1) Ber. : C 16.3 H 2.7 N 3.8
Gef. : C 16.3 H 2.7 N 3.7
^{1}H-NMR : $\delta = 1.73$ (s, 9H).
^{19}F-NMR : $\delta = -76.78$ (s, 3F).
^{11}B-NMR : $\delta = +1.91$ (d, ^{11}B) ; J (B, H) = 142 Hz.
IR : 1493 (m), 1256 (s), 1200 (vs, br), 1162 (s), 1138 (s), 1125 (s), 1111 (m), 1098 (m), 1020 (s), 979 (m), 938 (m, br), 860 (m), 586 (m), 500 (m, br) cm^{-1}.
MS : 369 (0.2)M^+.

LITERATUR

[1] A. Haas, "The Element Displacement Principle : A New Guide in p-Block Element Chemistry", *Adv. Inorg. Chem. Radiochem.*, **28**, 167 (1984).
[2] A. Haas und F. Weiss, *Z. anorg. allg. Chem.*, **518**, 234 (1984).
[3] A. Haas, "Perfluorhalogenorgano-Verbindungen der Hauptgruppen-elemente, Band 12, Teil III" in Gmelins Handbuch der Anorganischen Chemie, Verlag Chemie, Weinheim 1973.
[4] M. Häberlein, Dissertation Bochum, 1975.
[5] B. Koch, Dissertation Bochum, 1975.
[6] W. Gombler, *Z. Naturforsch.*, **36b**, 535 (1981).

Revue Roumaine de Chimie, 31, *11—12*, 935—942 (1986)

Professor P. SPACU zum 80. Geburtstag gewidmet.

ÜBER REAKTIONEN DES TETRAFLUOR-1,2-ETHANDISULFENYLDICHLORIDS MIT ALKINEN UND KETONEN

HERBERT W. ROESKY und NASREDDINE BENMOHAMED

Institut für Anorganische Chemie der Universität Göttingen, Tammannstraße 4, D-3400 Göttingen

Eingegangen am 8. Mai 1986

The reaction between C_2F_4 with elemental sulfur yields $C_2F_4S_3$ (**1**) and $C_2F_4S_4$ (**2**). Both compounds react with chlorine yielding $ClS-CF_2-CF_2-SCl$ (**3**). This bis-sulfene-chloride reacts with acetylene or phenylacetylene affording the six-membered compounds **4** and **5**, respectively. Ketones $R-CH_2CO-CH_3$ ($R=H$, CH_3, C_2H_5, Cl) react with **3** giving the five membered rings **6a-d**. From acetylacetone and **3** one obtains **7**. Cycloalkanones with 5, 6 or 7-membered rings react with **3** at the α-CH_2 group giving spiro-compounds **8**—**10**, respectively. All compounds were characterized by ^1H—, ^{13}F—, ^{13}C-NMR, mass spectra and elemental analyses.

Die Reaktion von C_2F_4 mit elementarem Schwefel führt zu $C_2F_4S_{3,4}$ **1** und **2**. Diese Verbindungen reagieren mit elementarem Chlor zu $ClSCF_2CF_2SCl$ **3**. Das Bissulfensäurechlorid **3** kann man mit $HC\equiv CH$ und $PhC\equiv CH$ unter HCl-Abspaltung zu den sechsgliedrigen Ringen **4** und **5** umsetzen. Die Ketone $R-CH_2-CO-CH_3$ ($R=H$, CH_3, C_2H_5, Cl) reagieren mit **3** zu den fünfgliedrigen Ringen **6a-d**. Aus Acetylaceton und **3** gewinnt man **7**. Cyclopentanon, -hexanon und -oktanon reagieren mit **3** in Nachbarstellung zur Ketogruppe mit einer Methylengruppe unter Bildung der Spirocyclen **8**, und **10**. Die Verbindungen werden durch ^1H-, ^{19}F-, ^{13}C-NMR, Massenspektren und Elementaranalysen charakterisiert.

EINLEITUNG

Nach Krespan und Brasen [1,2] reagiert Tetrafluorethen mit elementarem Schwefel bei 445°C zu Tetrafluor-1,2,3-trithiolan **1** und Tetrafluor-1,2,3,4-tetrathian **2**:

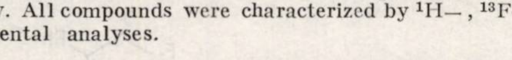

1 2

Das Rohprodukt aus **1** und **2** wird mit überschüssigem Chlor umgesetzt, dabei entstehen nahezu quantitativ $ClSCF_2CF_2SCl$ **3** und SCl_2, die sich leicht durch Destillation trennen lassen.

Kürzlich haben wir zeigen können, daß **3** mit funktionellen Stickstoffbasen zu interessanten Heterocyclen führt.[3]

In diesem Beitrag berichten wir über Reaktionen von **3** mit Alkinen und Ketonen.

SYNTHESEN

$ClSCF_2CF_2SCl$ **3** reagiert mit Ethin in Gegenwart von Aluminiumtrichlorid unter HCl-Eliminierung in geringer Ausbeute zum sechsgliedrigen Heterocyclus **4**

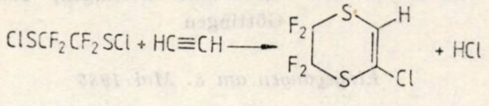

$ClSCF_2CF_2SCl + HC\equiv CH$
F_2
S
H
F_2
S
Cl
+ HCl

4

Dabei wird ein Chloratom vom Schwefel auf den Kohlenstoff übertragen. **4** ist eine gelbe Flüssigkeit, die bei 30°C und 0,05 Torr siedet. Ähnlich verhält sich $PhC\equiv CH$, jedoch ist für diese Reaktion kein Katalysator erforderlich und die Ausbeute von **5** liegt bei 40 Prozent.

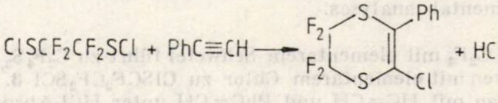

$ClSCF_2CF_2SCl + PhC\equiv CH$
F_2
S
Ph
F_2
S
Cl
+ HCl

5

Die Reaktionen, die zu **4** und **5** führen, haben gemeinsam, daß zur HCl-Abspaltung keine Base erforderlich ist.

Acyclische Ketone der Zusammensetzung 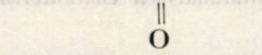 $R-CH_2-\underset{\underset{O}{\|}}{C}-CH_3$ reagieren mit $ClSCF_2CF_2SCl$ exotherm, dabei erfolgt die Substitution nur an einem Kohlenstoffatom in Nachbarstellung zur Ketogruppe. Man erhält die fünfgliedrigen Heterocyclen **6**.

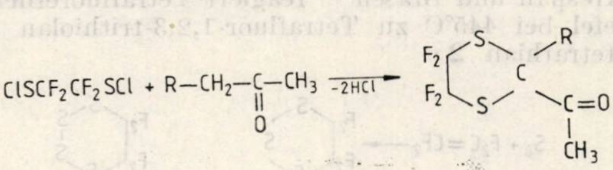

$ClSCF_2CF_2SCl + R-CH_2-C(=O)-CH_3$
-2HCl
F_2
S
R
C
F_2
S
C=O
CH_3

6

6a R = H
6b R = CH_3
6c R = C_2H_5
6d R = Cl

Die fünfgliedrigen Ringe **6a–d** entstehen in guten Ausbeuten. Es sind gelbgefärbte Flüssigkeiten. Im Reaktionsablauf von **6** spielt die Stabilität des Carbanions und die damit verbundene leicht Deprotonierung eine wesentliche Rolle.

Bei den Reaktionen von Ketonen mit $ClSCF_2CF_2SCl$ wurde die Bildung siebengliedriger Ringe nicht beobachtet. Ein Grund dafür dürfte die hohe Stabilität der fünfgliedrigen Heterocyclen sein

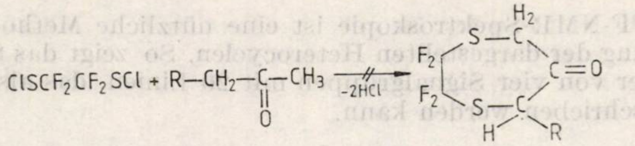
ClSCF2CF2SCl + R–CH2–C–CH3
O
-2HCl
F2
F2
S
S
H2
C
C=O
C
H
R

Acetylaceton und $ClSCF_2CF_2SCl$ ergeben ebenfalls einen fünfgliedrigen Kohlenstoff-Schwefel Ring **7** unter Abspaltung von zwei Molekülen Chlorwasserstoff.

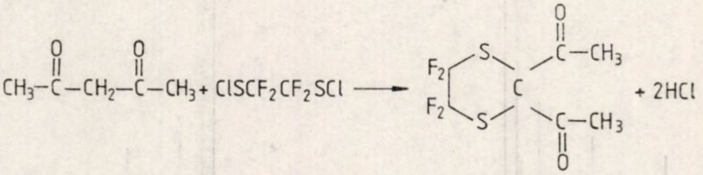
O
O
CH3–C–CH2–C–CH3 + ClSCF2CF2SCl
F2
F2
S
S
C
C–CH3
C–CH3
O
O
+ 2HCl

7

Die cyclischen Ketone, Cyclopentanon, -hexanon und -octanon, führen zu den Spirocyclen **8–10**.

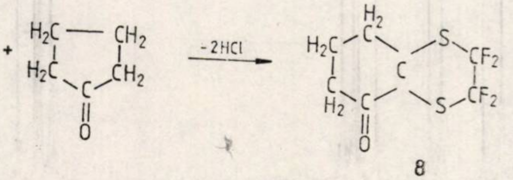
+
H2C
CH2
H2C
CH2
C
O
-2HCl
H2
H2C
C
C
S
CF2
CF2
S
H2
C
O

8

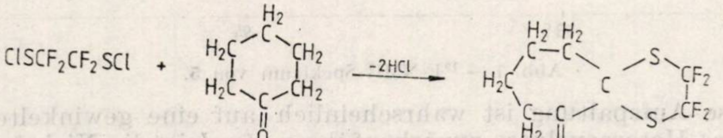
ClSCF2CF2SCl
+
H2
H2C
CH2
H2C
CH2
O
-2HCl
H2 H2
H2C
C
S
CF2
CF2
H2
O

9

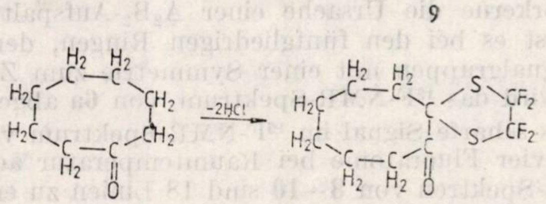
H2 H2
H2C
CH2
H2C
CH2
H2
O
-2HCl
H2 H2
H2C
S
CF2
H2C
S
CF2
H2 H2
O

10

Bei diesen Reaktionen werden stets die Wasserstoffatome an einem Kohlenstoffatom in Nachbarstellung zur Ketogruppe substituiert. Die Ausbeuten der Verbindungen **8**–**10** sind nahezu quantitativ. Die Titelverbindung ist ein vielseitiges Reagenz für die Darstellung von Heterocyclen.

NMR-UNTERSUCHUNGEN

Die ^{19}F-NMR-Spektroskopie ist eine nützliche Methode zur Strukturaufklärung der dargestellten Heterocyclen. So zeigt das Spektrum von **5** ein Muster von vier Signalgruppen mit 20 Linien, das als ein AA'XX'-System beschrieben werden kann.

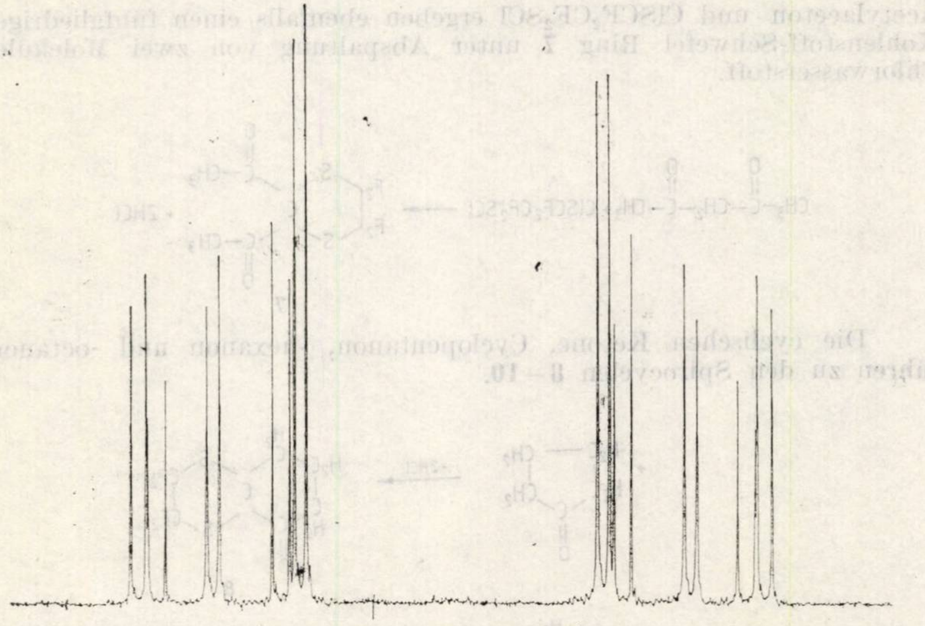

Abb. 1 — ^{19}F-NMR-Spektrum von **5**.

Diese Aufspaltung ist wahrscheinlich auf eine gewinkelte Konformation des Heterocycluses zurückzuführen. In **4** ist die Nichtäquivalenz der Fluorkerne die Ursache einer A_2B_2-Aufspaltung im ^{19}F-Spektrum. Anders ist es bei den fünfgliedrigen Ringen, deren ^{19}F-NMR-Spektren drei Signalgruppen mit einer Symmetrie zum Zentrum zeigen. In der Abb. 2 wird das ^{19}F-NMR-Spektrum von **6a** abgebildet.

Das scharfe Signal im ^{19}F-NMR-Spektrum von Verbindung **7** zeigt daß die vier Fluoratome bei Raumtemperatur äquivalent sind. In den ^{19}F-NMR-Spektren von **8**–**10** sind 18 Linien zu erkennen, sie kann man als A_2B_2-System höherer Ordnung deuten.

Aufgrund der ^{13}C-NMR-Spektren von **8**—**10** können wir ausschließen, daß die Substitution an zwei Kohlenstoffatome des Ketons erfolgt. Das Signal des quartären Kohlenstoffes in Nachbarstellung zur Carbonylgruppe spricht deutlich für die Spiroverbindung. Wir beobachteten im protonenentkoppelten Spektrum von **10** sowohl eine Fernkopplung zwischen dem Kohlenstoffatom der CH$_2$-Gruppe in α-Stellung zu dem quartären Kohlenstoffatom als auch dem Carbonylkohlenstoffatom selbst mit des vier Fluorkernen der CF$_2$-Gruppen. Bei **8** wird eine entsprechende Kopplung nur mit zwei Fluorkernen beobachtet (Abb. 3 und Abb. 4). Dies kann so gedeutet werden, daß in **10** die erwähnten C-Atome und F-Atome einander sehr nahe kommen, dies ist aufgrund von Molekülmodellen in **8** nicht der Fall.

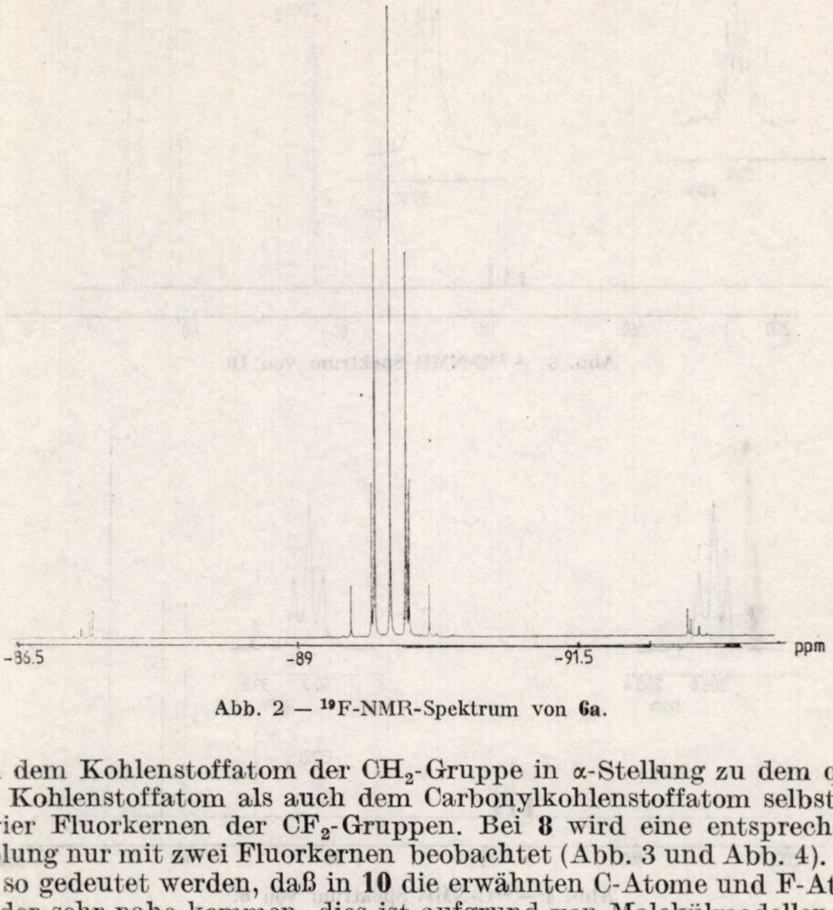

Abb. 2 — ^{19}F-NMR-Spektrum von **6a**.

EXPERIMENTELLER TEIL

Alle Arbeiten wurden unter Feuchtigkeitsausschluß durchgeführt. — ^{1}H-, ^{19}F- und ^{13}C-NMR-Spektren : Bruker 60E (60 MHz), WP8SY, AM250. — Als Standard verwandten wir TMS bzw. CFCl$_3$.

IR-Spektren : Perkin-Elmer Spektrograph 735 B. — Massenspektren : MAT CH5 (70 eV), MAT 8230 (70 eV). Elementaranalysen : Mikroanalytisches Labor Beller, Göttingen

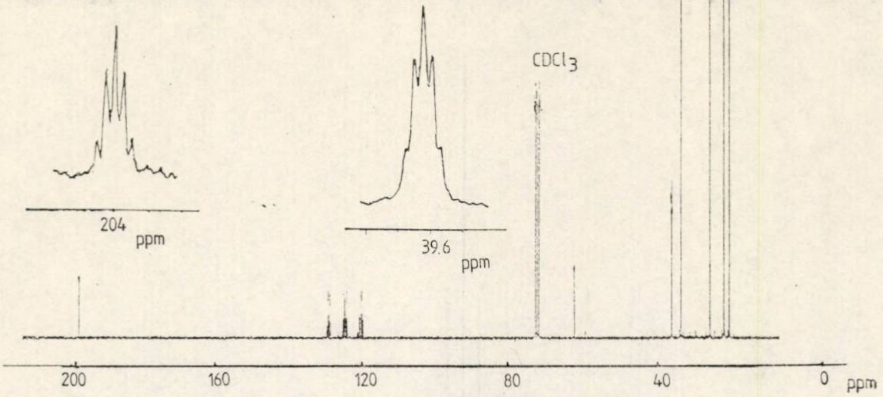

Abb. 3 — ^{13}C-NMR-Spektrum von **10**.

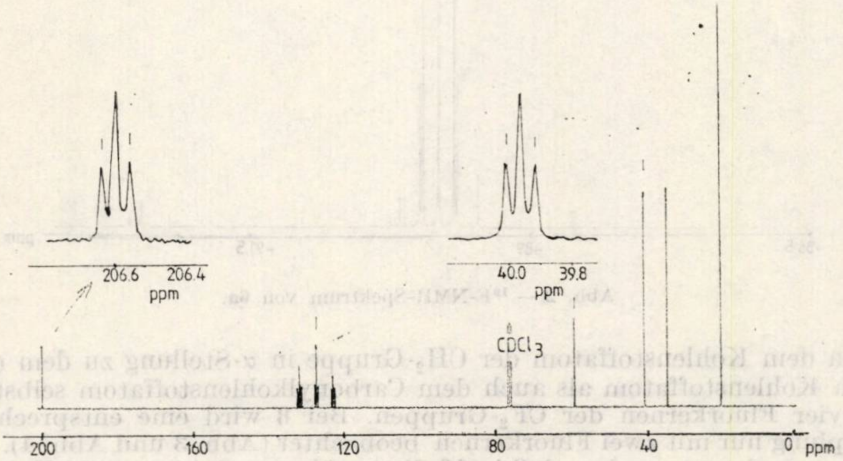

Abb. 4 — ^{13}C-NMR-Spektrum von **8**.

ARBEITSVORSCHRIFT FÜR 4

In ein Druckgefäß werden 7.34 g (30 mmol) $ClSCF_2CF_2SCl$, 20 mL CH_2Cl_2 und katalyitische Mengen $AlCl_3$ gegeben und mit flüssiger Luft gekühlt. Danach kondensiert man äquimolare Mengen Ethin ein. Die Reaktionsmischung wird unter starkem Rühren auf Raumtemperatur erwärmt. Schließlich wird der Feststoff durch Filtration entfernt und das Filtrat unter reduziertem Druck destilliert.

$C_4HClF_4S_2$(**4**) : Sdp. 30°C/0.05 Torr, Ausb. 7 %. — IR : 3050 st, 2900 s, 1150 sst, 1225 sst, 1190 sst, 1010 sst, 900 sst, 850 sst, 800 sst, 770 sst, 750 st, 700 st cm^{-1} — MS : $m/z = 224$ (M, 80 %), 124 (M-C_2F_4, 70 %), 63 (CFS, 10 %). — ^{19}F-NMR ($CDCl_3/CFCl_3$) : $\delta = -87.8$ (t), -89.7 (t) ppm, ^3J (F, F) = 10.6 Hz. — ^{1}H-NMR ($CDCl_3$/TMS) : $\delta = 5.3$ (s) ppm. — ^{13}C-NMR ($CDCl_3$/TMS) : $\delta = 132.2$ (s), 128.7 (t), 114.7 (s) ppm, ^1J (C, F) = 297.3, ^2J (C, F) = 33.7 Hz

$C_4HClF_4S_2$ (224.6) Ber. C 21.62 F 33.08 S 28.60
Gef. C 20.9 F 32.9 S 27.4

ALLGEMEINE ARBEITSVORSCHRIT FÜR 5–10

7.34 g (30 mmol) $ClSCF_2CF_2SCl$ werden tropfenweise und unter Eiskühlung zu äquimolaren Mengen Alkin oder Keton gegeben. Nach der Zugabe rührt man die Reaktionsmischung so lange, bis die Gasentwicklung aufhört. Anschließend werden die leicht flüchtigen Produkte bei 10 Torr abgezogen und der Rückstand unter reduziertem Druck fraktioniert.

$C_{10}H_5ClF_4S_2$ (**5**) : Sdp. 79°C/0.05 Torr, Ausb. 40 %. — IR : 3090 m, 1590 sst, 1225 sst, 1120 sst, 1110 sst, 1020 sst, 900 st, 750 st, 620 m cm^{-1}. — MS : $m/z = 300$ (M, 100 %), 200 ($M-C_2F_4$, 55 %), 164 ($C_2F_4S_2$, 60 %), 100 (C_2F_4, 50 %) — ^{19}F-NMR ($CDCl_3/CFCl_3$) : $\delta = -93.3$ (m), -93.5 (m), -94.0 (m) ppm. — ^{1}H-NMR ($CDCl_3$/TMS) : $\delta = 7.4$(m). —
$C_{10}H_5ClF_4S_2$ (300.7) Ber. C 39.46 H 1.67 S 21.30
Gef. C 40.0 H 1.8 S 20.0

$C_5H_4F_4OS_2$ (**6a**) : Sdp. 61°C(0.05 Torr, Ausb. 95 %. — IR : 2925 m, 1720 sst, 1410 st, 1300 sst, 1220 sst, 1150 sst, 1100 sst, 1015 sst, 925 sst, 650 st, 575 sst cm_^{1}. — MS : $m/z = 220$ (M, 3 %) 177 ($C_2F_4S_2CH$, 30 %), 100 (C_2F_4, 10 %), 43 (CH_3CO, 100 %). — ^{19}F-NMR ($CDCl_3/CFCl_3$) ; $\delta =$ $= -89.9$ (m) ppm. — ^{1}H-NMR ($CDCl_3$/TMS) : $\delta = 5.0$ (t), 2.4 (s) ppm, $^{4}J(H, F) = 5Hz$. — — ^{13}C-NMR ($CDCl_3$/TMS) : $\delta = 25.6$ (s), 47.8 (s), 130.2 (t), 198.0 (t) ppm, $^{1}J(C, F) = 291.7$, $^{2}J(C, F) = 29.3$, $^{4}J(C.F) = 2.6$ Hz.
$C_5H_4F_4OS_2$ (220.2) Ber. C 27.72 H 1.81 S 29.9
Gef. C 27.4 H.1.9 S 28.9

$C_6H_6F_4OS_2$ (**6b**) : Sdp. 40°C/0.05 Torr, Ausb. 90 %. — IR : 2920 s, 1725 sst, 1450 m, 1395 s, 1375 m, 1250 sst, 1200 sst, 1150 st, 1110 st, 1090 sst, 1025 sst, 925 st, 650 m cm^{-1}. — MS : $m/z = 234$ (M, 3 %), 191 (M-CH_3CO, 100 %). — ^{19}F-NMR ($CDCl_3/CFCl_3$) : $\delta = -88.9$(m) ppm. — ^{1}H-NMR ($CDCl_3$/TMS) : $\delta = 1.9$(m), 2.5(s). — ^{13}C-NMR ($CDCl_3$/TMS) : δ 24.3(s), 28.9(s), 60.3(s), 130.7(t), 200.3(s) ppm, J (C, F) = 291.30, ^{2}J (C, F) = 29.8 Hz.
$C_6H_6F_4OS_2$ (234.2) Ber. C 30.70 H 2.56 S 27.35
Gef. C 30.8 H 2.7 S 27.0

$C_7H_8F_4OS_2$ (**6c**) : Sdp. 33°C/0.05 Torr, Ausb. 85 %. — IR : 3000 sst, 2950 st, 2900 m, 1725 sst, 1450 sst, 1425 st, 1395 st, 1350 sst, 1245 sst, 1190 sst, 1125 sst, 1100 sst, 1025 sst, 925 sst, 850 s, 750 s, 650 st, 600 st cm^{-1}. — MS : $m/z = 248$ (M, 2.0 %), 205 (M-CH_3CO, 100 %), 43 (CH_3CO, 100 %). — ^{19}F-NMR ($CDCl_3/CFCl_3$) : $\delta = 89.0$(m). — ^{1}H-NMR ($CDCl_3$/TMS) : $\delta = 1.0$ (t), 2.2 (m), 2.4 (s) ppm, J (C, H) = 7.2 Hz. — ^{13}C-NMR ($CDCl_3$/TMS) : $\delta = 10.1$ (s), 25.5(s) 34.3 (s), 130.2 (t), 200.5 (s) ppm, $^{1}J(C, F) = 293.7$, $^{2}J(C, F) = 30.8$ Hz.
$C_7H_8F_4OS_2$ (248.2) Ber. C 33.87 H 3.20 S 25.80
Gef. C 34.2 H 3.2 S 25.7

$C_5H_3ClF_4OS_2$ (**6d**) : Sdp. 42°C/0.05 Torr, Ausb. 78 %. — IR : 2950 m, 1725 sst, 1400 m, 1370 s, 1250 sst, 1150 sst, 1100 sst, 1025 sst, 925 st, 810 m, 790 m, 750 m, 700 s, 650 m, 600 m cm^{-1}. — MS : $m/z = 254$ (M, 2 %), 219 (M-Cl, 15 %), 211 (M-CH_3CO, 20 %). — ^{19}F-NMR ($CDCl_3$/TMS) = $= \delta = -90.0$ (m) ppm. —^{1}H-NMR ($CDCl_3$/TMS) : $\delta = 2.5$ (s). — ^{13}C-NMR ($CDCl_3$/TMS) :$\delta =$ $= 23.1$ (s), 83.3 (t), 129.8 (t), 190.1 (t) ppm, ^{1}J (C. F) = 291.3, ^{2}J (C. F) = 29.0, $^{3}J(C, F) =$ $= 3.8$, $^{2}J(C,F) = 2.4$ Hz. $C_5H_3ClH_4OS_2$ (254.5) Ber. C 23.62 H. 1.18 S 25.19
Gef. C 23.8 H.1.3 S 24.8

$C_7H_6F_4O_2S_2$(**7**) : Sdp. 78°C/0.05 Torr, Ausb. 90 % — IR : 2910 m, 1725 sst, 1350 st, 1240 sst, 1175 st, 1125 sst, 1100 sst, 1015 sst, 925 st, 650 st cm^{-1}. — MS : $m/z = 262$ (M, 1 %), 100 (C_2F_4, 10 %) — ^{19}F-NMR ($CDCl_3/CFCl_3$) : $\delta = -90.8$ (s) ppm. — ^{1}H-NMR ($CDCl_3$/TMS) : $\delta = 2.5$(s) ppm. — ^{13}C-NMR ($CDCl_3$/TMS) : $\delta = 25.9$(s), 70.7 (s), 134.4 (t), 197.4 (t), J(C,F) = 291.7, $^{2}J(C, F) = 28.9$, $^{4}J(C, F) = 1.7$ Hz.
$C_7H_6F_4O_2S_2$ (262.2) Ber. C 32.06 H 2.29 S 24.42
Gef. C 32.5 H 2.2 S 24.5

$C_7H_6F_4OS_2$ (**8**) : Sdp. 61°C/0.05 Torr, Ausb. 95 %). — IR : 3000 st, 2950 st, 2900 st, 1775 sst, 1475 st, 1450 st, 1405 st, 1320 m, 1270 m, 1250 sst, 1100 sst, 1000 sst, 950 sst, 925 sst, 895 st, 875 m, 800 sst, 650 st, 600 st cm^{-1}, — MS : $m/z = 246$ (M, 45 %). — ^{19}F-NMR ($CDCl_3/CFCl_3$) : : $\delta = -87.3$ (m). — ^{1}H-NMR ($CDCl_3$/TMS) : $\delta = 2.0$ (q), 2.4 (t), 2.5 (t) ppm, J (H, H) = 7.2 Hz. — ^{13}C-NMR ($CDCl_3$/TMS) : $\delta = 19.0$(s), 33.7(s) 39.9(s), 59.3(t), 130.8(t), 200.6(t) ppm. — $^{1}J(C, F) = 290.5$, ^{2}J (C, F) = 27, ^{4}J (C, F) = 2.7 Hz.
$C_7H_6F_4OS_2$ (246.2) Ber. C 34.10 H 2.43 S 26.00
Gef. C 34.0 H 2.5 S 25.6

$C_8H_8F_4OS_2$ (**9**) : Sdp. 75° C/0.05 Torr, Ausb. 90 % — IR : 2900 sst, 2850 sst, 1740 sst, 1450 sst, 1325 st, 1300 sst, 1250 sst, 1150 sst, 1100 sst, 1050 sst, 950 sst, 850 st, 800 m, 790 s, 700 s 650 m, 600 m cm^{-1}. — MS : $m/z = 260$ (M^+, 40 %), 216 (M^+-CH_3CO, 100 %). — ^{19}F-NMR ($CDCl_3/CFCl_3$) : $\delta = -88.3$ (m) ppm. — ^{1}H-NMR ($CDCl_3$/TMS) : $\delta = 2.7$(m), 2.5 (m), 1.9(m) ppm. — ^{13}C.-NMR ($CDCl_3/TMS$): $\delta = 23.8$(s), 26.7(s), 38.6(s), 45.1(s), 65.1(t), 130.0 (t), 200.1(t) ppm. — $^1J(C, F) = 291$, $^2J(C, F) = 27$, $^4J(C, F) = 2.8$ Hz

$C_8H_8F^{\circ}OS_2$ (260.2) Ber. C 36.92 H 3.07 S 24.61

Gef. C 38.6 H 3.3 S 23.5

$C_{10}H_{12}F_4OS_2$ (10): Sdp. 90°C/0.05 Torr, Ausb. 80 %. — IR: 2950 sst, 2870 st, 1725 sst, 1475 st, 1450 st, 1325 m, 1245 sst, 1190 sst, 1100 sst, 1025 sst, 925 st, 900 m, 850 m, 800 m, 790 m, 670 s 650 s cm^{-1}. — MS: $m/z = 288$ (M, 15 %). — ^{19}F-NMR ($CDCl_3/CFCl_3$): $\delta = -87.7$(m). — — ^{1}H-NMR ($CDCl_3/TMS$): $\delta = 2.6$(m), 1.9(m), 1.7(m), 1.5(m), 1.3(m) ppm. — ^{13}C-NMR ($CDCl_3/TMS$): $\delta = 23.8$(s), 25.2(s), 25.3(s), 29.3(s), 37.3(s), 66.9(q), 130.2(t), 204.0(q) ppm $^1J(C, F)) = 289.4$, $^2J(C, F) = 28.6$, $^4J(C, F) = 1.6$ Hz.

$C_{10}H_{12}F_4OS_2$(288.3) Ber. C 41.60 H 4.10 S 22.20

Gef. C 42.2 H 4.4 S 21.9

LITERATUR

[1] C. G. Krespan und W. R. Brasen, *J. Org. Chem.*, **27**, 3995 (1962).

[2] C. G. Krespan, U.S.P. 3099688 (1963): *Chem. Abstr.*, **60**, 1597 (1964).

[3] H. W. Roesky, A. Thiel, M. Noltemeyer und G. M. Sheldrick, *Chem. Ber.*, **118**, 2811 (1985).

Revue Roumaine de Chimie, **31**, *11–12*, 943–948 (1986)

Dedicated to Professor P. SPACU on his 80th anniversary

THE POSITION OF 4,4′-BIPYRIDYL IN THE SPECTROCHEMICAL SERIES FOR NICKEL(II) COMPLEXES

MARIUS ANDRUH *, C. I. LEPĂDATU ** and MARIA BREZEANU *
* Faculty of Chemical Technology, Laboratory of Inorganic Chemistry, Dumbrava Roșie 23, Bucharest, Romania
** Center of Chemical Physics, ICECHIM, Splaiul Independenţei 202, Bucharest, Romania

Received July 20, 1985

The parameters Dq^z for 4,4′-bipyridyl were calculated from the electronic spectra of Ni(II) complexes. They were compared with those of pyridine in similar compounds. The calculations made for weak and strong field couplings show that both ligands have practically the same position in the spectrochemical series of Ni(II). Two new Ni(II) complexes of general formulas $[Ni(TAAB)(4,4'\text{-bipy})](ClO_4)_2 \cdot 2H_2O$ and $[Ni(TAAB)Py_2](ClO_4)_2 \cdot 2\ H_2O$ (where TAAB = tetrakis-anhydro-aminobenzaldehyde) have been synthetized.

1. INTRODUCTION

The increasing number of papers or the transition-metal complex compounds containing 4,4′-bipyridyl as ligand made necessary a study of its position in the spectrochemical series. Due to the position of the donor atoms, this ligand, in contrast with 2,2′-bipyridyl, generates polynuclear complexes [1-3] :

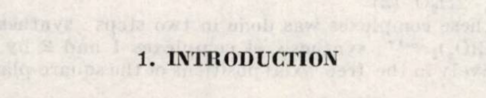

The position of a ligand in the spectrochemical series can be determined in different ways :

(i) the estimation of the splitting parameter 10 Dq from the $d-d$ transitions of $[ML_6]^q$ complexes [4];

(ii) the estimation of Dq^{xy} and Dq^z parameters for *trans*-$[MA_4L_2]^q$ (D_{4h} symmetry in the frame of the crystal field theory [5,6]). In this latter case, the calculation can be easily performed for Ni (II), Co(III) and Cr(III) complexes, having a nondegenerate electronic state.[7-9]

(iii) if the number of the absorption bands split by the anisotropy between A and L ligands in *trans*-$[MA_4L_2]$ complexes allows the separate estimation of the Angular Overlap Model parameters, a bidimensional σ and π spectrochemical series for ligands can be easily built. [10-14]

The present note deals with the tetragonal Ni(II) complexes with macrocyclic ligands, of the type :

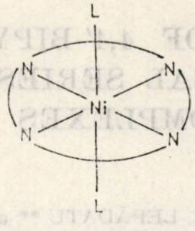

in order to see the effects produced by the tetragonal ligand field on the electronic states of the transition-metal ion. Such complexes are suitable for the calculation of Dq^z parameters of different axial ligands, L, because, for a given macrocyclic ligand, Dq^{xy} parameter remains practically constant in the series $[Ni(II)(MAC)L_2]X_2$, when MAC is the macrocyclic ligand, the same for a given series of complexes.[15]

The calculations have been made using both strong and weak field coupling, without configuration interaction.

2. EXPERIMENTAL

New complexes containing the macrocyclic ligand tetrakis-anhydroaminobenzaldehyde (TAAB) were synthetized. The elemental and physico-chemical analyses lead to the formulas :
$[Ni(TAAB)(4,4'\text{-bipy})](ClO_4)_2 \cdot 2H_2O$ (**1**) and
$[Ni(TAAB)Py_2](ClO_4)_2 \cdot 2H_2O$ (**2**)

The synthesis of these complexes was done in two steps : synthesis of the diamagnetic compound $[Ni(TAAB)](ClO_4)_2$ [16,17] ; synthesis of complexes **1** and **2** by addition of 4,4′-bipyrydyl or pyridine respectively in the free axial positions of the square-planar $[Ni(TAAB)](ClO_4)_2$ complex :

The second step of synthesis was achieved by treatment of warm saturated aqueous solution of perchlorate complex with corresponding amounts of 4,4′-bipyridyl or pyridine respectively. The obtained compounds were filtered and dried under vacuum on P_2O_5.

Analytical data :

Compound **1** : Found 52.5 % C ; 4.0 % H ; 9.9 % N ; 8.1 % Cl ; calculated : 52.9 % C ; 3.7 %H ; 9.8 %N ; 8.2 %Cl

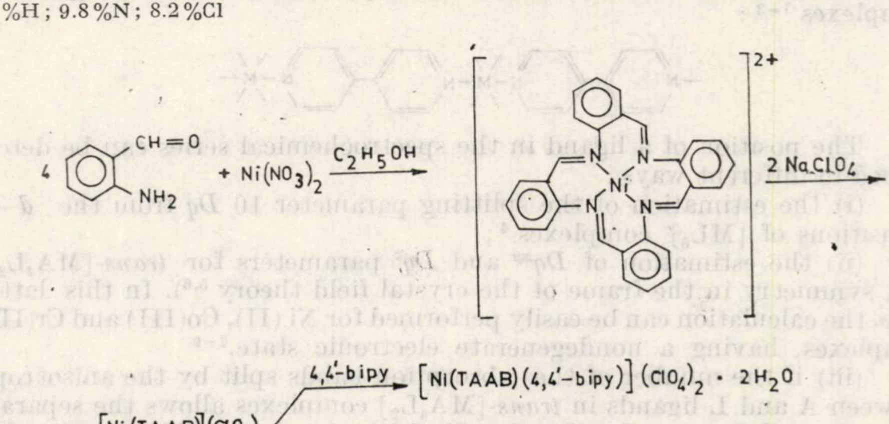

Compound **2** : Found 53.1 % C ; 3.7 % H ; 9.5 % N ; 8.0 % Cl calculated : 53.0 % C ; 3.9 % H ; 9.7 % N ; 8.2 % Cl.

The hexacoordination was attributed to these compounds by means of their electronic spectra and magnetic measurements. The effective magnetic moment of the two complexes indicates ion a high spin electronic configuration for Ni(II) (see below).

3. RESULTS AND DISCUSSION

The electronic spectra of the two complexes undoubtedly indicate a D_{4h} environment for the Ni (II) ions, the ligands L = 4,4′-bipyridyl and pyridine being placed on axial positions :

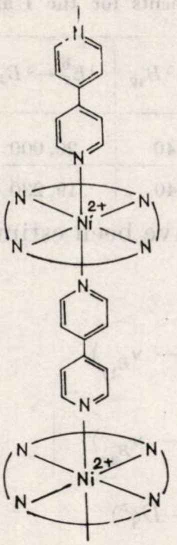

N
N
N
N
N
2+
Ni
N
N
N
N
N
N
2+
Ni
N
N

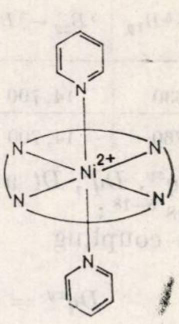

2.

Figure 1 gives the energy diagram for the Ni(II) ion in a weak field of O_h and D_{4h} symmetries. Figure 2 gives the Ni(II) energy diagram for the same symmetries in a strong field coupling. Table 1 summarizes the

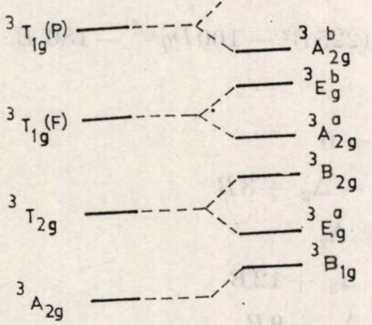

$^3T_{1g}(P)$
$^3E_g^c$
$^3A_{2g}^b$
$^3T_{1g}(F)$
$^3E_g^b$
$^3A_{2g}^a$
$^3T_{2g}$
$^3B_{2g}$
$^3E_g^a$
$^3A_{2g}$
$^3B_{1g}$
O_h
D_{4h}

Fig. 1. — Energy level diagram for Ni(II) ion in a weak field of O_h and D_{4h} symmetries.

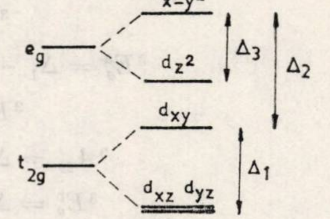

$d_{x^2-y^2}$
e_g
d_{z^2}
Δ_3
Δ_2
d_{xy}
t_{2g}
Δ_1
d_{xz} d_{yz}
O_h
D_{4h}

Fig. 2. — Energy level diagram for Ni(II) ion in a strong field coupling of O_h and D_{4h} symmetries.

absorption maxima of the *d—d* transitions of the two complexes, as well as the paramagnetic moments measured at room temperature (298 K).

In a series of complexes of the type *trans*-[Ni(II)(MAC)L$_2$] the position of $^3B_{2g} \leftarrow {}^3B_{1g}$(10 Dq^{xy} or Δ_2) transition does not depend on the nature of the axial ligands. Indeed, in the high spin complexes [Ni (TAAB) (NCS)$_2$] and [Ni(TAAB)(N$_3$)$_2$], the mentioned transition has the energy 14,650 and 14,734 cm^{-1} respectively.[15]

Table 1

Absorption maxima (cm^{-1}) and magnetic moments for the **1** and **2** complexes

Compound	$^3E_g^a \leftarrow {}^3B_{1g}$	$^3B_{2g} \leftarrow {}^3B_{1g}$	$^3A_{2g}^a \leftarrow {}^3B_{1g}$	$^3E_g^b \leftarrow {}^3B_{1g}$	μ_{eff}(M.B.)
1	11, 630	14, 700	17, 540	20, 000	3, 12
2	11, 760	14, 700	17, 240	19, 230	3, 09

Parameters Dq^{xy}, Dq^z, Dt and Ds have been estimated from the following relationships [5–18]:

I. Weak field coupling

$$Dq^{xy} = \frac{1}{10}(\nu_{B_{2g}} - \nu_{B_{1g}})$$

$$Dq^z = \frac{1}{10}(2\nu_{E_g^a} - \nu_{B_{2g}})$$

$$Dt = \frac{4}{7}Dq^{xy} - Dq^z)$$

$$Ds = \frac{1}{6}\left[(\nu_{E_g^b} - \nu_{A_{2g}^a}) + \frac{5}{4}Dt\right]$$

$$E = (E_g^b \leftarrow B_{1g}) = R(-) + 2Ds + \frac{3}{4}Dt$$

where $R(-) = \frac{1}{2}[15B + 30\, Dq^{xy} - (225B^2 - 100Dq^{xy^2} - 180\, B \cdot Dq^{xy})^{1/2}]$

II. Strong field approach

$$^3B_{1g} = 0$$

$$^3E_g^a = \Delta_1 + \Delta_2 - \Delta_3 + 3B$$

$$^3B_{2g} = \Delta_2$$

$$^3A_{2g} = \Delta_2 - \Delta_3 + 12B$$

$$^3E_g^b = \Delta_1 + \Delta_2 + 9B$$

$$Dq^z = \frac{1}{10}\Delta_2 + \frac{1}{5}\Delta_1 - \frac{3}{20}\Delta_3$$

$$10\ Dq^{xy} = \Delta_2$$

The two types of parameters can be correlated as follows:

$$\Delta_1 = 3\,Ds - 5Dt\,;\ \Delta_3 = 4Ds + 5\,Dt$$

and hence the molecular orbital parameters:

$$\mathrm{d}\sigma = -\frac{3}{8}\Delta_3\,;\ \mathrm{d}\pi = -\frac{1}{2}\Delta_1$$

Table 2 presents the values of these parameters calculated as above.

Table 2

Calculated spectral parameters (cm^{-1}) for the two complexes

	$[Ni(TAAB)\ (4,4'\text{-bipy})](ClO_4)_2 \cdot 2H_2O$		$[Ni(TAAB)\ (Py_2)](ClO_4)_2 2H_2O$	
	weak	strong	weak	strong
Dq^{xy}	1470	1470	1470	1470
Dq^z	856	714	882	755
Dt	351	432	336	408
Ds	483	619	465	522
Δ_1	−306	−305	−295	−475
Δ_2	14700	14700	14700	14700
Δ_3	3687	4636	3540	4132
$\mathrm{d}\sigma$	−1383	−1739	−1328	−1550
$\mathrm{d}\pi$	153	152	148	238
B	376	623	301	556

One observes that Dq^z parameter obtained with both methods takes close values for the two complexes:

$$Dq^z(4{,}4'\text{-bipy}) \approx Dq^z(\mathrm{Py})$$

To verify the Dq^z-values thus obtained, they were compared with those for similar Ni(II) complexes [2,3,5]:

	$NiPy_2Br_2$	$Ni(4,4'\text{-bipy})NBr_2$	$NiPy_2Cl_2$
$Dq^{xy}(cm^{-1})$	580(Br^-)	520 (Br^-)	600(Cl^-)
$Dq^z(cm^{-1})$	1020 (Py)	1060(4.4'-bipy)	1080 (Py)

As may be seen, the ligands 4,4'-bipyridyl and pyridine have close positions in the spectrochemical series, *i.e.* they have the same strength of the metal-ligand bond. Another remark is that the Dq^z values for 4,4'-bipyridyl and pyridine in $[Ni(TAAB)(4,4'\text{-bipy})](ClO_4)_2 \cdot 2H_2O$ and $[Ni(TAAB)\ Py_2]\ (ClO_4)_2 \cdot 2H_2O$ are obviously different from those for the same ligands in $Ni(4,4'\text{-bipy})\ Br_2$ and $NiPy_2Br_2$, namely Dq^z decreases as Dq^{xy} increases. A similar difference is observed with Dq^z values for other complexes having the same axial ligand[5,15]

	$[Ni(NH_3)_4(NCS)_2]$	$[Mi(TAAB)(NCS)_2]$
$Dq^{xy}(cm^{-1})$	1103(NH_3)	1465(TAAB)
$Dq^z(cm^{-1})$	1075 (NCS^-)	801(NCS^-)

This observation suggests the existence of a *cis*-effect in these Ni(II) complexes,[15] *i.e.* Dq^{z}-value is strongly influenced by the field strength of the in-plane ligand, Dq^{xy}.

The concluding result of this note is that the studied ligand, 4,4′-bipyridyl, belongs to the following sequence of the spectrochemical series for the Ni(II) ion :

$$\text{Py} \approx \text{4,4'-bipy} > \text{NCS}^- > \text{Cl}^- > \text{Br}^-$$

This result is useful for the study of other Ni(II) complexes containing the mentioned ligand.

REFERENCES

[1] A. Anagnostopoulos, *J. Inorg. Nuclear Chem.*, **35**, 3366 (1973).
[2] J. R. Ferraro and K. C. Davis, *Inorg. Chim. Acta*, **3**, 686 (1969).
[3] I. S. Ahuja and R. Singh, *Indian J. Chem.*, **12**, 107(1974).
[4] C. K. Jørgensen, "Absorption Spectra and Chemical Bonding in Complexes", Pergamon, Oxford, 1962.
[5] A. B. P. Lever, *Coord. Chem. Rev.*, **3**, 119 (1968).
[6] A. B. P. Lever, *Adv. Chem. Ser.*, **62**, 430 (1966).
[7] C. I. Lepădatu, *Rev. Roumaine Chim.*, **10**, 1093(1965).
[8] C. I. Lepădatu, *Rev. Roumaine Chim.*, **11**, 489 (1966).
[9] C. I. Lepădatu, *Rev. Roumaine Chim.*, **11**, 937 (1966).
[10] D. W. Smith, *Struct. and Bond.*, **35**, 88(1978).
[11] J. K. Burdett, *Adv. Inorg. Chem. Radiochem.* **21**, 113(1978).
[12] M. Andruh, C. I. Lepădatu and M. Brezeanu, *Rev. Roumaine Chim.*, **25**, 811 (1980).
[13] M. A. Hitchman, *Inorg. Chem.*, **11**, 2387 1972).
[14] C. Furlani, G. Mattogno, A. Monaci and F. Tarli, *Inorg. Chim. Acta*, **4**, 187 (1970).
[15] L. Martin. C. R. Sperati and D. H. Busch, *J. Amer. Chem. Soc.*, **99**, 2968, (1977).
[16] G. A. Melson and D. H. Busch, *J. Amer. Chem. Soc.*, **86**, 4834 (1961).
[17] G. A. Melson and D. H. Busch, *J. Amer. Chem. Soc.*, **86**, 4830 (1966).
[18] R. A. D. Wentworth and T. S. Piper, *Inorg. Chem.*, **4**, 709 (1965).

Revue Roumaine de Chimie, 31, *11–12*, 949–953 (1986)

Herrn Professor SPACU zum 80. Geburtstag gewidmet

DIE CYCLOTETRAPHOSPHANE $(Me_3C)_3P_4H$ UND $(Me_3C)_3P_4[P(CMe_3)Cl]$

G. FRITZ und K. STOLL
Institut für Anorganische Chemie der Universität Karlsruhe

Eingegangen am 3. Mai, 1986

The cleavage of the P-Si bond in $(Me_3C)_3P_4(SiMe_3)$ **1** with CH_3OH or the reaction of $LiP_4(CMe_3)_3$ **2** with H_2O or CH_3OH as well yield $(Me_3C)_3P_4H$ **3**, which forms colorless, needle shaped crystals, m.p. 104 ± 1°C. $(Me_3C(_3P_4[P(CMe_3)Cl]$ **4** is obtained by P-Si cleavage in **1** with $(Me_3C)PCl_2$ or by the reaction of $LiP_4(CMe_3)_3$ **2** with $(Me_3C)PCl_2$. The colorless crystals of **4** are needle shaped, m.p. 101 ± 2°C. The data of NMR-spectra and mass spectrometric investigations of the compounds **3** and **4** are given.

Sowohl die Spaltung der P-Si-Bindung im $(Me_3C)_3P_4(SiMe_3)$ **1** mit CH_3OH als auch die solvolytische Spaltung der P-Li-Bindung im $LiP_4(CMe_3)_3$ **2** mit H_2O oder CH_3OH führen zum $(Me_3C)_3P_4H$ **3**. **3** bildet farblose, nadelförmige Kristalle, Smp. 104 ± 1°C. Durch Umsetzung von $(Me_3C)_3P_4(SiMe_3)$ **1** mit $(MeC)PCl_2$ entsteht under P-Si-Spaltung in **1** das $(Me_3C)_4P_4[P(CMe_3)Cl]$ **4**. **4** bildet sich auch bei der Umestzung von $LiP_4(CMe_3)_3$ **2** mit $(Me_3C)PCl_2$. Die farblosen Kristalle von **4** sind nadelförmig, Smp. 101 ± 2°C. Es werden die Daten der NMR-Spektren und der massenspektrometrischen Untersuchung der Verbindungen **3** und **4** angegeben.

1. EINLEITUNG

Vorausgehende Untersuchungen an silylierten Cyclotetraphosphanen zeigen, daß das chemische Verhalten dieser Verbindungen durch den Silylierungsgrad bestimmt wird[1]. Während $P_4(SiMe_3)_4$, $(Me_3C)P_4(SiMe_3)_3$ und cis-$(Me_3C)_2P_4(SiMe_3)_2$ mit LiBu unter Ringöffnung durch Spaltung einer P-P-Bindung reagieren, bilden trans-$(Me_3C)_2P_4(SiMe_3)_2$ und $(Me_3C)_3P_4(SiMe_3)$ **1** mit LiBu unter Spaltung einer P-Si-Bindung die Phosphide $LiP_4(CMe_3)_2(SiMe_3)$ bzw. $LiP_4(CMe_3)_3$ **2**,[2] unter denen das Phosphid **2** das beständigere ist. Im folgenden wird über Substitutionsreaktionen am Gerüst des $(Me_3C)_3P_4(SiMe_3)$ **1** bzw. $LiP_4(CMe_3)$ $_3$**2** berichtet, die zu den Verbindungen $(Me_3C)_3P_4H$ **3** und $(Me_3C)_3P_4[P(Me_3)Cl]$ **4** führen.

2. ERGEBNISSE DER UNTERSUCHUNG

2.1. Das $(Me_3C)_3P_4H$ 3

Aus älteren Untersuchungen ist bekannt, daß sich die P-Si-Bindung in Silylphosphanen mit Alkoholen unter Ausbildung der P-H-Gruppe spalten läßt.[3] Diese Reaktion ist auf Verbindung **1** übertragbar. Wird

$(Me_3C)_3P_4(SiMe_3)$ **1** (gelöst in Toluol) bei 50°C mit überschüssigem CH_3OH versetzt, so erfolgt die Umsetzung nach Gl. (1), die nach 15 h zu Verbindung **3** mit einer Ausbeute von ca. 80 % (nach ^{31}P-NMR-Spektrum) führt.

$$\underset{\mathbf{1}}{(Me_3C)_3P_4(SiMe_3)} + CH_3OH \rightarrow \underset{\mathbf{3}}{(Me_3C)_3P_4H} + H_3COSiMe_3 \qquad (1)$$

Als Nebenprodukte (mssenspektrometrisch nachweisbar) bilden sich die Verbindungen $(M_3C)_4P_5H$ und $(Me_3C)_5P_6H$. Dies ist auf die thermisch begünstigte Dismutierung des Vierringgerüstes von **3** zurückzuführen. Nach Abdestillieren aller flüchtigen Bestandteile aus der Reaktionslösung läßt sich Verbindung **3** durch Sublimation (40–50°C, 10^{-4} Torr) aus dem Rückstand in Form farbloser, nadelförmiger Kristalle isolieren, die nach Umkristallisieren aus wenig Pentan spektroskopisch rein sind; Smp 104 ± 1°C. Verbindung **3** bildet sich quantitativ bei der Umsetzung von $LiP_4(CMe_3)_3$ **2** mit H_2O oder MeOH im Molverhältnis 1 : 1. Präparativ erfordert dieser Weg jedoch einen größeren Aufwand, da **2** aus $(Me_3C_3)P_4(SiMe_3)$ **1** gebildet wird.

Das ^{31}P-NMR-Spektrum von Verbindung **3** ist in Abb. 1 wiedergegeben. Es zeigt drei Signalgruppen im Intensitätsverhältnis 1 : 2 : 1, die den P-Atomen der Verbindung eindeutig zuzuordnen sind. Benachbarte Me_3C-Gruppen am P-Vierring von **3** liegen in transoider Anordnung

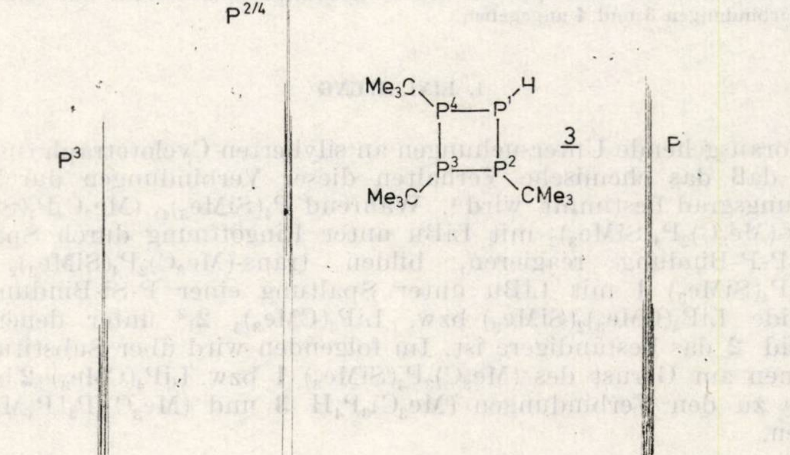

Abb. 1. — ^{31}P-NMR-Spektrum des Cyclotetraphosphans **3**.

vor , da P^2 und P^4 chemisch, im ^1H-entkoppelten Fall auch magnetisch äquivalent sind.

Das ^1H-NMR-Spektrum von **3** zeigt im Me_3C-Bereich zwei triplettierte Dubletts. Im P-H-Bereich beobachtet man bei 3,65 ppm das erwartete Resonanzsignal, das zu allen P-Atomen des Vierringes Kopplungen aufweist. Die Gesamtintegration H : CMe_3 entspricht mit 1 : 27 dem Erwartungswert. Die NMR-Daten von $(Me_3C)_3P_4H$ **3** sind in Tab. 1, die Ergebnisse der massenspektrometrischen Untersuchung in Tab. 2 zusammengestellt.

Tabelle 1

$^{31}P\{^1H\}$ und ^1H—NMR-Daten der Verbindungen **3** und **4**

Nr.	Verbindung*	δ(P)/(H) [ppm]		J(P, P)/J(P,H) [Hz]		J(P, P)/J(P, H)[Hz]	
3	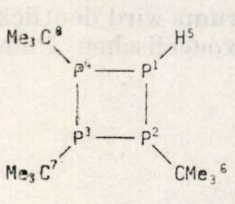	(1)	−181	(1, 2)=(1, 4)	93		
		(2)=(4)	− 74	(1, 3)	19		
		(3)	− 19	(2, 3)=(3, 4)	137		
		(5)	3, 65	(1, 5)	186, 0	(1, 6)=(1, 8)	0, 9
		(6)=(8)	1, 16	(2, 5)=(4, 5)	31, 9	(2, 7)=(4, 7)	0, 8
		(7)	1, 25	(2, 6)=(4, 8)	13, 4	(3, 6)=(3, 8)	0, 9
				(3, 5)	13, 2		
				(3, 7)	13, 2		
	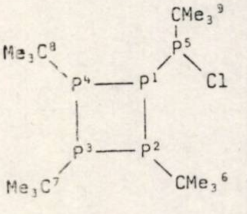	(1)	−110	(1, 2)	144	(2, 3)=(3, 4)	147
		(2)	− 53	(2, 3)	7	(2, 4)	11
		(3)	− 30	(1, 4)	121	(2, 5)	102
		(4)	− 55	(1, 5)	228	(3, 5)	10
		(5)	+142			(4, 5)	182
		(6)	1, 27	(2, 6)	13, 1	(1, 6)=(3, 6)	0, 8
		(7)	1, 30	(3, 7)	13, 2	(1, 8)=(3, 8)	0, 7
		(8)	1, 24	(4, 8)	13, 1	(2, 7)=(4, 7)	0, 8
		(9)	1, 30	(5, 9)	13, 4	(5, 8)	0, 7

* gemessen in C_6D_6 (ca. 0,2 m) bei 23°C. Hochfeldverschiebungen sind mit negativen Vorzeichen versehen;

Kopplungskonstanten werden ohne Vorzeichen angegeben.

Standardsubstanzen : H_3PO_4 (85 %, ext.) bzw. TMS (intern).

Tabelle 2

Exackte Massenbestimmung von $P_4(CMe_3)_3H$ **3** und $(Me_3C)_3P_4[P(CMe_3)Cl]$ **4**

Verbindung	exackte Masse		gemessen	Diff. [mn]	I rel. [%]
3	$P_4C_{12}H_{28}$	M	296, 1153	1, 1	17, 4
	$P_4C_8H_{19}$	M-CMe_3	239, 0445	0, 8	16, 5
	$P_4C_4H_{10}$	M-2 CMe_3	181, 9772	3, 9	2, 1
4	$P_5C_{16}H_{36}Cl$	M	418, 1193	0, 0	7, 2
	$P_5C_{16}H_{36}$	M-Cl	383, 1533	2, 8	0, 2
	$P_5C_{12}H_{27}Cl$	M-CMe_3	361, 0481	−0, 8	2, 2
	$P_4C_{12}H_{27}$	M-$P(CMe_3)Cl$	295, 1061	−0, 2	13, 4

Verdampfungstemperatur **3** und **4**: 30°C; I rel. = 100 % für CMe_3^+ bei **3** und **4**.

2.2. Das $(Me_3C)_3P_4[P(CMe_3)Cl]$ 4

Für die Bildung der Verbindung **4** kann die Möglichkeit der Si-P-Spaltung mit Elementhalogeniden eingesetzt werden, die bei Verwendung eines Phosphorchlorides zur Ausbildung einer neuen P-P-Bindung führt.[4] Demgemäß verläuft die Umsetzung nach Gl. (2).

$$\underset{\mathbf{1}}{(Me_3C)_3P_4SiMe_3} + (Me_3C)PCl_2 \rightarrow \underset{\mathbf{4}}{(Me_3C)_3P_4[P(CMe_3)Cl]} + Me_3SiCl \qquad (2)$$

Die Bildung von **4** kann auch durch Umsetzung von $LiP_4(CMe_3)_3$ mit (Me_3C) PCl_2 erfolgen. In beiden (Fällen entsteht **4** in hohen Ausbeuten) und kann durch Kristallisation oder durch Sublimation (85°C/10^{-4} Torr) rein erhalten werden. **4** bildet farblose, nadelförmige Kristalle, Smp. 101 ± 2°C.

Das linienreiche $^{31}P\{^1H\}$-NMR-Spektrum von **4** zeight fünf intensitätsgleiche Signalgruppen, die mit Ausnahme von P^2 und P^4 eindeutig zuzuordnen sind (Abb. 2). Bei der Interpretation des Spektrums wird deutlich, daß sich die Beträge der $^2J(P,P)$-Kopplungen zur exocyclischen Phosphingruppe (102 und 182 Hz) deutlich von den übrigen Kopplungskonstante nunterscheiden. Diese liegen in der für cyclische Tetraphosphane zu erwartenden Größenordnung. Deshalb ist anzunehmen, daß die freien Elektronenpaare der P-Atome (2), (4), (5) aufeinander zuweisen, wobei die Wechselwirkung P^4-P^5 am stärksten ausgeprägt ist (entsprechend P^2-P^5 bei vertauschter Zuordnung der chemischen Verschiebungen von P^2

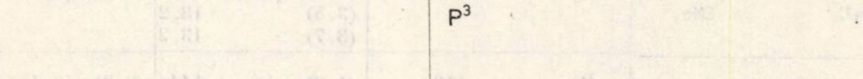

Abb. 2. — $^{31}P\{^1H\}$-NMR-Spektrum von Verbindung **4** bei 23°C.

und P^4). Vergleichbare Größenverhältnisse von J(P, P) findet man in den analog aufgebauten Verbindungen $(Me_3C)_3P_4[P(CMe_3)H]$ [5] und $(Me_3C)_2P_4(PBu_2)(SiMe_3)$.[6]

Das ^{1}H-NMR-Spektrum von **4** zeigt teilweise Überlagerungen der Resonanzlinien der chemisch in äquivalenten Me_3C-Gruppen. Die getroffenen Zuordnungen (Tab. 1) wurden durch ^{31}P-Entkopplungsexperimente bestätigt.

3. EXPERIMENTALLE EINZELHEITEN

Darstellung von $P_4(CMe_3)_3H$ **3** : Die Lösung von 5 g (13,6 mmol) $P_4(CMe_3)_3SiMe_3$ **1** in 50 mL Toluol wird mit 5 mL (3,9 g ; 123,5 mmol) Methanol versetzt und 15 h unter Rühren auf 40°C erwärmt. Nach Abdestillieren des Lösungsmittels und der leicht flüchtigen Anteile bei Unterdruck kann $P_4(CMe_3)_3H$ **3** durch Sublimation (10^{-4} Torr/40°C) abgetrennt und durch Kristallisation aus wenig n-Pentan gereinigt werden. Ausbeute : 2,2 g (7,4 mmol ; 55 % d.Th.).

Die Verbindung **3** bildet sich quantitativ bei der Umsetzung von $LiP_4(CMe_3)_3$ **2** mit H_2O oder mit Methanol im Molverhältnis 1 : 1 in THF als Lösungsmittel.

Darstellung von $P_4(CMe_3)_3[P(CMe_3)Cl]$ **4** : Eine Lösung von 3,3 g (9 mmol) $P_4(CMe_3)_3SiMe_3$ in 40 mL THF wird mit 1,7 g (10,7 mmol ; 19 % Überschuß) $P(CMe_3)Cl_2$ in 10 mL THF versetzt und 4 d bei 60°C gerührt. Nach Abdestillieren des Lösungsmittels und der leicht flüchtigen Anteile (20°C/10^{-3} Torr) wird der gelbe, feinkristalline Rückstand in 20 mL n-Pentan augenommen, vom Unlöslichen (geringer Anteil) abfiltriert und bei −78°C kristallisiert. Man erhält als erste Kristallfraktion 1,1 g der Verbindung **4**, nach Aufarbeitung der Mutterlauge weitere 1,3 g. Gesamtausbeute : 2,4 g (5,7 mmol ; 65 % d.Th.).

Darstellung von **4** *aus* $LiP_4(CMe_3)_3 \cdot 2{,}3\ THF$ **2** : Eine Lösung von 1,6 g (3,4 mmol) **2** in 150 mL Benzol wird mit 0,65 g (4,1 mmol ; 20 % Überschuß) $P(CMe_3)Cl_2$ in 10 mL Benzol versetzt und 3 h bei 20°C gerührt. Die ursprünglich orangerote Phosphidlösung färbt sich dabei blaßgelb und wird trübe durch das gebildete LiCl. Nach Abfiltrieren des LiCl und Abdestillieren des Lösungsmittels sowie der leicht flüchtigen Anteile verbleibt ein gelber, feinkristalliner Rückstand. Durch Sublimation (85°C/10^{-4} Torr) wird daraus Verbindung **4** in Form farbloser, nadelförmiger Kristalle zugänglich.

LITERATUR

[1] G. Fritz und K. Stoll, *Z. anorg. allg. Chem.*, im Druck

[2] G. Fritz, J. Härer und K. Stoll, *Z. anorg. allg. Chem.*, **504**, 47 (1983).

[3] G. Fritz und H. O. Bergernoff, *Z. anorg. allg. Chem.*, **279**, 250 (1957).

[4] G. Fritz und J. Härer, *Z. anorg. allg. Chem.*, **481**, 185 (1981).

[5] M. Baudler und H. Tschäbunin, *Z. anorg. allg. Chem.*, **511**, 77 (1984).

[6] G. Fritz und T. Vaahs, unveröffentlicht.

Revue Roumaine de Chimie, 31, *11–12*, 955–962 (1986)

Dedicated to Professor P. SPACU on his 80th birthday

THE BONDING IN DIALKYLDITHIOPHOSPHINATO METAL COMPLEXES.

A MOLECULAR ORBITAL STUDY OF BIS(DIMETHYLDITHIOPHOSPHINATO)NICKEL(II)

IOAN SILAGHI-DUMITRESCU and IONEL HAIDUC *
Chemistry Department, University of Cluj-Napoca, R–3400 Cluj-Napoca, Romania

Received May 17, 1986

The isobidentate behaviour of dithiphosphinato ligands R_2PS^{2-} is investigated by the CNDO/2 SCF-MO method. Metal-sulfur bonds are realized mainly through nickel *4s, 4p* and to a smaller extent, $3d_{xy}$ orbitals, with the proper combinations of ligand orbitals. Lower degree of covalency than in dithiophosphato nickel complexes is found. A peculiar consequence of the orbital mixing in the NiS_2P four-membered ring is the remarkable high metal-phosphorus transannular interaction. The main contributions to these ring molecular orbitals are visualized in the text by approximate pictures. Electron density analysis shows an unexpected increase on the phosphorus atom, when going from the free to the coordinate ligand. This is due to the redistribution of the sulfur electrons and causes a slight increase in the phosphorus-sulfur bond order and force constant.

INTRODUCTION

The metal complexes of dithiophosphorus ligands (dithiophosphates and dithiophosphinates) are intensively investigated due to their remarkable properties and often unexpected structures.[1–5] In the past few years our laboratory was actively interested in this field.[6–13] The peculiarities of dithiophosphato ligands

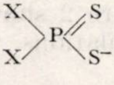

stem from the presence of two sulfur atoms, which makes possible several ways of coordination (Fig. 1).

Most of these coordination patterns are firmly established by X-ray structural investigations.[1] The isobidentate behaviour (Fig. 1b) is a typical and most frequent case in transition metal complexes. It involves equal metal-sulfur and phosphorus-sulfur bond lengths, respectively. The resulting four-membered metallocycle is a particular case of inorganic (carbon-free) chelate rings.[2]

---

* Author to whom correspondence should be addressed

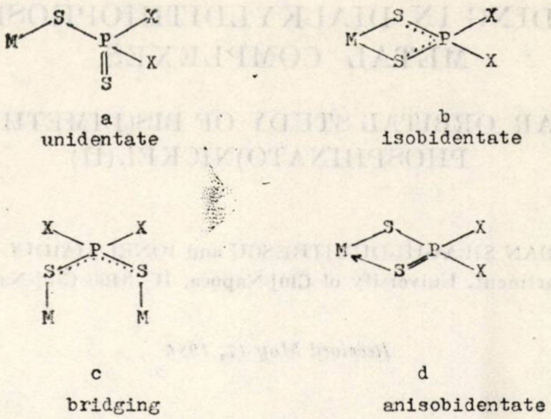

a unidentate

b isobidentate

c bridging

d anisobidentate

Fig. 1. — Main coordination patterns of dithiophosphato ligands. For other coordination patterns see ref.[1]

We carried out a CNDO/2 SCF molecular orbital treatment[14] of this coordination pattern, in order to get a deeper insight into the electronic structure of these compounds. Semiempirical MO calculations have already been published for dithiophosphato (X = OH, M = Mn, Fe, Co, Ni, Cu[15,16]; X = OEt, M = Ni[17,18]) and dithiophosphinato metal complexes (X = H, F, M = Cu, VO^{2+})[19] but the use of different levels of approximation by different authors (CNDO/2 with various parameters of Extended Huckel) makes the comparison of the results rather problematic. To avoid discrepancies resulted from different parametrizations, in this work we performed CNDO/2 calculations on bis(dithiophosphinato) nickel(II) (X = methyl or H) and also on the corresponding free ligands This way, electronic changes accompanying chelation become clearer and more consistent conclusions can be drawn.

CALCULATIONS

a) *Molecular geometry.* Figure 2 shows the molecular model and the coordinate system used in calculations.

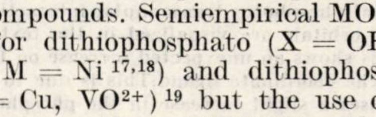

Fig. 2. — The molecular model and the coordinate axes system for $Ni[S_2PH_2]_2$.

Geometrical parameters are taken from ref. 20. For bis(dithiophosphinato)nickel(II), $Ni(S_2PH_2)_2$, a hypothetical geometry, with $R_{PH}=1.10$ Å and tetrahedral angles around the phosphorus atom was assumed. All the other bond lengths and bond angles are as in the bis(dimethyldithiophosphinato)nickel(II).[20]

b) *Basis orbitals and parametrization.* Valence orbitals for hydrogen and carbon atoms have been used within the original parameter framework of Pople [14] and Santry and Segal [21] for phosphorus and sulfur respectively. The 4*s*, 4*p* and 3*d* orbitals of nickel were used with the parameters proposed by Baetzold.[22]

All calculations were performed on a Felix C256 computer, using a modified version of PARAMOL-2 program, originally written by Zhogolev and Volkov.[23]

METAL *d*-ORBITAL LEVELS

It is well known that UV photoelectron spectra provide useful information which usually can be correlated with the MO energy levels. Unfortunately, to our best knowledge, for the title compounds no such spectra have been published so far. The only related data available are those reported by Myers [17] and Fragala [24] for alkyldithiophosphato transition metal complexes and Andreocci [25] and Furlani [26] for difluorodithiophosphinato transition metal complexes. In all these spectra, the metal part contributions are quite similar: $Ni(S_2PF_2)_2$ exhibits a broad peak centered at 8.76 eV and $Ni[S_2P(OEt)_2]_2$ two peaks at 7.24 and 8.37 eV respectively; these were assigned to metal *d*—electron ionization potentials (for a detailed disscussion see ref. [26]). Our calculations put four of the five metal *d* orbitals between 8.688 and 8.678 eV. This range compares well with the above mentioned observable peaks. The higher energies of metal *d* orbitals in dialkyldithiophosphinato complexes are probably caused by the lower electronegativity of CH_3 groups than those of F or OR substituents on phosphorus. The relative ordering of the five metal orbitals can be judged from several points of views:

a) Crystal field arguments suggest for a Ni^{2+} ion, in a D_{4h} environment the following splitting pattern:

$$d_{xz} < d_{yz} < d_{z^2} < d_{x^2-y^2} < d_{xy}$$

b) Circular magnetic dichroism data on the other hand order these as follows: [27]

$$d_{z^2} < d_{x^2-y^2} < d_{xz} \approx d_{yz} < d_{xy}$$

c) Electronic spectra of Cavell and coworkers [28] seem to support the extreme parts of these orderings but $d_{x^2-y^2}$ is placed above the (d_{xy}, d_{yz}) tandem:

$$d_{z^2} < d_{xz} \approx d_{yz} < d_{x^2-y^2} < d_{xy}$$

d) The CNDO/2 calculations also predict that the most destabilized orbital is d_{xy} thus lending further support to the crystal field predictions :

$$d_{xz} < d_{z^2} < d_{yz} < d_{x^2-y^2} < d_{xy}$$

TOTAL ENERGY

The total energy of the two dithiophosphinato systems has been expressed in terms of mono and diatomic contributions : E_A and E_{AB}.[29] Some relevant pairs of atoms and their interaction energies are given in Table 1.

Table 1

Covalent diatomic components of total energies in dithiophosphinato- and -phosphato complexes (a.u.)

E_{AB}	$Ni[S_2P(CH_3)_2]_2$ *	$Ni[S_2PH_2)_2$ *	$Ni[S_2P(OH)_2]_2$ **
Ni-S	−0.4210	−0.4423	−1.33
P...Ni	−0.1925	−0.1058	−0.41
$S...S^{intra}$	0.0117	0.0094	0.021
$S...S^{inter}$	0.0095	0.0009	0.029

* This work
** Ref. [15,16]

The metal-sulfur component of the total energy has a smaller value in dithiophosphinato than in dithiophosphato complexes thus reflecting a smaller degree of covalency. This finding excelently correlates with a smaller Ni—S force constant found in bis(dimethyldithiophosphinato) Ni(II) [30] than in bis(dimethyldithiophosphato)Ni(II). [31] Another point of interest is the relatively high value of Ni...P component, denoting an important transannular interaction. Note that this represents one third of the main Ni—S interaction. The same ratio was also found in dithiophosphato metal complexes.[15,16] To prove that this is not a simple artefact of the calculation procedure *i.e.* of the energy partitioning, we quote the unusual high values of the Ni...P Urey-Bradley force constants previously reported from normal coordinate analyses.[30,31] Figure 3 shows the approximate picture of the NiS_2P four membered ring of $Ni(S_2PH_2)_2$. It can be seen that certain molecular orbital fragments do match nickel and phosphorus atomic orbital lobes in such a way that may generate Ni...P transannular bonding interactions.

It is remarkable that such kind of "through-space" interactions between chemically "non-bonded" atoms are no more exotic findings in inorganic chemistry, and many other examples are known by now in the chemistry of inorganic rings (Reference [32] quotes only a few of such examples).

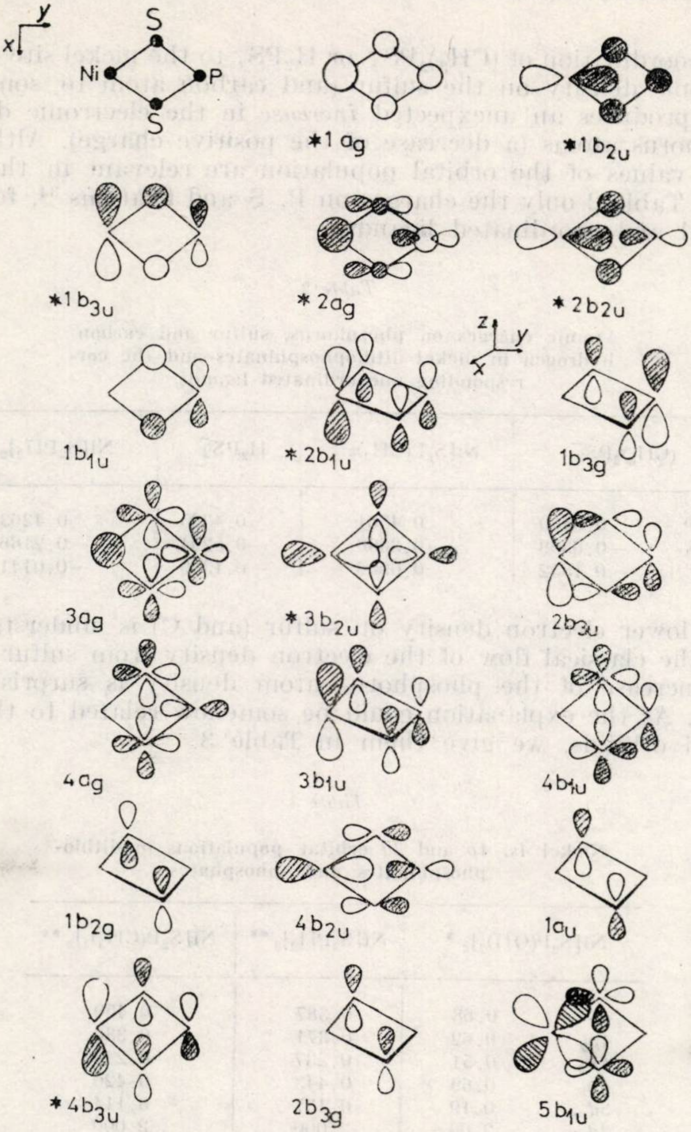
y
x
S
Ni
P
S
*1ag
*1b2u
*1b3u
*2ag
*2b2u
z
x
1b1u
*2b1u
1b3g
3ag
*3b2u
2b3u
4ag
3b1u
4b1u
1b2g
4b2u
1au
*4b3u
2b3g
5b1u

Fig. 3. — Approximate description of the main molecular orbitals of $Ni[S_2PH_2]_2$. D_{2h} point group symmetry notations are used but only one ring part of these mo's is displayed. Those mo's responsible for Ni ... P transannular interaction are marked by an asterisk.

In the model hypothetical compound $Ni(S_2PH_2)_2$ the S...S interligand interactions are about one order of magnitude smaller than the intraligand S...S interactions. In the methyl derivative the difference is not so shocking, nevertheless, it may justify to some extent the 1M : 1L model often used in the normal coordinate analysis of the vibrations of these compounds.[30, 31, 33]

ELECTRONIC POPULATION, BOND ORDERS AND FORCE CONSTANTS

The coordination of $(CH_3)_2PS_2^-$ or $H_2PS_2^-$ to the nickel site diminishes the electronic density on the sulfur (and carbon atom to some extent) but, also, produces an unexpected *increase* in the electronic density on the phosphorus atoms (a decrease of the positive charge). Although the individual values of the orbital population are relevant in this respect, we give in Table 2 only the charges on P, S and C atoms [34], for the uncoordinated and coordinated ligands.

Table 2

Atomic charges on phosphorus, sulfur and carbon/hydrogen in nickel dithiophosphinates and the corresponding uncoordinated ligands

	$(CH_3)_2PS_2^-$	$Ni[S_2P(CH_3)_2]_2$	$H_2PS_2^-$	$Ni[S_2PH_2]_2$
P	0.6400	0.4501	0.4325	0.4263
S	−0.6399	−0.3090	−0.5294	−0.2186
C/H	−0.1552	−0.0906	−0.1369	−0.0141

The lower electron density on sulfur (and C) is understandable in terms of the classical flow of the electron density from sulfur to nickel, but the increase of the phosphorus atom density is surprising at the first sight. As the explanation could be somehow related to the population of Ni orbitals, we give them in Table 3.

Table 3

Nickel 4*s*, 4*p* and 3*d* orbital populations in dithiophosphinates and -phosphates

	$Ni[S_2P(OH)_2]_2$ *	$Ni[S_2PH_2]_2$ **	$Ni[S_2P(CH_3)_2]_2$ **
$4s$	0.68	0.387	0.450
$4p_y$	0.62	0.371	0.380
$4p_z$	0.51	0.237	0.240
$4p_x$	0.69	0.443	0.420
$3d_{xy}$	0.19	0.137	0.114
$3d_{yz}$	2.00	2.000	2.000
$3d_{z^2}$	1.99	1.997	1.997
$3d_{xz}$	2.00	2.000	2.000
$3d_{x^2-y^2}$	1.99	1.990	1.990

* ref.[15,16]
** this work

It can be noticed that besides 4*s* and 4*p*, only $3d_{xy}$ has changed its population relative to the free Ni^{2+} cation. This means that the metal-ligand bonding is realized mainly through Ni 4*s*, 4*p* and $3d_{xy}$ orbitals and the proper combinations of the ligand orbitals. The same metal orbitals were found by Pilipenko *et al.* to be involved in bonding in dithiophosphato metal complexes.[15,16] One may refer to Fig. 3 for a qualitative description of the ring molecular orbitals. As the figure is selfexplanatory no other comments are necessary. Thus the return to the large decrease in the electronic density on sulfur can be formaly explained by a partial electron flow to the nickel ion and also to the phosphorus atom. The latter is enhanced by the occupied *3d* orbitals on Ni, which exert a repulsive effect on the sulfur *p* electrons. This way, the positive charge on phosphorus is diminished and the P—S bond order increases. Hence, a greater P—S force constant is expected in the chelate ring than in the uncoordinated anion. The same result has been found by normal coordinate analysis.[30]

Wiberg bond indices[35] are given in Table 4.

Table 4

Wiberg bond indices and stretching force constants in $Ni[S_2P(CH_3)_2]_2$ and $Ni[S_2PH_2]_2$

	$Ni[S_2P(CH_3)_2]_2$ *			$Ni[S_2PH_2]_2$	
	W	f_{AB}	f_{AB}^{exp}	W	f_{AB}
Ni-S	0.6124	1.24	1.18	0.5634	1.19
P-S	0.8752	2.09	2.99	1.2765	2.91
P-C	0.9746	2.53	2.83	—	—
P-H	—	—	—	0.9747	3.26
C-H	0.9891	5.26	5.40	—	—

* experimental force constants, mdyne/Å, taken from ref. [30]

The Ni—S bond order is quite low suggesting a relatively low degree of covalency. The P—S bond order in the methyl derivative is also smaller than expected, probably due to the smaller basis set on phosphorus (no *3d* orbitals included in calculations for this compound). When phosphorus *3d* orbitals are taken into account as in $Ni(S_2PH_2)_2$, a reasonable P—S bond index is obtained. These bond indices are good starting points for empirical estimation of the stretching force constants.

REFERENCES

[1] I. Haiduc, *Revs. Inorg. Chem.*, **3**, 353 (1981).
[2] I. Haiduc and I. Silaghi-Dumitrescu, *Coord. Chem, Revs.*, 1986, accepted for publication.
[3] I. Haiduc, *Rev. Chim. (București)*, **33**, 234 (1982).
[4] J. R. Wasson, G. M. Woltermann and H. J. Stoklosa, *Fortschr. Chem. Forsch.* (Topics Curr. Chem.), **35**, 65 (1973) : W. Kuchen and H. Hertel, *Angew. Chem.*, **81**, 127 (1969) ; *Angew. Chem. Internat. Ed. Engl.*, **8**, 89 (1969).
[5] K. C. Molloy and J. J. Zuckerman, *Acc. Chem. Res.*, **16**, 386 (1983) ; RC. Mehrotra, G. Srivastava and B. P. S. Chauhan, *Coord. Chem. Revs.*, **55**, 207 (1984).
[6] D. B. Sowerby and I. Haiduc, *Inorg. Chim. Acta*, **17**, 15 (1976).
[7] D. B. Sowerby and I. Haiduc, *Inorg. Nucl. Chem. Lett.*, **1** , 791 (1976).

[8] I. Haiduc and M. Curtui, *Synth. React. Inorg. Metalorg. Chem.*, **6**, 125 (1976).

[9] M. Curtui and I. Haiduc, *J. Inorg. Nuclear Chem.*, **43**, 1076 1981).

[10] J. L. Lefferts, K. C. Molloy and J. J. Zuckerman, I. Haiduc, C. Guţă and D. Ruse, *Inorg. Chem.*, **19**, 1662, 2861 (1980).

[11] I. Haiduc, C. Silvestru and M. Gielen, *Bull. Soc. chim. belges*, **92**, 187 (1983).

[12] R. Constantinescu, F. Martinaş and I. Haiduc, *Inorg. Chim. Acta*, **19**, 105 (1976).

[13] R. Micu-Semeniuc, L. Silaghi-Dumitrescu and I. Haiduc, *Inorg. Chim. Acta*, **17**, 5 (1976); **33**, 281 (1979).

[14] J. A. Pople and G. A. Segal, *J. Chem. Phys.*, **43**, S 129, 136 (1965).

[15] A. T. Pilipenko, L. I. Savranskii, A. I. Zubenko, V. P. Kobylyashii and A. L. Rosenfeld *Doklady Akad. Nauk S.S.S.R.*, **243**, 378 (1979).

[16] A. T. Pilipenko, L. I. Savranskii and A. I. Zubenko, *Koord. Khim.*, **7**, 25 (1981).

[17] K. Myers and G. Andermann, *J. Phys. Chem.*, **77**, 280 (1973).

[18] D. V. Sokol'skii, L. M. Kurashvilli, I. B. Bersuker, S. S Budnikov and I. A. Zavorohina, *Doklady Akad. Nauk S.S.S.R.*, **198**, 126 (1971).

[19] H. J. Stoklossa, G. L. Seebach and J. R. Wasson, *J. Phys. Chem.*, **78**, 962 (1974).

[20] P. E. Jones, G. B. Ansell and L. Katz, *Acta Cryst.*, B**25**, 1939 (1969).

[21] D. P. Santry and G. A. Segal, *J. Chem. Phys.*, **47**, 158 (1967).

[22] R. C. Baetzold, *J. Chem. Phys.*, **55**, 4355, 4363 (1971).

[23] D. A. Zhogolev and V. B. Volkov, "Metody, Algoritmy i Programy dlya Kvantovo-Khimicheskih Raschetov Molekul", Kiev, Naukova Dumka, 1976.

[24] I. Fragala, D. S. Giuffrida, E. Ciliberto and G. Condorelli, *Chimical Industrial (Milan)*, **58**, 656 (1976).

[25] M. V. Andreocci, P. Dragoni, A. Flamini and C. Furlani, *Inorg. Chem.*, **17**, 291 (1978).

[26] C. Furlani and C. Cauletti, *Struct. and Bonding*, **35**, 119 (1978).

[27] O. Looney and B. E. Douglas, *Inorg. Chem.*, **9**, 1955 (1970).

[28] R. G. Cavell, M. Byers, E. D. Day and P. M. Watkins, *Inorg. Chem.*, **11**, 1958 (1972).

[29] H. Fischer and H. Komar, *Theor. Chim. Acta*, **16**, 163 (1970).

[30] I. Silaghi-Dumitrescu and I. Haiduc, *Rev. Roumaine Chim.*, **25**, 815, 823 (1980).

[31] W. Rudzinski, G. F. Behnke and Q. Fernando, *Inorg. Chem.*, **19**, 1206 (1977).

[32] a) P ... P interactions in $(X_2PN)_3$: D. R. Armstrong, G. H. Langmuir and P. G. Perkins, *J. Chem. Soc., Chem. Commun.*, 464 (1972); J. P. Foucherrand and J. F. Labarre, *Phosphorus*, **3**, 265 (1974);

b) Al ... N interactions in $Me_2NAlH_2)_3$: M. Pelissier, J. F. Labarre, L. V. Vilkov, A. Golubinsky and V. S. Mastryukov, *J. Chim. phys.*, **71**, 702 (1974);

c) S ... S interactions in N_4S_4 : P. Cassoux, J. F. Labarre, O. Glemser and W. Koch, *J. Mol. Struct.*, **13**, 405 (1972);

d) Si ... Si interactions in cyclodisiloxanes (-silazanes); T. Kudo and S. Nagase, *J. Amer. Chem. Soc.*, **107**, 2589 (1985), see also, I. Silaghi-Dumitrescu and I. Haiduc, *Inorg. Chim. Acta*, **11**, 159 (1986).

[33] I. Haiduc, I. Silaghi-Dumitrescu, R. Grecu, L. Silaghi-Dumitrescu and R. Constantinescu, *J. Mol. Struct.*, **114**, 467 (1984).

[34] A complete orbital population is available on request.

[35] K. B. Wiberg, *Tetrahedron*, **24**, 1083 (1968).

Revue Roumaine de Chimie, **31**, *11–12*, 963–972 (1986)

Professor P. SPACU zum 80. Geburtstag gewidmet

RÖNTGENOGRAPHISCHE UND IR-SPEKTROSKOPISCHE UNTERSUCHUNGEN DER THERMOLYSE VON ALKALIPENTAFLUOROALUMINATHYDRATEN

U. BENTRUP und L. KOLDITZ

Zentralinstitut für Anorganische Chemie der Akademie der Wissenschaften der DDR, Berlin-Adlershof

Eingegangen am 10. Mai 1986

The thermolysis of $M^I_2AlF_5 \cdot H_2O$($M = NH_4$, K, Rb) was investigated by X-ray diffraction and IR-spectroscopy in a temperature range of 20–600°C. Different behaviour on thermal treatment can be observed depending on the kind of water bonding. By comparison of the isomeric compounds $Rb_2AlF_5 \cdot H_2O$ and $Rb_2[AlF_5(H_2O)]$ – the latter was prepared now – this fact can be clearly shown. Pentafluoroaluminate hydrates with lattice water and chains of AlF_6 octahedra are much more stable than compounds with coordinated water and isolated $[AlF_5(H_2O)]$ octahedra. In the first case dehydration is detected at essentially higher temperatures. The dehydrated products $M^I_2AlF_5$ can be obtained only from the compounds with lattice water. Hydrates with coordinated water were decomposed by dehydration into M^IAlF_4 and $M^I_3AlF_6$. At higher temperatures hydrolysis of $M^I_2AlF_5$ and M^IAlF_4 is observed.

Die Thermolyse von $M^I_2AlF_5 \cdot H_2O$($M = NH_4$, K, Rb) wurde im Temperaturbereich 20–600°C rötgenographisch und IR-spektroskopisch untersucht. In Abhängigkeit von der Art der Wasserbindung wird ein unterschiedliches Verhalten bei thermischer Behandlung beobachtet. Besonders aus dem Vergleich der Hydratisomeren $Rb_2AlF_5 \cdot H_2O$ und $Rb_2[AlF_5(H_2O)]$-letzteres wurde neu dargestellt – wird deutlich, daß Pentafluoroaluminathydrate mit Gitterwasser und AlF_6-Oktaeder-Ketten wesentlich stabiler bzw. schwerer zu entwässern sind als die mit koordinativ gebundenem Wasser und isolierten $[AlF_5(H_2O)]$-Oktaedern. Wasserfreie Produkte M_2AlF_5 sind nur von den Hydraten mit Gitterwasser erhältlich. Hydrate mit koordinativ gebundenem Wasser dismutieren bei Wasserabgabe sofort in M^IAlF_4 und $M^I_3AlF_6$. Bei höherer Temperatur ist Hydrolyse von $M^I_2AlF_5$ und M^IAlF_4 zu beobachten.

1. EINLEITUNG

Alkalipentafluormetallathydrate dreiwertiger Me-Kationen sind vom strukturellen Standpunkt aus in zwei verschiedene Gruppen einzuordnen. Für die erste Gruppe sind MeF_6-Oktaederketten charakteristisch, die durch dazwischen eingelagerte Alkalikationen und Wasser stabilisiert werden.

Die zweite Gruppe ist dadurch gekennzeichnet, daß isolierte $[MeF_5(H_2O)]$-Oktaeder als bestimmendes Strukturelement auftreten.

Im speziellen Fall des Aluminiums sind die Pentafluoroaluminathydrate und deren Strukturen vom Ammonium, Kalium und Rubidium bekannt; zum Teil liegen auch IR-Spektroskopische Untersuchungen vor.

Die Struktur des orthorhombischen $(NH_4)_2AlF_5 \cdot H_2O$ ist von Knop und Mitarbeitern[1] bestimmt worden. Sie ist gekennzeichnet durch das Vorhandensein isolierter $[AlF_5(H_2O)]$-Oktaeder, die durch Wasserstoffbindung der Form F ... H–O–H ... F' verbunden sind und sich in Zick-Zack-Ketten parallel zur o-Achse anordnen. Diese Ketten sind abwechselnd innerhalb und zwischen den Schnichten durch normale, teilweise etwas gekrümmte N-H...F – und N-H...F'-Wasserstoffbindung verbunden.

Bei den orthorhombischen Verbindungen $K_2AlF_5 \cdot H_2O$ und $Rb_2AlF_5 \cdot H_2O$ liegen leicht geknickte Ketten von über jeweils zwei Ecken *trans*-verknüpften AlF_6-Oktaedern vor[2,3]. Alkalikationen und Wassermoleküle befinden sich zwischen diesen Ketten. Zwischen den Wassermolekülen und F-Atomen der angrenzenden Oktaeder tritt Wasserstoffbindung auf, durch welche die Kettenstruktur stabilisiert wird.

IR-spektroskopisch lassen sich beide Strukturgruppen der Pentafluorometallathydrate gut unterscheiden. Bukovec und Mitarbeiter[4] haben dazu wesentliche Beiträge geleistet. Auch andere Autoren[5,6] diskutieren anhand IR-spektroskopischer Untersuchungen die Art der Wasserbindung bei diesen Verbindungen.

Prinzipiell ist zu unterscheiden, ob es sich um Gitterwasser (Gruppe 1) oder koordinativ gebundenes Wasser (Gruppe 2) handelt.

Demnach liegt die Valenzschwingung des Wassers bei Gruppe 1 um 3 300–3500 cm^{-1}; bei Verbindungen der Gruppe 2 um ca. 300–400 cm^{-1} erniedrigt bei 3100 cm^{-1}. Die Deformationsschwingungen des Wassers liegen im selben Bereich, sind bei Verbindungen der Gruppe 2 jedoch wesentlich schwächer. Die Librationsschwingungen haben etwas höhere Frequenzen als die gleichen Schwingungen der Gruppe 1 und sind stärker ausgeprägt.

Die wasserfreien Alkalipentafluoroaluminate sind im Prinzip durch thermische Entwässerung unter Inertgas erhältlich,[2,7] jedoch erscheint es nach[3] fraglich, ob die Kettenstruktur ohne die stabilisierende Wirkung des Wassers überhaupt existent ist.

Für Verbindungen der Gruppe 2 ist ohnehin eine geringere Stabilität bei thermischer Behandlung und eine starke Umorientierung im Gitter bei Verlust von Wasser zu erwarten.

Besonders diese letztgenannte Problematik sollte im Rahmen unserer Untersuchungen näher beleuchtet werden und ist Gegenstand des vorliegenden Berichts.

2. ERGEBNISSE

2.1. Allgemeines

Wir haben in unsere Untersuchungen sowohl Verbindungen der Gruppe 1 als auch der Gruppe 2 einbezogen. Alle Verbindungen sind analytisch, röntgenographisch und IR-spektroskopisch charackterisiert worden

(Tab. 1). Durch eine spezielle Synthesevariante gelang es, neben dem bekannten $Rb_2AlF_5 \cdot H_2O$ eine noch nicht beschriebene, der Strukturgruppe 2 zuzuordnende Verbindung $Rb_2[AlF_5(H_2O)]$ darzustellen, d.h., von der Rb-Verbindung sind zwei Hydratisomere existent.

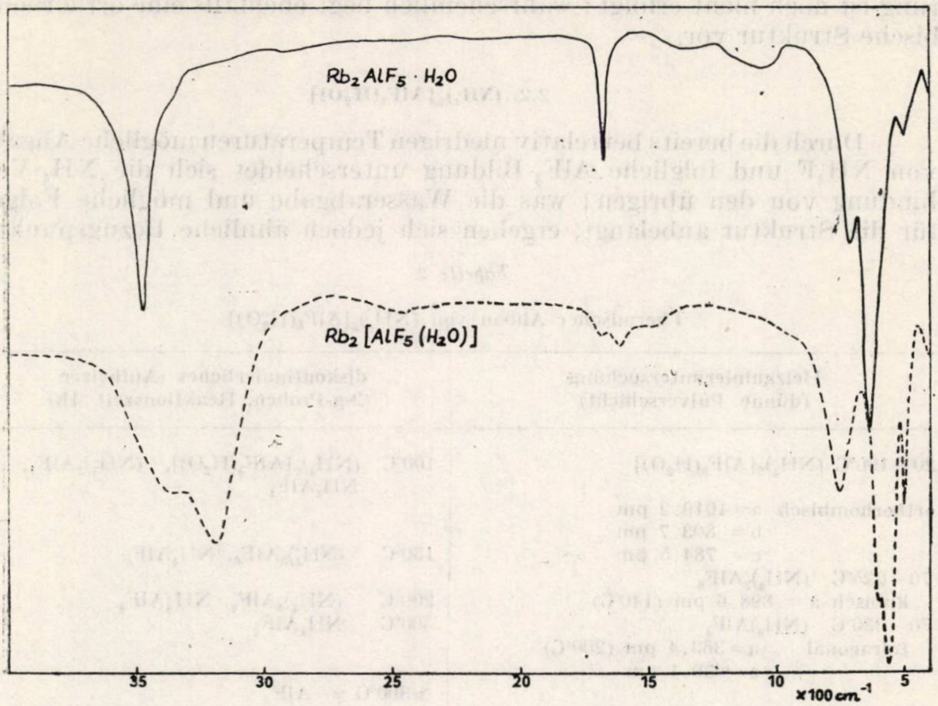

Abb. 1. — Ir-Spektren von $Rb_2AlF_5 \cdot H_2O$ und $Rb_2[AlF_5(H_2O)]$.

Tabelle 1

Schwingungsfrequenzen (cm^{-1}) der untersuchten Verbindungen $M^I_2AlF_5 \cdot H_2O$

	$K_2AlF_5 \cdot H_2O$	$Rb_2AlF_5 \cdot H_2O$	$Rb_2[AlF_5(H_2O)]$	$(NH_4)_2[AlF_5(H_2O)]$
$\nu(H_2O)$	3480 vs	3475 vs	3350 s 3200 s	3175 s
$\nu(H_2O)$	1665 vs	1675 vs	1690 w 1615 w	1620 w
lib (H_2O)	735 m	705 m	755 s	855 m 740 s
ν_3	520 m 645 vs	500 m 630 vs	504 s 563 vs	510 s 575 vs

Diese Einordnung der Verbindung stützt sich auf die für Gruppe 2 charakteristischen starken Banden bei 3200 cm^{-1} (νH_2O) und 755 cm^{-1} (lib H_2O) (Abb. 1) sowie die im Vergleich zu $Rb_2AlF_5 \cdot H_2O$ erniedrigte

ν_3(Al-F)-Bande bei 565 cm^{-1}; letztere ist typisch für das Vorhandensein isolierter AlF_6-bzw. [$AlF_5(H_2O)$]-Oktaeder.[8] Letztlich sind die IR-Spektren der Rb- und NH_4-Verbindung sehr ähnlich (Tab. 1), so daß die Zuordnung zu Gruppe 2 gerechtfertigt wird. Eine röntgenographische Indizierung ist noch nicht erfolgt; wahrscheinlich liegt ebenfalls eine orthorhombische Struktur vor.

2.2. $(NH_4)_2[AlF_5(H_2O)]$

Durch die bereits bei relativ niedrigen Temperaturen mögliche Abgabe von NH_4F und folgliche AlF_3-Bildung unterscheidet sich die NH_4-Verbindung von den übrigen; was die Wasserabgabe und mögliche Folgen für die Struktur anbelangt, ergeben sich jedoch ähnliche Bezugspunkte.

Tabelle 2

Thermischer Abbau von $(NH_4)_2[AlF_5(H_2O)]$

Heizguinieruntersuchung (dünne Pulverschicht)	diskontinuierliches Aufheizen (2-g-Proben, Reaktionszeit 1h)
20–190°C $(NH_4)_2[AlF_5(H_2O)]$	100°C $(NH_4)_2[AlF_5(H_2O)]$, $(NH_4)_3AlF_6$, NH_4AlF_4
orthorhombisch a = 1019.2 pm b = 803.7 pm c = 784.5 pm	150°C $(NH_4)_3AlF_6$, NH_4AlF_4
70–225°C $(NH_4)_3AlF_6$ kubisch a = 898.6 pm (140°C)	200°C $(NH_4)_3AlF_6$, NH_4AlF_4
70–330°C $(NH_4)AlF_4$ tetragonal a = 363.4 pm (200°C) c = 639.1 pm	300°C NH_4AlF_4
155–550°C γ–AlF_3 tetragonal a = 355.2 pm (400°C) c = 605.7 pm	>300°C γ–AlF_3
über 550°C amorph	

Die beim thermischen Abbau erhaltenen Produkte sowohl bei Zersetzung in dünner Schicht als auch bei Verwendung größerer Probemengen sind in Tab. 2 aufgeführt. Es sollte noch vermerkt werden, daß Zersetzungs- und Umwandlungstemperaturen in dünner Schicht grundsätzlich tiefer liegen und damit nicht unmittelbar vergleichbar mit Untersuchungen größerer Probemengen sind.

Prinzipiell zeigt sich jedoch, daß die Struktur mit der Abgabe von Wasser instabil wird, d.h., es erfolgt eine Dismutierung in NH_4AlF_4 (Schichtstruktur, Verknüpfung der AlF_6-Oktaeder über vier Ecken: $[AlF_2F_{4/2}]$), und $(NH_4)_3AlF_6$ (isolierte AlF_6-Oktaeder). Eine vollständige Entwässerung wird erst bei 150°C erreicht; der Masseverlust beträgt dann 10,6 % (theoret. 10,3 %). Der weitere Verlauf der thermischen Zersetzung erfolgt in bekannter Weise [9,10] durch Abgabe von NH_4F über NH_4AlF_4 bis hin zum γ-AlF_3. Der gleiche schematische Verlauf ergibt sich aus den Heizguinieruntersuchungen. Die ermittelten Gitterkonstanten von $(NH_4)_3AlF_6$, NH_4AlF_4 und γ-AlF_3 entsprechen den bei erhöhter Temperatur etwas aufgeweiteten Gittern.

2.3. $K_2AlF_5 \cdot H_2O$

Bukovec und Mitarbeiter[4] geben für die Entwässerung einen Temperaturbereich von 70–180°C an, wobei das DTG-Minimum bei 150° liegt. Aus unseren Untersuchungen folgt (Tab. 4), daß eine vollständige Entwässerung erst oberhalb 200°C erreicht wird. Eine Dismutierung setzt nicht ein, vielmehr entsteht neben etwas $KAlF_4$ eine Phase, die sich tetragonal indizieren läßt. Entwässert man $K_2AlF_5 \cdot H_2O$ bei 300°C im Inertgasstrom, erhält man auch diese Phase mit dem gleichen in Abb. 2 dargestellten Ir-Spektrum, aber ohne Verunreinigung mit $KAlF_4$.

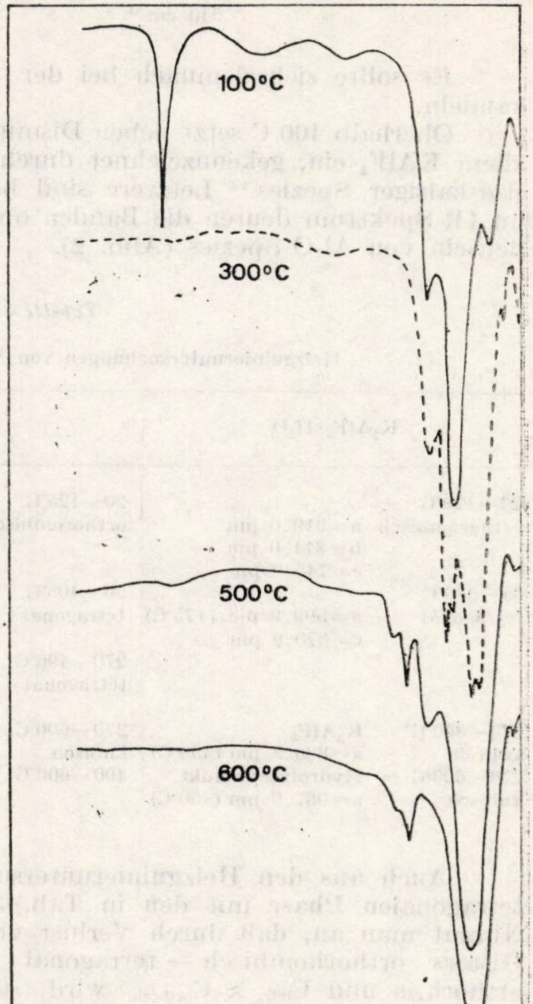

Abb. 2. — IR-Spektren (Ausschnitt) der bei thermischer Behandlung von $K_2AlF_5 \cdot H_2O$ erhaltenen Produkte.

---

[4] — c. 2473

Vergleicht man das IR-Spektrum mit dem von Bukovec und Mitrabeiter[11] für Tl_2AlF_5 gemessenen, so ergibt sich bezüglich der Banden für ν_3(Al-F) eine gute Übereinstimmung:

Tl_2AlF_5 : 675 cm^{-1} tetr. Phase : 650 cm^{-1}, 670 cm^{-1}

540 cm^{-1} 578 cm^{-1}, 555 cm^{-1}

Es sollte sich demnach bei der tetragonalen Phase um K_2AlF_5 handeln.

Oberhalb 400°C setzt neben Dismutierung auch Hydrolyse von vor allem $KAlF_4$ ein, gekennzeichnet durch Bildung von K_3AlF_6 und sauerstoffhaltiger Spezies.[12] Letztere sind bei 500–600°C amorph; lediglich im IR-Spektrum deuten die Banden oberhalb 800 cm^{-1} auf das Vorhandensein von Al-O-Spezies (Abb. 2).

Tabelle 3

Heizguinieruntersuchungen von $M_2AlF_5 \cdot H_2O$, M= K, Rb

$K_2AlF_5 \cdot H_2O$		$Rb_2AlF_5 \cdot H_2O$		$Rb_2[AlF_5(H_2O)]$
20–120°C orthorombisch	a=919.0 pm b=811.0 pm c=745.0 pm	20–125°C orthorombisch	a=960.4 pm b=837.8 pm c=754.2 pm	20–180°C
65–380°C tetragonal	a=599.9 pm (175°C) c=370.9 pm	50–405°C tetragonal	a=628.2 pm(220°C) c=376.9 pm	
		270–490°C tetragonal	$RbAlF_4$ a=519.3 pm (340°C) c=634.6 pm	175–450°C
270–600°C kubisch	K_3AlF_6 a=860.3 pm (450°C)	270–600°C kubisch	Rb_3AlF_6 a=896.8 pm (505°C)	175–600°C
270–600°C kubisch	Hydrolyseprodukt a=987.0 pm (450°C)	400–600°C	Hydrolyseprodukt	430–600°C

Auch aus den Heizguinieruntersuchungen folgt die Bildung einer tetragonalen Phase mit den in Tab. 3 angegebenen Gitterkonstanten. Nimmt man an, daß durch Verlust von Wasser eine Umwandlung des Gitters orthorhombisch → tetragonal erfolgt, wobei $a_{tetr.} \approx (a + b)$ orthorh./s und $c_{tetr.} \approx c_{orthorh.}$ wird, so würde man erhalten: $a_{tetr.} = 865$ pm, wobei sich $a/\sqrt{2} = 611{,}6$ pm ergibt und $c_{tetr.} = 745$ pm, wobei $c/2 = 372{,}5$ pm ist.

Die Werte kommen denen der erhaltenen tetragonalen Phase sehr nahe, so daß es sich hierbei um eine Hochtemperaturform von K_2AlF_5 handeln sollte. Nach Brosset[2] ist K_2AlF_5 orthorhombisch; HT-Phasen sind nicht untersucht worden.

In der Heizguinieraufnahme ist kein $KAlF_4$ nachweisbar; vielmehr erfolgt Hydrolyse unter Bildung von K_3AlF_6 und einem noch nicht näher charakterisierbaren kubischen Hydrolyseprodukt.

2.4. $Rb_2AlF_5 \cdot H_2O$ und $Rb_2[AlF_5(H_2O)]$

Aus Tab. 4 wird deutlich, daß $Rb_2AlF_5 \cdot H_2O$ wesentlich stabiler bzw. schwerer zu entwässern ist als das Hydratisomere, d.h., Gitterwasser ist wesentlich schwieriger zu entfernen als koordinativ gebundenes.

Tabelle 4

Thermolyse von $M_2AlF_5 \cdot H_2O$, M= K, Rb — Phasenzusammensetzung in Abhängigkeit von der Temperatur (2-g-Proben, Reaktionszeit 1 h)

Temperatur (°C)	$K_2AlF_5 \cdot H_2O$	$Rb_2AlF_5 \cdot H_2O$	$Rb_2[AlF_5(H_2O)]$
100	$K_2AlF_5 \cdot H_2O$	$Rb_2AlF_5 \cdot H_2O$	$Rb_2[AlF_5(H_2O)]$ $RbAlf_4$ $RbAlF_6$
200	$K_2AlF_5 \cdot H_2O$	$Rb_2AlF_5H_1O$	$RbAlF_4$ $Rb_2AlF_5 \cdot H_2O$
300—400	$KAlF_4$ tetr. Phase′	$Rb_2AlF_5 \cdot H_2O$ Rb_3AlF_6 $RbAlF_4$ tetr. Phase″	Rb_3AlF_6 $RbAlF_4$ tetr. Phase″
500—600	K_3AlF_6	Rb_3AlF_6 Hydrolyseprodukt	Rb_3AlF Hydrolyseprodukt

tetragonale Phase′: a = 1217 pm c = 1090 pm
tetragonale Phase″: a = 1460 pm c = 1190 pm

Auch im Falle der Rb-Verbindung wird (hier jedoch neben Dismutierungsprodukten) eine tetragonale Phase gebildet. Ob diese in reiner Form durch Entwässerung unter Inertgas erhältlich ist, konnte noch nicht überprüft werden.

Daß bei Heizguinieruntersuchungen (Tab. 3) auch $RbAlF_4$ gefunden wurde, weist aber darauf hin, daß Rb_2AlF_5-sofern existent — wesentlich leichter dismutiert als die entsprechende K-Verbindung.

Oberhalb 400°C setzt auch hier Hydrolyse ein (u.a. gekennzeichnet dadurch, daß im IR-Spektrum die Bande bei 720 cm^{-1} verschwindet und bei 600°C nur noch die für Rb_3AlF_6 typische Bande bei 575 cm^{-1} vorhanden ist.), wobei eine nähere Charakterisierung des Hydrolyseprodukts noch nicht möglich ist.

Die Heizguinieraufnahme von $Rb_2[AlF_5(H_2O)]$ weist die größere Instabilität bei Verlust von Wasser deutlich aus; die Dismutierungsprodukte $RbAlF_4$ und Rb_3AlF_6 treten auf, wobei bei höheren Temperaturen die bereits beschriebene Hydrolyse von $RbAlF_4$ einsetzt.

Zu bemerken ist vor allem noch die Tatsache, daß die Art der Wasserbindung vor der vollständigen Entwässerung wechselt, wie aus dem Vergleich der IR-pektren bei 100 und 200°C (Abb. 3) und der zwischenzeitlichen Bildung von $Rb_2AlF_5 \cdot H_2O$ (Tab. 4) deutlich wird.

3. Zusammenfassende Diskussion

Aus den IR-spektroskopischen und Heizguinieruntersuchungen der thermischen Entwässerung von Pentafluoroaluminat-hydraten konnte das unterschiedliche Verhalten der nach Art der Wasserbindung in zwei Gruppen auftretenden Verbindungen nachgewiesen werden.

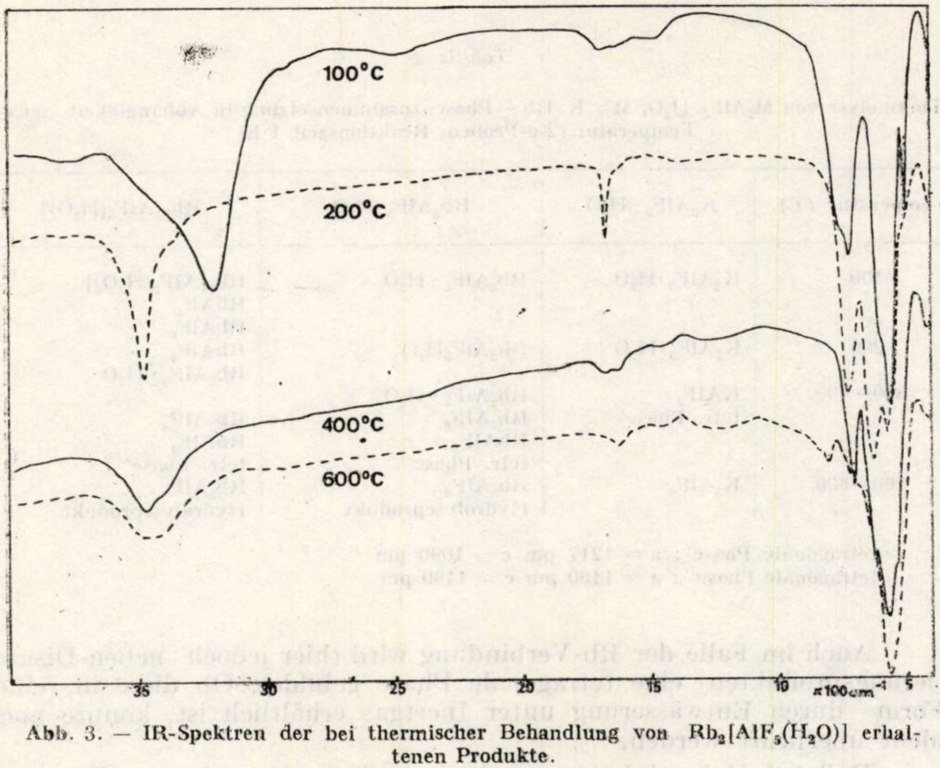

Abb. 3. — IR-Spektren der bei thermischer Behandlung von $Rb_2[AlF_5(H_2O)]$ erhaltenen Produkte.

Pentafluoroaluminathydrate mit koordinativ gebundenem Wasser und isolierten $[AlF_5(H_2O)]$-Oktaedern (NH_4 — u. Rb-Verbindung) lassen sich bei tieferen Temperaturen und im wessentlichen ohne Hydrolyse entwässern. Da die Wasserabgabe eine starke Störung der Oktaedersymmetrie bedingt, erfolgt die Absättigung der Koordination am Al sowohl durch Bildung von M^IAlF_4 als auch $M^I_3AlF_6$, d.h., kondensierte und isolierte AlF_6-Oktaeder.

Pentafluoroaluminate mit AlF_6-Oktaederketten und Gitterwasser (K- und Rb-Verbindung) sind thermisch wesentlich stabiler. Eine vollständige Entwässerung wird erst oberhalb 300°C möglich. Das reine wasserfreie Produkt ist bislang nur von der K- Verbindung bekannt. Bei höheren Temperaturen tritt sowohl Dismutierung als auch Hydrolyse auf. Hydrolyseprodukte sind wahrscheinlich Fluoroxoaluminate, da Al_2O_3, wie in anderen Fällen nachgewiesen,[12] nicht gebildet wird.

Schematisch lassen sich die beschriebenen Prozesse mit folgenden Gleichungen beschreiben:

$$2(NH_4)_2[AlF_5(H_2O)] \rightarrow (NH_4)_3AlF_6 + NH_4AlF_4 + 2H_2O \tag{1}$$

$$(NH_4)_3AlF_6 \rightarrow NH_4AlF_4 + 2NH_4F$$

$$NH_4AlF_4 \rightarrow \gamma AlF_3 + NH_4F$$

$$2Rb_2[AlF_5(H_2O)] \rightarrow Rb_3AlF_6 + RbAlF_4 + 2H_2O \tag{2}$$

$$3RbAlF_4 \xrightarrow{\text{Hydrolyse}} Rb_3AlF_6 + \text{Hydrolyseprodukt} + HF$$

$$\begin{tikzcd}
2M^I_2AlF_5 \cdot H_2O \arrow[r] & 2M_2AlF_5 \arrow[r, "\text{Dismutierung}"] \arrow[d, dashed] & M^IAlF_4 + M^I_3AlF_6 \arrow[dl, "\text{Hydrolyse}"] \\
 & Rb_3AlF_6 + \text{Hydrolyseprodukt} + HF &
\end{tikzcd}$$ (3)

4. EXPERIMENTELLES

Darstellung der untersuchten Verbindungen

$(NH_4)_2[AlF_5(H_2O)]$: durch Fällung aus Floroaluminiumsäurelösung mit $NH_3(g)$.[13]

$K_2AlF_5 \cdot H_2O$: aus KF-haltiger Fluoroaluminiumsäurelösung durch Fällung mit EtOH.

$Rb_2[AlF_5(H_2O)]$: Aus einer Rb-haltigen Fluoroaluminiumsäurelösung (Molverhältnis Rb : Al = 1 : 1) wird zunächst ein saures Rb-Fluoroaluminat mit EtOH gefällt, welches abfiltriert wird. Durch Schütteln dieses Niederschlags mit Wasser erhält man als Rückstand das Hydrat.

$Rb_2AlF_5 \cdot H_2O$: durch Lösen von $Rb_2[AlF_5(H_2O)]$ in 40 %iger HF und anschließendem Eindampfen bis zur Trockne.

Analytik

Fluorid wurde nach Seel,[14] Aluminium nach Aufschluß mit $K_2S_2O_7$ komplexometrisch mit Xylenolorange, Ammonium nach Kjeldahl, Kalium und Rubidium nach Aufschluß mit $NaHSO_4$ mit Natriumtetraphenyloborat bestimmt.

Die Thermolyse wurde zum einen in dünner Pulverschicht mit Hilfe von Hochtemperatur-Röntgenuntersuchungen (Heizguinieraufnahmen) verfolgt. Es wurde dynamisch mit einer Aufheizgeschwindigkeit von 2,5 grd/min von 20 auf 600°C aufgeheizt. Zum anderen wurden 2g-Proben jeweils 1h bei entsprechenden Temperaturen (50—600°C) erhitzt, und die Phasenzusammensetzung röntgenographisch bestimmt sowie IR-spektroskopisch (KBr-Preßling, Specord IR — 75) verfolgt.

LITERATUR

[1] O. Knop, T. S. Cameron, S. P. Deraniyagala, und D. Adhikesavalu, *Can. J. Chem.*, **63**, 516 (1985).

[2] C. Brosset, Doctoral dissertation, Stockholm 1942, *Structure Reports*, **19**, 324 (1955).

[3] J. -L. Fourquet, F. Plet und R. De Pape, *Rev. Chim. Miner.*, **18**, 19 (1981).

[4] P. Bukovec, B. Orel und J. Siftar, *Monatshefte Chem.*, **104**, 194 (1973) ; **105**, 1299 (1974).

[5] E. N. Deichman, Yu. Ya. Kharitonov und A. A. Schachnasarjan, *Zh. Neorg. Khim.*. **16**, 3271 (1971).

[6] K. I. Petrov, I. V. Tananajev und T. B. Vorotilina, *Zh. Neorg. Khim.*, **16**, 1534 (1971),

[7] J. Schooman, E. E. Hellstrom und R. A. Huggins, *J. Solid State Chem.*, **18**, 325 (1976).

[8] U. Bentrup, R. Stodolski und L. Kolditz, *Z. Chem.*, im Druck.

[9] D. B. Shinn, D. S. Crocket und H. M. Haendler, *Inorg. Chem.*, **5**, 1927 (1966).

[10] L. K. Beck, B. Haendler Kugler und H. M. Haendler, *J. Solid State Chem.*, **8**, 312 (1973).

[11] P. Bukovec, B. Orel und J. Siftar, *Monatshefte Chem.*, **102**, 885 (1971).

[12] U. Bentrup un L. Kolditz, *Z. anorg. allg. Chem.*, im Druck.

[13] DD-Patent WP CO1F 284070/5, 10.12.1985.

[14] F. Seel, E. Steigner und J. Burger, *Angew. Chem.*, **76**, 532 (1964).

Revue Roumaine de Chimie, 31, *11–12*, 973–980 (1986)

Dedicated to Professor P. SPACU on his 80th anniversary

HYDROTHERMAL CRYSTALLIZATION OF ZEOLITE Na-X

E. PINCOVSCHI and M. MERCHEŞ
Polytechnic Institute, Department of Inorganic Chemistry
Splaiul Independenţei 313, 76206 Bucharest, Romania

Received May 18, 1986

Some of the processes suggested or applied for the manufacture of zeolite Na-X, stipulate a technologically difficult step of quiescent aging, followed by another lengthy stage of hydrothermal crystallization. Careful consideration of the parameters which control the synthesis, namely alkalinity, mixing rate, temperature of mixing, stirring during crystallization, etc., allows to shorten appreciably the time required for complete crystallization of zeolite Na-X on the laboratory scale. Tentative methods are given to eliminate the aging step of the gel precipitated from sodium aluminate and silicate solutions.

INTRODUCTION

Commercial utilization of synthetic zeolites is based on their selectivity as sorbents and filters at the molecular level, [1] ion exchange properties [2] and catalytic activity as well.[3–10]

Among the about 100 types of synthetic zeolites, zeolite X has an important practical significance due to a wide variety of applications including the removal of water and carbon dioxide from the air being fed to oxygen /nitrogen eigenfactors, separation of xylenes in petrochemical industry [11,12] and removal of sulfur compounds from reformer recycle hydrogen and isomerization feed. [13]

Because of the large number of zeolities[14–17] which can be obtained in the 4-component system, $Na_2O - Al_2O_3 - SiO_2 - H_2O$, it is necessary, in order to get a certain lattice type in pure form, to work under strictly defined conditions. Among the critical parameters there are the type of SiO_2 used, the quantitative ratios between all the starting components, the temperature and the reaction time. In addition, it has been found that another critical parameter, in the synthesis of the highly porous faujasite structure, is whether or not the reaction mixture is stirred during gel preparation, heating to the crystallization temperature and crystallization itself. Thus, stirring is accompanied by the gradual formation of an undesirable zeolite, referred to as B or P and characterized [18] by narrow pore openings and low adsorption capacity, as well.

Commercial manufacture of molecular sieves without continuous mechanical stirring is extremely difficult due to heat transfer problems which prevent an efficient heating of the reaction mixture and keep the crystallization temperature at a constant level. These difficultis have resulted in the development of processes for the manufacture of zeolite Na—X on a commercial scale which requires a lengthy aging step, hot-mixing of the reactants or seeding.[19-21] Some of the processes applied, although use stirring, provide a zeolite Na—X unstable to dehydration — rehydration cycles and consequently with variable adsorption capacity.

In the present work we attempted to improve the economy of faujasite synthesis by reducing to a minimum the time needed for complete crystallization and by eliminating the aging step. For this purpose 59 compositions of sodium aluminosilicate gel were crystallized under a range of conditions, by varying : alkalinity, mixing, rate temperature of mixing, stirring during crystallization and the additives.

EXPERIMENTAL

As starting materials for zeolite synthesis were used commercial-grade waterglass type SE (26.62 SiO_2, 8.89 Na_2O, 64.49 H_2O), alumina trihydrate (61.67 Al_2O_3, 38.23 H_2O) and sodium hydroxide (77.03 Na_2O, 22.87 % wt/wt H_2O), characterized by chemical analysis.

The mixing of the reactants took place at room temperature for all samples (except samples Nos. 29, 33 and 50—55 prepared at 80°C) in a centrifugal pump, by dropping in the aqueous sodium aluminate over diluted sodium silicate solution. The resulting sodium aluminosilicate gel was subjected immediately to hydrothermal crystallization, under continuous mechanical stirring, at 98°C. All the time the ratio solid/liquid was kept constant with an adequate reflux cooler. After the digestion period the mother liquor was filtered off in a Buchner funnel. In some cases the mother liquor was preserved for chemical analysis. Occluded liquor in the filter cake was removed by additional water washing until the pH of the slurry was about 9.5.

Evolution of the synthesis was followed by optical microscope examination, X-ray powder patterns, thermal analysis, adsorptive capacity for benzene (using a McBain type of balance), and chemical analysis.

RESULTS AND DISCUSSION

Preliminary work, given partially in Table 1, has confirmed the best reaction mixture-composition (expressed in oxide mole fractions as 0.41 SiO_2 ; 0.08 Al_2O_3 ; 0.51 Na_2O), hydrogen concentration (2.8—

Table 1

Preliminary results[a)]

Exp. No.	Initial anhydrous gel composition (mole fr.)			Hydrogel conc. (mol/L)	Phase[b)] comp.	Adsorption[c)] Capacity C_6H_6 (wt %)
	SiO_2	Al_2O_3	Na_2O			
1	0.444	0.170	0.386	4.37	P	—
2	0.395	0.131	0.474	5.5	HS	—
4	0.390	0.130	0.470	2.82	A	—
6	0.392	0.089	0.519	3	X+(P)	15
22	0.410	0.080	0.510	3.3	X+((P))	21
23	0.410	0.080	0.510	2.82	X+((P))	20

[a)] Samples crystallized in quiescent conditions.

[b)] The phases in parantheses appear in small ( ) or very small (( )) amounts. (Valid for all the Tables which follow).

[c)] The quantity adsorbed (293°K), 28 torr) is given as the weight in grams of benzene per 100 grams of dehydrated zeolite (400°C, 10^{-2} torr). (Valid for all the Tables which follow).

3.3 moles/l), the need to add the major part of the excess alkali to the silicate and the benefit to pour,during mixing, the aluminate over diluted silicate solution.

The temperature of activation during adsorption capacity measurements was indicated by thermal analysis. A typical derivatogram is presented, for sample No. 10, in Fig. 1.

It has been established [22] that Ostwald's rule of polymorphs formation is applicable to synthesis of zeolize Na—X as :

$$\text{amorphous} \longrightarrow \text{faujasite} \rightarrow \text{gysmodine type Na—P}$$

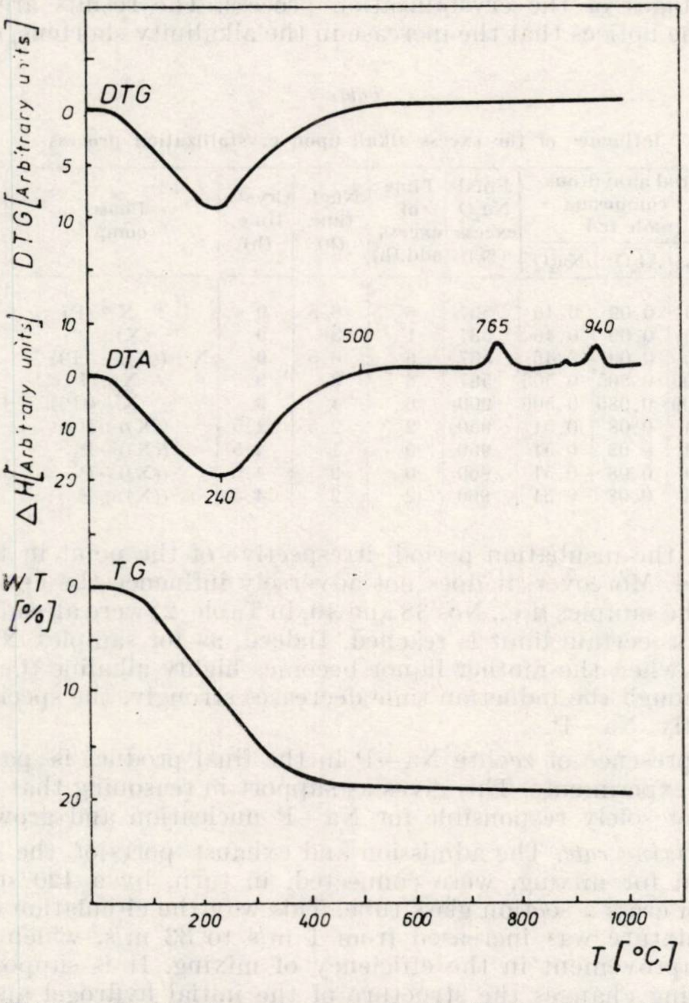

Fig. 1. — Derivatogram of sample No. 10. Heating rate 9°/min. (*T* — tempeature, TG, DTA, DTG — thermogravimetric, differential thermal and differential thermogravimetric analysis curves, respectively).

that is, zeolite Na$-$X appears to be less stable thermodynamically with respect to zeolite Na$-$P.[23] The time scale for this sequence could be changed by varying the reaction parameters.

a. *Alkalinity*. It is known [24] that the excess alkali per $Al_2O_3 \geqslant 300\%$ suppresses the nucleation and crystal growth of zeolite Na$-$P in favour of Na$-$X. However, the upper limit of this excess has not been established. On the other hand, when the total Na_2O amount in the oxide composition of the reaction mixture is doubled,[25] the nucleation rate of zeolite Na$-$A increases about 20-fold.

Consequently, the excess alkali was increased, in our samples, from about 400% to 960%, by adding a certain amount of NaOH solution at different stages of the crystallization process. The results are given in Table 2. One notices that the increase in the alkalinity shortens, sometimes drastically, the incubation period, irrespective of the point in time when it is applied. Moreover, it does not adversely influence the crystallization process if the samples (i.e., Nos 38 and 40, in Table 2) were already nucleated, unless a certain limit is reached. Indeed, as for samples Nos 45, 46, 54 and 55, when the mother liquor becomes highly alkaline (i.e., $\geqslant 950\%$ Na_2O), although the induction time decreases strongly, the species generated is mostly Na$-$P.

Table 2

Influence of the excess alkali upon crystallization process

Exp. No.	Initial anhydrous gel composion (mole fr.)			Final Na_2O excess (%)	Time of excess add.(h)	Nucl. time (h)	Cryst. time. (h)	Phase comp.	Adsorbtion capacity C_6H_6 (wt%)
	SiO_2	Al_2O_3	Na_2O						
26	0.45	0.09	0.46	537	6	6.5	9	X+(P)	19
27	0.45	0.09	0.46	537	1	3	9	(X)+P	6
28	0.45	0.09	0.46	537	6	6.5	9	X+((A))+((P))	21
38	0.409	0.805	0.506	587	6.5	3	9	X+(P)	17
40	0.409	0.085	0.506	900	6	4	9	X+((P))	23
45	0.41	0.08	0.51	950	2	2.5	4.5	((X))+P	1
46	0.41	0.08	0.51	950	0	1	4.5	((X))+P	3
54	0.41	0.08	0.51	960	0	2	4.5	((X))+P	2
55	0.41	0.08	0.51	960	2	2	4.5	((X))+P	2

The presence of zeolite Na$-$P in the final product is paradigmatic for all our experiments. This gives as support in reasoning that the excess alkali is not solely responsible for Na$-$P nucleation and growth.

b. *Mixing rate*. The admission and exhaust ports of the centrifugal pump, used for mixing, were connected, in turn, by a 420 sq.mm and 12.5 sq.mm cross a section glass tube. This way the circulation rate of the reaction mixture was increased from 1 m/s to 33 m/s, which allowed a sizeable improvement in the efficiency of mixing. It is supposed that a better mixing changes the structure of the initial hydrogel and modifies its nucleation capacity in the favor of zeolite Na$-$X at the expense of zeolite Na$-$P. Consequently, the adsorption capacity for benzene (last column in Table 3) increases for samples Nos 37, 39, 41 and 56 with respect to samples Nos 43, 59 and 59. Phase composition, as revealed by X-ray patterns (column 7 in Table 3) and the chemical analysis of the final product (Cf. Table 4) support this observation. For some of the samples (i.e., Nos 41, 46, etc.), the unit cell parameter (24.86 A) calculated from the X-ray patterns, is in good agreement with admitted literature values for approximately 75 Al atoms/unit cell. The same good agreement could be noticed from Table 4, for the first and the last samples, in what the SiO_2/Al_2O_3 ratio is concerned.[19]

Table 3

Influence of stirring during hydrogel precipitation upon the crystallization process[a)]

Exp. No.	Initial anhydrous gel composition (mole fr.)			Cryst. time (h)	Pipe cross section (mm^2)	Phase comp.	Adsorption capacity C_6H_6 (wt %)
	SiO_2	Al_2O_3	Na_2O				
37	0.409	0.085	0.506	7	12.5	X+((P))	24
39	0.409	0.085	0.506	9	12.5	X+(A)+((P))	18
41	0.43	0.08	0.49	6.5	12.5	X+((P))	23
43	0.409	0.085	0.506	8	420	X+P	11
56	0.43	0.08	0.49	10.5	12.5	X+((P))	23
58	0.43	0.08	0.49	13	420	X+P	13
59	0.43	0.08	0.49	10	420	((X))+P	4

[a)] Samples stirred at low speed during crystallization.

Table 4

Effect of the rate of stirring during crystallization[a)]

Exp. No.	Zeolite composition (moles/Al_2O_3)			Cryst. time (h)	Stirring rate (rpm)	Phase comp.	Adsorption Capacity C_6H_6 (wt %)
	Na_2O	SiO_2	H_2O				
41	0.97	2.84	6.59	6.5	60	X+((P))	23
47	0.98	2.29	4.87	5	250	(X)+P	5
49	1.03	2.40	4.62	5	250	((X))+P	2
56	1.09	2.84	5.04	10.5	60	X+((P))	23
Grace Co. SPA	1.13	3.30	2.82	—	—	X	24

[a)] Initial anhydrous gel composition as for sample No. 56 in Table 3.

c. *Influence of stirring during crystallization.* It is admitted that the increase in the stirring rate during crystallization reduces very much the amount of zeolite Na—X in the final product and therefore the adsorption capacity for benzene. One argues [27] that stirring induces collision nucleation which appears to promote the competitive formation of Na—P.

Using two stirring rates, of 60 and 150 rpm, we obtained better results, evaluated after the phase composition and the adsorption capacity, in the first case. They are consistent with the above mentioned observations. For the sake of comparison, the last row of Table 4, presents pertinent data for a Grace Comp. Na—X molecular sieve.

In this study we arrived at another interesting result, namely, the more efficient and prolonged the stirring during mixing step, the less "mechanically sensitive" are the samples in the course of the crystallization period. As a result, they could be stirred at a low speed during the digestion stage. This way the required time to complete crystallization is reduced, i.e., from 9 h, as for sample No. 39 (stirred only 10 min.) to 6.5 — 7 h for samples Nos 41 and 37, respectively (each stirred 30 min.), in the circumstances that the phase composition and the absorption capacity are improved (Cf. Table 3).

d. *Temperature of mixing*. As mentioned above, two mixing temperatures : were used : 25 and 80°C. The results, presented in Table 5, appear to be independent of this parameter.

Table 5

Relationship between the temperature of mixing and the quality of the final product

Exp. No.	Initial anhydrous gel composition (mole fr.)			Mixing temp. (°C)	Cryst time (h)	Adsorption capacity C_6H_6 (wt %)
	SiO_2	Al_2O_3	Na_2O			
29	0.41	0.08	0.51	80	4.5	5
31	0.41	0.08	0.51	25	6	8
33	0.41	0.08	0.51	80	6	8
36	0.41	0.08	0.51	25	5	6

e. *Seeding*. Provided the conditions are right for the evolution of zeolite Na—X, the usual incubation period can be shortened by appropriate seeding with microcrystals ($\leqslant 1\mu m$) of zeolites A or X.[28,29] Such a procedure was followed in the present work, with the hope to decrease both the amount of zeolite Na—P in the final product, by consuming the nutrients for its growth, and the overall time required for the synthesis. Some of the results are summarized in Table 6. Unexpectedly, we found that the seeds of zeolite A neither shortened the incubation period nor

Table 6

Influence of seeding[a)]

Exp. No.	Seed Nature	Amount of seeds (wt %)	Cryst time (h)	Phase comp.	Adsorption capacity C_6H_6 (wt %)
24A	A	8	21	A+(X)+(P)	5
24B	—	—	21	X+(P)	16
25	A	3	6	X+P	9
30	X	6	6	X+((P))	21
34	X	6	6	X+(P)	18
35	X	3	6	X+((P))	20

[a)] Seeds were added to the initial gel of composition as for sample No. 56 in Table 3. No mechanical stirring during crystallization, except when sampling.

improved the phase composition. Moreover, the sample No. 25 consisted of almost equal amounts of zeolite X and P, while in the case of the sample No. 24A, the dominant phase was zeolite A.

Seeding with zeolite X, on the other hand, had a positive influence with respect to unseeded samples (*i.e.*, sample No. 24B).

f. *Mother liquor composition.* In order to better characterize the crystallization process we determined the chemical composition of the mother liquor for the most of the samples. A typical composition is 88 Na_2O ; $3SiO_2$; 0.6 g Al_2O_3/l. It is interesting to note that for the samples which crystallized into a more siliceous zeolite (*i.e.*, sample Wo. 56) the amount of Al_2O_3 in the mother liquor is larger (1.5 g/L).

Previous work has drawn the attention on the need for a "faujasite crystal directing mixture" [30] and an "active silica source", in which traces of alumina were detected. Due to its content in Na_2O and even in Al_2O_3, the mother liquor can be a valuable diluting medium for the silicate solution required in the synthesis.

Table 7

Crystallization in the presence of organic substances a)

Exp. No.	Time of addition (h)	Cryst. time (h)	Adsorption capacity C_6H_6 (wt %)
45	—	5	1
50 b)	0	5	10
52 c)	1	5.5	12
53 d)	1	4.5	3

a) Anhydrous initial gel composition as for sample No. 56 in Table 3.
b) n-tributylamine ;
c) amylamine
d) benzoic acid.

g. *Additives*. It has been pointed earlier that in the case of the zeolite Na–X synthesis it is probable to appear by concentration fluctuation, either simultaneously or successively, nuclei of more than one species. As n – tributylamine [33] is one of the largest molecules which can penetrate the pores of zeolite Na–X, we crystallized some samples in its presence. It was hoped to positively influence the nucleation and crystal growth either by adsorption on the precursor species or by template effect. Similar considerations were responsible for using benzoic acid and amylamine. All the additives amounted 0.005 M for each mole of Al_2O_3 present in the parent gel. Table 7 reveals the positive influence of the amines.

CONCLUSIONS

1. For a good yield of zeolite Na–X synthesis an efficient mixing (approximately 30 min.) of the initial hydrogel is indispensable. With this provision the mixture can be stirred at low speed during crystallization period.

2. Mixing can take place at room temperature.

3. The increase of the Na_2O amount in the parent gel shortens the induction stage. However, a Na_2O excess $\geqslant 950\%$ promotes nucleation and growth of zeolite Na–P.

4. Seeding of the fresh precipitated gel with 3—10 wt% of zeolite X microcrystals reduces the incubation period and this way, the overall time required for the complete crystallization.

5. The best crystallized samples, even if they contain tiny amounts of zeolite Na—P, have an adsorption capacity for benzene very close to or equal with an imported Na—X molecular sieve.

REFERENCES

[1] D. W. Breck, "Zeolite Molecular Sieves. Structure, Chemistry and Use", Wiley Interscience New York, 1974 p. 593.
[2] R. M. Barrer, "Hydrothermal Chemistry of Zeolites", Acad. Press London, New York, 1982, p. 31.
[3] P. B. Weisz, *Pure Appl. Chem.* **52**, 2091 (1980).
[4] J. A. Rabo (Ed.), "Zeolite Chemistry and Catalysis", Amer. Chem. Soc. Monograph No. 171, 1976.
[5] S. L. Meisel, *Phil. Trans. Roy. Soc. London*, **300 A**, 157 (1981).
[6] C. D. Chang and A. J. Silvestri, *J. Catal.*, **47**, 249 (1977).
[7] P. B. Weisz, *Erdöl u. Kohle*, **18**, 527 (1965).
[8] W. W. Kaeding and S. A. Butter, *J. Catal.*, **61**, 155 (1980).
[9] M. Ziolek and Z. Dudzik, *Zeolites*, **1**, 117 (1981).
[10] R. P. Townsend Ed.), "Properties and Applications of Zeolites", The Chemical Society, London, 1980, p. 84.
[11] P. E. Eberly Jr. and W. F. Arey, U.S. Pat. 3.126.425 (1964).
[12] R. N. Fleck and C. G. Wright, U.S.Pat. 3.114.782 (1963).
[13] S. A. Conviser, *Oil Gas J.*, **63**, 130 (1965).
[14] D. W. Breck and E. M. Flanigen, "Molecular Sieves", Society of Chemical Industry, London, 1968, p. 47.
[15] S. P. Zhdanov, "Molecular Sieves", Society of Chemical Industry, London, 1968, p.62.
[16] J. L. Guth, P. Collins and R. Wey, *Bull. Soc. Fr. Mineral. Crystall ogr.*, **93**, 59 (1970).
[17] E. E. Senderov and N. I. Khitarov, "Zeolites, Their Synthesis and Conditions of Formation in Nature", Nauka, Moscow, 1970, p. 125.
[18] R. M. Milton, U. S. Pat. 3.008.803 (1961).
[19] R. M. Milton, U.S. Pat. 2.882.244 (1959).
[20] G. T. Kerr, *J. Phys. Chem.*, **72**, 1385 (1968).
[21] E. F. Freund, *J. Cryst. Growth*, **34**, 11 (1976).
[22] F. G. Dwyer and P. Chu, *J. Catal.*, **59**, 263 (1979).
[23] D. W. Breck, "Zeolite Molecular Sieves. Structure, Chemistry and Use", Wiley Interscience, New York, 1974.
[24] R. M. Barrer, J. W. Baynham, F. W. Bultitude and W. M. Meier, *J. Chem. Soc.*, **1**, 95 (1959).
[25] W. Meise and F. E. Schwochow, in "Molecular Sieve", Eds. W. M. Meier and J. B. Uytterhoeven, American Chemical Society Advances in Chemistry Series, No. 121 1973, p. 169.
[26] D. W. Breck, "Zeolites Molecular Sieves. Structure. Chemistry and Use", Wiley Interscience, New York, 1974, p. 94.
[27] E. F. Freund, *J. Cryst. Growth*, **34**, 11 (1976).
[28] L. Puppe, G. Ulisch and F. Schwochow (to Bayer Aktiengesellschaft Leverkusen, Germany), I.S. Pat. 4.007.253 (1977).
[29] H. Kacirek and H. Lechert, *J. Phys. Chem.*, **80**, 1291 (1976).
[30] J. Ciric, I. Pitman and L. J. Reid Jr., Audubon, N. J. (to Mobil Oil Corp.), U.S. Pat. 3.433.589 (1969).
[31] T. V. Whittam, (to Peter Spence Ltd.) Brit. Pat., 1.17.463 (1969).
[32] T. V. Whittam, (to I.C.I.Ltd.), Brit. Pat. 1.450.411 (1976).
[33] L. Pauling, "Nature of the Chemical Bond", 3rd Ed., Cornell University Press, Ythaca, N. Y. (1960).

Revue Roumaine de Chimie, **31**, *11–12*, 981–986 (1986)

Dedicated to Professor P. SPACU on his 80th anniversary

CONTRIBUTIONS TO THE STUDY OF COBALT (II) DIOXYGEN COMPLEXES

GH. MARCU, AL. BOTAR and ADRIANA NAUMESCU
Institute of Chemistry, Cluj-Napoca, Romania

Received May 15,1986

New methods for the synthesis of Co(Salen) and Co(Br-Salen) complexes were elaborated and their adducts with molecular oxygen, in the crystalline form, were isolated by dissolving in dimethyl-formamide. The IR study confirmed the existence of adducts of type 1 : 2, $[Co(Salen)]_2 \cdot O_2 \cdot (DMF)_2$ and $[Co(Br\text{-}Salen)]_2O_2(DMF)_2$ respectively. It was verified practically that one oxygen mole is absorbed by two complex moles. The oxygen absorption is influenced by solvent and the nature of the complex, being a reversible process which can be repeated even after 50 cycles, without the decomposition of the initial substances. At the same time, the quaternary ammonium salts of the $(R_4N)_5[PCoW_9Mo_2O_{39}]$ and of the $(R_4N)_8[P_2CoW_{16}MoO_{61}]$ heteropolyanions with cobalt as heteroatom, which are unknown in the literature, were synthesized. These complexes were able to reversibly absorb O_2 at temperatures under −20°C and the process can be repeated more than ten times without decomposition of the initial substances.

INTRODUCTION

Generally the complex compounds and particularly the cobalt compounds as molecular oxygen carriers have been the subject of numerous investigations.[1–15] Until recently the molecular oxygen adducts of Co(II) complexes have been formulated as dimers. Recent investigations point out the existence of 1 : 1 type adducts. The Co(II) complexes with different Schiff bases have been proved to be the most important, from the applicative point of view, among Co(II) compounds which exhibit reversible absorption-desorption properties of molecular oxygen.

The coordination compounds with molecular oxygen named also synthetic oxygen carriers are of major interest for biochemistry, in elucidation of problems concerning the oxygen binding in the natural oxygen carriers such as hemoglobin and hemocyanin, constituting a veritable model for the study of reversible oxygenation mechanisms. Since the oxygen reversible attachment to systems containing transition metals with variable oxidation states and different complexing and chelating agents is a topical problem,[16–17] our investigations were directed to the elaboration of new and more efficient methods for the synthesis of some Co(II) complexes with Schiff basses such as Co(Salen) and Co(Br-Salen), exhibiting oxygen absorption-desorption properties (Salen =N,N′-bis-salicylidene-ethylenediamine).

At the same time, on the basis of the present knowledge according to which one or more constitutional water molcules[17–18] exist in the heteropolyanion structures, we have attempted to obtain — by removal of these molecules — a new kind of complex with coordinative unsaturated "holes" and with possible reversible absorption properties towards small gas molecules particularly the molecular oxygen. With this aim in view new Co(II) heteropolyanions of the type $(R_4N_5)[PCoW_9Mo_2O_{39}]$ and $(R_4N)_8[P_2CoW_{16}MoO_{61}]$ were synthesized and examined.

RESULTS AND DISCUSSION

The first part of the research presents two new methods for synthesis of Co(Salen) and Co(Br-Salen), which were obtained in the crystalline form, inactive towards molecular oxygen in this solid state.

Very reactive solutions were obtained by dissolving these complexes in DMF. The adducts with molecular oxygen of the 1 : 2 type, namely : $[Co(Salen)]_2O_2\ (DMF)_2$ and $[Co(Br\text{-}Salen)]_2O_2(DMF)_2$ were isolated from the above solutions after three-day-staying. The results of the elemental analysis are given in table 1.

Table 1

The elemental analysis of the complexes studied

Compound	C, %		H, %		Co, %	
	Calculated	Found	Calculated	Found	Calculated	Found
Co(Salen)	59.08	59.9	4.31	4.50	18.14	18.31
Co(Br-Salen)	39.77	39.3	2.48	2.51	12.21	12.13
$[Co(Salen)]_2O_2(DMF)_2$	55.08	54.6	5.11	5.03	14.22	14.12
$[Co(Br\text{-}Salen)]_2O_2(DMF)_2$	39.80	40.22	3.32	3.25	10.31	10.32

It has been proved that the adducts with oxygen are air-stable but they are decomposed by moderate heating or by treating them with chloroform or benzene, when the molecular oxygen releases and the initial complex is regenerated.

Table 2 shows that dimethylformamide (DMF) and eventually dimethylsulphoxide (DMSO) are the most adequate solvents, which can be taken into account in order to render soluble and to activate the studied complexes.

The systematic study of the molecular oxygen absorption in DMF solutions by Co(Salen) and Co(Br-Salen) complexes respectively as follows from Table 3 certifies the fact that in the forming process of the corresponding adducts with molecular oxygen, a part of the solvent coordinates around the cobalt so one solvent molecule occupies a coordination place according to the reaction :

$$2Co(Salen) + O_2 + 2L \rightleftarrows [(Co\text{-}Salen)]_2O_2L_2$$

where L = DMF. Practically one absorbed oxygen molecule corresponds to two adduct molecules which is in accordance with the literature.

The oxygen absorption process is influenced by the solvent, the nature of the complex and by the substitution in aromatic ring. Thus Co-Salen absorbs molecular oxygen more rapidly than Co-Br-Salen, as follows from Table 4. The absorption-desorption properties of the molecular oxygen have been proved to be reversible even after 50 cycles without the degradation of the initial complexes (Table 5).

Table 2

The influence of the solvent on the oxygenation of Co(Salen) and Co(Br-Salen)

Complex	Solvent (L)	Sample weight (mg)	The amount of absorbed O_2 (mg)
Co(Salen)	DMF	15.2	0.746
	DMSO	15.2	0.648
	PyO	15.2	0.320
	THF	15.2	0.050
Co(Br-Salen)	DMF	15.2	0.507
	DMSO	15.2	0.428
	PyO	15.2	0.214
	THF	15.2	0.020

Table 3

The study of the O_2 absorption by Co(Salen) and Co(Br-Salen) in DMF

Complex	Sample weight (mg)	The average amount of the absorbed O_2 (mg)	The amount of absorbed O_2 on two complex moles, (g)
Co(Salen)	15.7	0.772	33.05 (~1 mole)
Co(Br-Salen)	15.5	0.512	32.87 (~1 mole)

The experiments were quantitatively performed by heating in vacuum at 60—80°C or by treating with chloroform or benzene.

In order to elucidate the structure of the adducts with molecular oxygen, the IR spectroscopy was used. By examining the absorption IR spectra it can be stated that the lack of some very intense bands in the case of the adducts with molecular oxygen — (of type 1 : 2) which can be assigned to the O_2 group, is probably due to a symmetrical arrangement of the oxygen atoms around the metal. An idealized structure of the adducts of type $(\text{Co-Salen})_2O_2L_2$, where L = DMF is in accordance with some data from the literature, is given in figure 1. According to this, oxygen and the additional ligand occupy the axial positions of an octa-

Table 4

The O_2 absorption by Co(Salen) and Co(Br-Salen) after 50 cycles of absorption-desorption

Complex	Sample weight (mg)	The average amount of the absorbed O_2 (mg)	The amount of absorbed O_2 on two complex moles (g)
Co(Salen)	15.4	0.737	32.36 (~1 mole)
Co(Br-Salen)	15.5	0.489	31.39 (~1 mole)

Table 5

The elemental analysis of the heteropolyanions with cobalt (II) as heteroatom

Complex		K	P	W	Mo	Co	H_2O
$K_5[PCoW_9Mo_2O_{39}]$	Calculated	6.17	0.98	52.20	6.05	1.86	12.93
	Found	6.02	0.94	52.61	6.23	1.78	12.94
$K_8[P_2CoW_{16}MoO_{61}]$	Calculated	6.16	1.22	57.93	5.88	1.16	12 05
	Found	6.23	1.16	58.40	5.36	1.18	12.08

hedral configuration. Thus, the L ligand being in *trans* position towards the oxygen compensates the shifted charge from cobalt to oxygen, so that the presence of the σ donors leads to the stabilization of the cobalt-oxygen bonds.

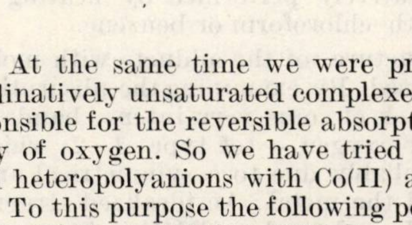

Fig. 1. — The possible structure of $[Co(Salen)]_2O_2 . L_2$ where L = DMF.

At the same time we were preoccupied by the obtention of new coordinatively unsaturated complexes possessing in their structure "holes" responsible for the reversible absorption properties of small gases, respectively of oxygen. So we have tried the synthesis of some new unsaturated heteropolyanions with Co(II) as heteroatom.

To this purpose the following potassium salts were first synthesized : $K_5[PCoW_9Mo_2O_{39}(H_2O)] \cdot 22H_2O$ and $K_8[P_2CoW_{16}MoO_{61}(H_2O)] \cdot 34H_2O$ containing in their structure one constitutional water molecule (Table 5). Then, by treating them with a tetraalkylammonium salt R_4N where

$R > C_4H_9$ new unsaturated heteropolyanions of type $(R_4N)_5(PCoW_9Mo_2O_{39})$ and $(R_4N)_8(P_2CoW_{16}MoO_{61})$ respectively were obtained. The potassium salts of the synthesized heteropolyanions treated with tetraalkylammonium salts precipitate the quaternary ammonium salts of the unsaturated heteropolyanions which are isolated by filtration or extraction in toluene or in another proper organic solvent.

The experiments performed with these complexes dissolved in some organic solvents at temperatures under −20°C, point out that they are able to absorb-desorb the molecular oxygen; this process can be repeated more than ten times without destroying the initial heteropolyanions.

The fact is concomitant with a change of colour from pink to green for the derivatives with molecular oxygen. The isolation of solid adducts with molecular oxygen was not yet successful.

EXPERIMENTAL

Synthesis of N N'bis-salicylidene-ethylenediamine cobalt(II) or Co(Salen). 0.11 moles N N' bis-salicyclidenethylenediamine or Salen are dissolved in 700 mL absolute ethanol at 60—70°C in a nitrogen current purified of oxygen traces. The resulting solution is treated with 0.11 moles of $Co(CH_3COO)_2 \cdot 4H_2O$ dissolved in absolute ethanol (pre-boiled and refluxed for 15 minutes) after which is slowly cooled at room temperature. A crystalline brown-violaceous product is separated from the solution, which is then filtered, washed with absolute ethanol, then with diethyl ether and dried in vacuum. The yields and the results of the elemental analysis are given in table 1. The synthesized crystalline product is air stable, very little soluble in ethanol by heating and easily soluble in dimethylformamide (DMF) and in dimethylsulphoxide (DMSO).

Synthesis of N N' bis (5 Br-salicylidene-ethylenediamine cobalt(II) or Co(Br-Salen). A suspension of 0.06 moles $Co(CH_3COO)_2 \cdot 4H_2O$ in 200 mL absolute ethanol (previously refluxed for 30 minutes) is added slowly in small portions to a solution containing 0.06 moles Br-Salen in 900 mL ethanol at 70°C. The reaction is performed in inert atmosphere by passing a nitrogen current. After 15 minutes of reflux, it is cooled at room temperature. Dark-brown crystals are separated from the solution, filtered off, washed with ethanol, diethyl ether and dried in air. The yields and the results of the elemental analysis are given in Table 1. The synthesized complex is air stable, very little soluble in absolute ethanol by heating and easily soluble in DMF or DMSO.

Synthesis of $K_5[PCoW_9Mo_2O_{39}(H_2O)] \cdot 22H_2O$ is performed by treating a solution containing 0.005 moles $K_7PW_9Mo_2O_{39} \cdot 13H_2O$ in 75 mL water at 70°C with 0.005 moles of $Co(CH_3COO)_2 \cdot 4H_2O$. The obtained red-rose solution is cooled by staying at room temperature, is filtered from the eventually precipitated traces, and then it is cooled at −20°C. Red and well shaped crystals are separated; they are then washed with cool water and dried in air. The elemental analysis is given in Table 5.

Synthesis of $K_8[P_2CoW_{16}MoO_{61}(H_2O)]34H_2O$ is performed by treating 0.002 moles of $K_{10}P_2W_{16}MoO_{61} \cdot 19H_2O$ in 75 mL water at 70°C with a solution containing 0.002 moles $Co(CH_3COO)_2 \cdot 4H_2O$ in 25 mL water. From the red-dark solution red well shaped crystals are separated by cooling and slowly evaporation for a few days, at room temperature. They are filtered off, washed with cool water and dried in air. The elemental analysis is given in Table 5.

REFERENCES

[1] T. Tsumaki, *Bull. Soc. Japan*, **13**, 252 (1938).

[2] M. Calvin, R. H. Bailes and W. K. Wilmarth, *J. Amer. Chem. Soc.*, **68**, 2254 (1946).

[3] M. Calvin and C. H. Barnelew, *J. Amer. Chem. Soc.*, **68**, 2267 (1946).

[4] L. H. Vogt, N. M. Faigenbaum and S. E. Wiberley, *Chem. Rev.*, **63**, 269 (1963).

[5] H. P. Fritz and G. Gretner, *Inorg. Nucl. Chem. Let*, **3**, 141 (1967).

[6] F. Calderazzo, C. Floriani and J. F. Salzman, *Inorg. Nucl. Chem. Lett.*, **2**, 379 (1966).

[7] L. Waska, *Science*, **140**, 809 (1963).

[8] C. Floriani and F. Calderazzo, *J. Chem. Soc.(A)*, **1969**, 946.
[9] A. L. Crumbliss and F. Basolo, *Science*, **164**, 1168(1969).
[10] F. Miller, J. Simplicio and R. G. Wilkins, *J. Amer. Chem. Soc.*, **91**, 2775 (1969).
[11] M. Calligaris, D. Minichelli, G. Nardin and L. Randaccio, *J. Chem. Soc. (A)*, **1970**, 2411.
[12] N. Arika and T. Harno, *J. Mol. Catal.*, **7**, 179 (1980).
[13] K. B. Yatsimirskii and Yu. I. Bratuskho, *Dokl. Akad. Nauk SSSR*, **252**, 376 (1980).
[14] K. Mutso and K. Euchii, *Inorg. Chem.*, **19**, 1871 (1980).
[15] T. D. Smith and J. R. Pulbrow, *Coord. Chem. Rev.*, **39**, 295 (1981).
[16] Gh. Marcu, Plenary Lecture Delivered at the 2nd National Congress of Chemistry, September 7—10/1981, Bucharest, Romania, p. 180—194.
[17] Gh. Marcu, "Chimia compușilor coordinativi", Editura Academiei R.S.R., Bucharest, 1984.
[18] S. Kirschner, "Inorganic Synthesis" Vol. 23, p. 186—191, Wiley New York, 1985.

Revue Roumaine de Chimie, **31**, *11–12*, 987–993 (1986)

Dedicated to Professor P. SPACU on his 80th anniversary

COMPLEX COMPOUNDS OF Hg(II) WITH THIOBENZOPIPERIDIDES AND THIOBENZOMORPHOLIDES

D. NEGOIU[a], S. NEAGOE[b], CORNELIA CERCASOV[a], MARIA NEGOIU[a], IOANA SARAMET and C. TOMA[d]

[a] Polytechnical Institute of Bucharest, Faculty of Chemical Technology, 1, Str. Polizu, 78126-Bucharest—Romania

[b] Institute of Petroleum and Gas, 3, Sos. București-Ploiești, 2000-Ploiești, Romania

[c] Institute of Medicine and Pharmacy, Faculty of Pharmacy, 6, Str. Traian Vuia, 70139-Bucharest — Romania

[d] I.C.I.T.P.R. — Ploiești, 291, B-dul Republicii, 2000-Ploiești — Romania

Received May 9, 1986

Eight complex compounds of Hg(II) with thioamides of the thiobenzopiperidides and thiobenzomorpholides class were synthesized and analyzed. The formulation of the obtained compounds was made on the basis of elemental chemical analysis, determination of molecular mass and thermal analysis. It has been established by conductimetric determination that the respective compounds are non-electrolytes. The structural formulation of the studied compounds was made using spectral analysis IR, UV-VIS and ^{1}H-NMR.

Mercury has a special affinity for the sulphur atom. The marked donor character of sulphur allows the achievement of coordinative bonds. Thus, attempts were made to obtain complex of mercury(II) with thioamides.[1]

Literature offers certain data on some methods determining mercury with thioamides.[1-3]

The following forms were prepared with thiobenzamide compounds : $HgCl_2 \cdot 2C_6H_5\,CSNH_2$ and $HgCl \cdot C_6\,H_5\,CSNH$.

With Hg(II) tetramethylurea (tmu) forms compounds in which each of the Hg(II) atoms is linked to two molecules of ligand through the sulphur atom. The IR spectra of these compounds indicate corresponding frequencies to the Hg—S bond, suggesting a tetrahedral configuration.[4]

The authors [5] have also prepared and studied certain complex compounds of Hg(II) with thioamides.

This work presents the results of the study on complex compounds of Hg(II) with thioamides of the thiobenzopiperidides (a) and thiobenzomorpholides (b) class also known in the specialty literature [6-8]:

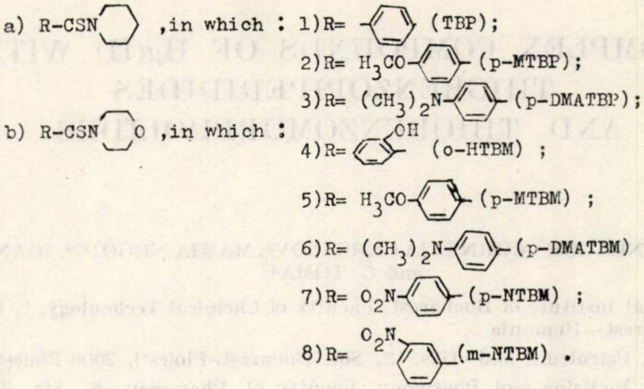

RESULTS AND DISCUSSIONS

The complex compounds of Hg(II) with thioamides of the thiobenzopiperidides and thiobenzomorpholides class are microcrystalline powders having the following colours : white, yellow or orange with higher melting points than the corresponding ligands. They are easily soluble in dimethyl sulphoxide (DMSO), dimethylformamide (DMF), dichloroethane (CH_2Cl_2), camphor, sparsely soluble in nitromethane and insoluble in acetone. These were obtained through similar methods. A solution of 0.1 M thioamide in acetone is added, while stirring to an aqueous solution of $HgCl_2$ 0.1M. According to the nature of the thioamide, the precipitate appears instantaneously or after about 1/2 hour. After one hour the formed precipitate is filtered, washed in water and acetone and then is dried in vacuum.

The results of the elemental chemical analysis are given in Table 1. These results suggest the following formulations : $[HgLCl_2]$ in which L = lingands 1 . . . 7 table 1 and $[HgL_2Cl_2]$ in which L = m-NTBM.

The determinations of molecular mass [9] and the measurements of molar conductibility,[10] whose values are presented in Table 2 confirm the formulation of the general type of complex compounds established on the basis of elemental chemical analysis.

To determine the molecular masses we used camphor as a solvent. The experimental values obtained confirm those calculated theoretically. The molar conductibilities were determined in DMSO and the obtained values confirm the fact that the respective compounds are non-electrolytes. Hence, the general formulations suggested for the compounds of Hg(II) with thioamides of the thiobenzopiperidides and thiobenzomorpholides series are correct.

Table 1

Elemental chemical analysis of the complex compounds of Hg(II) with thioamides

Compound	Element analysed (%) theor./exptl.					M.p.	Colour
	Hg	C	H	S	Cl		
[Hg(II)-TBP]	42.09 41.99	30.22 30.00	3.15 3.08	6.71 6.60	14.87 14.62	220	white
[Hg(II)—(p-MTBP)]	39.60 39.50	30.80 31.54	3.35 3.95	6.31 6.04	14.00 14.11	168	white
[Hg(II)-(p-DMATBP)]	38.61 38.72	32.34 33.00	3.85 3.12	6.16 5.85	13.64 13.25	230	yellow
[Hg(II)-(p-MTBM)]	39.45 39.85	28.31 28.60	2.16 1.98	6.29 5.89	13.94 14.21	98	white
[Hg(II)-(p-DMATBM)]	38.46 38.60	29.91 30.32	3.45 4.08	6.13 6.33	13.59 13.98	118	orange
[Hg(II)-(o-HTBM)]	40.56 40.42	26.69 26.28	2.63 2.55	6.47 7.00	14.33 14.31	238	white
[Hg(II)-(p-NTBM)	38.32 38.16	25.21 25.00	2.29 2.25	6.11 5.55	13.54 13.28	219	white
[Hg(II)-(m-NTBM)]	25.86 25.77	34.04 34.28	3.09 3.00	8.25 7.97	9.14 9.68	169	white-yellow

Table 2

The molecular masses and molar conductivities of the complex compounds of Hg(II) with thioamides

Compound	Molecular masses		Concentration ($X \cdot 10^{-4}M$)	Molar conductivity ($\Omega^{-1}cm^2 \cdot mole^{-1}$)
	Theor.	Exptl.		
[Hg(TBP)Cl$_2$]	476.50	462.42	8.70	2.72
[Hg(p-MTBP)Cl$_2$]	506.50	489.00	16.68	3.47
[Hg(p-DMATBP)Cl$_2$]	519.50	445.62	5.48	2.98
[Hg(p-MTBM)Cl$_2$]	—	—	8.16	1.50
[Hg(p-DMATBM)Cl$_2$]	521.50	487.80	5.08	10.23
[Hg(o-HTBM)Cl$_2$]	494.50	438.83	2.04	3.22
[Hg(p-NTBM)Cl$_2$]	523.50	505.81	6.87	1.94
[Hg(m-NTBM)$_2$Cl$_2$]	775.50	764.00	4.25	0.63

THERMAL ANALYSIS

We studied the thermal behaviour of certain complex compounds of Hg(II) with thiobenzopiperidide (TBP) *p*-dimethylamino-thiobenzopiperidide (p-DMATBP) and *o*-hydroxy-thiobenzomorpholide (*o*-HTBM).

The analysis of the ATD, TGD and TG diagrams indicates a similar thermal behaviour and thermal stability of these compounds up to temperatures of 150°C. By increasing the temperature, two marked endothermal effects appear with all compounds : the first around 220°C and the second between 320 and 390°C, after which the oxidation process of the organic substance begins and concludes at a) 645°C for the [Hg(TBP)Cl_2] compound ; b) 680°C for the [Hg(*p*-DMATBP)Cl_2] compound ; c) 730°C for the [Hg(*o*-HTBM)Cl_2] compound.

Concurrently with the decomposition and oxidation of the organic substance the volatilization of mercury is also taking place, a fact which did not allow for the checking of the molar ratio of metal to ligand.

IR SPECTRA

The IR spectra of the thioamides and the corresponding complex compounds that were obtained with Hg(II) are systematized in Table 3.

Table 3

Characteristic IR frequencies of the complex compounds of Hg(II) with thioamides (cm^{-1})*

Compound	SPECTRAL RANGE			
	1530—1490 $\nu_{CN}+\delta_{NH_2}$	1400—1200 $\nu_{CC}+\nu_{CN}$	1200—1000 $\nu_{NCS}+\gamma_{NH_2}$	1000—850 $\nu_{C=S}$
[Hg(TBP)Cl_2]	1540sh	1298w 1250s 1210m	1140w	1015s
[Hg(p-MTBP)Cl_2]	1510m	1270w 1245w 1210w	1175m 1140w 1125w	1020sh
[Hg(p-DMATBP)Cl_2]	1510sh	1275sh 1240m 1215sh	1195w 1175w 1140w	1020w
[Hg(p-MTBM)Cl_2]	1510w	1275s 1235w	1180s	1040m
[Hg(p-DMATBM)Cl_2]	1510sh	1290m 1265sh	1160sh	1030w
[Hg(o-HTBM)Cl_2]	1535sh	1300m 1265m 1205w	1160w	1030s
[Hg(p-NTBM)Cl_2]	1505w	1310m 1265w 1210w	1180s	1030s
[Hg(m-NTBM)Cl_2]	1500w	1300w 1270w 1215w	1170w	1030m

* Abbreviations : s = strong ; m = medium ; w = week ; sh = shoulder.

The comparative analysis of the spectra of the ligands and the complex compounds allows for certain assessments on the nature of chemical bonds.

The interpretation of spectral data leads to the conclusion that in all the studied complex compounds except $[Hg(m-NTBM)_2Cl_2]$ thioamides function as bidentated ligands in which the sulphur and nitrogen atoms are donor atoms.

The arguments for the achievement of the chemical bond in complex compounds through the sulphur atom of the thioamidic grouping under the "thioceto" form, are :

a) changes in the band from 1020 to 1040 cm^{-1} which expresses an important contribution of the $> C = S$ bond and which appears in compounds either at lower frequencies, or at the same frequency but in both cases with a decreased intensity and sometimes much enlarged.

b) changes in the bands between 1200 and 1000 cm^{-1} assigned to the coupled vibrations $\nu_{NCS} + \nu_{NH_2}$ of the thioamides spectra, which in the spectra of the complexes appear displaced either towards lower frequencies or towards higher frequencies but with changed intensity.

The proofs concerning the participation of the nitrogen atom out of the thioamido groups in achieving chemical bonds are given by the change in the bands ranging from 1530 to 1490 cm^{-1} assigned to coupled frequencies $\nu_{CN} + \nu_{NH_3}$ of thioamides which in complex compounds appear at higher frequencies except for the $[Hg(m-NTBM)_2Cl_2]$ compound in whose spectrum no visible changes appear in this range. This proves that when Hg(II) is complexed with m − NTBM the binding of the ligand with the central metallic ion is made through the sulphur atom alone.

This is also confirmed by the fact that no changes occur in the band of the 1400—1200 cm^{-1} range assignable to vibrations $\nu_{CC} + \nu_{CN}$ of thioamides. In the case of the other complex compounds the band of the 1400—1200 cm^{-1} range undergoes changes showing the involvement of the nitrogen atom in coordination.

SPECTRA OF THE VISIBLE ULTRAVIOLET

The spectra of the visible ultraviolet of the complex compounds of Hg(II) with thioamides of the thiobenzopiperidides and thiobenzomorpholides class were made in solid state after pelletizing in MgO.

The aspect of the curves in this range confirms the fact that the central metallic ion Hg(II) has the electronic configuration of d^{11} for which the theory of the crystalline field does not envisage any band in the visible range.

Bands characteristic for ligands appear in the ultraviolet range of the spectrum.

^{1}H-NMR SPECTRA

The coordination manner of ligands with the central metallic ion is also confirmed by the NMR spectra. The NMR spectrum of the $[Hg(p-MTBM)Cl_2]$ compound and of the p − MTBM ligand has been registered.

The spectrum of complex compounds shows a slight descreening of the aromatic protons and of those neighbouring the nitrogen atom of the morpholinic cycle. This behaviour suggests a coordination of the ligand through the sulphur and nitrogen atoms.

EXPERIMENTAL

Reagents : $HgCl_2$ 0.1 M solution
Thioamides : 0.1 M solution in acetone.

The complex compounds of Hg(II) with thiobenzopiperidides and thiobenzomorpholides were obtained by the same general method : to 10 cm^3 solution of 0.1 M $HgCl_2$ we added the solution in acetone of the corresponding thioamide in small portions and under continuous stirring, until complete precipitation. The precipitate was filtered through a G_4-grade sintered glass filter, washed in a 1 : 2 acetone — water solution, with ethanol and dried under vaccum. The obtained crystals are white , yellow or orange (Table 1).

Instrumentation : The IR spectra of the thioamides and the complex compounds were recorded with Carl Zeiss Jena UR-20 spectrophotometer, with samples prepared as pellets in anhydrous KBr. The UV-VIS electronic reflectance spectra were recorded with a Carl Zeiss Jena VSU-1 spectrophotometer, using MgO pellets. Electrical conductivity measurements were carried out with a Radelkis OK-102/1 conductimeter.

CONCLUSIONS

The conclusion was reached that the complex compounds of Hg(II) with tertiary thioamides of the thiobenzopiperidides and thiobenzomorpholides class are of the following form : $[HgLCl_2]$ or $[HgL_2Cl_2]$.

The elemental chemical analysis determinations of molecular mass indicate a 1 : 1 mercury : ligand molar combination ratio except for the compound obtained with *m*-nitrothiobenzomorpholide (*m*-NTBM).

The thermogravimetric analysis shows the great thermal stability of the synthesized compounds. This recommends the use of the respective ligands as reactives for determining Hg(II).

The determinations of molar conductivity showed that the studied compounds are nonelectrolytes which suggests a donor-acceptor bond between ligand and the central metallic ion.

The analysis of the infrared, visible-ultraviolet and ^1H-NMR spectra allows for the establishment of the structural formulas of the studied compounds. This indicate that the ligand is bidentated, the coordination being achieved both through the sulphur atom and the nitrogen atom.

The thioamidic grouping participates in complexing under "thioceto" form.

For the $[HgLCl_2]$ complex combinations the structures were assigned :

I. 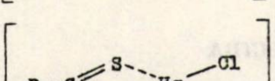

in which: $R_1 = C_6H_5-$, $CH_3O-C_6H_4-$, $(CH_3)_2N-C_6H_4-$;

II. 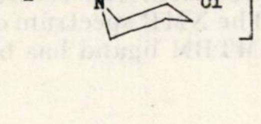

in which: $R_2 = CH_3O-C_6H_4-$, 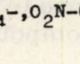

-, $(CH_3)_2N-C_6H_4-$, $O_2N-C_6H_4-$;

The following structure was assigned to $[HgL_2Cl_2]$ complex compounds :

III.

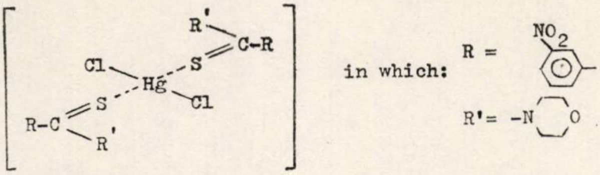

In the case of mercury the nature of thioamide and its substitutes does not specifically determine the type of coordination. The appearance of the compound with 2 : 1 ligand-metal molar ratio can be due to the nitro group attracting the electrons from the *meta* position which has a greater influence on the conjugation of the thio-amidic grouping thus determining the decrease of the basicity of the nitrogen atom in the morpholinic cycle.

REFERENCES

[1] S. Neagoe, Doctoral Thesis, 1983, Polytechnical Inst. of Bucharest, Bucharest — Romania.

[2] D. Negoiu and V. Mureșan, *Anal. Univ. Buc. Chim.*, **1**, 121 (1971).

[3] D. Negoiu, V. Mureșan and Cornelia Fulea, *Anal. Univ. Buc. Chim.*, **2**, (1973).

[4] M. N. Hughes, *Coord. Chem. Rev.*, **37**, 297 (1981).

[5] D. Negoiu, S. Neagoe and Ioana Saramet, *Rev. Roumaine Chim.*, **29**, 275 (1984).

[6] F. Cornea, C. Cercasov and M. Ciureanu, *Spectrochim. Acta*, **36A**, 775 (1980).

[7] C. Cercasov, F. Cornea, M. Ciureanu, M. Hillebrand, V. E. Sahini and E. Volanschi, *Org. Mag. Resonance.*, **20**, 217 (1982).

[8] C. P. Leopardi, O. Fabre, D. Zimmermann, J. Reisse, F. Cornea and C. Fulea., *Canad., J. Chem.*, **55**, 2649 (1977).

[9] I. Tănăsescu and M. Ionescu, "Lucrări practice de chimie organică", vol. II, Ed. Tehnică. Bucharest, p. 143, 1975.

[10] W. J. Geary, *Coord. Chem. Rev.*, **7**, 81 (1971).

Revue Roumaine de Chimie, 31, *11–12*, 995–999 (1986)

Dedicated to Prof. Dr. Doc. P. SPACU on the occasion of his 80th anniversary

SOLUTION PROPERTIES OF ULTRAHIGH MOLECULAR WEIGHT POLYMERS (PLEISTOMERS). 14*

SOLVENT EFFECT ON THE UNPERTURBED DIMENSIONS OF POLY(BUTYL METHACRYLATE) CHAINS

CRISTOFOR I. SIMIONESCU, SILVIA IOAN** and BOGDAN C. SIMIONESCU
Department of Organic and Macromolecular Chemistry, Polytechnic Institute Jassy, R 6600 Jassy, Romania
** "P. Poni" Institute of Macromolecular Chemistry, R 6600 Jassy, Romania

Received May 25, 1986

The paper reports the possibilities of determining the unperturbed dimensions of ultrahigh molecular weight poly(butyl methacrylate). A correction term, depending on the exponent *a* of the Mark-Houwink relation, is introduced into the Stockmayer-Fixman-Burchard equation.

The systematic characterization of ultrahigh molecular weight polymers (pleistomers) raises a number of problems, and the specialty literature contains few references on this subject. However, in the last years, some papers dealt with the application of the now classical techniques of polymer characterization (e.g., light scattering, viscometry) in studying the solution properties of pleistomers.[1–4]

The most important parameters describing polymers in dilute solutions are the molecular weight, the perturbed and unperturbed dimensions, the second virial coefficient and the intrinsic viscosity. A number of methods are available and currently used for the determination of unperturbed dimensions of polymer molecules, *e.g.*, light scattering and/or viscosity measurements of polymer solutions at the theta temperature; it is possible to find suitable expressions relating the intrinsic viscosity in good solvents (or other characteristic parameters of the chain) to the molecular weight by following a mathematical extrapolation procedure. Very often, however, the experimental obtention of a theta-temperature (or theta-solvent) is difficult or even impossible, especially for pleistomers. Likewise, for these polymers, the known extrapolation procedures [5,6] yield much higher values of the unperturbed dimensions due to the curvatures of the linear dependences as given by the experimental points for high excluded volume. In this context, the present paper is aimed at showing that by introducing a correction term depending only on one parameter it becomes possible to obtain the unperturbed dimensions for very high molecular weights. The new parameter is a smooth function of the exponent *a* of the Mark-Houwink equation. Poly(butyl methacrylate) (PBuMA) was used as investigated material.

---

* Note 13 : *Eur. Polym. J.*, in press.

EXPERIMENTAL

PBuMA samples were obtained by plasma-induced polymerization; the conditions of this new polymerization technique were previously described in detail.[7,8] The samples were submitted to fractionation by use of toluene — methanol mixtures as solvent — precipitant systems.

Viscosity measurements were carried out in methyl ethyl ketone (MEK), benzene (B), dioxane (D) and cyclohexanone (C), while light scattering measurements were performed in MEK, at 25°C.

Previous studies on pleistomers established the concentration domains [9] (diluted — semidiluted — concentrated) based on different theoretical models, gave details on the used experimental techniques and discussed the experimental data based on the existing theories on excluded volume effect.[10–15] The possible error sources affecting the analysis of the excluded volume effect for ultrahigh molecular weight PBuMA were also presented.[16;17]

Table 1 gives the weight-average molecular weights and the intrinsic viscosities of the studied samples.

Table 1

Weight-average molecular weights ($\overline{M}_w$) and intrinsic viscosities * $[\eta]$ of PBuMA samples

Sample	$\overline{M}_w \cdot 10^{-6}$ mol·g^{-1}	$[\eta]$, dl·g^{-1}			
		MEK	B	D	C
1	9.59	7.18	—	—	—
2	12.31	8.56	—	—	7.22
3	12.71	8.82	12.26	—	—
4	13.33	—	—	7.44	—
5	14.17	—	13.31	7.58	7.93
6	15.20	9.97	13.87	8.00	8.18
7	15.90	10.35	14.52	—	8.62
8	16.80	10.60	—	8.44	8.77
9	17.90	11.31	15.79	8.65	—
10	18.37	11.51	—	—	—
11	20.66	12.53	17.51	9.84	—
12	21.63	12.96	—	—	—
13	24.50	—	—	—	11.29

* Calculated by averaging the values obtained by use of the equations of Huggins, Kraemer, Martin, Schulz-Blaschke and Fedors [14].

RESULTS AND DISCUSSION

Among the methods currently used to linearize the viscosity-molecular weight relation, able to yield the unperturbed dimensions and the long-range interaction parameter, B, the best known is the Stockmayer-Fixman-Burchard plot [5,6]:

$$[\eta]/M^{1/2} = K_\theta + 0.51\ \Phi_0\ B\ M^{1/2} \qquad (1)$$

with $(K_\theta/\Phi_0)^{2/3} = \langle 6S_0^2\rangle/M$ and $\Phi_0 = 2.51 \cdot 10^{21}$, where $[\eta]/M^{1/2}$ is plotted as a function of $M^{1/2}$. It has been shown by Cowie [18] and others that this plot yields a linear relation only for molecular weights above about 4.10^4 and up to about 10^6.

For high excluded volume effects, *e.g.*, for pleistomers, the situation is more complicated. Moreover, it was observed that the exponent a in the Mark-Houwink relation $[\eta] = K\ M^a$ is not a constant. In all cases there is a deviation from linearity for very large molecular weights, and the exponent a can be considered as constant only for molecular weights varying in well-established limits.

This paper presents a new method for the determination of K_θ from equation (1) for ultrahigh molecular weight polymers by introducing a correction depending on the a coefficient of the Mark-Houwink relation.

Figure 1 depicts the $[\eta]/M^{1/2} = f(\mathrm{M}^{1/2})$ dependence according to equation (1) and to the data from Table 1. One can observe a linearization of the experimental data in the $9 \cdot 10^6 - 24 \cdot 10^6$ molecular weight range.

The data yield values of the K_θ parameter, respectively $< S_0^2 > / M$, depending on the used solvent and are higher as compared to that obtained in a theta solvent (DMF, 23.6°C) by use of light scattering technique (previous data [10,11]). Table 2 summarizes the results obtained by extrapolation to molecular weights tending to zero.

In Figure 2, ΔK_θ was plotted as a function of the Mark-Houwink coefficient a. Evidently, for $a = 0.5$, ΔK_θ has to be zero, and it has to increase with increasing solvent quality. However, it is remarkable to see that there is practically a linear relationship between ΔK_θ and a (within the limit of experimental errors : $\pm 15\%$ for $\overline{M}_w$; $\pm 1.2\%$ for $[\eta]$; $\pm 8.7\%$ for K_θ), yielding the relation :

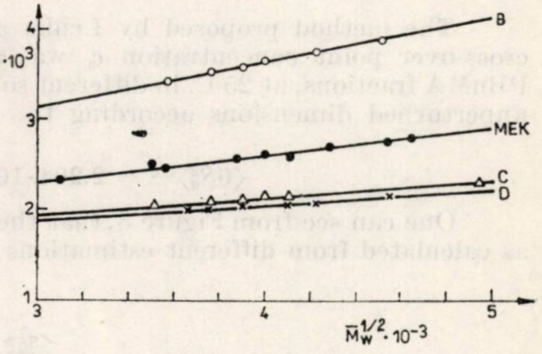

Fig. 1. — Plot of $[\eta]/M^{1/2}$ versus $M^{1/2}$ for PBuMA samples in B, MEK, C and D at 25°C.

$$\Delta K_\theta = -1{\cdot}71(6).10^{-3} + 3.4(3) \cdot 10^{-3}\ a \qquad (2)$$

or

$$\Delta K_\theta = 34.3 \cdot 10^{-4}(a - 0.5) \qquad (3)$$

Table 2

Values of K_θ parameters, $<S^2>/M$ and of the slopes obtained from Figure 1 (according to equation (1)) for PBuMA samples in B, MEK, C and D, with the exponents a from the Mark-Houwink relation[14], as well as the deviation from the value determined[10,11] in a theta solvent (ΔK_θ)

Solvent	a	$K_\theta \cdot 10^3$	$\Delta K_\theta \cdot 10^3$ *	$\langle S_0^2\rangle / M \cdot 10^{17}$	Slope $\cdot 10^6$
B	0.774	1.570	0.854 ± 0.074	1.218	0.52
MEK	0.726	1.400	0.684 ± 0.060	1.129	0.30
C	0.648	1.300	0.584 ± 0.050	1.075	0.20
D	0.630	1.155	0.439 ± 0.040	0.993	0.21
DMF (θ solv.)	0.500	0.716	—	0.724	—
in different solvents (eq. (4))[15]	0.500	0.793	—	0.773	—

* $\Delta K_\theta = K_{\theta \text{experimental}} - K_{\theta \text{DMF}}$

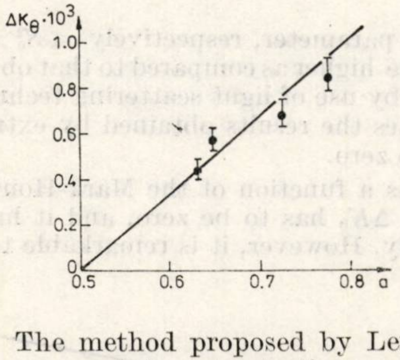

Fig. 2. — Plot of ΔK_θ versus Mark-Houwink coefficient a, for the systems mentioned in Table 2.

The method proposed by Lenka *et al.* [19] for the evaluation of the cross-over point concentration c_0 was also used (viscometric data) for PBuMA fractions, at 25°C, in different solvents[15], in order to determine the unperturbed dimensions according to

$$\langle 6S_0^2\rangle^{1/2} = 2.204 \cdot 10^{-8} (M/c_0)^{1/3} \tag{4}$$

One can see from Figure 3, that the most probable value for $\langle S_0^2\rangle/\text{M}$, as calculated from different estimations of c_0, is $0.773 \cdot 10^{-17}\,\text{cm}^2$, in very

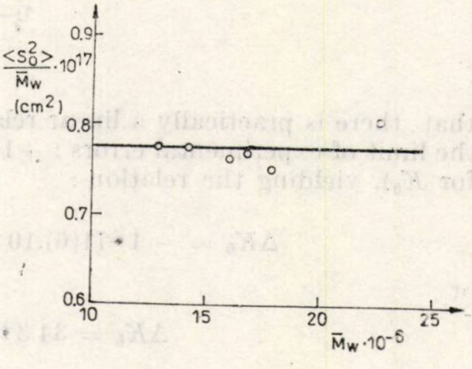

Fig. 3. — $<\overline{S_0^2}>/M$ dependences as a function of $\overline{M}_w$, calculated according to equation (3), for PBuMA samples 3, 5, 6 8, 9 and 11 (Table 1). The full line represents the average established by the least squares method.

good agreement with that obtained from light scattering measurement in theta-solvent (DMF at 23.6°C) [10,11] and with the corrected value $(0.724 \cdot 10^{-17}\,\mathrm{cm}^2)$, by ΔK_θ, according to equation (3) already established (see Table 2).

CONCLUSIONS

The use of the classical extrapolation relations for the determination of the unperturbed dimensions of macromolecular chains has to be applied with great care to pleistomers for high excluded volume.

The present paper introduces a correction term depending only on one parameter (the exponent a of the Mark-Houwink equation) for the estimation of the real value of K_θ and of the unperturbed dimensions of pleistomers, respectively. The resulted correction is correlated to the previous data [10,11,15] obtained in a theta-solvent (DMF, at 23.6°C) for PBuMA, and to those determined according to the method of Lenka *et al*[19].

REFERENCES

[1] Y. Miyaki, Y. Einaga and H. Fujita, *Macromolecules*, **11**, 1180 (1978).
[2] Y. Einaga, Y. Miyaki and H. Fujita, *J. Polym. Sci., Polym. Phys. Ed.*, **17**, 2103 (1979).
[3] C. I. Simionescu, B. C. Simionescu and S. Ioan, *Macromolecules*, **18**, 1995 (1985).
[4] C. I. Simionescu, B. C. Simionescu and S. Ioan, *J. Macromol. Sci.-Chem.*, A**22**, 765 (1985).
[5] W. H. Stockmayer and M. Fixman, *J. Polym. Sci. (C)*, **1**, 137 (1963).
[6] W. Burchard, *Makromol. Chem.*, **50**, 20 (1961).
[7] B. C. Simionescu, A. Natansohn, C. Ananiescu, M. Leancă and C. I. Simionescu, *Polym. Bull.*, **3**, 247 (1980).
[8] B. C. Simionescu, M. Leancă, C. Ananiescu and C. I. Simionescu, *Polym. Bull.*, **3**, 437 (1980).
[9] S. Ioan, B. C. Simionescu, I. Neamţu and C. I. Simionescu, *Polymer Commun.*, **27**, 113 (1986).
[10] C. I. Simionescu, B. C. Simionescu and S. Ioan, *J. Polym. Sci., Polym. Lett. Edn.*, **3**, 12 (1985).
[11] C. I. Simionescu, S. Ioan and B. C. Simionescu, 27th Microsymposium on Macromolecules "Physical Optics of Dynamic Phenomena and Processes in Macromolecular Systems", Prague, July, 16—19, 1984, pp. P 64—1.
[12] B. C. Simionescu, S. Ioan and C. I. Simionescu, *J. Polym. Sci.*, in press.
[13] S. Ioan, B. C. Simionescu and C. I. Simionescu, to be published.
[14] C. I. Simionescu, I. Neamţu, S. Ioan and B. C. Simionescu, *Polymer*, in press.
[15] C. I. Simionescu, S. Ioan and B. C. Simionescu, *Eur. Polym. J.*, in press.
[16] S. Ioan, C. Sava and B. C. Simionescu, *Bull. Polytechnic Inst. Jassy*, XXXI(XXXV), Special Issue, 117 (1985).
[17] S. Ioan, A. Leonte, C. Sava, B. C. Simionescu and C. I. Simionescu, *Acta Polym.*, in press.
[18] J. M. G. Cowie, *Polymer*, **7**, 487 (1966).
[19] S. Lenka, P. L. Nayak and M. Dash, *J. Macromol. Sci. — Chem.*, **A19**, 321 (1983).

Revue Roumaine de Chimie, **31**, *11–12*, 1001– 1011 (1986)

Dedicated to Professor P. SPACU on his 80th anniversary

CARBONIUM ION REACTIONS. XVII*

REARRANGEMENTS OF DIBENZOBICYCLO[3.2.1]OCTANE AND DIBENZOBICYCLO[3.2.2]NONANE DERIVATIVES

MICHAELA STĂNESCU, M. ELIAN and ECATERINA CIORĂNESCU
Centre of Organic Chemistry, Spl. Independenţei 202 B, 78100 Bucharest, Romania

Received May 18, 1986

The trifluoroacetolyses of alcohols **3** and **4** proceed with rearrangement leading to compounds with one more carbon atom in the saturated bridge. The two systems present different behaviours regarding the position of the substituent (methyl or phenyl) in the reaction products, namely alcohols **3** generate bridge-substitututed and bridgehead-substituted compounds, while alcohols **4** generate only bridge-substituted compounds. This different behaviour is most probably due to steric factors.

The solvolyses of double bond-unsubstituted [1,2] or -substituted [3–5] tosylates **1** with side-chain of one or two carbon atoms were described in previous papers. It was shown that, depending on the reaction conditions (kinetic or thermodynamic control), the main products of the methyl- or phenyl-substituted tosylates **1** were **2a** or **2b**.

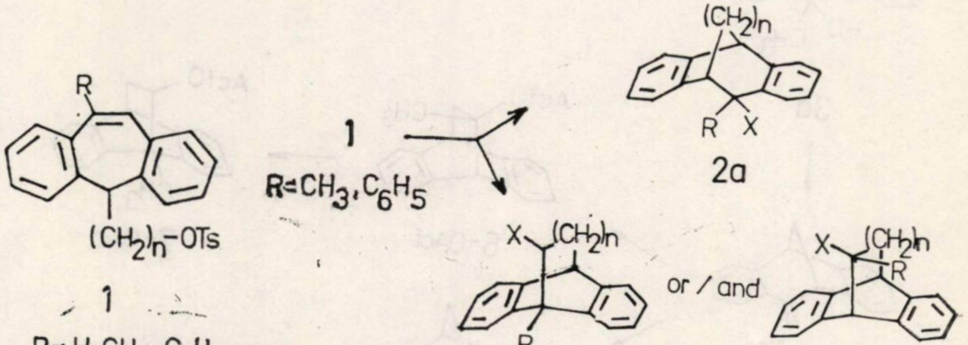

1

2a

2b

This paper presents the solvolytic behaviour of alcohols **3** and **4**, closely related to the primary solvolytic reaction products of tosylates **1** ($R=CH_3$ and C_6H_5).

---

* Part XVI, M. Banciu, Phan Le Thuy and Ligia Stănescu, *Rev. Roumaine Chim.*, **24**, 957 (1979).

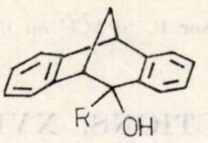

3a R = CH_3
3b R = C_6H_5

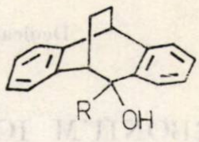

4a R = CH_3
4b R = C_6H_5

RESULTS

Alcohols **3a**,[6] **4a**[5] and **4b**[5] were synthesized according to the literature data. Alcohol **3b** was obtained from the corresponding ketone [7] and phenylmagnesium bromide.

The solvolyses were conducted in trifluoroacetic acid (AcfOH) at 25°, with a molar ratio acid *vs.* alcohol 10/1. The reaction course was followed by v.p.c. The reaction was stopped at the selected time intervals by dilution with water and neutralization with sodium carbonate. The reaction products were isolated by column chromatography or preparative v.p.c. Their structure was determined by elemental analysis, IR and ^{1}H-NMR spectroscopy or comparison with authentic samples for the known compounds.

Solvolysis of alcohol **3a**. In trifluoroacetic acid, alcohol **3a** led by a clean and rapid dehydration to hydrocarbon **5**. According to the ^{1}H-NMR spectrum this reaction was completed in a few minutes.

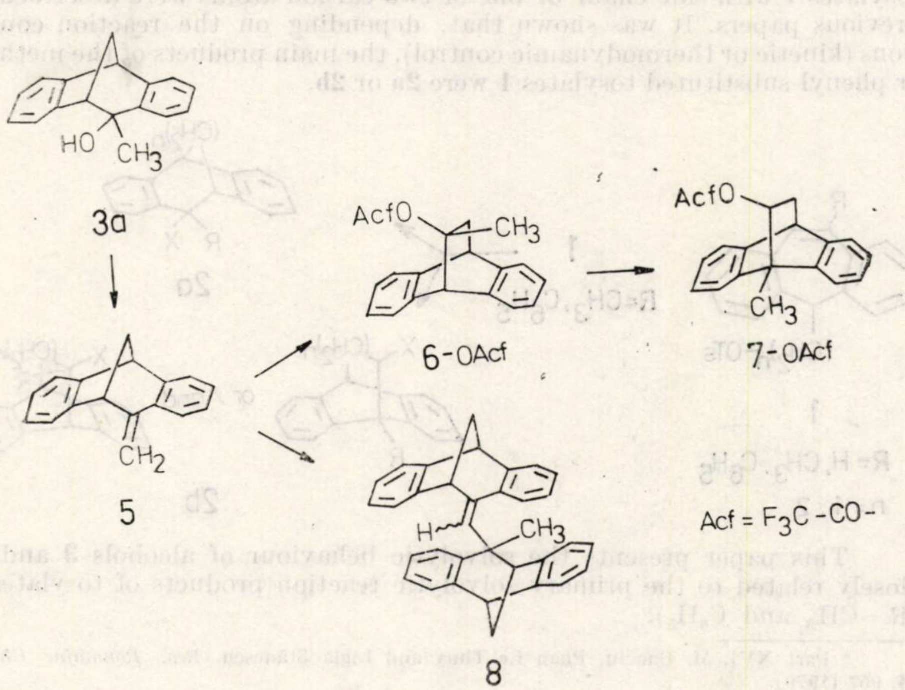

At longer reaction time hydrocarbon **5** was converted into trifluoroacetates **6**-OAcf and **7**-OAcf with dibenzobicyclo[2.2.2]octane skeleton and the dimeric hydrocarbon **8** (Table 1). Dimer **8** was formed only at the beginning of the reaction (the first 15 minutes) while the concentration of hydrocarbon **5** was still high. The dimer concentration remained practically unchanged till the end of the reaction. These observations proved that **8** was generated directly from the hydrocarbon **5** and was stable under the reaction conditions. Trifluoroacetate **6**-OAcf, with the methyl group linked to the bridge, was rapidly formed and rearranged subsequently into the trifluoroacetate **7**-OAcf with the substituent at the bridgehead position.

Table 1

Trifluoroacetolysis of alcohol **3a**

Time (h)	Product % (v.p.c.)				
	5	**6**-OAfc	**7**-OAfc	**8**	Other compounds
0.08	100.0	—	—	—	—
0.25	11.9	39.6	29.0	14.5	5.0
0.50	9.2	33.5	42.0	10.0	5.3
1.25	4.6	28.0	50.0	10.4	7.0
2.00	0.5	18.0	65.0	10.1	6.4
3.00	—	13.0	70.0	8.0	9.0

The transformation of system **6** into **7** was independently proved in a control experiment; alcohol **6**-OH[8] gave in trifluoroacetic acid a mixture consisting of **6**-OAcf and **7**-OAcf. Trifluoroacetate **7**-OAcf was stable under the reaction conditions, while the corresponding acetate **7**-OAc was converted into **7**-OAcf. The control experiments proved that although the ionization of **7** is possible, its reaarrangement to **6** does not occur. Most probably, the compound substituted at the bridgehead position (**7**-OAcf) is the thermodynamically stable product.

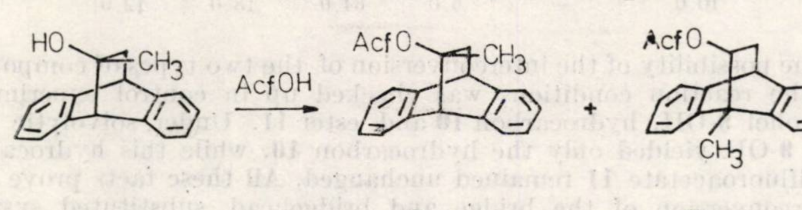

6 - OH 6 - OAcf 7- OAcf

Solvolysis of alcohol **3b**. The solvolysis of alcohol **3b** gave rise to a mixture of three compounds **9**−**11** with dibenzobicyclo[2.2.2]octane skeleton. In ester **9**-OAcf and hydrocarbon **10**, the phenyl group is linked to the bridge, while in the trifluoroacetate **11** it stands at the bridgehead position. Table 2 presents the evolution of the reaction. Obviously, during the reaction the ester **9**-OAcf was partially transformed into hydrocarbon **10**. After three hours, when the starting material had almost entirely vanished, the only reaction was the conversion of ester **9**-OAcf into hydrocarbon **10** so the ratio between the bridge substituted (**9**-OAcf + **10**) and bridgehead substituted compounds (**11**) remained constant (4.2/1).

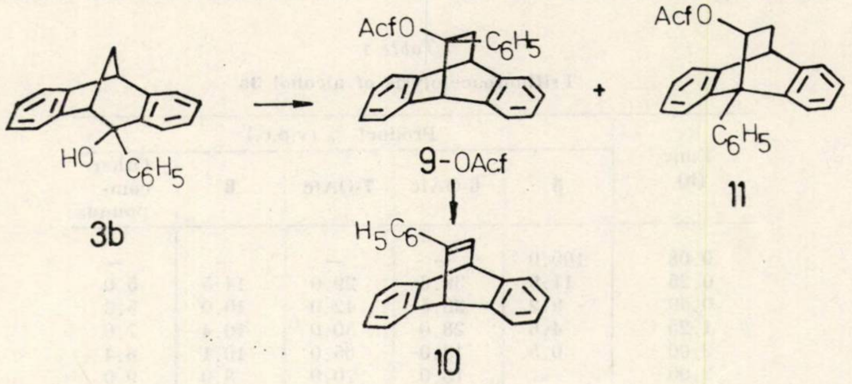

Table 2
Trifluoroacetolysis of alcohol 3b

Time (h)	Products % (v.p.c.)				
	3b	**9-OAfc**	**10**	**11**	Other compounds
0.5	52.0	41.0	2.5	2.0	2.5
1.0	39.8	46.4	3.0	7.2	3.6
2.0	15.5	65.0	4.0	13.5	2.0
3.0	5.0	69.0	8.0	16.0	2.0
4.0	1.5	62.0	15.0	18.0	3.5
5.0	1.5	53.0	25.0	18.0	2.5
10.0	—	6.0	64.0	18.0	12.0

The possibility of the interconversion of the two types of compounds under the reaction conditions was checked up in control experiments with alcohol **9**-OH, hydrocarbon **10** and ester **11**. Under solvolytic conditions, **9**-OH yielded only the hydrocarbon **10**, while this hydrocarbon and trifluoroacetate **11** remained unchanged. All these facts prove that no interconversion of the bridge and bridgehead substituted systems occurs.

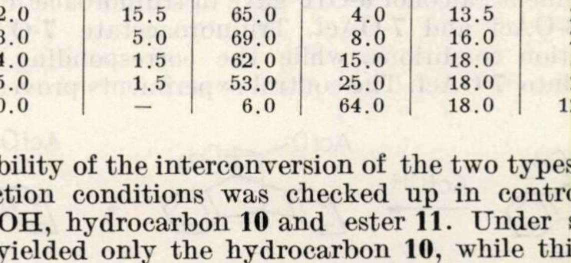

Solvolysis of alcohol **4a**. In trifluoroacetic acid, alcohol **4a** gave rapidly and entirely hydrocarbon **12** (in 5 minutes, **12** was the only detectable compound). At longer time a mixture of three compounds with dibenzobicyclo[3.2.2]nonane skeleton was obtained, namely ester **13**-OAcf and hydrocarbons **14** and **15** (see Table 3).

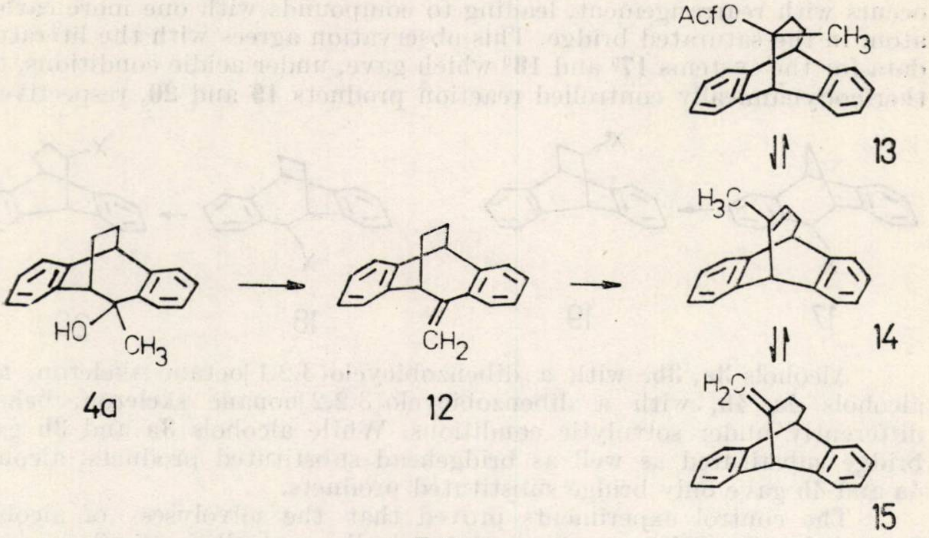

Table 3
Trifluoroacetolysis of alcohol **4a**

Time (h)	Products % (v.p.c.)			
	12	**13**-OAcf	**14**	**15**
0.08	98.0	—	—	—
6.0	15.0	16.8	43.6	24.6
24.0	1.5	10.5	54.0	34.0

Control experiments with the reaction products **13**—**15** proved that under solvolytic conditions, any of these compounds were converted after 24 h into an equilibrium mixture consisting of **13**-OAcf (11%), **14**(55%) and **15**(34%). In all these compounds, the substituent is linked to the three-membered bridge. No bridgehead substituted compound had been detected.

Solvolysis of alcohol **4b**. Under solvolytic conditions, alcohol **4b** was transformed rapidly and completely into hydrocarbon **16**, with a dibenzobicyclo[3.2.2]nonane skeleton and the phenyl substituent at the bridge. No other reaction products have been detected.

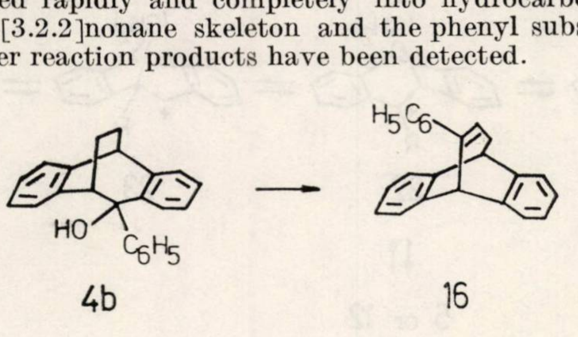

DISCUSSION

The solvolysis in trifluoroacetic acid of alcohols **3a, b** and **4a, b** occurs with rearrangement, leading to compounds with one more carbon atom in the saturated bridge. This observation agrees with the literature data for the systems **17**[9] and **18**[2] which gave, under acidic conditions, the thermodynamically controlled reaction products **19** and **20**, respectively.

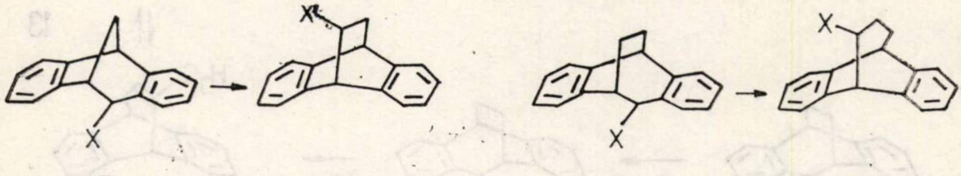

17 19 18 20

Alcohols **3a**, **3b**, with a dibenzobicyclo[3.2.1]octane skeleton, and alcohols **4a**, **4b**, with a dibenzobicyclo[3.2.2]nonane skeleton, behave differently under solvolytic conditions. While alcohols **3a** and **3b** gave bridge substituted as well as bridgehead substituted products, alcohols **4a** and **4b** gave only bridge substituted products.

The control experiments proved that the solvolyses of alcohols **3a** and **4a** ($R=CH_3$) are thermodynamically controlled. Similar experiments indicated that the two types of solvolysis products (**9** + **10** and **11**) of alcohol **3b** are formed by irreversible paths under the reaction conditions. The fact that alcohol **4b** gave only one product (**16**), which was stable under the reaction conditions, was not conclusive concerning the reaction control (thermodynamic *vs.* kinetic).

A general reaction scheme describing the transformations of alcohols **3** and **4** involves at least the ions **21**–**24**.

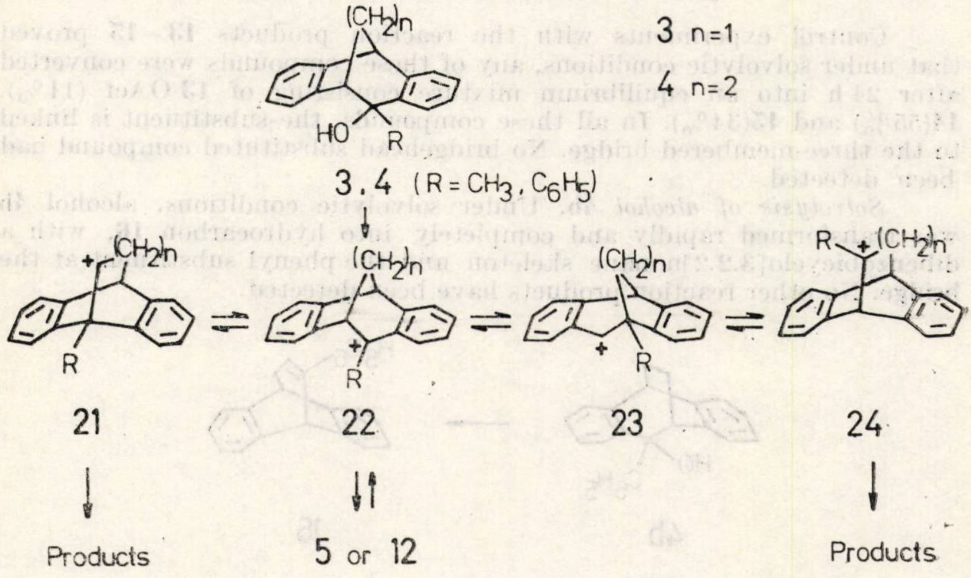

The ionization of alcohols **3** and **4** leads to the tertiary benzylic ion **22**. For alcohols **3a** and **4a** (R$=CH_3$), this ion is in equilibrium with the corresponding exomethylenic hydrocarbon representing the kinetically controlled product (**5** and **12**, respectively). Ion **22** has two additional reaction paths besides the above mentioned one. Phenyl migration from the β position leads to ion **21**, precursor of the bridgehead substituted products. The second reaction path involves the 1,2 migration of the saturated bridge giving the benzylic ion **23**, followed by the phenyl migration which generates the tertiary ion **24**, precursor of the bridge substituted products. The nonclassical ion **25** and the phenonium ions **26** and **27** may be as well involved in the transformations **22** ⇌ **23**, **22** ⇌ **21** and **23** ⇌ **24**, but most probably these are high energy intermediates or transition states in these reactions.

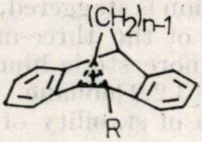

25

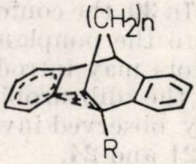

26

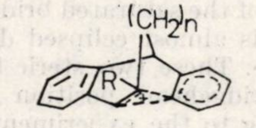

27

Bridge substituted compounds have been identified among reaction products in all the solvolytic reactions described above. Therefore, the reaction path involving the saturated bridge migration is proper to all investigated systems (**3**, **4** → **22** → **23** → **24**). The bridge migration reaction path in these systems is well documented by Cristol and coworkers[10]; the deuterium substituted compounds **28** and **29** equilibrate in acidic medium (acetic acid and perchloric acid).

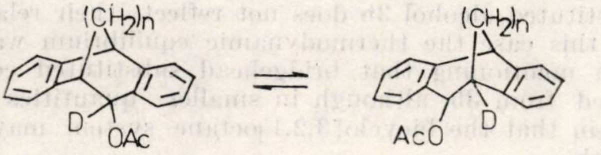

28 29

The solvolytic behaviour under thermodynamically controlled conditions of the methyl substituted alcohols **3a** and **4a** deserves further comments. While the major product of the trifluoroacetolysis of alcohol **3a** is a bridgehead substituted compound (**7**) generated by ion **21** (R$=CH_3$, n $= 1$), alcohol **4a** is entirely transformed into bridge substituted products (**13**–**15**) originating from the precursor **24** (R$=CH_3$, n $= 2$). The thermodynamic control of the reaction being established, these observations reflect the stability difference of the two types of compounds for the dibenzobicyclo-octane and -nonane skeletons. The solvolytic behaviour of alcohol **3a** may be assumed as a "normal" one, the most stable product (**7**-OAcf) being the most difficultly ionisable one under the reaction conditions. Indeed, the trifluoroacetate **7**-OAcf is in equilibrium with the secondary ion **21**

($R = CH_3$, $n = 1$), which is more reactive than the tertiary one **24**. The solvolytic behaviour of alcohol **4a** shows a change in the reaction pathway. All the reaction products originate from the tertiary ion **24** ($R = CH_3$, $n = 2$), indicating that in this case the bridgehead substituted compounds are less stable than the bridge substituted ones.

Most probably, this stability inversion is steric in nature. Inspection of the steric models suggests two possible explanations for the different stability of the bridgehead substituted compounds **30** and **31**. The bicyclo[2.2.2]octane skeleton **30** is more folded than the bicyclo[3.2.2]nonane one **31**. In **31**, the R group and the indicated hydrogen atoms of the aromatic rings are almost coplanar generating probably a more severe crowding in **31** than in **30**. Additionally, the bridgehead substituent R is in a different relation to the substituents of the neighbouring carbon atom of the saturated bridge. In **30**, the conformation is staggered, while in **31** it is almost eclipsed due to the nonplanarity of the three-membered bridge. These two steric factors may introduce more steric hindrance at the bridgehead position of the dibenzobicyclo[3.2.2]nonane skeleton, leading to the experimentally observed inversion of stability of the products originating from ions **21** and **24**.

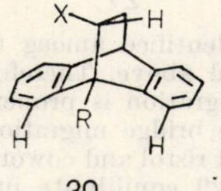

30

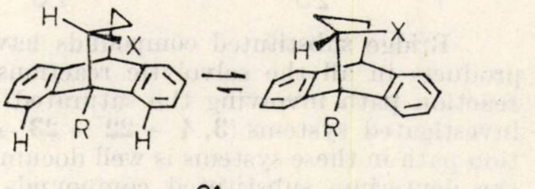

31

The distribution of the reaction products in the solvolysis of the phenyl substituted alcohol **3b** does not reflect their relative stabilities, because in this case the thermodynamic equilibrium was not reached. It is worth mentioning that bridgehead substituted compounds were also obtained from **3b**, although in smaller quantities than from **3a**, proving again that the bicyclo[3.2.1]octane system may react on both reaction paths.

EXPERIMENTAL

Melting points are uncorrected. IR spectra were recorded with a double-beam C. Zeiss Jena UR-20 spectrophotometer and ^1H-NMR spectra on a Varian A-60A spectrometer using TMS as internal standard. The v.p.c. analyses were performed on a Carlo Erba model D chromatograph with flame ionization detector, 2 m column (10% silicone oil QF1 on Chromosorb Q, 80–100 mesh), carrier gas nitrogen at 180°. The v.p.c. separations were carried out on a preparative Carlo Erba model GV chromatograph with a 2 m column (10% silicone oil QF1 on Chromosorb W, 30–60 mesh), carrier gas nitrogen, at 200°.

10,11-Dihydro-11-phenyl-5,10-methano-5*H*-dibenzo[*a*,*d*]cyclohepten-11-ol-(3b). A solution of 2.2 g (10 mmoles) of 10,11-dihydro-5,10-methano-5*H*-dibenzo[*a*, *b*]cyclohepten-11-one [7] in 50 mL anhydrous ethyl ether was treated with a solution of C_6H_5MgBr (prepared from 1 g Mg and 5 g C_6H_5Br) in 50 mL anhydrous ethyl ether, under dry nitrogen. After 3 h at reflux the mixture was worked out in the usual way. 2.4 g (80%) of a crystalline product were obtained; m.p. 149–150° (methanol).

Found: C, 88.90 ; H, 6.32 %. $C_{22}H_{18}O$ requires : C, 88.56 ; H, 6.08 %.

IR spectrum (CCl_4 ; cm^{-1}) : ν_{OH} 3580 m.

NMR spectrum (CCl_4 ; δ, ppm) : 2.32 (s, 1H, OH), 2.48 (m, 2H, H_{12}), 3.55 (t, J = 3.5 Hz, 1H, H_{10}), 3.98 (t, J = 3.5 Hz, 1H, H_5) and 7.1—7.8 (m, 13H, H_{arom}).

9,10-Dihydro-11-phenyl-9,10-ethanoanthracen-11-ol (9-OH). From 2.2 g (10 mmoles) 9,10-dihydro-9,10-ethanoanthracen-11-one [12] and C_6H_5MgBr as described above, 2.43 g (82 %) **9**-OH were obtained ; m.p. 150—151° (methanol).

Found: C, 88.25 ; H, 6.25 %. $C_{22}H_{18}O$ requires : C, 88.56 ; H, 6.08 %.

IR spectrum (CCl_4 ; cm^{-1}) : ν_{OH} 3586 m.

NMR spectrum (CCl_4 ; δ, ppm) : 1.76 (s, 1H, OH), 2.02 (dd, J = 2.5 ; 14 Hz, 1H, H_{12}), 2.66 (dd, J = 2.5 ; 14 Hz, 1H, H_{12}), 4.19 (s, 1H, H_{10}), 4.41 (t, J = 2.5 Hz, 1H, H_9) and 6.7—7.6 (m, 13H, H_{arom}).

9,10-Dihydro-11-methyl-9,10-propanoanthracen-11-ol (13-OH). By the same method from the corresponding ketone [2] (2.3 g, 10 mmoles) and CH_3MgI, alcohol **13**-OH was prepared (2.3 g, 90 %) ; m.p. 98—99° (aq. ethanol).

Found: C, 85.50 ; H, 7.24 %. $C_{18}H_{18}O$ requires : C, 85.38 ; H, 7.24 %.

IR spectrum (CCl_4 ; cm^{-1}) : ν_{OH} 3585 m.

NMR spectrum ($CDCl_3$; δ, ppm) : 1.15 (s, 3H, CH_3), 1.0—2.0 (m, 5H, $H_{12,13}$ + OH), 3.81 (s, 1H, H_{10}), 3.95 (t, J = 3.5 Hz, 1H, H_9) and 7.1—7.5 (m, 8H, H_{arom}).

General procedure for trifluoroacetolyses. A $CHCl_3$ solution of the alcohol **3a** (**3b**, **4a** or **4b**) was treated with AcfOH with stirring at room temperature. The reaction mixture was neutralized with a solution of Na_2CO_3 (10 %) and extracted with $CHCl_3$. The organic extracts were combined, washed with cold water, dried (Na_2SO_4), evaporated and separated by elution or v.p. chromatography.

For analytical studies, from the reaction mixture, aliquots of 0.1 mL were withdrawn at selected time intervals and worked up as described above. The residue was analysed by v.p.c.

The trifluoroacetolysis of 10,11-dihydro-11-methyl-5,10-methano-5*H*-dibenzo [*a*,*d*]cyclohepten-11-ol (3a). A solution of 2.36 g (10 mmoles) alcohol **3a** in 1 mL $CHCl_3$ and 5 mL AcfOH was stirred for 3 h. The residue resulted after the standard work up was treated with methanol (10 mL). The obtained precipitate was filtered and washed with additional methanol (10 mL). *10,11-Dihydro-11-[(10, 11-dihydro-5,10-methano-5H-dibenzo[a, d]cyclohept-11-ylidene) methyl]-11-methyl-5,10-methano-5H-dibenzo[a,d]cycloheptene* (**8**) was isolated as a white solid ; m.p. 260—265° (cyclohexane).

Found: C, 93.63 ; H 6.20 %. $C_{17}H_{28}$ requires : C, 93.97 ; H, 6.03 %.

IR spectrum (CS_2, CCl_4 ; cm^{-1}) : 760i, 1438 m, 1472 m, 2950 m, 3024 w, 3082 w.

NMR spectrum ($CDCl_3$, δ, ppm) : 1.55 and 1.70 (two singlets, 3H, CH_3), 2.5—2.8 (m, 4H, H_{12}), 3.50 (m, 2H, H_5), 4.05 (m, 2H, H_{10}), 6.45 and 6.50 (two singlets, 1H, H_{olef}) and 7.0 — 7.5 (m, 8H, H_{arom}). The spectrum corresponds with a 1 : 2 mixture of the two possible stereoisomers of **8**.

The oily residue resulted after the methanol evaporation was separated by preparative v.p.c.

9,10-Dihydro-11-methyl-9,10-ethanoanthracen-11-ol trifluoroacetate (**6**-OAcf) was isolated as an oily product. Treated with $LiAlH_4$ it gave the corresponding alcohol **6**-OH, identified by comparison with an authentic sample.[8]

9, 10-Dihydro-10-methyl- 9,10-ethanoanthracen-11-ol trifluoroacetate (**7**-OAcf) resulted also as an oily compound.

IR spectrum (CCl_4 ; cm^{-1}) : ν_{CO} 1780 vi.

NMR spectrum ($CDCl_3$; δ, ppm) : 1.58 (dt, J = 13 and 2.7 Hz, respectively, 1H, H_{12}), 1.92 (s, 3H, CH_3), 2.58 (ddd, J = 2.7 ; 8.5 ; 13 Hz, 1H, H_{12}), 4.24 (t, J = 2.7 Hz, 1H, H_9), 5.01 (dd, J = 2.7 ; 8.5 Hz, 1H, H_{11}) and 7.0—7.5 (m, 8H, H_{arom}).

0.1 g of **7**-OAcf were treated in the usual way with $LiAlH_4$. Alcohol **7**-OH (0.07 g, 90 %) was identical with the alcohol prepared by Hart and coworkers.[12]

*10,11-Dihydro-11-methylene-5,10-methano-5*H*-dibenzo*[a,d]*cycloheptene* (**5**) was identified at a short reaction time (5 min) by its known NMR-spectrum.[13]

Alcohol **6**-OH (0.1 g, 0.4 mmoles) in 0.5 mL $CHCl_3$ was stirred with 2 mL AcfOH, 3 h at room temperature. The residue resulted after the work up was v.p.c. analysed (40 % **6**-OAcf and 60 % **7**-OAcf).

The trifluoroacetolysis of 10,11-dihydro-11-phenyl-5,10-methano-5*H*-dibenzo[*a*,*d*] cyclohepten-11-ol (3b). 2.9 g (10 mmoles) alcohol **3b** in 1 ml $CHCl_3$ were stirred with 6 mL AcfOH 10 h. The oily residue (2.1 g 70%) was separated by elution chromatography on neutral alumina.

The first fraction (petroleum ether b.p. 36—38°) gave 1.3 g *9,10-dihydro-11-phenyl-9, 10-ethenoanthracene* **(10)** as a yellow oil wich crystallized in time ; m.p. 72—73°.

Found: C, 93.99 ; H, 6.01 %. $C_{22}H_{16}$ requires : C, 94.15 ; H, 6.20 %.

IR spectrum (CS_2, CCl_4 ; cm^{-1}) : 710 vi, 755 vi, 762 vi, 1460 m, 2860 m, 3020 m and 3070 m.

NMR spectrum (CCl_4 ; δ, ppm) : 5.02 (d, J=6.5 Hz, 1H, H_9), 5.33 (t, J=1.5 Hz, 1H, H_{10}) and 6.5—7.5 (m, 14H, $H_{arom-olef}$).

The next fraction (1 : 1 petroleum ether : ethyl ether) gave the *9,10,dihydro-10-phenyl-9,10-ethanoanthracen-11-ol trifluoroacetate* (**11**).

Found: C, 73.30 ; H, 4.09 %. $C_{24}H_{17}F_3O_2$ requires : C, 73.09 ; H, 4.34 %.

IR spectrum (CCl_4 ; cm^{-1}) : ν_{CO} 1780 vi.

NMR spectrum ($CDCl_3$; δ, ppm) : 1.58 (dt, J = 13 and 2.5 Hz, respectively, 1H, H_{12}), 2.58 (ddd, J = 2.5 ; 8.5 ; 13 Hz, 1H, H_{12}), 4.37 (t, J = 2.5 Hz, 1H, H_9), 5.77 (dd, J = 2.5 ;8.5 Hz, 1H, H_{11}) and 6.5—7.5 (m, 13H, H_{arom}).

The last fraction (ethyl ether) gave *9,10-dihydro-11-phenyl-9,10-ethanoanthracen-11-*ol *trifluoroacetate* (**9**-OAcf) which was reduced to the corresponding alcohol **9**-OH and identified by comparison with an authentic sample.

Alcohol **9**-OH (0.1 g, 0.34 mmoles) in 0.5 mL $CHCl_3$ and 2 mL AcfOH gave after 10 h at room temperature hydrocarbon **10** (spectral and v.p.c. analyses).

The trifluoroacetolysis of 10,11-dihydro-11-methyl-5,10-ethano-5-*H* dibenzo[*a*,*d*]cyclohepten-11-ol (4a). A solution of 2.5 g (11 mmoles) alcohol **4a** in 0.5 mL $CHCl_3$ and 6 mL AcfOH was stirred for 10 h. The mixture resulted after the usual work up was separated by preparative v.p.c.

*9,10-Dihydro-11-methylene-9,10-propanoanthracene (***15***)* is an oily product.

Found: C, 93.06 ; H, 7.15 %. $C_{18}H_{16}$ requires : C, 93.11 ; H, 6.89 %.

IR spectrum (CS_2, CCl_4 ; cm^{-1}) : 760vi, 890i, 2860m, 2935m, 3025m, 3075 m.

NMR spectrum (CCl_4 ; δ, ppm) : 1.7—2.3 (m, 4H, $H_{12,13}$), 4.05 (t, J = 4Hz, 1H, H_9), 4.57 (s, 1H, H_{10}), 4.65 (s, 1H, H_{olef}), 4.90 (s, 1H, H_{olef}) and 7.0—7.4 (m, 8H, H_{arom}).

9,10-Dihydro-11-methyl-9,10-propenoanthracene (**14**) was identified by comparison with an authentic sample.[5]

9,10-Dihydro-11-methyl-9,10-propanoanthracene-11-ol trifluoroacetate (**13**-OAcf) was isolated as a white solid ; mp. 101—103°C. After reduction with $LiAlH_4$ alcohol **13**-OH was obtained, identical with a sample synthesized as described above.

*10,11-Dihydro-11-methylene-5,10-ethano-5*H*-dibenzo*[*a*,d]*cycloheptene* (**12**) was identified by spectral analyses in the reaction mixture at a short time (5 min).

Hydrocarbon **14** (0.2 g) in 0.2 mL $CHCl_3$ and 3 mL AcfOH gave after 24 h stirring at room temperature a mixture of : 58 % **14**, 33 % **15** and 9 % **13**-OAcf. In the same conditions **15** and **13**-OH gave 54 % **14**, 38 % **15**, 8 % **13**-OAcf and respectively 55 % **14**, 34 % **15** and 11 % **13**-OAcf.

The trifluoroacetolysis of 10,11-dihydro-11-phenyl-5,10-ethano-5*H*-dibenzo[*a*,*d*]cyclopten-11-ol-(4b). A solution of **4b** (3.1 g, 10 mmoles) in 1 mL $CHCl_3$ was stirred with 6 mL AcfOH 1h. The usual work up gave 2.6 g (80 %) *9,10-dihydro-11-phenyl-9,10-propenoanthracene* (**16**)[5].

ACKNOWLEDGEMENTS: We wish to thank Mrs. Ligia Stănescu for v.p.c analyses and Mr. F. Chiraleu for NMR spectra.

REFERENCES

[1] E. Ciorănescu, A. Bucur, M. Elian, M. Banciu, M. Voicu and C. D. Nenitzescu, *Tetrahedron Letters*, **1964**, 3855 ; E. Ciorănescu, A. Bucur, M. Elian and C. D. Nenitzescu, *Rev. Roumaine Chim.*, **10**, 149 (1965) ; E. Ciorănescu, A. Bucur, M. Elian, M. Banciu, M. Voicu and C. D. Nenitzescu, *ibid.*, **10**, 161 (1965).

[2] E. Ciorănescu, M. Banciu, R. Jelescu, M. Rentzea, M. Elian and C. D. Nenitzescu, *Tetrahedron Letters*, **1969** ; 1971 ; *Rev. Roumaine Chim.*, **14**, 911 (1969).

[3] M. Stănescu, E. Ciorănescu to be published.

[4] M. Stănescu, *Ph. D. Thesis*, Bucharest, 1982.

[5] M. Stănescu, G. Mihai, L. Stănescu and E. Ciorănescu, *Rev. Roumaine Chim.*, **24**, 197 (1979).

[6] M. Avram, I. G. Dinulescu, C. D. Nenitzescu, R. A. Y. Jones, A. R. Katritzky and R. J. Wyatt, *Rev. Roumaine Chim.*, **18**, 441(1973).

[7] S. J. Cristol, F. P. Parungo and D. E. Plorde, *J. Amer. Chem. Soc.*, **87**, 2870 (1965).

[8] V. J. Shiner and J. S. Humphrey, *J. Amer. Chem. Soc.*, **85**, 2416 (1963).

[9] S. J. Cristol, F. P. Parungo, D. E. Plorde and K. Schwarzenbach, *J. Amer. Chem. Soc.*, **87**, 2879 (1965) ; E. Ciorănescu, A. Mihai, G. Mihai, M. Elian and C. D. Nenitzescu, *Rev. Roumaine Chim.*, **10**, 175 (1965) ; E. Ciorănescu, A. Bucur, F. Badea, M. Rentzea and C. D. Nenitzescu, *Tetrahedron Letters*, **1969**, 1867.

[10] S. J. Cristol, R. J. Bopp and E. Johnson, *J. Org. Chem.*, **34**, 3574 (1969) ; S. J. Cristol and R. J. Bopp, *ibid.*, **39**, 1336 (1974) ; S. J. Cristol and A. L. Noreen, *ibid.*, **41**, 4016 (1976).

[11] S. Wawzonek and S. V. Hallum, *J. Org. Chem.*, **18**, 288 (1953).

[12] H. Hart, D. L. Dean and D. N. Buchanan, *J. Amer. Chem. Soc.*, **95**, 6294 (1973).

[13] D. A. Cullison and R. K. Hill, *Tetrahedron Letters*, **1972**, 3747.

Revue Roumaine de Chimie, **31**, *11–12*, 1013–1018 (1986)

Dedicated to Professor P. SPACU on his 80th anniversary

MOLECULAR COMPLEXES WITH AROMATIC CATIONS AS ELECTRON ACCEPTORS. VII.[1]

SPECTROMETRIC, CONDUCTIMETRIC, AND DIPOLAR DATA OF PHENYL-SUBSTITUTED PYRYLIUM SALTS WITH TETRACYANO-*PARA*-QUINODIMETHANE ANIONS

MIHAELA BUGEANU[a], V. E. SAHINI[b], V. T. CIORBA[c] and A. T. BALABAN[c]

[a] Polytechnic Institute, Faculty of Electronics and Telecommunication, Department of Physics, Splaiul Independenţei 313, 76206 Bucharest, Romania

[b] Polytechnic Institute, Department of Physical Chemistry, Blvd. Republicii 13, Bucharest, Romania

[c] Polytechnic Institute, Department of Organic Chemistry, Splaiul Independenţei 313, 76206 Bucharest, Romania

Received May 18, 1986

Several parameters were determined for a series of pyrylium salts with $[TCNQ_2]^{\cdot -}$ anions and 2,4,6-triphenyl, 2,3,5,6-tetraphenyl, and 2,3,4,5,6-pentaphenyl substituents : solvatochromy of electronic absorption spectra, dipole moments, vibrational and conductimetric data.

INTRODUCTION

Previous parts of this series [1] examined change-transfer (CT) spectra from the anion (iodide, thiocyanate, selenocyanate, 2-aza-1,1,3,3-tetraphenylpropenide) to substituted pyrylium cations ; in the preceding part,[1] a new method was reported for preparing pyrylium salts having anions derived from 7,7′,8,8′-tetracyano-*para*-quinodimethane (TCNQ) ; electronic absorption as well as ESR data were described.

Change-transfer or donor-acceptor complexes [2] are normally formed by neutral electron donors (*e.g.* a molecule having unshared electrons such as ethanol, or π-electrons such as naphthalene), and neutral electron acceptors (*e.g.* elemental iodine which gives a brown ethanolic solution, or a polynitroaromatic compound such as picric acid, which gives a crystalline adduct with naphthalene). In particular cases, however, the donor-acceptor pair may be charged, and this is illustrated by pyrylium or pyridinium salts : whenever the anion can function as electron donor, the salts have deeper colours than is the case when the anion is perchlorate or tetrafluoroborate ; Kosower examined extensively pyridinium salts.[2]

The tetracyano-*para*-quinodimethane radical anion may lead to 1 : 1 or 1 : 2 complexes, i.e. [pyrylium]$^+$ [TCNQ]$\cdot^-$ or [pyrylium]$^+$ [TCNQ]$_2^{\cdot-}$, as known from literature data.[3] Spectral studies [4] and conductimetric data showed that some of the TCNQ complexes, *e.g.* those with tetrathiofulvalene or tetraselenofulvalene, possess interesting properties of organic metals.[5] Although the hope of obtaining superconductivity with organic materials has not been achieved with TCNQ complexes but with other compounds, the study of spectral properties and of the conductivity of TCNQ complexes led to interesting conclusions.[6,7]

The first preparation of TCNQ was reported in 1960, and details appeared in 1962.[8] At the same time, among other CT complexes, the salts of TCNQ with the 2,4,6-triphenylpyrylium cation were reported.[9,10]

The present paper reports further data on the electronic structure of the CT complexes between pyrylium cations with phenyl substituents and the 7,7′,8,8′-tetracyano-*para*-quinodimethane radical anions.

EXPERIMENTAL

The complexes studied are of type Π^+ (TCNQ) (TCNQ$\cdot^-$), where Π^+ are the 2,4,6-tri-, 2,3,5,6-tetra-, and 2,3,4,5,6-penta-substituted phenyl derivatives of the pyrylium cation. In addition to such 1 : 2 Π(TCNQ)$_2$ complexes, a 1 : 1 complex was also obtained with pentaphenylpyrylium. The substances were purified by recrystallization from acetonitrile, and their preparation was reported in the preceding part.[1]

Commercial solvents have been used and dioxane was dried on calcium chloride.

Solutions of low concentrations ($10^{-4}-10^{-5}$ mol/L) were used for spectrophotometric measurements, and 10^{-4} mol/L for dielcometric and conductimetric measurements.

The IR spectra were obtained in KBr disk with a "Specord IR" spectrophotometer.

The spectral measurements were carried out with a „Specord UV-VIS" spectrophotometer, and the dielcometer measurements with on Oehme 600 RL dielcometer.

The refractive indices were measured with an Abbé refractometer and the conductances with a conductimeter ; these measurements were performed at 25°C. Paramagnetic sensitivities were determined with a balance of the Guy type.

EXPERIMENTAL RESULTS

The above Π^+TCNQ$\cdot^-$ complexes mentioned were studied spectrally in different aprotic solvents, finding evidence of a shoulder within the 470 – 500 nm region which was attributed to the CT complex.

In order to determine the λ_{max} of the CT band for these complexes, differential spectroscopy was applied : the compensation in the solvent cell was carried out with the corresponding pyrylium perchlorate and (in separate experiments) TCNQ. The results of spectrophotometric measurements are presented in table 1.

A bathochromic shift with the polarity of the solvent appears. Enhancement of the band intensity was noticed for the tetrasubstituted complex. The spectra of the complexes also present a band within the range 15 000 – 16 000 cm^{-1} (625 – 670 nm) ; the band is very intense, and affected bathochromically by increasing the polarity of the solvent and hypsochromically with the increase in the number of substituents per cycle.

In the solvents mentioned in table 1 both the band of free TCNQ and that of the radical-anion can also be noted between 12 000 and 13 000 cm^{-1} (770–830 nm).

Table 1

Solvatochromy of one absorption band λ_{max}^{CT} (nm) in the electronic spectrum of the TCNQ-pyrylium salt complexes

Solvent	Dioxane	Chloroform	1,2-Dichloroethane	Acetonitrile
2,4,6-Triphenyl	450	462	465	468
2,3,5,6-Tetraphenyl	472	475	478	481
2,3,4,5,6-Pentaphenyl 1 :2	481	485	487	491
2,3,4,5,6-Pentaphenyl 1 :1	490	492	496	498

The dipole moment measurements were carried out at 25°C, in dioxane solvent by the Guggenheim method (considering the complex but slightly ionized in the solvent and therefore assimilable with a polar molecule).

The values of the dipole moments obtained are given in table 2. These values range from 6.3 to 6.9 D, showing a high polarity of the bond in the complex.

Table 2

Dipole moments of the TCNQ-pyrylium salt complexes (Debye units)

Complex	μ_{exp}
2,4,6-Triphenyl	6.51
2,3,5,6-Tetraphenyl	6.82
2,3,4,5,6-Pentaphenyl 1 :2	6.31
2,3,4,5,6-Pentaphenyl 1 :1	6.52

The IR spectra of the complexes were studied, noting slight differences between the stretching frequencies for $C\equiv N$, $-C=C-$, $C-C\equiv N$ in the complex and in free TCNQ; similarly, for the stretching vibration (ring breathing) and the asymmetrical stretching vibration of the C–C bonds in the pyrylium ring of the complex as compared with the corresponding perchlorate.

The shifts of the vibrations obtained amount to 5–13 cm^{-1} and indicate the formation of a change transfer complex even in the electronic ground state. All these bands show an increased intensity as compared to the intensities of the donor and acceptor bands. The bands and shifts are shown in table 3.

The stability constants of the complexes were obtained by processing the electronic absorption band of the complex.

Table 3

Differences (cm^{-1}) between the infrared spectra of the TCNQ-pyrylium complexes and the corresponding perchlorates

Band in unperturbed cation/TCNQ complex	TCNQ 2200–2250	TCNQ 1500–1600	Π 1300–1400	Π 1100–1200	TCNQ 800–900
2,4,6-Triphenyl	11.8	1.5	2.1	10.9	0.7
2,3,5,6-Tetraphenyl	11.5	1.7	2.2	10.5	0.9
2,3,4,5,6-Pentaphenyl 1 :2	10.8	1.2	1.7	11.2	1.1
2,3,4,5,6-Pentaphenyl 1 :1	10.5	1.6	1.5	11.6	0.8

The stability constant K is expressed in terms of the initial concentration C_0 of the complex introduced into the acetonitrilic solution. The constants show a slight variation with the nature of the cation (Table 4).

Table 4

Stability constants of the TCNQ-pyrylium salt complexes in acetonitrile

Complex	Stability constant K[$L.mol^{-1}$]
2,4,6-Triphenyl	3.9
2,3,5,6-Tetraphenyl	2.8
2,3,4,5,6-Pentaphenyl 1 : 2	3.1
2,3,4,5,6-Pentaphenyl 1 : 1	2.9

The literature mentions that the $M^+(TCNQ)(TCNQ^{\cdot -})$ complexes are strongly ionized in polar solvents when M^+ is a metallic cation. Starting from this idea we have tried to establish whether the complexes of the pyrylium salts have ionogenic capacity, assuming that in solution the equilibrium is of the form :

$$D^+(TCNQ)(TCNQ^{\cdot -}) \rightleftarrows D^+ + TCNQ + TCNQ^{\cdot -}$$

The behaviour in solution of these complexes was analysed conductimetrically in solutions of various concentrations $c \cong 10^{-4}$ mol/L in dioxane, in a thermostat at 25°C. The conductance of the solutions was measured at various concentrations of the soluion. The molar conductivities were calculated, applying an Onsager type equation ; the molar conductivity was represented versus $\sqrt{c}$. Extrapolation at infinite dilution afforded Λ_∞ values. The curve presented the behaviour of a weak electrolyte. The ionization degree and the ionization constant for these complexes were calculated as shown in table 5.

It may be seen from table 5 that increasing substitution in the cycle diminishes the ionization constant.

The enthalpy of the dissociation process was calculated by Van't Hoff's relationship, measuring the constants within the 25–45°C range. Magnetic sensitivity measurements indicated the presence of an unpaired electron, $\mu = 1.53\ \mu_B$.

Table 5

Ionisation constants and thermodynamic functions of the TCNQ-pyrylium salt complexes (in 1,2-dichloroethane)

Complex	α	$k_{\text{ionis}} \cdot 10^{-5}$	ΔH^c_{298}(kcal/mol)
2.4,6-Triphenyl	0.35	3.15	7.8
2,3,4,6-Tetraphenyl	0.28	2.8	6.5
2,3,4,5,6-Pentaphenyl 1 :2	0.14	1.8	6.2

DISCUSSION

The experimental data obtained were obtained for studying the electronic structure of the tetracyano-*para*-quinodimethane complexes. The electronic and IR spectroscopy data suggested that these are weak complexes. The stability constants lend support to this assumption.

The electronic structure may be described by two limiting structures : an ionic one, I (as in perchlorates), and a charge-transfer one II.

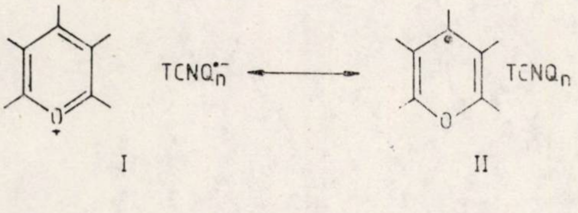

I II

The ESR spectroscopic data[1] and the newly measured paramagnetism data confirm the presence of the unpaired electron.

The weight of the ionic limiting structure I in the wave function is important in the ground state ; the degree of substitution of the pyrylium cation has a detectable influence on all data referring to the CT complex : it is apparent that the electronically excited state has a substantial contribution of structure II.

The fact that the 2,3,5,6-tetraphenyl-substituted compound has no phenyl group able to delocalize the unpaired electron in the CT-structure II (it is known[11] that the spin density in pyranyl radicals is the highest in the γ-position, as indicated in formula II) may be correlated with this compound having an unusual intensity of the CT bond and the highest dipole moment.

REFERENCES

[1] Part VI, V. T. Ciorba, S. Bădilescu, A. Meghea, I. Schiketanz and A. T. Balaban, *Rev. Roumaine Chim.*, **29**, 817 (1984) ; part V, A. T. Balaban, and M. Paraschiv, *ibid.*, **27**, 813 (1982) ; part IV, S. Bădilescu, L. Manu and A. T. Balaban, *ibid.*, **24**, 947 (1979) ; part III, S. Bădilescu, and A. T. Balaban, *Spectrochim. Acta*, **32 A**, 1311 (1976).

[2] R. S. Mulliken, *J. Am. Chem. Soc.*, **72**. 600 (1950) ; R. S. Mulliken, and W. B. Person, *Ann. Rev. Phys. Chem.*, **13**, 107 (1962) ; G. Briegleb, "Elektronen-Donator-Acceptor-Komplexe", Springer Verlag, Berlin, 1961 ; E. M. Kosower, "An Introduction to Physical Organic Chemistry", Wiley, New York, 1961, p. 301.

[3] A. Lombardo and T. R. Fico, *J. Org. Chem.*, **44**, 209 (1979).

[4] W. E. Wentworth, G. W. Drake, and W. Kirch, *J. Chem. Educ.*, **41**, 373 (1974).

[5] W. J. Gunning and A. J. Neeger, *Solid State Commun.*, **29**, 585 (1979) ; S. Kogoshima, T. Ishigwea, T. D. Schultz, Y. Tomkiewicz, *Solid State Commun.*, **28**, 485 (1978).

[6] D. J. Calvin and J. A. Bard, *J. Am. Chem. Soc.*, **102**, 5435 (1980).

[7] H. Strzelecka, W. Schönfelder and J. Rivory, *Mol. Cryst. Liq. Cryst.*, **53**, 611 (1979).

[8] D. S. Acker, and W. R. Hertler, *J. Am. Chem. Soc.*, **84**, 3370 (1962) ; D. S. Acker et al., *ibid.* **82**, 6408 (1960).

[9] Q. R. Melby, R. J. Herder, W. R. Hertler, W. Mahler, R. E. Benson and W. E. Machel *J. Am. Chem. Soc.*, **84**, 3374 (1962).

[10] J. W. Siemons, P. E. Bierstedt and R. G. Kepler, *J. Chem. Phys.*, **39**, 3528 (1963).

[11] A. T. Balaban, A. Dinculescu et al., "Pyrylium Salts", Adv. Heterocyclic Chem., Suppl. Vol. 2 (A. R. Katritzky, ed.), Academic Press, New York, 1882, p. 195.

Revue Roumaine de Chimie, 31, *11–12*, 1019–1024 (1986)

Dedicated to Professor P. SPACU on his 80th anniversary

PHOTOCHEMICAL RING CONTRACTION OF 8-DIAZO-DIBENZO[*c,e*]TRICYCLO[$5.3.0.0^{2,10}$]DECA-3,5-DIEN-9-ONE

M. BANCIU,[a] M. ELIAN,[b] ANCA BANCIU,[b] C. DRĂGHICI [b]
and ECATERINA CIORĂNESCU [a,b]

[a] Laboratory of Organic Chemistry – TCH ; Polytechnic Institute ; 76206 Bucharest 16, Romania
[b] Center of Organic Chemistry – ICECHIM, Bucharest, Romania

Received May 15, 1986

Dibenzo[*c,e*]tricyclo[$5.3.0.0^{2,10}$]deca-3,5-dien-9-one (**1**) was converted successively into the 8-hydroxymethylene derivative **4** and diazoketone **3**. On UV irradiation of **3** the dibenzo[*c,e*]tricyclo[$5.2.0.0^{2,9}$]nona-3,5-dien-8-yl-carboxylic acid (**6**) and its methyl ester **7** were obtained as derivatives of a new polycyclic system.

INTRODUCTION

In connection with other investigations of this laboratory we described some years ago [1] the synthesis of dibenzo[*c, e*]tricyclo-[$5.3.0.0^{2,10}$]-deca-3,5-dien-9-one (**1**) through intramolecular cyclization of the diazomethylketone **2c** obtained from the acid **2a**.

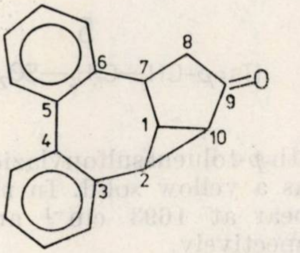

1

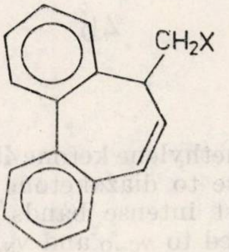

2 a; X=COOH
b; X=COCl
c; X=$COCHN_2$

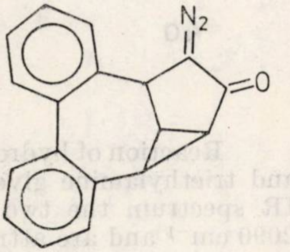

3

The ketone **1** proved to be a valuable intermediate in the synthesis of a new dibenzo $(CH)_{10}$ hydrocarbon.[2] On the other hand, an interesting rearrangement of derivatives with the skeleton **1** into triphenylene derivatives was observed in acidic medium.[1] It seemed appropriate to know also if the strained system **1** could be converted into a more strained one (e.g. containing annelated three-, four- and seven-membered rings). In this paper we describe the photochemical ring contraction of the diazoketone **3** related to the ketone **1**.

RESULTS AND DISCUSSION

In order to synthesize the diazoketone **3** the general reaction of Rosenberger *et al.*[3] between hydroxymethylene derivatives of ketones and *p*-toluenesulfonylazide was applied.

Condensation of ketone **1** with purified ethyl formate in the presence of sodium methoxide afforded the formyl ketone **4** as a white solid. As its ^{1}H-NMR spectrum shows, the formyl-derivative is totally tautomerized to the enolic form **4b**. Thus, the ^{1}H-NMR signal of $=CH-O$ proton from **4b** appears at $\delta = 6.5$ ppm and the enolic OH proton signal occurs (in $CDCl_3$) at $\delta = 9.7$ ppm (broad singlet) indicating intramolecular hydrogen bridging. Similar shifts towards α-hydroxymethylene ketonic forms were observed for 2-formyl-cyclohexanone[4] as well as for different dibenzo-derivatives.[5]

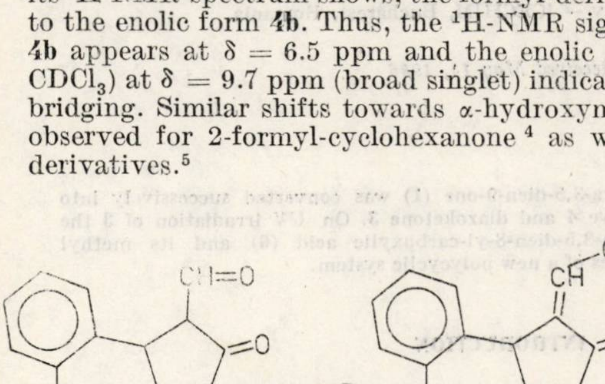

4a 4b

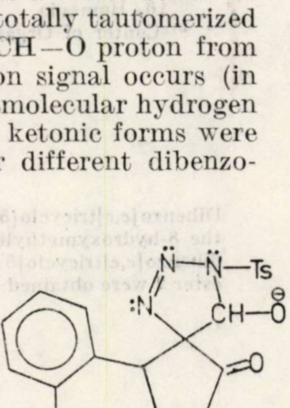

5

(Ts = *p*-$CH_3-C_6H_4-SO_2-$)

Reaction of hydroxymethylene ketone **4b** with *p*-toluenesulfonylazide and triethylamine gives rise to diazoketone **3** as a yellow solid. In the IR spectrum the two most intense bands appear at 1693 cm^{-1} and 2090 cm^{-1} and are attributed to $\nu_{C=O}$ and ν_{N_2} respectively.

The formation of **3** from **4b** could be explained by a cyclic intermediate **5**, in agreement with the accepted mechanism[3] of this reaction.

UV-Irradiation of cyclic α-diazoketones is a well-known alternative procedure of the Wolff rearrangement proceeding usually with ring contraction;[6] this reaction was used very recently by Agosta *et al.*[7] for synthesis of very strained [4.4.4.5] phenestrane derivatives. The UV-illumination of **3** in dioxane : water affords as reaction product the acid **6** whereas UV irradiation in methanol gives rise to the ester **7**. The same methyl ester **7** was obtained on treatment of **6** with ethereal diazomethane.

The structure of **6** and its methyl ester **7** resulted from spectral data. The UV-spectrum showed a biphenyl moiety, the absorption band at 263 nm being in the range of related systems.[8]

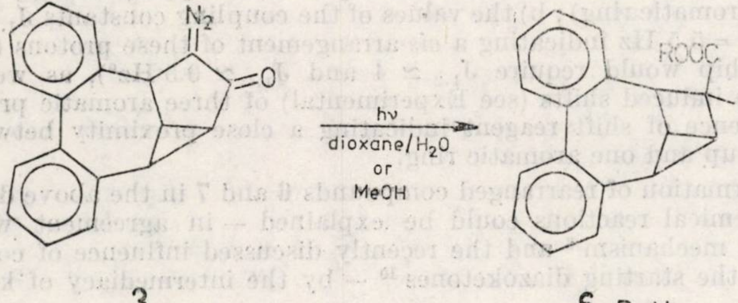

3

6; R=H
7; R=Me

The chemical shifts and coupling constants in the ^{1}H-NMR spectrum of **7** were approximated from the data obtained in the absence or in the presence of the chemical shift reagent d$_{27}$-Eu(FOD)$_3$ (see Experimental). The crude parameters were refined by simulation of the five-proton spectrum H^1–H^5 (Fig. 1).

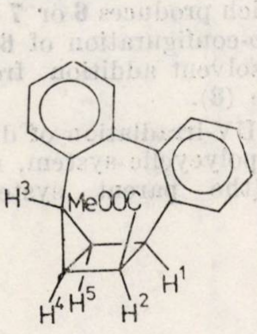

7

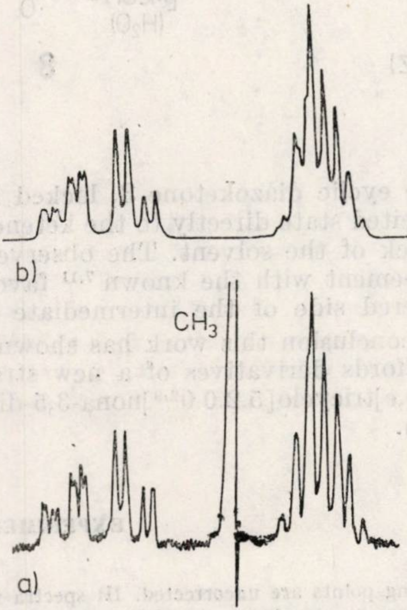

Fig. 1. Observed (a) and simulated (b) ^{1}H-NMR spectra of H^1–H^5 in **7**.

All the coupling constants (see Experimental) compare favourably with the corresponding ones in bicyclo[2.1.0] pentane derivatives [9] indicating a *cis*-stereochemistry for all the protons H^1-H^5.

The *endo*-configuration of the carbomethoxy group resulted from : a) the abnormal chemical shift of CH_3 ($\delta = 2.93$ ppm, strongly shielded by one aromatic ring) ; b) the values of the coupling constants $J_{1,2} = 11.0$ and $J_{1,4} = 5.5$ Hz indicating a *cis*-arrangement of these protons (a *trans*-relationship would require $J_{1,2} \simeq 4$ and $J_{1,4} \simeq 0.5$ Hz[9]), as well as c) the large induced shifts (see Experimental) of three aromatic protons in the presence of shift reagent indicating a close proximity between the ester group and one aromatic ring.

Formation of rearranged compounds **6** and **7** in the above described photochemical reactions could be explained — in agreement with the accepted mechanism [6] and the recently discussed influence of conformations of the starting diazoketones [10] — by the intermediacy of ketene **8**.

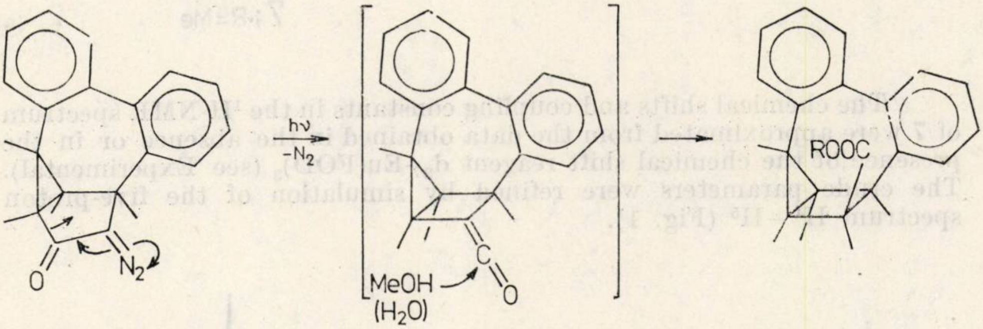

3 (*s*–Z) **8** **6**; R=H **7**; R=Me

The cyclic diazoketone **3**, locked in *s*–*Z* conformation, gives rise in the excited state directly to the ketene **8** which produces **6** or **7** by further attack of the solvent. The observed *endo*-configuration of **6** and **7** is in agreement with the known [7,11] favoured solvent addition from the less-hindered side of the intermediate ketene (**8**).

In conclusion this work has shown that UV-irradiation of diazoketone **3** affords derivatives of a new strained polycyclic system, namely dibenzo[*c*,*e*]tricyclo[5.2.0.0^{2,9}]nona-3,5-diene (the parent system for **6** and **7**).

EXPERIMENTAL

Melting points are uncorrected. IR spectra were recorded with a double-beam UR-20 Carl Zeiss Jena spectrophotometer, UV spectra with a SPECORD UV-VIS Carl Zeiss Jena double beam spectrophotometer; ^{1}H-NMR spectra were registered on a VARIAN A60-A spectrometer using TMS as internal standard.

8-Hydroxymethylene-dibenzo[c,e]*tricyclo*[5.3.0.$0^{2,10}$]*-deca-3,5-dien-9-one* (**4b**)

In a 100 mL three-necked flask provided with stirrer and reflux condenser sodium methoxide was prepared from 0.35 g (0.0152 g-atoms) sodium and 10mL anhydrous methanol. The remaining methanol was distilled off then 10 mL anhydrous benzene were added. The obtained suspension was cooled in an ice bath and a solution of ketone **1**[1] (2 g ; 8.1 mmoles) and freshly distilled anhydrous ethyl formate (1.1 g ; 14.8 mmoles) in 10 mL anhydrous benzene was dropped with vigorous stirring during 1.5 hrs. After six hours of stirring at room temperature the reaction was left overnight. The yellowish-brown reaction mixture was treated with 10 mL cold water then extracted with six 20 mL-portions of 1N-NaOH solution. The combined alkaline solutions were extracted with 20 mL benzene then acidified with dil.HCl. The oily product formed was thoroughly ether extracted. The ethereal solution obtained was washed with water, dried and evaporated *in vacuo* affording 1.57 g (72 %) of hydroxymethylene ketone **4b**, mp.. 161 – 3° (ethanol). Found : C, 83.10 ; H, 5.02 ; $C_{11}H_{14}O_2$ requires : C, 83.19 ; H, 5.14 %.

IR spectrum (CCl_4 ; cm^{-1}) : 842 m, 853 m, 930 w, 958 m, 980 m, 1120 m, 1180 s, 1200 m, 1390 m, 1485 m, 1610 m, 1680 vs, 2900 w and 3040 m.

^{1}H-NMR spectrum ($CDCl_3$; δ ppm) : 2.15 – 3.10 (m ; 3H ; cyclopropanic H) ; 4.2 – 4.45 (m ; 1H ; H^7) ; 6.5 (d ; J = 2 Hz ; 1H ; =CH–0) ; 6.9 – 7.6 (m ; 8H ; Harom) ; 9.70 (large s ; 1H ; OH).

8-Diazo-dibenzo[c,e]*tricyclo*[5.3.0.$0^{2,10}$]*deca-3,5-dien-9-one* (**3**)

p-Toluenesulfonyl azide[12] (1.08 g ; 5.5 mmoles) was added with stirring over a cooled suspension of hydroxymethylene ketone **4b** (1.5 g ; 5.5 mmoles) in 50 mL anhydrous diethylether. Over this mixture triethylamine (0.6 g ; 0.83 mL ; 5.9 mmoles) was dropped with stirring and cooling (0°C) during two hours. After six hours of additional stirring at room temperature the reaction was left overnight. Decomposition with 25 mL water was followed by separation of the ethereal layer and ether extraction (4 × 15 mL) of the aqueous one. The combined ethereal solutions were washed with water, dil. HCl, again with water, dried and evaporated *in vacuo*. The oily solid obtained was filtered and washed with few drops of anhydrous diethylether affording **3** (0.45 g ; 30.5 %) as yellow crystals with m.p. 168 – 170° (dec.).

IR spectrum (CCl_4 ; cm^{-1}) : 970 m, 1240 m, 1330 m, 1345 s, 1453 w, 1493 w, 1693 vs ($\nu_{C=0}$), 2090 vs (ν_{N_2}), 2900 w and 3040 w.

^{1}H-NMR spectrum (d_6-DMSO ; δ ppm) : 2.1 – 3.0 (m ; 3H ; cyclopropanic H) ; 4.96 (splitted doublet ; 1H ; H^7) ; 7.2 – 7.6 (m ; 8H ; Harom).

Dibenzo[c,e]*tricyclo*[5.2.0.$0^{2,9}$] *nona-3,5-dien-8-yl carboxylic acid* (**6**).

In a 50 mL quartz flask a solution of diazoketone **3** (0.2 g ; 0.74 mmoles) in dioxane (25 mL) and water (6 mL) was illuminated with a medium pressure UV-Hg lamp (150 watt, Pyrex filter) for 18 hrs (during which time the evolution of nitrogen ceased). The solution was evaporated *in vacuo* and the residue was treated with 50 mL diethylether. The whole mixture was thoroughly extracted with 10 % NaOH solution (5 × 20 mL). The cooled combined alkaline solutions were acidified with dil. HCl. The precipitate was extracted with diethylether and the ethereal layer was washed with water, dried, decoloured with charcoal, filtered and evaporated *in vacuo* affording the acid **6** (0.1 g ; 52 %) as a white solid with m.p. 255 – 6° (ethanol).

IR spectrum (KBr ; cm^{-1}) : 740s, 762s. 1260 m, 1280 s, 1328 m, 1420 m, 1445 m, 1490 m, 1695 vs (ν_{CO}), 2400 – 3300 large.

UV spectrum (MeOH ; λ_{max} nm : ε_{max} 209 (23700) ; 263 (8400) ; 299 (sh, 750).

^{1}H-NMR spectrum (d_6-DMSO, δ ppm) : 2.0 – 2.6 (m ; 3H ; $H^{3,4,5}$) 3.35 – 4.05 (m ; 2H ; $H^{1,2}$) ; 7.0 – 7.5 (m ; 8H ; Harom) ; 10.9 (large s ; 1H ; COOH) (for proton numbering see formula **7**).

8-*Carboxymethyl-dibenzo*[c,e]*tricyclo*[5.2.0.$0^{2,9}$] *nona*-3,5-*diene* (**7**)

a) *Through UV-irradiation of diazoketone* **3**

A solution of diazoketone (0.2 g ; 0.74 mmoles) in 120 mL anhydrous methanol was UV-irradiated for 24 hrs in the conditions described above for the acid **6**. The reaction mixture was filtered and evaporated *in vacuo* affording the solid ester **7** (0.125 g ; 61 %) with m.p. 138 – 140° (ethanol).

IR spectrum (CCl_4 ; cm^{-1}) : 1060 m. 1220 s, 1450 m, 1500 m, 1745 vs (ν_{CO}), 2960 w and 3 060 w.

UV spectrum (MeOH ; λ_{max} nm ; ε_{max} 213 (19500) ; 263 (7800) ; 296 (sh, 750).

^{1}*H-NMR spectrum* ($CDCl_3$, δ ppm) (for proton numbering see formula **7**) : 2.0–2.7 (m ; 3H ; H^3, H^4, H^5) ; 2.93 (s ; 3H ; CH_3) ; 3.57 (m ; 1H ; H^2) ; 4.03 (m ; 1H ; H^1) ; and 7.0–7.5 (m ; 8H ; Harom). The following parameters were obtained by simulation (see also fig. 1) : $\delta_1 = 4.03$; $\delta_2 = 3.57$; $\delta_3 = 2.53$; $\delta_4 = 2.43$; $\delta_5 = 2.28$ ppm ; $J_{1,2} = 11.0$; $J_{1,3} = 1.5$; $J_{1,4} = 5.5$; $J_{2,5} = 5.0$; $J_{3,4} = 5.5$; $J_{3,5} = 5.5$ and $J_{4,5} = 4.9$ Hz. The molar induced shifts in the presence of d_{27}-Eu$(FOD)_3$ were : 3.01(CH_3) ; 2.52 (H^2) ; 2.17 (2Harom) ; 1.87 (H^3) ; 1.74 (1Harom) ; 1.45 (H^1) and 1.35 (H^4 and H^5).

b) *Through esterification of the acid* **6**

Treatment of the acid **6** with a slight excess of ethereal diazomethane afforded the methyl ester **7**, identical in all respects with that obtained by photochemical rearrangement of **3**.

REFERENCES

[1] M. Banciu, Phan Le Thuy, M. Elian, C. Drăghici and E. Ciorănescu, *Rev. Roumaine Chim*, **26**, 1115 (1981).

[2] M. Banciu, M. Elian, Phan Le Thuy, C. Drăghici and E. Ciorănescu, *Rev. Roumaine Chim*, **27**, 19 (1982).

[3] M. Rosenberger, P. Yates, J. B. Hendrickson and W. Wolf, *Tetrahedron Letters*, **1964**, 2285.

[4] K.v. Auwers and H. Jacobsen, *Liebigs Ann. Chem.*, **426**, 161, 224 (1922) ; cf. *Chem. Zentr.*, **1922**, I, 635.

[5] M. Banciu, Phan Le Thuy and L. Stănescu, *Rev. Roumaine Chim.*, **24**, 957 (1979) ; M. Banciu *Rev. Roumaine Chim.*, **27**, 769 (1982).

[6] W. Kirmse, "Carbene, Carbenoide und Carbenanaloge", Verlag Chemie, Weinheim 1969, p. 166.

[7] V. Bhaskar Rao, C. F. George, S. Wolff and W. C. Agosta, *J. Amer. Chem. Soc.*, **107**, 5732 (1985).

[8] G. H. Beaven, G. R. Bird, D. M. Hall, E. A. Johnson, J. E. Ladburg, M. S. Leslie and E.E. Turner, *J. Chem. Soc.*, **1955**, 2708 ; E. Ciorănescu, M. Banciu, M. Elian, A. Bucur and C.D.Nenitzescu, *Liebigs Ann. Chem.*, **739**, 121 (1970).

[19] E. Block, H. W. Orf and R.E.K. Winter, *Tetrahedron*, **28**, 4483 (1972).

[10] H. Tomioka, H. Okuno and Y. Izawa, *J. Org. Chem.*, **45**, 5278 (1980).

[11] J. Meinwald and P. G. Gassmann, *J. Amer. Chem. Soc.*, **82**, 2857 (1960) ; K. B. Wiberg, L. K. Olli, N. Golembeski and R. D. Adams, *J. Amer. Chem. Soc.*, **102**, 7467 (1980).

[12] W. v. E. Doering and C. H. de Puy, *J. Amer. Chem. Soc.*, **75**, 5955 (1953).

Revue Roumaine de Chimie, **31**, *11–12*, 1025–1030 (1986)

Dedicated to Professor P. SPACU on his 80th anniversary

SYNTHESIS OF 1α,2α- AND 1β,2β-ISOMERS OF 5,9-METHANO-5*H*-BENZO[3,4]CYCLOBUTA[1,2] CYCLOHEPTENES[1]

ANGELA POPESCU, LUMINIȚA PÂRVULESCU, LIGIA STĂNESCU
and MIRCEA D. GHEORGHIU *
Department of Organic Chemistry, Polytechnic Institute, Bucharest 16,
Romania 76206

Received May 12, 1985

5,9-Methano-*5H*-benzo[3,4]cyclobuta[1,2]cycloheptenes 1 and 2, belonging to the class of benzopolycyclic compounds $C_{14}H_{14}$, were obtained in good yields by reduction of the dichloroderivatives 3 and 4 respectively. ^{1}H-, ^{13}C-NMR and mass spectral data of 1 and 2 are presented and discussed.

INTRODUCTION

Bicyclo[3.2.1] octenes **1** and **2****, and their substituted derivatives are virtually unknown. A few years ago [2] we mentioned the synthesis of dichloroderivatives **3** and **4** from the *exo*- and *endo*-benzocyclobutabicyclo[2.2.1]heptene derivatives **5** and **6** *via* Makosza reaction (chloroform, aqueous solution of sodium hydroxide and the presence of phase transfer catalyst triethylbenzylammonium chloride).

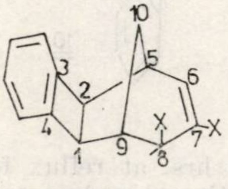

1 X=H
3 X=Cl

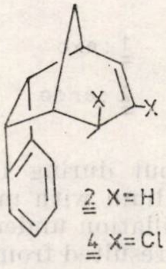

2 X=H
4 X=Cl

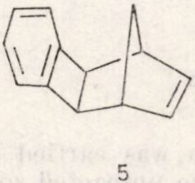

5

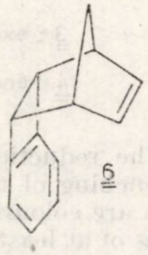

6

---

* Correspondence author

** Hereafter called benzocyclobutabicyclo[3.2.1]octene. However, the carbon atoms numbering is according to *Chem. Abstracts* and corresponds to the nomenclature mentioned in the title.

We now report the synthesis and spectral characteristics of the parent hydrocarbon **1** and **2**. In this way our novel examples extend the class of bicyclo[3.2.1]octene derivatives **7**–**9**, which in the last 25 years received a high interest from the chemical and spectroscopical points of view;

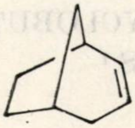

7

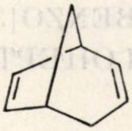

8

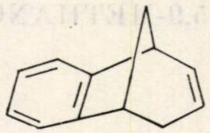

9

for instance, homoaromaticity,[3a] a versatile route to benzobarrelene,[3b] bent allenes,[3c] photoelectron spectroscopy studies,[3d] are just a few of the highlights of the domain.

DISCUSSION

A. Synthesis of *exo*- and *endo*-benzocyclobutabicyclo[3.2.1]octenes 1 and 2

When dichloroderivatives **3** and **4** were subjected to reduction with sodium and t-butanol in ether at reflux, under nitrogen, benzocyclobutabicyclo[3.2.1]octenes **1** and **2** were obtained in yields of 79% and 74%, respectively.

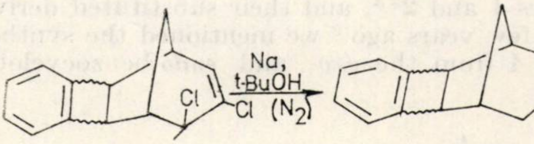

3 : exo
4 : endo

1 : exo
2 : endo

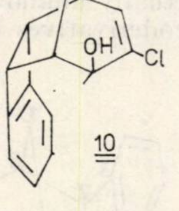

10

The reduction was carried out during 18 hrs. at reflux followed by quenching of the unreacted sodium with methanol and water. Both alkenes are colourless liquids. Distillation under reduced pressure yielded samples of at least 94% purity, as resulted from GLC assessment.

It is interesting to note that an alternative, but so far less convenient synthetically pathway to hydrocarbon **2**, is an elimination of hydroxyl and chlorine substituents from the derivative **10**. Thus by treating the *endo*-benzocyclobutabicyclo[3.2.1]octene derivative **10** with lithium and t-butanol, alkene **2** results in only 20% yield. A rationale of this conversion is at present only speculative.

Dichloroderivatives **3** and **4** result in our new version of synthesis in better yields than in our previous report.[2] However in both syntheses, the present one and the previous version, dichlorocarbene precursors were added to the bicyclo [2.2.1] heptene derivatives **5** and **6**. Using ethyl trichloroacetate and sodium methoxide as dichlorocarbene precursor,[3b] instead of the condition of Makosza reaction (see Introduction), the yield of dichloroderivatives was improved from 50 % to 97 % for **4** and from 65 % to 91 % for isomer **3**.

B. Spectral data

The chemical shifts of the protons bonded to the benzocyclobutabicyclo[3.2.1]skeleton are presented in fig. 1. The assignments were made by double and triple resonance experiments and comparison with the related structures.[4]

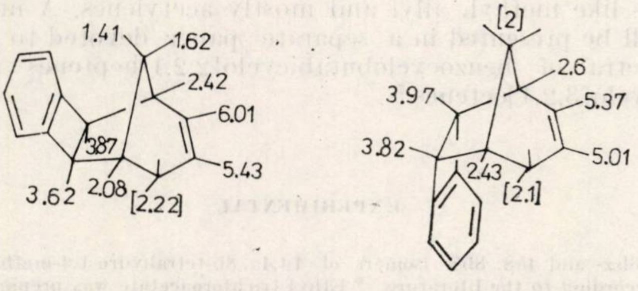

Fig. 1. — Chemical shifts for the protons of the benzocyclobutabicyclo[3.2.1]octene **1** and **2**. Figures in square brackets indicate approximate centres of complicated multiplets.

The ^{13}C-chemical shifts are presented in fig. 2. The assignments are also made in comparison with the related structures.[5]

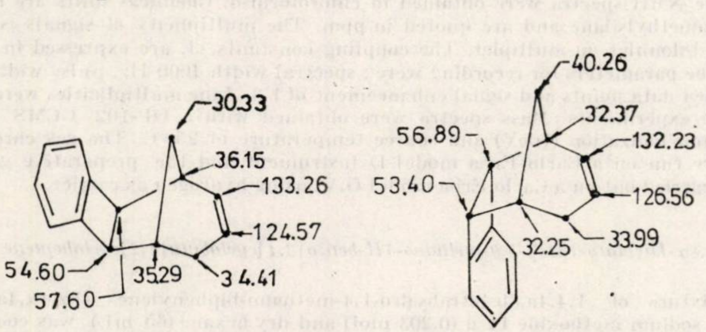

Fig. 2. — The ^{13}C chemical shifts of the carbon atoms belonging to benzocyclobutabicyclo[3.2.1]octene **1** and **2**.

Both ^{1}H- and ^{13}C-NMR support nicely the *endo*- and *exo* configuration of the benzocyclobuta moiety. *Exo*-configuration, due to the anisotropic effect of the aromatic ring will shield the proton pointing toward the ring. This H_{10}^{syn} has the chemical shift at $\delta = 1.41$ ppm, while the same proton has in **2** the chemical shift centered at $\delta = 2$ ppm. The difference in the chemical shifts of the carbon belonging to the methylene bridge, as it may be seen from fig. 2, is about 10 p pm, with the more shielded chemical shift in the *exo* hydrocarbon. Therefore, we believe that the ^{13}C-NMR is a powerful tool in defining the configuration of the benzocyclobuta moiety in the *exo*-annelated bicyclo[3.2.1]octene compounds. A similar conclusion results from the analysis of ^{13}C chemical shift of the same carbon atom from other benzocyclobuta-substituted skeleton.[6]

The mass spectra for both isomers **1** and **2** are very similar both in *m/ze* values of fragments and their intensities. Therefore with this method one cannot distinguish between the *exo*- or *endo*-configurations of the benzocyclobuta moiety. Both alkenes present fragments at 77, 89, 102, 115, 128(100%), 141, 152, 167 and the molecular ion at 182. We believe that the mass spectra can be rationalized by accepting as fragments groups like methyl, allyl and mostly acetylenes. A more detailed discussion will be presented in a separate paper devoted to the analysis of mass spectra of benzocyclobutabicyclo[2.2.1]heptenes and benzocyclobutabicyclo[3.2.1]octenes.[7]

EXPERIMENTAL

The 4aα, 8bα- and 4aβ, 8bβ- isomers of 14,4a, 8b-tetrahydro-1,4-methanobiphenylene were obtained according to the literature.[8,9] Ethyl trichloroacetate was prepared in 85–95% yield from trichloroacetic acid, dry ethanol and sulphuric acid. Water was removed continuously by azeotropic distillation with carbon tetrachloride[10].

IR spectra were recorded in CS_2 and CCl_4, with Jena UR-20, Specord 71-IR and Perkin-Elmer-621 spectrophotometers.

^{1}H-NMR were obtained with Varian EM-360L instrument, ^{13}C-NMR were recorded with a Varian FT-80A instrument.

All the NMR spectra were obtained in chloroform-d. Chemical shifts are referenced to internal tetramethylsilane and are quoted in ppm. The multiplicity of signals is abbreviated as s-singlet, d-doublet, m-multiplet. The coupling constants, J, are expressed in Hz. For the ^{13}C-spectra the parameters for recording were : spectral width 4000 Hz, pulse width 20μs, pulse delay 3s, 16384 data points and signal enhancement of 1.3. Line multiplicities were obtained by off-resonance experiments. Mass spectra were obtained with a DP-102 GCMS spectrometer using electron ionization (70eV) and source temperature of 250°C. The gas chromatographic analyses were run on a Carlo Erba model D instrument and the preparative gas chromatography was carried out on a Carlo Erba model G.V, using hydrogen as carrier.

7,8α-Dichloro-1β,2β-5,9-methano-5H-benzo[3,4]cyclobuta[1,2]cycloheptene (**4**)

A mixture of 1,4,4a,8b-tetrahydro-1,4-methano-biphenylene (1α,4α,4aβ,8bβ) 7.6g (0.045 mol), sodium methoxide 11 g (0.203 mol) and dry hexane (65 mL) was cooled in an ice bath and vigorously stirred while ethyl trichloroacetate 35.4 g (0.185 mol) was added dropwise during 2 hrs. The reaction temperature was maintained below 5°C throughout the addition. After 4 hrs at 0°C, the mixture was allowed to warm gradually to ambient temperature and was stirred for 12 hrs, before being poured into ice water (150 mL). The organic layer was separated and the water layer was extracted with ether (3×50 mL). Combined organic layers were washed with water and brine, dried over $MgSO_4$ anh. and the solvent was evaporated. The unreacted alkene was separated by distillation at reduced pressure (b.p. 82–84°C/2 mmHg) leaving the title compound as a residue, a viscous brown oil (97%, lit [2] 50%), which crystalized on standing. Cromatography on SiO_2 with petroleum ether (b.p. 35°C) gave a pure sample of the title compound (white crystals m.p. 139–140°C, uncorrected). IR and ^{1}H-NMR spectra are identical with those reported previously[2].

7,8α-Dichloro-1α,2α-5,9-methano-5H-benzo[3,4]cyclobuta[1,2]cycloheptene (**3**).

The compound was obtained in analogous experimental conditions. The work up of the reaction mixture ended with vacuum distillation of unreacted alkene (b.p. 82—84°C/2 mmHg). The title compound as a residue is a viscous brown oil (91 %, lit[2] 65 %), crystallized on standing. Cromatography on SiO_2 with petroleum ether (b.p. 35°C) gave a pure sample (m.p. 140—141°C, uncorrected).

5,9-Methano-5H-benzo[3,4]cyclobuta[1,2]cycloheptene (1α,2α) (**1**)

Metallic sodium 3.6 g (0.156 mol) was suspended into 40 mL anhydrous ether. This was mechanically stirred at gentle reflux under a nitrogen atmosphere while a mixture of 4 g (16 mmol) of **3**, 9.6g (0.13 mol) t-butanol in ether (15 mL) was added dropwise during 20 minutes. After stirring at reflux for 18 hrs, heating was discontinued and methanol (20 mL) and then water (50 mL) were added dropwise while cooling in an ice bath. The mixture was poured into water (50 mL) and the organic layer was separated. The water layer was extracted with ether (3×30 mL). Combined organic layers were washed with water and brine, dried over $MgSO_4$ anh. and solvent was evaporated. Distillation at reduced pressure yielded the title compound (79 %, b.p. 103—105°C/2 mmHg).

$C_{14}H_{14}$(182.25) Calcd. : C 92.26 H 7.74
Found : C 92.10 H 7.85

IR (cm^{-1}) : 3063, 3022, 2940, 2830, 1450, 733, 680.

H-NMR : 1.41 (H_{10}^{syn}, d, J = 12), 1.62 (H_{10}^{anti}, d, J = 12), 2.08 (H_9, m), 2.22 (H_8^{exo}, H_8^{endo}, m), 2.42 (H_5, m, J = 4), 3.62 (H_4, d, J = 3.5), 3.87 (H_2, d, J = 3.5), 5.43 (H_7, m, J=10), 6.01 (H_6, m, J = 4.10), 7.1 (5H).

^{13}C-NMR : 30.33, 54.60, 57.60, 121.65, 121.75, 124.57, 127.28, 133.26, 146.51, 147.07.

MS (intensity %) : 182(50.7), 181(16.3), 167(52.2), 166(14.5), 165(20.8), 154(12.9), 153(12.7), 152(13.5), 141(39.9), 129(16.2), 128(100), 116(39.6), 115(43.3), 104(12.3), 103(10.4), 102(22.6), 91(13.4), 89(17.7), 77(22.2), 76(13.2), 67(11.4).

5,9-Methano-5H-benzo[3,4]cyclobuta[1,2]cycloheptene (1β,2β) (**2**)

The compound was obtained similarly with the 1α, 2α isomer (*vide infra*), as a colourless liquid with b.p. 104°C/2 mmHg. An analytical sample of **2** was obtained by preparative GLC (using a SE 54 column, operated at 70—240°C, with a rate of 10°C/min., hydrogen as carrier, with a flow of 1 mL/min., injection at 250°C).

$C_{14}H_{14}$(182.25) Calcd. : C 92.26 H 7.74
Found : C 91.50 H 8.15

IR (cm^{-1}) : 3060, 3026, 2930, 2825, 1452, 1426, 745, 694.

^{1}H-NMR : 2. (H_{10}^{syn}, H_{10}^{anti}, m), 2.1 (H_8^{exo}, H_8^{endo}, m), 2.43 (H_9, m), 2.6 (H_5, m), 3.82 (H_1, m), 3.97 (H_2, m), 5.01 (H_7, m, J = 10), 5.37 (H_6, m, J = 5.5), 7. (5H).

^{13}C-NMR : 32.25, 32.37, 33.99, 40.26, 53.40, 56.89, 123.29, 123.13, 126.07, 126.56, 132.23, 147.38, 148.17.

MS (intensity %) : 182(53.8), 181(27.8), 168(14.8), 167(94.2), 166(31.4), 165(43.1), 154(22.07) 153(27.7), 152(29.4), 142(14.5), 141(92.8), 129(18.4), 128(100), 116(34.3), 115(35.2), 104(10), 102(13.8), 89(12.9), 83(13.9).

REFERENCES

[1] Taken in part from the Ph.D.Thesis of A. P. Presented in part at the 2nd National Congress of Chemistry, Bucharest, 7—10 September 1981 and at the 4th Congress of Chemistry and Chemical Engineering, Bucharest, 17—18 November 1985, Abstract p. 44.

[2] L. Pârvulescu and M. D. Gheorghiu, *Rev. Roumaine Chim.*, **22**, 1089 (1977).

[3] a F. A. Carey and R. J. Sundberg, "Advanced Organic Chemistry", 2nd Edition, Part A, Plenum Press, New York, 1984, p. 474 ; J. B. Grutzner and W. L. Jorgensen, *J. Amer. Chem. Soc.*, **103**, 1372 (1981) ; E. Kaufmann, H. Mayr, J. Chandrasekhar and P. von Ragué Schleyer, *ibid.*, **103**, 1375 (1981) and literature cited therein.
b R. P. Johnson, A. Exarchon, C. W. Jefford and R. C. Hahn, *J. Org. Chem.*, **42**, 3758 (1977).
c M. Balci and M. Harmandar, *Tetrahedron Letters*, **25**, 237(1984) and literature cited therein.
d L. N. Domeelsmith, P. D. Mollere, K. N. Houk, R. C. Hahn and R. P. Johnson, *J. Amer. Chem. Soc.*, **100**, 2959 (1979).

[4] R. De Selms and C. M. Combs, *J. Org. Chem.*, **28**, 2206 (1963) ; S. Winstein, M. Ogliaruso, M. Sakai and J. M. Nicholson, *J. Amer. Chem. Soc.*, **89**, 3656 (1967) ; J. M. Brown, E. N. Cain and M. C. Mc Ivor, *J. Chem. Soc.* (*B*), **1971**, 730 ; Z. Goldschmidt and U. Gutman *Tetrahedron*, **30**, 3327 (1974).

[5] J. B. Stothers and C. T. Tan, *Can. J. Chem.*, **55**, 841 (1977).

[6] M. D. Gheorghiu and E. Olteanu, manuscript to be submitted.

[7] M. D. Gheorghiu, A. Popescu and L. Pârvulescu, to be published.

[8] H. E. Simmons, *J. Amer. Chem. Soc.*, **83**, 1657 (1961) ;
M. N. Paddon-Row and R. Hartcher, *ibid.*, **102**, 662 (1980).

[9] M. P. Cava and M. J. Mitchell, *J. Amer. Chem. Soc.*, **81**, 5409, (1958).

[10] W. E. Parham and E. E. Schweizer, *J. Org. Chem.*, **24**, 1733 (1959) ; E. J. Salmi and R. Korte, *Ber. dtsch. Chem. Ges.*, **72**, 790 (1939).

Revue Roumaine de Chimie, **31**, *11–12*, 1031–1039 (1986)

Hommage au Professeur P. SPACU
à l'occasion de son 80e anniversaire

PRINCIPALES RÉACTIONS DE L'ATOME DE COBALT DANS LA VITAMINE B_{12} ET DANS LES COMPLEXES MODÈLES DU GROUPE DES COBALOXIMES

MARIE-HÉLÈNE DARBIEU

Laboratoire de Chimie de Coordination et UER des Sciences Pharmaceutiques, 35, Chemin des Maraîchers, 31400 Toulouse, France.

Reçu le 12 mai 1986

This paper is aimed at comparing cobaloxime models to vitamin B_{12} in order to verify the different reactivities of the cobalt atom (Co(I), Co(II), Co(III)) and to confirm the dependence of the Co-C bond reactivity on certain factors, including the importance of the nature of axial and equatorial ligands.

La volonté de comprendre les mécanismes chimiques des réactions ayant comme site la méthylcobalamine a conduit un certain nombre de chercheurs à imaginer et à élaborer des molécules plus simples conçues comme « modèles » pour disposer de situations parfaitement déterminées et caractérisables.
Le but de cet article est donc de comparer un de ces « modèles » connu sous le nom de « Cobaloxime », à la Vitamine B_{12} afin de vérifier les différentes réactivités de l'atome de Cobalt sous ses trois degrés d'oxydation principaux : (Co(I), Co(II), Co(III) et de confirmer que la réactivité de la liaison Co-C est sous la dépendance étroite de certains facteurs parmi lesquels figure l'importance de la nature des ligands axiaux et équatoriaux.

INTRODUCTION

Les complexes de cobalt ayant un système chélatant quadridentate et une structure électronique délocalisée, représentent de bons modèles pour les coenzymes du groupe des cobalamines. Mais plusieurs de ces complexes conviennent aussi pour l'étude des facteurs qui influencent le mécanisme et la réversibilité de la formation d'adduit avec l'oxygène moléculaire. Ils sont donc considérés comme des transporteurs biologiques d'oxygène.

L'utilisation de complexes modèles contribue donc à une meilleure compréhension du mode d'action des coenzymes corrinoïdes dans les réactions enzymatiques mais elle élargit aussi notre connaissance sur les propriétés et les réactions des composés organo-cobaltiques.

Ce présent article résume les principales réactions de l'atome de cobalt dans la Vitamine B_{12} et dans les composés modèles type « Cobaloximes ».

QUELQUES FAITS HISTORIQUES

L'importante découverte de Lenhert et Hodgkin qui affirmèrent en 1955 que la Vitamine B_{12} renfermait une liaison Co—C, indiquait en même temps, pour la première fois, que des réactions organométalliques se produisent dans les systèmes biologiques. Il parait donc raisonable d'affirmer que le ligand macrocyclique modifie de manière significative les propriétés du cobalt, le rendant capable de former une liaison Co-C stable alors qu'avant cette découverte, on pensait que les complexes de cobalt étaient trop instables pour permettre l'établissement d'une telle liaison.

C'est en 1964 que Schrauzer et Kohn [1] ont annoncé que les réactions de l'atome de cobalt dans la Vitamine B_{12} pouvaient être simulés avec des complexes beaucoup plus simples. Les complexes de cobalt du diacétyl dioxime ressemblent si étrangement à la Vitamine B_{12} que le nom de « Cobaloxime » leur a été donné.

Depuis de nombreuses publications ont confirmé la validité de ces complexes comme « molécules modèles ».[2]

RELATIONS STRUCTURALES ENTRE COBALAMINE ET COBALOXIMES

A. Structure de la Vitamine B_{12}

Les cobalamines forment une famille étendue de composés organométalliques et ont en commun une structure moléculaire complexe (Fig. 1).

L'étude cristallographique aux Rayons X montre que la molécule est caractérisée par un élément métallique, le cobalt, et qu'elle peut être divisée en deux grandes parties :

— un groupe planaire,
— un nucléotide.

1°) *Le groupe planaire*

Il comprend :

a) Un macrocycle, le noyau corrine, constitué par quatre noyaux pyrrole, A, B, C, D substitués par différents radicaux :

— méthyle : CH_3
— acétamide : CH_2CONH_2
— propionamide : $CH_2CH_2CONH_2$

reliés entre eux par trois ponts carbonés comprenant six doubles liaisons conjuguées.

b) Un atome de cobalt, hexacoordiné, qui établit des liaisons :

— d'une part, avec les quatre atomes d'azote des noyaux pyrrole,

— d'autre part, avec des substituants situés au dessus et au dessous de cette structure.

— Au dessous de la structure plane, on trouve un nucléotide.

— Au dessus est fixé un groupement X qui permet de caractériser chacun des différents facteurs présentant une activité vitaminique.

X = CN → Cyanocobalamine
= OH → Hydroxocobalamine
= CH_3 → Méthylcobalamine
= Adénosyl → Adénosylcobalamine

2°) *Le Nucléotide*

Il se situe au dessous de la structure plane. Il est formé :

— d'une base azotée, le 5,6-diméthylbenzimidazole (Bzm) ;

— d'un sucre, le ribose ;

— d'une molécule d'acide phosphorique. Il s'agit donc du diméthyl-5,6-benzimidazole-ribose-3-phosphate.

Le nucléotide est doublement rattaché au groupe planaire :

— par une liaison entre le noyau corrine D et le groupement phosphate.

— par une autre liaison entre l'atome de cobalt et l'azote du noyau benzimidazole.

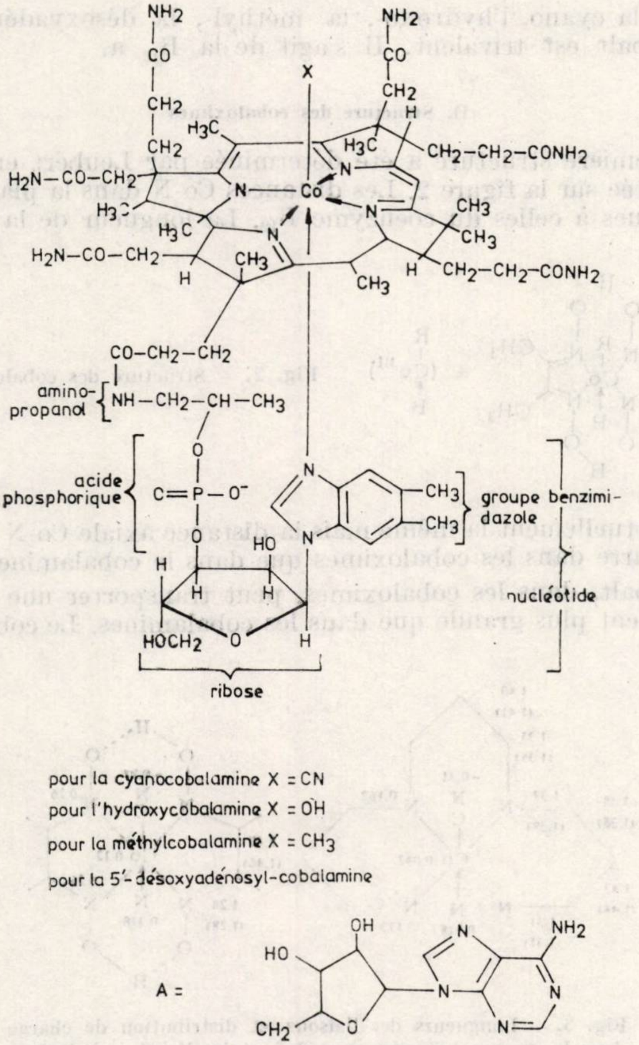
X
amino-propanol
acide phosphorique
groupe benzimidazole
nucléotide
ribose
A =

pour la cyanocobalamine X = CN
pour l'hydroxycobalamine X = OH
pour la méthylcobalamine X = CH_3
pour la 5'-désoxyadénosyl-cobalamine

Fig. 1. — Structure de la Vitamine B_{12}.

Remarques : 1) Dans la vitamine B_{12} a, les substituants périphériques protègent le groupement chromophore contre une attaque déshydrogénante. 2) Les chaînes propionamides dotent la molécule d'un caractère hydrophile mais les nombreux substituants servent de points d'attachement de la Vitamine B_{12} sur les apoenzymes ou pour le transport des protéines. 3) La base axiale fixée en sixième position fonctionne comme agent protecteur car la liaison Co-C est susceptible d'un clivage réducteur par attaque axiale. Dans les « cobamides », le ligand axial manque, mais la partie ribose phosphate est toujours présente. Si cette dernière partie est enlevée par hydrolyse acide, on obtient les « cobinamides ».[3] 4) Les formes réduites de la Vitamine B_{12} sont représentées par « B_{12}r » (Cobalamine II) et B_{12} s (Cobalamine I).

Dans la cyano, l'hydroxo-, la méthyl-, la désoxyadénosyl-cobalamine, le cobalt est trivalent. Il s'agit de la B_{12} a.

B. Structure des cobaloximes

La première structure a été déterminée par Leubert en 1967.[4] Elle est représentée sur la figure 2. Les distances Co-N dans la plan sont à peu près identiques à celles du coenzyme B_{12}. La longueur de la liaison Co-C est aussi virtuellement la même mais la distance axiale Co-N este quelque peu plus courte dans les cobaloximes que dans le cobalamines (Figure 3).

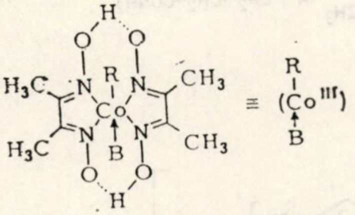

Fig. 2. — Structure des cobaloximes.

La cobalt, dans les cobaloximes, peut transporter une charge positive légèrement plus grande que dans les cobalamines. Le cobalt, dans les

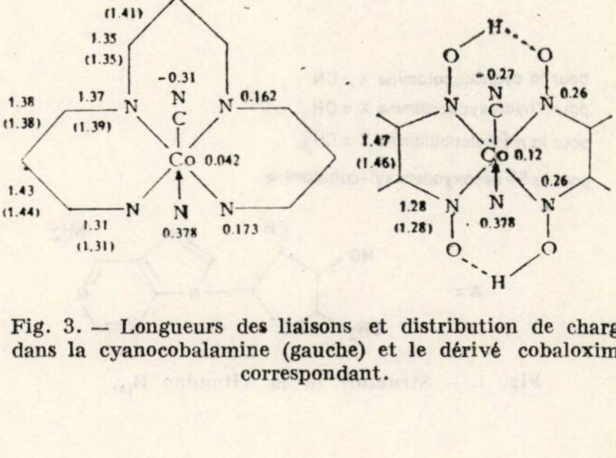

Fig. 3. — Longueurs des liaisons et distribution de charge dans la cyanocobalamine (gauche) et le dérivé cobaloxime correspondant.

cobaloximes, est aussi trivalent et les formes réduites sont représentées par le terme « cobaloxime II » ou « cobaloxime I ». La base axiale est représentée par B.

La figure 4 est un tableau récapitulatif de ces différents composés.

Cobalamines	Cobamides	Cobinamide	Cobaloximes
Cobalt III + Subst. Corrine + Ribose phosphate + 5.6 Diméthyl Benzimidazole + R	Cobalt III + Subst. Corrine + Ribose phosphate	Cobalt III + Subst. Corrine	Cobalt III + Subst. Bis glyoxal dioxime + Base + R

Fig. 4. — Tableau récapitulatif des différentes nomenclatures.

C. Considérations générales sur la réactivité de l'atome de cobalt

L'activité biologique des coenzymes de la Vitamine B_{12} est sans aucun doute associée à la présence de l'atome de cobalt dont les potentiels d'oxydo-réduction sont modifiés par incorporation dans le système corrine.

1°) *Le Cobalt I : Structure électronique et caractère nucléophile*

Dans les dérivés cobalt I, le métal est dans une configuration d^8 à spin apparié. Deux électrons occupent l'orbitale faiblement antiliante $3d_{z^2}$ et la distribution électronique résultante est responsable de la forte réactivité nucléophile du cobalt I.

Dans les cobaloximes, le cobalt I interagit avec les bases, ce qui entraîne des changements dans le spectre d'absorption et la réactivité chimique. Cette interaction modifie la distribution électronique de l'orbitale d_z^2.

Les bases fortes comme OH^- augmentent la densité électronique sur le Cobalt, les bases azotées insaturées abaissent la densité électronique par des interactions de type $d_\pi - p_\pi$. Ceci entraîne une légère diminution du caractère nucléophile.

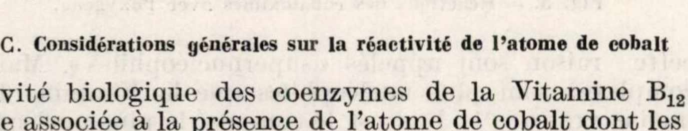

La position de la Vitamine B_{12} s et des complexes modèles de Co^I dans l'échelle de Pearson est représentée sur la figure 5.[5] On peut s'apercevoir que les dérivés de Co^I sont les plus puissants nucléophiles connus

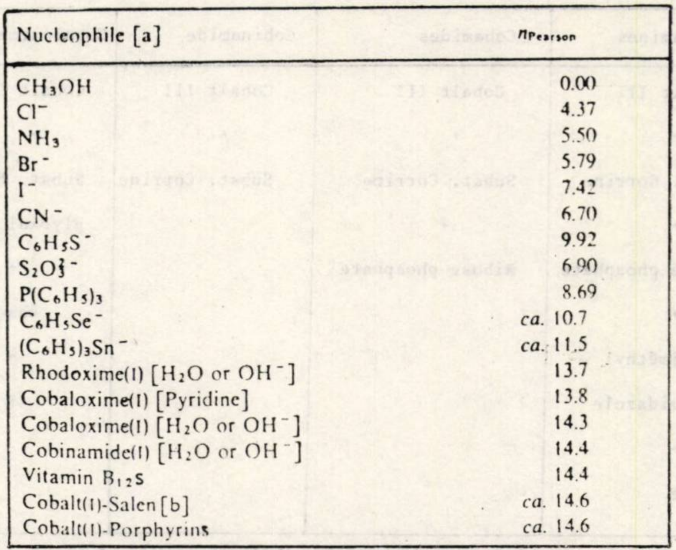

Nucleophile [a]	$n_{Pearson}$
CH_3OH	0.00
Cl^-	4.37
NH_3	5.50
Br^-	5.79
I^-	7.42
CN^-	6.70
$C_6H_5S^-$	9.92
$S_2O_3^{2-}$	6.90
$P(C_6H_5)_3$	8.69
$C_6H_5Se^-$	*ca.* 10.7
$(C_6H_5)_3Sn^-$	*ca.* 11.5
Rhodoxime(I) [H_2O or OH^-]	13.7
Cobaloxime(I) [Pyridine]	13.8
Cobaloxime(I) [H_2O or OH^-]	14.3
Cobinamide(I) [H_2O or OH^-]	14.4
Vitamin $B_{12}s$	14.4
Cobalt(I)-Salen [b]	*ca.* 14.6
Cobalt(I)-Porphyrins	*ca.* 14.6

Fig. 5. — Réactions des cobaloximes avec l'oxygène.

et pour cette raison sont appelés « supernucléophiles ». Mais, même si certains complexes sont plus nucléophiles que la Vitamine $B_{12}s$, il n'en reste pas moins vrai que la $B_{12}s$ est le composé le plus nucléophile trouvé dans la nature. La vitamine $B_{12}s$ et les cobaloximes I se décomposent dans les solutions neutres ou faiblement alcalines. La décomposition est accélérée en présence de catalyseurs métalliques comme le platine.

Le Co^I, supernucléophile, réagit avec les agents alkylants conventionnels pour donner des complexes organo-cobaltiques. Il s'agit de réactions de substitution nucléophile.

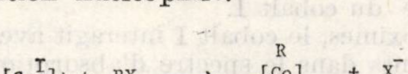

$$[Co^I]^- + RX \longrightarrow \overset{R}{[Co]} + X^-$$

2°) *Structure électronique et réactivité des dérivés* Co^{II}

a) Dans la vitamine $B_{12}r$ et les dérivés Co^{II} des cobaloximes, le cobalt est dans une configuration d^7. L'électron non apparié occupe l'orbitale $3d_z^2$. Les mesures RPE montrent que le ligand axial 5,6-diméthylbenzimidazole dans la vitamine $B_{12}r$ est lié au cobalt. Les cobaloximes (II) forment des adducts 1 : 1 et 1 : 2 avec une grande variété de bases.[6]

b) La vitamine $B_{12}r$ et les cobaloximes II réagissent aussi avec l'oxygène pour former des complexes « peroxo ». Les peroxocobalamines peuvent être considérées comme des complexes formés par « transfert de charge » qu'on peut représenter par deux structures limites :

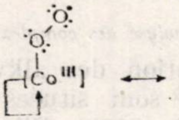

Les cobaloximes II réagissent également avec l'oxygène pour donner trois composés différents (figure 6).

Les péroxocobalamines en solution montrent un spectre RPE qui est virtuellement identique à celui des péroxocorrines (figure 6a). Mais les cobaloximes II peuvent aussi former des « μ péroxodimères de type 6b ». Cette forme tend à se convertir en radicaux « μ péroxo », vraisemblablement par la voie d'une dismutation (figure 6c).

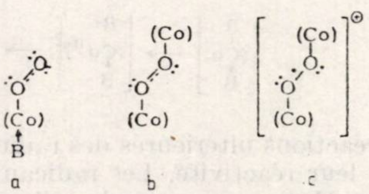

Fig. 6. — Situation des complexes de cobalt dans l'échelle de Pearson.

c) Les cobaloximes II se dismutent en solution alcaline et donnent des dérivés Co^{III} et Co^{I}. La même réaction peut se produire avec la vitamine $B_{12}r$ mais plus lentement.

3°) *Réactivité des dérivés Co^{III}*

a) *Formation de la liaison Co-C*

Les premiers dérivés organocobaltiques des corrines et des cobaloximes ont été préparés par réaction des dérivés Co^{III} correspondant avec les halogénures des organomagnésiens. Bien que les complexes organocobaltiques de la vitamine B_{12} et des composés modèles soient habituellement décrits comme des complexes Co^{III}, ce formalisme peut conduire à ignorer la haute covalence de la liaison Co-C. Il est plus réaliste de décrire la nature de la liaison Co-C en terme de structures limites de a à c.

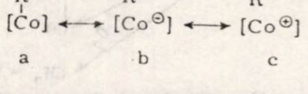

L'interaction de l'orbitale du carbone sp^3 avec les orbitales $3d_{z}^{2}$, $4p_z$ et 4s est responsable de la stabilisation de la liaison. Les liaisons axiales des cobaloximes et des cobalamines possèdent une énergie à peu près semblable.[7]

Le substituant organique R est influencé, à travers l'atome de cobalt, par la base axiale B et vice-versa. Il s'agit d'un effet *trans* ou d'un effet de conjugaison verticale. Si le substituant R est en hybridation sp^2 ou sp, des interactions supplémentaires de type π se produisent avec les orbitales $3d_{xz}$ et $3d_{yz}$ du cobalt, ce qui explique l'effect de stabilisation.

Les liaisons axiales peuvent réagir avec les orbitales du système équatorial. Aussi, les liaisons axiales se trouvent délocalisées sur l'ensemble de la molécule. Il s'agit d'un effet « *cis* ».

b) *Photolyse et thermolyse des complexes méthylés*

Dans les spectres d'absorption des alkylcobaloximes, les bandes de faible et de moyenne intensité sont situées dans un domaine compris entre 350 et 470 nm ($\varepsilon = 1000-3000$). Elles ont été attribuées aux transitions entre liaisons axiales.

Une irradiation des alkylcobaloximes avec une lumière de longueur d'onde comprise entre 500 et 350 nm, entraîne une occupation des orbitales moléculaires antiliantes, ce qui induit le clivage de la liaison Co-C. Durant les processus d'excitation, des étapes intermédiaires se produisent pour conduire en fin de réaction à des radicaux libres R· et à des fragments de cobaloximes II.

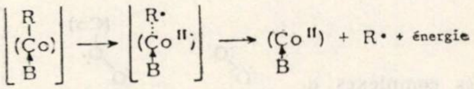

Les réactions ultérieures des radicaux libres dépendent de leur structure et de leur réactivité. Les radicaux méthyle se recombinent avec les cobaloximes II avec une grande efficacité, si la photolyse a lieu dans des conditions strictement anaérobiques. On peut dire que les méthylcobaloximes et les méthylcobalamines sont assez résistants à la photolyse dans ces conditions. Mais, ces radicaux méthyle peuvent aussi diffuser en dehors de la sphère de coordination du cobalt. Par dimérisation, ils forment de l'éthane, ou par enlèvement d'hydrogène, du méthane. La photolyse de ces composés dans des solvants alcooliques, en particulier l'isopropanol, favorise les réactions d'abstraction d'hydrogène. On observe alors exclusivement la formation de méthane (Fig. 7).

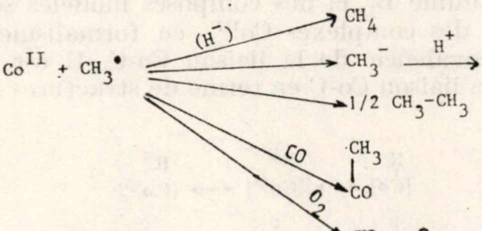

Fig. 7. — Devenir des radicaux méthyle.

Si les complexes méthylés du cobalt sont photolysés en présence d'ions CN^-, le méthane devient le produit principal. La coordination axiale du CN^- sur le cobalt augmente la densité électronique du cobalt. Ceci favorise la réduction des radicaux méthyle.

La photolyse, en milieu aérobique, des complexes méthylés se complique par suite de réactions d'oxydation du radical. Par la voie d'intermédiaires type péroxyde, du formaldéhyde se forme à partr des radicaux méthyle.

— Les complexes de cobalt sont stables jusqu'à une température de l'ordre de 170° et se décomposent à une température supérieure par suite d'un clivage homolytique de la liaison Co—C.

— La photolyse de la méthylcobaloxime en présence de vitamine $B_{12}r$ donne lieu à la formation de petites quantités de méthylcobalamine ; la vitamine B_{12} agit ainsi en tant que radical piège. Le benzène peut également piéger les radicaux méthyle et produit par photolyse du toluène.

— Le clivage de la liaison covalente Co—C peut se faire par attaque nucléophile, électrophile mais aussi par clivage réducteur. La méthylcobalamine et les méthylcobaloximes réagissent avec des nucléophiles comme les ions thiolate (RS-), Cl^-, Br^-, I^-, CN^-, $P(C_6H_5)_3$, mais aussi avec les supernucléophiles Co I eux mêmes.[8]

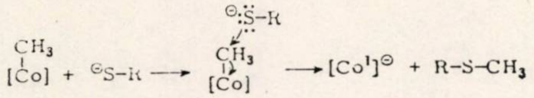

— Pour illustrer l'attaque électrophile, on peut citer l'action des complexes méthylés avec les ions métalliques. Par exemple, la méthylcobalamine et la méthylcobaloxime peuvent réagir avec l'ion mercurique pour donner des sels alkylmercuriques. Mais, la liaison Co—C peut être aussi clivée par des ions comme Au^{3+}, Tl^{3+}, Pt^{2+}, Pd^{2+}.[9]

Ces réactions interviennent dans les réactions de biométhylation nocives pour l'environnement et pour la santé de l'homme par suite de la formation de ces alkyl-métaux.

CONCLUSION

Le fait que la réactivité du cobalt dans la vitamine B_{12} puisse être étudiée à l'aide de complexes modèles permet de rationaliser cet aspect de la chimie de coordination. Il est intéressant de souligner la stabilité et la réactivité non usuelle de ces composés.

La plupart des réactions envisagées ont permis de confirmer la similitude de comportement entre les complexes modèles et la vitamine B_{12}, aussi bien du point de vue qualitatif que quantitatif. Cette étude offre un intérêt certain car elle permet de situer la position des cobaloximes dans le domaine de la Chimie de la Vitamine B_{12}.

Or, ces composés modèles sont d'un emploi plus facile, aussi bien du point de vue de la préparation que de la réactivité car ils sont de structure beaucoup moins complexe.

BIBLIOGRAPHIE

[1] G. N. Schrauzer et J. Kohnle, *Chem. Ber.*, **97**, 3056 (1964).
[2] G. N. Schrauzer, *Angew. Chem. Int. Ed. Engl.*, **15**, 417 (1976).
[3] J. M. Pratt, « *Inorganic Chemistry of Vitamin B_{12}* », Academic Press, London 1972.
[4] G. Lenhert, *Chem. Comm.*, **1967**, 980.
[5] R. G. Pearson, H. Sobel, J. Songstad, *J. Amer. Chem. Soc.*, **90**, 319 (1968).
[6] G. N. Schrauzer, R. J. Windgassen, *Chem. Ber.*, **99**, 602 (1966).
[7] G. N. Schrauzer, L. P. Lee, J. W. Sibert, *J. Amer. Chem. Soc.*, **92**, 2997 (1970).
[8] E. A. Stadbauer, R. J. Holland, G. N. Schrauzer, *Bioinorg. Chem.*, **4**, 67 (1974).
[9] G. Agnes, S. Bendle, H. O. Hill, R. J. Williams, *Chem. Comm.*, **1971**, 850
[10] J. M. Wood, *Naturwissenschaften*, **62**, 1 (1975).

Revue Roumaine de Chimie, 31, *11–12*, 1041–1046 (1986)

Dedicated to Professor P. SPACU on his 80th anniversary

CRITERIA FOR NUCLIDES ORDERING AND OBSERVED REGULARITIES

EMIL PETROVICI, EUGENIA NARTEA and GHEORGHE MARA
"Traian Vuia" Polytechnic Institute, Timișoara, Romania

Received May 31, 1986

The number of stable nuclei and the total number of the knwon ones are presented in three graphs, as a function of the increasing values for Z, N and A (the number of isotopes, isotones and isobars). Some rules are stated as a function of discontinuities in nuclear stability. Five discontinuities are concentrated around the values $Z = 61$, $N = 84-87$ and $A = 147$ and 149 ; in this domain there is a "nuclear stability disaster". From the graphs one can find those values for Z, N and A for which the probability of discovering new radioactive nuclides is greater.

Usually, the atomic nuclear species — the nuclides — are represented in the first quadrant of a system of rectangular axes by plotting on the abscissa the number of protons, Z, and on the ordinate, the number of neutrons, $N = A - Z$. The mass number of nuclides, A, is ranging on the bisector and the values are read on oblique lines, perpendicular to that bisector. Such a representation which offers many advantages, has also one great disadvantage, namely that it does not permit to read, directly, the influence of each nuclear component on the nature of each nuclide.

In the present paper, the ordering of the existing nuclides is presented in graphs which contain the number of stable nuclides, and the total number of known ones. The difference gives the unstable nuclides. Three graphs are given, as follows : the first has on the abscissa the number of protons, Z (Fig. 1), the second, the number of neutrons, N (Fig. 2) and the third, the number of nucleons, A (Fig. 3). Each graph has on the ordinate the number of nuclides having constant abscissa : isotopes, isotones and isobars, as total number (the higher values), as well as the number of the stables ones (the lower values). In other words, each graph contains the same number of nuclides — 264 stable nuclides and the total of them, namely 1679 known since 1970 (for each of them 2 mm correspond on the abscissa, 5 mm on the ordinate, and a surface of 10 mm^2).

Examination of these graphs shows that the total known nuclides have a much greater variation on the ordinate, as the values increase on the abscissa, than the number of the stable ones which remains constant.

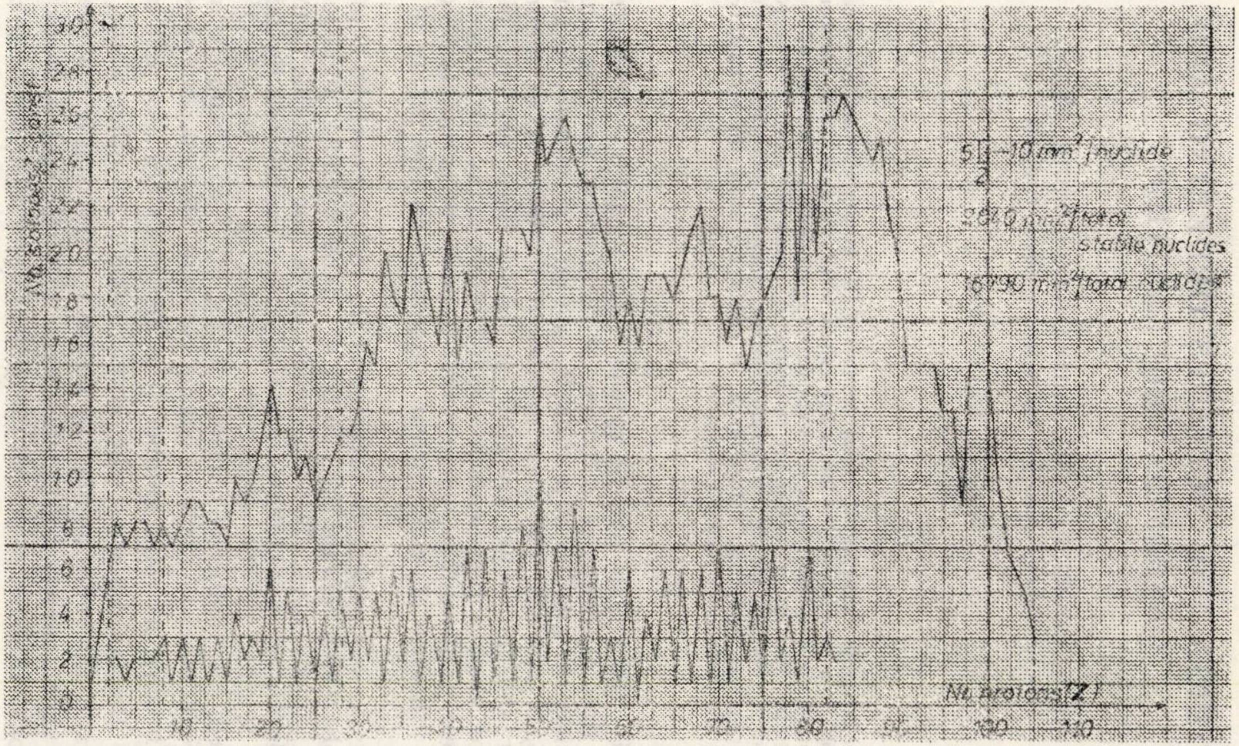

Fig. 1. — The total number of isotopes and that of the stable ones (lower values) for each value of atomic number, Z.

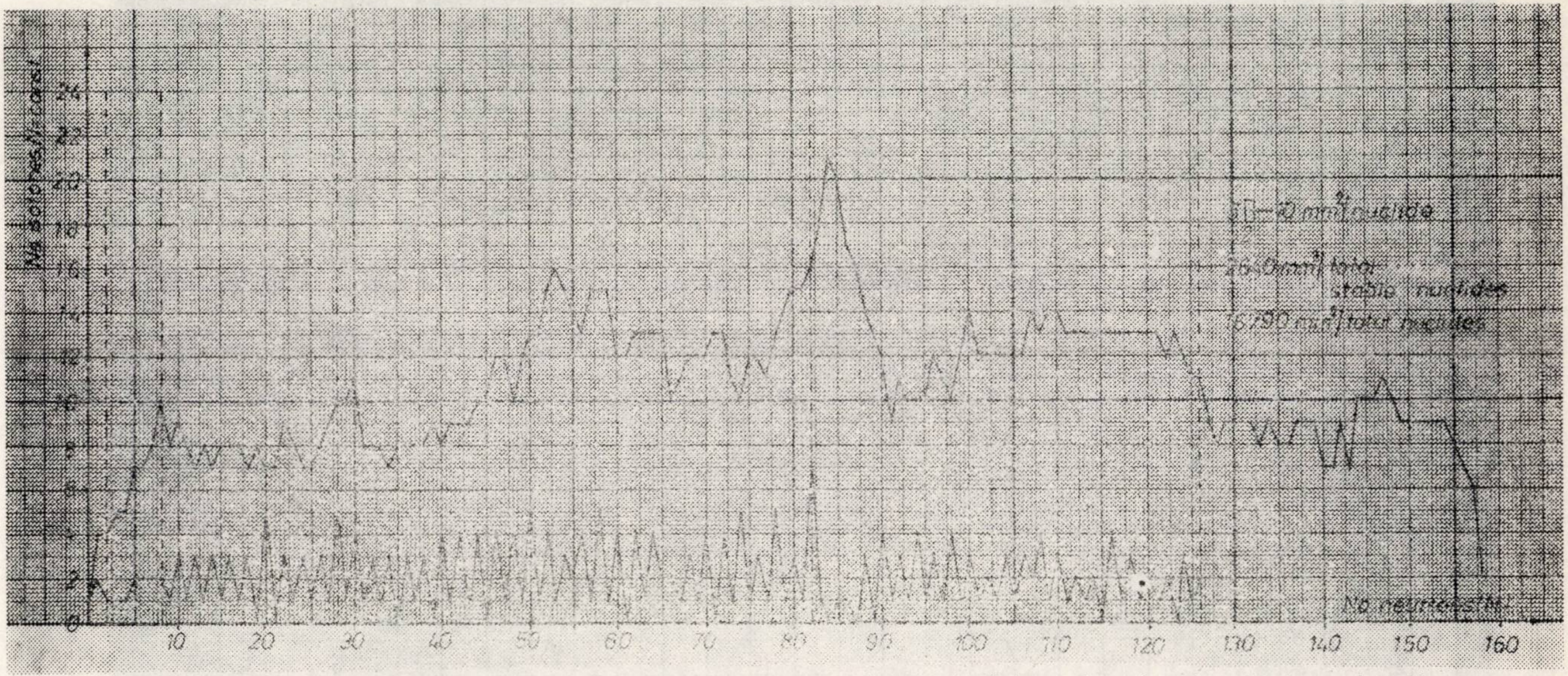

Fig. 2. — The total number of isotones and that of the stable ones (lower values) for each value of neutronic number, N.

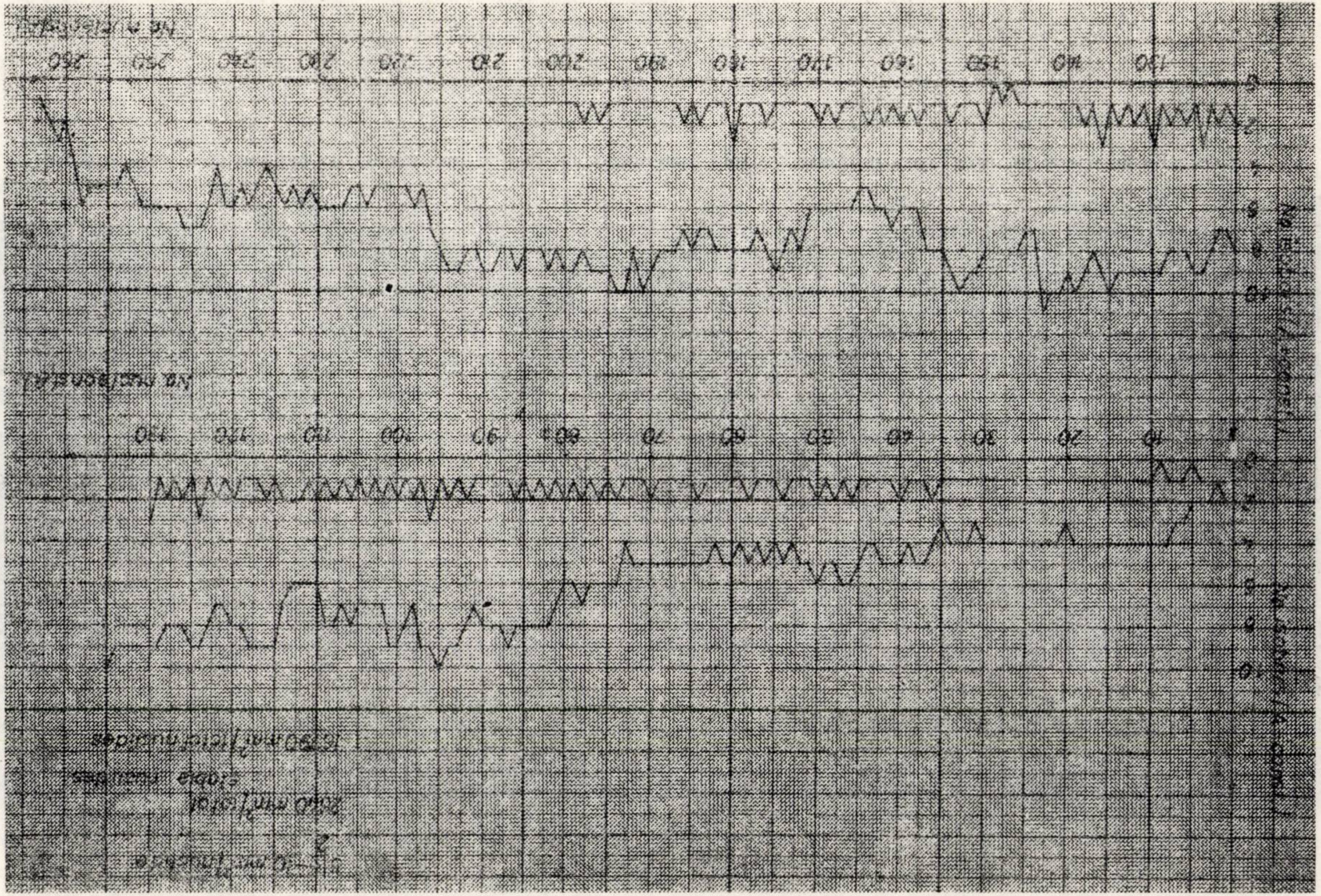

Fig. 3. — The total number of isobars and that of the stable ones (lower values) for each value of mass number, A.

On the other hand, there are to be expected additions to the graphs concerning the total number of nuclides, as new nuclidic systems are discovered.

The interpretation of these graphs allows us to find some known data about the nuclides, but, at the same time, it offers the possibility of new interpretations and anticipations.

In the present paper new data and regularities are given, first concerning the stable nuclides, then the radioactive ones. The known isotopes and their mass numbers can be found in any isotopes table (*e.g.* in C. Drăgulescu and E. Petrovici, "Introducere în chimia anorganică modernă", Ed. Facla, Timişoara, 1973, tables nos 1 and 2).

The graphs show that whereas all the known nuclidic species cover all the integer numbers up to $Z = 105$, $N = 158$ and $A = 262$, the stable nuclides present stability discontinuities, as follows : the stable isotopes, up to $Z = 83$, present two discontinuities; the stable isotones, up to $N = 126$, present twelve discontinuities; the stable isobars, up to $A = 209$ have four discontinuities. The nuclear stability was conventionally taken for those nuclides whose half-life is greater than 2×10^{17} years (therefore the last stable nuclide was considered to be ^{209}Bi, whose $T_{1/2} = 2.5 \times \times 10^{17}$ years).

Examination of these graphs evidences that the regularities observed are valid only for the abscissa values greater than 10. Up to 10 there are deviations which can be observed in all the three figures on the lower curves. In this range there are two stable nuclides with the mass numbers A and A + 1, for odd values of Z — 4 of the total five existent — as well as for odd values of N — 3 of the total four existent. From the five odd-odd stable nuclides four are situated at the beginning. Two isobaric discontinuities — out of all four — are placed at $A = 5$ and $A = 8$. All these cases justify why the stated rules do not apply for less than values 10 on the abscissa.

A general rule states that the discontinuities in nuclear stability appear for odd values for Z, N, and A. Exceptions are for ($Z = 0$), $N = 84$ and $A = 8$. Another general rule states that only one stable nuclide having odd values for Z, N, and A, exists for each numerical value of them. The most numerous and obvious deviations are found for odd values of Z. These deviations obey another rule — the isotopes rule — which may be formulated as follows : an element with odd Z has two stable isotopes only if their mass numbers are odd A and A + 2. To this last rule is connected the rule of isotones which may be formulated as follows : if one element with odd Z has stable isotopes with odd A and A + 2 values then the A + 1 isotope has no stable isotone, the number of A + 1 — Z neutrons being not able to form any stable nuclide. In the case of 10 discontinuities, among the 12 existent, the number of neutrons corresponds to the value of A + 1 — Z, where Z is odd and A and A + 2 — odd too — correspond to the stable isotopes.

An observation of major importance consists in the fact that the two neutronic discontinuities — excepted from the above stated rule — at $N = 84$ and $N = 87$ are found at the convergency with the protonic discontinuity, at $Z = 61$ and at the two nucleonic discontinuities, at $A = 147$ and $A = 149$. Figure 2 offers the best way to visualize the fact that the five discontinuities – of three different types – appear as values between N = 84 and N = 87, just at the place where the most numerous unstable isotones are known. Thus appears clearly a zone which may be called a "gap of nuclear instability" as a result of a "nuclidic stability disaster".

The reverse of the rule of isotopes is also valid, *i.e.* : two stable nuclides with odd N have as mass numbers odd A and A + 2 values. The A + 1 isotone has no stable isotopes, for N = 55 and Z = 43 (at Z = 61 – the second protonic discontinuity – there is a multiple focused instability, as it has been mentioned before).

Some observations can be made concerning the unstable nuclides as a function of the number of the known ones. Thus, the isotopes (Fig. 1) are concentrated mostly at Z = 31–40, 46–58, and 78–90. Most of the isotones (Fig. 2) are concentrated at N = 50–55, 78–90, 105–126 and 144–148. The isobars (Fig. 3) in greater number are at A = 80–110, 115–145, 152–155 and 189–215. Between these maxima there are "gaps" – a relatively small number of known nuclides. Such minima are situated at Z = 23–33, 41–49, 59–80 and 91–100; at N = 9–29, 31–45, 55–80, 90–110, and 125–155; at A = 8–30, 50–74, 101–130, 155–191 and 215–262. Inside these gaps there exists a greater probability that new unstable nuclides might be discovered.

The data recorded in the present paper may serve as starting points for discovering the causes standing behind them and – implicitly – contribute to a better understanding of the internal constitution of the atomic nuclei.

Revue Roumaine de Chimie, **31**, *11—12*, 1047—1054 (1986)

Hommage au Professeur P. SPACU à l'occasion de son 80e anniversaire

CORRÉLATION DANS LES SPECTRES D'ABSORPTION EN INFRA-ROUGE ET DE RAYONS X, DE QUELQUES COMPLEXES DE TYPE REINECKE

N. CALU, G. BRÎNZAN et N. BÎLBĂ

Institut Polytechnique « Gh. Asachi » de Iassy
Faculté de Technologie Chimique
Splai Bahlui 71, 6600 Iași, Romania

Reçu le 12 mai 1986

The Reinecke type complexes, with the $[Cr(NCS)_4L_2]^-$ ion, present some specific properties as a function of organic base L. These properties have been investigated through IR spectrophotometry and X-ray diffraction spectra. Thus, the stretching frequencies ν_{CN} and ν_{CS}, as well as the deformation frequency δ_{NCS}, give evidence of CrN bonds, with the SCN^- ligand. By graphic representation $K_{CrN} = f(K_b)$ – a direct proportionality relation between force constant and base character of the ligand – the stretching frequency ν_{CrN} was localized in the 320—390 cm^{-1} region. At the same time, linear relations between spectral parameters of complexes, have been established. The Reinecke type complexes have a simple cubic elemental cell, with a_0 : 14.82—23.40 Å, as a function of the organic base L.

Les complexes de type Reinecke avec l'ion $[Cr(NCS)_4L_2]^-$, présentent quelques propriétés spécifiques en fonction de la base organique L. Ces propriétés sont investiguées par spectroscopie en infra-rouge et de rayons X. Ainsi, à partir des fréquences caractéristiques en infra-rouge ν_{CN}, ν_{CS} et δ_{NCS}, on a mis en évidence des liaisons de type CrN de l'ion NCS^-. En s'appuyant sur des représentations graphiques $K_{CrN} = f(K_b)$, une fonction de proportionnalité directe, on a localisé les fréquences caractéristiques ν_{CrN} dans le domaine : 320—390 cm^{-1}. De même, on a défini une série de relations de proportionnalité directe ou inverse, entre les paramètres spectraux des complexes. Par diffraction des rayons X, on a établi que les complexes de type Reinecke ont une cellule élémentaire cubique primitive, avec a_o : 14,82—23,40 Å.

1. INTRODUCTION

Les complexes de type Reinecke, avec l'ion $[Cr(NCS)_4L_2]^-$ contiennent la base organique L comme constituent variable. Par son caractère nucleophile, sa configuration moléculaire et par les intéractions de la sphère de coordination, la base L confère aux complexes de cette série certaines particularités. De telles particularités ont été saisies lors de l'analyse thermique, spectroscopie d'absorption en ultra-violet, visible et infra-rouge etc.[1-8]

En ce sens, dans ce travail, on présente les données obtenues concernant l'étude d'une série de complexes de type Reinecke par spectroscopie d'absorption en infra-rouge (IR) et de rayons X. Ces données permettent l'établissement de certaines corrélations entre le caractère basique du ligand L et la constante de force de la liaison métal-ligand, ainsi que l'éclaircissement du mode de liaison entre Cr(III) et le ligand bifonctionnel SCN^-.

2. PARTIE EXPÉRIMENTALE

La synthèse des complexes $LH[Cr(NCS)_4L_2]\cdot \times H_2O$, avec $LH = NH_4^+$ ou LH^+ et $L = NH_3$ ou base organique, a été effectuée d'après un procédé approprié,[9] à base d'un rapport optimal des réactants pour chaque produit.[1]

Les données de l'analyse quantitative et celles de l'analyse thermique sont en accord avec les formules chimiques de ces complexes.[2]

Les spectres IR des complexes, en pastilles de bromure de potassium, ont été enregistrés à l'aide d'un spectrophotomètre UNICAM SP−100.

Les spectres de diffraction des rayons X ont été obtenus avec le diffractomètre T.U.R. M−62. Les diffractogrammes ont été obtenus à base de la radiation K_α du cuivre, avec le filtre de nickel, la vitesse de rotation de l'échantillon étant 0,5 degré/min. et celle d'enregistrement de 600 mm/h.

3. RÉSULTATS ET DISCUSSIONS

3.1. Spectres IR

Les données expérimentales de l'analyse spectrale en IR des complexes concernés, tableau 1, montrent que la liaison métal-ligand est de type Cr(III) − NCS . .,[10−13] à savoir :

— les fréquences des vibrations de valence ν_{CN}, assez intenses, avec déformations éventuellement pics, sont situées dans le domaine 2050−2090 cm^{-1} ;

— les fréquences des vibrations de valence ν_{CS}, moins intenses, sont situées dans le domaine 800−820 cm^{-1} ;

— les fréquences de déformation δ_{NCS}, d'intensité moyenne, apparaissent dans le domaine 460−480 cm^{-1}.

L'identification des vibrations caractéristiques ν_{CrN} constitue un aspect très important, car elles apportent des informations directes sur la liaison métal-ligand. Dans ce but, en s'appuyant sur les données de la littérature concernant les fréquences ν_{MN} de certains amino-complexes,[14,15] on a établi des relations linéaires entre la constante de force, K, et le caractère basique des ligands, pK_b. Finalement, on a déterminé expérimentalement les fréquences caractéristiques de l'anion complexe $[Cr(NCS)_6]^{3-}$, qui sert à l'obtention des dérivés de type Reinecke étudiés.

Ainsi, on constate que dans le domaine 320−390 cm^{-1}, les complexes présentent des vibrations de groupement qui peuvent être ordonnées selon le caractère basique des ligands L. En fait, on admet que les vibrations de valence ν_{CrN} sont situées dans ce domaine et surtout entre 340 et 360 cm^{-1}, avec les valeurs de K_{CrN} :$0,7507\cdot 10^5$ respectivement $0,8910\cdot 10^5$ dyn. cm^{-1}.

D'autre part, on mentionne que les vibrations ν_{CrN} des complexes de type Reinecke sont dues tant aux liaisons CrN de l'ion NCS^-, qu'à celles CrN de la base organique. Par conséquent, elles peuvent produire

Tableau 1

Données concernant les spectres IR dans la série des complexes de type Reinecke, $[Cr(NCS)_4L_2]^-$

Numéro d'ordre	L des complexes	ν_{NC} cm^{-1}	ν_{CS} cm^{-1}	δ_{NCS} cm^{-1}	ν_{CrN} cm^{-1}	Observations
0	1	2	3	4	5	6
1	L_0 : SCN^-	2080	820	472	352	$pK_b = 11,54$
2	L_{01} : NH_3	2090	820	463· (497)	340	$pK_b = 4,74$
3	L_{11} : n-propylamine	2060	(820)	478	358	$pK_b = 3,33$
4	L_{12} : n-butylamine	2060	(820)	475	358 ; 348	$pK_b = 3,38$
5	L_{13} : tri n-propylamine	2073	813	478	360	
6	L_{14} : triethylamine	2048	830	476	356	$pK_b = 3,25$
7	L_{15} : tri n-butylamine	2060	(815)	478	354	
8	L_{21} : aniline	2080	800	477	365 ; 340	$pK_b = 9,41$
9	L_{22} : N,N-dimethylaniline	2073	825	478	358	$pK_b = 9,89$
10	L_{23} : benzylamine	2060	813	475	359	$pK_b = 4,64$
11	L_{24} : phenylbenzylamine	2062	(817)	470	354	
12	L_{25} : 4-methylaniline	2075	822	480	347 ; 318, 384	$pK_b = 8,92$
13	L_{26} : 2,3-dimethylaniline	2070	817	480	348	
14	L_{27} : 2,4-diamino-1-methylbenzene	2067	820	473	354	
15	L_{28} : 4-aminoanisole	2073	805 (825)	479	344 ; 357	
16	L_{29} : 4-aminophenetole	2080	810 (825)	481	350 ; 378	$pK_b = 8,74$
17	L_{31} : α-naphtylamine	2060	800	475	360 ; 350	$pK_b = 10,07$
18	L_{32} : β-naphtylamine	2050	810 (820)	475	351	$pK_b = 9,88$
19	L_{41} : pyridine	2055	800	480	356 ; 322, 380	$pK_b = 8,85$
20	L_{42} : 4-methylpyridine	2050	820	480	363 ; 328, 390	$pK_b = 8,00$
21	L_{43} : 2,2′-dipyridil	2050	800	476	356	$pK_b = 9,60$
22	L_{44} : 2-methylquinoline	2060	807	478, (463)	355	
23	L_{51} : morpholine	2054	820	479	372	
24	L_{52} : scopolamine	2070	805	480	356	
25	L_{53} : pilocarpine	2060	815 (825)	480	360	$pK_b = 7,15$

de bandes normales, ou déformées, et avec pics, ceci en fonction de la force de ces liaisons, des effets électroniques aux niveaux des liaisons, éventuellement de la scission en champ cristallin.

3.1.1. *Relations linéaires dans la série de données spectrales en IR, des complexes de type Reinecke*

A la base de la loi de Hooke on a établi pour la constante de force[16] la relation :

$$K = 0{,}6494\ \bar{\nu}^2 \approx 0{,}65\ \bar{\nu}^2 \qquad (1)$$

où :

$\bar{\nu}$ = fréquence caractéristique de groupement, en tant que numéro d'onde, en cm^{-1}.

À l'aide de la constante de force qui est, par ailleurs, dépendante de la force de la liaison, on a représenté graphiquement la fonction :

$$K_i = f(pK_b) \tag{2}$$

où :

$K_i = K_{\mathrm{CrN}}$, K_{CN} et K_{NCS} ;

$pK_b = -\lg K_b$; K_b étant la constante de basicité des ligands L.

Des représentations graphiques de type (2), comme celle de la figure 1, on fait une série d'observations.

a. Dans la représentation $\mathrm{K}_{\mathrm{CrN}} = f\,(pK_b)$, les constantes de force augmentent avec la diminution des valeurs pK_b entre 11,5 et 6–5, ce qui implique un accroissement de la force de liaison métal-ligand. Dans ce domaine on définit la droite p (fig. 1).

Mais les bandes d'absorption peuvent être déformées ou scindés qui s'écartent souvent de la droite p (tableau 1 et figure 1).

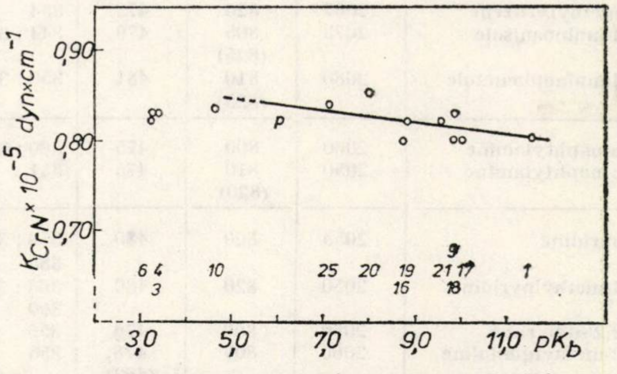

Fig. 1. — Représentation graphique $K_{\mathrm{CrN}} = f\,(pK_b)$, dans la série des complexes de type Reinecke : a. les données expérimentales obtenues pour différents complexes, sont présentées suivant le numéro d'ordre des ligands correspondants du tableau 1 ; b. dans le cas des bandes scindées on a pris en considération celle avec l'intensité maximale.

Les complexes avec $pK_b \gtrsim 5$ sont situés au-dessous de la droite p (fig. 1). Dans de tels cas, les interactions de la sphère de coordination affaiblissent, entre autre, la force de la liaison CrN avec les ligands SCN$^-$.

b. Dans la représentation $K_{\mathrm{CN}} = f\,(pK_b)$, les constantes de force augmentent d'habitude avec l'accroissement des valeurs pK_b, ce qui permet de définir la droite de type i. Par conséquent, la force de la liaison CN s'affaiblit au fur et à mesure que le caractère basique des ligands L croit.

c. Dans la représentation $K_{NCS} = f(pK_b)$, les constantes de force augmentent d'habitude avec la diminution des valeurs pK_b; ainsi on définit une droite de type p.

Avec les points des droites p et i obtenues, on a effectué de nouvelles représentations $K_i = f(pK_b)$, en coordonnés à l'échelle plus grande, qui ont permis le calcul de nouveaux paramètres – le coefficient angulaire et l'ordonnée à l'origine. Avec ces derniers paramètres, on a défini les équations suivantes entre K_i et pK_b :

$$K_{CrN} = -6{,}40 \cdot 10^2\, pK_b + 8{,}78 \cdot 10^4 \tag{3}$$

$$K_{CN} = 8{,}61 \cdot 10^3 pK_b + 2{,}70 \cdot 10^6 \tag{4}$$

$$K_{NCS} = -1{,}42 \cdot 10^3 pK_b + 1{,}61 \cdot 10^5 \tag{5}$$

De même, on a représenté graphiquement la fonction :

$$K_i = f(\mathrm{CrN}) \tag{6}$$

où :

$$K_i = K_{NC},\ K_{CS} \text{ et } K_{NCS}$$

Des représentations graphiques de type (6), comme celle de la figure 2, on fait une autre série d'observations.

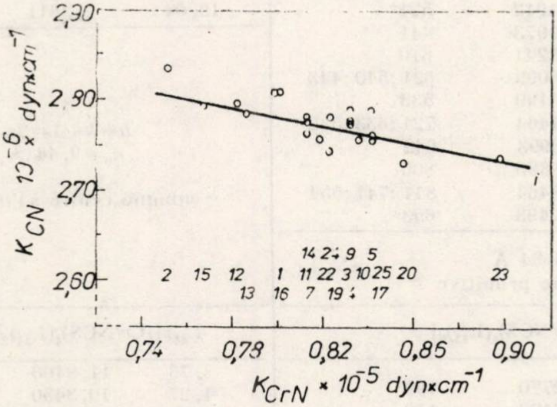

Fig. 2. – Représentation graphique $K_{CN} = f(K_{CrN})$ dans la série des complexes de type Reinecke – la notation et la sélection des données ont été faites conformèment aux points a et b, de la figure 1.

a. Dans la représentation $K_{CN} = f(K_{CrN})$ on définit la droite $\boldsymbol{i}$, de la figure 2, c'est-à-dire une relation de proportionnalité inverse. Evidemment, la force de la liaison CN diminue au fur et à mesure que la force de la liaison CrN croit – due à l'effet de coordination.

b. Dans la représentation $K_{CS} = f(K_{CrN})$ on définit une droite de type i, qui correspond à une relation de proportionnalité inverse.

c. Dans la représentation $K_{NCS} = f(K_{CrN})$ on définit une droite de type p, respectivement une relation de proportionnalité directe.

Les équations établies entre K_i et K_{CrN} sont les suivantes :

$$K_{CN} = -4{,}66K_{CrN} + 3{,}15 \cdot 10^6 \tag{7}$$

$$K_{CS} = -2{,}03K_{CrN} + 5{,}93 \cdot 10^5 \tag{8}$$

$$K_{NCN} = 0{,}62\, K_{CrN} + 9{,}53 \cdot 10^4 \tag{9}$$

En se basant sur les équations (7—9), et en sachant l'une des fréquences caractéristiques impliquée, on peut approximer la position des autres fréquences dues au ligand SCN^- et aux liaisons CrN, pour les complexes de type Reinecke.

Tableau 2

Données des diffraction de rayons X, pour quelques complexes de type Reinecke

$K_3[Cr(NCS)_6] \cdot 4\ H_2O$			$NH_4[Cr(NCS)_4(NH_3)_2] \cdot H_2O$		
θ_{hkl}	d_{hkl}	hkl	θ_{hkl}	d_{hkl}	hkl
2, 47	17, 8730	110	4, 68	9, 4404	110
5, 32	8, 3074	220	6, 63	6, 6713	200
6, 16	6, 1781	310	9, 39	4, 7210	220
8, 14	5, 4399	411 ;330	11, 52	3, 8568	222
9, 08	4, 8808	332	12, 46	3, 5700	321
9, 40	4, 7160	422	13, 30	3, 3482	400
9, 98	4, 4445	511 ;333	14, 14	3, 1530	411
10, 59	4, 1912	521	19, 04	2, 3611	440
11, 11	3, 9973	441			
11, 62	3, 8241	610			
12, 32	3, 6099	621 ;540 ;443			
12, 64	3, 5199	533			
14, 17	3, 1464	721 ;633 ;552	$h+k+1=2n$		
14, 29	3, 0993	642	$a_0 = 9{,}44$ Å		
15, 46	2, 8895	800			
15, 70	2, 8464	811 :741 ;554	cubique centré à i'intérieur		
16, 27	2, 7493	653			
$a_0 = 16{,}34$ Å cubique primitive					

$L_{41}[Cr(NCS)_4(L_{41})_2]$			$L_{44}H[Cr(NCS)_4(L_{44})_2] \cdot 2H_2O$		
			3, 73	11, 8400	111
2, 29	19, 2770	100	4, 27	10, 3450	200
3, 10	14, 2430	110	5, 95	7, 4350	220
3, 76	11, 7460	111	8, 32	5, 3230	440
6, 17	7, 1665	221	9, 76	4, 5437	332
6, 98	6, 3383	311	10, 33	4, 2955	500 ;430
7, 57	5, 8469	320	11, 41	3, 8935	521
10, 46	4, 2427	422	11, 89	3, 7385	522 ;441
10, 93	4, 0623	511 ;333	12, 86	3, 4607	611 ;532
11, 54	3, 8502	521	13, 14	3, 8882	620
12, 37	3, 5955	530 ;433	13, 60	3, 2757	541
12, 68	3, 5090	600 ;442	14, 20	3, 1399	631
17, 62	2, 5446	820 ;644	17, 20	2, 6048	733
$a_0 = 14{,}82$ Å cubique primitive			$a_0 = 15{,}07$ Å cubique primitive		

3.2. Spectres de rayons X

Des diffractogrammes enregistrés sur les complexes de type Reinecke, on a déterminé les angles de diffraction caractéristiques θ_{hkl}, les distances interplanaire d_{hkl}, les indices Miller hkl, les intensités relatives $I/I_0 \cdot 100$ (I_0 étant l'intensité du pic le plus fort) et les valeurs approximatives des paramètres a_0 de la cellule élémentaire (tableaux 2 et 3).

Pour définir la cellule élémentaire on a utilisé le procédé d'indexation pour le système cubique [17-19], dont les résultats sont portés dans le tableau 2.

Tableau 3

Données de diffraction de rayons X, pour quelques complexes de type Reinecke.

$NH_4[Cr(NCS)_4(L_{51})_2] \cdot 2\ H_2O$			$NH_4[Cr(NCS)_4(L_{22})_2] \cdot H_2O$		
θ_{hkl}	d_{hkl}	hkl	θ_{hkl}	d_{hkl}	hkl
3,98	11,0970	210	3,85	11,4720	210
4,60	9,6042	211	4,97	8,8908	221
5,14	8,5975	220	5,25	8,4179	310
7,42	5,9644	400	5,57	7,9357	311
8,06	5,4935	331	6,37	6,9424	321
10,13	4,3793	521	8,73	5,0748	510 ;431
10,66	4,1639	530 ;433	8,85	5,0066	511 ;333
10,82	4,1031	531	9,57	4,6330	440
12,01	3,7017	541	9,73	4,5575	522 ;441
12,41	3,5841	630 ;542	10,09	4,3965	531
13,28	3,3531	640	10,29	4,3120	610
13,80	3,2291	642	10,44	4,2507	611 ;532
17,14	2,6136	920 ;760	10,93	4,0623	541
			11,13	3,9902	533
			12,73	3,4965	642
			13,11	3,3958	731 ;553
a_0= 17,05 Å cubique primitive			a_0= 18,51 Å cubique primitive		

$NH_4[Cr(NCS)_4(L_{31})_2]$			$NH_4[Cr(NCS)_4(L_{15})_2]H_2O$		
3,61	12,2330	211	3,73	11,8400	220
6,25	7,0752	411	3,93	11,2380	300
7,01	6,3113	332	7,53	5,8777	440
7,17	6,1712	422	8,69	5,0980	541
7,97	5,5552	520 ;432	10,05	4,4138	642
9,09	4,8754	611 ;532	10,57	4,1990	732 ;651
9,81	4,5207	622	10,73	4,1371	800
10,57	4,1990	711	10,89	4,0770	811 ;741, 554
10,85	4,0919	721 ;633	11,25	3,9482	653
11,21	3,9621	722 ;544	11,37	3,9070	822 ;660
11,45	3,8801	731 ;553	11,45	3,8801	830 ;661
12,25	3,6302	820 ;644	11,69	3,8015	662
12,45	3,5728	653	11,87	3,7447	752
12,77	3,4847	831 ;750 ;743	12,25	3,6302	911 ;753
a_0= 21,19 Å cubique primitive			a_0= 23,40 Å cubique primitive		

A partir de ces données, on peut conclure comme suit :

a. le complexe Reinecke, $NH_4[Cr(NCS)_4(NH_3)_2]\cdot H_2O$, contient une cellule élémentaire de type cubique centré à l'intérieur, avec $a_0 = 9{,}44$ Å ;

b. les complexes de type Reinecke, $LH[Cr(NCS)_4L_2]\cdot \times H_2O$, contiennent une cellule cubique primitive, avec $a_0 = 14{,}82-23{,}40$ Å.

Les différences structurales entre les complexes de type Reinecke sont dues aux constituants L, à savoir les bases organiques.

BIBLIOGRAPHIE

[1] G. Brînzan, *Teză de Doctorat*, Inst. Polit. Iași, 1983.
[2] N. Calu, L. Odochian, G. Brînzan et N. Bîlbă, *J. Thermal Anal.*, **30**, 541 (1985).
[3] I. Gănescu, C. Várhelyi, F. Futó et G. Brînzan, *Z. anorg. allg. Chem.*, **439**, 282 (1978).
[4] I. Gănescu, C. Várhelyi, G. Brînzan et M. Proteasa, *Z. anorg. allg. Chem.*, **423**, 259 (1976).
[5] M. Cioică, I. Gănescu et C. Lepădatu, *Z. physik. Chem. Neue Folge*, **97**, 41 (1975).
[6] A. W. Adamson, *J. Amer. Chem. Soc.*, **80**, 3183 (1958).
[7] J. Zsakó, C. Várhelyi, D. Oprescu et I. Gănescu, *Acta Chim. Acad. Sci. Hung.*, **97**, 159 (1978).
[8] J. Zsakó, C. Várhelyi, I. Gănescu et D. Oprescu, *Ann. Soc. Chim. Polonorum*, **48**, 1141 (1974).
[9] I. Gănescu et C. Várhelyi, *Monatsh. Chem.*, **95**, 372 (1966).
[10] D. C. H. Michell et R. J. Williams, *J. Chem. Soc.*, **1960**, 1912.
[11] J. Lewis, R. S. Nyholm et P. W. Smith, *J. Chem. Soc.*, **1961**, 4590.
[12] M. Brezeanu et P. Spacu, « Chimia Combinațiilor Complexe », Ed. Did. și Ped. București Ed. II, 1974, p. 124.
[13] K. Nakamoto, « Infrared Spectra of Inorganic and Coordination Compounds », John Wiley and Sons, Inc,. New York, London, 1963, p. 173.
[14] H. Block, *Trans. Faraday Soc.*, **55**, 667 (1959).
[15] B. Powell et N. Sheppard, *J. Chem. Soc.*, **1956**, 3108.
[16] A. T. Balaban, M. Banciu, et I. Pogany, « Aplicații ale Metodelor Fizice în Chimia Organică », Ed. Științifică și Enciclopedică, București, 1983, p. 13.
[17] Powder Diffraction Fille, « Search Manual-Organic and Inorganic Compounds », J.C.P.D.S., 4, 1973.
[18] H. G. Stout et H. L. Jensen, « X-Ray Structure Determination », McMillan Co., 1968.
[19] H. Lipson et H. Steeple, « Interpretation of X-Ray Powder Diffraction Patterns », Mc.Millan Co., 1970.

Revue Roumaine de Chimie, **31**, *11–12*, 1055–1064 (1986)

INDEX DES AUTEURS

A

ABDALLA E. B., voir HABIB O.M.O. 629
AGARWAL R. and BAHADUR P. Study of α-diazoketones from nicotinyl and furoyl chlorides and higher diazoalkanes. 297
AGARWAL R. K. and S. K. GUPTA, Magnetic and spectral studies of lanthanide perchlorate complexes of 2-ethoxy-carbonylamino-pyridine-N-oxide 585
ALARCÓN O. M., voir LEON N. 353
ALBU I. voir CHIFU E. 105
ALEXANDROAIE M., voir POPOVICI EV. 419
ANAÇ OLCAY, Some observations on the catalytic and direct photolytic reactions of *cis*-cyclodecene and *cis*-bicyclo[3.3.0.]oct-2-ene with dimethyldiazomalonate . 787
ANDRUH M. and C. I. LEPADATU, MARIA BREZEANU, The position of 4,4'-bipyrydyl in the spectrochemical series for nickel(II) complexes 943
ARIAS C., voir CAYRE I. 727
ARVAY Z., voir BARTHA E. 519
AVILA-DIAZ L. A., voir SILAGHI DUMITRESCU L. 335
AVRAM M., voir IORDACHE F. 261

B

BACALOGLU R. and HANS-HORST GLATT, MAMADOU FOULA BARRY, C. CSUNDERLIK, Imines of aminoazoles. III. Basicity constants of heterocyclic imines in the series of benzylidene-amine-benzothiazoles, -benzoxazole, benzimidazoles, -thiazole and- triazole (in German) 283
— , voir GLATT H. H. 273
BACALOGLU R. and L. COTARCA, A. IŞFAN, C. IŞFAN, High-performance liquid chromatography of 2,4,6-haloalkyl-1,3,5-triazines 403
BADEA F. and A. T. BALABAN, A. DUMITRIU, F. IORDACHE, A. MEGHEA, L. STOENESCU, Carbanions and free radicals derived from 1,2-diphenylpyrazolidine -3,5-diones. II. Trapping of the free radicals derived from diethyl fluoro-malonate, n-butyl-, and phenyl-malonate 119
— , voir IORDACHE F. 26
— , voir STOENESCU M. 507
BADIGER B. M. and S. A. PATIL, S. M. KUDARI, V. H. KULKARNI, Magnetic and spectral properties of cobalt(II) and copper(II) complexes with 3-substituted-4-(5'-substituted-salicylidene/2'-hydroxyacetophenoncimine)-1,2,4-triazoles . 849
BAHADUR P., voir AGARWAL R. 297
BALABAN A. T. and G. MARTON, I. SCHIKETANZ, Reaction of pyrylium salts with nucleophiles. XVIII. Synthesis of 4(*p*-n-butoxyphenyl)-2,6-dimethylpyridine and of 2,6-dimethyl-4(*p*-n-pentylphenyl)-pyridine 37
— , voir BADEA F. 119
BALABAN A. T., Chemical graphs. Part 44. Isomer enumeration for substituted saturated polyhedral valence isomers of annulenes 679
— — Part. 45. Edge-labelled graphs as unsaturated valence isomers of annulenes; application of Pólya's theorem 695
— — Part. 46. Enumeration of valence isomers of adamantane using Pólya's theorem 795
— , voir BUGEANU M. 1013
BĂLĂNESCU E, voir CALU N. 71
BÂLDEA I., voir ZSAKÓ J. 443
BANCIU ANCA, voir BANCIU MIRCEA 1019
BANCIU M. and DANA ELIAN, M. ELIAN, LIGIA STĂNESCU, ECATERINA CIORĂNESCU, 4b,10b-dihydrochrysene, a new dibenzo$(CH)_{10}$ hydrocarbon 503
— and M. ELIAN, ANCA BANCIU, C. DRĂGHICI, E. CIORANESCU, Photochemical ring contraction of 8-diazo-dibenzo[*c*, *e*]-tricyclo [5.3.0.0.2,10]-deca-3,5-dien-9-one . 1019
BARAKAT M. A., voir OSMAN A. N. 615
BĂRBÎNŢĂ V., voir VÎLCU R. 657
— , voir VÎLCU R. 741
— ; voir VÎLCU R. 839

BARRIOS H., voir R. SÁNCHEZ-OBREGÓN . . . 709
BARRY M. F., voir GLATT H.-H. . . . 273
— , voir R. BACALOGLU . . . 283
BARTHA E. and Z. ARVAY, A. C. RĂZUŞ, Synthesis of benzospiro[2, 4]heptane derivatives . . . 519
BELDIE C. and N. HURDUC, A. ONU, I. G. POINESCU, Thermal behaviour of some styrene-methylmethacrylate copolymers . . . 31
BENMOHAMED N., voir ROESCHI H. W. . . . 935
BENTRUP U. and L. KOLDITZ, Roentgenographic and IR-spectroscopic investigations of the thermolysis of alkali pentafluoroaluminate hydrates (in German) . . . 963
BERDAN I., voir CALU N. . . . 71
— , voir CALU N. . . . 217
BEZAK E., Studies on 4-alkylpyridines usability for extraction of Co(II), Ni(II), Cu(II), Zn(II) and Cd(II) complexes from nitrate solutions . . . 411
BÎLBĂ N., voir CALU N. . . . 1047
BOTAR AL., voir MARCU GH. . . . 981
BOTOACĂ M., voir GLATT H.-H. . . . 273
BOTOACĂ SAVU SIMONA, voir GLATT H.-H. . . . 273
BRÂNZAN G. voir CALU N. . . . 1047
BRÂNZOI V. and AHMED KABIR, M. CIOPEC, Corrosion kinetics or Armco iron in aqueous solution of citric acid . . . 473
— — — , Corrosion of steel C-95 in aqueous hydrochloric acid in the presence and absence of organic inhibitors . . . 571
BREZEANU M., voir PATRON L. . . . 811
— , voir ANDRUH M. . . . 943
BRUMĂ M. and GH. DUMITRESCU, E. DUMITRESCU, Modified copolymers with radioprotective action . . . 163
BRUYLANTS A., Early and contemporary scientific links between Romania and Belgium . . . 923
BUDIU T., voir VĂŢULESCU R. . . . 199
BUDIU T., voir VĂŢULESCU R. . . . 209
BUDIU T., voir VĂŢULESCU R. . . . 345
BUGEANU M. and V. EM. SAHINI, V. T. CIORBA, A. T. BALABAN, Molecular complexes with aromatic cations as electron acceptors. VII. Spectrometric, conductometric and dipolar data of phenyl-substituted pyrylium salts with tetracyano-*para*-quinodimethane anions . . . 1013
BURGUERA J. L., voir LEÓN N. . . . 353
BURGUERA M., voir LEÓN N. . . . 353

C

CALU N. and E. BĂLĂNESCU, I. BERDAN, I. SANDU, Complex compounds of Mn(III) and Mn(IV). II. The system Mn(III, IV)—2-amino-phenol-4-sulfone acid (in French) . . . 71
CALU N. and I. SANDU, I. BERDAN, Preparation and characterization of active forms of manganese dioxide for dry galvanic elements and systems (in French) . . . 217
CALU N. and G. BRÂNZAN, N. BÎLBĂ, IR and X-ray spectral correlations of some Reinecke type complexes (in French) . . . 1047
CAPITÁN F. and P. ESPINOSA, F. MOLINA, L. F. CAPITÁN-VALLVEY, Study of metallic complexes of Schiff bases derived from 2-thiophene-carboxaldehyde, 2-pyridinecarboxaldehyde and o-aminobenzenethiol (in Spanish) . . . 897
CAPITÁN-VALLVEY L. F., voir CAPITÁN F. . . . 897
CĂLUŞARU A., voir SAVIUC E. . . . 753
CARTIANU D. Dissipative structures in reaction-diffusion systems as synchronization phenomena . . . 175
CAYRE I. and C. ARIAS, C. RUEDA, Rheological characteristics of sodium carboxymethylcellulose solutions at low shear rate. The evaluation of parameters thermodynamics. The effects of the dextran's addition (in Spanish) . . . 727
CEBA M. ROMÁN and J. C. JIMÉNEZ SÁNCHEZ, T. GALEANO DÍAZ, Kinetic determination of Co(II) based on its catalytic effect on atmospheric oxidation of 1,3-cyclopentandione bis(4-methylthiosemicarbazone) (in Spanish) . . . 889
CECAL AL. and D. CIOBANU, I. SANDU, Use of beta-rays back-scattering in the study of corrosion process of some carbon steel samples in acid solutions . . . 451

CERCASOV C., voir NEGOIU D. 987
CHAAR M.A., voir NICOLESCU I. V. 99
CHIRALEU F., voir IORDACHE F. 261
CHIRCA M.S., voir IONESCU N. 671
CHIRIAC C. I., A convenient method for the synthesis of 1,3,4-oxadiazoles from diaroylhydrazines under mild conditions using phosphorus trichloride-dimethylformamide adduct as reagent 51
— , Phosphorous acid-iodine as reagent for the synthesis of 1,3,4-oxadiazoles from diacylhydrazines 159
— , Amides from N-acylphthalimides and aliphatic amines 525
— , Synthesis of aromatic thioureas 625
CHIFU E., and I. ALBU, C. I. GHEORGHIU, E. GAVRILĂ, M. SĂLĂJAN, M. TOMOAIA-COTIȘEL, Marangoni flow—induced by temperature gradients—against gravity forces 105
CIOBANU D., voir CECAL AL. 451
CIOMÂRTAN D., voir DAVID V. 823
CIOPEC M., voir BRÂNZOI V. 473
— , voir BRÂNZOI V. 571
CIORĂNESCU ECATERINA, voir BANCIU M. 503
— , voir STĂNESCU M. 1001
— , voir BANCIU M. 1019
CIORBA V. T., voir BUGEANU M. 1013
CIBURA K. and A. HAAS, Reactions on tetracoordinated boron: advances in trimethyl-aminoborane-chemistry (in German) 927
COCÂRLĂ I., voir GORDUZA V. 661
COLȚEA P. voir SCHWARTZ R. 481
COMBIER A. LABLACHE, voir SURPĂȚEANU GH. 371
COTÂRCĂ L., voir BACALOGLU R. 453
COTÂRȚĂ ADINA, voir STERNBERG S. 431
CONȚESCU A., voir PATRON L. 341
— , voir PATRON L 811
CRISTESCU CAROL, *as*-Triazine derivatives with potential therapeutic action. XXI. Synthesis of 4-thioxo-5(fluoro-benzyl)thio-6-azauracil derivatives and their nucleosides 881
CRUCEANU M., voir POPOVICI E. 419
CSUNDERLICK C., voir GLATT H.-H. 273
— , voir BACALOGLU R. 283
CUETO G. LÓPEZ and A. ALONSO MATEOS. Study on controlled-potential coulometric anodic oxidation of the binuclear Mn(III)-cyanide complex. III. Correction of positive and negative kinetic currents for its coulometric determination. Electrolytic formation of the binuclear cyanide complex of Mn(III)— Mn(IV) (in Spanish) 9
CUETO G. LÓPEZ andA. A. ALONSO MATEOS, Coulometric study at controlled potential of the anodic oxidation of the binuclear cyanide complex of Mn(III). Part II. Oxidation at +0.80 volts vs. SCE: Faraday currents, kinetic currents (in Spanish) 237

D

DARBIEU MARIE-HÉLÈNE, Main reactions of the cobalt atom in vitamin B_{12} and in model complexes from the cobaloxime group (in French) 1031
DAVID V. and CIOMÂRTAN D., On the spectral analytical measuring processes regarded as information processes 823
DAL SASSO LILIAM INÉS, voir REZENDA MARCOS CAROLI 323
DEMETER-VODNÁR J., voir ZSAKÓ J. 443
DIAZ T. GALEANO, voir CEBA M. ROMAN 889
DOCA N. and E. SEGAL, Dehydrogenation kinetics of low aliphatic alcohols on copper catalysts. II. Preparation, stabilisation and catalytic activity of Cr—O—Cu and Mn—O—Cu system 567
DOGAR F. and L. SILAGHI-DUMITRESCU, R. GRECU, I. HAIDUC, Amine adducts of nickel(II) diphenyldithiophosphinate with substituted ethylenediamines 79
DONIA S. G., voir SHAMS N. A. 541
DUBEY R. C., voir NATH NARENDRA 57
DULMAN V., voir HAGIU C. 909

DUMITRESCU GH., voir BRUMĂ M. 163
DUMITRESCU E., voir BRUMĂ M. 163
DUMITRIU A., voir BADEA F. 119
DUMITRIU EMIL, voir OPREA SPIRIDON 425
DUPRET C., voir VIDAL B. 773

E

EL-GAWAD I.I.ABD, voir KHALIL A. M. 901
ELIAN DANA, voir BANCIU M. 503
ELIAN M., voir BANCIU M. 503
— , voir STĂNESCU M. 1001
— , voir BANCIU M. 1019
EL-KHAMRY ABDEL MOMEN A. and M. E. SHABAN, M. M. HABASHY, Synthesis and reactions of 6-aryl-4,5-dihydropyridazin-3(-2H)-ones . . . 387
ESPINOSA P., voir CAPITÁN F. 897
ETMAN H. A., voir KHALIL A. M. 901

F

FECHETE D., voir GLATT H. H. 273
FILIP P., voir GEORGESCU E. 365
FILOTI G., voir NICOLESCU I. V. 99
FRITZ G. and K. STOLL, The cyclotetraphosphanes $(Me_3C)_3P_4H$ and $(Me_3C)_3 P_4 [P (CMe_3) Cl]$ (in German) 949
FULEA A. O. Concerning "The relation between moments of inertia, steric crowding and librational motion in molecules. Effects on NMR spectra" 309

G

GĂINAR I., voir VÎLCU R. 657
— , voir VÎLCU R. 741
— , voir VÎLCU R. 839
GĂNESCU I., voir VÁRHELYI CS. 291
GARTNER M. and M. VASS, Elipsometric spectroscopy of pure and CO covered gold films 589
GAVRILĂ E., voir CHIFU E. 105
GEORGESCU E.I. and FLORENTINA GEORGESCU, M. D. GHEORGHIU, P. FILIP, MAGDA PETROVANU, Dipolar derivatives in the quinazoline series. V. Inactivation of quinazolinium-ylids : a new approach towards novel pyrrolo[1, 2-c] quinazoline derivatives (in French) 365
GEORGESCU FLORENTINA, voir GEORGESCU E. I. 365
GHEORGHIU C. voir PATRON I. 341
GHEORGHIU C. I., voir CHIFU E. 105
GHEORGHIU D. M., voir GEORGESCU E. I. 365
— , voir POPESCU ANGELA 1025
GHIRVU C., voir GORDUZA V. 661
GIURGINCA M., voir IVAN G. 857
GLATT H.-H. and M. F. BARRY, C. CSUNDERLIK, R. BACALOGLU, M. BOTOACĂ, S. SAVU-BOTOACĂ, D. FECHETE, Imines of aminoazoles. II. Synthesis and characterization of some imines of 2-amino-benzothiazoles benzoxazole thiazole and 3-amino-1,2,4-triazole (in German) 273
— , voir BACALOGLU R. 283
GORDUZA V. and I. COCÂRLA, G. CHIRVU, L. WAGNER, V. PESCARU, Studies on the reactivity of benzimidazolone derivatives, based on the electronic spectra and molecular diagrams 661
GRANDCLAUDON P., voir SURPĂŢEANU GH. 371
GRECU M., voir POPOVICI EVELINE 419
GRECU R., voir DOGAR F. 79
GÜNAYDIN KERIMAN and Ü. OYMAN, Investigation of dehydration products of aryl and arylalkyl cyclododecanols 497
GUPTA S. K., voir AGARWAL R. K. 585
GUPTA U., voir RAO A.L.J. 93
GUŢUL M., voir MANDRAVEL C. 819

H

HAAS A., voir CIBURA K. 927
HABASHY M. M., voir EL-KHAMRY A. M. 387
HABIB O.M.O. and A. M. KHALIL, E. M. KANDEEL, E. B. ABDALLA, Syntheses and reactions of some new 4-(*p*-substituted ciannamoyl) phenyl-3'4'-xylene sulphonates of expected potential biological activity 629
— , voir KHALIL A.M. 901
HAGIU C. and M. TALABA, V. DULMAN, A. TALABA, Ammonium polyphosphates. Obtention of ammonium polyphosphates by warm ammoniation of orthophosphoric acid 909
HAIDUC I., voir DOGAR F. 79
— , voir SILAGHI DUMITRESCU L. 335
— , voir SILAGHI DUMITRESCU L. 955
HAMED A. A., voir SHAMS N. A. 541
HANTZ A., voir MARCU GH. 227
— , voir VÁRHELYI CS. 291
HAWA S. K., voir SHARMA S. 581
HILLEBRAND M., and M. IOVU, N. NICOLAU, E. VOLANSCHI, Spectral study of the anion radicals provided by some nitro- and amino-ethers 43
— , and V. EM. SAHINI, Electronics pectra of some heteroaromatic cation-radicals 649
HULEA V., voir OPREA SPIRIDON 427
HURDUC V., voir BELDIE C. 31

I

IOAN SILVIA, voir SIMIONESCU Cr. I. 995
IONESCU N. I., and M. S. CHIRCA, D. I. MARCHIDAN, Thermal effect and oscillation in the catalytic oxidation of methanol 671
IORDACHE F., voir BADEA F. 119
IORDACHE F. and F. CHIRALEU, L. STĂNESCU, F. BADEA, M. AVRAM, Bicyclo-[2.2.2]octane derivatives. III. Stereoisomeric 2,3,5,6-tetracarbomethoxy-bicyclo-[2.2.2]octanes 261
IOVU M., voir HILLEBRAND M. 43
IȘFAN ANABELA, voir BACALOGLU R. 403
IȘFAN C., voir BACALOGLU R. 403
ISMAIL M. M. and M. S. MOHAMED, Cyclization of ethyl cyanoacetate and 3,5-dichlorosalicylaldehydes with ketones by means of ammonium acetate 393
— , and M. S. MOHAMED, Synthesis of certain substituted benzopyranopyridine and pyrimidine ring systems 533
— , voir OSMAN A. N. 625
IVAN G. and M. GIURGIUNCA, Substituted and solvent effects in the absorption spectra of nitroso-aromatic derivatives 857

J

JADON S. P. S., voir SHARMA H. K. 305
JUHÁSZ A., voir SCHWARTZ R. 131
— , voir SCHWARTZ R. 481

K

KABIR AHMED, voir BRĂNZOI V., 473
— , voir BRÂNZOI V. 571
KADI H. and D. P. LAZĂR, Identification of aromatic hydrocarbons in petroleum fractions. IV. IR Spectral analysis (in French) 149
KANDELL E. M., voir HABIB O.M.O. 629
KHALIL A. M., voir HABIB O.M.O. 629
KHALIL A. M. and O. M. O. HABIB, I. I. ABD EL-GAWAD, H. A. ETMAN, Synthesis and reactions of some new isoquinoline-1-carbonitrile derivatives 901
KHURANA D. P. and TANEJA A. D., J. S. TYAGI, Spectroscopic determination of enethiol content of substituted pyridyl-thioureas in different solvents 761
KOLDITZ L., voir BENTRUP U. 963
KUDARI S. M., voir BADIGER B. M. 849
KUDESIA V. R., voir KUMARI R. 869
KULKARNI V. H., voir BADIGER B. M. 849
KUMAR ATUL, voir PURI B.K. 85

KUMARI R. and A. D. TANEJA, U. P. KUDESIA, Effects of solvents on the spectra of some substituted acetoacetarylamides 869

L

LAZĂR D. P., voir KADI H. 149
LĂZĂRESCU V. and O. RADOVICI, M. VASS, Cyclic voltammetry studies on oxygen/silver system 461
LEÓN N. and J. L. BURGUERA, M. BURGUERA, O. M. ALARCÓN, Determination of cobalt and manganese in blood serum by flow injection analysis and atomic absorption spectroscopy 353
LEPĂDATU C. I., voir ANDRUH M. 943
LINGVAY I., voir STERNBERG S. 3

M

MĂNĂILĂ R., voir NICOLESCU I. V. 99
MANDRAVEL C. and M. GUŢUL, M. TOMESCU, Synthesis and characterization of the Pd(II), Cd(II) and Hg(II) complex compounds with carbazole derivatives 819
MANDRIC GH. and G. NEAMŢU, S. PECINCU, G. RĂCARU, High temperature polymers. VI. Polybenzimidazole-amide-imides 25
MARA GH. voir PETROVICI EMIL 1041
MARCHIDAN D. I., voir IONESCU N. I. 671
MARCU GH., voir VĂŢULESCU R. 199
— , voir VĂŢULESCU R. 209
— , and A. HANTZ, M. SOMAY, CS. VÁRHELYI, F. TOLEA, Study on some cobalt(III) dioximine chelate adducts with tertiary phosphines 227
— , voir VĂŢULESCU R. 345
— and AL. BOTAR, A. NAUMESCU, Contribution to the study of cobalt(II) dioxygen complexes 981
MARTON G., voir BALABAN A. T. 37
MATEOS A. ALONSO, voir CUETO G. LÓPEZ 9
— , voir CUETO G. LÓPEZ 237
MATEOS E. J. MARTIN, voir MENDEZ J. H. 597
MATHUR S. P., voir SHARMA S. 581
MEGHEA A., voir BADEA F. 119
MÉNDEZ J. H. and A. ALONSO MATEOS, E. J. MARTÍN MATEOS, Gravimetric determination of mercury and cadmium *via* formation of ion pairs $[C_4H_9)_4N]_2$ $[HgI_4]$ and $[C_4H_9)_4N]_2$ $[CdI_4]$ (in Spanish) 597
MERCHES M., voir PINCOVSCHI E 973
MIHAI GH., voir STĂNESCU M. 507
MISRA U. S., voir NATH NARENDRA 57
MOHAMED M. S., voir ISMAIL M. M. 393
— , voir ISMAIL M. M. 533
MOLINA F., voir CAPITAN F. 897
MORARU GH., voir VĂŢULESCU R. 345
MUNTEANU G., voir PATRON L. 811

N

NARTEA E., voir PETROVICI EMIL 1041
NATH NARENDRA and R. C. DUBEY, U. S. MISRA, Kinetics of oxidation of digol by vanadium(V) in aqueous sulphuric and hydrochloric acid medium 57
— , and L. P. SINGH, Kinetics and mechanism of osmium(VIII) catalysed oxidation of benzyl alcohol and benzylamine by alkaline hexacyanoferrate(III) ion 489
NEAMŢU S., voir MANDRIC GH. 25
NEGOIU D. and S. NEAGOE, CORNELIA CERCASOV, M. NEGOIU, I. SARAMET and C. TOMA, Complex compounds of Hg(II) with thiobenzopiperidides and thiobenzomorpholides 987
NEGOIU MARIA, voir NEGOIU D. 987
NICOLAU N., voir HILLEBRAND M. 43
NICOLESCU I. V. and R. MĂNĂILĂ, M. A. CHAAR, G. FILOTI, Structure and properties of the ZnO. nFe_2O_3 catalysis system in the oxydehydrogenation reaction. I. 99
— , voir SĂNDULESCU I. 375

O

ONU A., voir BELDIE C. 31

OPREA SPIRIDON and E. DUMITRIU, V. HULEA, KAYED YOUSEF, Activity and selectivity of neodymium exchanges zeolites in the alkylation reaction of toluene with methanol 425

ORTIZ B., voir SANCHEZ OBREGON R. 709

OSMAN A. N. and M. M. ISMAIL, M. A. BARAKAT, Synthesis and biological activity of certain nicotinic acid derivatives 615

OYMAN Ü., voir GÜNAYDIN K. 497

P

PAPA I., voir VÁRHELYI CS. 291

PAL I., voir VĂŢULESCU R. 199

— , voir VĂŢULESCU R. 209

PÂRVULESCU V., voir SĂNDULESCU I. 375

PATRON L. and A. CONTESCU, GH. ROLEA, C. GHEORGHIU, Preparation and properties of a novel Pd(II)-Sn(II) complex 341

PATRON L. and A. CONŢESCU, G. MUNTEANU, M. BREZEANU, E. SEGAL, Coordination compounds as raw materials for mixed oxides. III. Trinuclear, exocentered, carboxylate compounds containing Fe(II,III,III) 811

PATIL S. A., voir BADIGER B. M. 849

PECINCU S., voir MANDRIC GH. 25

PÉREZ de MARQUEZ OLGA, Mechanistic and synthetic aspects of the anodic oxidation of the 1,4-dimethoxybenzene (in Spanish) 637

— , Anodic oxidation of alkylbenzenes in dry acetonitrile 711

PESCARU V., voir GORGUZA V. 661

PETRESCU V., voir STERNBERG S. 431

PETROVANU M., voir GEORGESCU E. I. 365

PETROVICI EMIL and E. NARTEA, GH. MARA, Criteria nuclides ordering and observed regularities 1041

PINCOVSCHI E. and M. MERCHEŞ, Hydrothermal crystallization of zeolite Na-X 973

PÎRVULESCU L., voir POPESCU A. 1025

POINESCU, I. G., voir BELDIE C. 375

POPA A., voir SĂNDULESCU I. 375

POPESCU ANGELA and L. PÎRVULESCU, L. STĂNESCU, M. D. GHEORGHIU, Synthesis of 1α,2α- and 1β, 2β-isomers of 5,9-methano-5*H*-benzo [3, 4]cyclobuta-[1, 2]cycloheptenes 1025

POPOVICI EVELINE and M. CRUCEANU, M. GRECU, A. VASILE, M. ALEXANDROAIEI, Synthetic zeolites for detergent conditioning. II. On zeolite — surfactant — bleaching agent systems 419

PURI B. K. and A. KUMAR, M. SATAKE, Spectrophotometric determination of cadmium and lead after adsorption of their n-butylxanthates onto microcrystalline naphthalene and replacement by copper 85

R

RADOVICI O., LĂZĂRESCU V. 000

RĂCARU G., voir MANDRIC GH. 25

RAO A.L.J. and U. GUPTA,Extraction spectrophotometric determination of nickel and palladium using cyclohexylthioglycolate (CyHTG) as a reagent 93

RĂZUŞ AL., voir BARTHA E. 519

REZENDE MARCOS CAROLI and DAL SASSO LILIAM INÈS, Polarity of salt solutions. A general empirical equation 323

ROBERT J. E., voir XICLUNA A. 143

ROESKY W. H. and N. BENMOHAMED, On reactions of tetrafluoro-1,2-ethanedisulfenyl-dichloride with alkynes or ketones (in German) 935

ROLEA GH., voir PATRON L. 341

RUEDA C., voir CAYRE I. 727

S

SADEK H., voir SIDAHMED I.M. 327

SAHINI V. EM., voir HILLEBRAND M. 649

— , voir BUGEANU M. 1013

SĂLĂJAN M., voir CHIFU E. 105
SALEM S. M., voir SIDAHMED I. M. 327
SÁNCHEZ J. C. JIMÉNEZ, voir CEBA M. R. 889
SÁNCHEZ OBREGÓN R. and H. BARRIOS, B. ORTIZ, F. YUSTE. Diels-Alder reaction of *trans,trans*-1,4-diacetoxy-1,3-butadiene and 1,2-pentadien-4-one 709
SANDU I., voir CALU N. 71
— , voir CALU N. 217
— , voir CALU N. 451
SĂNDULESCU D., voir VASILESCU ELIZA-MANUELA 605
SĂNDULESCU I. and V. PÂRVULESCU V., E. SZABO, A. POPA, I. V. NICOLESCU, Styrene hydrogenation on supported Pd and Pd-Co/$\gamma-Al_2O_3$ catalysts 375
SARAMET I., voir NEGOIU D. 987
SATAKE M., voir PURI B. K. 85
— , voir SHARMA S. 581
SAVA D., voir VÎLCU R. 657
— , voir VÎLCU R. 741
SAVIUC E. and A. CĂLUŞARU, Rate constants and activation energies of Cr(II) to Cr(III) oxidation reaction by hydroxylamine in normal and heavy water 753
SCHWARTZ R. and A. JUHÁSZ, The synthesis of some 3-oxo-4-ene-B-nor-derivatives. Oppenauer oxidation of 3β-hydroxy-5-ene-B-nor-steroids with Al_2O_3 131
SCHWARTZ R. and ANIKO JUHÁSZ, PETRONELA COLŢEA, Comparative study of the IR spectra of some B-nor and natural steroids 481
SCHIKETANZ I., voir BALABAN A. T. 37
SEKHAR V. c. and K. N. THIMMAIAH 719
SEGAL E., voir DOCA N. 567
— , voir PATRON L. 811
SHABAN M. E., voir EL KHAMRY A. M. 387
SHAKER S. A., voir SHAMS N. A. 541
SHAMS N. A. and A. A. HAMED , S. G. DONIA, S. A. SHAKER, Synthesis of 4-aroyl-4,5-dihydro-2-(3H)-furanones and their reactions with some nucleophiles 541
SHARMA H. K. and A. K. YADAV, S. P. S. JADON, Characterization of the complexes of Ti (III) and Zr(IV) with tetrathiazylhydrofluoride by UV, EPR and XRD spectra 305
SHARMA SAROJ and S. K. HAWA, S. P. MATHUR, M. SATAKE, Spectrophotometric determination of palladium(II) with N-naphthyl-N'-pyridylthiourea 581
SIDAHMED I. M. and SADEK H., S. M. SALEM, Types of solvents interactions in water-glycerol mixtures 327
SILAGHI-DUMITRESCU L., voir F. DOGAR 79
— and L. A. AVILA-DIAZ, IONEL HAIDUC, Dimethyl- and diphenyldithioarsinates of some main group metals 335
— and IONEL HAIDUC, The bonding in dialkyldithiophosphinate metal complexes. A molecular orbital study of bis(dimethyldithiophosphinate)nickel(II) 955
SIMIONESCU CR. I. and S. IOAN, B. C. SIMIOMESCU, Solution properties of ultrahigh molecular weight polymers (pleistomers). 14. Solvent effect on the unperturbed dimensions of poly(butyl methacrylate) chains 995
SIMIONESCU BOGDAN, voir SIMIONESCU Cr. 995
SINGH L. P., voir NATH N. 489
SOMAY M., voir MARCU GH. 227
STĂNESCU L., voir IORDACHE F. 261
— , voir POPESCU A. 1025
STĂNESCU LIGIA, voir BANCIU M. 503
STĂNESCU MICHAELA and F. BADEA, GH. MIHAI, The acetolysis of ditosylates with a bicyclo[4.4.0]decane skeleton 507
STĂNESCU M., and M. ELIAN, ECATERINA CIORĂNESCU, Carboniumion reactions. XVII. Rearrangements of dibenzobicyclo[3.2.1]octane and dibenzobicyclo[3.2.2.]nonane derivatives 1001
ŞTEFAN M. and C. STOICESCU, Kinetics of the methoxylation of o-chloronitrobenzene 269
STERNBERG S. and M. UNGUREANU, I. LINGVAY, Study of polarization of the semiconductor silicon-electrodes in ammonium fluoride solutions 3
— and T. VIŞAN, V. PETRESCU, A. COTÂRŢĂ, Electrochemical reactions of cupric and cupreous ions in lithium chloride — potassium chloride eutectic. III. Cyclic voltammetry 431
STOENESCU L., voir BADEA F. 119

STOICESCU C., voir ŞTEFAN M. 269

STOLL K., voir FRITZ G. 949

SURPAŢEANU GH. and P. GRANDCLAUDON, A. LABLACHE COMBIER, Theoretical study of the reactivity of benzo[b]-thiophenes with heterocyclic amines and their anions (in French) 371

SZABO E., voir SĂNDULESCU I. 375

T

TALABA ANA, voir HAGIU C. 909

TALABA MIHAI, voir HAGIU C. 909

TALABĂ MIHAI, Computer use of nitrophosphate fertilizers. Computer-aided analysis of the nitric decomposition of phosphatic raw materials 547

TANEJA A. D., voir D. P. KHURANA 761

— , voir KUMARI R. 869

TERDIC M. H., Disubstituted phenothiazones. IV. Chloro-4-nitro- and -7-nitro-phenothiazin-3-ones 137

THAKER B. T. and PURNIMA B. THAKER, Synthesis and characterization of mixed ligand Schiff base complexes formed by template method 52

THAKER B. PURNIMA, voir THAKER B. T. 529

THIMMAIAH K. N. and V. C. SEKHAR, Hydrazine carbothioamide-2-[(4-hydroxy-3-methoxyphenyl)methylene] as a sensitive reagent for rapid spectrophotometric determination of palladium(II) and copper(II): analysis of alloys and minerals 719

TOLEA F., voir MARCU GH. 227

TOMESCU M., voir MANDRAVEL C. 819

TOMOAIA COTISEL M., voir CHIFU E. 105

TYAGI J. S., voir KHURANA D. P. 761

U

UNGUREANU M., voir STERNBERG S. 3

V

VÁRHELYI CS., voir MARCU GH. 227

VÁRHELYI CS. and I. GĂNESCU, A. HANTZ, I. PAPA, A new Reinecke salt analogues with dibutylphenylphosphine and diphenylethylphosphine (in German) 291

— voir, ZSAKO J. 443

VARMA R. P. and A. K. VIRMANI, Studies on physical properties of cadmium soaps. III. Dehydration and thermal decomposition studies of soaps be thermogravimetry 63

VASILE A., voir POPOVICI EV. 419

VASILIU OPREA CL. and F. WEINER, Modification of structure and properties of PVC-S by the processing on rollers in the presence of some new filling materials 17

VASS M., voir LĂZĂRESCU V. 461

— , voir GARTNER M. 589

VASILESCU ELIZA-MANUELA and D. SĂNDULESCU, Molecular compounds with some alkyl aryl ethers. I. Charge transfer complexes 605

VĂŢULESCU R. and T. BUDIU, GH. MARCU, I. PAL, Heteropolytungstates with Ti(IV) and Ni(II). VI. The behaviour of the Ni(II)-undecatungstotitanate(IV) and Ni(II)-pentatungstotitanate(IV) anions towards cationites in acidic and neutral media 199

VĂŢULESCU R. and T. BUDIU, GH. MARCU, I. PAL, Heteropolytungstates with Ti(IV) and Ni(II). VII. The stability of Ni(II)-undecatungstotitanates(IV) and Ni(II)pentatungstotitanate(IV) anions in aqueous solution 209

— and T. BUDIU, GH. MARCU and GH. MORARU, Heteropolytungstates with Ti(IV) and Ni(II). VIII. Crystal data for the potassium and ammonium salts of the Ni(II)-undecatungstotitanate(IV) anion 345

VIDAL B. and C. DUPRET, Enlargement of transitions and relative order of band heights. Application to incidence of remote interactions and solvation on the UV spectra of some phenylalkylamines 773

VÎLCU R. and V. BĂRBÎNŢĂ, I. GĂINAR, D. SAVA, Estimation of chemical nonhomogeneity of polymers using the interrelation structure-entropy-information. I. The use of the tracer method 657

— and V. BĂRBÎNŢĂ, I. GĂINAR, D. SAVA, Estimation of chemical nonhomogeneity of polymers using the interrelation structure-entropy-information II. Computing program and results 741
— and V. BĂRBÎNŢĂ, I. GĂINAR, Determination of chemical non-homogeneity of polymers according to the chain length at fractionation. The use of double standardization by tracing method 839
VIRMANI A. K., voir VARMA R. P. 63
VIŞAN T., voir STERNBERG S. 431
VLĂDEA R. Catalytic influences in electrooxidation of olefins in nonaqueous solutions. IV. Reaction mechanism for olefin oxidation in methanol 169
VOLANSCHI E., voir HILLEBRAND M. 43

W

WAGNER L., voir GORDUZA V. 661
WEINER F., voir VASILIU OPREA CL. 17

X

XICLUNA A. and J. E. ROBERT, ^{1}H-NMR Spectral study of ethyl 3,5—diphenyl-3,5-dihydrothiophene-2-carboxylate (in French) 143

Y

YADAV A. K., voir SHARMA H. K. 305
YOUSEF KAYED, voir OPREA SPIRIDON 425
YUSTE F., voir R. SÁNCHEZ OBREGON 709

Z

ZSAKÓ J. and J. DEMETER-VODNÁR, I. BÂLDEA, CS. VÁRHELYI, Kinetics and mechanism of substitution reactions of complexes. LVIII. Hg(II) assisted aquation of *cis*-$[(Co(en)_2Br(\gamma\text{-picoline})]^{2+}$ 443

Revue Romaine de Chimie, 31, *11 – 12*, 1065 – 1069 (1986)

INDEX DES SUJETS

Absorption spectra of nitroso aromatic derivatives. Substituent and solvent effect in the—. GH. IVAN and M. GIURGINCA 857
Acetolysis of ditosylates with a bicyclo[4.4.0]decane skeleton, M. STĂNESCU, F. BADEA and GH. MIHAI 507
Adducts cobalt(III) dioximine chelate with tertiary phosphines. Study on some — GH. MARCU, A. HANTZ, M. SOMAY, CS. VARHELYI and F. TOLEA 227
4-Alkylpyridines usability for extraction of Co(II), Cu(II), Zn(II), Ni(II) and Cd(II) complexes from nitrate solution. Studies on — E. BEZAK 411
Amides from N-acylphthalimides and aliphatic amines, C. I. CHIRIAC 525
Amine adducts of Ni(II) diphenyldithiophosphinate with substituted ethylenediamines, FL. DOGAR, L. SILAGHI DUMITRESCU, R. GRECU and I. HAIDUC . . . 79
Ammonium polyphosphates. Obtention of ammonium polyphosphates by warm ammoniation of ortophosphoric acid. C. HAGIU, M. TALABA, V. DULMAN and ANA TALABA 909
Anion-radicals provided by some nitro- and amino-ethers. Spectral study of the—, M. HILLEBRAND, M. IOVU, N. NICOLAU and EL. VOLANSCHI 43
Anodic oxidation of the binuclear cyanide complex of Mn(III). Part III. The electrolytical preparation of the Mn(III) — Mn(IV) binuclear cyanide complex, G. LÓPEZ CUETO and A. ALONSO MATEOS 9
Anodic oxidation of the 1,4-dimethoxybenzene. Mechanistic and synthetic aspect of the — OLGA PÉREZ DE MÁRQUEZ 637
Anodic oxidation of alkylbenzenes in dry acetonitrole. OLGA PÉREZ DE MÁRQUEZ 711
Aromatic hydrocarbons in different petroleum fractions. Identification of —. IV. IR spectral analysis. HOCINE KADI and D. P. LAZAR. 149
Aromatic thioureas. Synthesis of—C. I. CHIRIAC 625
4-Aroyl-4,5-dihydro-2(3H)-furanones and their reactions with some nucleophiles. Synthesis of-, N. A. SHAMS, A.A. HAMED, S. G. DONIA and S. A. SHAKER 541
6-Aryl-4,5-dihydropyridazin-3-(2H)-ones. Synthesis and reactions of — ABDEL MOMEN A. EL-KHAMRY, MOHAMED E. SHABAN and M. M. HABASHY . . 387
Benzopyranopyridine and pyrimidine ring systems. Synthesis of certain — , M.M. ISMAIL and M. S. MOHAMED 533
Benzospiro[2,4]heptane derivatives. Synthesis of — E. BARTHA, Z. ARVAY and A. C. RĂZUŞ 519
Benzo(b)-thiophenes with heterocyclic amines and their anions. GH. SURPĂŢEANU, P. GRANDCLAUDON and A. LABLACHE COMBIER 371
Beta ray back-scattering in the study of corrosion process of some carbon steel samples in acid solutions. Use of —. AL. CEAL, D. CIOBANU and I. SANDU . . . 451
Bicyclo[2.2.2]octane derivatives. III. Stereoisomeric 2,3,5,6-tetracarbomethoxy-bicyclo[2.2.2]octanes, F. IORDACHE, F. CHIRALEU, L. STĂNESCU, F. BADEA and MARGARETA AVRAM 261
Book reviews 113—116, 255—257, 361 — 362, 457 — 458, 737, 833 — 836, 915 — 917
Cadmium and lead after adsorption of their n-butylxanthates onto microcrystalline naphthalene and replacement by copper. Spectrophotometric determination of —, B. K. PURI, ATUL KUMAR and M. SATAKE 85
Cadmium soaps. III. Dehydratation and thermal decomposition studies of soaps by thermogravimetry. Studies on physical properties of— , R. P. VARMA and A. K. VIRMANI 63
Carbanions and free radicals derived from 1,2-diphenylpyrazolidine-3,5-diones. II. Trapping of the free radicals derived from diethyl fluoro-malonate, n-butyl-, and phenyl-malonate. F. BADEA, A. T. BALABAN, A. DIMITRIU, F. IORDACHE, A. MEGHEA and L. STOENESCU 119
Carbonium ion reactions XVII. Rearrangements of dibenzobicyclo[3.2.1]-octane and dibenzobicyclo[3.2.2]nonane derivations. M. STĂNESCU, M. ELIAN and E. CIORĂNESCU 1001

Catalysts system $ZnO.nFe_2O_3$. Structure and properties of the oxydehydrogenation reaction (I). I. V. NICOLESCU, R. MANAILA, M. A. CHAAR and G. FILOTI 99
Catalytic oxidation of methanol. Thermal effect and oscillation in the — , N. I. IONESCU, M. S. CHIRCA and D. I. MARCHIDAN 671
Chemical graphs. Part. 44. Isomer enumeration for substituted saturated polyhedral valence isomers of annulenes, A. T. BALABAN 679
— — Part. 45. Edge-labelled graphs as unsaturated valence isomers of annulenes; applications of Pólya's theorem. A. T. BALABAN 695
— — Part 46. Enumeration of valence isomers of adamantane using Pólya's theorem. A. T. BALABAN 795
Chemical nonhomogeneity of polymers using the interrelation structure-entropy-information. I. The use of the tracer method. R. VÎLCU, V. BĂRBÎNȚĂ, I. GĂINAR and D. SAVA 657
— — — — — II. Computing program and results, R. VÎLCU, V. BĂRBÎNȚĂ, I. GĂINAR and D. SAVA 741
— — — — Chemical non-homogeneity of polymers according to the chain length at fractionation. The use of double standardization by tracing method. Determination of — , R. VÎLCU, V. BĂRBÎNȚĂ and I. GĂINAR 839
Cobalt(II) and copper(II) complexes with 3-substituted-4-(5′-substituted-salicylidene/2′-hydroxyacetophenoneimine)-1, 2,4-triazoles. Magnetic and spectral properties of — . B. M. BADIGER, S. A. PATIL, S. M. KUDARI and V. H. KULKARNI 849
Cobalt and manganese in blood serum by flow injection analysis and atomic absorption spectroscopy. N. LÉON. J. L. BURGUERA, M. BURGUERA and O. M. ALARCÓN 353
Cobalt atom in vitamin B_{12} and in model complexes from the cobaloxime group MARIE-HÉLÈNE DARBIEU 1031
Cobalt(II) dioxygen complexes. Contributions to the study of — , GH. MARCU, AL. BOTAR and A. NAUMESCU 981
Complex compounds of Hg(II) with thiobenzpiperidides and thiobenzomorpholides. D. NEGOIU, S. NEAGOE, C. CERCASOV, M. NEGOIU, I. SARAMET and C. TOMA 987
Complexes of Ti(III) and Zr(IV) with tetrathiazyl hydrofluoride by UV, EPR and XRD spectra. Characterization of the — , H. K. SHARMA. A. K. YADAV and S.P.S. JADON 305
Complex Mn(III) and Mn(IV). Part. II. System Mn(III, IV)-2-aminophenol-4-sulfone acid. N. CALU, E. BĂLĂNESCU, I. BERDAN and I. SANDU 71
Complex Pd(II)—Sn(II). Preparation and properties of — , L. PATRON, A. CONȚESCU, GH. ROLEA and C. GHEORGHIU 341
Computer use of nitrophosphate fertilizers. M. TALABA 547
Coordination compounds as raw materials for mixed oxides. III. Trinuclear, oxo-centered, carboxylate compounds containing Fe(II, III, III). L. PATRON, A. CONTESCU, G. MUNTEANU, M. BREZEANU and E. SEGAL 811
Copolymers modified with radioprotective action, M. BRUMA, GH. DUMITRESCU, and E. DUMITRESCU 163
Copper catalysts II. Preparation, stabilisation and catalytic activity of Cr-O-Cu and Mn-O-Cu systems. Dehydrogenation kinetics of low aliphatic alcohols on — . N. DOCA and E. SEGAL 567
Corrosion kinetics of Armeo iron in aqueous solution of citric acid, V. BRÂNZOI, AHMED KABIR and MIHAI CIOPEC 473
Corrosion of steel C-95 in aqueous hydrochloric acid in the presence and absence of organic inhibitors. V. BRÂNZOI, A. KABIR and M. CIOPEC 571
Coulometric study at controlled potential of the anodic oxidation of the binuclearcyanide complex of Mn(III). Part II. Oxidation at A+ 0.80 volts vs. SCE. Faraday curents G. LÓPEZ CUETO and A. A. MATEOS 237
Cyclic voltammetry studies on oxygen/silver system. V. LĂZĂRESCU, O. RADOVICI and M. VASS 461
Cyclization of ethyl cyanoacetate and 3,5-dichlorosalicylaldehyde with ketones by means of ammonium acetate. M. M. ISMAIL and M. S. MOHAMED 393
Dehydration products of aryl and arylalkyl cyclododecanols. Investigation of — . K. GÜNAYDIN and Ü. OYMAN 497
Dialkyldithiophosphinate metal complexes. A molecular orbital study of bis(dimethylthiophosphinate nickel (II). The bonding in — I. SILAGHI DUMITRESCU and I. HAIDUC 955

α-Diazoketones from nicotinyl and furoyl chlorides and higher diazoalkanes. Study of —. R. AGARWAL and P. BAHADUR 297

Diels-Alder reaction of *trans*, *trans*-1,4-diacetoxy-1,3-butadiene and 1,2-pentadien-4-one. R. SANCHEZ-OBREGÓN, H. BARRIOS, B. ORTIZ and F. YUSTE 709

Digol by vanadium(V) in aqueous sulphuric acid hydrochloric acid medium. Kinetics of oxidation of — , N. NATH, R. C. DUBEY and U. S. MISRA 57

4b, 10b-dihydrochrysene, a new dibenzo$(CH)_{10}$ hydrocarbon. M. BANCIU, DANA ELIAN, M. ELIAN, LIGIA STĂNESCU and E. CIORĂNESCU 503

Dimethyl- and diphenyldithioarsinates of some main group metals. L. SILAGHI DUMITRESCU, L. A. AVILA-DIAZ and I. HAIDUC 335

3,5-Diphenyl-3,4-dihydrothiophene-2-carboxylate. Study of ^{1}H-NMR of the — . A. XICLUNA and J. E. ROBERT 143

Dissipative structures in reactions-diffusion systems as synchronization phenomena. D. CARTIANU 175

Early and contempory links between Romania and Belgium, ROBERT BRUYLANTS 923

Electrochemical reactions of cupric and cupreous ions in lithium chloride-potassium chloride eutectic. III. Cyclic voltammetry. S. STERNBERG, T. VISAN, V. PETRESCU and A. COTARTA 431

Electronic spectra of some heteroaromatic cation-radicals. M. HILLEBRAND and V. EM. SAHINI 649

Electrooxidation of olefins in non-aqueous solution. Catalytic influence in — IV. Reaction mechanism for olefin oxidation in methanol. R. VLĂDEA 169

Ellipsometric spectroscopy of pure and CO covered gold films, M. GARTNER and M. VASS 589

Enethiol content of substituted pyridyl-thioureas in different solvent. Spectroscopic determination of—. D. P. KHURANA, A. D. TANEJA and J. S. TYAGI. . . . 761

2,4,6-Haloalkyl-1,3,5-triazines. High performance liquid chromatography of. — . R. BACALOGLU, L. COTARCA, ANABELA IȘFAN and C. IȘFAN 403

Heteropolytungstates with Ti(IV) and Ni(II). Part VI. The behaviour of the Ni(II)-undecatungstotitanate(IV) and Ni(II)-pentatungstotitanate (IV)anions towards cationites, in acidic and neutral mdia, R. VĂȚULESCU, T. BUDIU, GH. MARCU and I. PAL 199

— — — Part. VII. The stability of Ni(II)-undecatungstotitanate (IV) and Ni(II)-pentatungstotitanate(IV) anions in aqueous solution 209

— — — Part VIII. Crystal data for the potassium and ammonium salts of the Ni(II) undecatungstotitanate(IV)anion. R. VATULESCU, T. BUDIU, GH. MARCU and GH. MORARU 345

Hydrothermal crystallization of zeolite Ni-X. E. PINCOVSCHI and M. MERCHEȘ 973

Imines of aminoazoles. II. Synthesis and characterization of some imines of 2-aminobenzothiazoles benzoxazole thiazole and 3-amino-1,2,4-triazole. H. H. GLATT, M. F. BARRY, C. CSUNDERLIK, R. BACALOGLU, M. BOTOACĂ, S. SAVU-BOTOACĂ and D. FECHETE 273

— — — III. The basicity constants of heterocyclic imines from the benzylidine-amino-benzothiazoles, -benzoxazole, benzimidazoles, -thiazole and -triazole series. R. BACALOGLU, H. H. GLATT, M. F. BARRY and C. CSUNDERLIK 283

IR Spectra of some B-NOR and natural steroids. Comparative study of the — , R. SCHWARTZ, A. JUHÁSZ and P. COLTEA 481

1α,2α- and 1β,2β-Isomers of 5,9-methano-5*H*-benzo-[3,4]cyclobuta[1,2]cycloheptenes. A. POPESCU, L. PÎRVULESCU, L. STĂNESCU and M. D. GHEORGHIU . . . 1025

Isoquinoline-1-carbonitrile derivatives. Synthesis and reactions of some new. — A. M. KHALIL, O. M. O. HABIB, I. I. ABD EL-GAWAD and H. A. ETMAN . . . 901

Lanthanide perchlorate complexes of 2-ethoxycarbonylamino-pyridine-N-oxide. Magnetic and spectral studies of — , R. K. AGARWAL and S. K. GUPTA 585

Manganese dioxide used in the structure of electrochemical and electronic systems. Synthesis and activation of the — , N. CALU, I. SANDU and I. BERDAN 217

Marangoni flow — induced by temperature gradients — against gravity forces. E. CHIFU, L. ALBU, C. I. GHEORGHIU, E. GAVRILĂ, M. SALAJAN and M. TOMOAIA-COTISEL. 105

Mercury and cadmium via formation of ion pairs $[C_4H_9)_4N]_2[HgI_4]$ and $[(C_4H_9)N]_2$ $[CdI_2]$. Gravimetric determination of — J. HERNANDEZ MÉNDEZ, A. ALONSO MATEOS and E. J. MARTIN MATEOS 597

Methoxylation of o-chloronitrobenzene. Kinetics of the — . M. STEFAN and C. STOICESCU 269

Mixed ligand Schiff base complexes formed by template method. B. T. THAKER and PURNIMA B. THAKER 529

Molecular complexes with aromatic cations as electron acceptors VII. Spectrometric, conductometric and dipolar data of phenyl-substituted pyrylium salts with tetracyano-*para*-quinodimethane anions — M. BUGEANU, V. EM. SAHINI, V. T. CIORBA and A. T. BALABAN 1019

Molecular compounds with some alkyl aryl ethers. I. Charge transfer complexes. ELIZA-MANUELA VASILESCU and D. SANDULESCU 605

Neodymium exchanged zeolites in the alkylation reaction of toluene with methanol. Activity and selectivity of —, S. OPREA, E. DUMITRIU, V. HULEA and K. YOUSEF 425

Nickel and palladium. Extraction spectrophotometric determination of —. using cyclohexylthioglycolate as a reagent. A.L.J. RAO and USHA GUPTA 93

Nickel(II) complexes. The position of 4,4′-bipyridyl in the spectrochemical series for —. M. ANDRUH, C. I. LEPĂDATU, M. BREZEANU 943

Nicotinic acid derivatives. Synthesis and biological activity of certain — . A. N. OSMAN, M.M.ISMAIL and M. A. BARAKAT 615

Nuclides ordering and observed regularities. Criteria for — . E. PETROVICI, E. NARTEA and GH. MARA 1041

1,3,4-Oxadiazoles from diaroylhydrazines under mild conditions using phosphorus trichloride-dimethylformamide adduct as reagent. A convenient method for the synthesis of — . C. I. CHIRIAC 51

Oxidation of 1,3-cyclopentandione bis(4-methylthiosemicarbazone). Kinetic determination of Co(II) based on its catalytic effect on atmospheric—. M. ROMAN CEBA, J. C. JIMÉNEZ SANCHEZ and T. GALEANO DIAZ 889

Oxidation of benzyl alcohol and benzylamine by alkaline hexacyanoferrate(III) ion. Kinetics and mechanism of osmium(VIII) catalysed, N. NATH and L. P. SINGH 489

Oxidation reaction Cr(II) to Cr(III) by hydroxylamine in normal and heavy water. Rate constants and activation energies of —. E. SAVIUC and A. CĂLUȘARU 753

3-Oxo-4-ene-B-nor-derivatives. Oppenauer oxidation of 3β-hydroxy-5-ene-B-bor-steroids with Al_2O_3. R. SCHWARTZ and A. JUHASZ 131

Pd(II), Cd(II) and Hg(II) complex compounds with carbazole derivatives. Synthesis and characterization of the — C. MANDRAVEL, M. GUȚUL and M. TOMESCU 819

Phenothiazones disubstituted. IV. Chloro-4-nitro-and-7-nitro-3H-phenothiazin-3-ones. M. H. TERDIC 137

Phosphorous acid-iodine as reagent for the synthesis of 1,3,4-oxadiazoles from diacylhydrazines. C. I. CHIRIAC 159

Photochemical ring contraction of 8-diazo-dibenzo[*c*,*e*]-tricyclo[5.3.0.0.2.10]-deca-3,5-dien-9-one. M. BANCIU, M. ELIAN, A. BANCIU, C. DRĂGHICI and E. CIORANESCU 1019

Photolytic reactions of *cis*-cyclodecene and *cis*-bicyclo[3.3.0]oct-2-ene with dimethyldiazomalonate. Some observations on the catalytic and direct. — OLCAY ANAÇ 787

Polarity of salt solutions: a general empirical equation. MARCOS CAROLI REZENDE and LILIAM INES DAL SASSO 323

Polarization of the semiconductor silicon electrodes in ammonium fluoride solutions. S. STERNBERG, M. UNGUREANU and. I. LINGVAY 3

Polybenzimidazole-amide-imides. High temperature polymers. VI. GH. MANDRIC, G. NEAMTU, S. PECINCU and. G. RACARU 25

PVC-S by processing on rollers in the presence of some new filling materials. Modification of structure and properties of — . Cl. VASILIU OPREA and FELICIA WEINER 17

Pyrylium salts with nucleophiles. XVIII. Synthesis of 4 (*p*-*n*-butoxyphenyl)-2,6-dimethylpyridine and of 2,5-dimethyl-4 (*p*-*n*-pentylphenyl)-pyridine. Reaction of —. A. T. BALABAN, G. MARTON and I. SCHIKETANZ 37

Quinazoline series. V. Inactivation of quinazolium-ylids: a new approach towards novel pyrrola[1,2-quinazoline derivatives. E. I. GEORGESCU, FL. GEORGESCU, M. D. GHEORGHIU, P. FILIP and M. PETROVANU 365

Reactivity of benzimidazolone derivatives, based on the electronic spectra and molecular diagrams. V. GORDUZA, I. COCARLA, C. CHIRVU, L. WAGNER and V. PESCARU 661

Reagent for rapid spectrophotometric determination of palladium(II) and copper(II): analysis of alloys and minerals. K. N. THIMMAIAH and V. C. SEKHAR 719

Relation between moments of inertia, steric crowding and librational motion in molecules. Effects on NMR spectra. ADRIAN O. FULEA 309

Roentgenographic and IR-spectroscopic investigations of the thermolysis of alkali pentafluoroaluminate hydrates. U. BENTRUP and L. KOLDITZ 963

Solvent interactions in water-glycerol mixtures. Types of — , I. M. SIDAHMED, H. SADEK and S. M. SALEM 327

Spectral analytical measuring processes regarded as information processes, V. DAVID and D. CIOMÂRTAN 823

Spectra of some substituted acetoacetarylamides. Effects of solvents on the — . R. KUMARI, A. D. TANEJA, V. P. KURDESIA 869

Spectrophotometric determination of palladium(II) with N-naphthyl-N'-pyridylthiourea. S. SHARMA. S. K. HAWA, S. P. MATHUR and M. SATAKE 581

Styrene hydrogenation on supported Pb and Pd-Co/γ-Al_2O_3-catalysts. I. SANDULESCU, V. PARVULESCU, EL. SZABO, ALEX. POPA and I. V. NICOLESCU . . . 375

Styrene-methylmethacrylate copolymers. Thermal behaviour of some — . C. BELDIE, N. HURDUC, A. ONU and I. C. POINESCU 31

Solution reactions of complexes. Kinetics and mechanism of. — .LVIII. Hg(II) assisted aquation of *cis*-$[(Co(en)_2Br(\gamma\text{-picoline})]^{2+}$ J. ZSAKO, J. DEMETER-VODNAR, I. BALDEA and CS. VARHELYI 443

Substitution reactions of $K_3(Cr(NCS)$ with dibuthylphenylphosphines and diphenylethylphosphines. CS. VARHELYI., I. GANESCU, A. HANTZ and I. PAPA 291

Synthesis and reactions of some new 4-(*p*-substituted cinnamoyl)phenyl-3',4'-xylene sulphonates of expected potential biological activity. O. M. O. HABIB, A. M. KHALIL, E. M. KANDEEL and E. B. ABDALLA 629

Synthetic zeolites for detergent conditioning. II. On zeolite-surfactant-bleaching agent systems. Ev. POPOVICI, M. CRUCEANU, M. GRECU, A. VASILE and M. ALEXANDROAIEI 419

Tetracoordinated boron: advances in trimethyl-aminoborane-chemistry. Reactions on —. K. CIBURA and A. HAAS 927

Tetrafluoro-1,2-ethanediosulfenyldichloride with alkynes of ketones. H. W. ROESKY and N. BENMOHAMED 935

2-(2-Thienyl)benzothiazole and 2(2-pyridylbenzothiazoline with different metallic salts. F. CAPITAN, P. ESPINOSA, F. MOLINA and L. F. CAPITAN-VALLVEY 897

as-Triazine derivatives with potential therapeutic action. XXI. Synthesis of 4-thioxo-5(fluoro-benzyl)thio-6-azauracil derivatives and their nucleosides. C. CRISTESCU 881

Ultrahigh molecular weight polymers (pleistomers). 14. Solvent effect on the unperturbed dimensions of poly(butyl methacrylate)chains. Solution properties of. —. Cr. I. SIMIONESCU, S. IOAN and B. SIMIONESCU 995

50 draieuri
nifedipin
„TERAPIA"
Intreprinderea de
medicamente
Cluj-Napoca

SYNONYMS : ADALAT — BAYER

Drajées containing 0.010 g nifedipin (dimethyl ester of 1,4-dihydro-2,6-dimethyl)-4-(0-nitrophenyl)-(pyridine-3,5 dicarbonic acid).

PHARMACOTHERAPEUTICAL ACTION :

Antianginose through the inhibition of the transmembraneous penetration of calcium ions into the coronary and myocardial fibres. By this mechanism the preparation reduces the activity of the calcium ion-dependent contractile system, lowers oxygen consumption in the myocardium, produces relaxation of the coronary vessel walls thus increasing their lumen and blood flow as well as the oxygen supply, improving the energy balance and tolerence of the myocardium to hypoxia.

INDICATIONS :

Chronic ischemic cardiopathy, long-term prophylaxis of anginose attacks.

COUNTERINDICATIONS :

Acute myocardial infarction, pregnancy.

ADVERSE REACTIONS :

occasionally cephalea, vertigo, sensation of intracranial pressure, congested face, sickness, oedema.

PRESENTATION :

Flasks containing 50 drajées each.

50 coated pills
nifedipin
MADE IN ROMANIA
Sole exporter:
CHIMIMPORTEXPORT
Bucharest
50 draieuri
nifedipin
„TERAPIA"
Intreprinderea de
medicamente
Cluj-Napoca

PRODUCED BY :

I. M. Terapia, Cluj-Napoca, Romania

SOLE EXPORTER :

I. C. E. "CHIMICA", Splaiul Independenței, 202 A, Bucharest, Romania, Telex 11489/10073 danaz r, Telephone: 49.50.10; 49.26.20

engineering

iprochim

ROMANIA

Si vous êtes intéressés à choisir une solution économique d'investissements dans l'industrie chimique, vous pouvez vous adresser en toute confiance à

IPROCHIM – ROMANIA

IPROCHIM – c'est une compagnie d'engineering, ayant un profil complexe, spécialisée en industrie chimique inorganique, industrie organique de base, industrie des engrais et industrie pétrochimique.

Pour toutes les usines chimiques et pétrochimiques existantes en Roumanie, IPROCHIM a élaboré indépendamment ou en collaboration avec des entreprises bien réputées, des études et toute la documentation de détail, donnant en même temps son avis pour la construction, le montage et la mise en fonction de toutes les installations de son profil.

Le potentiel technique dont IPROCHIM dispose, l'expérience accumulée pendant plus de 38 ans, l'étroite coopération avec les instituts de recherche, les centres universitaires et avec d'autres compagnies d'engineering du pays ainsi que la vaste coopération avec les autres compagnies étrangères, constituent la garantie de la qualité des services qu'IPROCHIM peut assurer, en assumant ses responsabilités pour :

- études de faisabilité, d'emplacement, de profil, d'optimisation et études technico-économiques ;
- cahiers de charges pour la réalisation des objectifs chimiques ;
- expertises techniques pour les installations en fonction visant leur modernisation ;
- documentation de licence et savoir-faire ;
- engineering de base (basic design) et projets d'exécution ;
- complexes pour les installations chimiques et pétrochimiques « à clef à main » ;
- organisation de la direction, du fonctionnement et de l'entretien des installations chimiques ;
- organisation des laboratoires de contrôle des procédés technologiques ;
- assistance technique à la construction, au montage et à la mise en marche des installations ;
- instruction du personnel d'opération et de contrôle dans les installations industrielles ;
- réalisation des maquettes de plan général et de montage des équipements, tuyauterie et contrôle ;
- calcul des installations et des équipements par des programmes propres.

Signe de notre capacité technique, sauf les plates-formes industrielles chimiques du pays, c'est l'élaboration des projets pour toute une série d'objectifs industriels importants réalisés à l'étranger, dont on mentionne les derniers :

- Installations de soude calcinée en Egypte et en Iran ;
- Installations d'engrais en Turquie, Syrie, Chine ;
- Installations d'acide sulfurique en Turquie, Egypte, Syrie ;
- Installations de Vitamine C en Corée Démocratique et au Mexique ;
- Installation d'aldéhyde phormique en URSS ;
- Installation de fibres de nitrile polyacrylique en Corée Démocratique ;
- Installation de bichromate de sodium en Turquie ;
- Installation d'aniline en URSS.

Les services sont offerts à l'exportation par l'intermédiaire des entreprises de commerce extérieur : ROMCONSULT, INDUSTRIALEXPORTIMPORT, UZINEXPORT et GEOMIN.

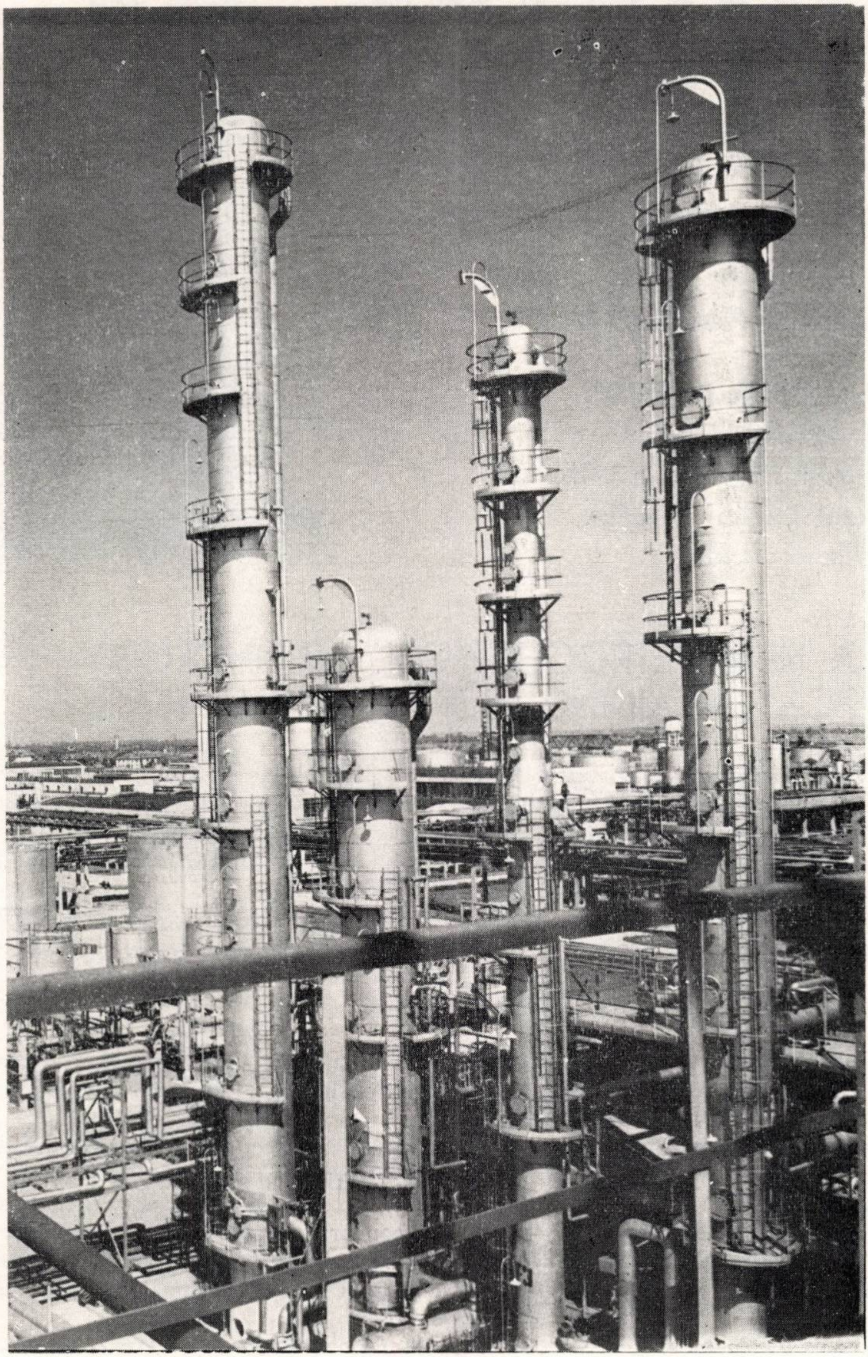

IPROCHIM
COMPAGNIE D'ENGINEERING POUR L'INDUSTRIE CHIMIQUE

**Roumanie – Bucarest – 19–21 Rue Mihai Eminescu – Téléphone 49.64.48 ;
49.47.57, Telex 11907 Cab. TX. 735 IITPIC**

INSTITUTUL
CENTRAL
DE CHIMIE

i.c.i.t.p.r

INSTITUTUL DE CERCETĂRI,
INGINERIE TEHNOLOGICĂ
ŞI PROIECTARE PENTRU RAFINĂRII
Ploieşti, B-dul Republicii 291A,
Cod 2000 Telex: 93.40

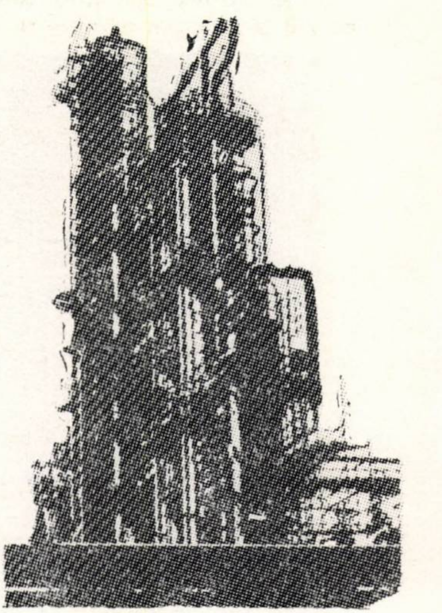

A NEW PETROCHEMICAL TECHNOLOGY FOR OBTAINING HIGH PURITY BUTENES

ICITPR Ploieşti (Institute of Research, Technological Engineering and Design for Refineries) has patented a technology for chemical conversion of isobutene contained in C_4 hydrocarbon mixtures by its reaction with methanol on macroporous cationites. The new technology assures a high degree of isobutene conversion to methyl tert-butyl ether (MTBE), a high-octane component that can substitute tetraethyllead in motor-gasoline.

The linear butenes with a maximum content of 0.2% isobutene, produced by MTBE technology, constitute the ideal feedstock for producing 1,3-butadiene by oxidative dehydrogenation.

A brief description of the technology

MTBE and the mixture of linear butenes are obtained under very advantageous conditions from the C_4 cut obtained in the pyrolysis process. The flow-sheet shows the reaction, fractionation and recovery stages of the process.

The moderately exothermal reaction is achieved by contacting the homogeneous liquid phase that contains the reagents, with the static bed of macroporous cationite in the R_1 reactor. The specific shape of the etherification reactor ensures a high efficiency; in the case of a feedstock concentrated in isobutenes (35—50%), the conversion attains values of 94—95%. The formation of MTBE at moderate temperatures and pressures is characterized by a very high selectivity (above 98%), the other olefins present in the system having a role of inert medium.

The efluent from reactor R_1 is separated by fractionation in the column C_1 and MTBE of 98—99% purity results. The fraction of separated hydrocarbons at the top of the column, with a content of 3—5% isobutene and 2—3% methanol, is directed towards the second stage of the reaction in the reactor R_2 with cationite where, under specific temperature conditions and excess of methanol, the isobutene conversion attains the final values of 99.5—99.8%.

The effluent from the reactor R_2 is subjected to fractionation in column C_2. MTBE and the excess of methanol at the bottom of the column is fed to reactor R_1 and the volatile product is extracted with water in column C_3 for removing the methanol, the methanol being subsequently recovered from the water in column C_4.

Under normal operating conditions of the catalytic bed and in the absence of metal cations and of nitrogen bases in the feed, the catalyst life can surpass three years.

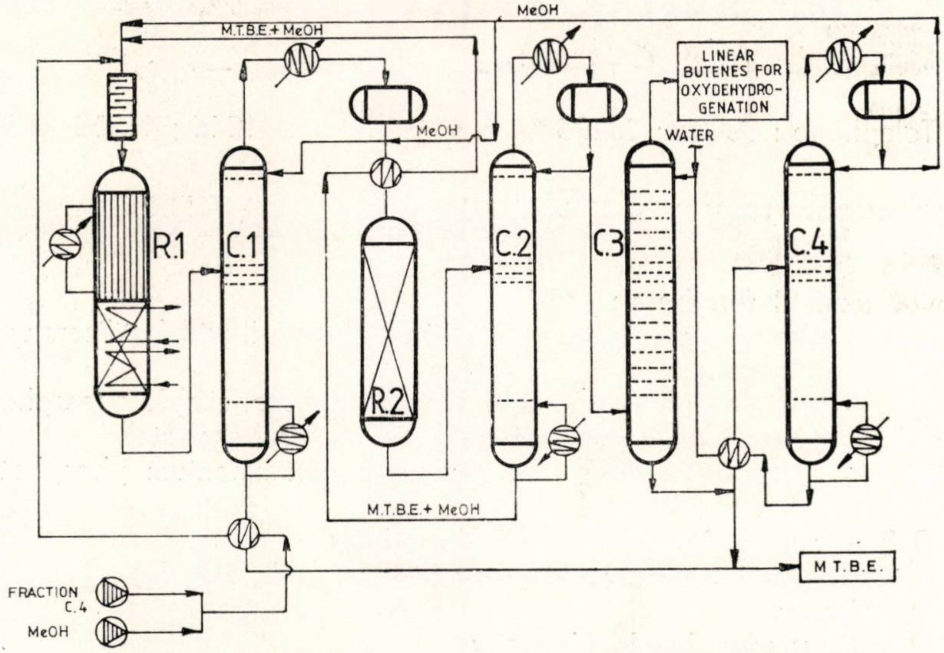

Flow-sheet of the ICITPR technology for obtaining simultaneously MTBE and linear butenes with a low content of isobutene.

Performance of the process

Characteristics of the finished products

MTBE for motor-gasoline		Linear butenes for oxydehydrogenation	
MTBE	min. 98 %	Isobutene	max. 0.2 %
C_4 hydrocarbon	max. 0.3 %	Methanol	max. 10 ppm
Methanol	max. 1 %	MTBE	max. 10 ppm
Diisobutene	max. 0.5 %	Water	5 ppm
Tert-butanol	max. 0.2 %		

Consumption of raw materials and utilities per ton of MTBE

	MTBE from C_4 pyrolysis cut		MTBE from catalytic cracking C_4 cut (15 % isobutene)
	One reaction step	Two reaction step	
Isobutene	670 kg	650 kg	650 kg
Methanol	365 kg	360 kg	365 kg
Low pressure steam	400 kg	700 kg	2200 kg
Cooling water (t=10°)	35 m^3	50 m^3	95 m^3
Electric energy	10 kWh	15 kWh	30 kWh

Process implementation

This process has been applied on an industrial scale in Romania. The plant produces linear butenes with a maximum 0.2% isobutene content (which are used for producing butadiene and 1-butene) and MTBE (that is used for increasing the octane number of the motor-gasoline).

CHEMICAL FERTILIZERS UNIT

— Craiova — Romania —

Telephone : 86405 ; 86496 Telex : 41246 ; 41353 ciich-r

PRODUCES AND DELIVERS

- **Chemical fertilizers :**
  - with nitrogen (urea, ammonium nitrate, liquid fertilizers with nitrogen)
  - with phosphorus (simple superphosphate, simple superphosphate with boron, concentrated superphosphate)
  - complexes (NPK – various types, diammonium phosphate, foliar fertilizers)
- **Inorganic and organic chemical products**
- **Condensed and liquefied gases (NH_3, O_2, N_2, SO_2 Ar)**
- **Polymers**
- **Catalysts for chemical industry**
- **Salts for treatment of metallic surfaces (degreasing salts, pickling, phosphatization, passivation)**

EXPORTERS:

CHIMICA

Foreign trade enterprise
Bucharest – ROMANIA
Splaiul Independenței 202A
Telephone : 495060
Telex : 11489 DANAZ-R
P.O. Box : 3915

DANUBIANA

Foreign trade enterprise
Bucharest – ROMANIA
Blvd. Republicii 10
Telephone : 156051 ; 156052
Telex : 11184 DANEX
P.O. Box : 1–74

DUNĂREA

Foreign trade enterprise
Bucharest – ROMANIA
Str. Varșovia 4
Telephone : 331681
Telex : 10435 DUNEX-R
P.O. Box : 63124

ORSZÁGOS MŰSZAKI
KÖZPONT
1883

NOTE POUR LES AUTEURS

La Revue Roumaine de Chimie publie des articles en anglais, français, russe, allemand ou espagnol. Les auteurs sont priés d'envoyer des articles et des comptes rendus inédits.

Les manuscrits seront dactylographiés à double interligne. La bibliographie, les tableaux et la légende des figures seront placés après le texte.

Si l'article fait partie d'une série numérotée, la partie précédente sera donnée comme première référence.

Chaque article sera précédée d'un résumé comprenant quinze lignes au maximum.

Les références bibliographiques dans le texte seront faites par des exposants sans parenthèses et paraîtront à la fin de l'ouvrage.

Les publications périodiques mentionnées dans la bibliographie seront présentées suivant les prescriptions internationales : le nom de l'auteur précédé de l'initiale du prénom, le titre du périodique abrégé conformément à « Chemical Abstract » et souligné par une ligne, le numéro du tome indiqué par des chiffres arabes et souligné par deux lignes, suivi de la première page de l'article : à la fin, l'année de la parution sera placée entre parenthèses. Le numéro de la revue ne sera pas indiqué si les pages du volume sont numérotées consécutivement.

Les textes des livrés ou traités inclueront : le nom des auteurs, précédés de l'initiale du prénom, le titre du livre entre guillements et sans être souligné, le numéro du tome précédé par l'abréviation « vol. » (ou « Bd. »), le numéro de l'édition, les éditions (the publisher), la localité de la parution du livre, l'année de la parution et la page de la référence précédée(s) par l'abréviation « p » (ou « S »).

Les brevets seront indiqués comme suit : l'auteur ou la firme, le pays et le numéro du brevet, la date de la revue (*Chem. Abstr.*). Par.ex. : M. Jones (to Union Carbide Co.). Brit. Pat. 610 238, 2 Sept. 1959 : et. *Chem. Abstr.*, **54**, 12808 (1960)

Si la référence n'a pas été lue en original, on indiquera aussi la revue de références consultée.

Les diagrammes seront tracés à l'encre de Chine sur papier calque. Les tableaux et les figures (en nombre strictement nécessaire), ainsi que les courbes dans les figures seront numerotés par des chiffres arabes. Leur explication sera donnée dans la légende des figures. Prière de ne pas inscrire les mêmes données dans les tableaux et les figures. Chaque tableau aura un titre. On indiquera dans le texte la place approximative des tableaux et des figures. Les formules chimiques seront incluses dans le texte ; en outre, elles seront transcrites sur papier calque, à l'encre de Chine.

Les auteurs sont priés d'indiquer les caractéres italiques (en soulignant les lettres au crayon), ainsi que tout autre caractère spécial : les préfixes, *ortho, meta, para, cis, trans*, etc. seront soulignés pour indiquer leurs caractères italiques, et ne seront jamais écrits avec des majuscules.

Aucune correction à la main ne sera admise sur le manuscrit. Les correction seront frappées à la machine. Les lettres grecques ou d'autres symboles spéciaux seront insérés à la main à l'encre clairement.

Le manuscrit sera signé par l'auteur.

Le titre courant aura 50 lettres au maximum.

L'entière responsabilité du contenu des articles appartient aux auteurs.

Sur demande on peut obtenir une note plus complète.

PRINTED IN ROMANIA

1986 NOV 25

TRAVAUX PARUS AUX ÉDITIONS DE L'ACADÉMIE DE LA RÉPUBLIQUE SOCIALISTE DE ROUMANIE

RAUL MIHAIL, ION GROZEANU, **Estimarea secvenţială aplicată sistemelor chimice, 1986, 406 p.**

M. BREZEANU, L. PATRON, M. ANDRUH, **Combinaţii complexe polinucleare şi aplicaţiile lor, 1986, 224 p.**

V. DRĂGUŢAN, A. T. BALABAN, M. DIMONIE, **Olefin Metathesis and Ring-Opening Polymerization of Cyclo-Olefins**, coédition avec John Wiley and Sons, 1985, 544 p.

C. LITEANU, I. RÎCĂ, **Optimizarea proceselor analitice**, 1985, 360 p.

N. PERESCU, **Chimia extracţiei cu solvenţi şi aplicaţii**, 1985, 212 p.

V. EM. SAHINI, N. HILLEBRAND, **Chimie cuantică în exemple şi aplicaţii**, 1985, 378 p.

GH. MARCU, **Chimia compuşilor coordinativi**, 1984, 415 p.

E. CORDOŞ, C. MANOLIU, **Spectrometria de absorbţie şi fluorescenţa atomică**, 1984, 178 p.

C. BODEA, **Tratat de biochimie vegetală**, p. II, vol. 5, 1984, 438 p.

ELENA CEAUŞESCU, **Cercetări în chimia şi tehnologia polimerilor**, 1983, 519 p.

N. ASANDEI, A. GRIGORIU, **Chimia şi structura fibrelor**, 1983, 395 p.

N. IONESCU, M. CĂLDĂRARU, **Oxidarea catalitică a olefinelor inferioare**, 1983, 178 p.

C. CAŞCAVAL, **Studiul polimerilor prin piroliză şi cromatografie de gaze**, 1983, 220 p.

C. I. SIMIONESCU, F. DANEŞ, **Originea vieţii**, 1983, 110 p.

C. BODEA (sous la direction), **Tratat de biochimie vegetală**, p. II, t. IV, 1982, 408 p.

I. G. MURGULESCU, RODICA VÎLCU, **Introducere în chimia fizică. Vol. III. Termodinamica chimică**, 1982, 624 p.

I. G. MURGULESCU, J. PĂUN, **Introducerea în chimia fizică. Vol. I. 3, Nucleul atomic, reacţii nucleare, particule elementare**, 1982, 606 p.

ELENA CEAUŞESCU, **Noi cercetări în domeniul compuşilor macromoleculari**, 1981, 536 p.

I. G. MURGULESCU, TATIANA ONCESCU, E. SEGAL, **Introducere în chimia fizică, Vol II. 2. Cinematică chimică şi cataliză**, 1981, 1024 p.

LYDIA-MARIA VAICUM, **Epurarea apelor uzate cu nămol activ. Bazele biochimice**, 1981, 218 p.

I. GĂLĂŢEANU, **Procese şi metode radiochimice în energetica nucleară**, 1981, 234 p.

O. IORDACHE, **Procese polistocastice la fenomenele de transfer**, 1981, 186 p.

CR. SIMIONESCU, VALERIA GORDUZA, **Polimeri biocompatibili şi biologic activi**, 1980, 479 p.

ELENA CEAUŞESCU, **Polimerizarea stereospecifică a izoprenului**, 1979, 307 p.

C. GH. MACAROVICI, **Analiza chimică cantitativă anorganică**, 1979, 457 p.

M. FLORESCU, **Metode ştiinţifice în dezvoltarea industriei chimice moderne**, 1979, 256 p.

A. T. BALABAN, I. GĂLĂŢEANU, G. GEORGESCU, LIGIA SIMIONESCU, **Compuşi marcaţi şi radiofarmaceutici cu aplicaţii în medicina nucleară**, 1979, 495 p.

I. G. MURGULESCU, E. SEGAL, **Introducere în chimia fizică. Vol. II. 1. Teoria molecular-cinetică a materiei**, 1979, 1036 p.

S. STERNBERG, FL. DANEŞ, **Termodinamica chimică aplicată** 1978, 400 p.

I. G. MURGULESCU, V. EM. SAHINI, **Introducere în chimia fizică. Vol. I. 2. Structura şi proprietăţile moleculelor**, 1978, 604 p.

I. ZUGRĂVESCU, MAGDA PETROVANU, **N-ylid chemistry**, coédition avec McGraw-Hil International Book Company, U.S.A., 1977, 396 p.

I. G. MURGULESCU, **Introducere în chimia fizică. Vol. I. 1. Atomi, molecule, legătură chimică**, 1976, 560 p.

ELENA CEAUŞESCU, **Research work on synthesis and characterization of macromolecular compounds, Contributions**, 1974, 251 p.

CR. SIMIONESCU, VIORICA RUSAN, V. POPA, **Chimia algelor marine**, 1974, 212 p., 1 pl.

T. ONCESCU, S. G. IONESCU, **Conversie fotochimică şi stocare de energie solară, 1985, 272 p.**

ISSN 0035–3930

I.P. INFORMAŢIA c. 2473

43 426

Lei 40

$ 80 (pour un abonnement annuel)